UNCLASSIFIED

AD NUMBER
AD380820
CLASSIFICATION CHANGES
TO: unclassified
FROM: confidential
LIMITATION CHANGES
TO: Approved for public release, distribution unlimited
FROM: Distribution authorized to U.S. Gov't. agencies only; Administrative/Operational Use; 30 NOV 1964. Other requests shall be referred to Federal Aviation Administration, Washington, DC.
AUTHORITY
FAA ltr, 10 Oct 1972; FAA ltr, 10 Oct 1972

THIS PAGE IS UNCLASSIFIED

Report No. PWA-2397-VOL-1 CONFIDENTIAL

30 November 1964

Copy # _____

ACCESSION NR
13

SUPERSONIC TRANSPORT AIRCRAFT ENGINE

PHASE II-A DEVELOPMENT PROGRAM.

VOLUME I

FINAL REPORT, 1 Jun-30 Nov 64.

PWA-E. H. Document Control
Eng. Sub-Control Station

Prepared Under Contract FA-SS-64-2

Number: 039-5-C1P-AYO

Period Covered
1 June 1964 through 30 November 1964

FAA SECURITY CONTROL
NO. 65 603-A-1

(FOR OFFICIAL USE ONLY)

DDC
MAY 8 1967

30 Nov 64

1v.

This document contains information affecting the national defense of the United States within the meaning of the Espionage Laws, Title 18 U S C, Sections 793 and 794. Its transmission or the revelation of its contents in any manner to an unauthorized person is prohibited by law.

Reproduction, distribution and use of this document are limited as specified in the contract under which it was prepared. Use for other than U. S. Governmental purposes is subject to prior approval of United Aircraft Corporation.

Approved by R. L. Toft

R. L. Toft
Project Engineer

Pratt & Whitney Aircraft DIVISION OF UNITED AIRCRAFT CORPORATION

EAST HARTFORD • CONNECTICUT

(287 500) CONFIDENTIAL

DOWNGRADED AT 3 YEAR INTERVALS;
DECLASSIFIED AFTER 12 YEARS.
DOD DIR 5200.10

Best
Available
Copy

NOTICES

When Government drawings, specifications, or other data are used for any purpose other than in connection with a definitely related Government procurement operation, the United States Government thereby incurs no responsibility nor any obligation whatsoever; and the fact that the Government may have formulated, furnished, or in any way supplied the said drawings, specifications, or other data, is not to be regarded by implication or otherwise as in any manner licensing the holder or any other person or corporation, or conveying any rights or permission to manufacture, use, or sell any patented invention that may in any way be related thereto.

Copies have been placed in the DDC collection. U.S. Government agencies may obtain copies from DDC. Other qualified DDC users may request, by submission of a DDC Form 1, through:

Director of Supersonic Transport Development
Federal Aviation Agency
Washington, D.C. 20553

Defense Documentation Center release to the Clearinghouse for Federal, Scientific, and Technical Information (CFSTI) and foreign announcement and dissemination are not authorized. The distribution of this report is limited because it contains technology identifiable with items excluded from export by the Department of State (U.S. Export Control Act of 1949 as amended).

Material in this publication relating to

JET FLAMEHOLDER

reveals subject matter contained in a patent application which has been placed under Secrecy Order by the Commissioner of Patents. This Secrecy Order has been modified by a "Permit A".

A Secrecy Order prohibits publication or disclosure of the invention, or any material information with respect thereto. It is separate and distinct, and has nothing to do with, the classification of Government contracts.

By statute, violation of a Secrecy Order is punishable by a fine not to exceed $10,000 and/or imprisonment for not more than two years.

A "Permit A" authorizes disclosure of the subject matter of the patent application to any person of the classes hereinafter specified if such person is known to be concerned directly in an official capacity with the subject matter, provided that all reasonable safeguards are taken to otherwise protect the invention from unauthorized disclosure. The specified classes are

(a) Any officer or employee of any department, independent agency, or bureau of the Government of the United States

(b) Any person designated specifically by the head of any department, independent agency or bureau of the Government of the United States, or by his duly authorized subordinate, as a proper individual to receive the disclosure of the above indicated application.

A "Permit A" also authorizes disclosure to the minimum necessary number of persons of known loyalty and discretion, employed by or working with United Aircraft Corporation or its licensees and whose duties involve cooperation in the development, manufacture or use of the subject matter by or for the Government of the United States, provided such persons are advised of the issuance of the Secrecy Order.

Should it appear necessary to make disclosures not authorized above, a request for modification of the Secrecy Order should be made through the Pratt & Whitney Aircraft Patent Engineer.

The foregoing does not in any way lessen responsibility for the security of the subject matter as imposed by any Government contract or the provisions of the existing laws relating to espionage and national security.

STATEMENT #3 CLASSIFIED

In addition to security requirements which apply to this document and must be met, each transmittal outside the agencies of the U.S. Government must have prior approval of FAA, Washington, D.C.

FOREWORD

This report describes the work which was accomplished by Pratt & Whitney Aircraft during the period 1 June 1964 through 30 November 1964 in accordance with the requirements of Contract FA-SS-64-2 entitled "Development of a Supersonic Transport Aircraft Engine - Phase IIA". The report is being submitted to fulfill the requirements of Item 20, Section C of the contract work statement for a final report describing in detail all work accomplished during this phase of the program.

This report is classified as CONFIDENTIAL in accordance with the provisions of DD Form 254 dated 9 September 1964 provided for this contract.

TABLE OF CONTENTS

FOREWORD	i
TABLE OF CONTENTS	ii
LIST OF ILLUSTRATIONS	xiv
Item 1 - SYSTEM ANALYSIS	1-1
Item 2 - PRELIMINARY DESIGN	
A. Aerodynamic Turbojet Studies	2-1
1. Introduction	2-1
2. Compressor	2-2
3. Main Burner	2-3
4. Turbine	2-6
5. Afterburning Turbojet - STJ222	2-6
6. Partial Afterburning Turbojet - STJ227	2-8
B. Mechanical Turbojet Studies	
1. Non-Afterburning Turbojet - STJ221	2-9
2. Afterburning Turbojet - STJ222	2-12
3. Partial Afterburning Turbojet - STJ227	2-13
C. Aerodynamic Turbofan Studies - STF219	2-14
1. General Description	2-14
2. Fan	2-15
3. High Pressure Compressor	2-17
4. Main Burner	2-19
5. Duct Heater	2-19
6. Turbine	2-22
D. Mechanical Turbofan Studies	2-26
1. Fan and Compressors	2-26
2. Diffuser	2-39
3. Combustion Chamber	2-42

DOWNGRADED AT 3 YEAR INTERVALS
NOT AUTOMATICALLY DECLASSIFIED AFTER 12 YEARS
DOD DIR 5200.10

TABLE OF CONTENTS (Cont'd)

4.	Turbine	2-48
5.	Turbine Shafts	2-57
6.	Number 3 Bearing Compartment and Supporting Structure	2-59
7.	Turbine Exhaust Section	2-61
8.	Number 4 Bearing	2-62
9.	Duct Heater	2-64
10.	Duct Heater Nozzle	2-70
11.	Ejector Reverser	2-71
12.	Assembly of Major Components	2-76
13.	Engine Assembly	2-81
14.	Preliminary Vibration Analysis	2-84
15.	Thrust Balance	2-86
16.	Fuel and Oil Heat Rejection Systems	2-88
17.	External Plumbing, Brackets, and Hardware	2-90
18.	Engine Mounts	2-93
19.	Engine Accessory Drives	2-96
20.	Engine Starting	2-98
E.	STF219 Cooled Turbine Design	2-100
1.	Introduction	2-100
2.	Approach	2-102
3.	Design Tools	2-103
4.	Design Problem	2-103
5.	Design Emphasis	2-105
6.	Heat Transfer and Life Analysis	2-105
7.	Environmental Conditions	2-106
8.	Specific Designs - 1st Turbine Vane	2-106
9.	Specific Design - 1st Blade	2-111
10.	Specific Design - 2nd Stage Vane	2-113
11.	Specific Design - 2nd Blade	2-114
12.	Specific Design - 3rd Vane	2-115
13.	Specific Design - 3rd Blade	2-116
14.	Future Growth	2-117
Item 3 - SPECIFICATIONS		3-1

DOWNGRADED AT 3 YEAR INTERVALS
NOT AUTOMATICALLY DECLASSIFIED AFTER 12 YEARS
DOD DIR 5200.10

TABLE OF CONTENTS (Cont'd)

Item 4 - COMPRESSOR DEVELOPMENT

A. Introduction 4-1

B. Experimental Program 4-1
1. Single-Stage Fan Rig 4-1
2. Two-Stage Fan Rig 4-3
3. Multistage Compressor 4-4

Item 5 - PRIMARY COMBUSTION

A. Introduction 5-1

B. Ram Induction Burner Testing 5-1
1. Program and Test Procedures 5-2
2. Test Results 5-3
3. Conclusions 5-4

C. Two-Dimensional Segmental Burner Rig Testing 5-4
1. Program and Test Procedures 5-4
2. Test Results 5-5
3. Conclusions 5-5

D. Showerhead Burner Testing 5-6
1. Program and Test Procedures 5-6
2. Test Results 5-6
3. Conclusions 5-6

E. Hot Cone Burner Testing 5-7
1. Program and Test Procedures 5-7
2. Test Results 5-7
3. Conclusions 5-8

F. Large-Scale Full-Annular Burner Rig Testing 5-9
1. Test Results 5-9
2. Conclusions 5-10

G. Advanced Primary Combustion Rig Testing 5-11
1. Program and Test Procedures 5-11
2. Test Results 5-12
3. Conclusions 5-12

DOWNGRADED AT 3 YEAR INTERVALS
DECLASSIFIED AFTER 12 YEARS
DOD DIR 5200.10

TABLE OF CONTENTS (Cont'd)

Item 6 - TURBINE DEVELOPMENT

A.	Introduction	6-1
	1. Single Specimen Tests to Optimize the Durability of Air Cooled Vanes and Blades	6-1
	2. Heat Transfer	6-2
	3. Performance Tests	6-2
	4. Engine Testing	6-2
B.	Single Specimen Rig Testing to Evaluate the Durability of Air Cooled Turbine Blades	6-2
	1. Description of Test Rig	6-3
	2. Thermal Shock Tests	6-3
	3. Clogging Tests	6-4
	4. Impact Tests	6-5
C.	Materials Laboratory Testing to Evaluate Blade and Materials Durability	6-5
	1. Blade Fatigue Tests	6-6
	2. Low Cycle Fatigue Tests	6-7
	3. Cyclic Creep Tests	6-7
	4. Cyclic Stress Rupture Tests	6-8
	5. High Temperature Fatigue Tests	6-8
D.	Investigation of the Heat Transfer Characteristics of Air Cooled Vanes in a Low Pressure Cascade Rig	6-9
	1. Description of Rig	6-9
	2. Test Results	6-10
E.	Investigation of Heat Transfer Characteristics of Air Cooled Turbine Vanes in a High Pressure Cascade Rig	6-10
F.	Heat Transfer Impingement Tests	6-10
G.	Testing of Air Cooled Vanes in a Hot Chocked Cascade Rig	6-11
	1. Description of Test Rig	6-11
	2. Test Program	6-12
H.	Aerodynamic Performance Testing of Turbine Vanes in a Plane Cascade Rig	6-12
	1. Film Cooled Vanes	6-12
	2. Transpiration Cooled Vanes	6-13

TABLE OF CONTENTS (Cont'd)

I.	Performance Testing of Film Cooled Blades and Vanes	6-14
	1. Description of Test Rig	6-14
	2. Description of Parts Tested	6-14
	3. Method of Test	6-16
	4. Test Results	6-16
J.	Evaluation of Full-Scale Turbine Blades and Vanes in a JT4 High Spool Engine	6-18
	1. Description of High Spool Engine	6-18
	2. Test Procedure	6-19
	3. Description of Film-Cooled Vanes and Blades Tested in High Spool Engine	6-19
	4. Description of Transpiration Cooled Blades and Vanes Used in High Spool Engine	6-21
	5. Description of Convectively Cooled Blades and Vanes Tested in High Spool Engine	6-23
	6. Tests of Convectively Cooled Blades in the JT4 High Spool Engine	6-23
	7. Initial Testing of Film and Transpiration Cooled Vanes and Blades in the JT4 High Spool Engine	6-25

Item 7 - AUGMENTORS

A.	Aerodynamic Flameholder Tests in Small-Scale Duct Heater Rigs	7-1
	1. Introduction	7-1
	2. Description	7-2
	3. Method of Test	7-3
	4. Test Results	7-4
	5. Discussion of Results	7-7
	6. Recommendations	7-8
B.	Ram Induction Burner Tests in Small-Scale Duct Heater Rigs	7-9
	1. Introduction	7-9
	2. Description	7-9
	3. Method of Test	7-10
	4. Test Results	7-11
	5. Recommendations	7-12

TABLE OF CONTENTS (Cont'd)

C. Heterogeneous Burner Tests in Small-Scale Duct Heater Rig 7-13
1. Introduction 7-13
2. Description 7-13
3. Method of Test 7-14
4. Test Results 7-15

D. Full-Scale Duct Heater Testing 7-16
1. Introduction 7-16
2. Description 7-16
3. Test Facility 7-17
4. Method of Test 7-18
5. Test Results 7-19
6. Recommendations 7-22

E. Small-Scale Afterburner Testing 7-23
1. Introduction 7-23
2. Description 7-23
3. Method of Test 7-24
4. Discussion of Results 7-25

Item 8 - EXHAUST SYSTEM

A. Introduction 8-1

B. Summary 8-2

C. Test Program 8-3
1. Nozzle Description 8-3
2. Test Facilities 8-4
3. Discussion 8-4

Item 9 - NOISE REDUCTION

A. Introduction 9-1

B. Review of Noise Suppression Devices 9-3
1. Exhaust Noise 9-3
2. Compressor Noise 9-7

DOWNGRADED AT 3 YEAR INTERVALS
DECLASSIFIED AFTER 12 YEARS
DOD DIR 5200.10

THIS DOCUMENT CONTAINS INFORMATION AFFECTING THE NATIONAL DEFENSE OF THE UNITED STATES WITHIN THE MEANING OF THE ESPIONAGE LAWS, TITLE 18, U.S.C., SECTIONS 793 AND 794. ITS TRANSMISSION OR THE REVELATION OF ITS CONTENTS IN ANY MANNER TO AN UNAUTHORIZED PERSON IS PROHIBITED BY LAW.

TABLE OF CONTENTS (Cont'd)

3.	Inlet Noise	9-11
4.	Fan Discharge Noise	9-11
5.	Application of Acoustic Test Experience to the SST Engine	9-12
C.	Inlet Duct Propagation Characteristics	9-14
1.	General Discussion	9-14
2.	Facilities	9-15
3.	Experimental Program	9-15
4.	Recommendations	9-19
5.	Analysis of Results	9-19
6.	Discussion of Results	9-20
D.	Sound Absorbing Materials	9-23
1.	Objective of Tests	9-23
2.	Description of Facilities	9-23
3.	Method of Test	9-24
4.	Results	9-26
5.	Effect of Results on SST Airplane Design	9-28
6.	Recommendations	9-28
E.	Exhaust Noise	9-28
1.	Introduction	9-28
2.	Description of Facilities	9-29
3.	Method of Test	9-30
4.	Results	9-33
5.	Recommendations	9-36
F.	Analysis of Total SST Airplane Noise	9-38
1.	Engine Size	9-39
2.	Engine Noise Levels	9-39
3.	Noise Suppression	9-40
4.	STF219 Engine Noise Levels	9-42
5.	Airplane Fly-Over Noise Levels	9-43

Item 9 - Appendix A

Item 9 - Appendix B

DOWNGRADED AT 3 YEAR INTERVALS
DECLASSIFIED AFTER 12 YEARS
DOD DIR 5200.10

THIS DOCUMENT CONTAINS INFORMATION AFFECTING THE NATIONAL DEFENSE OF THE UNITED STATES WITHIN THE MEANING OF THE ESPIONAGE LAWS, TITLE 18, U.S.C., SECTIONS 793 AND 794. THE TRANSMISSION OR REVELATION OF ITS CONTENTS IN ANY MANNER TO AN UNAUTHORIZED PERSON IS PROHIBITED BY LAW.

TABLE OF CONTENTS (Cont'd)

Item 10 - CONTROLS AND ACCESSORIES

A. Controls 10-1
1. Introduction 10-1
2. Description of Components 10-2
3. Control Methods 10-5
4. Engine Transient Performance 10-8
5. Thrust Reverser 10-11
6. Control Vendor Status 10-12
7. Control System Components 10-12

B. Accessories - Ignition System 10-13
1. Introduction 10-13
2. Components 10-14
3. Facilities 10-14
4. Test Procedure 10-15
5. Discussion of Results 10-16
6. Recommendations 10-20

Appendix 10-A
PWA Purchase Specification 819D
PWA Purchase Specification 858
PWA Purchase Specification 859
PWA Purchase Specification 860

Item 11 - BEARING AND SEAL DEVELOPMENT

A. Bearing Development 11-1
1. Introduction 11-1
2. Description 11-2
3. Method of Test 11-4
4. Test Results 11-5
5. Discussion of Results 11-7
6. Recommendations 11-8

B. Bearing Materials 11-9
1. Introduction 11-9
2. Description 11-9
3. Method of Test 11-10
4. Test Results 11-10
5. Discussion of Results 11-10
6. Recommendations 11-10

TABLE OF CONTENTS (Cont'd)

C. Seal Development 11-11
1. Introduction 11-11
2. Description 11-11
3. Method of Test 11-12
4. Test Results 11-13
5. Discussion of Results 11-14
6. Recommendations 11-15

D. Ring Seal Design 11-15
1. Introduction 11-15
2. Description 11-15
3. Method of Test 11-16
4. Test Results 11-16
5. Conclusions 11-17
6. Recommendations 11-17

Item 12 - FUELS

A. Introduction 12-1

B. Jet Fuel Survey 12-1
1. Fuel Inspection Data 12-3
2. Breakpoint Temperatures 12-3
3. Effect of Reservoir Heating 12-5
4. Fuel Lubricity 12-5

C. Investigation of the Effect of Oxygen Content on Fuel Thermal Stability 12-7

D. Review of Thermal Stability Requirements 12-11

E. Thermal Stability Improvement with Additives 12-17

Item 13 - LUBRICANTS

A. Introduction 13-1

B. Lubricant Environment 13-1
1. Temperature 13-2
2. Oil Tank Capacity 13-2
3. Air Contacting Oil 13-2
4. Bearings 13-2

DOWNGRADED AT 3 YEAR INTERVALS
DECLASSIFIED AFTER 12 YEARS
DOD DIR 5200.10

THIS DOCUMENT CONTAINS INFORMATION AFFECTING THE NATIONAL DEFENSE OF THE UNITED STATES WITHIN THE MEANING OF THE ESPIONAGE LAWS, TITLE 18, U.S.C., SECTIONS 793 AND 794. THE TRANSMISSION OR THE REVELATION OF ITS CONTENTS IN ANY MANNER TO AN UNAUTHORIZED PERSON IS PROHIBITED BY LAW.

TABLE OF CONTENTS (Cont'd)

5.	Alloys in Lubricating System	13-3
6.	Gears	13-3
7.	Elastomers	13-3
8.	Lubricant Viscosity	13-3
9.	Lubricant Volatility	13-3
C.	Gear Pitting Tests	13-4
D.	Discussion	13-4
Item 14 - INLETS		
A.	Engine - Inlet Compatiblity	14-1
1.	Introduction	14-1
2.	Discussion	14-1
3.	Conclusions	14-4
Item 15 - MATERIALS AND MANUFACTURING TECHNIQUES		
A.	Introduction	15-1
B.	Compressor Materials	15-1
1.	Disk Material Evaluations	15-1
2.	Disk and Blade Material Evaluations - Salt Corrosion	15-5
3.	Case Material Evaluations - Containment	15-6
C.	Turbine Materials	15-9
1.	Long-Time Creep Testing	15-9
2.	Programs for Fundamental Thermal Fatigue Testing	15-10
3.	Long-Time Erosion - Bar Testing	15-11
4.	Electron Microscopy and Phase - Identification Studies	15-11
Item 16 - OPERATIONS AND ECONOMICS		16-1
A.	Introduction	16-2
B.	Studies to Determine Optimum Engine Configuration	16-3
1.	Relative Engine Price	16-3
2.	Relative Development Cost	16-4
3.	Effect of Program Size	16-4

DOWNGRADED AT 3 YEAR INTERVALS
DECLASSIFIED AFTER 12 YEARS
DOD DIR 5200.10

TABLE OF CONTENTS (Cont'd)

4.	Effect of Design Cruise Mach Number	16-4
5.	Estimated Engine Labor Costs	16-4
6.	Analysis of Factors Affecting Engine Maintenance Material Cost	16-5
7.	Estimate of Engine Materials Costs	16-7
C.	Economic Factors	16-9
1.	Engine-Aircraft Matching	16-9
2.	Fuel Costs	16-10
3.	Oil Cost	16-10
4.	Depreciation	16-10
5.	Engine Prices	16-10
6.	Engine Development Costs	16-11
7.	Engine Labor Cost Estimates	16-12
8.	Engine Maintenance Material Cost Estimates	16-13

Item 16 - APPENDIX A

Item 16 - APPENDIX B

Item 17 - SUPPORTING DESIGN CONSIDERATIONS

A.	Reliability	17-1
1.	Introduction	17-1
2.	Comparative Reliability Analyses	17-2
3.	Failure Mode Analysis and Design Review	17-2
4.	STF219 Estimated Flight Reliability	17-3
5.	Engine Reliability Features	17-4
B.	Configuration Management	17-8
1.	Objective	17-8
2.	Discussion	17-8
C.	Weight and Configuration Control	17-10
1.	Weight Analysis	17-10
2.	Lightweight Design Features	17-11
3.	Weight Scaling	17-13
4.	Turbojet Weight Analysis	17-13
5.	Mixed Flow Afterburning Turbofan	17-14
D.	Value Engineering	17-14

DOWNGRADED AT 3 YEAR INTERVALS
DECLASSIFIED AFTER 12 YEARS
DOD DIR 5200.10

THIS DOCUMENT CONTAINS INFORMATION AFFECTING THE NATIONAL DEFENSE OF THE UNITED STATES WITHIN THE MEANING OF THE ESPIONAGE LAWS, TITLE 18, U.S.C., SECTIONS 793 AND 794. THE TRANSMISSION OR THE REVELATION OF ITS CONTENTS IN ANY MANNER TO AN UNAUTHORIZED PERSON IS PROHIBITED BY LAW.

TABLE OF CONTENTS (Cont'd)

E.	Maintainability	17-16
	1. Introduction	17-16
	2. Maintainability Engineering	17-16
	3. Comparison of Various Designs	17-17
	4. Flight Line Maintenance	17-17
	5. Hot Section Maintenance	17-18
	6. Field Repair	17-19
	7. Overhaul	17-21
	8. Maintenance Plan	17-21
F.	Safety	17-21
	1. Introduction	17-21
	2. Monitoring the Safety Aspects of Engine Design	17-22
	3. Fail-Safe and Redundant Features	17-22

DOWNGRADED AT 3 YEAR INTERVALS
DECLASSIFIED AFTER 12 YEARS
DOD DIR 5200.10

LIST OF ILLUSTRATIONS

SYSTEM ANALYSIS

1-1 Uninstalled Engine Performance of the STF219, STJ221, STJ222, STF223, and STJ227 Engines at Mach 2.7 at 65,000 Feet

1-2 Uninstalled Engine Performance of the STF219, STJ221, STJ222, STF223, and STJ227 Engines at Mach 3.0 at 75,000 Feet

1-3 Uninstalled Engine Performance of the STF219, STJ221, STJ222, STF223 and STJ227 Engines At Mach 0.9 at 36,150 Feet

1-4 Uninstalled Engine Performance of the STF219, STJ221, STJ222, STF223, and STJ227 Engines at Mach 0.6 at 15,000 Feet

1-5 Performance of the STF219 Engine With Cruise Turbine Inlet Temperatures of 1900°F and 2200°F and of the JT11F-3, -4 Engine at Mach 2.7 at 65,000 Feet

1-6 Performance of the STF219 Engine With Cruise Turbine Inlet Temperatures of 1900°F and 2200°F and of the JT11F-3, -4 Engine at Mach 3.0 at 75,000 Feet

1-7 Performance of the STF219 Engine With Cruise Turbine Inlet Temperatures of 1900°F and 2200°F and of the JT11F-3, -4 Engine at Mach 0.9 at 36,150 Feet

1-8 Performance of the STF219 Engine With Cruise Turbine Inlet Temperatures of 1900°F and 2200°F and of the JT11F-3, -4 Engine at Mach 0.6 at 15,000 Feet

LIST OF ILLUSTRATIONS (Con't)

PRELIMINARY DESIGN

2-1 Cross-Section of Nine Stage Compressor of STJ221 Engine

2-2 Flow Paths and Weights of Compressor Configurations Considered for STJ221 Engine

2-3 Predicted Performance of STJ221 Compressor

2-4 Schematic Diagram of Ram Induction Burner

2-5 Detailed Section of Scoop with Film Cooling Louvers on Ram Induction Burner

2-6 Temperature Profile Produced by Ram Induction Burner with Scoops Extending to the Middle of the Burner

2-7 Temperature Profile Produced by Ram Induction Burner with Limited Penetration

2-8 Penetration and Mixing Characteristics of the Downstream Row of Primary Ram Induction Burner Scoops

2-9 Flow Pattern in Recirculation Zone of Ram Induction Burner

2-10 Burner Liner to be Used in Secondary Scoop Design Studies

2-11 Burner Liner to be Used in Secondary Scoop Design Studies

2-12 STJ222 Afterburner

2-13 Typical Spray Ring-Flameholder Used in Afterburner of STJ222 Engine

2-14 Estimated Efficiency of Afterburner as a Function of the Fuel-to-Air Ratio

DOWNGRADED AT 3 YEAR INTERVALS
DECLASSIFIED AFTER 12 YEARS
DOD DIR 5200.10

LIST OF ILLUSTRATIONS (Con't)

2-15 Schematic Diagram of Tailpipe, Nozzle, and Turbine Exit Guide Vanes of STJ227 Engine

2-16 Cross-Sectional View of Integral Spray Bar-Flameholder-Exit Guide Vane Assembly

2-17 Schematic Diagram of STJ227 Partial Afterburner Showing Cooling Flow

2-18 Cross Sectional Drawing of STJ221 Engine

2-19 Cross Sectional Drawing of STJ222 Engine

2-20 Sectioned View of Alternate Spray Bar-Flameholder System for STJ222 Engine

2-21 Axial View of Alternate Spray Bar-Flameholder System for STJ222 Engine

2-22 Cross Sectional Drawing of STJ227 Engine

2-23 Cross Sectional Drawing of STF219-B Engine

2-24 Cross Sectional Drawing of STF219-L Engine

2-25 Schematic Diagram of Fan and Compressor of STF219 Engine

2-26 Predicted Performance Map for the STF219 Engine Fan

2-27 Two-Stage Fan Gas Path Comparison

2-28 Fan Pressure Ratio Compatibility

2-29 Fan Surge Line as a Function of Root Wheel Speed

2-30 Mean Line Air Triangles for the JT11F-11, 12 and the STF219 Fans for the Fan and Engine Portions of the Flow

LIST OF ILLUSTRATIONS (Con't)

2-31 Predicted Performance Map for the STF219 Engine High-Pressure Compressor

2-32 Mean Line Air Triangles for the JT11F-11, -12 and STF219 High-Pressure Compressors

2-33 Burner Characteristics at Sea-Level Take-Off Conditions for the STF219 and JT11F-11, -12 Engines

2-34 Schematic Diagram of Alternate Duct Heater for the STF219 Engine

2-35 Turbine Gas Path Dimensions

2-36 Relationships of Factors Considered in Optimizing the STF219 Turbine Parameters

2-37 Turbine Efficiency as a Function of Velocity Ratio

2-38 High Pressure Turbine Performance

2-39 High Pressure Turbine Inlet Flow Parameter

2-40 Low-Pressure Turbine Performance

2-41 Low-Pressure Turbine Inlet Flow Parameter

2-42 Engine Plus Fuel Weight of Single-Stage Low-Pressure Turbine Relative to Two-Stage Low Pressure Turbine as a Function of the Relative Maximum Diameter

2-43 Engine Plus Fuel Weight of Single-Stage Low-Pressure Turbine Relative to Two-Stage Low-Pressure Turbine as a Function of the Rotor Speed

2-44 Extended Root Blade with Mechanical Damping

2-45 Schematic Diagram of Diffuser of STF219 Engine

2-46 Schematic Diagram of Axially Split Annular Burner

LIST OF ILLUSTRATIONS (Con't)

2-47 Cross-Section of First-Stage Turbine Vane

2-48 Cross-Section of Second-Stage Turbine Vane

2-49 Cross-Section of First-Stage Turbine Blade

2-50 Schematic Diagram of Turbine, Turbine Exhaust Nozzle, and Number 3 Bearing Assembly

2-51 Schematic Diagram of Duct Heater for STF219 Engine

2-52 Duct Heater Nozzle and Ejector-Reverser for Lockheed

2-53 Duct Heater and Ejector Reverser for Boeing

2-54 Typical Thrust Reverser Segment

2-55 Major Assemblies of STF219 Engine

2-56 Duct Heater Nozzle and Ejector - Reverser Assembly

2-57 Resonance Diagram for First Rotor of STF219 Engine

2-58 Resonance Diagram for Second Rotor of STF219 Engine

2-59 Resonance Diagram for Fourth Rotor of STF219 Engine

2-60 Resonance Diagram for Seventh Rotor of STF219 Engine

2-61 Low Speed Rotor Stiff Bearing Mode Shape

2-62 High Speed Rotor Stiff Bearing Mode Shape

2-63 Internal Cooling and Thrust Balance Air System

2-64 Fuel-Oil System for STF219 Engine

LIST OF ILLUSTRATIONS (Con't)

2-65 Lockheed Mission Profile

2-66 Engine, Duct, and Total Fuel Flow Rates for Lockheed Mission

2-67 Estimated Total Engine System Heat Rejection Rate for Lockheed Mission

2-68 Estimated Duct Heater Fuel Pump Energy Input to Fuel as a Function of Duct Heater Fuel Flow for the Lockheed Mission

2-69 Boeing Mach Number Mission Profile

2-70 Boeing Altitude Mission Profile

2-71 Engine, Duct, and Total Fuel Flow Rates for Boeing Mission

2-72 Estimated Total Engine System Heat Rejection Rate for Boeing Mission

2-73 Estimated Duct Heater Fuel Pump Energy Input to Fuel as a Function of Duct Heater Fuel Flow for the Boeing Mission

2-74 Estimated Fuel and Oil Temperatures for the Lockheed Mission (Calculated by Lockheed)

2-75 Estimated Fuel and Oil Temperatures for the Boeing Mission (Fuel Temperatures Calculated by Boeing)

2-76 Typical Double-Wall Heat Shielding Structure

2-77 Typical Metal Foil Heat Shielding Structure

2-78 Typical Seals for STF219 Engine

2-79 Typical Tube Support and Clamping Configurations

2-80 Maneuver Loads for STF219 Engine Mounts

LIST OF ILLUSTRATIONS (Con't)

2-81 Maximum Flight Loads for Lockheed Engine

2-82 Maximum Flight Loads for Boeing Engine

2-83 Ultimate Lateral External Gust Loads for Boeing Aircraft

2-84 Engine Ground Handling Planes (Lockheed)

2-85 Engine Ground Handling Planes (Boeing)

2-86 Cross-Section of Accessory Drive Gearbox

2-87 Mounting System for Gearbox

2-88 Schematic Diagram of Gearbox

2-89 Right-Angle Power Take-Off Drive

2-90 Estimated Motoring Torque at Tower Shaft for Boeing Engine

2-91 Estimated Motoring Torque at Gearbox Shaft for Lockheed Engine

2-92 Estimated Starter Torque for Air Turbine Starter at Tower Shaft for Boeing Engine

2-93 Estimated Starter Torque for Air Turbine Starter at Gearbox Shaft for Lockheed Engine

2-94 Starter and Motoring Horsepower for Boeing Engine

2-95 Starter and Motoring Horsepower for Lockheed Engine

2-96 Effect of Temperature on Starter Motoring Torque

2-97 Impingement Heat Transfer Coefficient, Correlation of Experimental Results Obtained on Impingement Rig at Point of Impingement

LIST OF ILLUSTRATIONS (Con't)

2-98 100% Film Cooling Effectiveness at Trailing Edge Demonstrated in UAC Cascade Rig

2-99 18% Film Cooling Effectiveness at Leading Edge Demonstrated on Shielded Leading Edge Vane

2-100 Typical Transient Metal and Gas Temperatures

2-101 Average Gas Temperatures Entering Each Turbine Airfoil Row STF219 Supersonic Cruise

2-102 Tailored Spanwise Gas Temperature Variation First-Stage Turbine Vane

2-103 First-Stage Turbine Impingement Vane

2-104 First-Stage Turbine Impingement Vane. Spanwise Allowable and Predicted Metal Temperature

2-105 First-Stage Turbine Impingement Vane Showing Predicted Steady-State Metal Temperatures

2-106 First-Stage Turbine Detachable Leading Edge Shielded Vane

2-107 First-Stage Turbine Detachable Leading Edge Shielded Vane, Predicted Steady State, Metal Temperature °F

2-108 First-Stage Turbine Vane with Integrally Cast Leading Edge Shield

2-109 First-Stage Turbine Showerhead Blade

2-110 First-Stage Turbine Showerhead Blade Spanwise Allowable and Predicted Metal Temperature

2-111 First-Stage Turbine Showerhead Blade/Predicted Steady State Midspan Metal Temperature

LIST OF ILLUSTRATIONS (Con't)

2-112 First-Stage Turbine Blade with Integrally Case Leading Edge Shield

2-113 First-Stage Turbine Integral Cast Shield Blade Spanwise Allowable and Predicted Metal Temperature

2-114 First-Stage Turbine Integral Cast Shielded Blade/ Predicted Steady State Metal Temperature

2-115 Second-Stage Turbine Impingement Cooled Vane

2-116 Second-Stage Turbine Impingement Cooled Vane Spanwise Allowable and Predicted Metal Temperature

2-117 Second-Stage Turbine Impingement Cooled Vane/ Predicted Steady State Metal Temperature

2-118 Second-Stage Turbine Uncooled Blade Spanwise Allowable and Predicted Metal Temperature

2-119 Third-Stage Turbine Uncooled Vane Spanwise Allowable and Predicted Metal Temperature

2-120 Third-Stage Turbine Uncooled Blade Spanwise Allowable and Predicted Metal Temperature

COMPRESSOR DEVELOPMENT

4-1 Two-Stage Fan Rig First-Stage Rotor Assembly

4-2 Detail of Rotor Assembly with Welded Mid-Span Shrouds for Test in Single-Stage Fan Rig

4-3 Comparison of Single-Stage Fan Performance with Shroud Modifications

4-4 Assembled View of Two-Stage Fan Rig

4-5 Two-Stage Fan Rig Installed on Test Stand

4-6 Comparison of Original and Revised Flow Paths for Two-Stage Fan Rig

4-7 Multistage Variable-Geometry Compressor Rig Installed on Test Stand

4-8 Performance of Second Build of the Multistage Variable-Geometry Compressor Rig

4-9 Performance of Third Build of the Multistage Variable-Geometry Compressor Rig

4-10 Comparison of Multistage Compressor Efficiencies

PRIMARY COMBUSTION

5-1 Ram Induction Burner Test Section

5-2 Typical Burner Outlet Temperature Distribution Plot

5-3 Two-Dimensional Annular Burner

5-4 Two-Dimensional Annular Burner Rig Installation

5-5 Two-Dimensional Annular Burner (Shortened Version) Test Results

5-6 Showerhead Burner Configuration for Two-Dimensional Annular Testing

5-7 Schematic Diagram of Showerhead Burner Configuration

5-8 Schematic Diagram of Hot Cone Burner Front End.

5-9 Schematic Diagram of Full-Scale Annular Burner Rig

DOWNGRADED AT 3 YEAR INTERVALS
DECLASSIFIED AFTER 12 YEARS
DOD DIR 5200.10

LIST OF ILLUSTRATIONS (Con't)

5-10	SST Full-Scale Annular Burner Rig
5-11	Full-Scale Annular Burner Test Results
5-12	Effect of Inlet Trip on Inlet Total Pressure Profile
5-13	Average Exit Temperature Profile (Run 14)
5-14	Average Exit Temperature Profile (Run 15)
5-15	Isotherm Plot (Run 14)
5-16	Isotherm Plot (Run 15)
5-17	Advanced Primary Combustion Test Rig
5-18	Advanced Burner Configuration (Sch. I)
5-19	Advanced Burner Test Results
5-20	Advanced Burner Test Results
5-21	Advanced Burner Configuration (Sch. II)

TURBINE DEVELOPMENT

6-1	Film-Cooled Turbine Blade with 0.030 Inch Holes Drilled at 30° Angle to Leading Edge and 0.013 Inch Holes at 30° to Airfoil on Trailing Edge
6-2	Film-Cooled Turbine Blade with 0.030 Inch/30° Angle L. E. Holes and 0.013 Inch/30° Angle T. E. Holes Showing Cracks After 100 Cycles of Thermal Shock Testing
6-3	Convectively-Cooled Turbine Blade After 1000 Cycles of Thermal Shock Test (Showing Good Condition and Absence of Cracks)

DOWNGRADED AT 3 YEAR INTERVALS
DECLASSIFIED AFTER 12 YEARS
DOD DIR 5200.10

LIST OF ILLUSTRATIONS (Con't)

6-4	Turbine Blade Impact Test Rig
6-5	Convectively Cooled Blade After Impact Test
6-6	Film Cooled Blade with .030 Dia. Holes After Impact Test
6-7	Film Cooled Blade After Impact Test
6-8	Typical Turbine Blade Set-Up for High Temperature Testing
6-9	Low-Cycle-Fatigue (LCF) Test Rig
6-10	Low Cycle Fatigue Material Test Specimen
6-11	Cyclic-Creep Test Rig
6-12	Thermal Shock-Creep Specimen Undrilled
6-13	Thermal Shock-Creep Specimen Drilled
6-14	ARC Weld Creep Test Machine Cyclic Stress Rupture Tests
6-15	Smooth Cyclic Stress-Rupture Fatigue Specimen
6-16	High Temperature Reverse-Bending Fatigue Specimen
6-17	Vane Data Summary
6-18	Turbine Vane Incorporating Leading Edge Cooling Slots 0.008 Inch by 0.100 Inch Spaced 0.050 Inch Apart, 15° off Stagnation Line
6-19	Turbine Vane Showing 0.012 x 0.100 Inch Cooling Slots at L. E. Stagnation Line
6-20	Turbine Vane Configuration with Leading Edge Cooling Holes 0.40 Inch Diameter at 45° to L. E.

DOWNGRADED AT 3 YEAR INTERVALS
DECLASSIFIED AFTER 12 YEARS
DOD DIR 5200.10

LIST OF ILLUSTRATIONS (Con't)

6-21 Turbine Vane Featuring Film-Cooled Leading Edge. Coolant Injected into Spanwise Groove Along Stagnation Line

6-22 Turbine Vane Configuration with Film-Cooled Leading Edge Containing 0.012 x 0.100 Holes Behind an 0.025 Inch Thick Shield

6-23 Turbine Vane Configuration with Film-Cooled Leading Edge Containing 21 Holes, 0.030 Inch Diameter, Spaced 0.1 Inch Apart, Drilled at a 30° Angle to the Leading Edge

6-24 Turbine Vane Configuration with Film-Cooled Leading Edge Containing Five Rows of 0.013 Inch Diameter Holes

6-25 Turbine Vane Configuration with Film-Cooled Leading Edge Containing Shower Head Hole Scheme

6-26 Turbine Vane Configuration with Film-Cooled Leading Edge Containing Impingement Slots

6-27 Turbine Vane Configuration with Film-Cooled Leading Edge Containing Pierced Sheet (0.013" Dia. Holes)

6-28 Turbine Vane Configuration with Film-Cooled Leading Edge Containing Pierced Sheet (0.006" Dia. Holes)

6-29 Turbine Vane Configuration with Transpiration-Cooled Leading Edge Containing Poroloy

6-30 Turbine Vane Configuration with Impringement - And Film-Cooled Leading Edge Incorporating Umbrella Shield

6-31 Turbine Vane Configuration with Impringement - And Film-Cooled Leading Edge Incorporating Sugar Scoop Cut-Outs

LIST OF ILLUSTRATIONS (Con't)

6-32 Turbine Vane Configuration with Film-Cooled Leading Edge Incorporating Coanda Slot Scheme

6-33 Turbine Vane Configuration with Film-Cooled Trailing Edge (0.013" Dia. Holes)

6-34 Turbine Vane Configuration with Film-Cooled Trailing Edge

6-35 Turbine Vane Configuration with Film-Cooled Trailing Edge Containing Holes on Convex Side

6-36 Schematic of Turbine Vane with Leading Edge Slots at Stagnation Line

6-37 Schematic of Turbine Vane with Leading Edge Slots at Stagnation Line

6-38 Schematic of Turbine Vane With Leading Edge Cooling Slots as Shown on Figure 6-18

6-39 Schematic of Turbine Vane with Leading Edge Cooling Slots as Shown on Figure 6-19

6-40 Schematic of Turbine Vane with Leading Edge Cooling Slots as Shown on Figure 6-20

6-41 Schematic of Turbine Vane with Film-Cooled Leading Edge as Shown on Figure 6-21

6-42 Schematic of Turbine Vane with Film-Cooled Leading Edge as Shown on Figure 6-22

6-43 Schematic of Turbine Vane with Film-Cooled Leading Edge as Shown on Figure 6-23

6-44 Schematic of Turbine Vane with Film-Cooled Leading Edge as Shown on Figure 6-24

DOWNGRADED AT 3 YEAR INTERVALS
DECLASSIFIED AFTER 12 YEARS
DOD DIR 5200.10

THIS DOCUMENT CONTAINS INFORMATION AFFECTING THE NATIONAL DEFENSE OF THE UNITED STATES WITHIN THE MEANING OF THE ESPIONAGE LAWS, TITLE 18, U.S.C., SECTIONS 793 AND 794, THE TRANSMISSION OR THE REVELATION OF ITS CONTENTS IN ANY MANNER TO AN UNAUTHORIZED PERSON IS PROHIBITED BY LAW

LIST OF ILLUSTRATIONS (Con't)

6-45 Schematic of Turbine Vane with Film-Cooled Leading Edge as Shown on Figure 6-25

6-46 Schematic of Turbine Vane with Film-Cooled Leading Edge as Shown on Figure 6-26

6-47 Schematic of Turbine Vane with Film-Cooled Leading Edge as Shown on Figure 6-27

6-48 Schematic of Turbine Vane with Film-Cooled Leading Edge as Shown on Figure 6-28

6-49 Schematic of Turbine Vane with Transpiration-Cooled Leading Edge as Shown on Figure 6-29

6-50 Schematic of Turbine Vane with Impingement - and - Film-Cooled Leading Edge as Shown on Figure 6-30

6-51 Schematic of Turbine Vane with Impingement - and - Film-Cooled Leading Edge as Shown in Figure 6-31

6-52 Schematic of Turbine Vane with Film-Cooled Leading Edge as Shown on Figure 6-32

6-53 Schematic of Turbine Vane with Slotted Trailing Edge

6-54 Schematic of Turbine Vane with Film-Cooled Trailing Edge as Shown on Figure 6-33

6-55 Schematic of Turbine Vane with Film-Cooled Trailing Edge as Shown on Figure 6-34

6-56 Schematic of Turbine Vane with Film-Cooling Trailing Edge as Shown on Figure 6-35

6-57 Metal Temperature vs. Peripheral Distance Along the Foil - Coolant Slots on Stagnation Line

6-58 Metal Temperature vs. Peripheral Distance Along the Foil - Coolant Slots 15° to the Suction Side of the Stagnation Line

6-59 Metal Temperature vs. Peripheral Distance Along the Foil - Coolant Slots 15° to the Pressure Side of the Stagnation Line

DOWNGRADED AT 3 YEAR INTERVALS
DECLASSIFIED AFTER 12 YEARS
DOD DIR 5200.10

LIST OF ILLUSTRATIONS (Con't)

6-60 Metal Temperature vs. Peripheral Distance Along the Foil - Coolant Slots on Stagnation Line

6-61 Metal Temperature vs. Peripheral Distance Along the Foil - Coolant Holes Angled at 45° to the Stagnation Line

6-62 Metal Temperature vs. Peripheral Distance Along the Foil - Semicircular Groove Along Stagnation Line

6-63 Metal Temperature vs. Peripheral Distance Along the Foil - 30° Angled Holes

6-64 Metal Temperature vs. Peripheral Distance Along the Foil - "Showerhead" Vane

6-65 Metal Temperature vs. Peripheral Distance Along the Foil - Impingement Vane

6-66 Metal Temperature vs. Peripheral Distance Along the Foil - Porous Sheet Vane

6-67 Metal Temperature vs. Peripheral Distance Along the Foil - Porous Leading Edge

6-68 Metal Temperature vs. Peripheral Distance Along the Foil - "Umbrella" Vane

6-69 Metal Temperature vs. Peripheral Distance Along the Foil - "Sugar Scoop" Vane

6-70 Metal Temperature vs. Peripheral Distance Along the Suction Surface

LIST OF ILLUSTRATIONS (Con't)

6-71 United Aircraft Corporation Research Laboratory High Pressure Cascade Showing Infra-Red Scanning Devices

6-72 Shielded Leading Edge Vane Tested in High Pressure Cascade Rig

6-73 Turbine Vane with Leading Edge (Holes) and Trailing Edge (Slots) Cooling Schemes

6-74 Turbine Vane with Film-Cooled Porous Leading Edge and Slotted Trailing Edge

6-75 Film-Cooled Turbine Vane with Pierced-Sheet Leading Edge and Drilled-Hole Trailing Edge

6-76 Impingement Rig Test Section

6-77 View From Rear Showing Vane Cascades in Choked Cascade Thermal Shock Rig

6-78 Schematic of Choked Cascade Thermal Shock Rig

6-79 Vane Pack for Film-Cooled Vane Tests A. Plenum Chamber T/C. B. Plenum Chamber C. Leading Edge Cooling Air Holes

6-80 Pressure Ratio as a Function of Coolant Weight Flow

6-81 Pressure Loss Coefficient as a Function of Coolant Weight Flow

6-82 Coolant Parameters as a Function of Exit Mach Number

6-83 Coolant Parameters as a Function of Exit Mach Number

6-84 Schematic Diagram of JT12 Performance Rig Showing Blade and Vane Cooling Air Arrangement and Instrumentation System

LIST OF ILLUSTRATIONS (Con't)

6-85 JT12 Single-Stage Turbine Performance Rig

6-86 Blade and Vane Cooling Air Passage Configuration Evaluated in JT12 Performance Tests

6-87 JT12-Sized Film Cooled First-Stage Turbine Blade for Performance Test

6-88 JT12-Sized Film Cooled First-Stage Turbine Vane for Performance Test

6-89 Effect of Vane and Blade Cooling Airflow on Turbine Performance

6-90 Air Leakage Paths in JT12 Burner Turbine Rig

6-91 Effect of Blade Leakage on Turbine Performance

6-92 Comparison of the Effect of Off-Design Operation and Cooling Air Bleed on Turbine Performance

6-93 Effect of Blade and Vane Cooling Airflow on Rig Inlet Flow Parameter

6-94 Heated Inlet Hardware on Test Stand for High Spool Engine Test

6-95 Cooled Blade and Vane Test Rig Showing Heated Engine-Heated-Inlet Air Arrangement and Cooling Air Supply

6-96 JT12 Cooling Air Supply Engine Showing Cooling Air Bleed Ducting

6-97 JT4 High Spool Engine Showing Engine and Vane/Blade Cooling Air Supply
A. JT12 Cooling Air Supply Engine
B. Heater Burner
C. Chamber

DOWNGRADED AT 3 YEAR INTERVALS
DOD DIR 5200.10
CLASSIFIED AFTER 12 YEARS

LIST OF ILLUSTRATIONS (Con't)

6-98 JT4 High Spool Engine Showing Vane and Blade Cooling Air Manifold
A. Flow Control C. Vane Cooling Air
B. Bleed Stack D. Blade Cooling Air

6-99 JT4 Film Cooled Vane Five-Row Shower Head with 0.013-Inch Heads

6-100 JT4 Film Cooled Vane with Porous Leading Edge

6-101 JT4 Film Cooled Vane 11-Row Pierced Sheet Leading Edge

6-102 Impingement Vane Sectioned to Show Method for Cooling Leading Edge

6-103 JT4 Cooled Blade - 3 Row Shower Head (.013" Dia. Holes at 90° to Surface at Leading Edge) and .010" Dia. Holes at Trailing Edge (Pressure and Suction Sides) at 30° to Surface

6-104 JT4 Film Cooled Blade - 3 Row Shower Head (.013" Dia. Holes at 30° to Surface at Leading Edge) and .010" Dia. Holes at Trailing Edge (Pressure and Suction Side) at 30° to Surface

6-105 JT4 Cooled Blade - 3 Row Shower Head (.008" Dia. Holes at 90° to Surface at Leading Edge) and .010" Dia. Holes at Trailing Edge (Pressure Side Only) at 30° to Surface

6-106 JT4 Film Cooled Blade - 5 Row Shower Head (.008" Dia. Holes at 90° to Surface at Leading Edge) and .013" Dia. Holes at Trailing Edge (Pressure and Suction Sides) at 30° to Surface

6-107 JT4 Film Cooled Blade - 5 Row Shower Head (.008" Dia. Holes at 30° to Surface at Leading Edge) and .010" Dia. Holes at trailing Edge (Pressure and Suction Sides) at 30° to Surface

LIST OF ILLUSTRATIONS(Con't)

6-108 JT4 Film Cooled Blade 0.03-Inch Diameter Holes at 30° to Leading Edge

6-109 Narrow Land Blades - N155 Poroloy Skin - EB Weld Attachment (.040" Interface) Transpiration Cooled

6-110 Narrow Land Blades - N155 Regimesh Skin - Braze 82-18 Attachment - Transpiration Cooled

6-111 Wide Land Blades - L605 Regimesh Skin - EB Weld Attachment (.040" Interface) - Transpiration Cooled

6-112 Wide Land Blades - N155 Regimesh Skin - Braze 82-18 Attachment - Transpiration Cooled

6-113 Wide Land Blades - L605 Regimesh Skin - EB Weld Attachment (.072" Interface) - Transpiration Cooled

6-114 Wide Land Blade - L605 Regimesh Skin - EB Weld Attachment - H-47986 Transpiration Cooled

6-115 Wide Land Blade - N155 Poroloy Skin - EB Weld Attachment Transpiration Cooled

6-116 Wide Land Vanes - L605 Regimesh Skin - EB Weld Attachment - Transpiration Cooled

6-117 Wide Land Vane - N155 Poroloy Skin - EB Weld Attachment - Transpiration Cooled

6-118 Wide Land Vane - N155 Regimesh Skin - Braze 82-18 Attachment - Transpiration Cooled

6-119 JT4 Turbine Blade, .030" Sawtooth Cooling Passage Design, Material PWA-655

6-120 JT4 Turbine Blade, 11-Hole Cooling Passage Design, Material PWA-658 and PWA-663

DOWNGRADED AT 3 YEAR INTERVALS
DECLASSIFIED AFTER 12 YEARS
DOD DIR 5200.10

THIS DOCUMENT CONTAINS INFORMATION AFFECTING THE NATIONAL DEFENSE OF THE UNITED STATES WITHIN THE MEANING OF THE ESPIONAGE LAWS, TITLE 18, U.S.C., SECTIONS 793 AND 794. THE TRANSMISSION OR THE REVELATION OF ITS CONTENTS IN ANY MANNER TO AN UNAUTHORIZED PERSON IS PROHIBITED BY LAW.

LIST OF ILLUSTRATIONS (Con't)

6-121 PWA-657 Slotted Trailing Edge Vanes After 155 Cycles at 2235°F

6-122 PWA-657 Pedestal Trailing Edge Vanes After 155 Cycles at 2235°F

6-123 PWA-659 0.02-Inch Sawtooth Blades After 1030 Cycles At 2235°F

6-124 PWA 663 Eleven-Hole Blade After 1030 Cycles at 2235°F

6-125 PWA 659 $TaAl_3$ Coated 0.02-Inch Sawtooth Blade with Leading Edge Crack

6-126 PWA 658 Eleven-Hole Blade Showing Bowing and Leading Edge Crack

6-127 PWA 659 0.02-Inch Sawtooth Blade (Top) and PWA 658 Eleven-Hole Blade (Bottom) after 1030 Cycles at 2235°F

6-128 JT4 Turbine Vane Assembly with Film and Transpiration Cooled Vanes

6-129 JT4 Turbine Rotor Assembly with Film and Transpiration Cooled Blades

6-130 Measured vs. Predicted Metal Temperatures

AUGMENTORS

7-1 Schematic of Cross Jet Flameholder Installed in the 12" x 16" Rig

7-2 Cross Jet Flameholder Installed in the 12" x 16" Rig

7-3 12" x 16" Altitude Research Rig Simulating a 16" Segment of the STF219 Duct Heater

7-4 Duct Heater Performance at STF219 Cruise Conditions

LIST OF ILLUSTRATIONS (Cont'd)

7-5	Duct Heater Performance at STF219 Sea Level Acceleration Conditions
7-6	Duct Heater Performance at STF219 Transonic Conditions
7-7	Duct Heater Performance at STF219 Acceleration Conditions
7-8	Cold Flow Losses of Duct Heater System Utilized in Flight Performance Tests
7-9	Comparison of Jet Flameholder Performance in Air Cooled vs Water Cooled Rigs
7-10	Ignition Characteristics of the Cross Jet Flameholder With External Primary Fuel
7-11	A Typical High Speed Transducer Trace of the Ignition Pressure Pulse of the Duct Heater
7-12	Minimum Pressure Blowout of Typical Jet Flameholder
7-13	Initial Duct Burner Design, Model A
7-14	Latest Duct Burner Design, Model E
7-15	Comparison of Burner Combustion Efficiency
7-16	Comparison of Burner Pressure Loss
7-17	Diagramatic Illustration of Heterogeneous Burner - Model A
7-18	Photograph of Heterogeneous Burner - Model A
7-19	Rear View of Heterogeneous Burner - Model B
7-20	Test Results From Model A Heterogeneous Burner

CONFIDENTIAL

LIST OF ILLUSTRATIONS (Cont'd)

7-21 Test Results From Model B Heterogeneous Burner

7-22 Schematic of Full-Scale Duct Heater Test Rig

7-23 Full Scale Duct Heater Test Rig

7-24 Full Scale Duct Heater Rig Inlet Diffuser Assembly

7-25 Full Scale Duct Heater Rig Outer Wall Fuel Baffle

7-26 Full Scale Duct Heater Rig Jet Flameholder Installed

7-27 SST Full Scale Duct Heater Rig Jet Flameholder and Spray Rings Firey Cross Configuration

7-28 Full Scale Duct Heater Rig Porous Inner Cooling Liner

7-29 Partially Assembled Full Scale Duct Heater Rig Showing Transpiration Cooled Inner Body

7-30 SST Full Scale Duct Heater Rig Porous Outer Cooling Liner

7-31 SST Full Scale Duct Heater Rig Reinforced Combustion Chamber Outer Duct

7-32 Comparison of Full-Scale and Small-Scale Duct Heater Test Results at Low Temperature

7-33 Comparison of Full-Scale and Small-Scale Duct Heater Test Results at High Temperature

7-34 Full-Scale Duct Heater Rig Performance

7-35 Full-Scale Duct Heater Rig Cold Pressure Loss

7-36 Effect of Flameholder Air Temperature on Full-Scale Duct Heater Test Results

LIST OF ILLUSTRATIONS (Cont'd)

7-37 Effect of Flameholder Pressure Ratio on Full-Scale Duct Heater Test Results

7-38 Full-Scale Duct Heater Rig

7-39 Typical Heat-Shielded Orifice-Type Spraybar

7-40 12" x 16" Afterburner Segment Rig

7-41 Effect of Vitiation

7-42 Effect of Orifice Size

7-43 Effect of Increasing Width of F/H

7-44 Effect of Increasing the Number of Flameholders

7-45 Effect of Inlet Temperature on Combustion Efficiency

7-46 Stability Limits

EXHAUST SYSTEM

8-1 Wind Tunnel Test Data of First Freely Floating Co-Annular Blow-In-Door Ejector Model for Supersonic Transport

8-2 Summary of Data for Freely Floating Co-Annular Blow-In-Door Ejector Model

8-3 Effect on Performance of Blow-In-Door Position with Trailing Edge Flaps Fixed in Closed Position

8-4 Effect of Varying Trailing Edge Flap Position on Performance

8-5 Schematic Diagram of Forebody Venting Design

8-6 Effect of Forebody Venting on Performance Without Augmentation

DOWNGRADED AT 3 YEAR INTERVALS
DECLASSIFIED AFTER 12 YEARS
DOD DIR 5200.10

THIS DOCUMENT CONTAINS INFORMATION AFFECTING THE NATIONAL DEFENSE OF THE UNITED STATES WITHIN THE MEANING OF THE ESPIONAGE LAWS, TITLE 18, U.S.C., SECTIONS 793 AND 794. THE TRANSMISSION OR THE REVELATION OF ITS CONTENTS IN ANY MANNER TO AN UNAUTHORIZED PERSON IS PROHIBITED BY LAW.

LIST OF ILLUSTRATIONS (Cont'd)

8-7 Effect of Forebody Venting on Performance with Macimum Augmentation

8-8 Schematic Diagrams of Primary Engine Nozzles Evaluated

8-9 Characteristics of Primary Engine Nozzles Evaluated

8-10 STF219 Engine Operating Conditions Used for Exhaust Nozzle Models

8-11 Schematic Diagram of Model Simulating STF219 Ejector

8-12 Typical Effects of Shroud Exit Area and Blow-In Door Area on Ejector Performance at Sea Level Take-Off

8-13 Typical Effects of Shroud Exit Area and Blow-In Door Area on Ejector Performance at Mach 0.9 Cruise

8-14 Effect of Shroud Geometry on Transonic Blow-In Door Ejector Performance at Mach 1.2

8-15 Effect of Shroud Geometry on Supersonic Blow-In Door Ejector Performance at Mach 2.7 Cruise

8-16 Theoretical and Experimental Ejector Performance at Mach 2.6 Cruise

8-17 Scale Model STF219 Blow-In Door Ejector Performance and Phase IIA Model Specification Performance Requirements

8-18 Schematic Diagram of Co-Annular Blow-In Door Ejector-Reverser Models

8-19 Typical Effect of Bleed Flo Spoiler

LIST OF ILLUSTRATIONS (Cont'd)

8-20 Typical Effect of Flight Mach Number on Engine Flow, Fan Flow, and Reverse Thrust Coefficients with Four Blow-In Doors Blocked

8-21 Typical Effect of Fan-to-Engine Pressure Ratio on Engine Flow, Fan Flow, and Reverse Thrust Coefficients With Five Blow-In Doors Blocked

8-23 Schematic Diagram of Model Used to Simulate Partially Augmented Turbojet

8-24 Typical Effects of Shroud Exit Area and Blow-In Door Area on STJ227 Ejector Performance

8-25 Effect of Shroud Geometry on Transonic Blow-In-Door Ejector Performance of STJ227

8-26 Effect of Shroud Geometry on Supersonic Blow-In-Door Ejector Performance

8-27 Scale Model STJ227 Blow-In-Door Ejector Performance and Phase IIA Model Specification Performance Requirements

8-28 Schematic Diagrams of Plug Nozzles Tested

8-29 Typical Effect of Nozzle Area Ratio on Performance

8-30 Nozzle Performance With Truncated Plug

8-31 Effect of Plug Truncation on Nozzle Performance

8-32 Effect of Plug Contour on Nozzle Performance

8-33 Boat-Tail and Shroud Base Drag

8-34 Multiple Expansion Plug Nozzle Performance

8-35 Effect of Area Ratio on Multiple Expansion Plug Nozzle Performance

LIST OF ILLUSTRATIONS (Cont'd)

8-36 Effect of Plug Cone Half Angle on Multiple Expansion Plug Nozzle Performance

8-37 Effect of Plug Cone Angle on Multiple Expansion Plug Nozzle Performance

8-38 Scale Model Plug Nozzle Performance and Phase IIA Model Specification Performance Requirements

NOISE REDUCTION

9-1 Estimated STF219 Engine Noise Levels Compared With Current Turbojet and Turbofan Engine Noise Levels

9-2 Effect of Jet Relative Velocity on Sound Pressure Level

9-3 21-Tube Noise Suppressor Performance

9-4 Anechoic Chamber Showing Scale Model Exhaust Nozzle and Traversing Microphone Boom

9-5 Scale Model Exhaust Nozzles; Area Equivalent to Three-Inch Diameter Circular Nozzle

9-6 Experimental Jet Noise Suppressors

9-7 Rectangular Noise Suppressor Nozzle

9-8 Potential Noise Reduction From Mixing

9-9 Experimental Mixing Devices Acoustically Tested in Full Scale

9-10 JT3D Stator Vane Assemblies

9-11 Effect of Vane-to-Blade Spacing on Noise Level at Subsonic Blade Tip Speeds

9-12 Compressor Rotor with Blade Tips in Shrouded Through

9-13 Full-Scale Variable-Angle Vane Assemblies

DOWNGRADED AT 3 YEAR INTERVALS
NOT AUTOMATICALLY DECLASSIFIED AFTER 12 YEARS
DOD DIR 5200.10

LIST OF ILLUSTRATIONS (Cont'd)

9-14 Full-Scale Slanted Vane Assemblies

9-15 Various Blade Plan Forms Tested For Noise Generation

9-16 Stator and Turbulence-Generator Vane Configurations

9-17 Coanda Inlet Guide Vane

9-18 Resonant Absorber Shrouds

9-19 Sound Absorbent Inlets

9-20 Sonic Inlet Cowls

9-21 Full-Scale Fan Exit Duct Turbulence Generators

9-22 Sound-Reflecting Fan Exit Stator

9-23 28-Inch Diameter Compressor Rig and Drive Engine

9-24 Lockheed Shape Inlet

9-25 Boeing Shape Inlet with Partially Expanded Centerbody Configuration 2-B-2

9-26 Boeing Shape Inlet and Alternate Centerbodies

9-27 Long Inlet; Configuration 1-B-0

9-28 Sharp Lip Inlet; Configuration 2-B-0A

9-29 Performance Map of 28-Diameter Compressor Used for Noise Investigations

9-30 Results of Noise Tests

9-31 Sound Spectrum of 28-Inch Diameter Noise Rig

9-32 Effect of Inlet Mach Number on Noise Propagation

DOWNGRADED AT 3 YEAR INTERVALS
DECLASSIFIED AFTER 12 YEARS
DOD DIR 5200.10

THIS DOCUMENT CONTAINS INFORMATION AFFECTING THE NATIONAL DEFENSE OF THE UNITED STATES WITHIN THE MEANING OF THE ESPIONAGE LAWS, TITLE 18, U.S.C., SECTIONS 793 AND 794. THE TRANSMISSION OR THE REVELATION OF ITS CONTENTS IN ANY MANNER TO AN UNAUTHORIZED PERSON IS PROHIBITED BY LAW.

LIST OF ILLUSTRATIONS (Cont'd)

9-33 Sound Spectrum of 28-Inch Diameter Noise Rig with 54-Inch Cylindrical Extension

9-34 Typical Discrete Noise Directivity Patterns With and Without Fiberglas Lined Duct

9-35 Typical Directivity of Fundamental Discrete Frequency Noise for Axisymmetrical and Two-Dimensional Inlets

9-36 Effect on Average Noise Level of 54-Inch Extension of Inlet Duct

9-37 Reverberation Chamber Test Facility

9-38 Model Pulse-Jet Used as Noise Source in Reverberation Chamber Testing

9-39 STF219 Fan Discharge Duct Showing Location of Sound Absorption Materials

9-40 Fan Discharge Duct Model for Testing of Sound Absorption Materials

9-41 Sound Absorption Materials Tested in Fan Discharge Duct Model

9-42 Insertion Loss with Fan Duct Lining A

9-43 Insertion Loss with Fan Duct Lining B

9-44 Insertion Loss with Fan Duct Lining C

9-45 Insertion Loss with Fan Duct Lining D

9-46 Effect of Flow Velocity on Insertion Loss with Fan Duct Lining C

9-47 Insertion Loss with Fan Duct Lining C in One-Half Size Staggered Duct

9-48 Overall Diagram of Anechoic Chamber Test Facility

LIST OF ILLUSTRATIONS (Cont'd)

9-49 Natural Gas Fuel Supply System

9-50 Schematic Diagram of Burner Section in Anechoic Chamber

9-51 Primary and Secondary Throttling Valves

9-52 Water-Cooled Maximum Duct-Heating Nozzle Model Mounted on Test Rig

9-53 Schematic Diagram of Performance Instrumentation in Anechoic Chamber

9-54 Nozzle Aerodynamic Diagram

9-55 Schematic Diagram of Sound Data Processing System

9-56 Schematic Diagram of Sound Data Recording System

9-57 Sound Data Recording System

9-58 Interior of Anechoic Chamber Showing Microphone Boom and Test Model

9-59 Photograph of SNORE (Sequential Noise Output Recording Equipment)

9-60 Full-Scale Noise Predictions

9-61 Blow-In-Door Ejector Nozzle Models for Noise Tests

9-62 Nozzle Test Models Mounted on Rig

9-63 Tailpipe Temperature vs Primary Pressure Ratio

9-64 Duct Pressure Ratio vs Primary Pressure Ratio

9-65 Net Thrust vs Primary Pressure Ratio

9-66 Jet Velocity vs Primary Pressure Ratio

9-67 Jet Noise vs Pressure Ratio for Low Duct Pressure

LIST OF ILLUSTRATIONS (Cont'd)

9-68 Jet Noise vs Pressure Ratio for High Duct Pressure

9-69 Jet Noise vs Net Thrust for Low Duct Pressure

9-70 Jet Noise vs Net Thrust for High Duct Pressure

9-71 Comparison of SST Nozzle Models with SAE A-21 Committee Predictions

9-72 Effect of Engine Size on Community Noise

9-73 Trade-Off Between Community Noise and Airport Noise for a Typical SST Airplane

9-74 Sideline Noise at 1500 Feet From Centerline of STF219 Engine With No Noise Suppression

9-75 In-Flight Noise From STF219 Engine With No Noise Suppression

9-76 Sideline Noise at 1500 Feet From Centerline of STF219 Engine With Noise Suppression

9-77 In-Flight Noise From STF219 Engine With Noise Suppression

9-78 Noise Attenuation Due to Blow-In-Door Ejector

9-79 Estimated STF219 Engine Noise Levels Along a Line 500 Feet From and Parallel to One Engine

9-A-1 Sound Pressure Levels of Octave Band Containing Fundamental Blade-Passing Noise

9-B-1 Effect of Blow-In-Door Ejector on Exhaust Noise

9-B-2 Peak Discrete Frequency Fly-Over Noise Comparison for One Engine at Approach Thrust

LIST OF ILLUSTRATIONS (Cont'd)

CONTROLS AND ACCESSORIES

10-1 Schematic Diagram of Engine Control System

10-2 Illustration of Power Lever Operation

10-3 Engine Airflow Control - Method 1

10-4 Engine Airflow Control - Method 2

10-5 Illustration of Duct Fuel Flow Ratio Bias Reset for Thrust Cut-Back

10-6 Constant Cruising Mach Number Control Concept

10-7 Illustration of Rotor Speed Bias with Approach Speed Reset Lever Angle

10-8 Illustration of Approach Velocity Control Concept

10-9 Analog Program for STF219 Engine Low-Pressure Compressor

10-10 Analog Program for STF219 Engine Low-Pressure Compressor Discharge

10-11 Analog Program for STF219 Engine High-Pressure Compressor

10-12 Analog Program for STF219 Engine Primary Combustor Section

10-13 Analog Program for STF219 Engine High-Pressure Rotor Torque Balance

10-14 Analog Program for STF219 Engine Low-Pressure Rotor Torque Balance

10-15 Analog Program for STF219 Engine Duct Combustor Section

LIST OF ILLUSTRATIONS (Cont'd)

10-16 Analog Program for STF219 Engine Tailpipe and Thrust Calculation

10-17 Variation in Duct Area Control Parameter with Rotor Speed Showing Effect of Duct Lighting

10-18 Airflow Changes During Duct Lighting

10-19 Illustration of Transient Response During Lighting

10-20 Duct Heater Transient Response During Lighting

10-21 Analog Computer Traces of STF219 Engine Operating at 75,000 Feet, Mach 3.0 with Maximum Thrust With and Without Augmentation

10-22 Estimated Acceleration Time from Idle Thrust to Maximum Thrust for SST STF219 Engine

10-23 Estimated Acceleration Time from Idle Rotor Speed to Macimum Rotor Speed for SST STF219 Engine

10-24 Illustration of Power Lever Operation in Reverse Mode

10-25 Low-Tension Peripherally Cooled Exciter

10-26 Low-Tension Spiral-Wrapped Cooled Exciter

10-27 High-Tension Spiral-Wrapped Cooled Exciter

10-28 Test Results for Glow Plug Igniter

BEARING AND SEAL DEVELOPMENT

11-1 Typical Angular-Contact Thrust Bearing Used for Endurance Evaluation Test Under Simulated SST Engine Conditions

11-2 Schematic Diagram of Thrust Bearing Test Rig

11-3 Bearing Calibration Rig

LIST OF ILLUSTRATIONS (Cont'd)

11-4 Thrust Bearing Test Rig Installation Including (A) Rig in Stand for Operation, (B) Rig Housing with Bearings Removed, (C) Filter Control Valves, (D) Flowraters

11-5 Rotating Drum Oil Heater Installation Including (A) Mixing Valve, (B) Radiator, (C) Manifold Press. Control Valve, (D) Flow Indicators, (E) Remote Flow Control Valve, (F) Manifold, (G) Oil Heater

11-6 Weibull Distribution of M-50 Bearing Test Results

11-7 Thrust Bearing After 265 Hours of Endurance Test in 500°F PWA-524 Lubricant

11-8 Cage From Thrust Bearing Showing Deposits After 265 Hours of Endurance Test with 500°F PWA-254 Lubricant

11-9 Thrust Bearing Inner Race Showing Plugged Oil Grooves After 265 Hours of Endurance Test with 500°F PWA-524 Lubricant

11-10 Weibull Distribution of WD-65 Bearing Test Results

11-11 Outer Race Temperatures as a Function of Speed

11-12 Effect of Thrust Load Per Ball on Cage Speed

11-13 Single-Ball Fatigue Test Rig Showing (A) Lower Race, (B) Upper Race in Up Position, (C) Cage Holder

11-14 Schematic Diagram of Single-Ball Fatigue Test Rig

11-15 Installation of Rigs Including (Left to Right) Four Single-Ball Fatigue Rigs and High-Temperature Oil Rig (A).

11-16 Weibull Distribution of Ball Test in MIL-L-7808D Oil

11-17 Weibull Distribution of Ball Test in Type II Oil

LIST OF ILLUSTRATIONS (Cont'd)

11-18 Weibull Distribution of Ball Test in SATO 5180 Oil

11-19 Weibull Distribution of Ball Test in PWA-524 Oil

11-20 Schematic Diagrams of Face-Type Oil Seals

11-21 Component Parts of Oil Seal Testing Rig Including (A) Front Cover, (B) Rig Bearing, (C) Hub, (D) Oil Jet to Seal Plate, (E) Breather Manifold, (F) Shaft.

11-22 Face Seal High-Temperature Test Rig Installation

11-23 Radial Groove Type Ring Seal Design

11-24 Circular Groove Type Ring Seal Design

11-25 Ring Seal Design Test Shaft Including (1) Back-Up Plate, (2) Ring Seal and (3) Seal Plate

11-26 Ring Seal Test Shaft Stack-Up Including (1) Seal Plate, (2) Ring Seal, (3) Spacer, (4) Back-Up Plate, and (5) Spacer

11-27 Schematic Diagram of Seal Material Evaluation Test Rig

11-28 Installation of Ring Seal Test Rig Including (1) Air Heaters, (2) High Pressure Air Lines, (3) Stand Breather Line, (4) Thermocouple Conduit, (5) Rig Breather, (6) Drive Motors (Three 14 HP), (7) Gearbox Oil Drain, (8) Two-Speed Gearboxes, (9) Rig Drain, (10) Rig Oil Supply Manifold

11-29 Typical Rig Test Control Stand Including (1) Air Heater, (2) Fire Control, (3) Power Station to Control Heater, (4) Lewis Switch, (5) Potentiometer, (6) Pressure Gauges, (7) Rotometers, (8) Pressure Gages, (9) Heater Temperature Controls.

11-30 Ring Seal Test Data for Six-Inch Ring Seal Design - Circular Grooves

DOWNGRADED 3 YEAR INTERVALS
NO APPROVED APPLIED IN 12 YRS
DOD DIR 5200.10

LIST OF ILLUSTRATIONS (Cont'd)

11-31 Ring Seal Test Data for Eight-Inch Ring Seal Design - Circular Grooves

11-32 Ring Seal Test Data for Eight-Inch Seal Design - Radial Groove

11-33 Ring Seal Test Data - Eight-Inch Ring Seal Design - Radial Grooves

11-34 Ring Seal Test Data - Eight-Inch Ring Seal Design - Radial Grooves Radial Width Optimization

FUELS

12-1 Identification of Samples for Domestic Jet A and Jet A-1 Fuel Survey

12-2 Physical Properties of Domestic Jet Fuel Samples

12-3 Distillation Data Obtained on Jet A and Jet A-1 Fuel Samples Used in Domestic Fuel Survey

12-4 Summary of Tests to Determine Breakpoint Temperatures of Domestic Fuel Survey Samples in ASTM-CFR Fuel Coker

12-5 Summary of Tests to Determine Breakpoint Temperature of Domestic Fuel Survey Samples in CRC Research Fuel Coker

12-6 Summary of Breakpoint Temperatures of Domestic Fuel Survey Samples Based on Code 3 Preheater Deposits

12-7 Distribution of Preheater Breakpoint Temperatures as Determined in ASTM-CFR Fuel Coker

12-8 Preheater Breakpoint Temperature Distribution ASTM-CFR Fuel Coker

12-9 Domestic Jet Fuel Survey

LIST OF ILLUSTRATIONS (Cont'd)

12-10 Preheater Breakpoint Distribution of Survey Fuels

12-11 Domestic Jet Fuel Survey - Breakpoint Temperature Distribution in Tests With CRC Research Fuel Coker

12-12 Preheater Breakpoint Temperature Distribution CRC Research Fuel Coker (11 Samples)

12-13 Preheater Breakpoint Temperature Distribution CRC Research Fuel Coker (16 Samples)

12-14 Effect of Reservoir Fuel Heating on Preheater Breakpoint Temperature in CRC Research Fuel Coker

12-15 Breakpoint Profile Distribution of Survey Fuels

12-16 Lubricity Values of Domestic Survey Fuels

12-17 CRC Research Fuel Coker Tests for Determination of Preheater Breakpoint Temperature Standard Reservoir Configuration

12-18 Research Fuel Coker Tests for Determination of Preheater Breakpoint Temperature

12-19 Measured Fuel Oxygen Content During Research Fuel Coker Tests at 175F Reservoir Temperature 1.0±0.1 psia Reservoir Pressure

12-20 Typical Fuel Oxygen Content During Research Fuel Coker Test at Low Pressure Conditions

12-21 Thermal Stability Characteristics of West Coast Jet A-1 Fuel No. F-1497 in CRC Research Fuel Coker at 175°F Reservoir Temperature

12-22 Thermal Stability Characteristics of JP-5 Referee Fuel No. F1065 in CRC Research Fuel Coker at 175°F Reservoir Temperature

DOWNGRADED AT 3 YEAR INTERVALS
DECLASSIFIED AFTER 12 YEARS
DOD DIR 5200.10

THIS DOCUMENT CONTAINS INFORMATION AFFECTING THE NATIONAL DEFENSE OF THE UNITED STATES WITHIN THE MEANING OF THE ESPIONAGE LAWS, TITLE 18, U.S.C., SECTIONS 793 AND 794. THE TRANSMISSION OR THE REVELATION OF ITS CONTENTS IN ANY MANNER TO AN UNAUTHORIZED PERSON IS PROHIBITED BY LAW.

LIST OF ILLUSTRATIONS (Cont'd)

12-23 Thermal Stability Characteristics of East Coast Jet A-1 Fuel No. F-1498 in CRC Research Fuel Coker at 175°F Reservoir Temperature

12-24 Research Fuel Coker Tests for Determination of Preheater Breakpoint Temperature

12-25 Measured Fuel Oxygen Content During Research Fuel Coker Tests at 175F Reservoir Temperature 1.5 psia Reservoir Pressure

12-26 Typical Fuel Oxygen Content During Research Fuel Coker Test at Low Pressure Conditions

12-27 Thermal Stability Characteristics of West Coast Jet A Fuel No. F1497 in CRC Research Fuel Coker at 175°F Reservoir Temperature

12-28 Thermal Stability Characteristics of JP-5 Refernce Fuel No. F1065 in CRC Research Fuel Coker at 175F Reservoir Temperature

12-29 Thermal Stability Characteristics of East Coast Jet A-1 Fuel No. F1498 in Research Fuel Coker at 175F Reservoir Temperature

12-30 Breakpoint Distribution of Survey Fuels in Terms of Coker Metal Temperatures

12-31 Breakpoint Distribution of Survey Fuels in ASTM Research Coker as Related to Metal Temperature

12-32 Effect of Additive on Fuel Thermal Stability Modified (SSF Version) Fuel Coker Test 175F Reservoir

LUBRICANTS

13-1 Estimated Fuel and Oil Temperatures Versus Mission Time

13-2 Lubricant Test Environment

DOWNGRADED AT 3 YEAR INTERVALS
DECLASSIFIED AFTER 12 YEARS
DOD DIR 5200.10

LIST OF ILLUSTRATIONS (Cont'd)

13-3 Gear Pitting Fatigue Life in Ryder Gear Machine

13-4 Test Data Summary for L-919 Lubricant in the High Temperature Erdco Bearing Rig

INLETS

14-1 Effect of Vortex Generators on Boeing Inlet Distortion (Mach 2.5)

MATERIALS AND MANUFACTURING TECHNIQUES

15-1 Creep Properties of PWA 1007 Nickel-Base Alloy, Heats XFIR and XFKA

15-2 Stress-Rupture Properties of PWA 1007 Nickel-Base Alloy, Heats XFIR and XFKA

15-3 Tensile Properties of PWA 1007 Nickel-Base Alloy

15-4 Creep Properties of PWA 1003, PWA 1007, PWA 1010, PWA 1202, PWA 1203 and AMS 4928 Alloys

15-5 Estimated Stresses to Produce 0.1% Creep in PWA 1003, PWA 1007, PWA 1010, PWA 1202, PWA 1203, and AMS 4928 Alloys

15-6 Low-Cycle Fatigue Notched Test Results for PWA 1007 Nickel-Base Alloy

15-7 Combined-Load Test Data for PWA 1007 Nickel-Base Alloy

15-8 Combined-Load Notched Test Results for PWA 1007 and PWA 1010 Nickel-Base Alloys

15-9 Combined-Load Notched Test Results for PWA 1007 and PWA 1010 Nickel-Base Alloys

15-10 Combined-Load Notched Test Results for PWA 1007 and PWA 1010 Nickel-Base Alloys

LIST OF ILLUSTRATIONS (Cont'd)

15-11 Rotating Beam Test Data for PWA 1007 Nickel-Base Alloy

15-12 Rotating-Beam Fatigue Test Results for PWA 1007 and PWA 1010 Nickel-Base Alloys

15-13 Rotating-Beam Fatigue Test Results for PWA 1007 and PWA 1010 Nickel-Base Alloys

15-14 Rotating Beam Fatigue Test Results for PWA 1007 and PWA 1010 Nickel-Base Alloys

15-15 Low Cycle Fatigue Test Data for PWA 1007 Nickel-Base Alloy

15-16 Low Cycle Fatigue Test Results for PWA 1007 Nickel-Base Alloy

15-17 Low Cycle Fatigue Notched Test Results for PWA 1007 Nickel-Base Alloy

15-18 Cyclic Tension Fatigue Notched Test Data for PWA 1007 Nickel-Base Alloy

15-19 Cyclic Tension Fatigue Notched Test Data for PWA 1007 Nickel-Base Alloy

15-20 Cyclic Tension Fatigue Notched Test Results for PWA 1007 Nickel-Base Alloy

15-21 History and Composition of Materials Tested

15-22 Creep Properties of PWA 1003 Nickel-Base Alloy

15-23 Creep Properties of PWA 1010 Nickel-Base Alloy

15-24 Creep Properties of AMS 4928 Titanium Alloy

15-25 Creep Properties of PWA 1202 Titanium Alloy

15-26 Creep Properties of PWA 1203 Titanium Alloy

DOWNGRADED AT 3 YEAR INTERVALS
DECLASSIFIED AFTER 12 YEARS
DOD DIR 5200.10

LIST OF ILLUSTRATIONS (Cont'd)

15-27 Larson Miller Plot of Time to 0.1% Creep for Nickel-Base Alloys

15-28 Larson Miller Plot of Time to 0.1% Creep for Titanium Alloys

15-29 Tensile Properties of PWA 1003 Nickel-Base Alloy Heat Abet

15-30 Tensile Properties of PWA 1010 Nickel-Base Alloy Heat CGNJ

15-31 Tensile Properties of AMS 4928 Titanium-Base Alloy

15-32 Tensile Properties of PWA 1202 Titanium-Base Alloy

15-33 Tensile Properties of PWA 1203 Titanium-Base Alloy

15-34 Acceptance Data for 1.25-inch Bar Stock of PWA 1202 and AMS 4928 Titanium-Base Alloys

15-35 Stress Required to Produce Stress Corrosion Cracking and 0.1% Creep in 100 Hours for PWA 1202 And AMS 4928 Titanium-Base Alloys

15-36 Post-Exposure Tensile Test Results

15-37 Containment Properties for Candidate Case Materials

15-38 Creep Properties for PWA 658 and PWA 659 Cast Nickel-Base Alloys

15-39 Chemical Compositions of Creep Specimens

15-40 Creep Properties of PWA 658 and PWA 659 Cast Nickel-Base Alloys

15-41 Heat Treatments and Densities for Candidate Alloys

15-42 Stress for 1% Creep in 1000 Hours for Heat-Treated Nickel-Base Alloys

LIST OF ILLUSTRATIONS (Cont'd)

15-27 Larson Miller Plot of Time to 0.1% Creep for Nickel-Base Alloys

15-28 Larson Miller Plot of Time to 0.1% Creep for Titanium Alloys

15-29 Tensile Properties of PWA 1003 Nickel-Base Alloy Heat Abst

15-30 Tensile Properties of PWA 1010 Nickel-Base Alloy Heat CGNJ

15-31 Tensile Properties of AMS 4928 Titanium-Base Alloy

15-32 Tensile Properties of PWA 1202 Titanium-Base Alloy

15-33 Tensile Properties of PWA 1203 Titanium-Base Alloy

15-34 Acceptance Data for 1.25-inch Bar Stock of PWA 1202 and AMS 4928 Titanium-Base Alloys

15-35 Stress Required to Produce Stress Corrosion Cracking and 0.1% Creep in 100 Hours for PWA 1202 And AMS 4928 Titanium-Base Alloys

15-36 Post-Exposure Tensile Test Results

15-37 Containment Properties for Candidate Case Materials

15-38 Creep Properties for PWA 658 and PWA 659 Cast Nickel-Base Alloys

15-39 Chemical Compositions of Creep Specimens

15-40 Creep Properties of PWA 658 and PWA 659 Cast Nickel-Base Alloys

15-41 Heat Treatments and Densities for Candidate Alloys

15-42 Stress for 1% Creep in 1000 Hours for Heat-Treated Nickel-Base Alloys

DOWNGRADED AT 3 YEAR INTERVALS
DECLASSIFIED AFTER 12 YEARS
DOD DIR 5200.10
THIS DOCUMENT CONTAINS INFORMATION AFFECTING THE NATIONAL DEFENSE OF THE UNITED STATES WITHIN THE MEANING OF THE ESPIONAGE LAWS, TITLE 18, U.S.C., SECTIONS 793 AND 794. ITS TRANSMISSION OR THE REVELATION OF ITS CONTENTS IN ANY MANNER TO AN UNAUTHORIZED PERSON IS PROHIBITED BY LAW.

LIST OF ILLUSTRATIONS (Cont'd)

15-43 Stress for 1% Creep in 5000 Hours for Heat-Treated Nickel-Base Alloys

15-44 Thermal Fatigue Test Program

15-45 Typical PWA 657, PWA 659, and PWA 663 Thermal Fatigue Specimens before Coating and Testing. Parallel Gage Section is 1" Long With 0.480" OD and 0.320" ID.

15-46 Thermal Fatigue Data for Completed Specimens

15-47 Thermal Fatigue Data

15-48 Specimens Being Subjected to Erosion Testing

15-49 Specimen Heat Treatments and Exposure Conditions

15-50 X-Ray Diffraction Results

15-51 X-Ray Flourescence Results

OPERATIONS AND ECONOMICS

16-1 History of Powerplant Contribution to Aircraft Direct Operating Cost and Aircraft Capacity

16-2 History of Powerplant Contribution to Aircraft Direct Operating Cost

16-3 Estimated Relative Price of SST Study Engines

16-4 Estimated Effect of Program Size on SST Engine Price

16-5 Estimated Effect of Design Cruise Mach Number on Engine Unit Price and Total Development Cost

16-6 Quick Engine Change (Less Nacelle Structure) Unit Labor Man Hours Per Flight Hour - Turbojets and Turbofans

DOWNGRADED AT 3 YEAR INTERVALS
DECLASSIFIED AFTER 12 YEARS
DOD DIR 5200.10

THIS DOCUMENT CONTAINS INFORMATION AFFECTING THE NATIONAL DEFENSE OF THE UNITED STATES WITHIN THE MEANING OF THE ESPIONAGE LAWS, TITLE 18, U.S.C., SECTIONS 793 AND 794. THE TRANSMISSION OR THE REVELATION OF ITS CONTENTS IN ANY MANNER TO AN UNAUTHORIZED PERSON IS PROHIBITED BY LAW.

LIST OF ILLUSTRATIONS (Cont'd)

16-7 Estimation of Aircraft Quick Engine Change Unit Maintenance Labor Man Hours

16-8 Basic Data - Airline Reports to Cab

16-9 Quick Engine Change (Less Nacelle Structure) Unit Material Cost Per Hour vs. Gas Generator Take-Off Airflow

16-10 Material Cost Ratio vs. Bypass Ratio

16-11 Reference Specific Thrust vs. Bypass Ratio

16-12 Material Cost Ratio vs. Specific Thrust Ratio

16-13 Estimation of Aircraft Quick Engine Change Unit Material Costs Per Flight Hour

16-14 SST Cruise Environment & Duty Cycle Material Cost vs. Cruise Mach Number

16-15 SST Engine Maintenance Material Cost Increment for Variable Nozzle, Augmenter, Ejector and Reverser

16-16 Estimation of Engine Material Costs Per Flight Hour

16-17 Uninstalled Performance Comparison of Engines Studied During Phase II-A Evaluation

16-18 Anticipated Rate of TBO Progression

DOWNGRADED AT 3 YEAR INTERVALS
DECLASSIFIED AFTER 12 YEARS
DOD DIR 5200.10

LIST OF ILLUSTRATIONS (Cont'd)

SUPPORTING DESIGN CONSIDERATIONS

17-1 Typical Failure Mode Analysis for the STF219

17-2 Weight Summary for Boeing Installation STF219-B

17-3 Weight Summary for Lockheed Installation STF219-L

17-4 Adjusted Thrust-to-Weight Ratios vs Time for Supersonic Engines

17-5 Comparison of Engine Weight and Size

17-6 STJ221 Engine Weight vs Airflow

17-7 STJ222 Engine Weight vs Airflow

17-8 STJ227 Engine Weight vs Airflow

17-9 Estimated Relative Price vs Airflow of SST Engines Including Ejector Reverser

17-10 Estimated Relative Price vs Mach Number of SST Engines Including Ejector Reverser

17-11 STF219 Hot Section Maintenance

17-12 STF219 Major Disassembly Units

INTRODUCTION

The overall objectives of the program conducted under Contract FA-SS-64-2 were to prepare a preliminary design layout of a supersonic transport engine, conduct major component verification and initiate approximately full-scale component testing. This program was a continuation of the contractor's design and test effort on supersonic transport powerplants and was aimed at achieving further advances in engine design and component state-of-the-art over those submitted in the Phase I proposal for the supersonic transport engine.

~~In accordance with the requirements of Contract FA-SS-64-2,~~ the program described herein was divided into seventeen major areas of effort corresponding to the tasks listed in ~~Section C of~~ the contract work statement. These areas included systems analyses, the completion of a preliminary design layout of the engine and the preparation of model and performance specifications. Research and development effort was performed on compressors, primary combustion, turbines, augmentors, inlet and exhaust systems, noise research, controls and accessories, bearings and seals, fuels and lubricants, and materials and manufacturing techniques. Investigations were conducted in the areas of operations and economics and supporting design considerations such as maintainability, reliability and value engineering. A discussion of the work completed in each of these areas is presented in separate sections of the report in an order corresponding to the work statement items of the contract.

DOWNGRADED AT 3 YEAR INTERVALS
DECLASSIFIED AFTER 12 YEARS
DOD DIR 5200.10

SYSTEM ANALYSES



ITEM I - SYSTEMS ANALYSES

OBJECTIVE

The objective of the system analyses was to establish in conjunction with the airframe contractors those preliminary engine design requirements which affect the performance, operation, reliability, safety, maintainability, and economy of the commercial supersonic transport. The analyses were to be sufficiently complete to be used to establish the engine sizing and design at the end of the Phase II-A period.

SUMMARY

The Phase I evaluation results indicated that the proposed engines did not meet the SST program objectives. Consequently, the powerplant performance for Phase IIA was based on a more advanced technology. Since the advanced technology could possibly change the relative advantage of one engine cycle over another, several engines, each representing different cycles, were evaluated. Each engine was designed for a Mach 3 capability. The engines evaluated were the:

STF219	-	Duct Heating Turbofan
STJ221, 226, 228	-	Non-Auginented Turbojet
STJ222, 225	-	Full Afterburning Turbojet
STF223	-	Afterburning Turbofan
STJ 227	-	Partial Afterburning Turbojet

The design parameters for these engines are shown in Table I-1.

TABLE I-1

Phase IIA Engine Cycle Description

	Afterburning Turbofan STF219	Afterburning Turbojet STJ222	Partial Afterburning Turbojet STJ227	Dry Turbojet STJ221	Duct Heating Turbofan STF219
Over-All Pressure Ratio	11.0	9.3	9.3	7.5	11.0
Fan Pressure Ratio	2.3	--	--	--	2.7
Bypass Ratio	1.3	--	--	--	1.3
Nominal Airflow Size (lb/sec)	500	450	690	690	690
Take-Off and Acceleration Turbine Inlet Temperature (°F)	2300	2300	2300	2300	2300
Cruise Turbine Inlet Temperature (°F)	2200	2200	2200	2200	2200
Maximum Engine Diameter (in)	74	72	87	87	76
Engine Weight Including Ejector (lb)	7750	8400	11900	11650	8400
Relative Engine Cost	--	1.02	1.16	--	1.0

DOWNGRADED AT 3 YEAR INTERVALS
DECLASSIFIED AFTER 12 YEARS
DOD DIR 5200.10

The engine sizes were chosen such that the installed transonic acceleration thrust would be the same for each cycle. The airframe manufacturers were supplied with sufficient information to permit them to make a first approximation of the engine-aircraft performance. In addition, scale factors were supplied to permit the engine performance, weight, cost, and powerplant dimensions to be calculated for engines of other sizes.

Table 1-2 presents the uninstalled performance of the five engines at some of the critical flight conditions of the supersonic transport. The thrust specific fuel consumption values listed are based on the representative thrust requirements during supersonic cruise and subsonic part throttle operation. The fuel consumption for the critical flight conditions and a wide range of power settings are shown in Figures 1-1 through 1-4.

TABLE 1-2

Design Engine Uninstalled Performance Comparison

	STJ223	STJ222	STJ [illegible]	STJ221	STJ219
Take-Off Maximum Thrust	41800	41900	41 [illegible]	43700	42500
Nominal Airflow Size	500	450	69	690	600
Transonic Acceleration, Mach 1.2, 45000 Feet					
Thrust	17150	18330	24 [illegible]	[illegible]	18200
Specific Fuel Consumption	2.13	1.90	[illegible]	.25	1.84
Supersonic Cruise, Mach 2.7 at 65000 Feet, Thrust/Transonic Thrust 0.62					
Specific Fuel Consumption	[illegible]	1.44	[illegible]	1.41	.82
Supersonic Cruise, Mach 2.7 at 75000 Feet, Thrust/Transonic Thrust 0.59					
Specific Fuel Consumption	[illegible]	[illegible]	[illegible]	[illegible]	[illegible]
Subsonic Part Throttle, Mach 0.9 at 36150 Feet, Thrust/Transonic Thrust, 0.42					
Specific Fuel Consumption	0.92	.10	0	1.09	0.92
Subsonic Part Throttle, Mach 0.9 at 15000 Feet, Thrust/Transonic Thrust 0.42					
Specific Fuel Consumption	0.92	1.22	[illegible]	.80	0.91

*At Max Rating

The afterburning turbofan and the non-augmented turbojet cycles were not found to be competitive by the airframe contractors, and the study

DOWNGRADED AT 3 YEAR INTERVALS
DECLASSIFIED AFTER 12 YEARS
DOD DIR 5200.10

The engine sizes were [illegible] tion thrust would be [illegible] ers were supplied with [illegible] first approximation of the [illegible] scale factors were supplied [illegible] cost, and powerplant [illegible] sizes.

Table I-2 presents the unscaled performance [illegible] at some of the critical flight conditions [illegible] The thrust specific fuel consumption [illegible] representative thrust requirements during [illegible] sonic part throttle operation. The [illegible] flight conditions and a wide range of [illegible] Figures I-1 through I-4.

TABLE I-2

Design Engine Unscaled Performance [illegible]

	[illegible]	[illegible]	[illegible]	[illegible]	[illegible]
Take-Off Maximum Thrust	[illegible]	[illegible]	[illegible]	[illegible]	[illegible]
Nominal Airflow Size	[illegible]	[illegible]	[illegible]	[illegible]	[illegible]
Transonic Acceleration, Mach [illegible], 45000 Feet					
Thrust	[illegible]	[illegible]	[illegible]	[illegible]	[illegible]
Specific Fuel Consumption	[illegible]	[illegible]	[illegible]	[illegible]	[illegible]
Supersonic Cruise, Mach [illegible] at 65000 Feet, Thrust/Transonic Thrust 0.62					
Specific Fuel Consumption	[illegible]	[illegible]	[illegible]	[illegible]	[illegible]
Supersonic Cruise, Mach [illegible] at 75000 Feet, Thrust/Transonic Thrust 0.59					
Specific Fuel Consumption	[illegible]	[illegible]	[illegible]	[illegible]	[illegible]
Subsonic Part Throttle, Mach [illegible] at 36150 Feet, Thrust/Transonic Thrust 0.42					
Specific Fuel Consumption	[illegible]	[illegible]	[illegible]	[illegible]	[illegible]
Subsonic Part Throttle, Mach [illegible] at 45000 Feet, Thrust/Transonic Thrust 0.42					
Specific Fuel Consumption	0.32	[illegible]	[illegible]	[illegible]	[illegible]

FAI Max Rating

The afterburning turbofan and the non-augmented turbojet cycles were not found to be competitive by the airframe contractors, and the study

CONFIDENTIAL

of these engines was subsequently terminated. The detailed performance data for the remaining powerplants was calculated, and IBM performance decks were prepared. The final evaluation of the three remaining powerplants resulted in the selection of the STF219 duct heating turbofan engine by both airframe contractors, and IBM performance decks for the STF219 engine were delivered. Lockheed selected a 700 lb/sec airflow size for Mach 3 operation, and Boeing selected a 640 lb/sec airflow size for Mach 2.7 operation.

Table 1-1 indicates that the engines will operate with a turbine inlet temperature of 2300°F during acceleration and 2200°F during supersonic cruise. If SST service operation should be scheduled to commence during 1972, then the initial certification and service operation of the engine will probably have to be for a 1900°F cruise turbine inlet temperature and a 2000°F transonic acceleration turbine inlet temperature. Performance decks for the lower temperatures were supplied to the airframe manufacturers in addition to the decks for the higher temperatures.

The performance of the STF219 engine at the two turbine inlet temperature levels and the performance of the over-flowed JT11F-4 engine proposed for Phase I are presented in Table 1-3. More detailed performance data are given in Figures 1-5 through 1-8, showing the thrust specific fuel consumption as a function of thrust for supersonic cruise and for subsonic part-power operation.

TABLE 1-3

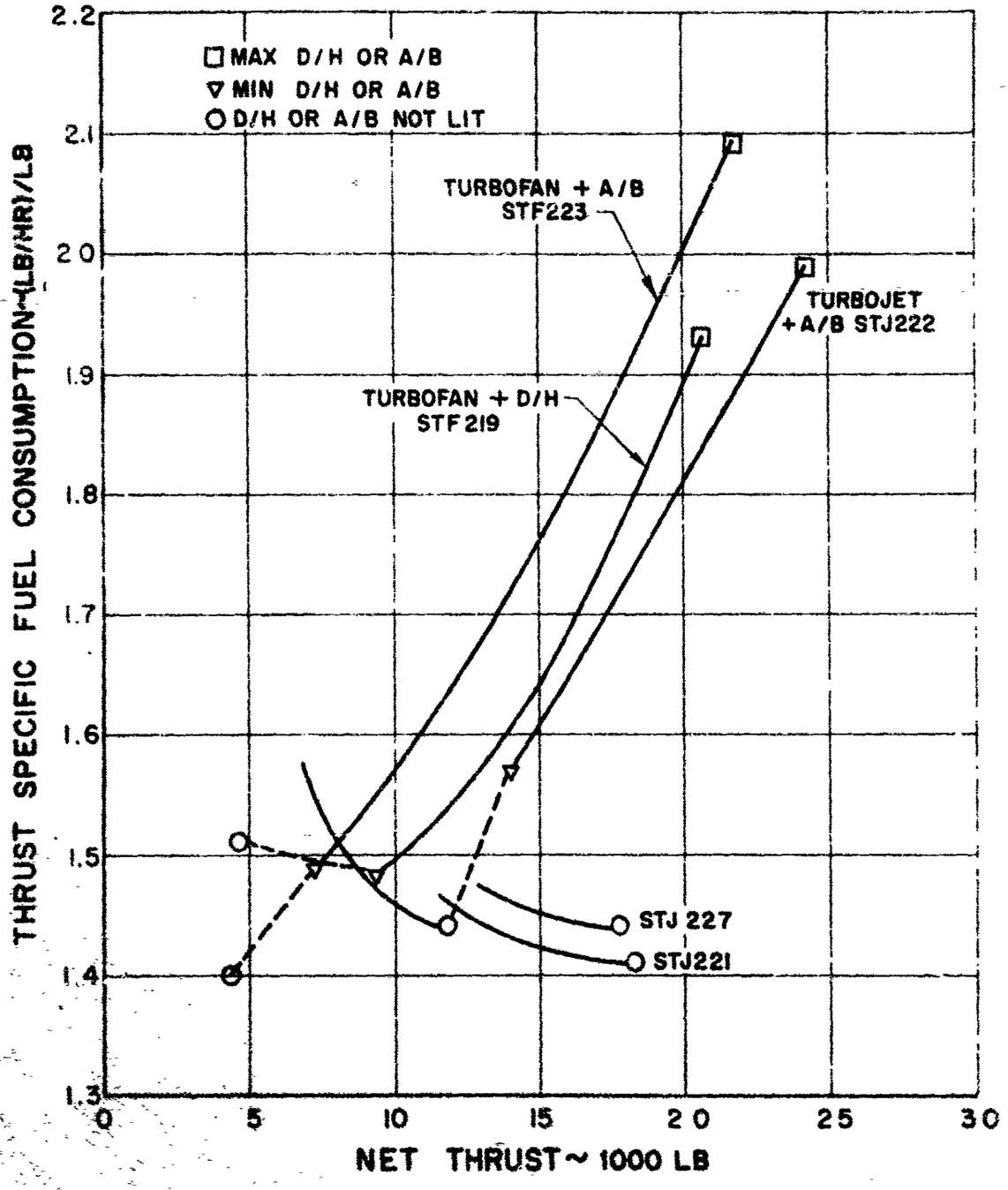
Performance of STF219 Engine and JT11F-4 Engine

	STF219 Design Engine	STF219 Initial Engine	JT11F-4 Variable Engine
Supersonic Cruise Turbine Temperature (°F)	2[illegible]	2[illegible]	2[illegible]
Take-Off Max Inlet Thrust (lb)	5[illegible]	1[illegible]	[illegible]
Airflow Size (lb/sec)	6409	6404	6[illegible]
Maximum Engine Diameter (in)	7[illegible]	7[illegible]	[illegible]
Engine Weight Including Ejector	9[illegible]	[illegible]	[illegible]
Transonic Acceleration, Mach [illegible] at [illegible] Feet			
Thrust	1440	1[illegible]00	[illegible]
Specific Fuel Consumption	1.[illegible]4	.[illegible]4	1.[illegible]7
Supersonic Cruise Mach 2.7 at [illegible] Feet Thrust [illegible] lb			
Specific Fuel Consumption	.[illegible]2	.[illegible]9	.[illegible]
Supersonic Cruise Mach [illegible] at [illegible] Feet Thrust [illegible] lb			
Specific Fuel Consumption	.[illegible]	.[illegible]	.[illegible]4
Subsonic Part Throttle, Mach 0.9 at [illegible] Feet, Thrust [illegible] lb,			
Specific Fuel Consumption	.92	0.89	0.99
Subsonic Part Throttle, Mach 0.6 at [illegible] Feet, Thrust [illegible] lb			
Specific Fuel Consumption	0.91	0.92	1.04

*Engines scaled from the nominal size of 700 lb/sec

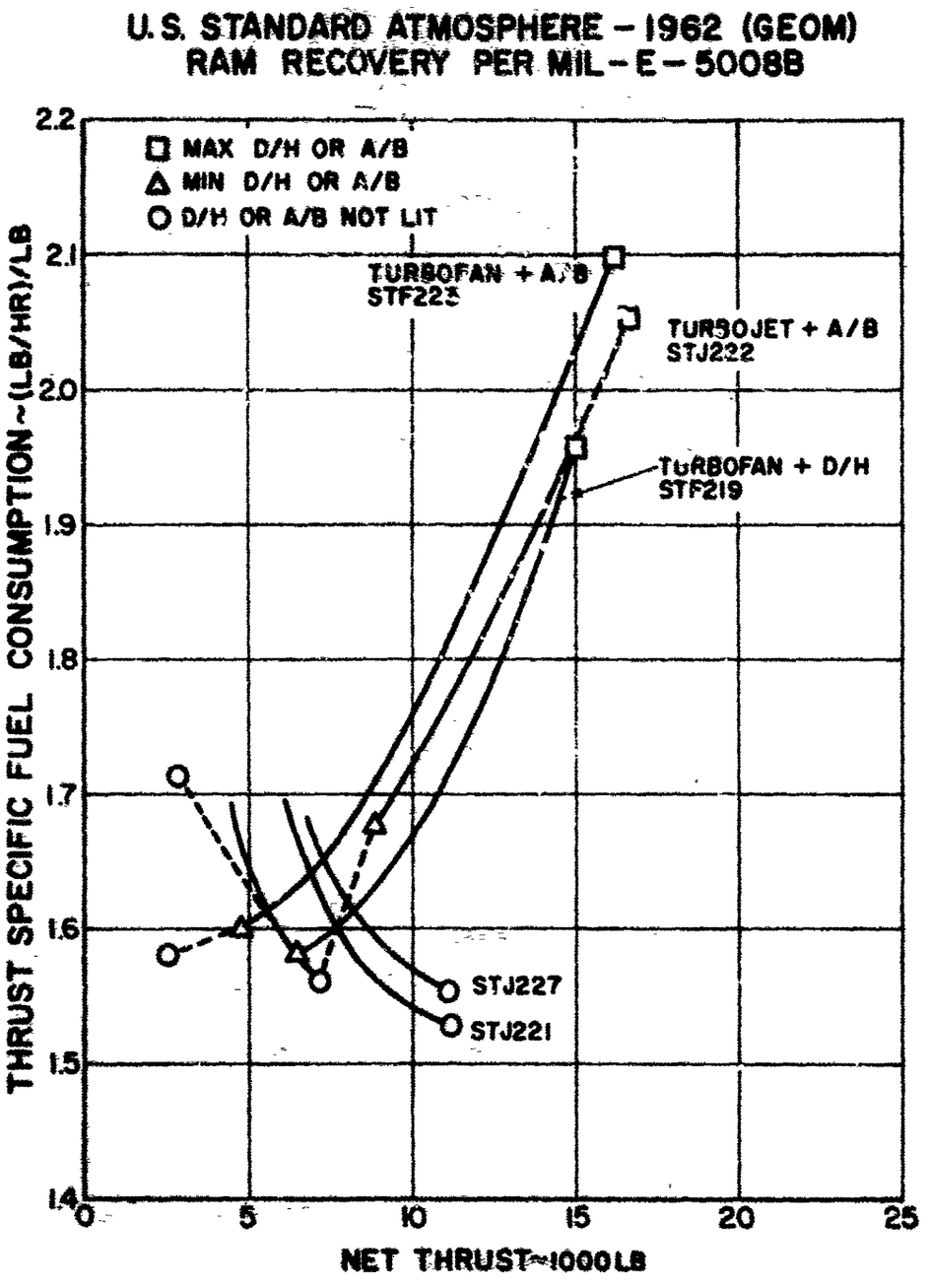
[illegible]
DOD DIR 5200.10

U.S. STANDARD ATMOSPHERE - 1962 (GEOM)
RAM RECOVERY PER MIL-E-5008B



UNINSTALLED ENGINE PERFORMANCE OF THE STF219, STJ221, STJ222, STF223 AND STJ227 ENGINES AT MACH 2.7 AT 65,000 FEET

Figure 1-1



UNINSTALLED ENGINE PERFORMANCE OF THE STF219, STJ221, STJ222, STF223, and STJ227 ENGINES AT MACH 3.0 at 75,000 FEET

Figure 1-2

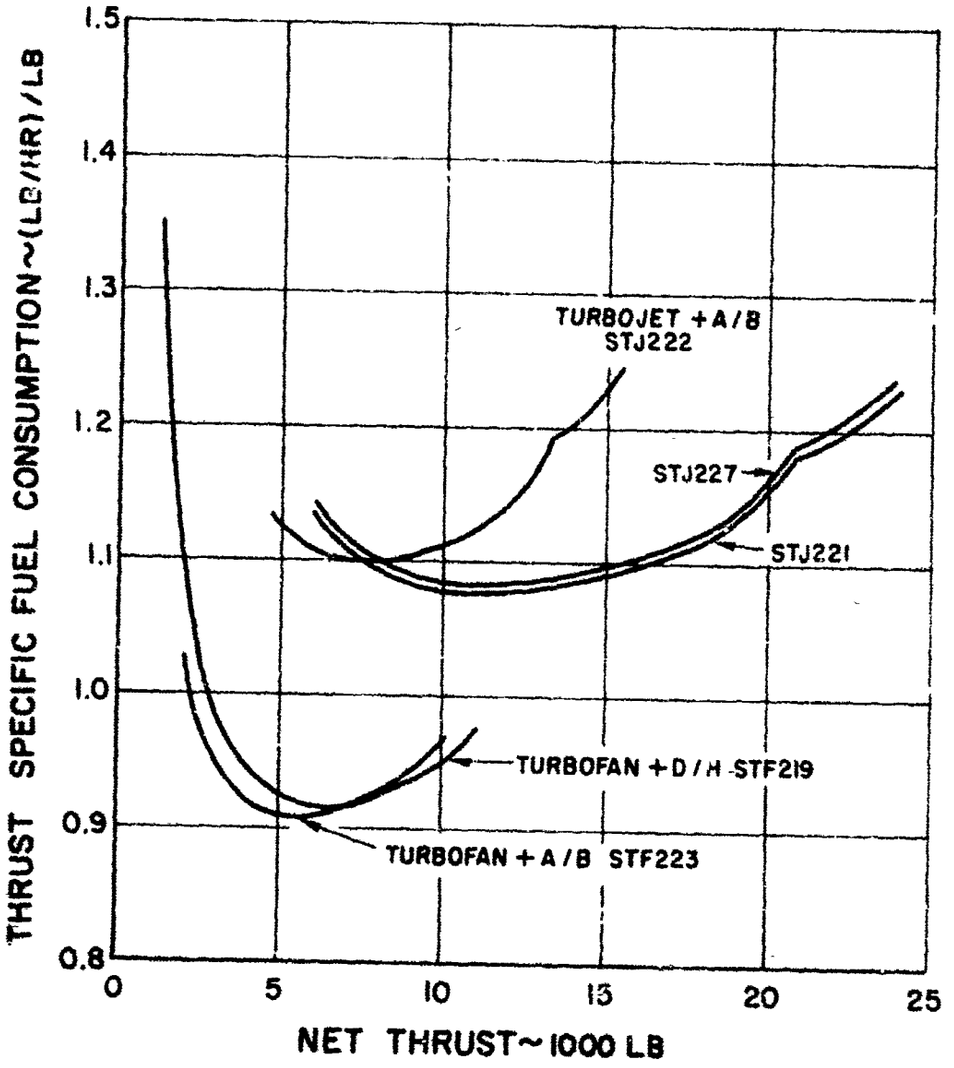
SECURITY MARKING

The classified or limited status of this report applies to each page, unless otherwise marked.
Separate page printouts MUST be marked accordingly.

THIS DOCUMENT CONTAINS INFORMATION AFFECTING THE NATIONAL DEFENSE OF THE UNITED STATES WITHIN THE MEANING OF THE ESPIONAGE LAWS, TITLE 18, U.S.C., SECTIONS 793 AND 794. THE TRANSMISSION OR THE REVELATION OF ITS CONTENTS IN ANY MANNER TO AN UNAUTHORIZED PERSON IS PROHIBITED BY LAW.

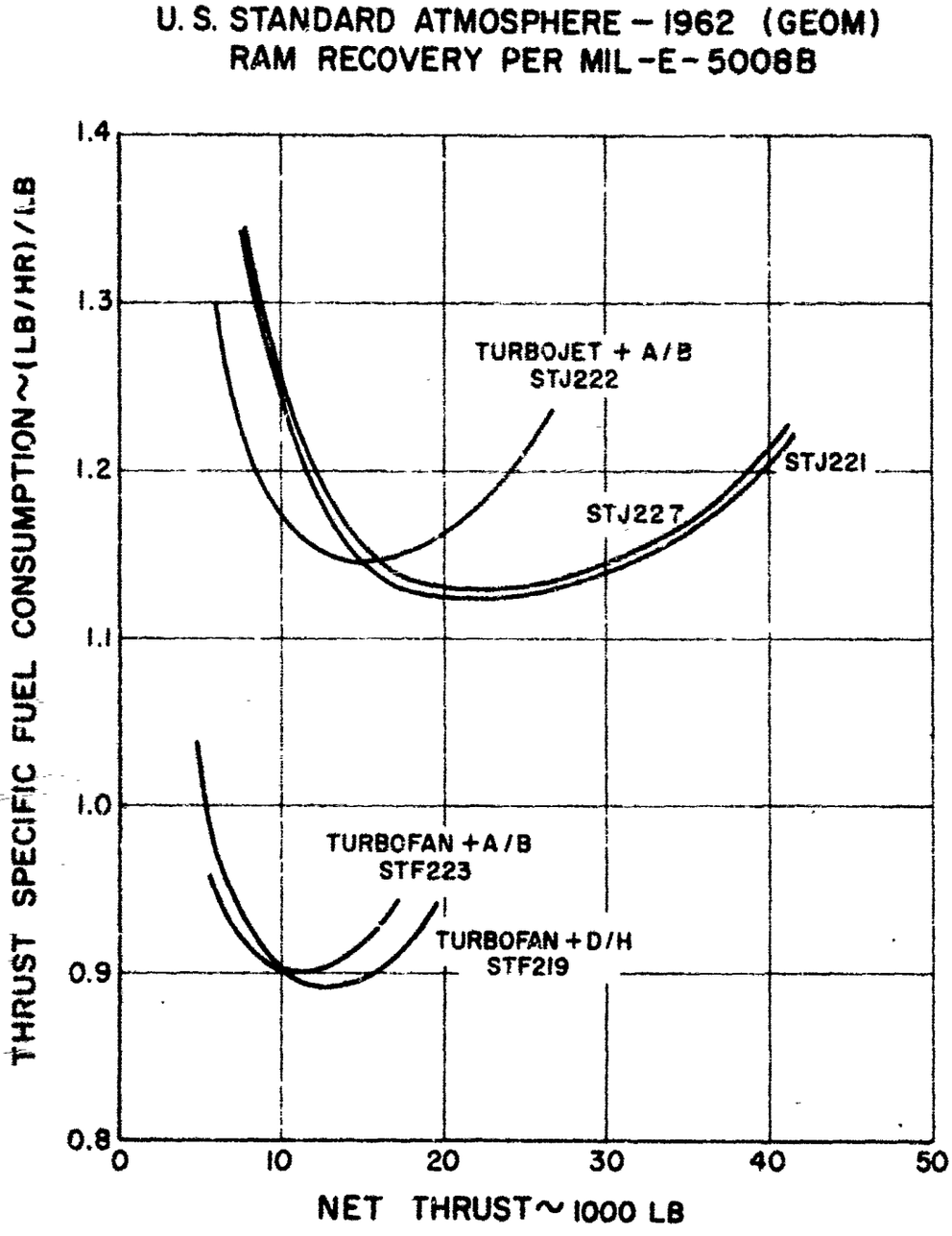
NOTICE: When government or other drawings, specifications or other data are used for any purpose other than in connection with a definitely related government procurement operation, the U. S. Government thereby incurs no responsibility, nor any obligation whatsoever; and the fact that the Government may have formulated, furnished, or in any way supplied the said drawings, specifications, or other data is not to be regarded by implication or otherwise as in any manner licensing the holder or any other person or corporation, or conveying any rights or permission to manufacture, use or sell any patented invention that may in any way be related thereto.

U.S STANDARD ATMOSPHERE-1962 (GEOM)
RAM RECOVERY PER MIL-E-5008B



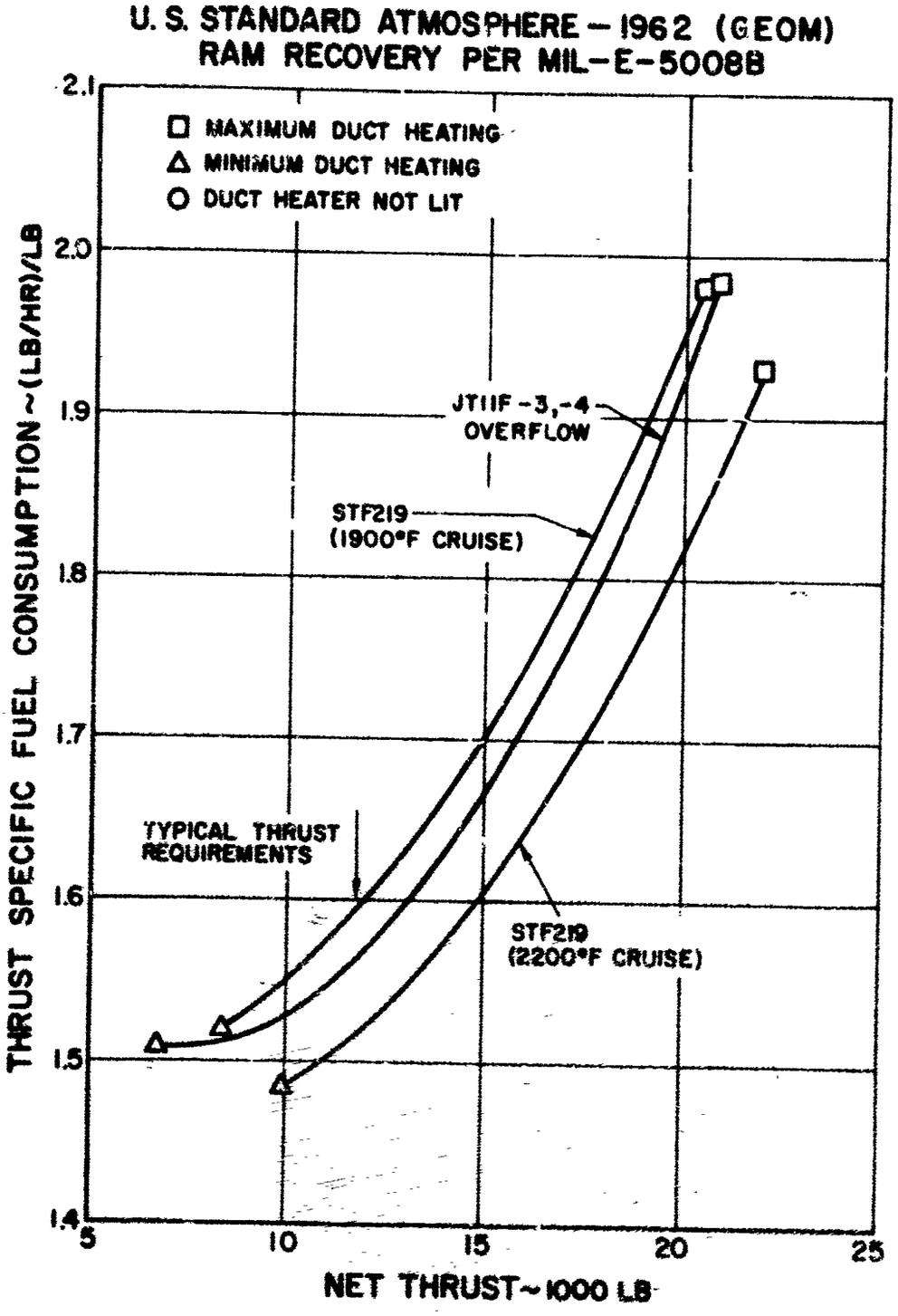
UNINSTALLED ENGINE PERFORMANCE OF THE STF219, STJ221, STJ222, STF223 AND STJ227 ENGINES AT MACH 0.9 AT 36,150 FEET

Figure 1-3



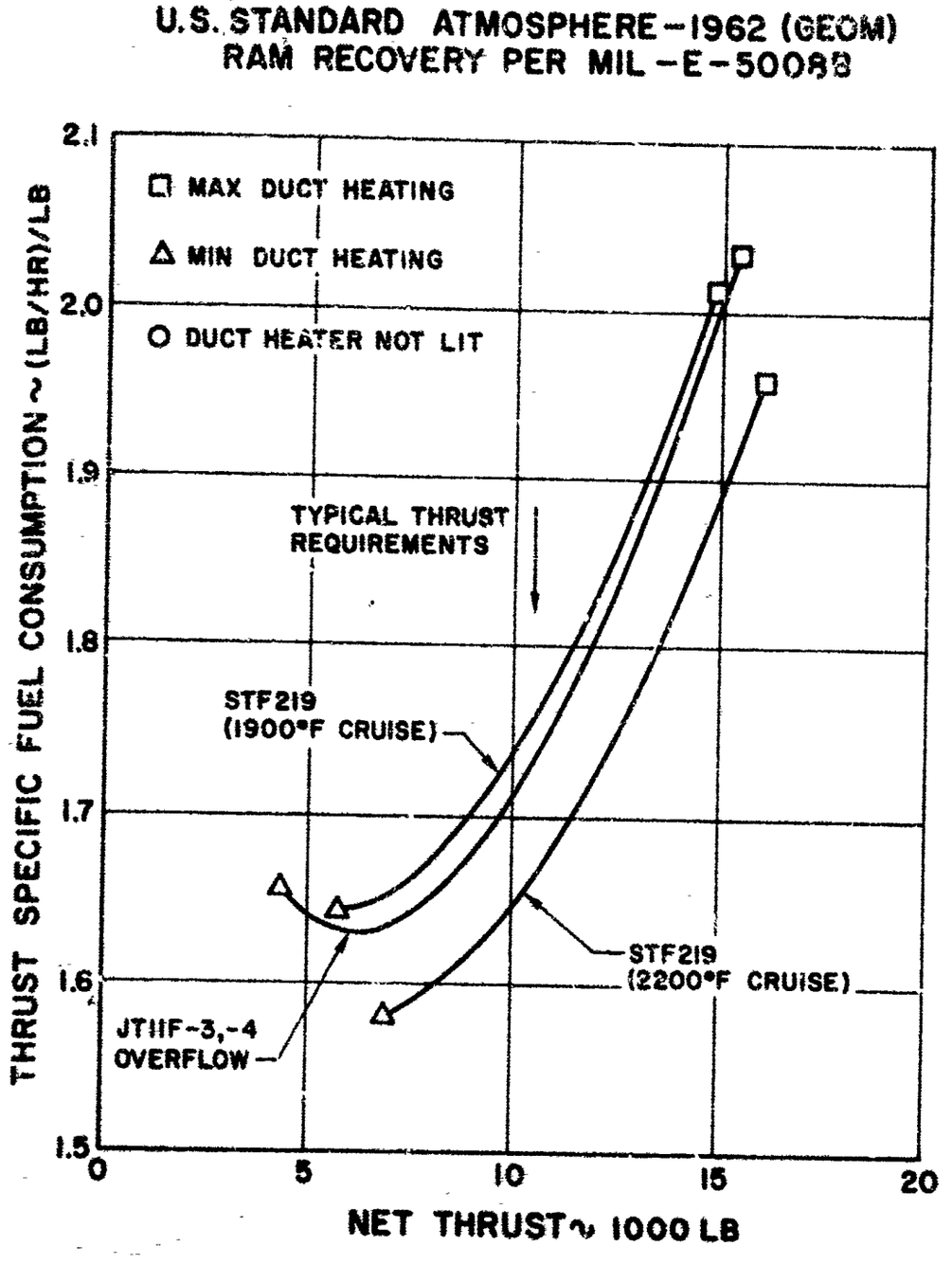
UNINSTALLED ENGINE PERFORMANCE OF THE STF219, STJ221, STJ222, STF223, AND STJ227 ENGINES AT MACH 0.6 AT 15,000 FEET

Figure 1-4



PERFORMANCE OF THE STF219 ENGINE WITH CRUISE TURBINE INLET TEMPERATURES OF 1900°F AND 2200°F AND OF THE JT11F-3, -4 ENGINE AT MACH 2.7 AT 65,000 FEET

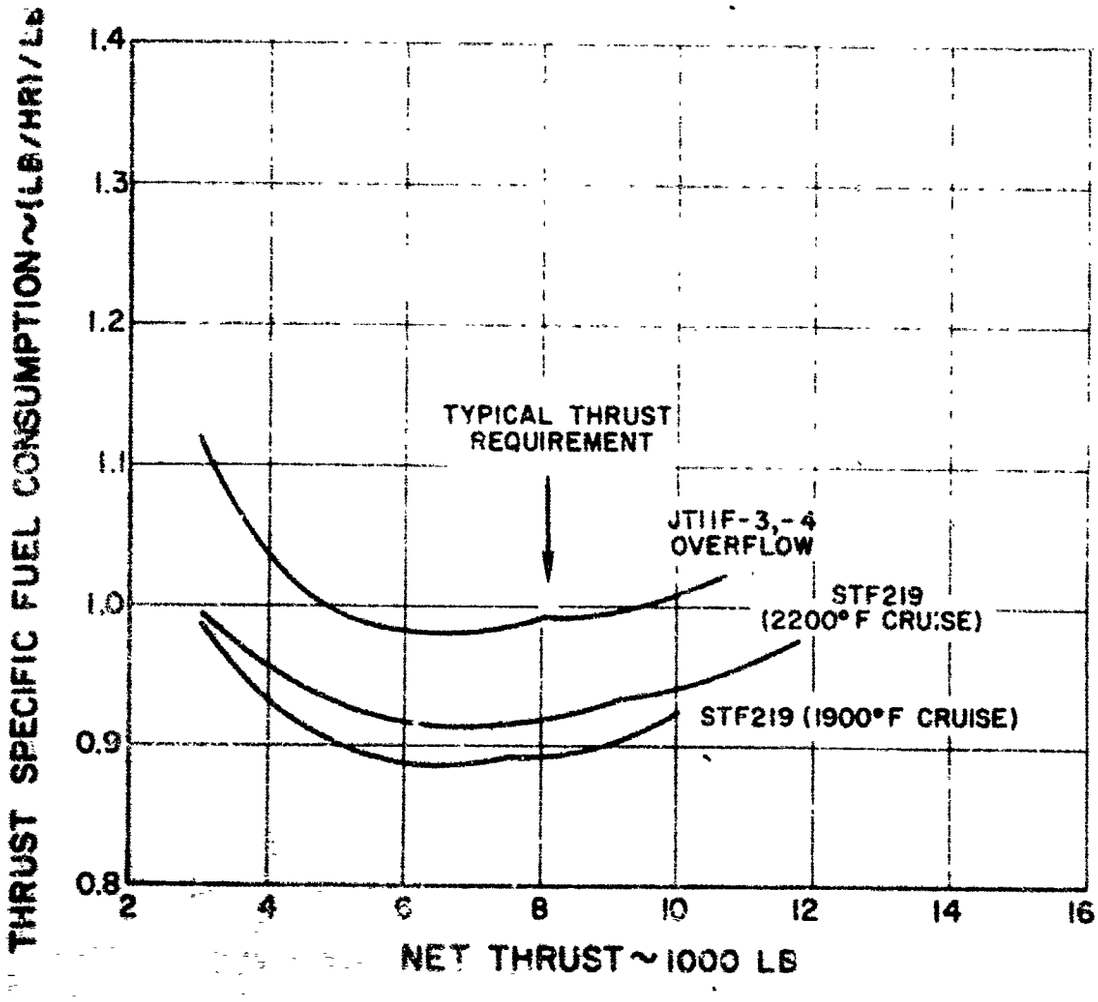
Figure 1-5



PERFORMANCE OF THE STF219 ENGINE WITH CRUISE TURBINE INLET TEMPERATURES OF 1900°F AND 2200°F AND OF THE JT11F-3, -4 ENGINE AT MACH 3.0 AT 75,000 FEET

Figure 1-6

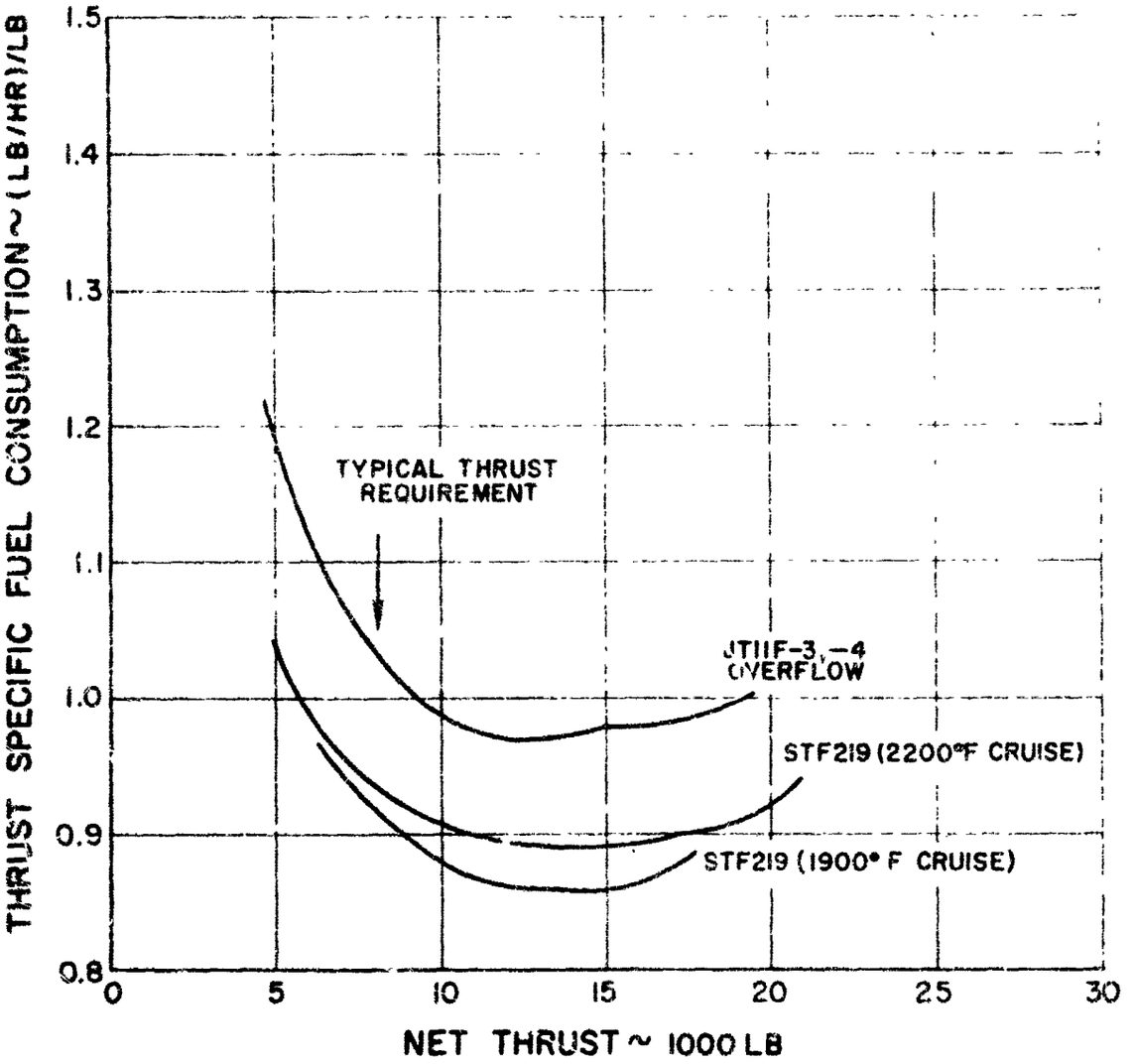
U.S. STANDARD ATMOSPHERE – 1962 (GEOM)
RAM RECOVERY PER MIL-E-5008B



PERFORMANCE OF THE STF219 ENGINE WITH CRUISE TURBINE INLET TEMPERATURES OF 1900°F AND 2200°F AND OF THE JT11F-3, -4 ENGINE AT MACH 0.9 AT 36,150 FEET

Figure 1-7

U.S. STANDARD ATMOSPHERE – 1962 (GEOM)
RAM RECOVERY PER MIL-E-5008B



PERFORMANCE OF THE STF219 ENGINE WITH CRUISE TURBINE INLET TEMPERATURES OF 1900°F AND 2200°F AND OF THE JT11F-3, -4 ENGINE AT MACH 0.6 AT 15,000 FEET

Figure 1-8

PRELIMINARY DESIGN



PRELIMINARY DESIGN

ITEM 2 - PRELIMINARY DESIGN

OBJECTIVE

The contractor shall prepare a preliminary layout design of the engine incorporating the requirements established under Item 1. The design shall contain sufficient detail to permit evaluation of all aspects of the engine and its components.

A. AERODYNAMIC TURBOJET STUDIES

1. INTRODUCTION

During the course of the Phase II-A study contract, a family of turbojet engines was studied with airflow rates ranging from 450 to 800 lb/sec. Thrust augmentation varying from zero to 40 per cent was evaluated. Each of the engines was designed to operate with a turbine inlet temperature of 2200°F at cruise and 2300°F for take-off and transonic acceleration. The design of these engines was based on the successful development and flight testing of the Mach 3 JT11 turbojet engine. The salient features of the turbojet engines studied are presented below:

Engine	Sea Level Take-Off Airflow (lb/sec)	Augmentation
STJ 221	690	None
STJ 226	800	None
STJ 222	450	40% max.
STJ 225	650	40% max.
STJ 227	800	15% max.

These engines are scaled versions of one another. They differ principally in physical size, weight, and the presence or absence of an afterburner. Each engine has a nine-stage axial-flow compressor which develops an optimum over-all cycle pressure ratio of 9.26:1 at standard-day, sea-level take-off conditions. The compressors are driven by two-stage air-cooled turbines. The engines are equipped with variable stagger

inlet guide vanes which are used during starting and also provide in-flight aerodynamic braking should an in-flight engine shut-down be required. A fifth-stage bleed is provided for use during starting. The afterburning STJ 222 and STJ 225 engines have provisions to continuously bleed some compressor fifth-stage air to cool the afterburner liner

These engines are designed with the advanced ram-induction annular burner proposed for all Pratt & Whitney Aircraf SST powerplants.

2. COMPRESSOR

The STJ221 engine compressor is described below in detail. The characteristics of the other compressors are similar to those of the STJ221 and were obtained by scaling to the corresponding engine airflow rates.

Figure 2-1 is a cross-section of the STJ-221 nine-stage compressor. The significant design parameters are shown in Table 2-1.

TABLE 2-1

STJ 221 Compressor Design Parameters
for Sea-Level Take-Off Operation

Number of Stages	9
Over-All Pressure Ratio	9.26
Corrected Rotor Speed (rpm)	4000
Corrected Weight Flow (lb/sec)	690
Specific Mass Flow (lb/sec/ft^2)	42
Corrected Inlet Tip Speed (ft/sec)	1093
Inlet Hub to Tip Diameter Ratio	0.477
Compressor Discharge Velocity (ft/sec)	600

Weight studies were performed to determine the optimum flow-path for this compressor. In these studies, the aerodynamic loading coefficients were held constant, and various levels of discharge velocity were investigated. Figure 2-2 shows the flow paths and the weights of the various configurations considered. The more important characteristics of each flow path are shown in Table 2-2.

inlet guide vanes which are used during starting and also provide in-flight aerodynamic braking should an in-flight engine shut-down be required. A fifth-stage bleed is provided for use during starting. The afterburning STJ 222 and STJ 225 engines have provisions to continuously bleed some compressor fifth-stage air to cool the afterburner liner

These engines are designed with the advanced ram-induction annular burner proposed for all Pratt & Whitney Aircraft SST powerplants.

2. COMPRESSOR

The STJ221 engine compressor is described below in detail. The characteristics of the other compressors are similar to those of the STJ221 and were obtained by scaling to the corresponding engine airflow rates.

Figure 2-1 is a cross-section of the STJ-221 nine-stage compressor. The significant design parameters are shown in Table 2-1.

TABLE 2-1

STJ 221 Compressor Design Parameters
for Sea-Level Take-Off Operation

Number of Stages	9
Over-All Pressure Ratio	9.26
Corrected Rotor Speed (rpm)	4000
Corrected Weight Flow (lb/sec)	690
Specific Mass Flow (lb/sec/ft^2)	42
Corrected Inlet Tip Speed (ft/sec)	1093
Inlet Hub to Tip Diameter Ratio	0.477
Compressor Discharge Velocity (ft/sec)	600

Weight studies were performed to determine the optimum flow-path for this compressor. In these studies, the aerodynamic loading coefficients were held constant, and various levels of discharge velocity were investigated. Figure 2-2 shows the flow paths and the weights of the various configurations considered. The more important characteristics of each flow path are shown in Table 2-2.

TABLF 2-2

Characteristics of Various Compressors
for STJ-221 Engine

Flow Path	Inlet (H/T)	Exit (H/T)	Axial Discharge Velocity (ft/sec)	Number of Stages	Relative Weight (Per Cent)
Constant mean diameter in stages 5 through 7	0.51	0.887	600	7	89
Constant mean diameter in stages 5 through 8	0.51	0.870	500	8	100
Constant mean diameter	0.51	0.856	600	8	78.2
Constant root diameter in stages 3 through 9	0.51	0.806	600	9	70.2

Note: Weight includes rotor, stator, and casing plus associated compressor hardware.

In the afterburning STJ 222, 225, and 227 engines, the compressor is continuously bled behind the fifth stator to provide cooling air for the afterburner centerbody and liners. At sea level take-off, the bleed air is about 2 1/2 per cent of the total flow. A small step in the outer case of the compressor provides room for a diffuser to recover a portion of the air velocity head. The predicted performance map of the compressor is presented in Figure 2-3.

3. MAIN BURNER

a. Design

The main burner is an advanced-design annular ram induction burner. Use of an annular burner permits the maximum utilization of available engine space by combining the burner and the diffuser in a common volume. The ram induction burner uses ram scoops to inject air into the burner with the desired velocities and at the desired locations as shown in Figure 2-4.

The ram induction liner differs from that of the conventional louvered liner such as proposed for the JT11F-11, -12 engine in that airflow into the conventional liner is accomplished by a static pressure gradient across the liner, whereas airflow into the ram induction liner is accomplished by ram pressure. In the conventional system, the penetration and mixing are a function of the static pressure differential at the secondary air holes coming through the liner. The major control over the turbulence level and resultant mixing in the combustion chamber is obtained through control of the static pressure drop across the liner. Hence, to increase the temperature rise in the burner of the JT11F-11, -12 engine without a large increase in length, it would be necessary to significantly increase the pressure drop. With the ram burner, however, the use of total pressure rather than static pressure permits a greater control over the mixing characteristics without incurring a significant pressure loss. The use of total pressure for penetration also requires less diffusion between the compressor and the burner shroud area, and, consequently, the diffuser pressure loss is lower.

A series of small scoops is used to promote good fuel-air mixing in the primary zone with an additional row of larger scoops providing the necessary mixing of air and hot gases in the secondary zone. Fuel is injected directly into the combustion chamber by means of swirl atomizing nozzles. Since the scoops provide a high level of turbulence and mixing, adequate fuel preparation can take place in the primary portion of the burner. Consequently, the primary scoop arrangement provides a mechanical method of fuel preparation and eliminates requirements for hot cone pre-mixing proposed for the JT11F-11, -12 engine.

The ram induction burner also provides certain structural advantages. First, because the shroud static pressure is low, the pressure load on the liner is less than that encountered in a more conventional design. Second, the high velocity flow over the liner and through the ram scoops provides basic cooling by convection. Supplementary film cooling is utilized to cool the surfaces which are exposed to the hot gases. Figure 2-5 shows a detailed section of a scoop with film cooling louvers on the portion exposed to the hot gas.

Transpiration cooling is used downstream of the scoops. Since the turbine inlet temperature is in the 2200 to 2300°F range, cooling of the secondary portion of the liner becomes more critical than in conventional burners Current engines operate at maximum turbine inlet temperatures of 2000°F and utilize 30 to 40 per cent of the air for film cooling. At the 2300°F temperature level, film cooling would require an excessive

amount of flow with a resultant distortion of the turbine inlet profile.

Transpiration cooling is also used at the front portions of the liner since the front end extends upstream into the diffuser and there is no significant flow of air over the fuel nozzle and swirler support bulkheads for convective cooling. The flow in this area is adequate, however, to provide transpiration cooling.

The extensive use of convective and transpiration cooling in the burner section significantly reduces the amount of film cooling required. Consequently, a greater portion of the airflow is available for tailoring the burner exit profile than in a liner using larger amounts of film cooling.

b. Testing

The feasibility of the ram induction principle has been demonstrated in rig tests. A preliminary series of tests was conducted to study the effectiveness of the secondary scoops and to establish the exit temperature profile.

Five configurations were tested. During these runs, penetration of the diluting air varied from excessive (producing a cold center at the exit) to insufficient (resulting in a hot core). No problems of scoop burning were encountered, even though the first design had scoops extending to within a half inch of the burner centerline. The temperature profiles produced by two of the configurations tested are shown in Figures 2-6 and 2-7. For the first of these, the secondary scoops extended to the middle of the burner, whereas for the second, the scoops were cut back to limit the penetration. These tests indicate the degree of control available and that some intermediate scoop length will provide a uniform radial temperature profile.

Water flow tests with ink injection were conducted to determine the burner flow patterns. Figure 2-8 shows the penetration and mixing characteristics of the downstream row of primary scoops. The ink pattern demonstrated that good penetration and mixing were achieved throughout the flow path in the secondary region. Figure 2-9 shows the flow pattern in the stable recirculation zone in the piloting region. The pattern reveals no definite axial flow indicating that the region upstream of the primary scoops has a very low velocity necessary for stable, efficient combustion.

These tests were conducted with a preliminary design burner. Two different burner liners were also used for studying the required secondary scoop configurations and are shown in Figures 2-10 and 2-11.

4. TURBINE

The turbojet engines studied used a two-stage turbine with air-cooled blades and vanes. The turbines were designed to operate with a turbine inlet temperature of 2300°F during take-off and transonic acceleration, and 2200°F during cruise. Although the cooling system is similar to that of the STF219 engine, the environmental temperatures for the second stage are approximately 50°F higher than in the turbofan engine because less work is extracted by the first stage in the turbojet. Identical blade and vane materials are used in the turbojet and turbofan engines.

5. AFTERBURNING TURBOJET - STJ 222

The afterburner used on the STJ 222 engine consists of a diffusing section, a combustion chamber, and a variable-area exhaust nozzle as well as a fuel distribution and flameholding system and liners to provide damping to suppress screech and to protect the structural case from high-temperature gas. The afterburner is shown in Figure 2-12, and the aerodynamic characteristics are shown in Table 2-3.

TABLE 2-3

STJ 222 Afterburner Characteristics

	Turbine Exit Temperature(°F)	Turbine Exit Mach No.	Mean Flameholder Mach No.	Mean Combustion Chamber Mach No.
Sea Level Take-Off	1829	0.36	0.25	0.20
Acceleration, Mach 1.2, 45000 feet	1786	0.40	0.27	0.21
Cruise, Mach 2.7, 65000 feet	1607	0.53	0.34	0.26
Cruise, Mach 3.0, 65000 feet	1621	0.51	0.33	0.25

The diffuser is necessary to reduce the turbine exit Mach number to a level at which combustion can be sustained and pressure losses can be kept to tolerable levels.

The fuel spray rings are integral with the flameholders so that all hardware can be fuel cooled for protection against the high turbine exit temperatures. A typical spray ring-flameholder is shown in Figure 2-13. Ignition is provided by a catalytic igniter which is integral with the fuel source.

A combination screech and cooling liner protects the outer structural case. The liner extends upstream to the spray ring plane to prevent fuel from entering the cooling air annulus between the liner and the case. The liner is convectively cooled by a combination of compressor discharge air and turbine case cooling air. The compressor discharge air is bled from the fifth compressor stage and comprises approximately 2 1/2 per cent of the total flow at sea level take-off conditions. The compressor air is carried to the afterburner by external ducts. The turbine case cooling air is scooped from the outer turbine gas path boundary layer. Use of the turbine gas for cooling reduces the amount of compressor bleed required and reduces the requirements for external cooling air supply ducts.

The afterburner nozzle is composed of hinged flaps which are actuated by hydraulic pistons. The flaps are cooled by the same air which is used to cool the afterburner liner. This air is injected over the flaps at the afterburner liner discharge location.

The STJ222 afterburner was designed to provide a high degree of augmentation at high efficiencies during transonic acceleration. It is capable of providing approximately 40 per cent net thrust at an efficiency of 93 per cent throughout the transonic acceleration region. It may also be used to provide a lower degree of augmentation during cruise, but at an efficiency level of approximately 85 per cent. Figure 2-14 shows the estimated efficiency of the afterburner as a function of the fuel-to-air ratio and shows the maximum efficiency available by optimizing the fuel distribution at all fuel-to-air ratios.

The change in efficiency from transonic acceleration to cruise conditions is a result of the change in the turbine exit temperature. During acceleration, the turbine exit temperature is high enough to cause spontaneous ignition of the fuel. During cruise, however, the turbine exit temperature is not high enough for diffusion burning to be maintained. Combustion stability then depends on the presence of the flameholder.

DOWNGRADED AT 3 YEAR INTERVALS
RELEASED AFTER 12 YEARS
DOD DIR 5200.10

The fundamental design concepts used in selecting the STJ 222 afterburner were derived by Pratt & Whitney Aircraft from testing and development of afterburners used on the J57, J58, and J75 engines, which are currently used to power a large number of military aircraft. The STJ 222 design, however, represents an improvement in the state of the art. Because of the high turbine exhaust temperatures, combustion can be stabilized at higher combustion chamber velocities and can be completed in less burning length. This yields a design which requires less diffusion and hence a smaller diffuser section along with shorter burning length than has been used in any previous afterburner design. The net result provides a higher augmentor thrust-to-weight ratio than any previous design.

6. PARTIAL AFTERBURNING TURPOJET - STJ 227

The afterburner for the STJ 227 engine differs significantly from conventional afterburners. The partial afterburner is shown in Figure 2-15. No diffuser is required since the Mach number at the flameholder plane does not exceed 0.35 and the turbine exit temperature is high enough to promote spontaneous combustion.

The spray bar-flameholder system is integral with the turbine exit guide vanes to reduce weight and drag. A cross section of a typical unit is shown in Figure 2-16. It was possible to integrate the flameholder assembly with the exit guide vanes in this engine because the high degree of swirl in the exit flow requires a row of cascade airfoils to provide the desired axial flow. Forty-five vanes are used and these provide a spray bar system capable of giving good fuel distribution over the airfoil.

The combustion chamber length from the flameholder to the nozzle throat is only 40 inches. This causes a reduction in combustion efficiency because some unburned fuel escapes as a result of insufficient residence time. Also, to minimize cooling requirements, the fuel is restricted to the mid portion of the flow path away from the walls. This imposes a peak temperature profile at the nozzle throat, which, combined with the combustion inefficiency, yields an afterburner efficiency of 80 per cent. This low level of efficiency is not detrimental to the mission, however, because the afterburner is only required for a short time and the resulting increase in fuel consumption is small.

Cooling of the tailpipe walls, plug nozzle, and turbine exit guide vanes is provided by a combination of compressor bleed air and turbine discharge boundary layer air. Figure 2-17 shows a schematic of the

cooling system. At sea level take-off conditions, approximately 2 1/2 per cent of the gas generator flow is bled from the compressor for cooling. Most of this air is used to cool the vanes and the fixed portion of the plug nozzle. Cooling of the vanes is required since the vanes provide the structural support for the plug nozzle and its associated hardware. Some of the vane cooling flow is bled out through the trailing edge to cool the spray bars to eliminate fuel gumming and coking. If the spray bars were subjected to the turbine exit temperature, the small fuel flows during filling and draining would not provide a sufficient heat sink and fuel decomposition would result. The compressor bleed air not used to cool the vanes and the plug nozzle is mixed with turbine discharge air to cool the tailpipe wall. Porous walls are used on both the tailpipe and the plug nozzle for transpiration cooling.

B. MECHANICAL TURBOJET STUDIES

Three of the turbojet engines for which aerodynamic studies were conducted were mechanically designed in sufficient detail to determine the structural arrangement, size, and weight of the engine. One engine of each type was studied, namely, the non afterburning STJ 221, the afterburning STJ 222, and the partial afterburning STJ 227 engines.

1. NON-AFTERBURNING TURBOJET - STJ 221

The design of the STJ221 engine is essentially the same as that of the gas generator portions of the other turbojets and is similar to the gas generator portion of the STF219 engine. The elements of the STJ221 engine which are similar to the corresponding elements in the STF219 engine are the design of the blades and disks and the blade attachments, the stacked disk and inner and outer spacer compressor rotor design, the use of carbon seals backed up by labyrinth seals (pressurized in bearing positions number two and three), the provision for blade containment, the use of abradable material over the blade tips, similar turbine vane and blade cooling, and the use of a ram induction annular combustor. The sections of the engine are bolted together at mating flanges. A cross-sectional drawing of the engine is shown in Figure 2-18.

The inlet of the gas generator is a single welded unit forming the inner and outer flow path walls and joined by aerodynamically shaped radially positioned inlet struts. The number one roller bearing and the associated seals are supported by a box structure formed at the inboard end of the struts. Within the bearing compartment is an oil scavenge pump driven from the front hub of the compressor rotor. The bearing compartment is oil jet cooled and lubricated and is protected from the surrounding environment by carbon ring seals backed up by labyrinth seals.

DOWNGRADED AT 3 YEAR INTERVALS
OR LASSIFIED AFTER 12 YEARS
DOD DIR 5200.10

The compressor inlet guide vanes are located behind the struts and may be rotated about their radial axes to improve the engine starting characteristics and to provide a rotor windmilling aerodynamic brake. The vanes are rotated by pneumatic actuators driving a synchronizing ring and levers on the outer stub shafts of the vanes.

Provision is made for anti-icing the inlet struts and the inlet guide vanes. When required, compressor discharge air flows radially inward through the inlet struts to a box manifold and then rearward through a group of axial pipes to the inboard ends of the inlet guide vanes. It flows radially outward through the vanes and then out through slits in the outer trailing edges of the vanes into the compressor flow path.

The compressor outer wall is formed by stacking and bolting short case and stator assemblies together, one for each of the nine stages. Each case and stator assembly provides an abradable shroud over the blade tips and also a box structure to which the outer ends of the forged stator vanes are welded. The inner ends of the vanes have integral tabs by which they are riveted to a diaphragm. The diaphragm supports the interstage seal rings by rivets and spacers in radially slotted holes to accommodate thermal growth. Similar construction is used in the J58 engine. Immediately to the rear of the fifth-stage stator, air is bled from the compressor to provide easier starting and cooling air for the afterburners. The air bled from the compressor during starting is discharged overboard through flap-type valves located in an annular bleed manifold enveloping the fifth- through eighth-stage compressor cases. The compressor exit guide vanes are made of rolled strip stock inserted into pre-punched slots in the inner and outer shroud rings and brazed in place. The inner shroud ring is bolted to the adjoining diffuser case flange and the outer shroud ring is supported by the ninth-stage compressor outer case with provisions for thermal expansion and fabrication tolerances.

The design of the compressor rotor is conventional. A front hub supports the first-stage disk and is followed by eight additional disks positioned axially by cylindrical inner spacers. Outer ring spacers are used to fix the location of the disk rims and to dampen axial vibrations. The outer ring spacers also carry knife edges to provide sealing against the ring seals on the stator diaphragms. Two sets of the bolts are used: one to join the disks, spacers, and hubs, and one to support the outer spacer between the eighth- and ninth-stage disks. The disks and spacers are designed with appropriate support to ensure concentricity at all operating conditions. An auxiliary disk is mounted on the ninth disk to support a knife-edge seal, help control the thrust balance, and prevent circulation of hot inner circumference boundary layer air around the disk.

The diffuser case is essentially a single welded unit consisting of inner and outer cases forming the flow path boundaries and joined by twelve aerodynamically shaped radial struts. An annular passage surrounds the outer wall forming a bleed air manifold. The manifold is reinforced with flanges that serve to transfer the engine thrust and the radial loads into the engine mounts. The number two bearing, a ball thrust bearing, is supported inside the inner diffuser flow path wall together with the associated carbon and labyrinth seals, an oil scavenge pump, and the tower shaft drives for the accessories. Supply lines for the bearing compartment, venting lines for the labyrinth seals, and pressure lines for thrust balancing are routed through the diffuser case struts. The rear inner flange of the diffuser case mates with the forward flange of a long shallow conical case supporting the number three roller bearing and seals; the rear flange of the middle diffuser case mates with the forward end of the combustor inner case; and the rear flange of the outer diffuser case mates with the forward flange of the combustor section front outer case. The fuel nozzles and the combustor are supported from the outer rear walls of the diffuser case.

The combustor rear outer case slides to the rear to provide access to the rear of the combustor, which, in turn, slides forward to provide access to the turbine nozzle vanes. Two igniter plugs protrude radially into the combustor through the outer rear wall of the diffuser. Suitable combustor section drain valves are provided in the bottom of the combustor cases to prevent accumulation of fuel in the inner bottom surface of the combustor case.

The forward outer flange of the turbine section mates with the combustion section rear case flange. The turbine rotor consists of a shaft, a second-stage turbine disk mounted on the conical end of the shaft, a first-stage disk overhung forward of the second-stage disk on its own integral cylindrical spacer, a front seal disk, and a conical seal spacer between the two stages. The rotor is supported on the Number 3 bearing and is splined to the compressor rear hub.

A variable-area exhaust nozzle is required in the STJ 221 engine to obtain the optimum performance at various flight conditions. The area is varied by moving the inner, central plug by a single hydraulic cylinder. The plug system is supported by the outer turbine exhaust case by a series of radial struts in the turbine exhaust stream.

The turbine exhaust outer case, the struts, and the fixed portion of the turbine exhaust inner wall are convectively cooled by a mixture of fifth-stage compressor bleed air and turbine case cooling air which flows between the inner and outer walls. The movable inner plug is also cooled convectively by compressor bleed air which flows through the rotor shaft and then between the inner and outer walls of the plug.

2. AFTERBURNING TURBOJET - STJ 222

The STJ222 engine is basically a scaled version of the STJ221 with the addition of an afterburner capable of providing full augmentation. The arrangement of the engine is shown in Figure 2-19.

The afterburner, which consists of a diffusing section, a combustion section, a variable-area exhaust nozzle, and a fuel distribution and flameholding system, is bolted to the rear flange of the turbine nozzle case.

The diffusing section is incorporated in the turbine nozzle case. An inner cone forms the inner wall of the diffusing section and is supported by 10 airfoil-shaped struts which are fusion butt welded to integral platforms machined on the inside of the outer turbine exhaust diffuser case and on the outside of the inner diffuser cone. The struts are protected from the turbine exhaust gases by sheet metal heatshields, and their aerodynamic shape tends to straighten the turbine exhaust flow.

The outer structural case of the afterburner forms the rear cylindrical section. The case is protected by a combination perforated screech and cooling nonstructural liner cooled convectively by a combination of compressor fifth-stage bleed air and turbine case cooling air.

The use of a combination fuel distribution and flameholder system is made possible by the high gas stream temperature which provides good combustion efficiency in a short burning length and allows flameholding from integral spray rings and flameholders. Six staggered spray ring-flameholder units, streamlined to reduce pressure losses, are used. The outer three are supported by the fuel supply lines from the outer case, whereas the inner three are supported from the inner cone and are supplied by fuel lines which pass through the exhaust struts. External fuel manifolds feed both sets of spray rings. An alternate spray-bar-flameholder system using 24 close-coupled low loss radial bars has also been designed and is shown in Figures 2-20 and 2-21.

DOWNGRADED AT 3 YEAR INTERVALS
NOT AUTOMATICALLY DECLASSIFIED AFTER 12 YEARS
DOD DIR 5200.10

The variable-area exhaust nozzle consists of a series of flap segments hinged from a supporting ring which is attached to the afterburner outer rear case. The flaps are operated by six hydraulic cylinders through a synchronization ring and suitable linkages. Cooling air which is used to cool the afterburner liner is injected over the flaps from the liner discharge location.

The blow-in-door ejector exhaust system and reverser system are similar to the corresponding systems for the STF219 engine. The ejector supporting beams are attached to the engine rear mount ring and to a rear ring supported from the afterburner outer structural case.

3. PARTIAL AFTERBURNING TURBOJET - STJ 227

The STJ 227 engine is basically a STJ 221 turbojet scaled for a 690 lb/sec airflow and provided with a short, lightweight afterburner capable of producing up to 15 per cent thrust augmentation. A cross-sectional drawing of the engine is shown in Figure 2-22.

The afterburner assembly is bolted to the rear end of the turbine outer case and includes a central movable plug, a plug support and actuation system, an exit guide vane and spray bar system, inner and outer liners, and the outer case.

The movable center plug provides a completely variable area orifice between the established limits. It is a double-walled Waspaloy sheet metal structure cooled by turbine disk cooling air. The cylindrical section of the plug is stiffened with a sheet metal box section that provides support for the rollers. The rollers ride in eight channel-section tracks with two rollers riding in each track. The tracks are located on a stiffened cylindrical ring which is part of the fixed support structure. A seal assembly consisting of a series of overlapping sheet metal sections is used to reduce the leakage past the movable plug.

The hydraulic actuator is attached to the fixed structure at the forward end and to the movable plug at the rear attachment point with ball joints. Fuel, held below 400°F by means of a continuous fuel recirculation system, is the actuating fluid. The fixed conical support structure, fabricated from Hastelloy X, is attached to a structural ring which transmits loads to the outer case through the turbine exit guide vanes. The guide vanes are fabricated from IN-100 alloy.

The fixed portion of the inner flow path is a double-walled structure cooled by compressor bleed air supplied through the exit guide vanes. The outer of the two walls is perforated.

The fuel spray bar system, fabricated from Hastelloy X, consists of 45 spray bars, each located directly behind a turbine exit guide vane. The spray bars are supported by the vanes and cooled by air supplied by the vanes to a temperature low enough to preclude fuel coking during lighting, shutdown, and low fuel flows. Flameholding is provided by the combined vane and spray bar structure. Fuel is supplied by the main fuel pump and catalytic igniters provide continuous ignition.

The outer liner is in two sections, both fabricated from Hastelloy X and cooled by a mixture of turbine case cooling air and compressor bleed air. The front section is bolted to the turbine outer case and supports the second-stage turbine blade tip seal, the exit guide vanes, and the fuel baffle perforated liner. Holes in the forward end of the liner introduce the cooling air flow into the afterburner cooling manifold. The rear outer liner is flexibly supported from 24 brackets on the inside of the outer case to permit thermal expansion. The rear liner is fabricated from perforated sheet metal and is convoluted to provide resistance to buckling.

C. AERODYNAMIC TURBOFAN STUDIES - STF 219

1. GENERAL DESCRIPTION

The STF219 turbofan engine is a two-spool engine with an optimum overall cycle pressure ratio of 11.88:1 at sea-level take-off conditions. The low-speed spool consists of a two-stage fan producing a 2.7:1 pressure ratio and a two-stage turbine. The high-speed spool consists of a five-stage constant mean diameter compressor producing a 4.4:1 pressure ratio and a single-stage turbine. The engine is shown in Figures 2-23 and 2-24.

At sea-level take-off conditions, the fan discharge air is divided between the engine and the bypass duct such that thirty per cent more air passes through the duct than through the engine. The air that enters the engine is compressed in the high-pressure compressor, heated in the combustion chamber, and expanded through the turbine. The air that is bypassed through the ducts flows through a diffuser and into the duct heater. During certain portions of the flight, the duct air is heated in the duct heater to provide additional thrust before being exhausted through a variable-area discharge nozzle.

The fixed portion of the inner flow path is a double-walled structure cooled by compressor bleed air supplied through the exit guide vanes. The outer of the two walls is perforated.

The fuel spray bar system, fabricated from Hastelloy X, consists of 45 spray bars, each located directly behind a turbine exit guide vane. The spray bars are supported by the vanes and cooled by air supplied by the vanes to a temperature low enough to preclude fuel coking during lighting, shutdown, and low fuel flows. Flameholding is provided by the combined vane and spray bar structure. Fuel is supplied by the main fuel pump and catalytic igniters provide continuous ignition.

The outer liner is in two sections, both fabricated from Hastelloy X and cooled by a mixture of turbine case cooling air and compressor bleed air. The front section is bolted to the turbine outer case and supports the second-stage turbine blade tip seal, the exit guide vanes, and the fuel baffle perforated liner. Holes in the forward end of the liner introduce the cooling air flow into the afterburner cooling manifold. The rear outer liner is flexibly supported from 24 brackets on the inside of the outer case to permit thermal expansion. The rear liner is fabricated from perforated sheet metal and is convoluted to provide resistance to buckling.

C. AERODYNAMIC TURBOFAN STUDIES - STF 219

1. GENERAL DESCRIPTION

The STF219 turbofan engine is a two-spool engine with an optimum overall cycle pressure ratio of 11.38:1 at sea-level take-off conditions. The low-speed spool consists of a two-stage fan producing a 2.7:1 pressure ratio and a two-stage turbine. The high-speed spool consists of a five-stage constant mean diameter compressor producing a 4.4:1 pressure ratio and a single-stage turbine. The engine is shown in Figures 2-23 and 2-24.

At sea-level take-off conditions, the fan discharge air is divided between the engine and the bypass duct such that thirty per cent more air passes through the duct than through the engine. The air that enters the engine is compressed in the high-pressure compressor, heated in the combustion chamber, and expanded through the turbine. The air that is bypassed through the ducts flows through a diffuser and into the duct heater. During certain portions of the flight, the duct air is heated in the duct heater to provide additional thrust before being exhausted through a variable-area discharge nozzle.

For subsonic commercial aircraft applications, Pratt & Whitney Aircraft has successfully met powerplant growth requirements by converting existing turbojet engines to turbofan engines by replacing several of the low-pressure-compressor stages with the number of fan stages required to produce the desired fan pressure ratios. The JT3D-1, the TF33P-7, and the JT8D-1 turbofan engines were all developed by this procedure. In each of these engines, many of the components were common to both the turbojet and turbofan engines, and commercial operators were assured of a continuity of proven hardware. However, the SST powerplant must provide drastic improvements in specific engine weight, increased flexibility in the stage matching between the fan and the engine compressor, and a capability of operating with a higher turbine inlet temperature if it is to meet the mission requirements. It is not believed that satisfactory results will be obtained by converting an existing turbojet engine into a turbofan engine.

The STF 219 engine was designed to meet the specific mission requirements. Unlike the JT11F-11, -12 engine, the fan is not integrally attached to the compressor shaft. By separating the fan from the compressor, the fan can operate at a lower rotational speed to provide better matching as well as a lighter, more versatile engine. Additional weight reduction is achieved by overhanging the fan stages and eliminating the inlet guide vanes and the associated anti-icing apparatus.

2. FAN

A cross-sectional view of the fan and compressor stage of the STF 219 is shown in Figure 2-25. The significant objectives and design parameters for the STF 219 fan are presented below.

Number of Stages	2
Pressure Ratio	2.70
Corrected Airflow (lb/sec)	600
Rotational Speed (rpm)	6100
By-Pass Ratio	1.30
Corrected Inlet Tip Speed (ft/sec)	1490
Inlet Hub-Tip Ratio	0.400
Discharge Mach Number	0.450
Rotor Maximum Relative Mach Number	1.47
Corrected Weight Flow Per Unit Annulus Area ($lb/sec/ft^2$)	41.6

The requirement for sufficient surge margin to ensure surge-free compressor operation was considered in the fan design. The pressure ratio available from the operating line to the stall line was selected to provide an adequate stall margin in the presence of inlet distortion and surge-free operation will result providing the distortion at the fan inlet does not exceed the limits specified in the model specifications presented in Item 3. The surge margin for the STF 219 engine at sea-level take-off conditions is 8 per cent as compared with 16 per cent for the JT11F-11, -12 engines. The reduced margin was made possible because recent duct heater rig test data indicates that satisfactory lights can be obtained with much lower fuel-to-air ratios than anticipated. Less surge margin would improve the steady-state engine performance, but would degrade the transient performance. Providing a larger stall margin would degrade the steady-state performance. The effect of inlet distortion on the engine performance is discussed in the section entitled Inlet-Engine Compatibility in Item 14. Provisions must also be made to ensure stable fan operation during reverse thrust operation and duct heater ignition. A predicted performance map for the STF219 engine is shown in Figure 2-26.

The fan pressure ratio is 2.70 as compared with 2.50 for the JT11F-11, -12 engine. Both fan stages provide approximately equal pressure ratios. Use of a higher pressure ratio produces a smaller fan duct diameter and a reduction in the over-all engine weight. Further increase in the fan pressure ratio would provide a still smaller duct diameter and lower engine weight, but the technical uncertainties involved are not justified by the present state of the art.

Transonic straight entry type airfoils are used for the fan. Titanium is used for the blades to permit high rotational speed to be used without exceeding the safe centrifugal stress limits. The fan blades are shrouded similar to other Pratt & Whitney Aircraft fans to ensure the aerodynamical and mechanical integrity of the blades. The shrouds do incur a small performance loss, but the alternative of increasing the chord size or the hub-to-tip diameter ratio would result in an excessive increase in weight. The stators have airfoils generated on a circular arc mean camberline with a 65 series thickness distribution.

No inlet guide vanes are used for this fan and the first stator provides the front bearing support. This design requires a large stator chord, but the weight involved is more than offset by the weight savings realized by the exclusion of the inlet guide vane assembly and the associated anti-icing system. The design produces an additional weight reduction by requiring a shorter low-speed shaft.

Elimination of the inlet guide vanes results in a high relative Mach number at the tips of the first-stage fan blades. The losses introduced, however, are partially offset by the elimination of the aerodynamic losses of the inlet guide vanes. Considerable testing has been conducted at Pratt & Whitney Aircraft to verify the feasibility of operating fans without inlet guide vanes, including testing in a supersonic cascade tunnel at Mach numbers above 1.00. These tests are described under Item 4 of this report. As shown in Figure 2-27, the STF 219 fan is well within the documented range for current fan testing.

The fan wheel speed for the STF 219 engine is lower than that for the JT11F-11, -12, and therefore the relative fan tip Mach number is also lower (1.47 for the STF-219 vs 1.60 for the JT11F-11, -12). However, as shown in Figure 2-28, the fan root exit wheel speed is greater than that of the TS-4 stage described in Volume EVI-10 of the Phase I final report, although both stages produce the same pressure ratio.

Figure 2-29 shows the fan surge pressure ratio requirements for the STF 219 engine together with those for the JT11F-11, -12 and several demonstrated production fans. The fan discharge Mach number for the STF 219 engine is higher than that for the JT11F-11, -12 fan (0.45 vs 0.36) to produce lower aerodynamic loading on the second-stage blades and vanes. The air triangles for the STF-219 and JT11F-11, -12 engines are presented in Figure 2-30.

3. HIGH-PRESSURE COMPRESSOR

The high-pressure compressor is designed to operate behind the 2.7:1 pressure ratio fan and produce a 4.4:1 pressure ratio so that the overall cycle pressure ratio is 11.88:1.

Other characteristics of the compressor are presented below:

Number of Stages	5
Engine Compressor Pressure Ratio	4.4
Corrected Weight Flow Per Unit Annulus Area (lb/sec/ft^2)	39.0
Rotational Speed (rpm)	8250
Corrected Inlet Tip Speed (ft/sec)	1122
Exit Velocity (ft/sec)	600
Inlet Hub-Tip Ratio	0.775

The compressor has a constant mean diameter to reduce the possibility of flow separation resulting from the slope of the walls and to reduce the possibility of the blades rubbing the cases when deflected. Use of a constant mean diameter compressor also permits the compressor discharge mean diameter to align with the optimum burner diameter. Studies were performed to determine if a weight savings could be realized by not using a constant mean diameter. The studies indicated that the weight savings were negligible and did not justify the additional complications of ducting the compressor discharge air to the burner inlet.

A starting bleed is not required for the STF 219 engine since only the high-pressure compressor is driven during starting whereas with the JT11F-11, -12 engine, both the fan and the compressor were driven during starting with an airflow 5.5 times greater than that of the STF-219 compressor. In addition, the JT11F-11, -12 engine had a more severe stage mismatch at idle as a result of its single rotor system. The elimination of the interstage bleed system provides a lighter engine with higher reliability, less complexity, and easier maintenance.

To provide a pressure ratio of 4.4:1 in five stages requires transonic blading in the early stages and high subsonic cascades in the later stage. The performance map for the high-pressure compressor is shown in Figure 2-31.

Test results obtained to date (see Item 4 of this report) with the five-stage SST compressor rig have demonstrated a surge line which is above the engine operating line at all required flight conditions.

In the STF 219 engine, airflow from the fan is accelerated from 615 ft/sec to 741 ft/sec as it passes through the intermediate case. This speed is maintained through the first high-pressure compressor stage, after which it is reduced by approximately 35 ft/sec in each stage, resulting in a compressor exit velocity of 600 ft/sec. In the JT11F-11, -12 engine, the compressor inlet velocity was 670 ft/sec and the discharge velocity from the high-pressure compressor was 540 ft/sec. Consequently, although the non-dimensional loading coefficients of the two engines are similar, the higher axial velocity in the STF 219 compressor results in a higher inlet tip wheel speed and a higher over-all pressure ratio (4.4 vs 3.8).

The feasibility of compressor designs incorporating multiple transonic stages to achieve high compression ratios in a limited number of stages has been demonstrated through testing. Pressure ratios and tip speeds

for some representative compressors are shown below.

	Pressure Ratio	Tip Speed (ft/sec)
NACA 5-Stage Compressor	4.91	1100
5 Stages of NACA 8-Stage Compressor	3.80	1167
5 Stages of J52 Low Pressure Compressor	3.80	1200
5 Stages of Light Weight Gas Generator	4.3	1140
STF-219 High-Pressure Compressor	4.4	1122

The velocity triangles for the STF-219 and JT11F-11, -12 compressors are shown in Figure 2-32.

4. MAIN BURNER

The STF 219 engine has been designed to operate with a turbine inlet temperature of 2200°F during cruise and of 2300°F from take-off through the transonic acceleration. Consequently, the main burner must provide a temperature rise 250°F greater than that of the main burners for the JT11F engines. In addition to providing a larger temperature rise than current burners, the STF 219 burner must produce a uniform temperature profile to prevent hot spots which would seriously damage the turbine. Consequently, an advanced ram-induction annular burner designed by Pratt & Whitney Aircraft will be used in the STF 219 engine. A discussion of the construction, method of operation, cooling requirements, and design test verification is included in the discussion of the turbojet engines, Section A-3, of this item. The characteristics of the burner, together with those of the burner for the JT11F-11, -12 engine, are presented in Figure 2-33 for sea-level take-off conditions.

An annular louvered burner has been designed and tested to provide an alternative to the ram-induction burner. The louvered burner utilizes the same design criteria as the louvered annular combustor being tested successfully in the STF 200 demonstrator engine.

5. DUCT HEATER

a. Current Design

Thrust augmentation for the STF 219 engine is provided by a combustion system in the fan duct. This "duct heater" extends rearward from the fan exit plane and includes a cascade diffuser, a fuel system and aerodynamic flameholder, and a variable-area exit nozzle.

The diffuser consists of two annular cascades which reduce the fan exit velocity to the level required for stable, efficient burning in the duct heater. The first cascade consists of four concentric rings of airfoils which are designed in accordance with the NACA 65 series and are 9 per cent thick with a 60° camber. Diffusion is accomplished in each of the cascades and in the duct between the cascades. This type of diffuser is 50 to 60 per cent shorter than a conventional straight-wall annular diffuser and produces essentially the same performance. Tests have been conducted to verify the diffuser design. The tests demonstrated that the offset cascade diffuser provides a total pressure exit profile which is much flatter radially than that produced by the conventional straight-wall annular diffuser, and hence is ideal for combustion. These tests demonstrated pressure losses somewhat higher than the design performance goal, but flat plate blades were used rather than airfoils, and it is expected that with airfoils the performance will meet the goals.

The combustion length for the STF 219 duct heater is 50 inches, which is 10 inches shorter than that for the JT11F-11, -12. The chamber was sized to provide a maximum Mach number (cold) of 0.175 throughout the normal flight spectrum to ensure that the required efficiency will be obtained. The combustion section is about the same volume as that of the JT11F-11, -12, however, and therefore the combustion mixture residence time and the resulting performance should be equivalent.

The jet flameholder is composed of both circumferential and radial elements. The resulting cross configuration provides a system of interacting flame fronts formed by short rows of holes aligned at right angles to each other. Tests have indicated that a wide range of augmentation levels can be achieved. Fuel is injected by a system external to the flameholder. In addition to providing more uniform fuel distribution, the external spray bars also provide a more uniform distribution of fuel droplet size and a simpler fuel pumping system since the fuel can be fed from the outer duct case rather than being carried across the duct and fed from between the engine outer case and the duct inner liner. Bleed air for the flameholder is supplied from the compressor. Earlier systems mixed hot combustion gases with the compressor bleed air to raise the temperature, but recent tests have indicated that the increase produced a negligible effect on the combustion efficiency and stability, and the simpler system is desirable.

The design of the duct heater provided for "soft" lighting. This ensures that the fan will not surge. Since severe and rapid increases in back pressure could cause fan surge and inlet disturbances, the duct nozzle was designed to open just prior to ignition.

This shifts the fan operating point away from the surge limit avoiding unacceptable back pressure increases which result from the inability of the duct nozzle and rotor speed to compensate rapidly enough for the sudden temperature rise produced by lighting. Studies have indicated that increasing the nozzle area by 9 per cent produces adequate protection. The increased duct flow produced decreases the fuel-to-air ratio, but studies have shown that the flow is still within the ignition limits, and, in fact the lowered efficiency produced reduces the temperature rise and the consequent back pressure pulse.

b. Alternate Duct Heater Design

An alternate duct heater for the STF 219 engine has been designed. The system uses a ram induction burner for primary augmentation to provide stable and efficient combustion. Secondary augmentation is provided by a conventional afterburner. A cross-section of the alternate duct heater is shown in Figure 2-34. The use of a ram-induction primary burner and an afterburner for secondary augmentation produces a system with the potential of very high efficiency. The ram induction burner provides ease of ignition, long igniter life, wide lean and rich blow-out limits, and combustion efficiencies in excess of 95 per cent for fuel-to-air ratios up to 0.025. The secondary zone provides the capability of local high heat release rates with combustion efficiencies in excess of 90 per cent for zone 2 fuel-to-air ratios between 0.020 and 0.038. The afterburner section includes variable-area spraybars with mixing devices (vortex generators) on the duct walls. The high velocity of air around the spraybar increases fuel break-up, atomization, and air-fuel mixing. The estimated performance of the duct heater is shown below.

	Sea-Level Take-Off	Mach 1.2 at 45,000 Feet	Mach 3.0 at 65,000 Feet
$\frac{W_d\sqrt{T_{t3}}}{P_{t3}}$	229	228	223
Diffuser Loss (%)	2	2	2
Burner Cold Loss (%)	4.2	4.2	4.12
Hot Momentum Loss (%)	4.4	5.0	1.5
Total Hot Loss (%)	10.6	11.2	8.62
Over-All Fuel-to-Air Ratio	0.053	0.054	0.021
Over-All Efficiency (%)	93.8	93.0	97.8

6. TURBINE

a. Introduction

A three-stage turbine with a single high-pressure stage and two low-pressure stages was selected for the STF219 engine. The flow path is shown in Figure 2-35.

Extensive mission analysis studies have indicated the desirability of high operating temperatures for good performance. Consequently, a turbine inlet temperature of 2300°F has been selected for sea level take-off and acceleration, and 2200°F has been selected for cruise. These high operating gas temperatures require that the first- and second-stage nozzle vanes and the first-stage blades be air cooled to provide adequate life. To reduce centrifugal blade stresses to desirable levels, blade tip shrouds have been removed from the first two stages. Extended roots and platform dampers have been incorporated to minimize vibration. High-aspect-ratio blading has been incorporated to produce a lightweight rotor.

The turbine efficiency requirements were determined through installed engine performance and weight optimization studies. These studies indicated that the best performance would be obtained through a proper balance between turbine weight and efficiency rather than by designing strictly for high efficiency. The resulting system has a combined efficiency of 88.1 per cent, which compares favorably with the efficiency of lower temperature engines as shown below.

	Number of High Pressure Stages	Number of Low Pressure Stages	Turbine Efficiency (Per Cent)
JT3	1	2	88.1
JT4	1	2	88.4
STF219	1	2	88.1

b. Cycle Optimization

The engine was designed to provide the maximum installed performance. A particularly significant factor is the engine diameter, which has a very strong influence on the installed engine weight and drag. One method of reducing the engine diameter is to increase the fan pressure ratio. A higher fan pressure ratio produces a higher duct flow density thereby requiring a smaller duct area. But the higher fan pressure ratio also reduces the pressure ratio required to be produced by the high pressure

compressor and consequently the work required by the high pressure turbine. The final result is a decrease in the diameter of the high pressure turbine provided the same velocity ratio is maintained. However, in order to increase the fan pressure ratio, the work required from the low pressure turbine is increased. If the increase is acquired by the addition of a second stage to the low pressure turbine, a diameter reduction can be realized and the two-stage turbine weighs very little more than the larger-diameter single stage turbine. Consequently cycle optimization indicated the desirability of a two-stage low pressure turbine. The interrelationships of the factors involved are shown in Figure 2-36.

c. Velocity Ratio-Efficiency Relationships

The turbine velocity ratio is a fundamental turbine performance parameter relating the available turbine work to the wheel speed through the expression:

$$\text{Velocity Ratio} = \sqrt{\frac{U^2}{2g\ J\Delta h}}$$

Where: U = wheel speed (ft/sec)
Δh = energy extracted (BTU/lb)
g = gravitational acceleration constant (ft/sec/sec)
J = Joule's constant (ft-lb/BTU)

A high velocity ratio usually indicates a low level of energy extraction which implies too heavy a turbine. However, two factors must be considered before a judgement is made. The first of these involves the relationship between the velocity ratio and turbine compactness. If the turbine diameter controls the over-all engine pod diameter, then it is desirable to reduce the design velocity ratio. If the rotor speed is held constant, the turbine weight is increased a small amount, but the over-all engine weight is significantly reduced. The second factor concerns the effect of rotor speed on velocity ratio and weight. Turbine blade stresses and rotor weights are proportional to the square of the rotor speed, and the velocity ratio is proportional to the rotor speed for a given work level. Reducing the turbine rotor speed reduces the turbine weight, but also reduces the compressor capability requiring the addition of more compressor stages. Consequently, there is an optimum rotor speed for the best rotor weight. However, reducing the velocity ratio also reduces the efficiency since higher blade turning angles must be used and because the higher relative velocities increase the blade friction losses. It is evident, therefore, that the turbine must be designed to provide the best combination of efficiency, weight, and size.

d. High-Pressure Turbine

Since the high pressure compressor requires a relatively high rotational speed, sufficient speed is available for a single-stage turbine to deliver the 109 BTU/lb required. The velocity ratio at the mean diameter for this turbine is 0.482 which is lower than the values for some existing military engines and implies a high level of stage loading and a certain efficiency penalty.

Turbine Mean Velocity Ratio

	JT3D-1	JT8D-1	JT4	STF219
High Pressure Turbine	0.540	0.512	0.523	0.482
Low Pressure Turbine	0.555	0.607	0.570	0.500

However, the lower velocity ratio provides the lower centrifugal blade stresses required for satisfactory operation in the high temperature environment. The resulting efficiency of the high pressure turbine is 87.3 per cent, as shown in Figure 2-37.

An exit Mach number of 0.52 was selected. As shown below, this is substantially higher than the exit velocity of engines operating at lower temperatures.

Turbine Exit Mach Number

	JT3D-1	JT8D-1	JT4	STF219
High-Pressure Turbine	0.369	0.355	0.452	0.520
Low-Pressure Turbine	0.417	0.412	0.498	0.570

The higher velocity is required, however, since the annulus height must be reduced in order to reduce the centrifugal stresses. For the STF219 engine, the first stage blades are 4.3 inches high and are subjected to a centrifugal root stress of 29,800 psi.

The predicted performance of the high-pressure turbine is shown in Figures 2-38 and 2-39.

e. Low-Pressure Turbine

Analytical design studies established that a two-stage low-pressure turbine would be required to meet the performance and weight requirements. The design mean velocity ratio is 0.50 and the turbine exit Mach number

is 0.57. Although the stage loading and Mach numbers are relatively high for a low-pressure turbine, the studies indicated that the weight savings and reduced centrifugal stresses justified the high values.

The over-all low-pressure turbine performance and the inlet flow parameter as a function of the turbine pressure ratio are shown in Figures 2-40 and 2-41.

Additional studies were conducted to ensure that the optimum design had been obtained. Consideration was given to three designs employing a single-stage low-pressure turbine. The diameter, rotor speed, and work extraction were maintained at the values for the two-stage turbine. The result was a weight reduction of 250 lb in the turbine. However, the mean velocity ratio was reduced 40 per cent and incurred an efficiency penalty of 8 percentage points in the turbine. To maintain the required thrust level, the entire engine would need to be scaled up in size, and to maintain the range with the higher specific fuel consumption, additional fuel would be required. The net effect was an increase in the aircraft take-off weight of 870 lb per engine.

This trend suggested that a three-stage turbine might provide better results than the two-stage turbine. The analysis indicated that a slight gain in efficiency could be achieved, but that no net reduction in aircraft take-off weight would be obtained. The results of the single- and three-stage turbine analyses are summarized below.

	Single-Stage	Two-Stage	Three-Stage
Over-all Efficiency	84.1	88.1	89.0
Turbine Weight Change (lb)	-250		+250
Engine Scaling Weight Change (lb)	+280		-62
Fuel Load Weight Change (lb)	+840		-188
Net Take-Off Weight Change (lb)	+870		0

Also considered were the effects of increasing the turbine diameter and rotational speed since restricting these parameters results in a performance loss requiring additional fuel and an increased engine size. Increasing the diameter of the low-pressure turbine required a comparable increase in the high-pressure turbine and also enlargement of the duct heater. These changes negate the advantages achieved by raising the fan pressure ratio, and, as shown in Figure 2-42, even with an increase of 12 per cent, the aircraft take-off weight with a one-stage turbine is not reduced to that for a two-stage turbine. Increasing the rotor speed would lower the fan performance. In addition, excessive centrifugal stress levels would be developed, which would aggravate an

already difficult cooling problem. But even if solutions were found for these problems, Figure 2-43 indicates that increasing the speed of a single stage would not reduce the aircraft take-off weight to the level obtained using the two-stage low pressure turbine.

f. Blade Solidity

The stage loading requirements were established with the selection of the velocity ratio, diameter, and rotor speeds on the basis of over-all engine performance. It remains, however, to determine the individual airfoil loading. Excessive loading results in flow separation and poor performance. Light loading results in an unnecessarily heavy turbine with poor efficiency. In addition, the increased number of blades presents more complicated cooling requirements. At Pratt & Whitney Aircraft, the Zweifel load coefficient is used to judge the severity of airfoil loading. High values of the load coefficient imply low blade solidity and therefore low turbine weight. For the STF219 engine, the requirements dictate that an increase in the design load coefficient be higher than in previous commercial engines. Studies were conducted to verify that higher values were permissible. Maximum wall pressure rise ($\Delta P/Q$) was carefully controlled to prevent separation. The load coefficients for the STF219 engine and representative commercial engines are presented below.

Average Airfoil Loading Coefficients

	JT3D-1		JT8D-1		JT4		STF219	
	Vane	Blade	Vane	Blade	Vane	Blade	Vane	Blade
Stage 1	0.482	0.977	0.464	0.935	0.525	0.955	0.5	1.0
Stage 2	0.680	0.944	0.766	0.985	0.825	0.712	0.9	1.0
Stage 3	0.775	0.945	0.837	0.898	0.738	0.963	0.9	1.0
Stage 4	0.701	0.898	0.793	0.816				

D. MECHANICAL TURBOFAN STUDIES - STF219

1. FAN AND COMPRESSORS

a. General Description

The STF219 engine includes a two-stage fan and a five-stage axial flow high-pressure compressor (see Figure 2-25). Air flows into the fan from the inlet and is subsequently split into two streams, one which flows through the high-pressure compressor, and one which passes into the discharge ducting. The main portion of the air entering the high-

already difficult cooling problem. But even if solutions were found for these problems, Figure 2-43 indicates that increasing the speed of a single stage would not reduce the aircraft take-off weight to the level obtained using the two-stage low pressure turbine.

f. Blade Solidity

The stage loading requirements were established with the selection of the velocity ratio, diameter, and rotor speeds on the basis of over-all engine performance. It remains, however, to determine the individual airfoil loading. Excessive loading results in flow separation and poor performance. Light loading results in an unnecessarily heavy turbine with poor efficiency. In addition, the increased number of blades presents more complicated cooling requirements. At Pratt & Whitney Aircraft, the Zweifel load coefficient is used to judge the severity of airfoil loading. High values of the load coefficient imply low blade solidity and therefore low turbine weight. For the STF219 engine, the requirements dictate that an increase in the design load coefficient be higher than in previous commercial engines. Studies were conducted to verify that higher values were permissible. Maximum wall pressure rise ($\Delta P/Q$) was carefully controlled to prevent separation. The load coefficients for the STF219 engine and representative commercial engines are presented below.

Average Airfoil Loading Coefficients

	JT3D-1		JT8D-1		JT4		STF219	
	Vane	Blade	Vane	Blade	Vane	Blade	Vane	Blade
Stage 1	0.482	0.977	0.464	0.935	0.525	0.955	0.5	1.0
Stage 2	0.680	0.944	0.766	0.985	0.825	0.712	0.9	1.0
Stage 3	0.775	0.945	0.837	0.898	0.738	0.963	0.9	1.0
Stage 4	0.701	0.898	0.793	0.816				

D. MECHANICAL TURBOFAN STUDIES - STF219

1. FAN AND COMPRESSORS

a. General Description

The STF219 engine includes a two-stage fan and a five-stage axial flow high-pressure compressor (see Figure 2-25). Air flows into the fan from the inlet and is subsequently split into two streams, one which flows through the high-pressure compressor, and one which passes into the discharge ducting. The main portion of the air entering the high-

pressure compressor is discharged into a diffuser and subsequently into the burner. A portion of the air, however, is bled off in front of the fourth stage to cool the compressor disk bores and the turbine.

The fan and compressor sections are separated by an intermediate section. The intermediate section supports the fan and compressor sections, and provides space and support for the Number 1 and 2 thrust bearings, heatshields, an oil scavenge pump, the towershaft and associated drive assemblies for the accessory gearbox, power take-off, and fan rotor tachometer pads. The outer portion of the intermediate case provides support for the accessory gear boxes, the power take-off drive provisions, and inflight aerodynamic brake actuators.

b. Fan

The rotating portion of the fan consists of two stages, a fan hub supporting both fan stages overhung from a single thrust bearing, and a coupling bolt to fasten the fan stages to the low-speed turbine shaft. Blades, disks, and hubs are all made of titanium alloy (PWA-1202). The overhung two-stage fan design is based on a similar design used successfully in the Pratt & Whitney Aircraft STF200 engine.

The first- and second-stage disks are separated by a conical flanged spacer which is integral with the second-stage disk. The disks and hub are fastened together at the first-stage disk.

The first- and second-stage fan blades have dovetailed roots which are inserted into conforming slots machined into the disk rim to constrain the blades radially. A tab on the forward side of the blade root prevents the blade from being driven rearward by the impingement of any ingested foreign objects. An annular ring attached to each disk prevents the blades from moving forward. The inner wall of the gas flow path is formed by adjacent blade root platforms.

Blade vibration is controlled by part-span shrouds. The shrouds are protrusions integral with the blades which are linked together by the contacting bearing surfaces of adjacent shrouds when the blades are assembled on the rotor disks. Vibrations normal to the plane of contact are resisted by the mechanical stiffness of adjacent blades, and vibrations parallel to the contact surface are dampened by frictional drag. The frictional force potential is provided by the natural untwisting tendency of the twisted airfoil under centrifugal loading. The contact areas are flame plated with tungsten carbide, and sufficient bearing area is provided to keep friction wear to acceptable levels. The airfoils are offset forward of the center of the dovetail attachment so that a centrifugal moment is induced to counteract the moment caused by the gas loading and to ensure optimum uniform attachment loading.

The first- and second-stage disk and blade assemblies are statically balanced to specified limits by adding balance weights to flanges on the disks. The disks are then dynamically balanced together to minimize rotor vibration. Suitable fits between mating parts are obtained to resist separation during all critical steady-state and transient operating conditions, thereby maintaining alignment and concentricity to maintain the dynamic balance.

Radial loads from the rotor are transmitted to the Number 1 bearing through the fan hub, which is supported by the thrust bearing and has mating splines to transmit torque loads to the low-speed turbine drive shaft. The splines are forward of the thrust bearing to ensure continued spline engagement and prevent serious turbine overspeeding should a major failure of the bearing occur.

A positive pressure differential is maintained across the front bearing compartment seal to prevent the possibility of oil leakage from the compartment. Pressurized air for this purpose is bled from behind the second-stage rotor, channeled up the side of the intermediate case, and vented through holes in the seal ring to a compartment outside of the carbon seal. The pressure in the compartment is maintained by a pair of knife-edge seals between the fan rotor hub and the thrust bearing support structure. An additional seal is located on the rear of the second-stage disk to reduce the thrust loading on the Number 1 bearing and consequently to increase the bearing life.

One interstage seal is used between the first and second fan stages. The seal is bolted to a flange on the integral conical spacer of the second-stage disk and rotates in close proximity to the stator seal ring. The clearance between the seal and the seal ring is as small as possible while still providing for the maximum tolerance buildup, the maximum radial differential thermal expansion encountered during steady-state operation, and elastic radial deflections during high-performance operations. These provisions will permit light, non-destructive rubbing during transient thermal or overspeed operation.

Blade tip clearances were similarly established with provision being made for the maximum tolerance buildup, the maximum differential radial and axial thermal growths anticipated during transient operation, radial elastic disk and blade growths during normal high-temperature operation, and for the anticipated effects of surge and for foreign object ingestion. To permit small clearances to be used, an abradable material is used inside the fan case. This will prevent severe blade-to-case rubbing resulting from blade deflections caused by foreign object ingestion

and will permit light, non-destructive rubbing during operation at the maximum adverse conditions.

Axial gaps between the forward side of the rotating parts and the adjacent stationary parts are established by providing for the maximum total tolerance accumulation, the maximum axial differential thermal growths during transient operations, the maximum net end play accumulation, the computed net intermediate case deflection, the maximum anticipated forward blade tip deflections resulting from foreign object ingestion, and deflection encountered during surges.

The axial gaps and seal land lengths between the rear side of rotating and adjacent stationary parts provide for the maximum total tolerance accumulation, the maximum axial differential thermal growths during transient operation, the maximum net end play accumulation, the estimated fan rotor hub net rearward deflection resulting from centrifugal loading, the maximum forward stator vane deflection resulting from gas loads during steady-state operation, the maximum rearward blade tip deflection resulting from foreign object ingestion, the maximum deflection during surges, and the maximum forward seal support diaphragm deflections resulting from steady-state pressure loads.

The first stage stator is made from forged titanium (PWA 1202). Integral platforms are forged at the inner and outer ends of the vanes to form the flowpath at the inside and to facilitate vane attachment at the outer end. The vane is attached to the front fan case by a foot at the rear of the platform and is held in place by an annular ring integral with the fan case at the front of the platform. The inner rear feet are riveted to an annular ring, and the inner forward feet are riveted to an annular diaphragm which is integral with the seal ring.

The fan cases, mount ring, and support cases are also made of titanium (PWA-1202) and are cantilevered from the front flange of the intermediate case. Within the fan cases are nickel-honeycomb liners coated with the abradable material discussed previously. The front part of the cases are thickened for blade containment purposes.

c. Intermediate Section

The intermediate section is, for the most part, a single welded AMS 5616 stainless-steel structure incorporating sections of the fan duct outer wall, the compressor flow path inner wall, and the rear portion of the splitter. Inside the compressor flow path inner wall is a box structure

which supports the thrust bearings. Attached to this welded structure are the second-stage stator vanes and the leading edge of the splitter.

Between the outer fan duct wall and the inner compressor wall are eight hollow machined struts. The compressor outer wall and fan duct inner wall are formed by welding sheet stock to contoured ribs on the sides of these struts. In the fan duct, the struts form the leading edges of the fan duct fairings. Four of the eight struts are used to transfer fluid to the inner portion of the engine. One strut houses two air lines, one to supply air for pressurizing the labyrinth seal in front of the Number 1 thrust bearing, and the other to vent the compartment in front of the inner box structure for thrust balancing. The three other struts supply oil to and remove scavenge oil and breather air from the bearing compartment.

In front of the strut system is the second-stage stator, which is variable for aerodynamic braking (discussed in the following section).

The box structure inside the compressor flow path inner wall provides a flange on the front inner section for mounting the Number 1 bearing support, an integral support for the Number 2 bearing on the rear section, and housings for the drive system of the three tower shafts.

Both the Number 1 and Number 2 bearings are single-thrust bearings sized for the design thrust load and a reasonable bearing life. The reliability obtained using a single Number 2 bearing has been determined by analysis and running times of engines using single Number 2 bearings to be no less than that obtained using multiple bearings. Both bearings are of the angular contact, ball bearing type, having split inner races and inner riding cages. The balls and races are fabricated of AMS 6490 material and the cages of AMS 6415 material.

The bearings are lubricated and cooled by oil injected under the races. Number 1 bearing oil is picked up from a jet by an oil scoop just behind the bearing. Number 2 bearing oil is collected in an angular cavity which is located forward of the accessory gear and which is held in place by the inner race retaining nut. In both cases, the oil then flows through a series of holes in the bearing liner to an annulus to cool the inner race, and then flows radially out to the bearing compartment through a series of holes in the seal rub plate. The oil also flows outward through a series of holes in the bearing liner to an annulus at the split inner race of the Number 2 bearing. The inner race has radial slots to centrifuge the oil into the bearing for lubrication.

The Number 1 and 2 bearing compartment contains three carbon face seals, two of which are bolted to the intermediate case. The third is fitted to the fan rotor hub. The carbon face seal forward of the Number 1 bearing has an oil-cooled rub ring, utilizing the oil from the Number 1 bearing cooling passages. A three-lip labrynth seal is employed for controlling air leakage in case of carbon seal malfunctions. Fan discharge air, being at a higher pressure than that maintained within the breather compartment, will always flow into the compartment and prevent contamination of the cabin pressurizing air from oil leakage past the seal face. A carbon face seal is used between the high- and low-speed rotor shafts within the bearing compartment. A three-lip labyrinth seal protects this area. The oil-cooled seal rub plate is supplied with oil from an integral annular cavity which is supplied by a jet. The carbon face seal behind the Number 2 bearing has a rub ring, using the oil from the bearing cooling passages. A three-lip labyrinth seal protects this area.

Oil supplied to the bearing compartment is routed through a perforated strainer and subsequently to the oil jets which meter the oil to the bearings and seals. The scavenge oil is returned to the gearbox by gravity when the gearbox is located on the bottom of the engine, and by a scavenge pump driven through a gear train by the high-pressure compressor rotor hub when the gearbox is on the side of the engine.

Two towershafts are required to transmit power radially from the high-pressure compressor shaft (compressor front hub) to the power take-off and accessory drive pads. A third tower shaft is required to transmit rotational speed from the fan rotor hub to a tachometer drive pad (AND 20005 XVB). The established power requirement for the aircraft accessory drive power take-off pad is 600 H. P.; for the side mounted gear box, 310 H. P.; and for the bottom mounted gear box, 150 H. P. Power for these towershafts is supplied by a spiral level gear integral with the Number 2 bearing sleeve fitted to the compressor hub. The tachometer towershaft is driven from the fan rotor hub through spur and bevel gears.

The spiral bevel pinions for the drives are supported by a ball and roller bearing assembly bolted into the inner box structure. The shaft connects to a stub shaft by a double spline coupling at the lower end. Loose fits at the coupling and at the shaft supports provide for possible misalignments.

Convoluted tubes are brazed to the outer portion of the outer towershaft bearing supports, and, at the other end, to the pedestals at the outer portion of the case. These tubes protect the struts and inner compressor wall from oil and, in conjunction with flanged bosses on the outside of the intermediate case, form sealed passageways to the accessory gearbox and the power take-off.

The intermediate case is attached to the rearward components at four locations. The outer fan duct wall extends to the rear and provides a flange for mounting the outer fan diffuser duct wall. The fan duct inner wall extends rearward and provides a sliding radial support for the inner diffuser duct wall. The outer compressor flow path wall extends rearward and provides a flange to support the gas generator and the outer shrouds of the compressor inlet guide vanes. On the inner compressor wall is a flange to which the inner shrouds of the inlet guide vanes are riveted.

d. Aerodynamic Brake

The basic concept and control of the aerodynamic brake remains essentially the same as for the JT11F-11, -12 engine.

The second-stage and fan exit vanes may be moved through an angle of 35 degrees from their normal positions. Changing the vane angles by 35 degrees will reduce the running cruise airflow by 50 per cent and will maintain a rotor speed between 1500 to 2000 rpm for emergency engine shutdown.

To withstand the high stresses produced by aerodynamic braking, the fan exit vanes are made from AMS 5667 nickel alloy. The second-stage vanes are subjected to lower stresses, and, therefore, PWA-1202 titanium alloy is used for these vanes.

The second-stage vanes are pivoted on spherical bearings at the inner shroud and universal joints at the splitter and at the outer case. The universal joint connects the second-stage vanes to the fan exit vanes and permits simultaneous rotation of the two sets of vanes.

The vanes are rotated by a unison ring connected by levers to the shaft extension on each outer vane. The unison ring is guided and supported by bumpers that ride on the outer case. Three pneumatic actuators spaced 120° apart operating through a bell crank move the unison ring tangentially and thus cause the vanes to rotate.

Power for the actuators will be provided by high-pressure gas bottles, preferably the same bottles used by the airframe for emergency control system power.

Due to the high pressure of the gas bottle system, the actuator diameters are approximately one-fourth that required for an engine-bleed-air-powered system. The reduced weight of the actuators over those provided for the JT11F-11, -12 engine should be adequate to overcome any weight addition resulting from the increased gas storage requirements in the aircraft emergency system. The smaller actuators are also more practical from the standpoint of accessory arrangement. These advantages, in addition to the desirability of using an actuating system which is independent of the engine subsystems, makes the use of gas bottles seem more attractive than the use of engine bleed air for actuator power.

The actuators are fitted with spring-operated plunger locks to hold the vanes in their normal operating position. When it is necessary to rotate the vanes, gas pressure on the locking plunger raises the plunger and permits gas to enter the piston chamber, thereby actuating the vanes.

e. High-Pressure Compressor

The stationary portion of the compressor consists of a series of short cases made of Inconel X nickel alloy (AMS 5667) and bolted together with vanes extending inward to channel shaped stiffening rings and the attached seal rings.

Each of the cases has two integral flanges at the ends for attachment to the adjacent cases. In addition, an intermediate circumferential groove is machined in each case to secure the rear feet of the associated vanes, and to the rear, a groove is provided for a flame-sprayed abradable coating to permit a reduced blade clearance to be used.

With the exceptions of the inlet and exit guide vanes, each vane is forged of Inconel X (AMS 5667) or Waspaloy (PWA 687) and includes integral channel section platforms at the tip. Each vane has a machined lip at the rear of the tip platform to engage the groove in the corresponding case. The flange is sandwiched between the flanges of adjacent cases. At the root, the radial legs on the vane platform are riveted to the channel-shaped stiffening ring. Because of the large number of vanes used, the vanes are electron-beam welded together in pairs before being assembled to the cases. The dual-vane design permits a wider bolt and rivet spacing to be used and results in stronger attachments.

The inlet guide vanes are also forged but are made of titanium alloy (PWA 1202) and are flanged at the rear rather than at the front. At the front tip, the inlet vanes are riveted directly to the intermediate

case. At the root, the inlet vanes have a channel-shaped platform, the front leg of which attaches to the inner intermediate case. Attachment at this point, however, must provide for thermal expansion, and, therefore, radial slots are machined into the front flange of the vane inner platform, and shouldered washers are installed which restrain tangential and axial movement but permit radial movement.

The exit guide vanes are contour rolled strip stock and are brazed to the inner and outer shrouds, all of which are Hastelloy X nickel alloy (AMS 5536 and AMS 5754). The front flange of the outer shroud is sandwiched between the flanges of the diffuser case and the rear compressor case.

Seal rings made of Hastelloy X (AMS 5754) are attached to the stiffening ring at the roots of the vanes. Provision is made to accommodate the differential thermal expansion between the seal and stiffening rings using the same technique used for the inlet guide vanes.

The rotating portion of the compressor consists of five rows of blades. Stages four through seven are joined and positioned axially by three cylindrical inner spacers. The third stage is overhung forward and positioned axially by a support cone secured to the front face of the fourth disk at the inner spacer diameter.

The blades have dovetail roots which are inserted into slots machined into the disk rims. Mechanical damping devices and extended blade roots are employed on stages three and seven to reduce the effects of blade vibrations resulting from the pressure impulse to which these stages are exposed. In these stages, the blades are restrained from axial movement by the side damper support plates which are riveted to the disks through holes in the lugs between the dovetail slots in the disk, as shown in Figure 2-44. The blades in stages four through six are restrained by tabs on the front and shear pin locks on the rear of the blades.

A series of outer spacers are positioned by piloting flanges on the disks to add stiffness to the disk rims and reduce blade tip deflections. One end of each of the through spacers is riveted to an adjoining pilot flange. Radial knife-edge seals are included on these spacers to provide the sealing required between stages. Two cones positioned between the third and fourth and between the sixth and seventh stages provide additional stiffness and support for the rotor.

The compressor blades are made of Incoloy 901 (PWA 1003) or Waspaloy (PWA 1007) nickel alloy, and the hubs, disks, and spacers are made of Incoloy 901 (PWA 1003), Waspaloy (PWA 1007), or Astroloy (PWA 1013)

nickel alloy, as required to satisfy the particular operating conditions in each stage of the two engine models.

Each disk and blade assembly and the front hub are statically balanced. The rotor shaft is dynamically balanced and then the rotor assembly is dynamically balanced as a unit by adding weights to flanges provided on the third-stage disk and the seventh-stage seal disk. Throughout the rotor structure, generous fillet radii, careful blending of intersecting surfaces, and the use of rounded or chamfered corners are provided to reduce stress levels in locations where stress concentrations occur.

The thrust loading on the rotor is transmitted to the Number 2 bearing from the outer spacers through the cone between the third- and fourth-stage disks and through the conical front hub. Radial loads are transmitted to the Number 2 bearing through the front hub and to the Number 3 bearing through a conical shaft secured by the tiebolts to the rear side of the seventh-stage disk. This shaft extends rearward to engage a spline on the high-speed turbine shaft.

A chamber formed behind the seventh-stage disk by two seals is fed free-stream compressor discharge air from two of the diffuser case struts. Air in this chamber controls the temperature on the seventh-stage rear rim face by preventing higher temperature boundary layer air from circulating in this area.

The cold static radial clearances of all knife-edge seals in the high-pressure compressor were made as small as possible while providing for the maximum tolerance buildup, the maximum radial differential thermal growths during high-performance steady-state operation, and the maximum elastic radial deflections during high-performance operation. Light, non-destructive rubbing will occur during transient thermal or overspeed operation during initial operation.

Blade tip radial clearances were established to provide for the maximum tolerance buildup, the maximum differential radial and axial thermal growth during transient operation, and radial elastic blade and disk growths at normal high-temperature operating speeds.

Axial gaps on the forward side of all rotating parts and adjacent stationary parts provide for the maximum total tolerance accumulation, the maximum axial differential thermal growths during transient operation, the estimated net forward deflection of the fan bell resulting from centrifugal action, the maximum forward blade tip deflections resulting from the steady-state gas loads, and the maximum forward blade tip deflection resulting from surge gas loads.

The axial gaps and the seal land lengths between the rear of the rotating parts and the adjacent stationary parts provide for the maximum tolerance accumulation, the maximum axial differential thermal growths during transient operation, the maximum net thrust bearing end play, the maximum disk rim deflection resulting from surge gas loads, the maximum forward stator vane deflections resulting from steady-state gas loads, and the maximum forward seal support diaphragm deflections resulting from steady-state static pressure loads.

f. Stress-Analysis Summary

The fan components were sized such that the resulting stresses would be equal or less than those in currently used components.

Since a support across the hot section of the duct to the rear of the inner engine is not practical in a duct heating engine, the inner engine is supported only at the front by the intermediate case struts. The cross-sectional moment of inertia of these struts was sized so that the stresses would not exceed 80 per cent of the 2 per cent yield strength of the material. Anticipated loading included maneuver loads, pressure loads, vibratory loads, loads induced by blade loss, and loads imposed by the rotor thrust bearings. The inner box structure was sized to restrict the deflection between the gas generator and the thrust bearings to within acceptable limits. The thickness of the bearing supports was determined on the basis of the radial spring rate, and in all cases the stresses are well below the material yield strength. The flange stresses were calculated by using a modified beam analogy method based on the loading which occurs during the maximum maneuvering condition during cruise at a high Mach number. This method was developed by Pratt & Whitney Aircraft and has been verified by extensive testing. The method includes the stresses induced by differential thermal expansion.

The greatest stresses in the high pressure compressor occur during cruise at Mach 3.0 at 65,000 feet. This section of the analysis is based on the maximum stresses resulting from deterioration, accumulated tolerances, and mismatch at the most adverse flight conditions. Typical dovetail attachment stresses are shown on the following page.

	Blade Root	Disk Lug
Material	PWA 1007	PWA 1007
Stress Rupture Design		
Speed (rpm)	8570	
Temperature (°F)	1288	
Operating Conditions	Mn 3.0 Cruise, 65,000 ft	
Neck Tensile Stress (psi)	13,900	15,800
6000-Hour Stress Rupture Strength (psi)	60,000	60,000
Neck Tensile Stress/6000 - Hour Stress Rupture Strength	0.232	0.264
Yield Design		
Speed (rpm)	8930	
Temperature (°F)	1288	
Operating Condition	Mn 3.0 Cruise	
Neck Tensile Stress (psi)	15,100	17,100
0.2% Yield Strength (psi)	106,000	106,000
Neck Tensile Stress/0.2% Yield Strength	0.070	0.062
Tooth Bending Stress (psi)	19,000	14,000
Tooth Bending Stress/0.2% Yield Strength	0.186	0.132
Tooth Bearing Stress (psi)	66,000	66,000
Tooth Bearing Stress/0.2% Yield Strength	0.622	0.622
Tooth Shear Stress (psi)	13,300	10,700
0.55 x 0.2% Yield Strength (psi)	58,300	58,300
Tooth Shear Stress/0.55 x 0.2% Yield Strength	0.228	0.184
Combined Stress (psi)	34,800	31,100
Combined Stress/0.2% Yield Strength	0.328	0.294
Vibratory Stress Design		
Combined Z-Ratio	4.80	-
SCF	2.22	-

On stages three and seven, the thick support struts produce excessive blade excitation, and an extended root design has been used to provide mechanical blade damping. The extended root permits motion of the blade platform in each of the fundamental vibration modes. A centrifugally loaded toggle pivots about a rivet attaching it to a side plate and bears against the under side of the blade platform. The friction developed between the toggle and the platform of the vibrating blade provides the required damping. The rubbing surfaces are flame plated to provide long life, but small amounts of wear will not alter the effectiveness of

the damper since changes in the contact load will be small. The damping system was designed to provide the optimum damping capacity at amplitudes where the vibratory stresses exceed 10,000 psi. Although the increased mass of the extended root increases the pull on the blade attachment, the damper effectively equalizes the bending moment distribution, and, therefore, no additional problems are produced.

The rotor disks were designed such that adequate burst and yield strength margines were provided and such that the creep growth, web, and bolt circle stresses were within the design limits. Typical stress data appear on the following page.

Calculations of stresses in the rotor tiebolts considered such factors as flexibility, thermal gradients, the poisson shrinkage of disks and spacers resulting from tangential and radial stresses, the thrust load on the rotor, and the centrifugal bending stress on the tiebolts. The maximum combined stresses produced by bolt tension and centrifugal loading may exceed the 0.2 per cent yield strength during transient acceleration, but the yield strength is not exceeded during steady-state operation.

The outer spacers are loaded centrifugally and by compressive forces produced by the axial gas loads. However, at the outer location, the cylinder radius is greater than the self-supporting radius at the high environmental temperatures and rotor speeds to which the rotor is exposed. Consequently, the spacer must be thick enough to restrain the bending at the center within acceptable limits. The bending stresses were set at 67 per cent of the stress which will produce rupture no sooner than 6000 hours of operation at maximum Mach 3.0 cruise temperature. The maximum allowable hoop stress was set at that which produces 0.1 per cent creep in 6000 hours of operation at Mach 3.0 cruise temperatures. Thicknesses determined by these criteria are adequate to resist buckling resulting from compressive axial loading.

The compressor vanes are deflected axially by gas loading and by the differential static pressure across the seals. The resultant load produces a bending moment on the vane.

The deflections and stresses were calculated by assuming that the vanes are variable-inertia twisted beams which deflect as guided cantilever beams. The inlet and exit guide vanes are supported against torque at both ends and were therefore assumed to deflect as fixed beams.

Based on the results of the analysis and on extensive experience in the analysis, testing, and development of gas turbine stators, suitable vane chord lengths and thickness ratio limits were selected to ensure that the stress and creep of the vanes will be kept within acceptable values.

the damper since changes in the contact load will be small. The damping system was designed to provide the optimum damping capacity at amplitudes where the vibratory stresses exceed 10,000 psi. Although the increased mass of the extended root increases the pull on the blade attachment, the damper effectively equalizes the bending moment distribution, and, therefore, no additional problems are produced.

The rotor disks were designed such that adequate burst and yield strength margines were provided and such that the creep growth, web, and bolt circle stresses were within the design limits. Typical stress data appear on the following page.

Calculations of stresses in the rotor tiebolts considered such factors as flexibility, thermal gradients, the poisson shrinkage of disks and spacers resulting from tangential and radial stresses, the thrust load on the rotor, and the centrifugal bending stress on the tiebolts. The maximum combined stresses produced by bolt tension and centrifugal loading may exceed the 0.2 per cent yield strength during transient acceleration, but the yield strength is not exceeded during steady-state operation.

The outer spacers are loaded centrifugally and by compressive forces produced by the axial gas loads. However, at the outer location, the cylinder radius is greater than the self-supporting radius at the high environmental temperatures and rotor speeds to which the rotor is exposed. Consequently, the spacer must be thick enough to restrain the bending at the center within acceptable limits. The bending stresses were set at 67 per cent of the stress which will produce rupture no sooner than 6000 hours of operation at maximum Mach 3.0 cruise temperature. The maximum allowable hoop stress was set at that which produces 0.1 per cent creep in 6000 hours of operation at Mach 3.0 cruise temperatures. Thicknesses determined by these criteria are adequate to resist buckling resulting from compressive axial loading.

The compressor vanes are deflected axially by gas loading and by the differential static pressure across the seals. The resultant load produces a bending moment on the vane.

The deflections and stresses were calculated by assuming that the vanes are variable-inertia twisted beams which deflect as guided cantilever beams. The inlet and exit guide vanes are supported against torque at both ends and were therefore assumed to deflect as fixed beams.

Based on the results of the analysis and on extensive experience in the analysis, testing, and development of gas turbine stators, suitable vane chord lengths and thickness ratio limits were selected to ensure that the stress and creep of the vanes will be kept within acceptable values.

Material	PWA 1007
Burst and Yield Design	
Speed (rpm)	8930
Average Temperature (°F)	1207
Average Tangential Stress (psi)	71,000
Yield Margin	1.17
Minimum Allowable Yield Margin	1.05
Burst Margin	1.40
Minimum Allowable Burst Margin	1.20
Maximum Web Radial Stress (psi)	68,000
Percent of Allowable Stress	98
Maximum Bolt Circle Radial Stress (psi)	61,000
Percent of Allowable Stress	97.5
Operating Condition	Mach 3.0 Cruise
Creep Design	
Speed (rpm)	8570
Average Temperature (°F)	1207
Average Tangential Stress (psi)	63,500
1.1 x 6000-Hour 0.1% Creep Strength (psi)	64,000
Percent of Allowable Stress	99
Operating Condition	Mach 3.0 Cruise
Low Cycle Fatigue Design	
Speed	8250
Bore Temperature (°F)	156
Rim Temperature (°F)	727
Maximum Stress (psi)	102,000
Minimum Stress (psi)	-2,500
Minimum Bore Low Cycle Fatigue Life (cycles)	40,000
Minimum Bolt Circle Low Cycle Fatigue Life (cycles)	30,000
Minimum Allowable Low Cycle Fatigue Life (cycles)	8,000
Operating Condition	Sea-Level Take-Off

2. DIFFUSER

a. General Description

The diffuser section (see Figure 2-45) of the STF219 engine consists of

a case, an exit guide vane and shroud assembly, annular burner supports, gas generator fuel nozzle supports, spark igniters, and certain fluid transfer tubes.

The primary function of the diffuser is to provide a modest reduction in the velocity of the compressor discharge air to a level suitable for the ram induction combustor. In addition, the diffuser acts as a structural component indirectly supporting the Number 3 bearing and the associated bearing compartment seals, and more directly supporting the burner, the spark igniters, and the gas generator fuel nozzle supports.

b. Physical Structure

The diffuser case assembly is the major component of the diffuser. This assembly is basically a weldment of two annular sections joined by struts. Inconel 718 nickel alloy (PWA 1009, PWA 1033) is used for the Mach 2.7 engine. Waspaloy (PWA 687, PWA 1030) is required for the higher temperatures and stresses of the Mach 3.0 engine.

The outer wall is machined from a forged ring. It is attached to the high-pressure compressor exit section at the front and to the outer combustor case at the rear by bolting at mating flanges. The case flares outward from front to rear at an angle of approximately 24 degrees. An annular box section, which incorporates two bleed air manifolds (one for compressor discharge total pressure air and one for compressor discharge static pressure air) separated by a structural bulkhead, is welded to the outside of the outer wall. The source of total pressure air for cabin pressurization and turbine blade cooling is from the center of the compressor discharge annular passage. Compressor discharge static pressure air is bled from openings in the diffuser passage outer wall and is used for applications relatively insensitive to air impurities, such as the aircraft inlet anti-icing air supply and to drive the duct heater fuel pump.

The inner case is joined to the outer case by 12 hollow sheet-metal struts. The ends of these struts are butt welded to airfoil-contoured platforms which are integral parts of the inner and outer cases. These struts carry thrust, high-speed rotor unbalance loads, and vibratory loads. The limiting strut stresses are those imposed by a static load equal to the centrifugal force of 10 per cent of the first-stage turbine blades. Since 10 per cent blade loss is an extreme failure, permanent deformation of the struts under these conditions is permitted. Integral airfoil-contoured platforms have been found to provide a good transition section with low stress concentration for transmitting the loads between

the struts and the cases. Conservative design stress levels are used to provide a suitable fatigue life.

A two-piece, forged, double scoop is welded into the leading edge of each strut to collect compressor discharge air from the center of the gas path. This air passes inward through the struts and is directed by ten transfer tubes to the first-stage of the turbine for cooling and thrust balancing and by two transfer tubes to a seal chamber at the outer rear of the seventh-stage compressor disk to pressurize it with air appreciably cooler than compressor inner boundary layer air. This cooler leakage air from the multi-lipped inner seal into the compartment behind the rear compressor disk produces an appreciably lower maximum disk operating temperature relative to that which would result from a system permitting boundary layer air leakage into the compartment. In addition, air scooped from the center of the compressor discharge annulus flows outward through the struts into the compressor discharge total pressure air manifold.

The struts also serve as passages for pressure and scavenge oil lines to the Number 3 bearing compartment, for pressurizing and vent lines to the front and rear bearing compartment labyrinth seals, and for venting the diffuser case inner compartment to the fan inlet for balancing the thrust on the high-speed rotor. All of the oil lines for the Number 3 bearing located inside the diffuser case struts are heat shielded. The inner diffuser wall is a single, conical section which flares rearward and outward at an angle of approximately 31.5 degrees and terminates with front and rear flanges. The front flange supports the compressor exit seals and the exit guide vane and shroud assembly. The rear flange supports the inner burner case. An intermediate flange is located just forward of the trailing edge of the struts to add structural stiffness. The compressor exit guide vane and shroud assembly is located at the front of the diffuser. Torque loads in the inner shroud are transmitted through twelve torque pins into the diffuser case. The outer shroud front flange is attached to the outer diffuser case front flange with flush countersunk screws for retention during assembly operations.

c. Stress Analysis

Stress analysis for the inner and outer case flanges was based on the theory of plates and shells with the minimum permissible flange thickness being determined by the thickness required to ensure gas-tight sealing. The inner wall is pressure buckling limited. The outer walls have greater internal pressures than external pressures and consequently

are hoop-stress limited. The outer wall thicknesses used were selected to provide a maximum stress of 80 per cent of the 0.2 per cent yield strength. The analysis used for determining the dimensions of the mounting flanges and intermediate stiffening flanges was based on the theories of three-concentric-ring compatibility discussed in NACA TN1310.

3. COMBUSTION CHAMBER

a. General Description

The combustion chamber section includes the compressor discharge air diffuser, the inner and outer combustion cases, the single annular combustion chamber, rear liner sections to the turbine nozzle, a fuel supply system of 24 fuel nozzles, and an ignition source consisting of 2 spark igniters.

In the high-velocity ram induction combustion chamber, only moderate diffusion of the compressor discharge flow occurs. The high momentum of the compressed air is utilized directly to inject primary and secondary air into the combustion chamber and to create intimate mixing of the fuel vapors, burned gases, and dilution air. The air is directed into the burner by means of ram air scoops with internal turning vanes to minimize pressure losses.

b. Physical Features

To control airflow and diffusion, the forward end of the combustor penetrates into the diffuser case to a point just behind the last compressor discharge stator. At this location, the air is separated into an inner, outer, and initial primary flow. The inner and outer flows are directed by the diffuser case and combustor walls to the main air injection areas. The initial primary air is diffused inside the forward cavity and injected into the combustion area through cast vane swirlers around each of the fuel nozzles. This air is used to initiate and stabilize combustion. The balance of the primary combustion air is injected through a series of cast ram air scoops in the inner and outer walls. There are three scoops, axially staggered, in each wall for each fuel nozzle. Immediately behind the last primary injection scoop, secondary dilution air is introduced through another series of scoops. These are shaped to ensure uniform mixing and dilution. There are two secondary scoops per nozzle in the inner and outer walls.

Fuel is injected through 24 individually removable, dual-orifice fuel nozzles to give a turn down ratio of 60:1. The pressurizing valves for

the dual-orifice system are incorporated in the nozzle housing as close as possible to the orifices to avoid the coking effects which occur in the interconnecting passages when the valves are located farther from the nozzle. The nozzle housings slide radially inward to engage a positioning groove in the cast swirler assemblies which are free to move within limits to accommodate mechanical tolerances and thermal displacement. Rotation of the swirlers is prevented by pins. The fuel nozzles are retained by flanges bolted to the outer wall of the diffuser case. The nozzle support structure has a sheet-metal heat shield attached in the region where it passes through the compressor discharge air annulus.

The front section of the combustor around the fuel nozzle discharge area is of welded double wall construction to ensure the cooling necessary for durability. The outer structural wall is perforated sheet metal. The inner wall is porous metal. The porous wall is attached to and supported by the perforated structural wall.

Ignition is provided by two electrical igniters which penetrate into the front section of the combustor. These igniters pass through the fan discharge duct and are individually removable without removing the duct. At the point of entering the combustor, the igniters pass through a floating eyelet which seals against air leakage and which accommodates mechanical tolerances and thermal displacements.

The front combustion section is retained in place by twelve radial pins. These pins are inserted from outside the diffuser case and pass within the trailing edge of the diffuser struts and into inserts in the combustor dome section. The combustion is thus positioned axially and concentrically. Radial clearance gaps at each pin allow for differential expansion between the case and the front combustor.

The inner and outer walls of the primary combustion section are formed from sheet metal to provide lightweight easily fabricated components. The turning vane cascade in each air scoop is a precision cast insert welded in place. Cooling of the sheet metal walls is achieved by a boundary layer film produced by a series of louvers.

The secondary injection ram scoops are formed sheet metal weldments. They serve to tie the inner combustion shell to the outer structural shell and give the burner mechanical stiffness. The outer shell is attached to the forward end of the combustion shell and to the extended dome.

The rear section of the combustor forms an annular passage for mixing and leads into the turbine section. It is composed of independent inner and outer shells, each of which is fabricated with a double-wall construction. In each shell, the outer wall is perforated sheet metal and the inner wall is convoluted porous metal for transpiration cooling. The rear sections are positioned axially at the rear by a bolting arrangement. They are free to float axially at the forward end and are supported radially by the forward combustion section. A machined, slotted ring provides the contacting support and also serves to establish a controlled cooling air film. The contacting surfaces between the rear of the combustion section and the forward air chute sections are hardfaced with chromium carbide to reduce wear.

Higher burner shroud velocities in conjunction with wall louver cooling have been shown to give satisfactory combustion wall temperatures in the limited rig testing to date. The secondary ram air scoops penetrating into the combustion zone have been shown by testing to have adequate cooling. Cooling is accomplished by the flow of air over the forward edges of the scoops. The rear inner and outer transition shells are efficiently cooled by transpiration. Combustor wall cooling flow requirements have been calculated to be 18 per cent of the total flow.

In the rear inner and outer liner sections, the perforated walls are sized to provide full structural support and to meter the cooling air. The porous walls are attached at either end and at convolution nodal points to the support shell. This construction was selected to ensure maximum durability and to minimize cooling air flows at the turbine inlet nozzle vanes.

The basic sheet metal of the combustor is Hastelloy X (AMS 5536) nickel alloy. Ram air scoops and front end section nozzle rings are cast Hastelloy X (AMS 5390). The air guide swirlers are cast Stellite 31 (AMS 5382) cobalt alloy. Combustor retaining pins are Waspaloy (PWA 1004) nickel alloy and the retaining inserts in the burner are L-605 (AMS 5759) cobalt alloy. These materials were selected because of their excellent resistance to high temperature oxidation, good wear properties, and extensive successful use in similar applications.

The bolting arrangement of the rear inner and outer transition shells allow them to be disengaged and to be moved forward to permit hot section inspection and replacement of the first-stage turbine nozzle vanes.

The outer combustion chamber case is in two sections. It is pressure limited and was designed to withstand the pressure differential between

the high pressure compressor discharge air and the lower fan duct pressure. At Mach 0.7 at sea level, this pressure will be 158.5 psi. The flange was designed to creep no more than 0.5 per cent in 6000 hours at Mach 3.0 at 65,000 feet. The front section of the outer case attaches to the rear of the diffuser case. The rear flange of the rear section joins with the turbine case and the end of the outer rear liner. Both sections of the outer case are flow-turned from a nickel-base alloy, Inconel 718 (PWA 1009) for the Mach 2.7 engine and Waspaloy (PWA 687) for the Mach 3.0 engine, with an integral front flange and a welded rear flange. Flow-turning eliminates longitudinal welds and permits higher allowable hoop stresses. Six integral machined bosses supply compressor discharge air to the duct heater. The fuel drain is located at the bottom rear of the case and prevents fuel from accumulating in the event of a false start. Design criteria for wall and flange thicknesses used were based on development experience on other engines.

The inner combustion chamber case is also in two sections and is made of Waspaloy. The front inner case forms the connecting structure between the diffuser case, the Number 3 bearing support, and the rear inner case. The rear inner case supports the turbine nozzle inner support case. Thus, the front inner case must withstand the radial loads produced by the Number 3 bearing, the blow-off loads and torques transmitted from the first turbine nozzle through the rear inner case, and buckling pressures. The allowable stress for the inner case was calculated to provide a 1.3 buckling margin, which has been found to be adequate for other Pratt & Whitney Aircraft engines. Stiffening to prevent buckling will be provided by internal radial ribs and external longitudinal ribs.

The rear outer combustion chamber case flanges permit it to move rearward over the turbine case for hot section inspection. The rear flange and its mating turbine case flange are scalloped to interlock over a common internal flange to allow assembly of the cases. The outer and inner rear liner sections of the combustion chamber can be moved forward over the primary and secondary ram air scoop sections. The inner rear combustion chamber case is designed to move to the rear over the turbine inner nozzle vane case. It is assembled by means of a scalloped front flange which passes through the scalloped front flange of the first-stage vane inner support. The turbine nozzle vane case assembly and the first-stage rotor disk seals can be moved forward around the rear inner combustion chamber case. The above procedures will permit inspection and replacement of individual nozzle vanes or first-stage turbine blades without further dismantling of the engine.

c. Alternate Design

A preliminary design for an axially split combustor which can be disassembled without removing the turbine is presented for comparison with the basic design and is shown in Figure 2-46. The construction of this combustion chamber is essentially the same as described for the basic STF-219 engine except for the addition of joints to permit disassembly.

The outer combustion chamber case is longitudinally split from the outer rear diffuser case flange to the turbine outer front flange in three places to facilitate handling and inspection. The rear outer combustor liner is made in two halves fastened together by two axial hinge pins inserted through a series of matching alternating hinges for the forward two-thirds of its length and a three bolt flange arrangement at its rear end which unites the longitudinal split. Axial retention is by nuts and bolts at the front turbine flange. Development testing is required to determine if there is a need for an overlapping joint in the porous section of this liner. The pins have puller heads to facilitate removal and are secured with stop lugs. The three bolts at the rear are also to be secured with self locking nuts with lockwired bolt heads.

The split outer primary and secondary ram air scoop section is made up of two halves fastened with six long axial bolts with the nuts permanently attached to the stiffening ribs at the rear of the nose cone section. Two of the bolts are inserted through a series of matching alternating hinges at the split joint. The bolt heads are secured by lockwire and puller grooves are machined on the bolt heads to facilitate removal. The four remaining bolts serve as additional tiebolts to share the axial load.

The split inner primary and secondary ram air scoop section is constructed similarly to the outer section. The rear inner liner is constructed in two halves joined by two axial hinge pins inserted through matching alternating hinges over the forward two-thirds of its length. These pins have a rear flange that is bolted to lugs attached to the rear portion of each half of the liner. A one bolt flange at the extreme end of the liner completes the split joint. All bolts are secured by self locking nuts and lockwired bolt heads. The hinge pin flange can be used as a puller device to facilitate removal. This liner is disconnected from the turbine nozzle vane ring at its rear and moved forward for removal. By reaching behind the liner, the bolts at the rear and the bolts holding the pin flanges can be removed. At this point the hinge pins are removed and the liner moved rearward

to clear the outer diffuser case flange for disassembly after the air scoop sections have been removed.

There is an overlapping joint construction between the rear portion of the nose cone and the forward portion of the ram air scoop section for sealing air leakage. To remove either the inner or outer air scoop sections, the hinge bolts are removed and the section moved rearward far enough to disconnect the seal joint and to clear the outer rear diffuser case flange.

The nose cone section is also comprised of two halves split in a plane midway between two nozzles and is held by three bolts at each split. The edges of the split porous inner liner are supported by ribs. Testing will be required to determine whether an overlapping joint is needed in this area. The three bolts joining the sections can be installed or removed through the access holes for the fuel nozzle supports. The nose cone is moved rearward to clear the outer rear diffuser case flange. This provides access to the three bolts and permits removal of the split sections.

Combustor removal procedure for the alternate design is similar to that employed with current Pratt & Whitney Aircraft engines with individual can burners. This familiar procedure may initially appear more attractive than the disassembly procedure for the basic design which involves removal of the turbine. However, the low turbine rotor, rear turbine case, and exhaust case assembly can be removed as a unit by uncoupling the shaft nut, fixturing the exhaust case to the rear end of the low speed turbine shaft, and unbolting the turbine case flange at the second-stage vanes. Subsequent removal of the second-stage vane assembly and first-stage turbine rotor, followed by the first stage vane assembly with the rear outer and inner combustion chamber cases, exposes all the combustor liners for removal if required. This disassembly procedure also has the advantage that the first- and second-stage blades, vanes, and disks are all separated from adjacent stages to permit thorough inspection and replacement when required.

Removal of the split combustor liners requires removal of at least two of the three split outer cases. The duct heater spray bars and jet flameholder must also be removed, which is necessary in the basic design only if removal of the fuel nozzles and the forward section of the combustor is required. After the outer cases are removed, the detailed removal of the liner components is accomplished as previously described by unfastening bolted and pinned attachments, a more complicated and time consuming procedure than for the basic design. A

DOWNGRADED AT 3 YEAR INTERVALS
DECLASSIFIED AFTER 12 YEARS
DOD DIR 5200.10

preliminary study by the Pratt & Whitney Aircraft Service Department indicates that burner removal time for the basic design should not be appreciably greater than for the split design, although more elaborate fixtures and hoisting equipment would be required. However, if turbine blades and vanes require replacement at the same time intervals as combustor parts, the split design is less attractive.

Combustor liner and turbine first-stage inspection can be accomplished more rapidly for the basic design, as fewer external parts must be removed. However, greater use of mirrors and borescopes is required since less liner surface is exposed to direct view through the smaller access opening.

Considering factors other than accessibility for maintenance, the alternate design involves some compromises in cost, performance, and development effort required. The outer cases with three longitudinal joints are more expensive to fabricate, are more difficult to seal to prevent external air leakage, and have lower allowable stresses than the flow-turned basic-design cases in which hoop stresses do not cross longitudinal welded joints. Some weight saving is realized, however, in that the longitudinal flanges weigh less than the two circumferential flanges that they replace. This helps to reduce the weight penalties incurred elsewhere in the split design, so that only a moderate increase in over-all weight results.

The choice between the two designs must be carefully weighed. The alternate split design is feasible, but any improvement in maintenance accessibility provided by the alternate design must be weighed against the performance, durability, and cost of the basic unsplit design.

4. TURBINE

a. General Description

The STF219 engine uses a single-stage high-pressure turbine and a two-stage low-pressure turbine. It is enclosed in a forged two-piece case bolted together at interlocking scalloped flanges. Fail-safe design has been used where possible to prevent a fractured vane or a shaft failure from producing a propagating failure.

b. Over-All Cooling System

Details of the cooling system are discussed in section E of this item.

c. Description of Stationary Parts

The outer turbine casing is in two sections, both of which are one-piece forgings of PWA 1004 Waspaloy. The front turbine case is flanged at the front and rear and contains two conical sections which meet at the minimum diameter. The front flange is scalloped to interlock with the scalloped rear flange of the outer combustion chamber case. The rear turbine case is a conical section flanged at the front and rear. The third-stage vane retention ring is sandwiched between the rear flange of the rear turbine case and the front flange of the turbine exhaust case. The three flanges involved are all deeply scalloped to reduce thermal stresses, to reduce weight, and to provide clearance for tubes passing over the flanges. Grooves and flanges integral with both turbine cases provide support for the turbine stators.

The first-stage vanes are cast from PWA 653 (WI-52), a cobalt base alloy which has excellent high-temperature strength, stress rupture, and creep properties. The vanes are air cooled and structurally supported against airfoil gas loads at the end wall attachment points. The flowpath across the vane is defined by integral inner and outer platforms. The outer support assembly of the first-stage vane consists of a vane support ring and a tube support ring which are riveted together to encase exhaust cooling air transfer tubes. The outer flange of the support ring is sandwiched between the interlocking turbine case and outer combustion case flanges and the retaining flange of the burner outer liner. The inner support for the first vane consists of the inner turbine nozzle vane case and an inner torque ring. The inner torque ring is riveted to the inner turbine case together with a second ring carrying knife edge seal lips extending rearward to the disk side plate seal surface. A rear flange on the inner case locates the inner torque ring and receives the thrust load of the vanes. The vane root attachments slide into tee slots which permit radial motion and are held in place by the rear flange of the inner rear combustion chamber liner, to which the forward flange of the vane support is bolted. Use of tee slots permits thermal expansion of the vane and prevents the Number 3 bearing load from being transmitted through the vanes. The inner and outer vane support loads are transferred to the inner and outer combustion chamber cases and subsequently to the diffuser case. However, since the inner combustion chamber case grows thermally more than the outer combustion chamber case, the inner portion of the first-stage vanes are displaced forward of the outer portion at assembly so that the vanes will be normal to the gas stream during engine operation The

ends of the transfer tubes are spherical to permit the vane roots to be tipped forward during assembly.

The first-stage turbine vanes, as shown in Figure 2-47, are cooled by impingement air on the leading edge and by film cooling on the trailing edge. This is one of several cooling schemes which may be used. Combustor secondary cooling air is introduced at the inner vane support from which it flows radially into a tube in the vane leading edge cavity. Orifices in the tube wall direct the cooling air to impinge on the vane leading edge inner surface and subsequently to flow along the chord to the finned inner surface of the leading edge cavity into a radial passage behind the tube. From this passage, the cooling air flows radially outward, through the transfer tube into the annular passage formed by the outer vane support and the turbine case, and then discharges through tubes in the fan duct.

Cooling air also flows from the outer end of the vane into a shell in the central vane cavity and is distributed radially through holes in the forward section of the shell. Subsequently, the cooling air flows rearward along the chord finned inner surface of the vane, and is discharged through slots in the vane surfaces just forward of the vane trailing edge. This provides film cooling of the trailing edge.

The second- and third-stage vanes are cast from PWA 658 nickel-base alloy and are cantilevered from the turbine case. The vanes are subjected to loading by gas pressure on the airfoils and inner vane supports and are secured front and rear by feet which are integral with the vane platforms and engage circumferential grooves in the turbine cases. The tangential shear loads are transferred to lugs on the first- and second-stage tip seals. The inner platforms of the second- and third-stage vanes are provided with lugs which engage mating lugs in an annular channel-shaped inner support fabricated from PWA 687 (Waspaloy). Rings carrying knife-edge seal lips are riveted to the forward inner edges of the annular channels.

The second-stage vanes are cooled by burner secondary air which flows through holes in the outer combustion chamber support diaphragm, between the first-stage vane extensions, through holes in the first-stage outer vane support inner flange, between the turbine case and the first stage blade tip seals, and through grooves in the turbine case lugs and vane feet. The second-stage vane is internally impingement cooled, as shown in Figure 2-48. Cooling air fills a central shell from which it passes through holes to impinge on the inside of the airfoil leading edge. It then flows rearward along the inner sides of the

ends of the transfer tubes are spherical to permit the vane roots to be tipped forward during assembly.

The first-stage turbine vanes, as shown in Figure 2-47, are cooled by impingement air on the leading edge and by film cooling on the trailing edge. This is one of several cooling schemes which may be used. Combustor secondary cooling air is introduced at the inner vane support from which it flows radially into a tube in the vane leading edge cavity. Orifices in the tube wall direct the cooling air to impinge on the vane leading edge inner surface and subsequently to flow along the chord to the finned inner surface of the leading edge cavity into a radial passage behind the tube. From this passage, the cooling air flows radially outward, through the transfer tube into the annular passage formed by the outer vane support and the turbine case, and then discharges through tubes in the fan duct.

Cooling air also flows from the outer end of the vane into a shell in the central vane cavity and is distributed radially through holes in the forward section of the shell. Subsequently, the cooling air flows rearward along the chord finned inner surface of the vane, and is discharged through slots in the vane surfaces just forward of the vane trailing edge. This provides film cooling of the trailing edge.

The second- and third-stage vanes are cast from PWA 658 nickel-base alloy and are cantilevered from the turbine case. The vanes are subjected to loading by gas pressure on the airfoils and inner vane supports and are secured front and rear by feet which are integral with the vane platforms and engage circumferential grooves in the turbine cases. The tangential shear loads are transferred to lugs on the first- and second-stage tip seals. The inner platforms of the second- and third-stage vanes are provided with lugs which engage mating lugs in an annular channel-shaped inner support fabricated from PWA 667 (Waspaloy). Rings carrying knife-edge seal lips are riveted to the forward inner edges of the annular channels.

The second-stage vanes are cooled by [illegible] air which flows through holes in the outer combustion chamber support diaphragm, between the first-stage vane shrouding rings, [illegible] the first-stage outer vane support inner flange, between the [illegible] and the first stage blade tip seals, and through grooves in the turbine case lugs and vane feet. The second-stage vane is [illegible] arrangement cooled, as shown in Figure 2-48. Cooling air flows [illegible] from which it passes through holes to impinge on the [illegible] of the leading edge. It then flows rearward along the [illegible]

CONFIDENTIAL

vane and is discharged through slots in the sides of the vane just forward of the trailing edge. The third-stage vanes are not cooled.

Many vane cooling configurations have been designed and tested, and extensive effort in this area will continue. There are a number of promising designs that have yet to be evaluated. The final vane cooling design for the STF219 engine can be determined only after extensive testing and engine development effort.

The blade tip seals are fabricated from Hastelloy X because of its high oxidation resistance and adequate strength for this application. The first-stage blade tip seal is held in place by the outer support of the first-stage vanes and by the second-stage vanes. The seal is cooled by high-pressure compressor air traveling between the seal and the diffuser case, and also by a flow of air which is metered through holes in the outer support and blankets the inner surface. The second-stage blade seal is held in place by the second- and third-stage vanes. The first-stage blade tip seal has a pressurized axial sealing ring in a groove at its forward edge which bears against the inner flange of the first-stage vane outer support. Replaceable wear rings are sandwiched between the first- and second-stage seal rear edges and the forward surfaces of the second- and third-stage vanes respectively. In addition, the first- and second-stage blade tip seals have torque lugs at the rear which engage grooves in the turbine case and then extend rearward into the flow passage in the outer front foot of the following vane. Adequate radial and axial clearances have been provided between the seal lugs and the case lugs to ensure that the relative thermal expansion of the parts will not constrain the seals during steady-state or transient operation. The third-stage blade tip seal is held in place by the third-stage vane retention ring and by a shoulder on the turbine exhaust case grooved to engage the seal torque lugs. The contact surfaces between the vanes and the seals are hardfaced to prevent galling.

Fail-safe design has been used in the turbine where possible. Each of the vanes are secured at both ends to prevent a part of a fractured or burned vane from being carried downstream. In addition, the knife-edge seals have been designed such that they do not restrict rearward travel of the rotor. Hence, in the event of a shaft failure, the rotor shifts axially into the stator dissipating the stored rotational energy within the engine, and battering the airfoils to reduce their torque input to the rotor. Containment of broken blades is provided partially by the turbine cases and the duct heater cases. The additional containment required is provided with the minimum addition of weight by the combined containment and heatshield liner located just inside the duct heater outer

vane and is discharged through slots in the sides of the vane just forward of the trailing edge. The third-stage vanes are not cooled.

Many vane cooling configurations have been designed and tested, and extensive effort in this area will continue. There are a number of promising designs that have yet to be evaluated. The final vane cooling design for the STF219 engine can be determined only after extensive testing and engine development.

The blade tip seals are fabricated from Hastelloy X because of its high oxidation resistance and adequate strength for this application. The first-stage blade tip seal is held in place by the outer support of the first-stage vanes and by the second-stage vanes. The seal is cooled by high-pressure compressor air traveling between the seal and the diffuser case, and also by a flow of air which is metered through holes in the outer support and blankets the inner surface. The second-stage blade seal is held in place by the second- and third-stage vanes. The first-stage blade tip seal has a pressurized axial sealing ring in a groove at its forward edge which bears against the inner flange of the first-stage vane outer support. Replaceable wear rings are sandwiched between the first- and second-stage seal rear edges and the forward surfaces of the second- and third-stage vanes respectively. In addition, the first- and second-stage blade tip seals have torque lugs at the rear which engage grooves in the turbine case and then extend rearward into the flow passage in the outer front foot of the following vane. Adequate radial and axial clearances have been provided between the seal lugs and the case lugs to ensure that the relative thermal expansion of the parts will not constrain the seals during steady-state or transient operation. The third-stage blade tip seal is held in place by the third-stage vane retention ring and by a shoulder on the turbine exhaust case grooved to engage the seal torque lugs. The contact surfaces between the vanes and the seals are hardfaced to prevent galling.

Fail-safe design has been used in the turbine where possible. Each of the vanes are secured at both ends to prevent a part of a fractured or burned vane from being carried downstream. In addition, the knife-edge seals have been designed such that they do not restrict rearward travel of the rotor. Hence, in the event of a shaft failure, the rotor shifts axially into the stator dissipating the stored rotational energy within the engine, and battering the airfoils to reduce their torque input to the rotor. Containment of broken blades is provided partially by the turbine cases and the duct heater cases. The additional containment required is provided with the minimum addition of weight by the combined containment and heatshield liner located just inside the duct heater outer

vane and is discharged through slots in the sides of the vane just forward of the trailing edge. The third-stage vanes are not cooled.

Many vane cooling configurations have been designed and tested, and extensive effort in this area will continue. There are a number of promising designs that have yet to be evaluated. The final vane cooling design for the STF219 engine can be determined only after extensive testing and engine development.

The blade tip seals are fabricated from Hastelloy X because of its high oxidation resistance and adequate strength for this application. The first-stage blade tip seal is held in place by the outer support of the first-stage vanes and by the second-stage vanes. The seal is cooled by high-pressure compressor air traveling between the seal and the diffuser case, and also by a flow of air which is metered through holes in the outer support and blankets the inner surface. The second-stage blade seal is held in place by the second- and third-stage vanes. The first-stage blade tip seal has a pressurized axial sealing ring in a groove at its forward edge which bears against the inner flange of the first-stage vane outer support. Replaceable wear rings are sandwiched between the first- and second-stage seal rear edges and the forward surfaces of the second- and third-stage vanes respectively. In addition, the first- and second-stage blade tip seals have torque lugs at the rear which engage grooves in the turbine case and then extend rearward into the flow passage in the outer front foot of the following vane. Adequate radial and axial clearances have been provided between the seal lugs and the case lugs to ensure that the relative thermal expansion of the parts will not constrain the seals during steady-state or transient operation. The third-stage blade tip seal is held in place by the third-stage vane retention ring and by a shoulder on the turbine exhaust case grooved to engage the seal torque lugs. The contact surfaces between the vanes and the seals are hardfaced to prevent galling.

Fail-safe design has been used in the turbine where possible. Each of the vanes are secured at both ends to prevent a part of a fractured or burned vane from being carried downstream. In addition, the knife-edge seals have been designed such that they do not restrict rearward travel of the rotor. Hence, in the event of a shaft failure, the rotor shifts axially into the stator dissipating the stored rotational energy within the engine, and battering the airfoils to reduce their torque input to the rotor. Containment of broken blades is provided partially by the turbine cases and the duct heater cases. The additional containment required is provided with the minimum addition of weight by the combined containment and heatshield liner located just inside the duct heater outer

DOWNGRADED AT 3 YEAR INTERVALS
DECLASSIFIED AFTER 12 YEARS
DOD DIR 5200.10

THIS DOCUMENT CONTAINS INFORMATION AFFECTING THE NATIONAL DEFENSE OF THE UNITED STATES WITHIN THE MEANING OF THE ESPIONAGE LAWS, TITLE 18, U.S.C., SECTIONS 793 AND 794. THE TRANSMISSION OR THE REVELATION OF ITS CONTENTS IN ANY MANNER TO AN UNAUTHORIZED PERSON IS PROHIBITED BY LAW.

case. The total containment thicknesses were determined by procedures which take into account strength and toughness factors for each different containment material at its maximum operating temperature.

Provision has been made for the inspection of the first-stage vanes and the first-stage turbine blades without necessitating a complete disassembly of the engine. The outer combustion chamber slides aft after the exhaust cooling air tubes are removed from the turbine case. The combustion chamber outer liner then slides forward and the vanes are visible. Individual vanes may be removed by sliding the inner combustion chamber liner forward after which the vane to be removed will slide out. The remaining vanes will be held in place by their respective transfer tubes. By removing the nuts on the forward flange of the inner turbine nozzle case, the entire first-stage vane assembly will slide forward over the inner rear combustion chamber case to provide access to the first-stage turbine blades.

d. Description of Rotating Parts

The high-pressure rotor consists of the first-stage turbine disk and blade assembly, the first-stage front disk seal and seal ring, the front disk seal support ring, the first-stage air seal ring, the first-stage turbine front shaft, and the rear inner knife-edge seal.

The disk and blade assembly, front seal disk support ring, and the rear inner knife seal are bolted to the rear flange of the turbine front shaft with eighteen one-half inch tiebolts. The front disk seal is self supporting, and is retained axially by a retaining ring bolted with twelve 1/4-inch bolts to the front disk seal support ring. The front disk seal fulfills two functions. It provides a sealing surface for the knife-edge seals mounted on the first stator inner support, and it provides a baffle to direct cooling air over the front face of the first-stage disk to the blade root attachments and through the first-stage blade foils.

Air sealing between the high- and low-pressure turbine rotors is provided by the rear inner knife-edge seal mounted on the rear face of the first-stage turbine disk at the bolt circle and a mating cylindrical seal surface attached to the low-speed rotor shaft. In addition, a knife-edge seal supported by the second-stage stator inner shroud mates with a cylindrical seal surface on the rear face of the first-stage turbine disk at the bolt circle to provide air sealing between the first-stage rotor and the second-stage stator.

The low-pressure rotor consists of the second-stage turbine disk and blade assembly, the second-stage front disk seal, the second-stage disk seal spacer, the second-stage air seal ring, the third-stage turbine disk and blade assembly, the inter-stage spacer and seal support, the low-pressure turbine rear hub, and the low-pressure turbine front shaft.

The rear flange of the low-pressure turbine front shaft, the second-stage disk seal spacer, the second-stage disk and blade assembly, the front flange of the low-pressure turbine rear hub, and the flange of the third-stage disk integral spacer are all bolted together with eighteen 5/8-inch tiebolts. The second-stage front seal disk is self-supporting and is retained axially by the shaft rear flange and the second-stage disk. Torque lugs on the inner circumference of the disk seal mate with slots in the second-stage front disk seal spacer, which is slightly thicker than the disk seal inner circumference to allow free radial growth. The torque lugs also hold the disk seal concentric with the rotor axis.

The cylindrical interstage spacer and seal support provides stiffening for the disks and raises the resonant vibration frequency of the third-stage disk out of the range of the frequency excited by the gas stream flow pattern produced by the turbine exhaust struts. In addition, the spacer supports the knife-edge seals which mate with the seal surface mounted on the third-stage stator inner shroud.

In all turbine stages, the blade roots are attached to the disks by a multiple serration "fir tree" root. This method provides an attachment which is designed to withstand fatigue and stresses resulting from centrifugal forces and aerodynamically excited vibrations. Experience has shown that this method of attachment is reliable and efficient. Similar to the JT11 engine, extended blade roots, in which the blade shank extends between the platform and the root attachment, are used for the first- and second-stage blades to displace the disk rim and the attachments away from the hot turbine gas stream and to facilitate their cooling. Air seal rings positioned by snap rings on the front faces of the first- and second-stage disks prevent uncontrolled flow of cooling air between the disk rims and the blade platforms. The blades in the first and second stages are retained axially by snap rings located in the front face of each disk rim. In the third stage, the blades are retained by rivets through the apex of the fir tree.

The low-pressure rotor consists of the second-stage turbine disk and blade assembly, the second-stage front disk seal, the second-stage disk seal spacer, the second-stage air seal ring, the third-stage turbine disk and blade assembly, the inter-stage spacer and seal support, the low-pressure turbine rear hub, and the low-pressure turbine front shaft.

The rear flange of the low-pressure turbine front shaft, the second-stage disk seal spacer, the second-stage disk and blade assembly, the front flange of the low-pressure turbine rear hub, and the flange of the third-stage disk integral spacer are all bolted together with eighteen 5/8-inch tiebolts. The second-stage front seal disk is self-supporting and is retained axially by the shaft rear flange and the second-stage disk. Torque lugs on the inner circumference of the disk seal mate with slots in the second-stage front disk seal spacer, which is slightly thicker than the disk seal inner circumference to allow free radial growth. The torque lugs also hold the disk seal concentric with the rotor axis.

The cylindrical interstage spacer and seal support provides stiffening for the disks and raises the resonant vibration frequency of the third-stage disk out of the range of the frequency excited by the upstream flow pattern produced by the turbine exhaust struts. In addition, the spacer supports the knife-edge seals which mate with the seal surface mounted on the third-stage stator inner shroud.

In all turbine stages, the blade roots are attached to the disks by a multiple serration "fir tree" root. This method provides an attachment which is designed to withstand fatigue and stresses resulting from centrifugal forces and aerodynamically excited vibrations. Experience has shown that this method of attachment is reliable and efficient Similar to the JT11 engine, extended blade roots, in which the blade shank extends between the platform and the root attachment, are used for the first- and second-stage blades to displace the disk rim and the attachments away from the hot turbine gas stream and to facilitate their cooling. Air seal rings positioned by snap rings on the front faces of the first- and second-stage disks prevent uncontrolled flow of cooling air between the disk rims and the blade platforms. The blades in the first and second stages are retained axially by snap rings located in the front face of each disk rim. In the third stage, the blades are retained by rivets through the apex of the fir tree.

Vibration damping for the first- and second-stage turbine blades is provided by cylindrical weights housed in protrusions integral with the front and rear first- and second-stage disk rims. Centrifugal force causes the weights to bear against the individual blade platforms to provide frictional damping of blade vibrations. This design concept has been successfully demonstrated in the J-58 engine.

The third-stage turbine blades have interlocking tip shrouds to control blade vibrations. The tip shroud bearing surfaces are hard-faced to prevent excessive wear. The tip shrouds also carry two knife-edge seals which mate with a stepped seal ring attached to the turbine case.

All of the turbine blades have integral platforms at the roots which extend to the front and rear to form cylindrical surfaces to mate with stationary interstage knife-edge seals. These seals prevent the hot turbine gases from circulating into the cavities between the disks and therefore the temperature gradient between the disk bore and rim is reduced together with the resultant thermal stresses. The outer surfaces of the platforms form the inner boundary for the gas path.

The primary element in the design of a turbine disk for satisfactory life is the selection of materials having the necessary properties to meet the requirements dictated by the levels of stress and temperature under which the disk must operate. The determination of the mechanical properties of these materials has been accomplished largely by Pratt & Whitney Aircraft, although these data were supported by material published by material producers, government agencies, research corporations, and full scale spin testing.

PWA 1007 nickel alloy has been selected for the first-stage turbine disk for the Mach 2.7 engine and for all three disks for the Mach 3.0 engine. PWA 1003 nickel alloy is adequate for the second- and third-stage disks for the Mach 2.7 engine. Experience with these materials in Pratt & Whitney Aircraft engines indicates that they will provide satisfactory life at the temperatures and stress levels predicted for the STF219 engines.

Pratt & Whitney Aircraft turbine blade materials are selected according to the operating conditions to achieve the best combination of

ductility, corrosion resistance, and high tensile and stress rupture properties. PWA 658 (IN 100) has been chosen as the blade material for all three turbine stages. Based on current engine experience, these materials show promise of demonstrating satisfactory blade attachment life at predicted temperatures and attachment stress levels.

Air for cooling the turbine parts is obtained from the fourth stage of the compressor and from the compressor discharge exit. Air from the fourth compressor stage initially cools various sections of the compressor, and subsequently flows to the turbine section through the annulus formed by the two shafts. The air surrounds and cools the bore of the first-stage turbine disk, passes through holes in the rear conical portion of the low speed turbine front shaft where it then surrounds and cools the bore of the second-stage turbine disk, and then passes through holes in the conical portion of the low speed turbine rear shaft to cool the bore and rear face of the third-stage turbine disk. This air is exhausted to the gas path at the rear of the third-stage blade platform.

For disk and blade cooling, compressor discharge air is piped directly to the compartment forward of the first-stage turbine front seal disk. A portion of this air passes through holes in the front disk seal support between the bolts to be directed over the front face of the first-stage turbine disk and subsequently into the rim at the apex of the blade attachments and into the individual blades.

One cooling scheme for the first-stage turbine blade (see Figure 2-49) uses film cooling for the leading and trailing edges. Cooling air is supplied to the blade at the blade root. From the root, it flows radially through the hollow blade convectively cooling the mid-chord section. At the front of the blade cavity, cooling air is ejected through holes to form an air film over the outer surface of the leading edge. At the rear of the cavity, the air is released through slots to form an air film over the trailing edge. This design is discussed in detail in section E of this item.

Many blade cooling configurations have been designed and tested and extensive effort in this area will continue. There are a number of

DOWNGRADED AT 3 YEAR INTERVALS
DECLASSIFIED AFTER 12 YEARS
DOD DIR 5200.10

promising designs that have yet to be evaluated. The final blade cooling design for the STF219 engine can be determined only after extensive testing and engine development effort.

The remainder of the high-pressure compressor discharge air for turbine cooling passes through holes between the first-stage tiebolts into the compartment between the first- and second-stage disks. From this point the flow divides into three parts. A portion leaks under a knife-edge seal to cool the rear face of the first-stage disk and subsequently past a second seal into the turbine gas stream. The second portion passes through holes near the inner circumference of the second-stage front seal disk to cool the front face of the turbine disk and the blade roots. The remainder of the flow passes through holes between the second-stage tiebolts into the chamber between the second- and third-stage disks. This air cools the rear face of the second-stage disk and the front face of the third-stage disk, and subsequently flows through holes on both sides of the seals on the outer spacer to cool the rims of the second- and third-stage disks. From here it leaks past the knife-edge seals into the turbine gas stream.

e. Turbine Rotor Balance

Before assembly, the high-speed front turbine shaft is dynamically balanced by removing material from the rear flange and by inserting plugs into the holes provided at the front of the shaft. The first-stage front disk seal is statically balanced by machining. The first-stage disk and blade assembly is statically balanced by pairing blades by the moment-weight method during assembly and subsequently inserting hollow plugs in the air holes between the tiebolt holes in the disk. The plugs are trapped in the disk after assembly by the adjacent flanges but permit cooling air to pass through the disk.

The turbine rotor is then assembled together with the Number 3 bearing compartment and support, the combustion chamber inner and outer cases, the first stage turbine stators, and the combustion chamber, the diffuser case, the previously balanced high-pressure compressor rotor and stator, and all associated hardware. The entire assembly is then balanced finally by adding weights to the flanges provided at the rear of the first-stage turbine disk and at the front of the third-stage compressor disk, making further disassembly and reassembly unnecessary.

The low-speed turbine front shaft is dynamically balanced by machining corrections in the flange provided just behind the high-pressure

compressor and in the inside of the rear flange. The second-stage front seal disk is statically balanced by machining corrections in the flanges at the front edge of the rim. The second- and third-stage blade-disk assemblies are assembled by the blade-pairing moment-weight method and then the second-stage assembly is balanced by the same method used for the first-stage assembly. The third-stage assembly is not statically balanced. The low-speed rotor is then assembled with the turbine rear case and the third-stage stators, and dynamically balanced by adding correction weights to the flange at the rear of the third-stage disk and to the flange just forward of the shaft rear flange.

f. Stress Analysis Summary

The front seal disks attached to the first- and second-stage disks are self-supporting and are designed to respond to thermal changes and centrifugal loading independent of the disks to which they are attached. The criteria for determining their design limits, however, are identical to those for the turbine disks.

The stresses and strains for the turbine components were determined by the use of moderately complex methods which enable the determination of stress redistribution within the components resulting from short time local yielding or long term creep. In addition, accurate methods evolved through an extensive program of material and stress evaluation were used to predict burst and yield speeds, transient yield growth, creep characteristics, and low-cycle fatigue characteristics of the turbine components, and, on the basis of these predictions, the turbine was designed to meet the life requirements of the engine.

5. TURBINE SHAFTS

a. General Description

The high-speed turbine shaft is coupled to the rear hub of the high-pressure compressor. The low-speed turbine shaft is coupled to the fan hub. In addition to transmitting torque, the two shafts form an annulus to carry cooling air from the compressor to the turbine. The low-speed turbine rear hub provides support for the low-speed turbine rotor.

b. Physical Structures

The high-speed turbine shaft is flanged at the rear and is bolted to the first-stage turbine disk. From the flange it extends forward and tapers

inward to join a cylindrical section which extends through the Number 3 bearing and terminates just beyond the bearing compartment. Holes are provided at the front end of the shaft for balance plugs. The inside of the shaft at the rear of the cylindrical section is splined to drive the high-pressure compressor rear hub. A shoulder on the inside of the shaft immediately behind the splined section provides a bearing surface for the coupling nut which screws onto the end of the high-pressure compressor rear shaft. At the junction of the tapered section and the rear flange of the high-speed turbine shaft, material is provided for the detail balancing of the shaft. The rear flange of the low-speed turbine shaft is bolted to the front face of the second-stage disk. From the flange, the shaft tapers to a cylindrical section and then extends forward to couple with the fan rear shaft just forward of the Number 1 bearing. Coupling is obtained through splines on the outside of the turbine shaft and on the inside of the fan hub. The shaft and hub are held together by a threaded coupling which screws into the low-speed turbine shaft and bears against a shoulder on the fan hub. Spacers are placed between the shoulder of the fan hub and the low-speed turbine shaft to absorb accumulated tolerances and accurately position the low-speed turbine rotor. Splines are provided at both ends of the coupling to permit it to be turned from either end of the engine.

An external flange just behind the seventh-stage compressor disk and an internal flange at the rear end of the shaft provide material for the detail dynamic balancing of the shaft.

The low-speed turbine hub is bolted at the front flange to the rear face of the second-stage disk. From the flange it tapers rearward to a cylindrical section supported by the Number 4 bearing.

c. Stress Analysis Summary

The shafts and hub are designed to withstand the stresses produced by a 10 per cent blade loss load. They were evaluated for torsional yield stress, creep stress, buckling stress, and critical speed. In all cases, the critical speed was the limiting factor. The shafts and hub for this engine provide a minimum critical speed margin of 20 per cent. Due to critical speed rather than stress limitation, PWA 1005 nickel alloy is adequate for these parts.

6. NUMBER 3 BEARING COMPARTMENT AND SUPPORTING STRUCTURE

a. General Description

The Number 3 bearing compartment assembly, shown in Figure 2-50, includes the Number 3 bearing, the inner and outer bearing support, the front and rear carbon face seal assemblies, the front and rear labyrinth seal assemblies, and insulation. The inner bearing support is made from AMS 5613 stainless steel, the outer support from PWA 687 (Waspaloy) nickel alloy, and the inner seal support from AMS 5613 stainless steel. The rear seal support and front and rear compartment cases are made of AMS 5667 (Inconel X) nickel alloy.

The Number 3 bearing supports the high-speed turbine rotor and is lubricated by a combined mist and jet oil system. The bearing compartment is sealed by carbon face seals which are loaded with fan discharge air to reduce the net seal loading and provide longer seal life. The carbon face seals are backed up by a labyrinth seal system.

b. Bearings

The Number 3 bearing is a preloaded roller bearing fabricated of AMS 6490 material stabilized to provide minimum distortion at 600°F. The rollers ride on a flanged inner race and are preloaded by an out-of-round outer race. When the out-of-round race is pressed into a round housing, two diametrically opposed points are produced which preload the bearing and prevent skidding of the rollers. The amount of preloading obtained is dependent on the degree of out-of-roundness and on the spring rate of the bearing inner support. This system has been successfully used in previous Pratt & Whitney Aircraft engines. AMS 6415 material is used for the bearing cage.

c. Seals

The front compartment is sealed by a primary carbon face seal and two sets of four-lip labyrinth seals, made from AMS 5667 material. The annular chamber between the outer support assembly and the front compartment case is pressurized with fan discharge air to provide back pressure for the seals.

The rear compartment is sealed by a primary carbon face seal and three sets of four-lip labyrinth seals. The innermost chamber formed by the rear labyrinth seal support and the first two sets of labyrinth

seals contains fan discharge air obtained from the front chamber through transfer tubes which are located between the main support flange bolts. The area outside the rear compartment case is pressurized with compressor discharge air, and, therefore, a third set of labyrinth seals was added to protect the first and second seals from exposure to high-temperature, high-pressure air. The area between the second and third seals is vented to the low pressure area outside the front compartment by a passage between the rear compartment case and the rear labyrinth seal supports. This passage passes between the support flange bolts and into the low-pressure area. Venting the compartment between the second and third rear seals prevents high-pressure air which leaks past the outer seal from pressurizing the first and second seals, and also prevents any oil which might leak past the first and second seals from contaminating the turbine cooling air supply.

d. Lubrication

The bearing is lubricated by an oil mist and cooled by oil flowing through slots in the bearing inner race. The oil supplied to the inner race is picked up from a stationary jet by rotating scoops located immediately forward of the bearing. Oil picked up by the scoops also cools the carbon face seals and the compartment inner wall. Accumulated oil in the compartment is removed by an ejector type scavenge pump.

e. Stress Analysis Summary

The bearing inner support is a conical segment attached to the rear end of the bearing outer race housing cylinder and extending forward and outward. The flange of the inner support is bolted between flanges on the front and rear shells of the compartment case. The conical section contains holes to control the torsional and two-point radial spring rates so that radial loads from the rotor will not cause significant changes in the slope of the outer race and consequent wear at the corners of the rollers. The holes maintain a relatively stiff radial support, but a relatively soft two-point spring load.

The outer support assembly is a second conical segment which transmits bearing loads from the compartment case flange to the rear flange of the inner combustion chamber case. The support has adequate stiffness to carry the bearing loads, but is designed to accept the stresses produced by the thermal differential expansion of the compartment case and the combustion case rear flange. The continued radial alignment of the bearing support to the combustion chamber is en-

sured by providing sufficient interference fit at the pilot diameters to preclude loosening by thermal expansion.

The bearing support structure is limited by the Mach 3 cruise, non-augmented flight condition. Design loads are caused by rotor unbalance, aerodynamic excitation, maneuvers, relative thermal expansion of components, operating pressure, and blade loss. By far the most significant load is that produced by possible blade loss. The bearing support is designed to withstand the dynamic load produced by blade loss represented by a static load equal to the centrifugal force of 10 per cent of the airfoils in any turbine stage.

The components were designed such that:

1. Under maximum operating and maneuver loading, tension, compression, or shear stresses shall not exceed 80 per cent of the 0.2 per cent yield strength or 67 per cent of the ultimate strength, whichever is less;

2. Under maximum operating and maneuver loading, bending stresses shall not exceed the 0.2 per cent yield strength;

3. Under combined operating, maneuver, and blade loss loading, tension or shear stresses shall not exceed the ultimate strength, and bending stresses shall not exceed the modulus of rupture; and

4. Vibratory stresses resulting from rotor unbalance and aerodynamic excitation shall not exceed the fatigue limit.

7. TURBINE EXHAUST SECTION

a. General Description

The turbine exhaust section is shown in Figure 2-50.

The airflow leaving the turbine passes through the exhaust system where it is straightened by twelve exit guide vanes, and subsequently into the exit area defined by the exhaust duct and the tail cone.

b. Physical Structure

The exhaust flow path is bounded by the inner and outer exhaust cases which are flow-turned from PWA 587 (Waspaloy) nickel alloy. The inner and outer cases are welded to the twelve exit guide vanes which

are fabricated from PWA 687 and PWA 1030 (Waspaloy). The vanes are protected from the hot turbine gases by heatshields of Hastelloy X and are cooled by the internal flow of cooling air from the fan duct. Some of the vanes have extra thickness to permit the passage of oil lines, breather tubes, and labyrinth-seal pressurizing air lines. These lines are flattened tubes surrounded by heat shields.

The exhaust duct is bolted to a flange at the rear of the outer exhaust case. The tail cone is bolted to the inner exhaust case.

8. NUMBER 4 BEARING

a. General Description

The Number 4 bearing is a roller bearing supporting the rear end of the low-speed shaft. Loads from the shaft are transmitted through the bearing supports to the inner exhaust case and through the exit guide vanes to the outer exhaust case. The bearings are made of PWA 724 or AMS 6490 stabilized for minimum distortion at 600°F. The cage is made of AMS 6415 material.

b. Physical Structure

The Number 4 bearing is designed to permit the relative axial thermal expansion differences between the shaft and the exhaust case by using a shouldered inner race and a long, unshouldered outer race. Both races are firmly clamped by long spanner nuts tightened to specified torque values and secured by riveting the nuts to the threaded members. During engine warmup, the case structure heats more rapidly than the shaft, and the roller bearing travels toward the front of the case. When the engine is shut down, the case cools more rapidly than the shaft, and the roller bearing travels toward the rear. At steady-state conditions, the bearing is at approximately the same position as at room temperature. Adequate clearance is provided to permit the rotor parts to clear the stationary parts during the transient expansions.

The outer race housing consists of a U-shaped section of PWA 1004 (Waspaloy) machined into individual fingers and having a conical section which is bolted to the exit guide vane assembly. The U-shaped section provides the desired spring rate for the rotor critical speed requirements. Deflections during large rotor overloads are limited by bumpers placed inside the U sections in line with the conical support section.

The bearing compartment consists of a flanged closed cylinder bolted to a cylindrical seal support at the bearing housing support. The bearing compartment is protected by heat shields and insulation.

The rear of the compartment has an insulated, removable cover to permit access to remove the jet oil supply tube and install a threaded fixture into the end of the oil tube and pump drive assembly. This fixture bolts to the exhaust case rear flange and locates the low rotor axially relative to the turbine cases during assembly and disassembly operations. It also prevents pivoting of the cases about the Number 4 bearing relative to the rotor to protect the turbine rotor seals during this operation.

The compartment is sealed by two pairs of carbon ring seals. The pairs are placed back-to-back with a light pressure applied against the angle faces by a wave-type spring washer to effect sealing both axially and radially. The seals are confined in a space formed by clamping the seal face plates, spacers, and inner bearing race against the shaft hub shoulder.

Two, four-knife-edge labyrinth seals are located forward of the carbon seals. The two seals seal against opposite sides of a replaceable cylinder riveted to the low speed shaft hub. These seals protect the bearing compartment from high-temperature gases by interposing fan discharge air between the carbon seals and disk hub cooling air. The inner seal is riveted to the oil seal ring flange and the outer seal to the integral seal and support shell.

To prevent buckling, a corrugated shell is welded to the back of the turbine exhaust nozzle. The inner skin and corrugated sheet are PWA 1030 (Waspaloy) and the flanges are PWA 678 (Waspaloy). Exhaust gas pressure and temperature instrumentation is mounted from bosses between the struts in the exhaust outer case. This instrumentation is accessible through the tailpipe of an installed engine for checking, and may be replaced if necessary by removing the fan duct inner liner.

c. Lubrication

Oil lines to the bearing compartment pass through the turbine exit guide vanes. Oil is supplied to the inside of the conical oil tube and pump drive assembly. It flows forward in the conical tube and through

slots in the forward edge into the rotor hub. It is then centrifuged to the forward portion of the hub where it passes radially outward to grooves in the seal plates and spacers and subsequently to the inner race of the bearing. The system provides two paths to the inner race so that, should the forward holes in the hub become plugged, the oil could pass behind the seals directly to the inner race.

Oil is returned to the oil tank in the front part of the engine by a gear-type scavenge pump located within the bearing compartment.

d. Stress Analysis Summary

The turbine exhaust and bearing support structure is limited by the Mach 3 flight condition. Design loads are caused by rotor unbalance, aerodynamic excitation, maneuvers, relative thermal expansion of components, operating pressure, and blade loss. The most significant load is that produced by possible blade loss. The support is designed to withstand the dynamic load produced by blade loss represented by a static load equal to the centrifugal force of 10 per cent of the airfoils in any turbine stage.

The components were designed such that:

1. Under maximum operating and maneuver loading, tension, compression, or shear stresses shall not exceed 80 per cent of the 0.2 per cent yield strength or 67 per cent of the ultimate strength, whichever is less;

2. Under maximum operating and maneuver loading, bending stresses shall not exceed the 0.2 per cent yield strength;

3. Under combined operating, maneuver, and blade loss loading, tension or shear stresses shall not exceed the ultimate strength, and bending stresses shall not exceed the modulus of rupture; and

4. Vibratory stresses resulting from rotor unbalance and aerodynamic excitation shall not exceed the fatigue limit.

9. DUCT HEATER

a. General Description

Thrust augmentation for the STF219 turbofan engine is provided by a fan duct combustion system commonly referred to as a duct heater.

To allow combustion in the fan stream, the fan exit air is diffused to a low velocity through the duct diffuser section. To initiate and maintain combustion in the relatively cool fan air stream, an aerodynamic or "jet" flameholder is used. Combustion continues in the duct heater combustion section, and the gas stream is exhausted through a variable-area exit nozzle. Ignition is provided by a torch-type igniter located upstream of the duct fuel spray rings. The duct heater is shown in Figure 2-51.

To accommodate the shorter length of the STF219 engine, an offset cascade type of diffuser is used instead of the straight-walled diffuser proposed for the JT11F-11, -12 engine.

The duct heater burning length is 60 inches which is a 10-inch reduction from the duct heater proposed in the Phase I study.

A cross-type aerodynamic flameholder consisting of both circumferential and radial elements fed by high-pressure, high-temperature air from the main engine combustion chamber secondary cooling air flows is used in the STF219 engine. The previously proposed design contained only one circumferential element. The fuel system for the aerodynamic flameholder now consists of externally fed spray rings. In the Phase I study, it was felt that internal injection of fuel would provide a means of premixing some partially vaporized fuel with the aerodynamic flameholder air to ensure efficient combustion. The cross-type flameholder has demonstrated more uniform distribution and increased combustion efficiency than demonstrated by the single-element unit. Fuel is supplied to secondary upstream spray rings and primary spray rings immediately downstream of the flameholder.

b. Physical Structure

The duct heater consists of a duct diffuser case, duct heater cases and liners, the aerodynamic flameholder and its air supply system and valves, two fuel spray rings, and the ignition system

The duct diffuser case is fabricated from AMS 4910 and AMS 4966 titanium alloys. It consists of an inner and outer case joined by eight hollow air-foil-shaped struts which run lengthwise through the diffuser section. Two sets of annular cascades reduce the fan exit velocity to the level required for stable, efficient combustion in the duct heater. The first cascade consists of four concentric rings of airfoils welded to supporting pylons and attached to the outer case between the struts. The second cascade consists of five concentric rings of airfoils supported in a similar manner. The vanes and sup-

porting pylons are fabricated from AMS 4966 titanium stock. The complete duct diffuser assembly is split at the engine vertical centerline to provide access to the fuel manifold and fuel, oil, and air lines which pass through these split struts and the two struts located on the engine horizontal centerline. The use of continuous lines from the internal to the external connections eliminates the possibility of internal leakage.

The four struts in the 45-degree positions are used to house the lines used to transmit compressor discharge air from the gas generator diffuser case air bleed manifold across the fan duct to the external connection for airframe use. External pads are provided at these strut locations for airframe cabin pressurization air and thermal anti-icing air connections.

The leading edges of all the fan duct diffuser struts match the trailing edge of the intermediate case struts to provide a smooth airfoil-shaped section.

The forward flange of the outer duct case attaches to the rear flange of the intermediate case. The forward end of the inner duct joins a flange on the intermediate case with a slip joint to provide for thermal growth and for radial and axial manufacturing tolerances.

The duct heater case is in three sections. The forward case and rear mount case are made from PWA 1202 titanium alloy, and the rear case is made from AMS 5616 and AMS 5508 stainless steel to withstand the slightly higher temperatures present in this area. Each of the cases is cylindrical and fastens to the adjacent sections at flanges. The forward case has provisions for the installation of the main engine igniter torque tubes, the secondary spray rings, the primary spray rings, the torch igniters, and the fuel drain plug. The rear mount case includes the rear engine mount ring. Both the rear mount case and the rear duct heater case have attaching points for the support of the exhaust-nozzle and ejector-reverser hardware.

The duct heater inner and outer liners consist of three major sections: the fuel baffle, the perforated screech liner, and a transpiration cooling liner. All liners are non-structural.

The fuel baffle forms the forward section of the liners and prevents fuel from entering the inner and outer cooling flow annular areas. The middle section of the liners is the screech liner, which is perforated with small holes whose open area is a predetermined percentage of the total area. This section absorbs the periodic combustion

porting pylons are fabricated from AMS 4966 titanium stock. The complete duct diffuser assembly is split at the engine vertical centerline to provide access to the fuel manifold and fuel, oil, and air lines which pass through these split struts and the two struts located on the engine horizontal centerline. The use of continuous lines from the internal to the external connections eliminates the possibility of internal leakage.

The four struts in the 45-degree positions are used to house the lines used to transmit compressor discharge air from the gas generator diffuser case air bleed manifold across the fan duct to the external connection for airframe use. External pads are provided at these strut locations for airframe cabin pressurization air and thermal anti-icing air connections.

The leading edges of all the fan duct diffuser struts match the trailing edge of the intermediate case struts to provide a smooth airfoil-shaped section.

The forward flange of the outer duct case attaches to the rear flange of the intermediate case. The forward end of the inner duct joins a flange on the intermediate case with a slip joint to provide for thermal growth and for radial and axial manufacturing tolerances.

The duct heater case is in three sections. The forward case and rear mount case are made from PWA 1202 titanium alloy, and the rear case is made from AMS 5616 and AMS 5508 stainless steel to withstand the slightly higher temperatures present in this area. Each of the cases is cylindrical and fastens to the adjacent sections at flanges. The forward case has provisions for the installation of the main engine igniter torque tubes, the secondary spray rings, the primary spray rings, the torch igniters, and the fuel drain plug. The rear mount case includes the rear engine mount ring. Both the rear mount case and the rear duct heater case have attaching points for the support of the exhaust-nozzle and ejector-reverser hardware.

The duct heater inner and outer liners consist of three major sections: the fuel baffle, the perforated screech liner, and a transpiration cooling liner. All liners are non-structural.

The fuel baffle forms the forward section of the liners and prevents fuel from entering the inner and outer cooling flow annular areas. The middle section of the liners is the screech liner, which is perforated with small holes whose open area is a predetermined percentage of the total area. This section absorbs the periodic combustion

energy fluctuations and prevents random pressure fluctuations from developing into cyclic vibrations of large amplitudes. To the rear of this section there are inner and outer transpiration cooled liners fabricated from porous metal. These liners protect the outer duct and engine cases from the high temperatures of the burning gases. They also form the outer wall of the annulus which carries fan discharge cooling air to the engine exhaust nozzle at the inner extremity of the fan discharge air passage. Fan discharge air is carried between the liners and the inner and outer cases through a series of liner supports that have graduated orifices to control the flow to every section of the liners, cases, and nozzle. The orifice areas are based on hole area only, and are unaffected by gaps between the outer liner and supports. At the end of the outer combustion case, cooling air is directed at the nozzle flaps to keep them from overheating, and, at the end of the inner case, air is directed into the exhaust stream. The outer rear section of the liner is convoluted circumferentially for reinforcement against buckling during duct heater operation. Longitudinal hot-section stiffeners are welded to the convolutions to prevent the convolutions from straightening out due to axial pressure loading, and to provide axial vibration control.

An additional liner of AMS 5536 material, located between the outer case and outer duct heater cooling liner and in the plane of the turbine blades, provides additional turbine blade containment. Design studies have shown that the necessary turbine blade containment can be provided at less weight by the addition of this liner in its relatively cool position than would be required by thickening the hotter turbine case.

High-temperature air is bled into the duct through the aerodynamic flameholder and is controlled by six piston-shuttle-type valves. These are mounted on the main engine combustion chamber outer case and are controlled remotely by the duct fuel control. With the fuel control in the "off" position, a two-way valve permits engine diffuser air to pass into one chamber of the control valve and actuate the piston to shut off the airflow. Moving the fuel control to the "on" position causes the two-way valve to vent the diffuser air overboard, allowing the combustion chamber air to enter the opposite end of the control valve. This air actuates the control valve to direct high-temperature air into the aerodynamic flameholder ring and subsequently into the duct stream.

Fuel is introduced into the duct through two separate systems. For

primary thrust augmentation (supersonic cruise operation), fuel is injected from a spray ring immediately downstream of the flameholder. This spray ring is a single circumferential tube supported by pylons from the outer case. For additional augmentation, fuel can be injected from the secondary spray rings located immediately upstream of the flameholder. The secondary fuel injection system consists of four circumferential tubes supported by pylons, and supplies fuel for additional augmentation at higher power settings.

The duct heater design is based on previous experience with afterburners for military jet engines. The duct heater, however, is expected to be more durable than are afterburners since the fan discharge air available for cooling is considerably cooler than the turbine discharge air used for afterburners.

c. Stress Analysis

The flanges on the outer duct diffuser case were analyzed using the theories of plates and shells and were designed to have stresses no greater than 80 per cent of the 0.2 per cent yield strength. The outer wall of the diffuser section is hoop stress limited with a maximum design stress of 80 per cent of the 0.2 per cent yield strength.

The heater duct cases are sized to resist buckling when subjected to maneuver loading with a safety factor of 1.3. The flanges were designed to resist blow-off and manuever loading with a maximum design stress equal to 80 per cent of the 0.2 per cent yield strength. The rear mount ring was designed to permit a displacement of the outer case from the normal position no greater than 0.2 inch.

The front liners and the containment heatshield liner were designed to resist vibratory loading. The rear outer liner is creep buckling limited and is designed to provide a buckling margin no smaller than 1.1 after 500 hours at Mach 3 at a minimum altitude of 58,500 feet or after 6,000 hours at Mach 3 at cruising altitude. The rear inner liner is hoop stress limited at the front with a maximum stress equal to 80 per cent of the 0.2 per cent yield strength. At the rear end, the rear inner liner is creep buckling limited and is designed in accordance with the criteria used for the rear outer liner.

d. Alternate Duct Heater Design

An alternate design of a ram induction type burner for the duct heater has been studied and is presented here as a possible alternative to the aerodynamic flameholder duct heater. Further development testing will be required to evaluate its full potential.

The ram induction duct heater (see Figure 2-34) for the STF219 engine burns fuel and air in an annular combustion chamber for primary augmentation, and in the air streams which bypass the combustor for additional augmentation.

Fan discharge air flows through the fan diffuser, where its velocity is reduced slightly. The relatively high residual velocity is utilized directly by the ram induction burner to inject primary combustion air into the combustion area. The high velocity ensures complete mixing for stable, efficient combustion. A dome extends forward of the burner into the forward duct heater case to separate the air into an inner, primary, and outer flow. The primary air enters the dome, where it is further diffused, and is then injected into the combustor through cast swirler vanes surrounding each fuel nozzle and through a series of chutes and turning vanes in the inner and outer walls of the combustor. The primary airflow is just sufficient to burn all the primary fuel.

When additional augmentation is required, fuel is injected into the two streams which bypass the main combustor. This fuel-air mixture is injected into the primary combustion stream by 69 vortex generators attached to the inner liner and by 96 vortex generators attached to the outer liner. The duct heater system, therefore, provides an augmentation potential ranging from very low to very high fuel-air ratios. The combustor has a single-thickness wall cooled by a boundary film along the inner surface. The dome section has a double wall with the outer wall being perforated and the inner wall porous for transpiration cooling. The combustor is supported at its forward end by eight radial pins which pass through the trailing edges of the forward duct heater case struts and into inserts in the dome section. The extended dome section is separate from the combustor but is integral with the forward duct heater case struts.

Primary fuel is injected through 48 dual-orifice fuel nozzles that are mounted in groups of 12 on 4 feeder manifolds located within the extended dome section of the combustor.

Secondary fuel is supplied through a series of variable-area pintle nozzles in the inner and outer spray rings.

Ignition for the duct heater is provided by two continuously operating electrical igniters which penetrate into the dome section of the burner. Secondary fuel flow is ignited by the combustion in the primary zone.

10. DUCT HEATER NOZZLE

The duct heater nozzle area is variable by a system of interlocking flaps and seal segments actuated by hydraulic pistons through a linkage system. Figures 2-52 and 2-53 show the duct heater nozzle and ejector reverser for Lockheed and Boeing, respectively.

The nozzle flaps are investment castings of PWA 658 (IN-100) nickel-base alloy. The flaps are stiffened by longitudinal and diagonal ribs on their outer surfaces to provide adequate rigidity to ensure that binding or seal leakage will not occur. Twelve flaps are used, and each forms one side of a twelve-sided truncated pyramid with the smaller end forming the nozzle. The flaps are hinged to the duct case. The varying gaps between the flaps are sealed with sheet metal segments which are retained by sockets in the flap hinge and which interlock with lugs along the sides of the adjacent flaps.

The flaps are actuated by hydraulic pistons which move a unison ring axially. Coupled to the ring are bell crank linkages which move the flaps. The unison ring serves to distribute the actuating load uniformly and ensures proper functioning of the nozzle flaps in the event of unsymmetrical loading.

The hydraulic actuators are pin mounted to brackets attached to the fan duct. Their shafts are attached to clevis fittings on the ring. The actuators are fabricated primarily of AMS 5643 (17-4PH) stainless steel to provide the proper strength and wear characteristics. Fuel, cooled by a continuous recirculation system, is supplied to the cylinders from the augmentation control.

Sealing is accomplished by a two-section shaft seal with a drain between the sections. The seal housing is designed such that recirculating fuel protects the seals from high temperatures. The seals are protected from contaminants by the cast iron bushing in which the shaft rides, which has two grooves to trap contaminants. The actuator cylinders and seal housings are designed to withstand fluid pressure surges.

The travel limits of the flaps are adjusted at the actuator. The minimum nozzle area is adjusted at the ends of the rods and the maximum

nozzle area is adjusted with stop nuts on the actuator shaft. In the event of a pressurizing system failure, the actuators would allow the flaps to open.

The actuator shafts are connected to a unison ring, which is a short sheet metal cylinder made from AMS 4910 and AMS 4926 titanium alloy and stiffened at both ends by rings with a square cross-section. Twelve rollers are equally spaced around the outside of the ring and attached to the stiffening rings. These rollers ride in axial channels in the ejector shroud support strut and prohibit circumferential motion of the ring while permitting axial motion with low friction. The roller system is designed to prevent cocking and binding of the ring when subjected to unsymmetrical loading.

To the rear, clevis fittings on the ring provide for the attachment of the bell crank linkage system. The bell crank provides a lever ratio of approximately 2:1 to reduce the required actuation forces. The linkages connect to the flaps at the center of the gas pressures so that the gas loads are concentrated on the link assembly and transmitted to the support strut of the ejector. The linkage system is made from Waspaloy (PWA 1061 and PWA 687) nickel alloy.

H. EJECTOR REVERSER

a. General Description

Thrust reversal is accomplished by an ejector-reverser system. The system incorporates a set of blow-in doors, trailing edge flaps, thrust reversal flaps, and a basic fixed structure or ejector shroud attached to the engine by integrally welded axial struts. The ejector reverser for Lockheed and Boeing are shown in Figures 2-52 and 2-53, respectively.

b. Ejector Reverser

The ejector shroud is the structural and load transmitting component of the ejector system. It serves as a housing and seal for the blow-in doors. It supports and stores the reverser flaps and actuating mechanism, and it provides an attachment ring for the trailing edge flaps.

Structurally, the ejector shroud is a cylinder fabricated from AMS 5542 (Inconel X) sheet, and is attached to the engine outer case by means of 12 equally spaced struts. The ejector and reverser loads are transmitted by these struts which are also fabricated from AMS 5542 (Inconel X) sheet. Each strut has a trapazoidal cross section and occupies 8 degrees of the shroud circumference. Lips on the outer edges of the struts provided to support and seal against the blow-in doors add an additional 1 degree of circumference, and therefore the struts cause a total blockage of blow-in-door flow of 108 degrees. The bending moment from the ejector shroud loading is carried by the support struts as either tension or compression with a sinusoidal distribution around the engine periphery. Shear forces are also sinusoidal but are displaced 90 degrees from the compressive or tensile forces. The struts also carry a uniform load caused by the axial differential pressures acting on the shroud, the reverser, and the tail-edge flaps.

Inside the struts are the hydraulic actuators for the reverser, and a number of bulkheads to stabilize the strut loading. The outer panel section of each support is removable to provide access to the reverser actuator.

The nose section and fillet pieces between the reverser flaps are secondary structures and form part of the aerodynamic throat surface of the ejector. When the reverser flaps are retracted, they provide the inner throat surface of the ejector shroud.

c. Blow-In Doors

Twelve blow-in doors are located around the ejector periphery in front of the shroud and between the support struts. They may be conical or canted slightly if required. For the Mach 2.7 airplane, AMS 4910 titanium alloy is used for the blow-in doors, and for the Mach 3 airplane, AMS 4910 material is used for the front section and AMS 5525 stainless steel for the rear section.

During normal operation, the blow-in doors are self actuating. Below Mach 1.3, the doors are generally open, and, above Mach 1.3, the doors are closed. During reverser operation, some of the doors are held open to exhaust the reversed gases, and others are held closed to protect particular areas of the airframe. The number of doors held closed depends on the requirements of the airframe manufacturer. Boeing requires five doors to be closed and Lockheed requires four to

be closed. Other blow-in door and ejector designs required to accommodate specific airframe specifications such as conical or tapered nacelle lines are possible.

Each blow-in door is fabricated in two sections, a forward section and a rear section. The use of two sections allows the doors to assume appropriate angles for inlet flow and yet return to a cylindrical configuration for supersonic flight. The doors are formed from two pieces; a smooth outer sheet, and an inner waffle sheet for reinforcement. Forged hinges are welded to each section, attaching them to the support struts. A set of links connects the two door sections to synchronize their action. When the doors are closed, they act essentially as a single plate supported by adjacent struts. The outer sheet acts like a membrane rigidly supported by the inner sheet, which transmits the load to the strut. During thrust reversing, the doors act as an overhung beam on two supports, with the longitudinal section of the sheet structure transmitting the pressure load into the hinge points of the actuating mechanism.

d. Thrust Reverser

The articulated flap design shown in Figure 2-54 is capable of ground or inflight reversing and null thrust, in addition to deflecting the thrust on the ground to prevent the exhaust jet from striking vulnerable objects. These functions are achieved by activating the reverser flaps in unison or singly either fully or partially as required. Particular arrangements have been coordinated with the airframe manufacturer.

The reverser flap assembly consists of a main flap, a tip flap (incorporating a cascade), an A frame link which attaches to the main flap, a link from the A frame to the tip flap, two adjustable stabilizing links from the A frame to the rear ring of the shroud, and one actuator link from the A frame to a track and roller assembly which guides the mechanism and the actuator.

The main flap and the tip flap are investment castings of PWA 655 (Inco 713C) nickel-base alloy. The flaps are strengthened and stiffened by longitudinal and lateral ribs on the rear surfaces. The flaps have a high stress margin, adequate rigidity, and were designed in accordance with good casting design practice. Rigidity is an important characteristic of the flaps since deflection could cause binding in the mechanism. To ensure smooth performance, the links are attached to the flap section at the longitudinal ribs on the rear surface. These ribs and hinge points are located to provide the best stability of the flap in the extended position while allowing proper clearances

for the folded retracted flap. The two hinge points on the main flap and the double link extending back from the flap to the rear shroud ring provide a stable four-point support.

The A frame link is forged but has machined ends and fittings. The remaining links are made of hollow tubes with forged fittings welded at each end, and are machined to accept a bearing. Some of the links include an adjustment nut for proper alignment during assembly.

Each flap is operated separately by its own actuator. Incorporated into the actuator is an inflight lock mechanism to hold the flaps in the retracted position when not in use. The locking mechanism consists of a locking pin, a piston, and a spring. The pin engages a groove in the head of the piston to lock the piston in place. The locking stroke and holding load is provided by the spring, hence, if hydraulic pressure is lost, the reverser flaps will remain locked in the stowed position. When the actuator is pressurized, the pressurizing fluid (fuel) enters the locking pin piston and disengages the pin. At the same time, the piston continues for a short stroke to open the port to the actuator cylinder. Use of a control valve in the locking cylinder ensures that the locking pin is removed before the actuator is pressurized.

An important characteristic of the articulated flap design is that the tip flap is extended and retracted rapidly. Hence, the major segment of the reverser is nearly fully extended before the tip section protrudes into the gas stream. This design permits the reverser flaps and the actuating mechanism to be subjected to lower stresses during extension than would be encountered if the tip were extended earlier.

Loading from the reverser flaps is transferred to the ejector shroud at the forward ring through the flap hinges and through the link to the roller and track assembly mounted in the support strut. Loading is transferred to the rear ring through the stabilizing links of the mechanism. These links are located so that the load reaction is taken through the shear section of the rear ring. Maximum loading occurs when the flap is fully extended and the flap and link mechanism is at its maximum mechanical advantage. Maximum stresses occur in the flaps at the points of attachment to the links and at the hinge fittings. The maximum stress in the A frame is from bending, whereas the maximum stresses in the other links are compressive.

One important feature of the reverser system is its ability to deflect the exhaust jet by actuating only a portion of the thrust reverser flaps to protect vulnerable areas from engine exhaust blast during engine

DOWNGRADED AT 3 YEAR INTERVALS
DECLASSIFIED AFTER 12 YEARS
DOD DIR 5200.10

THIS DOCUMENT CONTAINS INFORMATION AFFECTING THE NATIONAL DEFENSE OF THE UNITED STATES WITHIN THE MEANING OF THE ESPIONAGE LAWS, TITLE 18, U.S.C., SECTIONS 793 AND 794. THE TRANSMISSION OR THE REVELATION OF ITS CONTENTS IN ANY MANNER TO AN UNAUTHORIZED PERSON IS PROHIBITED BY LAW.

run-up at the airport facility. For deflecting the exhaust jet, best results will be obtained when the five top flaps are not fully activated. Also, it is desirable to have the movable tip section removed from the gas path. A mechanical lock in the actuator can be supplied to hold the reverser flap in a partially extended position for deflection purposes. The exhaust deflection capability adds no appreciable weight to the exhaust system.

Another important feature of the reverser is the cascade contained in the articulating flap. This cascade serves to spoil the forward thrust component produced by the hot inner engine gas stream. The hot gases are deflected against the inner nozzle wall during reverse while the cooler fan air is discharged forward through the open blow-in doors. This has the advantage of minimizing the temperature of any reversed air which might be reingested.

e. Cooling

To maintain temperatures within suitable limits for presently available materials, secondary air is required to film cool the inner injector surfaces during full duct heater operation above Mach 1. Two systems have been designed in coordination with the airframe manufacturers.

Lockheed System - For the Lockheed aircraft, cooling air at ram temperature is obtained from the aircraft inlet. It is brought back within the nacelle to a series of pressure-operated doors in front of the blow-in door hinge where it enters the area between the fan duct nozzle and the blow-in doors. A small portion of this air is routed into the ejector shroud cavity to protect the structural parts, the bearings, and the roller surfaces. The pressure-operated doors prevent exhaust gases from flowing forward through the cooling air system during the reversing mode and any operating conditions where the downstream pressure is greater than the upstream pressure.

Boeing System - For the Boeing airplane, cooling air is obtained from the aircraft inlet via the outer circumference of the engine inlet case at ram pressure and temperature. This air is ducted through several tubes to the rear mount ring through which it is distributed around the engine at the front of the ejector. Self-actuating check valves in the tubes prevent exhaust gases from flowing forward through the cooling system during the operating conditions mentioned in the preceeding paragraph.

DOWNGRADED AT 3 YEAR INTERVALS
DECLASSIFIED AFTER 12 YEARS
DOD DIR 5200.10

THIS DOCUMENT CONTAINS INFORMATION AFFECTING THE NATIONAL DEFENSE OF THE UNITED STATES WITHIN THE MEANING OF THE ESPIONAGE LAWS, TITLE 18, U.S.C., SECTIONS 793 AND 794. THE TRANSMISSION OR THE REVELATION OF ITS CONTENTS IN ANY MANNER TO AN UNAUTHORIZED PERSON IS PROHIBITED BY LAW.

f. Trailing Edge Flaps

Twenty-four trailing edge trapezoidal flaps are attached to the rear ring of the ejector shroud. The free-floating flaps are actuated by the difference in pressures on the inner and outer surfaces and vary the exit nozzle area within preset limits.

The flaps are made from PWA 1030 (Waspaloy) sheet attached to a framework of formed Waspaloy ribs. The integral frame structure is rigidly attached to a forging of PWA 687 Waspaloy designed to concentrate the flap loads at the tie-bolts. The tie-bolts, located near the center of pressure, have spherical ends to compensate for misalignment. The forward machined hinge fittings of PWA 687 are bolted to the trailing edge flaps at the longitudinal ribs for the maximum load distribution. When fully extended, the flaps are restrained by the tie-bolts. At the maximum inner position, the flaps rest against forged stops.

At the limits of travel, the loading on the flaps is similar to that of an overhung beam on two supports. Maximum loading occurs when the trailing edge flaps are against the outer stops.

A machined sleeve in the tie-bolt system permits the travel limits to be adjusted. Sealing between adjacent flaps is accomplished by overlapping sheet metal strips trapped against the upper and lower surfaces of the flaps by a tongue-and-groove construction.

12. ASSEMBLY OF MAJOR COMPONENTS

Assembly and disassembly of the major assemblies can be accomplished with the engine in a horizontal position provided the proper fixtures and procedures are used. Figure 2-55 shows the major assemblies of the engine. Figure 2-56 shows the assembly sections of the duct heater nozzle and ejector.

a. Fan Assembly

The first-stage rotor assembly, second-stage rotor assembly, first-stage stator assembly, and the first-stage rotor abradable seal, which comprise the fan section, are assembled as a complete unit during final engine assembly. The rotor is dynamically balanced by adding weights on both disks. Assembly and static balancing techniques are utilized to minimize unbalance in the correcting planes prior to final dynamic balancing of the rotor assembly.

b. Intermediate Section Assembly

The fan exit guide vanes are assembled to the splitter ring. The middle and rear fan cases are bolted together with the vanes and bushings sandwiched between the flanged joint. The second-stage vanes are installed in the splitter ring. The front and rear inner shroud cases are bolted together with the second-stage vanes and bushings sandwiched between the flanged joints. The levers, unison ring, and related hardware are installed to complete the subassembly of the aerodynamic brake. The front mount rear support case is positioned against the front flange of the intermediate case.

The aerodynamic brake subassembly is inserted inside the front mount rear support case and bolted to the intermediate case with the front mount rear support case flange sandwiched between these members. Radial bolts attach the splitter section to a support on the intermediate case struts. The other components including the tower shafts, Number 1 bearing and seals, Number 2 bearing and seals, support sections, and heat shielding are attached at final engine assembly. The accessory drive gearbox and lower tower shaft can be assembled or removed from the engine without disturbing other sections of the engine.

c. High-Pressure Compressor Assembly

The high-pressure compressor is assembled vertically beginning with the rear shaft. The seventh-stage rotor is installed over the tie bolts which are inserted through the shaft. The stator assemblies and rotor assemblies with their spacers and seals are installed alternately over the tie bolts. The rotor front spacer assembly and the compressor front hub are the final members installed over the tie bolts. The tabwashers and the tie bolt nuts are then installed. The nuts are secured after proper torque has been applied. The third-stage stator is positioned and the remaining third-stage rotor is attached to the front spacer assembly with bolts and tabwashers. The seventh-stage seal support is attached to the disk. The seventh-stage seal is bolted to the support. The stator cases may be bolted together after installing each stage or after the rotor assembly has been completed. The rotor is dynamically balanced by adding weights on the third-stage disk and the seventh-stage rotor seal. Pratt & Whitney Aircraft utilizes assembly and static balancing techniques to minimize unbalance in the correcting planes prior to final dynamic balancing of the rotor assembly.

d. High-Pressure Compressor and First-Stage Turbine Assembly

The first-stage tie bolts and their retaining rings are assembled on the

[illegible]

flange of the high-speed turbine shaft. The rear labyrinth seal-spacer is installed over the turbine shaft. The rear compartment case, rear labyrinth seal ring, rear labyrinth seal assembly, insulation assembly, and the rear face seal assembly are slid over the spacer. The rear face seal plate, the inner race and rollers of the Number 3 bearing, the oil scoop, the forward face seal plate, and the front labryinth seal and spacer are installed over the high pressure turbine hub. The retaining nut is threaded on the turbine shaft and torqued to a prescribed value. The Number 3 bearing support subassembly which contains the bearing outer race, spanner nut, tab washer, and flange seal is slid over the bearing rollers and piloted into the rear face seal support assembly. The rear labyrinth seal assembly is piloted onto the carbon seal support flange to complete the high turbine shaft, bearing, and rear compartment sub-assembly. Several temporary flange bolts and nuts may be used to hold the rear compartment together prior to completion of assembly procedures.

To start the assembly of the diffuser-burner section, the Number 3 bearing front compartment insulation and the compartment external support are slid over and assembled to the front face seal support assembly. The front labyrinth seal assembly is then piloted onto the compartment support flange. Several temporary bolts may be used to hold the forward compartment together prior to completion of assembly procedures.

The compressor seventh-stage rotor seal assembly is bolted to the front inner flange of the diffuser case. The combustion chamber inner front case is bolted to the diffuser case rear inner flange. The Number 3 bearing front compartment subassembly is piloted onto the combustion chamber inner rear flange and retained by several countersunk screws which facilitate assembly. All plumbing between the diffuser case and the bearing compartment is installed. The oil lines inside the Number 3 bearing front compartment are installed. The temporary flange bolts in the bearing front and rear compartments are removed. The flange seal is installed on the bearing support. The bearing front and rear compartments are bolted together, along with the high turbine shaft, bearing, and seal rotating parts. Access to these bolts is obtained by sliding the rear compartment case in the rearward direction. The rear compartment case and the high-pressure labyrinth seal ring are attached to the rear labyrinth seal ring assembly with flange bolts.

The front section of the annular burner is inserted in the rear section of the diffuser case and retained by radial pins assembled through the diffuser case. The combustion chamber outer front case is bolted to

the diffuser case rear flange. The combustor rear inner and outer liners are slid forward on the front burner section. The combustion chamber inner front case is assembled to the turbine nozzle inner case with flange bolts. The combustion chamber inner rear case is assembled to the first-stage vane inner support by sliding its scalloped front flange through the scalloped front flange of the vane support. The nozzle vanes are inserted into the vane inner and outer support rings. A temporary segmented bolted ring may be used to retain the vanes in the outer support ring. The nozzle vane subassembly is slid over the Number 3 bearing compartment until the trapped bolts in the rear flange of the inner front combustion chamber case engage the flange holes in the inner rear combustion chamber case. The nuts are assembled and tightened to a prescribed torque value. Radial bolts are assembled to anchored nuts which are attached to the burner inner liner. These bolts are not completely engaged until further assembly is completed.

The burner inner liner is slid to the rear and the radial bolts are aligned with the holes in the vane inner support ring. The bolts are tightened. The temporary segmented ring retaining the vanes to the outer support ring is removed. The burner outer liner is slid to the rear and assembled to the vane outer support ring. The combustion chamber rear outer case is assembled to the diffuser case and to the vane outer support ring.

The high pressure compressor exit guide vane assembly is assembled to the diffuser case by engaging slots in the vane inner shroud with the pins protruding from the case front inner flange.

A classified spacer, which positions the turbine rotor correctly, is installed on the compressor rotor rear hub. The compressor assembly and classified spacer are installed by engaging the compressor rear hub spline with those in the turbine hub. The block and the spanner nut are installed on the compressor hub and tightened to a prescribed torque value. The nut is secured by bending the washer tab. The first-stage turbine disk seal is attached to the plate support ring. This subassembly, rotor assembly, rotor rear seal, tabwashers, and nuts are assembled to the turbine hub. The complete assembly of the high-pressure compressor and the turbine is dynamically balanced by adding weights on the disks of the third stage compressor and the first stage turbine.

e. Low-Pressure Compressor Turbine Assembly

The second-stage turbine rotor assembly, the rear hub, and the seal disk assembly are assembled to the second-stage rotor shaft and may be retained by several temporarily installed bolts. The second-stage blade seal ring and ring seal are inserted into the turbine rear case. The second-stage rotor and shaft sub-assembly is inserted into the turbine rear case. The third-stage vanes are installed into the inner support ring and retained by attaching the rear seal. The third-stage vane subassembly is inserted into the turbine rear case with the vane lugs engaging those in the blade tip seal ring. Any temporarily installed bolts used to retain the members in the second-stage rotor subassembly must be removed. The outer spacer seal is piloted on the second stage disk. The third-stage blade seal ring is inserted behind the third-stage vanes and attached to the turbine case rear flange using several temporarily installed bolts. The third-stage rotor assembly is inserted behind the third-stage vanes and bolted to the second-stage rotor and shaft subassembly. Axial and radial positioning of the rotor relative to the stationary members, prior to final engine assembly, is accomplished by the use of proper fixtures. The rotor is dynamically balanced by adding weights on the low-pressure turbine shaft and on the third-stage disk. Pratt & Whitney Aircraft utilizes static balancing in the correcting planes during rotor assembly prior to final dynamic balancing of the completed rotor assembly.

f. Turbine Exhaust Assembly

The bearing outer race and spanner nut is installed on the bearing support. The oil scavenge pump is attached to the pump support which in turn is mounted on the rear side of the bearing support. The bearing front compartment subassembly consisting of the front labyrinth seal assembly, insulation assembly, and carbon liner assembly is positioned on the front face of the bearing support. The rear oil sump, insulation assembly, and heatshield assembly are attached to the rear face of the bearing support with bolts engaging the nuts anchored to the front labyrinth seal assembly. This complete compartment subassembly is bolted to the front flange of the turbine exhaust case. All tubes connected to both the bearing compartment and the turbine exhaust case are installed. The tail cone is bolted to the rear inner flange of the turbine exhaust case.

13. ENGINE ASSEMBLY

a. Intermediate Case Assembly

The subassembly of the towershaft gear and bearings is fastened to the towershaft mounting pad. The Number 2 bearing and classified spacer are slid onto the accessory drive gear. This group is installed in the intermediate case with the bearing outer race retained by a keywasher and nut. The carbon seal face plate is slid on the accessory drive gear. The rear carbon seal assembly with the face plate and heatshield are assembled to the intermediate case. The rear labyrinth seal is piloted on the carbon seal. By using proper fixtures, the high-pressure compressor and turbine rotor assembly section is assembled to the intermediate case assembly with the compressor front hub engaging into the accessory drive gear splines. The nut and retaining members lock the rotor assembly to the intermediate case assembly.

b. Low-Speed Turbine Assembly

The first-stage blade tip seal ring and ring seal are inserted and positioned in the turbine front case. The second-stage turbine vanes are inserted into the vane inner support ring and retained by attaching the rear seal to the support. The vane subassembly is inserted with the vane lugs engaging those in the first-stage blade tip seal ring. This vane and case subassembly is then bolted to the first-stage support ring. The low speed turbine rotor assembly is inserted behind the second-stage vanes and installed with the turbine rear case bolted to the front case. The low speed turbine rear bearing, carbon seals, and spacers are slid on and attached to the low-speed turbine shaft with the retaining nut. The oil scavenge pump drive shaft, seal, and seal plate are inserted into the rear hub and locked to the retaining nut.

c. Turbine Exhaust Assembly

The turbine exhaust assembly is slid over the bearing rollers on the turbine shaft. The turbine exhaust case is bolted to the turbine rear case with the third-stage blade seal sandwiched between the case flanges. Fixtures will be used to axially retain the low-speed rotor prior to assembly of the fan section to the intermediate case assembly.

d. Fan Section Assembly

The inner shaft seal face plate and laybrinth seal are attached to the front hub of the high-pressure compressor with the spanner nut. The nut is retained by bending a tab on the keywasher and then installing

the snap ring. Oil jets are installed. The front carbon seal assembly is slid over the fan rotor hub. The front bearing is installed on the bearing support and retained with the key washer and nut. This subassembly, oil scoop, face plate, and front labyrinth seal are slid onto the fan rotor hub. The tachometer gear is positioned on the oil scoop splines and the inner shaft carbon seal is slid over the fan hub behind this gear. The loose rotating members on the hub are retained by the spanner nut. This nut is secured by bending the tab on the key washer and then installing the snap ring. The inner shaft carbon seal assembly is slid on the seal support and retained by the spanner nut and key washer. The classified spacer positioning the low speed turbine rotor is installed. The fan rotor hub subassembly and heatshields are assembled to the intermediate case with the hub splines engaging the turbine shaft. The bearing face washer is installed on the hub. The low speed turbine rotor is locked to the fan rotor hub with the tiebolt and retained.

Air tubes are installed. The engine mount case is inserted and positioned against the engine mount support case. The fan section is inserted with the rotor engaging the trapped bolts in the rotor hub and the stator case mating with the middle fan case. Rotor bolt spacers and nuts including the first-stage blade retainers are installed. The engine mount case is slid forward to provide access for the installation of the fan case bolts. The engine mount case is slid rearward and bolted to the engine mount support case. The aerodynamic brake actuator mechanisms, actuators, and mounting brackets are installed.

e. Fan Diffuser Duct Assembly

The fuel nozzle flange seals are inserted over the fuel nozzles. The annular burner fuel nozzles are installed with the nozzle end inserted into the burner swirlers and the flange end attached to the diffuser case. One segment of the split fan diffuser duct is installed to the rear section of the intermediate case. All fuel and oil lines are assembled to the engine cases. The tubes are routed through the duct joints to simplify the installation of these lines. The second half of the split fan diffuser duct is installed and bolted to the intermediate case and to the other half of the fan diffuser duct.

f. Duct Heater Section

The front inner liner is slid over the compressor diffuser case and piloted on the fan diffuser duct. The flameholder air shutoff valves are attached to the combustion chamber case. The secondary fuel

DOWNGRADED @ 3 YEAR INTERVALS
DECLASSIFIED AFTER 12 YEARS
DOD DIR 5200.10

spray ring segments and fuel manifold and a segment of the front outer liner are attached to the forward duct heater case. This subassembly is slid over the engine and bolted to the rear flange of the fan diffuser duct. The flameholder segments are attached to the pads on the preassembled shutoff valves and on the combustion chamber case. The primary fuel spray ring segments are inserted into the outer liner and mounted to the forward duct heater case. The outer liner is positioned on the rear flange of the forward duct heater case. The inner cooling liner is slid over the engine and bolted to the front inner liner. The rear inner liner is slid over the engine and attached to the rear end of the inner cooling liner and the liner support ring. The exhaust nozzle subassembly is attached to the rear flange of the turbine exhaust case. The spark igniters and their related parts are installed.

g. Assembly of Duct Heater Nozzle and Ejector

The ejector can be completely assembled before being installed on the engine. The duct heater nozzle unison ring must be installed on the ejector support struts before installing the ejector shroud assembly to the engine, otherwise, the ejector assembly may be built up from the engine without using the ejector-reverser as a separate assembly. The assembly of the ejector-reverser will be explained as a complete unit before final assembly to the engine.

Beginning with the ejector shroud or afterbody, the reverser main flap and tip flap are assembled into the hinge fittings at their proper locations. From the rear of the ejector shroud, the linkage is assembled to the flaps and shroud. The reverser actuators are mounted in the support struts and connected to the reverser linkage and rollers. Adjustments for the flaps and linkages are made with adjustment nuts on the rear links and actuator rods.

Having completed the thrust reverser, the trailing edge flaps are attached to the shroud rear ring. They are assembled by inserting the seal segments and tie-bolts in sequence as the flaps are assembled. Access panels for the tie-bolts are fastened after all flaps are assembled and adjusted.

The blow-in doors are inserted between the support struts, and the hinges are assembled. The linkage for the reversing requirements on the doors is assembled from the inside together with the front and rear door synchronizing links. After making all adjustments, the duct heater nozzle links are attached to the support struts. The uni-

son ring with the rollers is inserted from the front into the roller tracks on the support struts. The flap connecting rod is installed between the flap bellcrank and unison ring.

The duct nozzle flaps with the seal segments are assembled onto the fan duct at the hinge fitting and the outer rear liner attached before the fan duct is installed into the ejector. A series of bolts are inserted at the rear fan duct ring and the engine mount, securing the fan duct and ejector. The duct burner nozzle actuators are mounted to the fan duct. At this point in the assembly, for Lockheed only, the secondary air valves with supporting hardware are assembled. After connecting the actuators to the unison ring, the nozzle flap links are assembled to the flaps, then the duct heater nozzle can be adjusted for proper minimum and maximum opening, with the adjustment stops on the actuators.

This ejector assembly is assembled to the main engine over the primary nozzle and is bolted to the fan duct heater flange. For the Boeing installation, the secondary air tubes and valves are installed. The supply and drain lines are connected to the actuators. The feed back system is installed and all access panels are fastened.

h. External Accessory Assembly

The towershaft and accessory drive gearbox assembly are installed. All engine accessories, electrical wiring, and tubing are now added to complete the assembly of the engine.

14. PRELIMINARY VIBRATIONAL ANALYSIS

a. Fan Stages

The first-stage blade chord was selected to provide adequate bird ingestion resistance.

The first-stage shroud was placed at a part span location to eliminate aerodynamic stall flutter which occurs at low corrected rotor speeds. Flutter resistance is thus provided by an increase in blade frequency and by damping through the proper selection of the shroud contact angle.

The first-stage fan integral hub location was set to prevent a 2 E standing wave resonance from occurring in the running range and to keep the 3 E resonance at low power.

The second-stage blade aspect ratio was selected as large as possible while still maintaining adequate flutter resistance, 2 E margin, and foreign object resistance. Rotor construction provides rim spacers to enforce a node at the disk rim and thus provide the maximum 2 E blade disk frequency for minimum weight.

The resonance diagrams shown in Figures 2-57 and 2-58 present calculated rotor stage natural frequencies and resonances.

b. Compressor Stages

The high-pressure compressor rotor stages (stages 3 through 7) for the STF219 are advanced, high work, high aspect ratio, light weight stages. The resultant higher aspect ratio is offset by optimizing the locations of the rim spacers and bolt circle to tune the coupled blade disk frequencies to eliminate a 2 E standing wave resonance from the engine running range. Stages 3 and 7 incorporate extended roots and friction damping to avoid high vibratory stress.

Figures 2-59 and 2-60 indicate typical compressor rotor stage resonance diagrams.

c. Turbine Stages

The first and second turbine stages incorporate extended root, friction damped blades to produce favorable vibration characteristics.

The third turbine stage employs light weight, tip shrouded blades. The tip shrouds provide the blade stiffening required by raising the cantilever mode frequency to a fixed pinned or shrouded mode. The tip shrouds also provide friction damping if they slip and a mechanical seal to reduce aerodynamic losses.

Shroud contact angles are set at least 12 degrees higher than the angle of blade tip motion in a pure cantilever mode to prevent the blade from vibrating in the first cantilever mode. Turbine tip shrouds are pretwisted to provide shroud contact forces for optimum damping and to control shroud wear.

The 3 turbine stages were designed to have 2 E and 3 E standing wave resonances outside the engine running range. The use of rim spacers has effectively reduced the stage weight by enforcing a disk mode at the point of spacer contact.

d. Critical Speeds

The STF219 engine adheres to the basic critical speed requirements established in the design criteria section of this report. The rotor design reflects the light, efficient components characteristic of advanced compressor and turbine design. The use of these components allows reduction in the rotor shaft and hub thicknesses. Greater thickness would be required to provide stiffness if heavier compressor and turbine components were used.

The compressor rotor of the STF219 is designed to the above stiff system criteria. Due to its length, the turbine rotor is designed to avoid rotor critical speeds in the operating range. The estimates of the STF219 stiff bearing critical speeds are tabulated below, and shapes corresponding to these preliminary estimates are shown in Figures 2-61 and 2-62.

	High Speed Rotor	Low Speed Rotor
Stiff Bearing Critical Speed (rpm)	11505	7933
Normal Operating Speed (rpm)	8650	6300
Ratio of Critical Speed to Maximum (Per Cent)	133	125

15. THRUST BALANCE

a. Introduction

The thrust bearing load is the summation of net axial aerodynamic and pressure loads on the compressor and turbine rotors. The tendency toward a wide bearing load variation between engine operating points is primarily a function of the engine matching characteristics altitude and Mach number requirements for the supersonic transport flight envelope. It is important that the wide variation never results in a "no load" situation on the thrust bearings in going from a net forward thrust condition to a net rearward thrust condition. As flight Mach number increases, the pressures at the front end of the engine tend to increase relative to those at the rear of the engine causing a net increase in rearward load. This characteristic has been utilized to advantage on the STF219 engine by designing the rotor thrust balance system to maintain a net rearward load on each rotor at all flight conditions. As the

aircraft progresses from sea level to higher altitudes, the load on the rotors tends to decrease as a result of lower pressures. This effect is, however, countered by the tendency toward greater rearward rotor loads resulting from increasing Mach number. Thus, at the high altitude, low pressure, high Mach number flight conditions the net rotor load is comparable to the low altitude, low Mach number, high pressure flight conditions. This approach eliminates the need for pressure modulation required in a system incorporating positive thrust load.

b. Design Approach

The primary areas used for rotor load adjustments are the internal cavities ahead and behind the high- and low-pressure compressor and turbine components. By venting two of these cavities directly to fan inlet pressure, which is primarily a function of ram pressure, an acceptable bearing life is obtained while still providing the system flexibility and the adjustments which may be necessary as a result of design modifications during the development phase. A brief summary of the design requirements of the internal cavities follows. The pressurizing airflow pattern is shown in Figure 2-63.

The fan front cavity and the high-pressure compressor front cavity are not pressurized. Pressurization in these areas would induce leakage into the fan and high-pressure inlet, resulting in reduced engine performance and compressor efficiency. Pressurization of these cavities would also increase fan and initial high-pressure compressor disk temperatures. It would then become necessary to replace the present titanium fan disks with steel disks and increase the high pressure compressor disk sizes at a substantial weight penalty.

The rear fan cavity is vented to the fan inlet pressure to obtain a rearward thrust loading on the low-speed rotor and minimize the effect of the fan pressure ratio on the rotor thrust. The seal isolating the cavity from the main gas path is located at a large diameter, but, the relatively low pressure differential across this seal produces almost negligible leakage. Vented air is piped out rather than vented through the front hub which would produce a hot recirculated boundary layer around the fan disks.

The high-pressure compressor rear cavity is also vented to the pressure upstream of the fan. This produces a pressure in the cavity slightly greater than the inlet ram pressure providing the desirable

net rearward loading on the high-speed rotor while maintaining a bias to the inlet ram pressure which is required for consistent rotor thrust loads.

The compressor rear seal is located at an intermediate diameter which has been chosen to obtain the desired bearing loads. A seal disk is incorporated to minimize seal clearances and therefore seal leakage from the primary engine gas path.

The turbine front seal is placed at a fairly large diameter and the disk face inboard of this seal is pressurized with 90 per cent of compressor exit pressure, which is consistent with blade cooling requirements.

The inter-turbine seals are located as required for thrust balance and turbine disk and blade cooling requirements. The cavity is pressurized slightly above the immediate turbine gas stream pressures to provide sufficient blade and disk cooling airflows.

The rear turbine cavity is unpressurized.

16. FUEL AND OIL HEAT REJECTION SYSTEMS

The fuel and oil systems used in the STF219 engine are shown in Figure 2-64. The system is substantially the same as that used in the JT11F-11, -12 engine. However, whereas only one fuel-oil cooler was used in the previous system, the present system uses two. In the earlier design, the cooler always worked at the maximum temperature limit and only the excess heat load was transferred to the duct heater circuit. Consequently, the fuel and oil supplied to the engine were at the maximum levels, whereas the fuel supplied to the duct heater was substantially lower.

The revised system, using two fuel oil coolers, equalizes the fluid temperatures and produces lower average main fuel and oil temperatures. The system is controlled by two bypass valves. One is operated by a control signal from the duct heater control and prevents the duct heater components cooled by fuel flow from overheating during low duct fuel flow operation. The second is a thermostatic valve which opens at the maximum fuel temperature limit. This valve will normally remain closed since the system is designed to maintain the duct heater fuel temperature at the equalized design values. However, during transient operation when overheating might otherwise occur, the thermostat will limit the fuel temperature. In addition to the temperature control of the duct heater fuel, a bypass line is provided to limit the fuel pressure drop during high duct heater flow rates.

The present system still incorporates a method for returning fuel to the airframe when supplementary cooling is required. Initially, this system was controlled by a thermostatic valve. However, the airframe manufacturers have expressed some concern regarding the reliability of the thermostatic system and Lockheed suggested that a manual valve controlled by the power lever be used to permit a constant metered return flow whenever the engine flow drops below some predetermined level.

An alternate system would use a manual valve in series with the thermostatic valve which would safeguard against the possibility of the thermostatic valve opening and initiating supplementary return flow when it was not required. A final safeguard would be to parallel the thermostatic valve with a manually operated bypass to ensure supplementary return flow in the event that the thermostatic valve failed closed.

During Phase II-A of the SST proposal, the problems associated with the engine fuel-oil heat rejection system were studied considering the integrated airframe, engine, and fuel requirements. It was immediately recognized that a unilateral approach was necessary to attack this problem, since the engine is bounded by a dual interface; i.e., the fuel inlet temperature to the engine pump is set by the airframe heat rejection and fuel flow requirements, and the fuel outlet temperature from the engine fuel control must satisfy the thermal stability limits of the fuel. Furthermore, the fuel inlet temperature to the engine pump can, in itself, be influenced by the engine heat rejection with a return line-to-tank system, and hence an iterative situation can arise.

For these reasons, it was decided that Pratt & Whitney Aircraft would calculate the total engine fuel-oil system heat rejection for various flight conditions and supply this information to the respective airframe manufacturers. They in turn would then determine the fuel temperatures leaving the engine fuel control based on their knowledge of the inlet temperatures to the fuel pumps and required fuel flows for various flight conditions. This approach resulted in a consistent and meaningful evaluation of the maximum fuel temperatures that would be encountered in the SST airplane.

Figures 2-65 through 2-68 present the data supplied to Lockheed and Figures 2-69 through 2-73 present the corresponding data for Boeing.

The total system heat rejection rates during unbraked and braked windmilling for the Lockheed 700 lb/sec flow engine are as follows:

	Unbraked Rotor		Braked Rotor	
Mach Number	Rotor Speed (rpm)	Heat Rejection Rate (BTU/min)	Rotor Speed (rpm)	Heat Rejection Rate (BTU/min)
3.0	6550	8700	3800	5810
2.5	5950	7420	3800	5160
2.0	4950	5680	3800	4460

For the Boeing engine, braked windmilling at Mach 2.7 results in a rotor speed of 7950 rpm and a total heat rejection rate of 4800 BTU/min. Of this, 3170 BTU/min are required for the engine lubrication system, 800 BTU/min for the engine fuel pump, and 830 BTU/min for the hydraulic pump and environment.

The estimated fuel and oil temperatures for the Boeing and Lockheed missions are presented in Figures 2-74 and 2-75. The temperatures shown for the Boeing aircraft descent are based on an assumed return line control valve maximum setting of 325°F. Fuel and oil temperatures were not calculated for operation before cruise since the fuel flow rates will be high and the temperatures will be low.

It is noted that the twin spool STF219 engine is significantly different from the JT11F engine with regard to fuel and oil heat rejection characteristics. A twin-spool engine inherently has higher heat rejection requirements than a single-spool engine because of the additional bearings and seals and higher rotor speeds. In addition, the STF219 engine heat rejection system was modified by the addition of a second cooler, and benefits from an evaluation of the thermal stability limit of Jet A fuels which indicated that fuel limits above 275°F can be achieved.

17. EXTERNAL PLUMBING, BRACKETS, AND HARDWARE

a. General Description

The plumbing associated with the STF219 engine will be designed to provide durability and accessibility. However, it was not possible to

provide a complete arrangement of all the external lines required for the STF219 engine in the time period of the Phase IIA program since an engine mock up is necessary to accomplish effective routing. Detailed coordination with the airframe manufacturer is essential to ensure proper accessibility and adequate clearance between adjacent lines and engine and airframe components and structure. Lines are carefully routed to avoid fluid traps and to accommodate thermal expansion. Proper support for the lines by clips and brackets must be provided to fix their position and avoid resonant vibrations.

The high environmental temperatures associated with the SST engine installation preclude the use of elastomer seals and dictate the use of stainless-steel lines and metallic seal joints. The use of solid (non-flexible) tubing and metallic seal joints compounds the problem of assembly and thermal growth. The lines, therefore, must be fabricated accurately to minimize assembly misalignment and must be routed so as to provide adequate flexibility to accommodate thermal expansion. Where flexibility cannot be provided by routing of the lines, bellows or slip-type joints are required to allow for misalignment and thermal growth.

The high environmental temperature will also require the use of heat-shielding on certain lines to minimize heating.

b. Material Selection

Fuel and hydraulic lines are fabricated from AMS 5571 on PWA 1060 (Inconel) tubing. Air and oil lines are fabricated from AMS 5571 stainless-steel tubing.

c. Heat Shielding

A number of effective methods for heatshielding lines may be used. Frequently within the engine structure, concentric, double-wall tubing is used with the stagnant air gap between the tubing walls providing the insulating medium. This construction is used for the oil lines passing through the diffuser case struts in the STF219 engine, and is shown in Figure 2-76. A similar construction is employed in the oil lines passing through the intermediate case struts and turbine exhaust struts. This method of insulating fluid lines is successfully used in many Pratt & Whitney Aircraft commercial and military engines.

The use of thermal insulation tape and an outer corrugated metal foil shield for insulating fluid lines has been used extensively in the J-58 engine. The insulating tape is spirally wound around the tubing and

the corrugated metal foil shielding is then applied in halves. The foil is supported by sleeve segments and secured by Inconel lockwire. Sections of foil shielding are joined by hoop bands. A detailed sketch of the shielding assembly is shown in Figure 2-77.

A recently developed approach to the heat absorption problem is the use of low-emissivity coatings on lines and engine components. The application of gold coatings to fluid lines and certain engine components is now being used in the J-58 engine and is replacing the previously mentioned tape and foil heat shielding. This coating may be applied to steel, titanium, or aluminum by applying several light coats of special gold paint with a short baking period of 900°F after each coat. The resulting coating is 0.0001 to 0.0002 inch in thickness, and may be exposed to temperatures up to 1000°F without deterioration. This process is controlled by specification PWA-55.

d. Seals and Fittings

A number of different non-elastomer seals are available which are being used on current production engines. Sketches of these seals are shown in Figure 2-78. The chevron seal is made up of V-shaped stainless-steel strips and is particularly effective for sealing high pressure fluids. The spiral-wound gasket consists of spiral windings of stainless steel and asbestos. It can be made in any size required and is useful at temperatures up to 800°F. Its use is limited to oil and gas sealing. The angle gasket is recommended for use at locations which require sealing of dissimilar material. It requires a small clamping force and is usable for gas, oil, or fuel.

The metal-to-metal cone fitting with a thin nickel gasket between the mating conical surfaces has been found to provide an extremely reliable seal for external plumbing connections. The conical gasket with a separate brazed on ferrule or a ferrule which is formed integral with the tube provides a reliable and safe tube joint which is easy to assemble and disassemble.

e. Clamps and Brackets

Brackets and clamps are used to prevent fatigue failure resulting from excessive vibration and to prevent the chafing of lines and adjacent parts. The brackets and clamps are so spaced as to provide a resilient support for the tubes.

Depending upon environmental temperatures, brackets are fabricated from AMS 5542 (Inconel X) or nickel cadmium plated AMS 5504 (type 410) stainless steel. Clamps are made from AMS 5542 and AMS 5510 (type 321) stainless steel and cushioned with teflon-impregnated asbestos, stainless steel, or Inconel wire mesh. In certain applications, it is necessary to interpose a stainless-steel sleeve between the tubing and the clamp to prevent chafing of the tube by the clamp cushioning material. The antichafing sleeve is brazed to the tube.

Typical methods of joining tubes to brackets or to each other are shown in Figure 2-79.

8. ENGINE MOUNTS

a. General Description

The gas generator is supported both axially and radially by the intermediate case. Loads in the intermediate case are transmitted to the outer duct and engine mount system. The mount system supports the engine in the aircraft and is designed to transfer vertical, side, thrust, and torque loads to the airframe structure.

The engine attachment points are designed so that a single system may be used for either right or left engines. The final selection of the mount systems depends on the specific airframe requirements and has been coordinated with the individual manufacturers.

b. Design Criteria

The significant loads acting on the mounting system are maneuver loads, thrust loads, and gust loads.

The maneuver loads for which the mounting system was designed are specified in Figure 2-80. It was assumed that the pitch and yaw maneuvers act about the engine center of gravity and that the maximum flight loads to which the front and rear mounts will be subjected are as indicated in Figures 2-81 and 2-82. These loads were determined on the basis of the most severe maneuver condition anticipated or in some cases by loading conditions determined in coordination with the airframe manufacturers. Combinations of loads other than those specified may also be acceptable, but these should be reviewed if such loading is anticipated.

c. Load Limits

The maximum allowable flight loads produce stresses that are less than or equal to either 80 per cent of the 0.02 per cent yield stresses or 75 per cent of the critical buckling stresses, as applicable. The ultimate loads are at least 150 per cent of the limit loads. At ultimate loading, the calculated stresses exceed the yield strengths. However, with these conditions, local yielding will occur and the load on the structure will be redistributed, thus reducing the chances of a complete material failure.

d. Lockheed System

The mount system for the Lockheed airframe consists of three rigid attachment points and a fourth resilient point to carry loads in the event that one of the rigid attachments fails.

The mount rings are located in two planes perpendicular to the engine axis. The forward ring is located in front of the fan and carries two mounting points, each on the horizontal centerline. These mounting points are designed for a rigid ball-type fitting on one side and a resilient ball-type fitting on the opposite side to carry thrust, vertical, and side loads.

The rear mount ring is located behind the blow-in-door hinge and provides two attachment points, one on each side of the engine, and both 32.86 degrees above the horizontal centerline. The rear mount is designed to carry vertical and side loads on one side and vertical loads on the other, although a resilient link will enable side loads to be carried at the second attachment point should the rigid side link fail.

Maximum loading occurs with one G down, one and one-half G forward, two G to the side, a yaw velocity of one radian per second accelerating at three radians per second at maximum thrust, or with six G down, one and one-half Gs forward, one G to the side, and maximum thrust.

Axial loads are transmitted by the rigid front mount and as a moment through the two side supports. The pad for attaching the mounting ball has been positioned as closely as possible to the outer engine case to keep the loading eccentricity to a minimum, thereby reducing the resulting deflections and stresses. The side loads are transmitted by two of the side supports, and the vertical loads are transmitted by two vertical supports at the rear and one at the front of the engine.

Roll moments are transmitted by the vertical supports on the rear mount ring, yaw moments are transmitted by the two side supports, and pitch moments by the vertical supports.

e. Boeing System

The front mount attachment points for the Boeing aircraft are located on the engine inlet face to support the inlet. The engine mount rings are located in two planes perpendicular to the engine axis. The front mount ring, which is located just forward of the fan, has two attachment points located 22.5 degrees on each side of the vertical centerline. One point is designed to carry vertical, side, and thrust loads through a pin fitting, and the other point is designed to carry vertical and side loads through a link.

The rear mount ring is attached to the airframe by a single attachment point on the vertical centerline just forward of the blow-in doors. Vertical and side loads are transmitted to the ring through a yoke which attaches at two locations 15 degrees on either side of the vertical centerline.

In addition to withstanding the maneuver loads, the mount system was designed to withstand gust loads in accordance with Figure 2-83. The load limits are 67 per cent of the ultimate gust loads, with one G down, and maximum thrust. Operational maximum loads occur with six Gs down, one G to the side, one and one-half G forward, and maximum thrust, or with gust loading, one G down and maximum thrust.

Axial loads are transmitted by the fixed front mount and a moment created by the vertical loads. The side loads are transmitted by the side supports and a moment created by the link support. Vertical loads are transmitted by the vertical supports and as a moment through the link support. Yaw moments are transmitted by the side supports and as a moment through the link support, and pitch moments are transmitted by the vertical supports and as a moment through the link support. Roll moments are transmitted by the two front attachment points.

f. Ground Handling Provision

Ground handling provisions have been closely coordinated with the airframe manufacturers. These provisions reflect considerations of internal (Pratt & Whitney Aircraft) ground handling equipment as well as the requirements of both airframe contractors. Since the

airframe manufacturer has traditionally been responsible for integrating ground handling equipment for installation and removal of the engine, Pratt & Whitney Aircraft has designed attachment points commensurate with details provided by both Boeing and Lockheed.

The powerplant will be delivered in two major assemblies. The first of these will consist of the gas generator and the fan duct diffuser. The second will consist of the ejector and the fan duct exhaust case. Provisions have been made to permit each unit to be handled independently and to permit the assembled units to be handled during installation.

Figures 2-84 and 2-85 show the ground handling provisions. The gas generator unit has two attachment points on the front mount ring and two brackets on the fan duct case. The rear of the gas generator is to be supported with a strap around the fan duct while installing the ejector since the brackets must be removed to attach the ejector. The ejector assembly is to be handled in a cradle which supports it at two points. Actual assembly will be made with the engine axis horizontal. After assembly, the engine should be handled by a cradle under the ejector and with the two attachments in the front mount ring.

For the Lockheed installation, an additional attachment hole has been placed at the top center of the front mount for hoisting the engine into the aircraft.

For the Boeing installation, two additional attachment points have been provided on the rear mount ring 15 degrees below the horizontal center line for handling the ejector.

19. ENGINE ACCESSORY DRIVES

The discussion presented here is limited to the basic characteristics of the engine accessory drive system. Specific arrangements have been developed in coordination with the particular airframe manufacturers involved.

The gearbox (see Figure 2-25) for the accessory drive system will house a major portion of the components supplying lubrication for the engine and has provisions for mounting and driving the engine accessories. The drive system will provide shaft speeds compatible with efficient accessory operation. The gearbox for the Lockheed installation is a welded unit using AMS 4901 and AMS 4921 titanium materials. The gearbox for the Boeing installation is cast high temperature magnesium (AMS 4418). Power is supplied to the drive system by a

towershaft driven by a pair of spiral bevel gears from the high-speed rotor shaft. Loose spline couplings are located on both sides of the towershaft to accommodate deflection and misalignment.

Power input to the drive system is 150 hp at maximum normal rotor speed for the Lockheed arrangement and 310 hp for the Boeing arrangement.

The gear trains within the gearbox are common for both aircraft manufacturers with the exception of the extra gear train required in the Boeing gearbox to drive two hydraulic pumps. The gearboxes also contain a main oil supply pump, a scavenge pump, an oil pressure regulating valve, and an overboard breather pressurizing valve operating in conjunction with a de-oiler.

The speed ratio and direction of rotation for all accessory pads are shown in Figure 2-86. Except for the high-speed rotor tachometer drive, all of the gear shafts are straddle mounted between anti-friction type bearings, and are lubricated by a combined oil jet and oil splash system. The gear trains are designed such that the maximum Hertz stress produced is no greater than 110,000 psi. Care was taken in the design of the gears to ensure that their resonant speeds are outside the operating ranges. Service experience has shown that a primary cause of gear failures is vibration at the mesh frequencies. To preclude such failures, gear designs are analyzed for resonance effects before the gears are fabricated, and, after fabrication, the gears are tested using strain gages to determine the actual resonant speeds and the severity of the effect. If necessary, the design is modified to avoid the resonant frequency.

Both the oil pressure pump and the scavenge pump are gear-type units which are installed as complete packages in the bottom of the gearbox. The oil in the system is filtered by cartridge filters consisting of stacks of 100-mesh screens and spacers. Pressure taps indicating filter pressure drop are provided for attachment to a cockpit warning light system. A redundant two filter system is used in conjunction with a bypass filter to provide for the event of the primary filter plugging. Upon leaving the filters, the oil is pumped to a spring-type pressure regulating valve which by-passes excess oil back to the pump inlet.

The gearbox breather system incorporates a centrifugal de-oiler to prevent oil from being lost overboard. The centrifuged breather air passes out of the system through the inside of the shaft to the pressure

regulating valve, which maintains a given pressure level within the gearbox.

Most of the accessory mounting pads are oriented perpendicular to the engine centerline and are angled inward to place the accessories as close to the engine as possible.

Pressurized oil is not supplied to any of the pads and high temperature synthetic rubber ring seals are used to prevent leakage between the pad and the accessory. Spring-loaded face type, two way carbon seals are used to contain the oil within the gearbox, and any oil which may accumulate due to leakage in the pad cavity is drained overboard.

The mounting pads for the fuel pump, fuel control, and the hydraulic pumps were designed to be in accordance with Aeronautical Specification 468B. The tachometer pad is supplied with a shaft speed of 4209 rpm and was designed to be in accordance with AND20005XV-B.

The gearbox mounting scheme is shown in Figure 2-87 and a schematic diagram of the gearbox is shown in Figure 2-88.

20. ENGINE STARTING

The STF219 engine will be started through a remote airframe-mounted gearbox. A power take-off pad located on the top of the engine at the intermediate case will provide the drive power for the Boeing engine. A right-angled step down gear box power take-off drive and decoupler will be furnished for Lockheed (see Figure 2-89).

The estimated engine motoring characteristics were determined on the basis of data and experience with the STF200 advanced turbofan engine and current production engines. The estimated motoring torque for the Boeing and Lockheed engines as a function of rpm at the power take-off pad is shown in Figures 2-90 and 2-91, respectively. As shown, the torque increases with rpm until the firing speed is reached, after which it decreases with rpm until it reaches zero at the self sustaining speed. It should be noted these curves reflect the difference in drive shaft speed at the power take off airframe attachment point.

Motoring torques were determined by calculating engine matching characteristics at various rotor speeds. For speeds up to the firing speed (4400 rpm at the towershaft for Boeing and 1750 rpm at the gearbox for Lockheed), no fuel is burned and there is no temperature

rise in the burner. For these conditions, matching of the high-pressure compressor is determined by the turbine flow characteristics. After the burner is lit, the high-pressure compressor has sufficient surge margin to allow the rotor to accelerate up the design operating line until the rotor is self-sustaining and the starter cut-off and idle speed is reached.

A curve of the starting torque as a function of rpm for one air turbine starter with proper intermediate gearing is shown in Figures 2-92 and 2-93. As shown, adequate torque is available over the entire range, and calculations indicate that the starting time would be approximately 13 seconds for the Boeing engine and 14.5 seconds for the Lockheed engine at standard-day conditions. A plot of motoring and starter horsepower as a function of rpm is shown in Figures 2-94 and 2-95.

Cold day starting requirements are shown in Figure 2-96. The decrease in air temperature causes an increase in the motoring torque, but the starter studied would be adequate for temperatures down to -40°F.

E. STF219 COOLED TURBINE DESIGN

1. INTRODUCTION

The STF219 turbine design has as its objective the ultimate attainment of a turbine inlet temperature of 2300° F for take-off and transonic acceleration and 2200° F for supersonic cruise in commercial service operation. This is an extremely ambitious goal and is, in our opinion, by far the greatest technical risk in the SST program. In order to fully appreciate the degree of the problem, one must be aware of the operating requirements and difficulties associated with the successful introduction of a new powerplant into commercial service.

First, experience has shown that a turbine must be developed to operate satisfactorily at temperature levels significantly higher than the average temperature which goes with the level of performance indicated by the engine rating. The distinction between a "rating" temperature and a development or "field" temperature is of major importance. Because of its importance, the background for this requirement will be discussed in some detail.

One reason for development of the hot section to higher temperatures is the requirement for establishment of a turbine out temperature limit for field use in the course of FAA certification of the engine. Since turbine temperature is not a direct measure of thrust, it must be used only as a monitor and, thus, the "field" limit must be set at some level higher than that needed to demonstrate engine performance for take-off and acceleration under ideal conditions. This increment must cover such factors as normal engine deterioration, control tolerances, cockpit instrumentation errors, etc. Past Pratt & Whitney Aircraft commercial experience indicates that a turbine out temperature increment equivalent to 60°-100° F T.I.T. must be allowed. It would certainly not be lower in the case of the SST.

Another cause for development of the hot section to temperatures above the "rating" temperature is the uneven temperature pattern of the gas entering the turbine. A highly developed combustor will show a Δ TVR of 1.10 or slightly less but this will mean hot spots 100° F above the

average gas temperature. Also allowance must be made for normal deterioration in the temperature pattern expected after long time service operation.

Information available on supersonic inlets indicates that the inlet distortion will be more severe than experienced in subsonic commercial aircraft and will persist through relatively long time periods at high turbine temperature levels. Inlet effects are known to carry through to the turbine resulting in local hot spots which inevitably will force development of the hot section to accept local temperatures 50° to 100°F higher than the "rating" temperature. Concerted effort over a period of years may be expected to improve inlet distortion and its effects on the turbine temperature pattern. If so, this would permit "rating" the engine closer to its development capability.

The above discussion reflects the most important factors which must be faced in establishing a design turbine inlet temperature for arriving at engine performance ratings. The net result of this is that it will be necessary to develop major elements of the hot section for a considerably higher temperature.

It is generally acknowledged that the creation of an SST airplane design which will be competitive with subsonic commercial transports in the same time period is a formidable task. To draw such a conclusion from comparative studies, it is necessary to assume that the SST aircraft will be available the same number of hours per day, will be as reliable, will have comparable TBO's, and will have competitive maintenance and overhaul costs. The failure of the SST to live up to these assumptions would result in substantially increased costs. The airlines would find it difficult, in our opinion, to cope with the economic problems which would arise if the SST fails to give satisfactory service from the outset.

It is the general experience of the industry that even a moderate increase in turbine temperature for commercial operation results in a quantity of unforeseen engine problems. Our experience is not unique in this regard. It is evident that despite the cross-flow of information from prior programs, and a very extensive engine development program conducted at turbine temperature levels significantly above the "rated" temperature we are unable to adequately evaluate by test prior to certification, all of the problems which will arise after the start of commercial service.

For the above reasons, it is our firm conviction that a design and development program aimed at 2300°F, turbine inlet temperature for acceleration and 2200°F for supersonic cruise will be no more than sufficient to assure acceptable engine durability at the initial airline service operating temperatures of 2000°F for acceleration and 1900°F, for supersonic cruise. As a part of this program the delivered prototype engines would be capable of operating at the 2200°F/2300°F temperature levels. Temperature increases beyond these initial production engine ratings must be firmly based on operational experience at the initial ratings supplemented by development testing and service testing at the higher temperature levels.

2. APPROACH

The effort during Phase IIA has been directed toward cooling vanes and blades in such a manner as to meet the special needs of different internal airfoil locations, i.e., leading edge, trailing edge, mid chord, etc. Emphasis was placed on efficient use of cooling air taking full advantage of improvements in cooling techniques, materials, and oxidation corrosion preventative coatings. Initially average metal temperatures were limited to 1600°F which is the upper limit of current subsonic commercial transports. As analysis progressed it became apparent that the cooling airflows required to do this job were inconsistent with good thermodynamic performance. Metal temperatures were therefore increased to a maximum value consistent with expected material and coating capabilities. This resulted in average metal temperatures of 1750°F at the most critical engine operating condition and permitted a reduction in cooling airflow of 36 per cent.

The complexities of the task at hand precluded the reduction of all the blade and vane design concepts to practice within the very short Phase IIA time period. More elaborate trades between the factors involved, i.e., cooling air, metal temperature, life and performance, remain to be exercised; however, evidence to date indicates that the ultimate requirements of a 2200 - 2300°F turbine inlet temperature, SST can be met through the application of a concentrated effort encompassing projected improvements in cooling technology, materials, and coatings.

3. DESIGN GOALS

The following design goals were established as necessary to meet performance objectives as well as commercial durability and service life.

- Turbine Inlet Average Gas Temperature - 2200°F at supersonic cruise
- Turbine Inlet Average Gas Temperature - 2300°F at SLTO and transonic acceleration
- Average Metal Temperature - 1750°F
- Engine Life - 5000 Hours

4. DESIGN PROBLEM

The design problem is one of complexity, durability, fabrication and inspection. Its complexity stems from the large number of variables which have a significant effect. Cooling air flow, pressure, and temperature; performance, life, and turbine inlet temperature and their effects on each other must be combined to yield functional hardware. Detailed studies of these parameters as they affect cooled turbine blades and vanes have shown that there are three primary factors which must be considered in designing for long airfoil life at high turbine inlet temperatures. These factors are creep life, cyclic life and resistance to erosion and corrosion.

a. Creep Life

Creep is a permanent deformation under stress and temperature over a period of time and is generally associated with the steady state, long time operating requirement. This requires that the average metal temperature at each spanwise location be held to levels consistent with airfoil stress rupture and creep requirements.

b. Cyclic Life

This is caused primarily by high metal temperature gradients resulting from rapid changes in external gas temperatures during transient operation. As turbine inlet temperature increases, it becomes increasingly difficult to maintain acceptable chord-wise temperature differences during acceleration and deceleration. During acceleration, the leading

and trailing edges heat up faster than the midchord region because of the higher heat transfer coefficient and lower mass of metal in these regions. The resulting gradients tend to be high and cause a loss of cyclic life. To avoid this, better cooling of the airfoil edges must be accomplished. Cooling is more difficult in the leading and trailing edge regions because of the limited space available for internal cooling passages in these areas. Some compromise of leading and trailing edge radii can be made without significantly affecting aerodynamic performance, thus somewhat reducing the heat transfer coefficients and relieving space limitations. Film cooling of the leading and trailing edges is an effective means of reducing the transient temperature differential since it reduces the heat transfer rate into these surfaces. However, it is difficult to establish a film on the leading edge of a foil for the following reasons:

1. Cooling air would have to be pumped to a pressure about 1.25 times compressor exit pressure in order to provide a film on the leading edge of the 1st stage inlet guide vanes. This could be accomplished by use of a turbine driven cooling air pump at a cost of some loss in performance, reliability, and a 125°F increase in cooling air temperature due to the pump temperature rise.

2. It appears that a porous surface or a surface with a large number of holes near the leading edge is required. This tends to compromise the mechanical integrity of the vanes or blades.

3. Another possible solution to the cyclic life problem is to employ the use of a nonstructural member at the leading edge of the airfoil which is free to thermally expand and contract independently of the rest of the part. This requires that the internal cooling passages be designed to cool this member or requires the use of materials not currently available.

c. Erosion and Corrosion

The surface phenomena of erosion and corrosion are respectively the wearing away of metal or the oxidation of metal caused by high temperature, high velocity gas streams. Protective coatings are necessary to prevent this phenomena from attacking the base metal of the airfoil. Coatings must be compatible with the material being coated and must be able to withstand some impact damage.

The solution of these severe cooling requirements has introduced a major structural problem which is the design and fabrication of a complex multipassage cooling configuration which retains the necessary structural integrity and which can be reliably inspected as a production and overhaul part. All of the above requirements must be met using an amount of cooling air consistent with good performance.

5. DESIGN EMPHASIS

Emphasis in phase IIA was placed on the efficient use of cooling air. Airfoil cooling air was distributed internally so as to meet the specific requirements of each location. The edges of the airfoil tend to be the hottest and hence were treated separately from the midchord section. Where required different types of cooling and, or, different amounts of cooling air were used at the edges than were used in the midchord section. This avoided both under or overcooling one section because the cooling requirement was incorrectly generalized based on another section. Cooling airflows were minimized by taking advantage of the excellent strength of advanced materials. As the metal temperature increases, the differential between relative external gas and the metal temperatures is decreased which results in a lower rate of heat input to the airfoil. In addition, the differential between the metal and coolant flow temperatures is higher which increases the heat capacity of the coolant. By utilizing the increased creep strength of the superior cast vane and blade alloys, a 36 per cent reduction in cooling airflow was affected.

This report describes the proposed blade and vane cooling schemes in detail and defines the design philosophy employed in establishing airfoil temperature and life. Several designs for the first stage vane and blade are proposed because development work on these airfoils is still too limited to permit selection of a single configuration at this time. It is to be noted that all configurations met or exceeded the design goals.

6. HEAT TRANSFER AND LIFE ANALYSIS

Unless otherwise specified, the analysis described below was used. External heat transfer coefficients were calculated employing the method of Ref. (1). Internal impingement coefficients shown in Figure 47 were used at the vane leading edge. They were calculated using test data developed at Pratt & Whitney Aircraft in a highly instrumented rig designed expressly to examine the capability of this type of cooling. A description of the rig is presented in item 6 of this report. Impingement

cooling produces heat transfer coefficients substantially greater than those which can be achieved with parallel flow. This cooling system allows the employment of the lowest temperature cooling air on the hottest portion of the vane, again an advantage which cannot be achieved with parallel flow. Internal heat transfer coefficients inside through holes in a foil were calculated using the standard procedures for channel flow Ref. (2). Fin efficiencies where used were calculated from Ref. (3). Film cooling effectiveness of 18 per cent was used on the leading edge while 100 per cent film effectiveness was used at the trailing edge. These values were based on test data shown in Figures 98 and 99. The tests were run in a choked vane cascade rig at the United Aircraft Corporation Laboratory under steady state conditions and showed that good correlation could be achieved between test data and calculations employing the method of Ref. (4).

Cyclic life was based on metal temperatures resulting from engine transients. Figure 100 shows typical transients used in the analysis. Creep life analysis was based on average chordwise metal temperature of 1750° F. or below.

7. ENVIRONMENTAL CONDITIONS

All airfoils were designed to operate at a gas temperature commensurate with a first stage turbine inlet temperature of 2300° F from SLTO through the transonic range and 2200° F at the supersonic cruise condition. Figure 101 shows the ideal average gas temperatures at the entrance to each air foil row. The gas temperature profile is tailored radially as shown in Figure 102 to minimize the temperature at the blade root where stresses are highest. A higher average turbine inlet gas temperature is possible in the turbine blading with a tailored radial temperature profile than with a flat profile.

8. SPECIFIC DESIGNS - 1st TURBINE VANE

The studies conducted have led to three candidate first turbine vane designs. All three employ impingement convective cooling of the most forward portion of the leading edge and film cooling of the trailing edge One design exhausts the leading edge cooling air to a low pressure region, while the other two exhaust this air into the gas path just behind the leading edge. The first configuration appears to be more desirable on a reliability basis because it does not require the boost in cooling air pressure level which the latter two do require.

a. Cooling System: Impingement - 1st Vane

Description - The vane has a constant cross sectional area with a 2.5 inch chord. Figure 103 shows the vane geometry. The main structural portion of the vane consists of a cast hollow airfoil section with slots placed in the trailing edge region on both suction and pressure surfaces. The hollow cavity is divided into two cooling compartments. Burner secondary air is supplied at the vane I. D. to the distribution tube in the leading edge compartment and is ejected at high velocity through slots onto the internal surface of the leading edge which has chordwise cooling fins. These fins provide an internal cooling area of 2 times that of the external heating area which results in excellent cooling effectiveness. After impinging on the leading edge, the air flows chordwise along the vane to the two exhaust manifolds which vent the air to the vane O. D. A sheet metal insert is placed into the rear central hollow cavity to provide a cooling air supply manifold and to form a regulating flow passage on both suction and pressure surfaces of the airfoil. The flow passage is formed by fins cast into the side walls of the vane and the outer wall of the sheetmetal insert. The fins, as before, increase the internal heat transfer area, increasing the heat transfer to the coolant. Burner secondary air fed into the insert, is ejected through slots at the leading edge of the insert, flows rearward in a chordwise direction convectively cooling both surfaces of the airfoil, and is ejected out the slots at the trailing edge of the vane film cooling the trailing edge. The lower external static pressures at the trailing edge of the vane do not pose a film cooling problem. However the high coolant side pressure increase required for film cooling the leading edge would necessitate the use of an additional pumping device to boost the pressure of the burner secondary air used for cooling. The added weight, complexity and inherent decrease of reliability involved in incorporating such a device gives preference to the internal fin design as opposed to the other designs presented.

Creep Life - The creep life of the vane is a function of the average metal temperature and the vane stress level. Figure 104 shows the average spanwise vane metal temperature variation for the vane cooling configuration using impingement cooling. Also shown are the allowable metal temperatures for several different materials. As indicated by the large margin between allowable and calculated metal temperatures, this design has a creep life well in excess of the 5000 hour engine life goal.

Cyclic Life - To determine the vane cyclic life, the chordwise temperature differential [illegible]rring during transient acceleration and deceleration were calcul[illegible] Typical transients are shown in Figure 100. The amount of tem[illegible]ature differential is an indication of the amount of thermal strain which will occur during the transient condition. This conclusion must be modified by a careful consideration of where the thermal difference occurs. If the part is affected by a linear temperature gradient and it is not restrained, no thermal stresses will arise. This vane experiences a calculated temperature difference of 200° F between the leading edge and a point on the convex surface at the 50 per cent chord location. This gradient is significantly larger than the steady state gradient because of the high response rate of the leading and trailing edge of the airfoil to changes in gas temperature. The edges heat and cool much more rapidly than the midchord section because of their smaller mass and higher external heat transfer coefficients. Since the vane is not constrained, some stress relieving bending will occur about the vane minimum axis of bending. A relaxation analysis was performed to determine the true cyclic stress. Based on this analysis a design life in excess of 5000 hours was predicted.

Erosion and Corrosion Life - The temperatures at the 75 per cent span location are shown in Figure 105. Adequate protection against corrosion and erosion can be provided using currently available coatings for the materials selected.

b. Cooling System: Detachable Shield - 1st Vane

Description - The cooling of this vane differs from the vane previously described only in the leading edge area. This vane has a detachable nonstructural shield which is cooled by internal jet impingement. Figure 106 shows the vane geometry which again incorporates two separate cooling systems, one for the leading edge and one for the midchord and trailing edge of the foil. The vane is cast in the configuration shown without the shield. A separate one-piece shield is then fitted to the vane leading edge. By fitting the shield in this manner, no mechanical bond is required, and the shield can expand and contract independent of the main portion of the vane, enhancing the cyclic life of the vane. Another advantage to be gained by this design is that a more highly corrosion resistant material can be used for the leading edge. Air is fed into the vane leading edge cavity aft of the shield from the O. D. of the vane. The air fed into this cavity is ejected

through the slots at the leading edge of the cavity, impinges directly on the inner surface of the shield, cooling the shield, and is expelled on either side of the shield, film cooling the suction and pressure surfaces of the airfoil.

Creep Life - The estimated average spanwise vane metal temperature for this vane is slightly less than that shown in Figure 104 for the impingement cooled vane. The bending stress is similar. As a result, the creep or "bow" life will be well in excess of 5000 hours.

Cyclic Life - The maximum temperature differential was computed to be 150°F during transient acceleration between the structural leading edge and the trailing edge. Although the response of the shield was calculated to be greater than any other portion of the vane, the cyclic life of the vane is not affected because the shield can grow independently of the remainder of the vane. The structural leading edge just back of the shield is the coolest portion of the vane. During a transient such as described in Figure 100, the local temperature difference between the shield and the structural leading edge just behind the shield is 200°F. This is due to the high response rate of the leading edge as it reacts to rapid changes in gas temperature during transient operation. This rate is significantly higher than the structural core due to the smaller mass and higher external heat transfer coefficients of the leading edge. If the shield were not free to grow independently a stress of 80,000 psi would result in this area. Since the temperature response is nearly linear from leading edge to trailing edge, no cyclic life limitation is foreseen.

Erosion and Corrosion Life - The temperatures at the 75 per cent span location are shown in Figure 107. As in the case of the previous design life is adequate.

c. Cooling System: Integrally Cast Shield - 1st Vane

Description - The only difference between this vane and the vane previously described is the leading edge cooling configuration. Figure 108 shows the vane geometry. The leading edge geometry consists of integrally cast shield members which are allowed to thermally expand independently of the main structural portion of the vane. Air is fed into the leading edge cavity aft of the shield from the O.D. of the vane. The air fed into this cavity is ejected through the slots at the leading edge of the cavity impinges directly on the inner surface of the shield, cooling

DOWNGRADED AT 3 YEAR INTERVALS
DECLASSIFIED AFTER 12 YEARS
DOD DIR 5200.10

the shield, and is expelled on either side of the shield, film cooling the suction and pressure surfaces of the airfoil. Mechanically interrupting the leading edge with slanted contours provides the concomitant advantage of aiding film stabilization.

Life - This vane has the same calculated life as the vane with the detachable shield leading edge.

d. Material Selection - 1st Vane

The 1st vane material selection criteria is derived from engine operating experience, standard laboratory test, and specific mission requirements. The selection of a vane material for the STF219 was the result of studies of development super alloys and current "Bill-of-Materials" alloys. These studies resulted in the selection of two materials for more detailed study and testing. The two materials chosen for detailed consideration for first vane use are WI-52 (PWA 653), B1900 (PWA 663).

First Choice - WI-52 is a cast cobalt base alloy which is widely used in current commercial production engines having as high as 5800 hours TBO. With the effectiveness of the proposed cooling schemes for the first vane, WI-52 has acceptable strength capabilities as shown in Figure 104. Because of the large amount of service experience with this alloy, it is the logical first material choice for the first stage vane until a more definitive evaluation can be made in the SST development program.

Alternate Material Choice - B1900 is a nickel-base cast alloy which has very good high temperature properties. Experimental engine test work is being conducted using this material for both blades and vanes. Test results have been excellent with B1900 showing one tenth the average vane bow of WI-52 vanes run for the same time. The material also shows good oxidation -- corrosion resistance. High temperature testing of coated B1900 vanes shows good resistance to sulfidation. Figure 104 shows the increased strengtn margin of B1900 over WI-52. Pilot lot experience is being started in commercial service.

9. SPECIFIC DESIGN - 1st BLADE

a. Cooling System: Showerhead Leading Edge - 1st Blade

Description - The blade selected has a 1.8 inch chord. Figure 109 shows the blade geometry which incorporates an extended root. In this blade, the leading edge cooling system consists of a multiplicity of small holes drilled or cast into the leading edge through which air is ejected. Cooling is effected by convection in the holes and the cooling air film which is formed on the leading edge surface. The remainder of the blade consists of a slotted film cooled trailing edge and a convectively cooled mid-chord section. The cooling air is introduced at the blade root attachment and passes through supply holes which extend from the base of the root attachment to the blade platform. The air then flows radially outward through the hollow blade supplying air to the leading and trailing edge. The air ejected through the trailing edge slots film cools the trailing edge. Wall to wall pedestals are cast in the coolant passage of the foil to provide structural integrity and a means of controlling coolant flow area. The hollow blade provides a means of limiting blade wall thickness to minimum dimensions thus minimizing the temperature gradient through the walls and reducing the cooling requirement. The pedestals in the coolant passage act as fins and turbulence generators and serve to increase the effective internal heat transfer area and heat transfer coefficient, and therefore the cooling efficiency. In contrast to the first vane situation, the pressure of the cooling air is adequate to force the air out the leading edge of the first blade without additional pumping.

Creep Life - The 1st turbine blade stress varies along the span from zero at the tip to a maximum of 29,800 psi at the airfoil root. The tailored spanwise temperature profile causes the blade to be creep limited near the mid span. Figure 110 is a graph of the average spanwise blade temperature. Also shown are the allowable metal temperatures for various materials considered for the 1st blade design. This design meets the 5000 hours engine life goal.

Cyclic Life - Cyclic life is adequate for 5000 hours engine life.

Erosion and Corrosion - Steady state temperatures at the mid span section are shown in Figure 111. The erosion and corrosion life, as in the case of the 1st vane is adequate.

b. Cooling System: Shielded Leading Edge - 1st Blade

Description - The only difference between the shielded leading edge blade shown in Figure 112 and the blade previously described is the geometry of the leading edge. In this blade, the leading edge shield is integrally cast. The air ejected through the leading edge slots impinges directly on the inner surface of the shield, cooling the shield and is ejected on either side of the shield, film cooling the suction and pressure surfaces of the airfoil. Again the cooling air pressure is adequate without additional pumping.

Creep Life - The shielded first blade stress is similar to that in the showerhead blade. The estimated average spanwise blade metal temperature variation is shown in Figure 113. The allowable metal temperatures for several materials are also plotted for comparison. The creep life will be adequate for 5000 hours engine life.

Cyclic Life - With the shielded leading edge cooling design the maximum chordwise temperature differential is 210°F. Once again the leading edge shield temperature is higher than that of the structural core. If the shield were not slotted, the high local thermal gradients between the shield and the main structure behind it would result in a stress of 80,000 psi. However since the slots in the shield permit it to expand or contract independently this is not a problem. Cyclic life is adequate for 5000 hours engine life.

Erosion and Corrosion Life - The blade temperatures at the stress limited midspan section are shown in Figure 114. The blade will achieve adequate life.

c. Material Selection - 1st Blade

The primary design considerations for blade materials are creep strength, ductility, density, and fatigue strength. These properties are used to predict blade growth and margin between design stress and failure stress. The percentage of creep used to establish design stresses is established from analyses of creep and stress rupture test data and actual engine test results and service experience. As in the vanes, the blades must have oxidation, erosion, and sulfidation resistance for long time use. A selection of three materials was made for

DOWNGRADED AT 3 YEAR INTERVALS
DECLASSIFIED AFTER 12 YEARS
DOD DIR 5200.10

THIS DOCUMENT CONTAINS INFORMATION AFFECTING THE NATIONAL DEFENSE OF THE UNITED STATES WITHIN THE MEANING OF THE ESPIONAGE LAWS, TITLE 18, U.S.C., SECTIONS 793 AND 794. THE TRANSMISSION OR THE REVELATION OF ITS CONTENTS IN ANY MANNER TO AN UNAUTHORIZED PERSON IS PROHIBITED BY LAW.

detailed study: IN-100 (PWA 658), SM-200 (PWA 659), and B-1900 (PWA 663). Comparative strengths of these materials are shown in Figures 110 and 113.

First Choice - IN-100 is a nickel base alloy which has excellent creep and fatigue strengths. Its ductility approaches current forged alloys and its density is low. Its creep strength compared to materials currently used in commercial production blades is approximately 100°F higher in temperature for a given stress. This temperature margin is bound to be valuable in development of the STF219 engine so IN-100 is the first material choice for this application. This alloy is used for blading in the J-58 engine.

Alternates - SM-200 is a nickel base alloy whose strength to density ratio is slightly better than that of IN-100. This alloy was first introduced in 1958 and has been developed as a proprietary alloy under partial sponsorship of Pratt & Whitney Aircraft. Considerable development experience has been attained in the J-58 development program. The early development experience gained with this alloy showed that it was subject to scatter in its ductility characteristics. Ductility characteristics have been substantially improved by imposing closer controls in the casting process. This alloy is being actively used in Pratt & Whitney Aircraft's high temperature research and development work. It has the potential of reaching the highest operating temperatures of any blade alloy available. Therefore, it must be considered a strong candidate for eventual use in the STF219 engine.

B-1900 is a nickel-base alloy which is considered also as an alternate 1st blade material choice. It is comparable to IN-100 on a strength to weight ratio basis. Experimental engine test work is being conducted using this material for both vanes and blades.

10. SPECIFIC DESIGNS - 2nd STAGE VANE

a. Cooling System - Impingement - 2nd Vane

Description - The vane has a chord of 2.2 inches. Figure 115 shows the vane geometry which incorporates a sheet metal insert centered inside the cast hollow vane cavity. Cooling air is introduced from the vane outer diameter into the hollow insert. The air is ejected through slots at the leading edge of the insert and impinges on the inner surface of the vane leading edge. The coolant then flows between the inner vane

surface and the outer insert surface in a chordal direction convectively cooling the midchord region of the vane. The air is then ejected through slots at the trailing edge, film cooling the trailing edge.

Creep Life - The creep life of the vane is a function of the average temperature and the vane stress level. The maximum vane bending stress due to airload at the cruise condition is 16,100 psi. Figure 116 shows the estimated average spanwise vane metal temperature variation. Also shown are the allowable metal temperatures for several different materials. The creep life of the 2nd stage vane will be well in excess of the 5000 hour goal.

Cyclic Life - Because the second vane is subjected to a lower temperature environment than the first vane, it is not necessary to mechanically isolate the leading edge of the vane from the remaining portion of the vane to achieve adequate cyclic life. Predicted maximum chordwise temperature gradient is 371°F. Predicted design cyclic life meets the 5000 hour engine life requirement.

Erosion and Corrosion Life - The vane temperatures at the 75 per cent span location are shown in Figure 117. The vane will have adequate life.

b. Material Selection - 2nd Vane

Requirements for the second vane materials are good erosion and corrosion resistance, good cycle fatigue strength, and adequate creep strength. The three materials chosen for detailed study are: IN-100 (PWA 658), B-1900 (PWA 663), and SM-200 (PWA 659). Because of the higher stresses due to gas loads in the second vanes than in the first vanes and the consequent need for a higher strength material, IN-100 was chosen as the first material choice for the 2nd vane. B-1900 has excellent strength and is being developed as potentially the best vane material. SM-200 is also an alternate material choice because of its high strength. Comparative strengths are shown in Figure 116.

11. SPECIFIC DESIGN - 2nd BLADE

The 2nd stage blade is uncooled and therefore the maximum temperature condition is SLTO.

a. Creep Life

The maximum centrifugal stress in the second blade is 24,000 psi. Figure 118 shows predicted average metal temperature and allowable temperature. The creep life meets the requirements for 5000 hour engine life.

b. Cyclic Life

Predicted design cyclic life is adequate for 5000 hour engine life.

c. Erosion and Corrosion Life

As in the case of the 1st Blade, life is adequate.

d. Material Selection - 2nd Blade

Material requirements for the 2nd blades are similar to the requirements for the 1st blades. The 2nd blades in general are subjected to a lower centrifugal stress and a lower cyclic thermal stress. Materials worthy of consideration for detailed s udy are IN-100 (PWA 658), B-1900 (PWA 663), SM-200 (PWA 659). Because of its high strength, good ductility, and light weight IN-100 was again chosen first material choice for the second blade.

12. SPECIFIC DESIGN - 3rd VANE

The 3rd vane is uncooled and therefore the maximum temperature condition is SLTO.

a. Creep

The maximum bending stress due to gas loads at SLTO conditions is 30,000 psi. The predicted average metal temperatures and allowable temperatures are shown in Figure 119. The curve snows that creep life meets the requirements for 5000 hour engine life.

b. Cyclic Life

Predicted cyclic life is adequate for 5000 hours engine life.

DOWNGRADED AT 3 YEAR INTERVALS
DECLASSIFIED AFTER 12 YEARS
DOD DIR 5200.10

THIS DOCUMENT CONTAINS INFORMATION AFFECTING THE NATIONAL DEFENSE OF THE UNITED STATES WITHIN THE MEANING OF THE ESPIONAGE LAWS, TITLE 18, U.S.C., SECTIONS 793 AND 794. THE TRANSMISSION OR THE REVELATION OF ITS CONTENTS IN ANY MANNER TO AN UNAUTHORIZED PERSON IS PROHIBITED BY LAW.

c. Erosion and Corrosion Life

Life is adequate.

d. Material Selection

The 3rd vane material requirements are similar to 2nd vane requirements. IN-100 (PWA 658), B-1900 (PWA 663), and SM-200 (PWA 659) are worthy of consideration in detailed study. IN-100 is again the first material choice.

13. SPECIFIC DESIGN - 3rd BLADE

The third stage blade is uncooled and therefore the maximum temperature condition is SLTO.

a. Creep

The centrifugal stress varies along the span from 2340 psi at the tip to 28,800 psi at the root during take-off and acceleration conditions. Maximum creep occurs near the hottest section at 75 per cent span. Figure 120 is a graph of average metal temperatures at take-off and cruise conditions versus allowable temperatures based on 3400 hours of T.O. and acceleration which is equivalent to 5000 hours of engine operation. Creep life exceeds the 5000 hour goal.

b. Cyclic Life

The third blades are not exposed to the thermal shock loads of the 1st and 2nd blades, and therefore, are not cyclic life limited.

c. Erosion and Corrosion

Life is adequate.

d. Material Selection

Materials requirements for the third blade are same as the the 2nd blade. Materials chosen for detailed study are IN-100 (PWA 658), B-1900 (PWA 663), and SM-200 (PWA 659). IN-100 is the 1st material choice for the third blade.

DOWNGRADED AT 3 YEAR INTERVALS
DECLASSIFIED AFTER 12 YEARS
DOD DIR 5200.10

THIS DOCUMENT CONTAINS INFORMATION AFFECTING THE NATIONAL DEFENSE OF THE UNITED STATES WITHIN THE MEANING OF THE ESPIONAGE LAWS, TITLE 18, U.S.C., SECTIONS 793 AND 794. ITS TRANSMISSION OR THE REVELATION OF ITS CONTENTS IN ANY MANNER TO AN UNAUTHORIZED PERSON IS PROHIBITED BY LAW.

14. FUTURE GROWTH

Achieving acceptable commercial life at 2200°F/2300°F turbine inlet temperatures as required of the STF219 in the SST flight profile was predicated on high temperature materials in current use, available oxidation and erosion resistant coatings, an 18 per cent film cooling effectiveness at the leading edge, and 100 per cent effectiveness for trailing edge films. These values of cooling film effectiveness are representative of the vane configurations which have been tested to date. It appears likely that continued effort will result in an improvement in leading edge film effectiveness. An increase in leading edge effectiveness to 50 per cent and utilization of this type of cooling in place of impingement cooling would result in a 28 per cent reduction in total cooling airflow requirements. Increased film cooling effectiveness coupled with improved materials provides a firm potential growth area for more effecien' and economical SST operation.

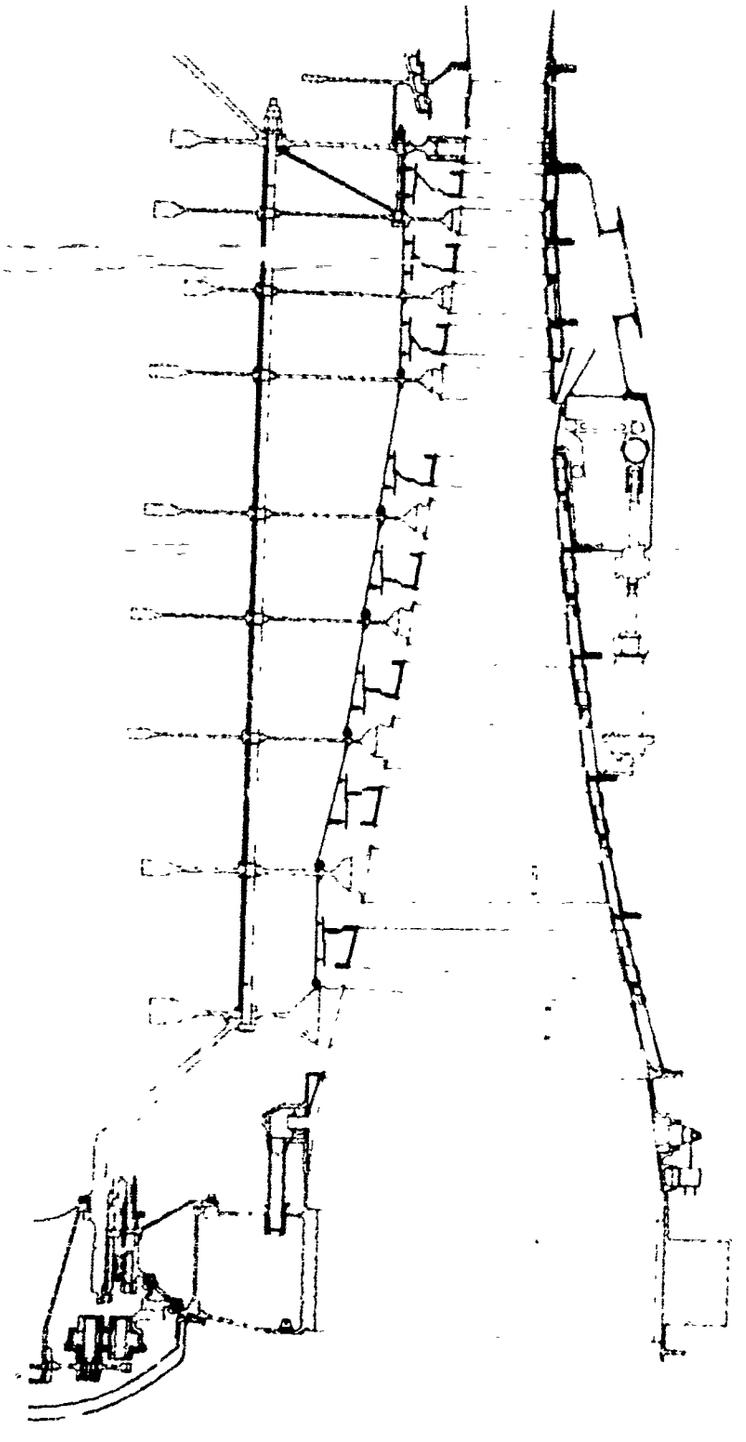
REFERENCES

(1) NACA RM-E50F02 entitled "Extension of Boundary Layer Heat Transfer Theory to Cooled Turbine Blades" by W. Byron Brown and Patrick L. Donoughe.

(2) Heat Transmission by William H. McAdams, Third Edition.

(3) Conduction Heat Transfer by P. J. Schneider.

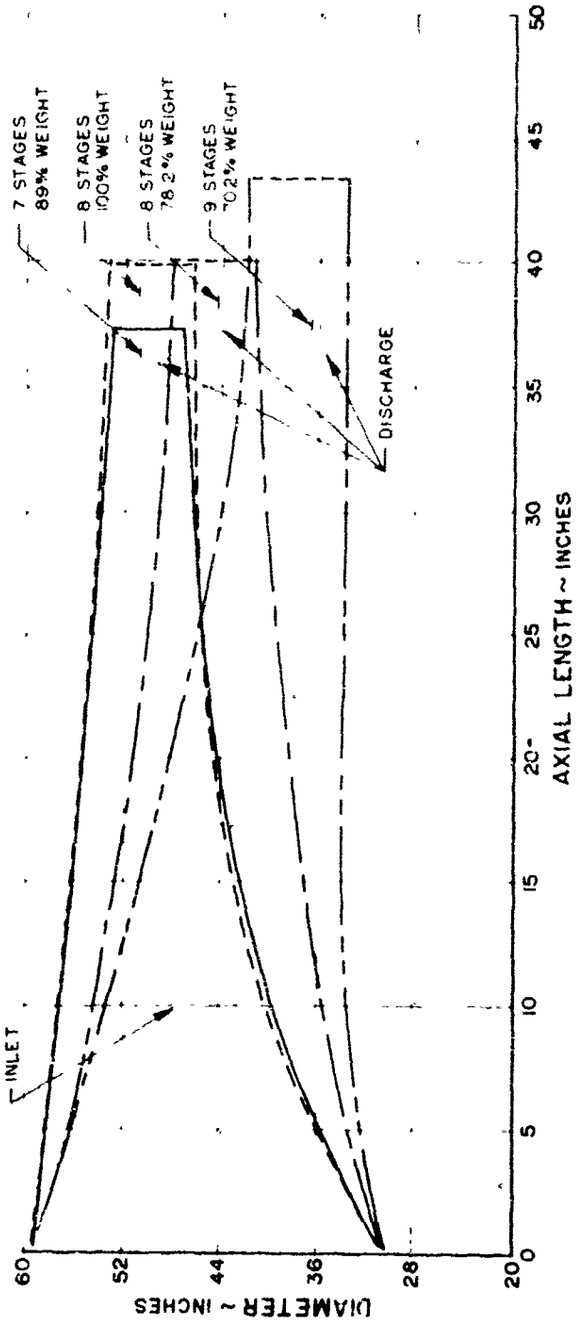
(4) J. P. Hartnett, R. C. Birkebak, and E. R. G. Eckert. "Velocity Distributions, Temperature Distributions, Effectiveness and Heat Transfer in Film Cooling of a Surface with a Pressure Gradient". Proceeding of the 1961 International Heat Transfer Conference.



CROSS-SECTION OF NINE STAGE COMPRESSOR OF STJ221 ENGINE

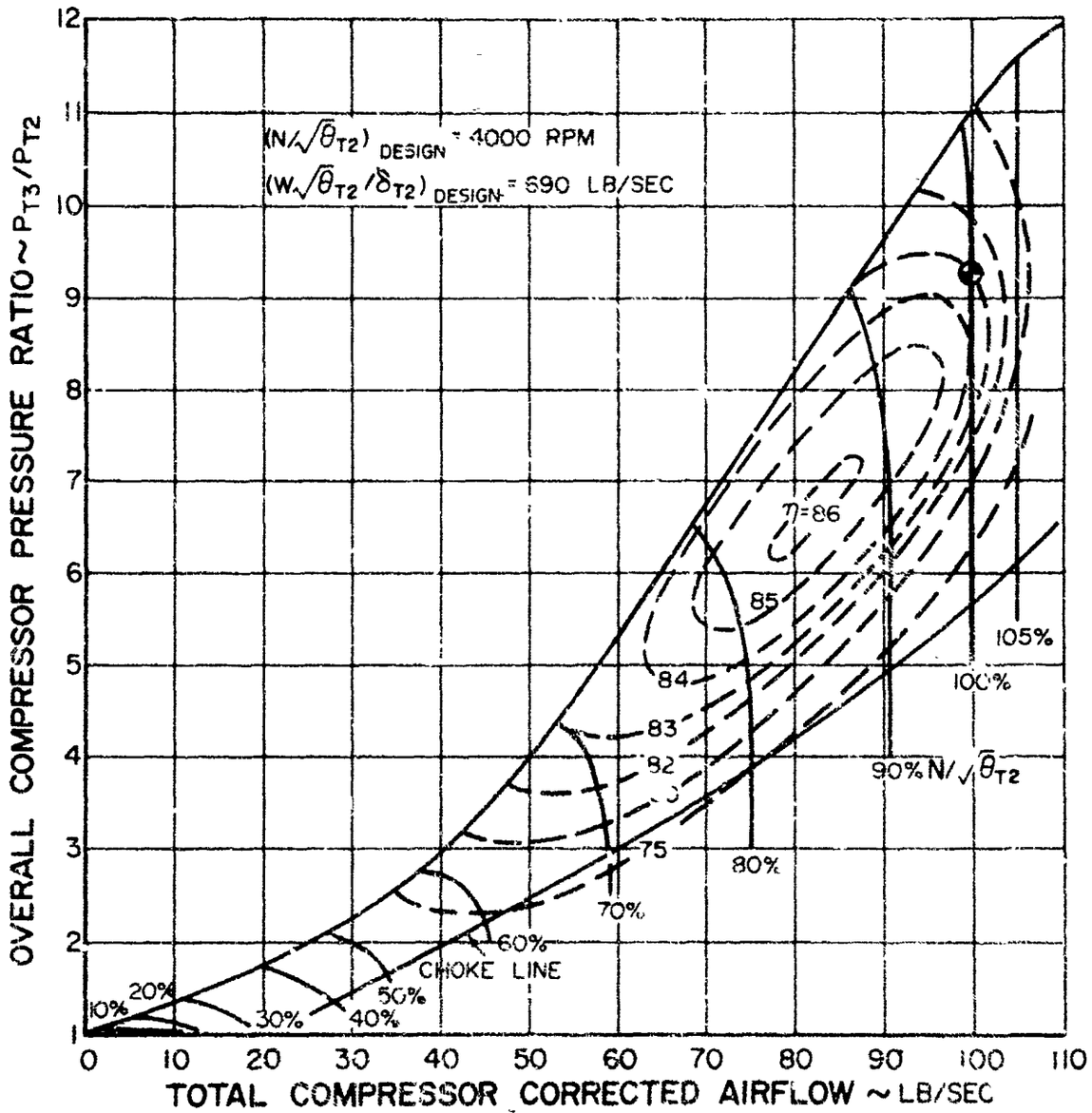
Figure 2-1

PER CENT WEIGHT	CORRECTED WHEEL SPEED	ROTOR NUMBER 1	2	3	4	5	6	7	8	9	10
89%	Um/√θ	943	943	910	880	841	804	775			
100%	Um/√θ	943	944	918	884	847	812	785	760		
78.2%	Um/√θ	944	881	835	796	757	728	698	678		
70.2%	Um/√θ	943	870	805	739	690	648	616	590	570	



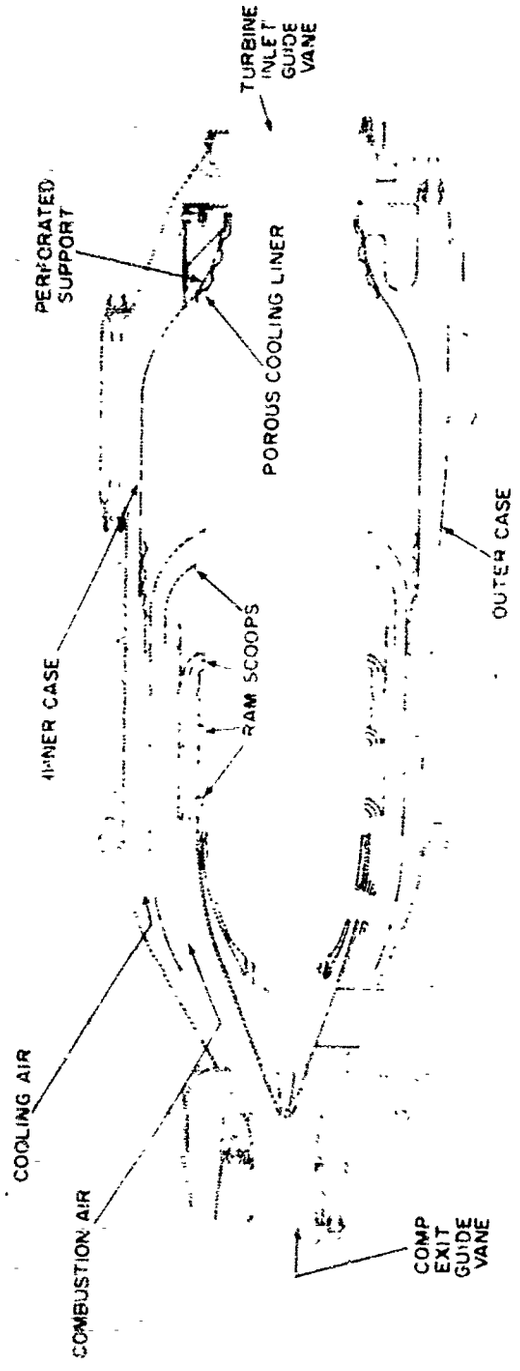
FLOW PATHS AND WEIGHTS OF COMPRESSOR CONFIGURATIONS CONSIDERED FOR STJ 221 ENGINE

Figure 2-2



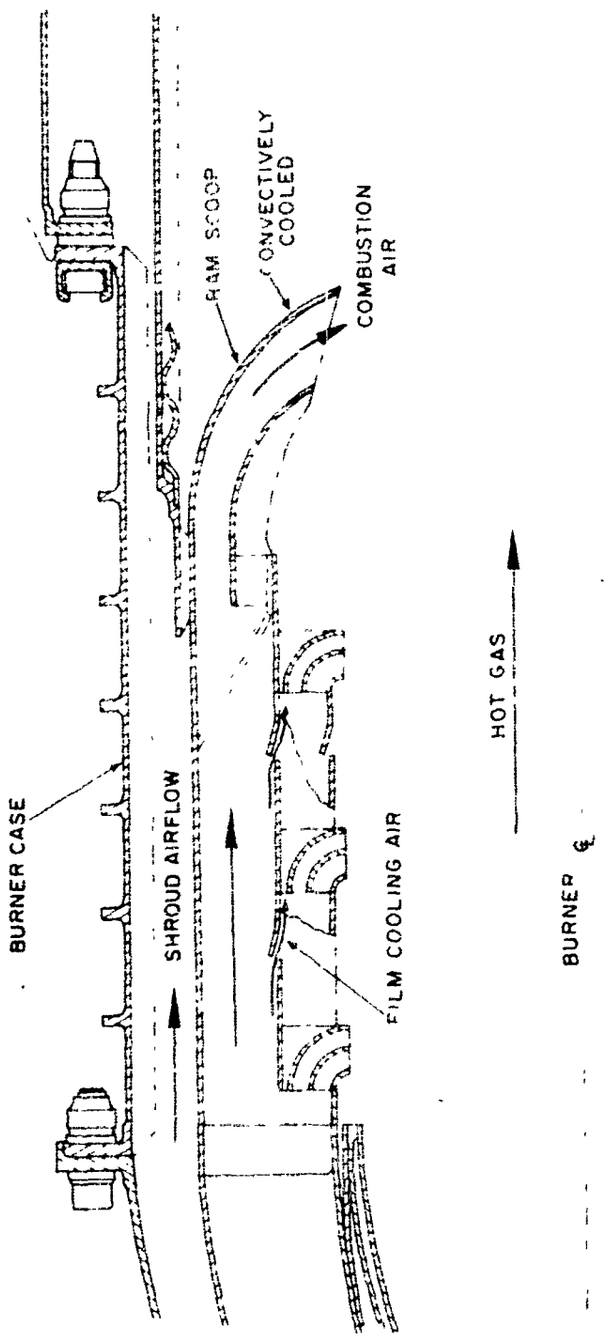
PREDICTED PERFORMANCE OF STJ 221 COMPRESSOR

Figure 2-3



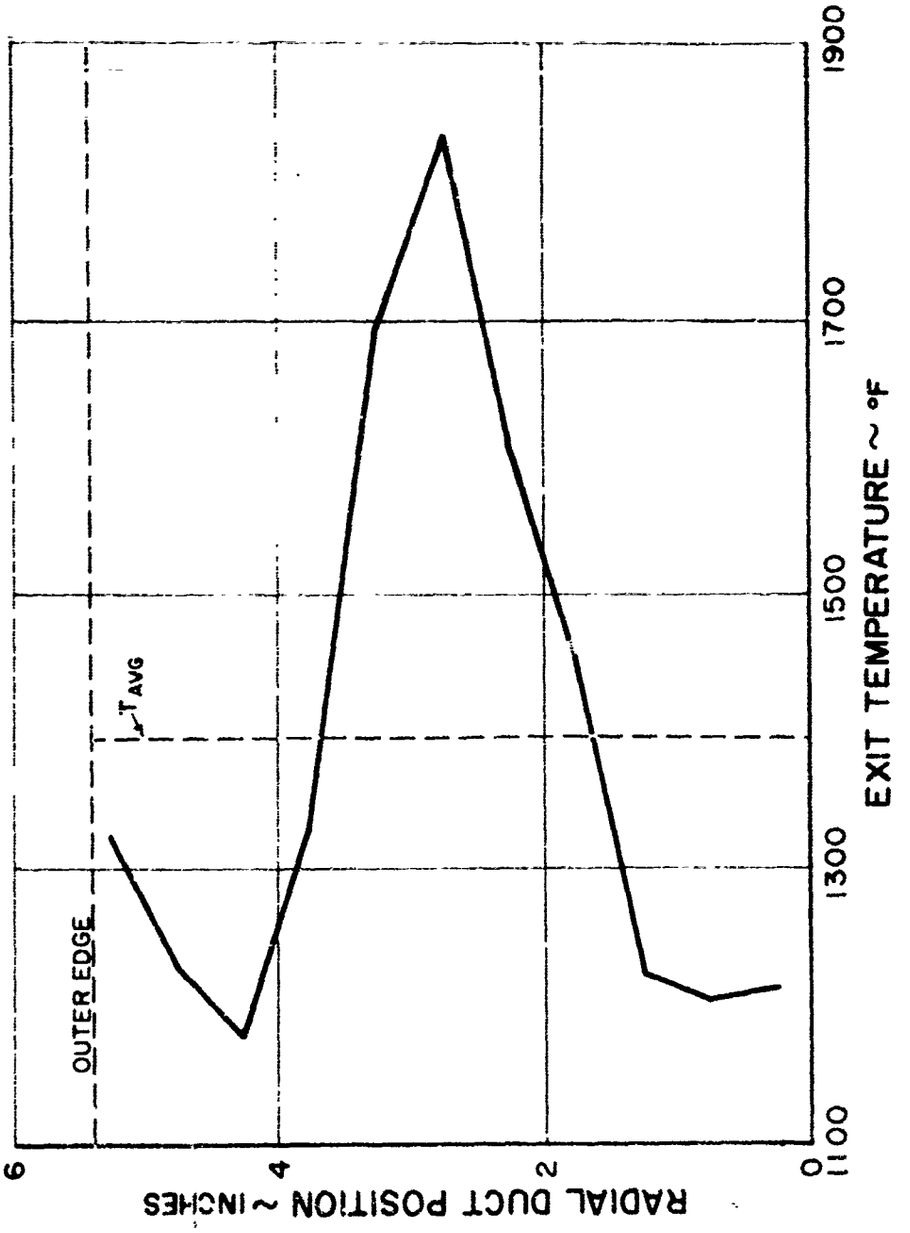
SCHEMATIC DIAGRAM OF RAM INDUCTION BURNER

Figure 2-4



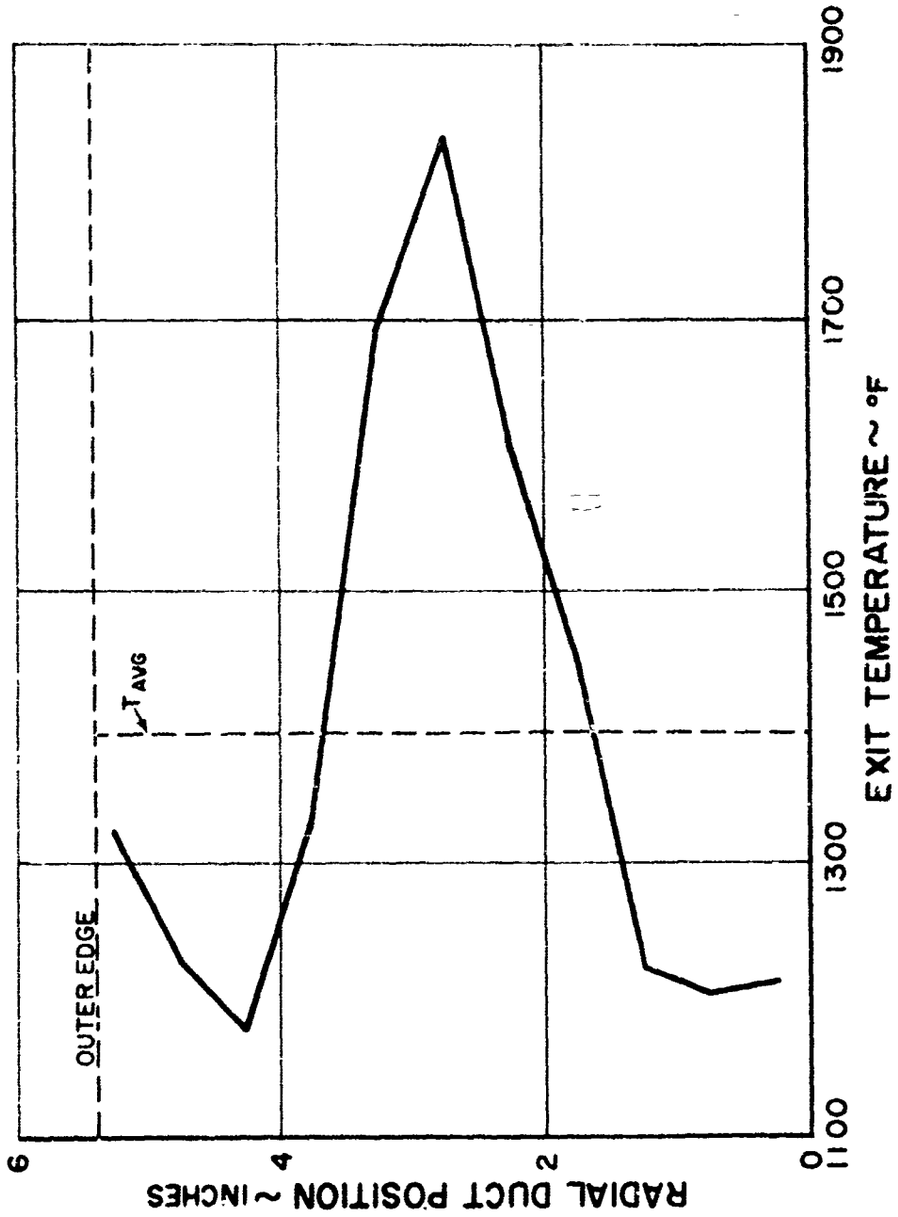
DETAILED SECTION OF SCOOP WITH FILM COOLING LOUVERS ON RAM INDUCTION BURNER

Figure 2-5



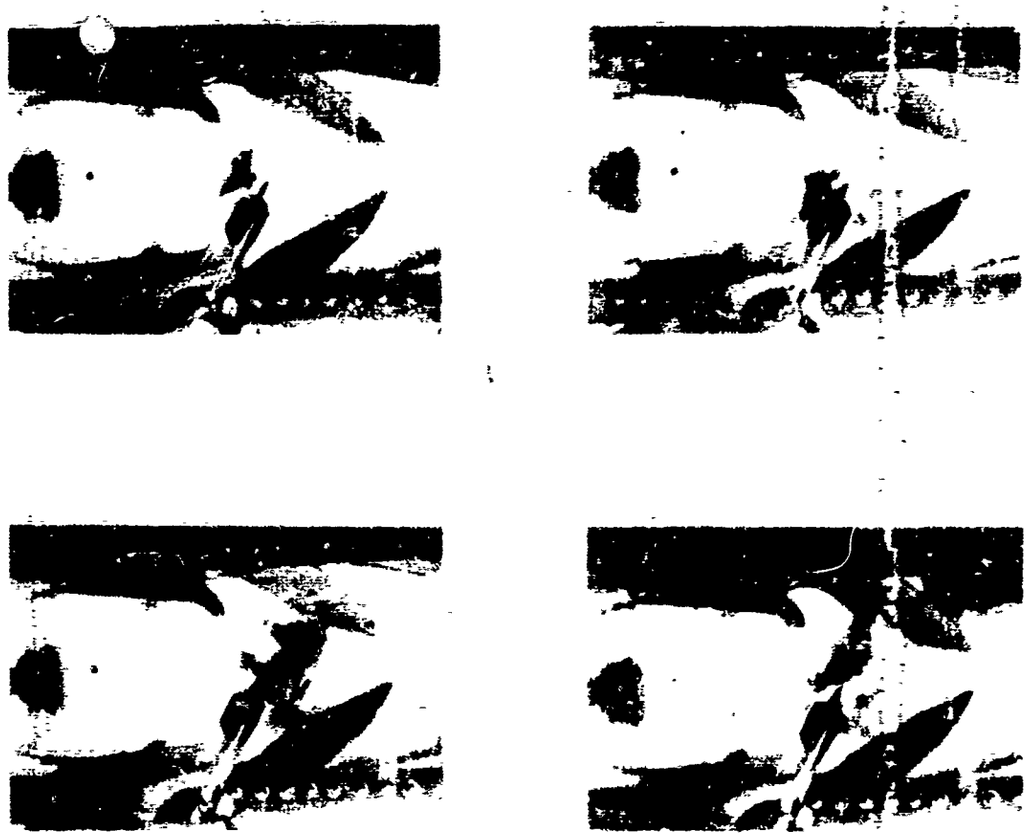
TEMPERATURE PROFILE PRODUCED BY RAM INDUCTION BURNER WITH SCOOPS EXTENDING TO THE MIDDLE OF THE BURNER

Figure 2-6



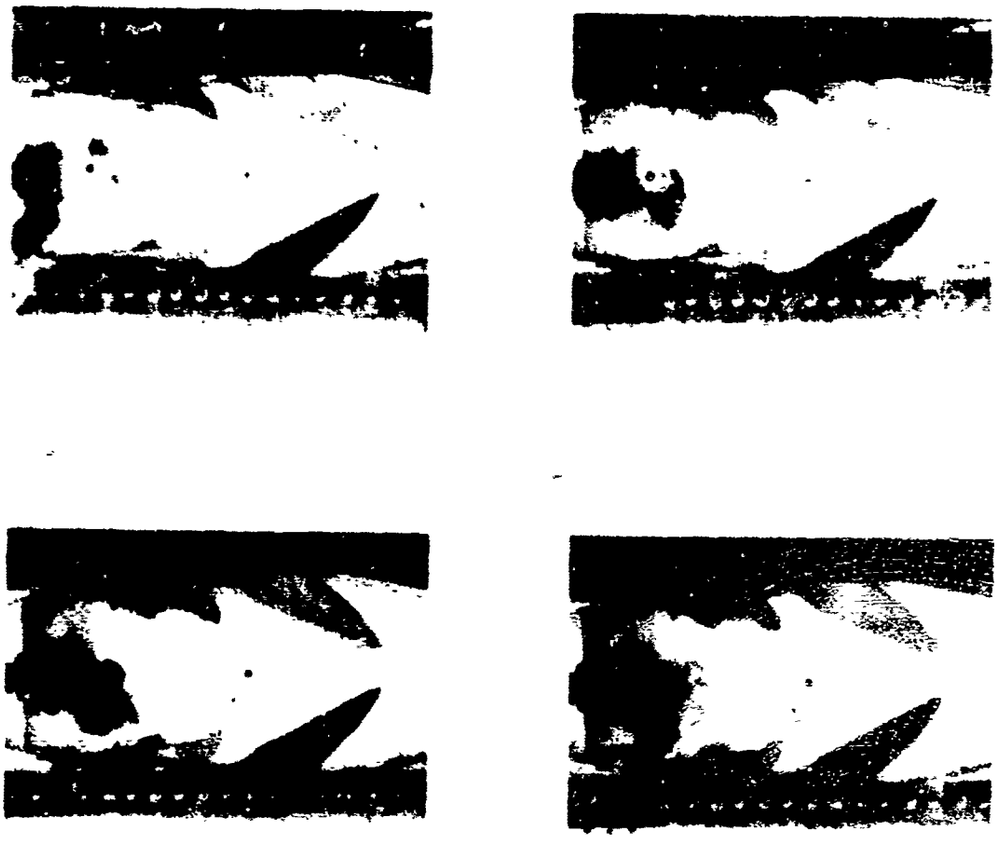
TEMPERATURE PROFILE PRODUCED BY RAM INDUCTION BURNER WITH LIMITED PENETRATION

Figure 2-7



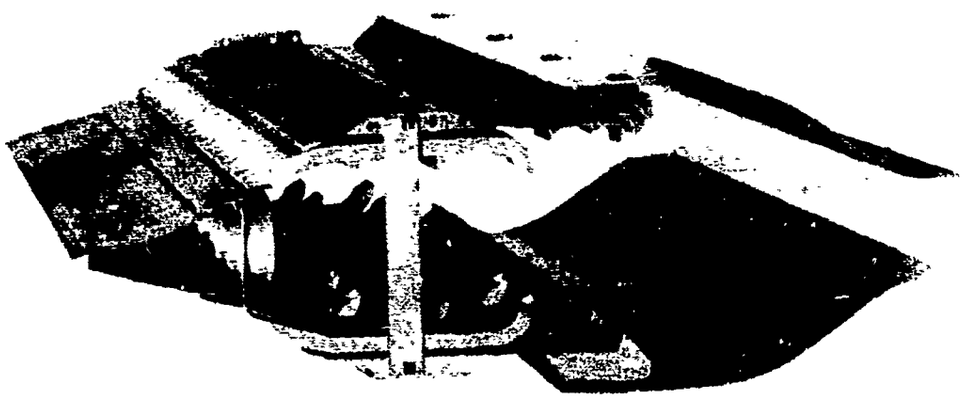
PENETRATION AND MIXING CHARACTERISTICS OF THE DOWNSTREAM ROW OF PRIMARY RAM INDUCTION BURNER SCOOPS

Figure 2-8



FLOW PATTERN IN RECIRCULATION ZONE
OF RAM INDUCTION BURNER

Figure 2-9



BURNER LINER TO BE USED IN SECONDARY SCOOP DESIGN STUDIES

Figure 2-10



FE-14756

BURNER LINER TO BE USED IN SECONDARY SCOOP DESIGN STUDIES

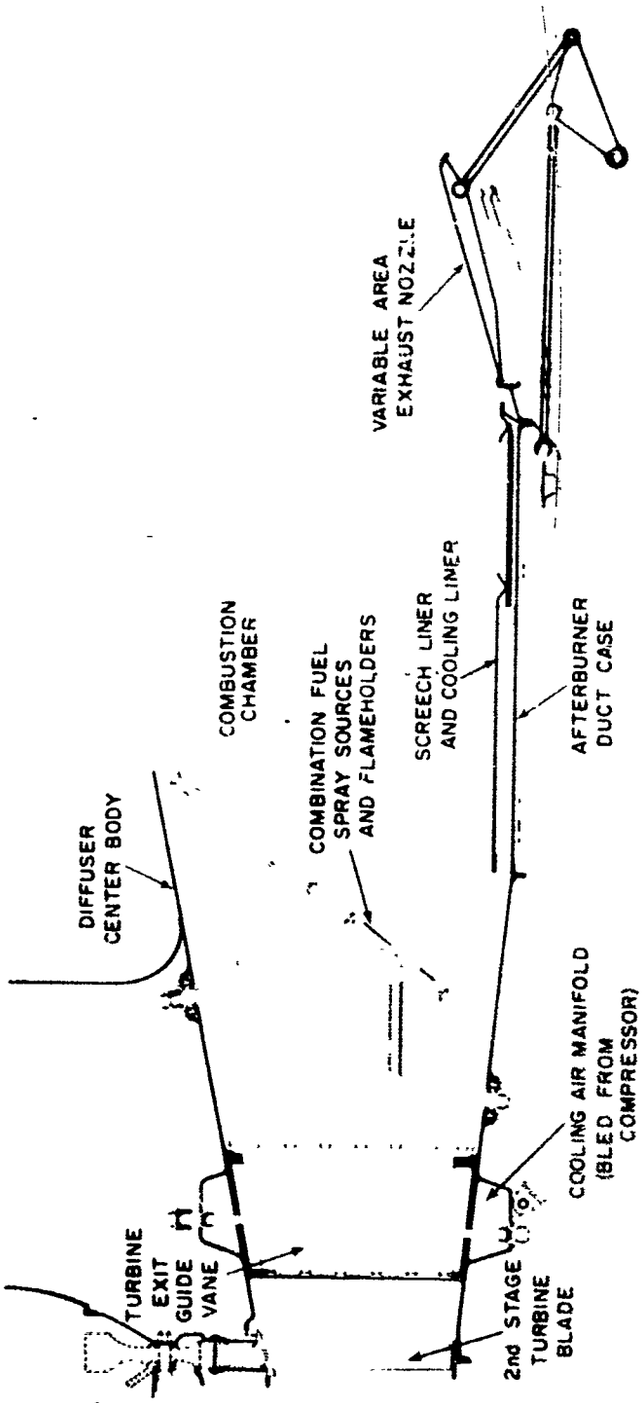
Figure 2-11

SECURITY MARKING

The classified or limited status of this report applies to each page, unless otherwise marked.
Separate page printouts MUST be marked accordingly.

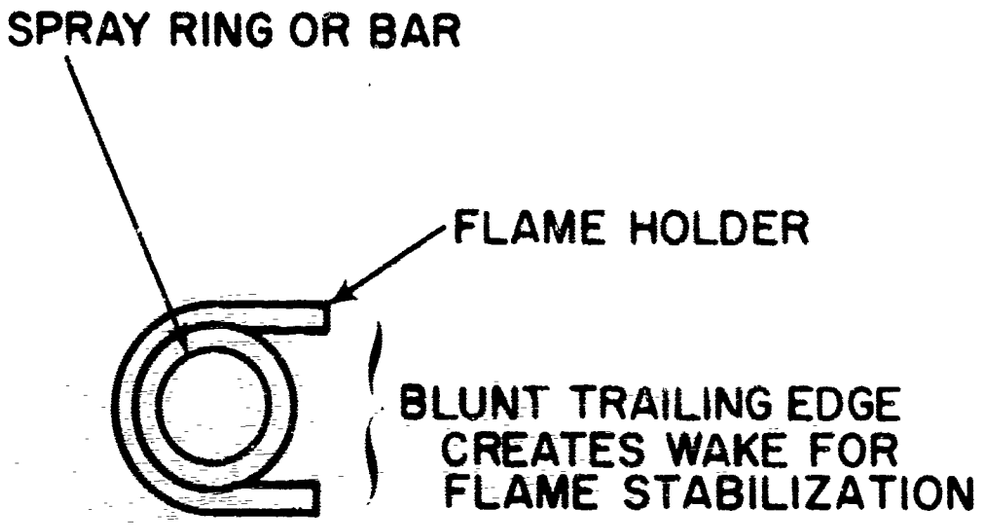
THIS DOCUMENT CONTAINS INFORMATION AFFECTING THE NATIONAL DEFENSE OF THE UNITED STATES WITHIN THE MEANING OF THE ESPIONAGE LAWS, TITLE 18, U.S.C., SECTIONS 793 AND 794. THE TRANSMISSION OR THE REVELATION OF ITS CONTENTS IN ANY MANNER TO AN UNAUTHORIZED PERSON IS PROHIBITED BY LAW.

NOTICE: When government or other drawings, specifications or other data are used for any purpose other than in connection with a definitely related government procurement operation, the U. S. Government thereby incurs no responsibility, nor any obligation whatsoever; and the fact that the Government may have formulated, furnished, or in any way supplied the said drawings, specifications, or other data is not to be regarded by implication or otherwise as in any manner licensing the holder or any other person or corporation, or conveying any rights or permission to manufacture, use or sell any patented invention that may in any way be related thereto.



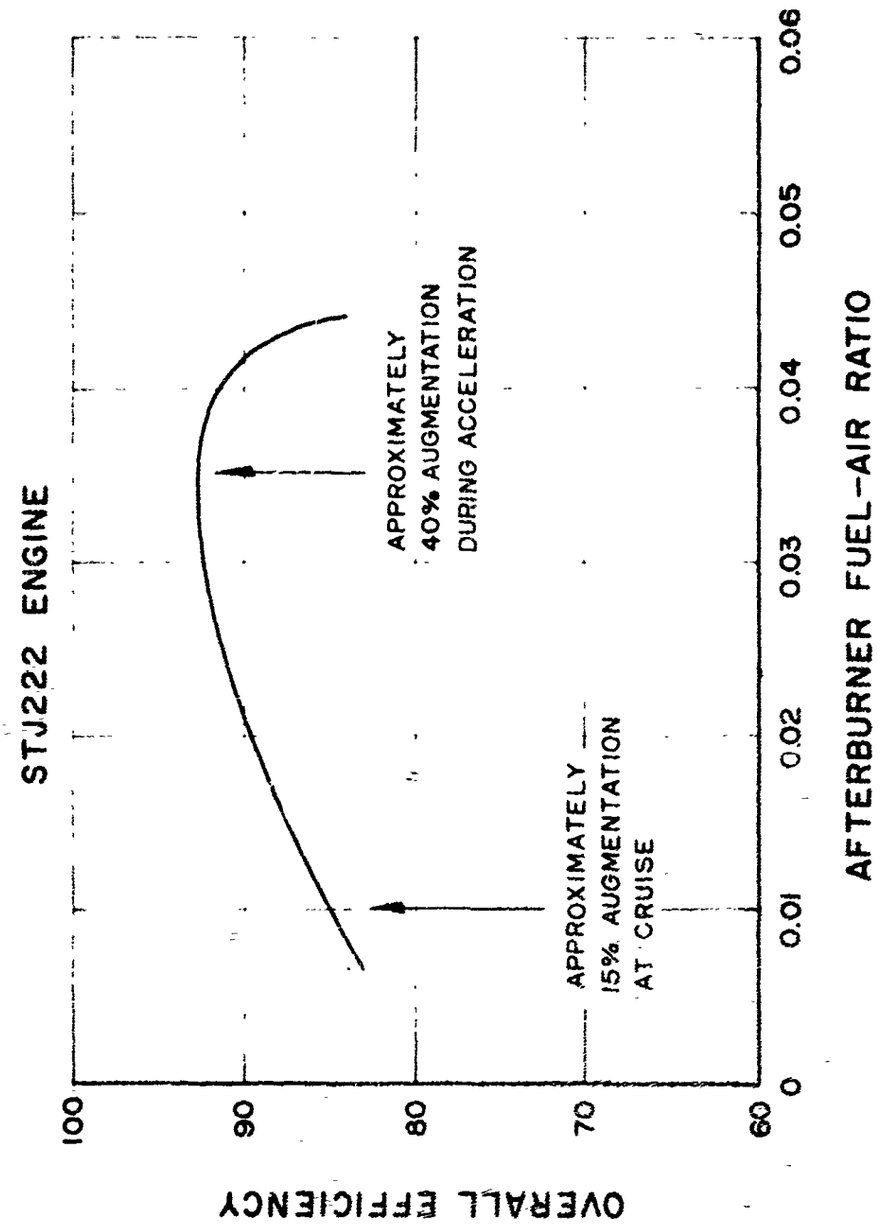
STJ 222 AFTERBURNER

Figure 2-12



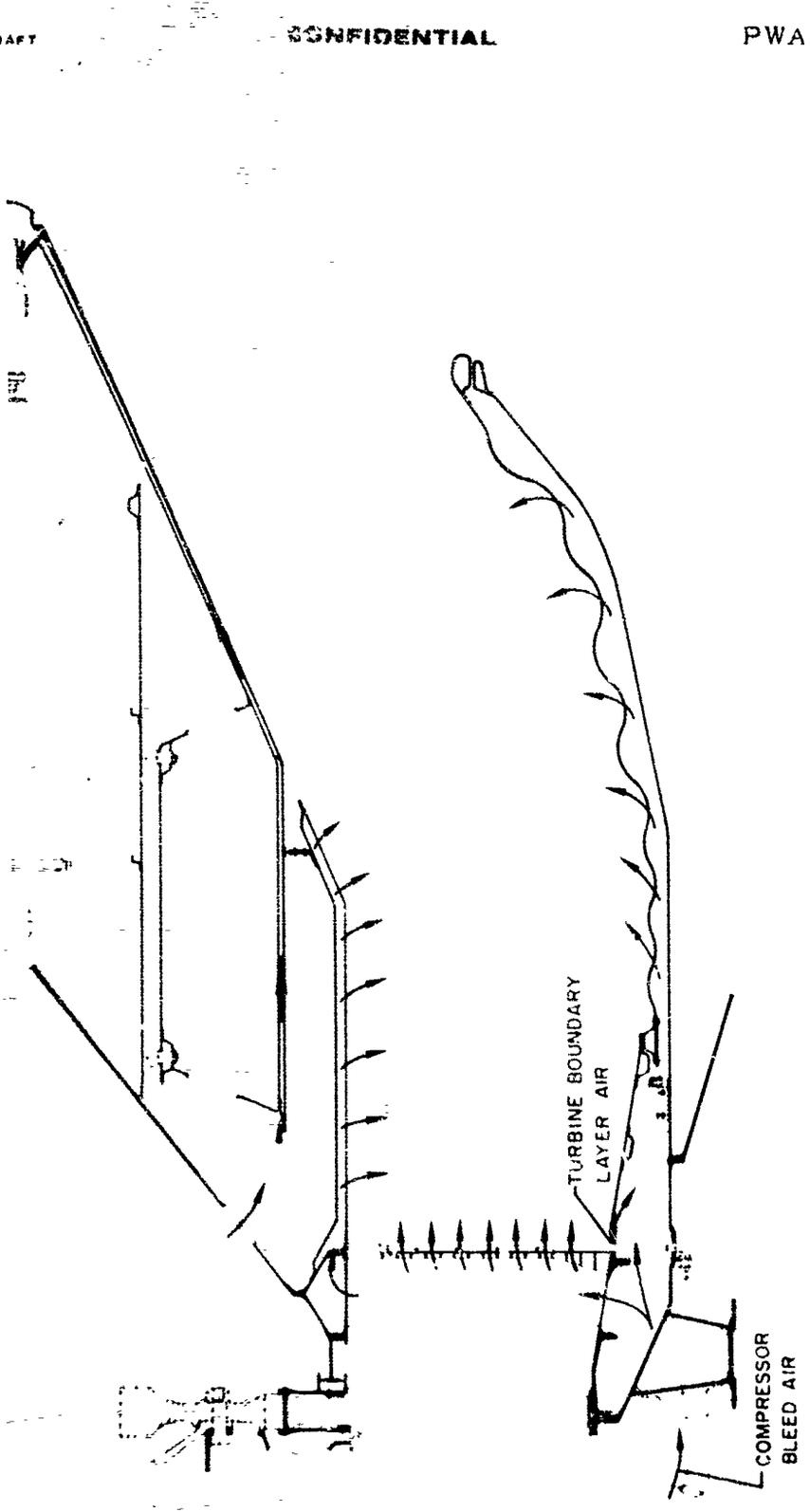
TYPICAL SPRAY RING-FLAMEHOLDER USED IN AFTERBURNER OF STJ 222 ENGINE

Figure 2-13



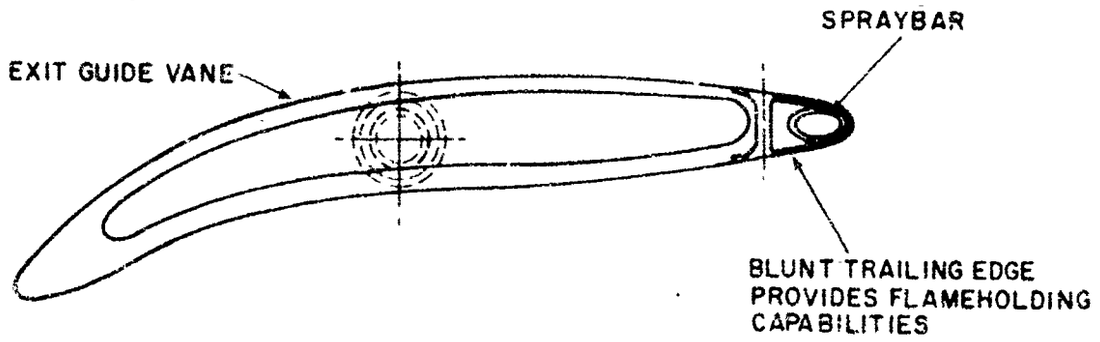
ESTIMATED EFFICIENCY OF AFTERBURNER AS A FUNCTION OF THE FUEL-TO-AIR RATIO

Figure 2-14



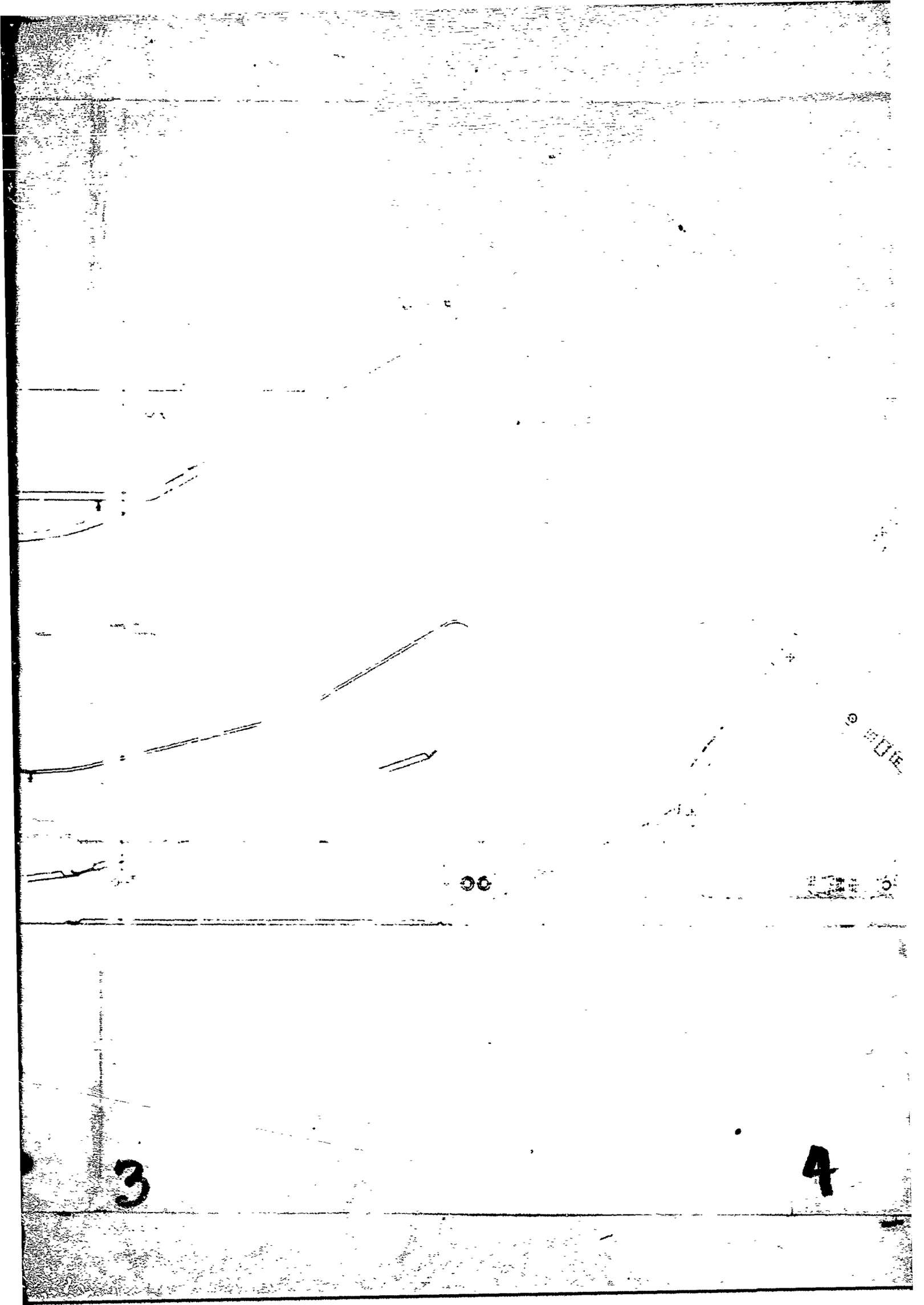
SCHEMATIC DIAGRAM OF TAILPIPE, NOZZLE, AND TURBINE EXIT GUIDE VANES OF STJ 227 ENGINE

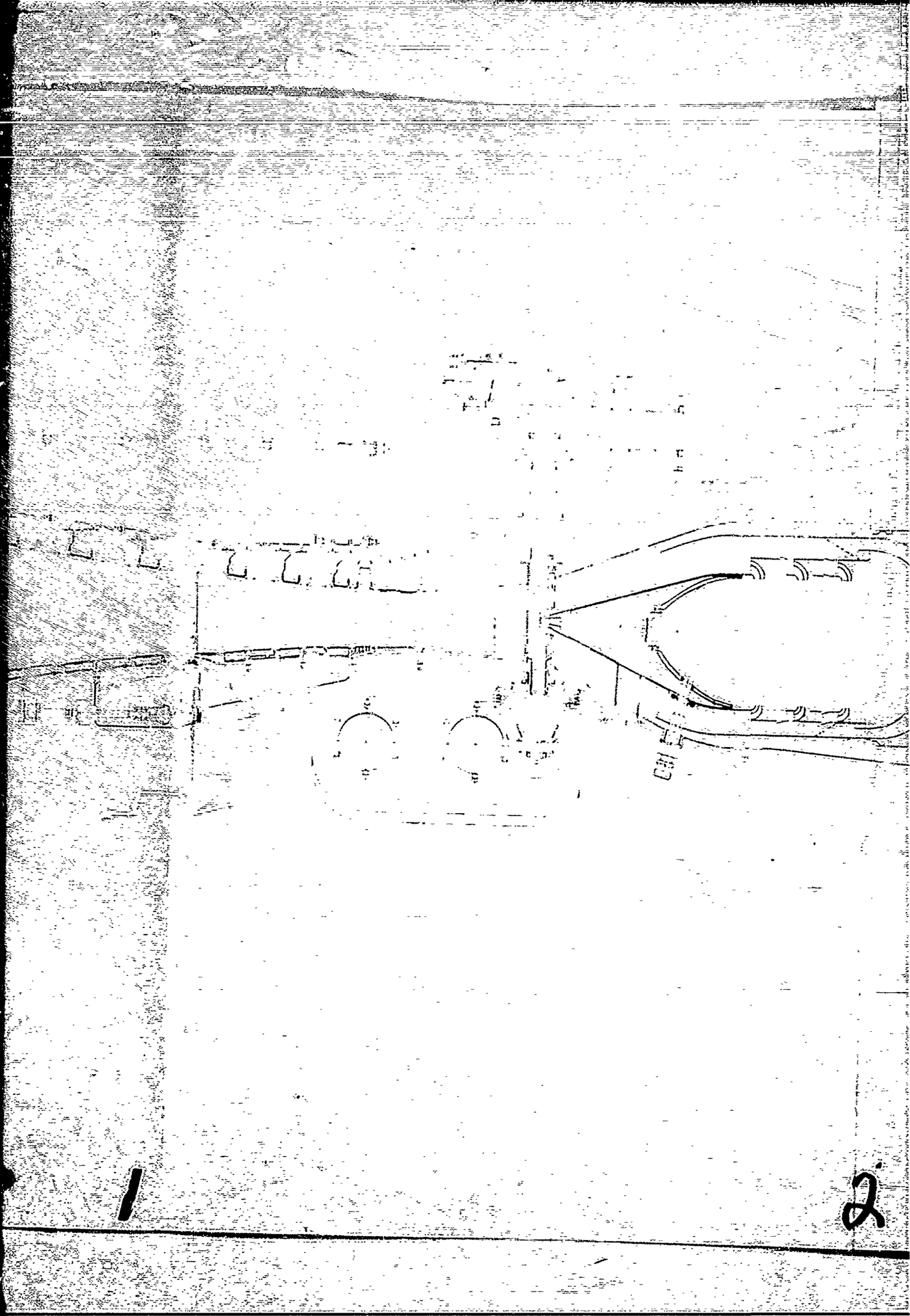
Figure 2-13

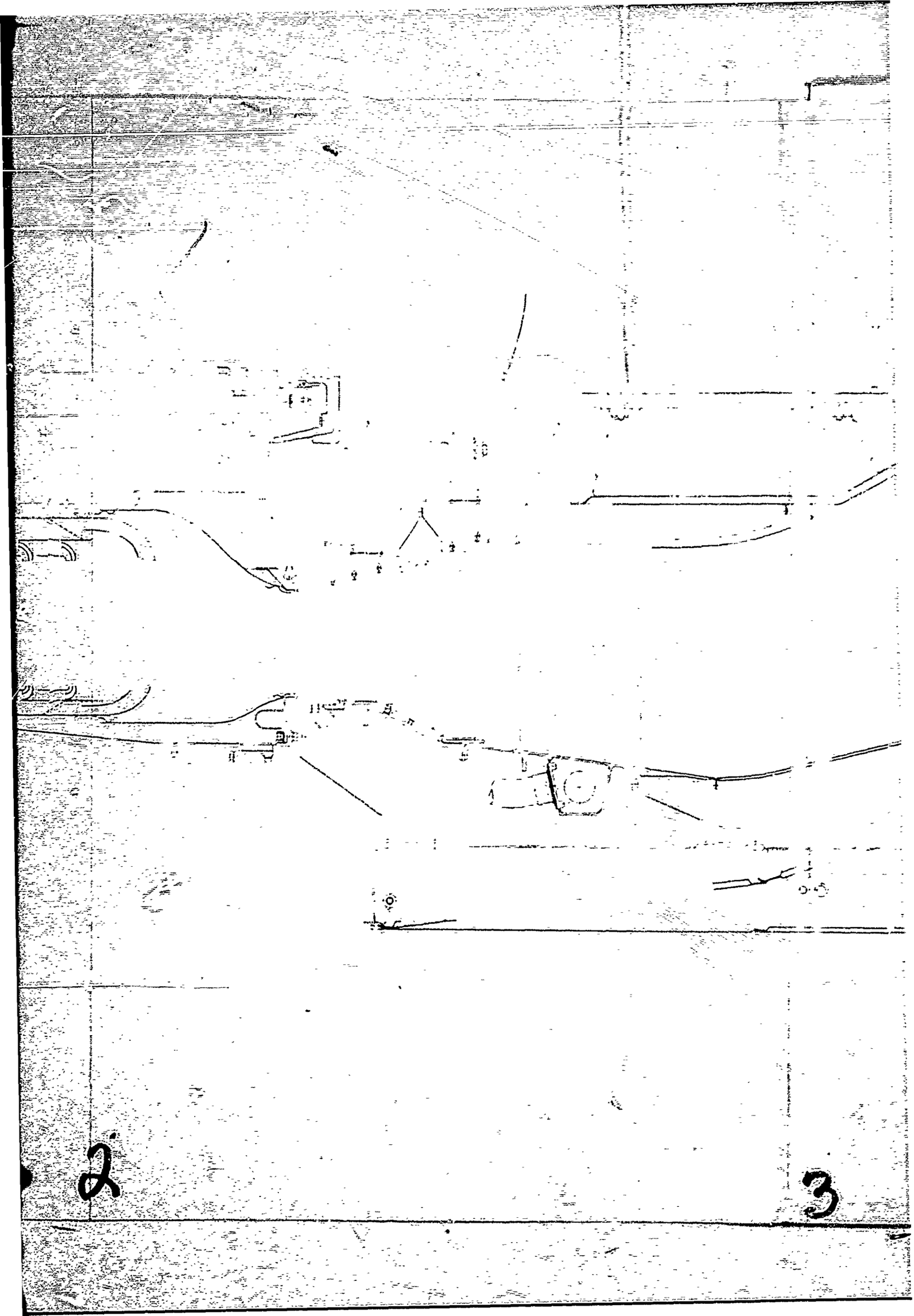


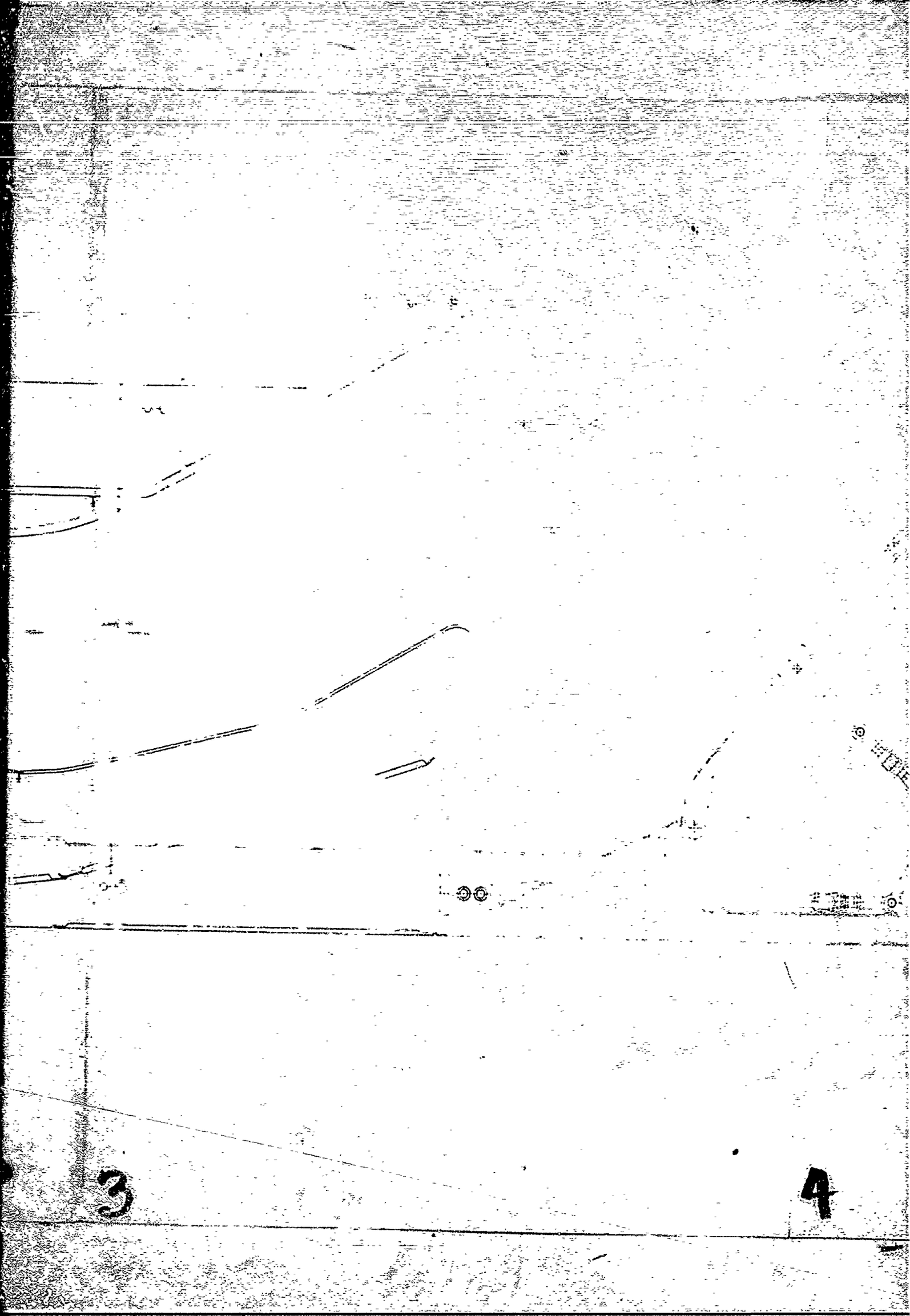
CROSS-SECTIONAL VIEW OF INTEGRAL SPRAY BAR-FLAMEHOLDER-EXIT GUIDE VANE ASSEMBLY

Figure 2-16



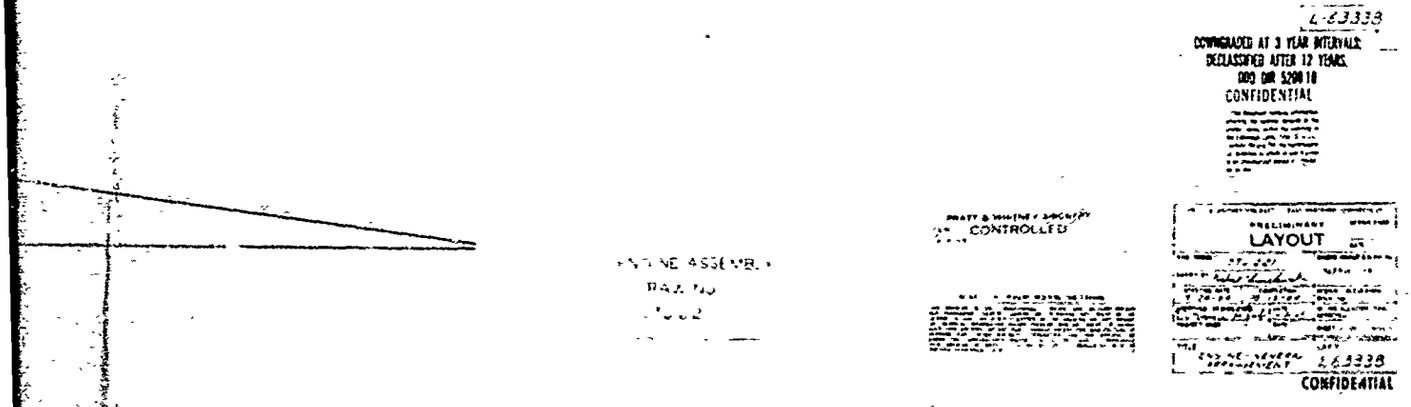






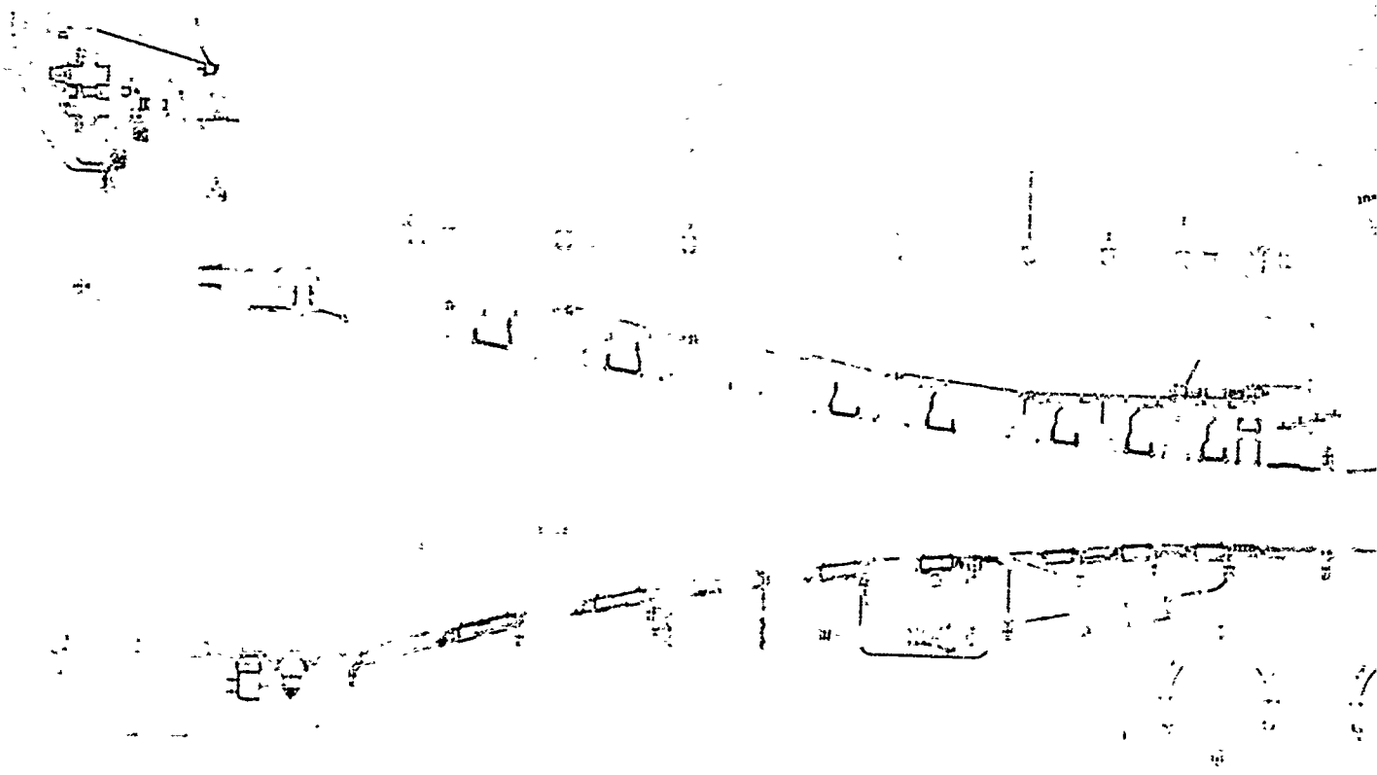
4

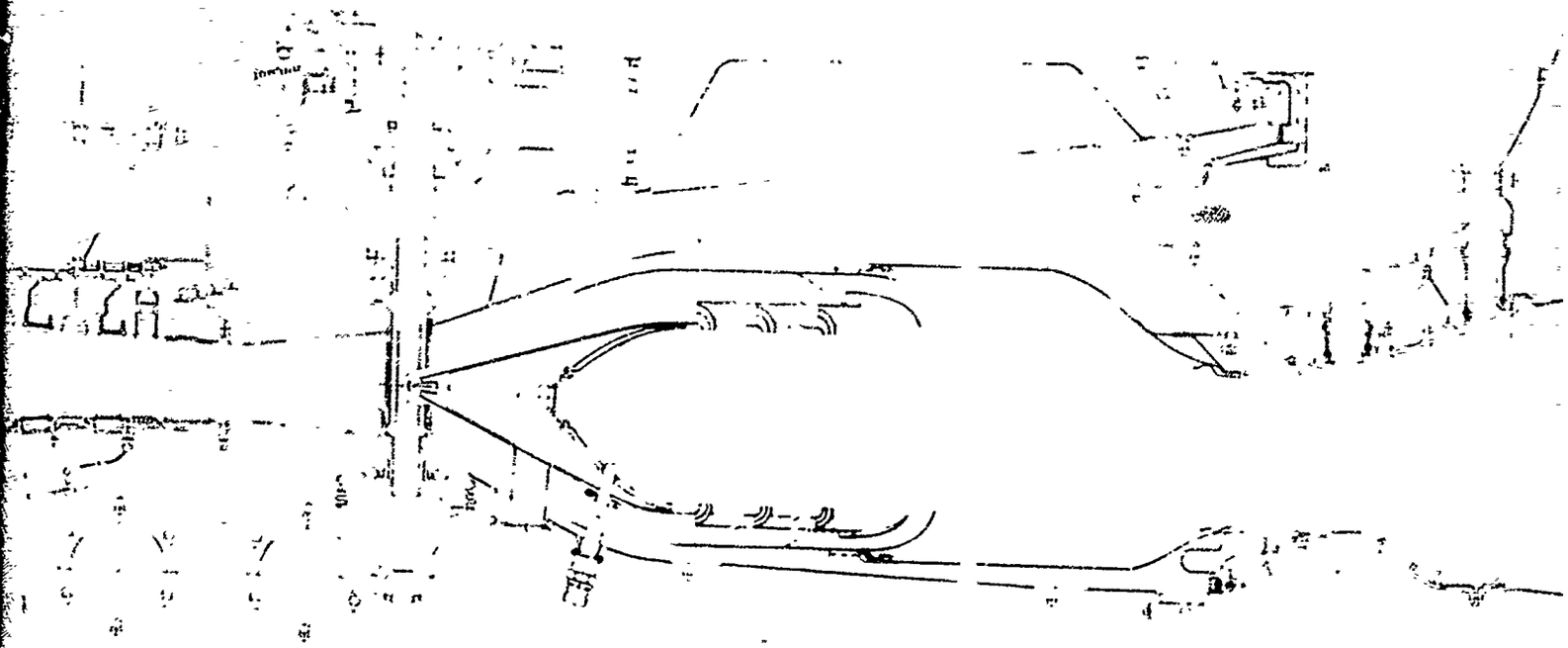
5

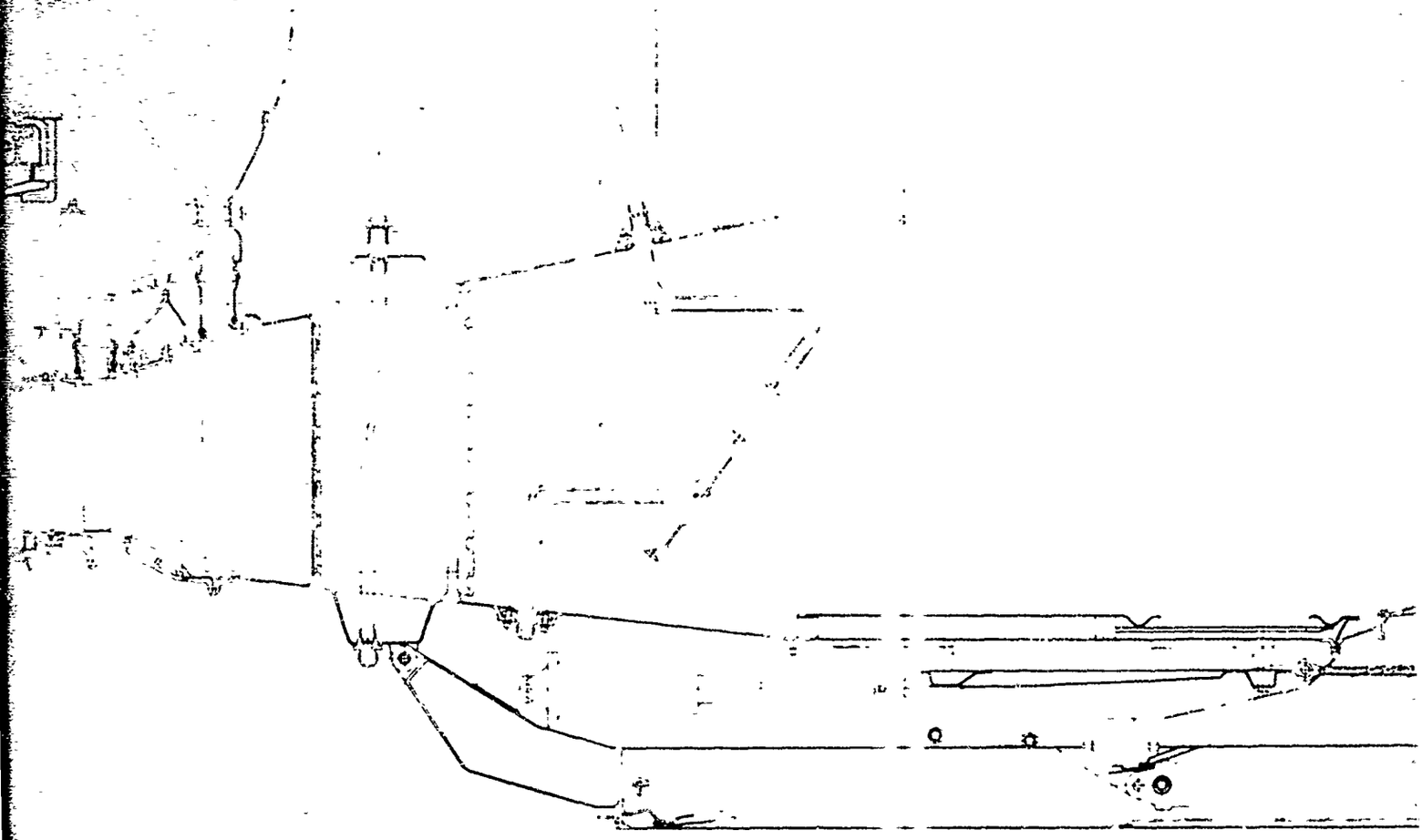


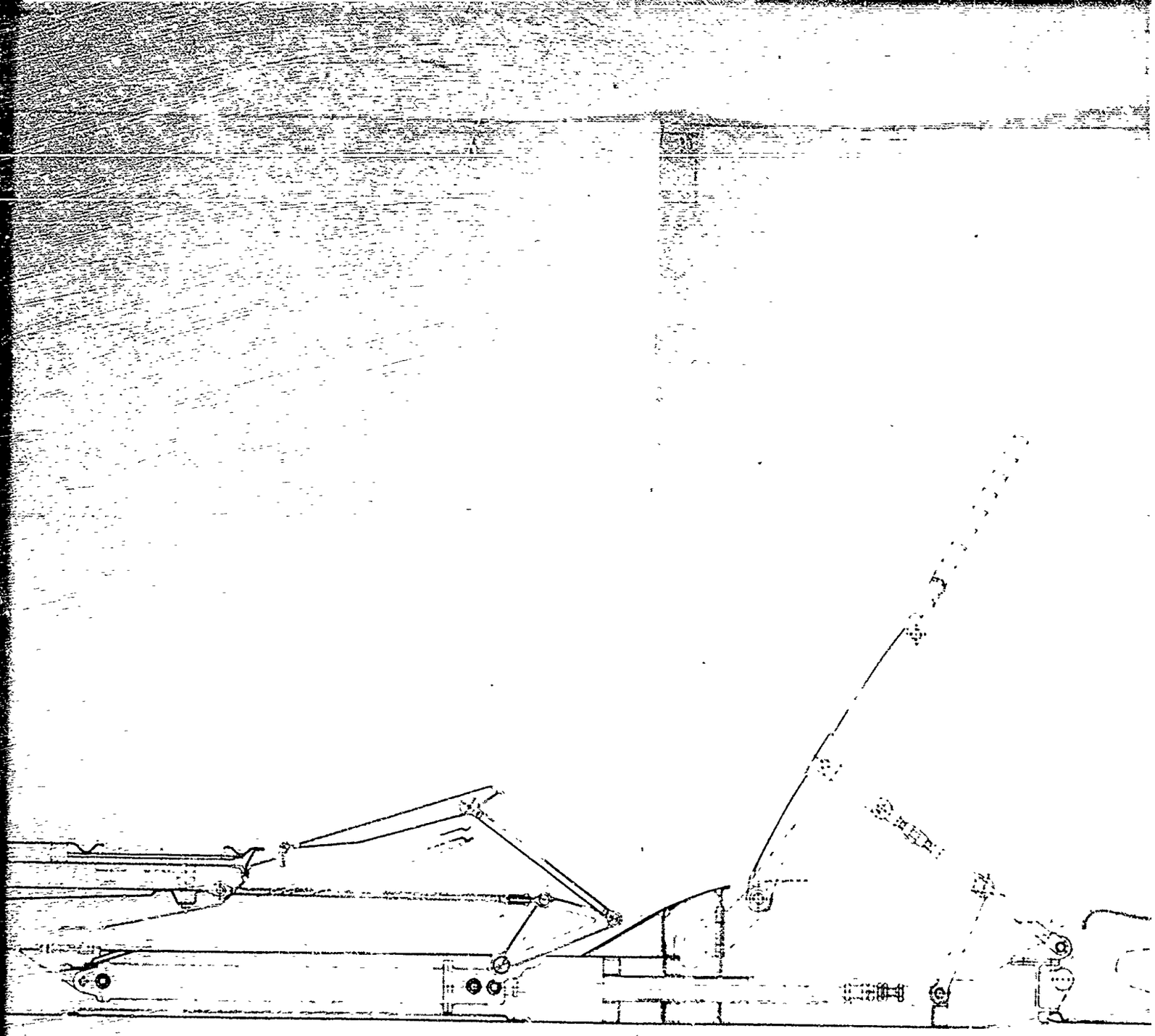
CROSS SECTIONAL DRAWING OF STJ 221 ENGINE

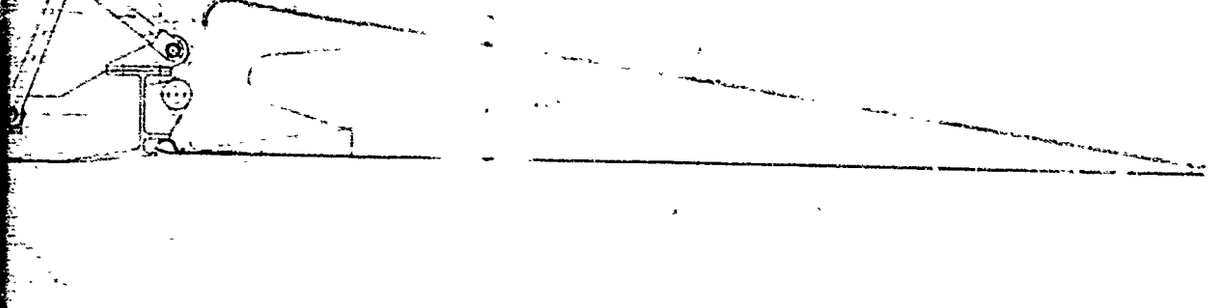
Figure 2-18











ENGINE ASSEMBLY
DRAWING
No. 62L

CROSS SECTIONAL D

Figure 1

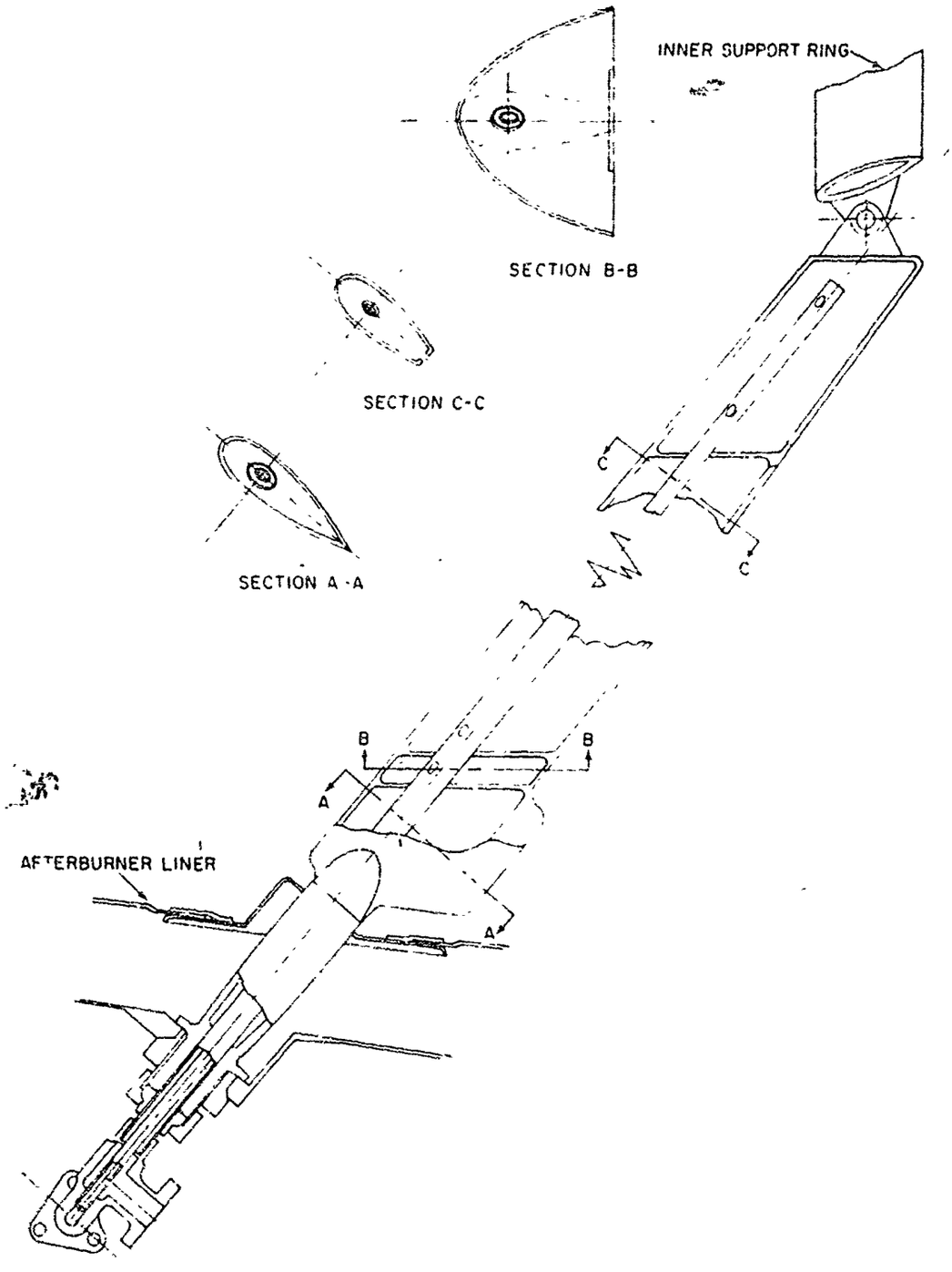
L-63339
DOWNGRADED AT 3 YEAR INTERVALS;
DECLASSIFIED AFTER 12 YEARS.
DOD DIR 5200.10
CONFIDENTIAL

CONTROLLED
LAYOUT
L-63339
CONFIDENTIAL

CROSS SECTIONAL DRAWING OF STJ 222 ENGINE

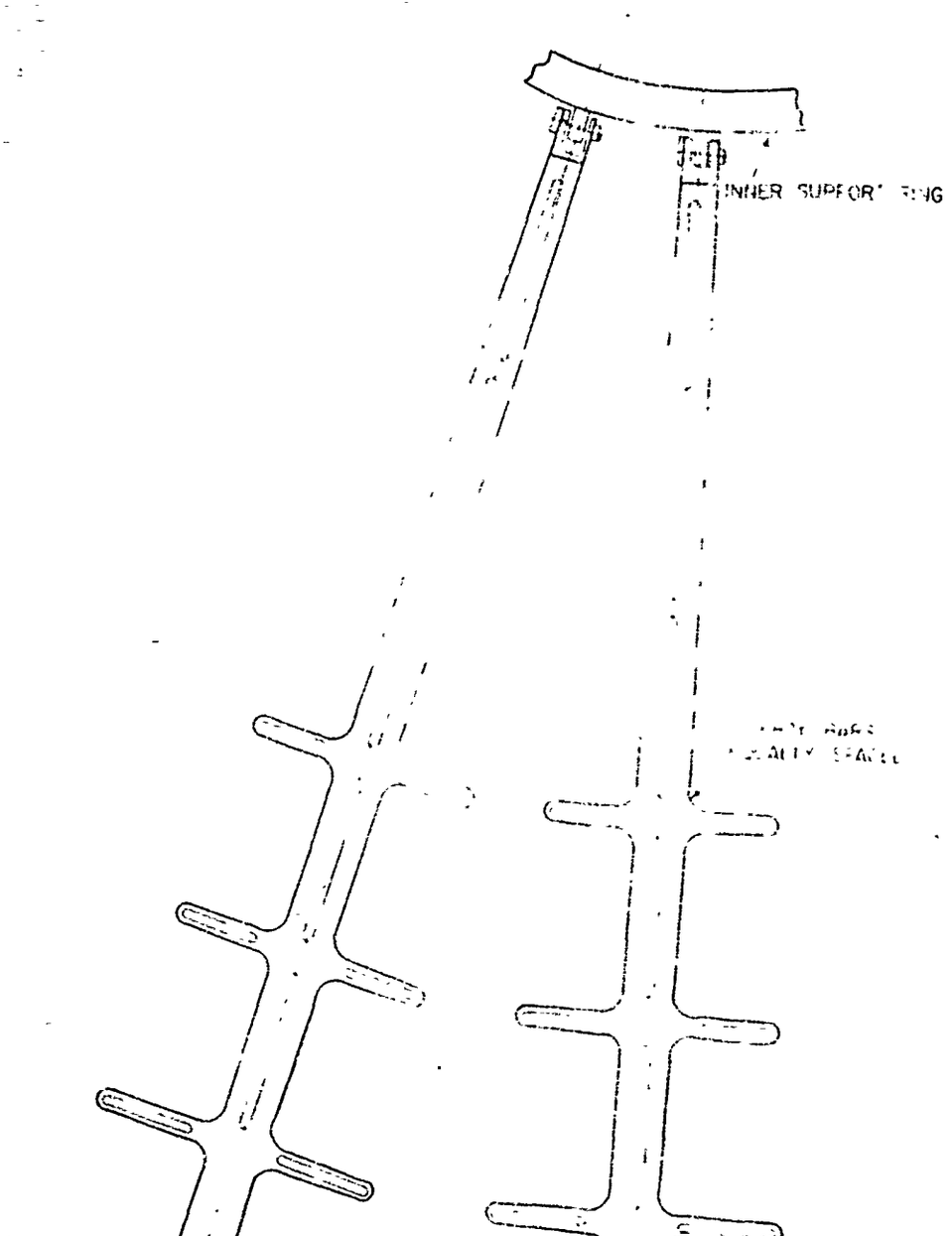
Figure 2-19

DOWNGRADED AT 3 YEAR INTERVALS;
DECLASSIFIED AFTER 12 YEARS.
DOD DIR 5200.10



SECTIONED VIEW OF ALTERNATE SPRAY BAR-FLAMEHOLDER SYSTEM FOR STJ 222 ENGINE

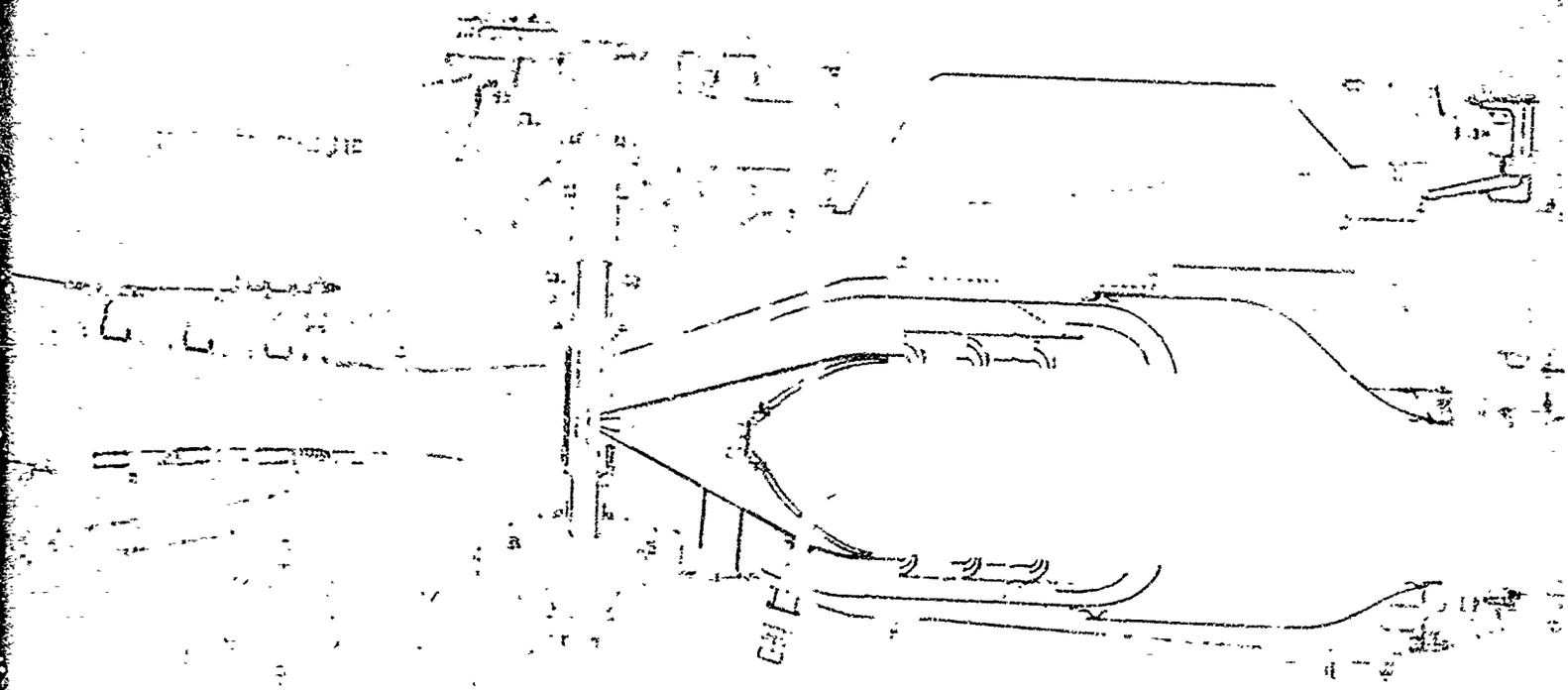
Figure 2-20

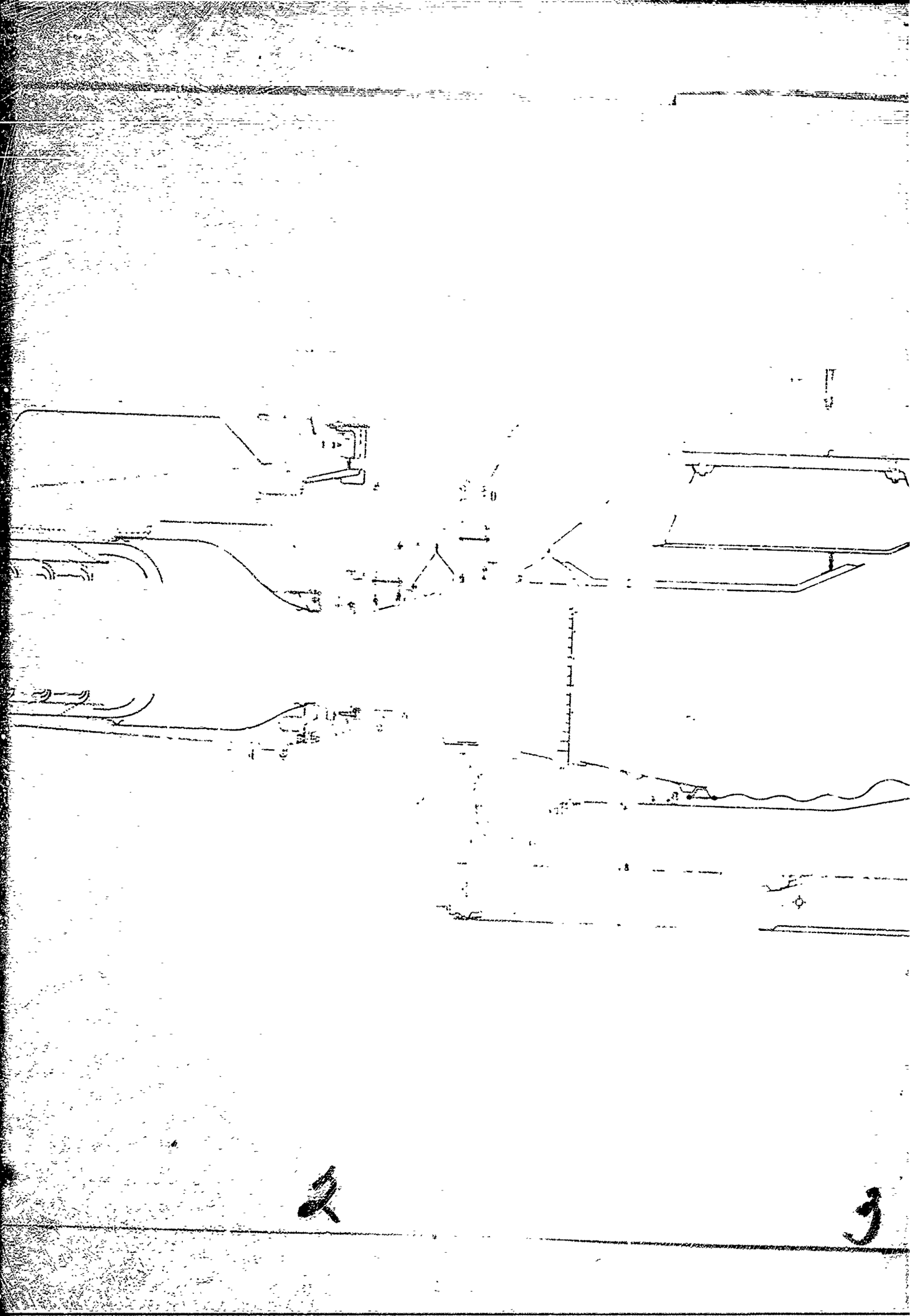


AXIAL VIEW OF ALTERNATE SPRAY BAR-
FLAMEHOLDER SYSTEM FOR STJ222 ENGINE

Figure 2-21







3

4

DOWNGRADED AT 3 YEAR INTERVALS
DECLASSIFIED AFTER 12 YEARS
DOD DIR 5200.10
CONFIDENTIAL

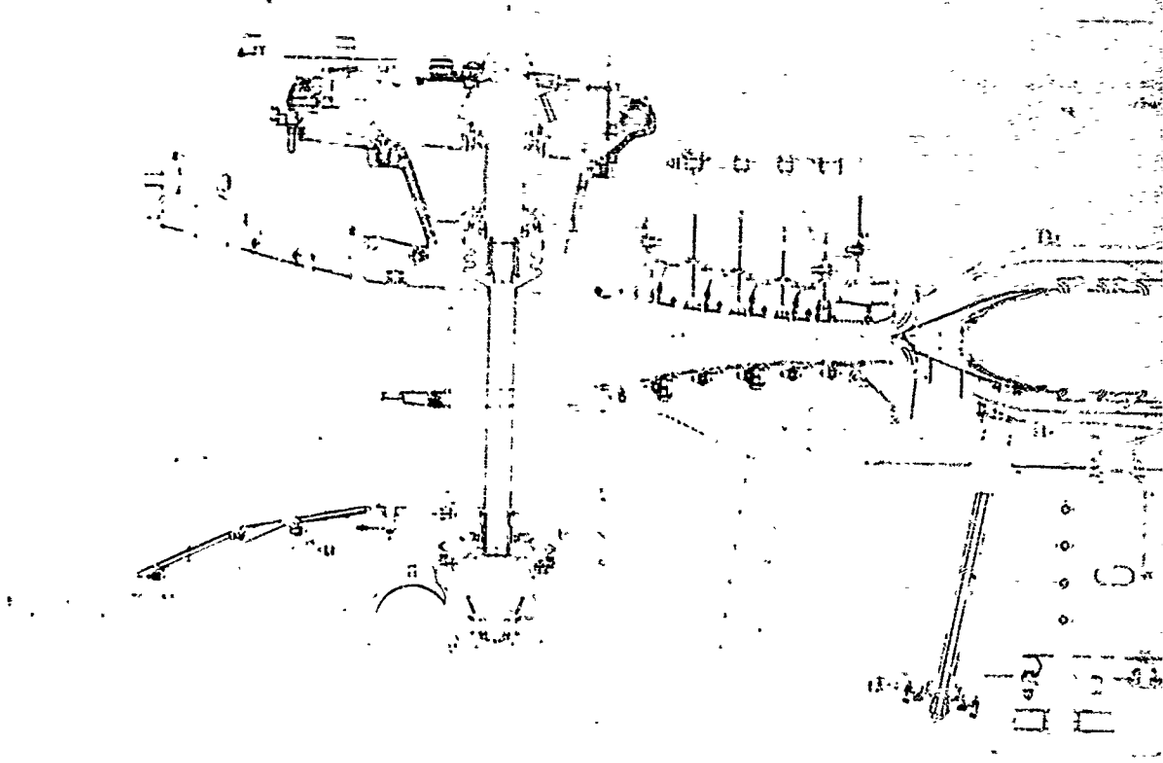
ENGINE ASSEMBLY
DRAWING
ST 227

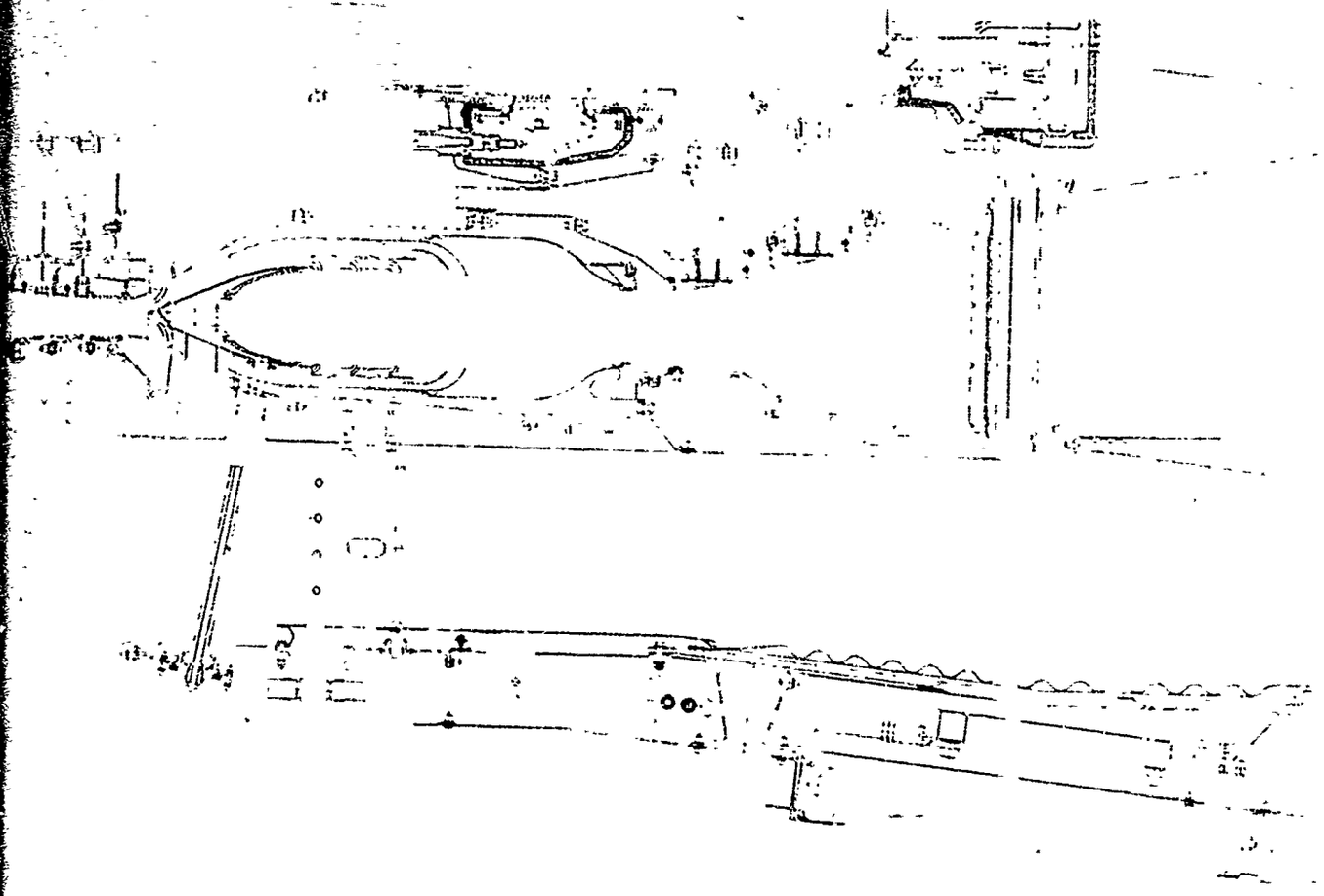
PRATT & WHITNEY AIRCRAFT
CONTROLLED

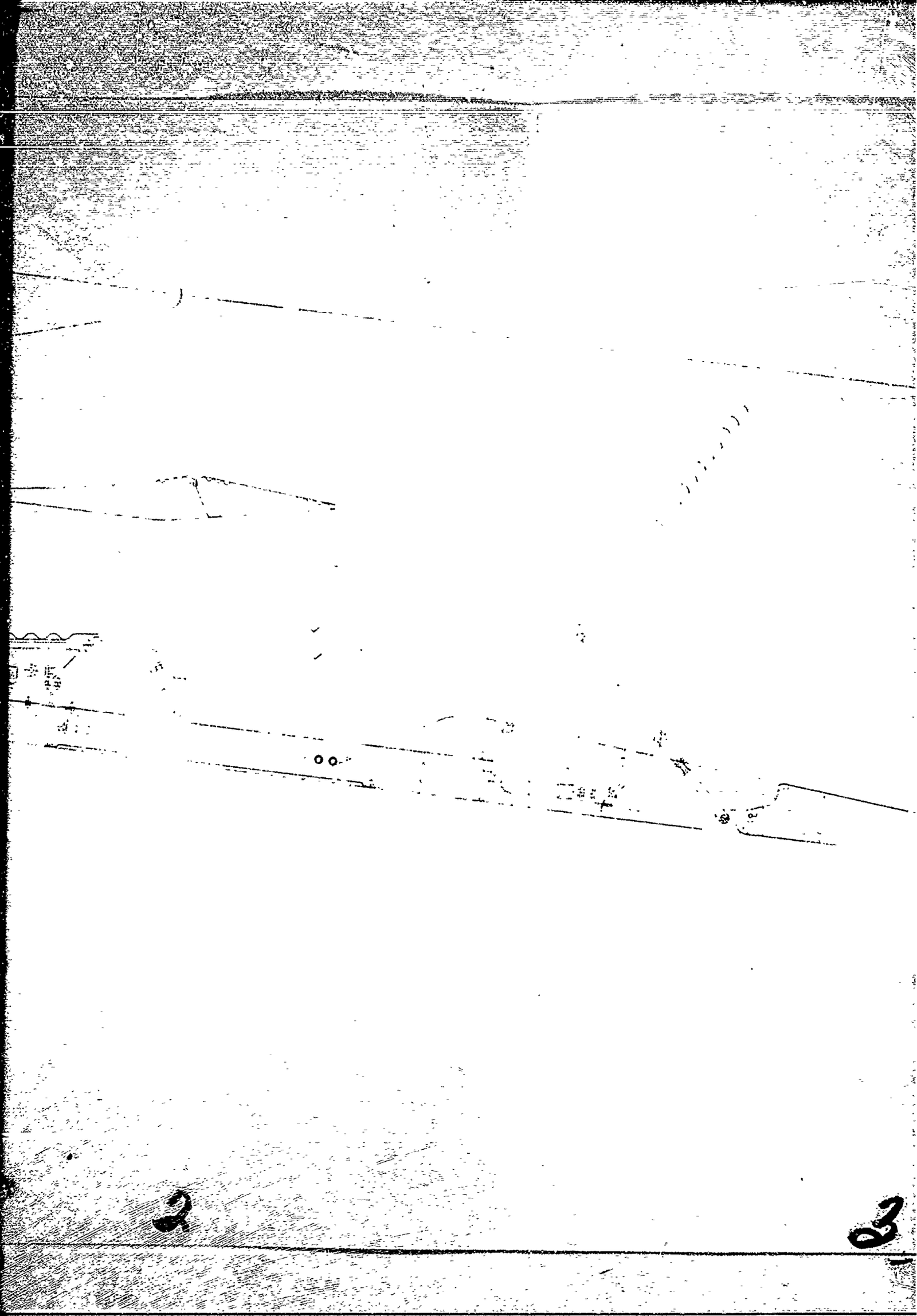
LAYOUT
CONFIDENTIAL

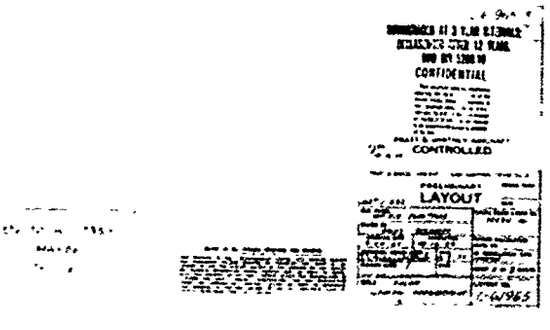
GROSS SECTIONAL DRAWING OF STJ 227 ENGINE

Figure 2-22



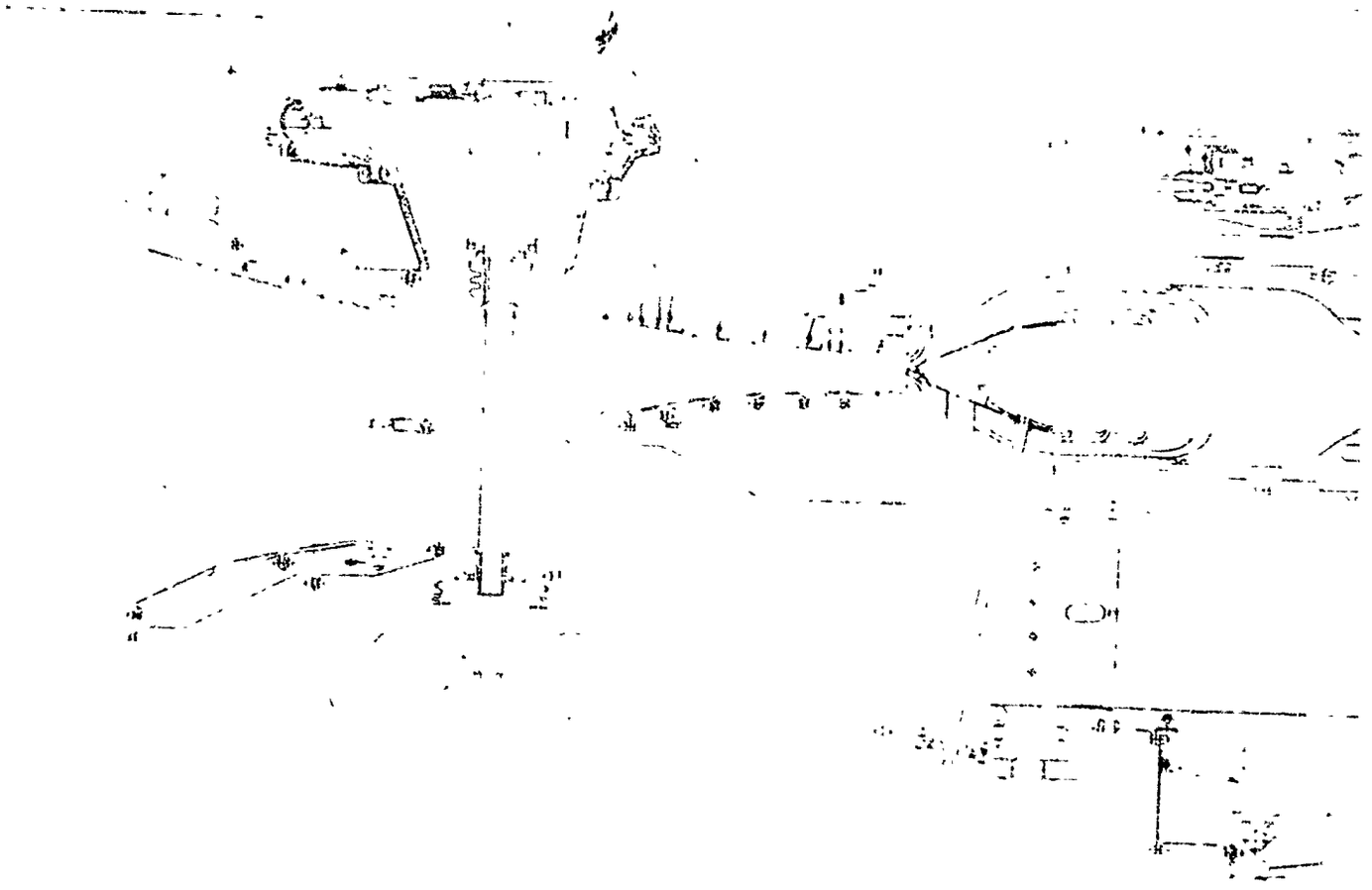


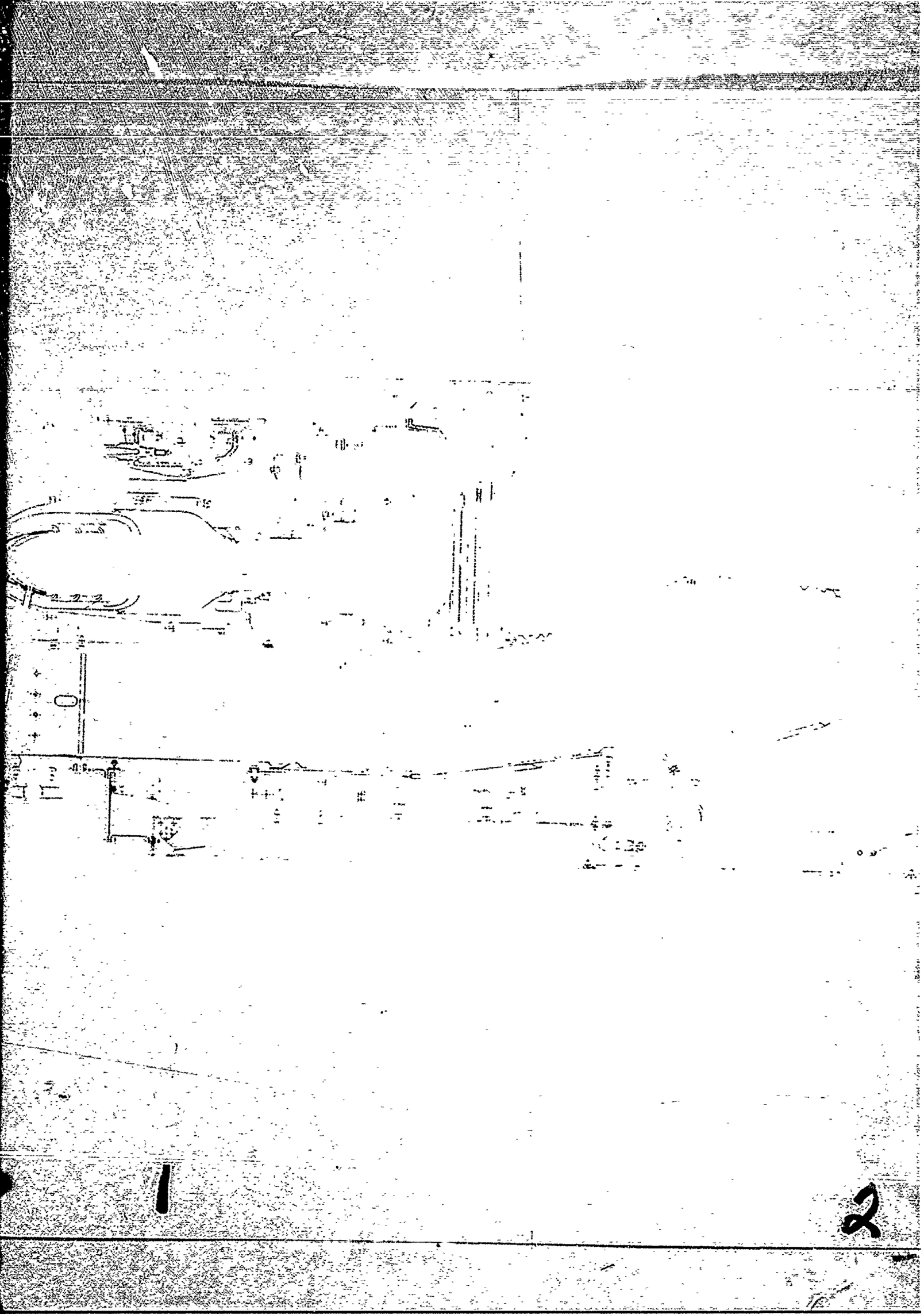




CROSS SECTIONAL DRAWING OF STF219-B ENGINE

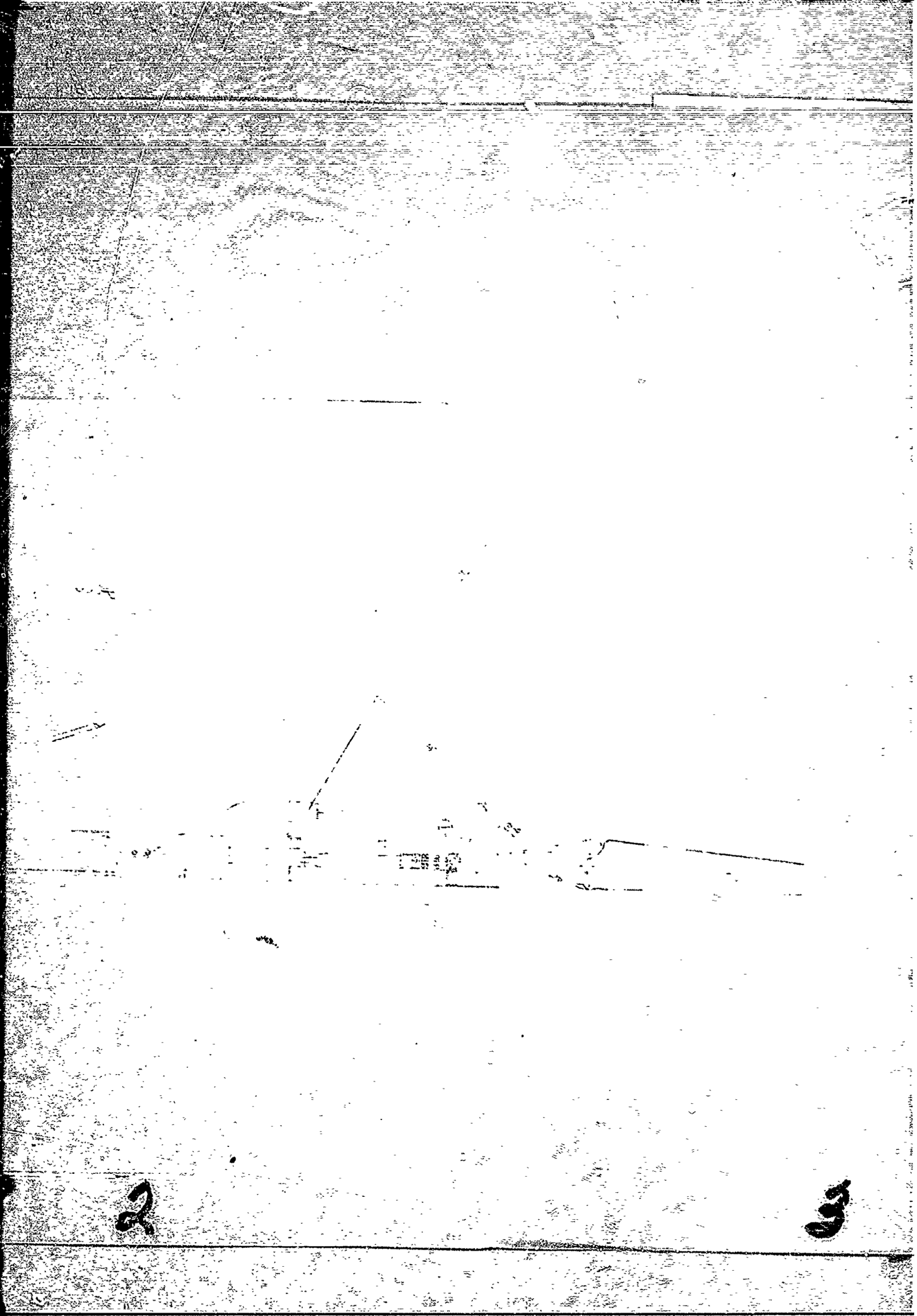
Figure 2-23

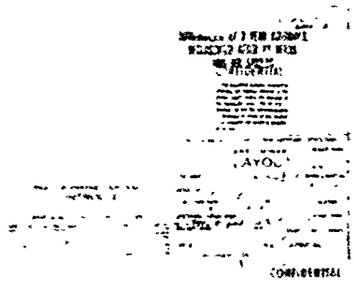




1

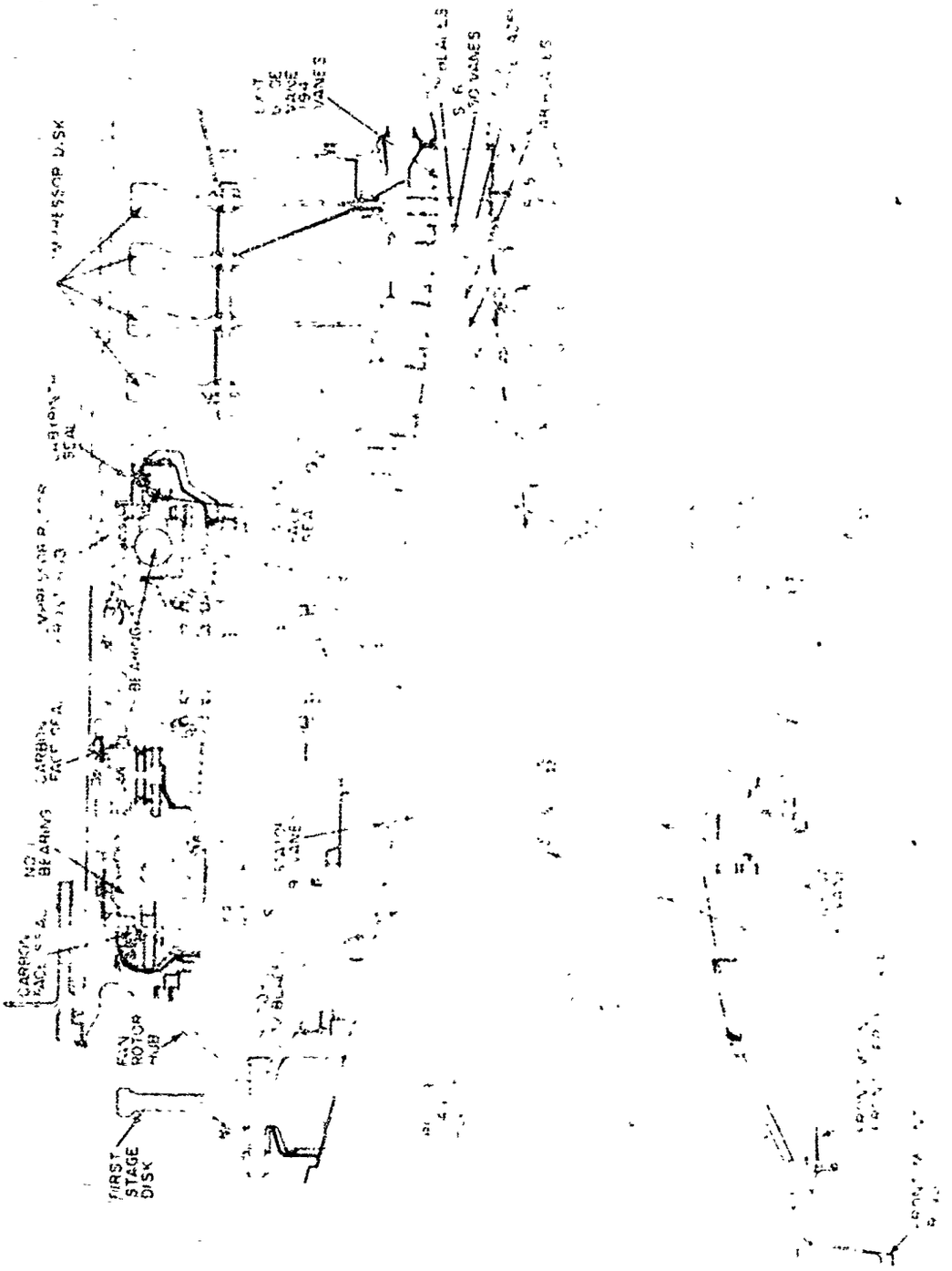
2





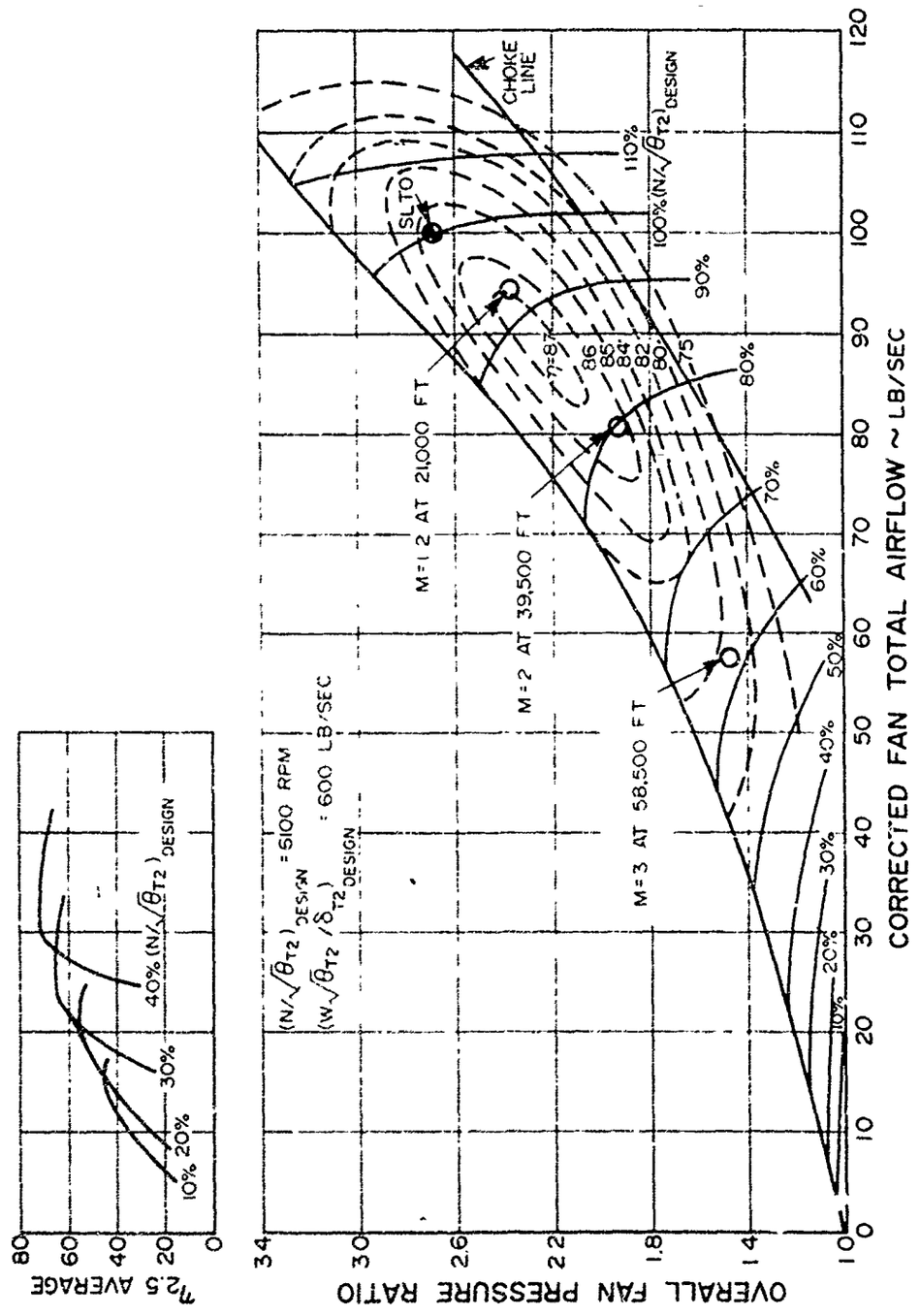
CROSS SECTIONAL DRAWING OF STF219-L ENGINE

Figure 2-24



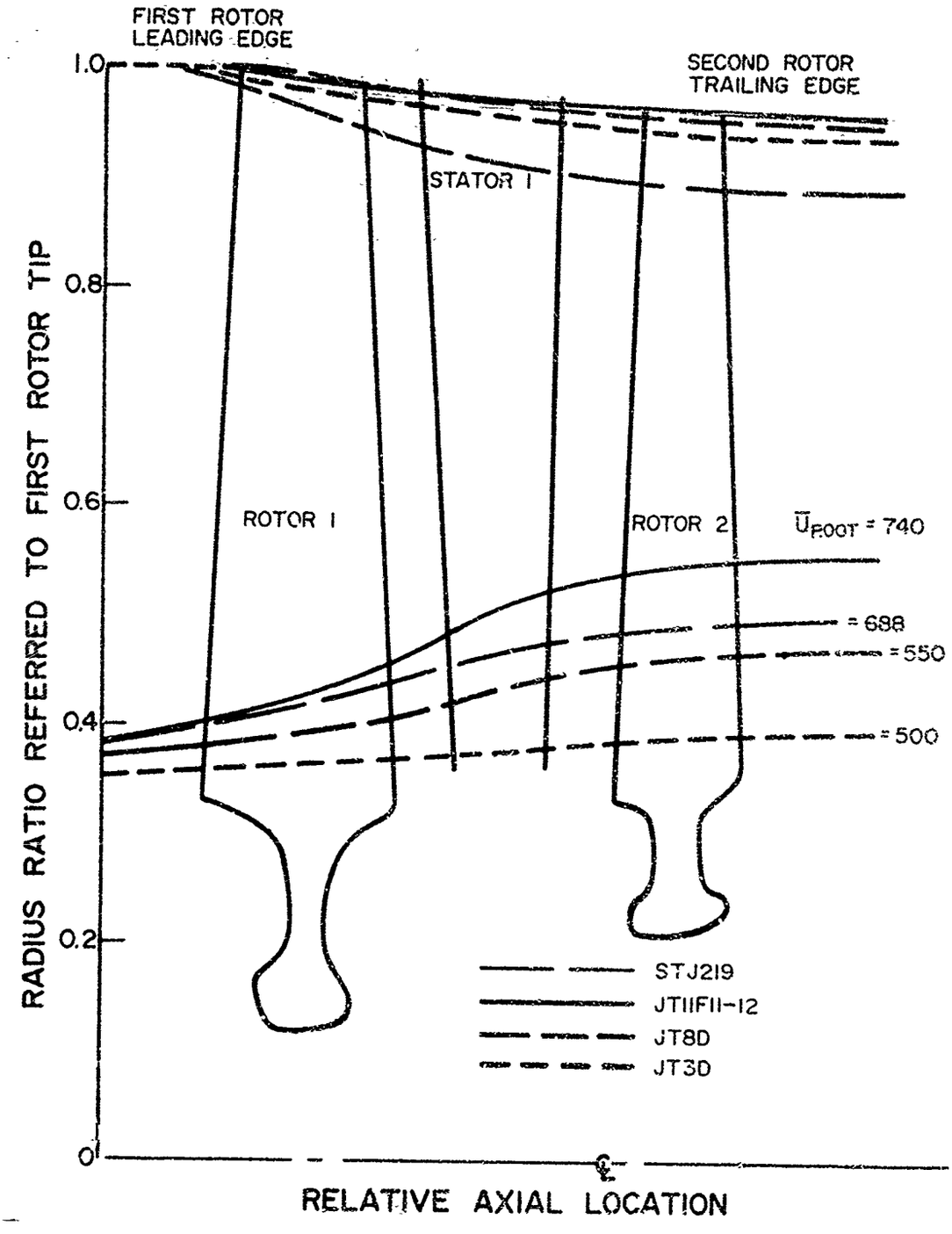
SCHEMATIC DIAGRAM OF FAN AND COMPRESSOR OF STF 219 ENGINE

FIGURE 2-25



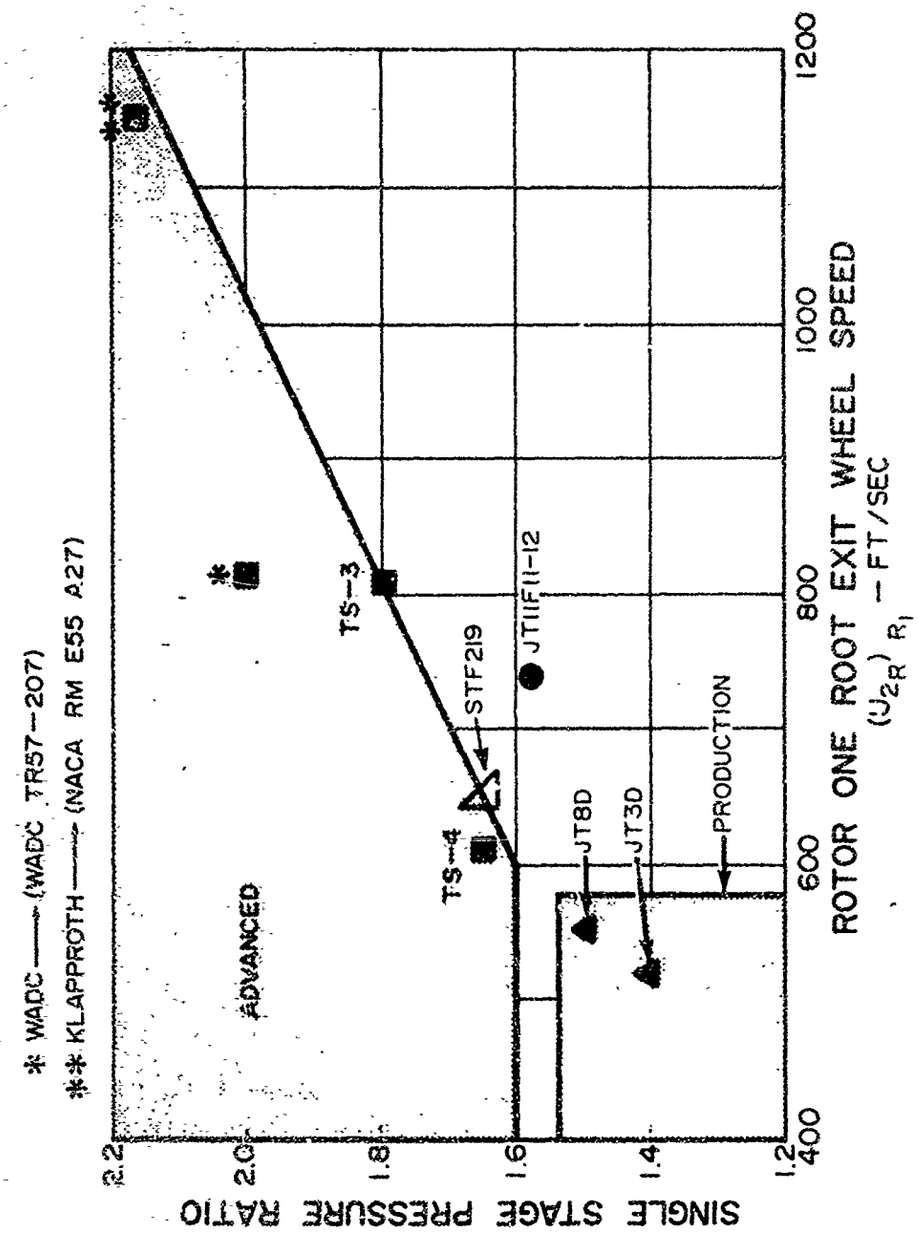
PREDICTED PERFORMANCE MAP FOR THE STF 219 ENGINE FAN

Figure 2-26



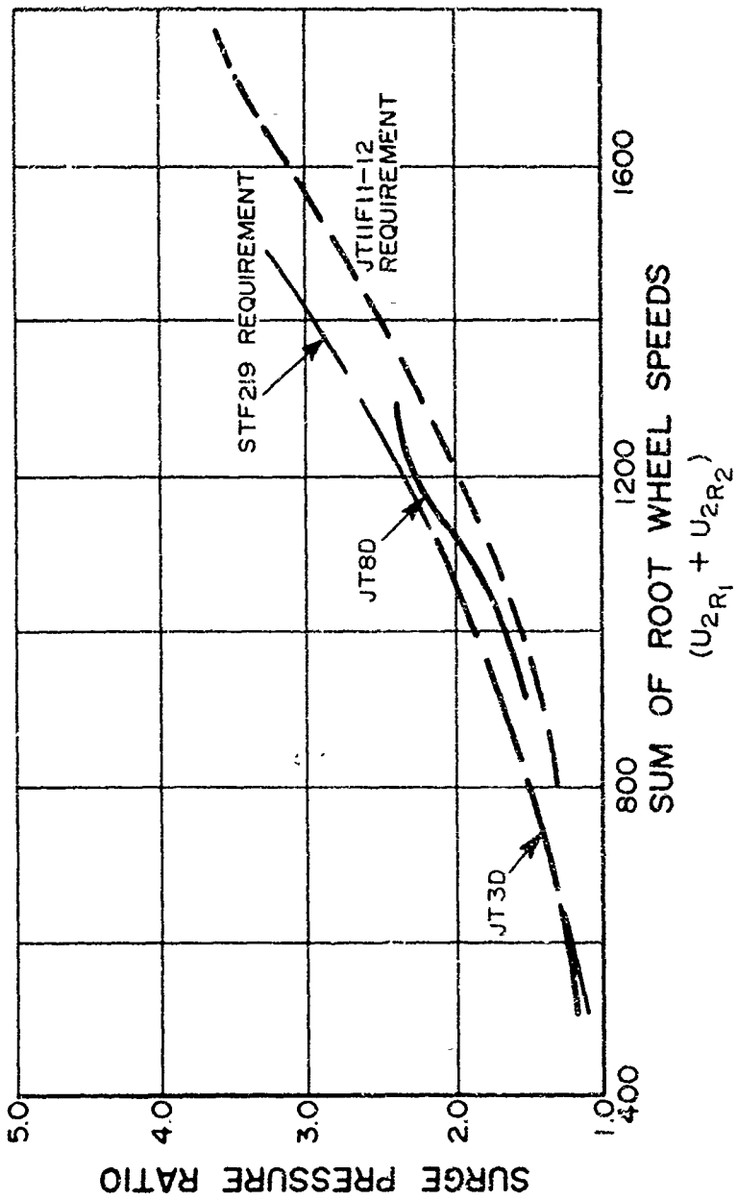
TWO-STAGE FAN GAS PATH COMPARISON

Figure 2-27



FAN PRESSURE RATIO COMPATIBILITY

Figure 2-28



FAN SURGE LINE AS A FUNCTION OF ROOT WHEEL SPEED

Figure 2-29

Station		$C_X\sqrt{\theta T2}$ (ft/sec)	$C_U\sqrt{\theta T2}$ (ft/sec)	$W_U\sqrt{\theta T2}$ (ft/sec)	$U/\sqrt{\theta T2}$ (ft/sec)	MREL (ft/sec)	MABS (ft/sec)	$\beta°$ (degrees)	$\alpha°$ (degrees)
		Fan (Duct Portion)							
R-1 Inlet	JT11F 11-12	681.8	0.0	1386.4	1386.4	1.44	0.636	29.16	90.0
	STJ w19 1a	680.8	0.0	1444.3	1267.5	1.35	0.646	28.24	90.0
R-1 Exit	JT11F 11-12	515.1	388.6	985.6	1374.2	0.958	0.565	28.5	54.02
	STJ 219 1b	650.6	477.8	987.7	1210.7	0.851	0.699	41.4	53.91
R-2 Inlet	JT11F 11-12 2a	623.8	0.0	1369.0	1369.0	1.28	0.531	24.5	90.
	STJ 219	651.9	0.0	1364.4	1262.6	1.16	0.555	28.5	90.0
R-2 Exit	JT11F 11-12 2b	460.7	410.6	950.3	1367.2	0.832	0.49	25.80	47.86
	STJ 219	553.8	565.8	829.8	1183.3	0.652	0.522	41.88	44.39
		Fan (Engine Portion)							
R-1 Inlet	JT11F 11-12 1c	658.4	0.0	914.3	934.3	1.046	0.618	35.17	90.0
	STJ 219	701.6	0.0	1101.5	847.8	1.029	0.657	39.61	90.0
R-1 Exit	JT11F 11-12 1d	539.2	500.6	810.6	965.6	0.624	0.643	49.19	47.46
	STJ 219	661.3	617.4	715.6	877.5	0.820	0.791	68.5	47.10
R-2 Inlet	JT11F 11-12 2c	624.4	0.0	1035.2	1034.6	1.041	0.543	31.19	90.0
	STJ 219	651.8	0.0	1102.8	889.1	0.94	0.556	36.22	90.0
R-2 Exit	JT11F 11-12 2d	490.0	524.8	822.7	1052.5	1.576	0.58	43.15	42.76
	STJ 219	624.6	685.1	862.6	900.0	0.535	0.749	42.46	71.07

MEAN LINE AIR TRIANGLES FOR THE JT11F-11, 17 AND THE STF 219 FANS FOR THE FAN AND ENGINE PORTIONS OF THE FLOW

Figure 2-30

Fan (Duct Portion)

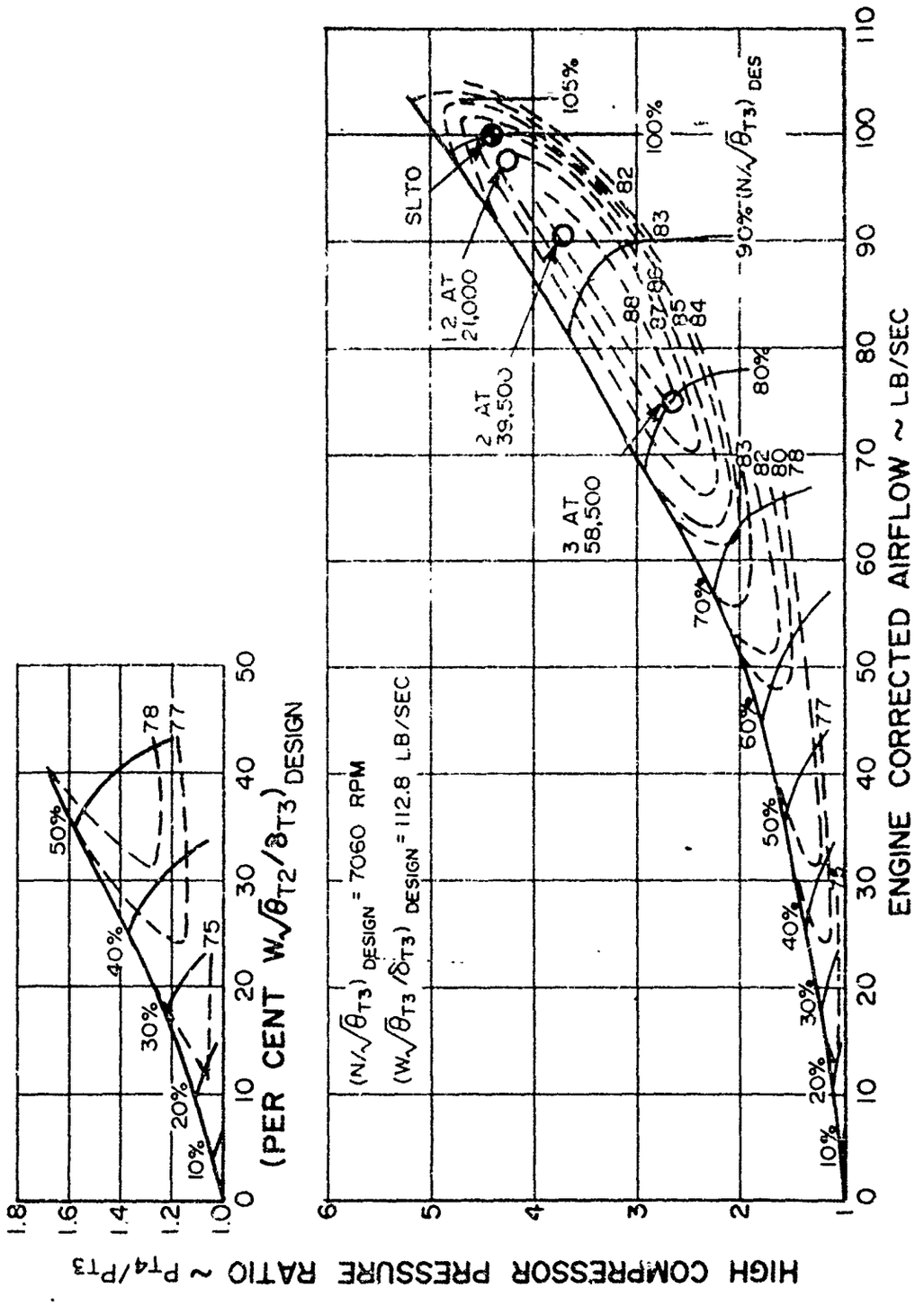
Station		$CX\sqrt{\theta T2}$ (ft/sec)	$Cu/\sqrt{\theta T2}$ (ft/sec)	$Wa\sqrt{\theta T2}$ (ft/sec)	$U/\sqrt{\theta T2}$ (ft/sec)	MREL (ft/sec)	MABS (ft/sec)	β° (degrees)	α° (degrees)
$R\text{-}1_{Inlet}$	JT11F 11-12	681.8	0.0	1386.4	1386.4	1.44	0.636	29.16	90.0
	STJ w/9 1a	680.8	0.0	1444.3	1267.5	1.35	0.646	28.24	90.0
$R\text{-}1_{Exit}$	JT11F 11-12	515.1	388.6	485.6	1374.2	0.958	0.565	28.5	54.02
	STJ 219 1b	650.6	477.8	987.7	1215.7	0.851	0.699	41.4	53.91
$R\text{-}2_{Inlet}$	JT11F 11-12 2a	623.8	0.0	1369.0	1369.0	1.28	0.531	24.5	90.
	STJ 219	653.9	0.0	1304.4	1202.6	1.16	0.555	28.5	90.0
$R\text{-}2_{Exit}$	JT11F 11-12 2b	460.7	416.9	850.3	1367.2	0.832	0.49	25.86	47.86
	STJ 219	553.8	565.8	829.8	1183.3	0.652	0.622	41.88	44.39

Fan (Engine Portion)

Station		$CX\sqrt{\theta T2}$ (ft/sec)	$Cu/\sqrt{\theta T2}$ (ft/sec)	$Wa\sqrt{\theta T2}$ (ft/sec)	$U/\sqrt{\theta T2}$ (ft/sec)	MREL (ft/sec)	MABS (ft/sec)	β° (degrees)	α° (degrees)
$R\text{-}1_{Inlet}$	JT11F 11-12 1c	658.4	0.0	934.3	934.3	1.016	0.618	35.17	90.0
	STJ 219	701.6	0.0	1101.5	847.8	1.029	0.657	39.61	90.0
$R\text{-}1_{Exit}$	JT11F 11-12 1d	530.2	500.0	865.6	965.6	0.621	0.641	49.19	47.10
	STJ 219	661.3	617.4	715.6	877.5	0.824	0.791	68.5	47.10
$R\text{-}2_{Inlet}$	JT11F 11-12 2c	624.4	0.0	1034.6	1034.6	1.041	0.543	31.19	90.0
	STJ 219	651.8	0.0	1163.6	889.4	0.94	0.556	36.22	90.0
$R\text{-}2_{Exit}$	JT11F 11-12 2d	490.6	524.8	522.7	1052.5	0.576	0.58	42.15	42.76
	STJ 219	624.6	685.1	662.6	900.0	0.535	0.749	42.46	71.07

MEAN LINE AIR TRIANGLES FOR THE JT11F-11, 12 AND THE STF 219 FANS FOR THE FAN AND ENGINE PORTIONS OF THE FLOW

Figure 2-30



PREDICTED PERFORMANCE MAP FOR THE
STF 219 ENGINE HIGH-PRESSURE COMPRESSOR

Figure 2-31

Station		$CX/\sqrt{\theta T_3}$ (ft/sec)	$Cu/\sqrt{\theta T_3}$ (ft/sec)	$Wu/\sqrt{\theta T_3}$ (ft/sec)	$U/\sqrt{\theta T_3}$ (ft/sec)	M_{REL} (ft/sec)	M_{ABS} (ft/sec)	β^* (degrees)	α^* (degrees)
$R-1_{Inlet}$	JT11F 11-12 3a	611.4	107.8	744.5	902.3	0.727	0.674	37.58	80.0
	STJ219	602.5	0	1004.2	1004.0	1.808	0.556	10.96	90.00
$R-1_{Exit}$	JT11F 11-12 5b	577.3	527.6	364.9	892.5	0.589	0.677	56.78	46.57
	STJ 219	562.5	415.4	581.7	997.1	0.699	0.602	43.53	53.06
$R-2_{Inlet}$	JT11F 11-12 4a	570.9	100.7	781.8	882.5	0.84	0.503	10.14	80.0
	STJ 219	591.9	31.4	961.0	992.4	0.3745	0.5118	31.63	86.96
$R-2_{Exit}$	JT11F 11-12 4b	547.8	509.3	364.1	873.4	0.551	0.627	55.33	47.08
	STJ 219	548.8	446.5	543.1	989.5	0.636	0.582	45.3	50.87
$R-3_{Inlet}$	JT11F 11-12 5a	573.0	102.1	762.3	864.4	0.79	0.485	37.22	80.0
	STJ 219	599.1	47.6	936.8	186.4	0.9088	0.4904	32.545	85.46
$R-3_{Exit}$	JT11F 11-12 5b	561.5	522.3	335.1	857.5	0.524	0.614	56.16	47.07
	STJ 219	545.9	440.7	544.8	985.5	0.1041	0.5496	45.06	51.08
$R-4_{Inlet}$	JT11F 11-12 6a	588.1	103.7	747.0	850.7	0.75	0.471	39.21	80.0
	STJ 219	568.8	75.6	910.6	985.6	0.833	0.445	32.01	82.43
$R-4_{Exit}$	JT11F 11-12 6b	539.9	482.3	366.5	848.7	0.500	0.556	55.83	48.23
	STJ 219	525.2	438.4	549.7	985.1	0.563	0.514	43.85	50.15
$R-5_{Inlet}$	JT11F 11-12 7a	525.7	92.7	754.1	846.8	0.696	0.404	34.88	80.0
	STJ 219	533.7	104.5	880.4	984.5	0.7664	0.405	31.23	82.43
$R-5_{Exit}$	JT11F 11-12 7b	479.4	393.7	453.0	846.8	0.489	0.459	46.62	50.6
	STJ 219	503.9	454.75	530.5	985.1	0.530	0.491	47.33	47.93

Velocities are corrective to standard atmospheric conditions at the engine compressor inlet (PT_3 = 14.7 PSIA, T_{T3} = 518.6°R)

MEAN LINE AIR TRIANGLES FOR THE JT11F-11, -12 AND STF 219 HIGH-PRESSURE COMPRESSORS

Figure 2-32

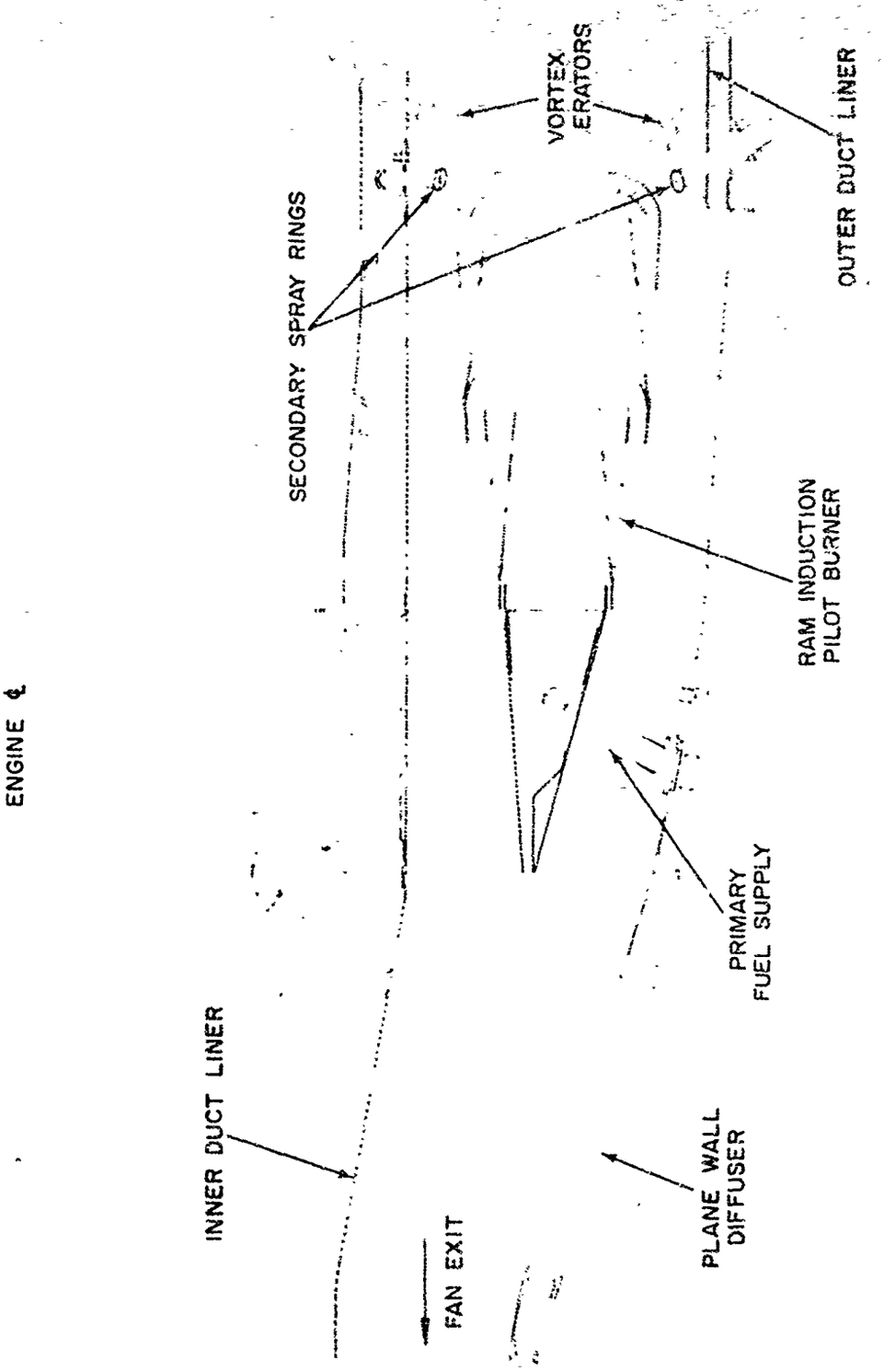
DOWNGRADED AT 3 YEAR INTERVALS
DECLASSIFIED AFTER 12 YEARS
DOD DIR 5200.10

	STF219	JT11F-11, -12
Outer Case Diameter (in)	39.8	41.98
Inner Case Diameter (in)	22.4	26.82
Liner Radial Height* (in)	7.7	7.58
Burner Centerline (in)	32.0	34.4
Liner Length (in)	21.94	26.5
Burner Section Length (in)	26.76	36.0
Burner Pressure Loss (Per Cent)	5.5	4.8
Burner Section Total Pressure Loss (Per Cent)	7.5	7.8
Burner Temperature Rise (°F)	1663	1386
Burner Exit Temperature (°F)	2300	2000
Liner Velocity (Based on Compressor Exit Conditions) (ft/sec)	117	150
Shroud Velocity (ft/sec)	412	270
Fuel Nozzle Type	Duel Orifice Integral Pressurizing Valve	Variable Area
Fuel Nozzle Number	24	24
Volumetric Heat Release Rate (BTU/hr/atm/ft^3)	4.5×10^6	
$\Delta TVR = \frac{\Delta T_{Max.\ Local}}{\Delta T_{Avg.}}$	1.11	1.15

* Tapered Liner - Nominal Values Tabulated

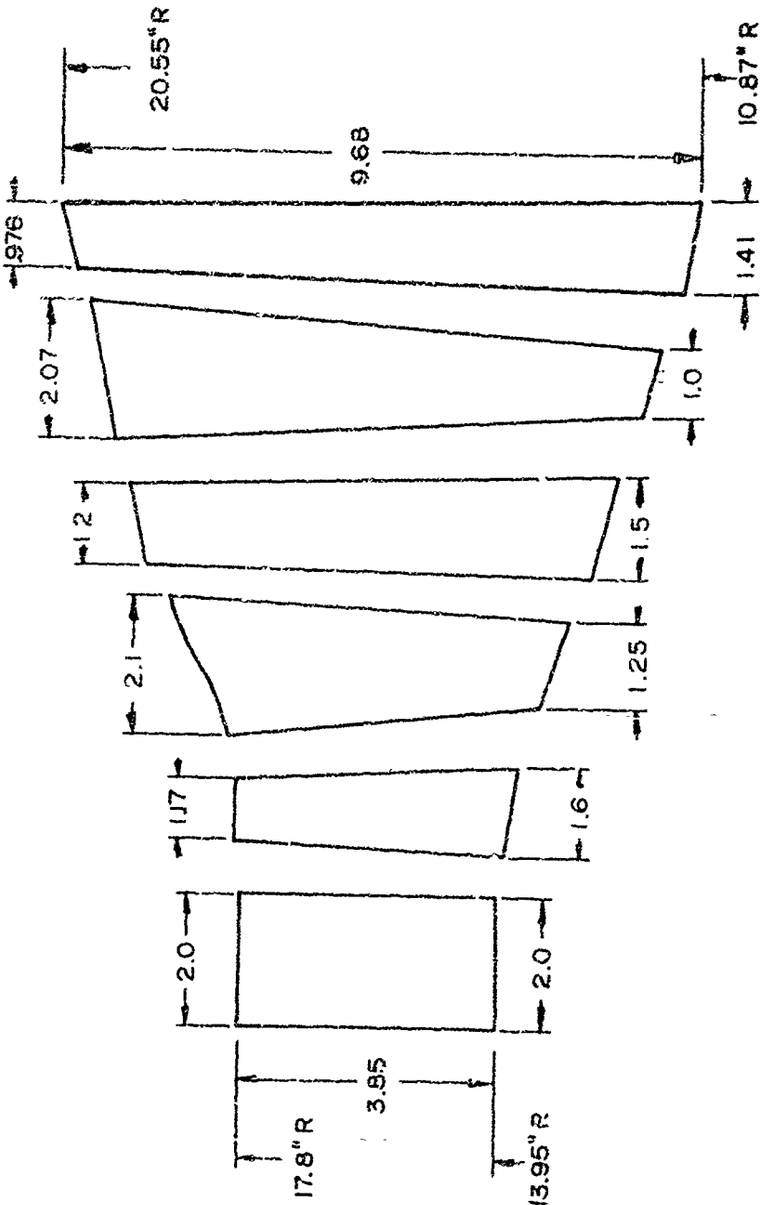
BURNER CHARACTERISTICS AT SEA-LEVEL TAKE-OFF CONDITIONS FOR THE STF 219 AND JT11F-11, -12 ENGINES

Figure 2-33



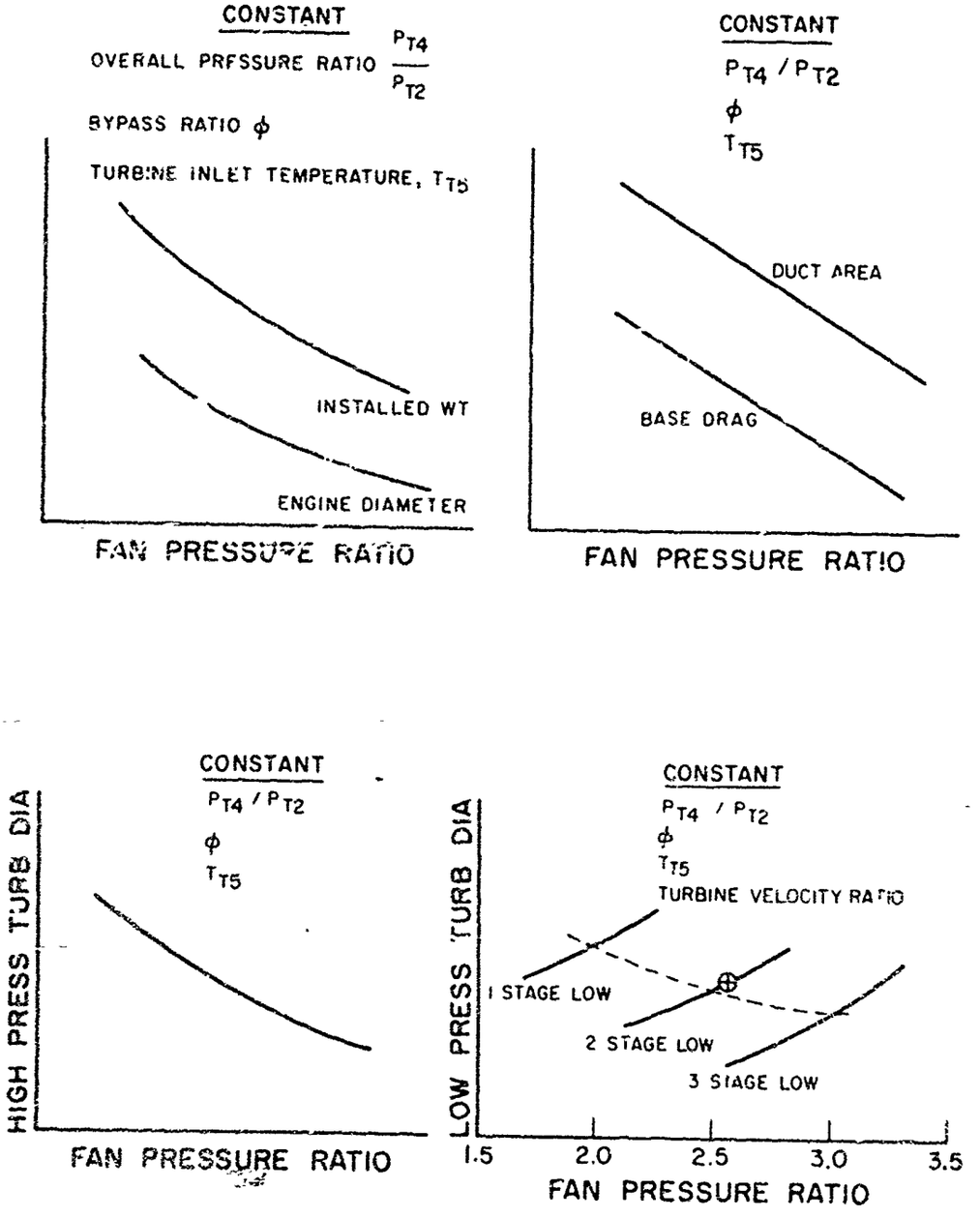
SCHEMATIC DIAGRAM OF ALTERNATE DUCT HEATER FOR THE STF 219 ENGINE

Figure 2-34



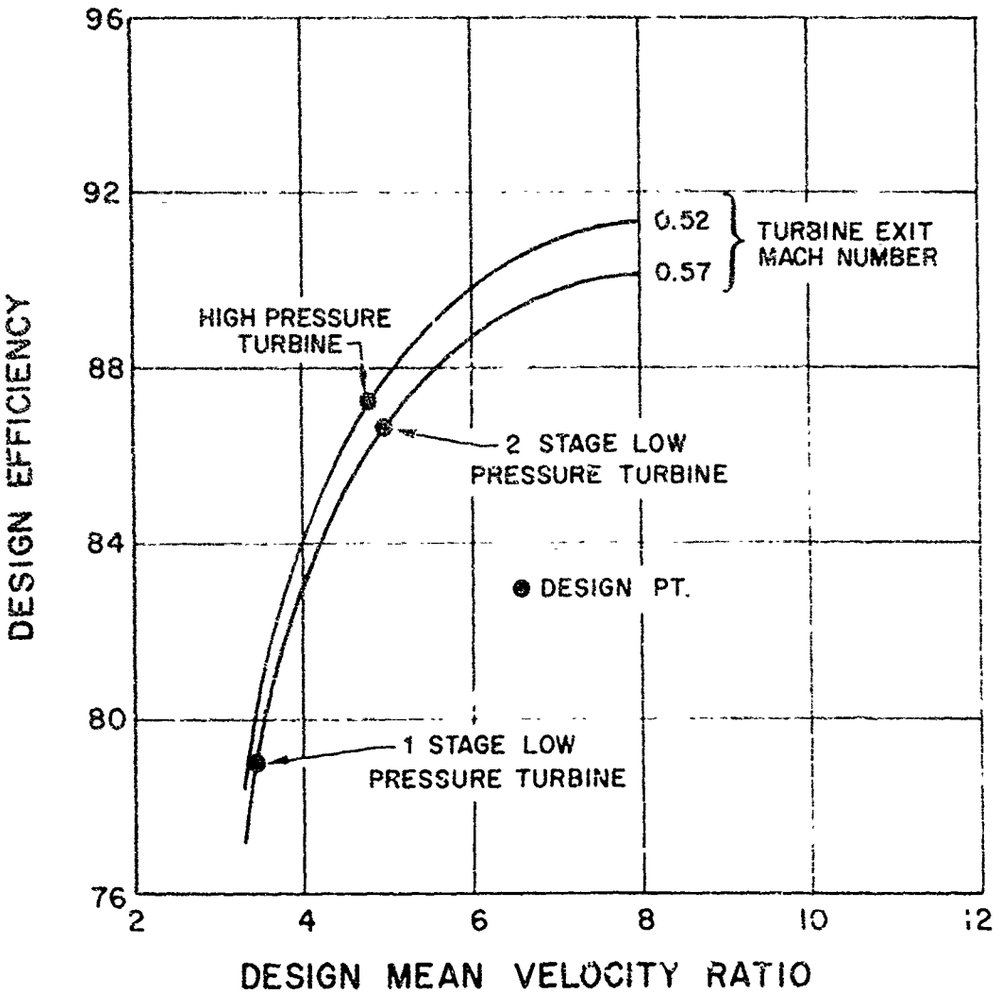
TURBINE GAS PATH DIMENSIONS

Figure Z-35



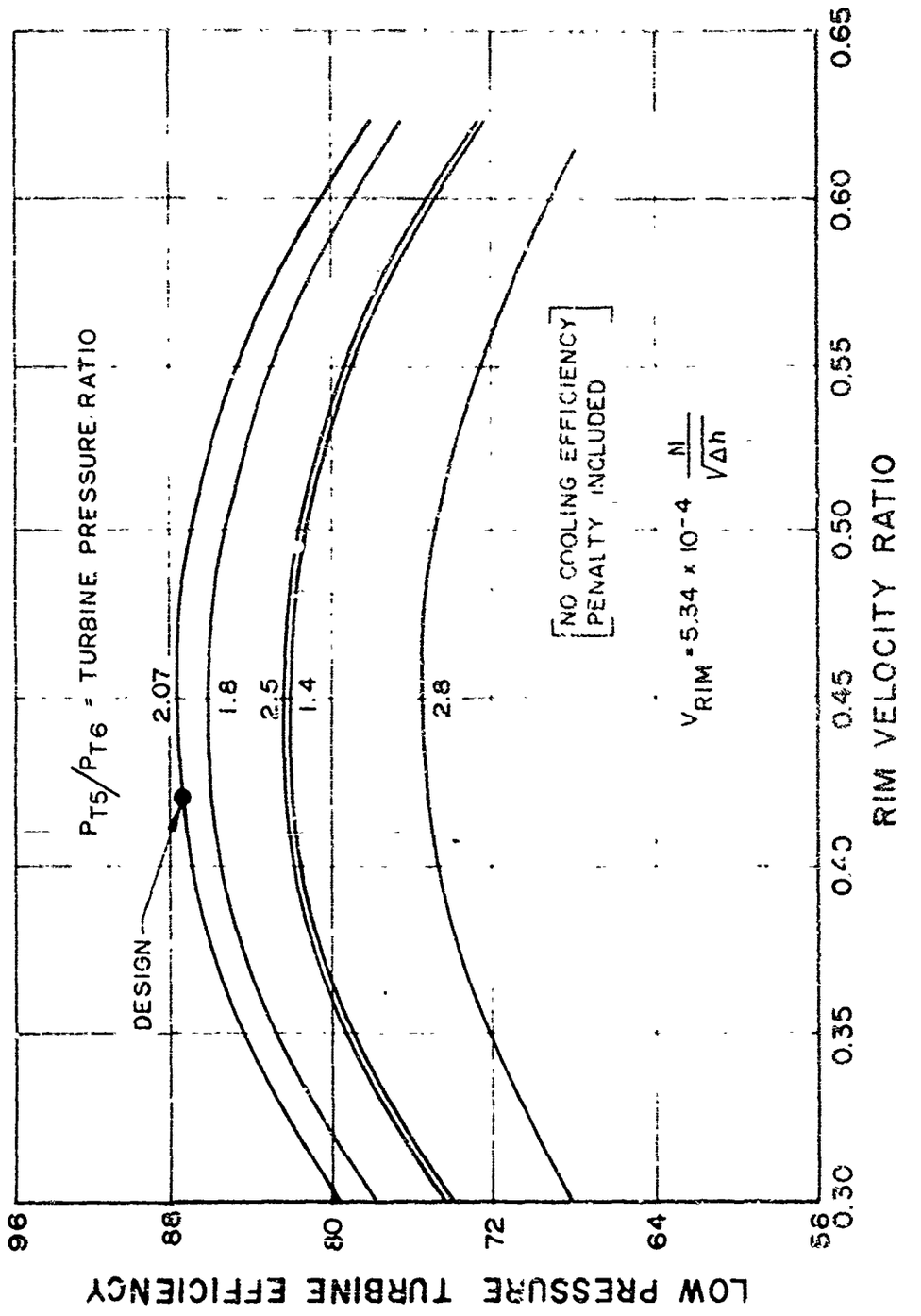
RELATIONSHIPS OF FACTORS CONSIDERED
IN OPTIMIZING THE STF 219 TURBINE PARAMETERS

Figure 2-36



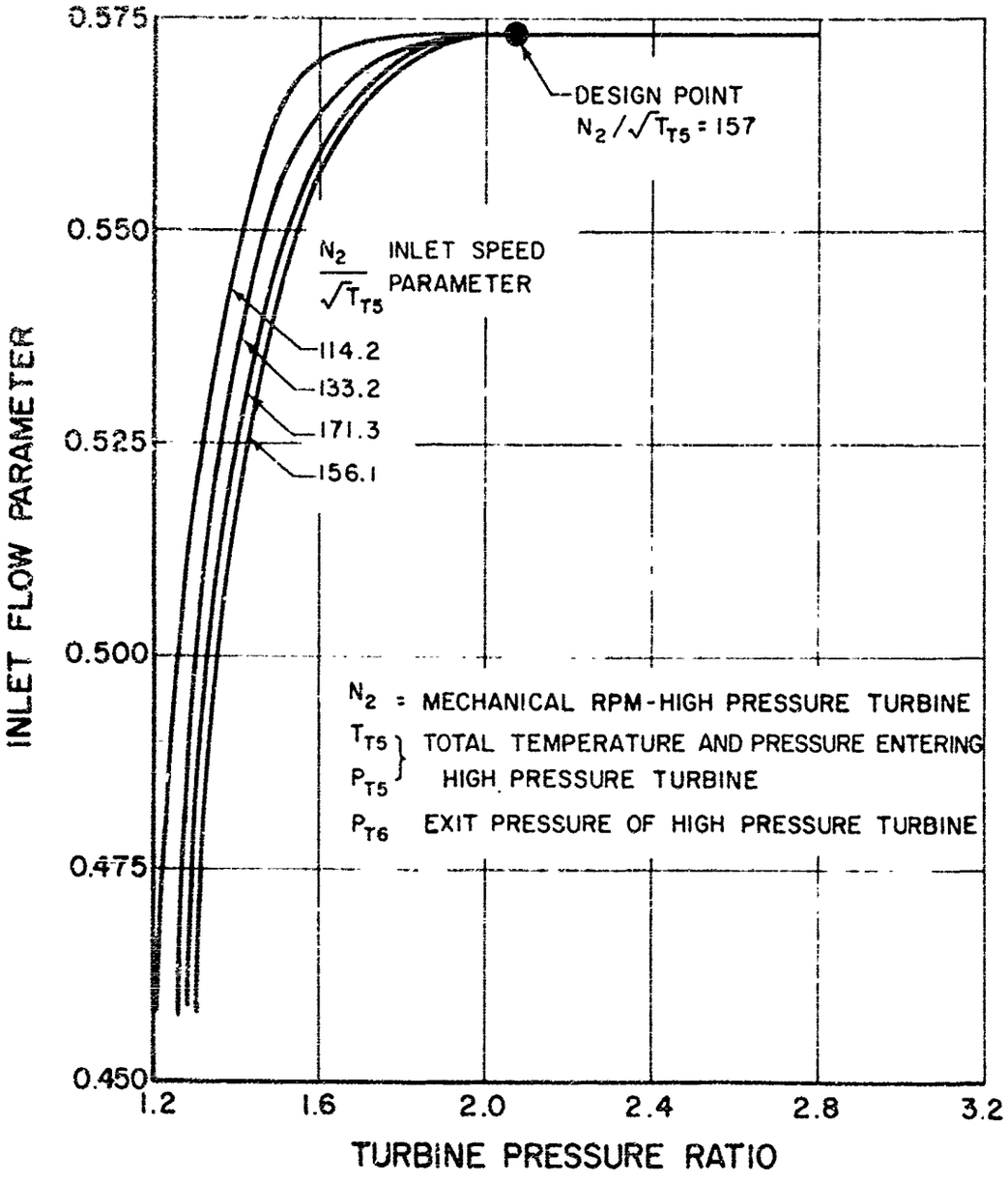
TURBINE EFFICIENCY AS A FUNCTION OF VELOCITY RATIO

Figure 2-37



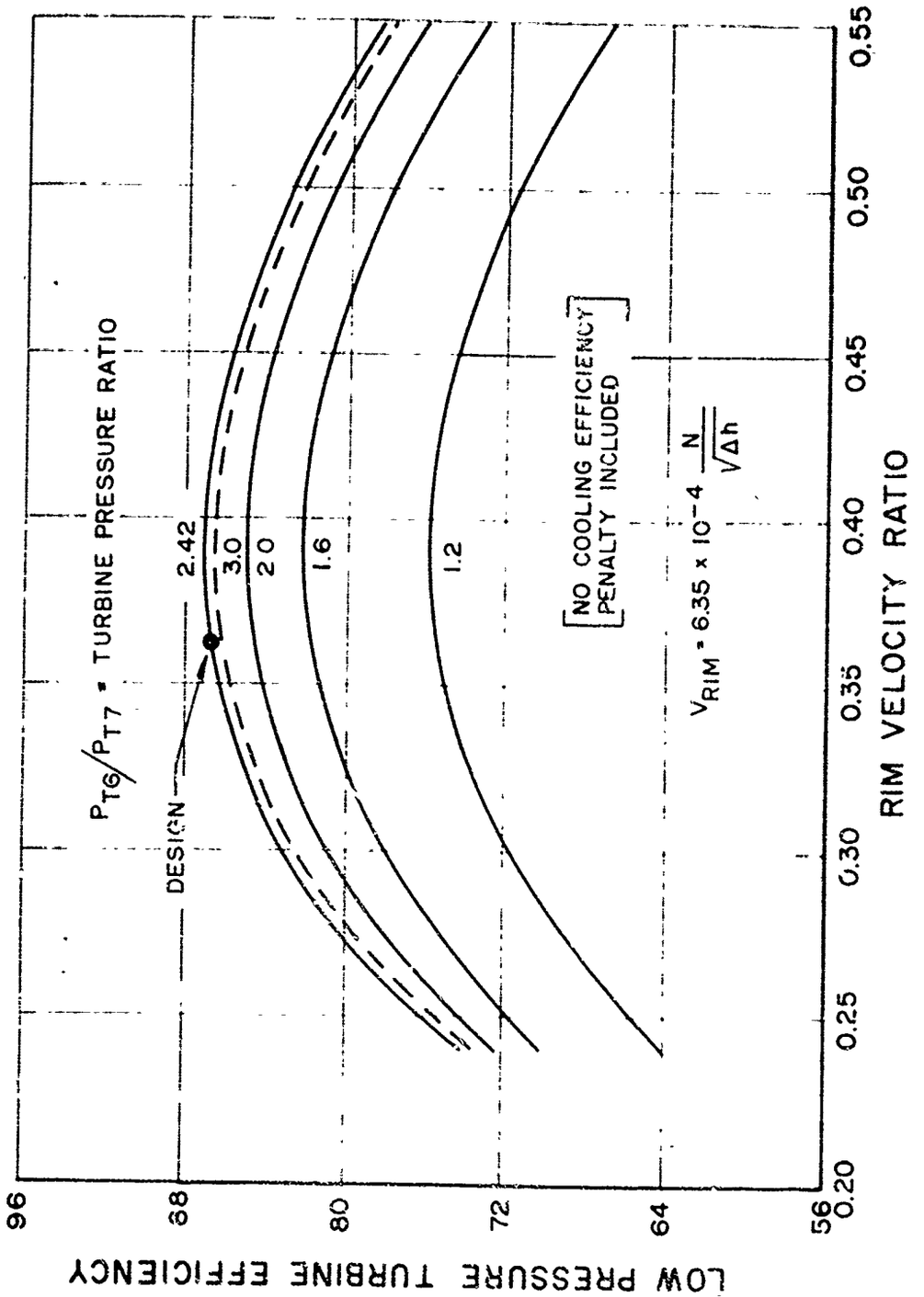
HIGH PRESSURE TURBINE PERFORMANCE

Figure 2-38



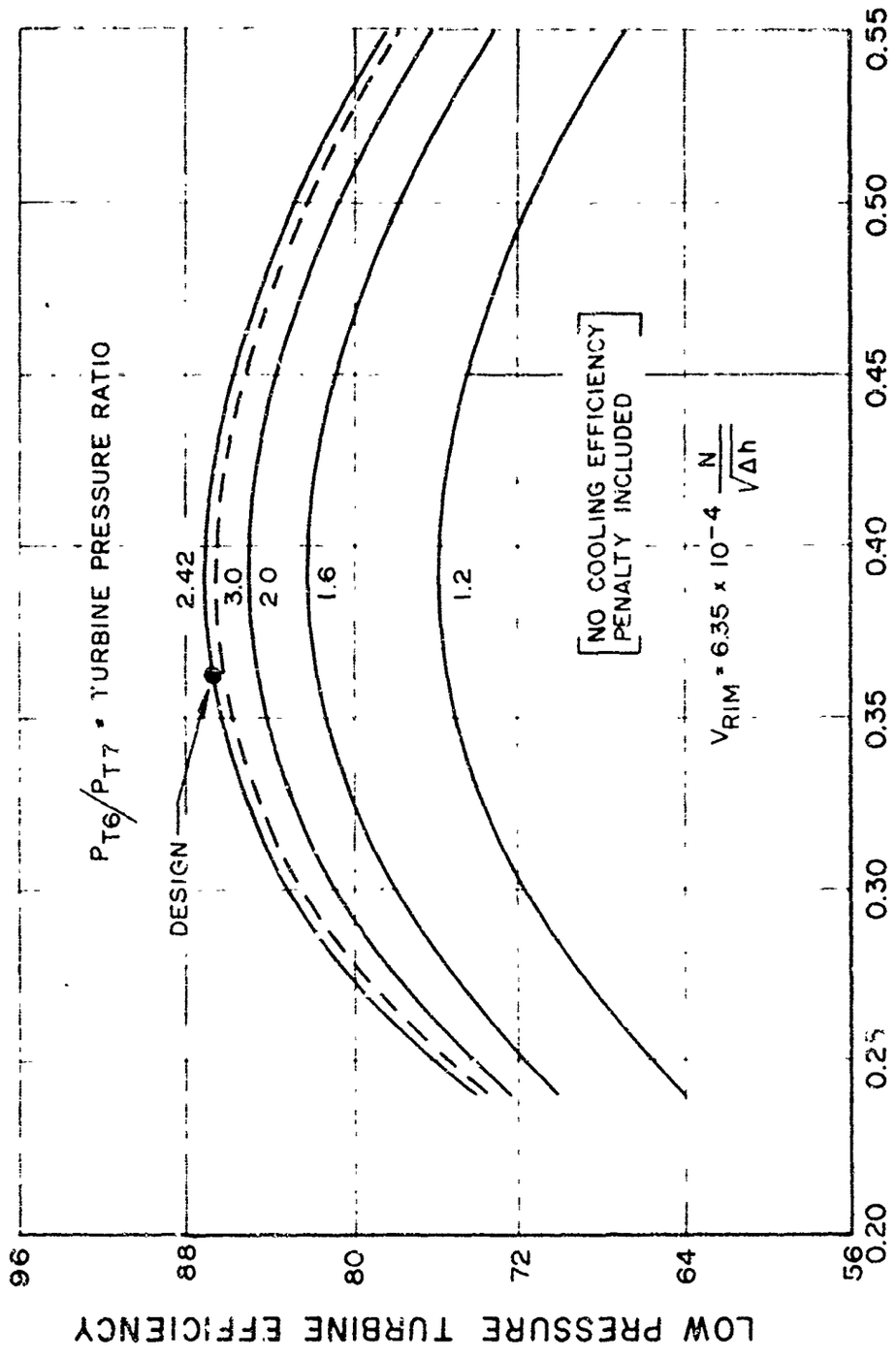
HIGH PRESSURE TURBINE INLET FLOW PARAMETER

Figure 2-39



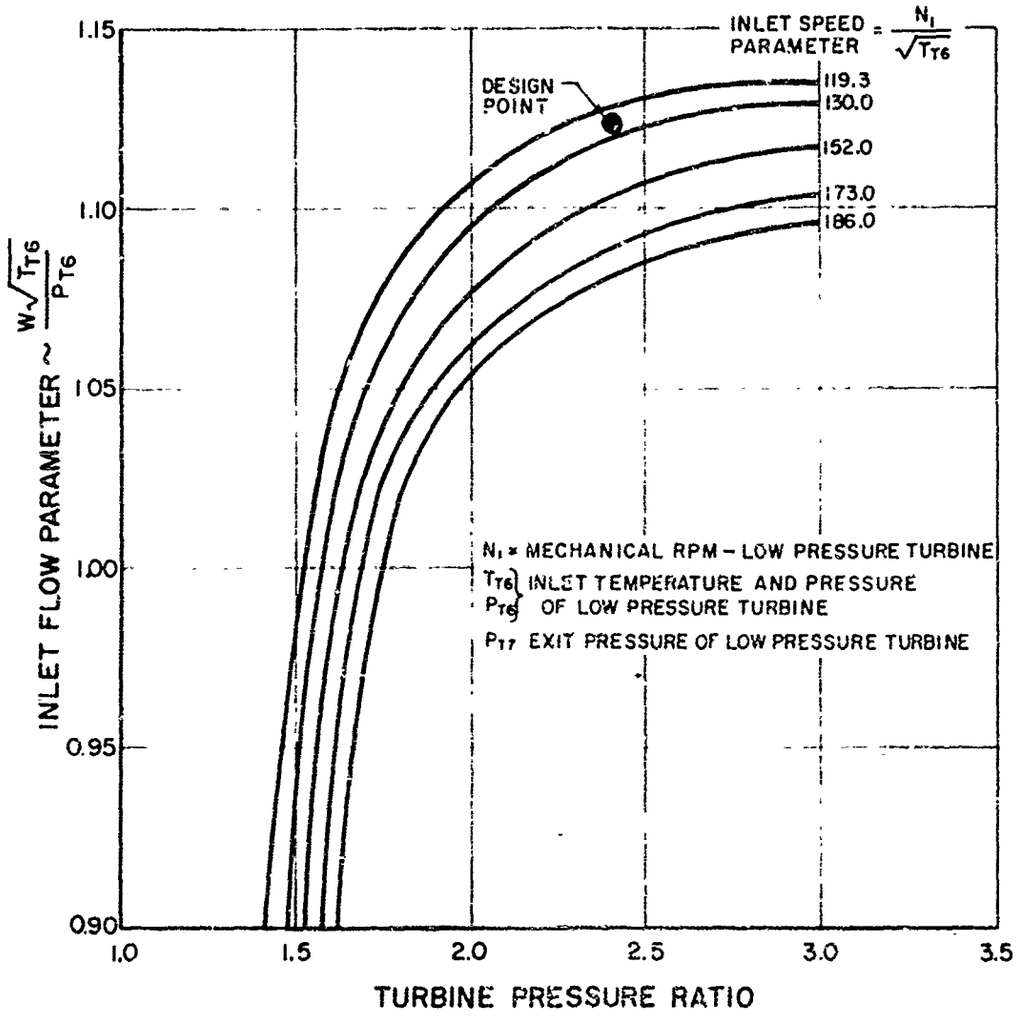
LOW-PRESSURE TURBINE PERFORMANCE

Figure 2-40



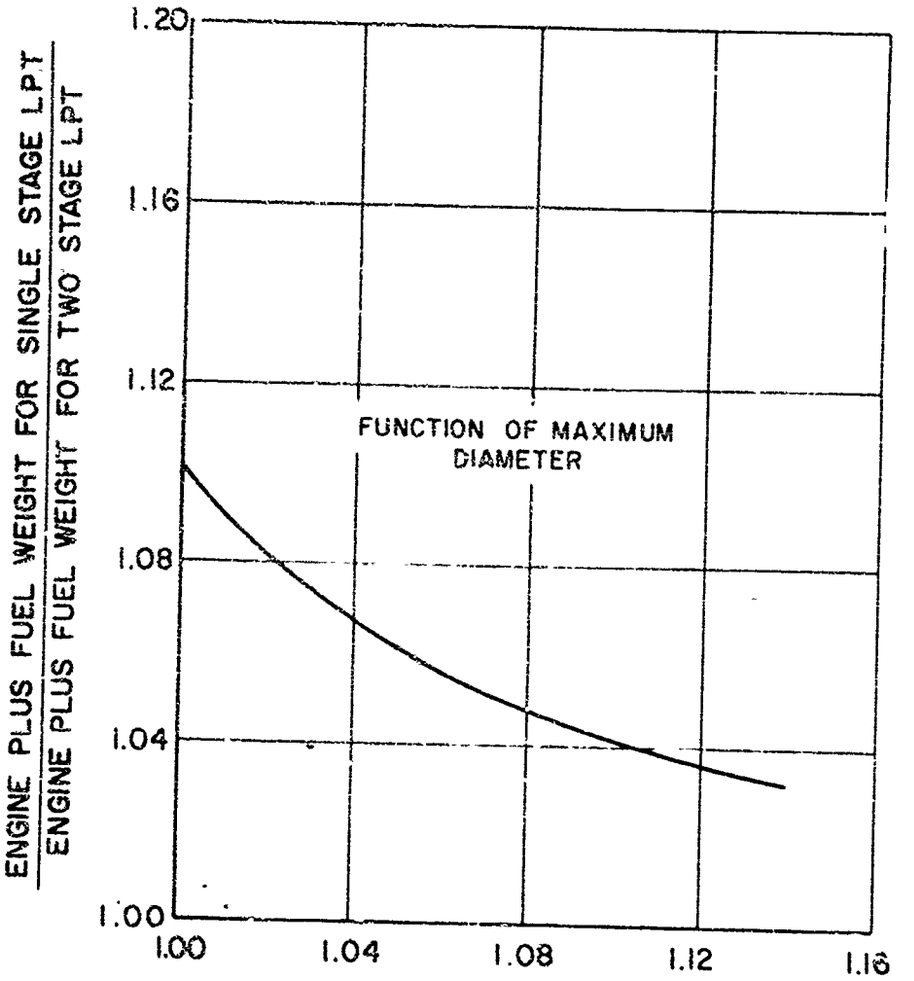
LOW-PRESSURE TURBINE PERFORMANCE

Figure 2-40



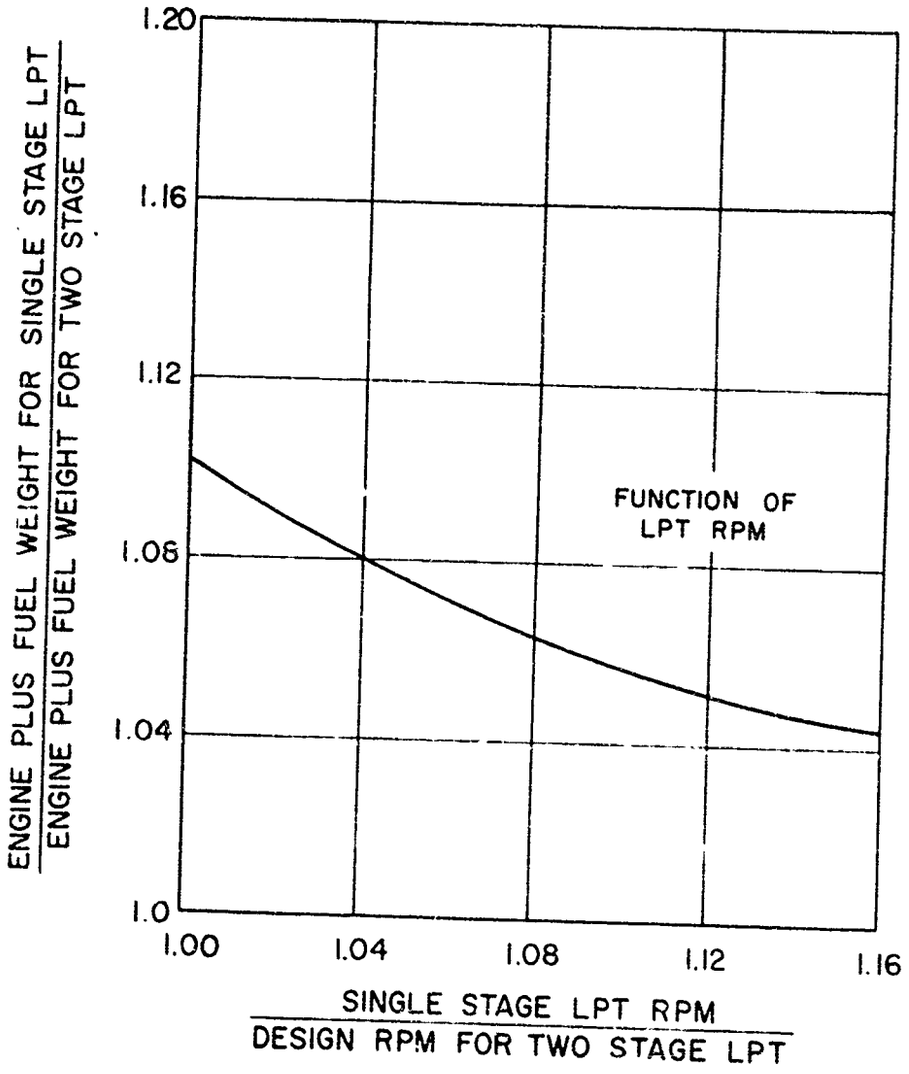
LOW-PRESSURE TURBINE INLET FLOW PARAMETER

Figure 2-41



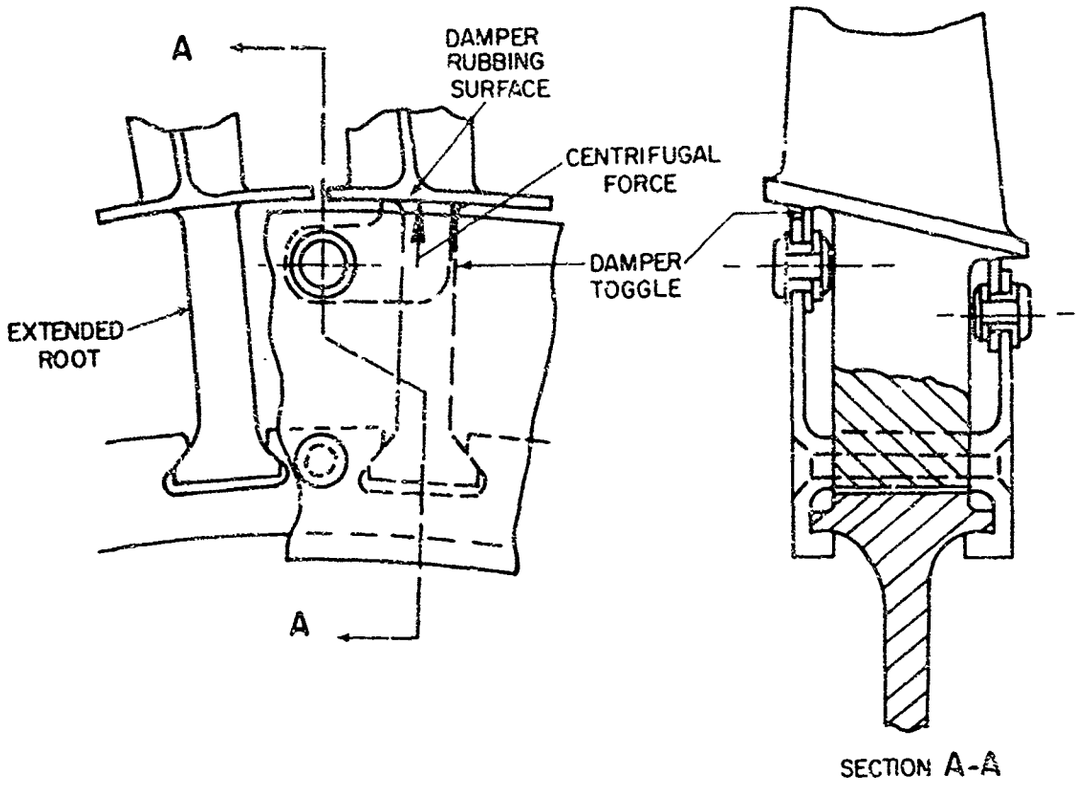
ENGINE PLUS FUEL WEIGHT OF SINGLE-STAGE LOW-PRESSURE TURBINE RELATIVE TO TWO-STAGE LOW PRESSURE TURBINE AS A FUNCTION OF THE RELATIVE MAXIMUM-DIAMETER

Figure 2-42



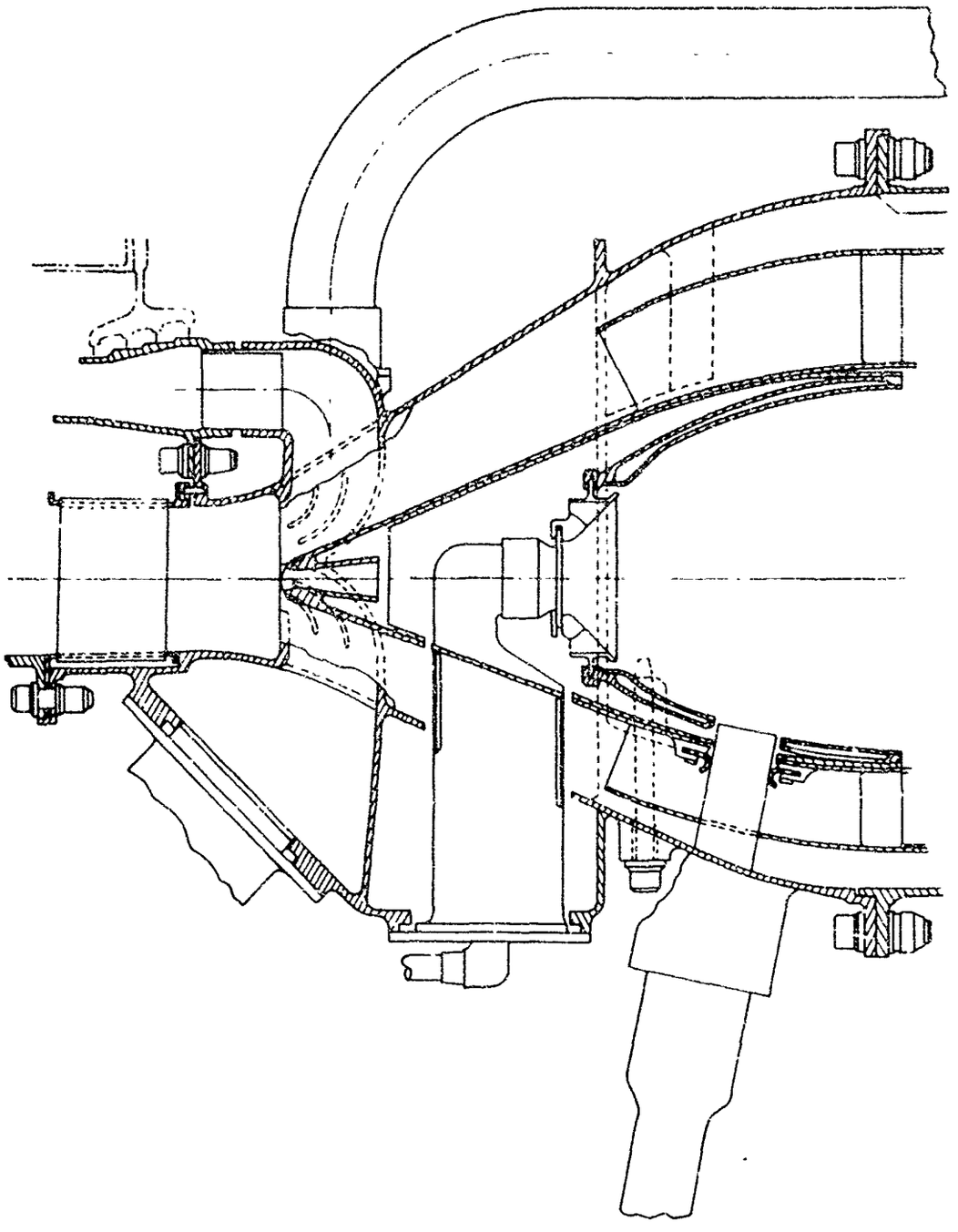
ENGINE PLUS FUEL WEIGHT OF SINGLE-STAGE LOW-PRESSURE TURBINE RELATIVE TO TWO-STAGE LOW-PRESSURE TURBINE AS A FUNCTION OF THE ROTOR SPEED

Figure 2-45



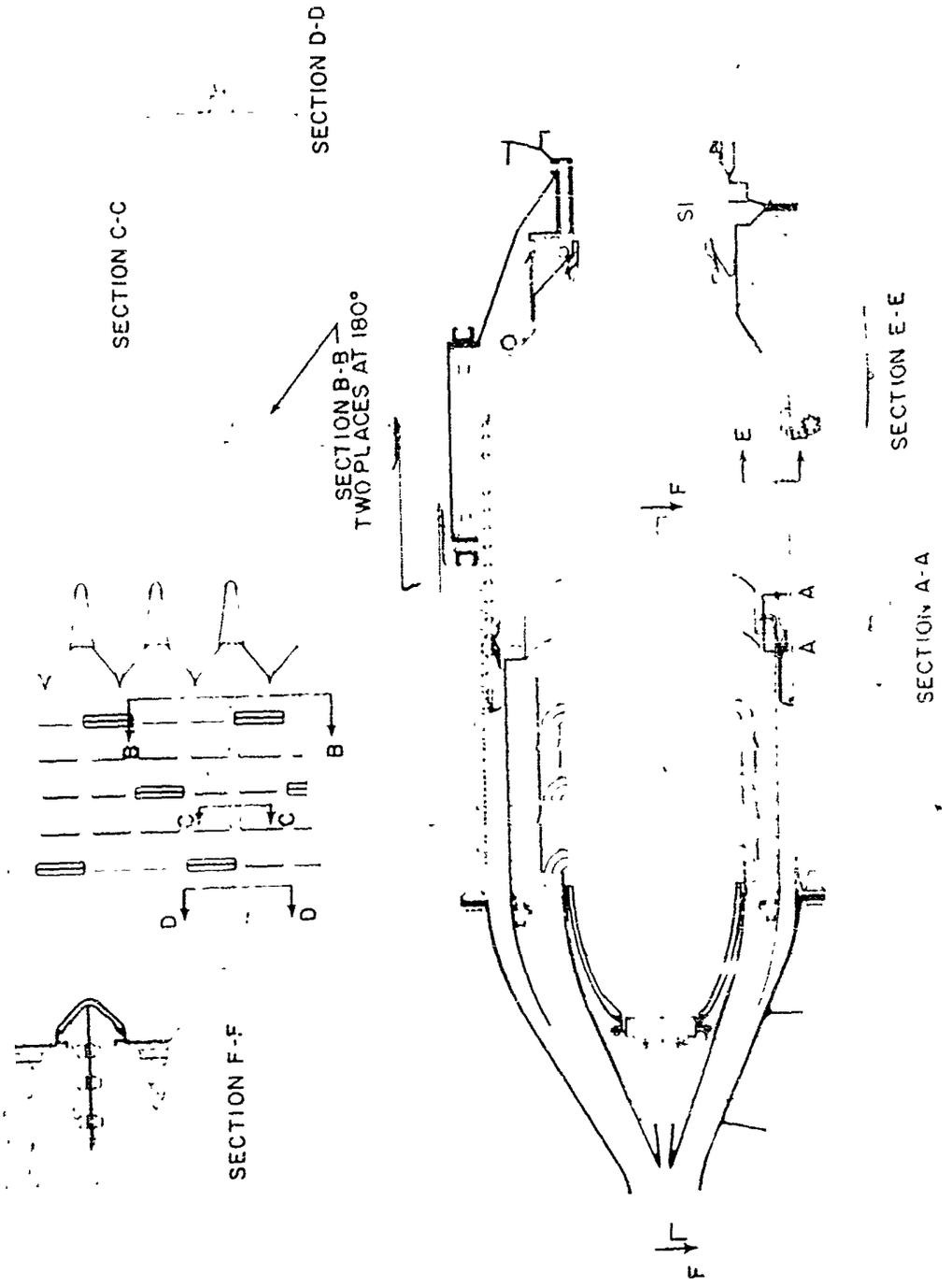
EXTENDED ROOT BLADE WITH MECHANICAL DAMPING

Figure 2-44



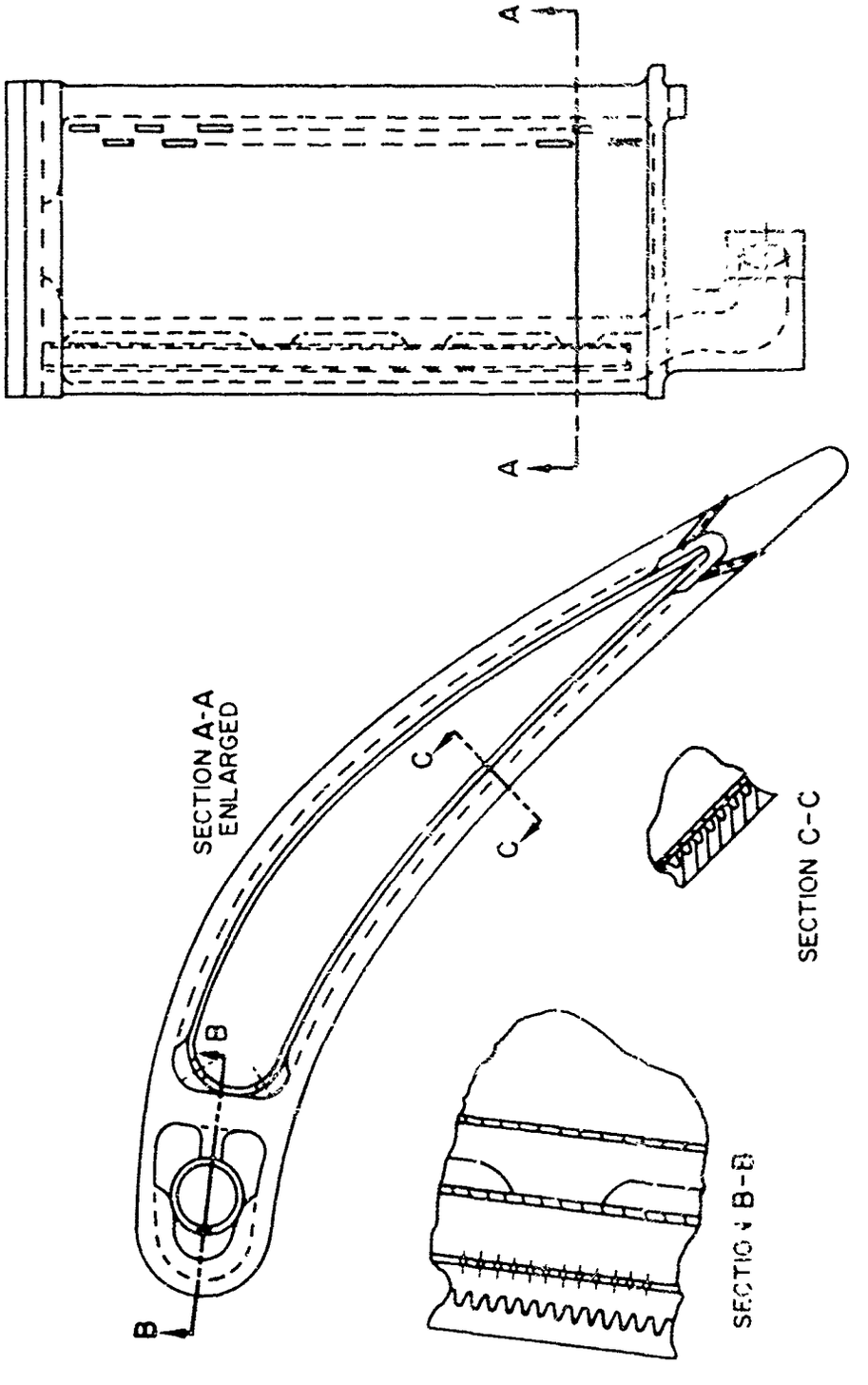
SCHEMATIC DIAGRAM OF DIFFUSER OF STF 219 ENGINE

Figure 2-45



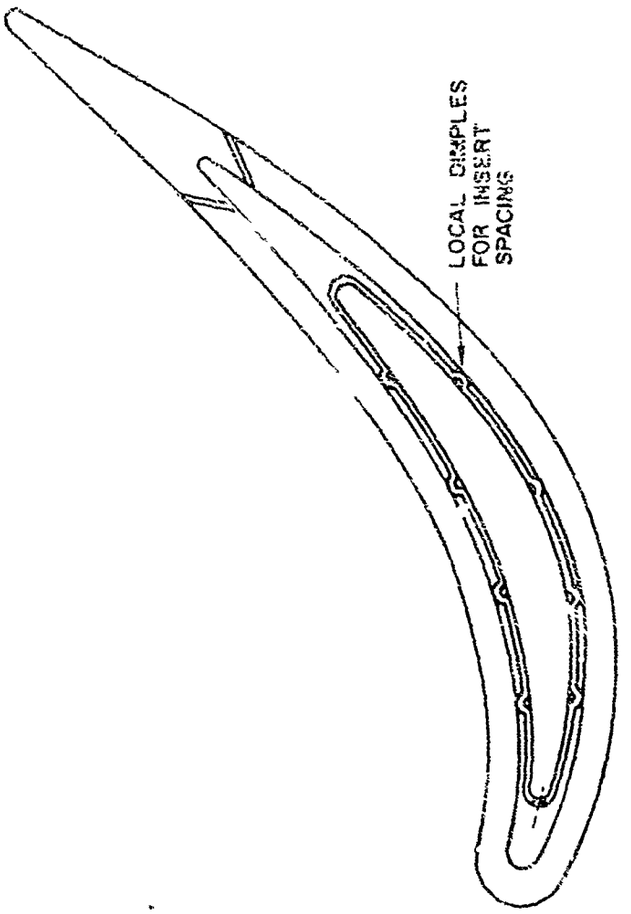
SCHEMATIC DIAGRAM OF AXIALLY SPLIT ANNULAR BURNER

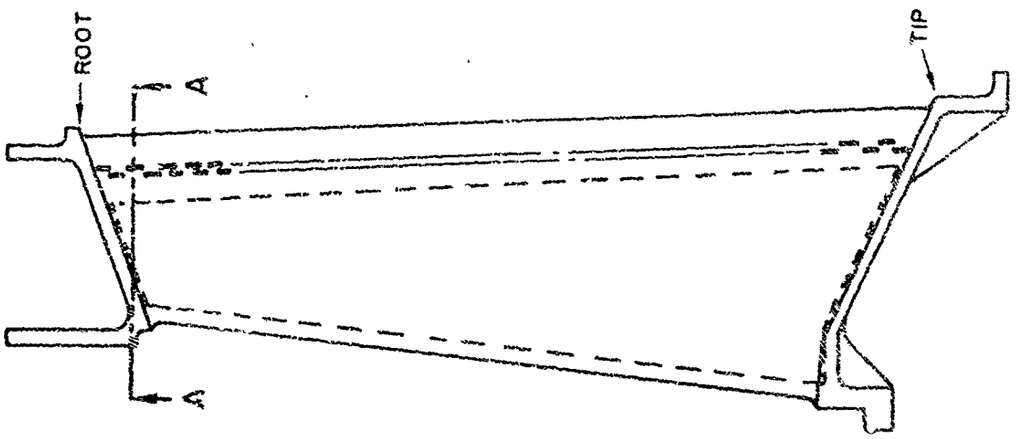
Figure 2-46



CROSS-SECTION OF FIRST-STAGE TURBINE VANE

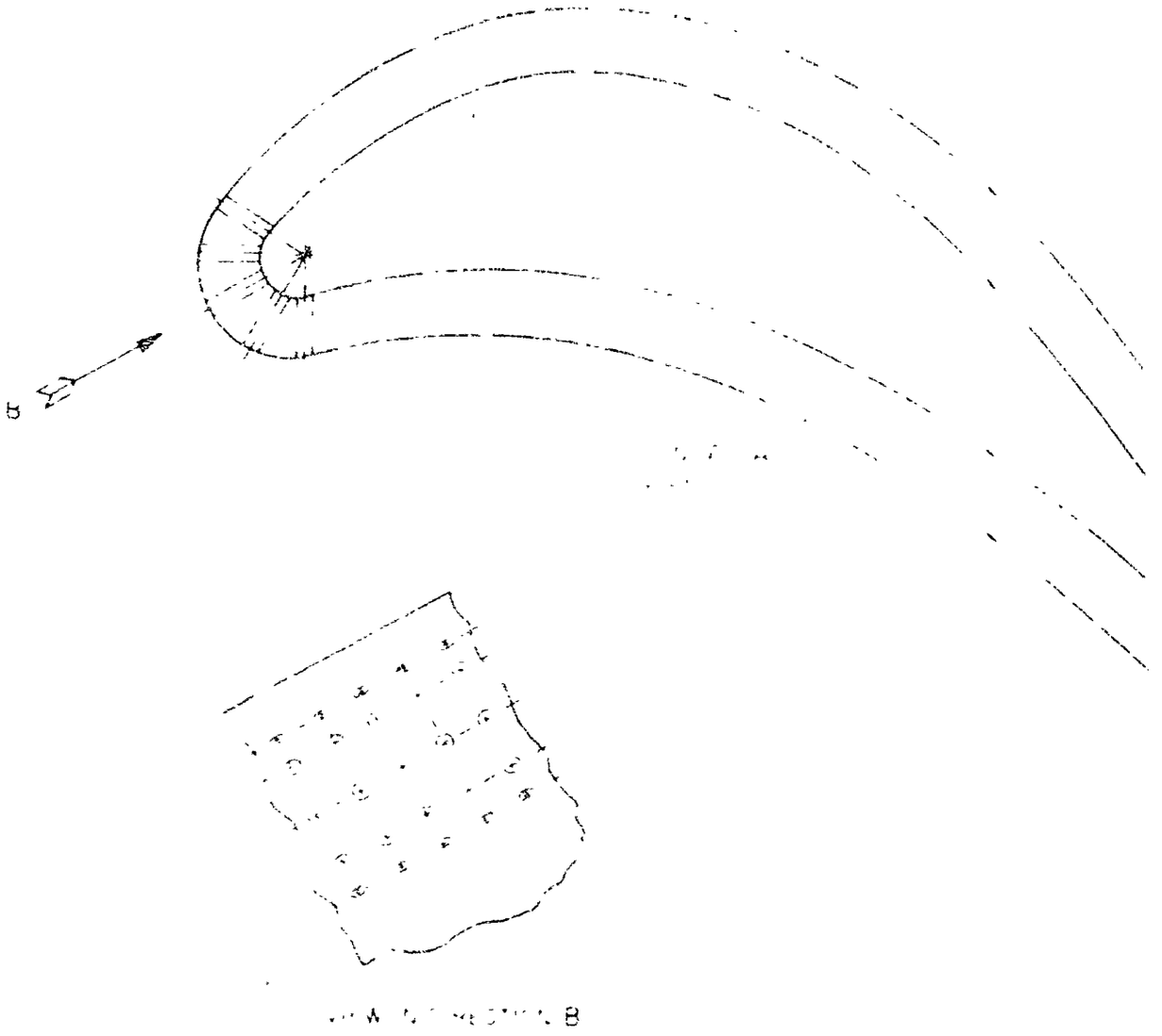
Figure 2-47

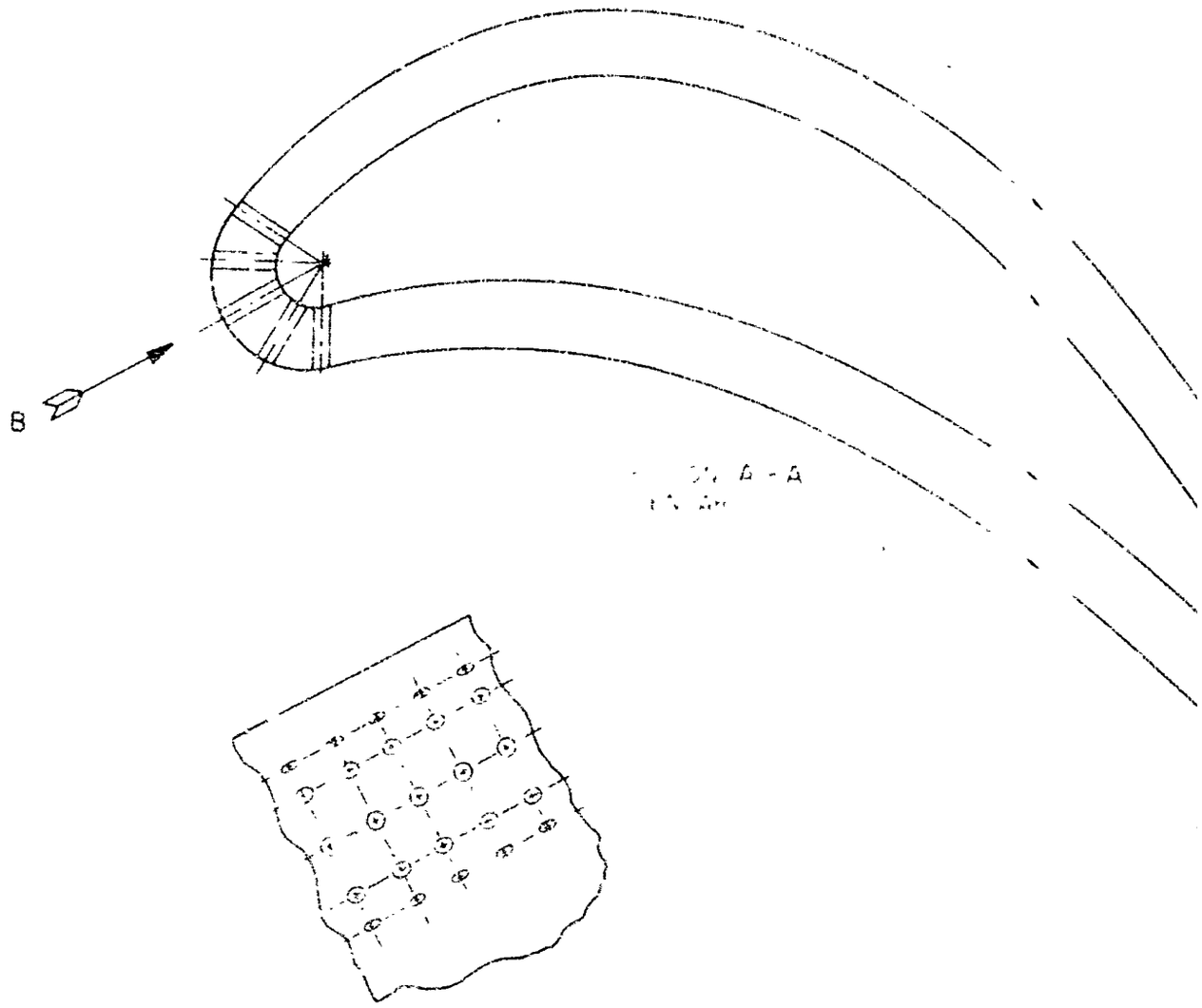




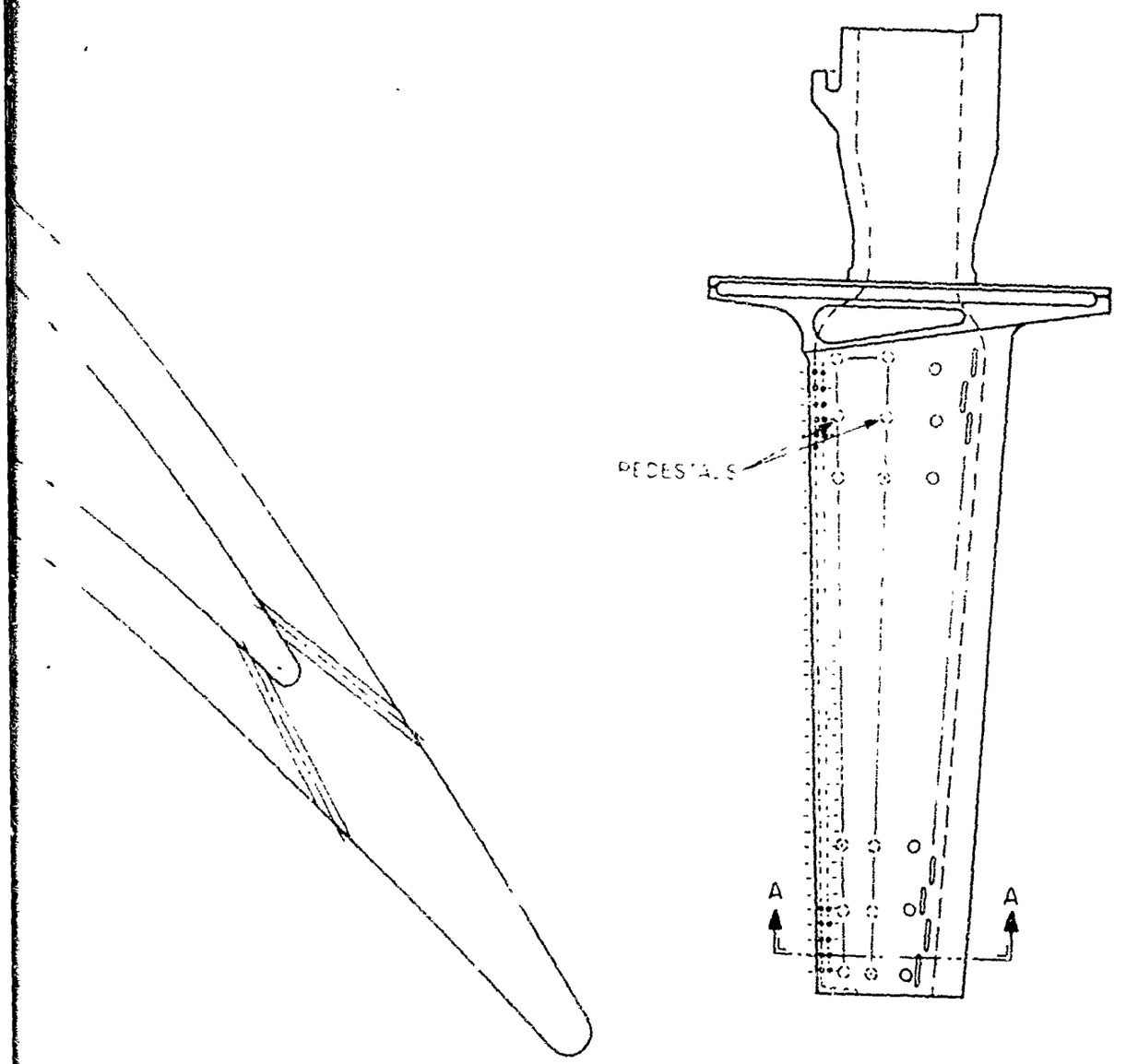
CROSS-SECTION OF SECOND-STAGE TURBINE VANE

Figure 2-48


B

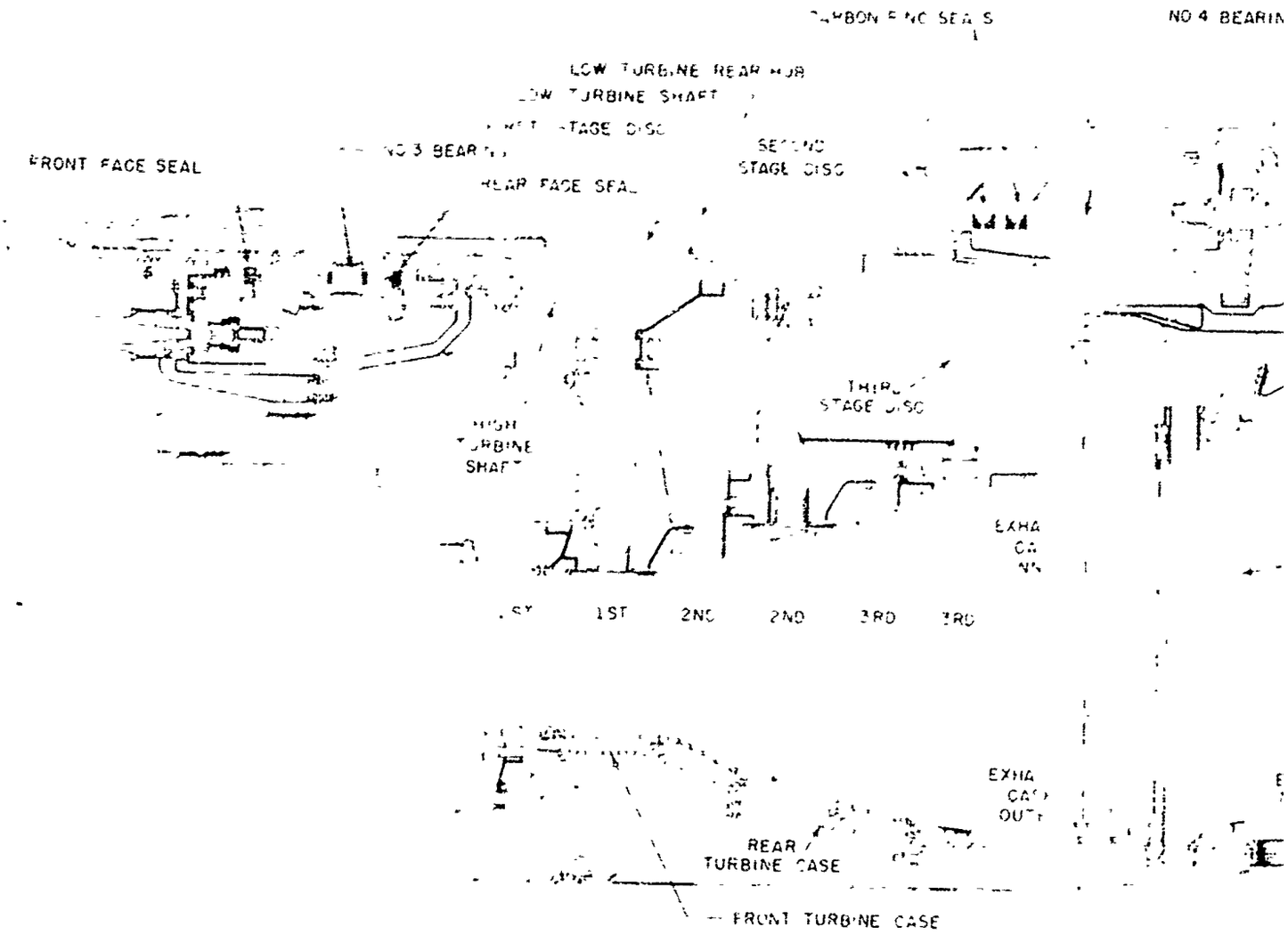


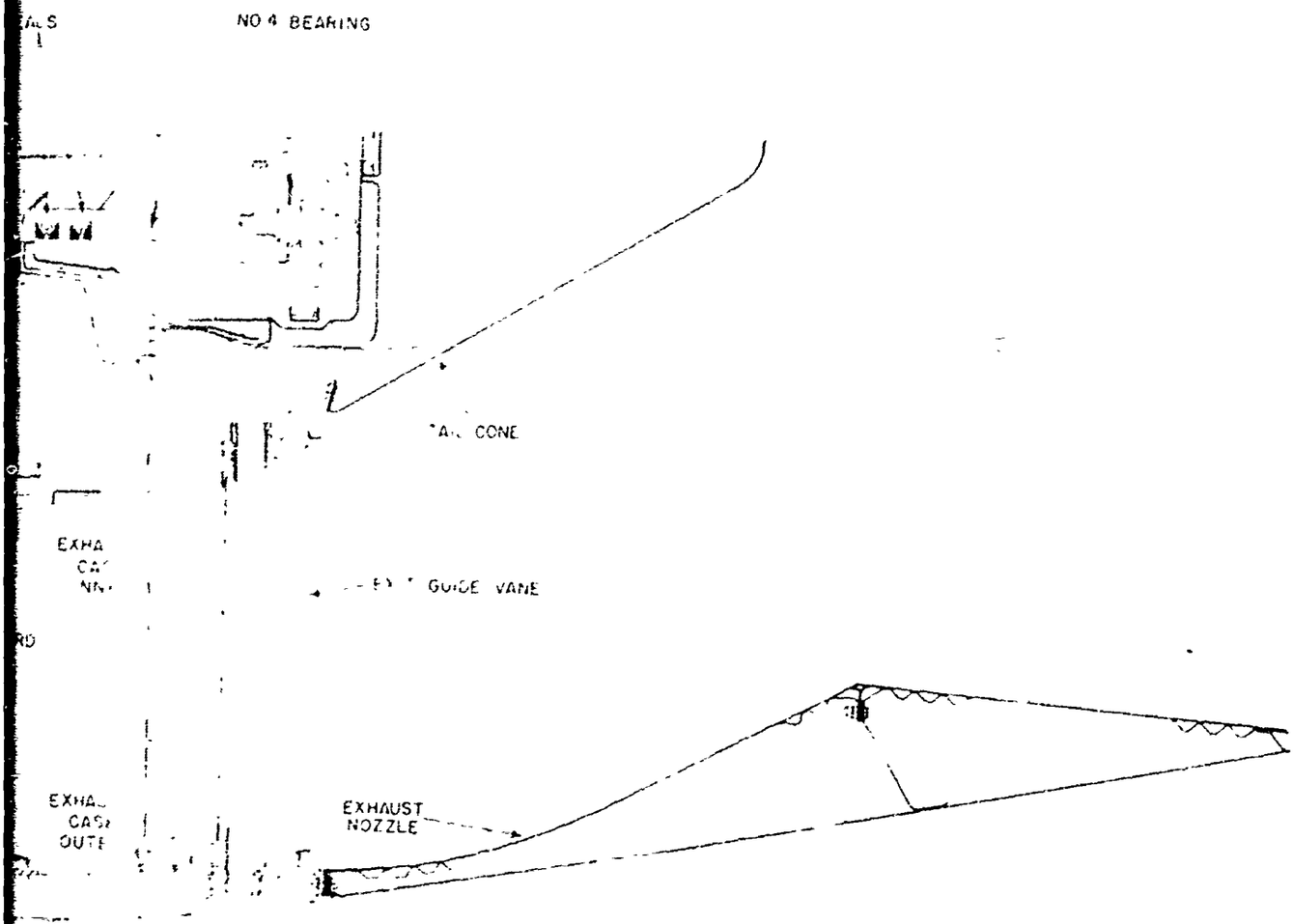
VIEW IN DIRECTION B



CROSS-SECTION OF FIRST-STAGE TURBINE BLADE

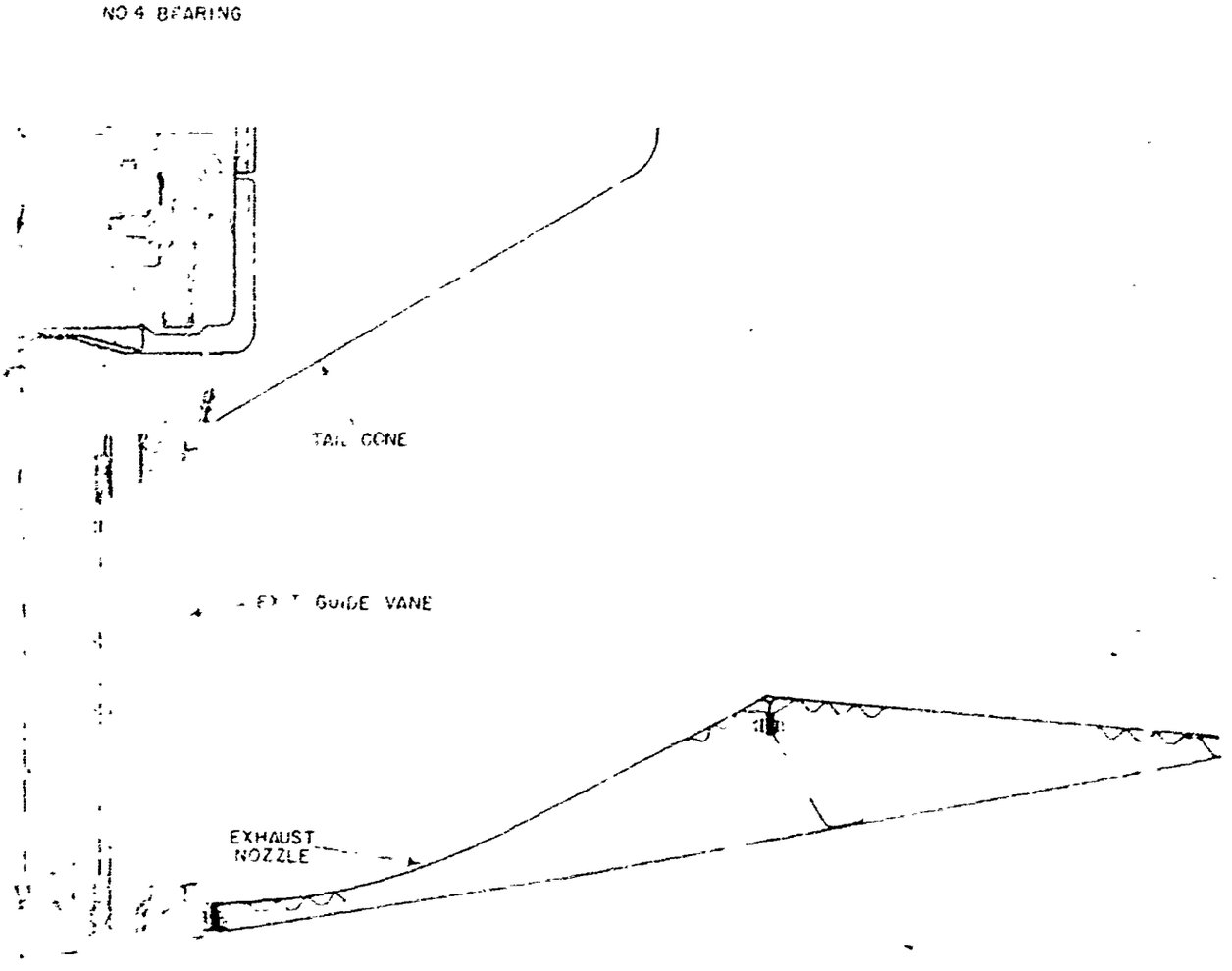
Figure 2-49


NO 4 BEARIN
LOW TURBINE REAR HUB
FRONT FACE SEAL
NO 3 BEARI
REAR FACE SEAL
SECOND
STAGE DISC
THIRD
STAGE DISC
HIGH
TURBINE
SHAFT
EXHA
CA
NO
1ST
2ND
2ND
3RD
3RD
EXHA
CA
OUT
REAR
TURBINE CASE
FRONT TURBINE CASE



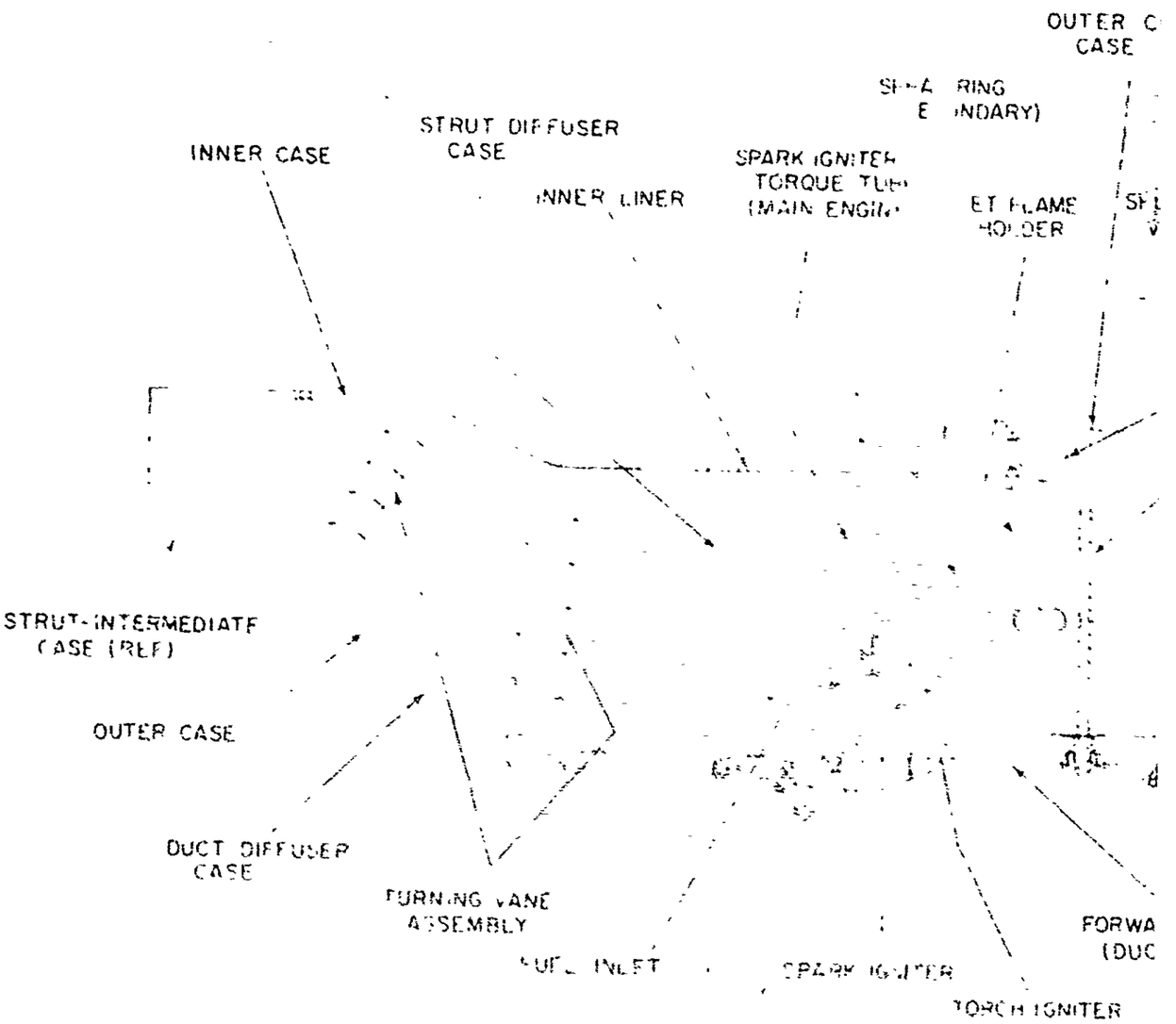
SCHEMATIC DIAGRAM OF TURBINE, TURBINE EXHAUST NOZZLE, AND NUMBER 3 BEARING ASSEMBLY

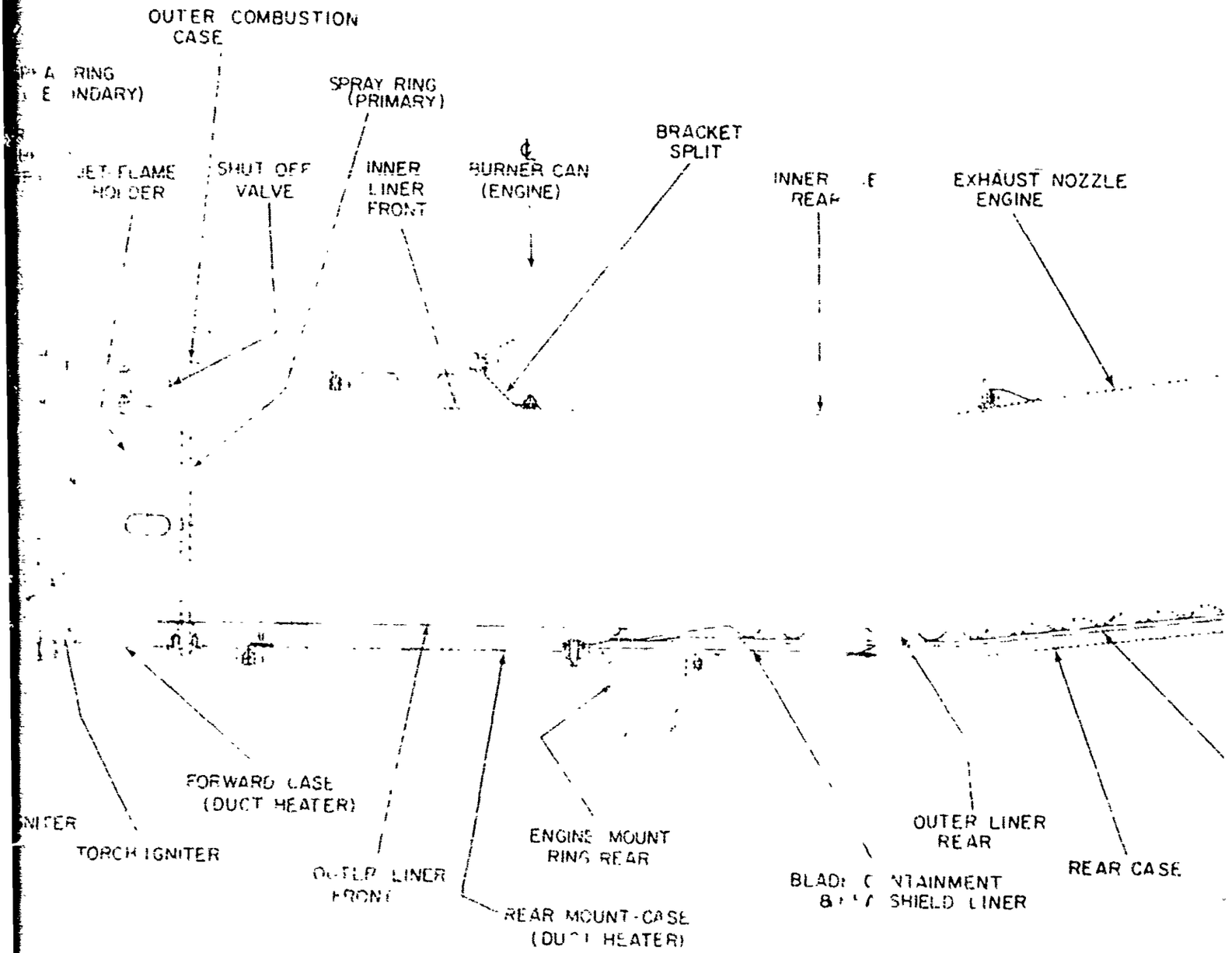
Figure 2-50



SCHEMATIC DIAGRAM OF TURBINE, TURBINE EXHAUST NOZZLE, AND NUMBER 3 BEARING ASSEMBLY

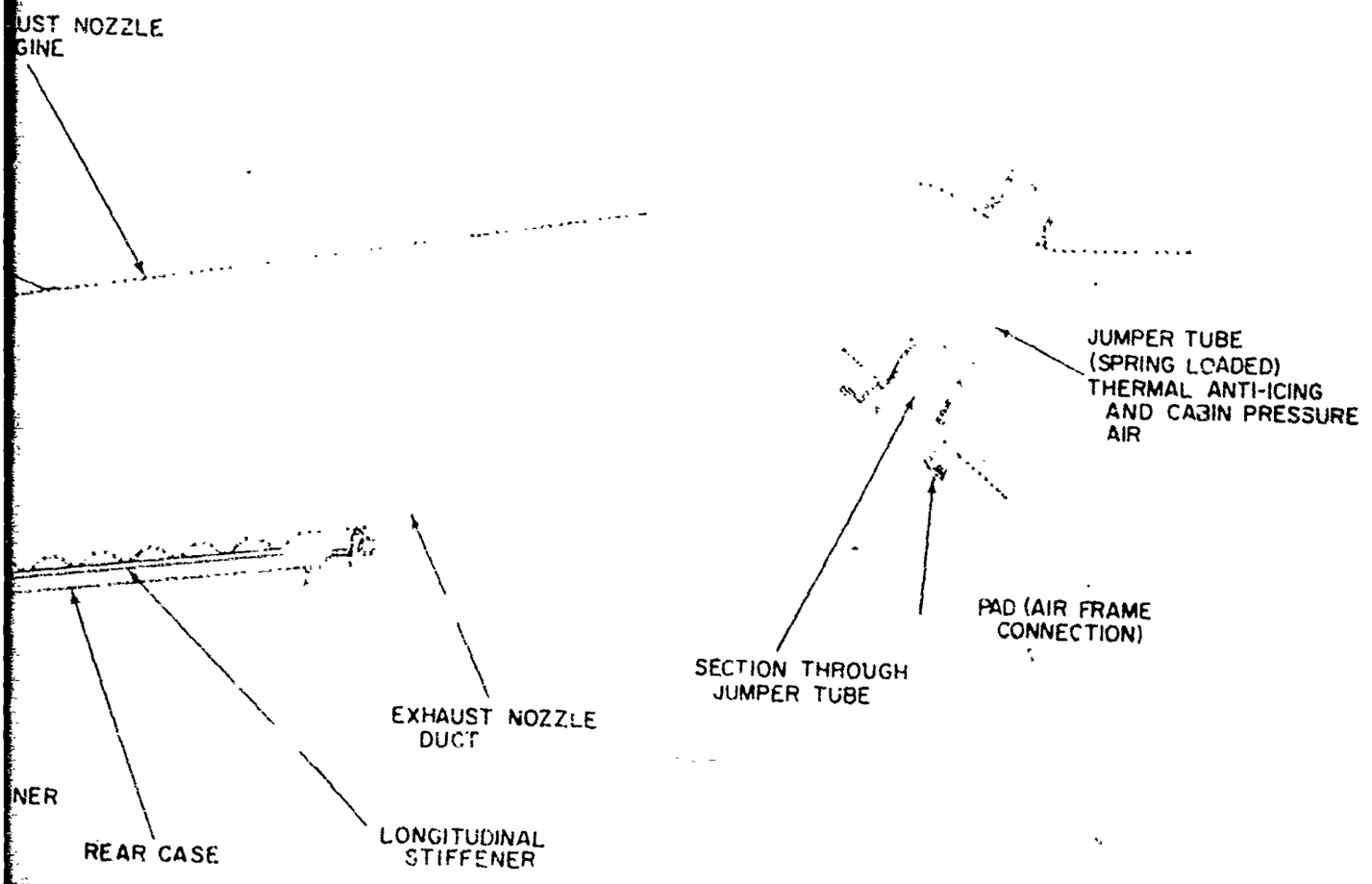
Figure 2-50


OUTER C
CASE
INNER CASE
STRUT DIFFUSER
CASE
INNER LINER
SPARK IGNITER
TORQUE TUB
(MAIN ENGI
ET FLAME
HOLDER
STRUT-INTERMEDIATE
CASE (REF)
OUTER CASE
DUCT DIFFUSER
CASE
TURNING VANE
ASSEMBLY
FORWA
(DUC
SPARK IGNITER
TORCH IGNITER


OUTER COMBUSTION CASE
SPRAY RING (PRIMARY)
BRACKET SPLIT
JET FLAME HOLDER
SHUT OFF VALVE
INNER LINER FRONT
BURNER CAN (ENGINE)
INNER
REAR
EXHAUST NOZZLE ENGINE
FORWARD CASE (DUCT HEATER)
TORCH IGNITER
ENGINE MOUNT RING REAR
OUTER LINER REAR
REAR CASE
REAR MOUNT-CASE (DUCT HEATER)

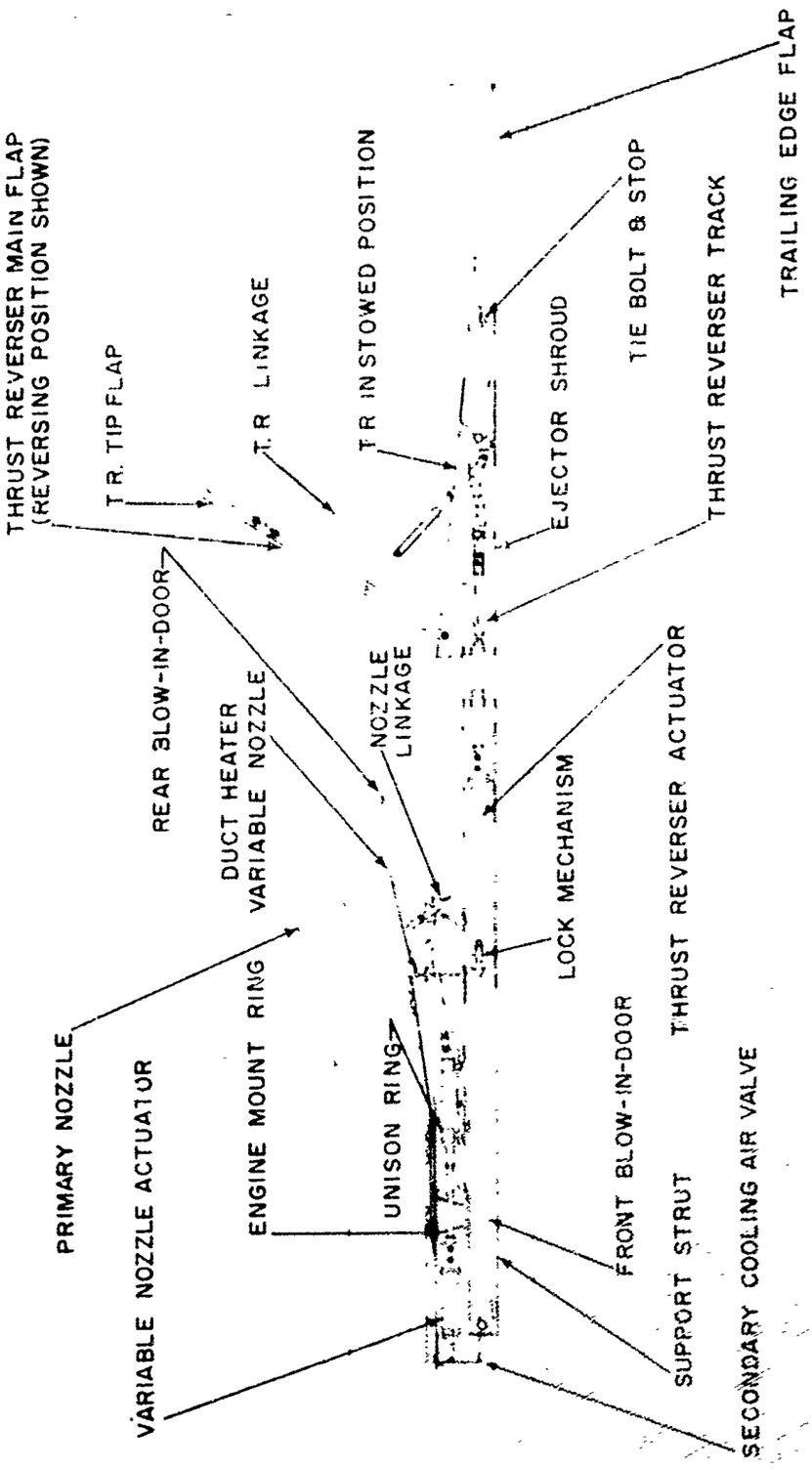
1

2



SCHEMATIC DIAGRAM OF DUCT HEATER FOR STF 219 ENGINE

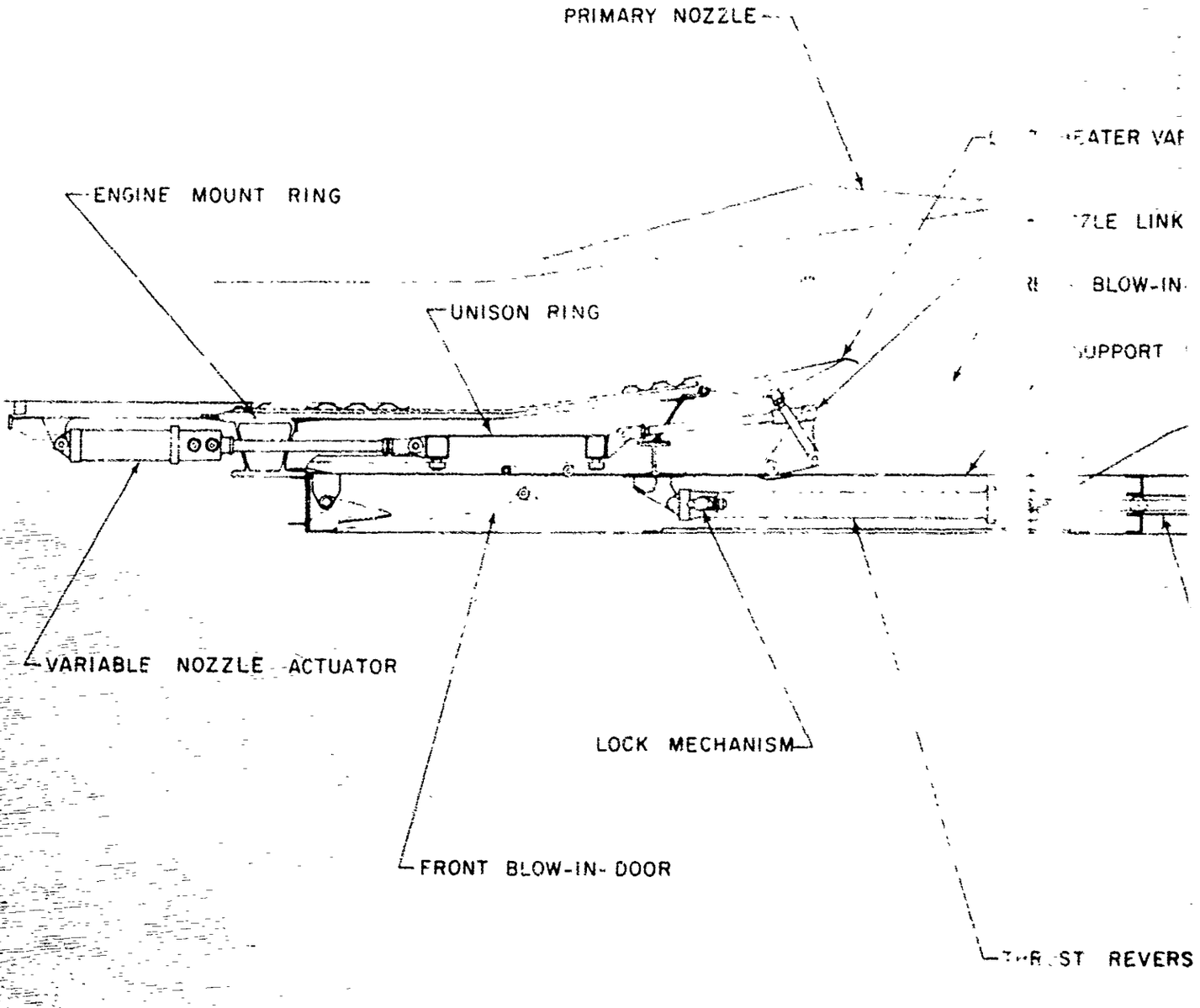
Figure 2-51

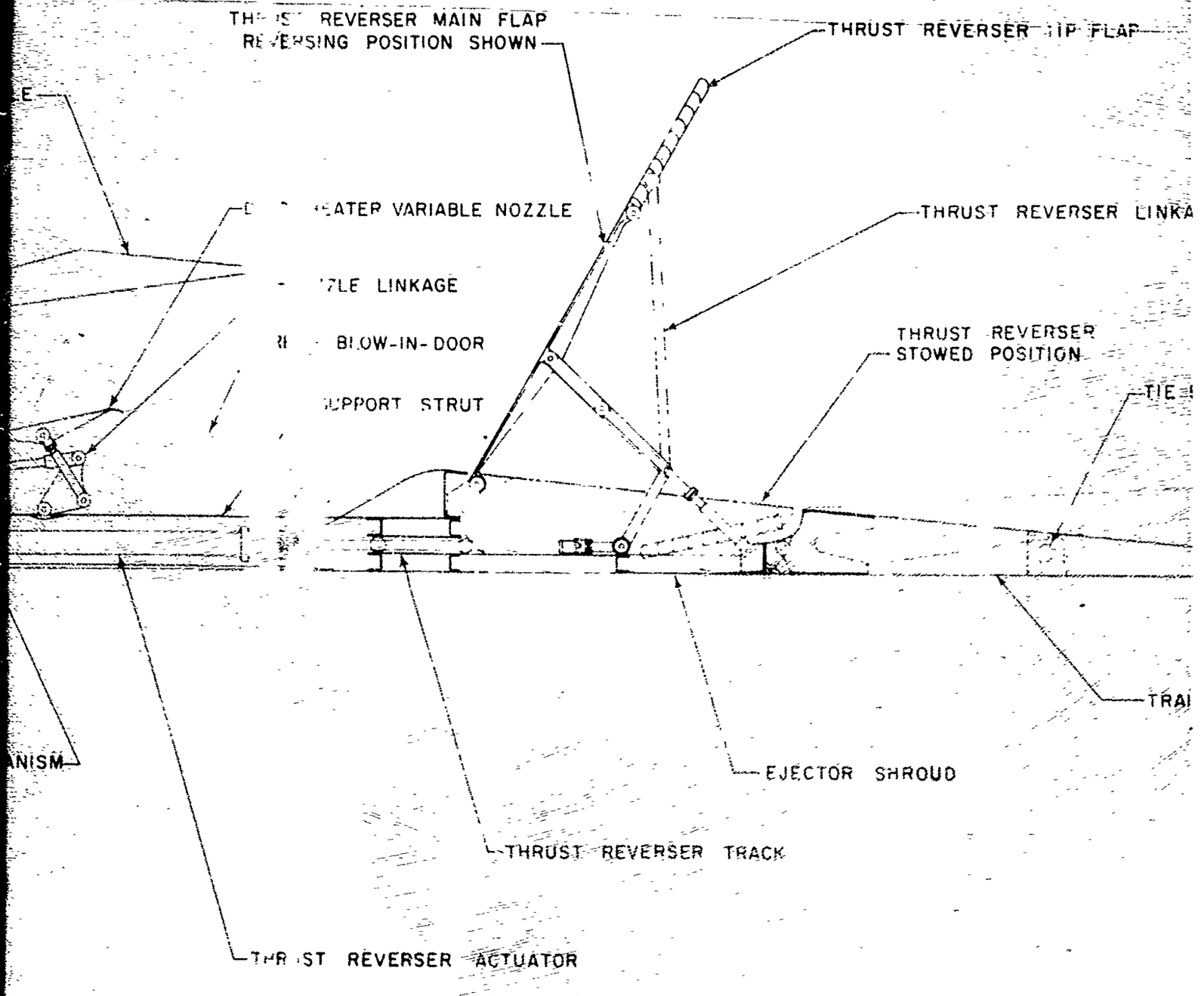


DUCT HEATER NOZZLE AND EJECTOR-REVERSER FOR LOCKHEED

Figure 2-52

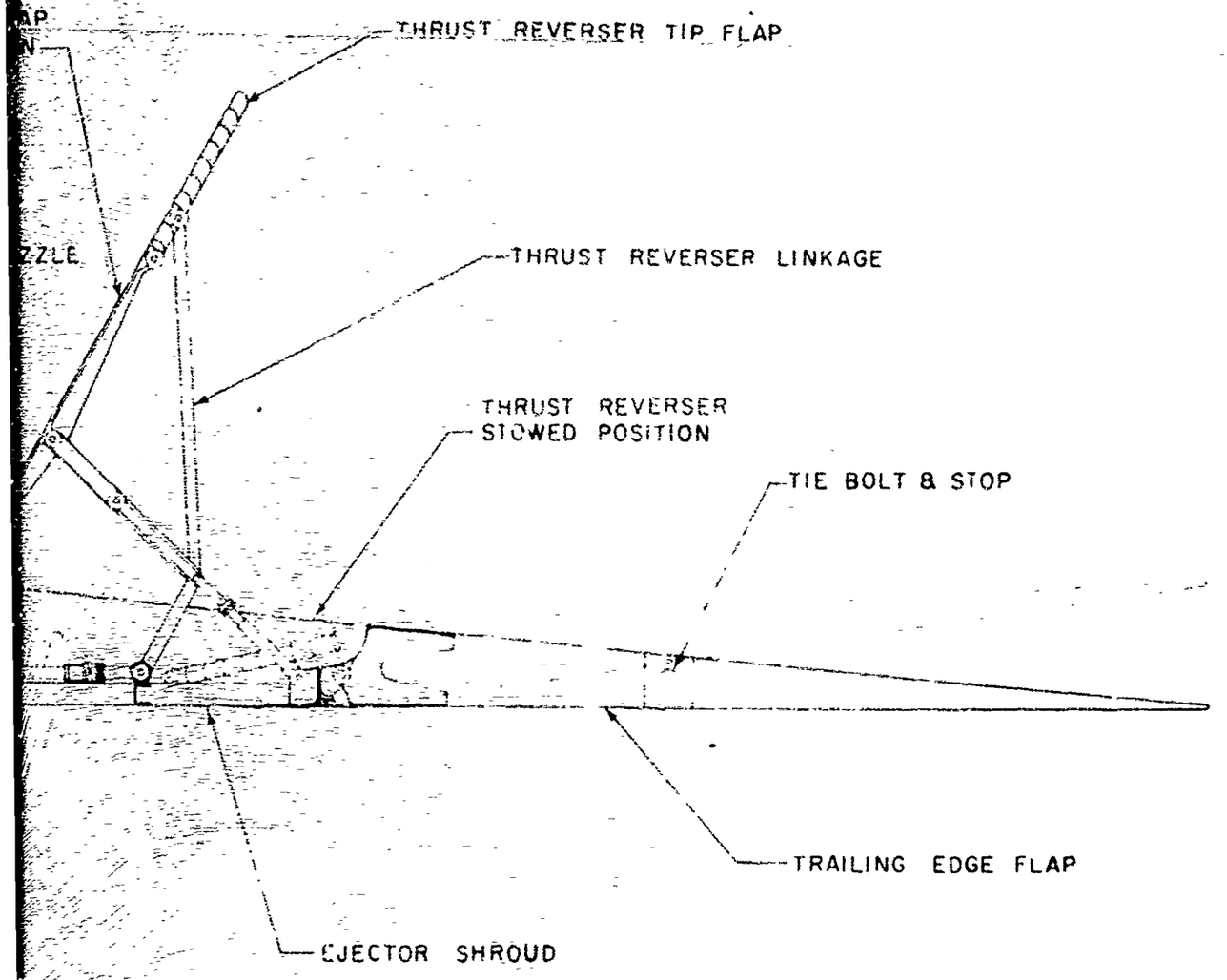
TH[illegible] REVERSER
R[illegible]SING POSIT





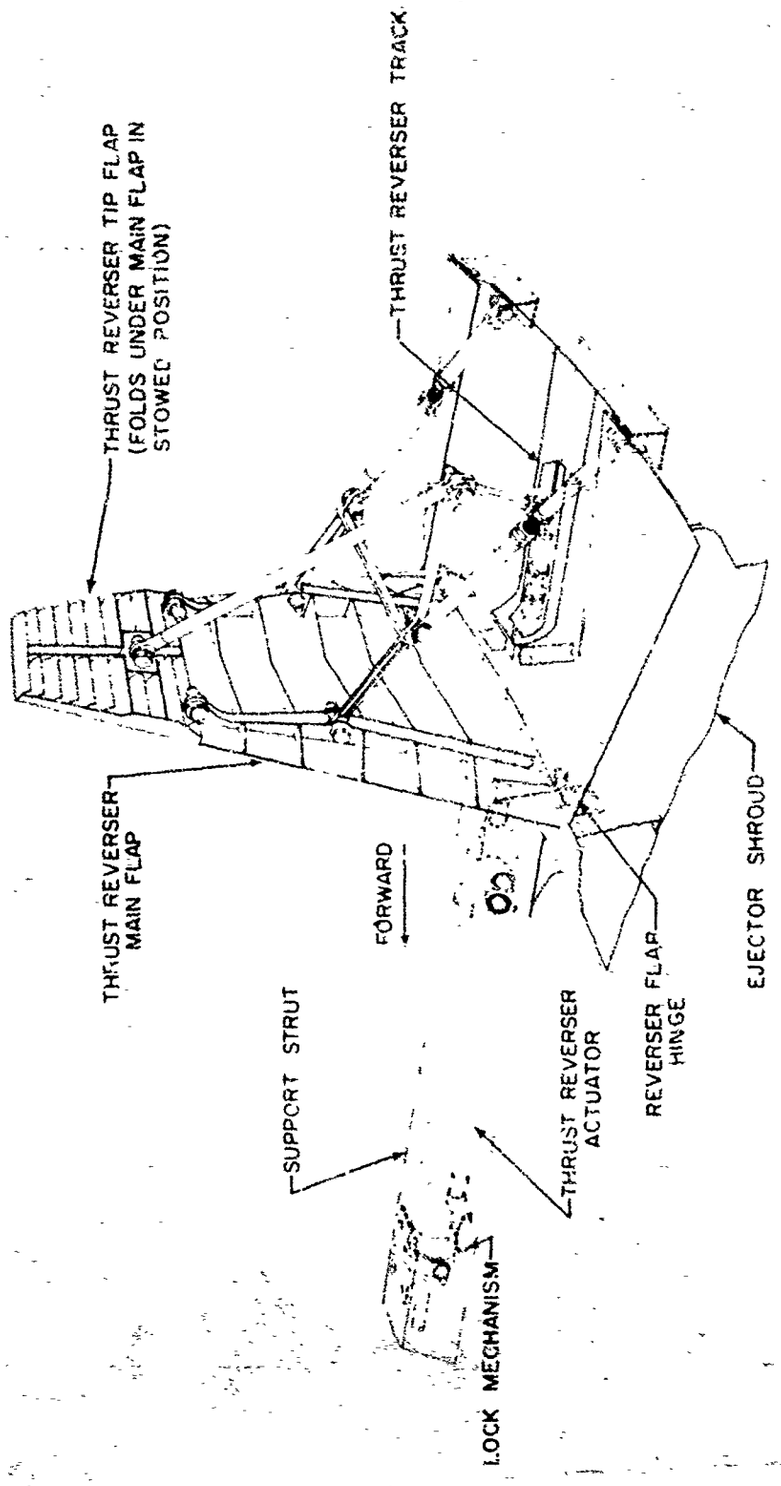
DUCT HEATER AND EJECTOR REV
BOEING

Figure 2-53



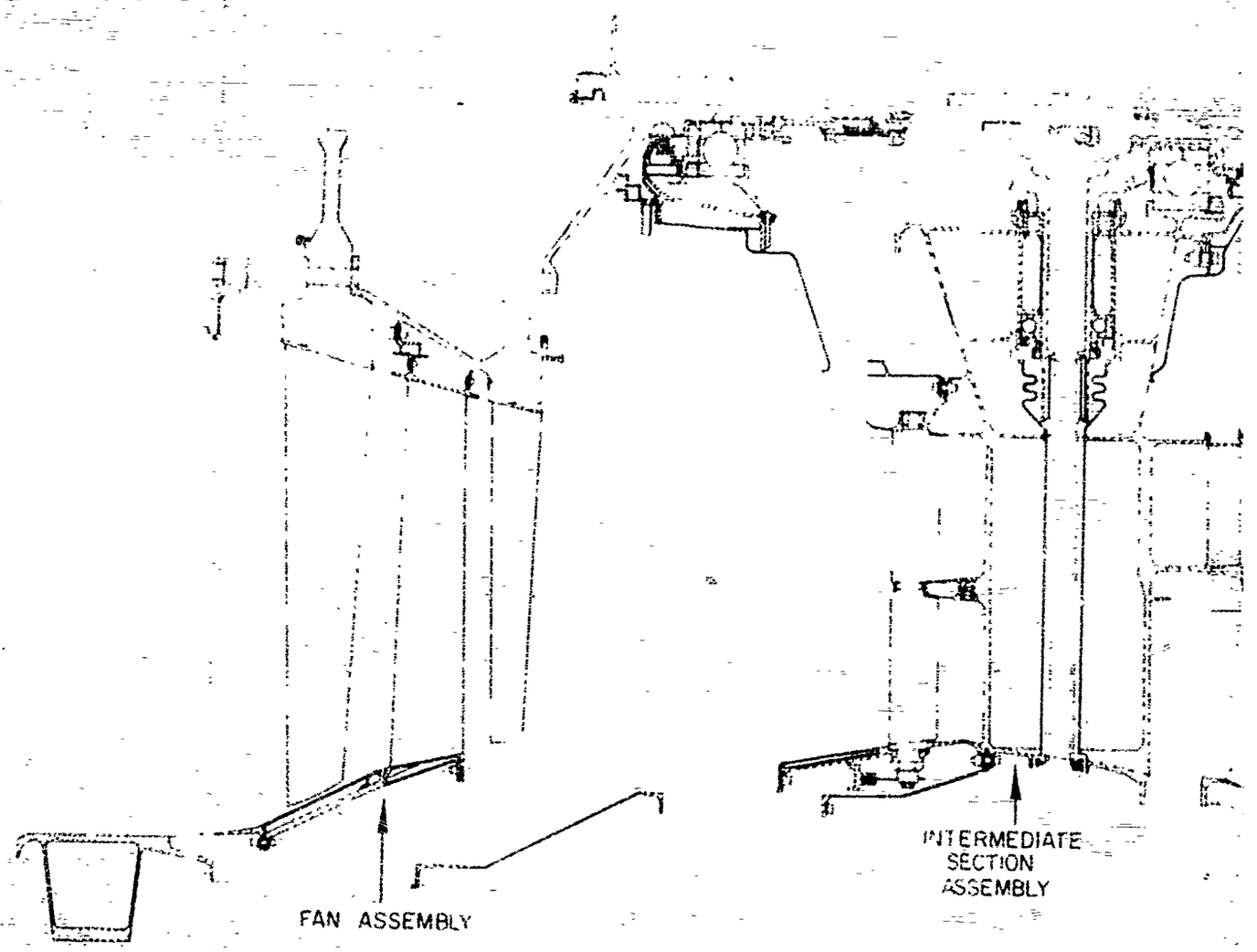
DUCT HEATER AND EJECTOR REVERSER FOR BOEING

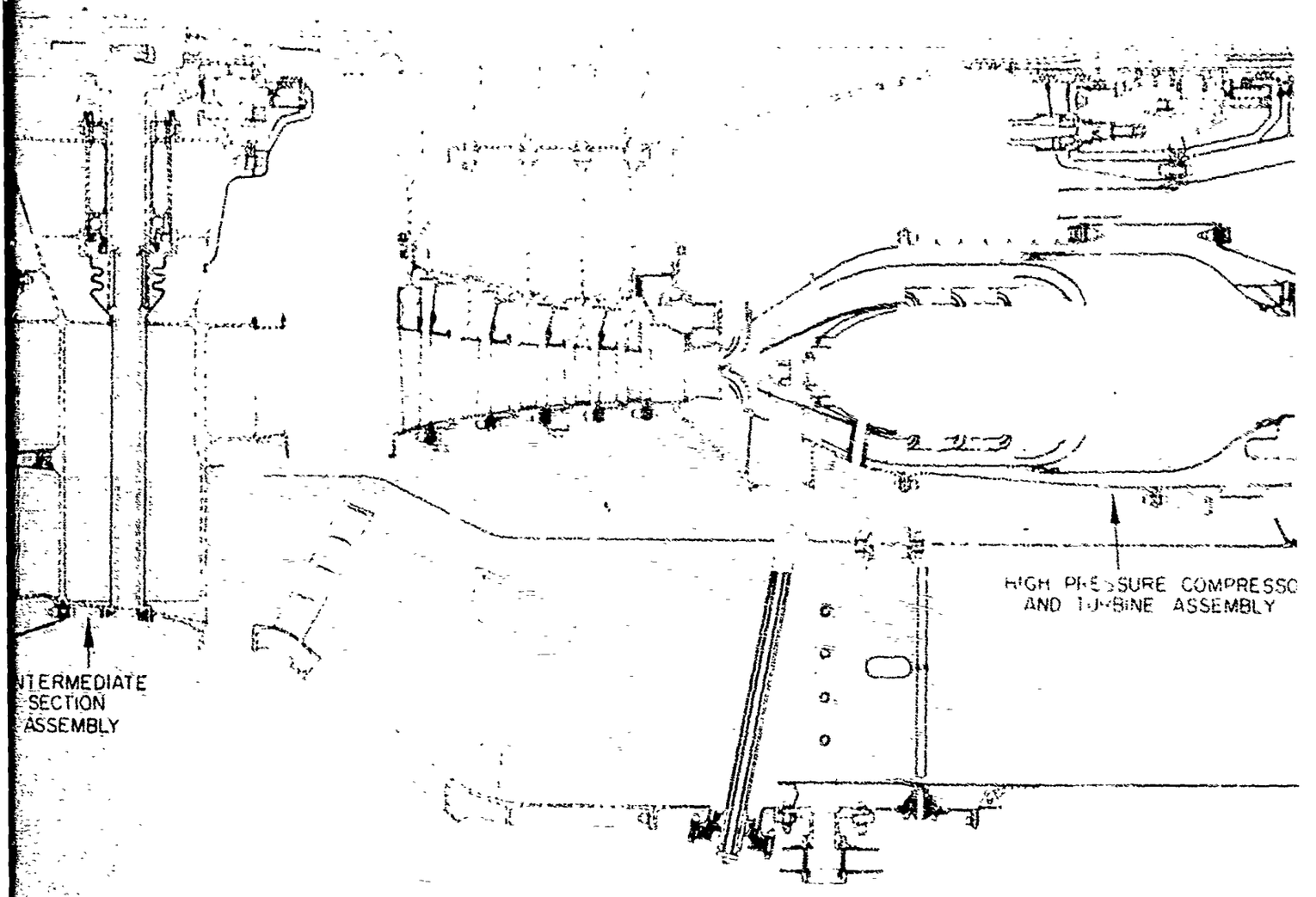
Figure 2-53



TYPICAL THRUST REVERSER SEGMENT

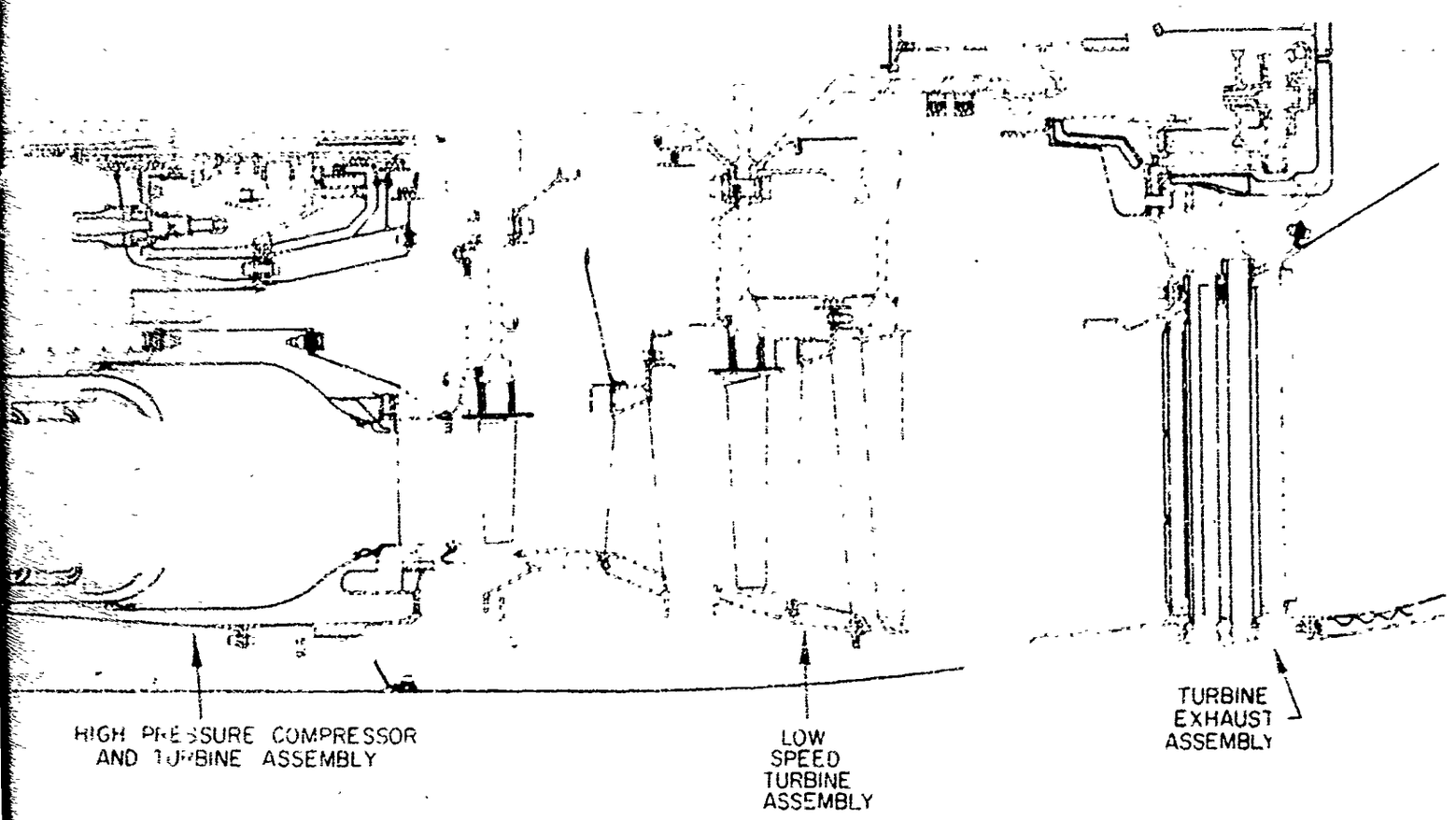
Figure 2-54


FAN ASSEMBLY
INTERMEDIATE
SECTION
ASSEMBLY

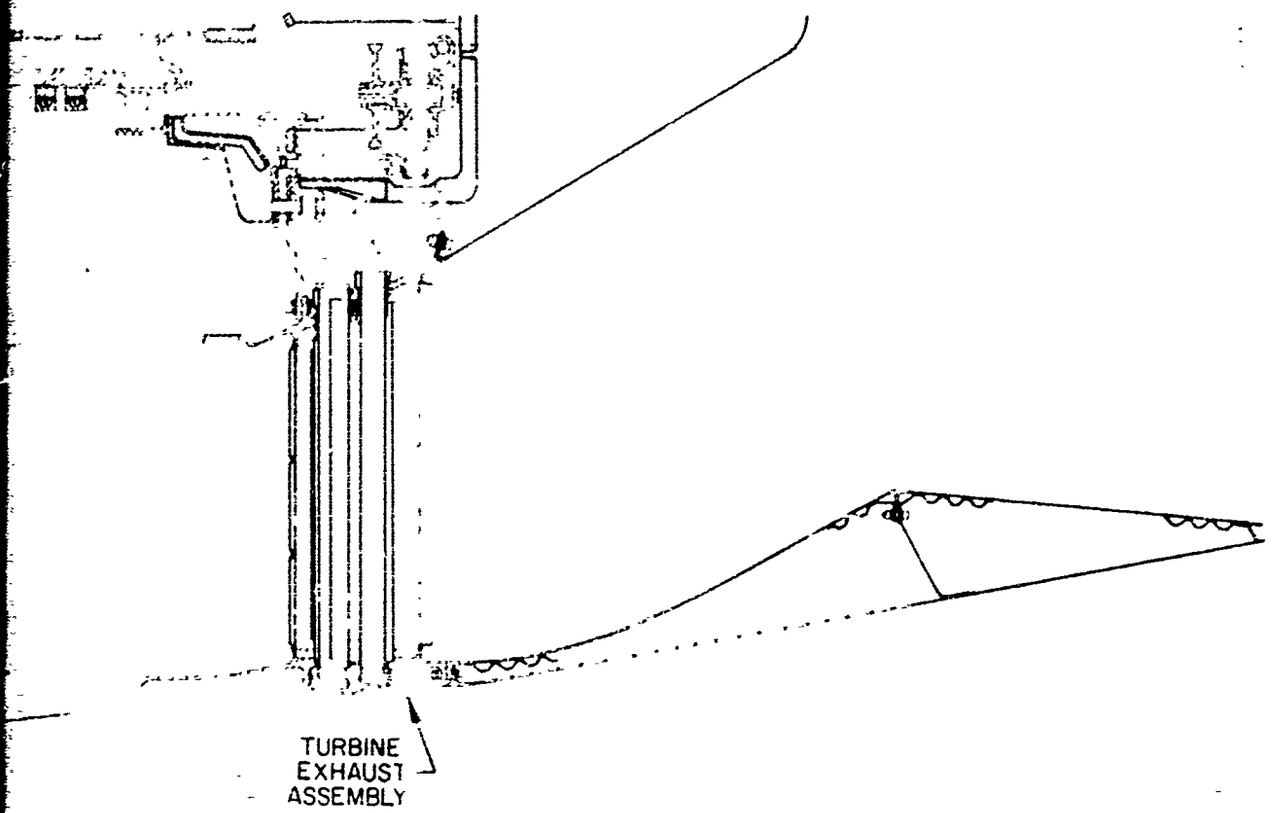

NTERMEDIATE
SECTION
ASSEMBLY
HIGH PRESSURE COMPRESSO
AND TURBINE ASSEMBLY

1

2

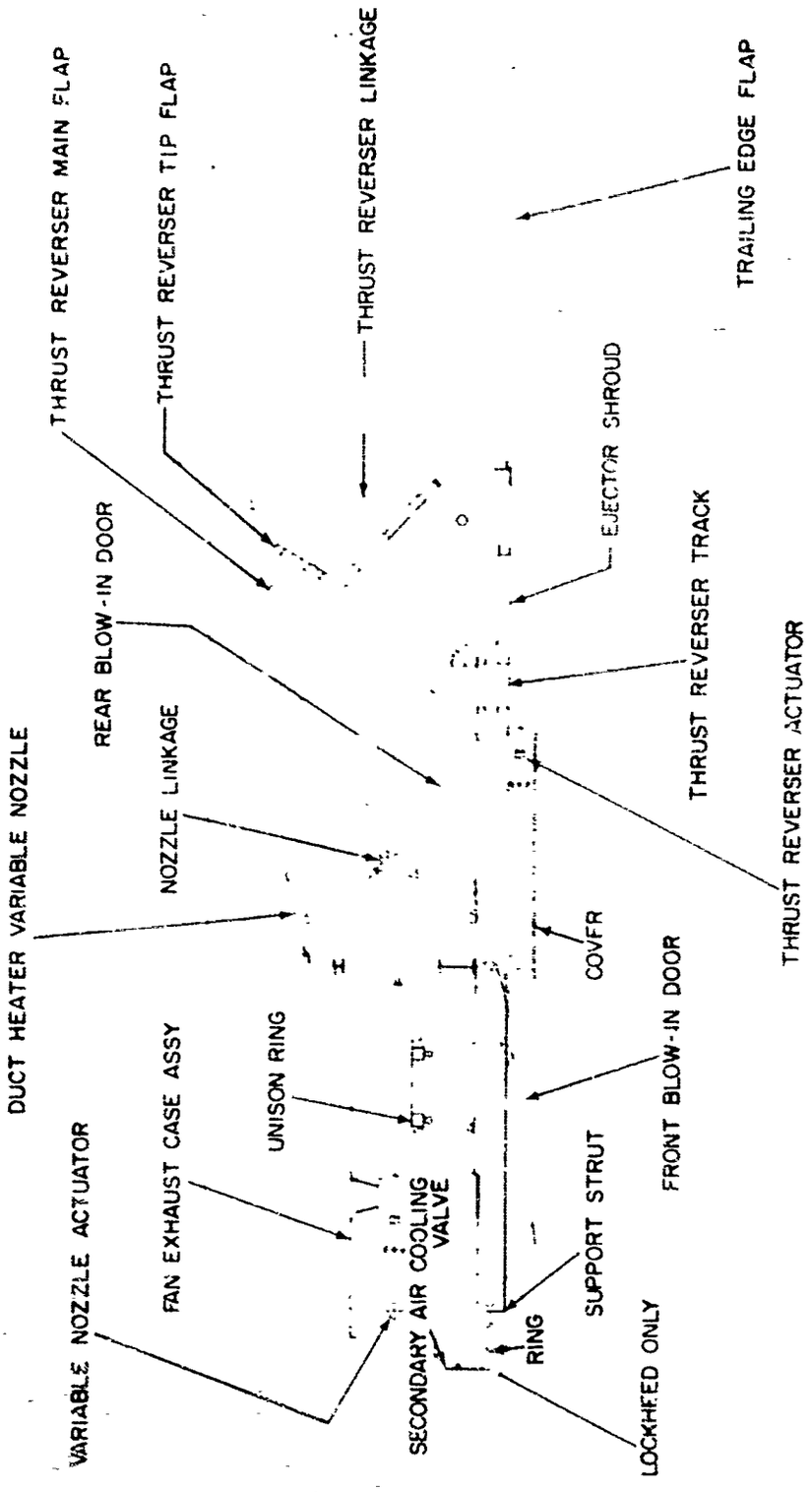

HIGH PRESSURE COMPRESSOR AND TURBINE ASSEMBLY
LOW SPEED TURBINE ASSEMBLY
TURBINE EXHAUST ASSEMBLY

MAJOR ASSE



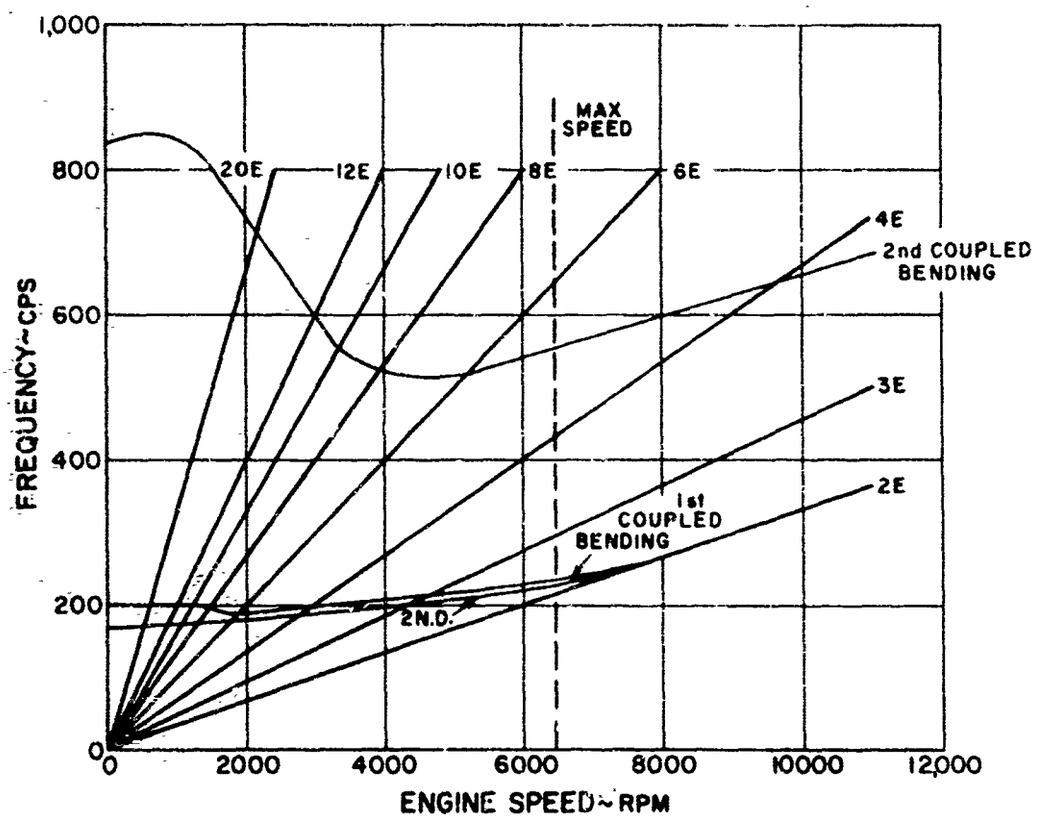
MAJOR ASSEMBLIES OF STF 219 ENGINE

Figure 2-55



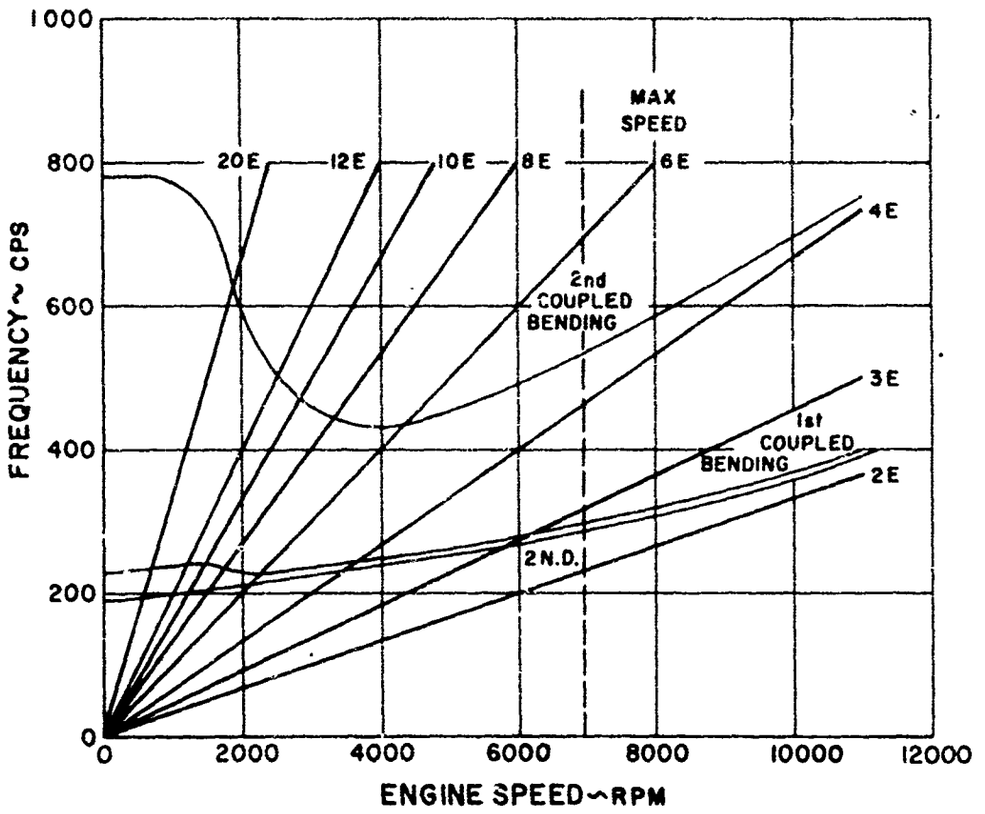
DUCT HEATER NOZZLE AND EJECTOR - REVERSER ASSEMBLY

Figure 2-56



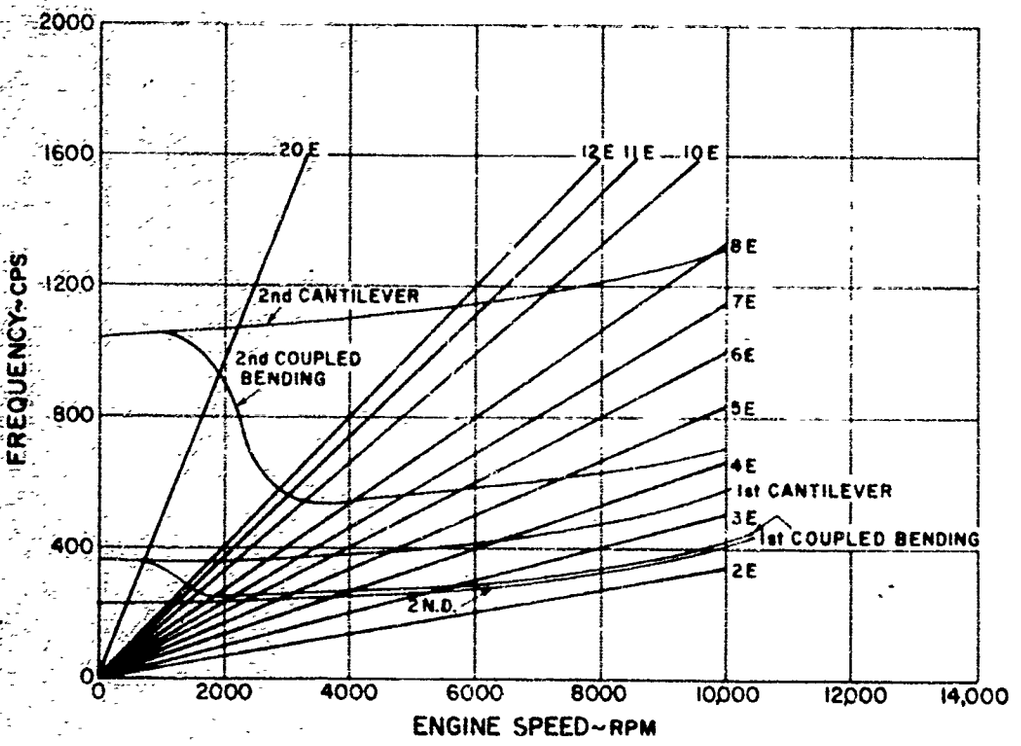
RESONANCE DIAGRAM FOR FIRST ROTOR OF STF 219 ENGINE

Figure 2-57



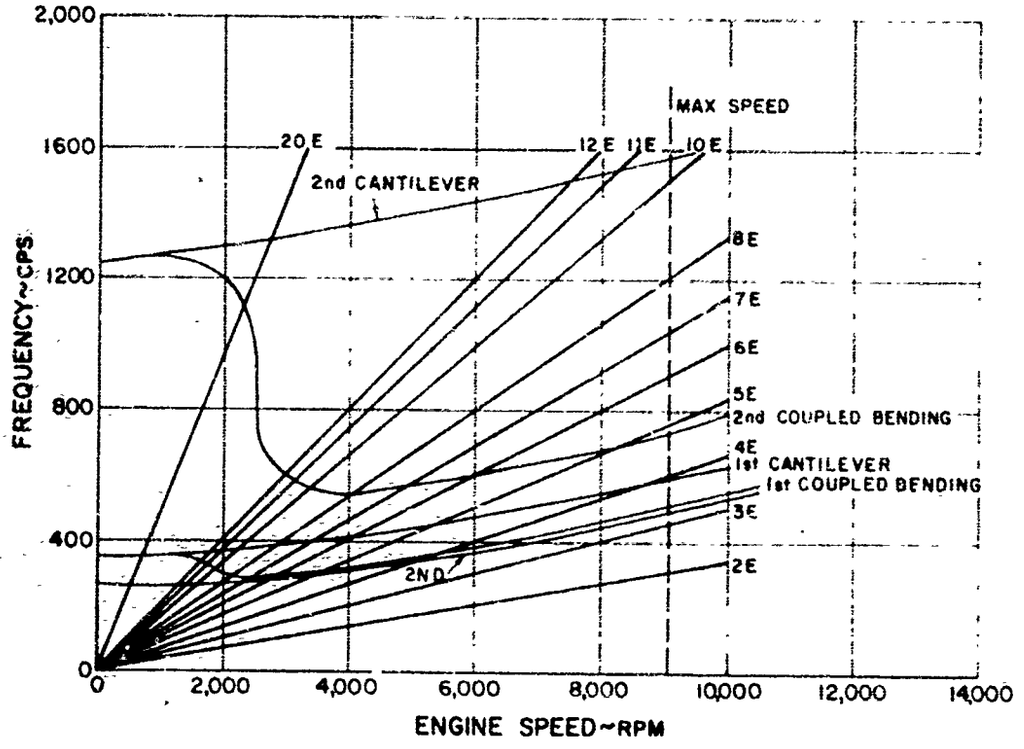
RESONANCE DIAGRAM FOR SECOND ROTOR OF STF 219 ENGINE

Figure 2-58



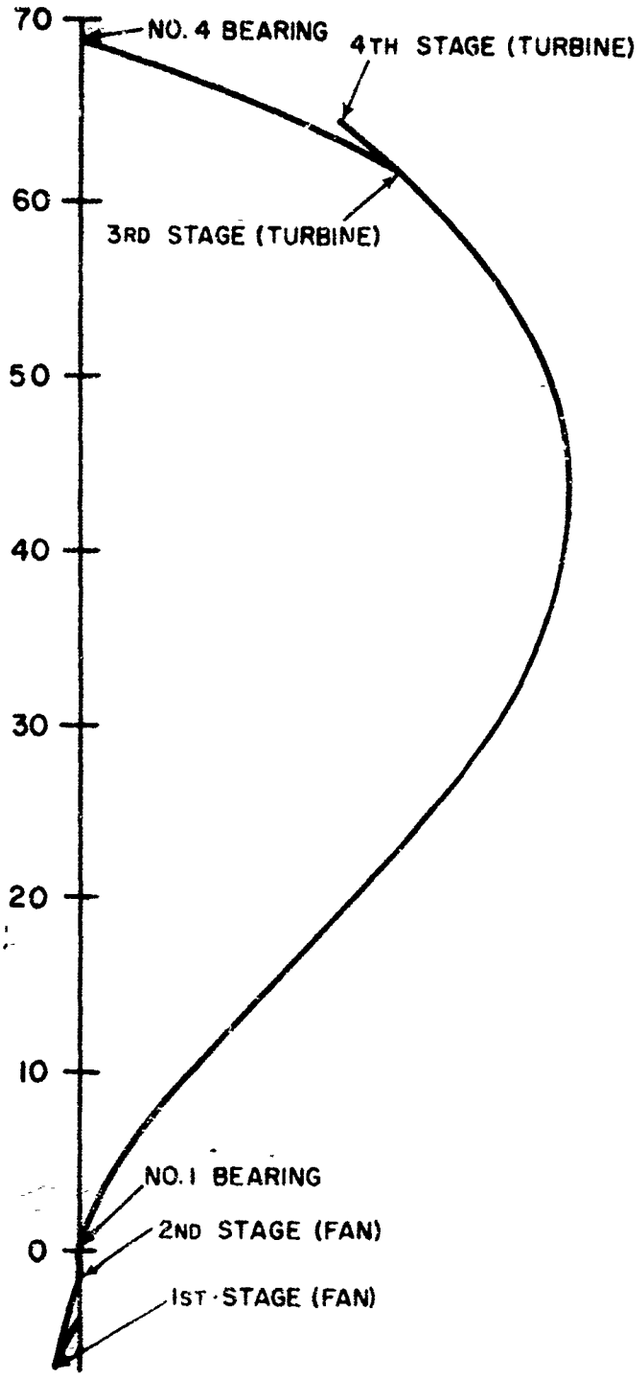
RESONANCE DIAGRAM FOR FOURTH ROTOR OF STF 219 ENGINE

Figure 2-59



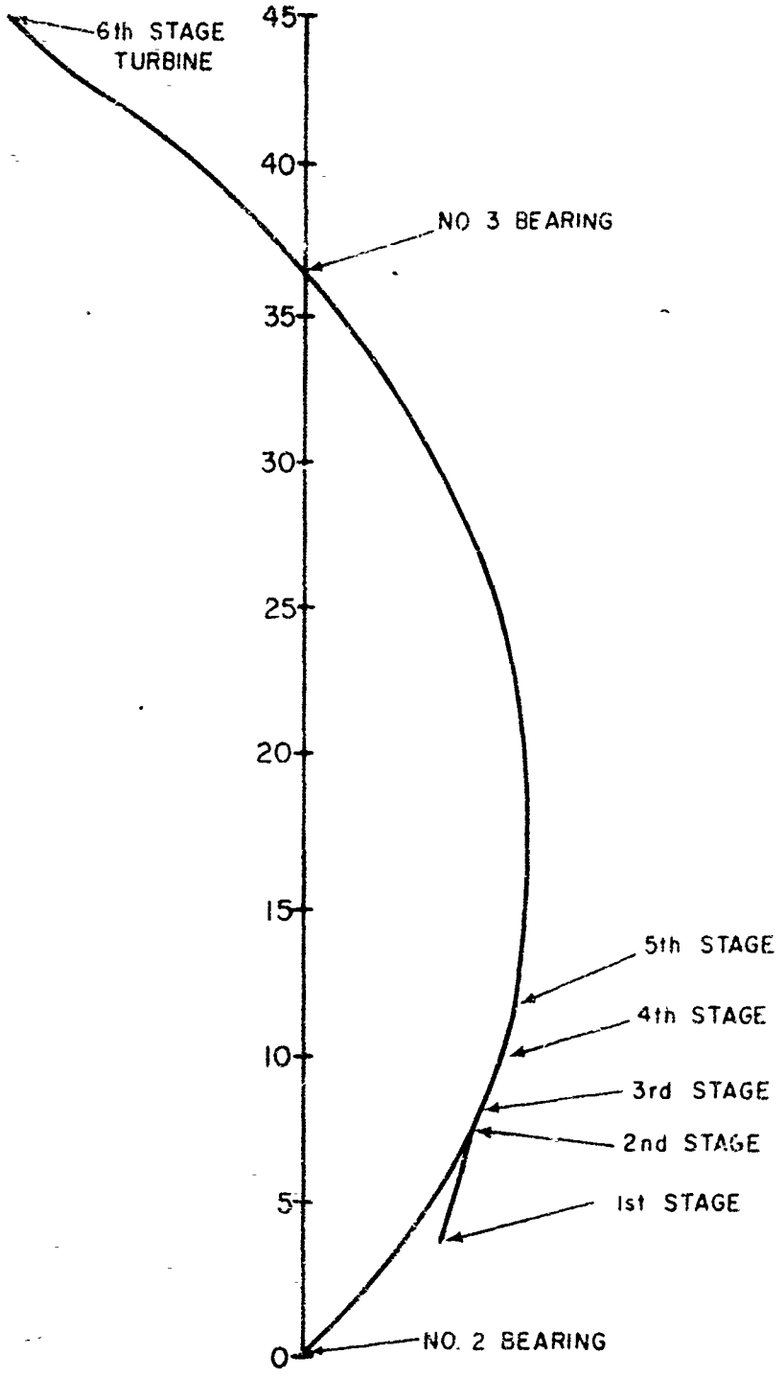
RESONANCE DIAGRAM FOR SEVENTH ROTOR OF STF 219 ENGINE

Figure 2-60



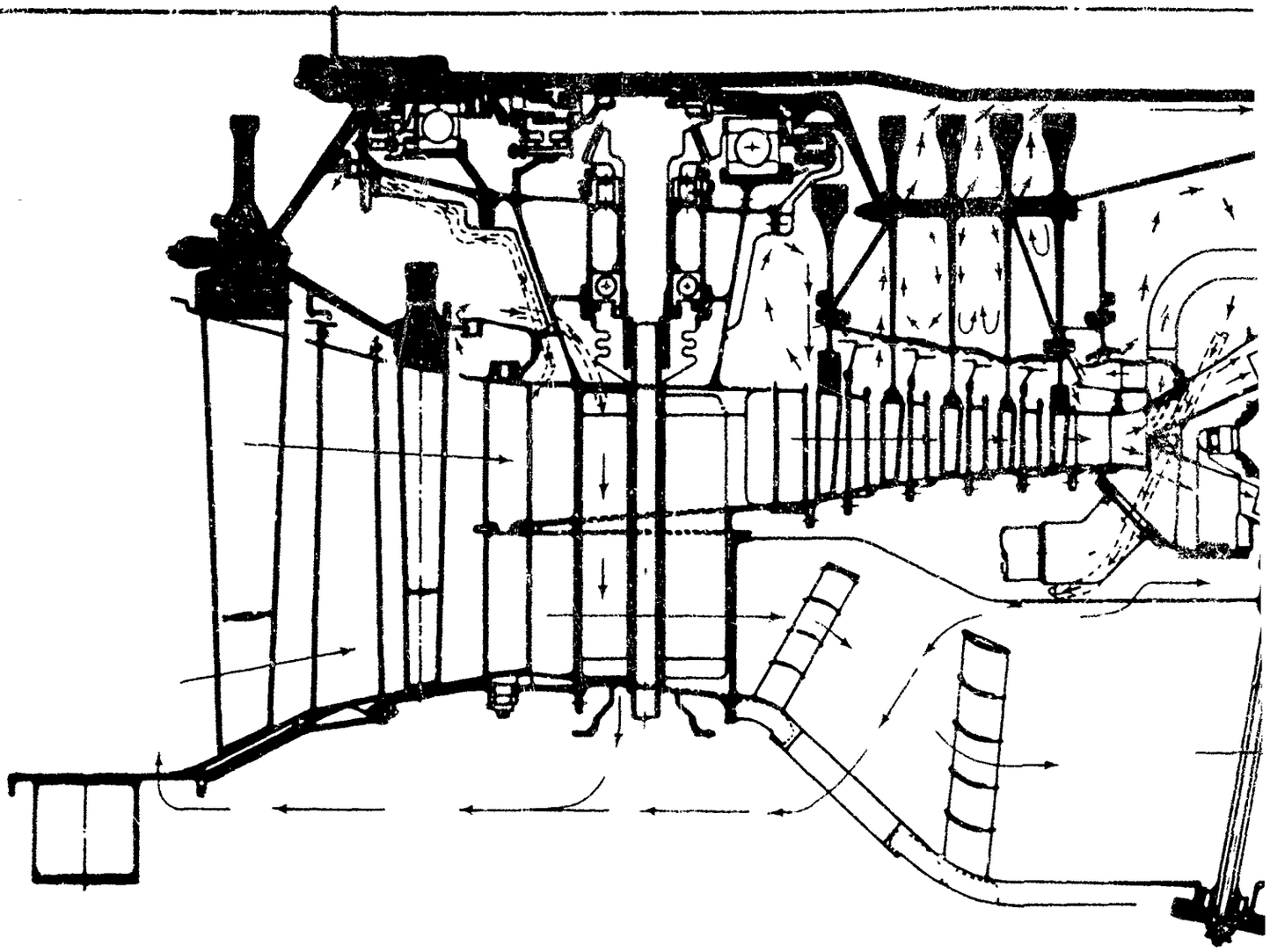
LOW SPEED ROTOR STIFF BEARING MODE SHAPE

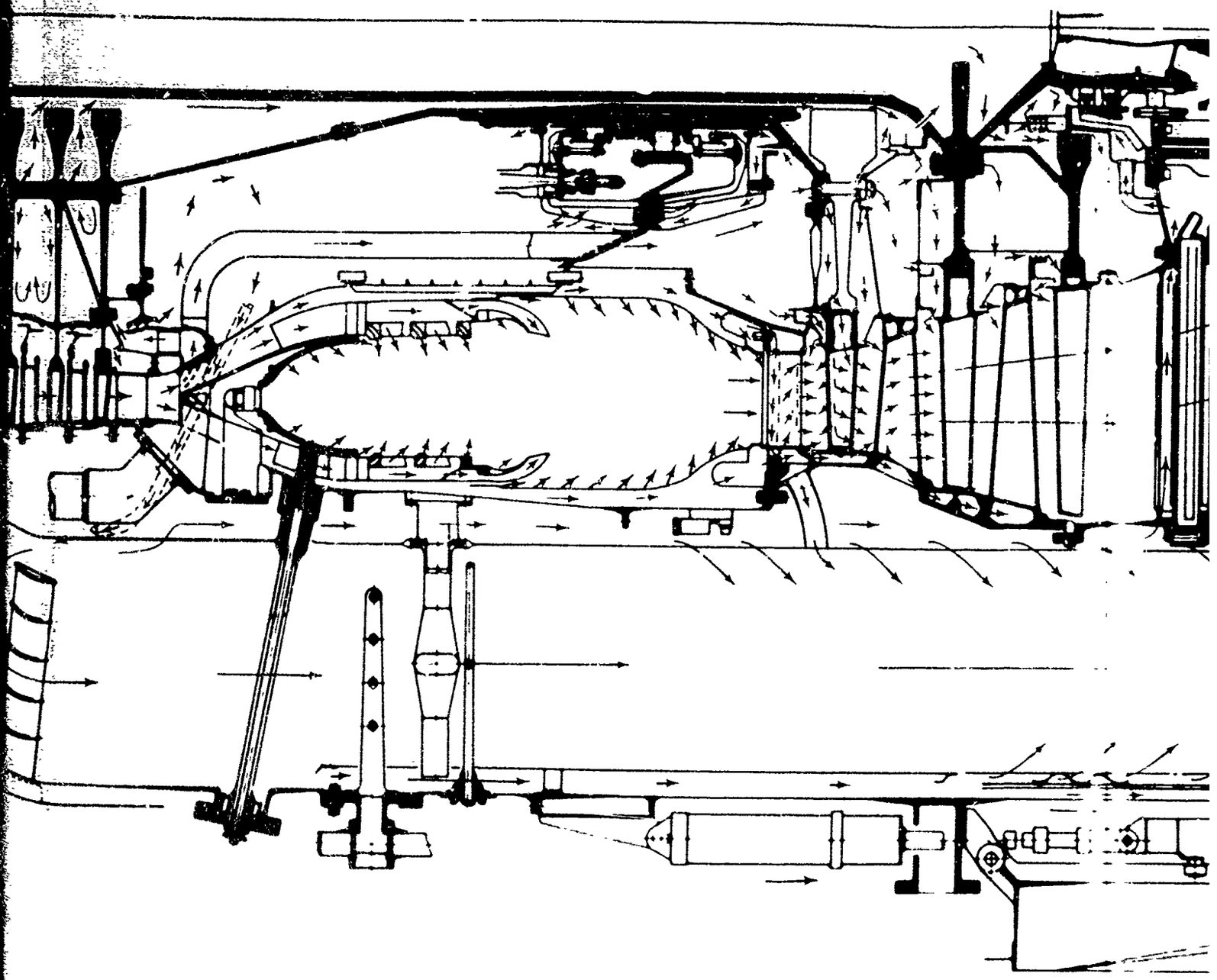
Figure 2-61



HIGH SPEED ROTOR STIFF BEARING MODE SHAPE

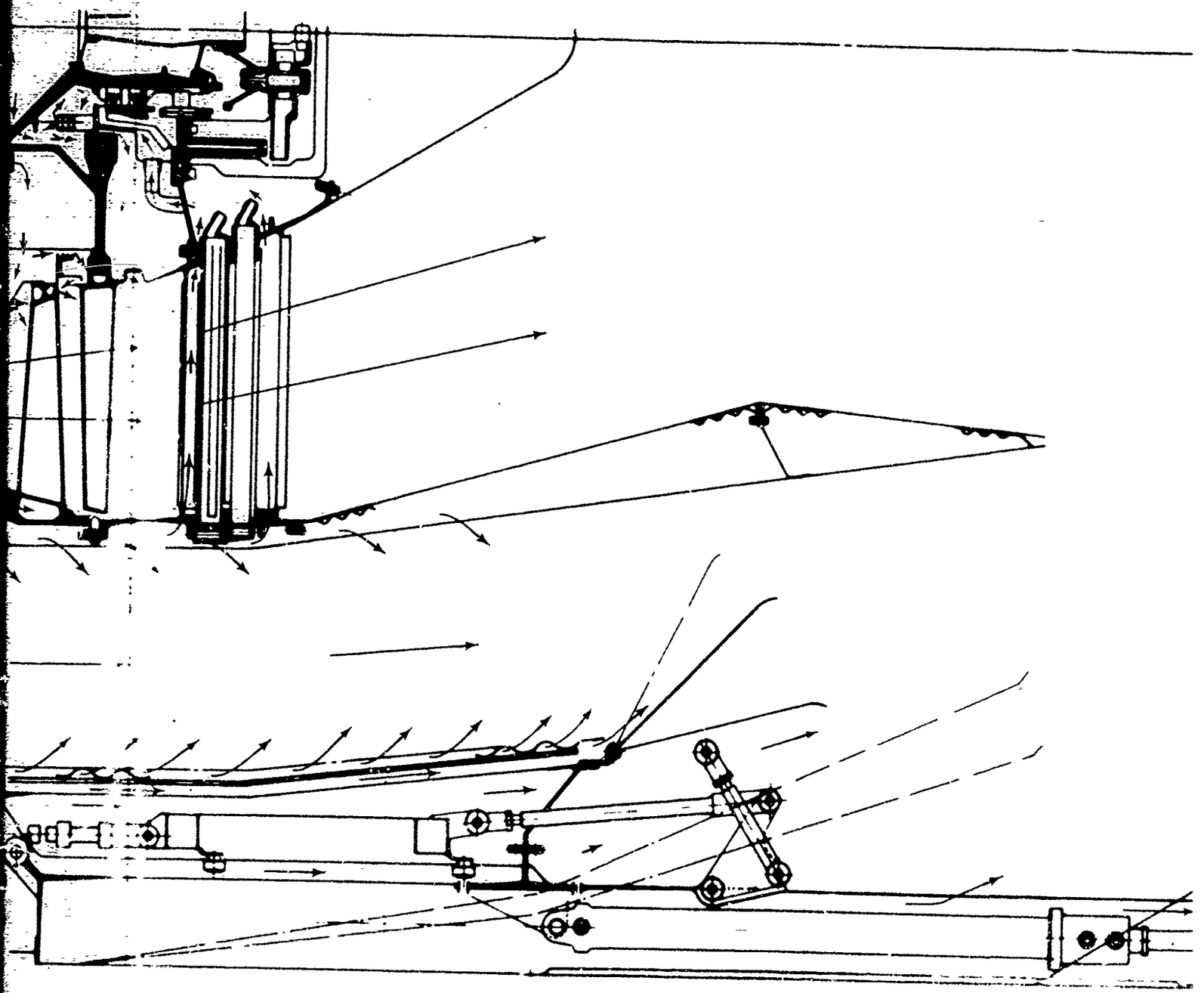
Figure 2-62

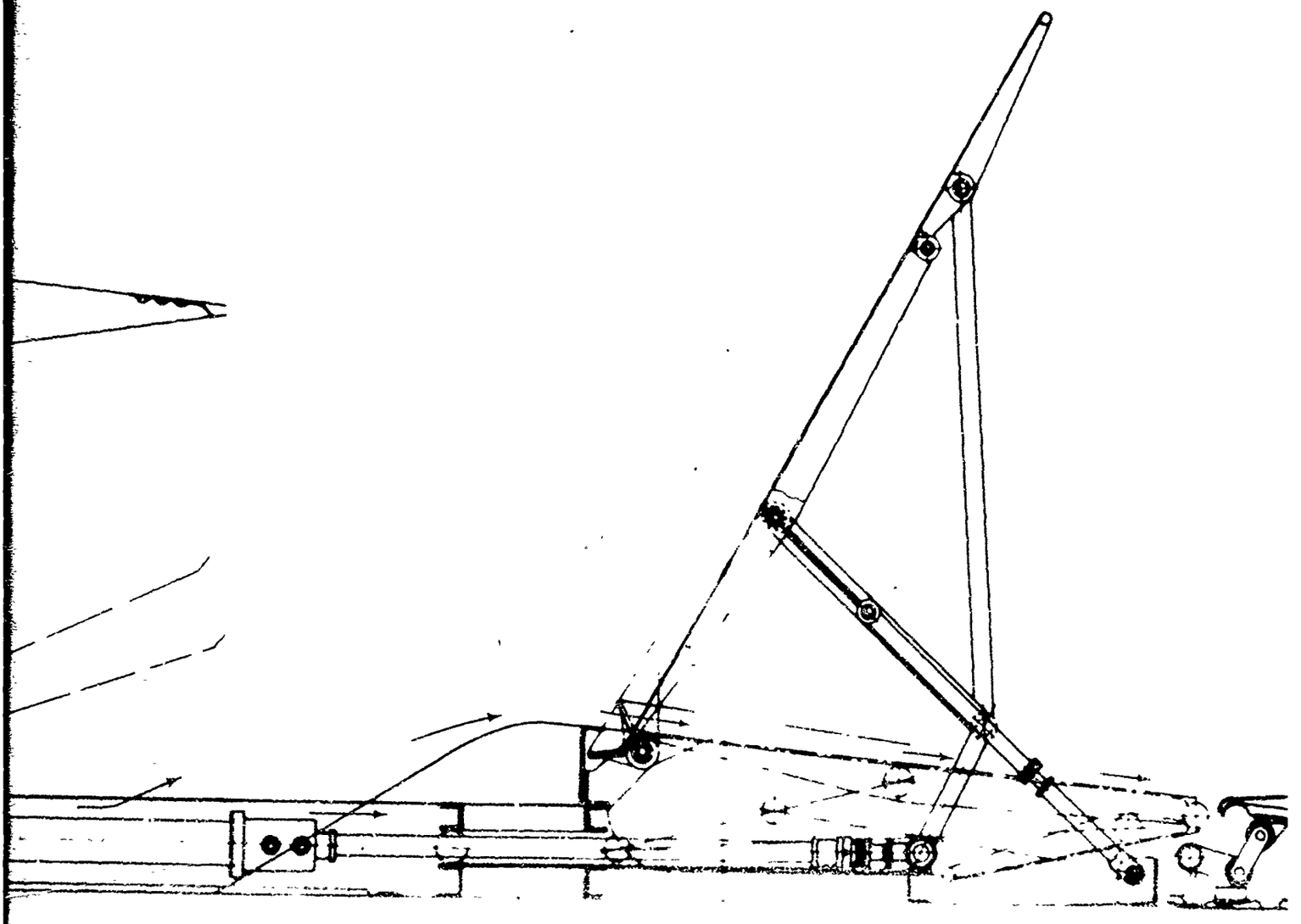




1

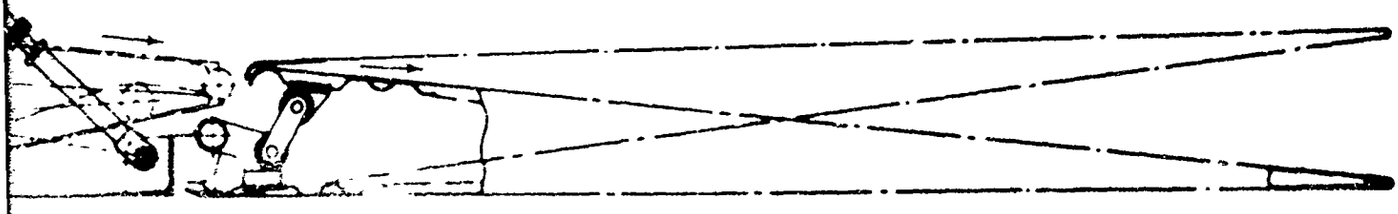
2



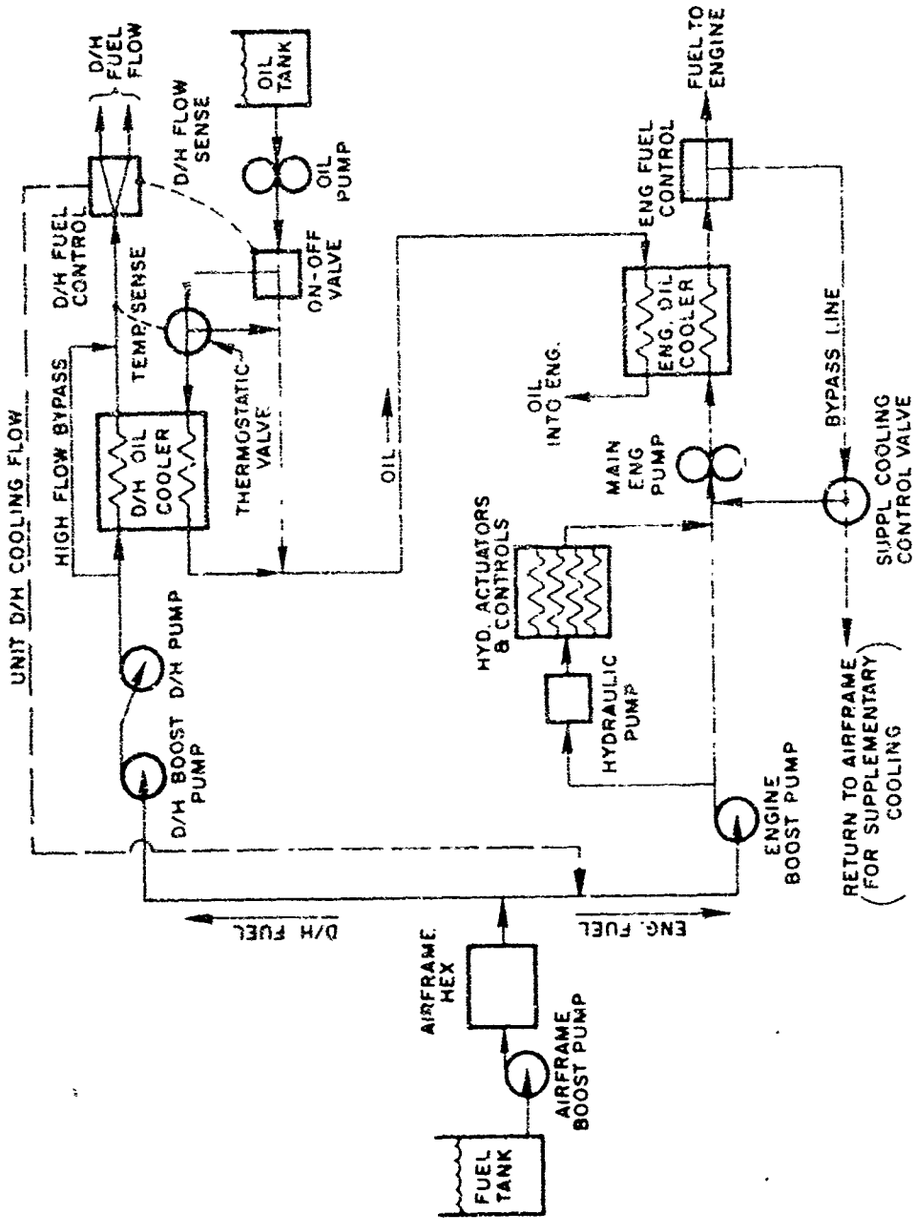


3

4

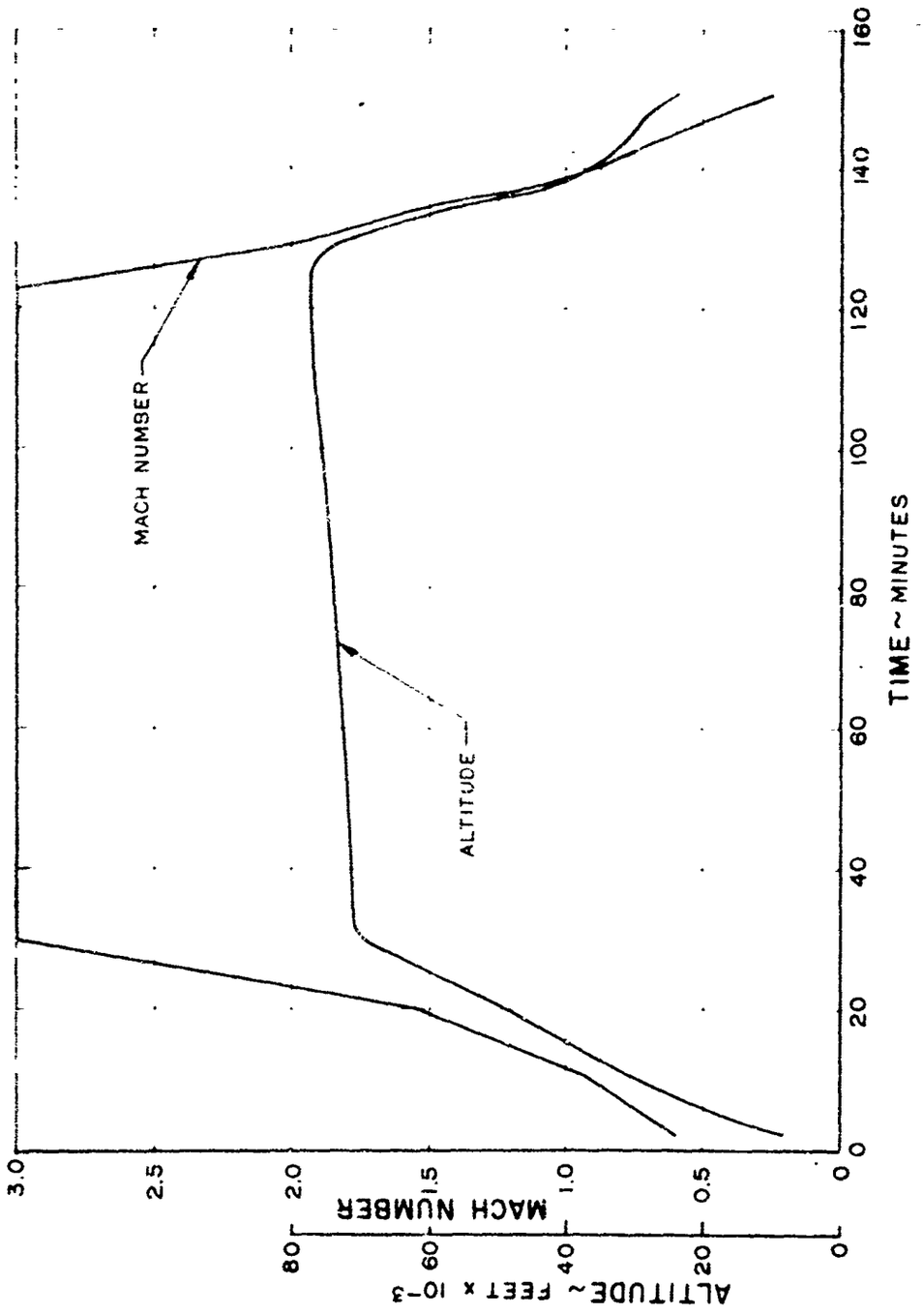


COOLING AND THRUST BALANCE AIR SYSTEM



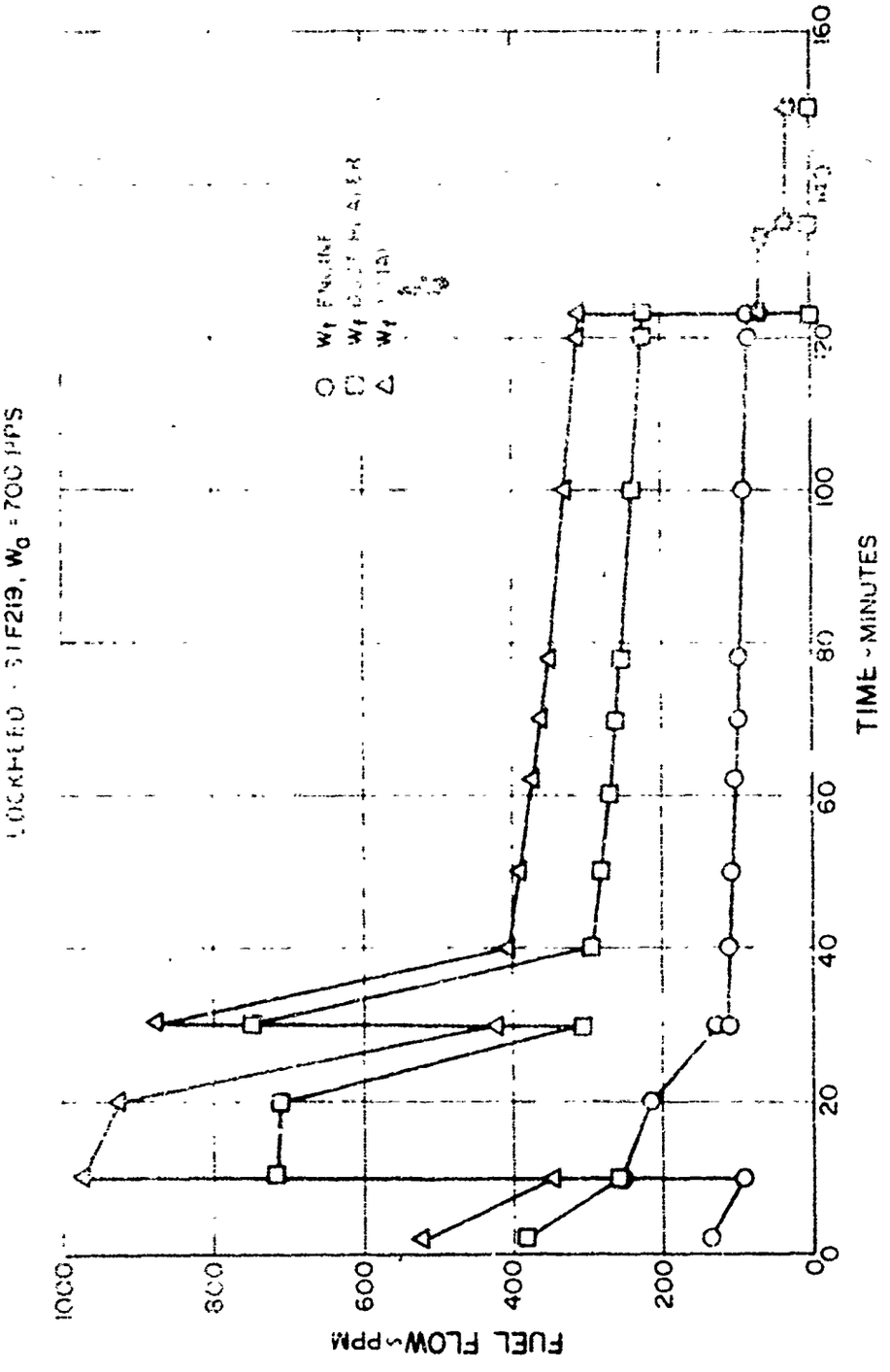
FUEL-OIL SYSTEM FOR STF 21Y ENGINE

Figure 2-64



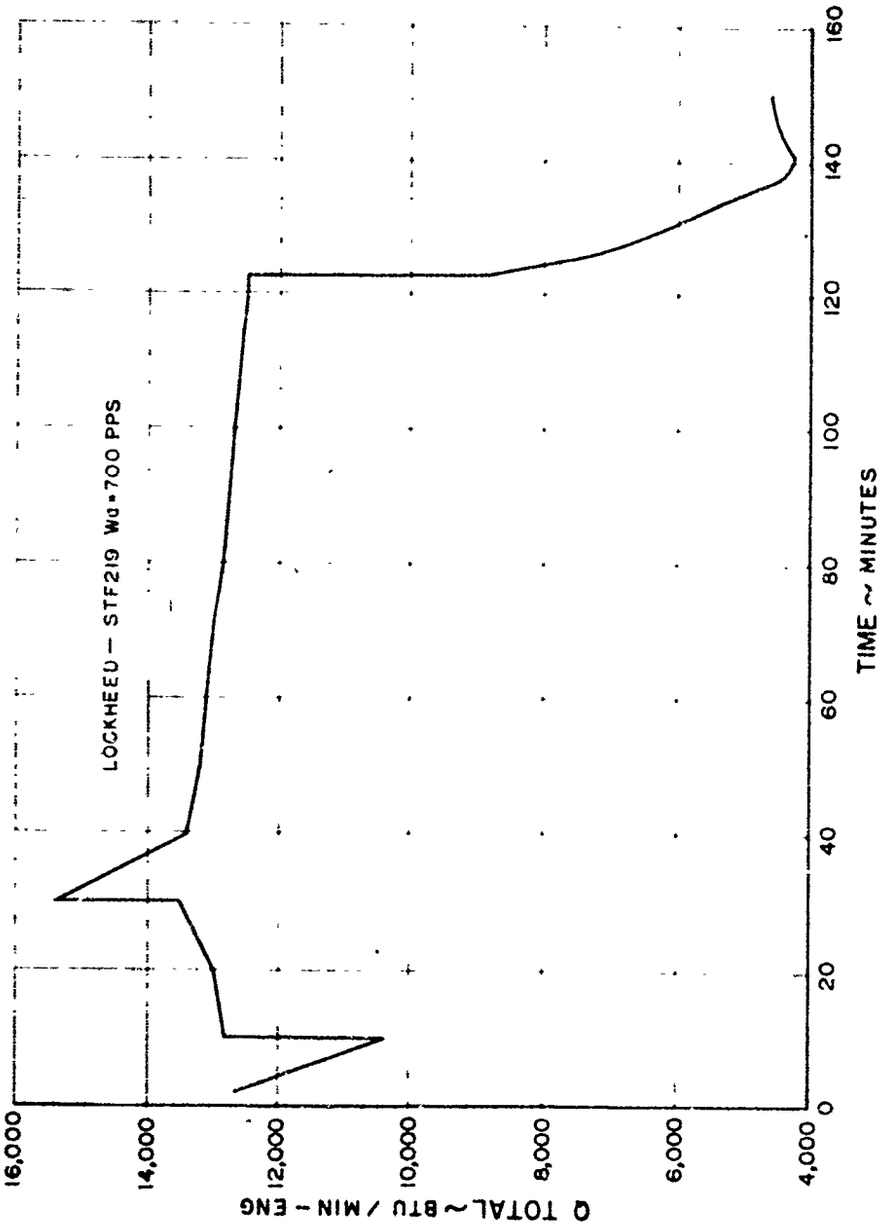
LOCKHEED MISSION PROFILE

Figure 2-65



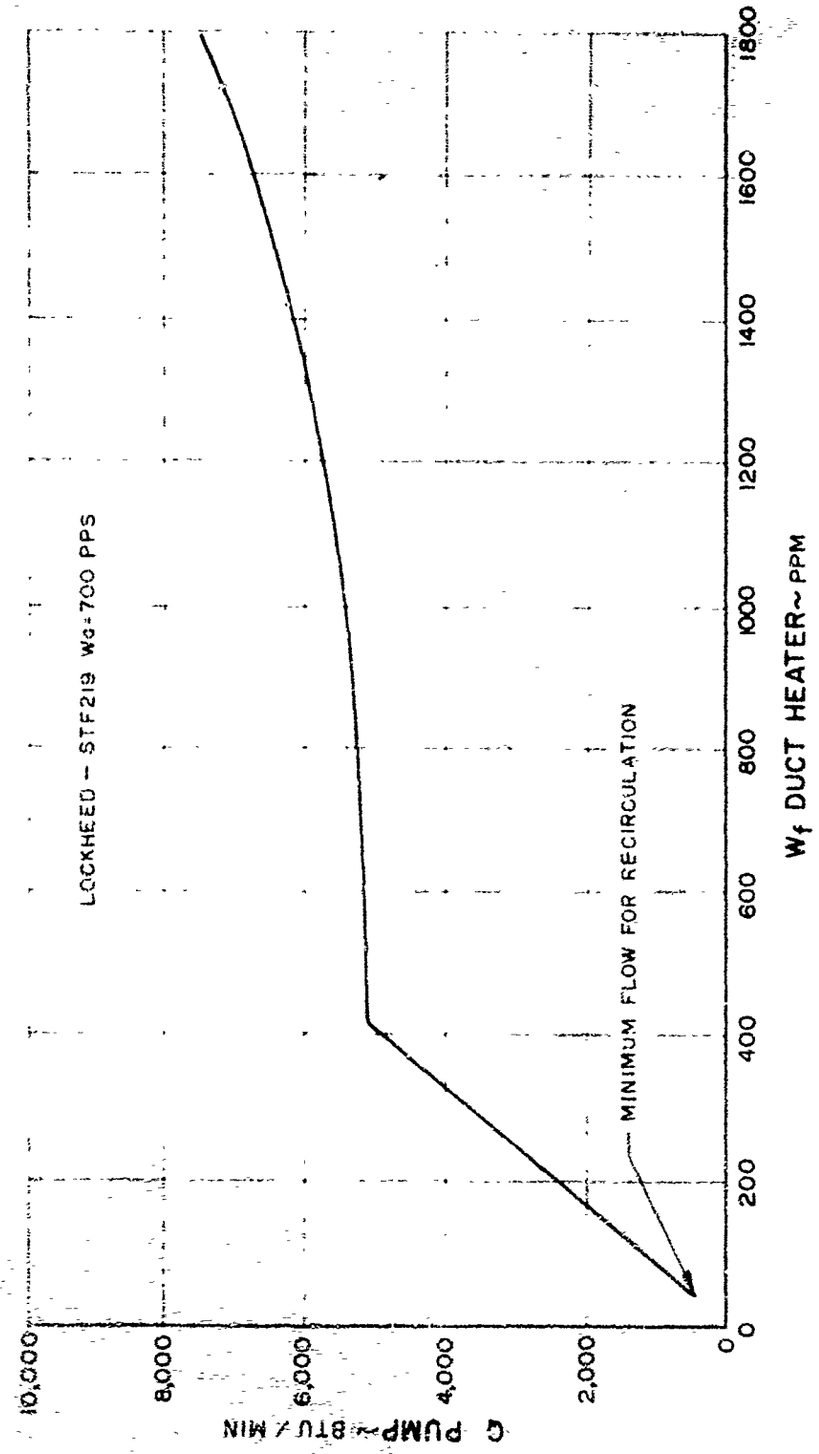
ENGINE, DUCT, AND TOTAL FUEL FLOW RATES FOR LOCKHEED MISSION

Figure 2-66



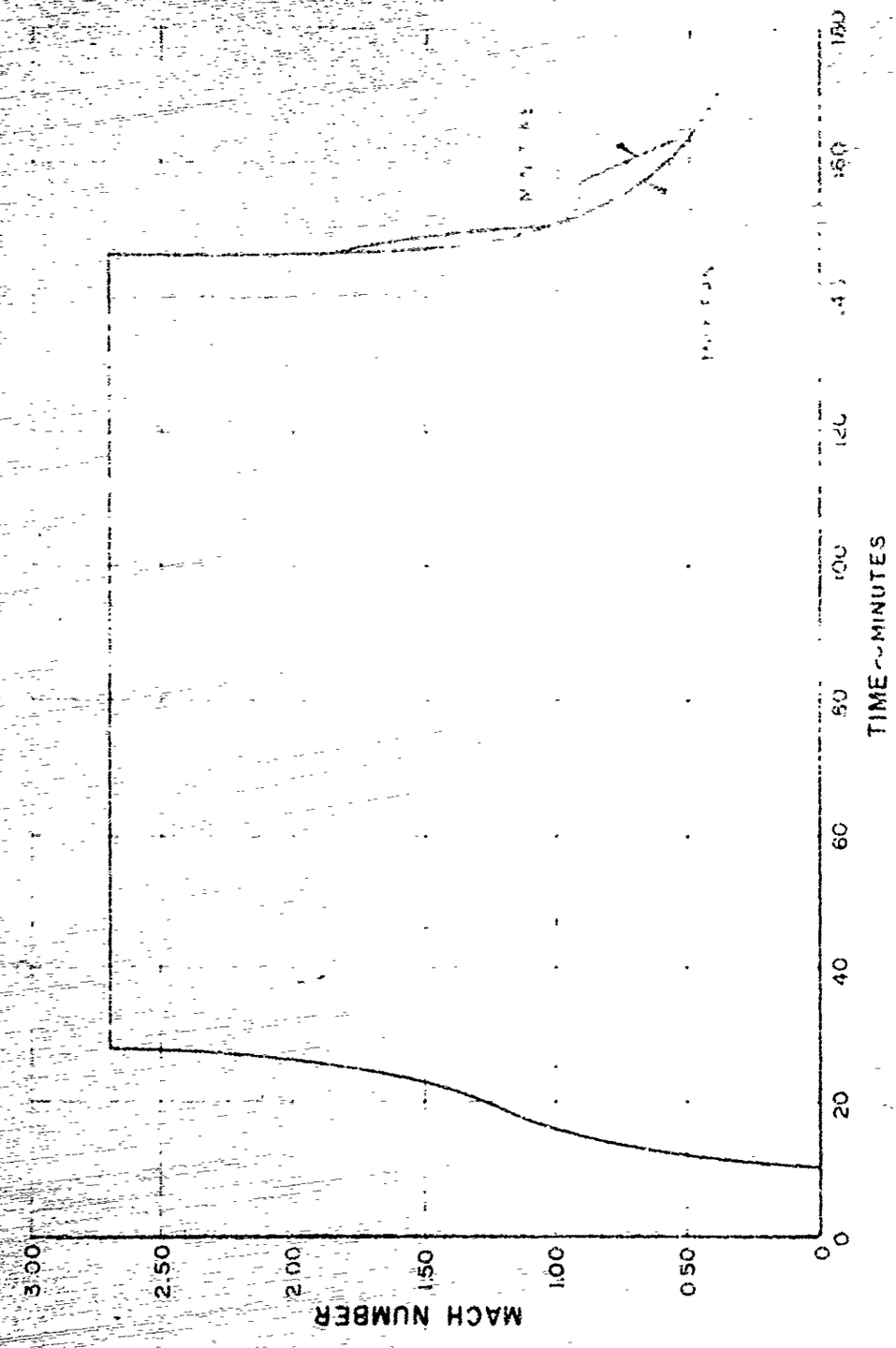
ESTIMATED TOTAL ENGINE SYSTEM HEAT REJECTION RATE
FOR LOCKHEED MISSION

Figure 2-67



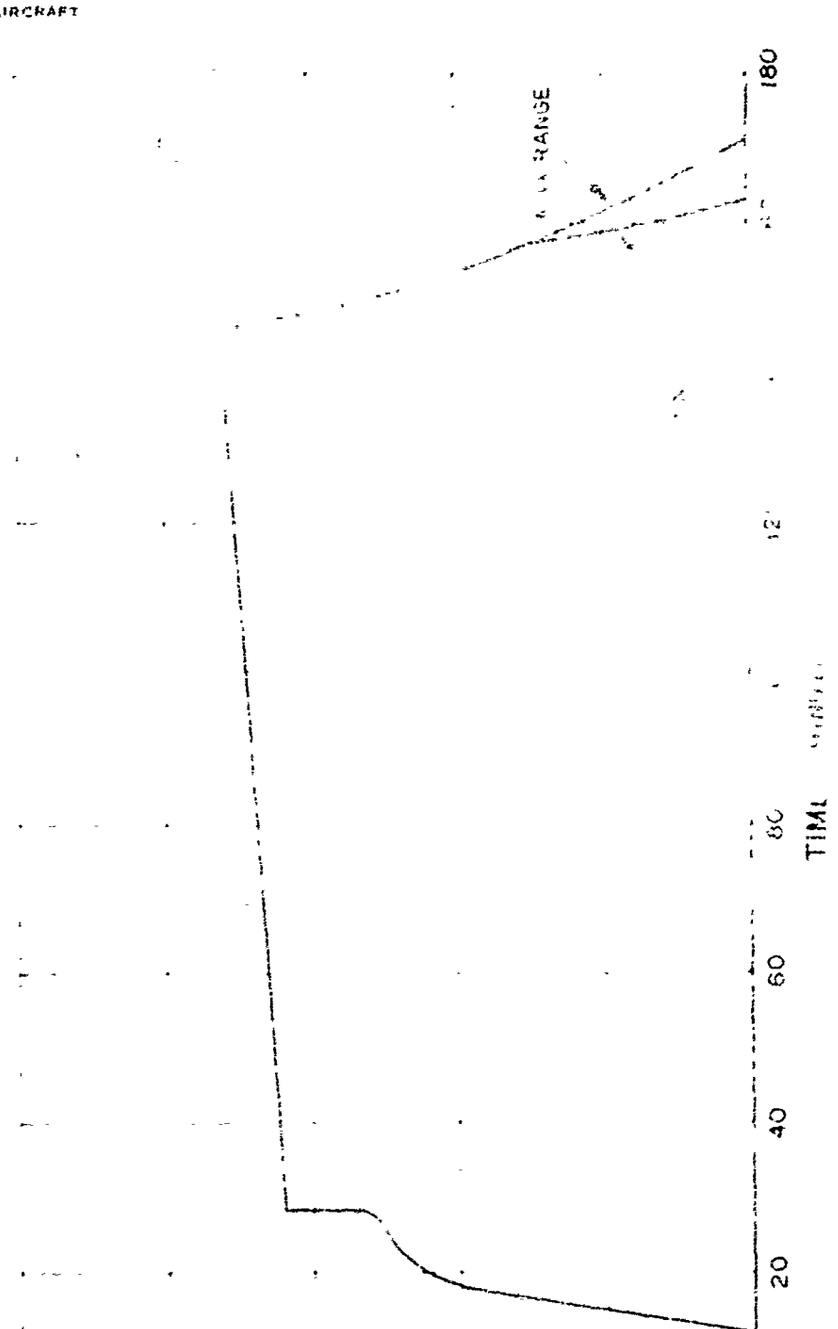
ESTIMATED DUCT HEATER FUEL PUMP ENERGY INPUT TO FUEL AS A FUNCTION OF DUCT HEATER FUEL FLOW FOR THE LOCKHEED MISSION

Figure 2-68



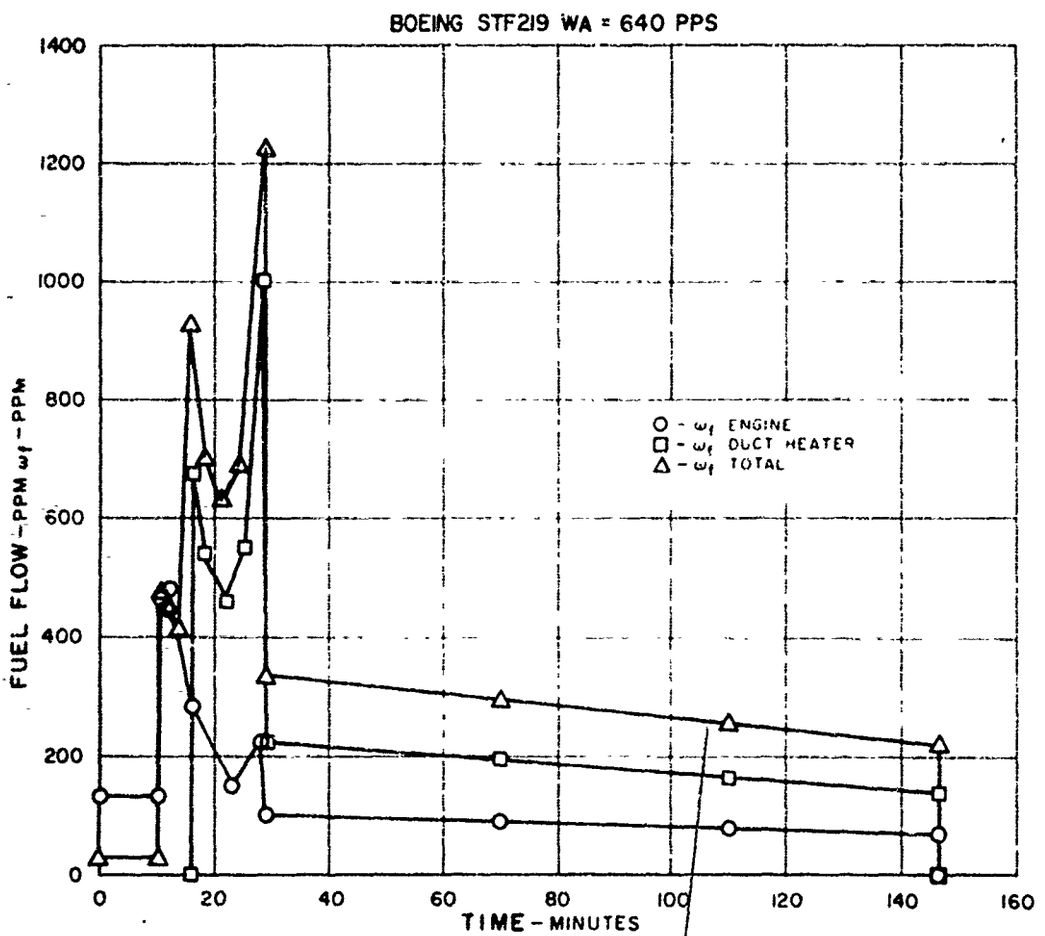
BOEING MACH NUMBER MISSION PROFILE

Figure 2-69



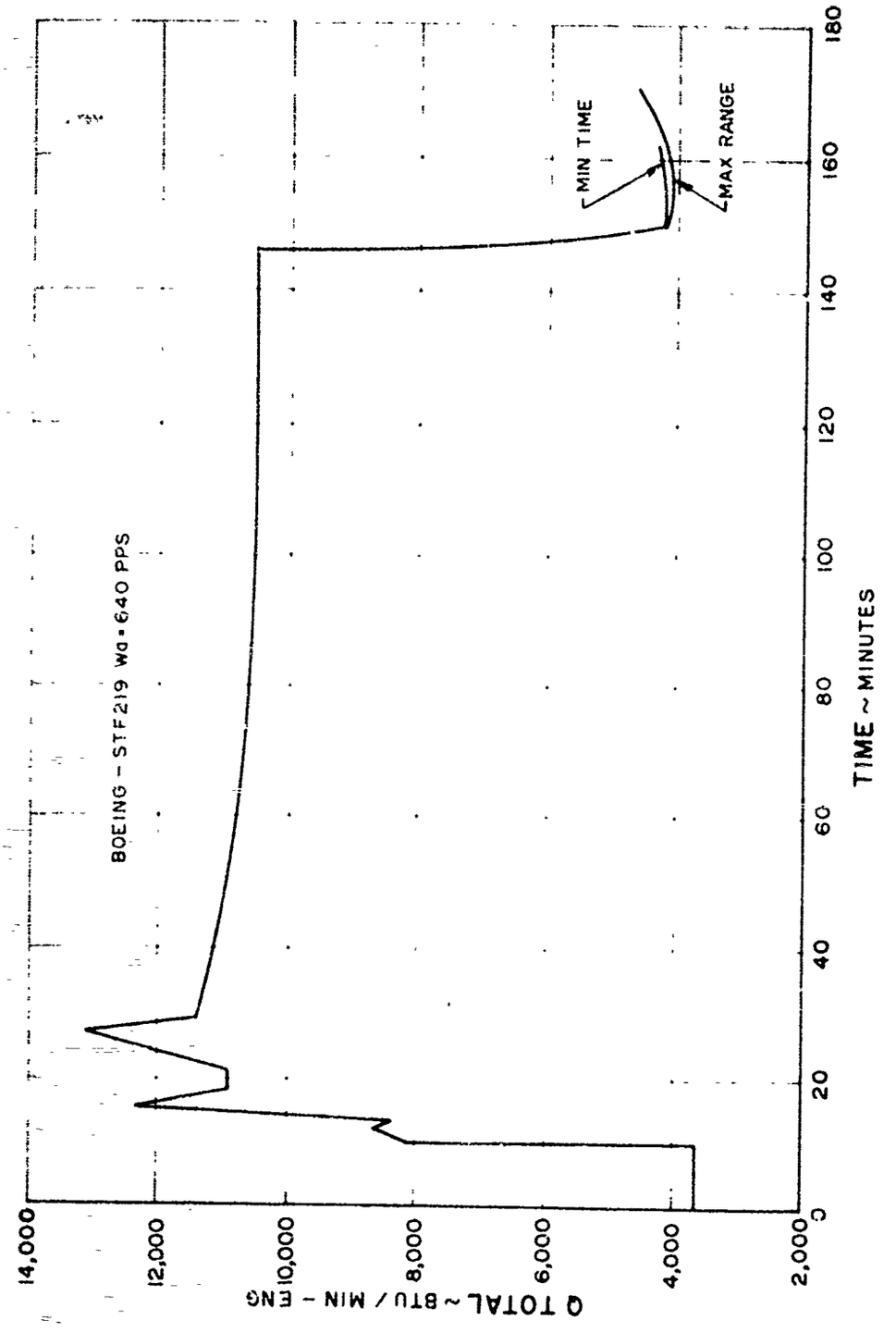
BOEING ALTITUDE MISSION PROFILE

Figure 2-70



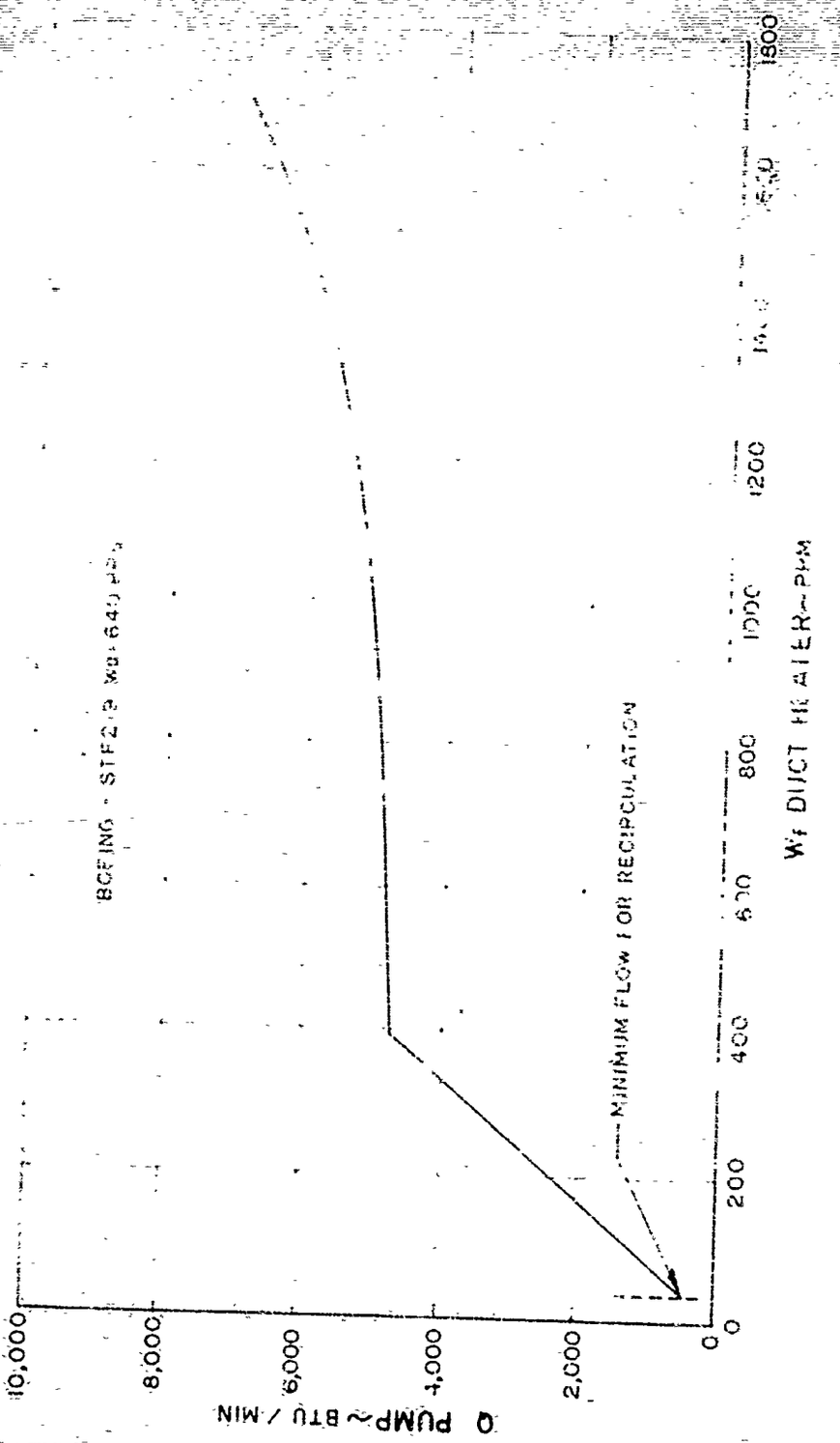
ENGINE, DUCT, AND TOTAL FUEL FLOW RATES FOR BOEING MISSION

Figure 2-71



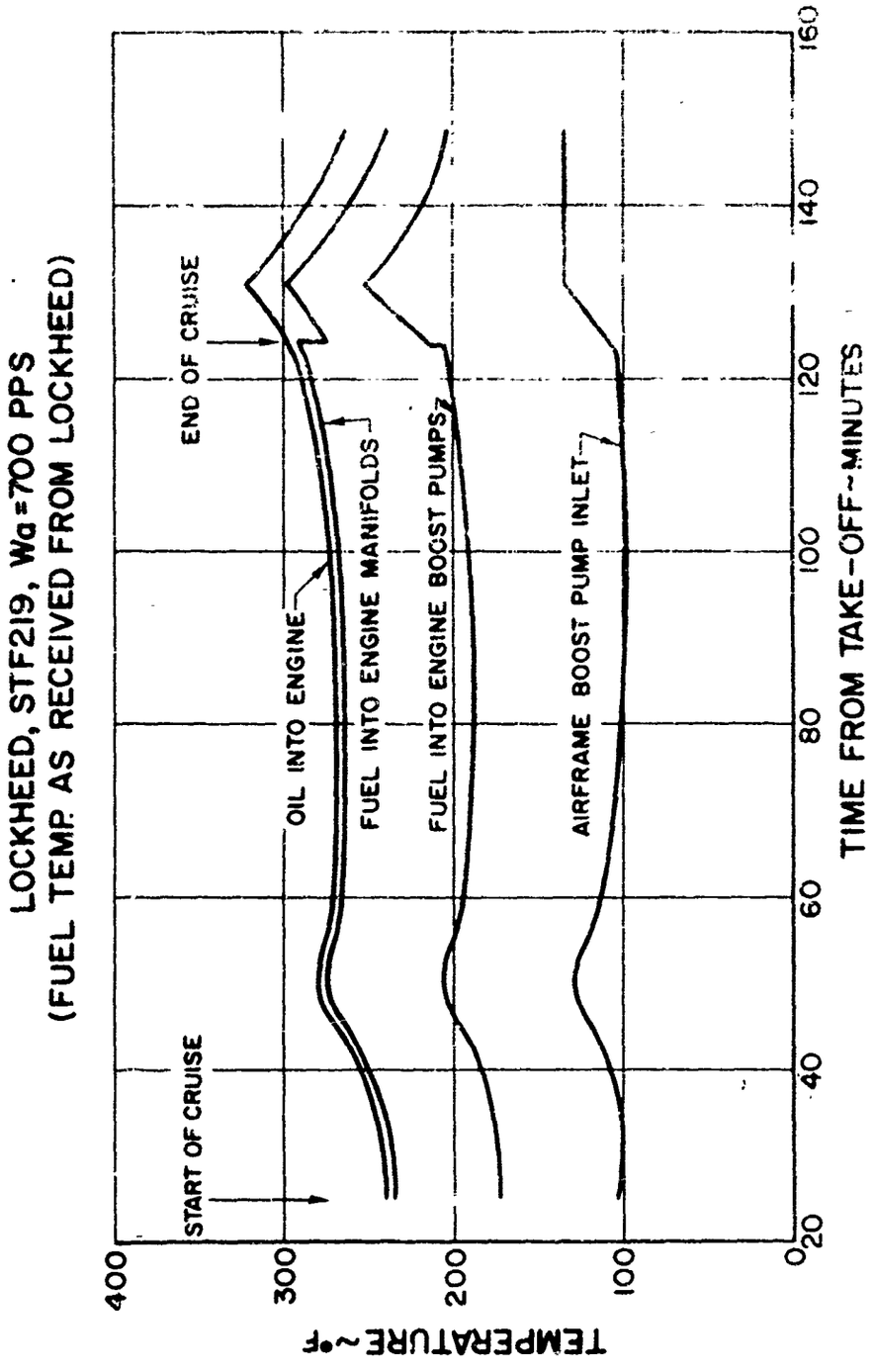
ESTIMATED TOTAL ENGINE SYSTEM HEAT REJECTION RATE
FOR BOEING MISSION

Figure 2-72



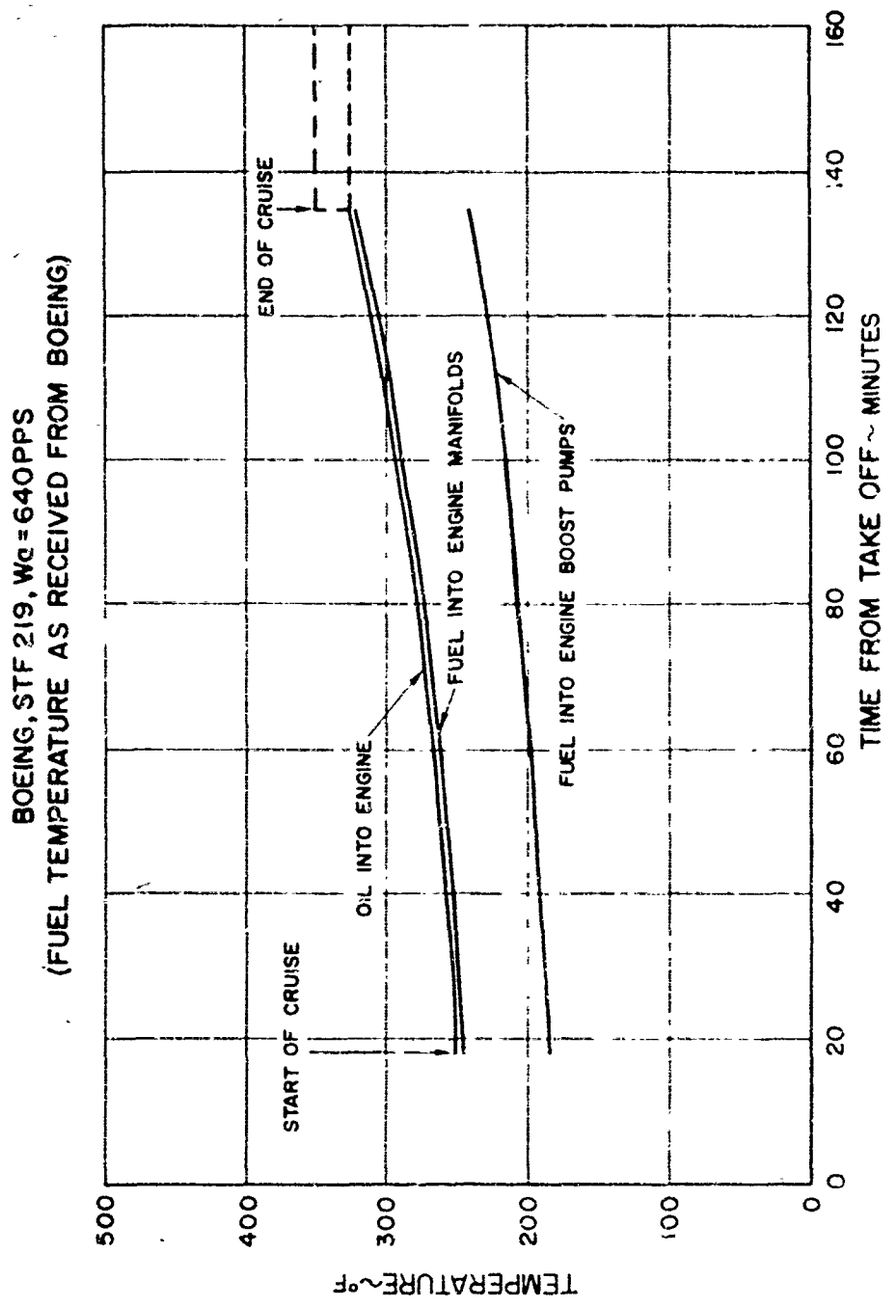
ESTIMATED DUCT HEATER FUEL PUMP ENERGY INPUT TO FUEL AS A FUNCTION OF DUCT HEATER FUEL FLOW FOR THE BOEING MISSION

Figure 2-73



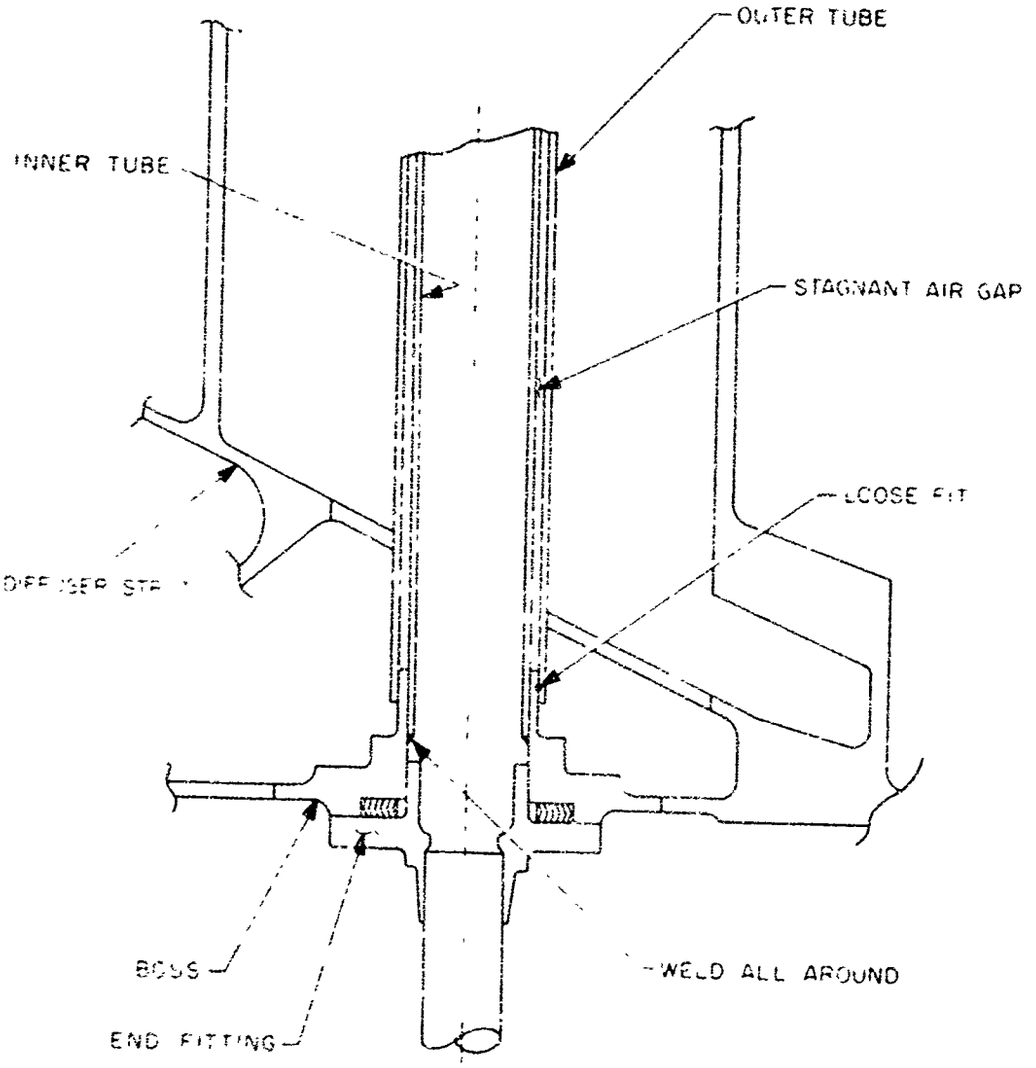
ESTIMATED FUEL AND OIL TEMPERATURES
FOR THE LOCKHEED MISSION
(CALCULATED BY LOCKHEED)

Figure 2-74



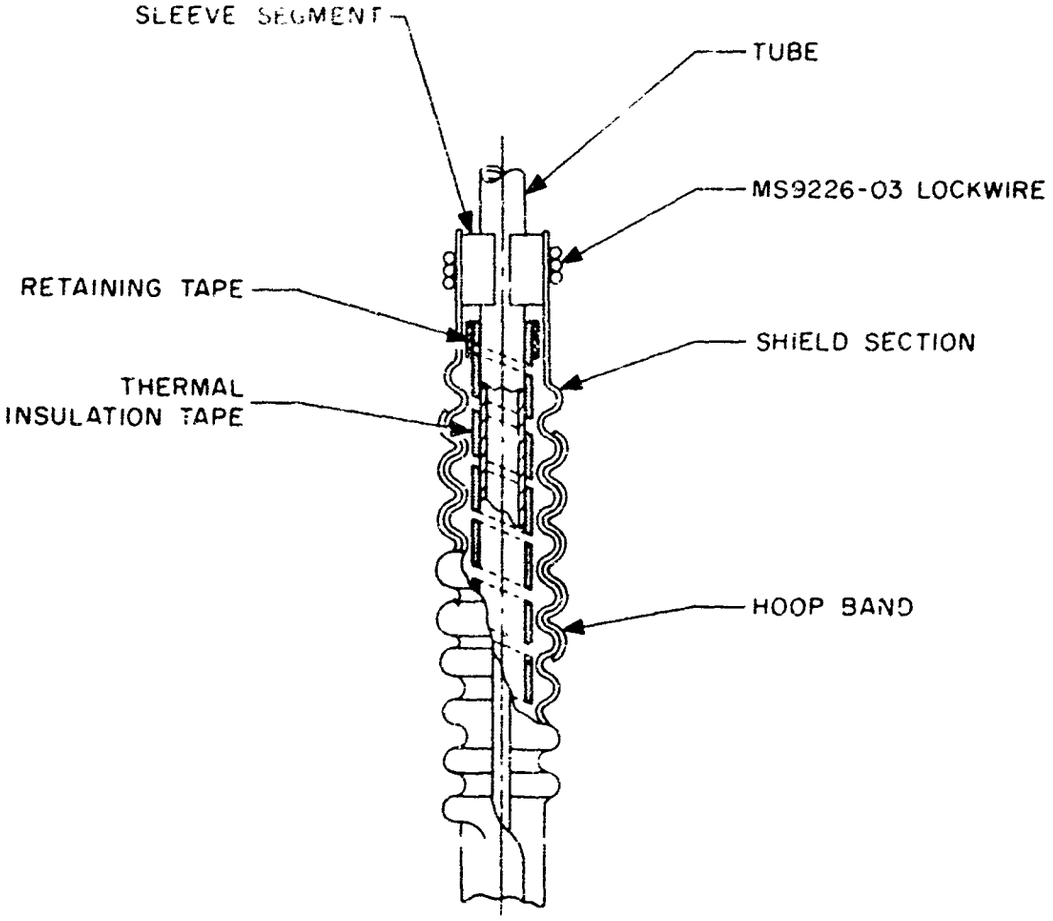
ESTIMATED FUEL AND OIL TEMPERATURES
FOR THE BOEING MISSION
(FUEL TEMPERATURES CALCULATED BY BOEING)

Figure 2-75



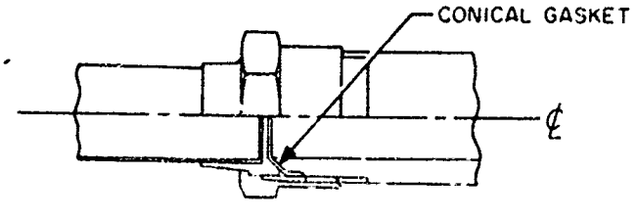
TYPICAL DOUBLE-WALL HEAT SHIELDING STRUCTURE

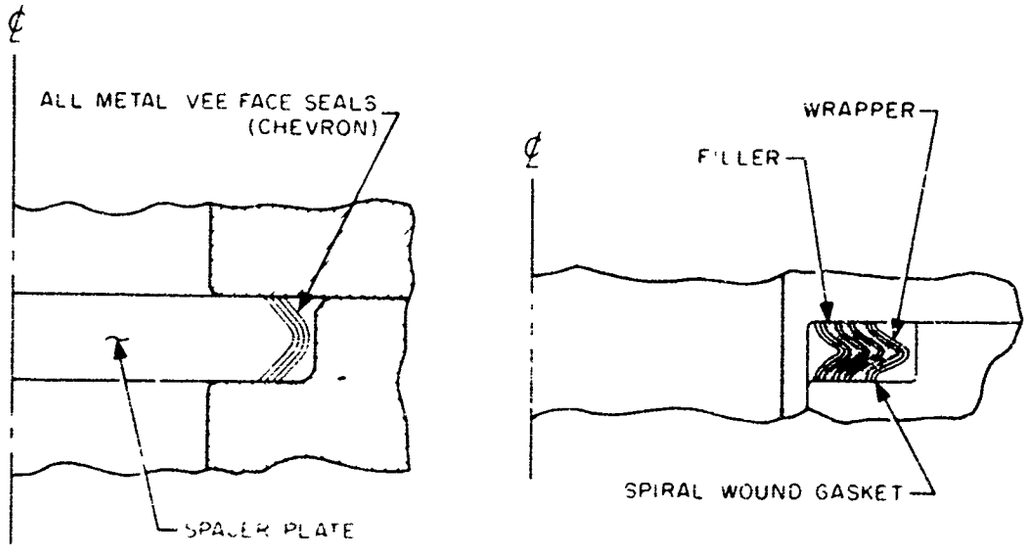
Figure 2-7

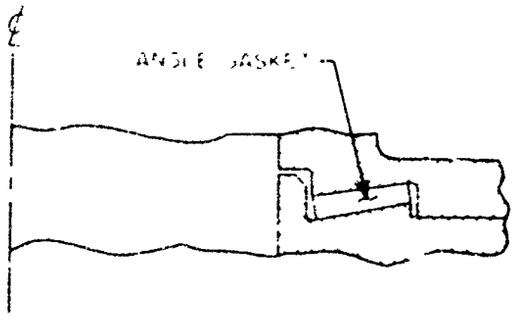


TYPICAL METAL FOIL HEAT SHIELDING STRUCTURE

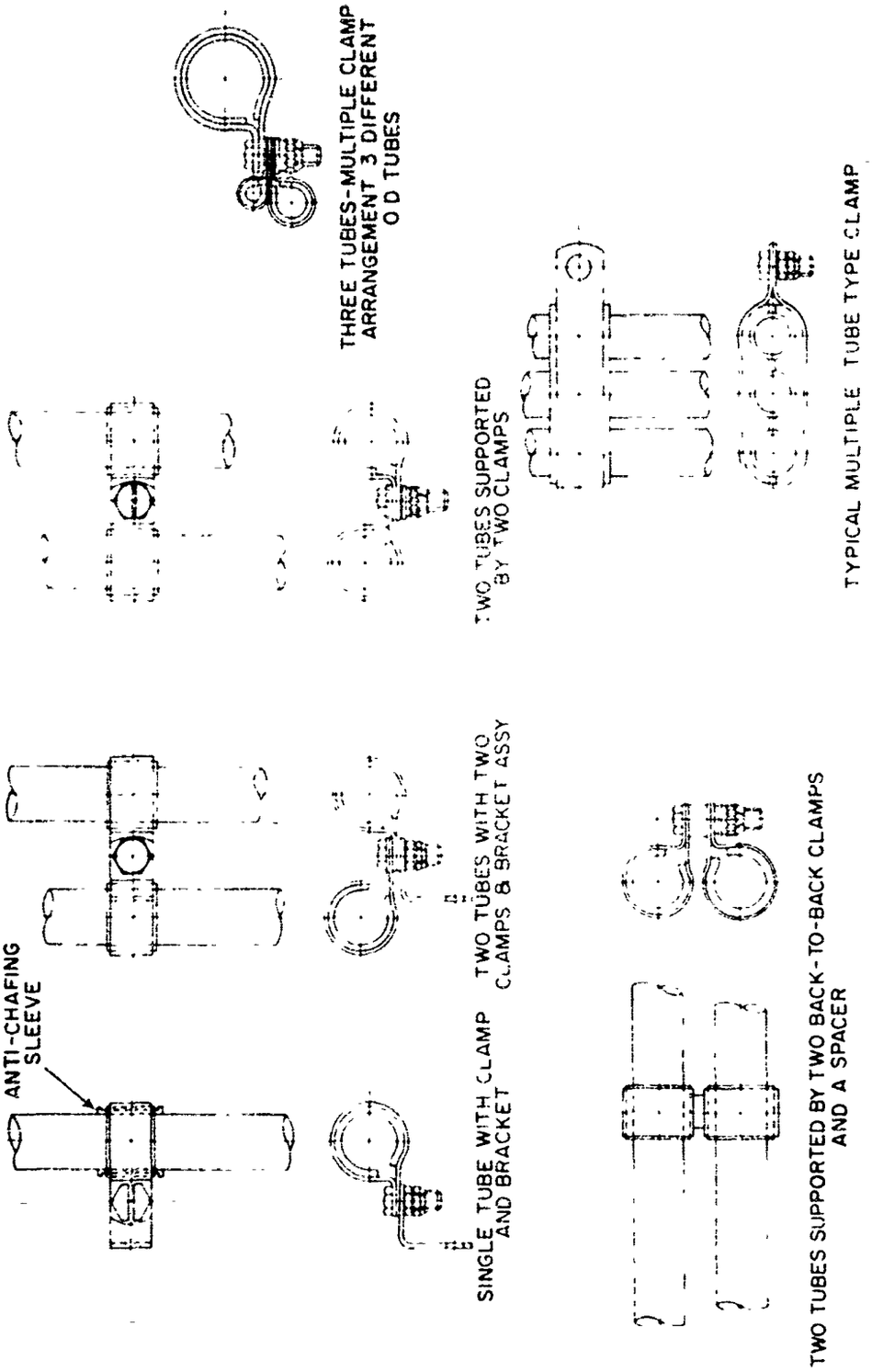
Figure 2-77





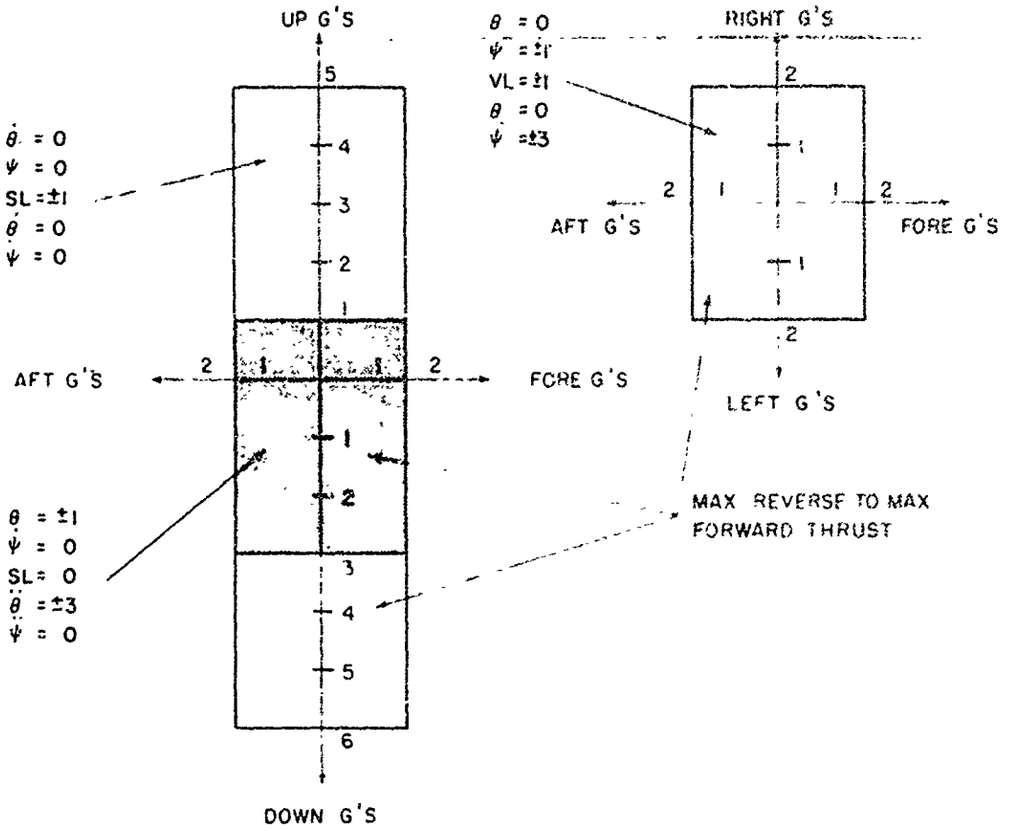


TYPICAL SEALS FOR STF 219 ENGINE



TYPICAL TUBE SUPPORT AND CLAMPING CONFIGURATIONS

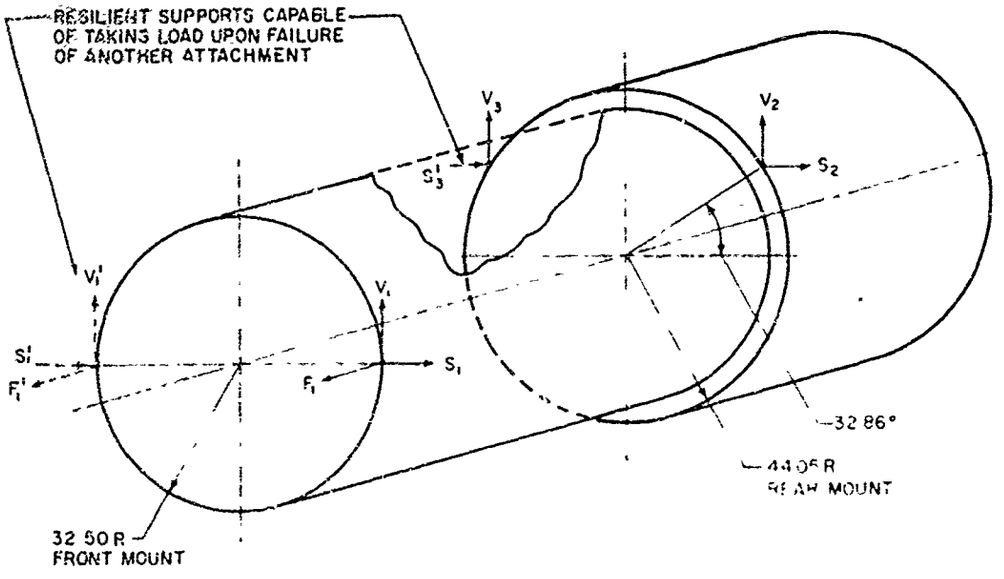
Figure 2-79



$\dot{\theta}$ AND $\ddot{\theta}$ ARE PITCHING VELOCITY AND ACCELERATION
$\dot{\psi}$ AND $\ddot{\psi}$ ARE YAWING VELOCITY AND ACCELERATION
SL = SIDE LOAD
VL = VERTICAL LOAD
G LOADS REFER TO INSTALLED ENGINE WEIGHT, WHICH INCLUDES ENGINE SUPPORTED EJECTOR AND INLET

MANEUVER LOADS FOR STF 219 ENGINE MOUNTS

Figure 2-80



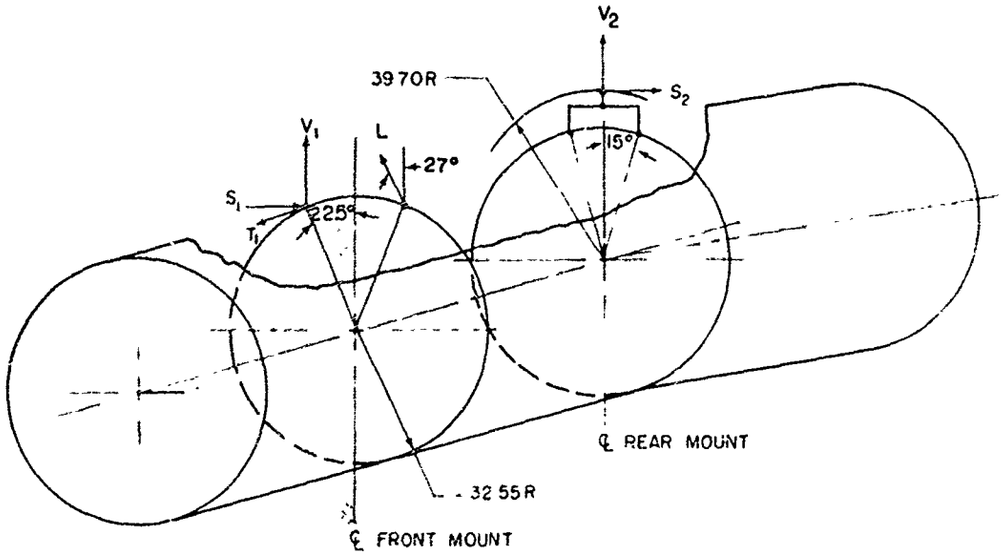
DISTANCE BETWEEN MOUNT PLANES ..... 76.6 IN
ENGINE WEIGHT ..... 10,225 LB
ENGINE C.G. FROM FRONT MOUNT ..... 70.00 IN AFT

THE ALLOWABLE LIMIT LOADS FOR EACH MOUNT ATTACHMENT POINT MUST SATISFY ALL EQUATIONS BELOW:

$\|V_1\| \leq 22{,}100$ LB	$\|V_1'\| \leq 22{,}500$ LB
$\|S_1\| \leq 29{,}700$	$\|S_1'\| \leq 19{,}800$
$\|F_1\| \leq 68{,}900$	$\|F_1'\| \leq 46{,}000$
$\|V_2\| \leq 27{,}200$	$\|S_1'\| \leq 19{,}800$
$\|S_2\| \leq 33{,}000$	
$\|V_3\| \leq 27{,}300$	

MAXIMUM FLIGHT LOADS FOR LOCKHEED ENGINE

Figure 2-81



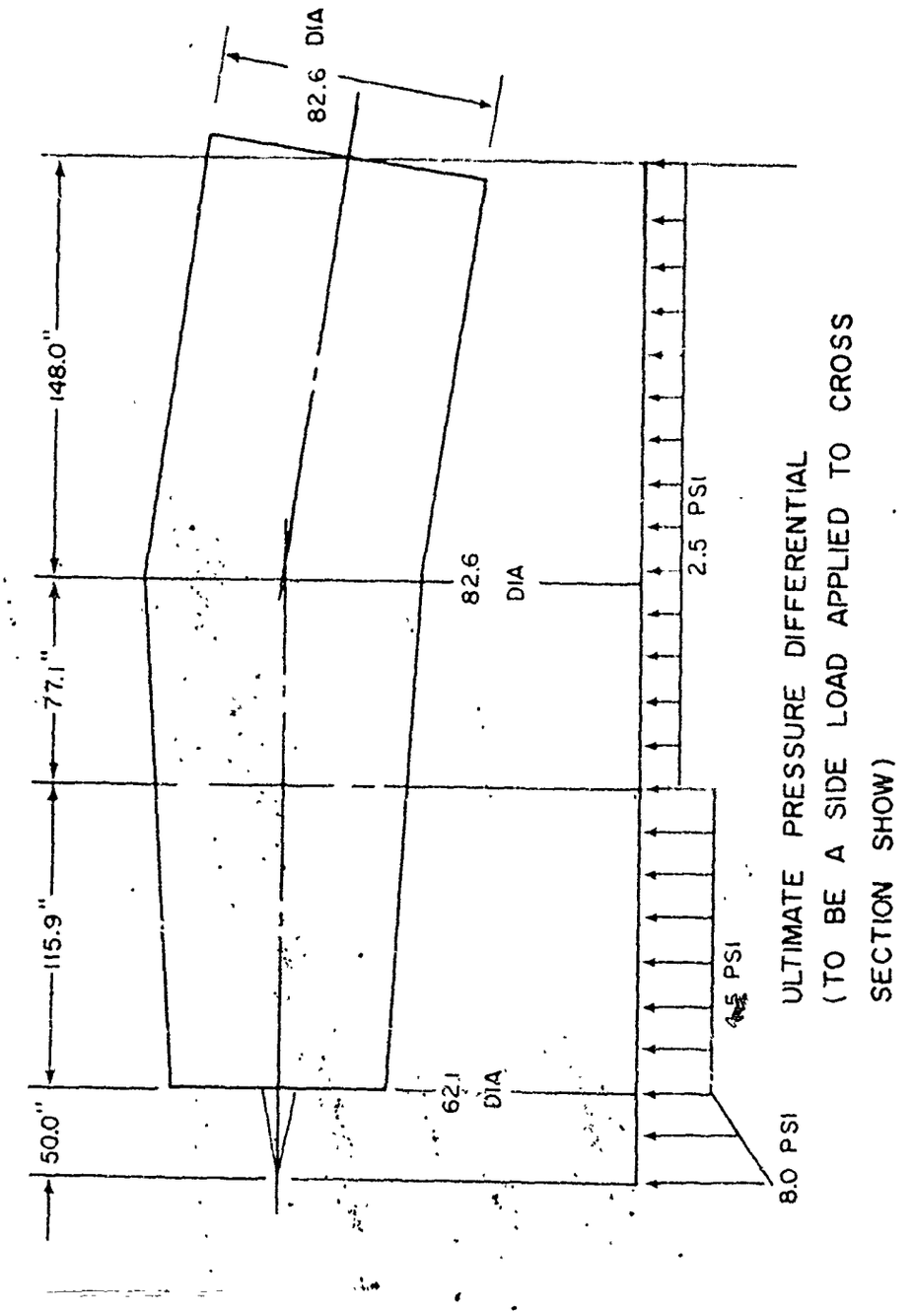
DISTANCE BETWEEN MOUNT PLANES _____ 83.60 IN.
ENGINE WEIGHT (INCLUDING INLET) _____ 11,170 LB
ENGINE C.G. FROM FRONT MOUNT _____ 70.00 IN AFT

THE ALLOWABLE LIMIT LOADS FOR EACH MOUNT ATTACHMENT POINT MUST SATISFY ALL EQUATIONS BELOW:

$$|V_1| \leq 80{,}000 \text{ LB}$$
$$|S_1| \leq 76{,}300$$
$$|T_1| \leq 75{,}000$$
$$|V_2| \leq 76{,}000$$
$$|S_2| \leq 15{,}400$$
$$|L| \leq 82{,}500$$

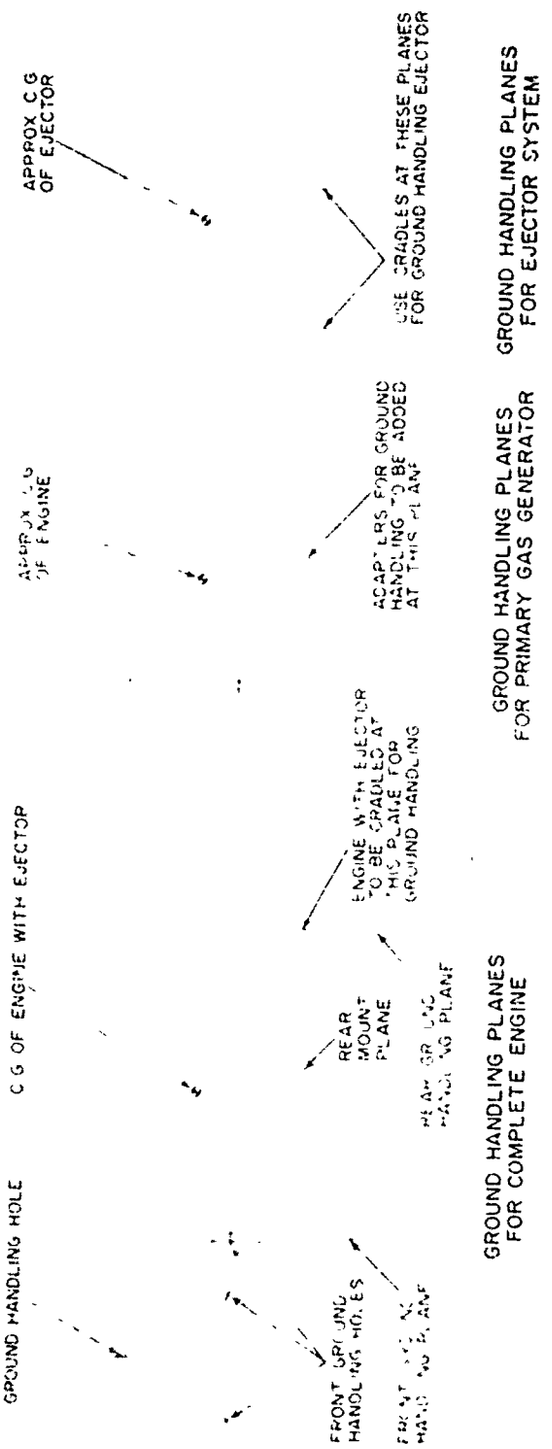
MAXIMUM FLIGHT LOADS FOR BOEING ENGINE

Figure 2-82



ULTIMATE LATERAL EXTERNAL GUST LOADS
FOR BOEING AIRCRAFT

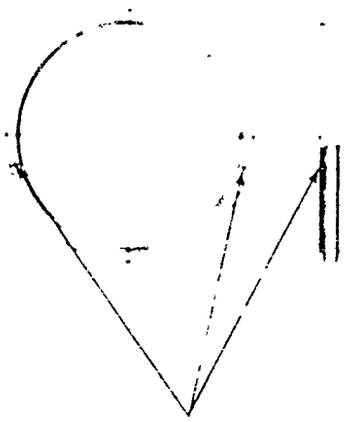
Figure 2-83



ENGINE GROUND HANDLING PLANES (LOCKHEED)

Figure 2-81

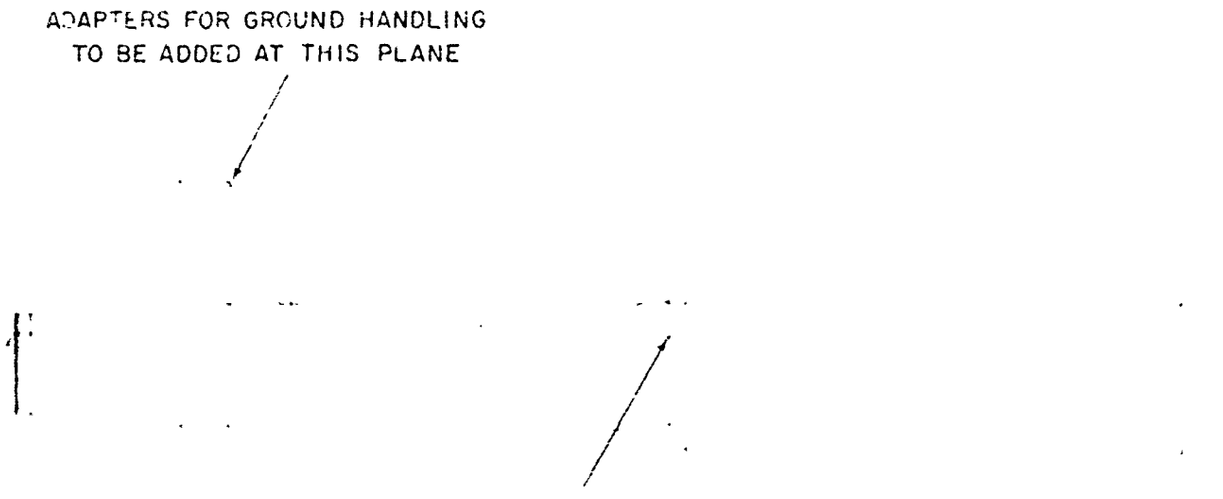
REMOVE THIS AIR DUCT
SECTION FOR DETACHING
EJECTOR SYSTEM



FRONT GROUND HANDLING HOLES

GROUND HANDLING PLANES FOR COMPLETE ENGINE

GROUN A

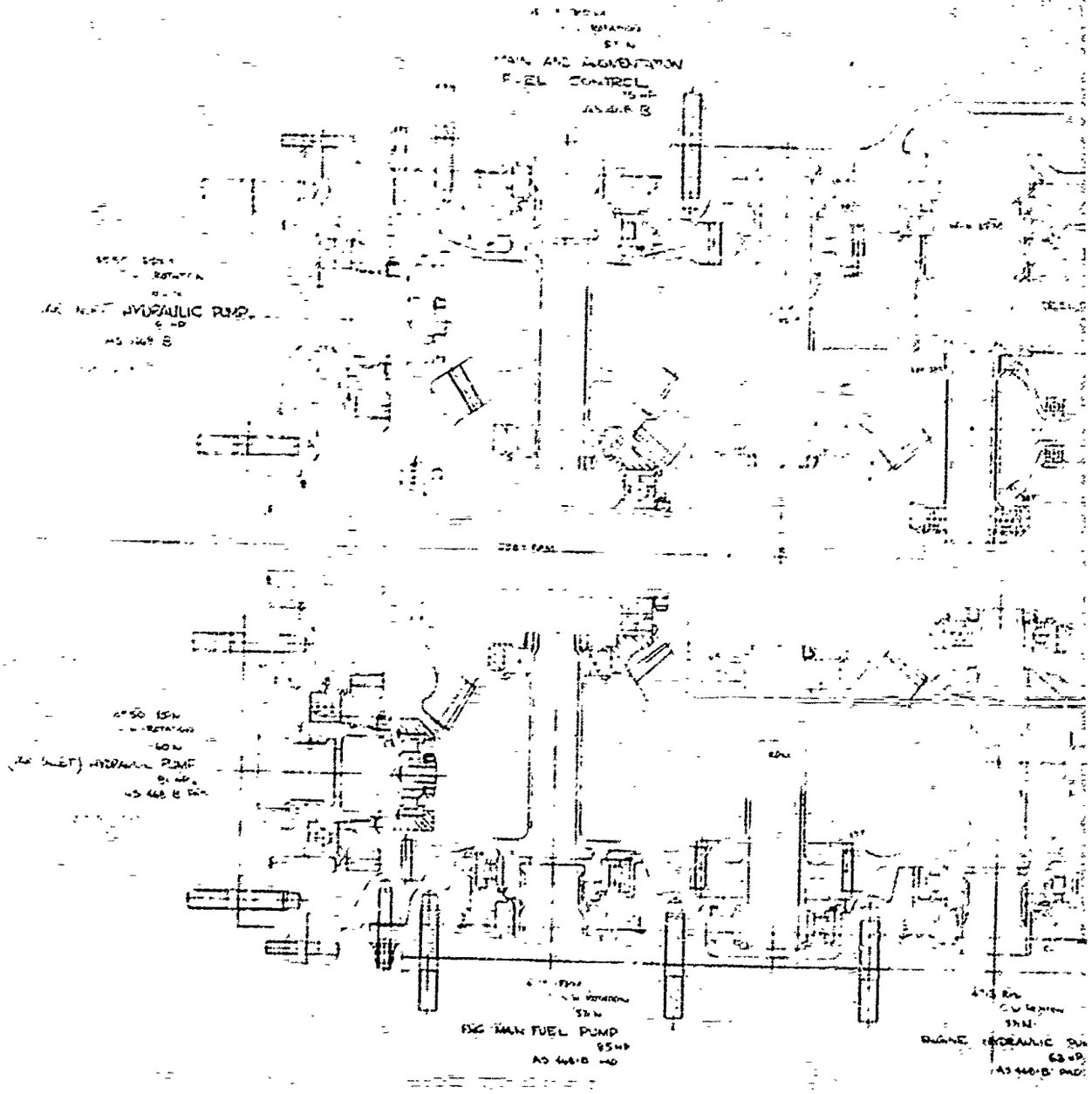


GROUND HANDLING PLANES FOR EJECTOR SYSTEM

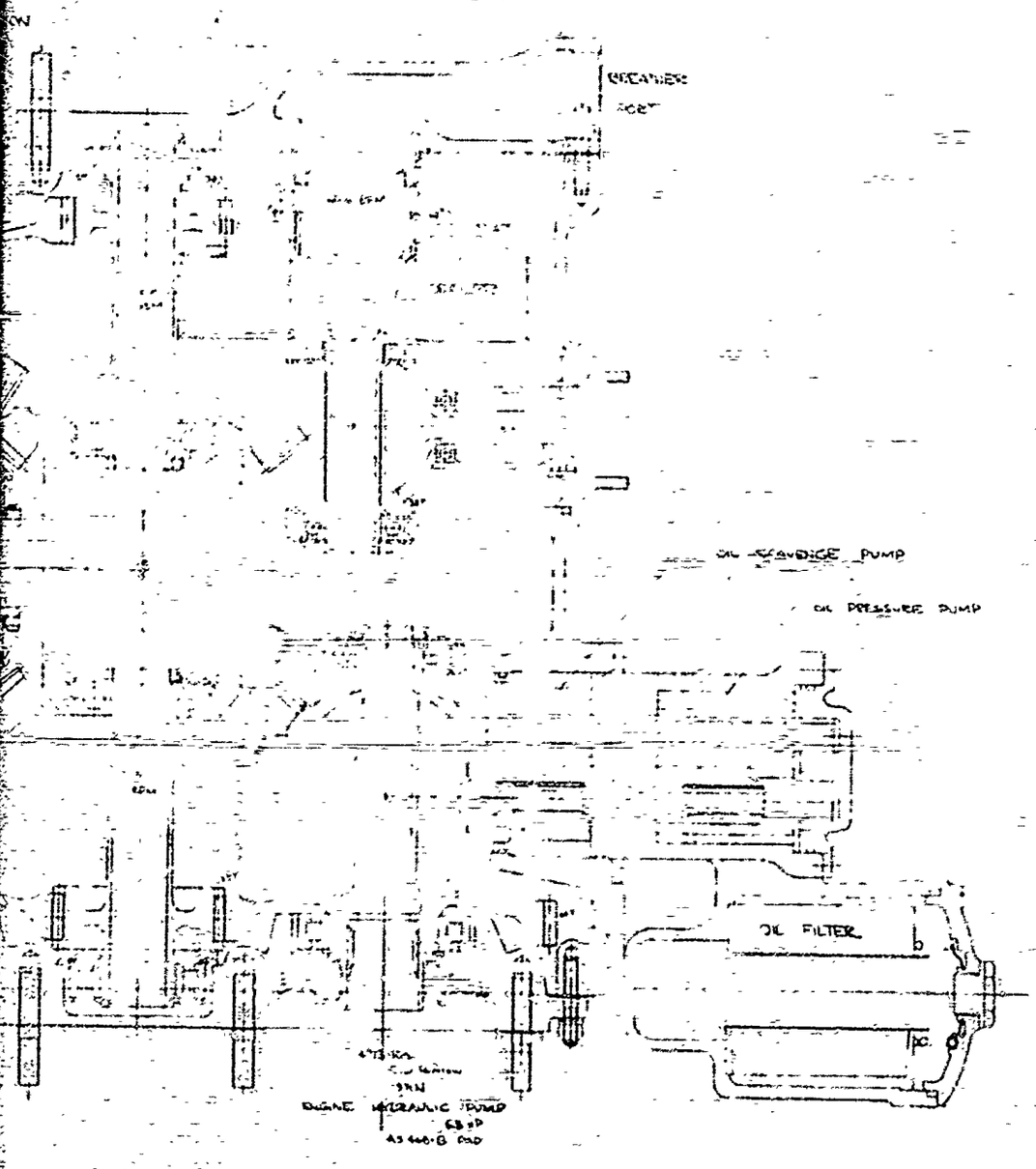
GROUND HANDLING PLANES FOR PRIMARY GAS GENERATOR

ENGINE GROUND HANDLING PLANES (BOEING)

Figure 2-85

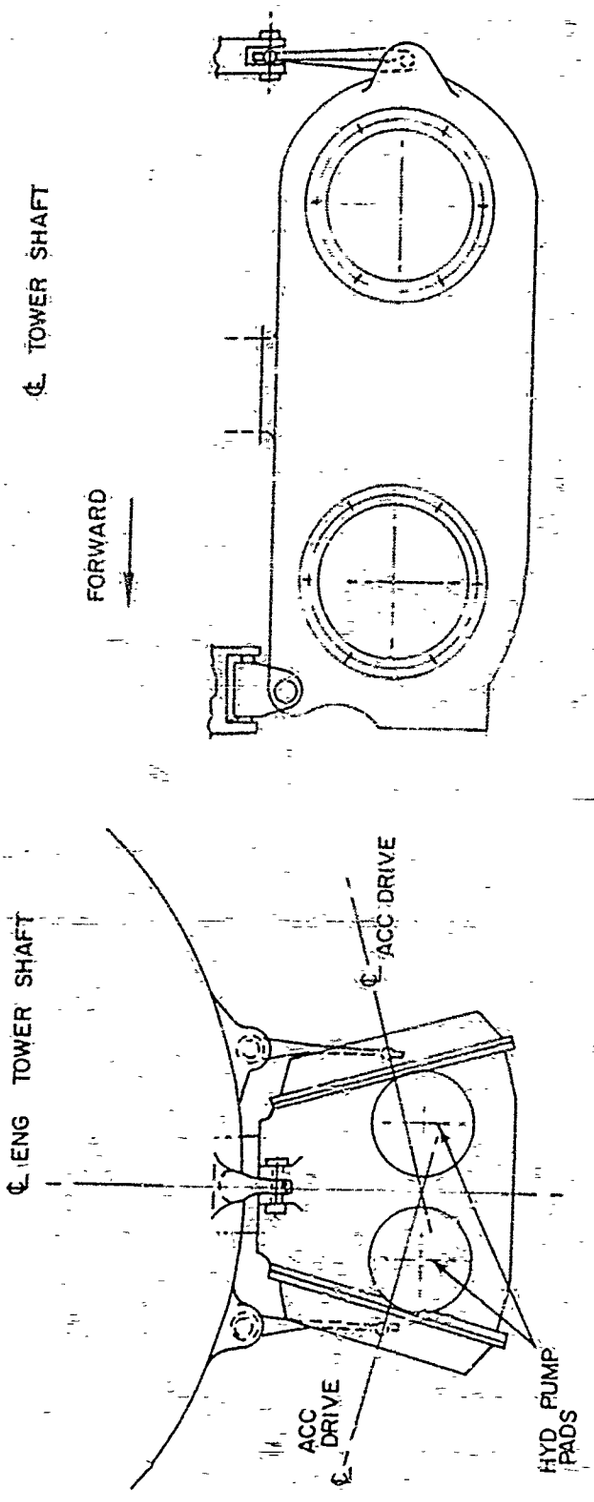


CROSS-SECTIO



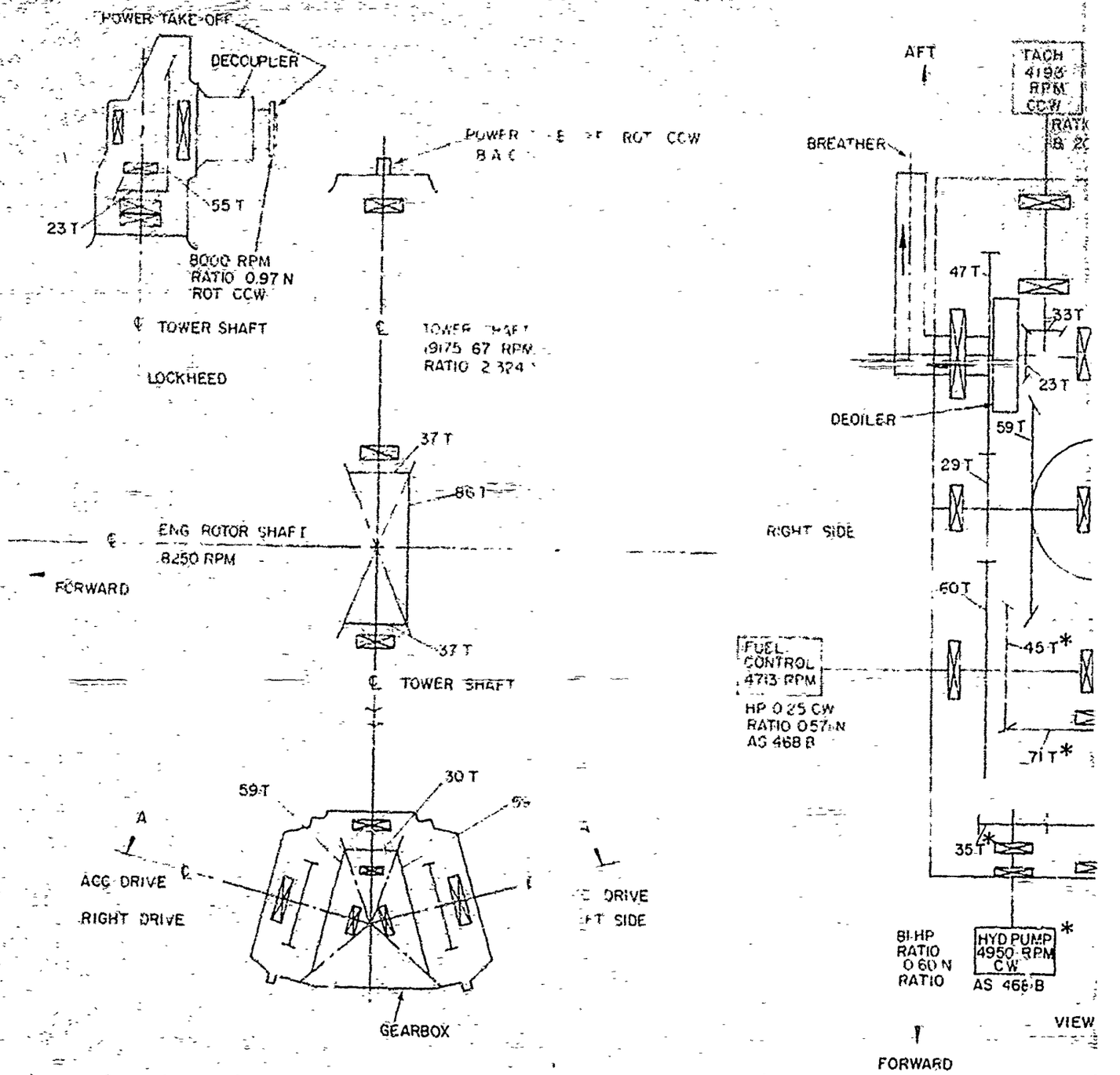
CROSS-SECTION OF ACCESSORY DRIVE GEARBOX

Figure 2-86



MOUNTING SYSTEM FOR GEARBOX

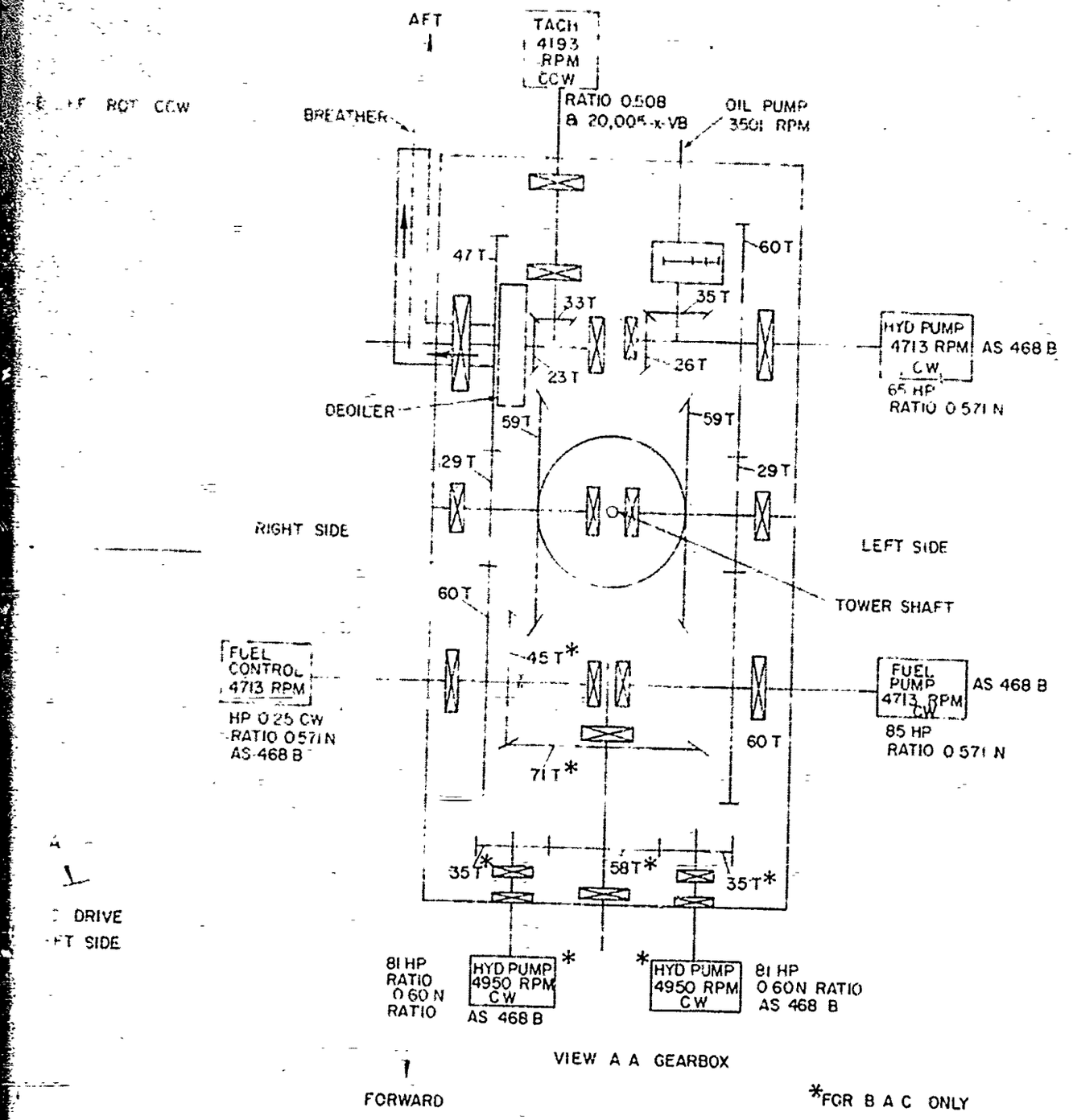
Figure 2-87



SCHEMATIC DIAGR

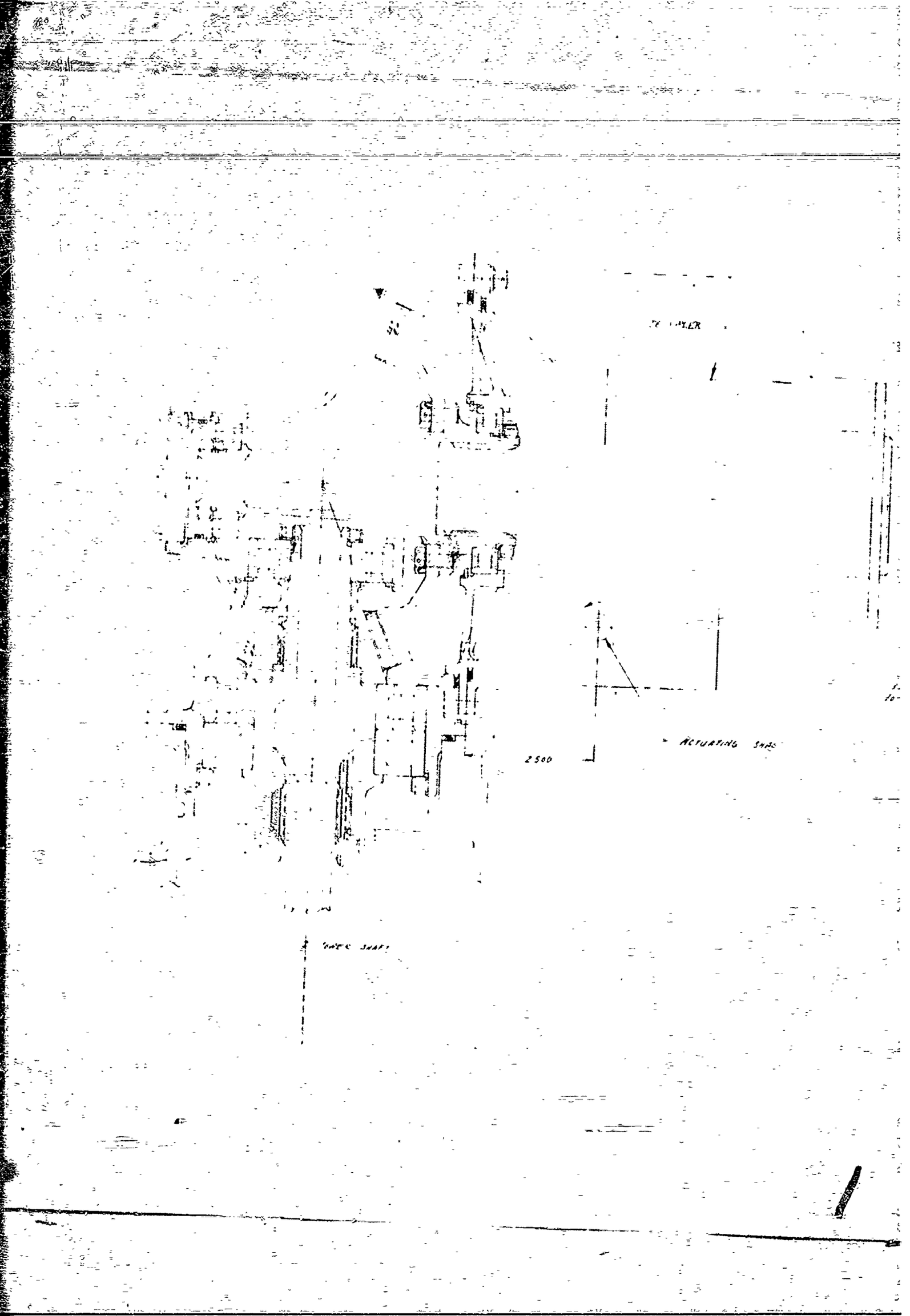
Figure

CONFI



SCHEMATIC DIAGRAM OF GEARBOX

Figure 2-88

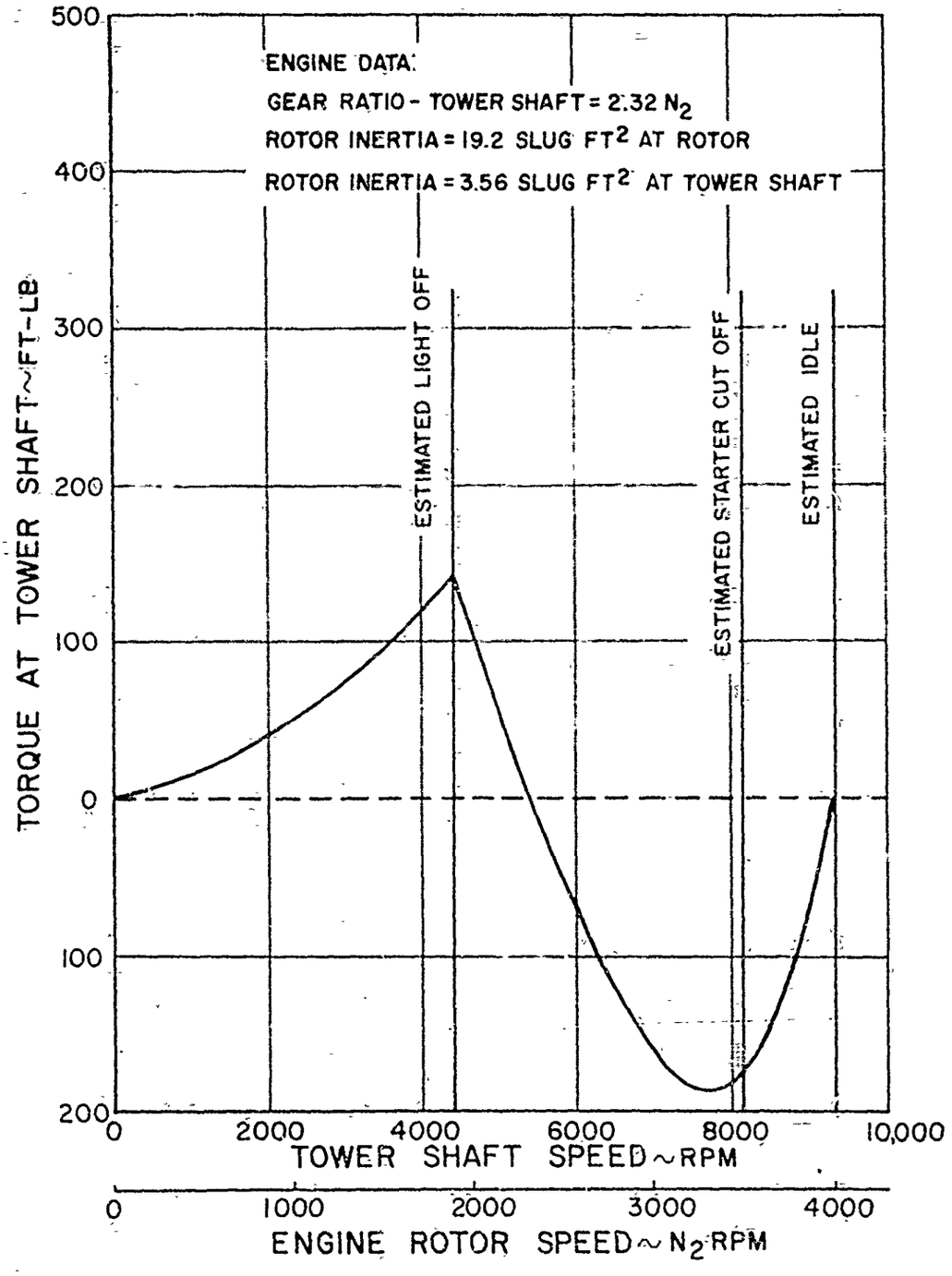

ACTUATING SHAFT
2500

RIGHT-ANGLE POWER TAK

Figure 2-89

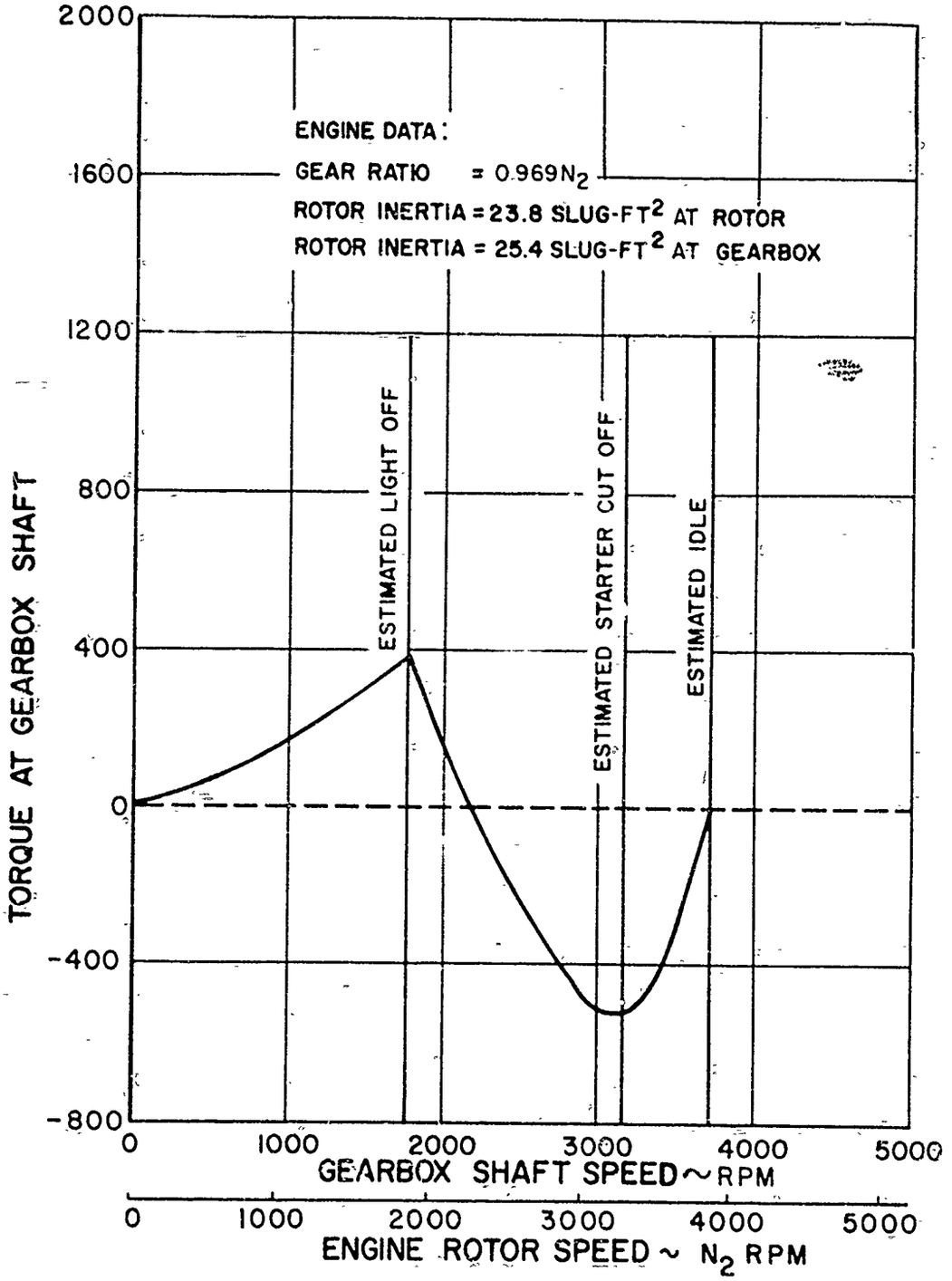
RIGHT-ANGLE POWER TAKE-OFF DRIVE

Figure 2-39



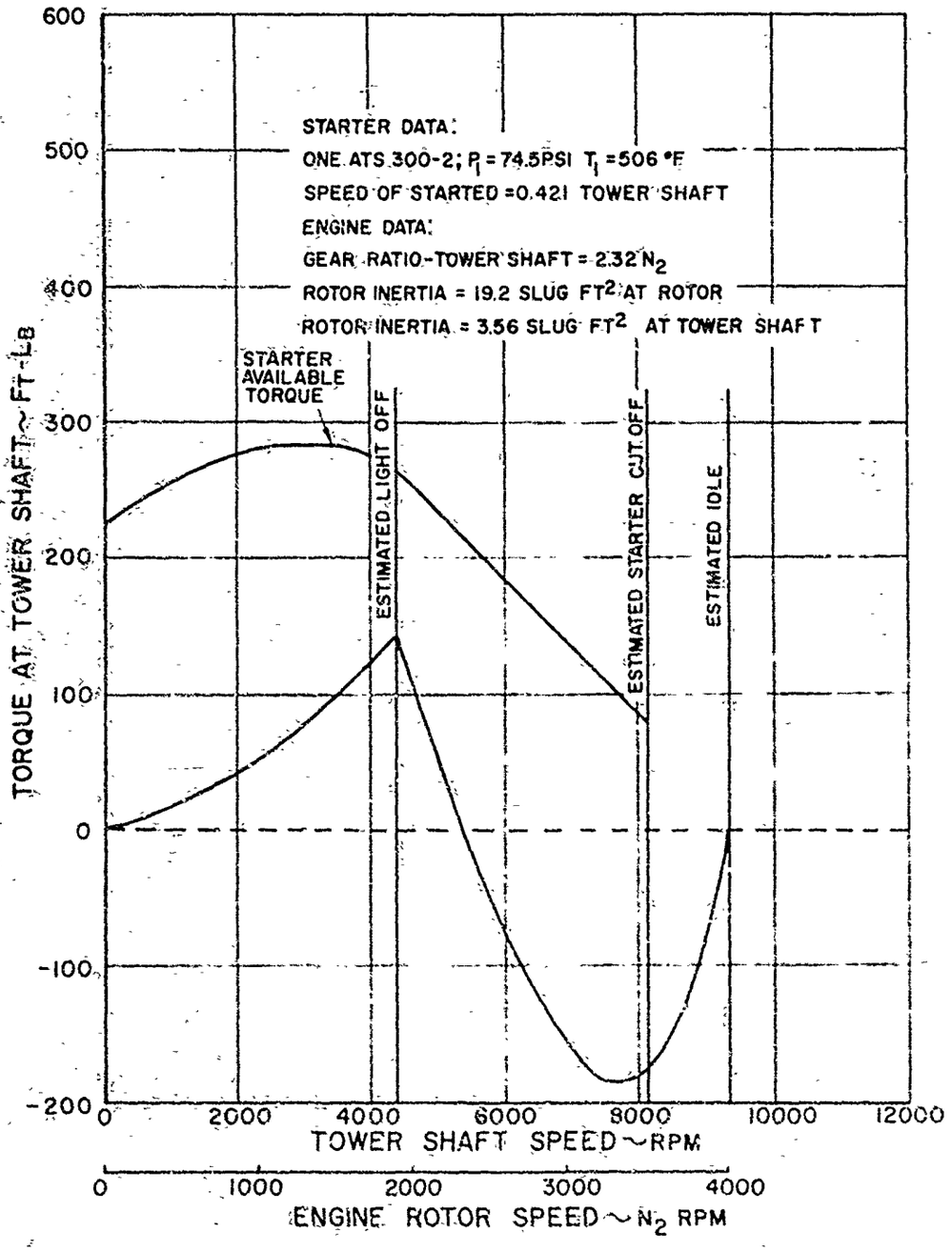
ESTIMATED MOTORING TORQUE AT TOWER SHAFT FOR BOEING ENGINE

Figure 2-90



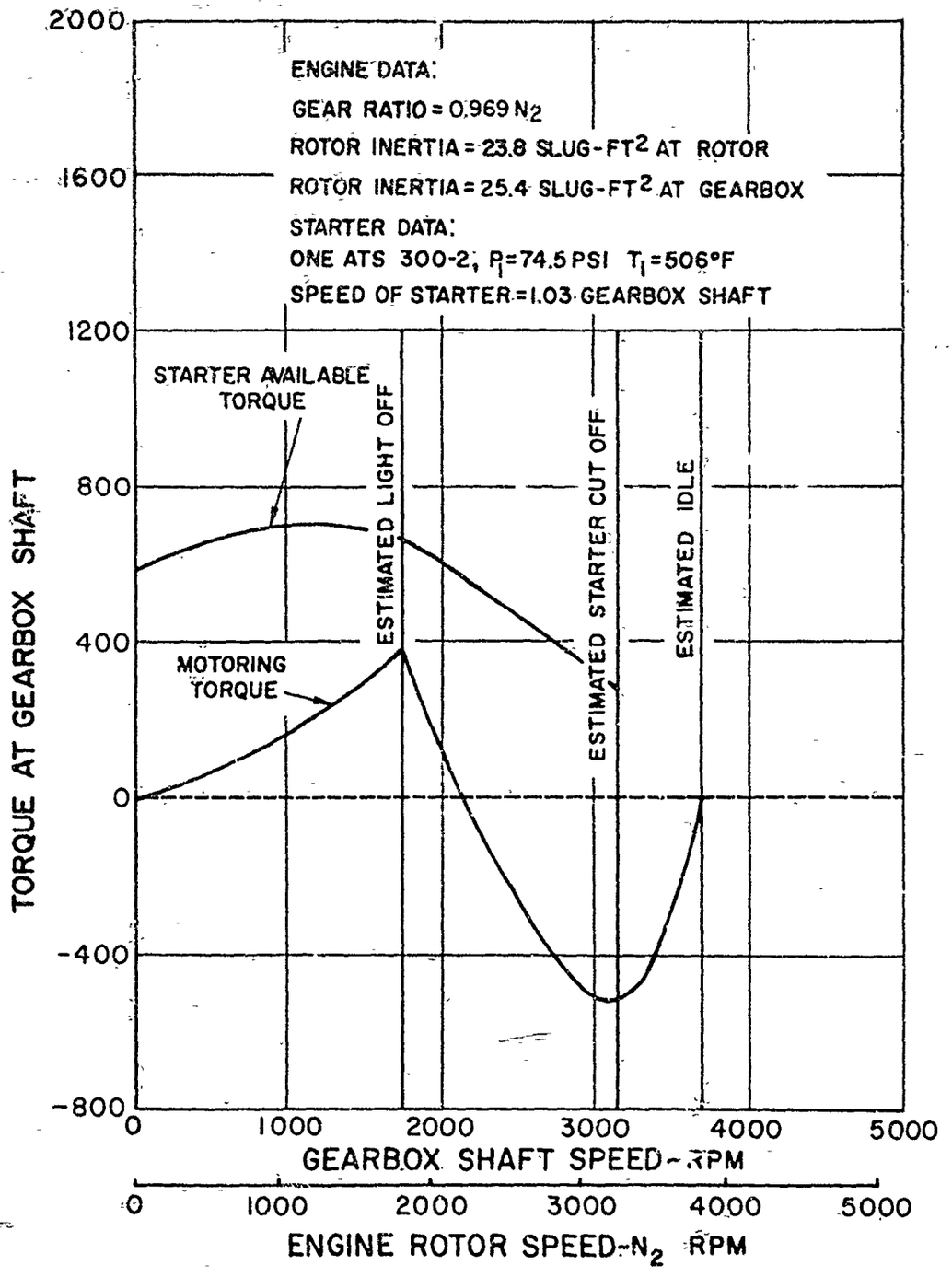
ESTIMATED MOTORING TORQUE AT GEARBOX SHAFT
FOR LOCKHEED ENGINE

Figure 2-91



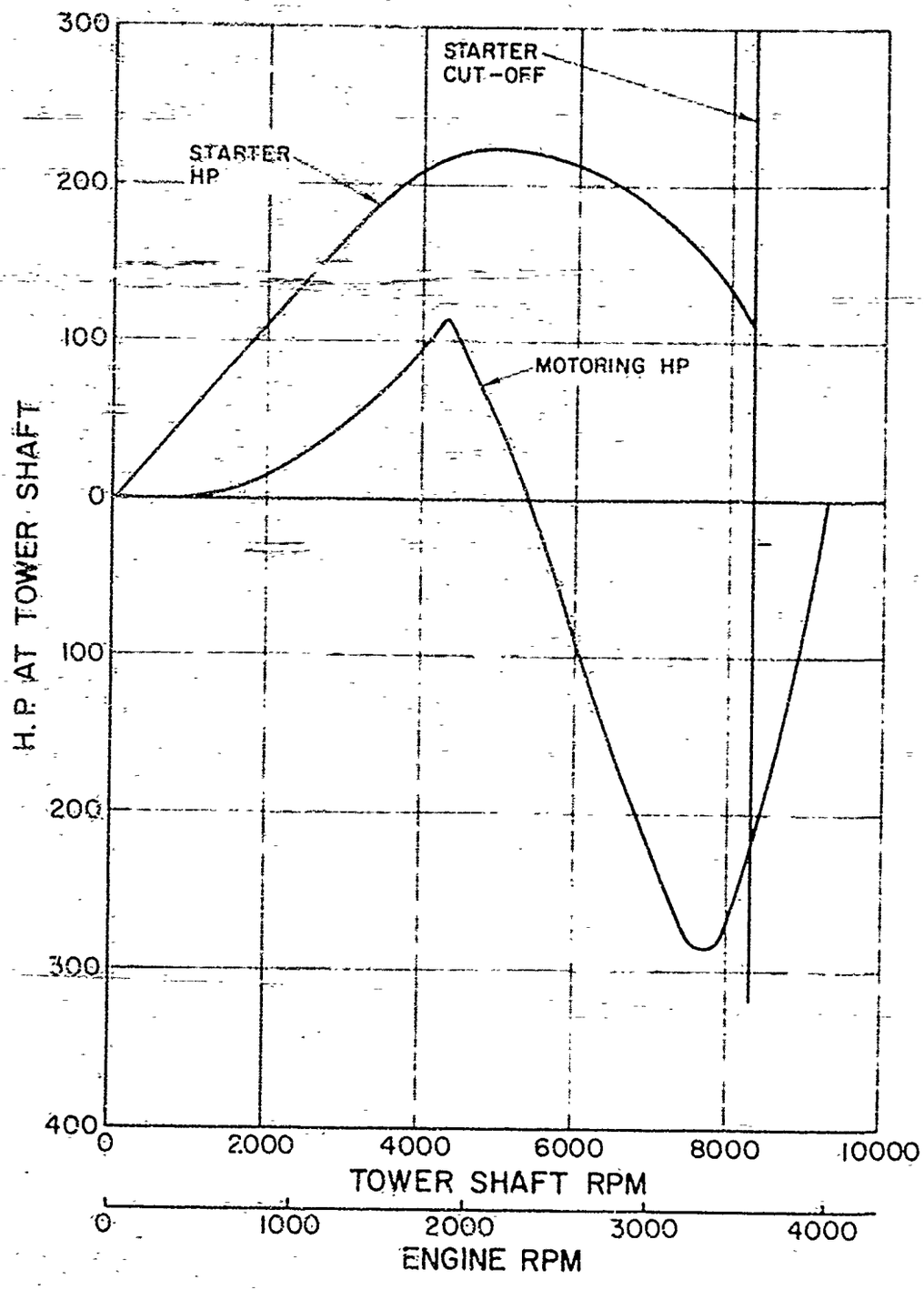
ESTIMATED STARTER TORQUE FOR AIR TURBINE STARTER AT TOWER SHAFT FOR BOEING ENGINE

Figure 2-42



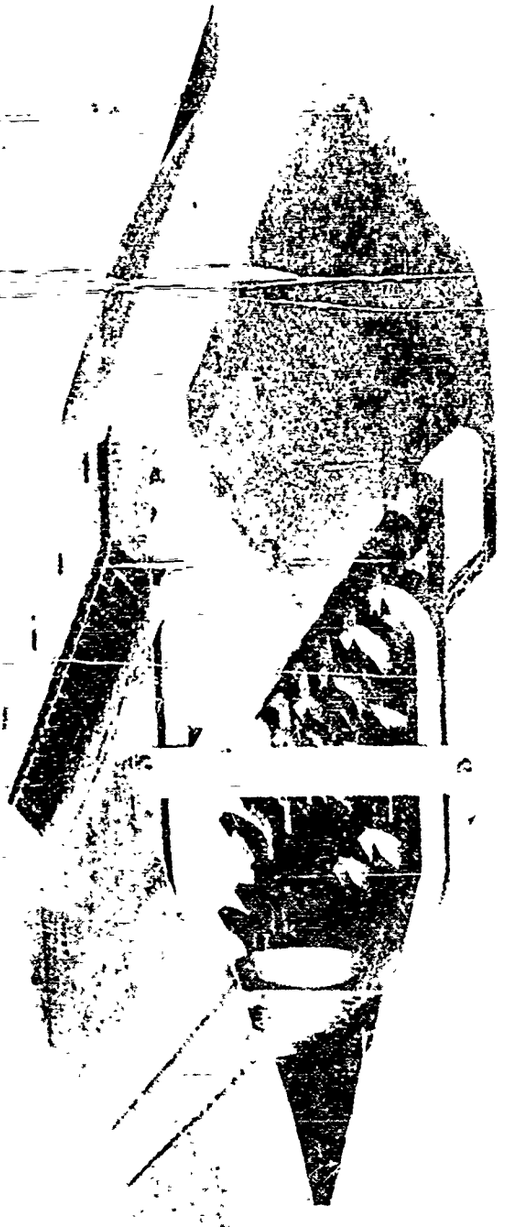
ESTIMATED STARTER TORQUE FOR AIR TURBINE STARTER AT GEARBOX SHAFT FOR LOCKHEED ENGINE

Figure 2-93



STARTER AND MOTORING HORSEPOWER FOR BOEING ENGINE

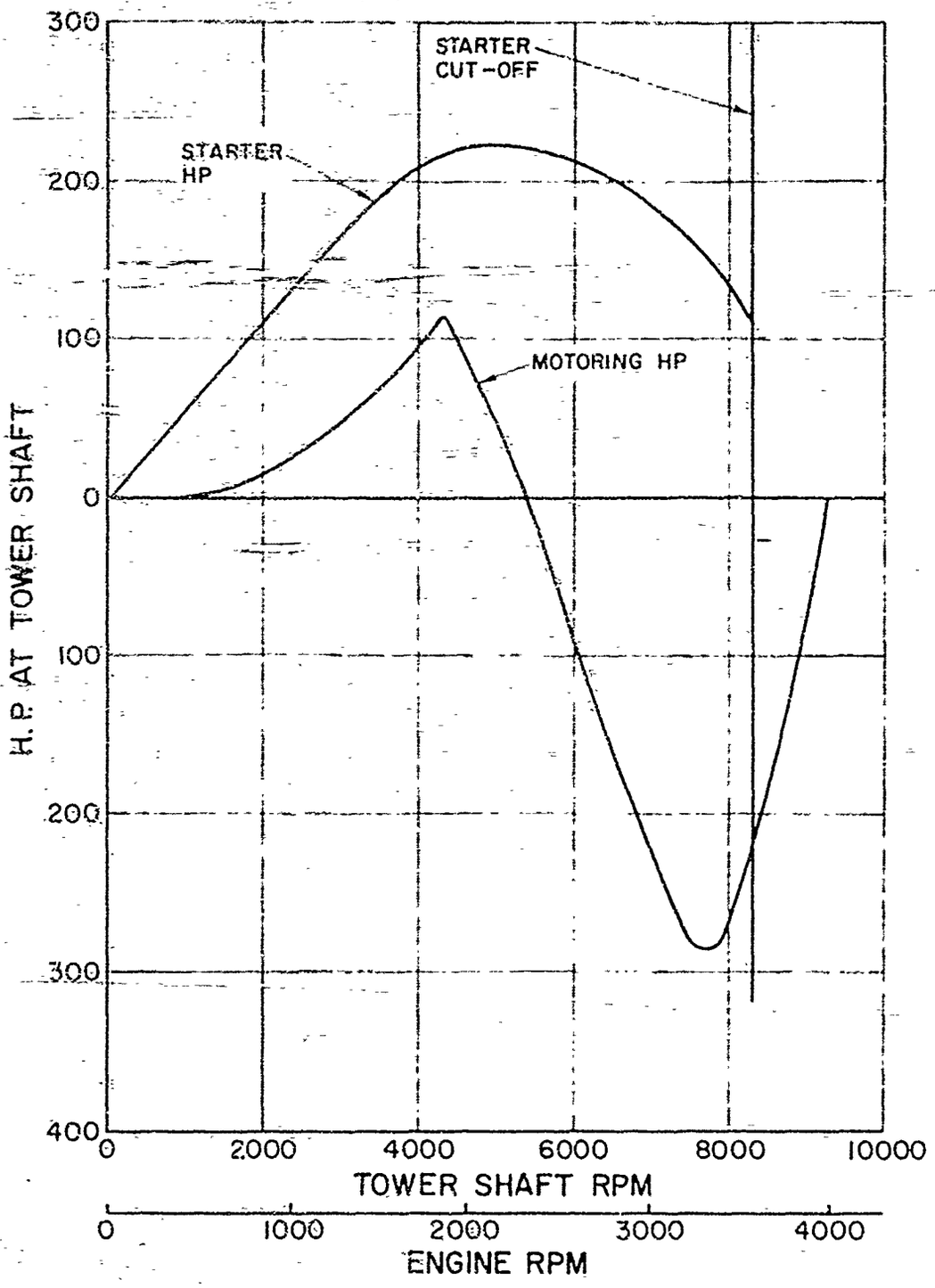
Figure 2-94



RAM INDUCTION BURNER TEST SECTION

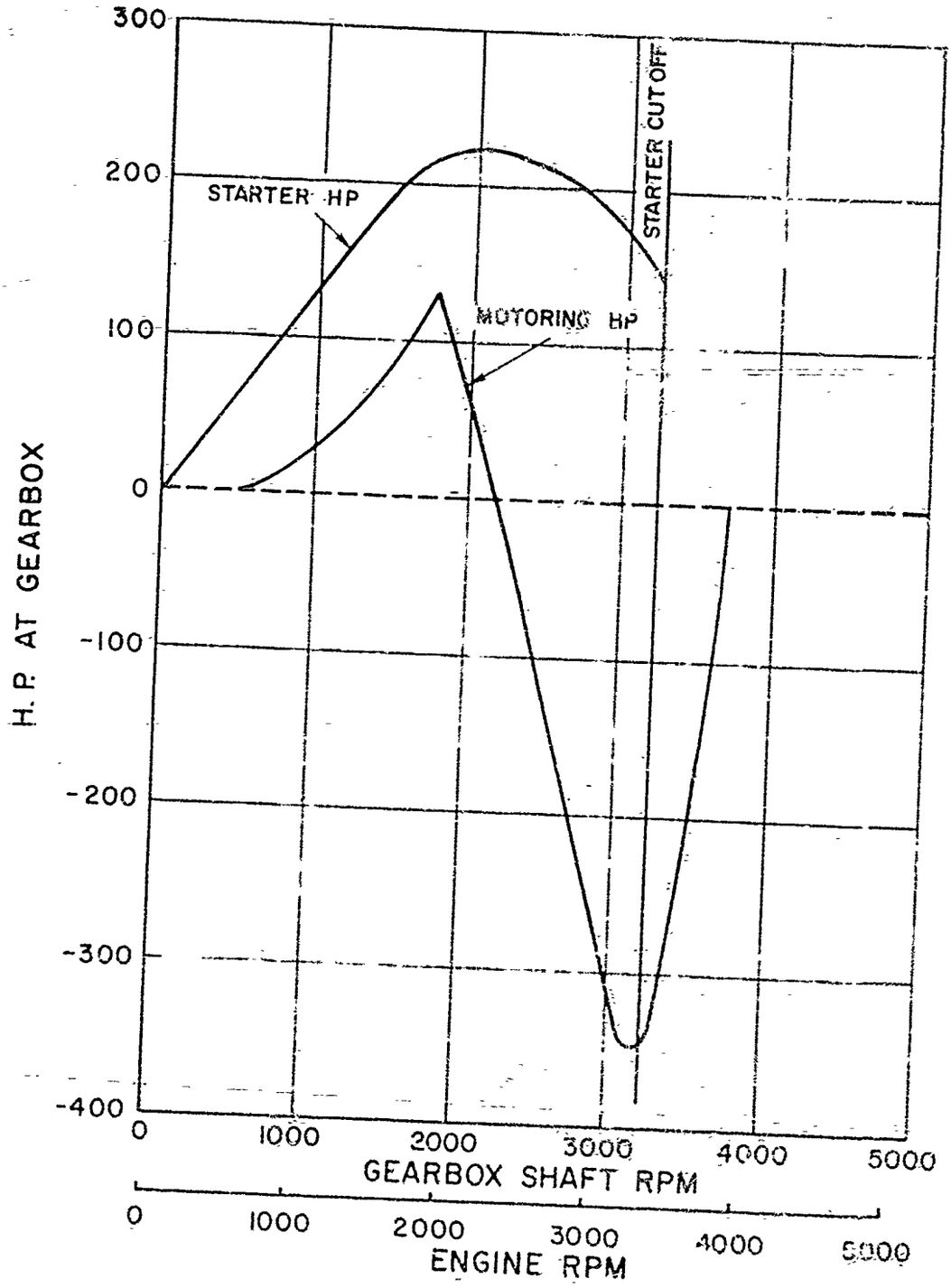
Figure 5-1

DOWNGRADED AT 3 YEAR INTERVALS
DECLASSIFIED AFTER 12 YEARS
DOD DIR 5200.10



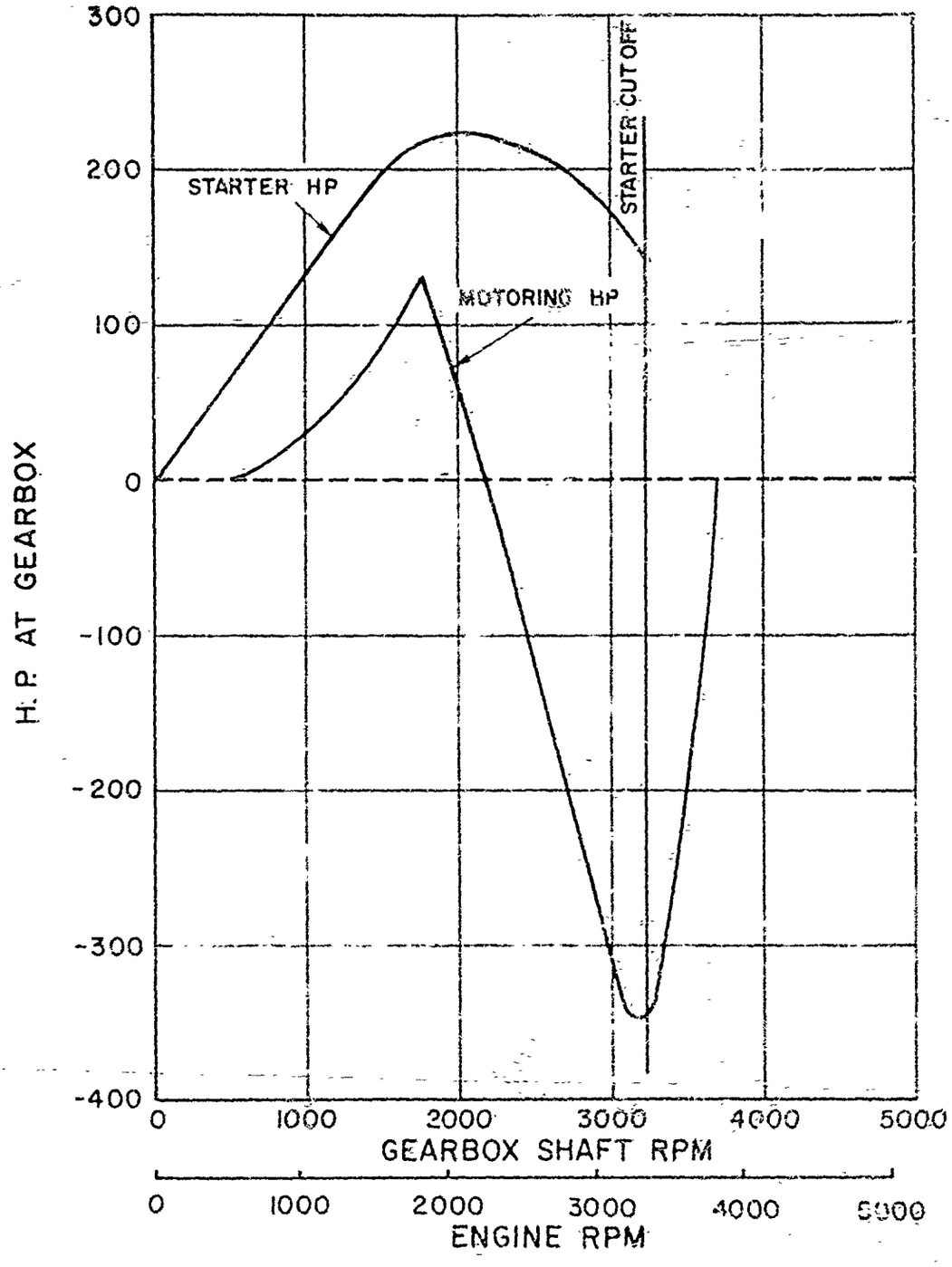
STARTER AND MOTORING HORSEPOWER FOR BOEING ENGINE

Figure 2-94



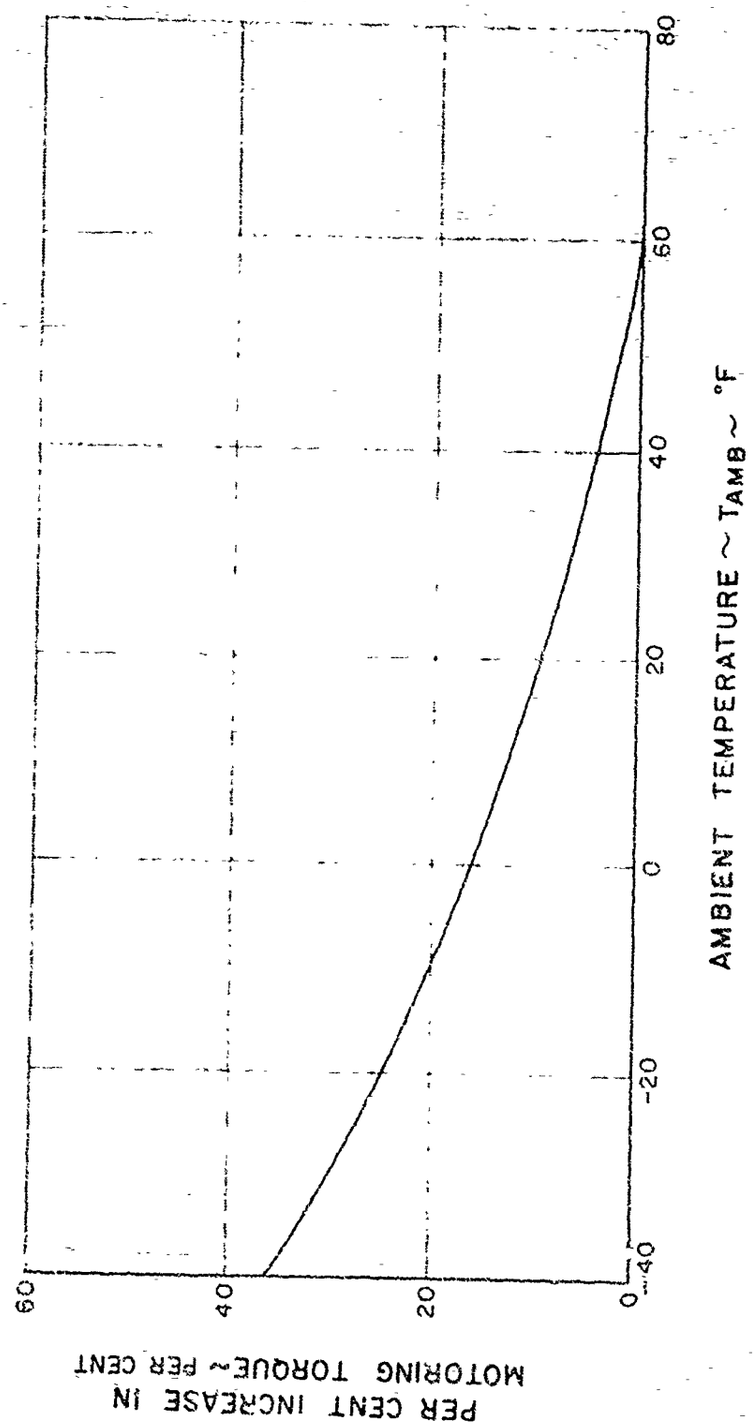
STARTER AND MOTORING HORSEPOWER FOR LOCKED ENGINE

Figure 2-95



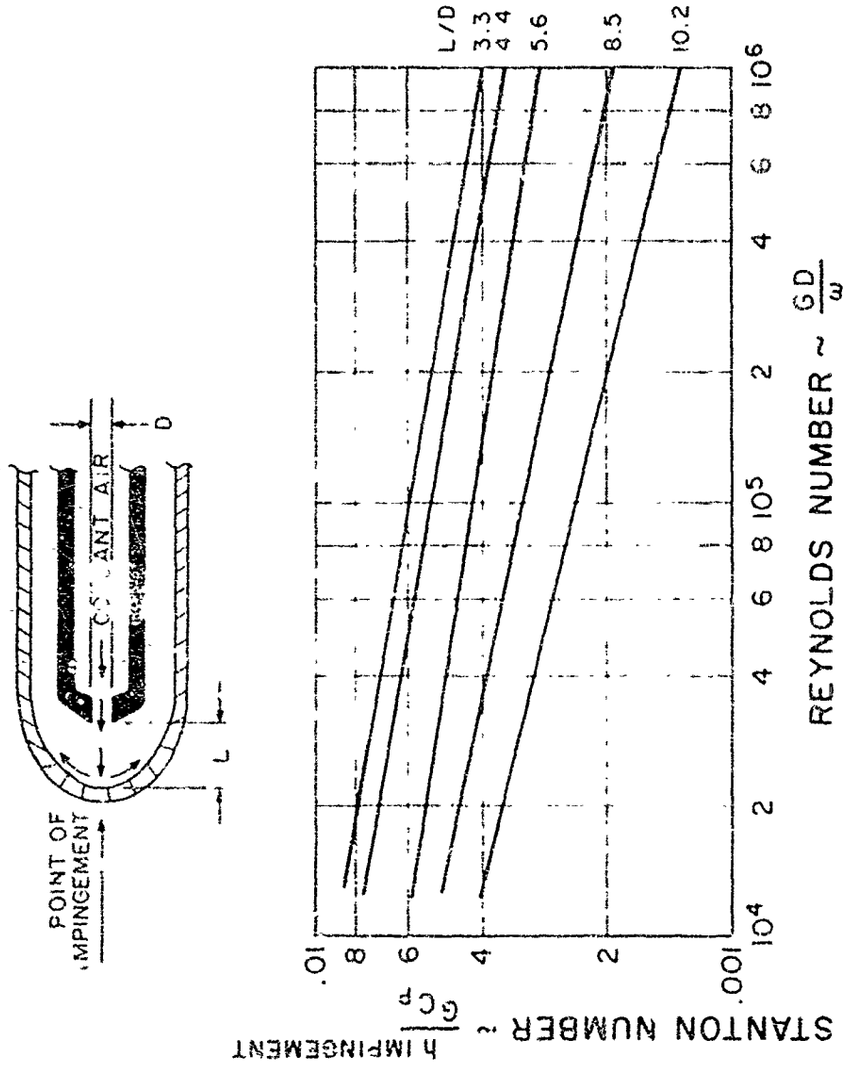
STARTER AND MOTORING HORSEPOWER FOR LOCKHEED ENGINE

Figure 2-95



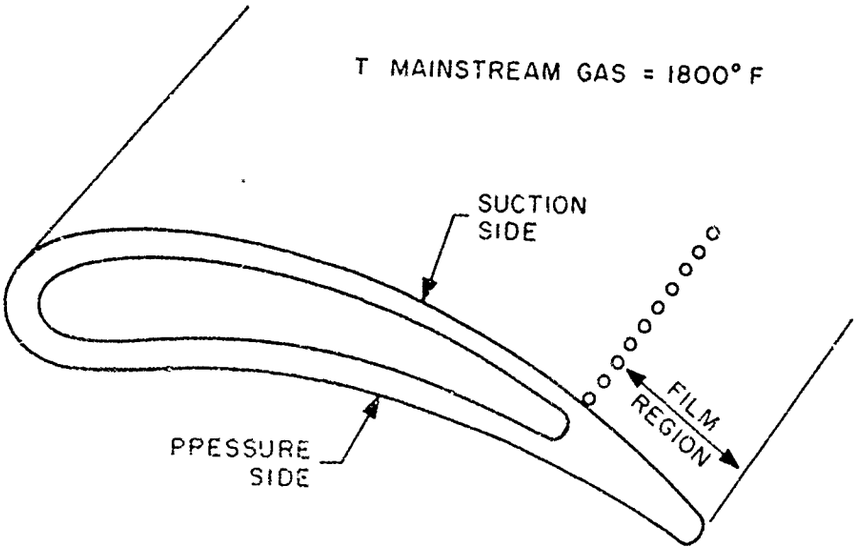
EFFECT OF TEMPERATURE ON STARTER MOTORING TORQUE

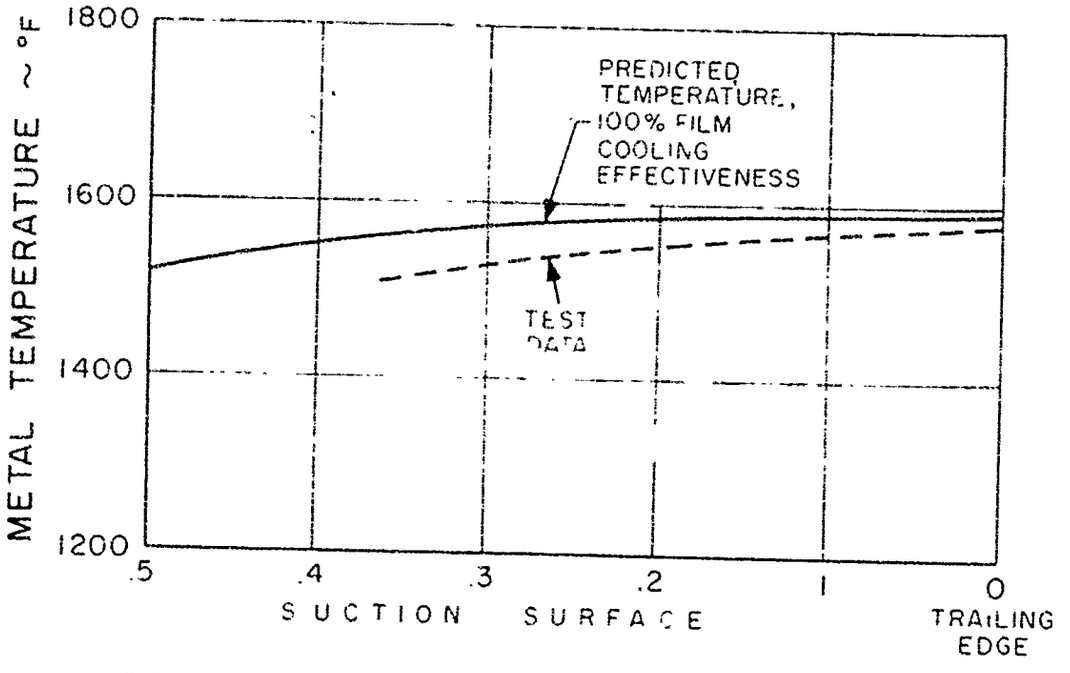
Figure 2-96



IMPINGEMENT HEAT TRANSFER COEFFICIENT, CORRELATION OF EXPERIMENTAL RESULTS OBTAINED ON IMPINGEMENT RIG AT POINT OF IMPINGEMENT

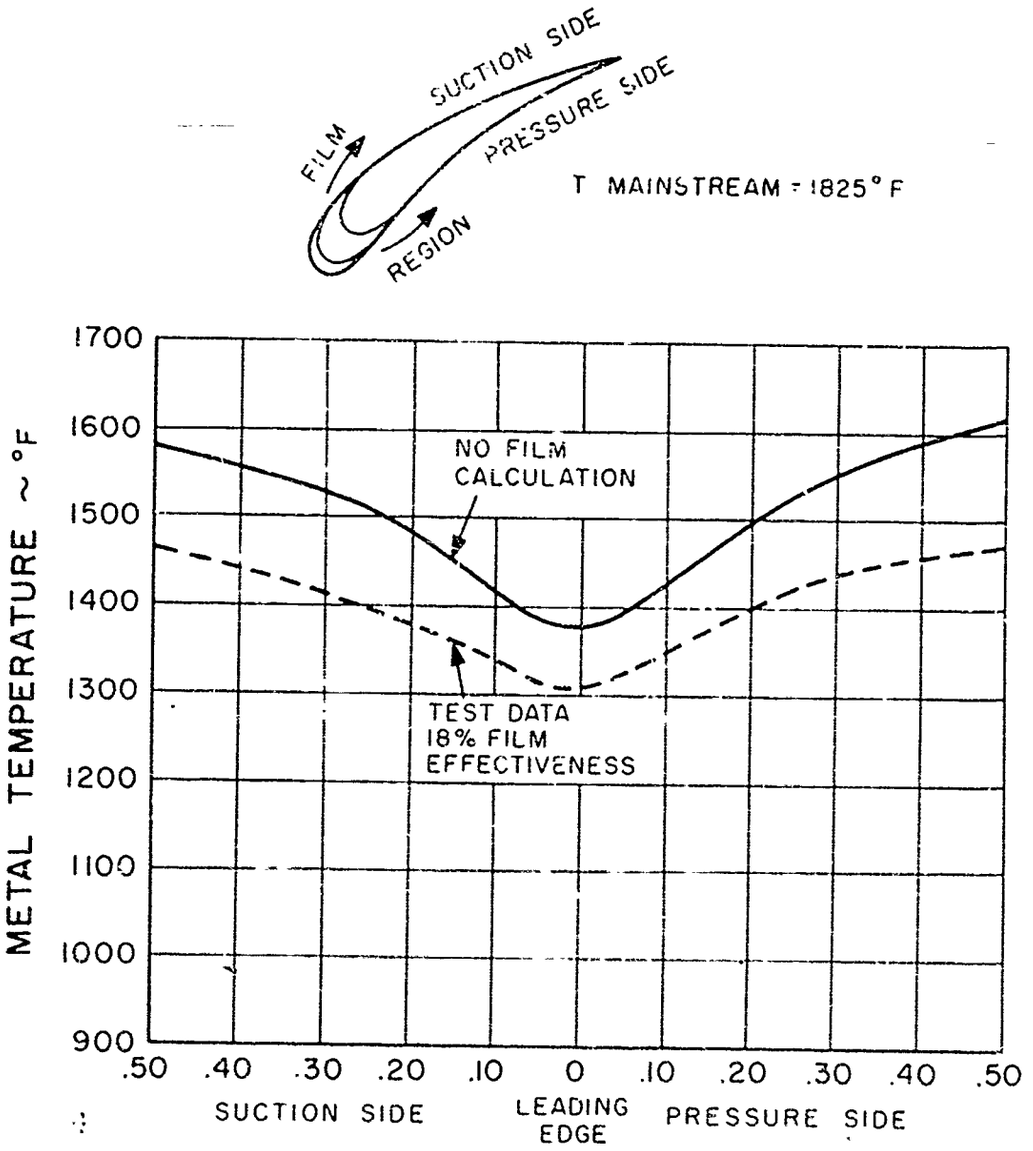
Figure 2-97





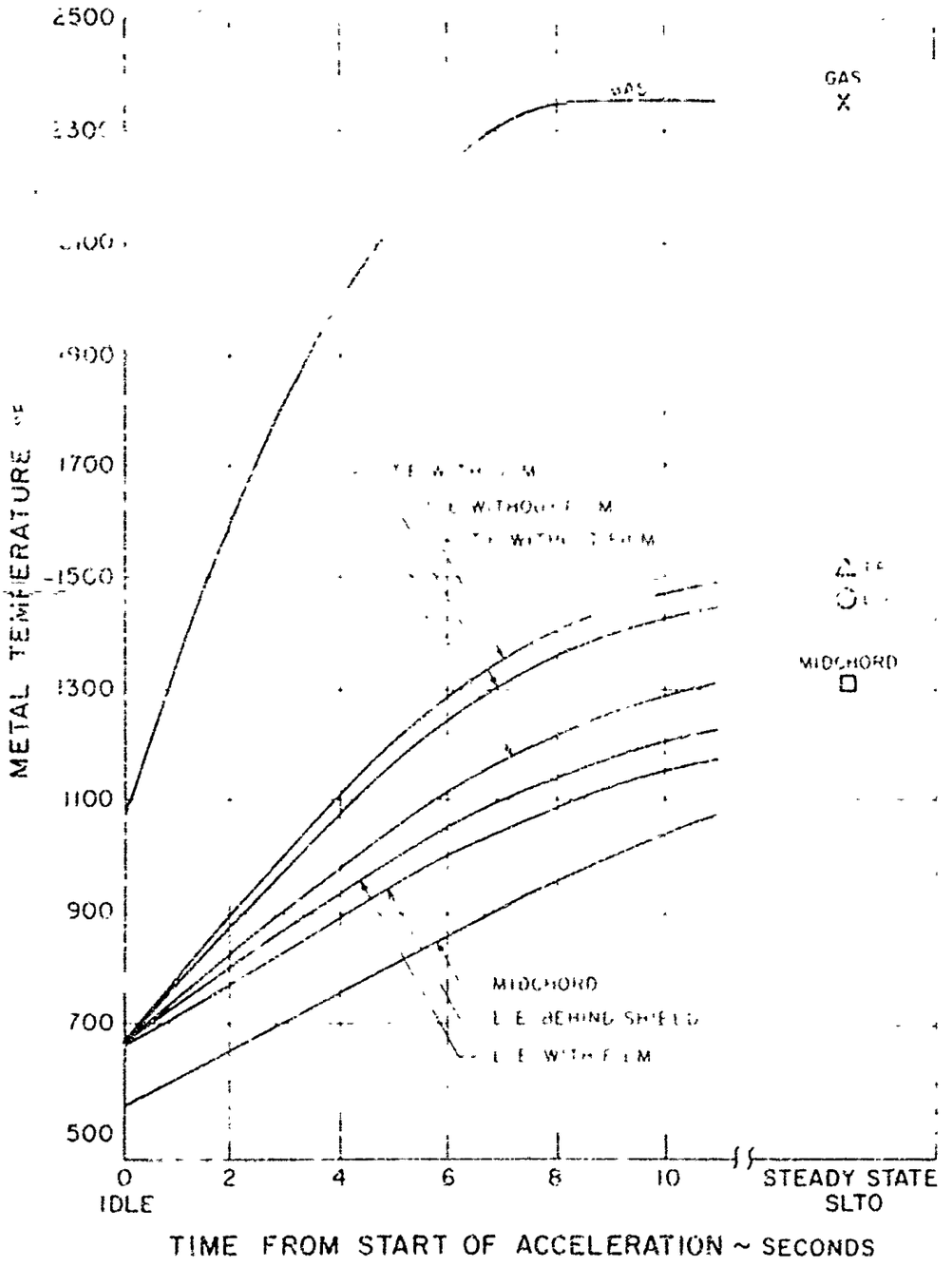
[illegible] FILM COOLING EFFECTIVENESS AT TRAILING EDGE
[illegible] OBSERVED IN FAN CASCADE RIG

Figure 4-45



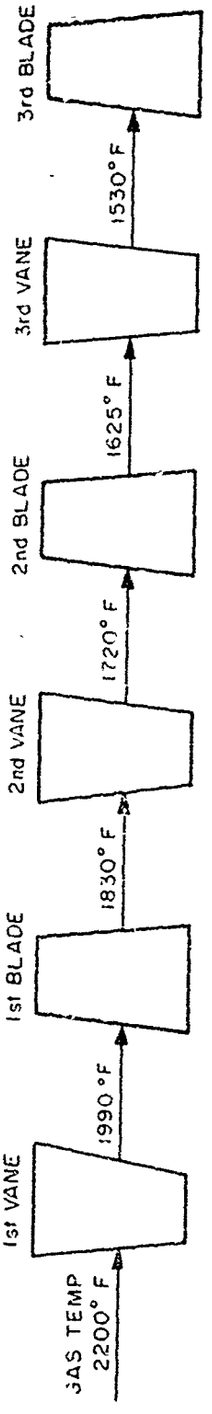
18% FILM COOLING EFFECTIVENESS AT LEADING EDGE DEMONSTRATED ON SHIELDED LEADING EDGE VANE

Figure 2-99



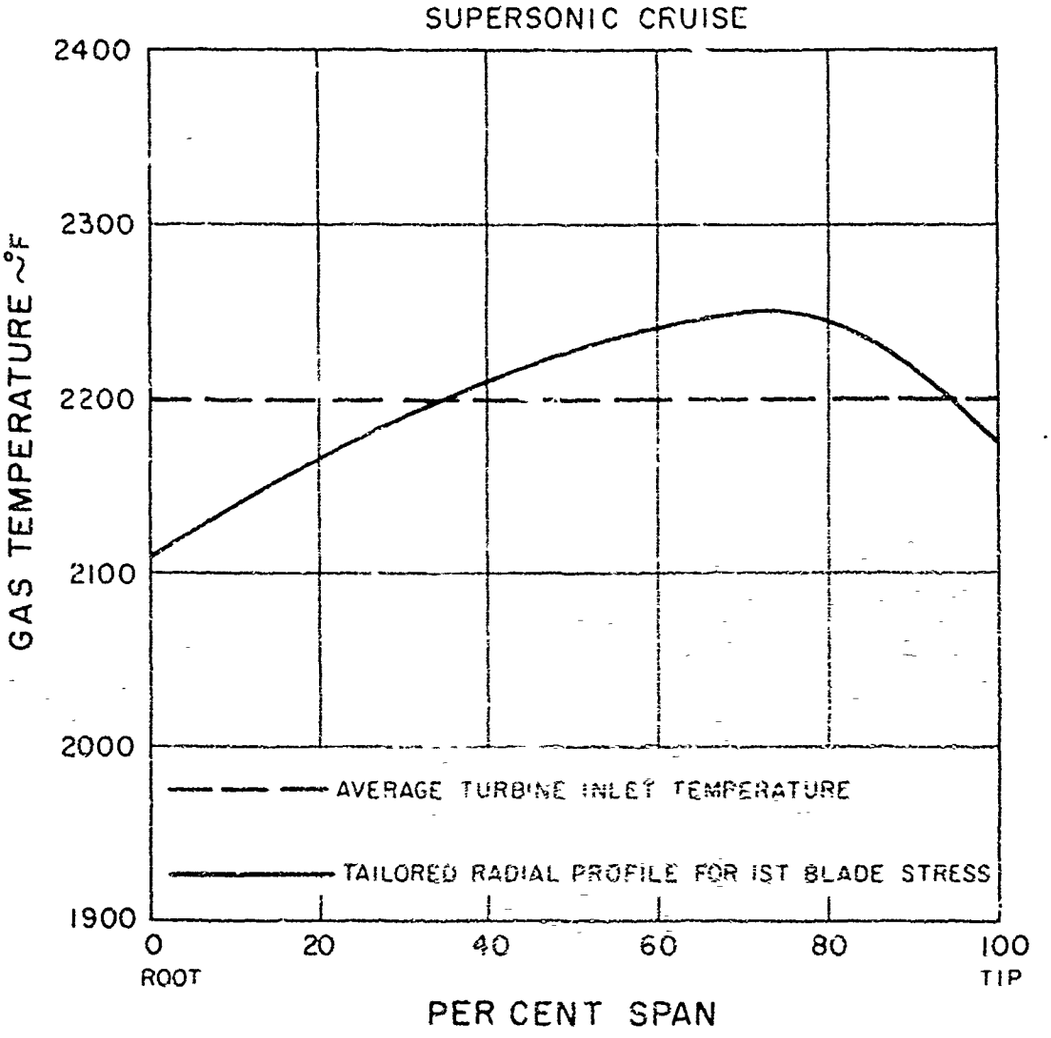
TYPICAL TRANSIENT METAL AND GAS TEMPERATURES

Figure 2-100



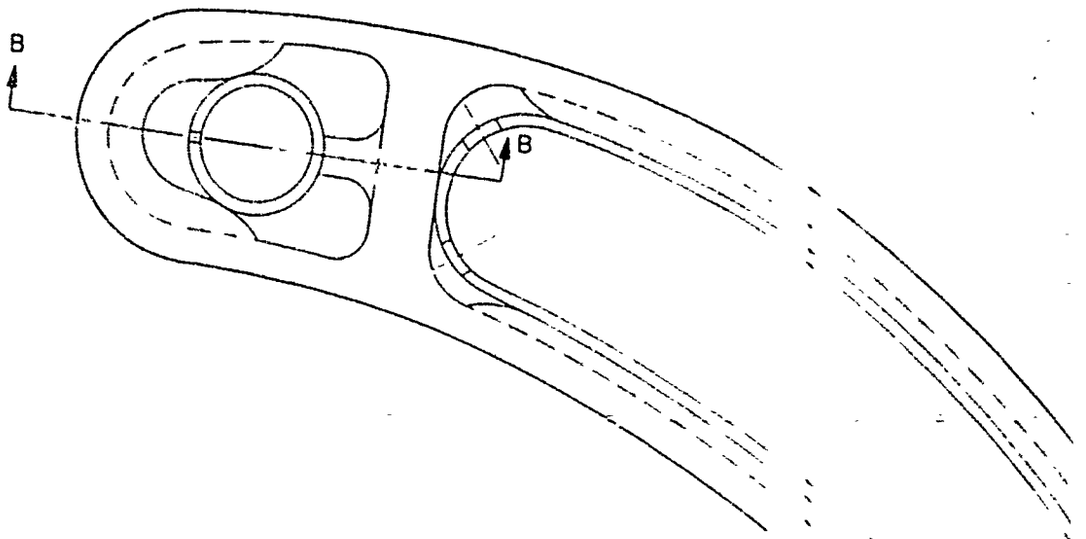
AVERAGE GAS TEMPERATURES ENTERING EACH TURBINE AIRFOIL ROW
STF219 SUPERSONIC CRUISE

Figure 2-101

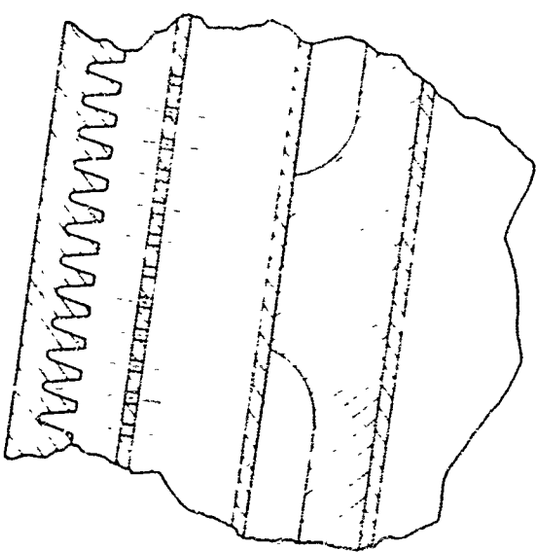


TAILORED SPANWISE GAS TEMPERATURE VARIATION
FIRST-STAGE TURBINE VANE

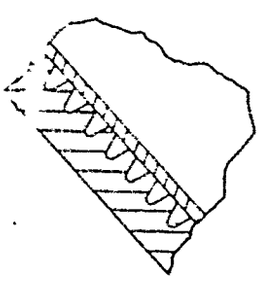
Figure 2-102



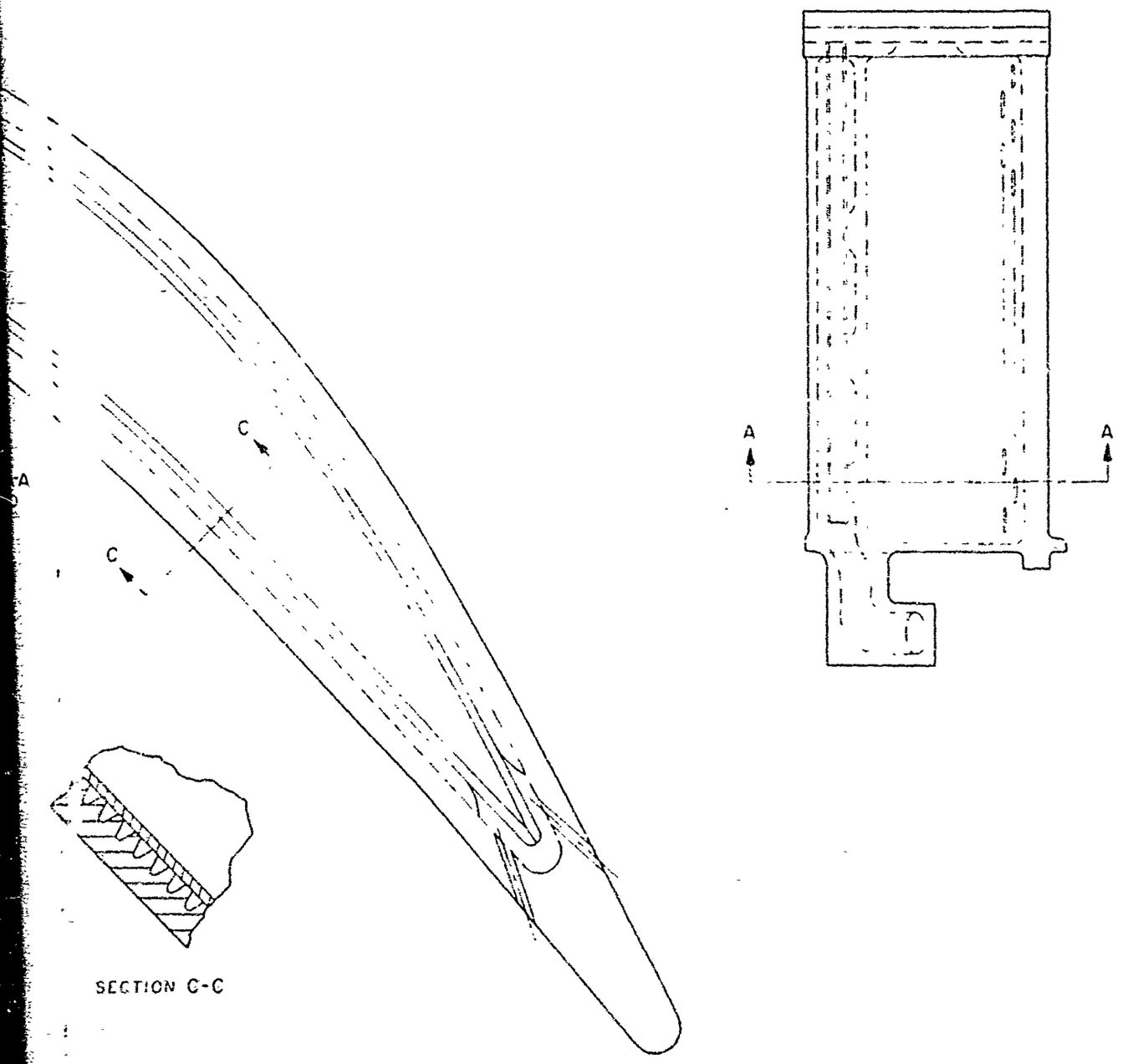
SECTION A-A
ENLARGED



SECTION B-B

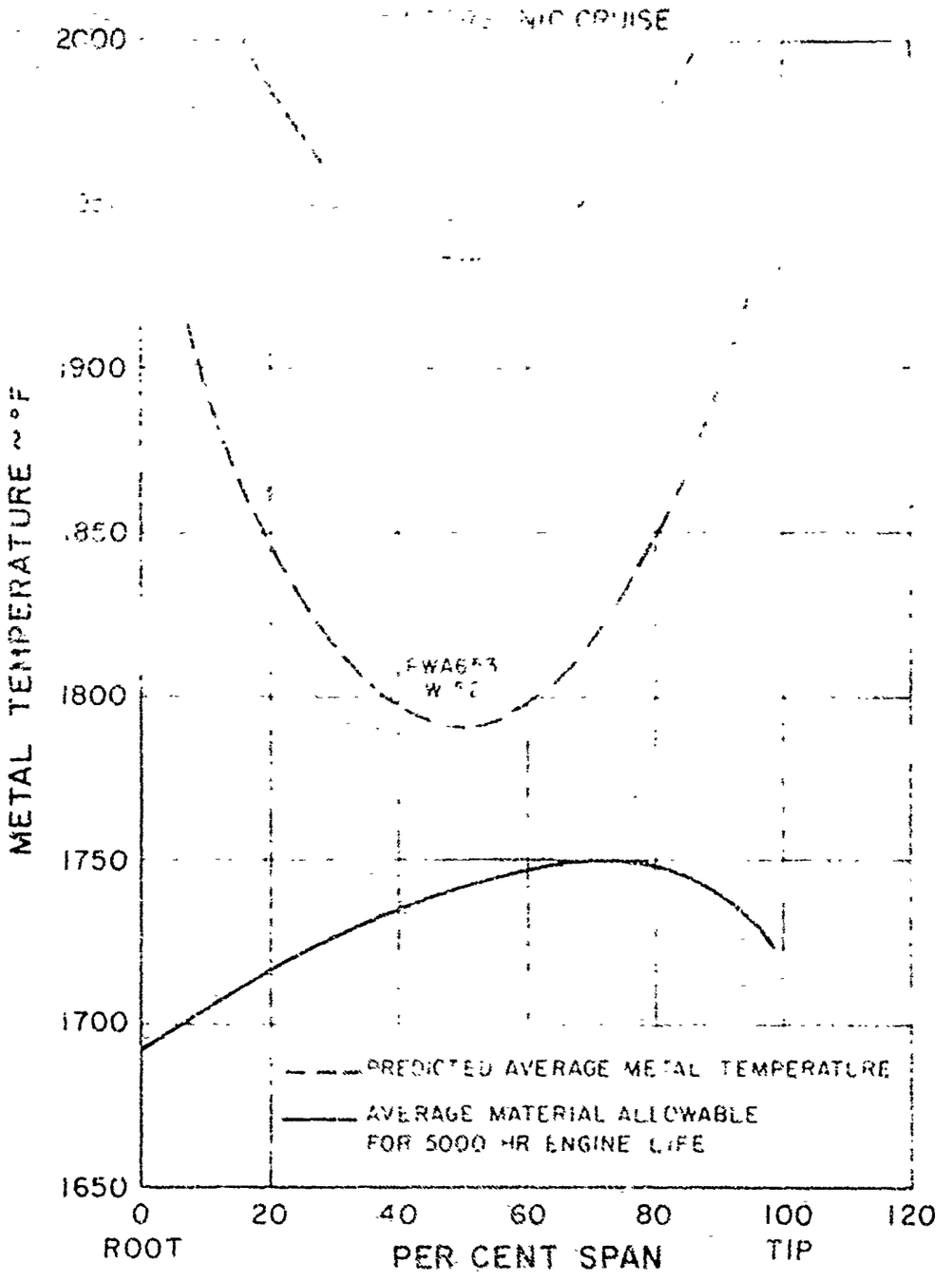


SECTION C-C



FIRST-STAGE TURBINE IMPINGEMENT VANE

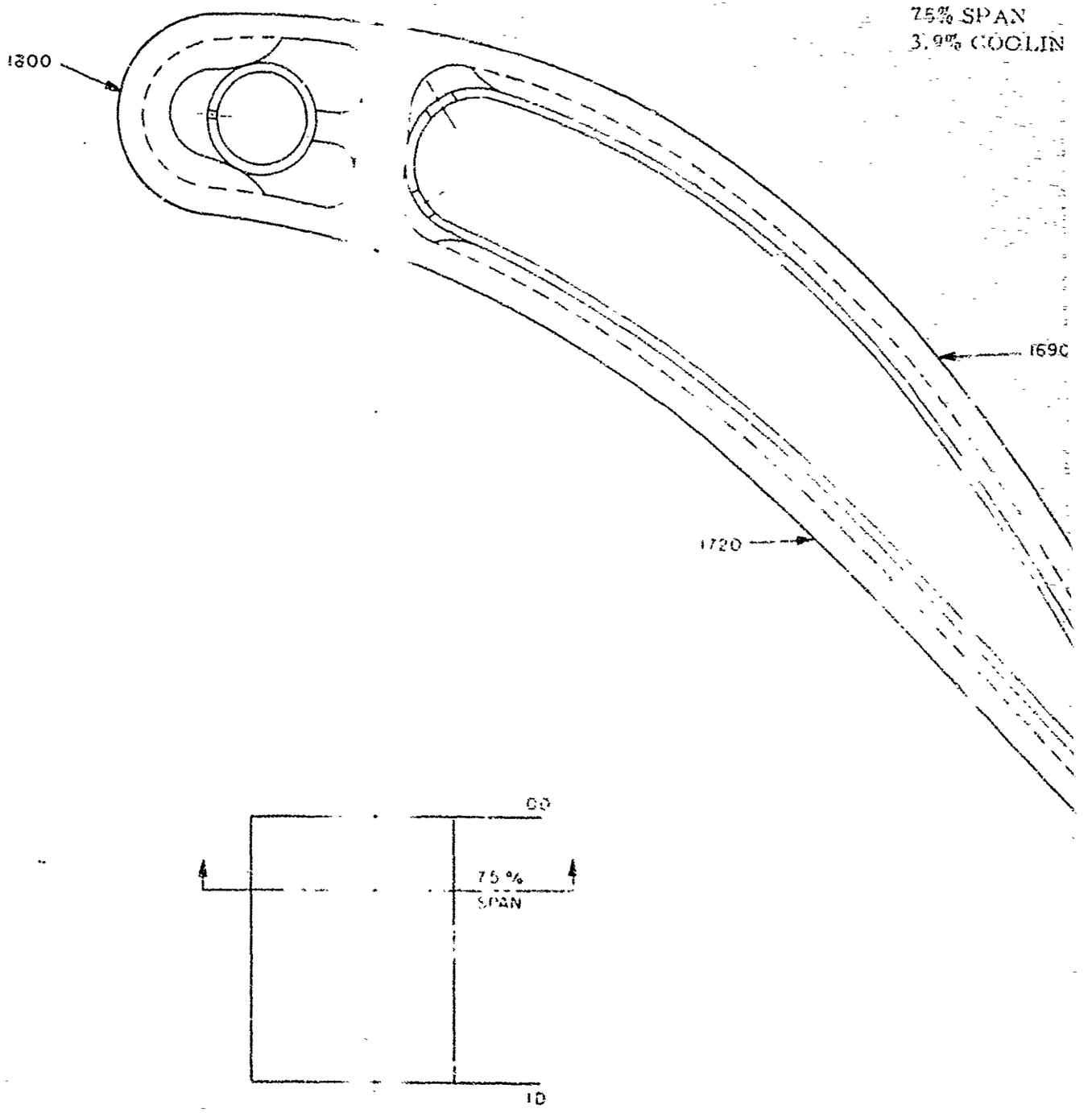
Figure 2-103



FIRST-STAGE TURBINE IMPINGEMENT VANE, SPANWISE ALLOWABLE AND PREDICTED METAL TEMPERATURE

FIGURE 2-104

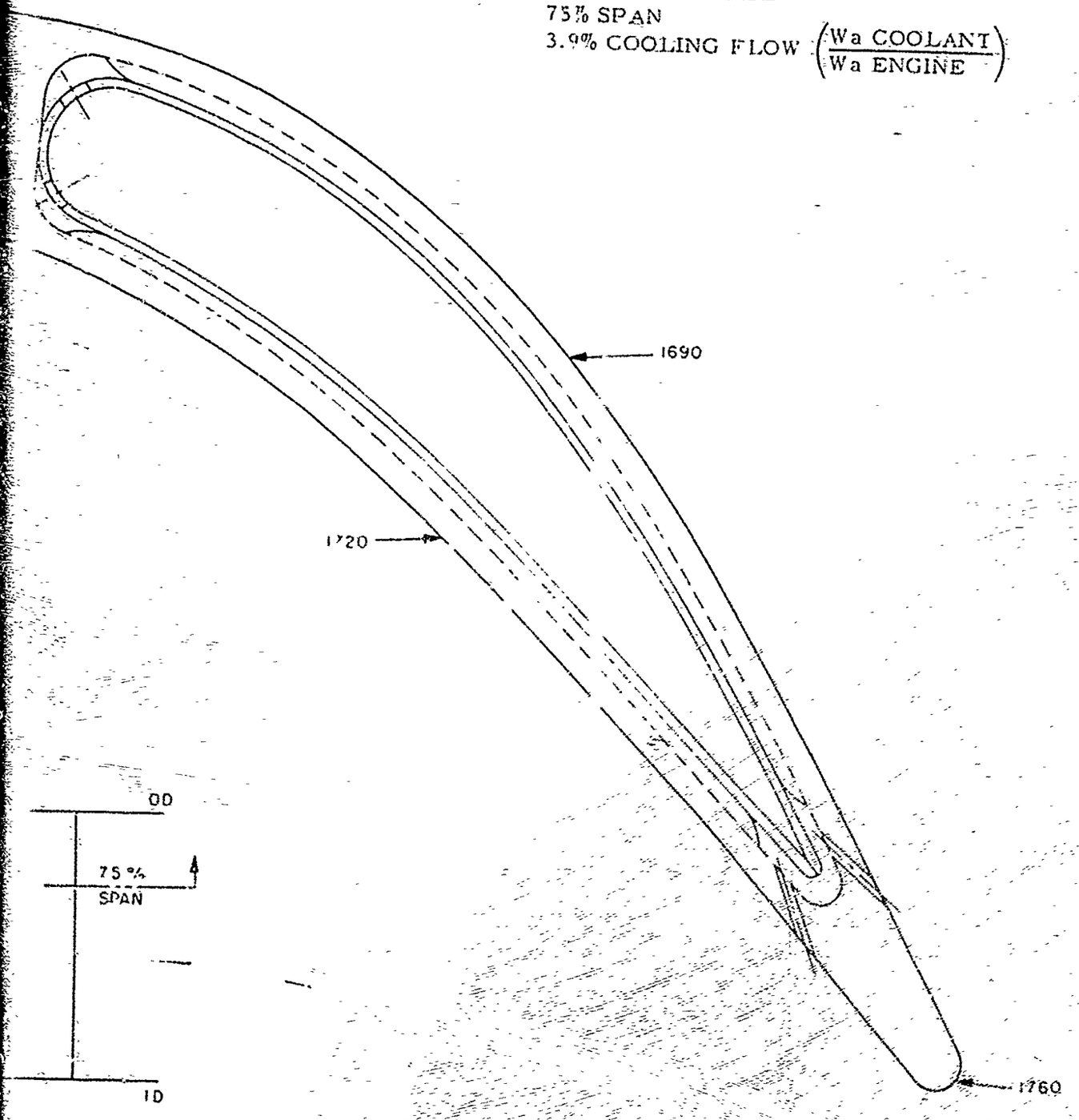
SUPERSONIC C
75% SPAN
3.9% COOLIN



FIRST-STAGE TURBINE IMPINGEMENT V
STEADY-STATE METAL TEMP

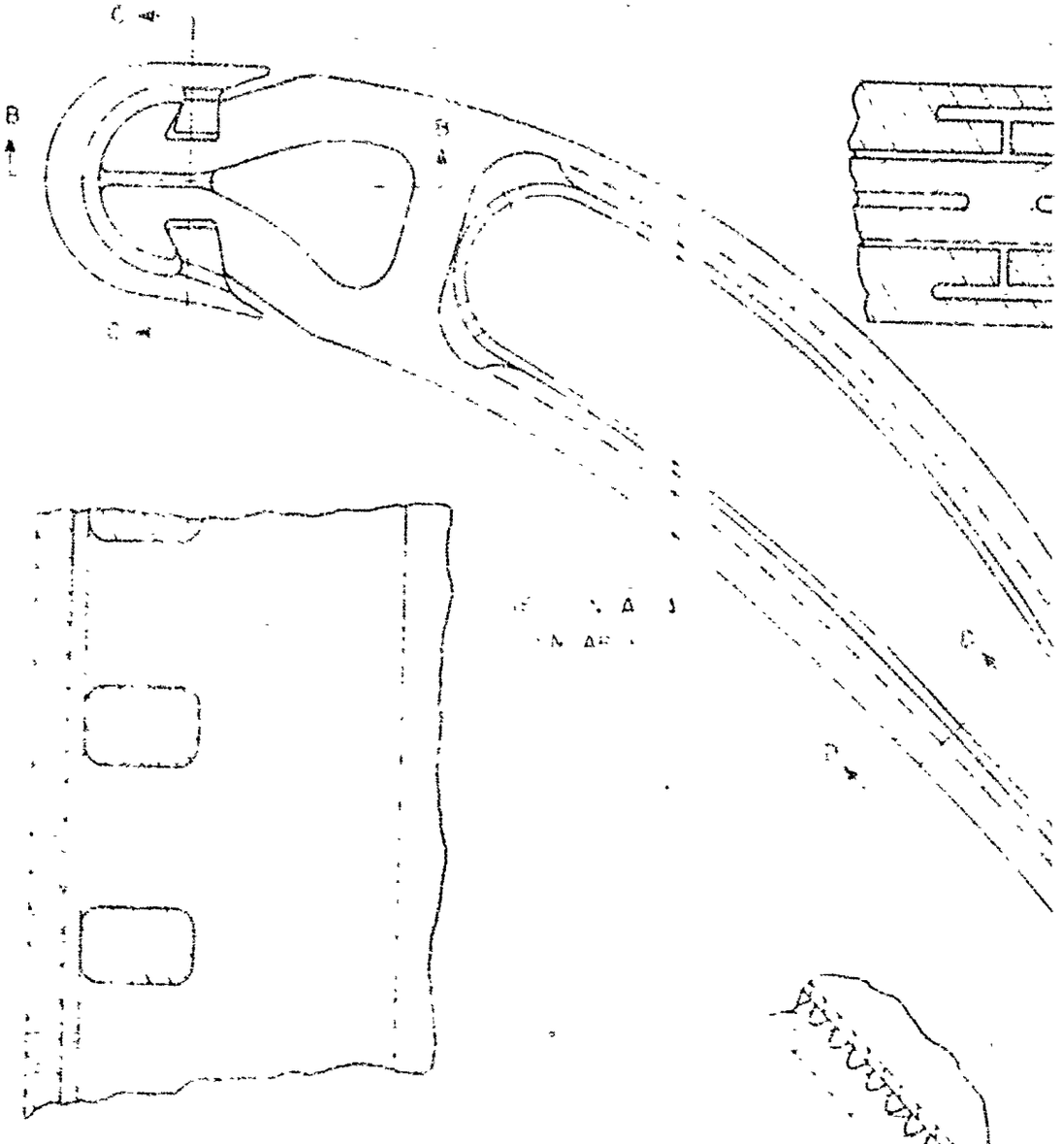
Figure 2-105

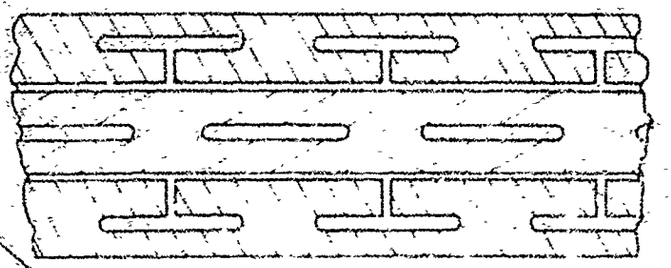
SUPERSONIC CRUISE
75% SPAN
3.9% COOLING FLOW $\left(\frac{\text{Wa COOLANT}}{\text{Wa ENGINE}}\right)$



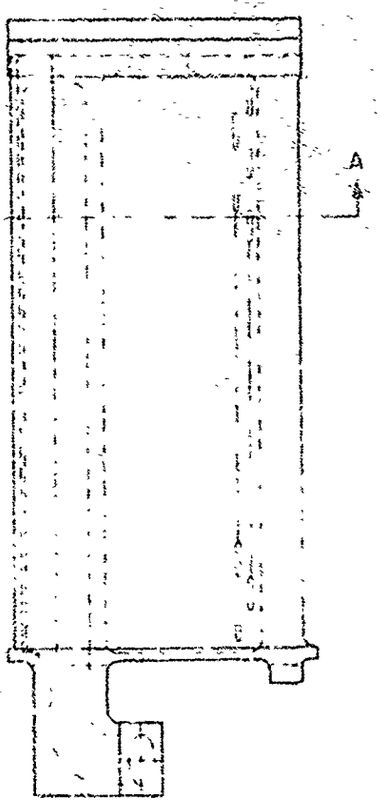
FIRST-STAGE TURBINE IMPINGEMENT VANE SHOWING PREDICTED STEADY-STATE METAL TEMPERATURES (°F)

Figure 2-105


C
B
B
C



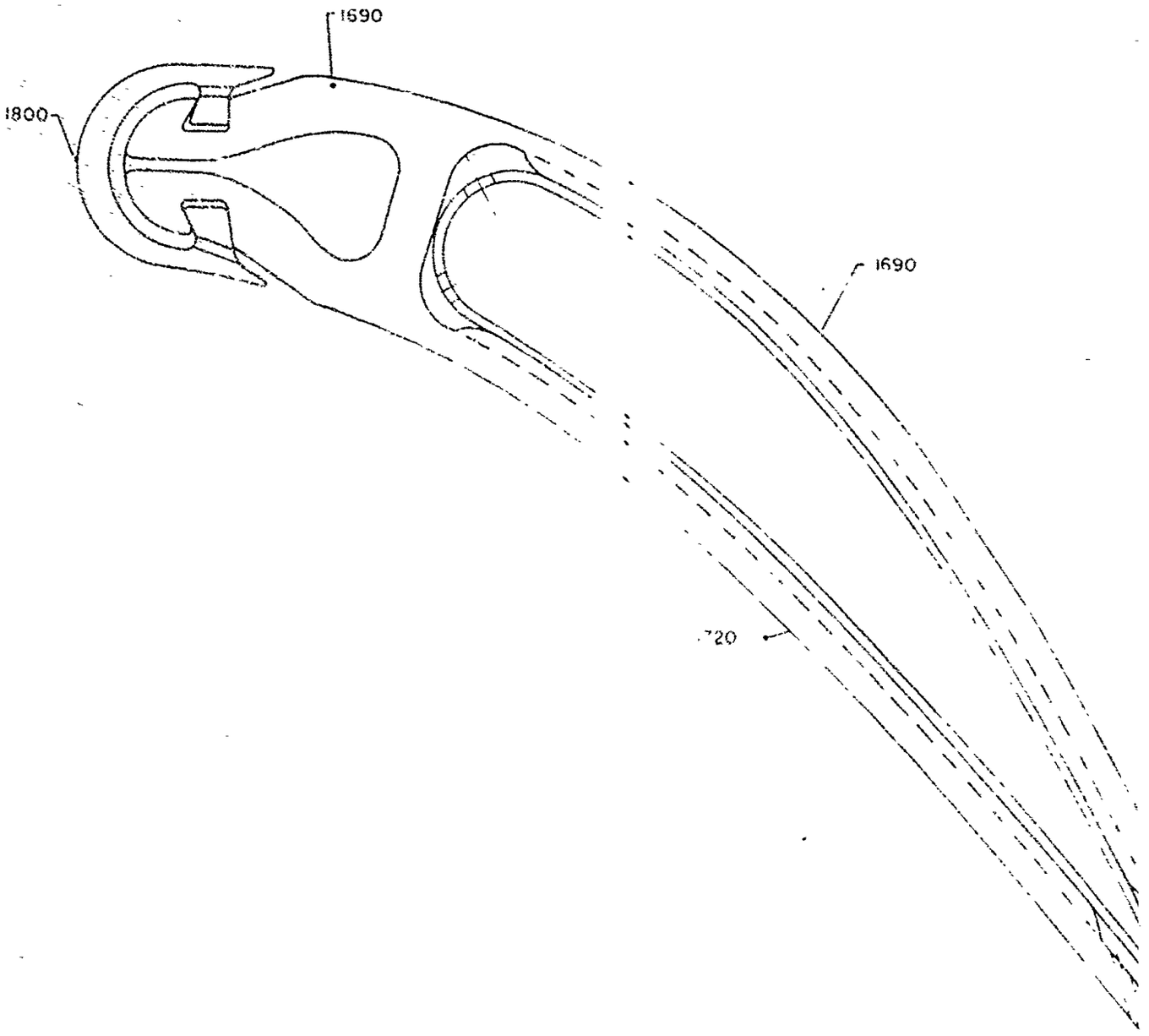
SECTION C~C



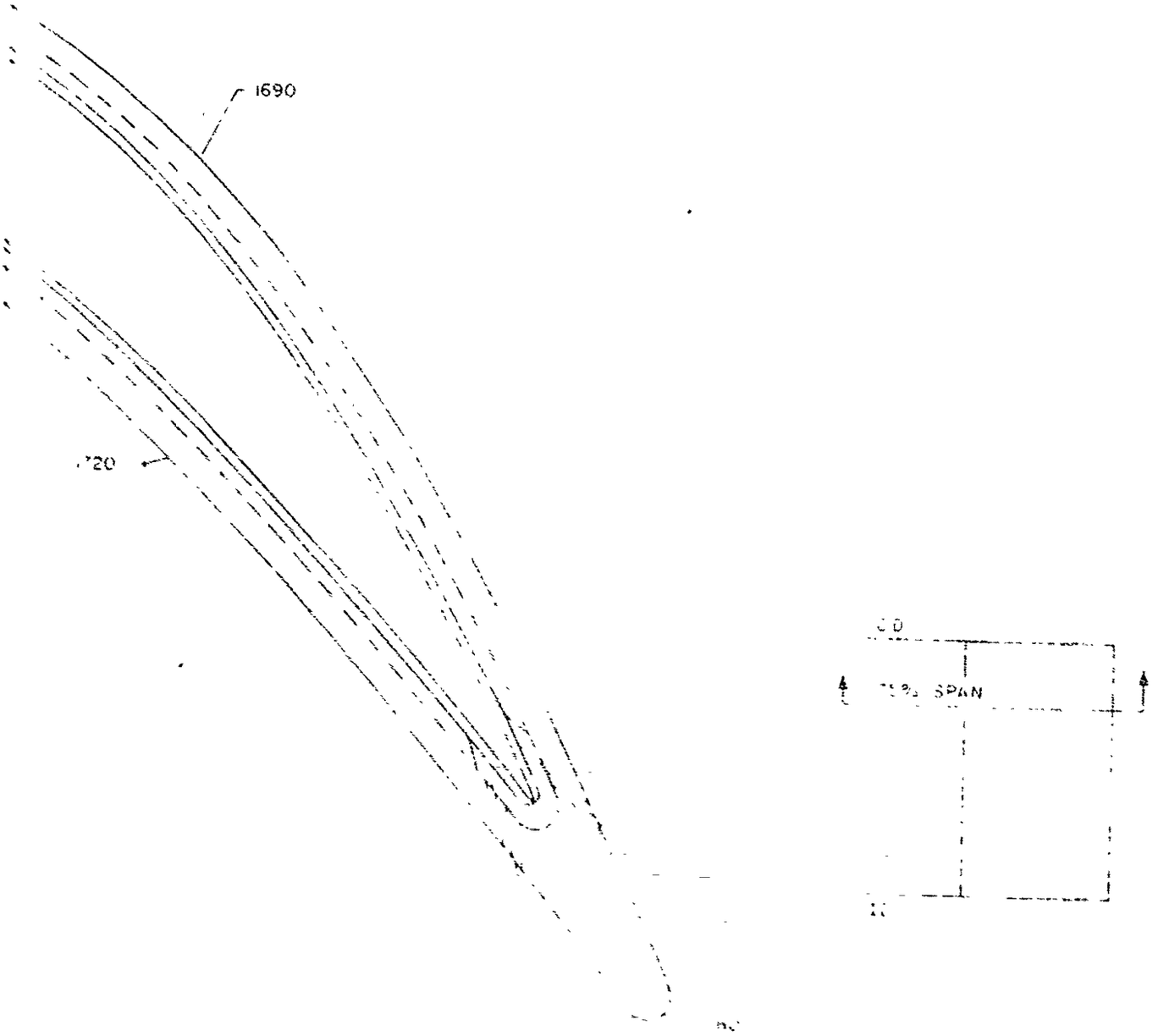
SECTION D~D

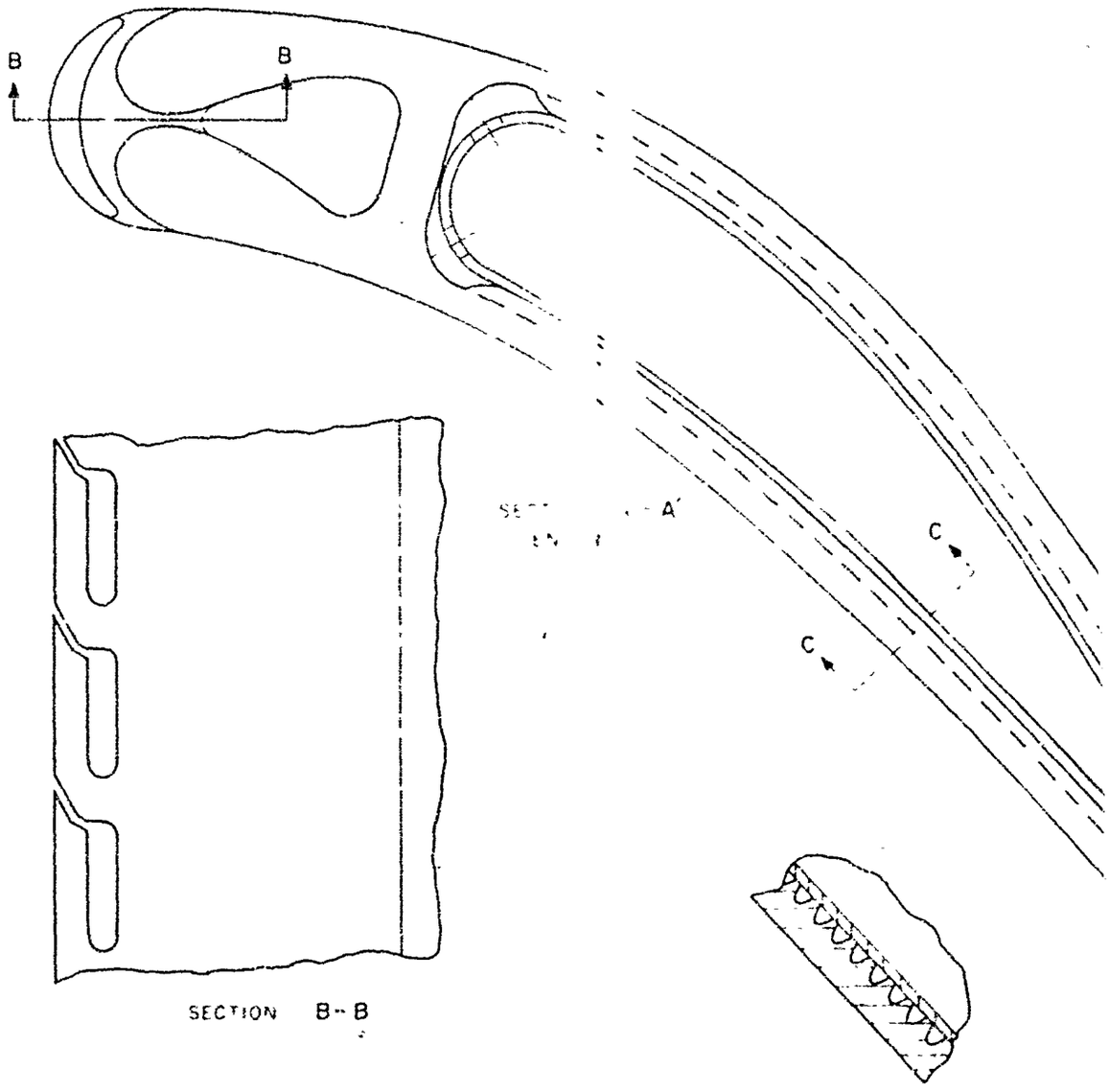
FIRST-STAGE TURBINE D[illegible] HAR[illegible] DO[illegible]
SHIELDED VANE

Figure 2-10b


1690
1800
1690
720

SUPERSONIC CRUISE
75% SPAN
3.5% COOLING AIRFLOW $\left(\frac{Wa\ COOLANT}{Wa\ ENGINE}\right)$



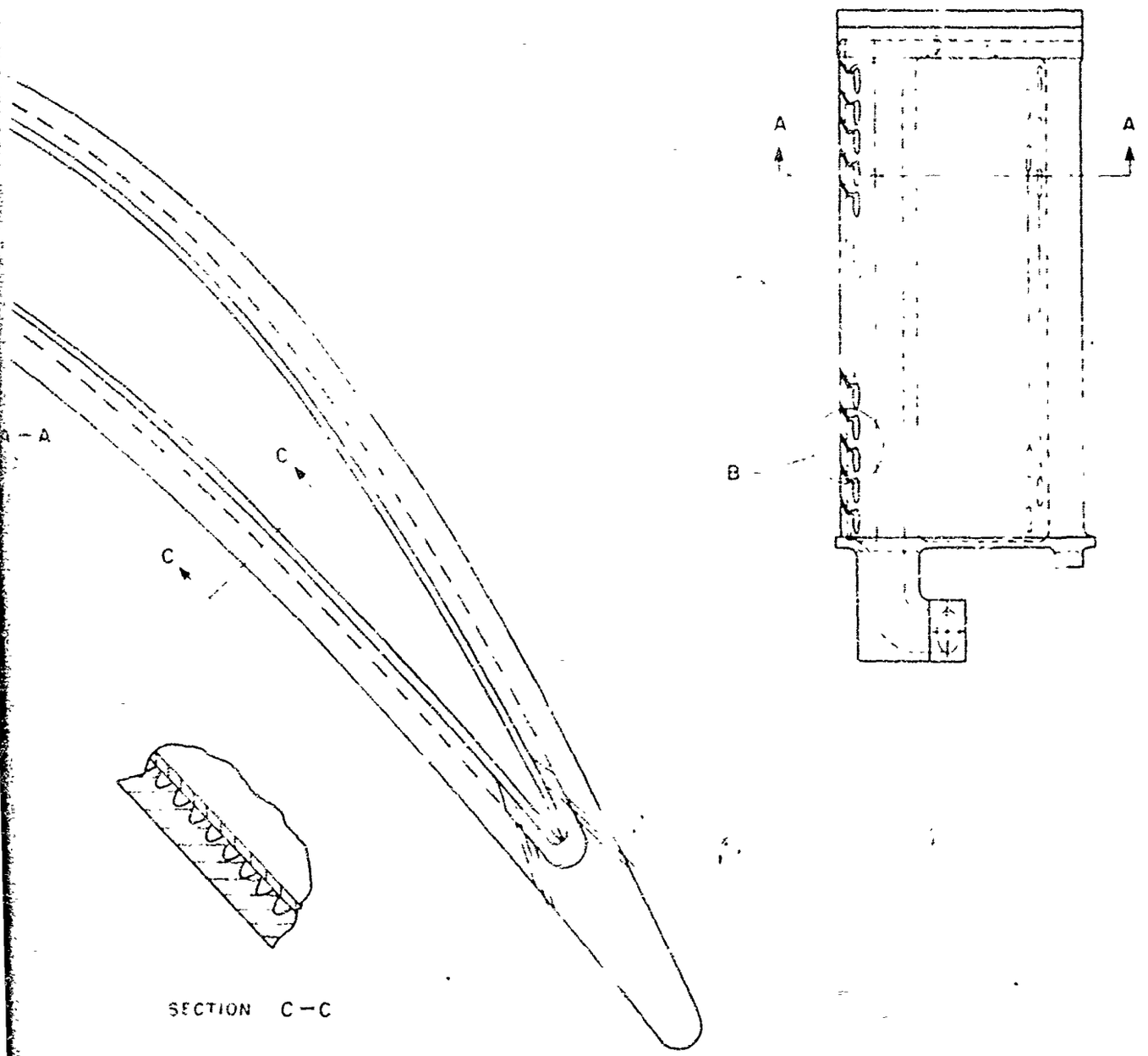


SECTION B-B

SECTION C-C

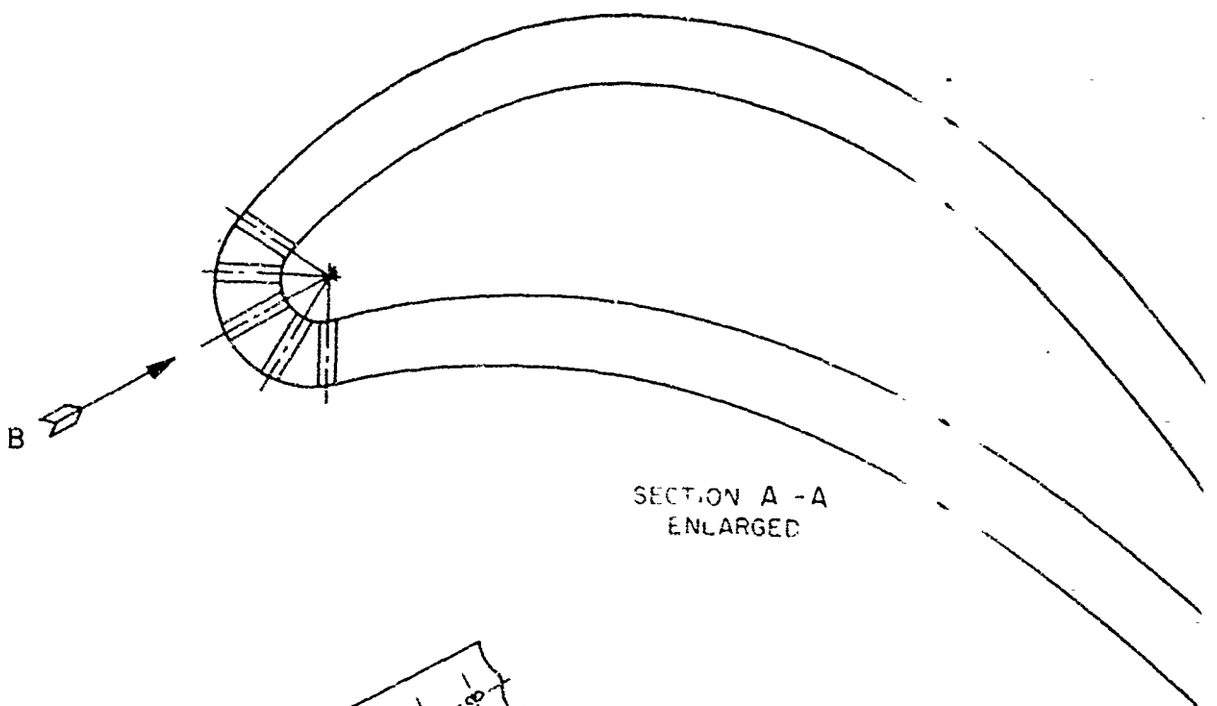
FIRST-STAGE TUI
L

SUPERSONIC CRUISE
3.5% Cooling Air

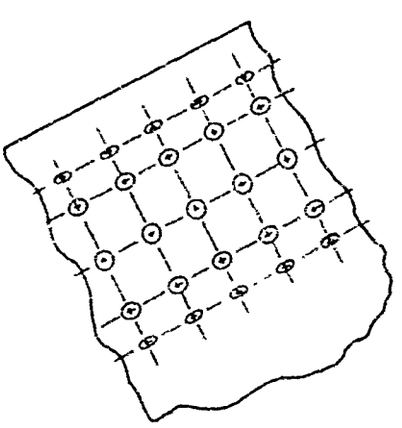


FIRST-STAGE TURBINE VANE WITH INTEGRALLY CAST LEADING EDGE SHIELD

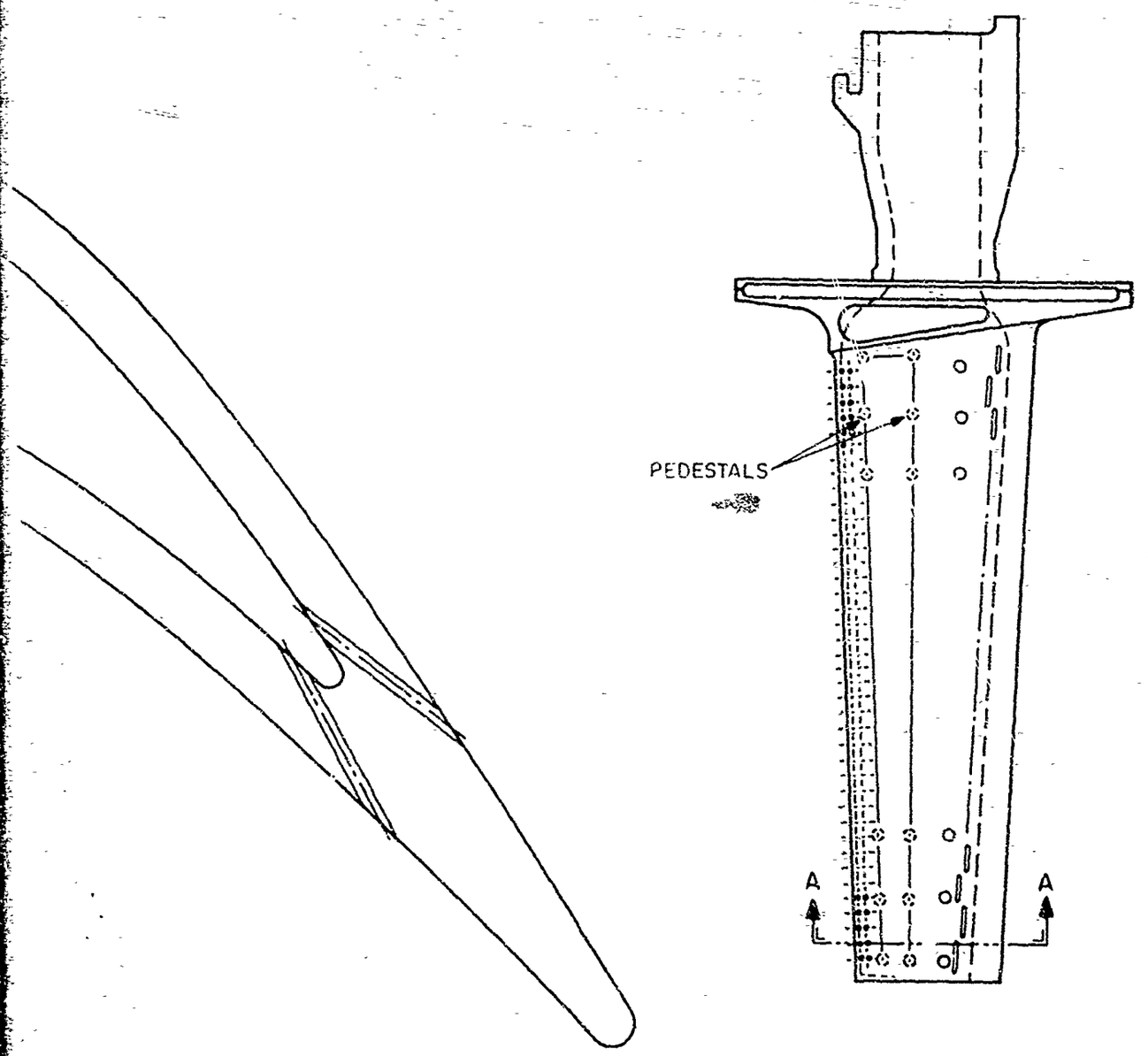
Figure 2-10a



SECTION A -A
ENLARGED

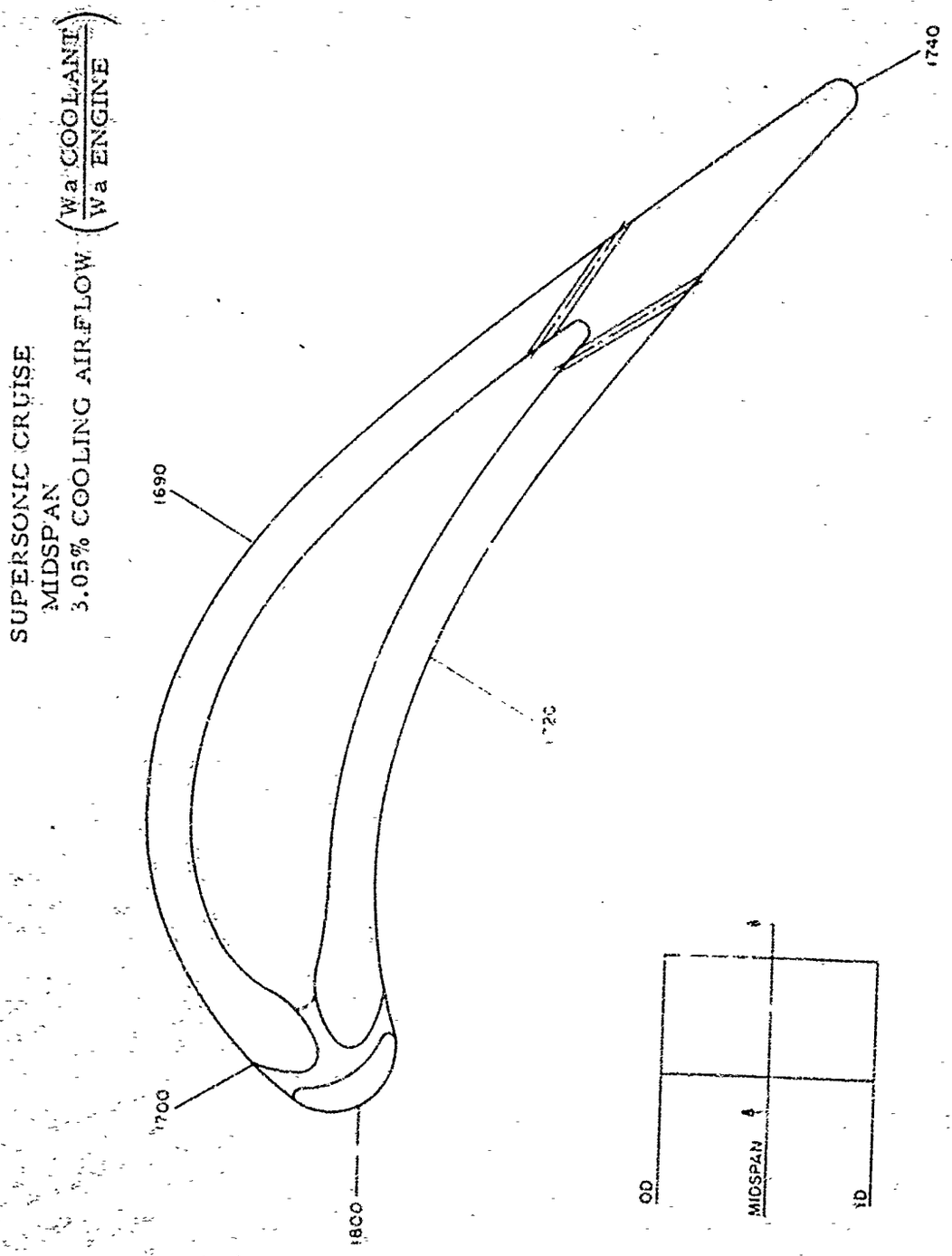


VIEW IN DIRECTION B



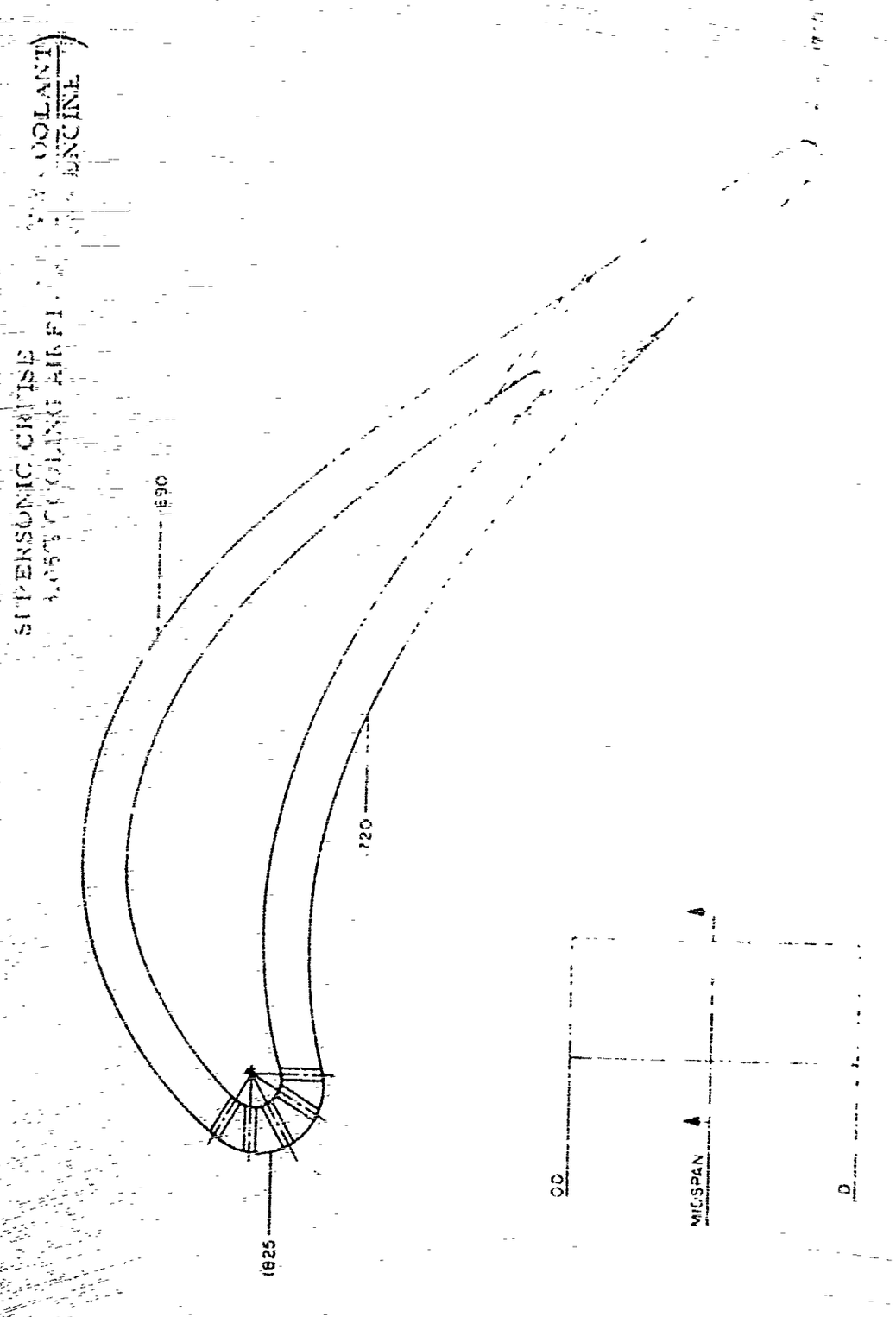
FIRST-STAGE TURBINE SHOWERHEAD BLADE

Figure 2-109



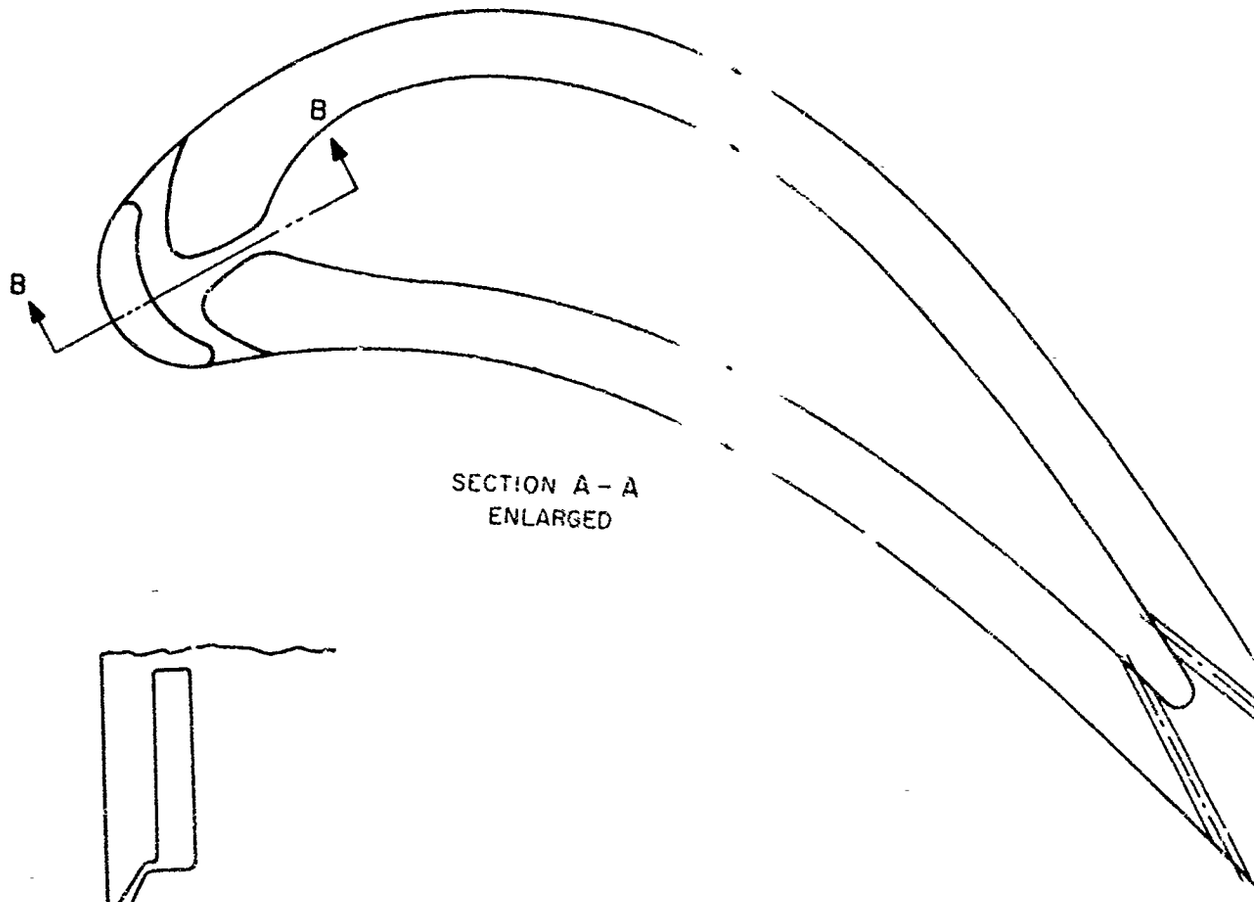
FIRST-STAGE TURBINE INTEGRALLY CAST SHIELDED BLADE/PREDICTED STEADY STATE METAL TEMPERATURE, °F

Figure 2-114

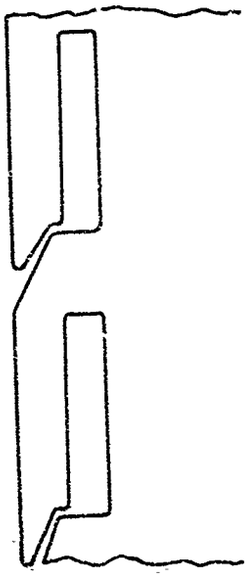


FIRST-STAGE TURBINE SHOWERHEAD BLADE/PREDICTED STEADY STATE MIDSPAN METAL TEMPERATURE, °F.

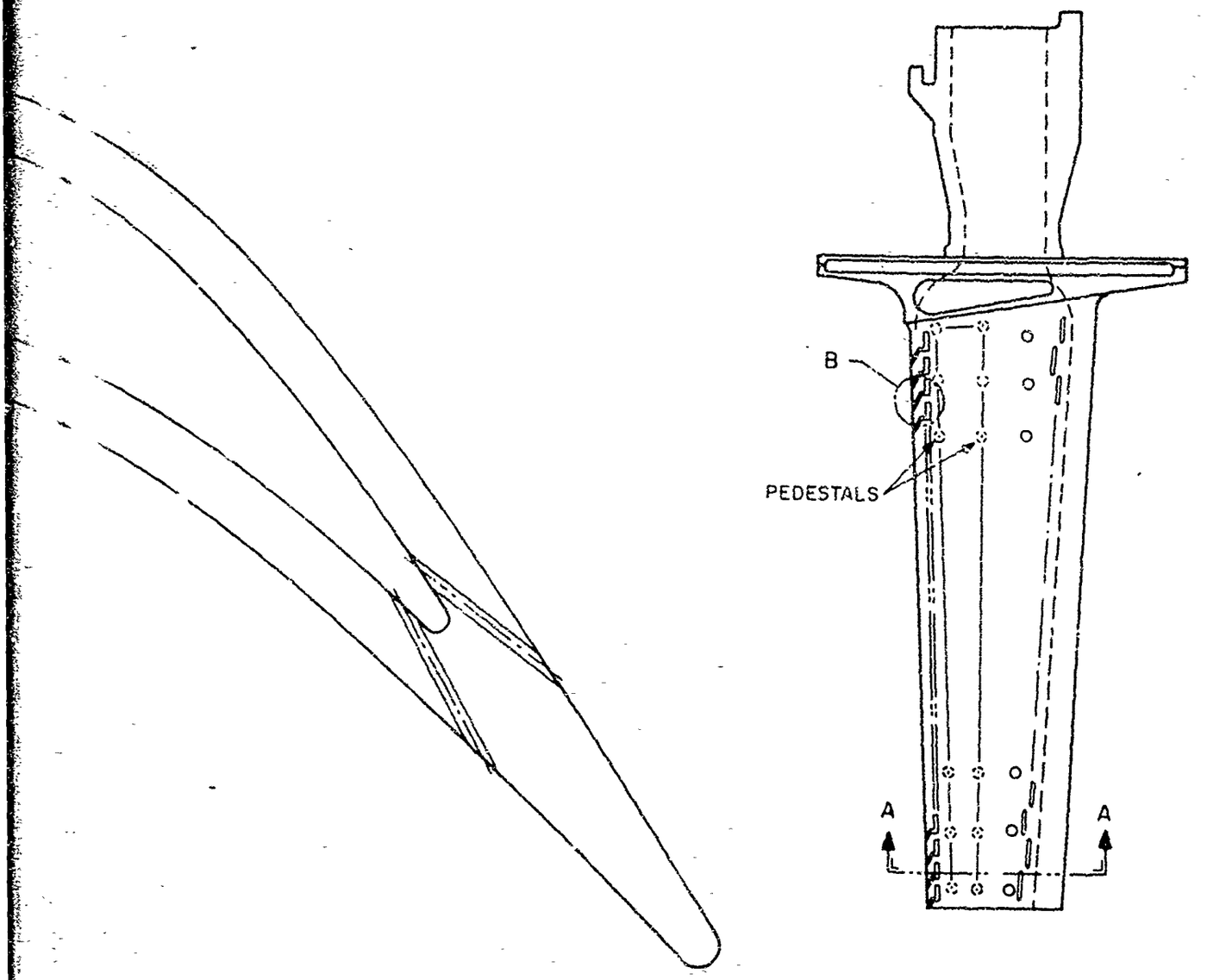
Figure 2-111



SECTION A – A
ENLARGED

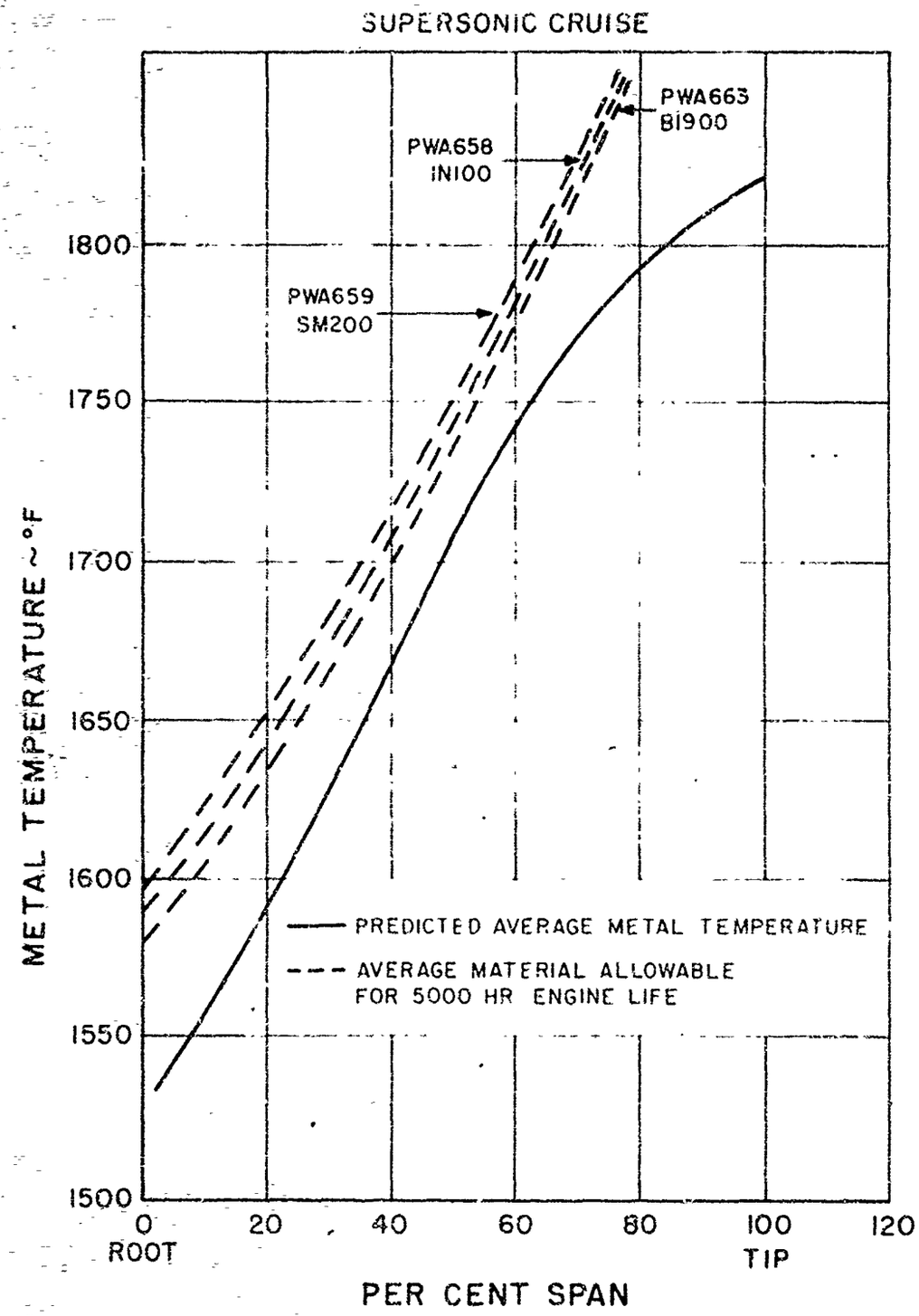


SECTION B – B



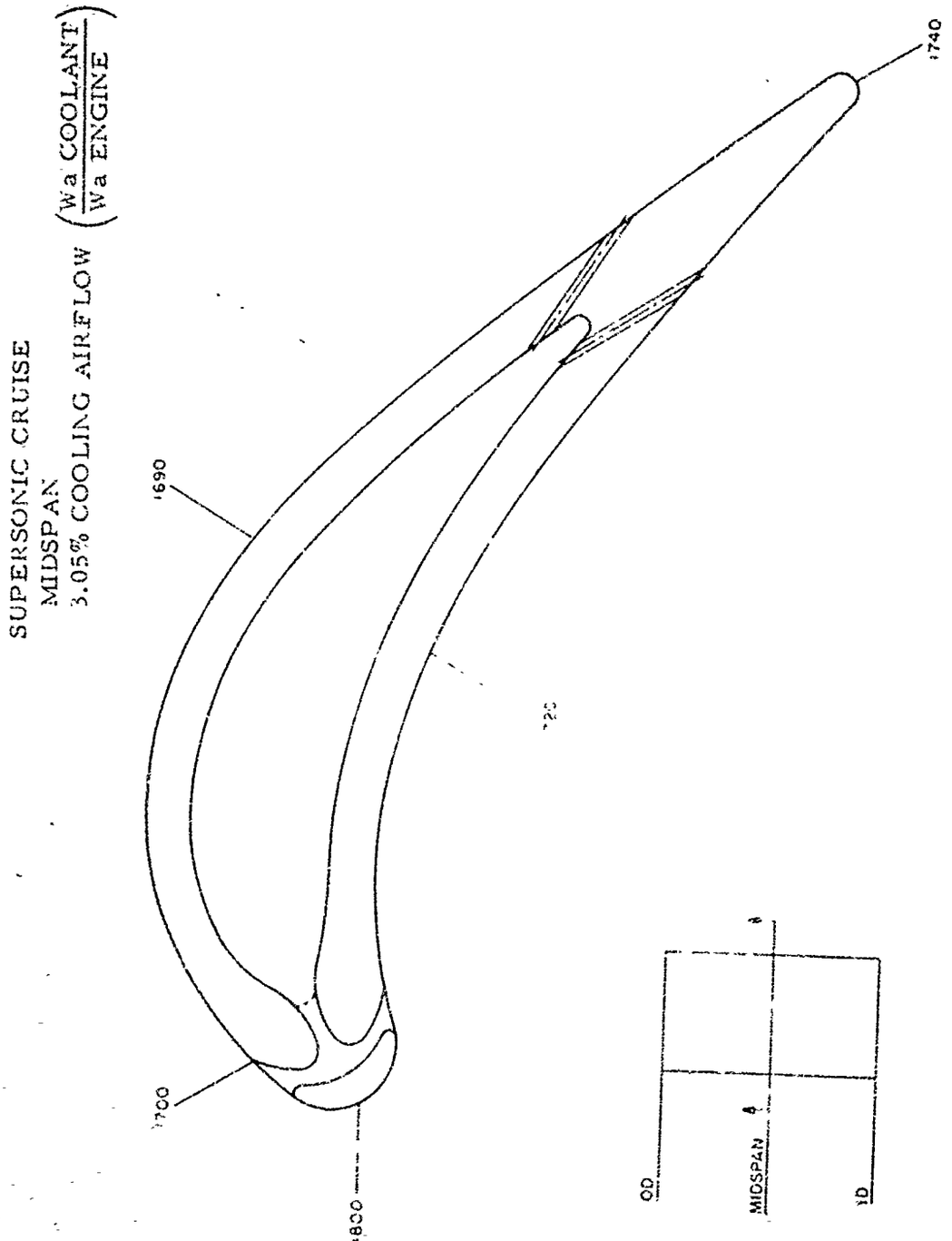
FIRST-STAGE TURBINE BLADE WITH INTEGRALLY CAST LEADING EDGE SHIELD

Figure 2-112



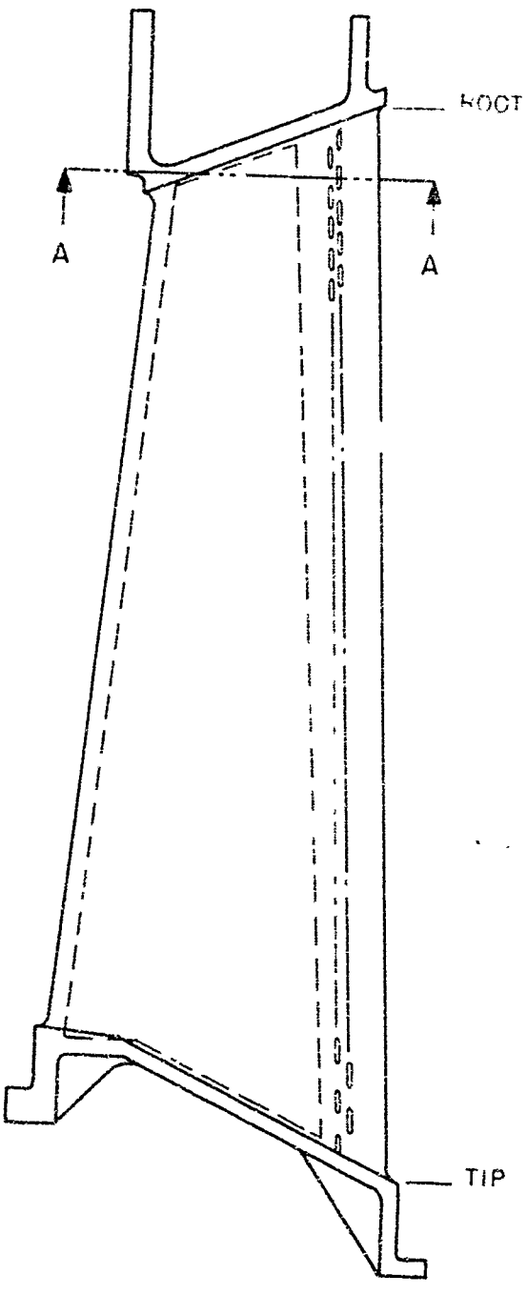
FIRST-STAGE TURBINE INTEGRAL CAST SHIELD BLADE SPANWISE ALLOWABLE AND PREDICTED METAL TEMPERATURE

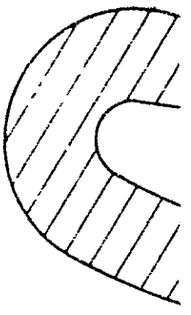
Figure 2-113



FIRST-STAGE TURBINE INTEGRALLY CAST SHIELDED BLADE/PREDICTED STEADY STATE METAL TEMPERATURE, °F

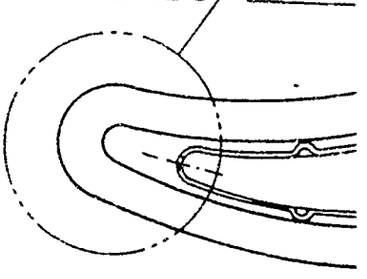
Figure 4-114



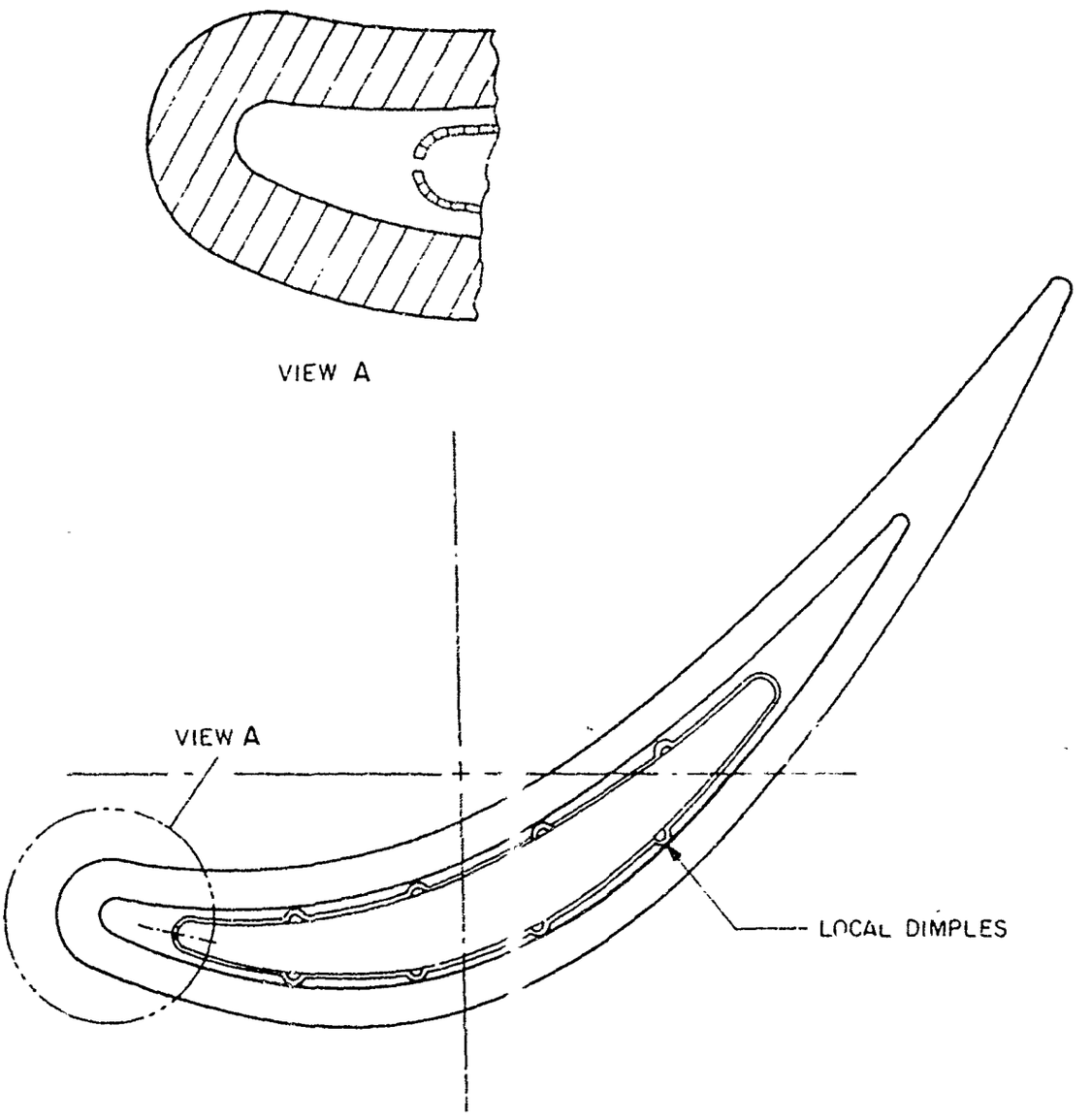


VIEW

VIEW A



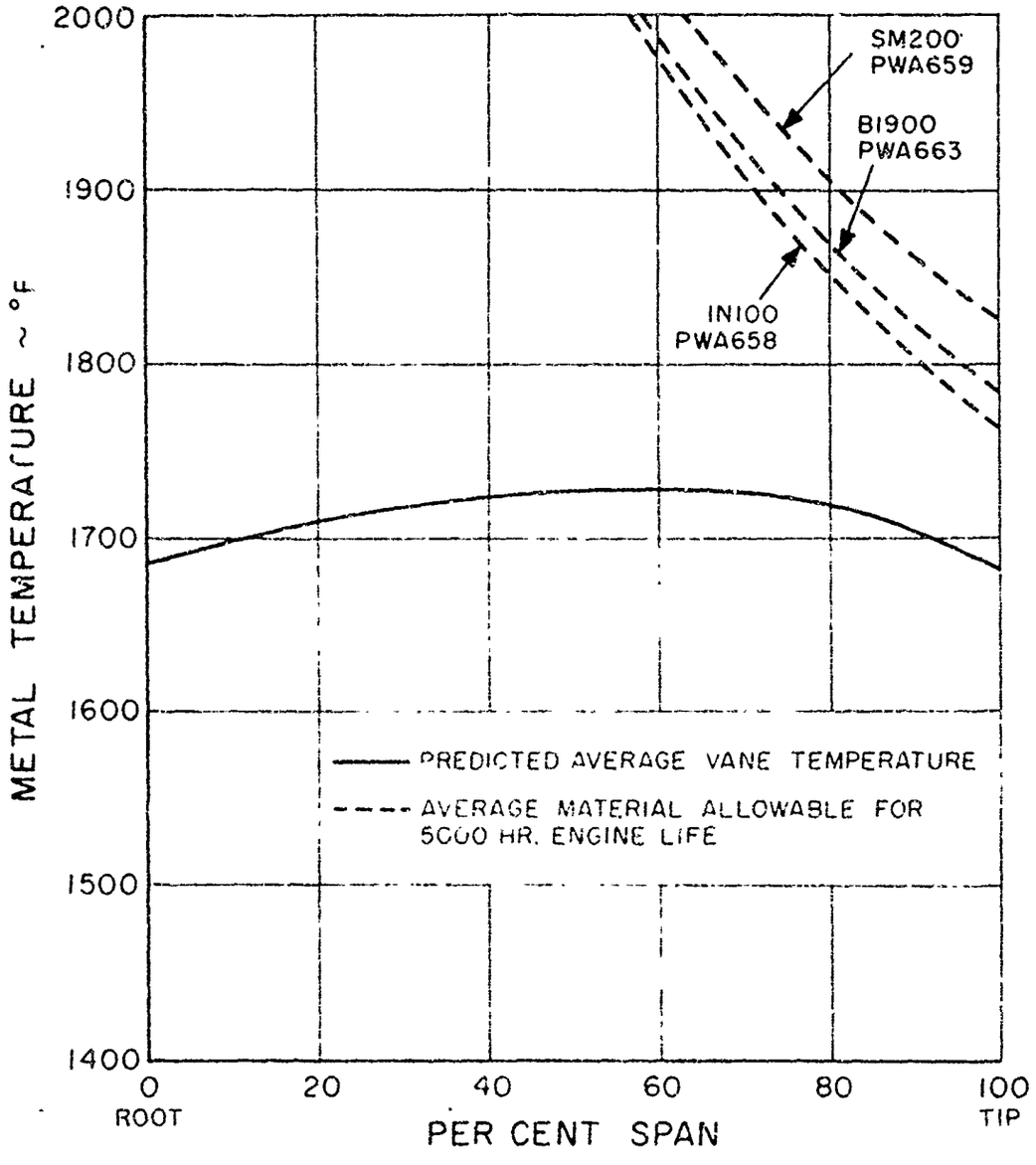
SECOND-STAGE



SECTION A - A

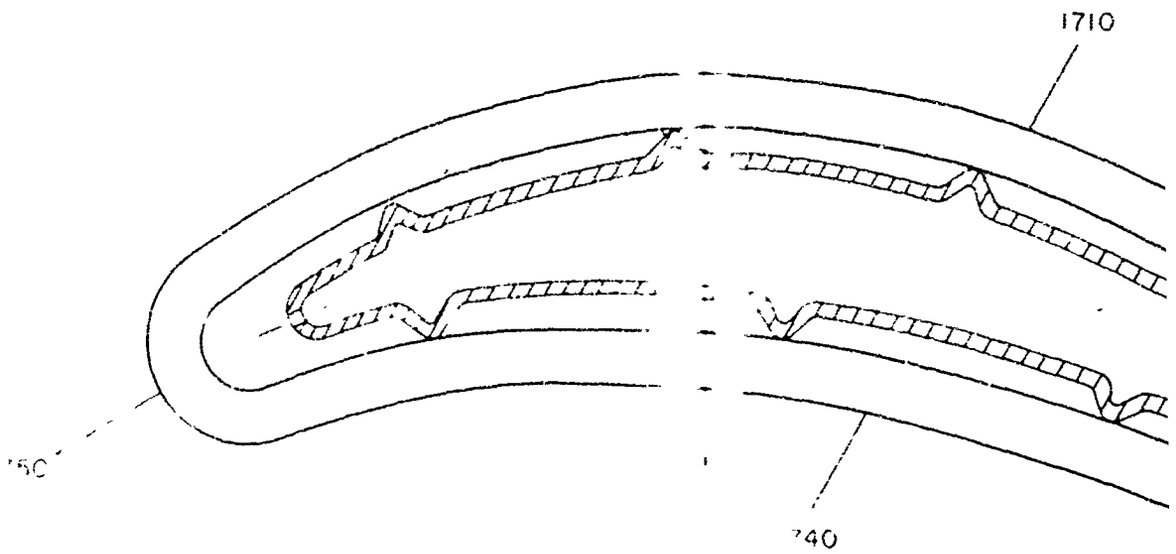
SECOND-STAGE TURBINE IMPINGEMENT COOLED VANE

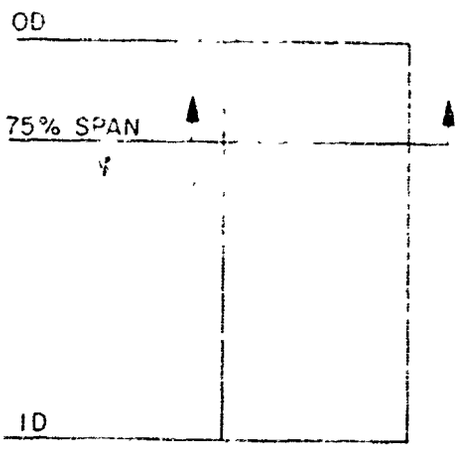
Figure 2-115



SECOND-STAGE TURBINE IMPINGEMENT COOLED VANE SPANWISE ALLOWABLE AND PREDICTED METAL TEMPERATURE

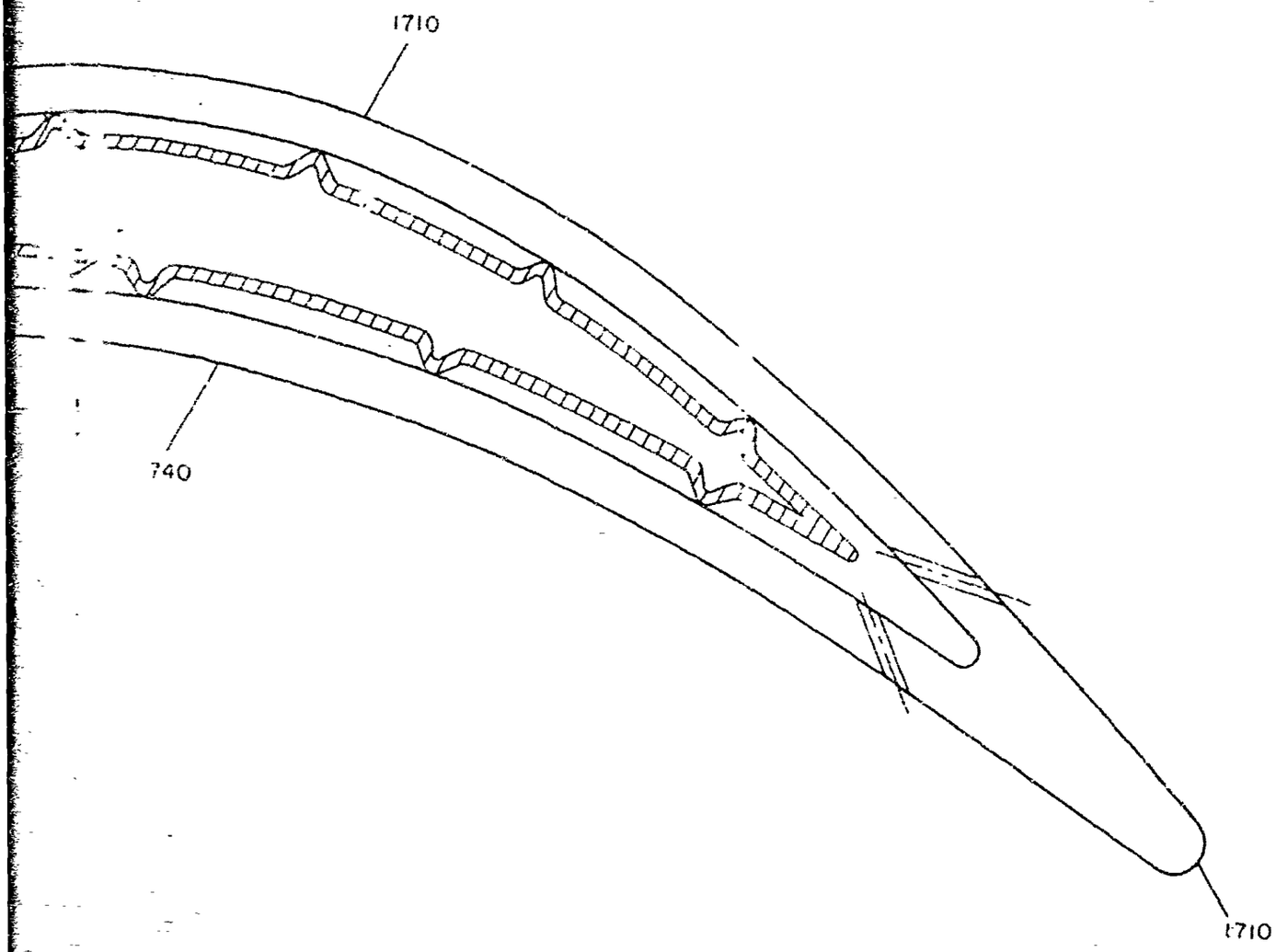
Figure 2-11c





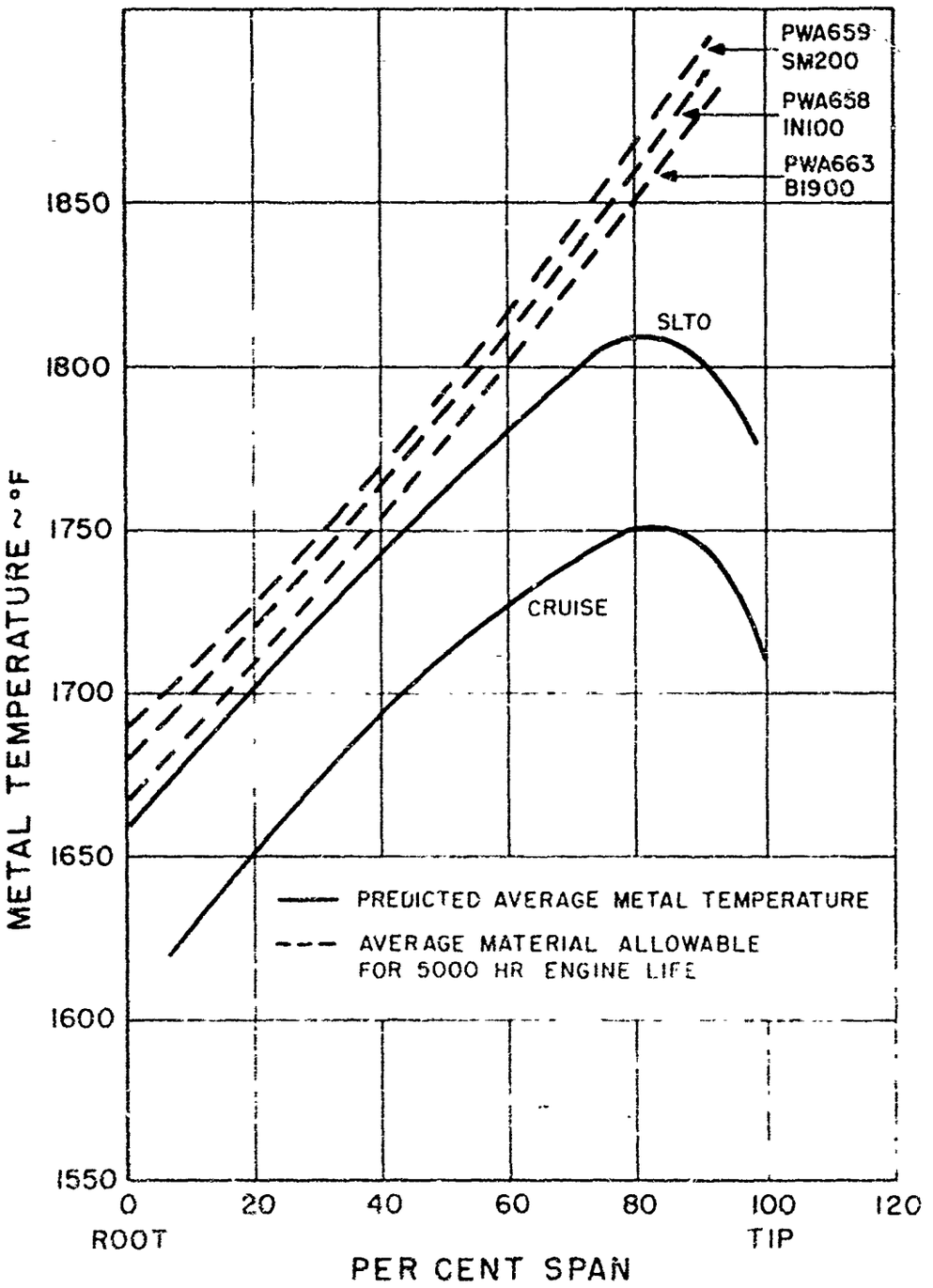
SECOND-STAG
S

SUPERSONIC CRUISE
75% SPAN
2.05% COOLING AIRFLOW $\left(\frac{W_a \text{ COOLANT}}{W_a \text{ ENGINE}}\right)$



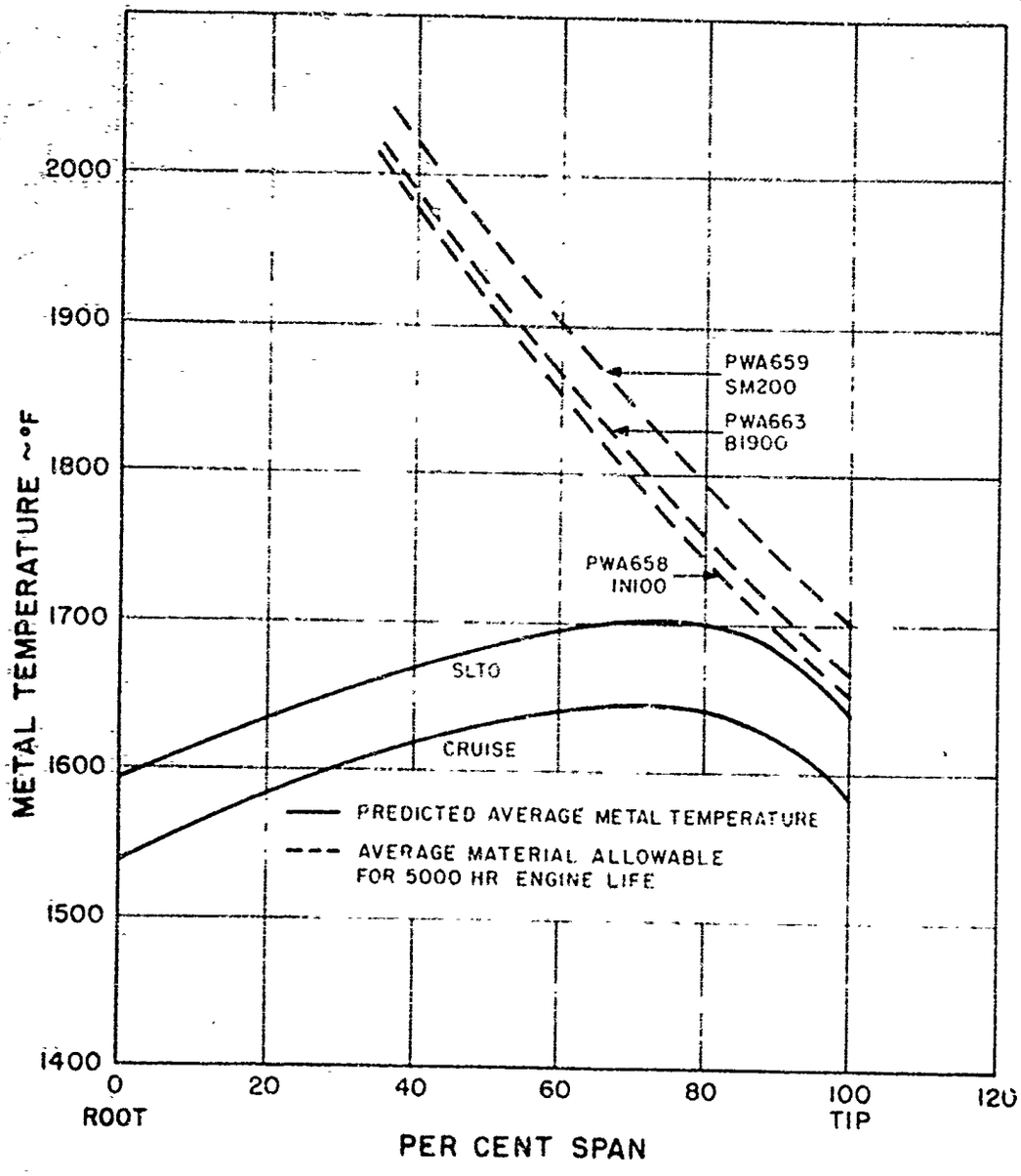
SECOND-STAGE TURBINE IMPINGEMENT COOLED VANE/PREDICTED STEADY STATE METAL TEMPERATURE °F

Figure 2-117



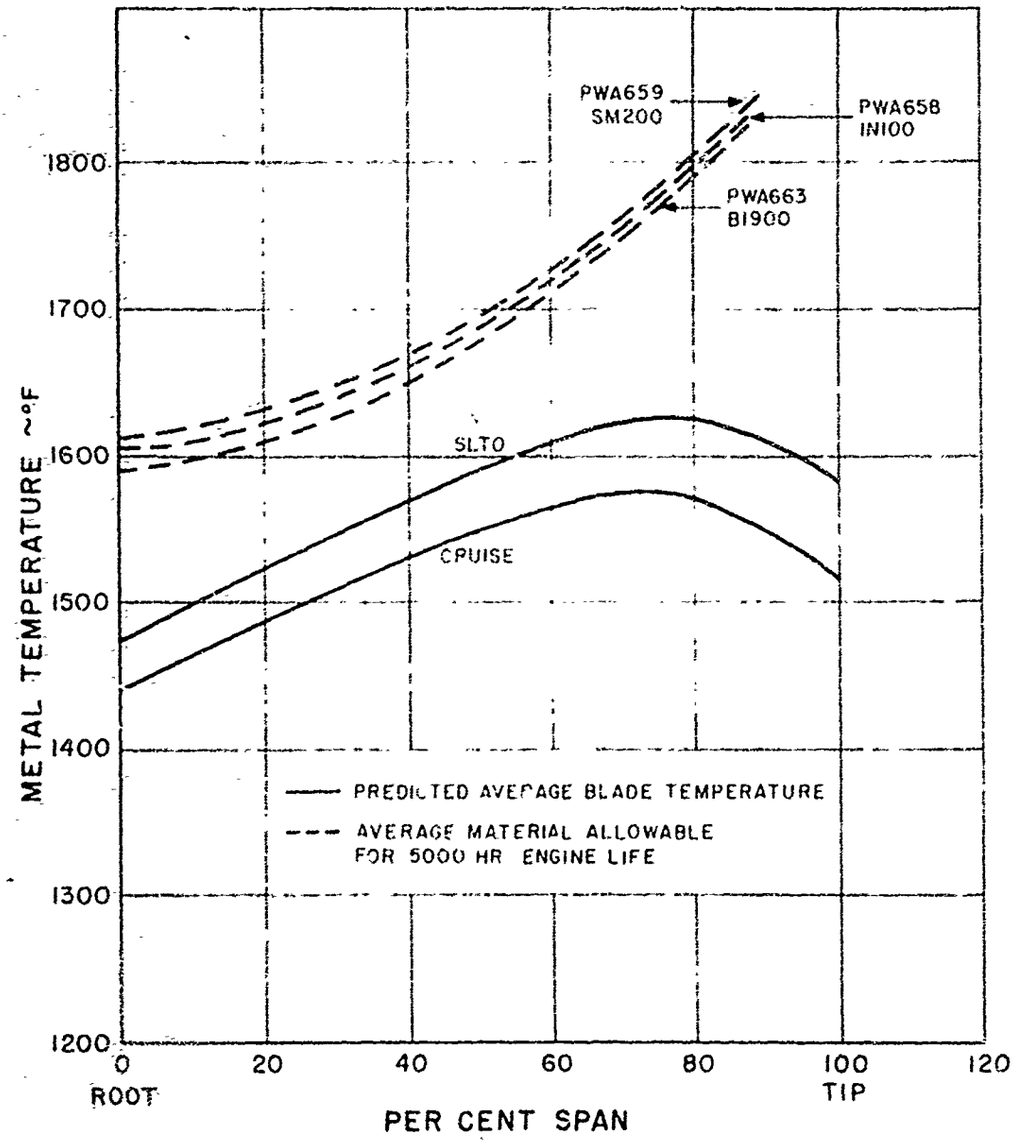
SECOND-STAGE TURBINE UNCOOLED BLADE SPANWISE ALLOWABLE AND PREDICTED METAL TEMPERATURE

Figure 2-118



THIRD-STAGE TURBINE UNCOOLED VANE SPANWISE
ALLOWABLE AND PREDICTED METAL TEMPERATURE

Figure 2-119



THIRD-STAGE TURBINE UNCOOLED BLADE SPANWISE ALLOWABLE AND PREDICTED METAL TEMPERATURE

Figure 2-120

SPECIFICATIONS

ITEM 3 - SPECIFICATION

SUMMARY

This item of the contract required that Pratt & Whitney Aircraft prepare and deliver preliminary coordinated engine model and performance specifications which shall apply specifically to the preliminary engine designs established under Item 2. These specifications, Pratt & Whitney Aircraft Engine Specification No. 2682 for the STF 219-L engine and Pratt & Whitney Aircraft Engine Specification No. 2681 for the STF 219-B Engine were transmitted to the FAA with PWA ltr LCM:mla-Adm. 1N Ref. No. 544A dated 30 October 1964 (CONF).

COMPRESSOR

ITEM 4 - COMPRESSOR DEVELOPMENT

OBJECTIVE

The objective of the Phase II-A program for this item of the contract was the continued development testing of the compressor directed toward the verification of compressor performance. The goal of the program was to develop a two-stage fan without inlet guide vanes having a pressure ratio of 2.5:1 with a design-point efficiency of 84 percent and a 10 percent surge margin, and a five-stage compressor having a pressure ratio of 4.3:1 with a design-point efficiency of 83 percent with a 10 percent surge margin, and a peak efficiency of 88 percent.

A. INTRODUCTION

Testing conducted during Phase II-A of the contract was directed toward the continued development of fan stages and a five-stage compressor designed to meet the performance goals required for the SST engine on an advanced technological level. Advanced levels of stage pressure ratio have been attained, and efforts now are directed toward improvements in stage and overall efficiency which permit advanced levels of engine performance.

B. EXPERIMENTAL PROGRAM

1. SINGLE-STAGE FAN RIG

The single-stage fan rig was brought into the Phase II-A program to augment stress-reduction development of the first-stage rotor of the two-stage fan. This stress-reduction development program was undertaken as a result of high stress levels encountered in initial tests of the two-stage fan rig. Total operating time on the single-stage fan during the Phase II-A program was seven hours.

Modifications made to this rig from the previous build, described in the final report PWA-2353 for the previous SST R&D contract [AF33 (657)-11189], included additional rotor camber to obtain a higher rotor pressure ratio and increased stator root convergence to reduce the

DOWNGRADED AT 3 YEAR INTERVALS
DECLASSIFIED AFTER 12 YEARS
DOD DIR 5200.10

THIS DOCUMENT CONTAINS INFORMATION AFFECTING THE NATIONAL DEFENSE OF THE UNITED STATES WITHIN THE MEANING OF THE ESPIONAGE LAWS, TITLE 18, U.S.C., SECTIONS 793 AND 794. THE TRANSMISSION OR THE REVELATION OF ITS CONTENTS IN ANY MANNER TO AN UNAUTHORIZED PERSON IS PROHIBITED BY LAW.

stator loading and losses. The mid-span shrouds at each alternate blade gap were welded together to reduce the possibility of a disk-blade-shroud coupled vibration mode and to achieve a significant reduction in rotor stress levels. This shroud configuration, termed a segmented shroud, has narrow shrouds located at 68.8 percent of the blade span. These shrouds have a root thickness-to-chord ratio of seven percent and an aspect ratio of 2.5.

This rotor assembly, without welded shrouds as shown in Figure 4-1, was originally tested in the two-stage fan rig, but the test was terminated because of excessive stresses. The welded-shroud version of the same rotor is shown in Figure 4-2.

On the first test of the segmented shroud configuration, the speed was held for a short time at 3,800 rpm, where the 2E resonance occurred. The following discussion of stresses during this test presents raw strain gage data for comparison only. At 3,800 rpm the stress at the root leading edge increased to ±15,000 psi; at the point of maximum thickness in the root and the point of maximum thickness above the shroud the stress increased to ±6,000 psi. Subsequent accelerations were made and the stress at the root leading edge was ±10,000 psi; at the points of maximum thickness the stress was ±4,000 psi. Since the speed was well below probable engine idle speeds, 2E resonance will not limit the safe operating region of this rotor. Above 4,000 rpm all stresses were below ±7,000 psi. A pressure ratio of 1.6:1 was achieved at design speed and no indication of flutter was encountered.

After operation of about one hour at design speed, a change was observed in the stress pattern at the maximum thickness point above the shroud. The stress at this point increased from ±5,000 to ±7,000 psi. Since the change in stress occurred with no apparent change in operating conditions, the rig was shut down for inspection. Cracks were found in two of the welded shrouds about 0.4 inch from the weld region. The cracked shrouds were rewelded, and additional strength was provided by increasing the shroud chord by weld puddling.

Analysis of the limited test data available from the single-stage fan rig indicates that the expected increase in rotor and stage pressure ratio was attained with no significant efficiency penalty compared to the original design of the stage. Analysis of the stress data show that the segmented shroud is at least as stable as the previous conventional shroud. Maximum rotor pressure ratio attained at design speed was 1.73:1 for the segmented shroud and 1.725:1 for the thick shroud.

Maximum stage pressure ratio attained at design speed was 1.68:1 for the segmented shroud and 1.69:1 for the thick shroud. Figure 4-3 shows that the pressure ratios with both shrouds were higher than in previous tests of this fan stage. A significant flow penalty resulted with the thick shroud. However, as a result of these tests, a thick shroud configuration with the shroud pitch angle changed for improved incidence was chosen for subsequent two-stage fan investigations.

2. TWO-STAGE FAN RIG

The two-stage fan rig, with its radius ratio of 0.35, is not a direct scale version of the STF219 engine fan, which has a radius ratio of 0.40. However, the relative performance goals based on this difference in radius ratio are comparable. Views of the assembled rig and its test stand installation are shown in Figures 4-4 and 4-5, respectively. Total operating time on the two-stage fan during the Phase II-A program was 4.5 hours.

The latest fan configuration incorporates first-stage blades with thick, conical mid-span shrouds; the blades are restaggered three degrees open as compared with previous tests in an attempt to regain the flow loss noted in the single-stage tests. The variable first-stage stator utilizes an increased number of "J"-airfoil vanes with an increased root convergence. The second-stage rotor blades have a thick shroud and an increased root diameter to match the first-stage stator convergence; the second-stage blades were recambered to maintain the previous average work level. The second-stage stator employs an increased root and tip convergence to decrease the stator loading and losses; in addition, the vanes were recambered to match the altered second-stage rotor. Finally, the exit guide vanes have been recambered to match the revised second stage. A comparison of the original design flow-path and the revised flow-path with increased root convergence is shown in Figure 4-6.

At the beginning of the test of this configuration, a complete stress survey was made with no abnormally high stresses recorded or observed. Shortly after beginning the next phase of the test, a failure of a second-stage blade occurred in an area of the blade not normally strain gaged and not considered as a high stress location. Continual stress monitoring during the test gave no indication of imminent failure. The blade failure occurred before any significant data were obtained. Investigation of the stress records and of the blade design are being continued in an effort to determine the cause of the failure.

3. MULTISTAGE COMPRESSOR

The six-stage variable stator compressor rig used in the previous SST contract, and shown in Figure 4-7, was converted to a five-stage rig by removal of the fifth-stage stator and sixth-stage rotor. This was done to make the revised compressor rig compatible with the pressure ratio requirement of 4.4:1 for the STF219 engine high-pressure compressor. The previous six-stage compressor rig had a design pressure ratio of 5.67:1. No external differences are obvious between the five- and six-stage compressor rigs. Three configurations of the five-stage rig were built and tested during the Phase II-A development program, and the total operating time on the rig was 78 hours.

The first build of the five-stage compressor rig utilized a reduced degree of reaction to provide an improved balance between rotor and stator inlet Mach numbers. Based on a gap-chord ratio correlation study, an increased number of rotor blades that were rest-ggered open were used in all stages in an effort to decrease rotor losses. In addition, cantilevered stator vanes were employed in stages three, four and five. In this design the inner stationary shrouds were removed from these stators to reduce the stator losses. All of these changes were directed toward an increase in the efficiency level.

Testing of this first build of the five-stage compressor was terminated before completion of the planned program because of an increase in stress and vibration levels. The teardown inspection revealed that the cantilevered third-stage stator vanes had rubbed through the rotating inner shroud, resulting in rotor imbalance and flow recirculation at the root of the stator vanes. Also, there was evidence of moderate rubbing of the rotor blade tips.

Analysis of the limited available data, which did not include the optimum stator setting, indicated a choked operating condition in the front stages and an accompanying flow penalty. The rubbing of the rotating inner shroud may have contributed to the observed flow penalty. A study of throat area correlations, made subsequent to the design of this configuration, predicted insufficient throat area in the rotors.

The second build of the five-stage rig was similar to the first five stages of Build 8 of the six-stage compressor (described in Report No. PWA-2353) except that the vanes in the first three stators and the blades in the third stage were uncambered at the leading edge. This was done to alleviate a choking condition that was indicated in the data analysis of Build 8A of the six-stage compressor rig.

DOWNGRADED AT 3 YEAR INTERVALS
DECLASSIFIED AFTER 12 YEARS
DOD DIR 5200.10

Analysis of the test data from the second build of the five-stage rig showed that the design pressure ratio was achieved at design speed with a flow capacity of 99 percent of the design value. Efficiency levels were better than any previously attained with the multistage compressor rig. The overall performance of this configuration compared with the desired performance, based on the prediction for the STF219 high-pressure compressor, is shown in Figure 4-8. To achieve the optimum performance of the second build of the compressor, it was necessary to rotate the first three stators in the closed direction by an amount approximately equal to the amount that the vanes were uncambered.

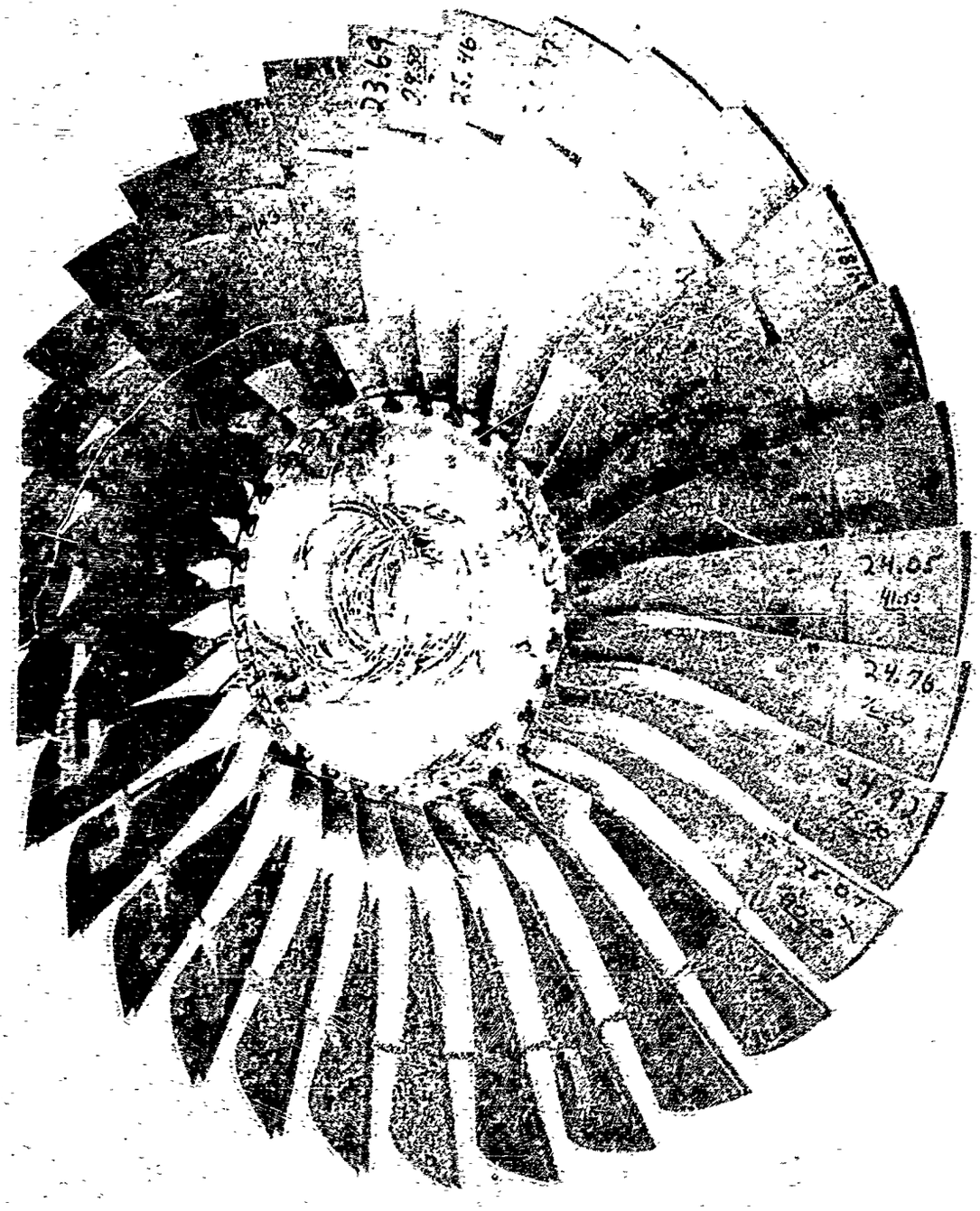
The third build of the five-stage rig was a revision of the low gap-chord ratio configuration of the first build. Compared to the first build, the third build used a first-stage rotor whose blades were restaggered two degrees closed, a second-stage rotor whose blades were restaggered one degree open and over-cambered at the trailing edge, and stator vanes in stages one through four that were uncambered and had a decreased gap-chord ratio.

Analysis of the test data from the third build of the five-stage compressor rig showed a significant improvement in performance over that of any previous configuration. Overall performance for build three, compared with the STF219 predicted performance, is shown in Figure 4-9. Figure 4-10 illustrates the efficiency gain achieved with this compressor configuration as compared with previous builds. Airflow capacity was 99.7 percent of the desired flow, and a design flow surge margin of 5.75 percent was achieved.

Following the calibration of the third build of the compressor, the part-span shrouds were removed from the first-stage rotor blades in an effort to further improve efficiency levels. However, excessive linear vibration permitted only preliminary operation and necessitated removal of the rig from the test stand before performance data could be obtained.

Test results from the multistage compressor rig to date indicate that, with continued development, the requirement for 83 per cent design point efficiency and a ten per cent surge margin can be met.

DOWNGRADED AT 3 YEAR INTERVALS;
DECLASSIFIED AFTER 12 YEARS
DOD DIR 5200.10



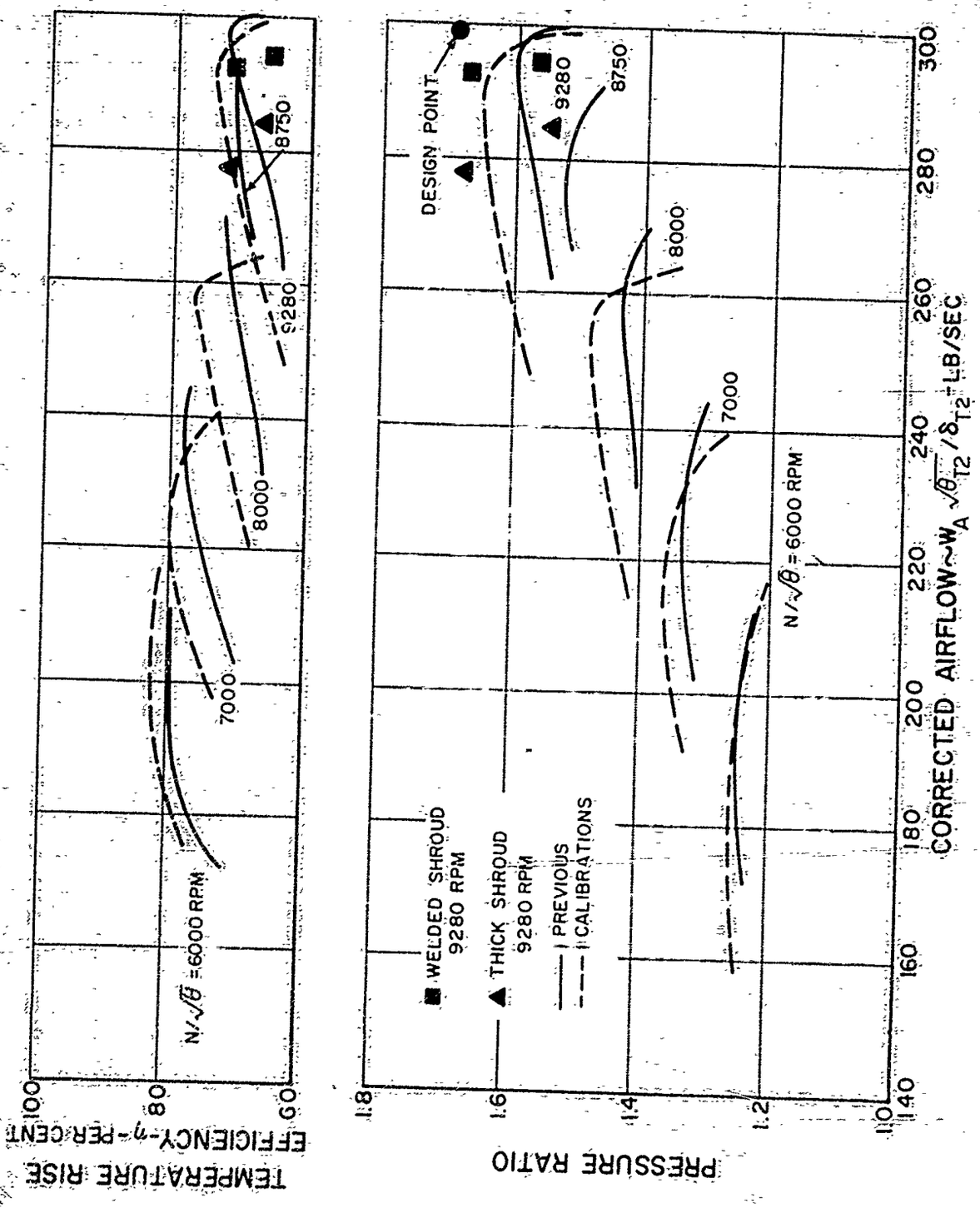
TWO-STAGE FAN RIG
FIRST-STAGE ROTOR ASSEMBLY

Figure 4-1



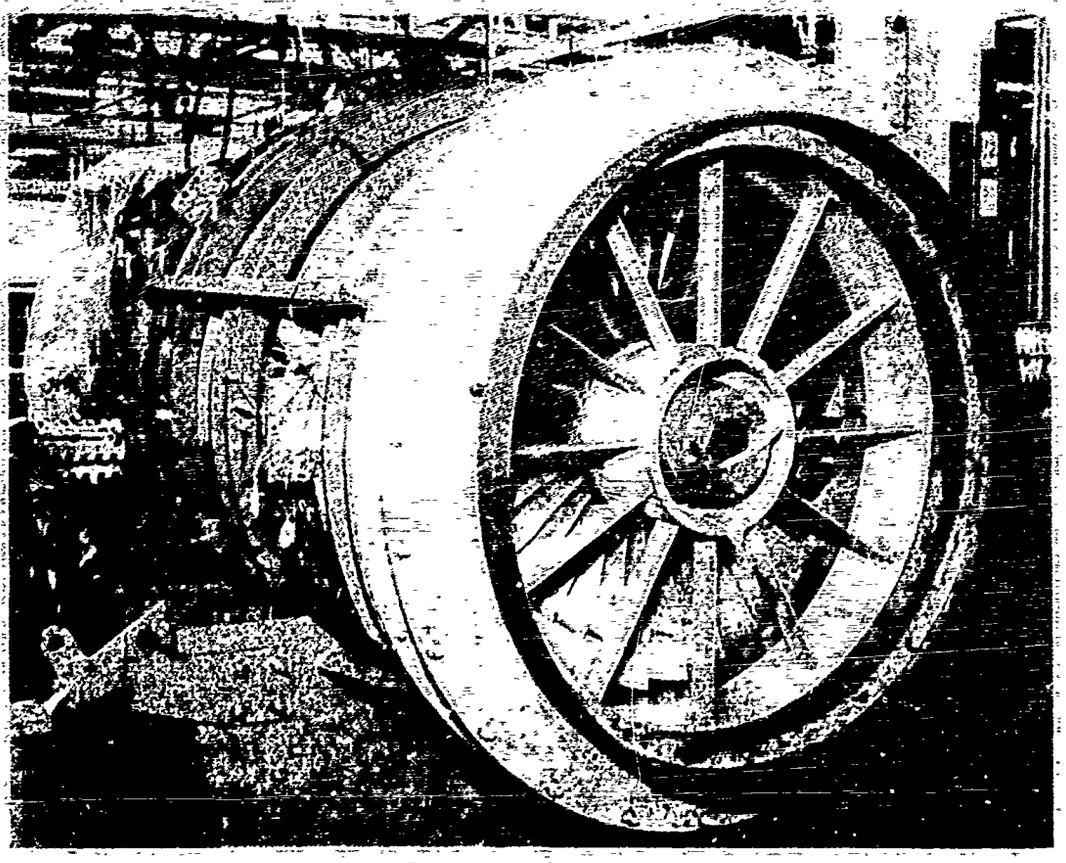
DETAIL OF ROTOR ASSEMBLY WITH WELDED MID-SPAN SHROUDS FOR TEST IN SINGLE-STAGE FAN RIG

Figure 4-2



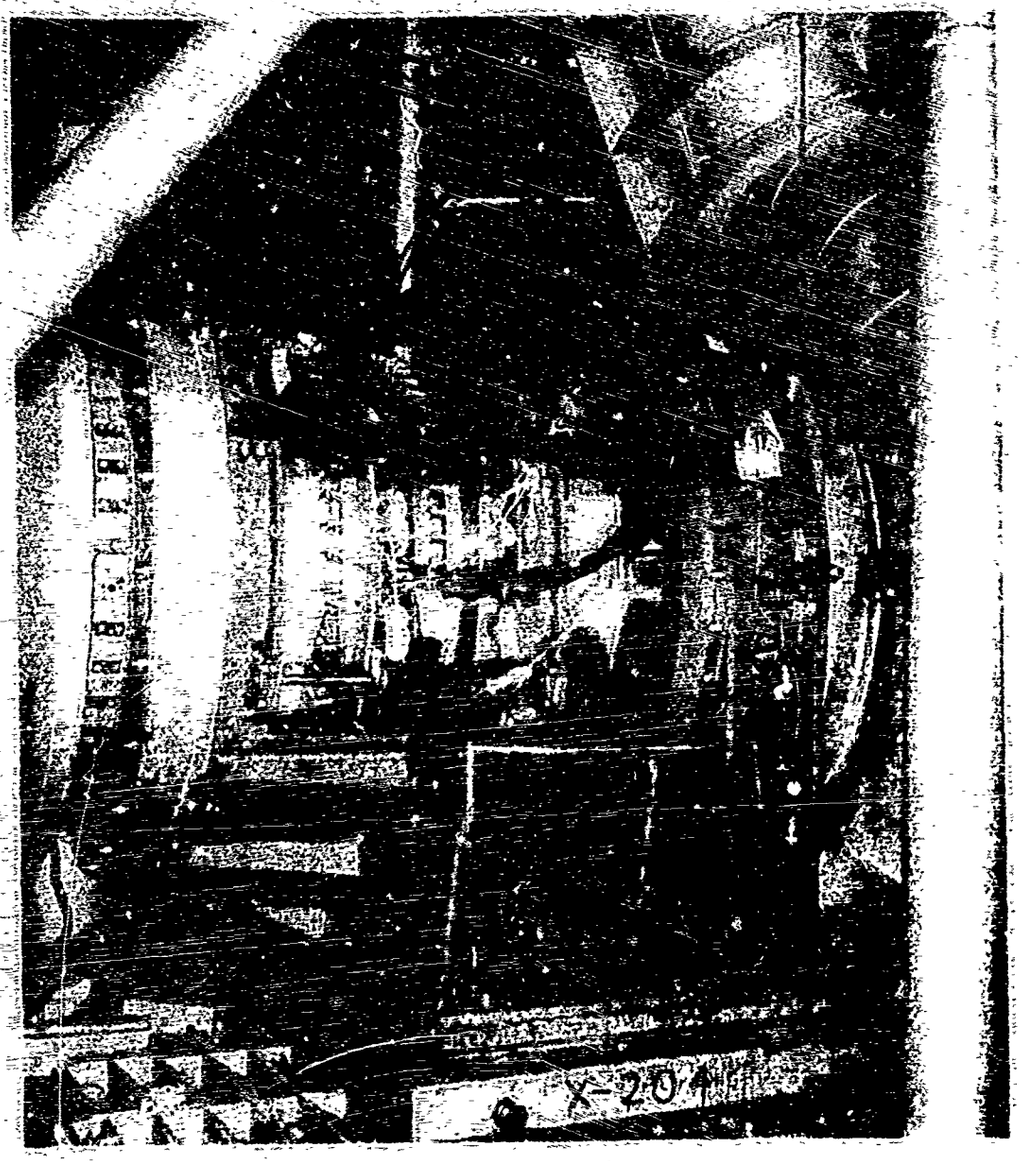
COMPARISON OF SINGLE-STAGE FAN PERFORMANCE WITH SHROUD MODIFICATIONS

Figure 4-3



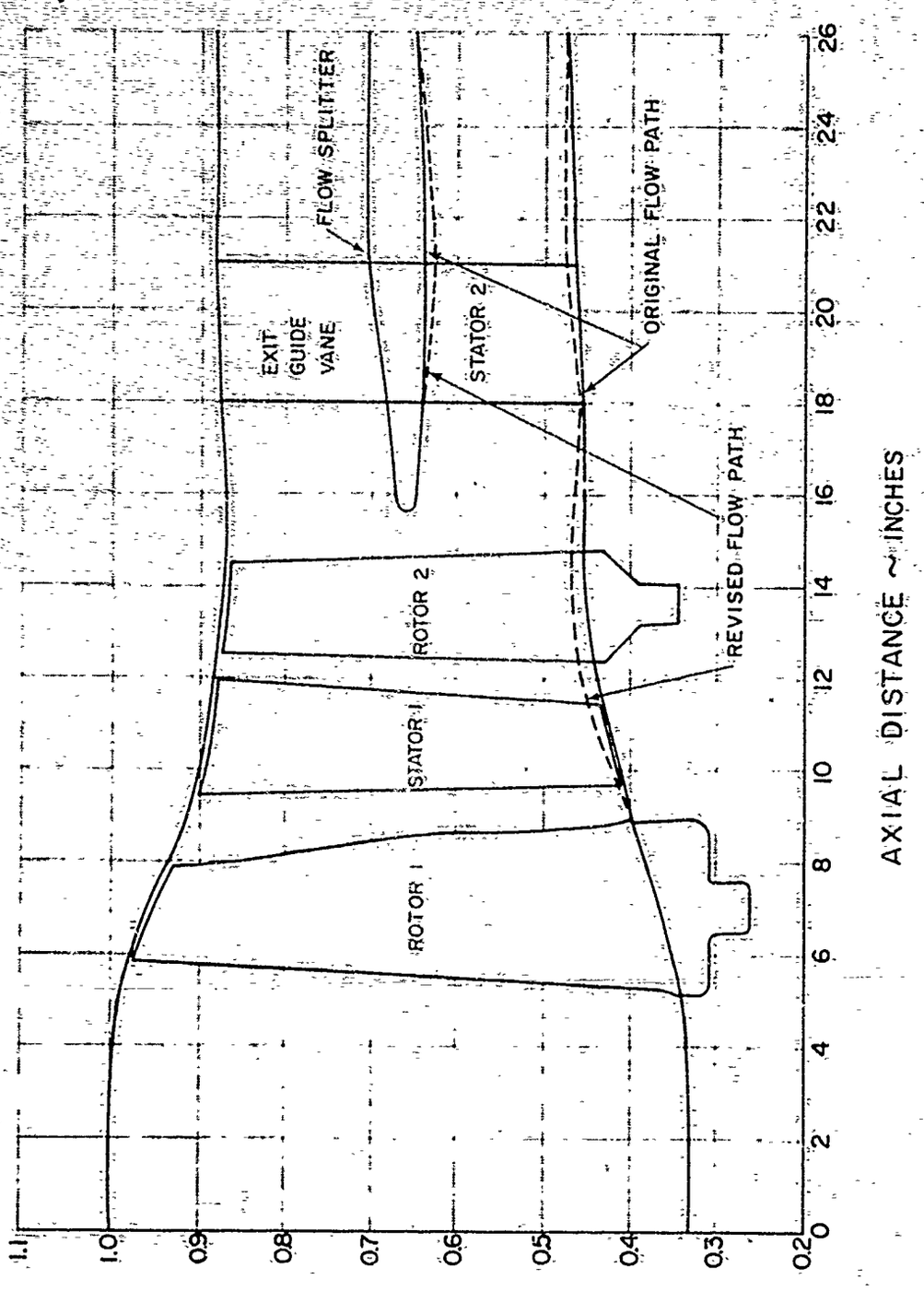
ASSEMBLED VIEW OF TWO-STAGE FAN RIG

Figure 4-4



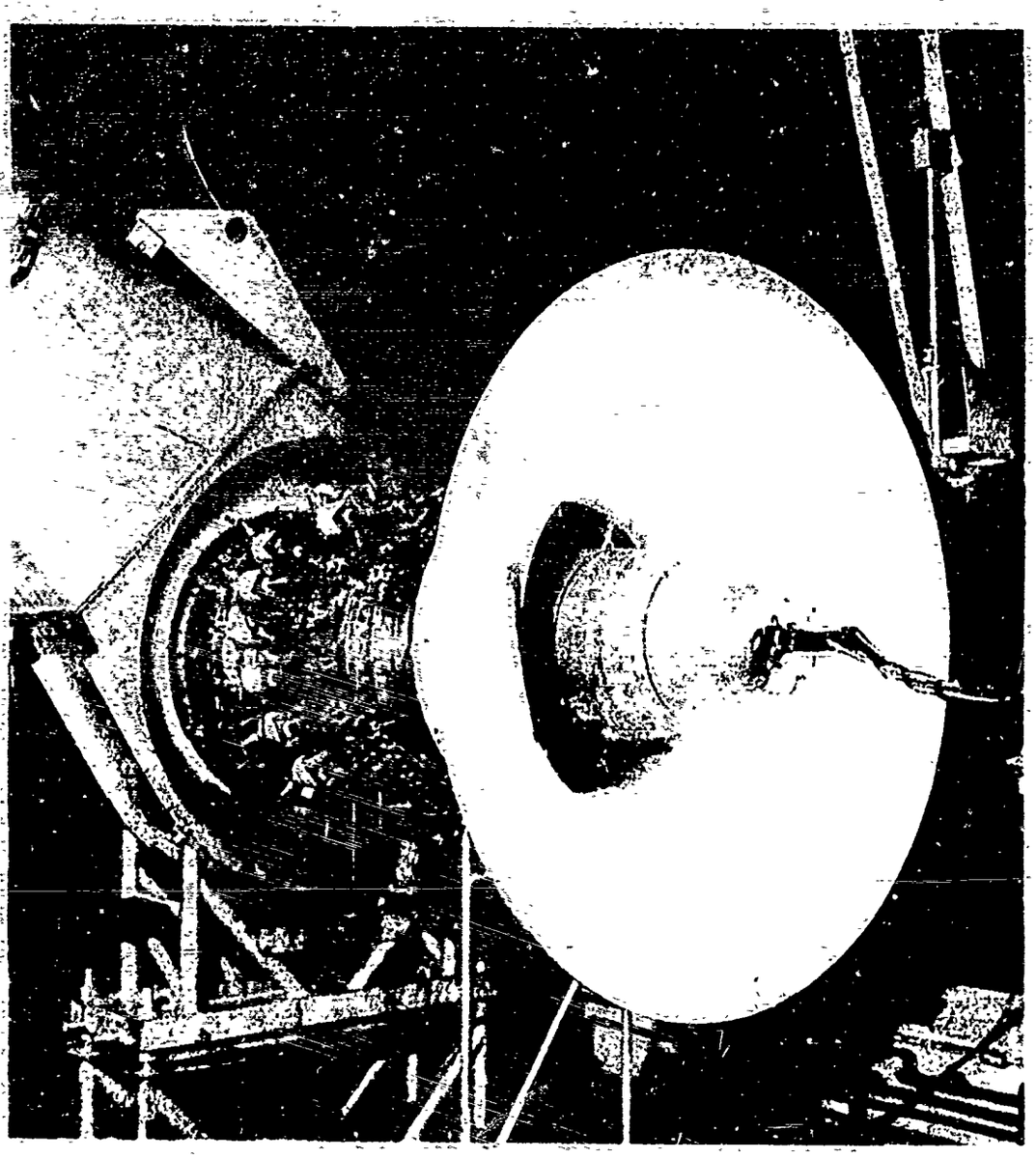
TWO-STAGE FAN RIG INSTALLED ON TEST STAND

Figure 4-5



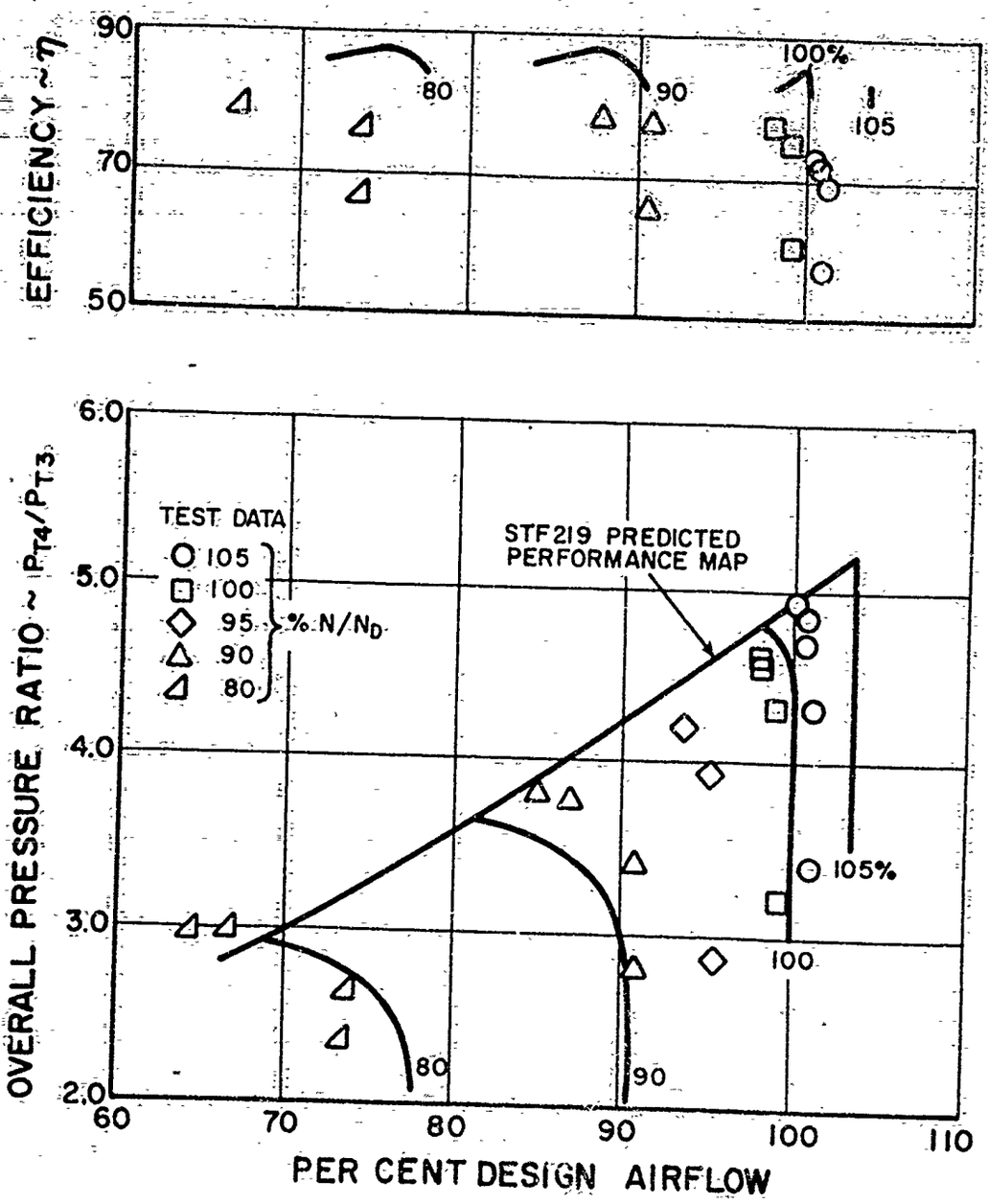
COMPARISON OF ORIGINAL AND REVISED FLOW PATHS FOR TWO-STAGE FAN RIG

Figure 4-6



MULTISTAGE VARIABLE-GEOMETRY COMPRESSOR RIG
INSTALLED ON TEST STAND

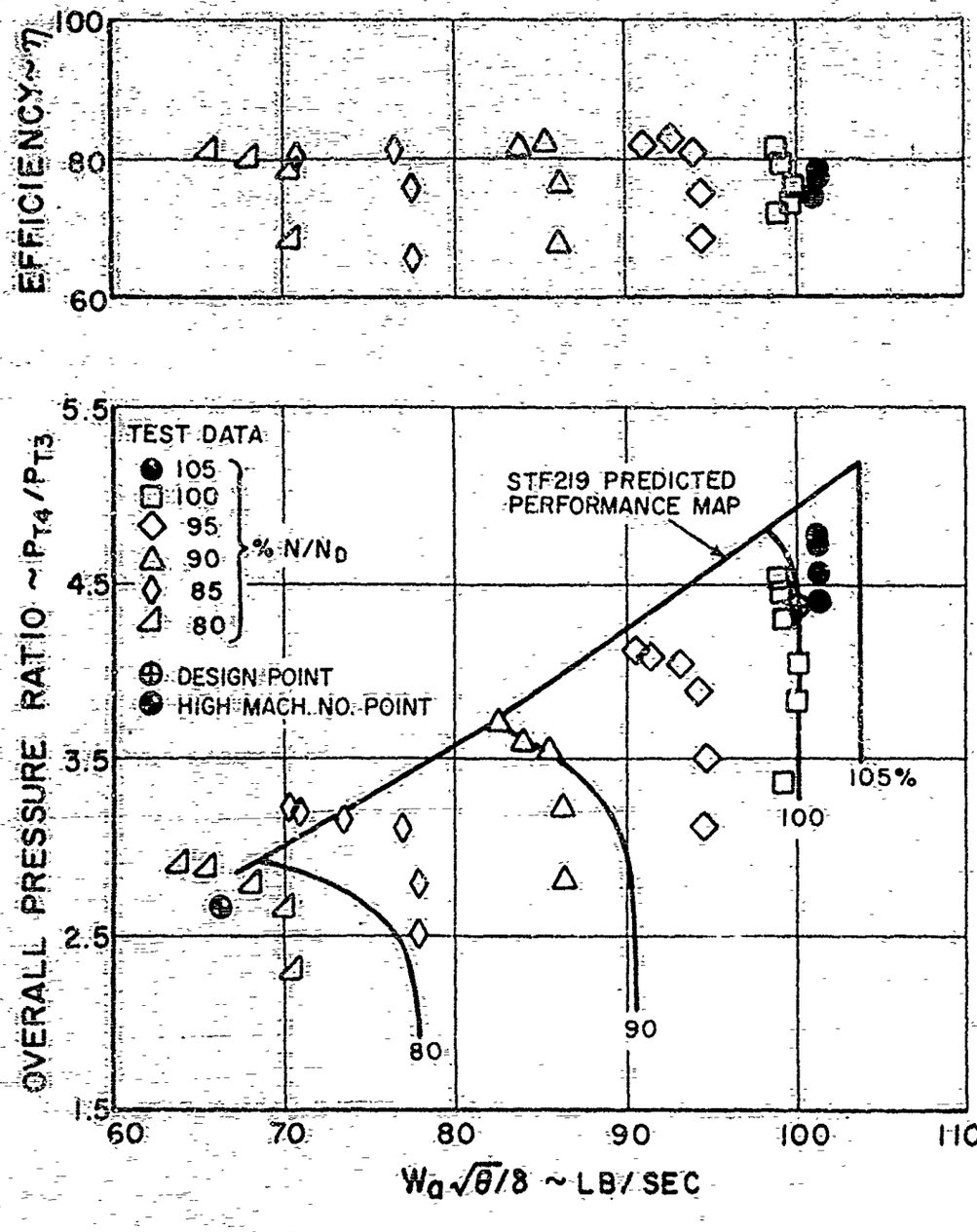
Figure 4-7



PERFORMANCE OF SECOND BUILD OF THE MULTISTAGE VARIABLE-GEOMETRY COMPRESSOR RIG

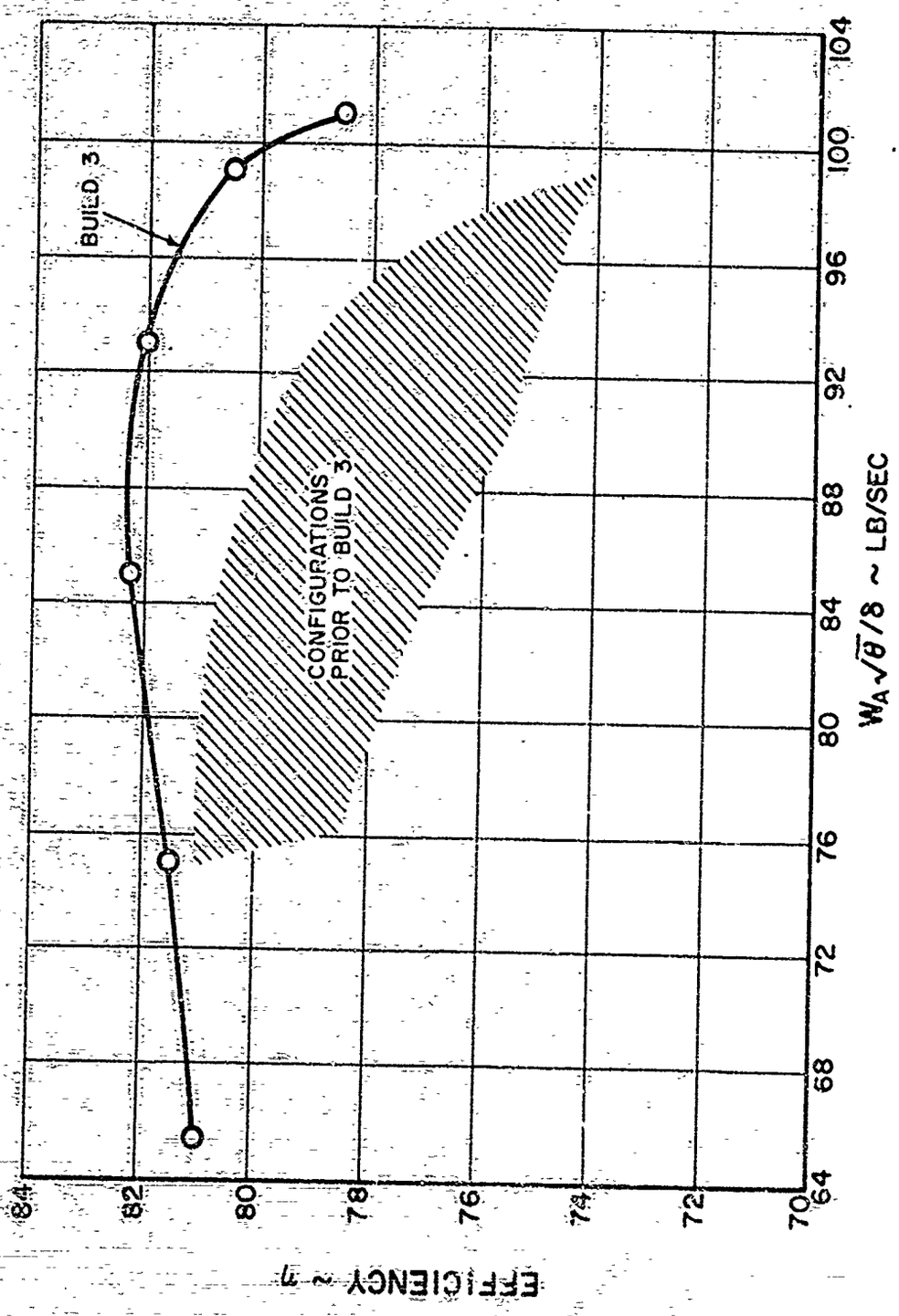
Figure 4-8

DOWNGRADED AT 3 YEAR INTERVALS
DECLASSIFIED AFTER 12 YEARS
DOD DIR 5200.10
THIS DOCUMENT CONTAINS INFORMATION AFFECTING THE NATIONAL DEFENSE OF THE UNITED STATES WITHIN THE MEANING OF THE ESPIONAGE LAWS, TITLE 18, U.S.C. SECTIONS 793 AND 794. THE TRANSMISSION OR THE REVELATION OF ITS CONTENTS IN ANY MANNER TO AN UNAUTHORIZED PERSON IS PROHIBITED BY LAW.



PERFORMANCE OF THIRD BUILD OF THE
MULTISTAGE VARIABLE-GEOMETRY COMPRESSOR RIG

Figure 4-9



COMPARISON OF MULTISTAGE COMPRESSOR EFFICIENCIES

Figure 4-10

COMBUSTION

ITEM 5 PRIMARY COMBUSTION

OBJECTIVE

This item of the contract required that Pratt & Whitney Aircraft conduct testing of engine combustor and combustor components directed toward verification of design characteristics.

The specific goals of these designs are:

1. A high heat release rate (5×10^6 BTU/hr./ft.^{3}/atm.)
2. A maximum pressure drop of six percent at sea level static conditions.
3. A combustion efficiency of 98.5 percent at sea level static conditions, and
4. Combustor exit temperature profiles not to exceed ΔT max/ ΔT avg. - 1.11

A. INTRODUCTION

Development testing with the object of attaining the goals listed above was conducted in four types of combustor rigs: a ram induction burner rig, two-dimensional segmented burner rigs, a large scale full-annular burner rig, and an advanced primary combustion rig.

B. RAM INDUCTION BURNER TESTING

To achieve the low engine weight desired, the primary burner section must be lighter and, therefore, smaller than the burner section in present production engines, but it must also provide a considerably higher temperature rise, good temperature profiles for the turbine, operate at high efficiency, and exhibit satisfactory durability. Prior to the start of this contract, Pratt & Whitney Aircraft designed a combination diffuser and burner which was unusually short and also held promise of low pressure loss. In this concept, air is ducted from

DOWNGRADED AT 3 YEAR INTERVALS
DECLASSIFIED AFTER 12 YEARS
DOD DIR 5200.10

THIS DOCUMENT CONTAINS INFORMATION AFFECTING THE NATIONAL DEFENSE OF THE UNITED STATES WITHIN THE MEANING OF THE ESPIONAGE LAWS, TITLE 18 U.S.C. SECTIONS 793 AND 794. THE TRANSMISSION OR THE REVELATION OF ITS CONTENTS IN ANY MANNER TO AN UNAUTHORIZED PERSON IS PROHIBITED BY LAW.

the diffuser to each hole in the burner, and turned into the burner by a low loss elbow or by turning vanes. Since the air is only diffused to the burner hole velocity, instead of to a much lower shroud velocity, much of the required diffuser length is eliminated, and some of the diffuser loss is avoided. This concept, referred to as "ram induction" because the velocity head of the air carries it into the burner, appears to provide one solution to the problem of shortening the burner section while maintaining or improving all other characteristics. Consequently, a portion of the primary burner effort under this contract has been directed towards investigating and developing this concept for application to the SST engine.

1. PROGRAM AND TEST PROCEDURES

Two basic configurations of burner rigs were used in this investigation. The first was a small sector burner incorporating two fuel nozzles, which was used for feasibility determination.

The second basic configuration, which is shown in Figure 5-1, simulates a straightened 72-degree arc of an annular main burner and incorporates eight fuel nozzles. The burner is approximately 24 inches wide and has a length approximating that of the SST diffuser and burner section.

The tests conducted to investigate and develop the ram induction primary burner included the following:

- Cold airflow tests of individual scoops of different designs to determine pressure drop and discharge airflow pattern.

- Airflow testing of the complete diffuser-burner combination to determine whether the cold pressure drop and general airflow characteristics were in agreement with predictions.

- Combustion tests were made to measure and record the overall characteristics of the system. In these tests, the complete burner-diffuser combination was operated essentially as it would be operated in an engine. From the data obtained during these tests, the following quantities were computed:

  - Burner exit temperature distribution parameter, Δ TVR ($T_{peak} - T_{inlet}/T_{average} - T_{inlet}$). The lower this number, the more uniform and desirable is the exit gas temperature pattern. Thus, the lower this number, the higher the turbine inlet temperature that can be attained without damaging the vanes or blades. This num-

ber was based on the values measured in the central 3/8 of the 24" annulus, which contained three fuel nozzles. This location was chosen to eliminate side wall effects.

- Overall pressure drop, ($\Delta P/P_i$). This is determined from the average inlet and exit pressure during both hot and cold tests.

- Combustion efficiency, ΔT measured average/ΔT ideal. These tests are run at lower pressures and lower inlet temperatures than those at which the flight engines operate. Thus, the burner efficiency in an engine is generally higher than that measured in the rig, and approaches 100%.

2. TEST RESULTS

For each test point run, a burner exit temperature distribution curve was plotted. The burner outlet temperature distribution gives the temperature at 3/4-inch horizontal increments across the 24-inch width of the outlet, and at 1/2-inch vertical increments up the 4-inch height. Only the middle 9 inches of the outlet has been used for calculation in order to eliminate side wall effects. Isotherms are drawn to show the distribution. A typical isothermal plot is shown in Figure 5-2.

Pressure drops ranging from four to ten percent were obtained at inlet Mach numbers ranging from 0.30 to 0.40. These low pressure drops, obtained with relatively high scoop entrance velocity, show the effectiveness of the ram induction scoops in utilizing velocity head to drive the air into the burner. The small amount of diffusion required with this system can be incorporated into the burner shroud and allows a very short combined diffuser and burner length.

In addition, the attainment of combustion intensities on the order of 6×10^6 BTU/hr/ft^3/atm is entirely feasible. This is attributed to the effectiveness of the scoops in turning the air into the burner and the resultant high degree of mixing. These good mixing characteristics contribute to the high heat release rates and the short length of the burner.

The operating range of the burner has been excellent. The design has been operated from .0005 to .030 fuel-air ratios. Combustion efficiencies ranging from 85 to 99 percent have been attained. The primary objective has been to obtain good outlet temperature control in

the short length of the burner system. Temperature profile control is the usual problem with high intensity or short length burner systems but good results have been obtained from this program. In one test, a ΔT max/ ΔT avg of 1.11 at .022 fuel-air ratio was obtained.

3. CONCLUSIONS

The results of the ram induction testing demonstrated the feasibility of this design in attaining acceptable burner performance within the length proposed for the burner SST engine. Specifically, the goals for the the SST primary burner have been met by this burner system as noted below.

- Heat Release Rate - The combustion intensity of 6×10^6 BTU/hr/ft^3/atm attained in this burner considerably exceeds the goal of 5×10^6 BTU/hr/ft^3/atm.

- Pressure Drop - Pressure drops have ranged from four to ten percent, with six percent representing a typical loss for sea level take-off conditions. This meets the goal drop of six percent.

- Combustion Efficiency - The goal efficiency of 98.5 percent was attained.

- Temperature Distribution Parameter - The goal value of a ΔTVR of 1.11 has been attained at .022 fuel-air ratio. This value should improve as fuel-air ratios are increased.

C. TWO-DIMENSIONAL SEGMENTAL BURNER RIG TESTING

Two-hundred and forty-eight hours of testing were completed on the two-dimensional burner rig during the contract period. The burner configuration which was tested most extensively is shown on Figure 5-3. This configuration is similar to the annular burner proposed as an alternative for the engine.

A sketch of the test setup may be seen in Figure 5-4. A heat exchanger supplies hot unvitiated air to the burner section. Inlet pressure and temperature instrumentation is used to determine the Mach number of the air approaching the test burner. A temperature-pressure rake at the rectangular burner exit is used to determine burner exit conditions.

1. PROGRAM AND TEST PROCEDURES

Two basically different types of runs were made on the two dimensional

DOWNGRADED AT 3 YEAR INTERVALS
DECLASSIFIED AFTER 12 YEARS
DOD DIR 5200.10

THIS DOCUMENT CONTAINS INFORMATION AFFECTING THE NATIONAL DEFENSE OF THE UNITED STATES WITHIN THE MEANING OF THE ESPIONAGE LAWS, TITLE 18, U.S.C., SECTIONS 793 AND 794. ITS TRANSMISSION OR THE REVELATION OF ITS CONTENTS IN ANY MANNER TO AN UNAUTHORIZED PERSON IS PROHIBITED BY LAW.

segmental rig. The first type is a standard performance run during which the liner velocity, inlet air temperature, and inlet pressure were held constant. The fuel flow was varied to attain predetermined burner fuel-air ratios and resultant burner temperature rises of 600°, 800°, 1000°, 1200°, 1400°, and 1600°F. For each of these temperature rises, the burner exit temperature was determined and values of ΔTVR, radial temperature profile, and burner efficiency were determined.

The second type of run was a cold-flow pressure loss test. Various airflows were passed through the burner, with the inlet temperature and pressure held constant. With no heat addition in the burner, the exit pressure was determined by means of a traverse at the burner exit. From those readings, a determination of the burner pressure loss was made at the various airflows. The testing was conducted at a liner velocity of 120 fps. The resulting liner loss was about three percent, which is equivalent to about 4.5 percent at a design velocity of 150 fps.

Various configuration changes were tested to investigate the effect and interaction of the following basic parameters:

- pressure loss
- hole area distribution
- number of holes/row
- axial location of each of five different rows

2. TEST RESULTS

In order to intensify the temperature variation at the burner exit, measurements of ΔTVR were obtained with a burner that was approximately four inches shorter than the SST design. Figure 5-5 shows the level of ΔTVR obtained with this shortened burner. A considerable improvement in ΔTVR is expected in a burner of the fully designed length.

3. CONCLUSIONS

The two-dimensional rig testing resulted in a heat release rate of over 5.69×10^6 BTU/hr/ft^3/atm being attained, which exceeded the goal of 5×10^6 BTU/hr/ft^3/ atm. The other results, i.e., a combustion efficiency of 100 percent and a pressure drop of only 5.35 percent, also exceeded the goal.

DOWNGRADED AT 3 YEAR INTERVALS
DECLASSIFIED AFTER 12 YEARS
DOD DIR 5200.10

THIS DOCUMENT CONTAINS INFORMATION AFFECTING THE NATIONAL DEFENSE OF THE UNITED STATES WITHIN THE MEANING OF THE ESPIONAGE LAWS, TITLE 18, U.S.C., SECTIONS 793 AND 794. THE TRANSMISSION OR THE REVELATION OF ITS CONTENTS IN ANY MANNER TO AN UNAUTHORIZED PERSON IS PROHIBITED BY LAW.

D. SHOWERHEAD BURNER TESTING

1. PROGRAM AND TEST PROCEDURES

A showerhead burner front-end was fabricated and tested in the two-dimensional burner rig. This design features a multiple-source, co-annular fuel-air and air injector front end. Figure 5-6 shows the finished part: Figure 5-7 shows the fuel-air path in the burner front end. Air is introduced through the front-end slot, and split into two passages, part going through the swirler and the rest remaining in the front-end chamber. The swirler air is mixed with fuel and discharged through many annular openings in the inner face. The front-end chamber air is introduced into the burner front end through tubes concentric with the fuel-air annuli. Many small fuel/air and air interfaces are set up which produce a high level of mixing in the burner front end. Since the inner face of the front end is adjacent to the flame, some preheating of the fuel-air mixture prior to injection into the burner proper should occur, very similar to the action that occurs in the hot-cone vaporizing burner. The showerhead burner, however, because of its inherent construction, introduces a more-evenly-dispersed fuel/air mixture across the front end.

2. TEST RESULTS

Limited testing was accomplished with this configuration. The few tests that were made showed that the showerhead produced a blue flame characteristic of a vaporizing type of burner. The individual injection ports appeared to be forming localized areas of combustion as planned. The snout inlet area was adjusted to determine its effect on burner performance. For the few tests completed, an increase or decrease of 50 percent in inlet area did not greatly affect ΔTVR. Increasing the fuel/air annulus area around the air tubes (in effect decreasing the fuel/air interface) increased ΔTVR.

3. CONCLUSIONS

The interactions of various features of the showerhead burner are many, so that extensive testing will be required to optimize these features and insure the best burner performance.

DOWNGRADED AT 3 YEAR INTERVALS
DECLASSIFIED AFTER 12 YEARS
DOD DIR 5200.10

E. HOT CONE BURNER TESTING

1. PROGRAM AND TEST PROCEDURES

One of the advanced concepts tested in the two-dimensional rig incorporates a hot-cone in the burner front end to pre-mix and partially vaporize the fuel prior to injection into the combusion chamber. Figure 5-8 shows a cross-section of this burner. About 10 percent of the engine airflow is admitted to the hot-cone section through holes in the blunt leading edge of the burner. Half of this air is admitted through swirlers to the vaporizing passages along with the fuel. The rich mixture ($F/A \approx 0.4$) in this passage allows mixing and vaporization of the fuel but prevents combustion upstream of the cone because the mixture is too rich to burn. This partially vaporized fuel-air mixture is then injected into the combusion region downstream of the cone through holes. The remainder of the air taken in through the blunt leading edge section is injected into the recirculation zone through additional holes. Ignition is provided in the recirculation region and additional combustion and dilution air is injected through holes in the liner walls to provide the desired temperature pattern and liner cooling. This additional air represents the bulk of the engine airflow which flows through the inner and outer diffusing passages into the liner shroud areas. The hot-cone principle which has been developed in can burner configurations by P&WA essentially increases fuel residence time in the combustion chamber and provides a means of initial fuel-air preparation. An increase in temperature rise capability of the burner for any given velocity, length, and pressure drop is expected with this configuration.

2. TEST RESULTS

Most of the work done on the annular burner used the standard liquid injector system for testing. The hot-cone optimization program was carried on as a separate feature using hole patterns and other variable items previously found acceptable in liquid-injection annular burner tests.

Initial tests of the vaporizing burner showed it to be compatible with similar liquid-injection burners. Its characteristic flame is basically blue; quite similar to a flame from a gaseous fuel, indicating that partial fuel vaporization is occurring in the front end. In this case, the burning mechanism appears different enough to warrant more detailed testing of the configuration.

DOWNGRADED AT 3 YEAR INTERVALS
DECLASSIFIED AFTER 12 YEARS
DOD DIR 5200.10

A series of tests were made to determine the effect of front-end airflow on the hot-cone burner. Air for the vaporizing passage is normally taken from the main air stream via a slot in the burner front end. For this series of tests, the slot height was changed to produce varying degrees of open area or, in effect, various air-flows to the front end.

Increasing the area by 25 percent greatly hurt performance, especially ΔTVR. With a 50 percent area increase, the burner stability was so poor at low temperature rises that a flame could not be sustained. At high temperature rises, the burner performed smoothly. Decreasing the inlet area did not produce a marked effect on burner stability or performance. It appears that this burner, like the liquid-injection burner, is highly sensitive to airflow in the front end.

Because of the sensitivity of the hot-cone to burner front-end airflow, the effect of slot feed hole area on burner performance was investigated. Blocking 50 percent of the slot feed hole area did not hurt performance at all. This is in line with results previously attained with can-type hot-cone burners. Blocking the slot feed holes entirely produced a slight loss in burner performance.

The effect of the slot feed lip was also investigated. Cutting back the slot feed lip with all slot feed holes open (in effect causing the slot feed air to enter the burner at a longer diameter) greatly increased the ΔTVR. Plugging the holes produced a ΔTVR similar to that encountered with the feed lip intact.

It appears that the slot feed air is necessary, at least to a certain extent (blocking it off entirely hurt ΔTVR), and if used in its full amount the diameter of the slot feed lip becomes very important.

3. CONCLUSIONS

Much testing remains to be done to fully optimize this configuration. The few short tests done so far have only served to indicate the complexity of the system and the interdependence of one variable on all of the others. Testing will proceed in an attempt to optimize this unique burner.

DOWNGRADED AT 3 YEAR INTERVALS
DECLASSIFIED AFTER 12 YEARS
DOD DIR 5200.10

THIS DOCUMENT CONTAINS INFORMATION AFFECTING THE NATIONAL DEFENSE OF THE UNITED STATES WITHIN THE MEANING OF THE ESPIONAGE LAWS, TITLE 18, U.S.C., SECTIONS 793 AND 794. ITS TRANSMISSION OR THE REVELATION OF ITS CONTENTS IN ANY MANNER TO AN UNAUTHORIZED PERSON IS PROHIBITED BY LAW.

F. LARGE-SCALE FULL-ANNULAR BURNER RIG TESTING

The large-scale full-annular burner rig incorporates burner liners simulating the STF219 alternate burner design. A schematic of the rig is shown in Figure 5-9: Figure 5-10 shows the assembled rig. A rotating temperature-and-pressure rake is provided to facilitate the determination of burner exit conditions. Instrumentation is similar to that of the two-dimensional segmental rig, and determination of pressure loss, burner efficiency, and burner ΔTVR are made in the same manner.

1. TEST RESULTS

Three significant tests were completed during the contract period on the large-scale full-annular burner rig, one test with a burner which was four inches shorter, and two tests with a burner which was one inch shorter than the proposed STF219 design. A total of 72 hours operating time was accumulated on the rig during the contract period.

The short (four inches less than SST) version of the full-annular burner attained an average ΔTVR of 1.20 at 1074°F ΔT without optimization using the hole pattern (Scheme 1, Mod. 3C) evolved in the two-dimensional rig. The ΔTVR level of the Scheme 1, Mod. 3C burner as compared to a previously tested configuration (Scheme 1, Mod. 8B), is shown in Figure 5-11. The application of results obtained in the two-dimensional program should lead to further optimization of the Scheme 1, 3C burner.

The short (one-inch less than SST) version of the full-annular burner was used for two significant tests, identified as Runs Nos. 14 and 15. Performance was obtained with a flow trip at the I.D. of the inlet to distort the profile (Run 14) and with a "clean" inlet (Run 15). Figure 5-12 shows the effect of the trip on the inlet total pressure profile. This is typical of the burner inlet profile that might be expected under actual engine conditions.

Run 14, with the distorted inlet profile was made at a temperature rise of approximately 1050°F and showed an average of the segmental ΔTVRs to be 1.25, with a minimum segmental ΔTVR of 1.11. This was the average of the ΔTVRs using all segmental ΔTVRs. Segment 10, however, was extremely high and appeared to be the result of a fuel leak, which would cause an abnormally high local temperature. Deletion of the segment 10 ΔTVR gave an overall average ΔTVR of 1.22 which was reasonable considering the high temperature rise and the early develop-

DOWNGRADED AT 3 YEAR INTERVALS
DECLASSIFIED AFTER 12 YEARS
DOD DIR 5200.10

THIS DOCUMENT CONTAINS INFORMATION AFFECTING THE NATIONAL DEFENSE OF THE UNITED STATES WITHIN THE MEANING OF THE ESPIONAGE LAWS, TITLE 18, U.S.C., SECTIONS 793 AND 794. THE TRANSMISSION OR THE REVELATION OF ITS CONTENTS IN ANY MANNER TO AN UNAUTHORIZED PERSON IS PROHIBITED BY LAW.

mental state of the combustor. The average exit temperature profile depicted in Figure 5-13 indicates that the warped inlet profile produced a cold O.D. at the plane of the turbine.

Run 15 without inlet distortion was made at a temperature rise of approximately 1530°F and produced an average of the segmental ΔTVRs of 1.29, with a minimum ΔTVR of 1.17. The ΔTVR level of Run 14 and 15 is also shown on Figure 5-11. The exit temperature profile for Run 15 (Figure 5-14) indicates that the O.D. was warmed somewhat and the I.D. cooled with the flat inlet pressure profile, as compared with the distorted profile. The sudden depression of temperature at the O.D. may have been due to the proximity of the instrumentation to the O.D. exit wall.

Figures 5-15 and 5-16 are the isotherm plots for Runs 14 and 15 respectively. Instrumentation failure allowed only a 180° traverse for Run 15 but past data have indicated that both sides of the exit annulus would be similar.

2. CONCLUSIONS

The burner used in Runs 14 and 15 was fairly sensitive to the incoming flow profile insofar as the exit temperature distribution was concerned; however, the affect on the ΔTVR level was less than expected. The hole pattern used in the longer burner was developed on the shorter version. It would appear that with some optimization of the hole pattern to better suit the long burner, a combustor capable of high temperature rise, together with low ΔTVR, can be attained. In fact, the best segment at the high (1530°F) ΔT point had a ΔTVR of 1.16 while at the 1050°F ΔT point the best segment had a ΔTVR of 1.11. These findings suggest development of a hole pattern to fit the inlet pressure profile and other features (probably shroud aerodynamics) to minimize circumferential variations.

G. ADVANCED PRIMARY COMBUSTION RIG TESTING

A program aimed towards the development of smaller main burners was initiated during the contract period. This program is an attempt to derive a philosophy of main burner design from ramjet technology based on concepts of high mass loading, reaction rate theory, and optimum mixing methods. Emphasis was placed on length reduction because shorter burners permit engine weight savings beyond that of the burner itself, i.e., shorter shafts and engine casing.

Primary objectives of the program were to:

Reduce present burner lengths by 50 percent.
Eliminate the inlet diffuser.
Utilize ram pressure to control burner airflow distribution.
Minimize pilot volume.
Determine optimum mixer schemes.

1. PROGRAM AND TEST PROCEDURES

A sea-level test stand was modified to accept a burner research rig. Figure 5-17 shows details of both the stand and rig. Pressure and temperature instrumentation was provided at both inlet and exit planes, as well as in the burner itself to meter internal airflow distributions. A high-temperature platinum/platinum-rhodium traversing rake was constructed to read 64 temperatures across the central eight inches of the burner exit.

The standard test procedure on each burner scheme was as follows:

a) A cold pressure loss run (8-10 data points) was made at inlet Mach Nos. of 0.1 through 0.6.

b) Performance data was obtained at fuel-air ratios from lean blow-out to 0.025 at an inlet Mach No. of 0.3.

c) Performance data was obtained at Mach No. 0.4.

For each data point, combustion efficiency, temperature rise, pressure loss, and local airflows were determined. A complete traverse of the exit plane was also made and the burner ΔTVR was computed. Forty hours of test time were accumulated on the advanced primary combustion rig during the contract period.

2. TEST RESULTS

Initial tests were conducted on the burner shown schematically in Figure 5-18. The burner configuration was approximately equivalent in length and volume to present main burners and was designed primarily for investigation of low-loaded pilot performance and for determination of the severity of the mixing problem without mixing bypass air. Results of the first tests are shown on Figure 5-19 and summarized below:

a) ΔTVR = 1.6 to 1.8

b) $\Delta P/P$ (cold pressure loss) = 6.5 percent at Mach No. 0.33

c) ΔT Maximum = 1200°

d) The use of four variations of fuel injector nozzles and orifices showed no discernible effect on performance.

The first major variation of the initial scheme consisted of installing flow turning sleeves at the shroud exit. Figure 5-20 shows the results of testing the modified burner and indicates that ΔTVR was reduced to 1.4 at the cost of one-half percent in pressure loss. A second configuration designed to lower cold pressure loss and double the pilot mass loading rate was installed for test. This scheme is shown schematically on Figure 5-21.

3. CONCLUSIONS

- During initial tests, with the shroud passage blocked, lean blowout occurred at 0.003 fuel-air ratio over inlet Mach Nos. of 1.0 to 0.6 and temperatures of 100°F to 600°F. Rich blowouts could not be obtained because of stand fuel limits. The mass loading parameter-$A/VP^2 \frac{(\text{lbs./sec.})}{(FT^3\,ATMOS^2)}$ - for the tested burner was 0.128, compared to a theoretical maximum of 26.0, indicating that pilot volume can be decreased.

- Pressure losses for the first conservatively-designed burner were not exhorbitantly high. A 6.5 percent $\Delta P/P$ was observed where 5.1 percent is expected of current state-of-the-art main burners.

DOWNGRADED AT 3 YEAR INTERVALS
DECLASSIFIED AFTER 12 YEARS
DOD DIR 5200.10

- Although the recorded ΔTVR were unacceptable for an engine application, it must be remembered that for the can tested no effort at all was made to mix the two streams. The relatively minor innovation of installing turning sleeves lowered ΔTVR to 1.4, indicating that even slight attempts to mix the streams produce significant results towards the goal of a ΔTVR of 1.10.

- Figure 5-18 shows that refinements to the front-end contours of the burner will effect a lower cold-pressure loss; the burner shown in Figure 5-21 is an example of such changes. It is expected that while ΔTVR may be lowered by introducing mixing losses, these losses can be compensated by improving front-end contours.

- Considering that the data obtained to date were from an initial, extremely conservative approach, the overall burner performance was close to that of present day main burners. It appears that much useful information concerning pilot loading, mixing losses and potential burner length reduction will be obtained from continued efforts in this program.

DOWNGRADED AT 3 YEAR INTERVALS
DECLASSIFIED AFTER 12 YEARS
DOD DIR 5200.10

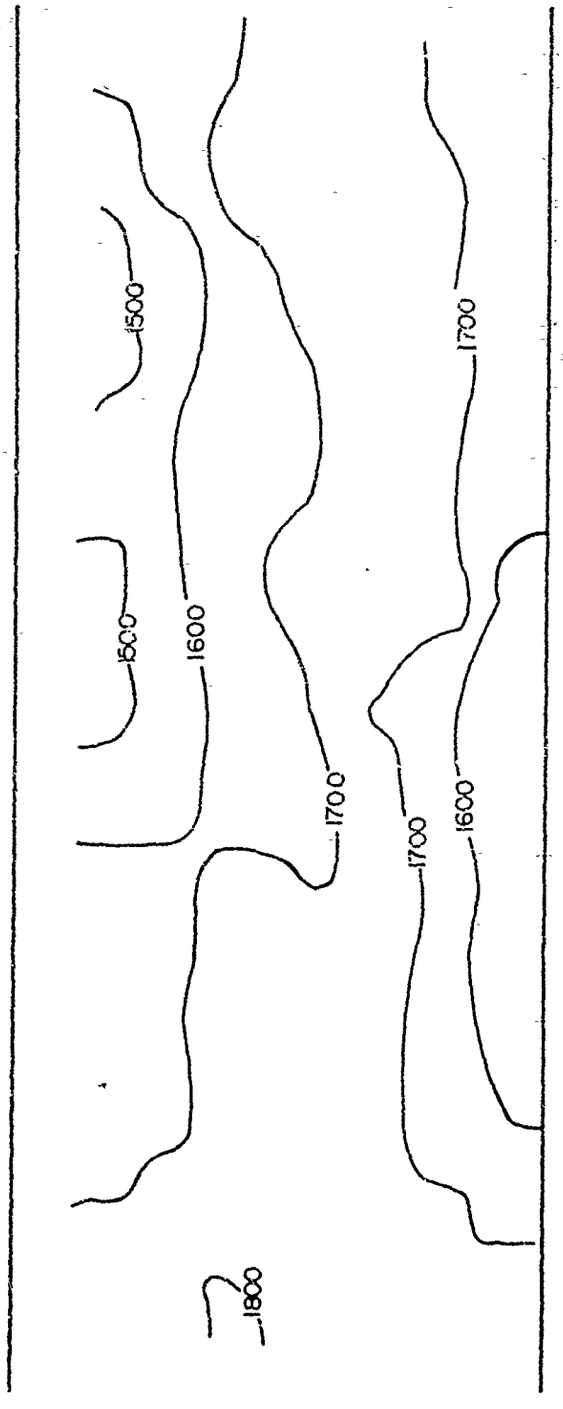
THIS DOCUMENT CONTAINS INFORMATION AFFECTING THE NATIONAL DEFENSE OF THE UNITED STATES WITHIN THE MEANING OF THE ESPIONAGE LAWS, TITLE 18, U.S.C., SECTIONS 793 AND 794. THE TRANSMISSION OR THE REVELATION OF ITS CONTENTS IN ANY MANNER TO AN UNAUTHORIZED PERSON IS PROHIBITED BY LAW.



RAM INDUCTION BURNER TEST SECTION

Figure 5-1

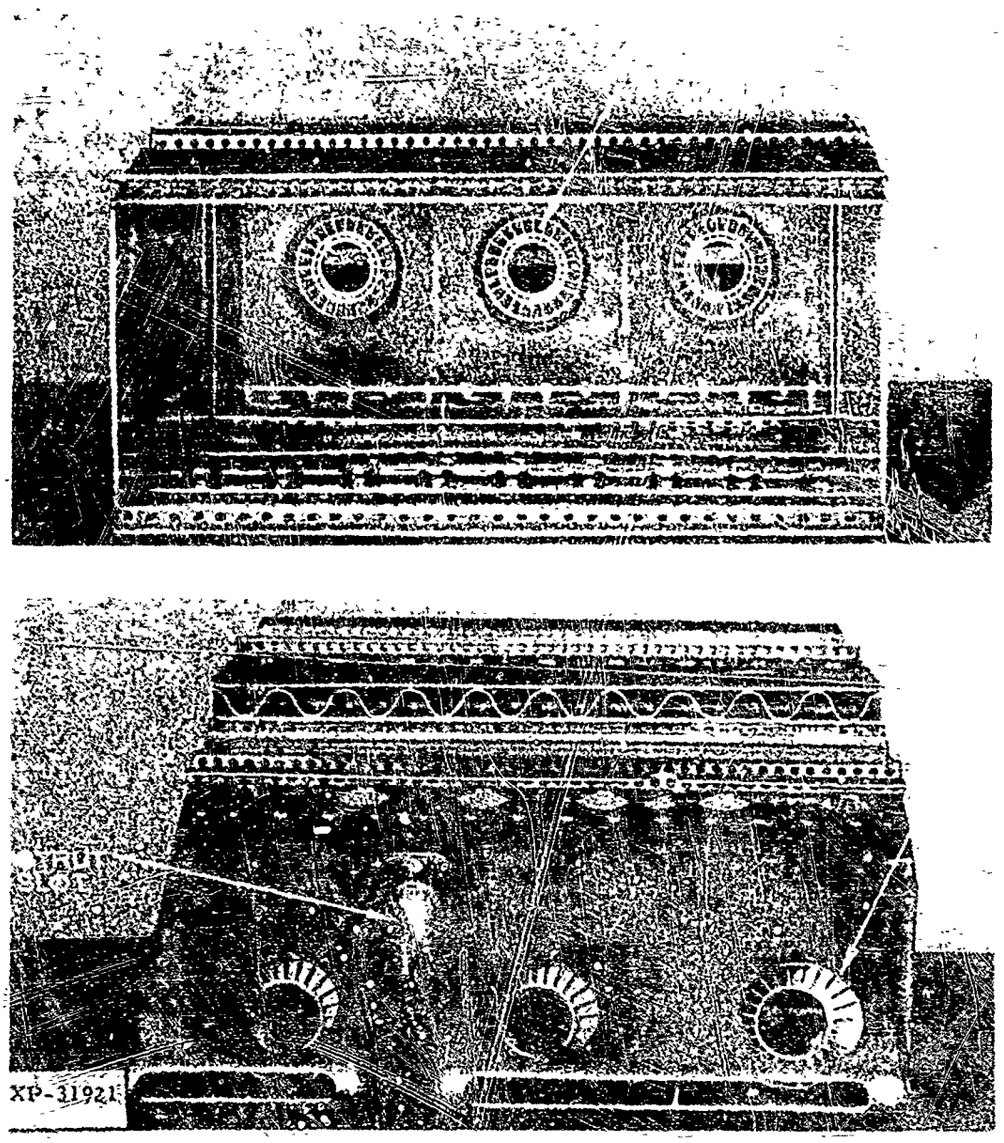
DOWNGRADED AT 3 YEAR INTERVALS
DECLASSIFIED AFTER 12 YEARS
DOD DIR 5200.10



TYPICAL BURNER OUTLET TEMPERATURE
DISTRIBUTION PLOT

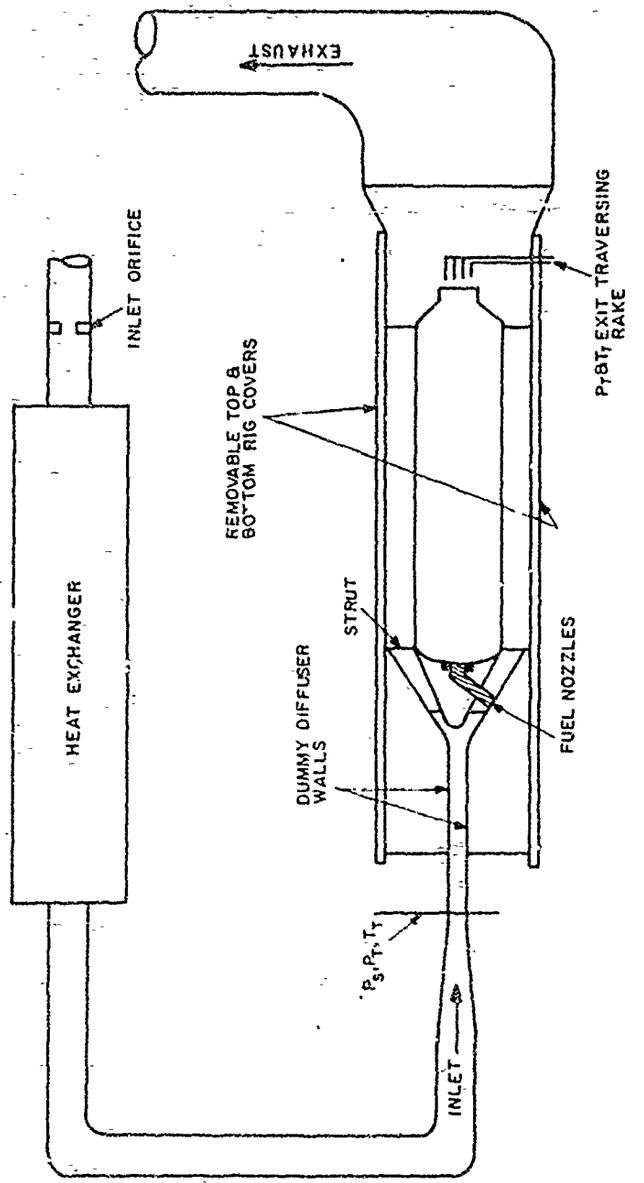
Figure 5-2

DOWNGRADED AT 3 YEAR INTERVALS
DECLASSIFIED AFTER 12 YEARS
DOD DIR 5200.10



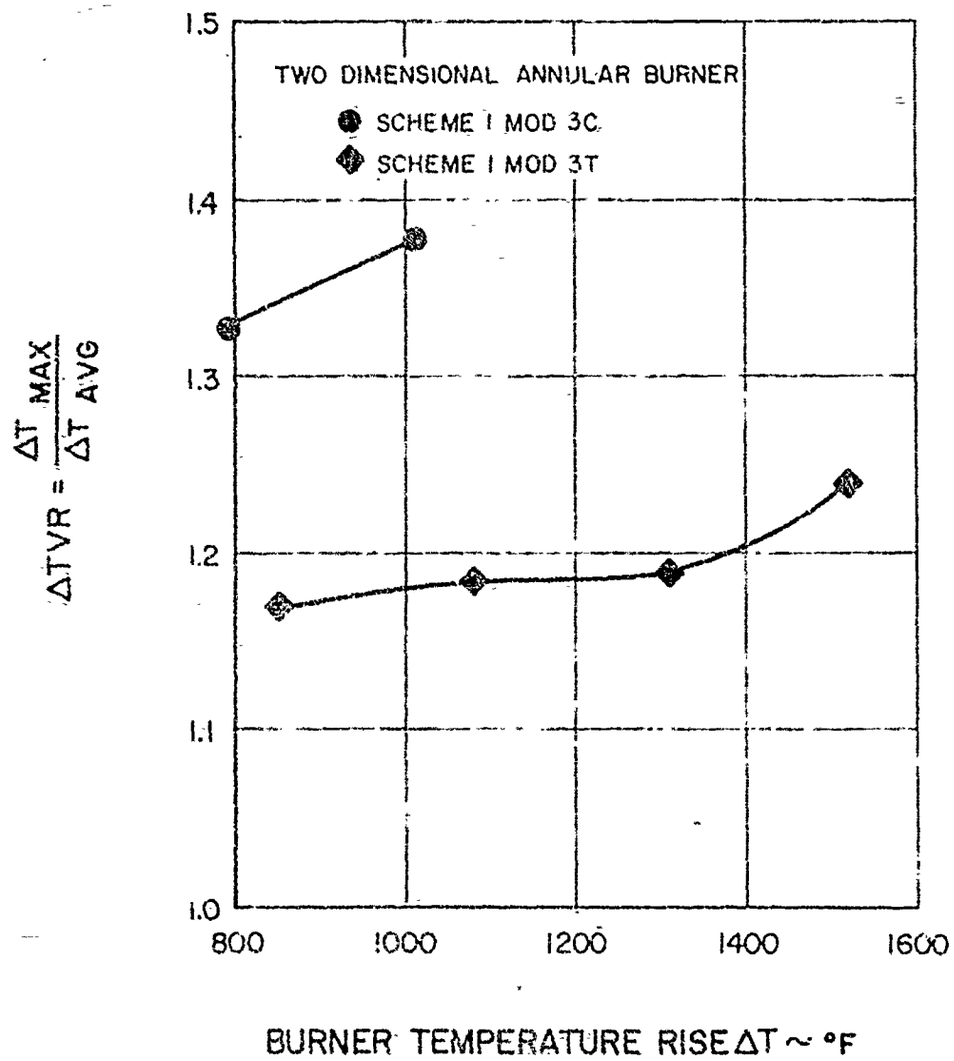
TWO-DIMENSIONAL ANNULAR BURNER

Figure 5-3



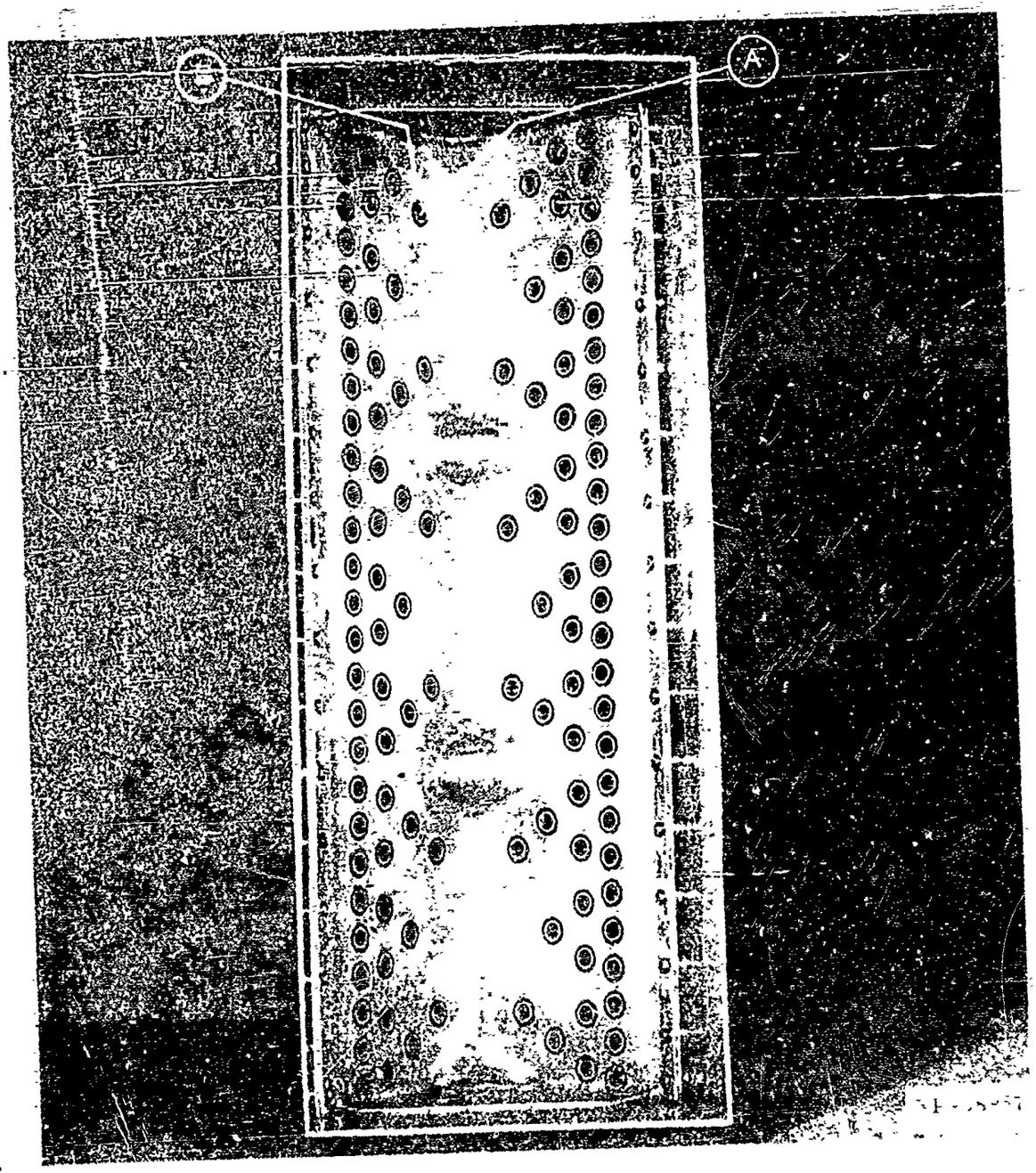
TWO-DIMENSIONAL ANNULAR BURNER RIG INSTALLATION

Figure 5-4



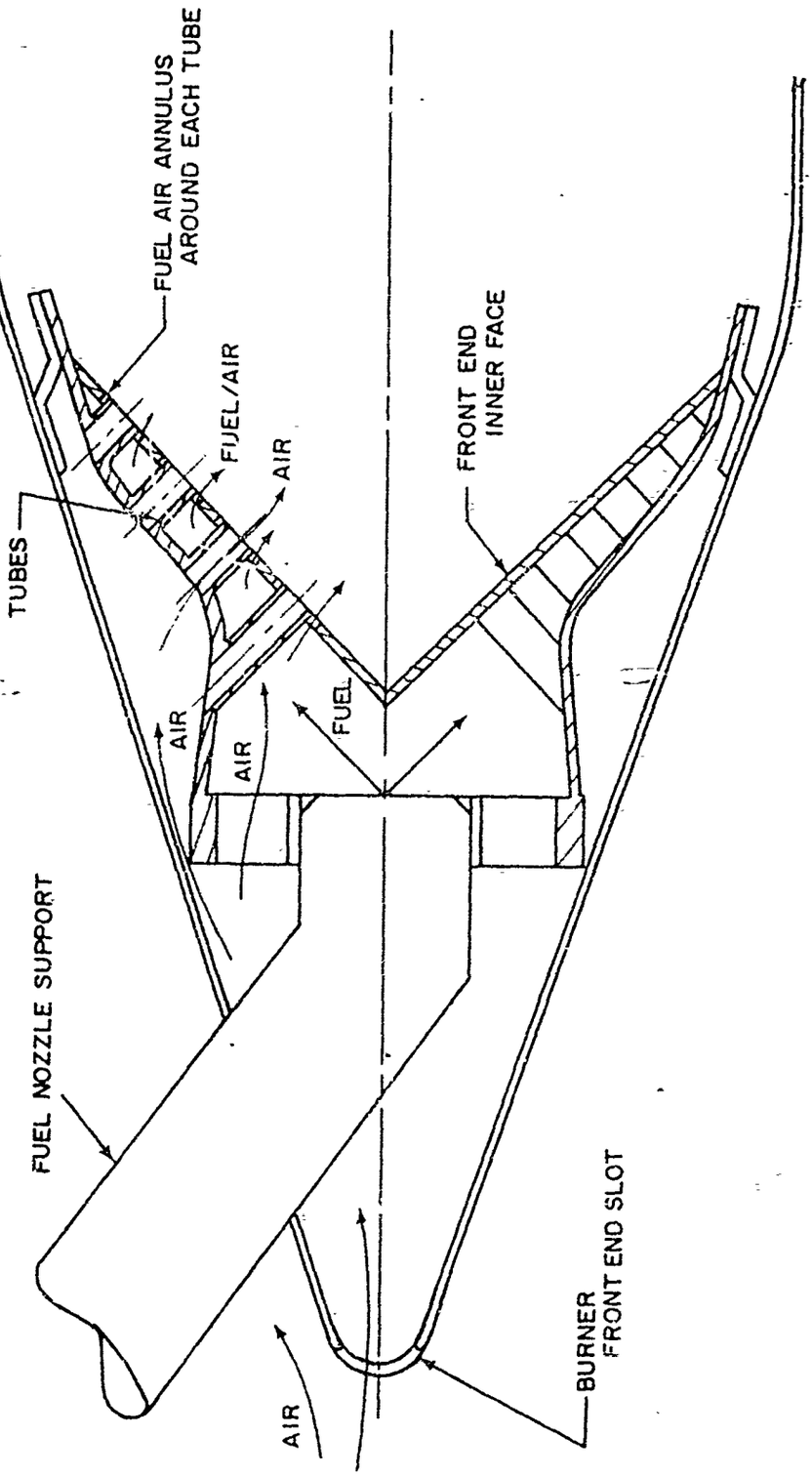
TWO-DIMENSIONAL ANNULAR BURNER
(SHORTENED VERSION) TEST RESULTS

Figure 5-5



SHOWERHEAD BURNER CONFIGURATION
FOR TWO-DIMENSIONAL ANNULAR TESTING
AIR TUBES (A) IN CENTER OF FUEL-AIR ANNULUS(B)

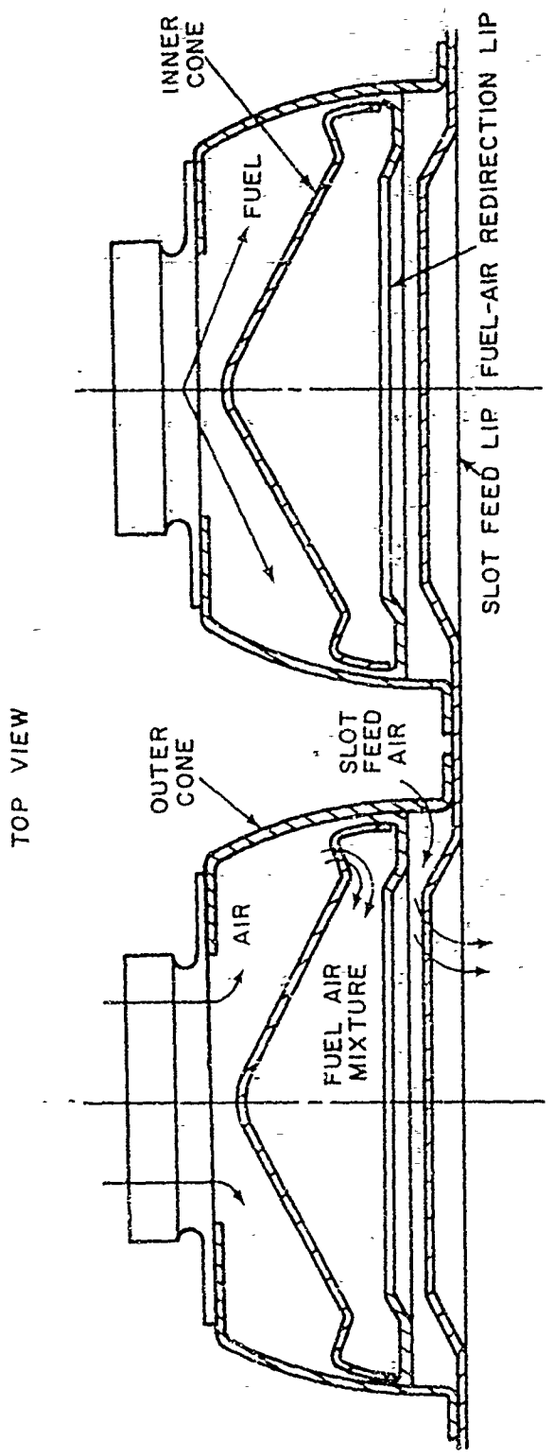
Figure 5-6



SCHEMATIC DIAGRAM OF SHOWERHEAD
BURNER CONFIGURATION

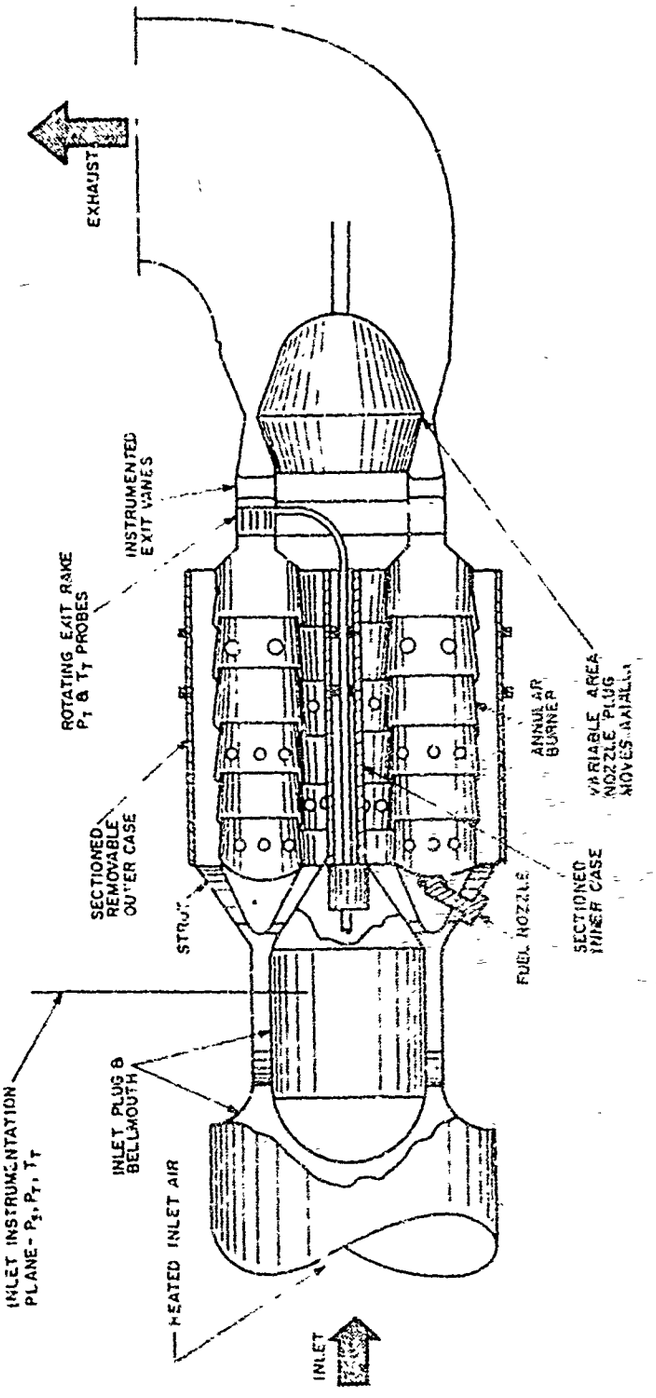
Figure 5-7

DOWNGRADED AT 3 YEAR INTERVALS
OR ARMED AFTER 12 YEARS
DOD DIR 5200.10



SCHEMATIC DIAGRAM OF HOT CONE BURNER
(FRONT SECTION)

Figure 5-8



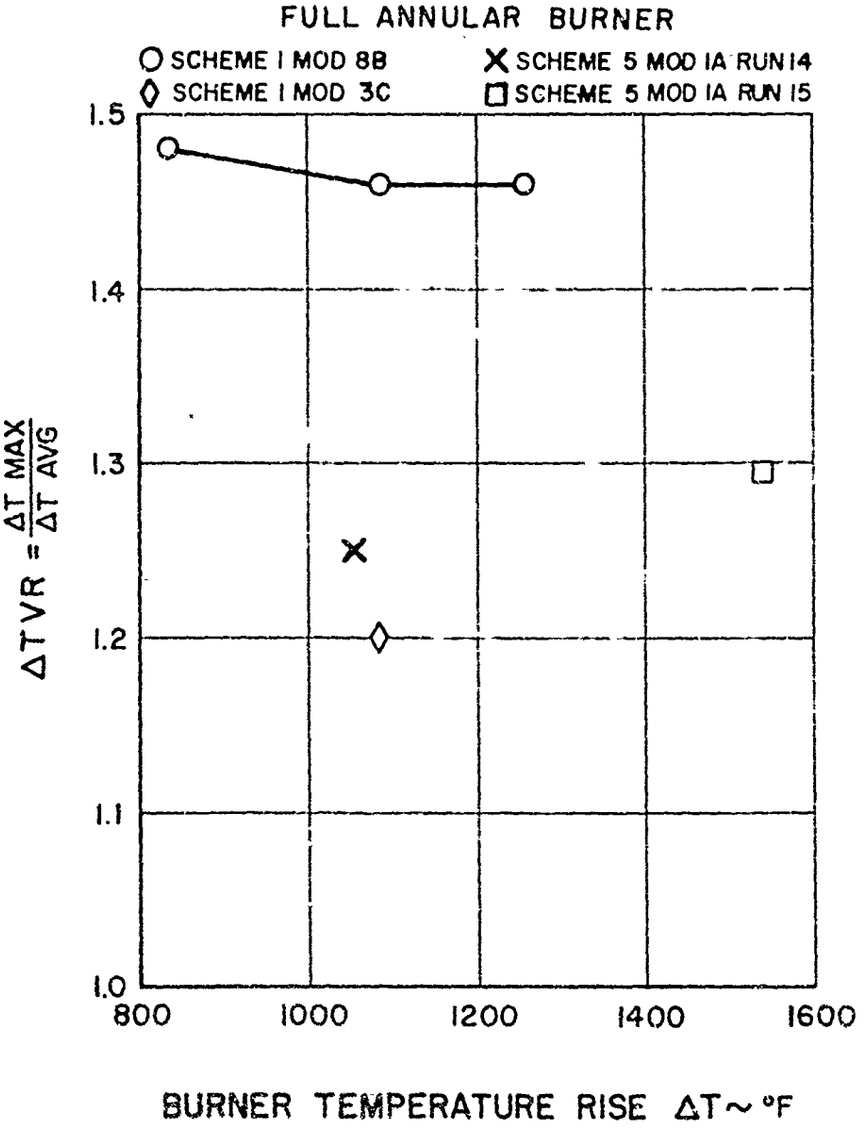
SCHEMATIC DIAGRAM OF FULL-SCALE ANNULAR BURNER RIG

FIG. 3-3



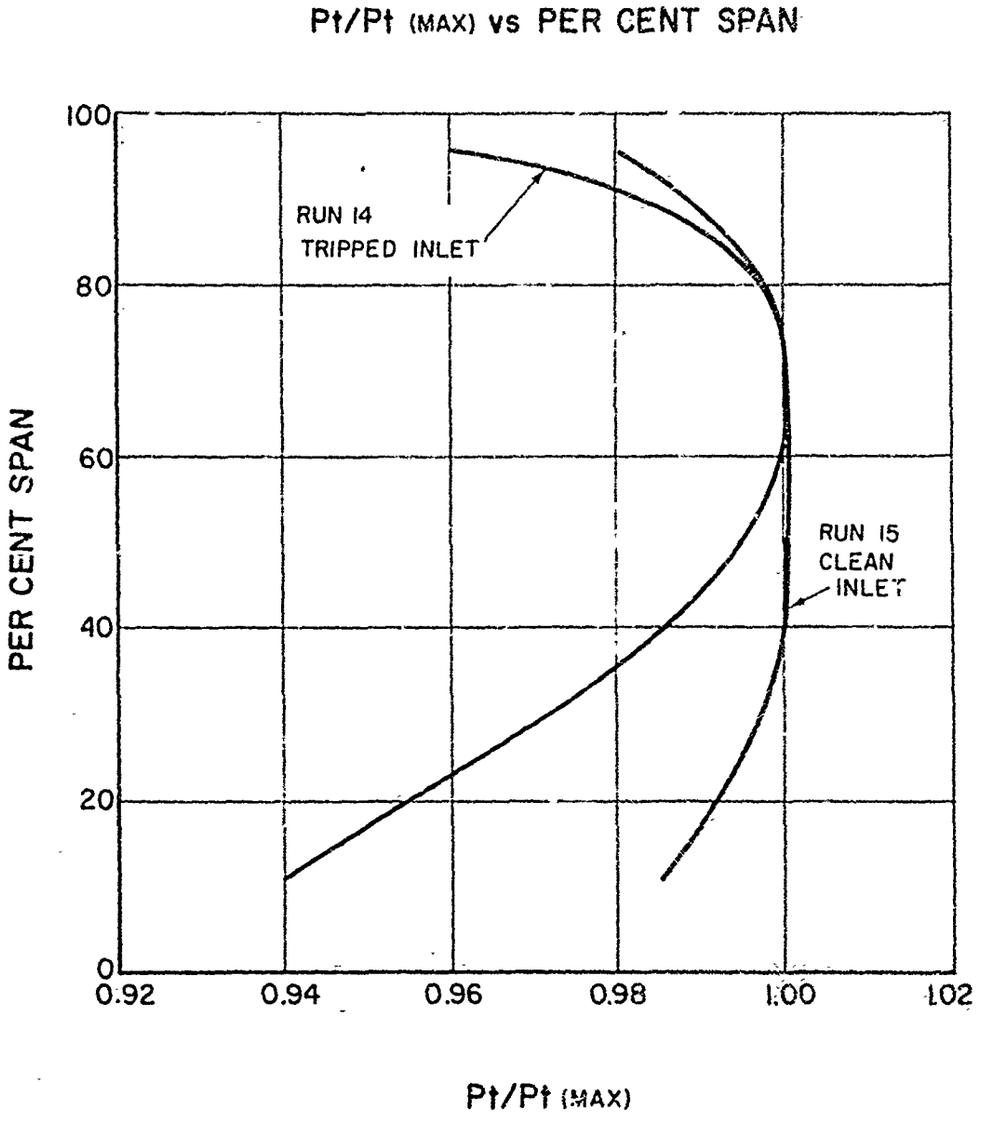
SST ENGINE FULL-SCALE ANNULAR
BURNER RIG

Figure 5-10



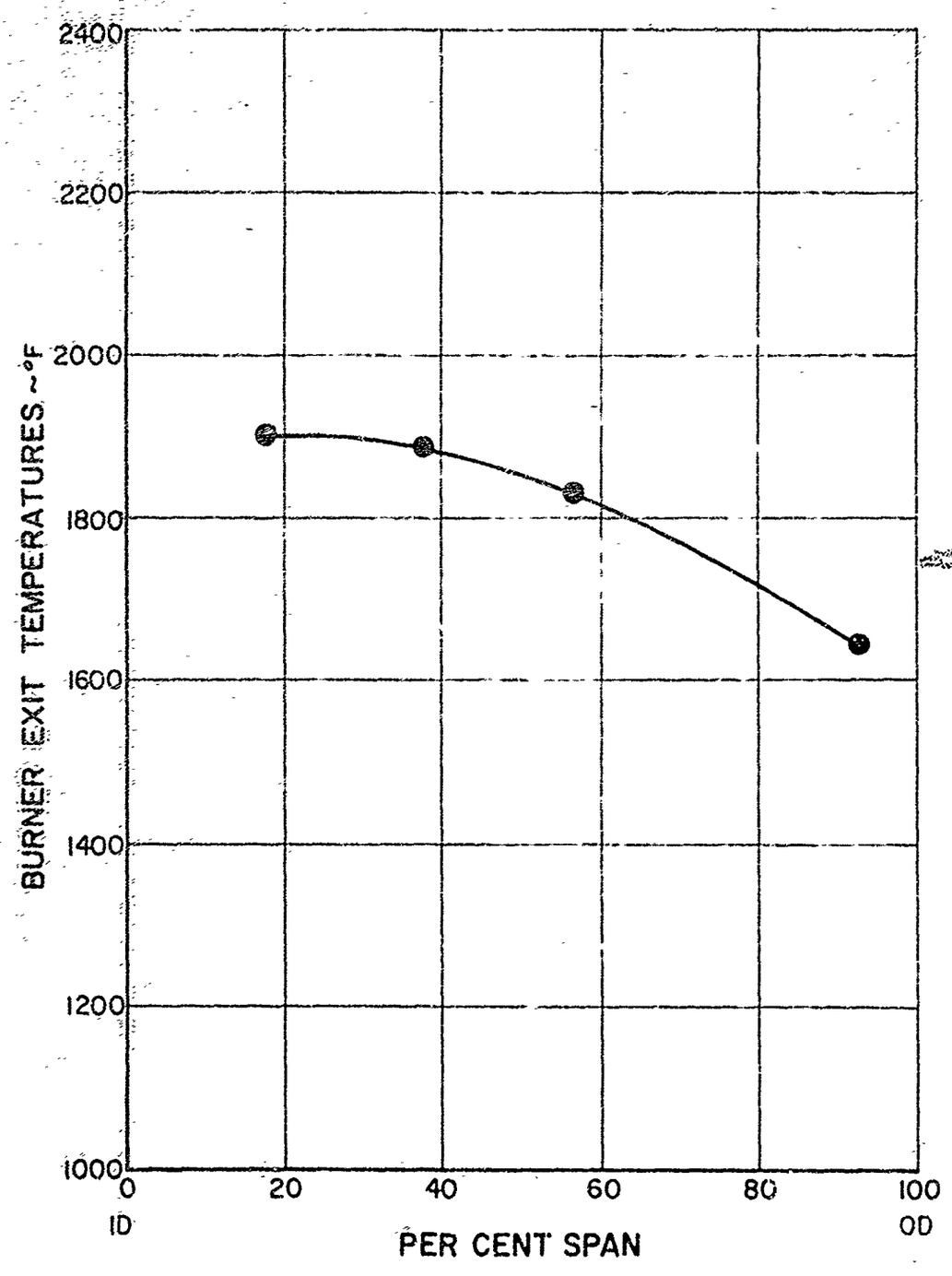
FULL-SCALE ANNULAR BURNER
TEST RESULTS

Figure 5-11



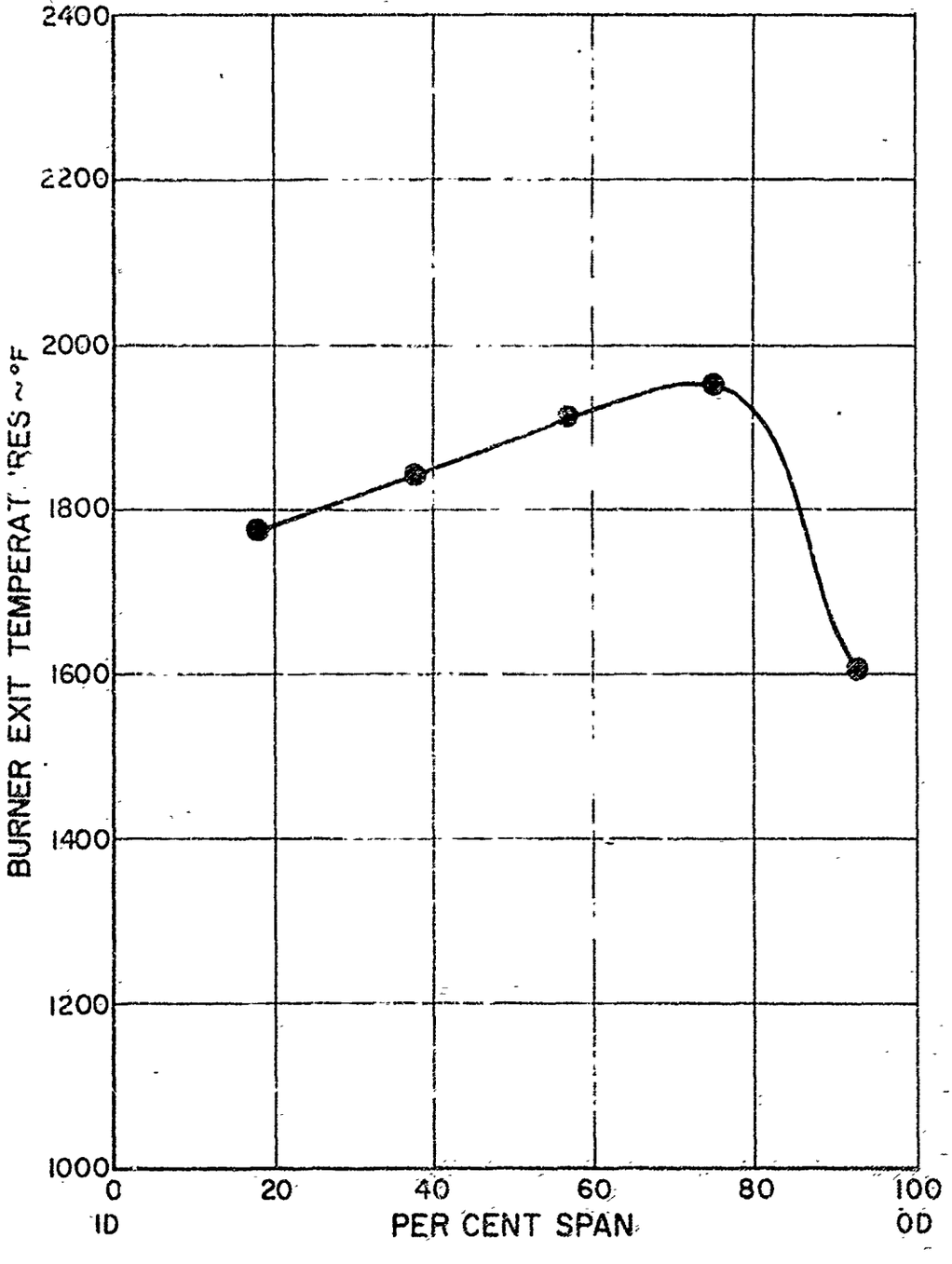
EFFECT OF INLET TRIP
ON INLET TOTAL PRESSURE PROFILE

Figure 5-12



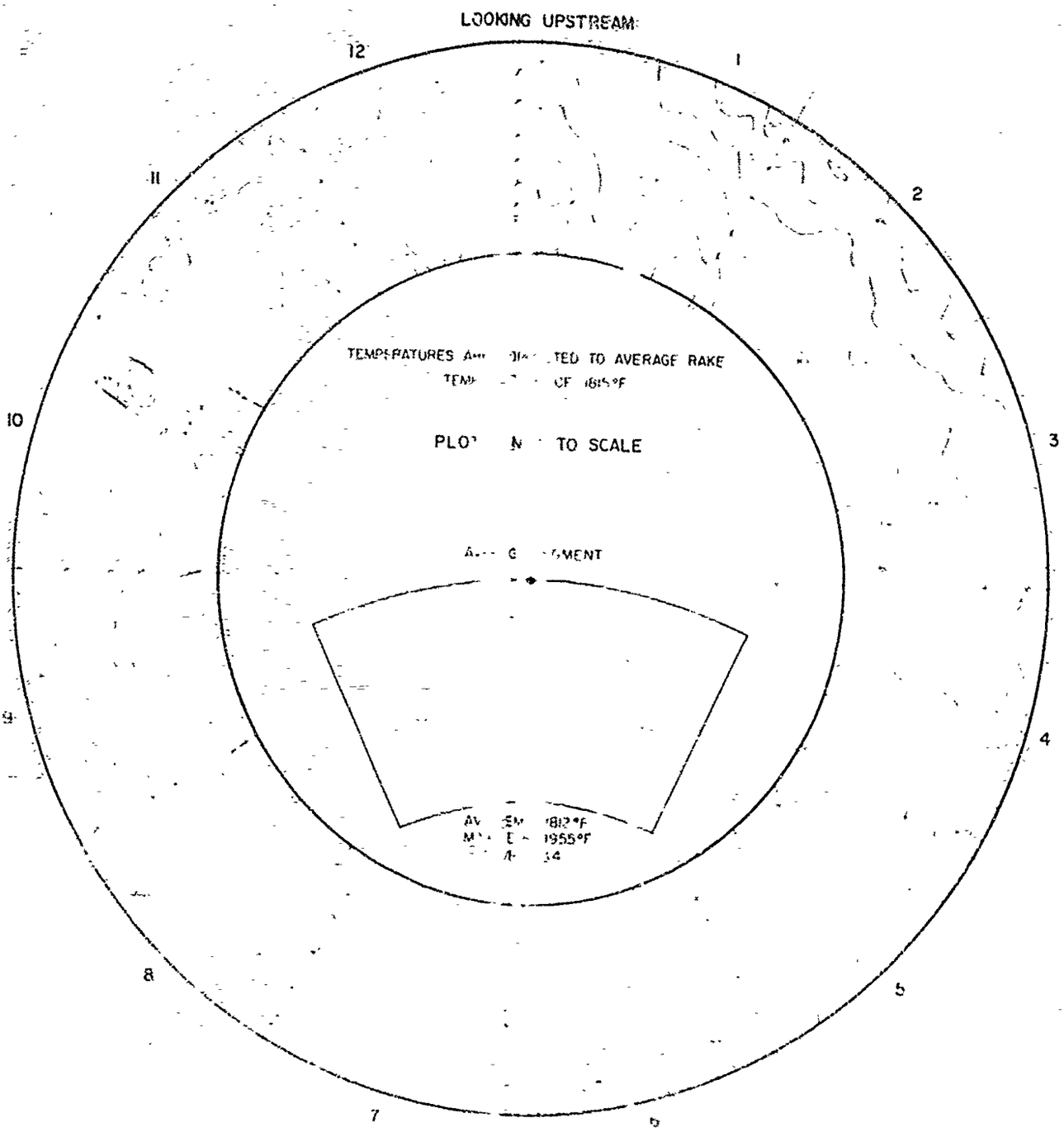
AVERAGE EXIT TEMPERATURE PROFILE (RUN 14)

Figure 5-13



AVERAGE EXIT TEMPERATURE PROFILE (RUN 15)

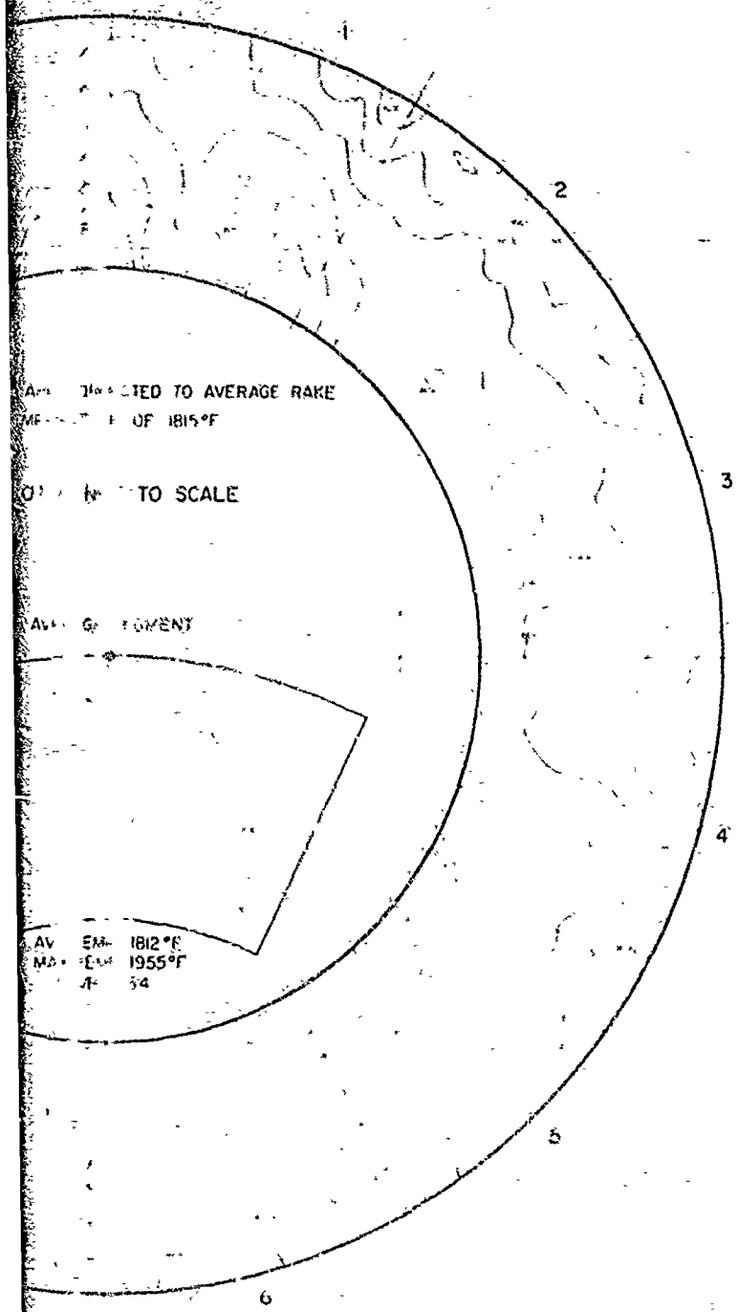
Figure 5-14


LOOKING UPSTREAM
12
1
2
3
4
5
6
7
8
9
10
11
TEMPERATURES ARE INDICATED TO AVERAGE RAKE
PLOT IS NOT TO SCALE

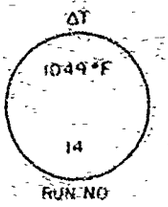
PRATT & WHITNEY AIRCRAFT

PWA-2397

LOOKING UPSTREAM



BURNER DISCHARGE TEMPERATURE PLOT
RIG NO 25003L STAND NO. X-125
TEST DATE 10/30/64
BURNER ANNULAR
SCH 5 MOD IA
FUEL TYPE JP5
VELOCITY INLET 529 FPS, LINER 120 FPS
AIRFLOW 84,377 PPH
AVG INLET AIR TEMP 600°F
AVG RAKE TEMP 1648°F
INLET TOTAL PRESS (IN. H_g ABS) 41.7



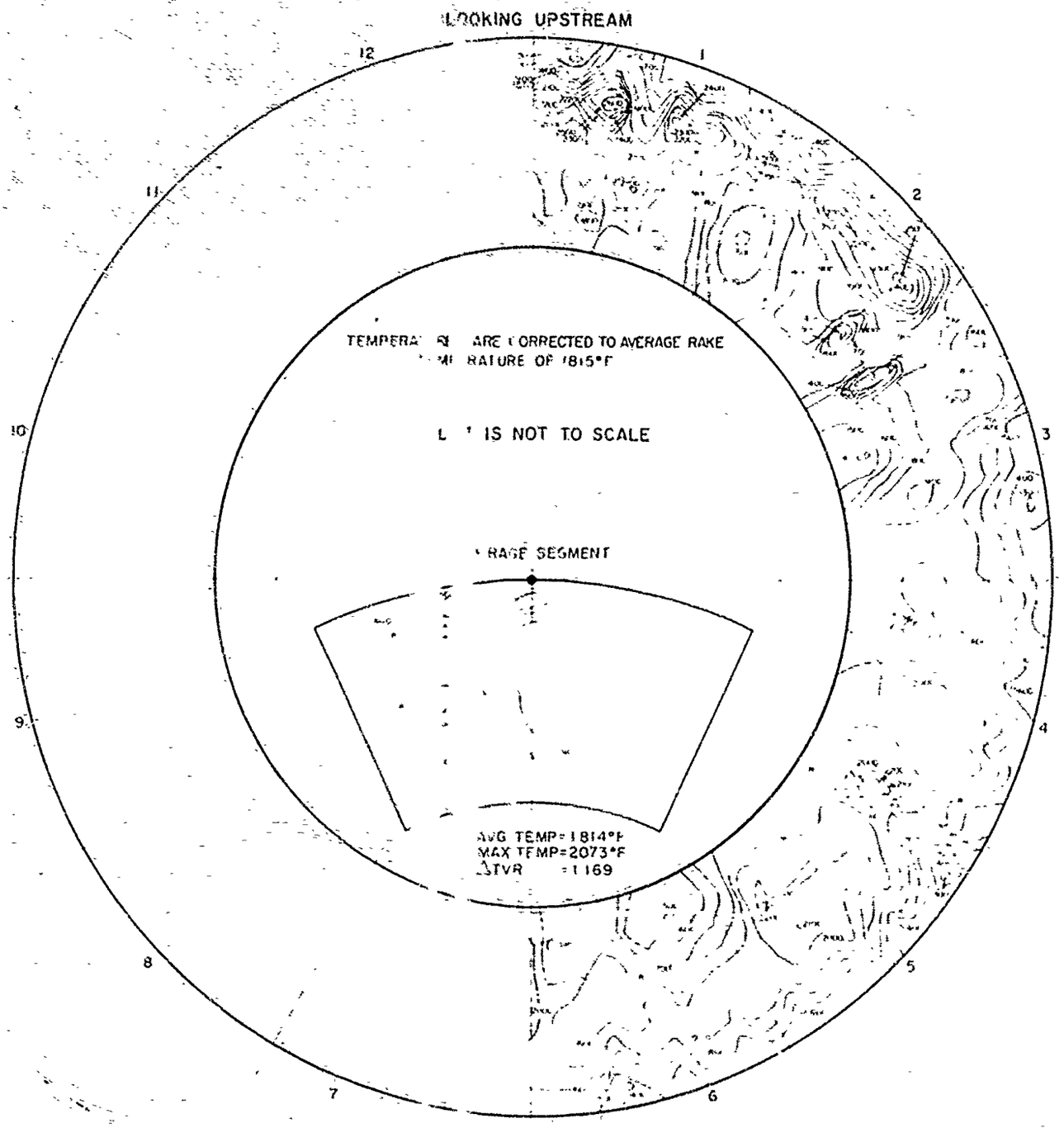
DISTORTED
INLET PROFILE

SEGMENT	1	2	3	4	5	6	7	8	9	10	11	12
AVG TEMP °F	1807	1699	1754	1800	1816	1754	1760	1937	1888	1881	1923	1850
MAX TEMP °F	2065	1931	1912	1994	1929	1931	1948	2072	2225	2470	2222	2253
ΔT	248	1249	1160	1188	1107	1179	1189	1219	1301	1556	1259	1372

AVG ΔT VR—12 SEGMENTS ~ 1.25
11 SEGMENTS ~ 1.22
(NO 10 OMITTED)

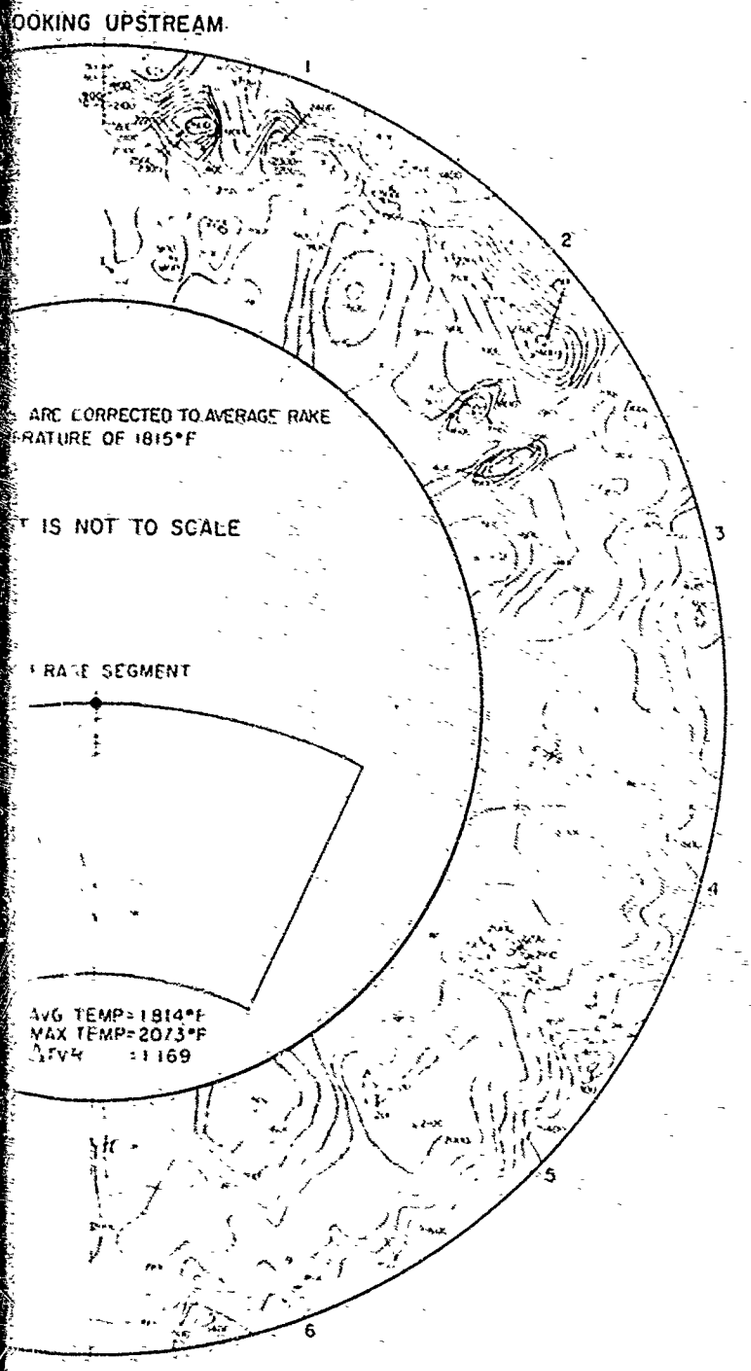
ISOTHERM PLOT

PRATT & WHITNEY AIRCRAFT



ISOTHERM PLOT (RU

Figure 5-16



BURNER DISCHARGE TEMPERATURE PLOT
RIG NO 25003L STAND NO. X-125
TEST DATE 11/4/64
BURNER ANNULAR
SCH 5 MOD 1A
FUEL TYPE JP5
VELOCITY INLET 503 FPS LINER 114 FPS
AIRFLOW 89,855 PPH
AVG INLET AIR TEMP 496°F
AVG RAKE TEMP 2028°F
INLET TOTAL PRESS (IN H_0 ABS) 42.14

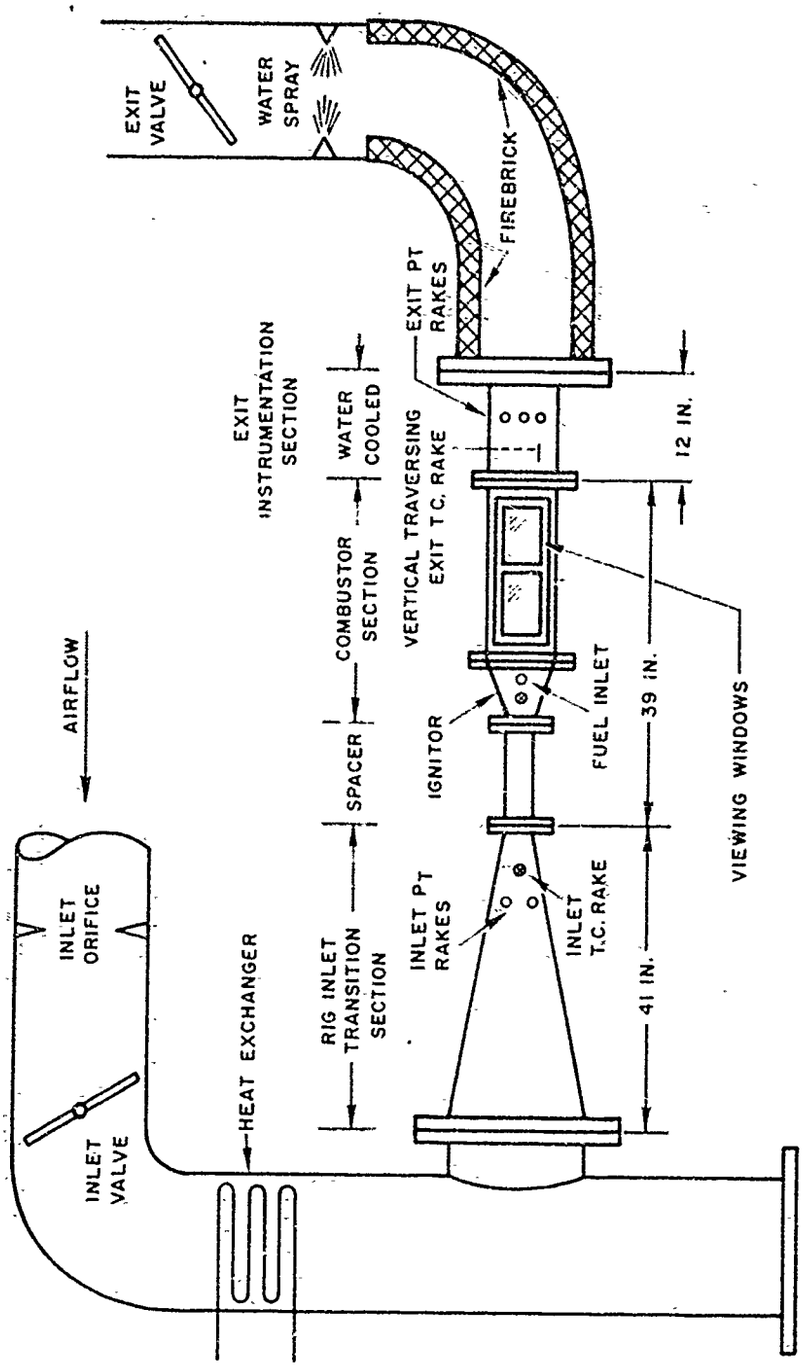
ΔT
1532°F
15
RUN NO

CLEAN INLET

SEGMENT	1	2	3	4	5	6
AVG TEMP °F	1948	1796	1675	1842	1846	1775
MAX TEMP °F	2637	2512	1932	2282	2282	2005
ΔTVR	1414	1474	1184	1282	1279	1167

ISOTHERM PLOT (RUN 15)

Figure 5-16

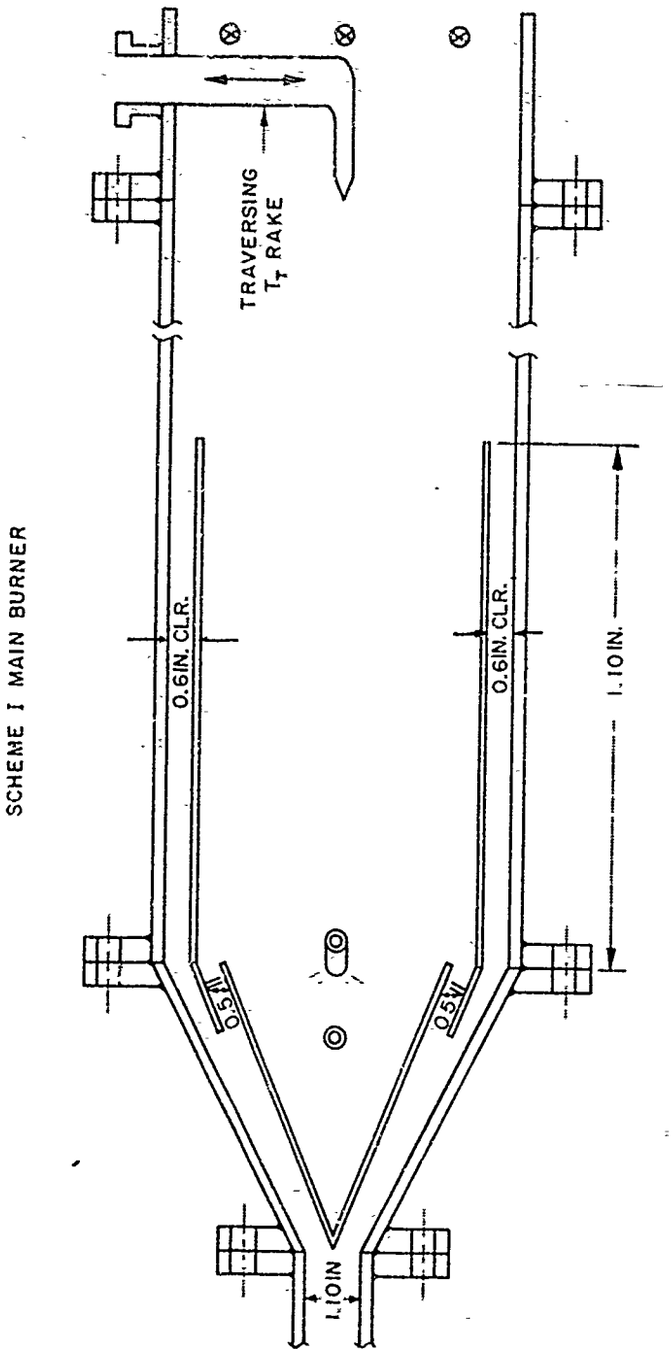


ADVANCED PRIMARY COMBUSTION TEST RIG

Figure 5-17

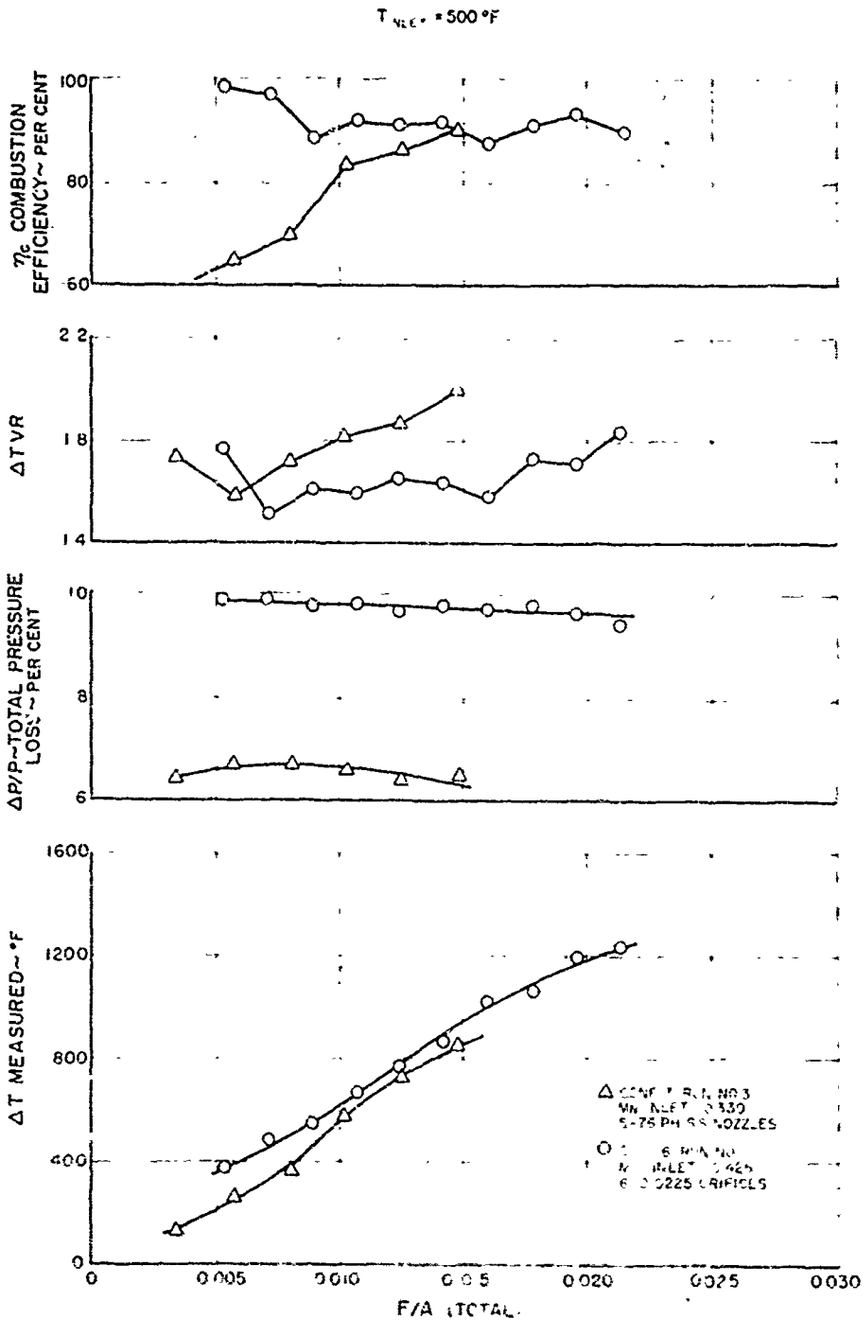
DOWNGRADED AT 3 YEAR INTERVALS
DECLASSIFIED AFTER 12 YEARS
DOD DIR 5200.10

THIS DOCUMENT CONTAINS INFORMATION AFFECTING THE NATIONAL DEFENSE OF THE UNITED STATES WITHIN THE MEANING OF THE ESPIONAGE LAWS, TITLE 18, U.S.C., SECTIONS 793 AND 794. ITS TRANSMISSION OR THE REVELATION OF ITS CONTENTS IN ANY MANNER TO AN UNAUTHORIZED PERSON IS PROHIBITED BY LAW.



ADVANCED BURNER CONFIGURATION

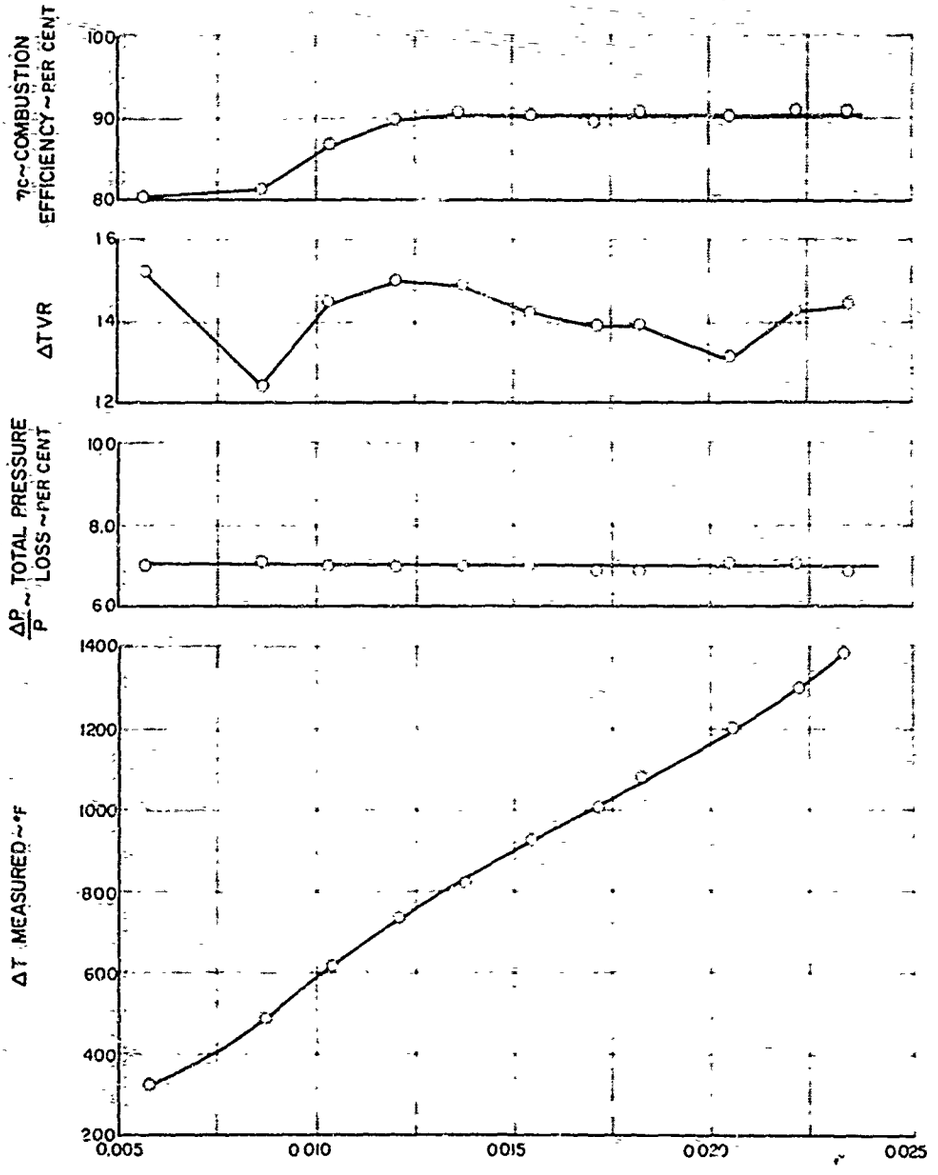
Figure 5-18



ADVANCED BURNER TEST RESULTS

Figure 5-19

T_{INLET} = 500°F
INLET MACH NO. = 0.330
CONFIG NO 6-B RUN NO 5

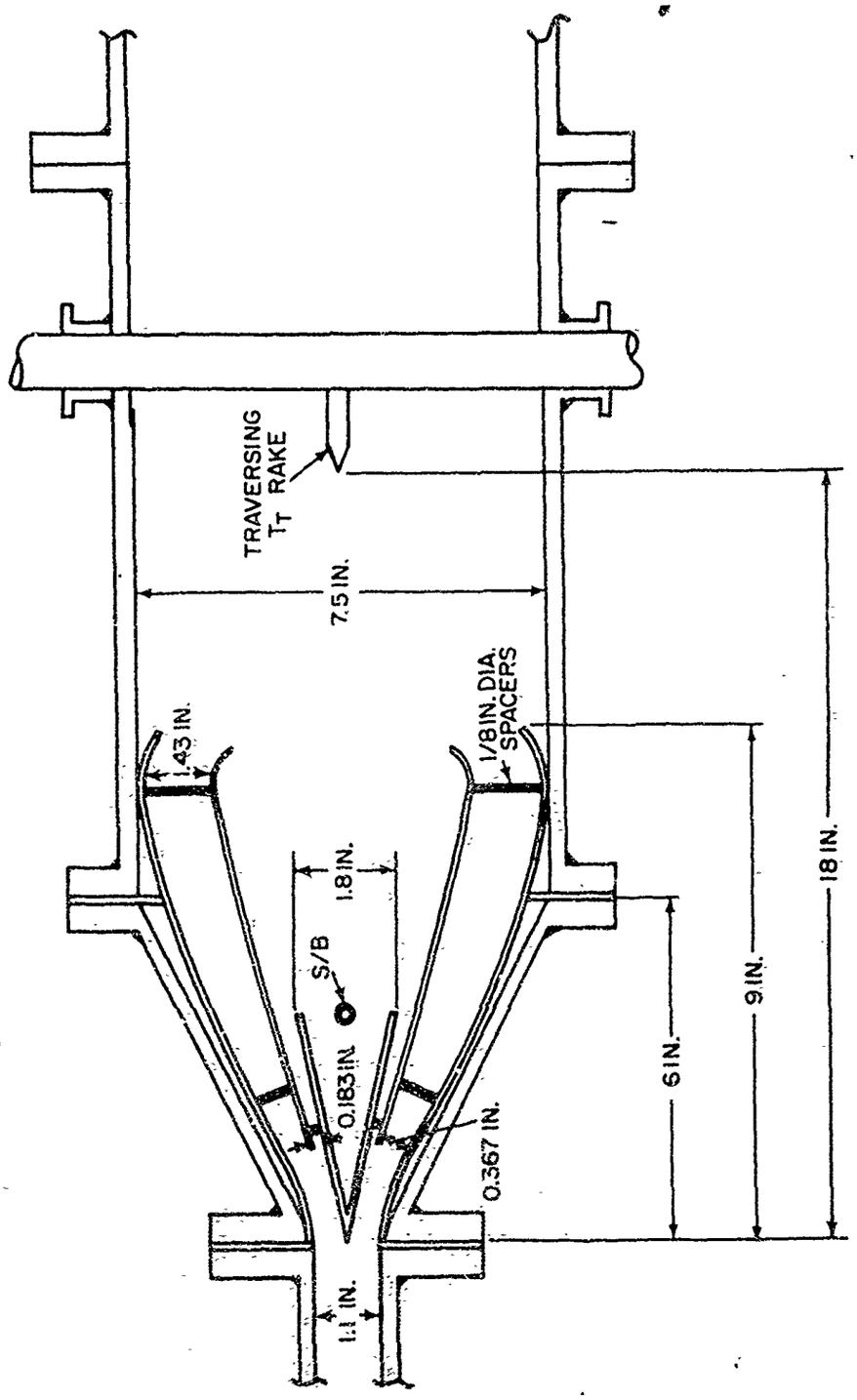


ADVANCED BURNER TEST RESULTS

Figure 5-20

DOWNGRADED AT 3 YEAR INTERVALS
DECLASSIFIED AFTER 12 YEARS
DOD DIR 5200.10

THIS DOC. CONTAINS INFORMATION AFFECTING THE NATIONAL DEFENSE OF THE UNITED STATES WITHIN THE MEANING OF THE ESPIONAGE LAWS, TITLE 18, U.S.C. SECS. 793 AND 794. THE TRANSMISSION OR REVELATION OF ITS CONTENTS IN ANY MANNER TO AN UNAUTHORIZED PERSON IS PROHIBITED BY LAW.



ADVANCED BURNER CONFIGURATION.

Figure 5-21

DOWNGRADED AT 3 YEAR INTERVALS
DECLASSIFIED AFTER 12 YEARS
DOD DIR 5200.10

THIS DOCUMENT CONTAINS INFORMATION AFFECTING THE NATIONAL DEFENSE OF THE UNITED STATES WITHIN THE MEANING OF THE ESPIONAGE LAWS, TITLE 18, U.S.C., SECTIONS 793 AND 794. THE REVELATION OF ITS CONTENTS IN ANY MANNER TO AN UNAUTHORIZED PERSON IS PROHIBITED BY LAW.

TURBINES



ITEM 6 - TURBINE DEVELOPMENT

OBJECTIVE

To conduct development testing of turbine components directed toward verification of the turbine design and to measure the effectiveness of turbine bucket and nozzle diaphragm cooling. The specific goals of this program were to advance the technology available for turbine design by conducting cyclic tests of turbine components employing advanced cooling techniques and to further substantiate the effect of turbine cooling on turbine performance parameters.

A. INTRODUCTION

An extensive program of laboratory, rig and engine testing was conducted to evaluate the capability of new blade and vane designs. This work included testing of advanced film and transpiration cooled turbine components as well as the further investigation of convectively cooled blade and vane designs. Because of the need to provide as much information as quickly as possible for the guidance of the STF219 development effort, the numerous test programs described below were conducted simultaneously rather than in series. Hardware was primarily of the JT4 size to expedite testing. Where possible existing parts were modified to permit the early evaluation of the various vane and blade schemes under consideration.

The turbine development program was divided into four principal areas of effort which are briefly defined below.

1. SINGLE SPECIMEN TESTS TO OPTIMIZE THE DURABILITY OF AIR COOLED VANES AND BLADES

In addition to the conventional stress rupture and erosion-corrosion testing which is described in Item 15 of this report, special tests were conducted to examine material behavior under conditions peculiar to turbine airfoils. Essentially all of the turbine blade and vane designs studied in this program incorporated internal passages for the cooling air and holes in the airfoil surface for the discharge of the cooling air. Therefore it was important to determine the effect of these holes on the structural capabilities of the airfoils. Tests were run using blade

DOWNGRADED AT 3 YEAR INTERVALS
DECLASSIFIED AFTER 12 YEARS
DOD DIR 5200.10

THIS DOCUMENT CONTAINS INFORMATION AFFECTING THE NATIONAL DEFENSE OF THE UNITED STATES WITHIN THE MEANING OF THE ESPIONAGE LAWS, TITLE 18, U.S.C., SECTIONS 793 AND 794. ITS TRANSMISSION OR THE REVELATION OF ITS CONTENTS IN ANY MANNER TO AN UNAUTHORIZED PERSON IS PROHIBITED BY LAW.

and vane specimens that had cooling passages representative of the airfoil holes in programs involving thermal shock tests, impact tests, fatigue tests, low cycle fatigue tests and combined thermal shock and creep tests to determine what property changes were associated with the cooling holes.

2. HEAT TRANSFER

Heat transfer tests were required to optimize the distribution of the cooling air passages in the airfoil in order to minimize thermal gradients and substantiate current design analysis procedures. In this program, the effect of film cooling as well as different means of establishing the film were evaluated. This investigation was conducted on single test specimens and on grouping of parts assembled to simulate engine configurations in a cascade rig.

3. PERFORMANCE TESTS

The effect of cooling air on the aerodynamic performance of the turbine is a function of the means used to re-introduce the cooling air into the engine cycle and the leakage incurred in routing the cooling air to the cooled parts. For this reason, investigations were conducted in a plane cascade rig at various coolant flow to determine the profile losses resulting from the discharge of the cooling air. In addition, tests were conducted in a full-scale rotating turbine rig to determine how the various blade and vane cooling schemes affected overall stage efficiency.

4. ENGINE TESTING

The final evaluation of any design must be accomplished through full-scale engine performance and endurance tests. In this phase of the turbine development effort, a JT4 high spool engine was used to conduct cyclic endurance tests on full-scale air-cooled blade and vane designs at conditions simulating operation in a supersonic transport powerplant.

B. SINGLE SPECIMEN RIG TESTING TO EVALUATE THE DURABILITY OF AIR COOLED TURBINE BLADES

As part of the development effort on air cooled turbine blades, test programs were undertaken to investigate the resistance of convectively cooled and film cooled blade designs to (1) thermal shock, (2) foreign

DOWNGRADED AT 3 YEAR INTERVALS
DECLASSIFIED AFTER 12 YEARS
DOD DIR 5200.10

THIS DOCUMENT CONTAINS INFORMATION AFFECTING THE NATIONAL DEFENSE OF THE UNITED STATES WITHIN THE MEANING OF THE ESPIONAGE LAWS, TITLE 18 U.S.C. SECTIONS 793 AND 794. THE TRANSMISSION OR THE REVELATION OF ITS CONTENTS IN ANY MANNER TO AN UNAUTHORIZED PERSON IS PROHIBITED BY LAW.

object damage at elevated temperature levels and (3) clogging caused by contaminants in the cooling air. This work was conducted on individual blade specimens rather than on a complete rotor assembly because of the speed, flexibility and low cost of this approach. A small burner rig, which is described below, was used in these programs.

1. DESCRIPTION OF TEST RIG

The test rig consisted essentially of a pipe containing a combustion chamber and a mount for the positioning the test blade downstream of the burner so that the hot gases impinged on the leading edge. The air was supplied to the combustion chamber by a commercial blower. If the test blades required cooling air, the latter was supplied from a high pressure source through a heater prior to entering the blades. Means were provided for varying cooling air pressure and temperature independently. Blade metal temperature were measured by an infrared scanning device.

2. THERMAL SHOCK TESTS

The thermal shock tests were accomplished by cycling the fuel flow to the combustion chamber with each cycle consisting of one minute at a high temperature level (to produce a 2000°F uncooled leading edge metal temperature in the blade) and one-half minute cold (170°F). If cooling air was used, it was preheated to 700°F; coolant flow rates were dependent upon the metal temperature desired.

Both film cooled and convectively cooled blades were tested in this program. The convectively cooled blades had hollow cores with internal radial cooling fins (the so-called sawtooth design*). The film cooled blades were of the same basic sawtooth design with the addition of a single row of .030" diameter holes drilled along the leading edge stagnation line and one row of .013 diameter holes drilled on both sides near the trailing edge. The holes were angled at 30° from the leading edge as shown in Figure 6-1. All blades were of PWA 659 material. Two blades of each type were tested with the following results:

*Two configurations of sawtooth blades were used in the overall program - a .030" sawtooth blade and a .020" sawtooth blade. These dimensions referred to the height of the radial cooling fins.

DOWNGRADED AT 3 YEAR INTERVALS
DECLASSIFIED AFTER 12 YEARS
DOD DIR 5200.10

THIS DOCUMENT CONTAINS INFORMATION AFFECTING THE NATIONAL DEFENSE OF THE UNITED STATES WITHIN THE MEANING OF THE ESPIONAGE LAWS, TITLE 18, U.S.C., SECTIONS 793 AND 794. ITS TRANSMISSION OR THE REVELATION OF ITS CONTENTS IN ANY MANNER TO AN UNAUTHORIZED PERSON IS PROHIBITED BY LAW.

Configuration	No. of Cycles	Results	Shown In
.030" Sawtooth (Film Cooled)	100	L. E. Crack**	Figure 6-2
.030" Sawtooth (Film Cooled)	500	L. E. Crack**	
Sawtooth - Basic	700	L. E. burned out due to rig malfunction	
Sawtooth - Basic	1000	No cracks, in good condition	Figure 6-3

3. CLOGGING TESTS

Tests were conducted to investigate the susceptibility of several air cooled blade designs to cooling hole blockage as a result of contaminants in the cooling air supply. Three blade configurations were evaluated. Two of these were identical with the ones used in the thermal shock program described above. The third incorporated the basic sawtooth configuration with the addition of five rows of .008 diameter holes drilled in the leading edges at a 30° angle. Blades of each design were installed in the rig noted in para. 1 above, and after establishing the desired temperature levels and cooling airflow, a predetermined quantity of Arizona Road Dust was injected into the cooling air stream. The quantity injected per cycle was gradually increased as the test progressed until clogging of the air passages occurred. An increase in leading edge metal temperature of 100°F above the original steady state temperature was considered to be evidence that some of the cooling passages had plugged.

The results of the clogging tests are given in the table below. This table lists the blade designs tested, the temperature level maintained for each test and the quantity of road dust (injected per test cycle) necessary to clog the blades.

**In both cases the cracks originated at the sharp-edges of the exit holes. The sharp edges resulted from use of existing parts which had small leading edge radii. This produced a large hole diameter/leading edge radius ratio.

DOWNGRADED AT 12 YEAR INTERVALS
DECLASSIFIED AFTER 12 YEARS
DOD DIR 5200.10

THIS DOCUMENT CONTAINS INFORMATION AFFECTING THE NATIONAL DEFENSE OF THE UNITED STATES WITHIN THE MEANING OF THE ESPIONAGE LAWS, TITLE 18, U.S.C., SECTIONS 793 AND 794. THE TRANSMISSION OR THE REVELATION OF ITS CONTENTS IN ANY MANNER TO AN UNAUTHORIZED PERSON IS PROHIBITED BY LAW.

Configuration	Initial Steady State L. E. Temp.	Quantity of Contaminant to Raise Temp. 100°F
Film Cooled (.030" dia holes)	1640°F	Unable to plug, maximum was 1 1/4 oz.
Film Cooled (.008" dia holes)	1680°F	1.0 oz.
Convectively Cooled (sawtooth design)	1820°F	Unable to plug, maximum was 1.0 oz.

Since the concentration of contaminant required to clog the cooling passages in any of these blade designs was much greater than anything that might be encountered in service, it was concluded that all three designs were satisfactory in this respect.

4. IMPACT TESTS

Tests to evaluate the impact resistance of air-cooled turbine blades were conducted in the rig described at the start of this section. For these tests, a projectile consisting of two 1/8" steel pellets brazed together and encased in lead was fired at the blade by a high velocity air gun (840 feet/sec-nozzle velocity) while the rig was being operated at elevated temperature levels. (2000°F leading edge temperature) The average weight of the pellet was 0.8 grams. The gun was aimed to strike the blade at a location considered appropriate based on field experience 1/8" from the leading edge. The test setup is shown in Figure 6-4.

Impact tests were conducted on all three of the blade configurations evaluated in the clogging tests described above. The post-test condition of the parts is shown in Figures 6-5, 6-6, and 6-7 demonstrating the good resistance of these blades to foreign object damage.

C. MATERIALS LABORATORY TESTING TO EVALUATE BLADE AND MATERIALS DURABILITY

As part . the development program on air-cooled blades and vanes, a series of laboratory tests were conducted at the Contractor's Materials Development Laboratory to determine the effect of drilling holes in

DOWNGRADED AT 3 YEAR INTERVALS
DECLASSIFIED AFTER 12 YEARS
DOD DIR 5200.10

THIS DOCUMENT CONTAINS INFORMATION AFFECTING THE NATIONAL DEFENSE OF THE UNITED STATES WITHIN THE MEANING OF THE ESPIONAGE LAWS, TITLE 18, U.S.C., SECTIONS 793 AND 794. THE TRANSMISSION OR THE REVELATION OF ITS CONTENTS IN ANY MANNER TO AN UNAUTHORIZED PERSON IS PROHIBITED BY LAW.

blade and vane materials using the Electrical Discharge Machining (EDM) process on the fatigue life and other physical properties of these materials. Three alloys, PWA-657, PWA-659, and PWA-689 were investigated using both test specimens and finished parts. These tests were divided into five separate programs which are outlined in the paragraphs below.

1. BLADE FATIGUE TESTS

Testing to determine the fatigue life of air cooled blades at elevated temperatures was conducted in the rig shown in Figure 6-8. This rig consisted of two main elements - a furnace used to heat the blade (to a temperature of 1400°F) and an electromagnet to provide excitation for the blades. The root end of the blade was brazed to a block inside the furnace while the tip of the blade protruded outside the furnace where it could be excited by the electromagnet. Magnetic blocks were welded to the tip of the blade to facilitate excitation. Stresses were measured by strain gages located on the convex side of the blade at the maximum airfoil root thickness. Testing was started at a relatively low stress level to obtain a runout condition, i. e., no failure after 10^6 cycles. After the initial tests, stress levels were increased with each successive blade to obtain a of stress vs cycles to failure.

A baseline runout value of 25,000 psi was established for the PWA-659 convectively cooled sawtooth blades. Subsequently four film-cooled blades of the so-called "showerhead" design were tested. These blades were similar to the sawtooth blades noted above except that the cooling tube exit area at the tip of the blades was reduced by seventy percent and five radial rows of .008" diameter holes were drilled in the region of the leading edge. Tests of the showerhead blades indicated a runout value of 15,000 psi.

In addition, three PWA-689 uncooled blades with slots (.010" wide and .075" deep) in the leading edges were run in the blade fatigue rig. The object of the latter tests was to determine the effect of the slots on blade durability. The runout value for these blades were determined to be 15,000 psi.

DOWNGRADED AT 3 YEAR INTERVALS
DECLASSIFIED AFTER 12 YEARS
DOD DIR 5200.10

THIS DOCUMENT CONTAINS INFORMATION AFFECTING THE NATIONAL DEFENSE OF THE UNITED STATES WITHIN THE MEANING OF THE ESPIONAGE LAWS, TITLE 18 U. S. C. SECTIONS 793 AND 794. THE TRANSMISSION OR THE REVELATION OF ITS CONTENTS IN ANY MANNER TO AN UNAUTHORIZED PERSON IS PROHIBITED BY LAW.

2. LOW CYCLE FATIGUE TESTS

Low cycle fatigue tests to determine the effect of drilled passages on the strength of test specimens fabricated from PWA-657 alloy were conducted in the rig shown in Figure 6-9. This rig was basically a hydraulically operated piston applying a cyclic tension-compression loading to a specimen maintained at a selected temperature level by a wire wound furnace. The procedure in making these tests was to apply an alternating load of ±60,000 psi at a frequency of 30 cycles/minute while maintaining the metal temperature at 1200°F.

Figure 6-10 shows a cross section view of a representative test specimen. Tests on undrilled PWA-657 specimens were run at stress levels of ±59,000 psi indicating a life of 3500 cycles to failure. Tests on drilled (.020" diameter) specimens of this material at the same stress demonstrated a life of 250 cycles to failure. The stress concentration factor for the drilled specimens was set at 2.8 which is considerably more severe than that used in normal design practice in order to accelerate the test.

3. CYCLIC CREEP TESTS

Cyclic creep tests were run on specimens of blade and vane alloys in the rig shown in Figure 6-11. Basically this rig consisted of a mechanical device which rotated and cycled a single test specimen between the flame of a small burner and a cold air jet while maintaining an axial stress of 20,000 psi on the specimen. Rotation of the test part was considered to be necessary to insure uniform heating and cooling of the entire part. During the test cooling air was passed through the central passage of the specimen.

The test procedure followed was to run twenty-five test cycles on the specimen, then shut down and make a visual examination and take creep measurements. The test was terminated whenever the examination revealed a crack. Each cycle consisted of fifteen minutes at a metal temperature of 1900°F and a stress of 20,000 psi followed by five minutes in a cold air jet with no load. During the entire cycle air was passed through the cooling air hole at a rate of 36 #/hr.

A cross-section of the standard undrilled specimen which was used as a baseline is shown in Figure 6-12. Figure 6-13 shows the same specimen but with the addition of EDM radial drilled holes. PWA-659 specimens with and without radial cooling holes were tested with no cracking

DOWNGRADED AT 3 YEAR INTERVALS
DECLASSIFIED AFTER 12 YEARS
DOD DIR 5200.10

THIS DOCUMENT CONTAINS INFORMATION AFFECTING THE NATIONAL DEFENSE OF THE UNITED STATES WITHIN THE MEANING OF THE ESPIONAGE LAWS, TITLE 18, U.S.C., SECTIONS 793 AND 794. THE TRANSMISSION OR REVELATION OF ITS CONTENTS IN ANY MANNER TO AN UNAUTHORIZED PERSON IS PROHIBITED BY LAW.

after 125 cycles. The test specimens incorporating radial cooling holes ran cooler (1750°F vs 1900°F), consequently the growth was less (0.9×10^{-3} vs. 3.7×10^{-3}). Identical tests, conducted on PWA-663 specimens, showed a growth after 100 test cycles of 11.0×10^{-3} for undrilled specimens and 1.0×10^{-3} for drilled specimens.

A similar series of tests was performed on radially drilled specimens of PWA-659 and PWA-663 material at 1900°F metal temperature for direct comparison with the undrilled specimens. Growth after seventy-five test cycles was 5.2×10^{-3} for the PWA-659 specimens and 1.0×10^{-3} for the PWA-663 specimens.

4. CYCLIC STRESS RUPTURE TESTS

Cyclic stress rupture tests were run on PWA 657 and PWA 659 materials at temperatures up to 1800°F using an arc weld creep test machine which had been modified to provide automatic cycling of the tensile load. The machine used for this test is shown in Figure 6-14. During the stress rupture tests, the rig was operated on a cycle which consisted of 30 minutes under load and 5 minutes with no load.

Tests were conducted to compare the life of undrilled PWA-657 specimens shown in Figure 6-15 with that of drilled specimens having .010" diameter holes at the grain boundary. Four specimens of each configuration were tested at a maximum stress level of 12,000 psi and a temperature of 1800°F. The undrilled specimens failed after an average of 190 hours and the drilled specimens failed after 150 hours. Tests on an undrilled specimen of PWA 659 material at a maximum stress level of 45,000 psi and a temperature of 1600°F resulted in a failure after 182 hours of testing.

5. HIGH TEMPERATURE FATIGUE TESTS

In another phase of the testing to determine the fatigue strength of turbine blade alloys, high temperature fatigue tests using specimens of PWA-659 alloy were performed in a Westinghouse Reverse Bending Fatigue Machine. These tests were conducted with the machine operating at 120 cps and a specimen temperature of 1600°F. Figure 6-16 shows a typical specimen used for this test. A failure was induced in this specimen after 5.4×10^6 cycles of testing at a load of 53,500 psi.

DOWNGRADED AT 3 YEAR INTERVALS
DECLASSIFIED AFTER 12 YEARS
DOD DIR 5200.10

THIS DOCUMENT CONTAINS INFORMATION AFFECTING THE NATIONAL DEFENSE OF THE UNITED STATES WITHIN THE MEANING OF THE ESPIONAGE LAWS, TITLE 18, U.S.C., SECTIONS 793 AND 794. THE TRANSMISSION OR THE REVELATION OF ITS CONTENTS IN ANY MANNER TO AN UNAUTHORIZED PERSON IS PROHIBITED BY LAW.

D. INVESTIGATION OF THE HEAT TRANSFER CHARACTERISTICS OF AIR COOLED VANES IN A LOW PRESSURE CASCADE RIG

An extensive experimental program was conducted to study the relative heat transfer characteristics of various turbine vane cooling schemes at the United Aircraft Research Laboratories in a low pressure heat transfer cascade rig. While all work was done on vanes, the results of this investigation are considered to be, in general, applicable to turbine blades as well. Since the objectives of the program were to compare the effectiveness of individual cooling schemes, the test vanes were designed to incorporate only the particular cooling scheme under investigation, i. e., if a particular leading edge configuration was being considered, provisions for cooling in the midchord and trailing edge regions were not included.

1. DESCRIPTION OF RIG

The test facility used for this program consisted essentially of a low pressure hot air source supplying air at temperatures up to 2025°F, a high pressure secondary source supplying cooling air and a test section. The test section consisted of one test vane and one slave vane on either side to provide the proper gas passage and a contoured end wall to provide the proper gas path for the slave vanes. Provisions were made for optically measuring the test vane metal temperatures using infra-red pyrometers.

The rig was calibrated so that, when the main air stream temperature was 2025°F, the test vane temperature, uncooled, was 1800°F at the leading edge and 1665°F at the trailing edge. (The difference between the test vane metal temperature and the gas stream was due to radiation and conduction of heat to the cooled outer walls of the rig.) Cooling effects were determined simply by measuring the test vane metal temperature using varying amounts of cooling airflow at a known temperature. To simulate engine conditions as closely as possible, the test section was operated at a choked pressure ratio.

DOWNGRADED AT 3 YEAR INTERVALS
DECLASSIFIED AFTER 12 YEARS
DOD DIR 5200.10

THIS DOCUMENT CONTAINS INFORMATION AFFECTING THE NATIONAL DEFENSE OF THE UNITED STATES WITHIN THE MEANING OF THE ESPIONAGE LAWS, TITLE 18, U.S.C., SECTIONS 793 AND 794. THE TRANSMISSION OR THE REVELATION OF ITS CONTENTS IN ANY MANNER TO AN UNAUTHORIZED PERSON IS PROHIBITED BY LAW.

2. TEST RESULTS

A total of forty-eight test runs were made during this contract period on approximately twenty turbine vanes employing various cooling schemes. Figure 6-17 summarizes all of the vanes tested and lists comparative leading and trailing edge temperatures at a common test condition and a common reference coolant flow rate. Figure 6-17 also provides references to Figures 6-18 through 6-70. The data obtained from this program were used as background information for the design of the blade and vane cooling schemes in the STF219 engine.

E. INVESTIGATION OF HEAT TRANSFER CHARACTERISTICS OF AIR COOLED TURBINE VANES IN A HIGH PRESSURE CASCADE RIG

A short program to investigate the heat transfer characteristics of air cooled turbine vane designs was conducted in a high pressure cascade rig at the United Aircraft Research Laboratory. This facility was similar to the low pressure cascade rig described in Section D except that it operated at engine pressure levels (up to 200 psia). The rig was run at inlet air temperatures of 2400°F for this program although it was capable of operation up to 3800°F. Figure 6-71 shows the rig and its components.

A shielded leading edge turbine vane was tested in this rig at an inlet air temperature of 2400°F and a pressure of 130 psia. A vane of this type is shown in Figure 6-72. At these conditions the cooling air flow supplied was not sufficient to provide adequate cooling for the leading edge shield. As a result the shield ran hot and collapsed. Three other air cooled vane configurations were prepared for testing in this rig. Because of lack of time, these parts were not evaluated during this report period; however, they will be tested under other funding. These vanes are shown in Figure 6-73 through 6-75.

F. HEAT TRANSFER IMPINGEMENT TESTS

Tests to determine local heat transfer coefficients in the internal airfoil passages of an air cooled vane were conducted in a heat transfer impingement rig. This rig was basically a five-times scale

model of the internal leading edge portion of a turbine vane and is shown in Figure 6-76. Local heat transfer coefficients were determined by measuring temperature change with time when sudden changes were made in the cooling airflow. The data in this program is summarized in Figure 2-97 of the preliminary design section of this report (Item 2).

G. TESTING OF AIR COOLED VANES IN A HOT CHOKED CASCADE RIG

Late in this report period, a turbine vane cascade rig designed for the thermal shock testing of air-cooled vanes at conditions simulating SST operation was installed in a test stand at the contractor's engineering laboratory. After the installation was completed, several performance calibrations were completed.

1. DESCRIPTION OF TEST RIG

The test vehicle which is shown in Figure 6-77 consisted of a translating water cooled vane holder, two cold air ducts, and a centrally-located hot gas duct. In operation, the vane holder, which had a capacity for testing twenty vanes (ten vanes per pack) simultaneously, was translated to a position in which ten vanes were exposed to the hot gas stream and ten to the cold gas stream. After a predetermined exposure period, the holder was moved rapidly in the reverse direction, exposing the ten heated vanes to the cold air stream and positioning the ten cold vanes in the hot gas stream. This alternate exposure to hot gas and cold air constituted one thermal shock cycle. A schematic diagram of hot choked cascade rig is shown in Figure 6-78.

During operation, air was supplied to the inlet of the cold air ducts and the central hot air duct at a temperature of 200°F and pressure up to 200" HgA. The air in the hot duct was preheated to test temperatures by engine-type burner cans using JP-4 fuel before being passed through the vane cascade, and finally into an exhaust plenum. The cold air was discharged directly from the supply plenum through the cold ducts and the vane cascade into the exhaust plenum where it was mixed with the exhaust gases from the hot duct. Pressure in the exhaust plenum was controlled by a back pressure valve to insure a choked flow across the vane pack.

DOWNGRADED AT 3 YEAR INTERVALS
DECLASSIFIED AFTER 12 YEARS
DOD DIR 5200.10

THIS DOCUMENT CONTAINS INFORMATION AFFECTING THE NATIONAL DEFENSE OF THE UNITED STATES WITHIN THE MEANING OF THE ESPIONAGE LAWS, TITLE 50 U.S.C. SECTIONS 793 AND 794. ITS TRANSMISSION OR THE REVELATION OF ITS CONTENTS IN ANY MANNER TO AN UNAUTHORIZED PERSON IS PROHIBITED BY LAW.

Air for the vane cooling passages was supplied to the test vanes from another compressor. The air was first passed through an alcohol burner to raise it to the temperature selected. It was then discharged into a plenum located at the bottom of the vane holder. From the plenum the air was supplied to each vane in the cascade and was discharged from there into the gas stream.

2. TEST PROGRAM

After the installation of the rig in a test stand was completed, calibrations were performed at an inlet pressure of 180 in. Hg and inlet temperatures of 1800°F and 1900°F in order to determine inlet temperature distribution. An analysis of the data revealed that changes in the burner exit profile were required to make the rig more representative of actual engine conditions. At the close of this report period, these changes were being accomplished in preparation for endurance testing to evaluate the thermal shock characteristics of several air cooled turbine vane configurations under other funding.

H. AERODYNAMIC PERFORMANCE TESTING OF TURBINE VANES IN A PLANE CASCADE RIG

A program of aerodynamic tests was conducted on air-cooled turbine vanes in a plane cascade rig for the purpose of obtaining data on the optimum location for the cooling air discharge holes. The plane cascade rig was basically a small wind tunnel with the capability of producing a choked flow across a cascade of four turbine vanes. It was used to evaluate the two-dimensional aerodynamic losses of several of the more promising film and transpiration cooled vane configurations being considered for the STF219 engine as described below.

1. FILM COOLED VANES

a. Description of Component

The film-cooled vane configuration tested in the plane cascade rig incorporated the basic JT4 vane design with the addition of .045" diam. holes drilled at a 45° angle in the vane leading edge stagnation line. The vane pack used in this test is shown in Figure 6-79.

DOWNGRADED AT 3 YEAR INTERVALS
DECLASSIFIED AFTER 12 YEARS
DOD DIR 5200.10

THIS DOCUMENT CONTAINS INFORMATION AFFECTING THE NATIONAL DEFENSE OF THE UNITED STATES WITHIN THE MEANING OF THE ESPIONAGE LAWS, TITLE 18, U.S.C., SECTIONS 793 AND 794. THE TRANSMISSION OR THE REVELATION OF ITS CONTENTS IN ANY MANNER TO AN UNAUTHORIZED PERSON IS PROHIBITED BY LAW.

b. Method of Test

The pressure profile behind the vanes was measured at different cooling air discharge rates, and the profile loss for each cooling flow rate computed.

c. Test Program

The initial run was a calibration to establish the relationship between the pressure ratio and the coolant weight flow. The resulting data is plotted in Figure 6-80. The vane pack was then tested at the design exit Mach number (M_n = .91) and the coolant weight flow varied to obtain the profile loss coefficient ($1 - \Phi^2$) vs % W_C as shown in Figure 6-81. Finally two pressure ratios were selected and maintained while the exit Mach number was varied over the engine operating regime. The results obtained during the latter test are shown in Figure 6-82.

2. TRANSPIRATION COOLED VANES

a. Description of Component

The transpiration cooled vanes evaluated in the plane cascade rig were of the same configuration as the brazed N-155 Rigimesh vanes tested in the high spool engine. (See Section J4). A vane pack consisting of four vanes was used in this test program.

b. Method of Test

The method of test for the transpiration cooled vanes was identical to that used for the film cooled vanes.

c. Test Results

The first step in this test was to establish the relationship of the coolant pressure-primary pressure ratio (Pc/Pp) and the coolant flow-primary flow rate (Wc/Wp). This was accomplished by maintaining the exit Mach number of approximately .91 (design exit Mach number) varying the ratio of cooling air total pressure (Pc/Pp) to maintain total pressure and recording the required data to determine the cooling air to mainstream weight flow (Wc/Wp).

DOWNGRADED AT 3 YEAR INTERVALS
DECLASSIFIED AFTER 12 YEARS
DOD DIR 5200.10

THIS DOCUMENT CONTAINS INFORMATION AFFECTING THE NATIONAL DEFENSE OF THE UNITED STATES WITHIN THE MEANING OF THE ESPIONAGE LAWS, TITLE 18 U.S.C. SECTIONS 793 AND 794. THE TRANSMISSION OR THE REVELATION OF ITS CONTENTS IN ANY MANNER TO AN UNAUTHORIZED PERSON IS PROHIBITED BY LAW.

Using this pressure-flow relationship, two pressure ratios (.95 and 1.11) were set and the Mach number varied over the engine operating regime. At each point taken, the exit air angle, profile loss coefficient and percent cooling air were measured. In addition, with no cooling air discharge, the exit air angle and profile loss coefficient were measured throughout the engine operating regime to establish a baseline for comparison. The results of this test are shown in Figure 6-83.

I. PERFORMANCE TESTING OF FILM COOLED BLADES AND VANES

As part of the development effort on film-cooled turbine vanes and blades, a series of performance tests were conducted in a JT12 rig to obtain quantitative data on the relation between cooling airflow quantity and turbine performance.

1. DESCRIPTION OF TEST RIG

The rig used for this program was essentially a JT12 engine with the compressor, burners and second-stage of the turbine removed. Figure 6-84 shows the basic arrangement of the test rig and indicates the method of supplying cooling air to the blades and vanes and the location and types of the instrumentation used. Figure 6-85 shows the installation of the rig in the test stand. High pressure air for the operation of the rig was provided by steam-driven air compressors capable of supplying air at pressures up to 200 inches of mercury and temperatures up to 215°F. Turbine shaft power was absorbed by a pair of electrical dynamometers connected in tandem.

2. DESCRIPTION OF PARTS TESTED

Convectively cooled blades and vanes, which had been fabricated for an endurance program during the previous FAA-sponsored contract, were reoperated and used for these tests. In re-operating the blades, the cooling air exit passages at the tips were sealed by welding. Slots for discharging the cooling air were machined in the leading edges and holes were drilled in the pressure (concave) and suction (convex) surfaces as shown in Figure 6-86. The leading edge slots were machined using the electrical discharge machining (EDM) process and were inclined 45 degrees with respect to the radial plane so that the cooling air would discharge toward the outside diameter of the turbine. The holes in the pressure and suction surfaces of the blades were drilled perpendicular to the radial plane at an average angle of 30 degrees to

DOWNGRADED AT 3 YEAR INTERVALS
DECLASSIFIED AFTER 12 YEARS
DOD DIR 5200.10

THIS DOCUMENT CONTAINS INFORMATION AFFECTING THE NATIONAL DEFENSE OF THE UNITED STATES WITHIN THE MEANING OF THE ESPIONAGE LAWS, TITLE 18, U.S.C., SECTIONS 793 AND 794. THE TRANSMISSION OR THE REVELATION OF ITS CONTENTS IN ANY MANNER TO AN UNAUTHORIZED PERSON IS PROHIBITED BY LAW.

the airfoil. Because of the twist of the turbine blades, this angle varied from approximately 15 degrees near the root to 45 degrees near the tip on the suction surface and 45 degrees near the root to 15 degrees near the tip on the pressure surface.

In reoperating the vanes for this test, the root (inside diameter) ends were sealed by welding. A cooling air supply boss was welded to the tip end of each vane and the remainder of the opening was filled with a plastic iron compound. Slots were machined in the leading edges and the pressure and suction surfaces as shown in Figure 6-86 using the EDM process. The leading edge slots were inclined 45 degrees with respect to the radial plane so that the cooling air would discharge toward the outside diameter of the turbine. Pressure and suction surface slots were machined perpendicular to the radial plane at a 30 degree angle to the airfoil surface. The vane airfoils were designed with no twist so this angle was constant over the entire span.

Photographs of a completed blade and vane are shown in Figures 6-87 and 6-88 respectively. Turbine specifications and cooling air flow areas are summarized below:

Turbine Specifications & Cooling Air Flow Areas

A. Nozzle

No. of vanes	58
Total flow area	50.8 sq. in.

B. Rotor

No. of blades	74
Total flow area	60.6 sq. in.

C. Cooling Air Flow Area

	Area/Vane Sq. In.	Area/Blade Sq. In.
Leading edge	0.01409	0.01410
Pressure surface	0.00550	0.00608
Suction surface	0.00550	0.00608
Total	0.02509	0.02626

3. METHOD OF TEST

The effect of cooling airflow on turbine performance was determined by setting and maintaining a given pressure ratio and rim velocity ratio while measuring turbine performance with different combinations of blade and vane cooling airflow. Test data were obtained at the design pressure ratio for three velocity ratio settings and at the design velocity ratio for one pressure ratio above and one pressure ratio below the design pressure ratio.

After completing the cooling airflow tests, the cooling holes in the airfoils of the blades and vanes were plugged and leakage calibration tests were run over the range of velocity ratio, pressure ratios and blade cooling supply pressures of interest. Leakage rates and their effect on turbine performance were measured at each velocity ratio for three blade and vane cooling air cavity supply pressures. The effect of leakage on performance was determined independently for the blades and vanes.

A test was also run with the leading edge slots in the blades plugged. Vane cooling airflow was not used for this test.

4. TEST RESULTS

Figure 6-89 shows the effect of the blade and vane cooling airflow (including leakage flow) upon turbine stage aerodynamic performance as measured in the JT12 turbine rig. With equal cooling airflow to the blades and vanes (including leakage) turbine stage efficiency was reduced 1/4 to 1/2 percent for each one percent of the total rig airflow diverted to turbine blade and vane cooling. As indicated in the curve referenced above, the effect of blade cooling airflow on turbine performance was three to five times greater than the effect of the same amount of vane cooling flow.

The change in turbine performance due to vane and blade cooling airflow appeared to be essentially independent of turbine pressure ratio and velocity ratio for the ranges tested. Therefore, the curves shown in Figure 6-89 do no distinguish between the data taken at different combinations of pressure ratio and velocity ratio.

Tests in the JT12 turbine rig showed that leakage accounted for approximately 65 percent of the cooling air supplied to the blades and vanes. Figure 6-90 indicates the probable leakage paths for this flow. Negligible leakage was assumed through the inside diameter labyrinth seal

since this seal was backed up by a carbon-type face seal on the turbine shaft and the only leakage path was through both of these seals in series.

Vane and blade leakage flow had differing effects on turbine performance. Vane leakage produced no measurable effect on turbine performance. Observations indicated that most of the vane leakage was through path B, shown in Figure 6-90, and entered the main flow path along the case outside diameter essentially parallel to the main flow stream.

Blade leakage, on the other hand, resulted in a penalty of approximately 0.2 percent in turbine aerodynamic performance for each percent of leakage expressed as a percent of total turbine airflow. Figure 6-91 shows a plot of the turbine aerodynamic performance penalty as a function of the ratio of blade leakage flow to total rig airflow.

These tests indicated that cooling air leakage is an integral part of turbine performance. Efforts should be made to minimize these leakage losses by improved sealing techniques.

The turbine performance penalty corrected to exclude leakage flow (with equal cooling air flow to the blades and vanes) was between 1/2 and 1 percent for each one percent of the total rig airflow diverted to turbine blade and vane cooling. This penalty would be valid for the ideal turbine with perfect seals. However, since the methods for sealing used in the JT12 turbine and consequently the magnitude of the leakage losses are essentially similar to those of an actual turbine, the penalty previously given for cooling airflow including leakage is considered to be more nearly applicable.

Tests with the blade leading edge slots plugged indicated that one third of the blade cooling airflow (exclusive of leakage) passed through the leading edge and that this flow produced approximately two-thirds of the blade cooling airflow penalty.

Figure 6-92 shows a comparison of the performance penalty for 15 percent cooling airflow (7 1/2 percent to the blades and 7 1/2 percent to the vanes including leakage) against that incurred by off-design operation. It will be noted that the performance penalty imposed by the cooling air is far greater than that imposed by off-design running. Figure 6-93 illustrates the effect of cooling air on the rig inlet flow parameter ($W_a \sqrt{T}/P$). As shown in this curve, the parameter decreases 0.7 percent with each percent of cooling airflow, indicating that 0.7 of each percent of cooling flow is choking the rotor.

DOWNGRADED AT 12 YEAR INTERVALS
DECLASSIFIED AFTER 12 YEARS
DOD DIR 5200.10

J. EVALUATION OF FULL-SCALE TURBINE BLADES AND VANES IN A JT4 HIGH SPOOL ENGINE

Since the final evaluation of any turbine blade or vane configuration must depend on its performance in an engine, development testing of full-scale convectively cooled, film cooled and transpiration cooled blades being developed in this program was undertaken in a JT4-size high spool engine at conditions simulating operation in a supersonic transport engine.

1. DESCRIPTION OF HIGH SPOOL ENGINE

The high spool engine used in this program was basically a JT4 engine with the low compressor and low turbine sections removed. This feature allowed extended operation at elevated temperatures with the minimum amount of operational problems; such as, deterioration of low turbine parts, overspeed of the low compressor and difficulties encountered with removal of the low turbine to replace test section vanes and blades.

The basic hardware consisted of a bellmouth inlet, a seven-stage compressor, complete diffuser and burner sections and a single stage turbine. The exhaust area was designed to produce optimum conditions required by the compressor for starting and continuous operation. The vehicle was equipped with instrumentation in the turbine section allowing for strain gage and thermocouple measurements through a slip ring assembly attached to the turbine shaft. In addition, the normal instrumentation requirements for measuring airflow, pressures and temperatures throughout the vehicle were incorporated.

In order to permit running at elevated turbine inlet temperatures at conditions simulating supersonic transport operation this engine was installed in a test stand incorporating provisions for heating the inlet air. Figure 6-94 shows a view of the heated inlet hardware which was provided for this test; Figure 6-95 shows a schematic diagram of the test installation. At the start of this contract, the turbine section of the JT4 high spool engine was modified to accept externally supplied blade and vane cooling air. The cooling air was supplied by an auxiliary JT12 engine with the cooling air bled off from the compressor discharge as shown in Figure 6-96. The JT12 engine was used in order to permit varying cooling airflow and pressure differentials independent of engine conditions. The vane and blade cooling air system incorporated a

DOWNGRADED AT 3 YEAR INTERVALS
DECLASSIFIED AFTER 12 YEARS
DOD DIR 5200.10

heater burner in the supply line to allow preheating the air to any desired temperature. An overall view of the JT4 engine installation including the vane and blade cooling air system is shown in Figure 6-97. A closeup of the engine showing the vane and blade cooling air manifolds is shown in Figure 6-98.

2. TEST PROCEDURE

After the engine has been assembled and all systems checked out, a short calibration was run to determine the correct turbine inlet-turbine discharge temperature relationship. This procedure was required since engine conditions make difficult the direct measurement of turbine inlet temperature; whereas, direct measurements of the turbine discharge temperature were available. After the relationship between turbine inlet and turbine discharge temperature was established, endurance testing was initiated. The engine was brought up to the maximum turbine inlet temperature desired, and at the completion of a predetermined time interval, the engine was idled back to the minimum turbine inlet temperature level established for the program, thereafter, the engine was cycled back and forth between these two temperature levels to expose the turbine vanes and blades to a thermal fatigue environment. The JT12 auxiliary blade and vane cooling air supply engine and the heated inlet facility were operational during the entire test. The heated inlet was cycled in unison with the high spool engine to produce the desired temperature conditions; however, the JT12 engine was not cycled but was maintained at one cooling air supply and pressure level throughout the test.

To insure that a repeatable cycle was obtained, the engine was controlled by a system of timers, solenoids and values that diverted a portion of the fuel flow to the engine and the heated inlet heater-burner to obtain the required idle turbine inlet temperature. Accelerations and decelerations were extremely rapid.

3. DESCRIPTION OF FILM COOLED VANES AND BLADES TESTED IN HIGH SPOOL ENGINE

Three of the four vane configurations fabricated for this program utilized PWA-657 slotted trailing edge vanes which had been fabricated for the previous FAA sponsored contract. The leading edges were modified and the trailing edge slots were closed by welding and new holes or slots were incorporated to film cool this portion of the vane.

The span-wise cooling passages were retained in the mid chord portions of the vanes to provide convective cooling for this section. These three film cooled vane configurations and a fourth, an impingement type vane, made up specially for this test, are shown in the figures listed below. These three film cooled vane configurations and a fourth, an impingement type vane, made up specially for this test, are shown in the figures listed below.

Configuration	Shown in
1. .013" diam Shower Head	Figure 6-99
2. Porous Leading Edge	Figure 6-100
3. Pierced Sheet Leading Edge	Figure 6-101
4. Impingement	Figure 6-102

Four film cooled blade configurations were designed and fabricated. As in the case of the vanes, these schemes were incorporated in existing convectively cooled blade designs because the length of the contract did not provide sufficient lead time to procure a totally new configuration. The leading edges of the blades were modified to incorporate provisions for film cooling as indicated in the tabulation below. In addition rows of .010" diameter holes were drilled in the trailing edge on both the pressure and suction sides at 30° to the blade surface to provide trailing edge coating.

Design	Shown in
Porous Leading Edge	Leading edge similar to that of vane shown in Fig. 6-74
"Sugar Scoop" Leading Edge	Leading edge similar to that of vane shown in Fig. 6-31
"Umbrella" Leading Edge	Leading edge similar to that of vane shown in Fig. 6-30.

Shower Head

1. 3 Rows of .013" dia. holes at 90° to L.E.	Figure 6-103
2. 3 Rows of .013" holes at 30° to L.E.	Figure 6-104
3. 3 Rows of .008" holes at 90° to L.E.	Figure 6-105
4. 5 Rows of .008" holes at 90° to L.E.	Figure 6-106
5. 5 Rows of .008" holes at 30° to L.E.	Figure 6-107
6. 1 Row of .030" holes at 30° to L.E.	Figure 6-108

The object of varying the hole arrangement in the shower head design were three fold. First, it was desired to determine the effect of differences in hole size. Secondly, the effect of angling the holes was

DOWNGRADED AT 3 YEAR INTERVALS
DECLASSIFIED AFTER 12 YEARS
DOD DIR 5200.10

investigated since an angled hole provides a larger passage and increased cooling due to convection. Finally, the extent of the area to be cooled was investigated by varying the number of cooling hole rows.

As in the case of the vanes, several trailing edge schemes were tested. In addition several showerhead schemes were run without trailing edge cooling for comparison.

4. DESCRIPTION OF TRANSPIRATION COOLED BLADES AND VANES USED IN THE HIGH SPOOL ENGINE

In the design of transpiration cooled blades structural integrity demanded the use of some type of support, referred to as a spar, around which a porous media, referred to as a skin, could be attached. This skin-spar construction was not peculiar to the blade alone but was used for the stationary turbine nozzle as well. Efforts to optimize a transpiration cooled blade and vane of the skin-spar construction resulted in the design of one basic spar design for the vanes and two basic spar designs for the blades for evaluation in the JT4 high spool engine. Both of the blade spar designs were redesigns of an existing convectively cooled blade.

The first blade spar design incorporated .015" deep radial grooves separated by raised portions or lands which are approximately .050" wide and numbered four on the concave airfoil surface and five on the convex.

The second blade design, herein referred to as the wide land blade spar, was an attempt to improve upon the cooling efficiency of the first design. The wide land spar used the same basic convectively cooled blade as did the narrow land, but the land width was increased to approximately 0.150" and the depth of the radial grooves was tapered from .050" at the root to .015" at the tip. These radial grooves were not produced by the EDM machining process but were cast directly in the blade. This wide land design afforded wider attachment surfaces promoting increased heating of the spar core and provides more coolant per unit area of porous skin thus more closely matching the thermal transient response characteristics of the core and skin to improve the thermal fatigue life.

An evaluation of candidate skin materials, including forming trials, led to the selection of three materials: N-155 Poroloy, N-155 Rigimesh,

and L-605 Rigimesh for evaluation in this program based on the following factors:

a. ductility and strength at high temperatures
b. fatigue strength
c. ability to be sinter bonded
d. weldability and brazeability

The following configurations were tested in the JT4 high spool engine:

BLADES

Configuration	Skin	Attachment	Shown In
Narrow land	N-155 Poroloy	E.B. Weld (.040" interface)	Fig. 6-109
Narrow land	N-155 Rigimesh	Braze 82-18	Fig. 6-110
Wide land	L-605 Rigimesh	E.B. Weld (.040" interface)	Fig. 6-111
Wide land	N-155 Poroloy	E.B. Weld (.072" interface)	
Wide land	N-155 Rigimesh	Braze 82-18	Fig. 6-112
Wide land	L-605 Rigimesh	E.B. Weld (.072" interface)	Fig. 6-113
Wide land	L-605 Rigimesh	E.B. Weld	Fig. 6-114
Wide land	N-155 Poroloy	E.B. Weld	Fig. 6-115

E.B. = Electron Beam

VANES

Configuration	Skin	Attachment	Shown In
Wide land	L-605 Rigimesh	E.B. Weld	Fig. 6-116
Wide land	N-155 Poroloy	E.B. Weld	Fig. 6-117
Wide land	N-155 Rigimesh	Braze 82-18	Fig. 6-118

E.B. = Electron Beam

DOWNGRADED AT 3 YEAR INTERVALS
DECLASSIFIED AFTER 12 YEARS
DOD DIR 5200.10

5. DESCRIPTION OF CONVECTIVELY COOLED BLADES AND VANES TESTED IN THE HIGH SPOOL ENGINE

The convectively cooled blades and vanes used in this program were identical to those designed and tested during the previous FAA-sponsored SST propulsion component program. The specific configurations and materials tested are shown in the table below:

Blade Design	Material	Shown In
.020" Sawtooth	PWA-659	--
.030" Sawtooth	PWA-655	Fig. 6-119
Eleven Hole	PWA-658, PWA-663	Fig. 6-120

Vane Design	Material
Slotted Trailing Edge	PWA-657
Pedestal Trailing Edge	PWA-657

6. TESTS OF CONVECTIVELY COOLED BLADES IN THE JT4 HIGH SPOOL ENGINE

The initial tests on the JT4 high spool engine were conducted using the convectively cooled vanes and blades listed in subsection 5 above. These tests were a continuation of the cyclic endurance program which had been started under the Commercial SST Propulsion Component Program, Contract AF 33(657)-11189. This program entailed the running of test cycles consisting of two minutes at high power (2235°F turbine inlet temperature) followed by two minutes at idle (1200°F). Under the previous contract, the engine had completed 767 test cycles with a set of convectively-cooled blades installed. The slotted and pedestal trailing edge vanes installed for this test had accumulated varying amounts of running time on previous programs.

Following a calibration to establish the turbine inlet temperature, cyclic endurance testing was started. After a total of 108 test cycles were completed, observations up the tailpipe revealed that one (1) vane was running excessively hot and consequently the engine was shut down to inspect the vanes. An examination revealed a considerable buildup of oxidation in the cooling passages which presumably had contributed to this failure. As noted previously, the vanes had accumulated considerable running time prior to the start of the current program. Since another turbine vane assembly with new slotted and pedestal

DOWNGRADED AT 3 YEAR INTERVALS
DECLASSIFIED AFTER 12 YEARS
DOD DIR 5200.10

trailing edge vanes was available at that time, this nozzle assembly was installed and the test resumed. The test was then continued for another 155 cycles (for a total of 1030 cycles on the blades).

At this time, the engine was disassembled to allow measurement and detailed examination of the blades and vanes. The condition of the slotted and pedestal trailing edge vanes was good, but as previously noted, these vanes were installed at the last inspection and had accumulated only 155 endurance cycles. The condition of typical slotted and pedestal trailing edge vanes at the time of this inspection is shown in Figure 6-121 and 6-122 respectively. The vane bow was:

	Bow		
	Avg.	Max.	Min.
Slotted T. E. Uncoated AMS-5382	.016"	.037"	.007"
Pedestal T. E. Uncoated AMS-5382	.005"	.009"	.003"

The blade assembly had completed 1030 cycles at the time of this inspection. The condition of typical sawtooth and eleven hole blades at this time is shown in Figures 6-123 and 6-124. One PWA-659, $TaAl_3$ coated .020" sawtooth blade had a 1/4" leading edge chordwise crack at approximately 70% span as shown in Figure 6-125. An examination of this blade showed the failure to be a result of a thin (.005) wall due to a core shift during fabrication. Two (2) other sawtooth blades had leading edge radial cracks which were attributed to thin walls resulting from core shifts.

All of the eleven-hole blades had bowed in the chordwise direction with the PWA-658 blades exhibiting more bow than the PWA-663 blades. One of the more severely-bowed PWA-658 blades showed fine cracks along the leading edge, as shown in Figure 6-126. A comparison of a bowed eleven-hole blade and a .020" sawtooth blade is shown in Figure 6-127. Because of the severity of the bow, the growth measurements on the eleven hole blade were of no value. The growth measurements recorded on the sawtooth blades were as follows:

	Avg.	Max.	Min.
.020" Sawtooth PWA-695 $TaAl_3$ coating	.016"	.025"	.010"
.030" Sawtooth PWA-655 JC-14L coating	.029"	.055"	.016"

DOWNGRADED AT 3 YEAR INTERVALS
DECLASSIFIED AFTER 12 YEARS
DOD DIR 5200.10

7. TESTING OF FILM AND TRANSPIRATION COOLED VANES AND BLADES IN THE JT4 HIGH SPOOL ENGINE

Following the tests noted in the preceding section, a combination of film and transpiration cooled blades were installed in the high spool engine. The turbine vane assembly with these parts installed is shown in Figure 6-128. This vane assembly incorporated the following combination of film and transpiration cooled vanes:

Number	Type	Configuration
14	Film Cooled	Porous Leading Edge
2	Film Cooled	Pierced Sheet
3	Film Cooled	Shower Head
6	Transpiration Cooled	Rigimesh
7	Transpiration Cooled	Rigimesh
3	Transpiration Cooled	Poroloy
34	Convectively Cooled	Pedestal Trailing Edge
11	Convectively Cooled	Slotted Trailing Edge

The turbine rotor assembly prior to installation in the engine is shown in Figure 6-129. This assembly included the following combination of film and transpiration cooled blades.

Number	Type	Configuration
5	Film Cooled	Three Row .013/30°
5	Film Cooled	Three Row .008/90°
5	Film Cooled	Five Row .008/90°
5	Film Cooled	Three Row .013/90°
7	Film Cooled	Five Row .008/30°
4	Film Cooled	Mod. H .030/30°
5	Transpiration Cooled	Rigimesh (L-605)
11	Transpiration Cooled	Rigimesh (N-155)
7	Transpiration Cooled	Poroloy (N-155)
5	Transpiration Cooled	WDL
37	Convectively Cooled	.020 & .030 Sawtooth

DOWNGRADED AT 3 YEAR INTERVALS
DECLASSIFIED AFTER 12 YEARS
DOD DIR 5200.10

During a shutdown of the engine with these parts installed, it was determined that the metering parts in the leading edge of the transpiration cooled vanes would not allow sufficient cooling of the leading edges. These vanes were removed and replaced with convectively-cooled parts.

The program planned to be run on this engine was to have been an initial calibration followed by cyclic endurance testing at the following conditions:

Two minutes at 2300°F Turbine inlet temperature
Two minutes at 1200°F Turbine inlet temperature
Cooling air temperature = 700°F
Snap (1 sec) "throttle" movements.

A calibration run was completed on this engine at low power settings. When the power was being increased to the planned program settings, a blade failure was experienced after five minutes at a turbine inlet temperature of 2175°F. An examination of the failed blade revealed parting of the porous skin from the core resulting in damage to the adjacent blades and the turbine seal.

The engine was rebuilt for a baseline run in preparation for the evaluation of film-cooled airfoils. For the baseline run, parts were instrumented in order to establish a comparison between predicted and measured blade and vane metal temperatures. A total of thirty-eight thermocouples were installed on the blades and twenty-nine on the vanes. Test results during this run indicated good agreement between predicted and measured temperatures. Typical results from one blade are presented in Figure 6-130. Having completed the instrumented run, the rotor was removed and blades incorporating the following film-cooled configurations were installed.

Configuration	Quantity
Five Rows of .008" Dia Holes at 30° to L.E.	2
Five Rows of .008" Dia Holes at 90° to L.E.	3
Three Rows of .008" Dia Holes at 90° to L.E.	5

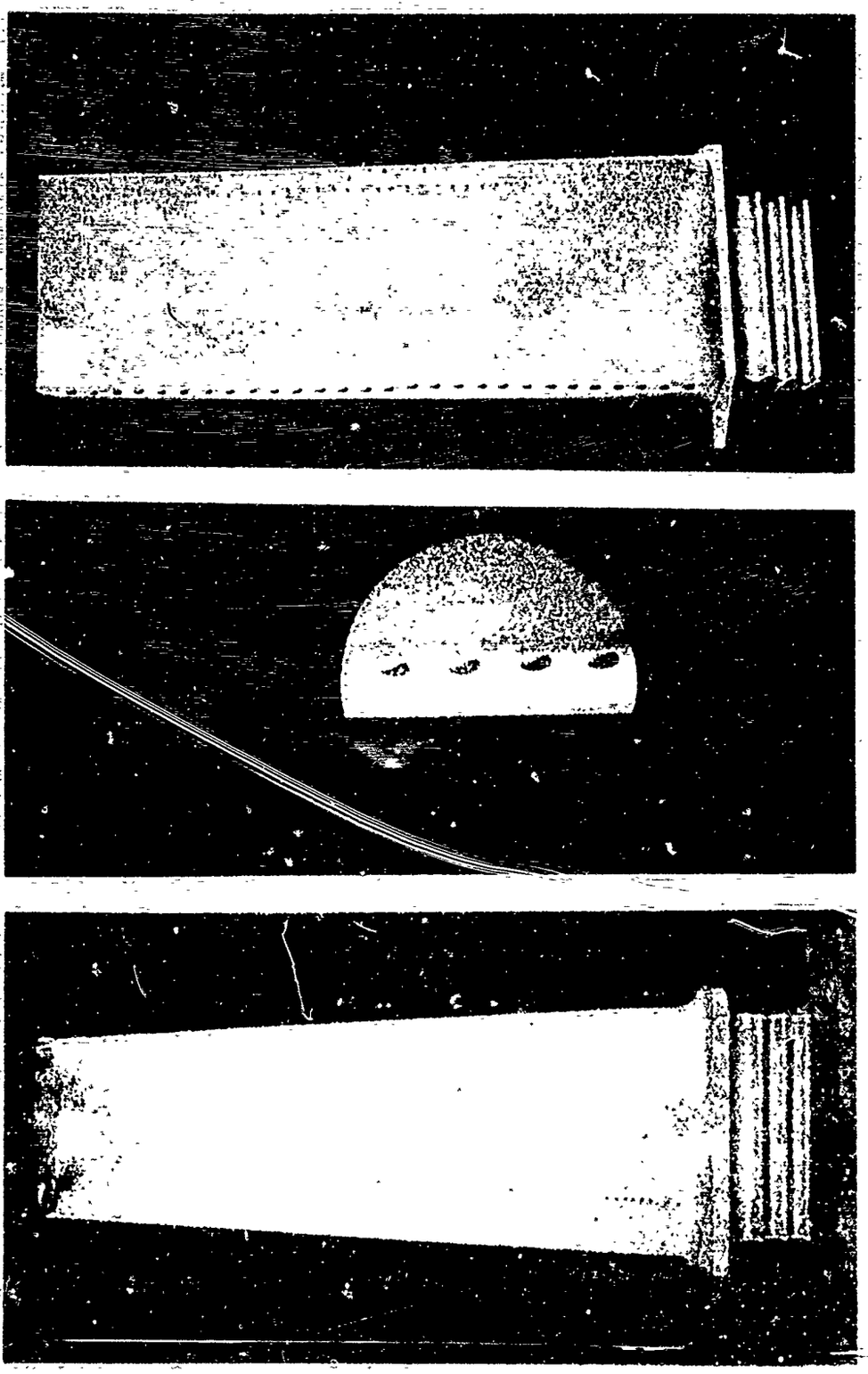
DOWNGRADED AT 3 YEAR INTERVALS
DECLASSIFIED AFTER 12 YEARS
DOD DIR 5200.10

THIS DOCUMENT CONTAINS INFORMATION AFFECTING THE NATIONAL DEFENSE OF THE UNITED STATES WITHIN THE MEANING OF THE ESPIONAGE LAWS, TITLE 18, U.S.C. SECTIONS 793 AND 794. ITS TRANSMISSION OR THE REVELATION OF ITS CONTENTS IN ANY MANNER TO AN UNAUTHORIZED PERSON IS PROHIBITED BY LAW.

Three Rows of .013" Dia Holes at 30° to L. E.	2
Three Rows of .013" Dia Holes at 90° to L. E.	3
One Row of .030" Dia Holes 30° to L. E.	4

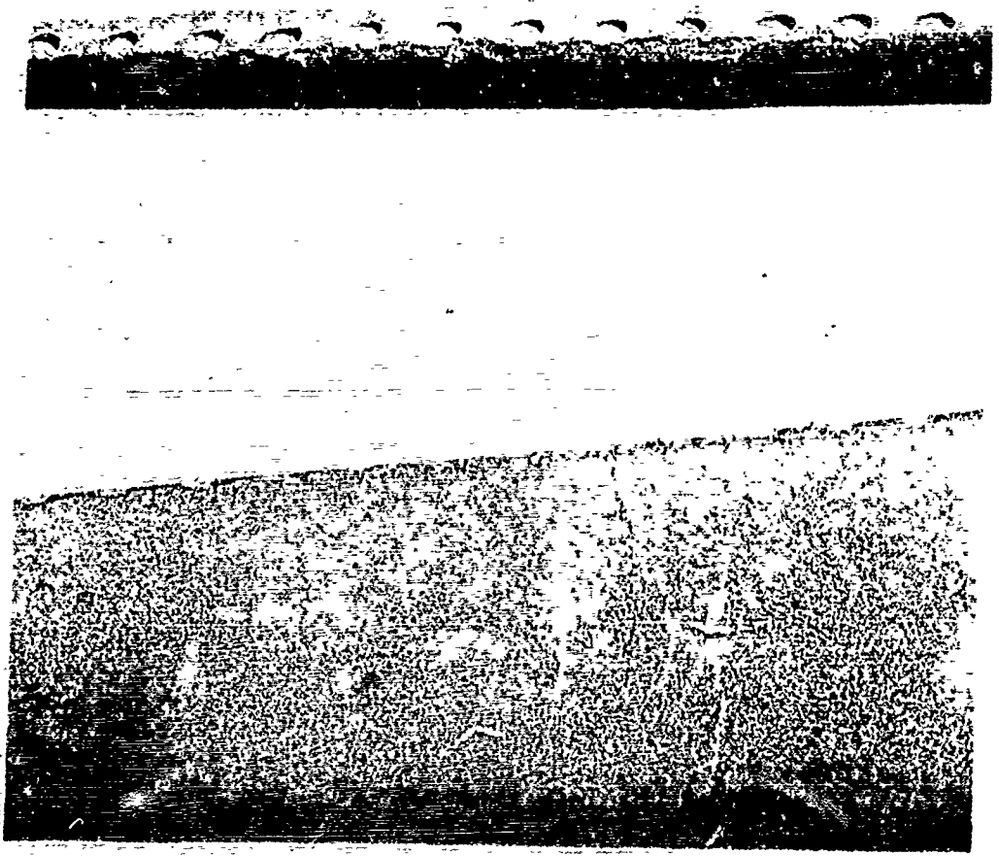
The remainder of the disc was assembled with convectively cooled blades. One hundred test cycles (of the type previously mentioned) were completed. At the end of this period, two blades were removed due to foreign-object damage. Microscopic examination of these blades revealed no significant damage. The blades were reinstalled and the cyclic endurance program continued. At the close of this report period 600 cycles of endurance testing had been accumulated on these blades.

DOWNGRADED AT 3 YEAR INTERVALS
DECLASSIFIED AFTER 12 YEARS
DOD DIR 5200.10
THIS DOCUMENT CONTAINS INFORMATION AFFECTING THE NATIONAL DEFENSE OF THE UNITED STATES WITHIN THE MEANING OF THE ESPIONAGE LAWS, TITLE 18, U.S.C., SECTIONS 793 AND 794. THE TRANSMISSION OR THE REVELATION OF ITS CONTENTS IN ANY MANNER TO AN UNAUTHORIZED PERSON IS PROHIBITED BY LAW.



FILM-COOLED TURBINE BLADE WITH 0.030 INCH HOLES DRILLED AT 30° ANGLE TO LEADING EDGE AND 0.013 INCH HOLES AT 30° TO AIRFOIL ON TRAILING EDGE

Figure 6-1



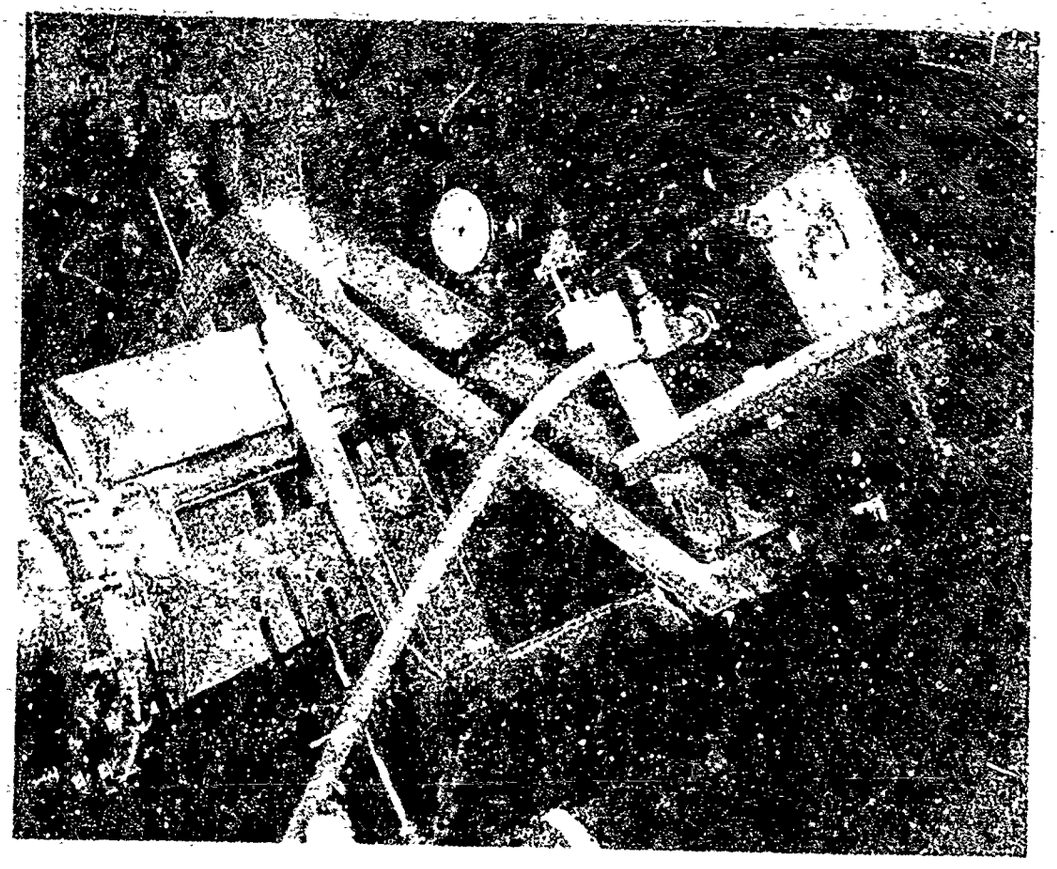
FILM-COOLED TURBINE BLADE WITH 0.030 INCH/30° ANGLE L.E. HOLES AND 0.013 INCH/30° ANGLE T.E. HOLES SHOWING CRACKS AFTER 100 CYCLES OF THERMAL SHOCK TESTING

Figure 6-2



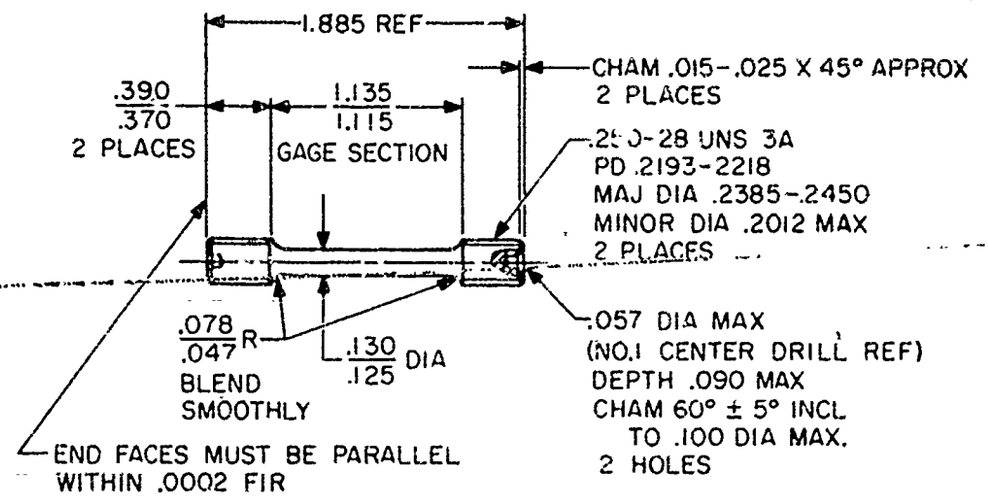
CONVECTIVELY-COOLED TURBINE BLADE AFTER 1000 CYCLES OF THERMAL SHOCK TEST
(SHOWING GOOD CONDITION AND ABSENCE OF CRACKS)

Figure 6-3



TURBINE BLADE IMPACT TEST RIG

Figure 6-4

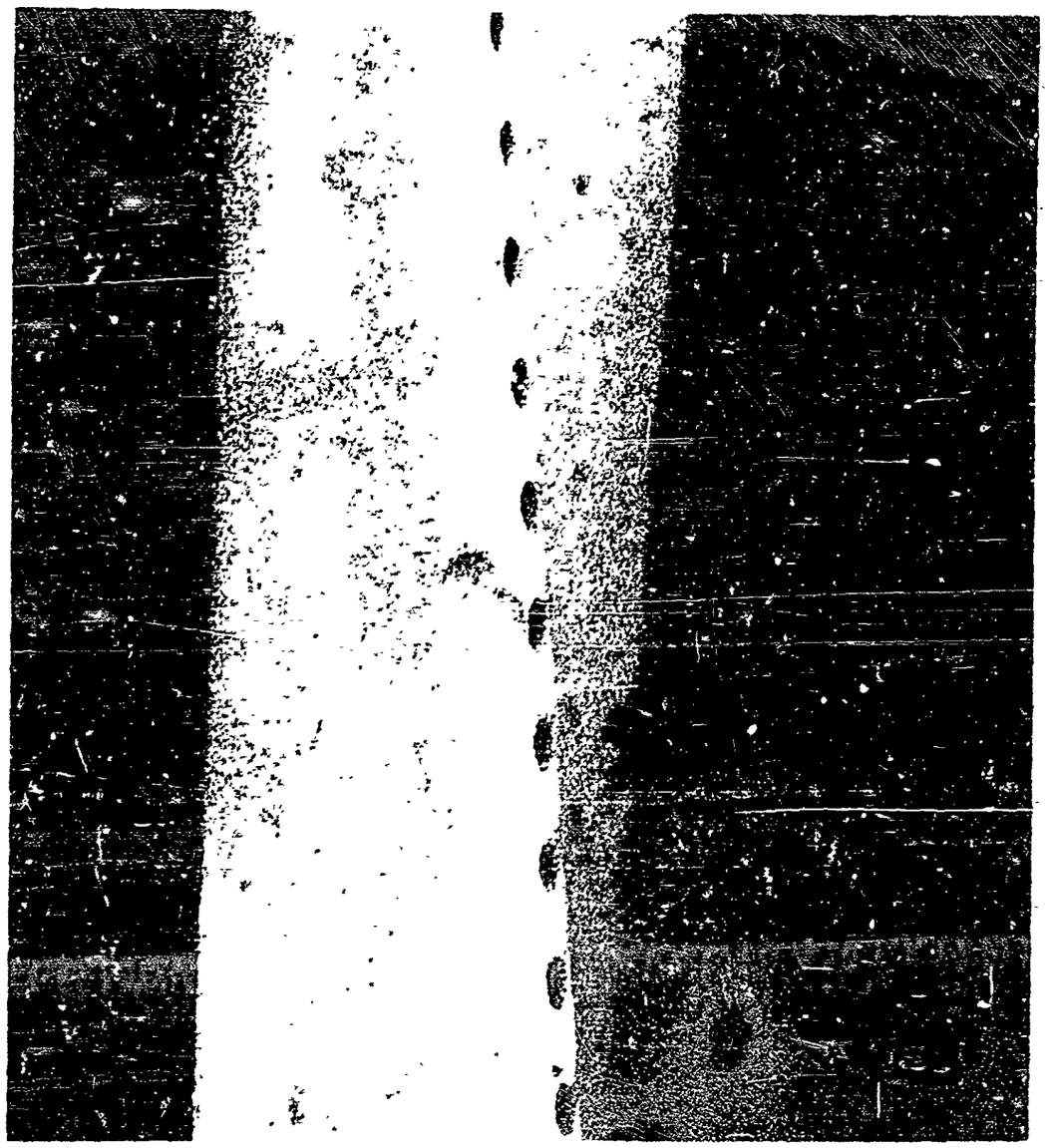


LOW CYCLE FATIGUE MATERIAL TEST SPECIMEN

Figure 6-10

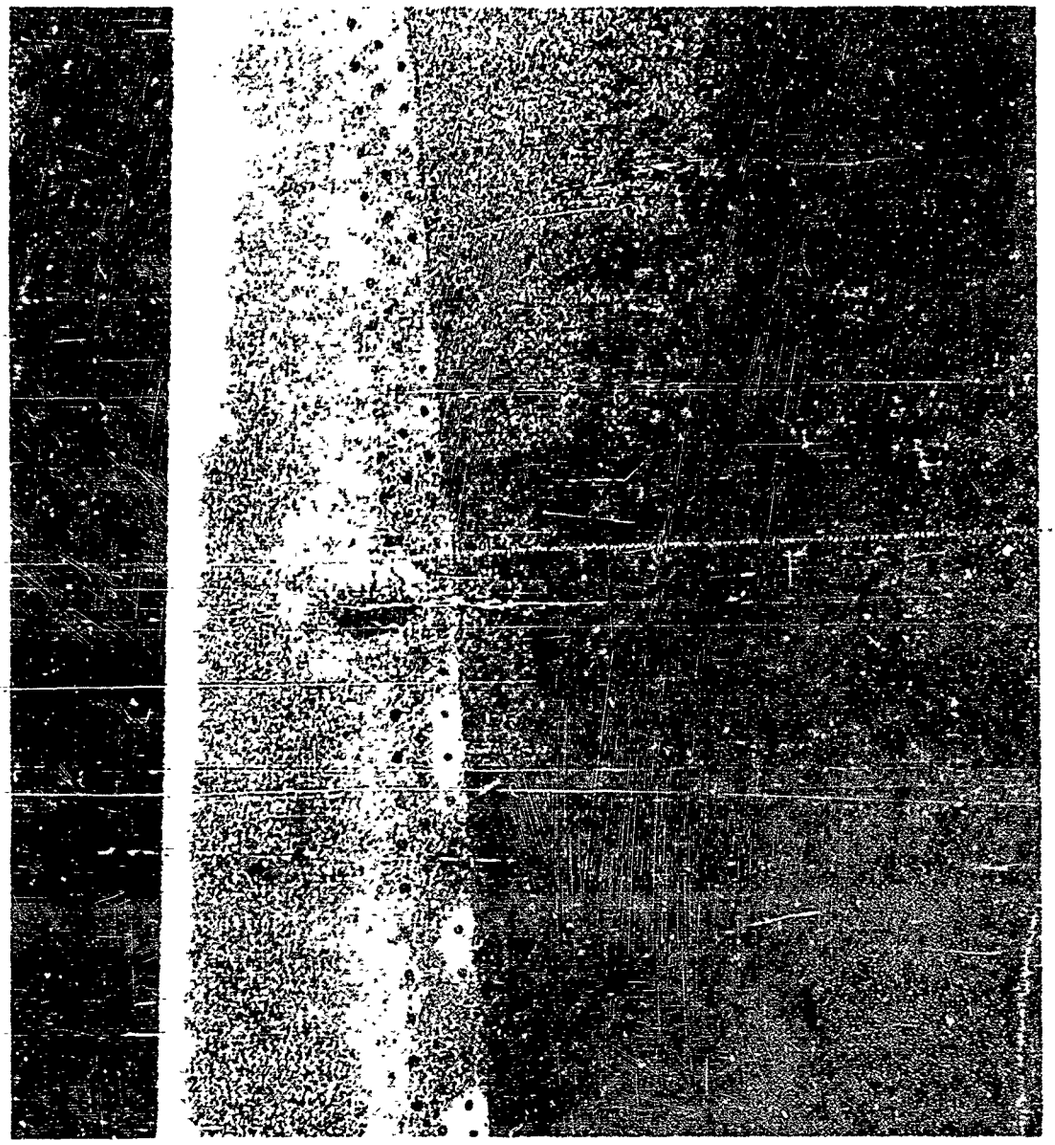
DOWNGRADED AT 3 YEAR INTERVALS
DECLASSIFIED AFTER 12 YEARS
DOD DIR 5200.10

THIS DOCUMENT CONTAINS INFORMATION AFFECTING THE NATIONAL DEFENSE OF THE UNITED STATES WITHIN THE MEANING OF THE ESPIONAGE LAWS, TITLE 18, U.S.C., SECTIONS 793 AND 794. THE TRANSMISSION OR REVELATION OF ITS CONTENTS IN ANY MANNER TO AN UNAUTHORIZED PERSON IS PROHIBITED BY LAW.



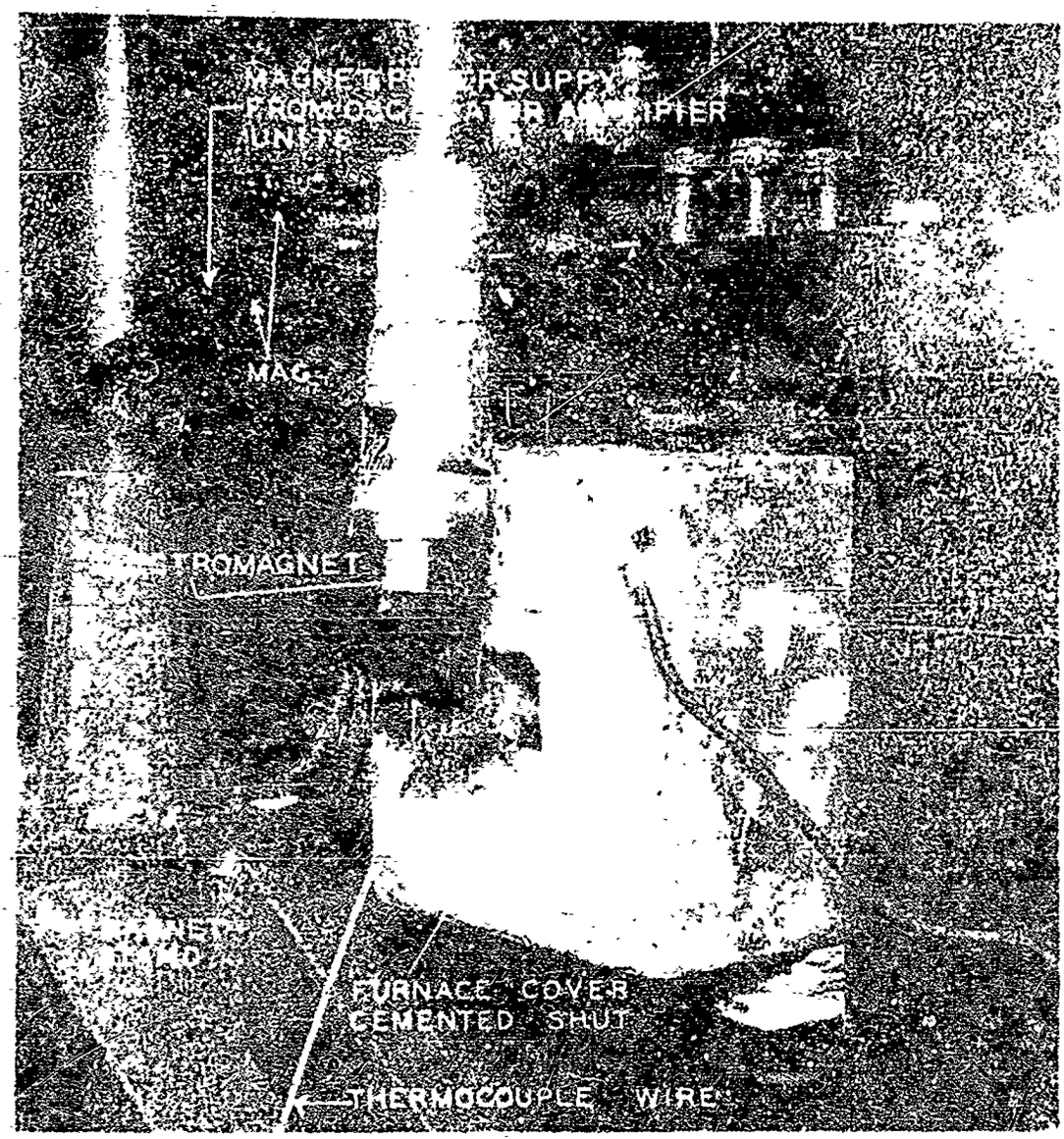
FILM COOLED BLADE WITH .030 DIA. HOLES AFTER IMPACT TEST

Figure 6-6



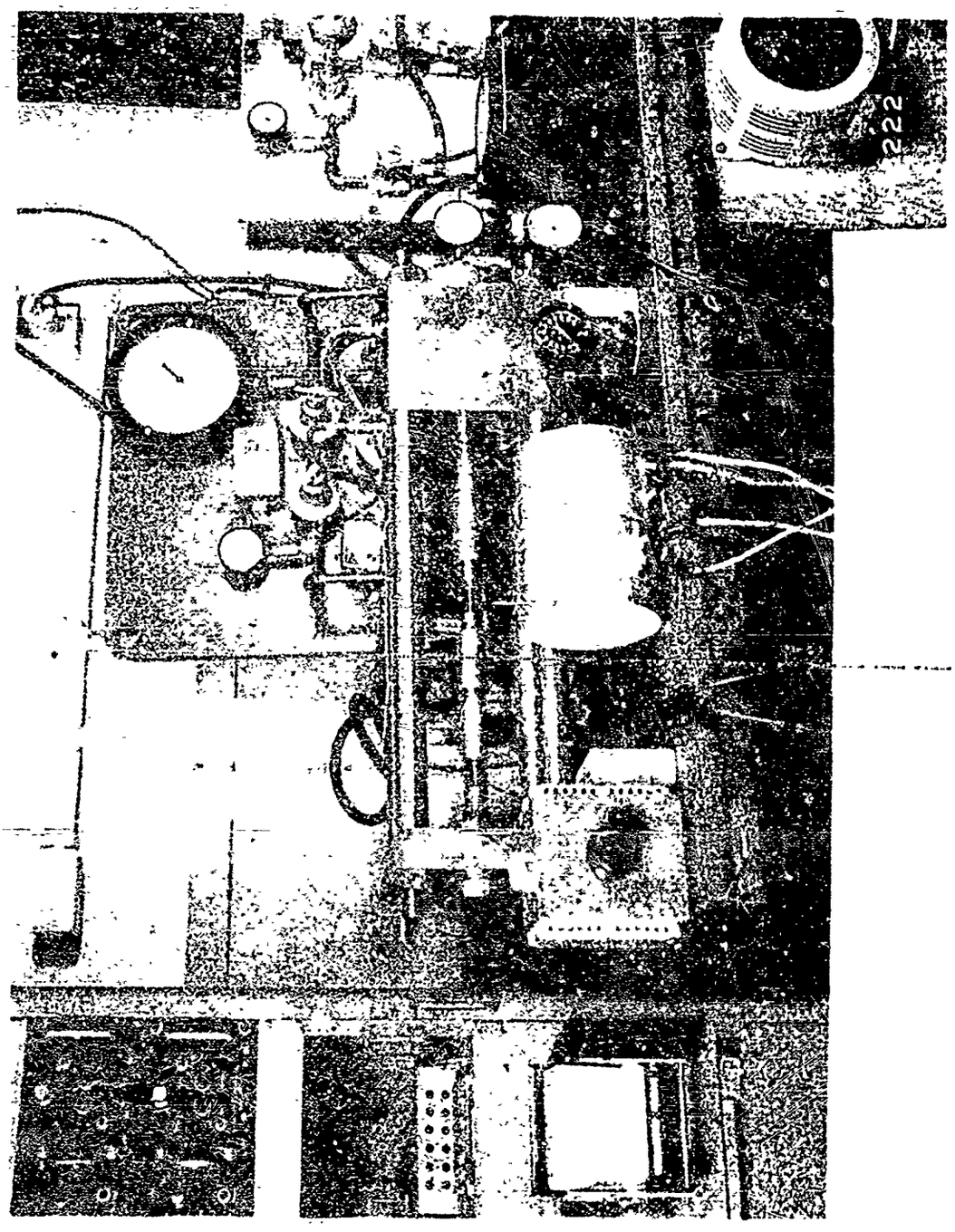
FILM COOLED BLADE AFTER IMPACT TEST

Figure 6-7



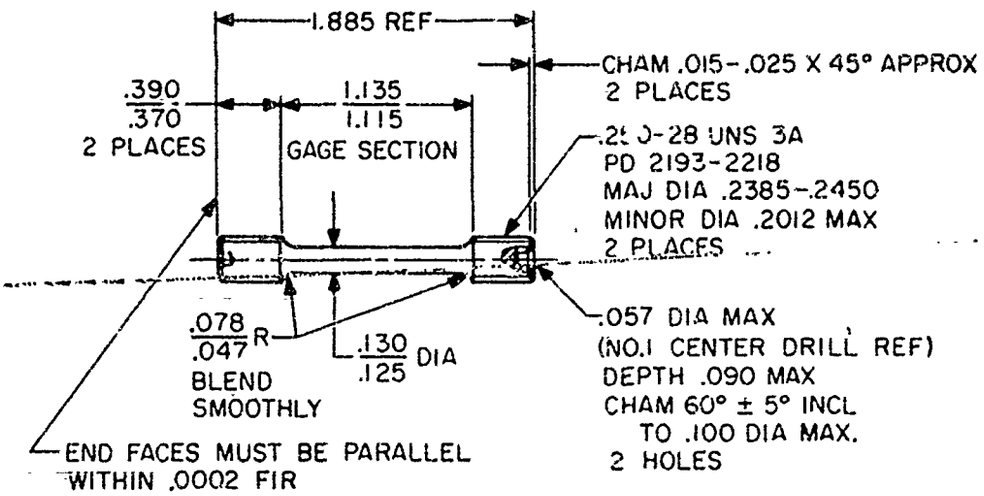
TYPICAL TURBINE BLADE SET-UP FOR HIGH TEMPERATURE TESTING

Figure 6-8



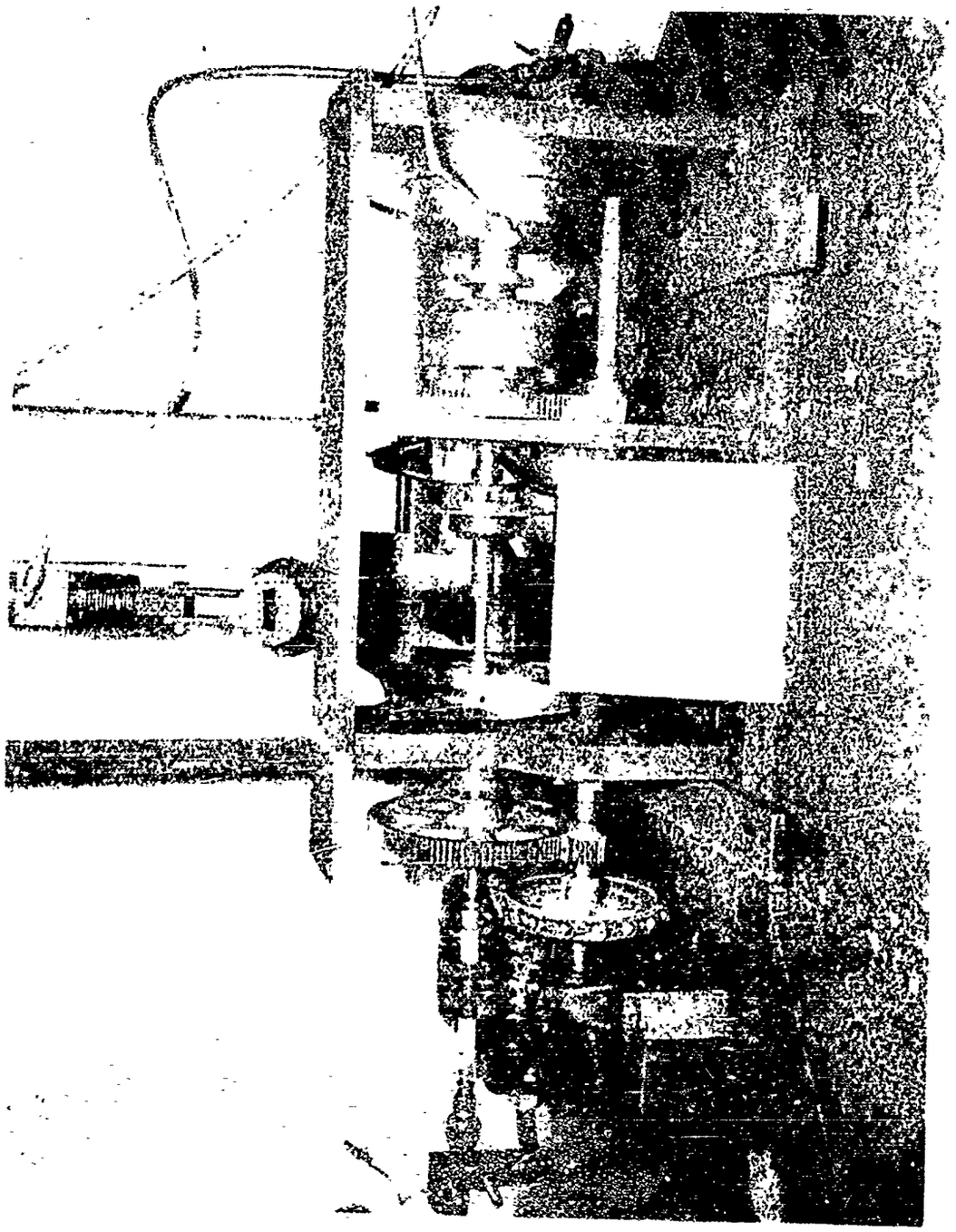
LOW-CYCLE-FATIGUE (LCF) TEST RIG

Figure 6-9



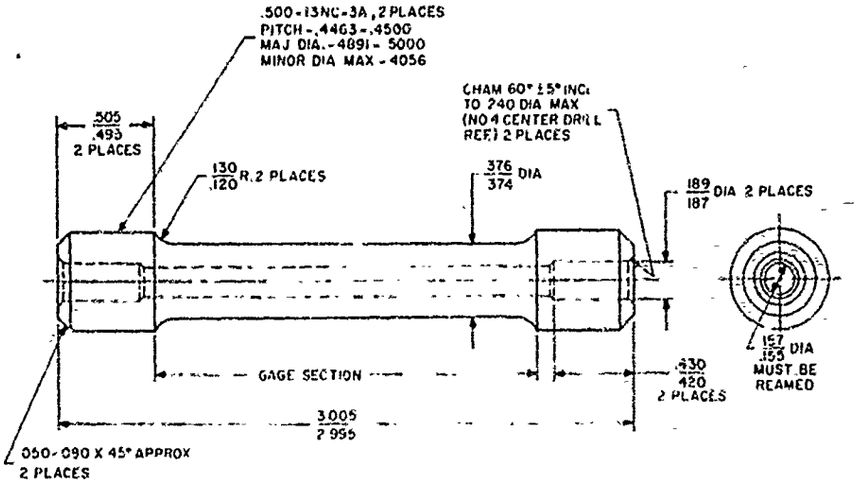
LOW CYCLE FATIGUE MATERIAL TEST SPECIMEN

Figure 6-10

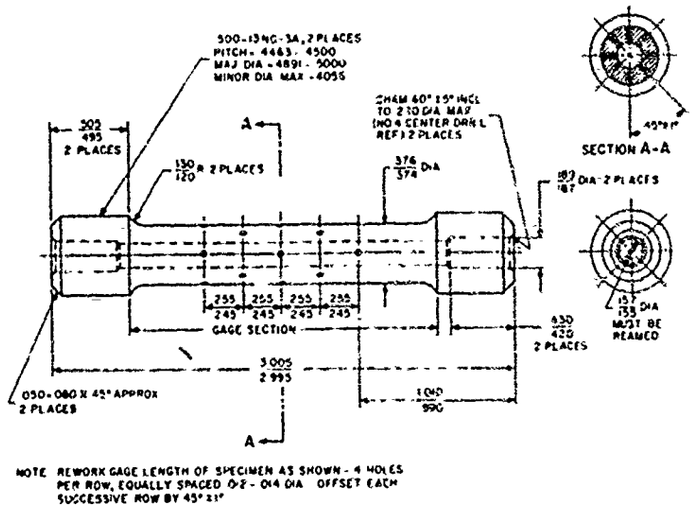


CYCLIC-CREEP TEST RIG

Figure 6-11



THERMAL SHOCK-CREEP SPECIMEN UNDRILLED



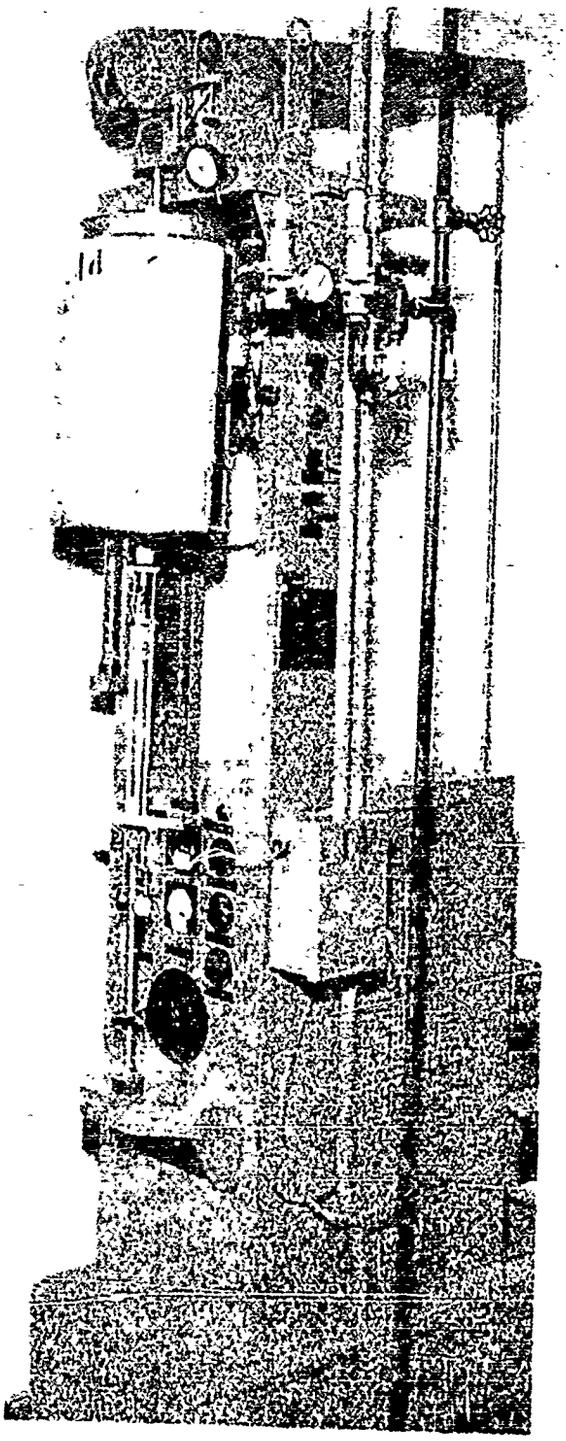
NOTE REWORK GAGE LENGTH OF SPECIMEN AS SHOWN - 4 HOLES PER ROW, EQUALLY SPACED .012 - .014 DIA OFFSET EACH SUCCESSIVE ROW BY 45° ±1°

THERMAL SHOCK-CREEP SPECIMEN DRILLED

Figure 6-12 and 6-13

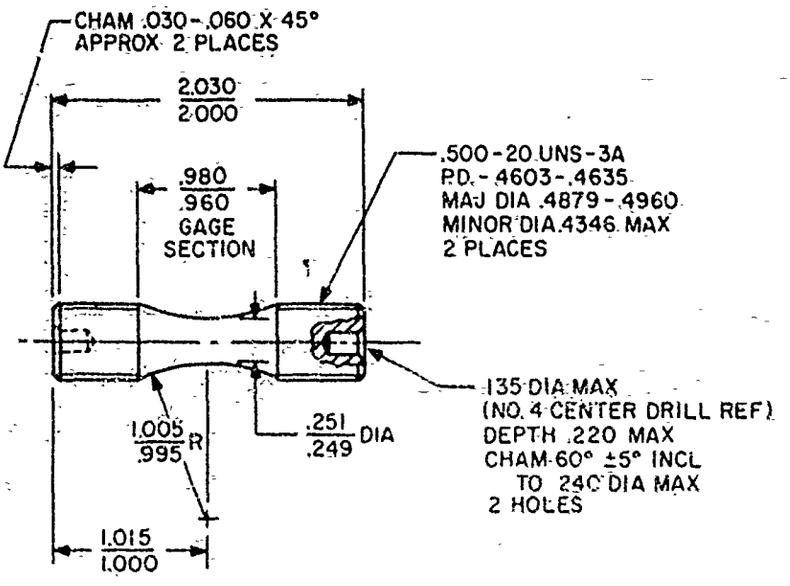
DOWNGRADED AT 3 YEAR INTERVALS
DECLASSIFIED AFTER 12 YEARS
DOD DIR 5200.10

THIS DOCUMENT CONTAINS INFORMATION AFFECTING THE NATIONAL DEFENSE OF THE UNITED STATES WITHIN THE MEANING OF THE ESPIONAGE LAWS, TITLE 18, U.S.C., SECTIONS 793 AND 794. THE TRANSMISSION OR THE REVELATION OF ITS CONTENTS IN ANY MANNER TO AN UNAUTHORIZED PERSON IS PROHIBITED BY LAW.

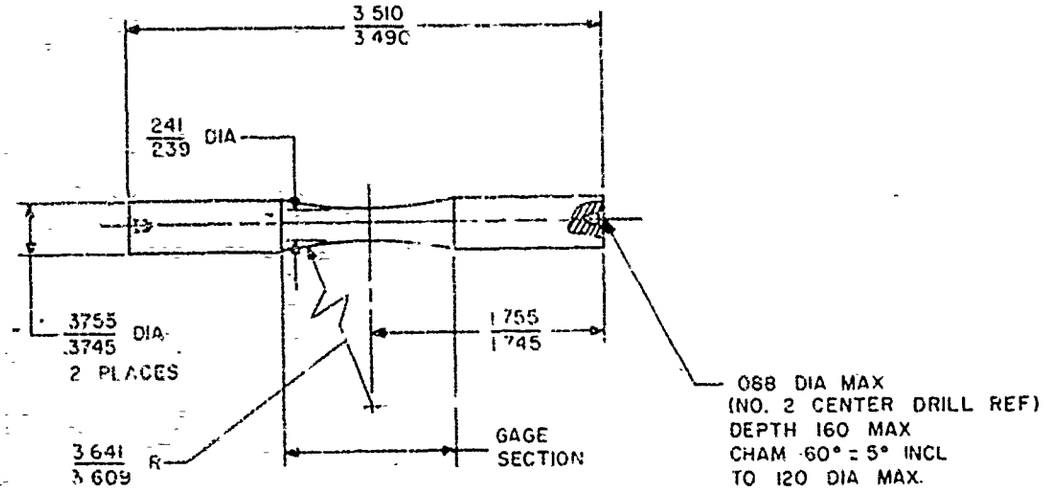


ARC WELD CREEP TEST MACHINE FOR CYCLIC STRESS RUPTURE TESTS

Figure 6-14



SMOOTH CYCLIC STRESS-RUPTURE FATIGUE SPECIMEN



HIGH TEMPERATURE REVERSE-BENDING FATIGUE SPECIMEN

Figures 6-15 and 6-16

DOWNGRADED AT 3 YEAR INTERVALS
DECLASSIFIED AFTER 12 YEARS
DOD DIR 5200.10

Item	Feature	Photo Fig. No.	Schematic Fig. No.	Data Fig. No.	Description	Minimum L.E. Temp. at Stated Flow
1	Film cooled L.E. coolant slots on stagnation line	-	6-37	6-57	14, 0.008" x 0.1" coolant slots, spaced 0.050" apart on the stagnation line.	1425°F at 14.4 #/hr.
2	Film cooled L.E. coolant slots 15° to suction side of stagnation line	-	6-36	6-58	Same slot dimensions as (1)	1550°F at 14.4 #/hr.
3	Film cooled L.E. coolant slots 15° to pressure side of stagnation line	6-18	6-38	6-59	Same slot dimensions as (1)	1460°F at 14.4 #/hr.
4	Film cooled L.E. coolant slots on the stagnation line	6-19	6-39	6-60	14, 0.012" x 0.1" coolant slots spaced 0.050" apart along the stagnation line.	1425°F at 17.7 #/hr.
5	Film cooled L.E. coolant holes angled at 45° to the gas stream	6-20	6-40	6-61	20, 0.040" dia. coolant holes spaced 0.1" apart along stagnation line, and angled 45° to gas stream.	1400°F at 15.95 #/hr.

Vane Data Summary (Sheet 1 of 6)

Figure 6-17 (1 of 6)

Item	Feature	Photo Fig. No.	Schematic Fig. No.	Data Fig. No.	Description	Minimum L. E. Temp. at Stated Flow
6	Film cooled L. E. spanwise coolant injection	6-21	6-41	6-62	A single 0.13" dia. coolant hole drilled in platform; coolant injected from hole into a blind semicircular groove running spanwise along the stagnation line.	1710°F at 14.0 #/hr.
7	Film cooled L. E. umbrella type (both ends attached)	6-22	6-42	-	A 0.025" thick shield 0.20" wide x 2.5" long attached at each end. 0.050" behind shield were 14, 0.012" x 0.1" coolant holes.	Data not available
8	Film cooled L. E. coolant holes angled 60° to gas stream	6-23	6-43	6-63	0.030" dia. coolant holes spaced 0.1" apart along the stagnation line and angled at 30° to the leading edge.	1260°F at 15.1 #/hr.

Vane Data Summary (Sheet 2 of 6)

Figure 6-7 (2 of 6)

CONFIDENTIAL

PRATT & WHITNEY AIRCRAFT

CONFIDENTIAL

Item	Feature	Photo Fig. No.	Schematic Fig. No.	Data Fig. No.	Description	Minimum L. E. Temp. at Stated Flow
9	Film cooled L. E. 5 row straight thru showerhead	6-24	6-44	6-64	5 rows, of ~41, 0.008" dia coolant holes. 1st row at the stagnation line; 1 row at ±45° from the stagnation line: 1 row at ±75° from the stagnation line.	1270°F at 14.796 #/ hr.
10	Film cooled L. E. 5 row straight thru showerhead	6-25	6-45	-	Same as (9) except coolant holes are 0.013" dia.	Not Available
11	Impingement cooled and film cooled L. E.	6-26	6-46	6-65	A 0.030" thick Hastelloy-x Shield attached all around. 14, 0.100 x 0.020" coolant slots spaced 0.060" apart behind the shield approx. 0.120". Coolant released along suction and pressure surfaces thru slots cut in shield	1300°F at 14.21 #/hr.

Vane Data Summary (Sheet 3 of 6)

Figure 6-17(3 of 6)

CONFIDENTIAL

PRATT & WHITNEY AIRCRAFT

CONFIDENTIAL

Item	Feature	Photo Fig. No.	Schematic Fig. No.	Data Fig. No.	Description	Minimum L. E. Temp. at Stated Flow
12	Film cooled L. E. porous sheet vane	6-27	6-47	6-66	L. E. of vane replaced by a porous sheet of same contour. Sheet was 2.0" long x 0.8" wide x 0.030 thick Waspalloy with 0.013" diameter holes drilled on an 0.060" x 0.093" spacing.	1380°F at 14.8 #/hr.
13	Film cooled L. E. porous sheet vane	6-28	6-48	-	Same as 12 except holes were 0.006" dia. on a 0.050" x 0.050" spacing.	Not Available
14	Transpiration cooled L. E. (Poroloy)	6-29	6-49	6-67	L. E. of vane replaced by an 0.030" thick sheet of 125-150 SCFM Poroloy of the same contour	1050°F at 14.8 #/hr.

Vane Data Summary (Sheet 4 of 6)

Figure 6-17 (4 of 6)

PRATT & WHITNEY AIRCRAFT

Item	Feature	Photo Fig. No.	Schematic Fig. No.	Data Fig. No.	Description	Minimum L. E. Temp. as Stated Flow
15	Impingement and film cooled L. E. umbrella type (single attachment point)	6-30	6-50	6-68	3, 0.290" wide x 0.580" long x 0.0275" thick curved shields attached to the vane at midpoints. To allow for thermal growth, behind each shield a distance of 0.165" on either side of the attachment point was a coolant slot 0.150" wide x 0.014" high.	1255°F at 15.02 #/hr.
16	Impingement and film cooled L. E. "Sugarscoop"	6-31	6-51	6-69	10 cylindrical cuts made in L. E. at an angle of 15° to Leading edge to a depth of 0.230". Behind each cut was an 0.0825" x 0.014" coolant slot.	1275°F at 14.417 #/hr.
17	Film cooled L. E. "Coanda"	6-32	6-52		6, 0.466" x 0.098" coolant slots on L. E. within a specially shaped groove.	Part failed during test

Vane Data Summary (Sheet 5 of 6)

Figure 6-17 (5 of 6)

CONFIDENTIAL

CONFIDENTIAL

PRATT & WHITNEY AIRCRAFT

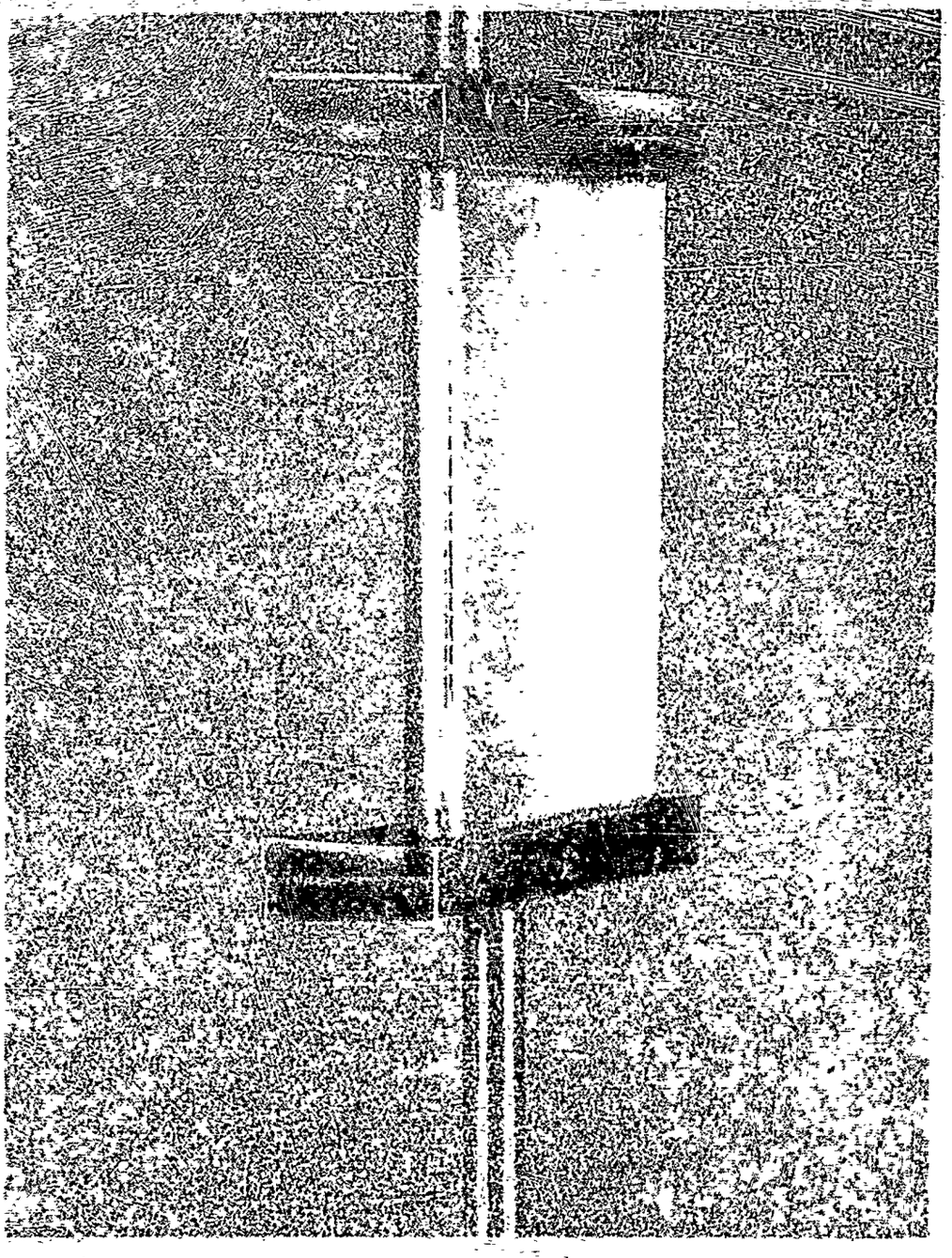
Item	Feature	Photo Fig. No.	Schematic Fig. No.	Data Fig. No.	Description	Minimum L. E. Temp. as Stated Flow
18	Convectively cooled T. E.	-	6-53	6-76	Internally slotted T. E.	No L. E. flow T. E. temp = 1520°F with comparable 4 lb/hr flow
19	Film cooled T. E. (suction side slots)	6-73	6-54	6-76	22, 0.013" dia. coolant holes spaced 0.090" ℄ to ℄ on a suction side spanwise line 0.40" from T. E.	No L. E. flow T. E. temp. at Wc = 4 lb/hr 1615
20	Film cooled T. E. (suction side slots)	6-73	6-54	6-76	Same as (19) except spanwise line is 1.40" from T. E.	No L. E. flow T. E. temp. at Wc = 4 lb/hr 1615°F
21	Film cooled T. E. (pressure side slots)	6-73	6-54	6-76	22, 0.013" dia. coolant holes spaced 0.090" apart ℄ to ℄ on a pressure side spanwise line 1.0" from T. E.	No L. E. flow T. E. temp. at 4 lb/hr = 1640

Vane Data Summary (Sheet 6 of 6)

CONFIDENTIAL

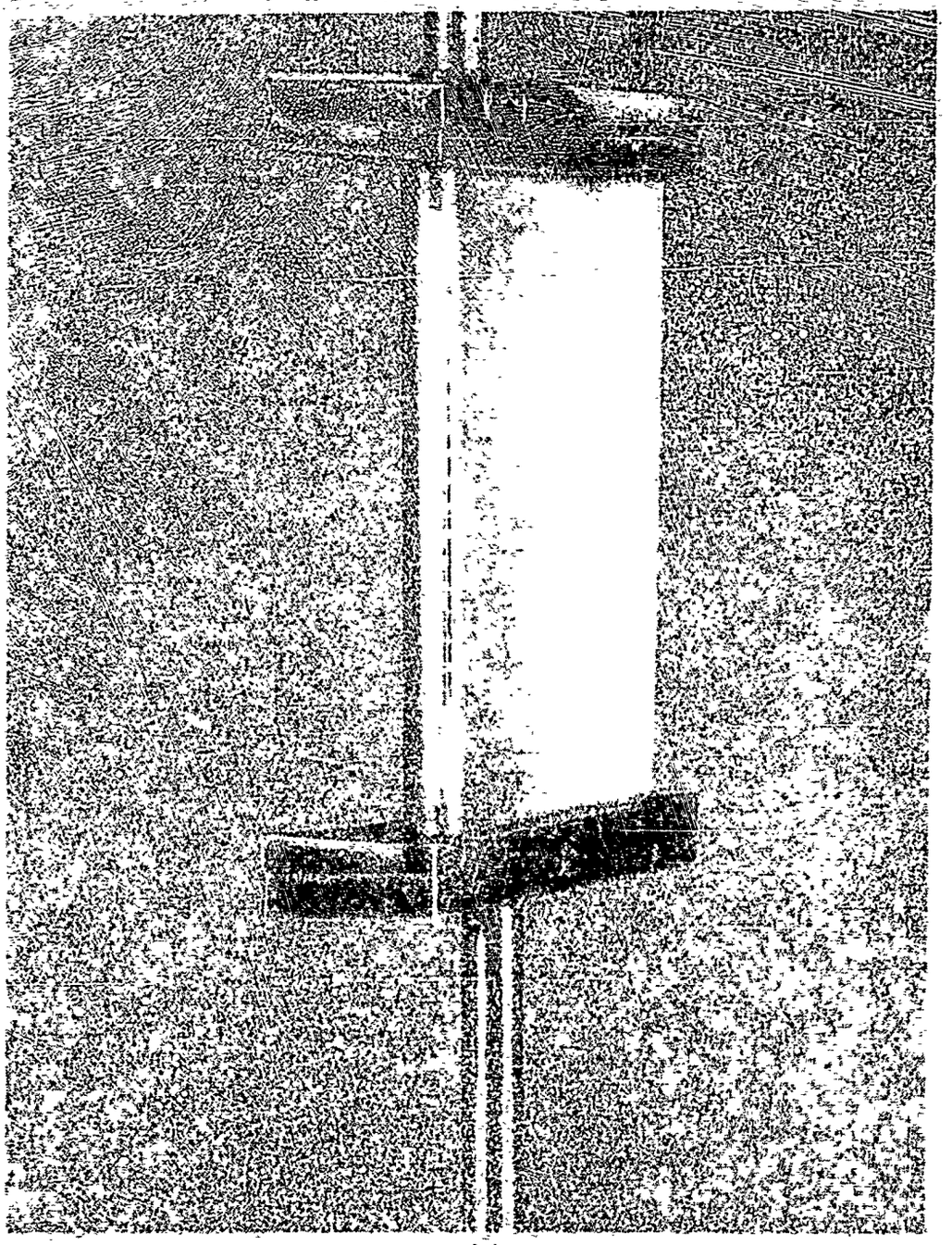
PRATT & WHITNEY AIRCRAFT

CONFIDENTIAL



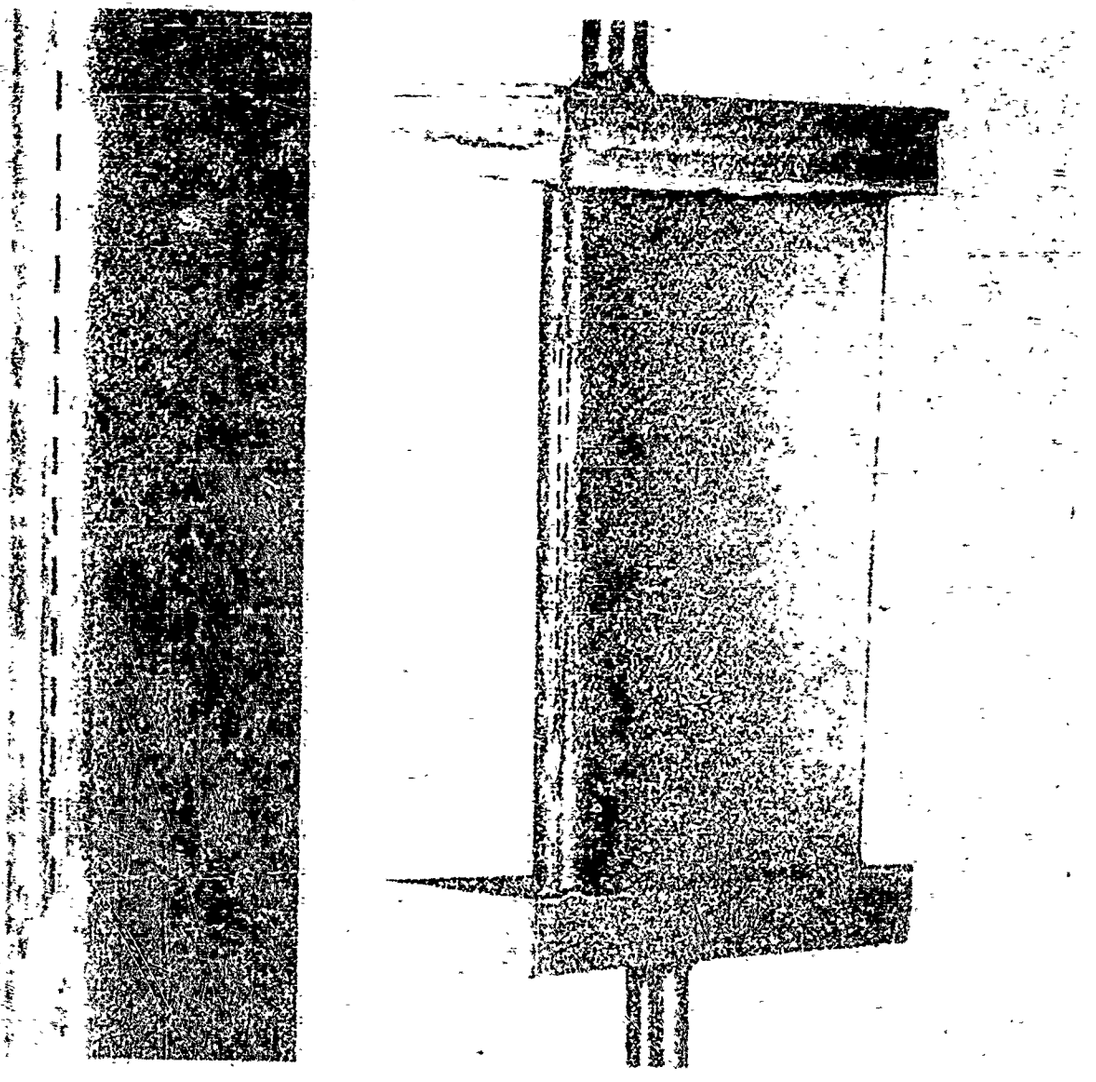
TURBINE VANE INCORPORATING LEADING EDGE COOLING SLOTS 0.008 INCH BY 0.100 INCH SPACED 0.050 INCH APART, 15° OFF STAGNATION LINE

Figure 6-18



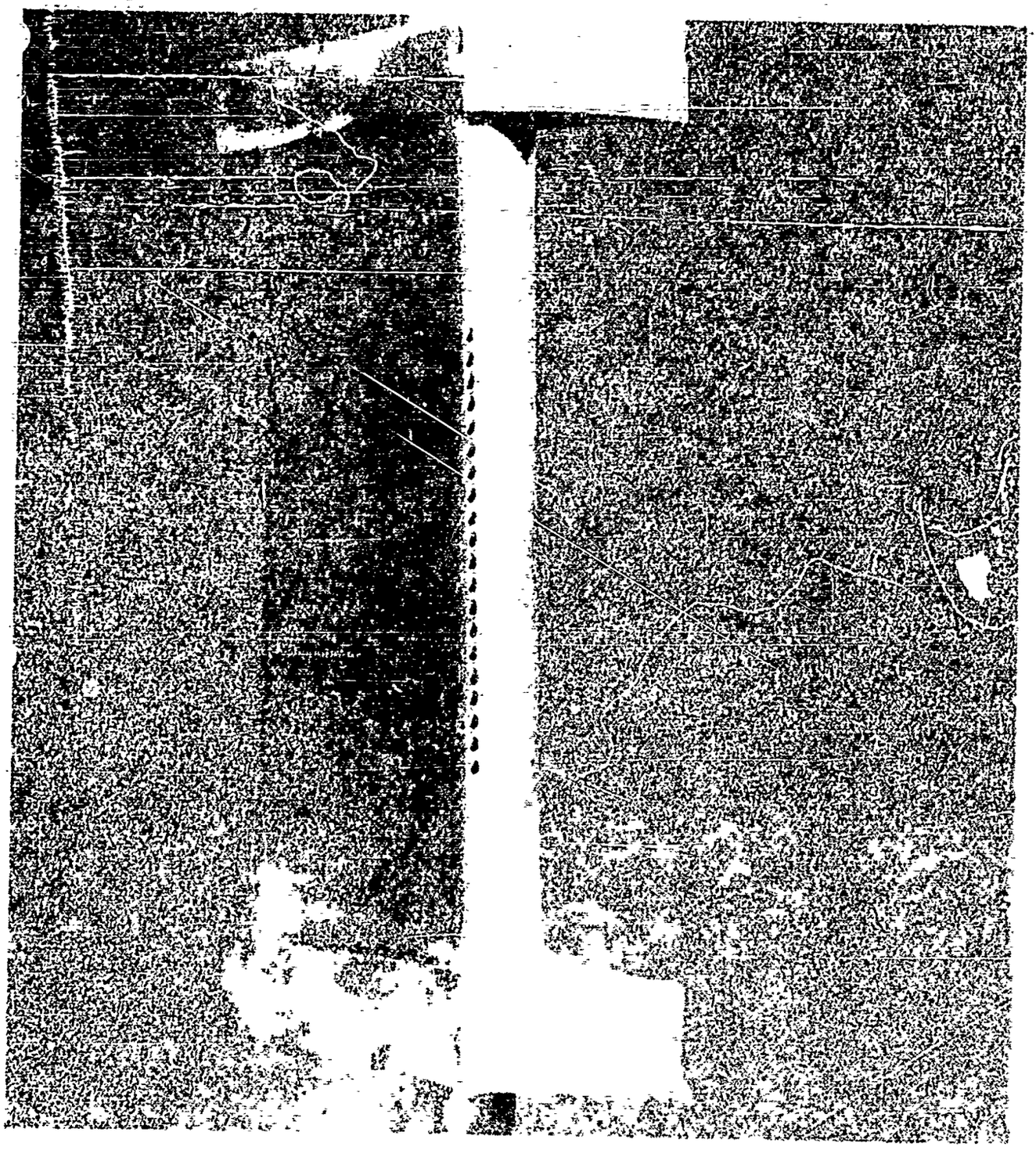
TURBINE VANE INCORPORATING LEADING EDGE COOLING SLOTS 0.008 INCH BY 0.100 INCH SPACED 0.050 INCH APART, 15° OFF STAGNATION LINE

Figure 6-18



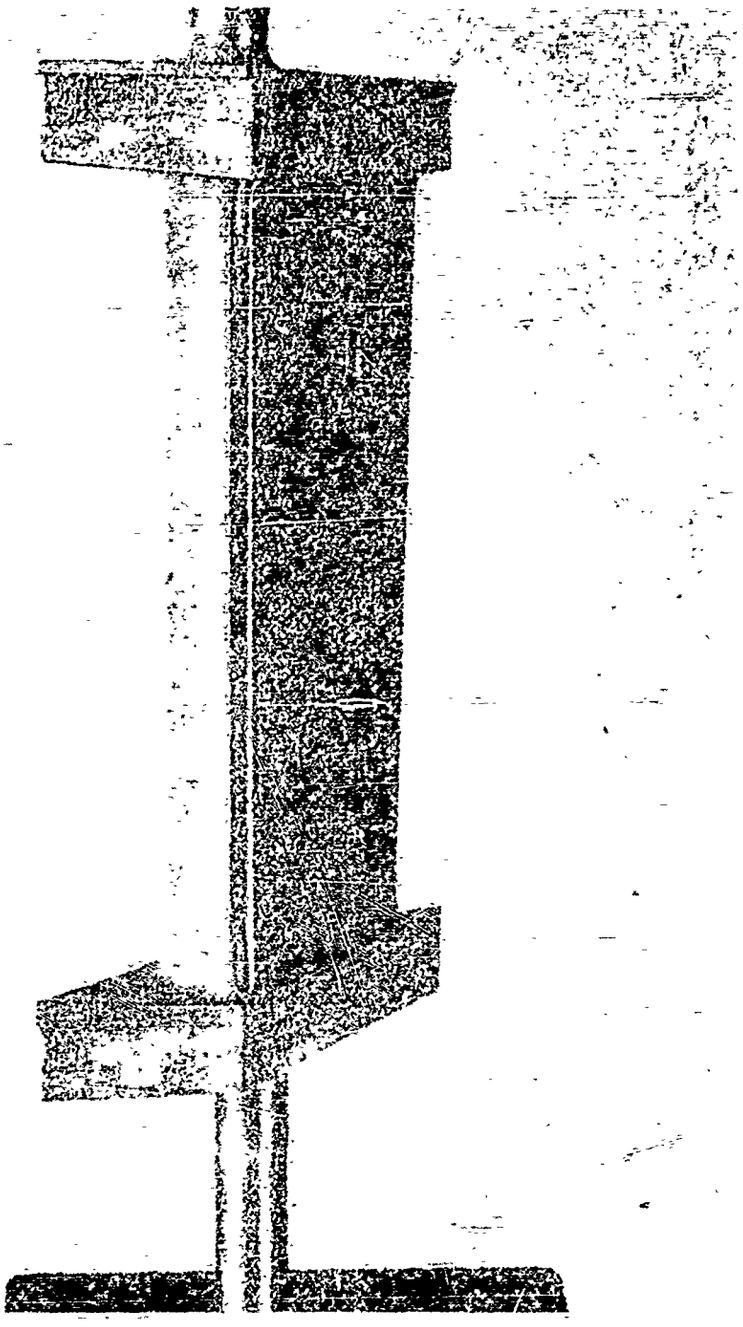
TURBINE VANE SHOWING 0.012 x 0.100 INCH COOLING SLOTS AT L.E. STAGNATION LINE

Figure 6-19



TURBINE VANE CONFIGURATION WITH LEADING EDGE COOLING HOLES 0.040 INCH DIAMETER AT 45° TO L.E.

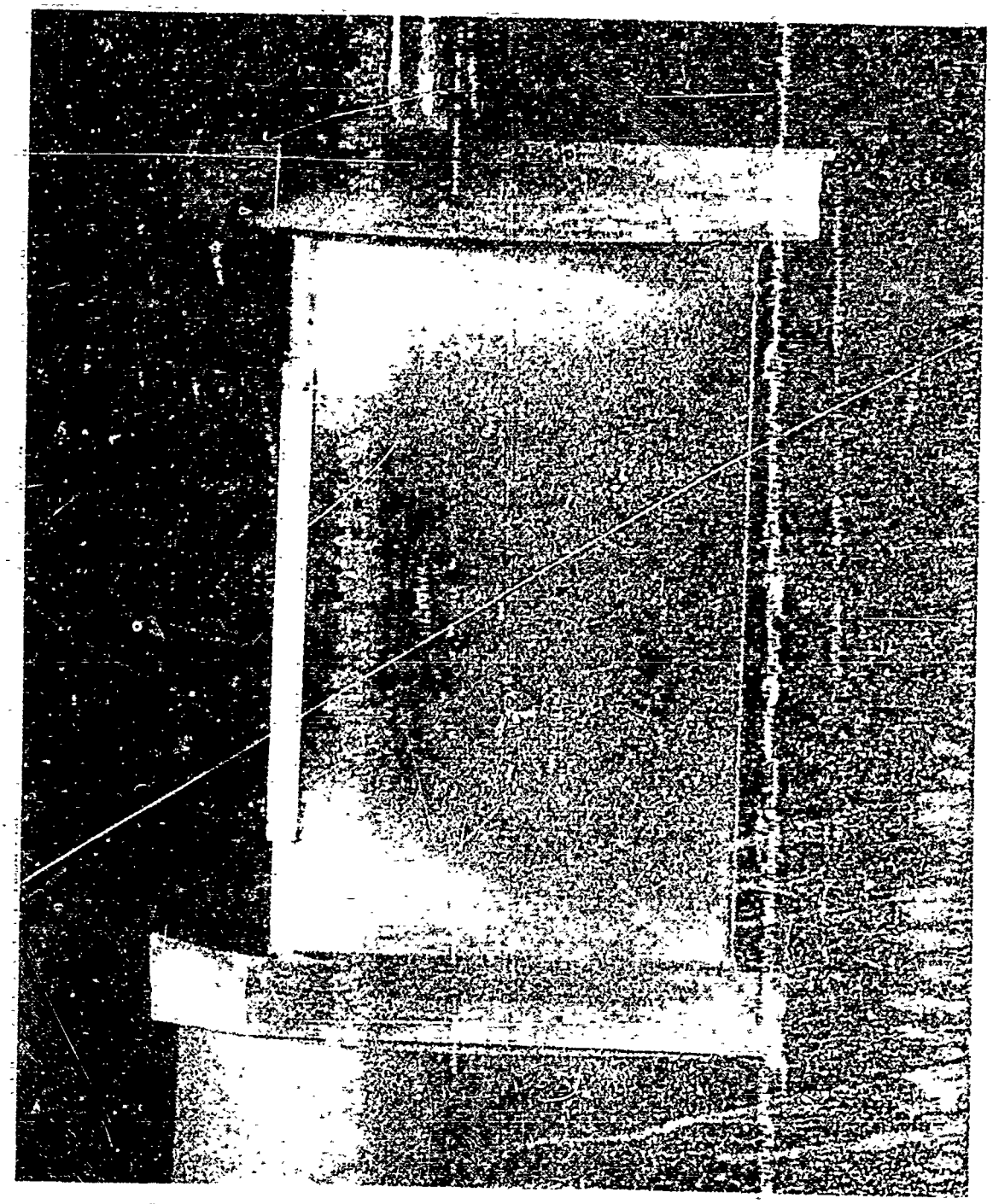
Figure 6-20



TURBINE VANE FEATURING FILM-COOLED LEADING EDGE COOLANT INJECTED INTO SPANWISE GROOVE ALONG STAGNATION LINE

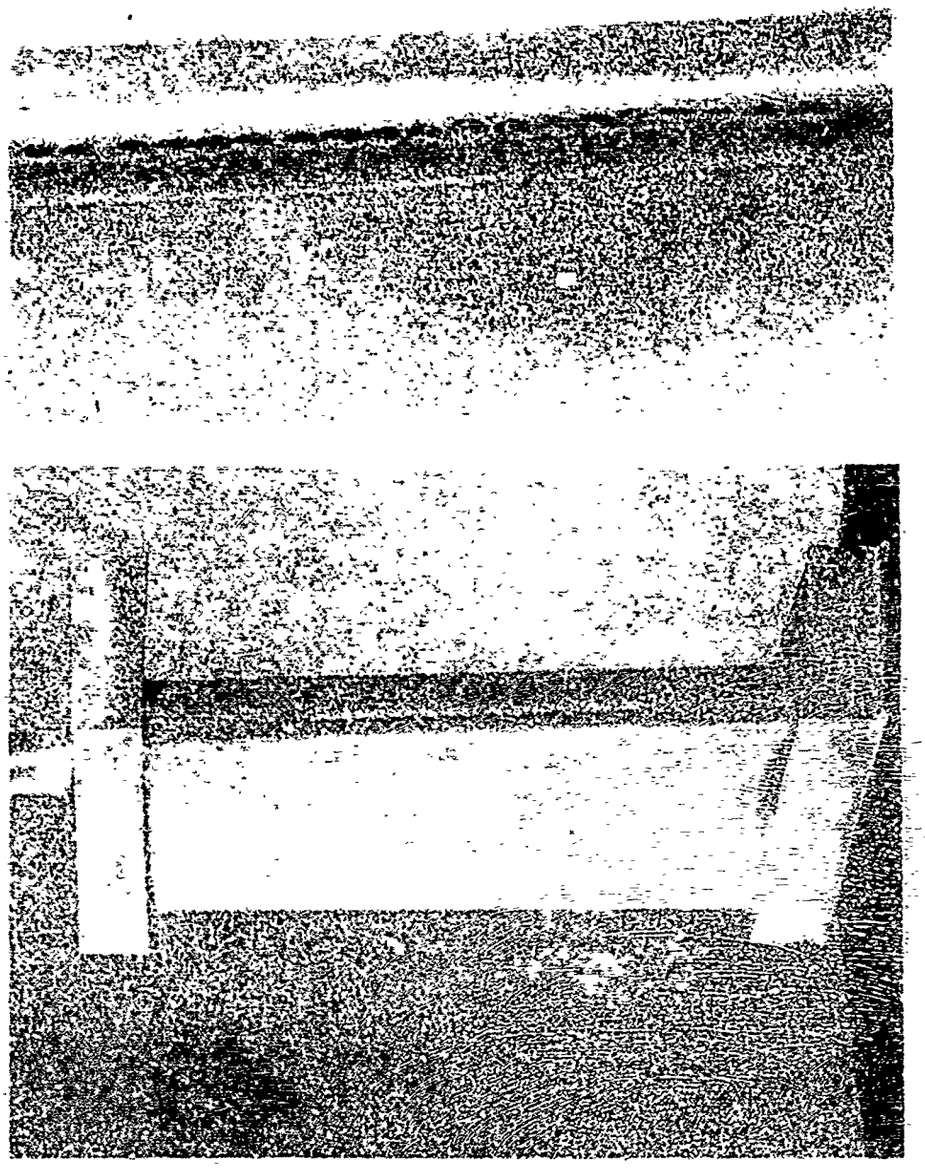
Figure 6-21

DOWNGRADED AT 3 YEAR INTERVALS
OR DECLASSIFIED AFTER 12 YEARS
DOD DIR 5200.10



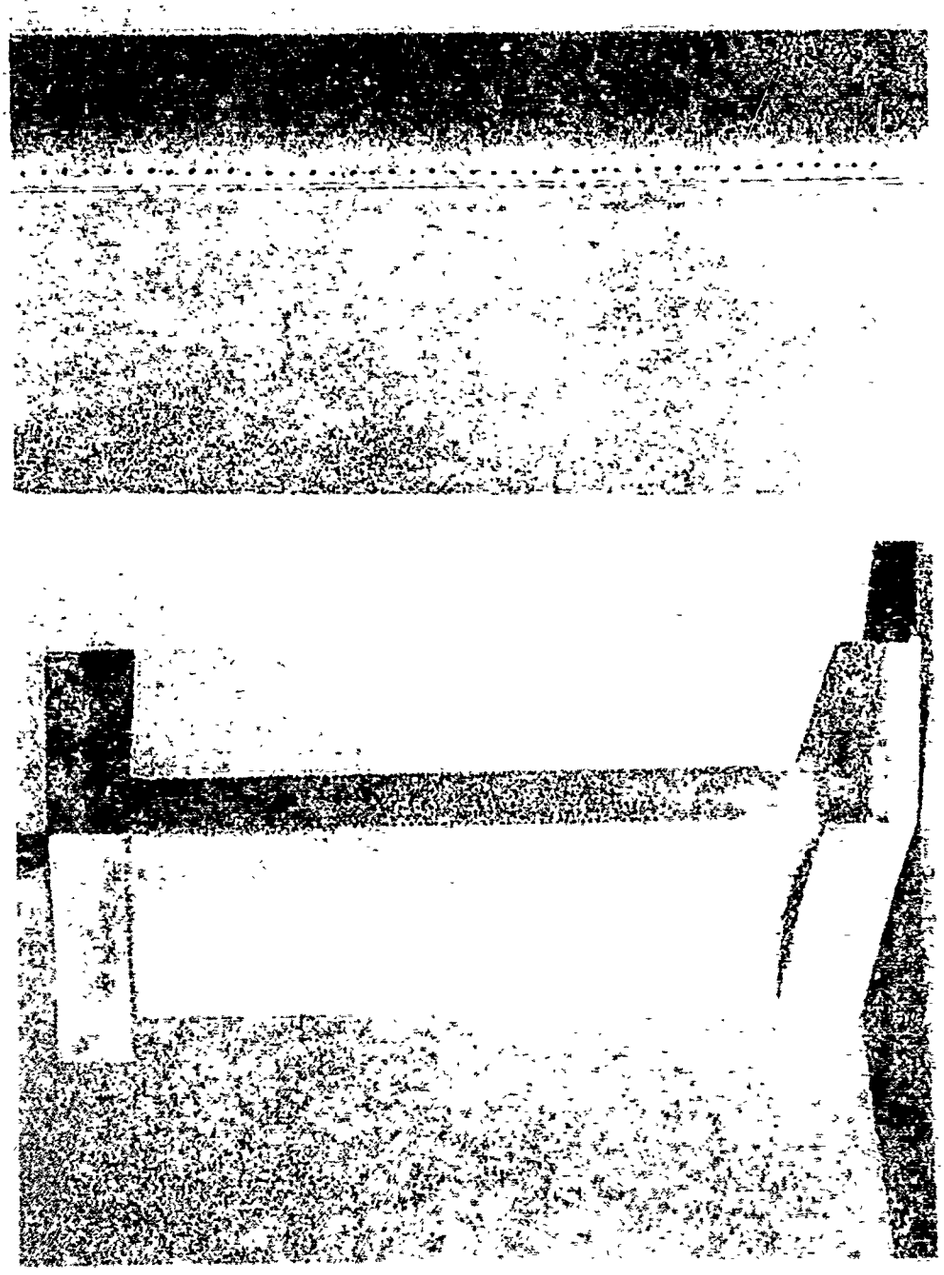
TURBINE VANE CONFIGURATION WITH FILM-COOLED LEADING EDGE CONTAINING 0.012 x 0.100 HOLES BEHIND AN 0.025 INCH THICK SHIELD

Figure 6-22



TURBINE VANE CONFIGURATION WITH FILM-COOLED LEADING EDGE CONTAINING 21 HOLES, 0.036 INCH DIAMETER, SPACED [illegible] APART, DRILLED AT A 45° ANGLE TO THE LEADING EDGE

Figure 6-23



...E WALL CONFIGURATION WITH FILM-COOLED LEADING EDGE CONTAINING
... ROWS OF ... INCH DIAMETER HOLES

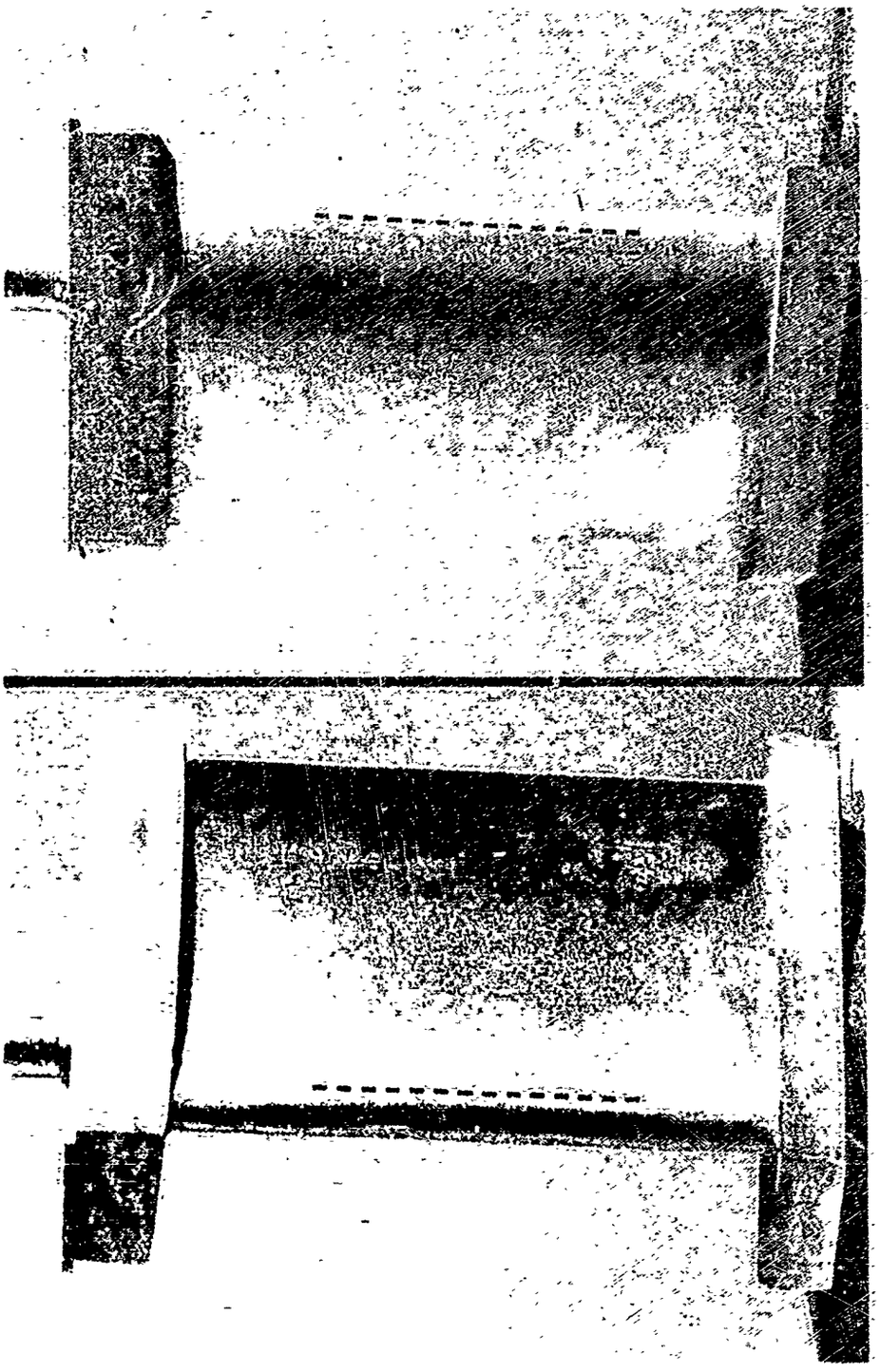
Figure 4-24



TURBINE VANE CONFIGURATION WITH FILM-COOLED LEADING EDGE CONTAINING SHOWER HEAD HOLE SCHEME

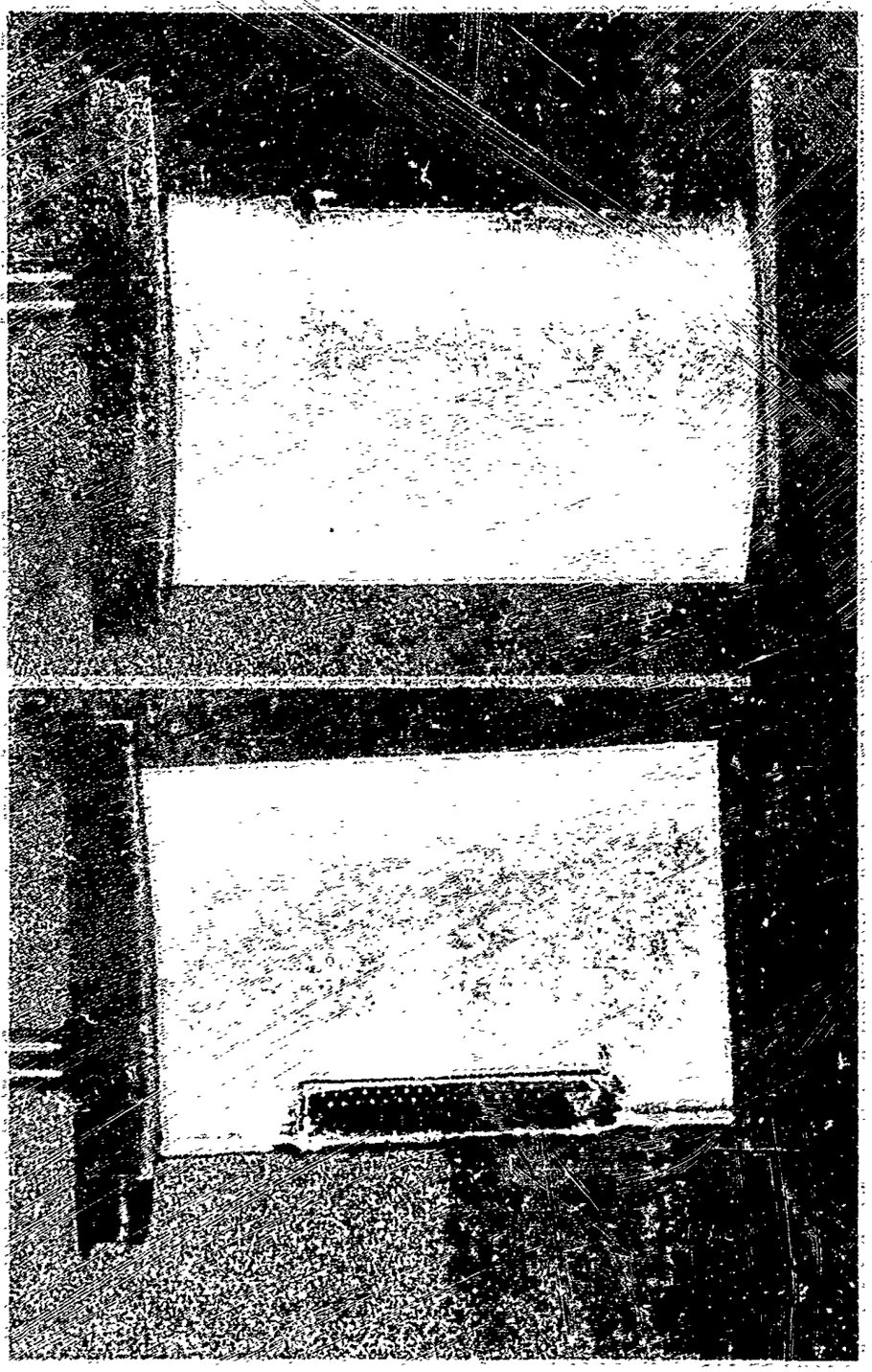
Figure 6-25

DOWNGRADED AT 3 YEAR INTERVALS
DECLASSIFIED AFTER 12 YEARS
DOD DIR 5200.10



TURBINE VANE CONFIGURATION WITH FILM-COOLED LEADING EDGE CONTAINING IMPINGEMENT SLOTS

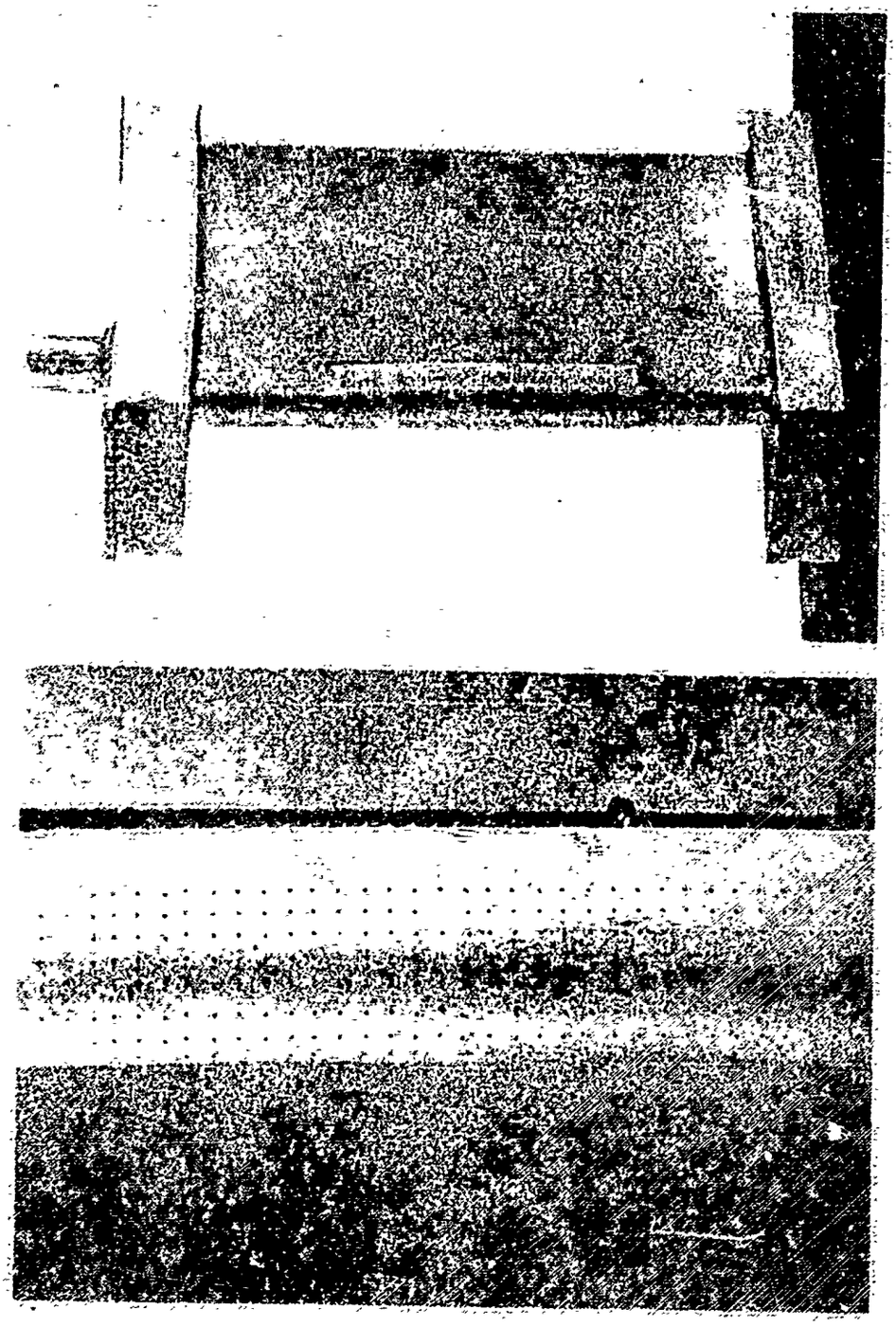
Figure 6-26



TURBINE VANE CONFIGURATION WITH FILM-COOLED LEADING EDGE CONTAINING PIERCED SHEET (0.013" DIA. HOLES)

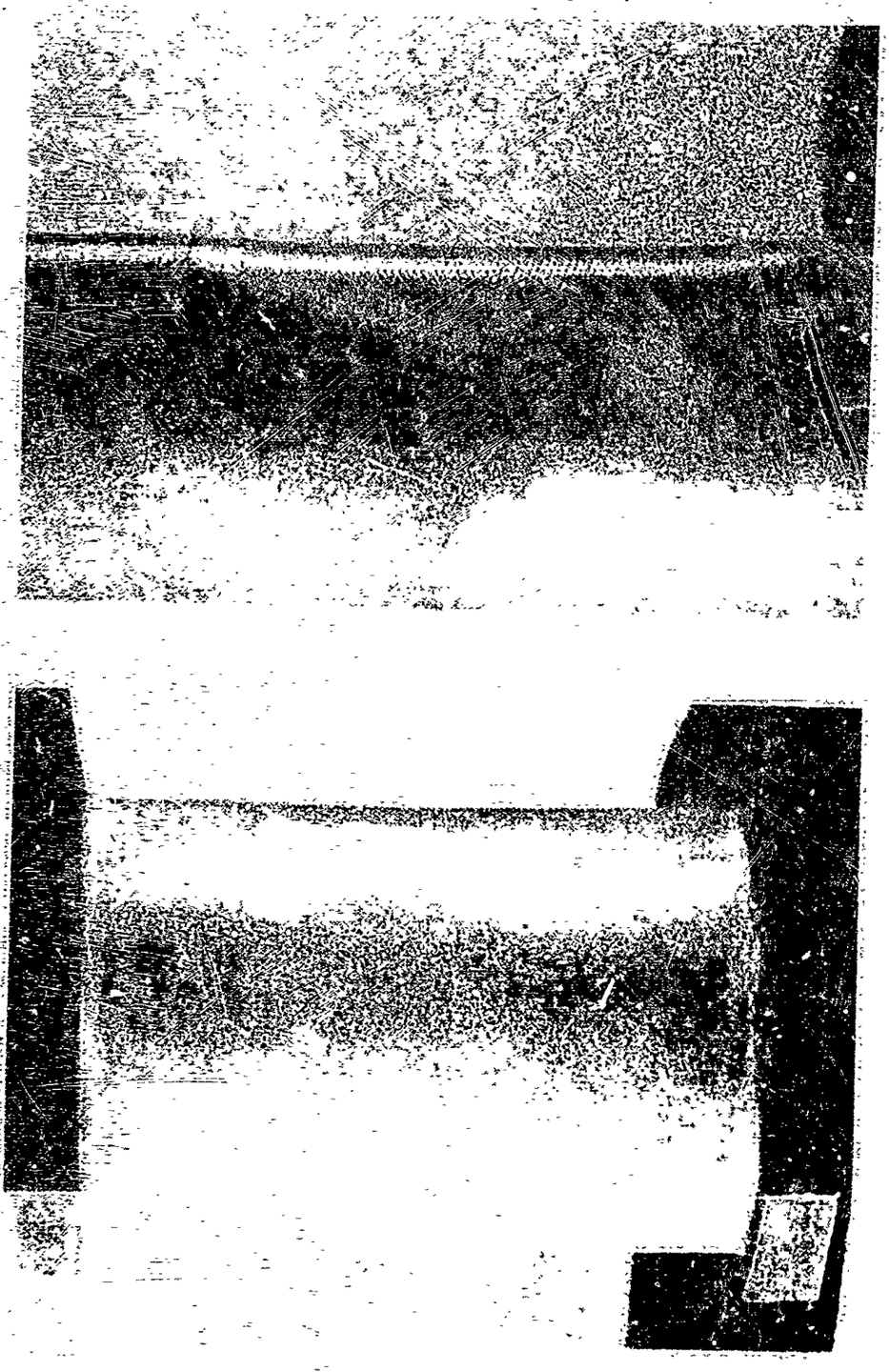
Figure 6-27

DOWNGRADED AT 3 YEAR INTERVALS
DECLASSIFIED AFTER 12 YEARS
DOD DIR 5200.10



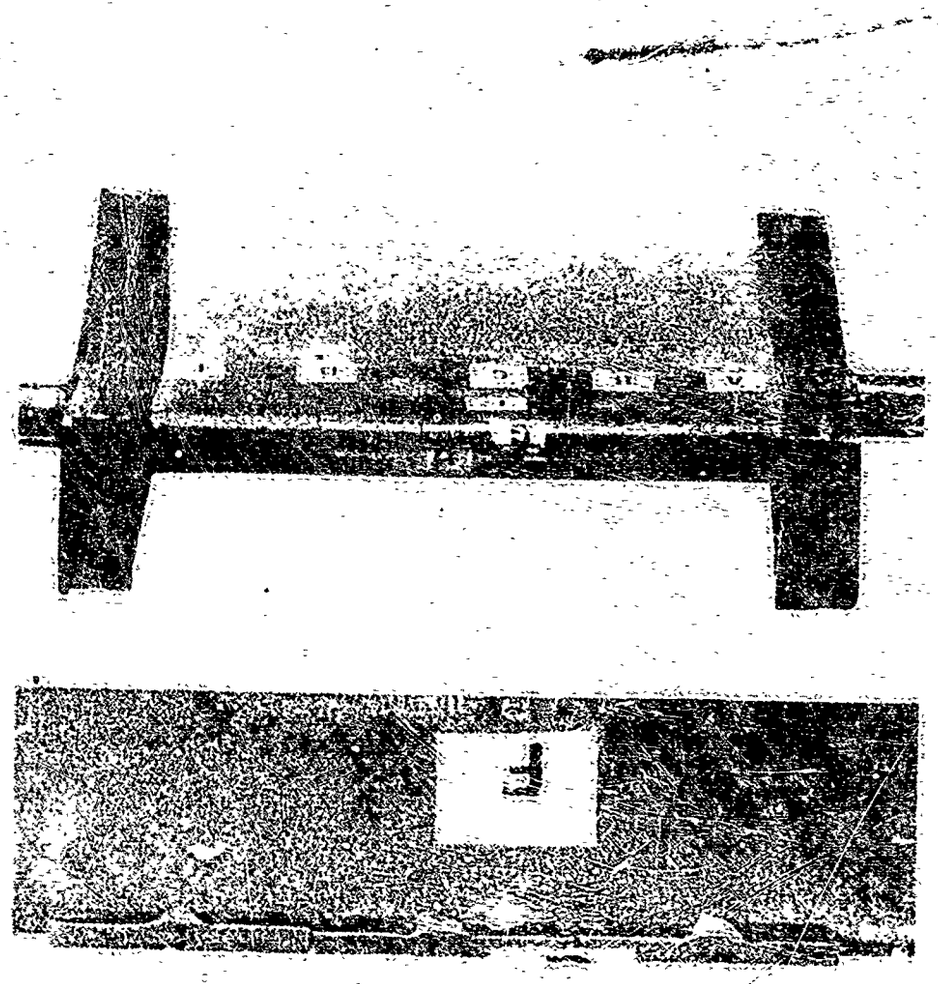
TURBINE VANE CONFIGURATION WITH FILM-COOLED LEADING EDGE CONTAINING PIERCED SHEET (0.006" DIA. HOLES)

Figure 6-28



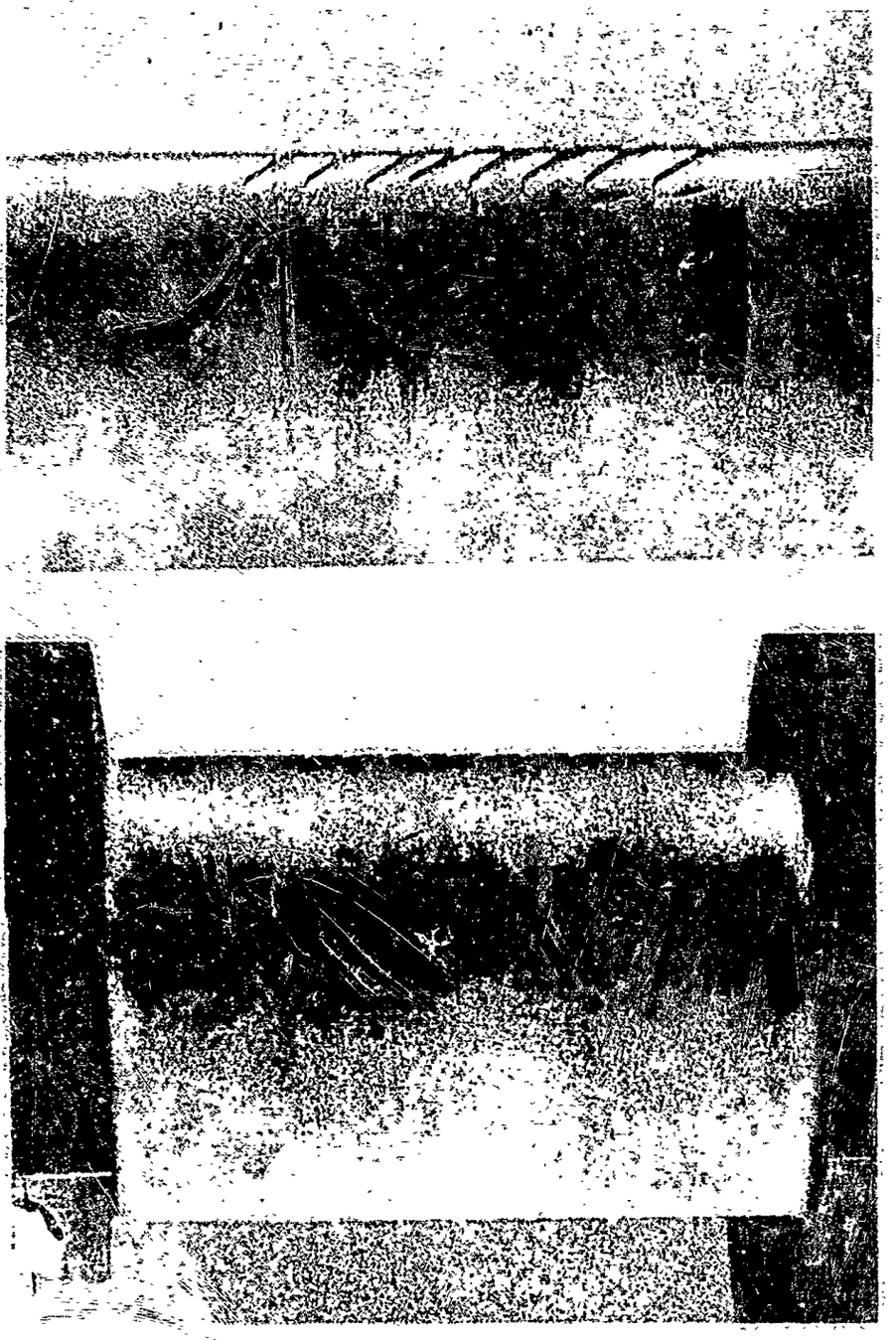
TURBINE VANE CONFIGURATION WITH TRANSPIRATION-COOLED LEADING EDGE CONTAINING POROLOY

Figure 6-29



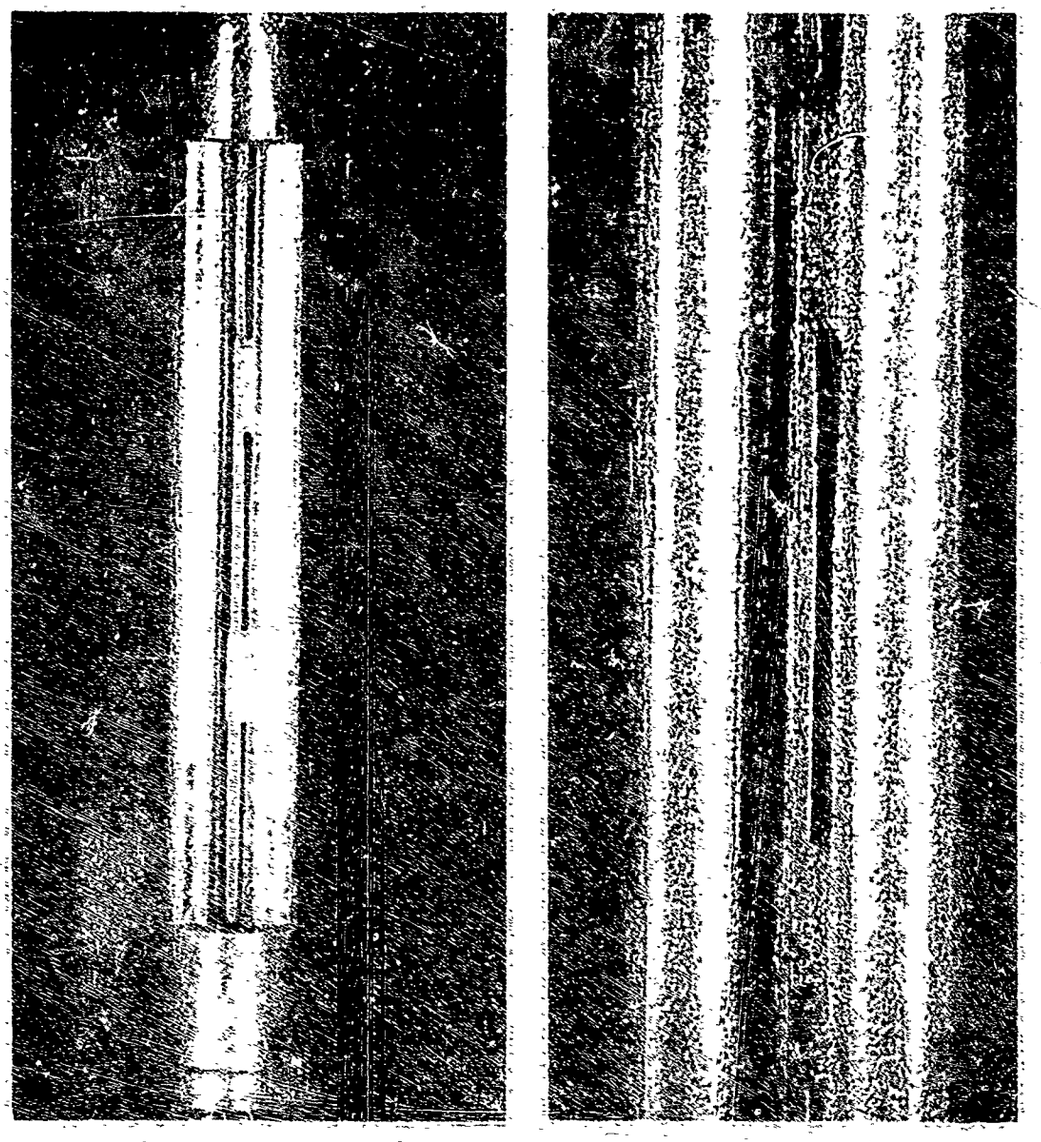
TURBINE VANE CONFIGURATION WITH IMPINGEMENT - AND FILM-COOLED LEADING EDGE INCORPORATING UMBRELLA SHIELD

Figure 6-30



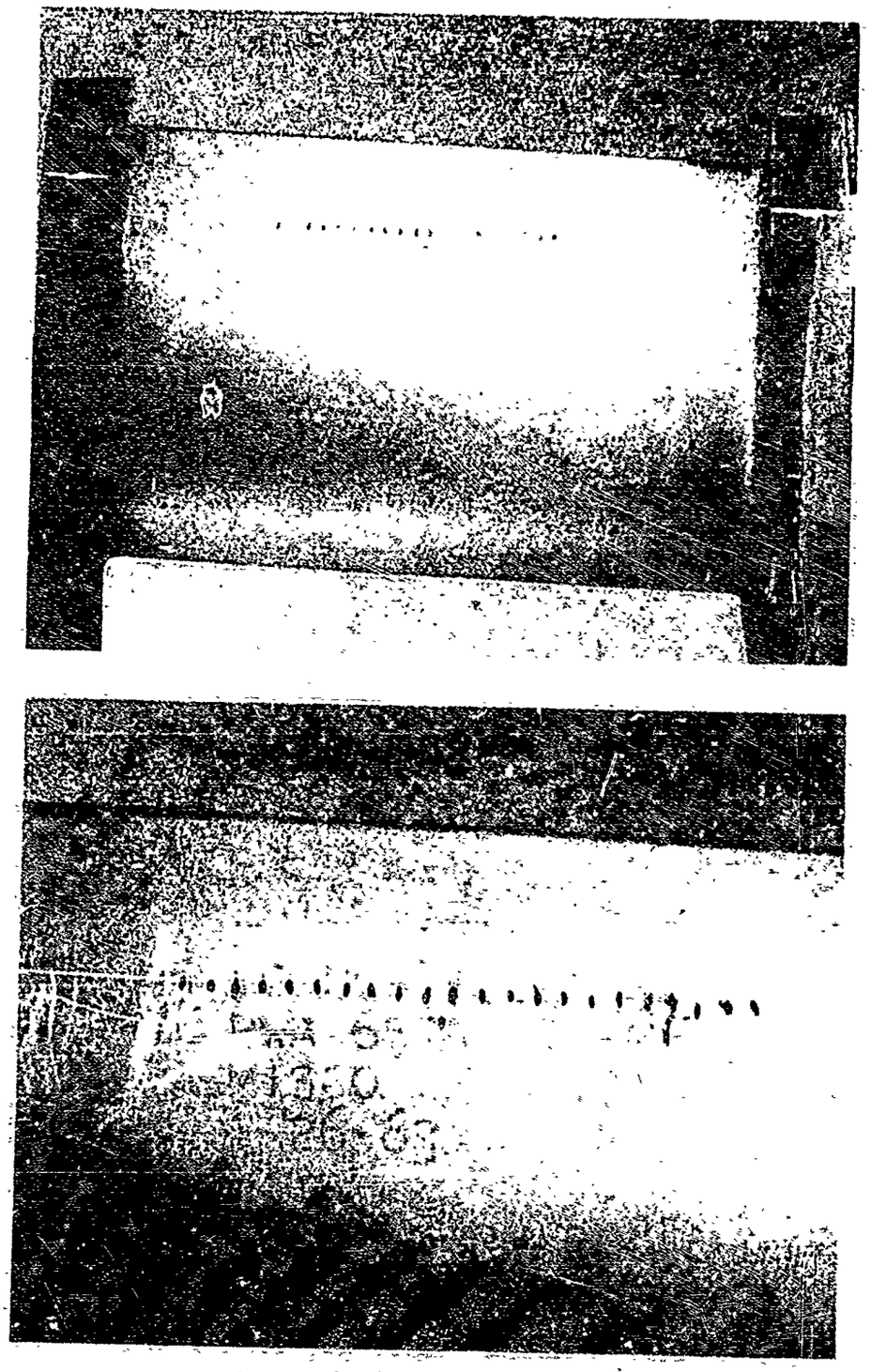
TURBINE VANE CONFIGURATION WITH IMPINGEMENT - AND FILM-COOLED LEADING EDGE INCORPORATING SUGAR SCOOP CUT-OUTS

Figure 6-31



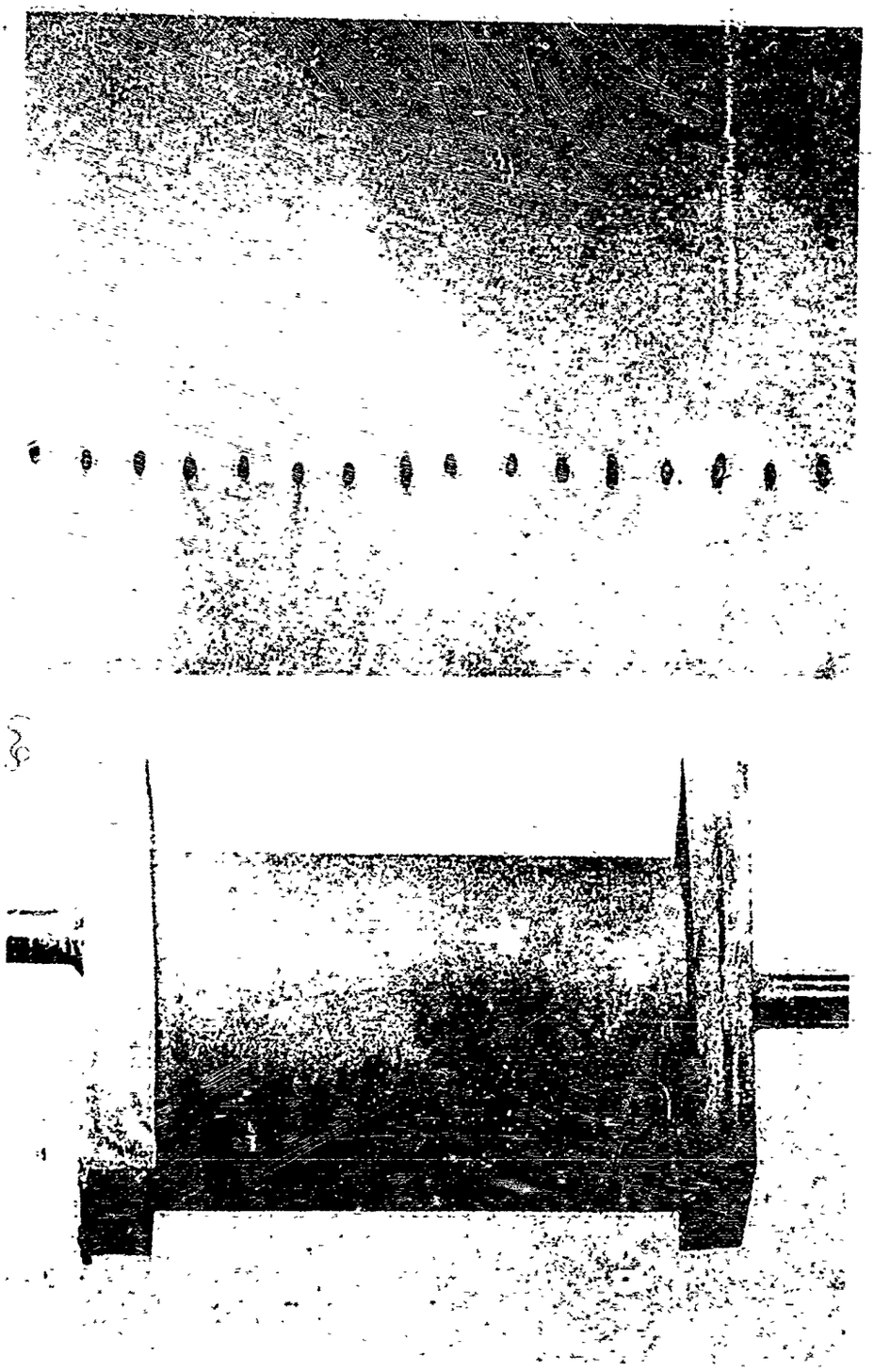
TURBINE VANE CONFIGURATION WITH FILM-COOLED LEADING EDGE INCORPORATING COANDA SLOT SCHEME

Figure 6-32



TURBINE VANE CONFIGURATION WITH FILM-COOLED TRAILING EDGE
(0.013" DIA. HOLES)

Figure 6-33

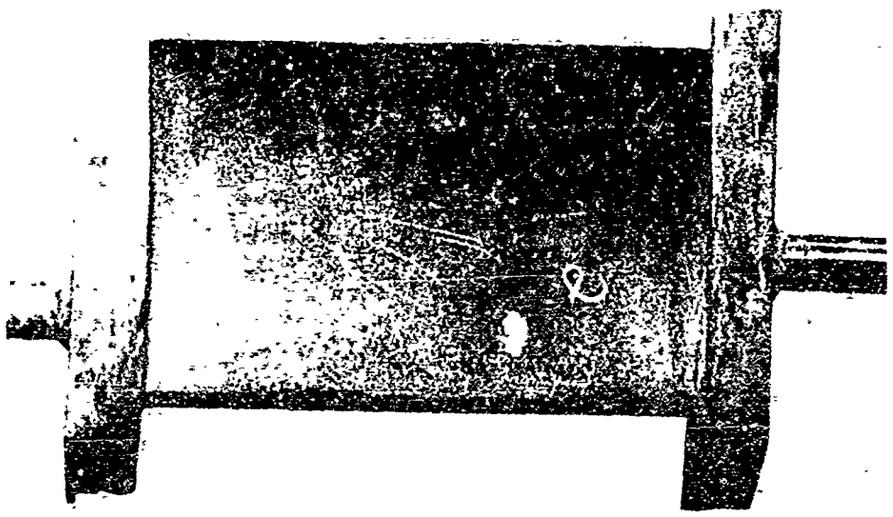


TURBINE VANE CONFIGURATION WITH FILM-COOLED TRAILING EDGE

Figure 6-34

DOWNGRADED AT 3 YEAR INTERVALS
DOD DIR 5200.10

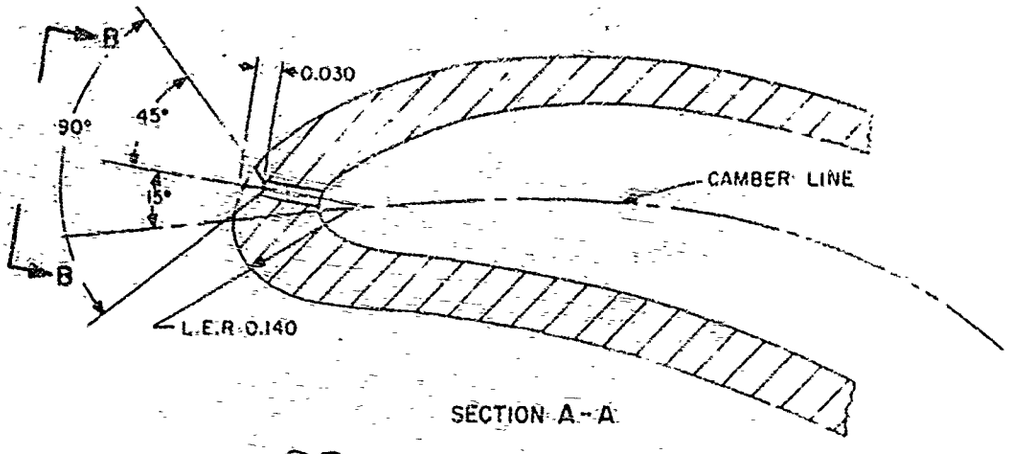




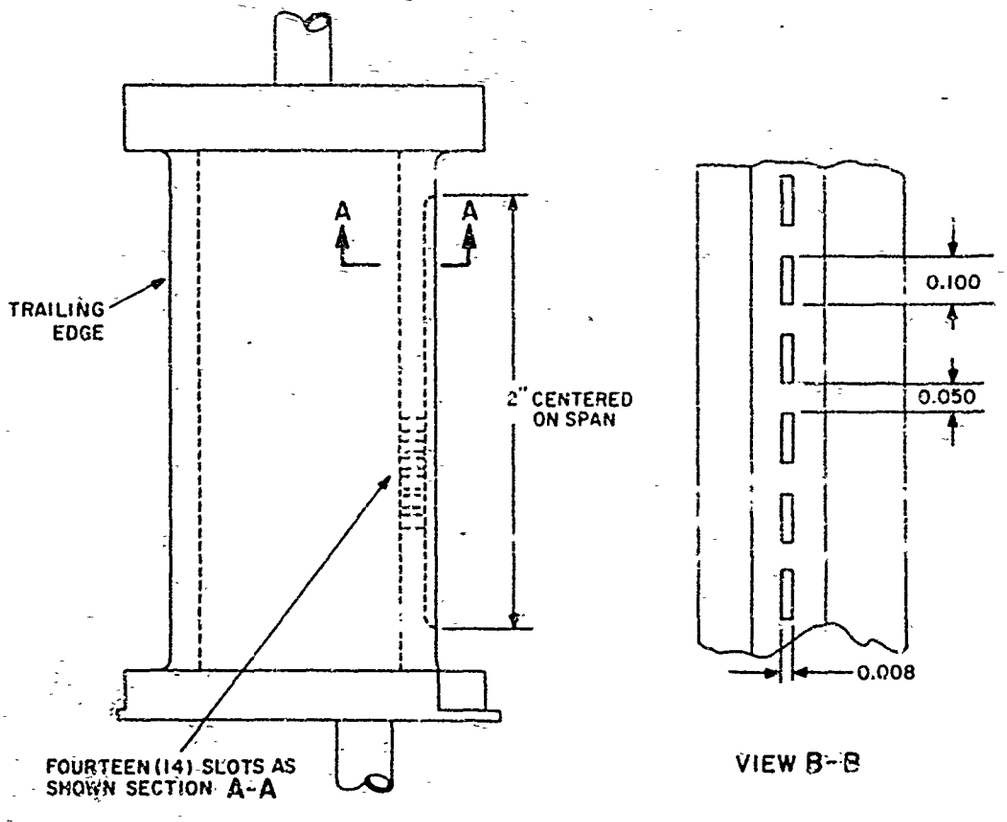
TURBINE VANE CONFIGURATION WITH FILM-COOLED TRAILING EDGE CONTAINING HOLES ON CONVEX SIDE

Figure 6-35

DOWNGRADED AT 3 YEAR INTERVALS
DECLASSIFIED AFTER 12 YEARS
DOD DIR 5200.10



SECTION A-A



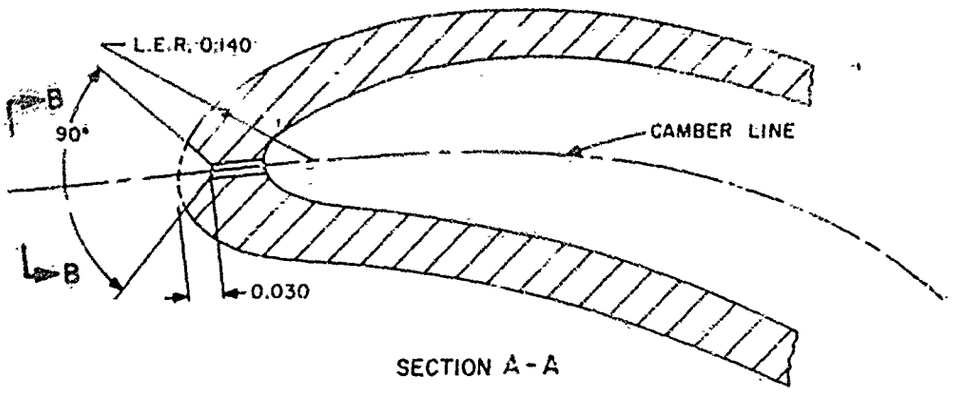
VIEW B-B

SCHEMATIC OF TURBINE VANE WITH LEADING EDGE SLOTS AT STAGNATION LINE

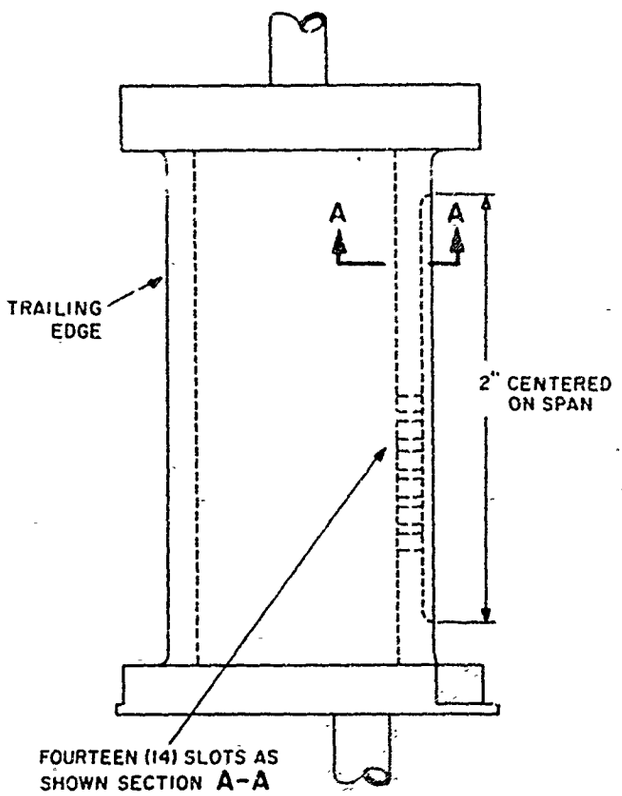
Figure 6-36

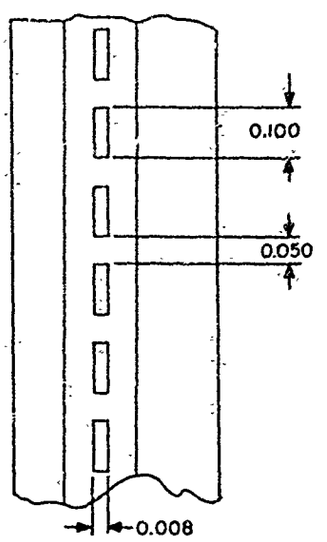
DOWNGRADED AT 3 YEAR INTERVALS
DECLASSIFIED AFTER 12 YEARS
DOD DIR 5200.10

THIS DOCUMENT CONTAINS INFORMATION AFFECTING THE NATIONAL DEFENSE OF THE UNITED STATES WITHIN THE MEANING OF THE ESPIONAGE LAWS, TITLE 18 U.S.C. SECTIONS 793 AND 794. THE TRANSMISSION OR THE REVELATION OF ITS CONTENTS IN ANY MANNER TO AN UNAUTHORIZED PERSON IS PROHIBITED BY LAW.



SECTION A-A



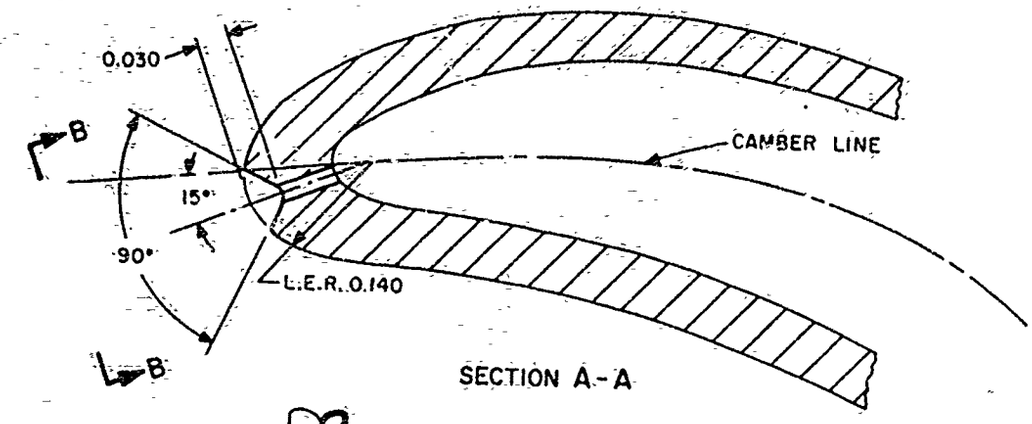


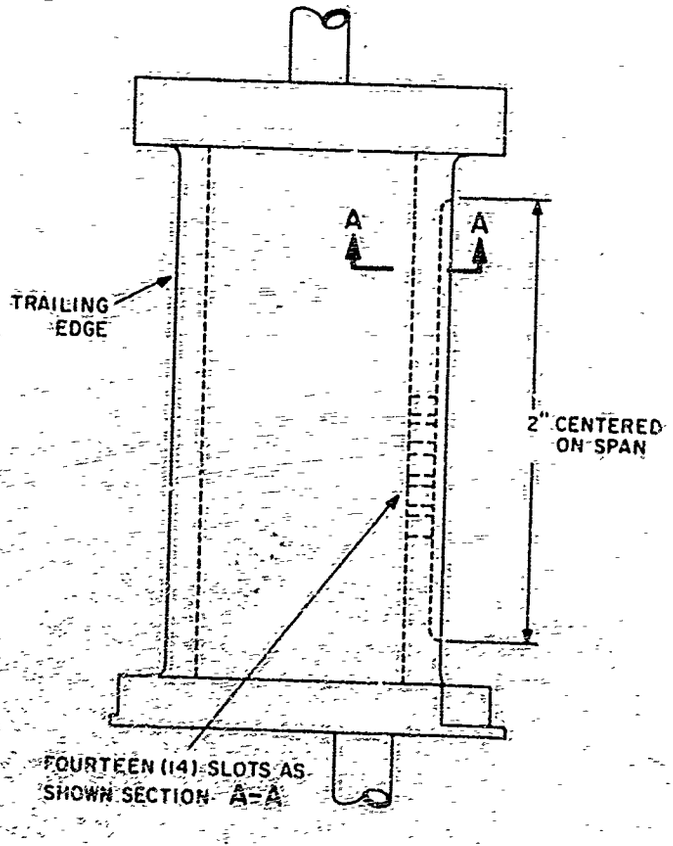
VIEW B-B

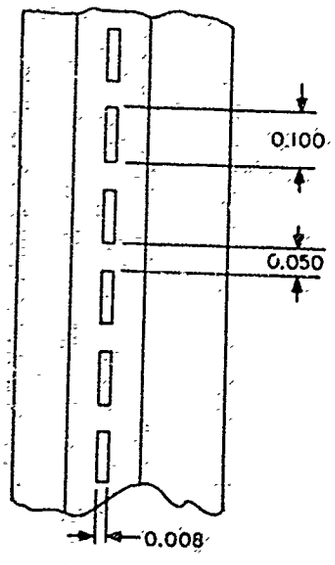
SCHEMATIC OF TURBINE VANE WITH LEADING EDGE SLOTS AT STAGNATION LINE

Figure 6-37

DOWNGRADED AT 3 YEAR INTERVALS
DECLASSIFIED AFTER 12 YEARS
DOD DIR 5200.10.

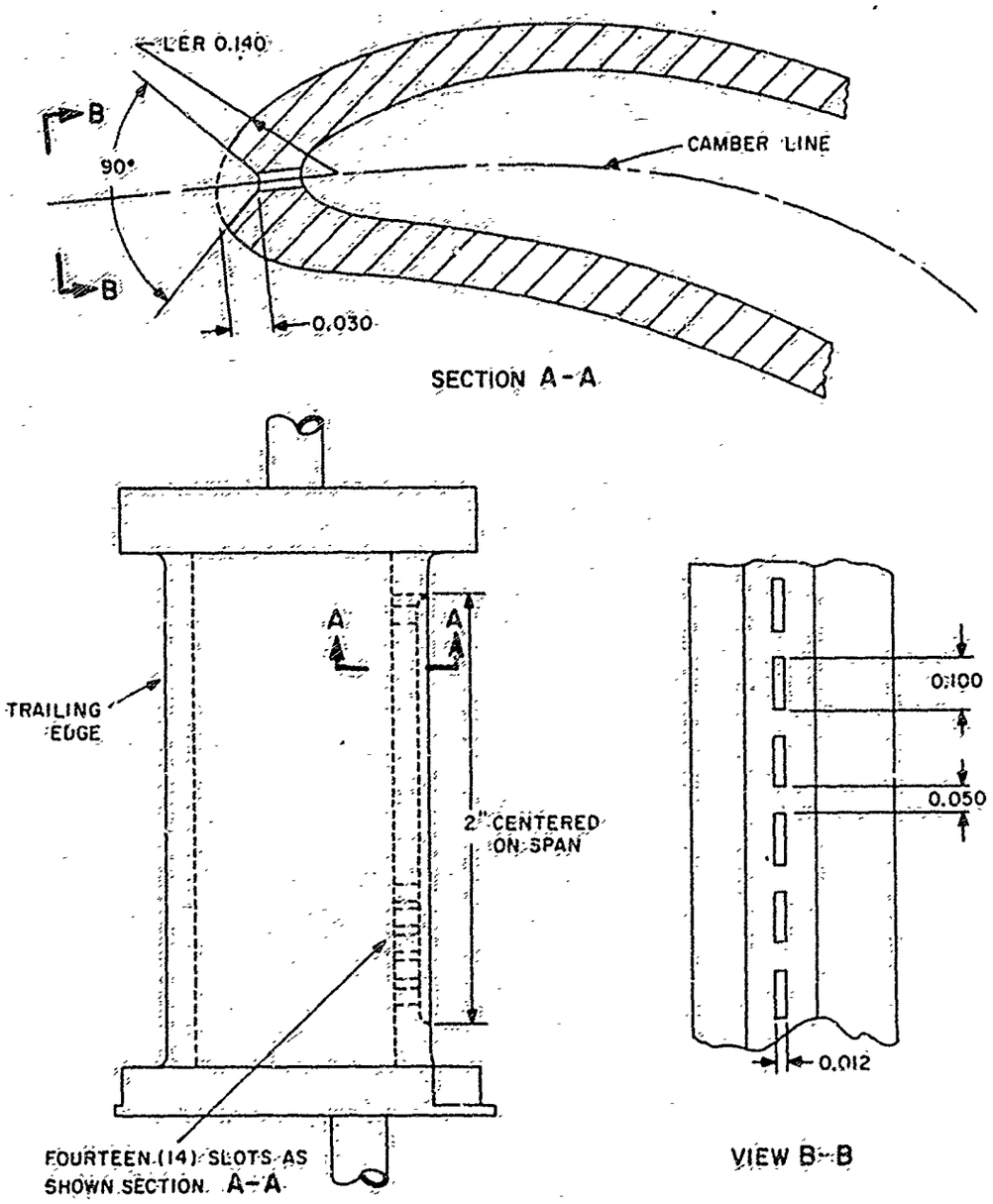






SCHEMATIC OF TURBINE VANE WITH LEADING EDGE COOLING SLOTS AS SHOWN ON FIGURE 6-18

Figure 6-38

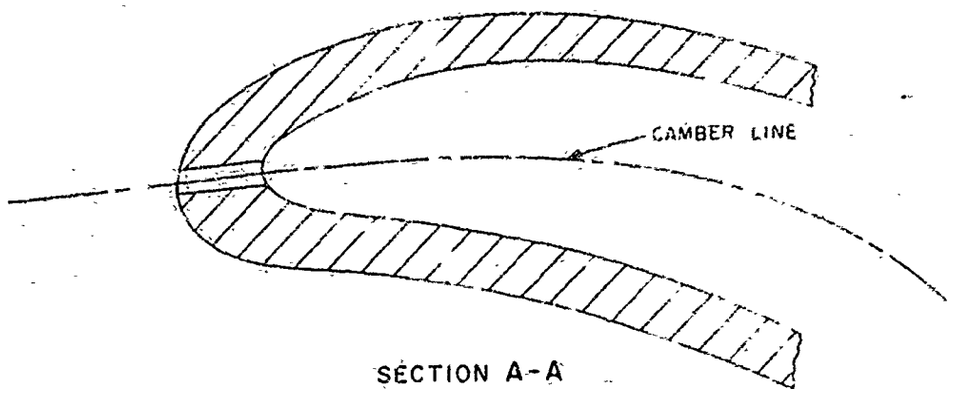


SCHEMATIC OF TURBINE VANE WITH LEADING EDGE COOLING SLOTS AS SHOWN ON FIGURE 6-19

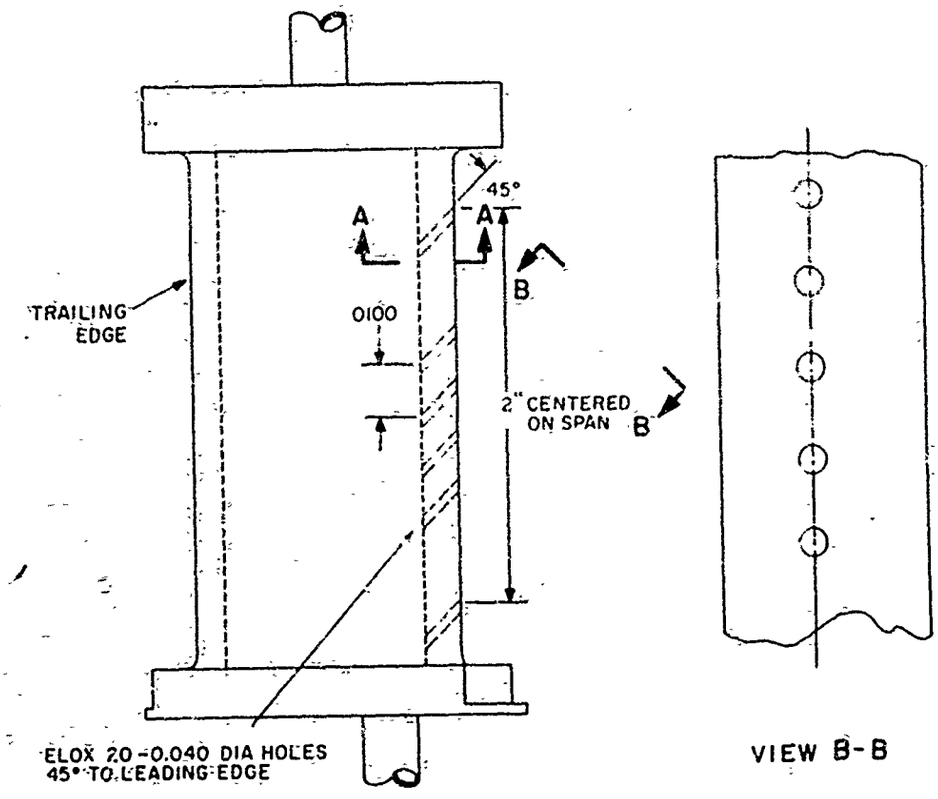
Figure 6-39

DOWNGRADED AT 3 YEAR INTERVALS
DECLASSIFIED AFTER 12 YEARS
DOD DIR 5200.10

THIS DOCUMENT CONTAINS INFORMATION AFFECTING THE NATIONAL DEFENSE OF THE UNITED STATES WITHIN THE MEANING OF THE ESPIONAGE LAWS, TITLE 18 U.S.C. SECTIONS 793 AND 794. THE TRANSMISSION OF THE REVELATION OF ITS CONTENTS IN ANY MANNER TO AN UNAUTHORIZED PERSON IS PROHIBITED BY LAW.



SECTION A-A

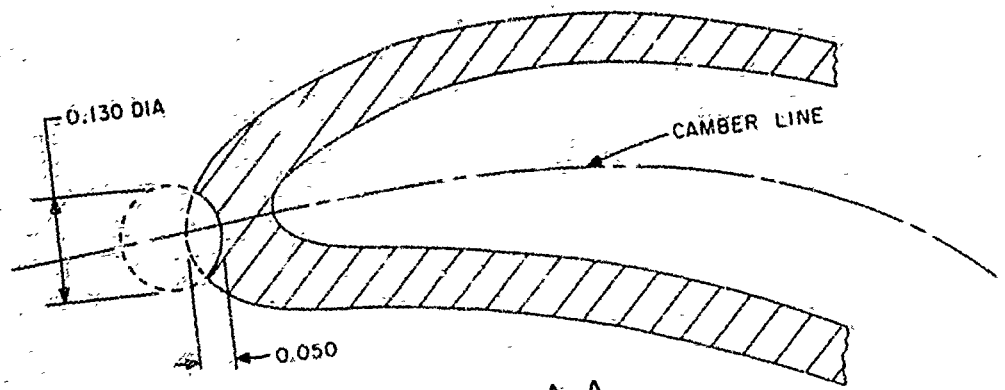


VIEW B-B

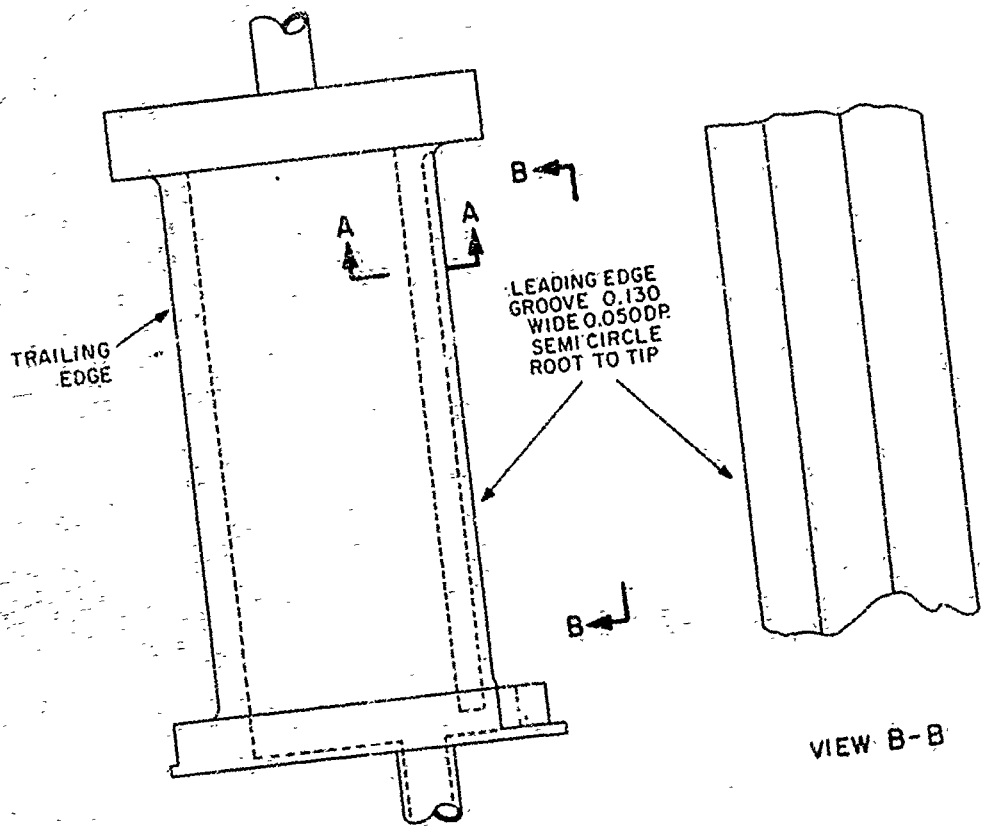
SCHEMATIC OF TURBINE VANE WITH LEADING EDGE COOLING SLOTS AS SHOWN ON FIGURE 6-20

Figure 6-40

DOWNGRADED AT 3 YEAR INTERVALS
DECLASSIFIED AFTER 12 YEARS
DOD DIR 5200.10



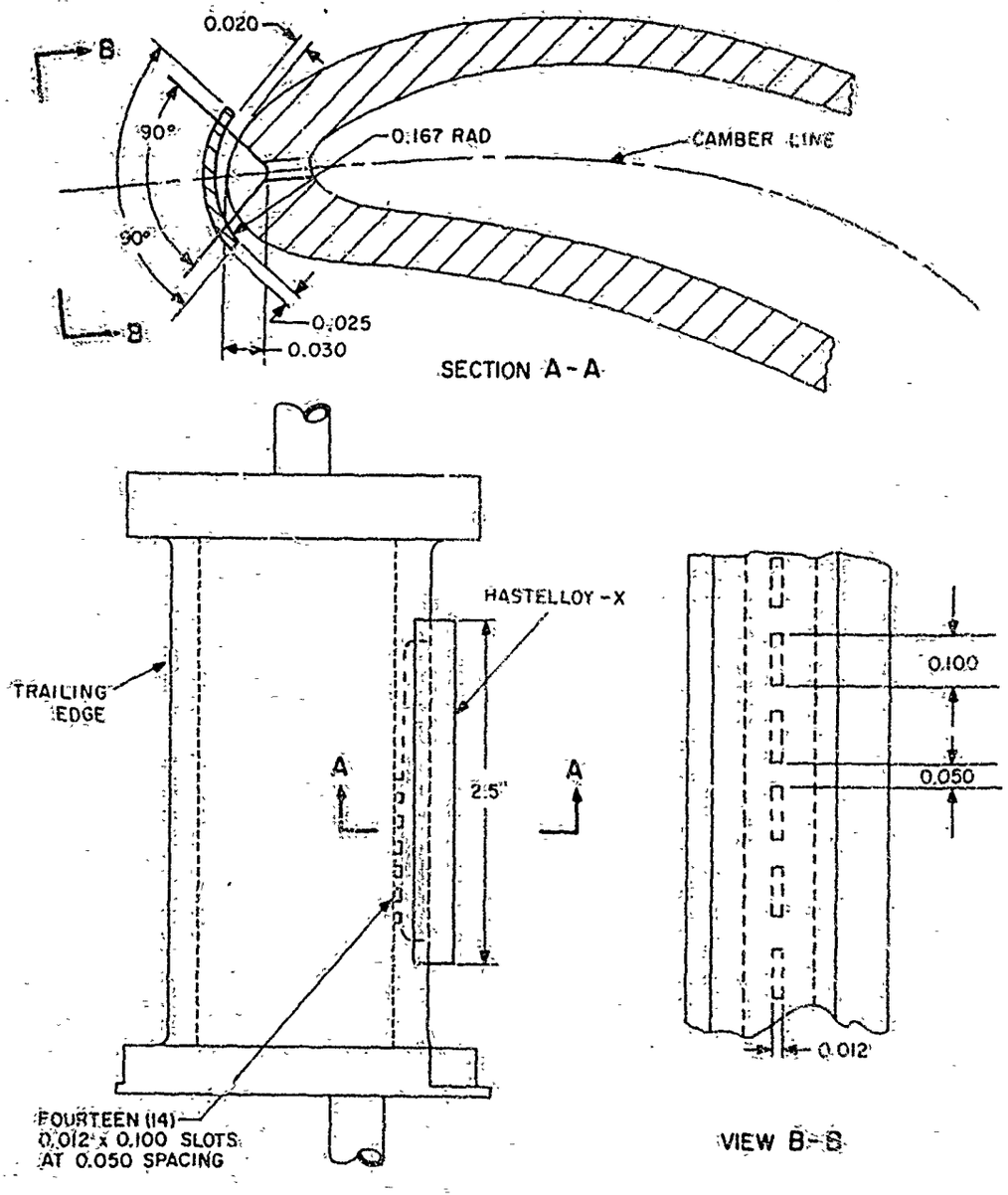
SECTION A-A



VIEW B-B

SCHEMATIC OF TURBINE VANE WITH FILM-COOLED LEADING EDGE AS SHOWN ON FIGURE 6-21 .

Figure 6-41

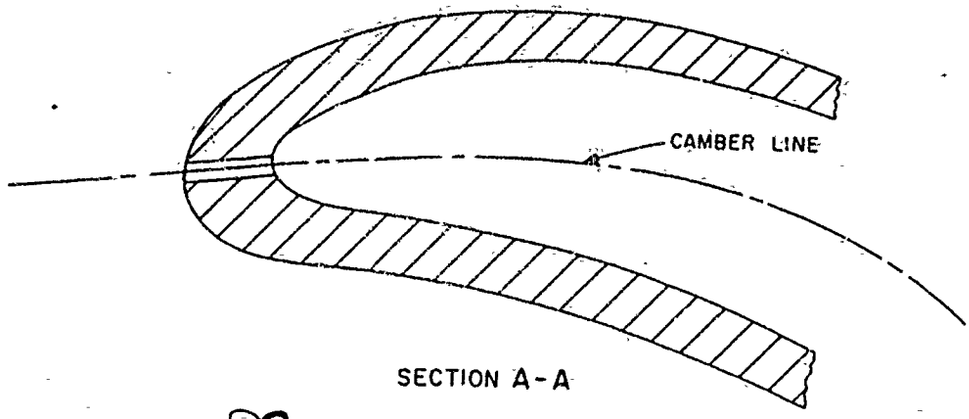


SCHEMATIC OF TURBINE VANE WITH FILM-COOLED LEADING EDGE AS SHOWN ON FIGURE 6-22

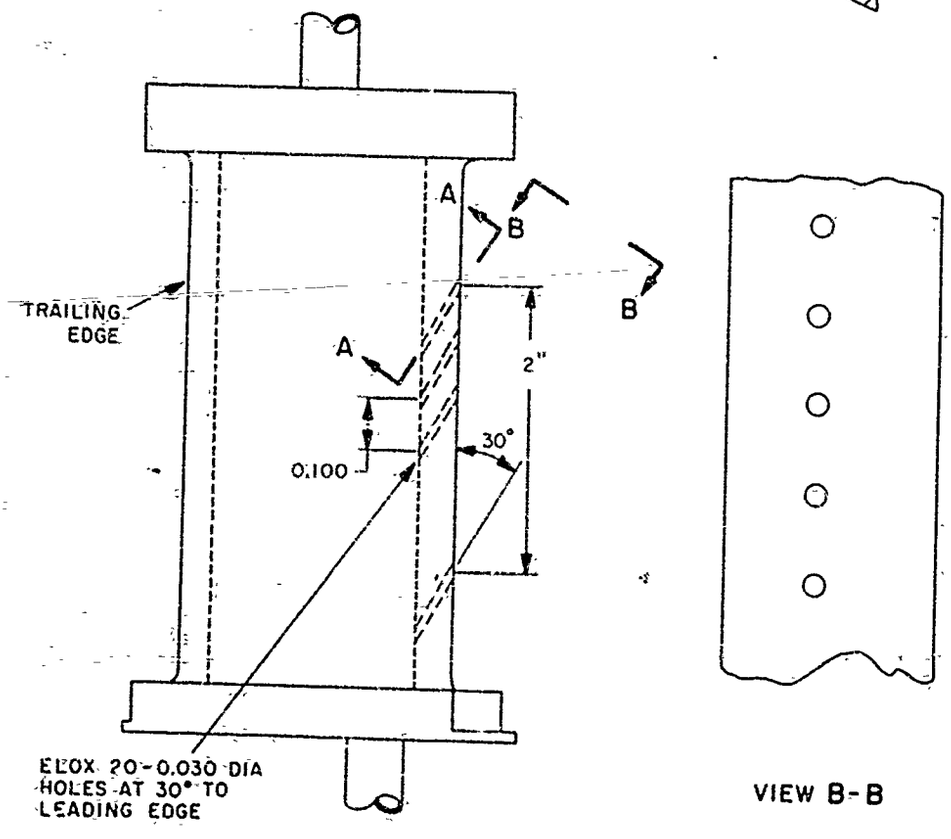
Figure 6-42

DOWNGRADED AT 3 YEAR INTERVALS
DECLASSIFIED AFTER 12 YEARS
DOD DIR. 5200.10

THIS DOCUMENT CONTAINS INFORMATION AFFECTING THE NATIONAL DEFENSE OF THE UNITED STATES WITHIN THE MEANING OF THE ESPIONAGE LAWS, TITLE 18, U.S.C., SECTIONS 793 AND 794. THE TRANSMISSION OR THE REVELATION OF ITS CONTENTS IN ANY MANNER TO AN UNAUTHORIZED PERSON IS PROHIBITED BY LAW.



SECTION A-A



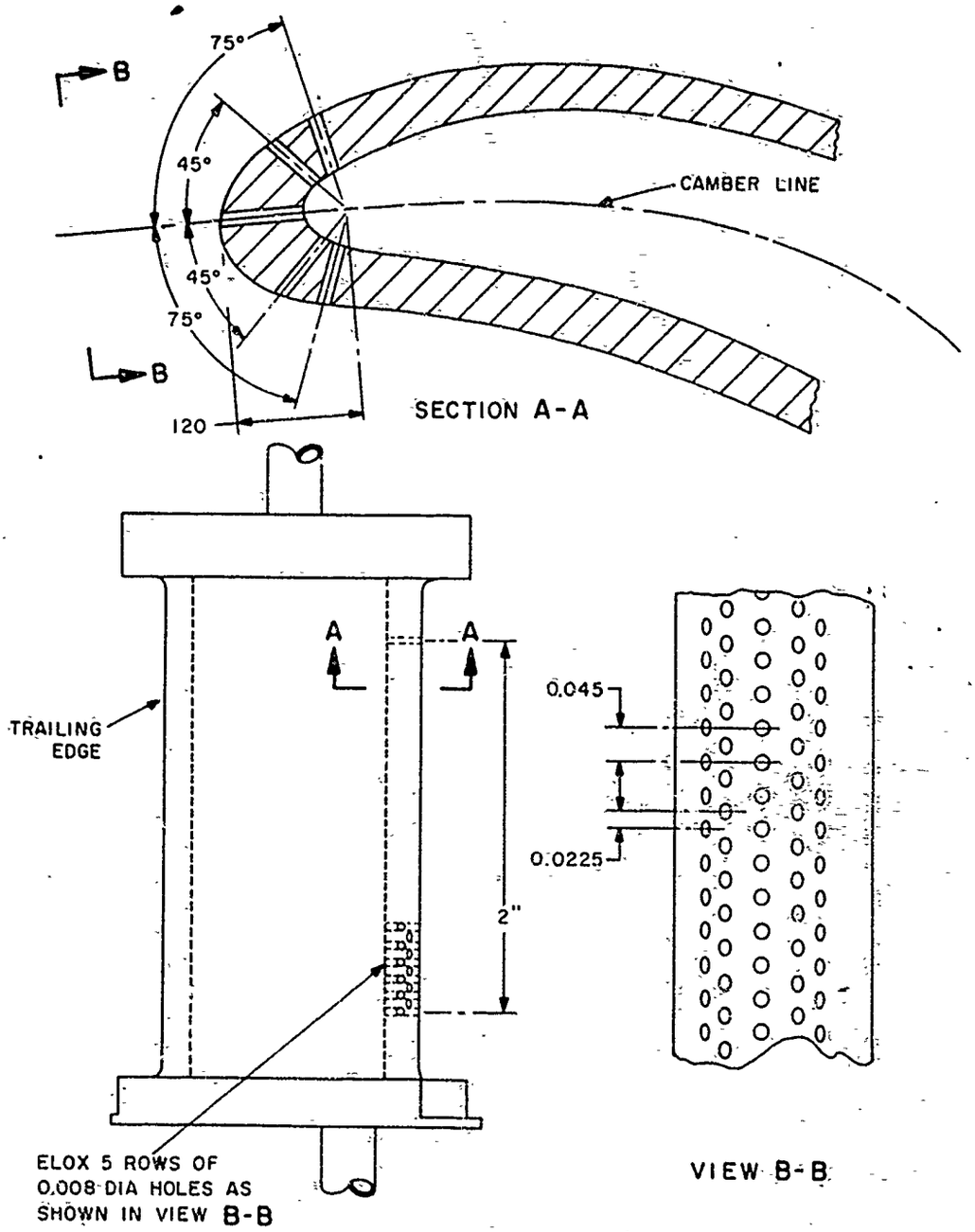
VIEW B-B

SCHEMATIC OF TURBINE VANE WITH FILM-COOLED LEADING EDGE AS SHOWN ON FIGURE 6-23

Figure 6-43

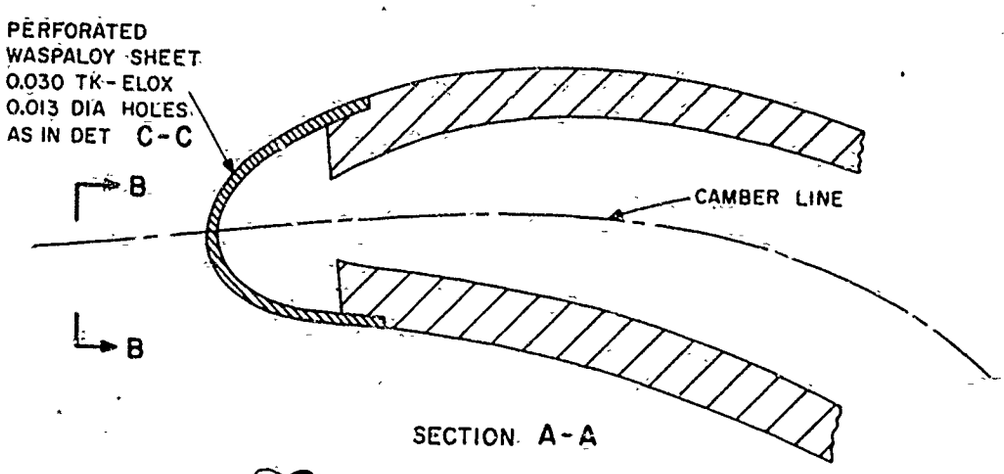
DOWNGRADED AT 3 YEAR INTERVALS
DECLASSIFIED AFTER 12 YEARS
DOD DIR 5200.10

THIS DOCUMENT CONTAINS INFORMATION AFFECTING THE NATIONAL DEFENSE OF THE UNITED STATES WITHIN THE MEANING OF THE ESPIONAGE LAWS, TITLE 18, U.S.C. SECTIONS 793 AND 794. THE TRANSMISSION OR THE REVELATION OF ITS CONTENTS IN ANY MANNER TO AN UNAUTHORIZED PERSON IS PROHIBITED BY LAW.

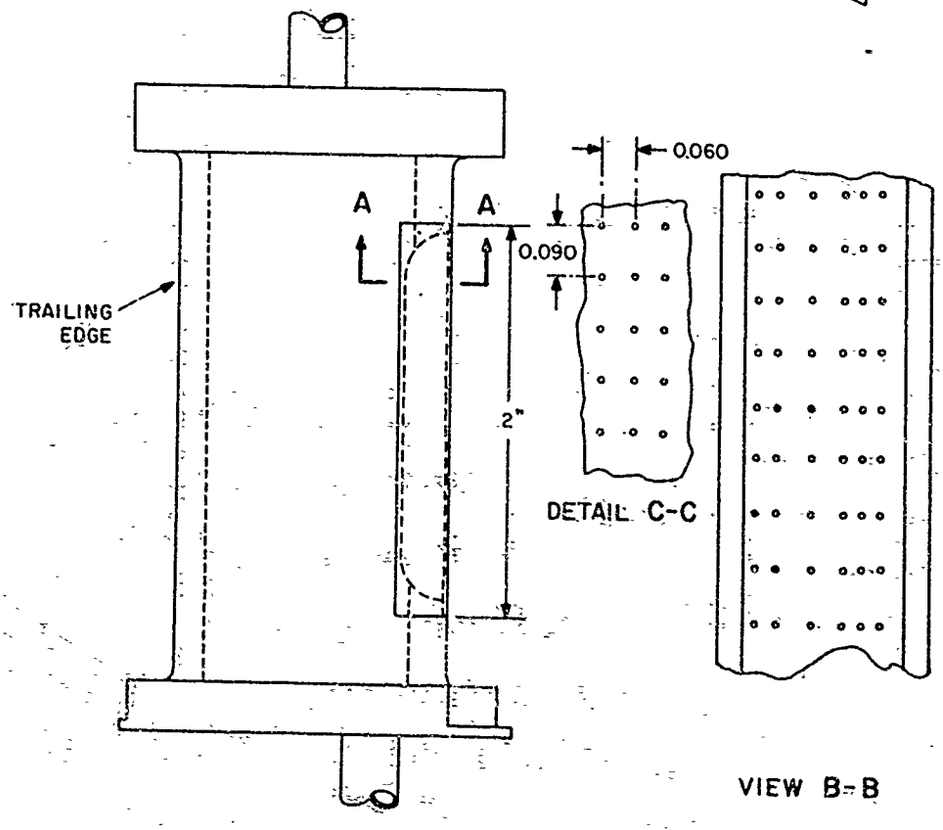


SCHEMATIC OF TURBINE VANE WITH FILM-COOLED LEADING EDGE AS SHOWN ON FIGURE 6-24

Figure 6-44



SECTION A-A

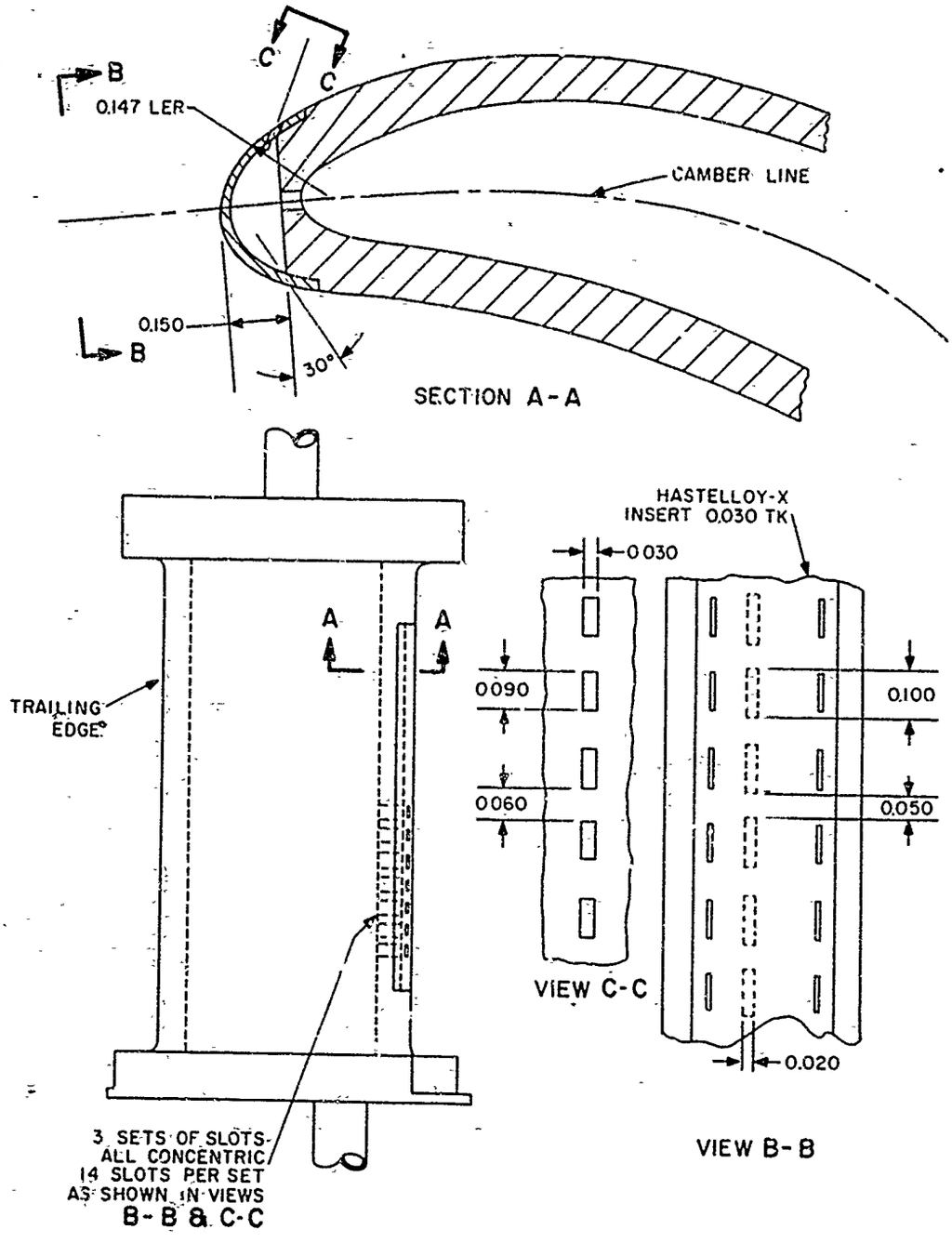


VIEW B-B

SCHEMATIC OF TURBINE VANE WITH FILM-COOLED LEADING EDGE AS SHOWN ON FIGURE 6-25

Figure 6-45

DOWNGRADED AT 3 YEAR INTERVALS
DECLASSIFIED AFTER 12 YEARS
DOD DIR 5200.10
THIS DOCUMENT CONTAINS INFORMATION AFFECTING THE NATIONAL DEFENSE OF THE UNITED STATES WITHIN THE MEANING OF THE ESPIONAGE LAWS, TITLE 18, U.S.C., SECTIONS 793 AND 794. THE TRANSMISSION OR THE REVELATION OF ITS CONTENTS IN ANY MANNER TO AN UNAUTHORIZED PERSON IS PROHIBITED BY LAW.

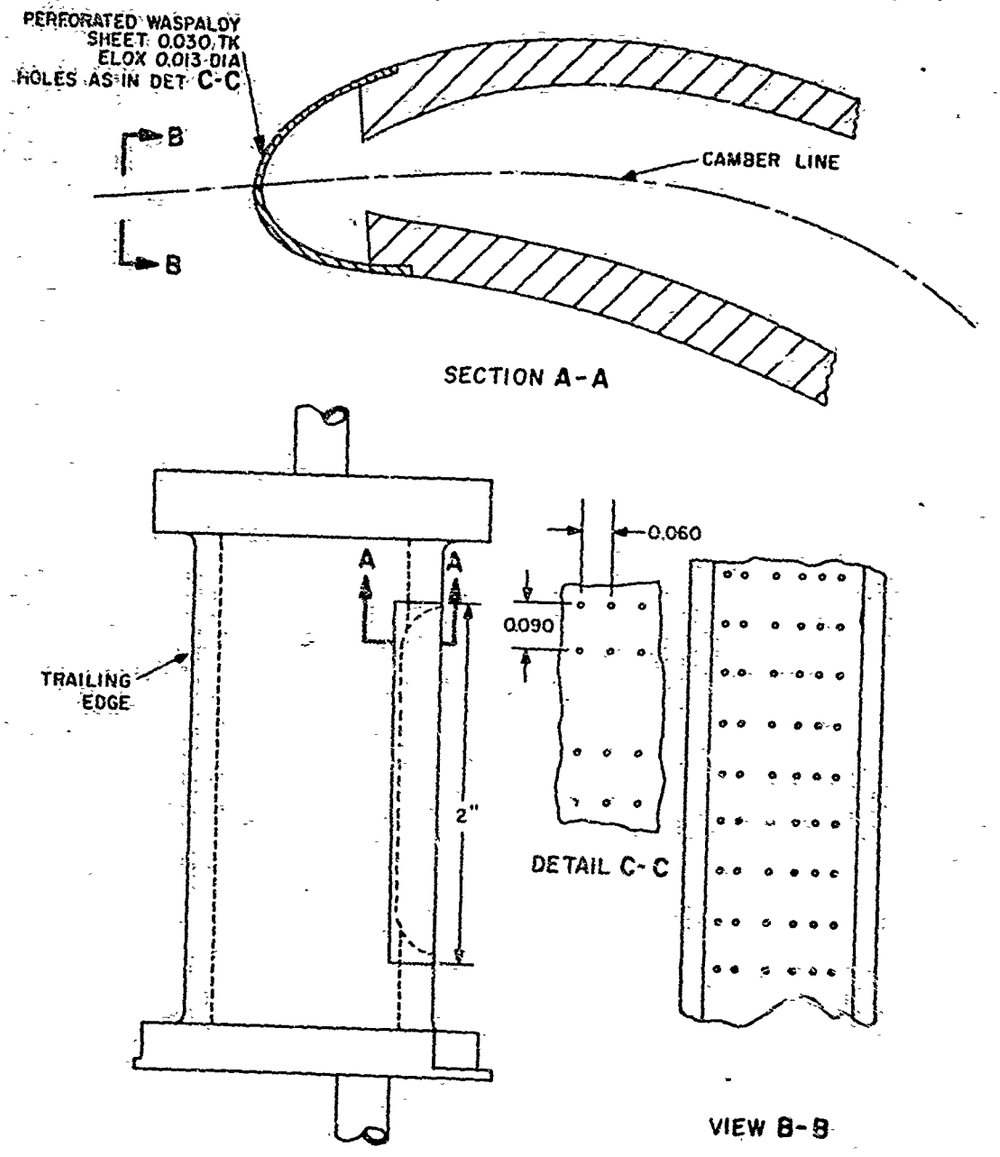


SCHEMATIC OF TURBINE VANE WITH FILM-COOLED LEADING EDGE AS SHOWN ON FIGURE 6-26

Figure 6-46

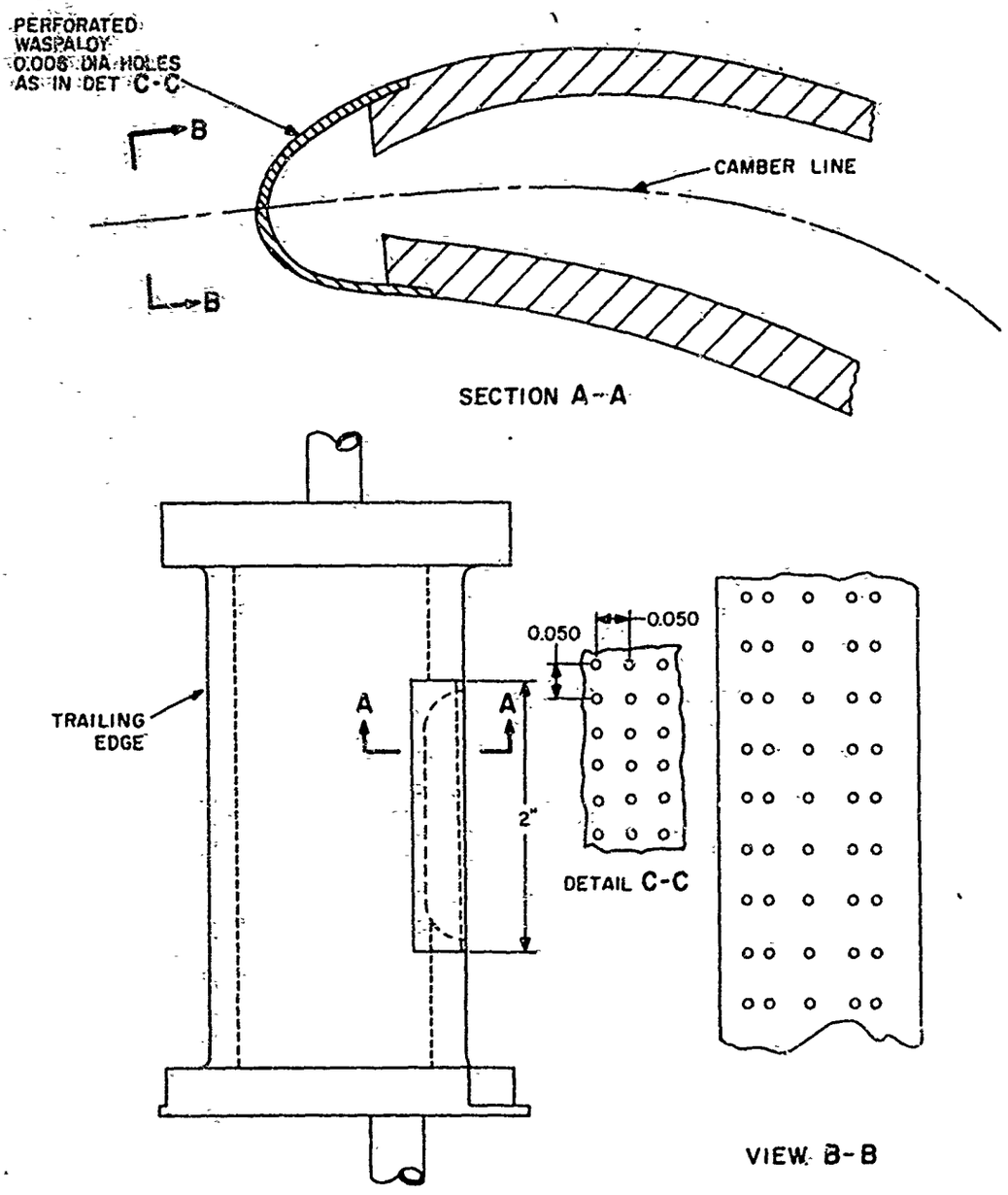
DOWNGRADED AT 3 YEAR INTERVALS
DECLASSIFIED AFTER 12 YEARS
DOD DIR 5.200.10

THIS DOCUMENT CONTAINS INFORMATION AFFECTING THE NATIONAL DEFENSE OF THE UNITED STATES WITHIN THE MEANING OF THE ESPIONAGE LAWS, TITLE 18 — U.S.C. SECTIONS 793 AND 794. ITS TRANSMISSION OR THE REVELATION OF ITS CONTENTS IN ANY MANNER TO AN UNAUTHORIZED PERSON IS PROHIBITED BY LAW.



SCHEMATIC OF TURBINE VANE WITH FILM-COOLED LEADING EDGE AS SHOWN ON FIGURE 6-27

Figure 6-47

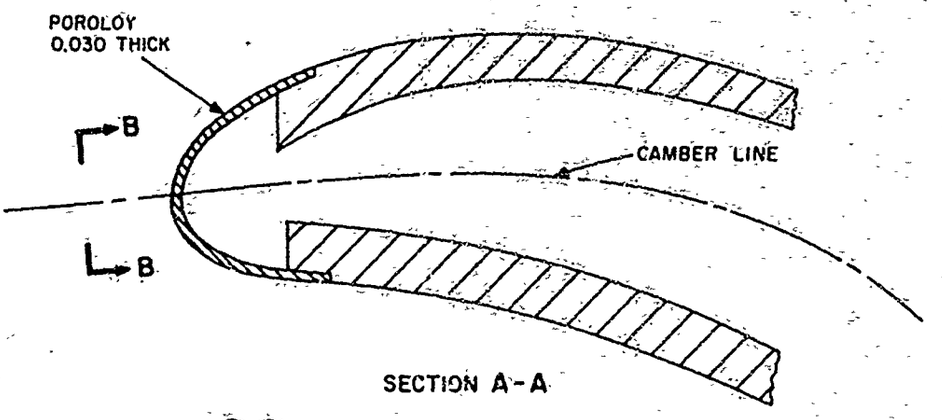


SCHEMATIC OF TURBINE VANE WITH FILM-COOLED LEADING EDGE AS SHOWN ON FIGURE 6-28

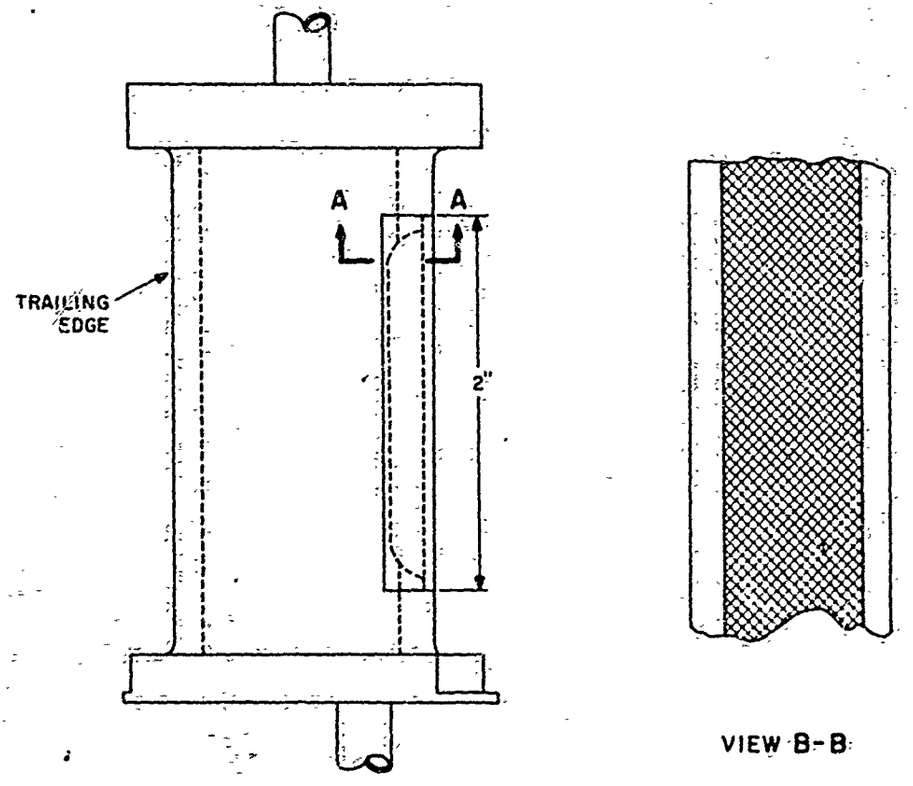
Figure 6-48

DOWNGRADED AT 3 YEAR INTERVALS
DECLASSIFIED AFTER 12 YEARS
DOD DIR 5200.10

THIS DOCUMENT CONTAINS INFORMATION AFFECTING THE NATIONAL DEFENSE OF THE UNITED STATES WITHIN THE MEANING OF THE ESPIONAGE LAWS, TITLE 18, U.S.C., SECTIONS 793 AND 794. THE TRANSMISSION OR THE REVELATION OF ITS CONTENTS IN ANY MANNER TO AN UNAUTHORIZED PERSON IS PROHIBITED BY LAW.



SECTION A-A



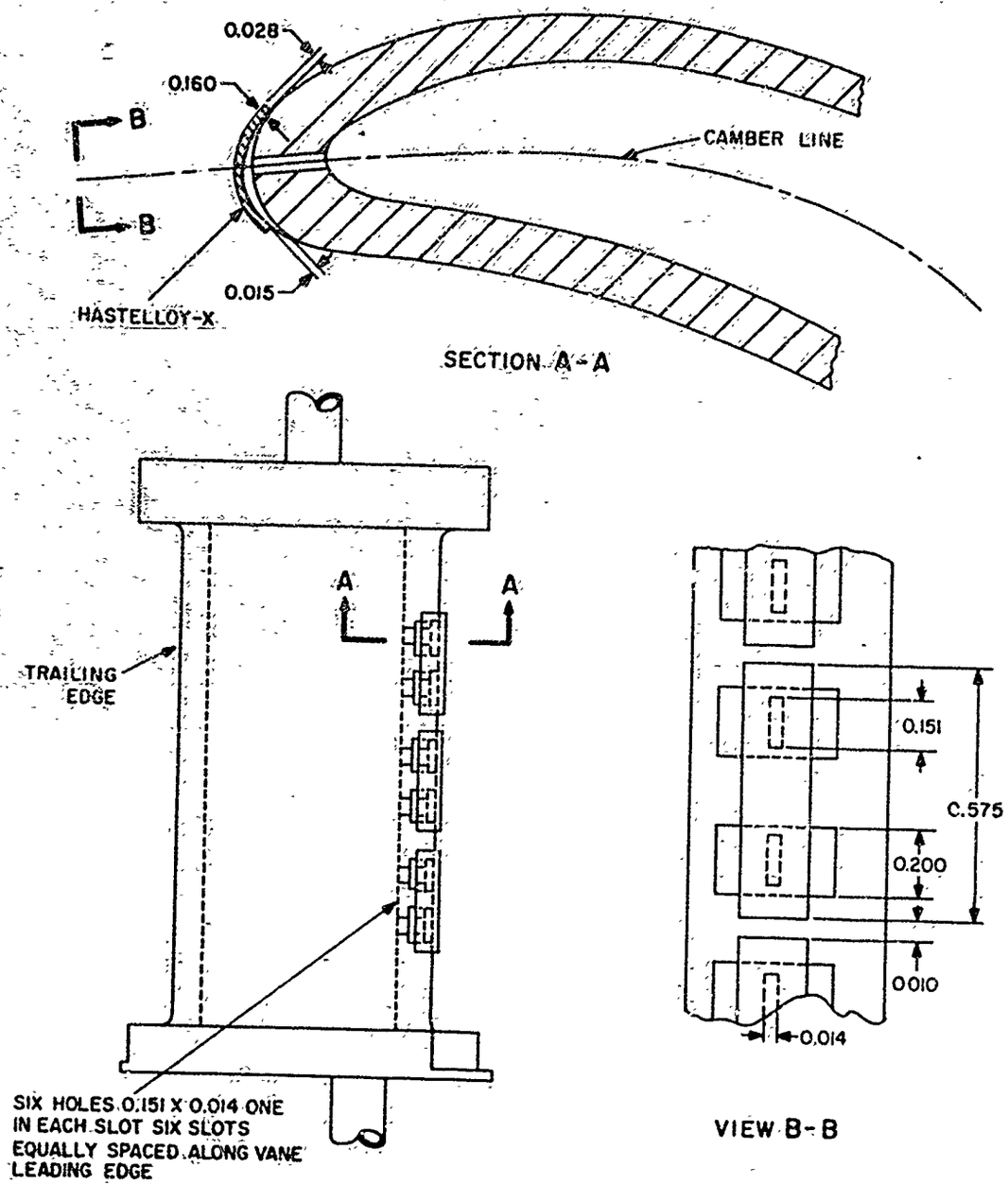
VIEW B-B

SCHEMATIC OF TURBINE VANE WITH TRANSPIRATION-COOLED LEADING EDGE AS SHOWN ON FIGURE 6-29

Figure 6-49

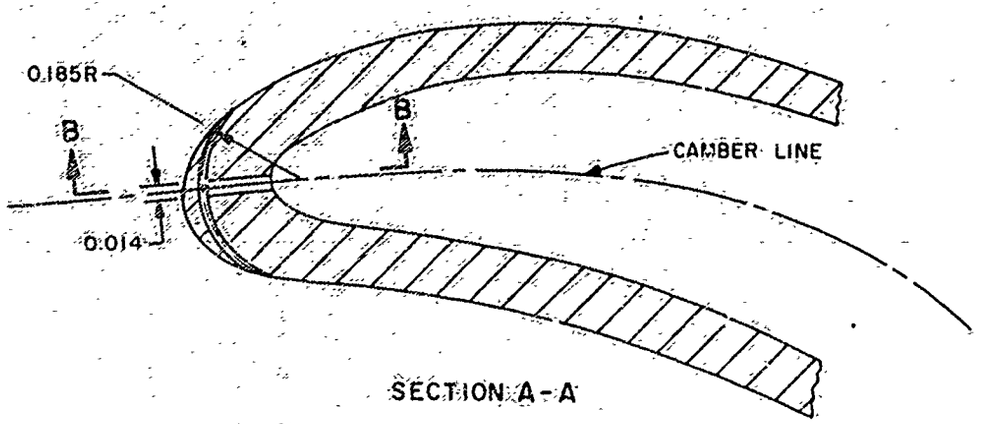
DOWNGRADED AT 3 YEAR INTERVALS
DECLASSIFIED AFTER 12 YEARS
DOD DIR 5200.10

THIS DOCUMENT CONTAINS INFORMATION AFFECTING THE NATIONAL DEFENSE OF THE UNITED STATES WITHIN THE MEANING OF THE ESPIONAGE LAWS, TITLE 18, U.S.C., SECTIONS 793 AND 794. THE TRANSMISSION OR THE REVELATION OF ITS CONTENTS IN ANY MANNER TO AN UNAUTHORIZED PERSON IS PROHIBITED BY LAW.

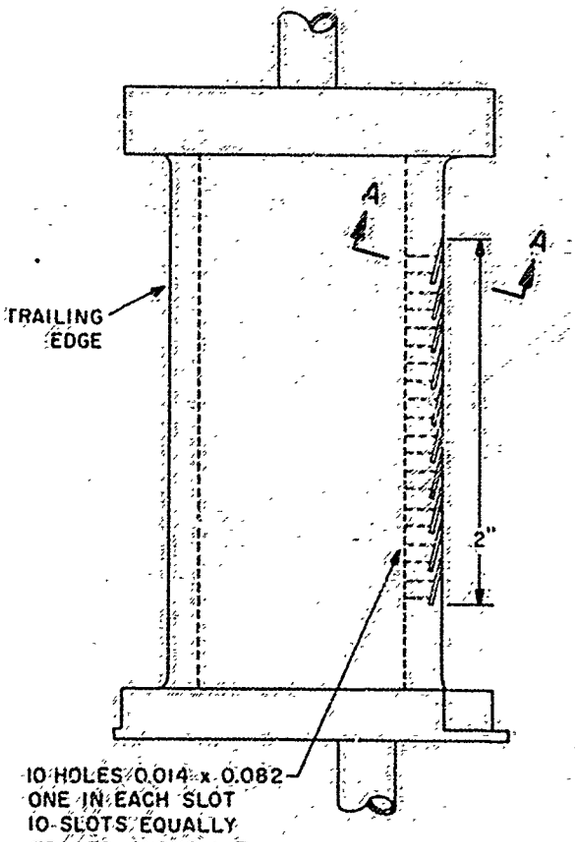


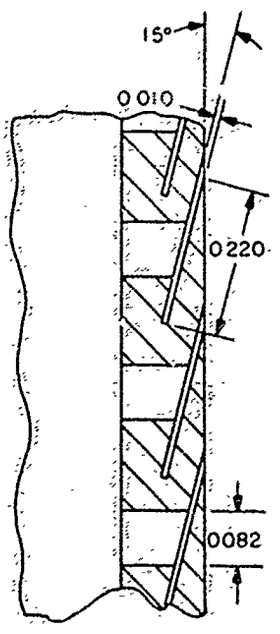
SCHEMATIC OF TURBINE VANE WITH IMPINGEMENT - AND - FILM-COOLED LEADING EDGE AS SHOWN ON FIGURE 6-30

Figure 6-50



SECTION A-A

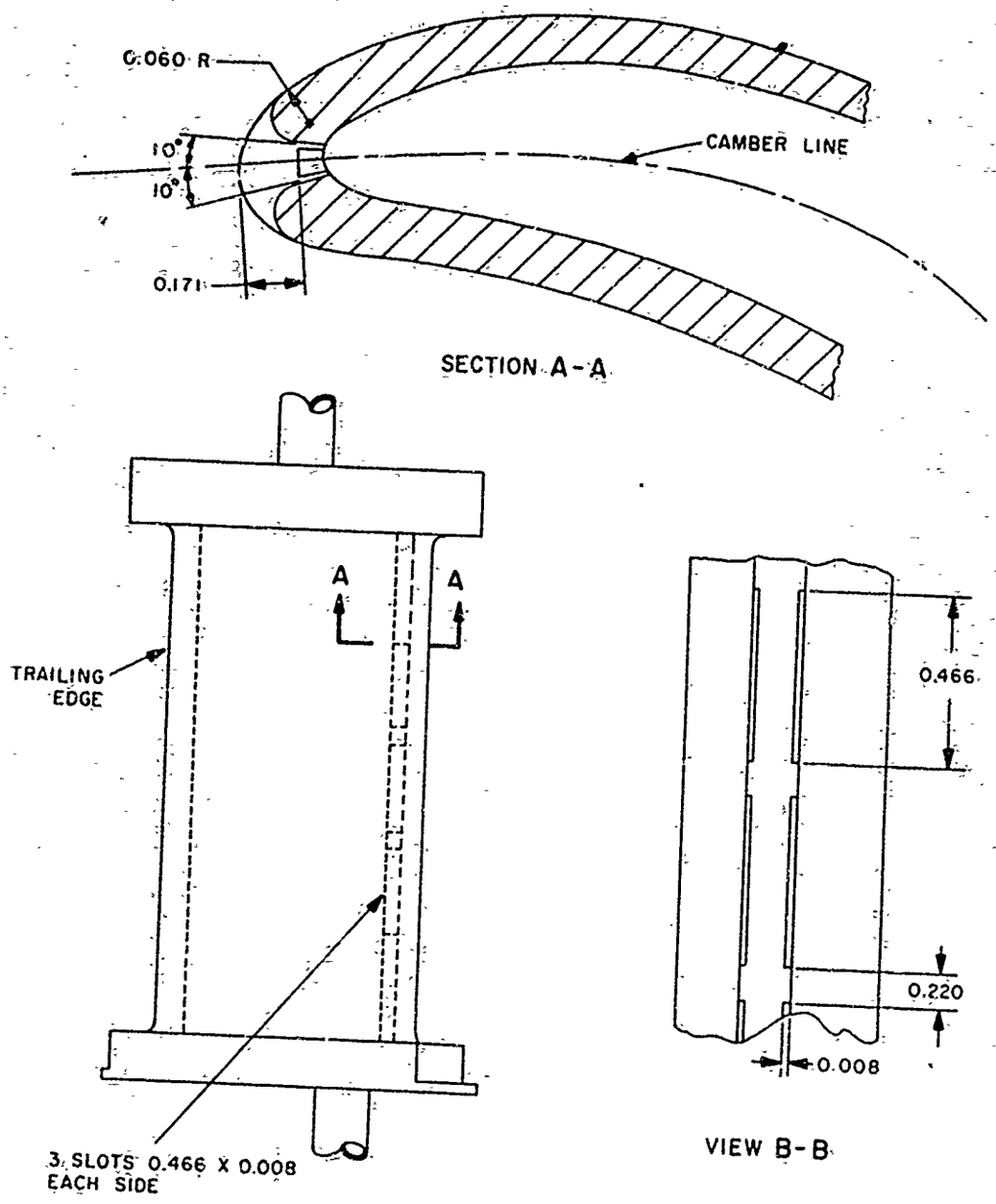




SECTION B-B

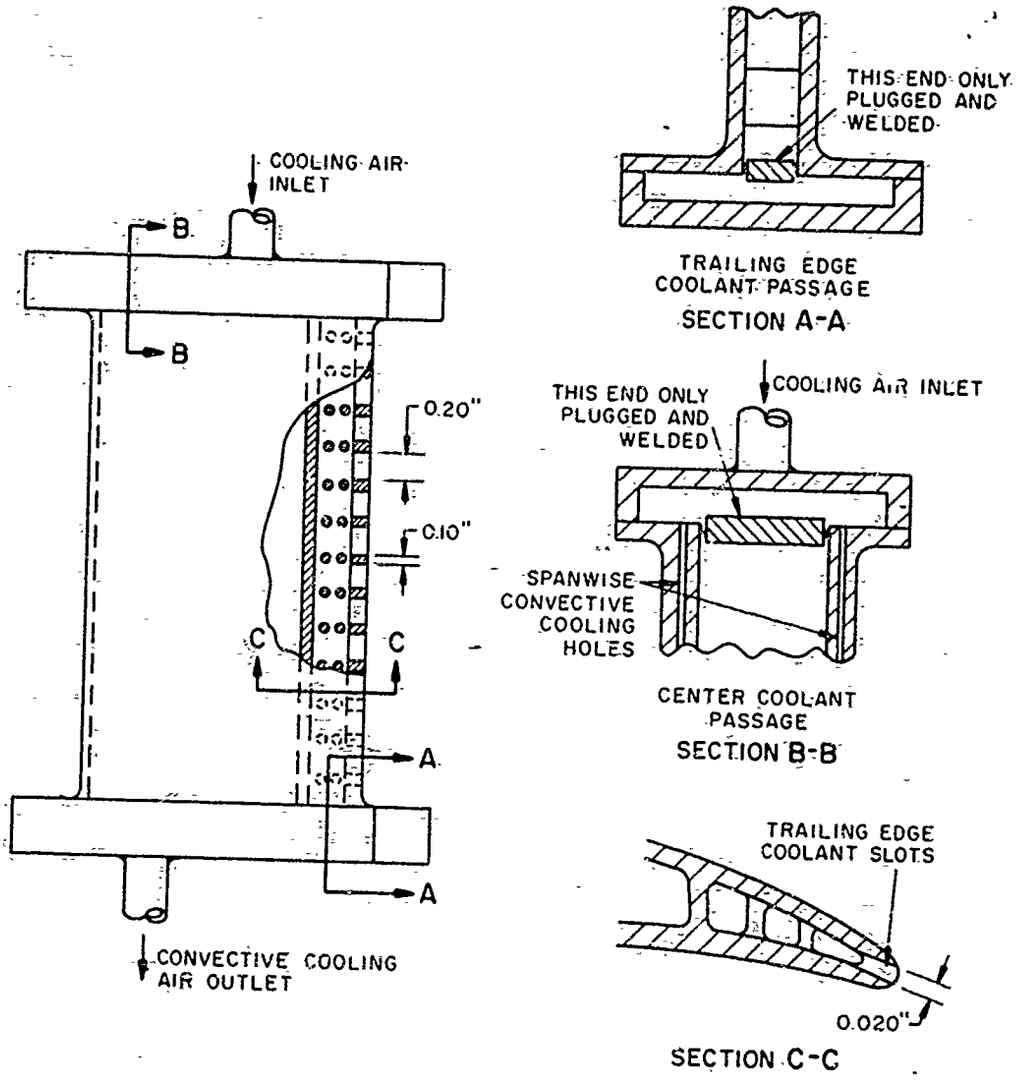
SCHEMATIC OF TURBINE VANE WITH IMPINGEMENT - AND FILM-COOLED LEADING EDGE AS SHOWN IN FIGURE 6-31

Figure 6-51



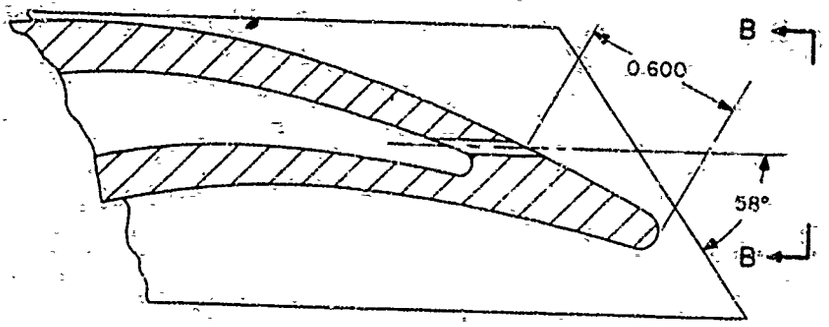
SCHEMATIC OF TURBINE VANE WITH FILM-COOLED LEADING EDGE AS SHOWN ON FIGURE 6-32

Figure 6-52

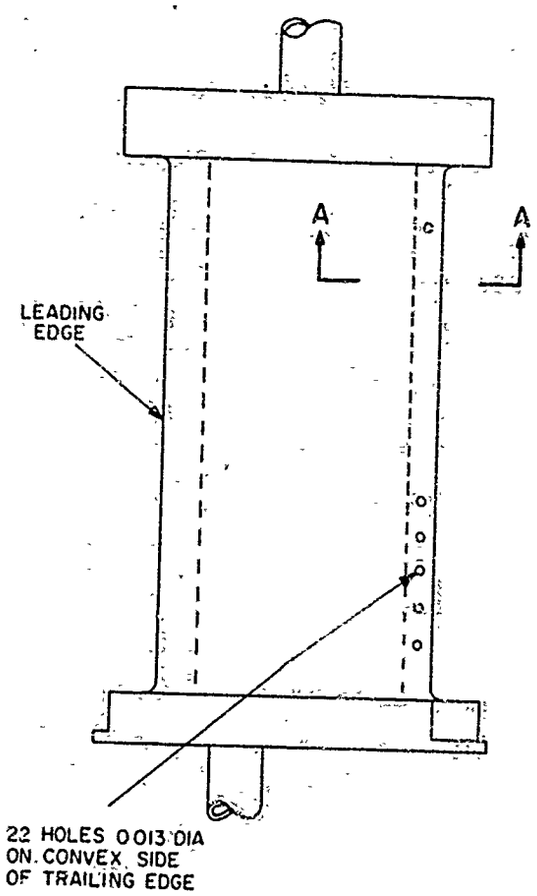


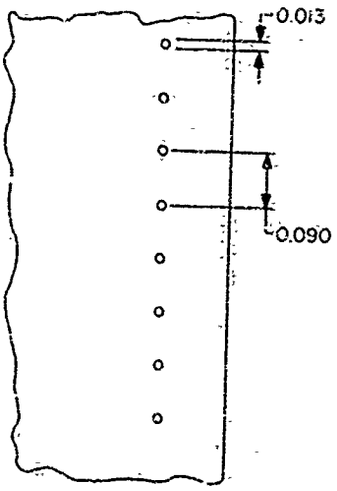
SCHEMATIC OF TURBINE VANE WITH SLOTTED TRAILING EDGE

Figure 6-53



SECTION A-A

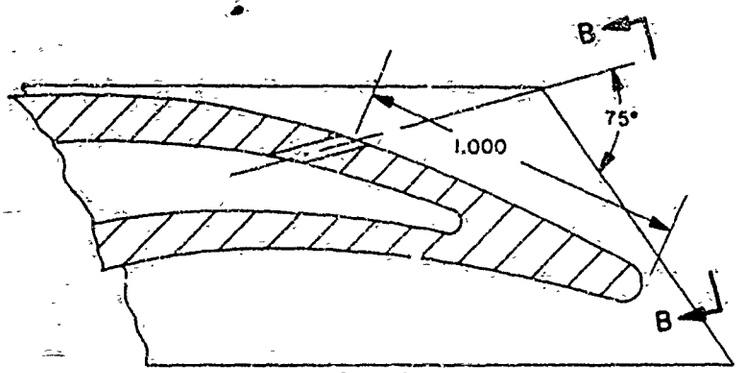




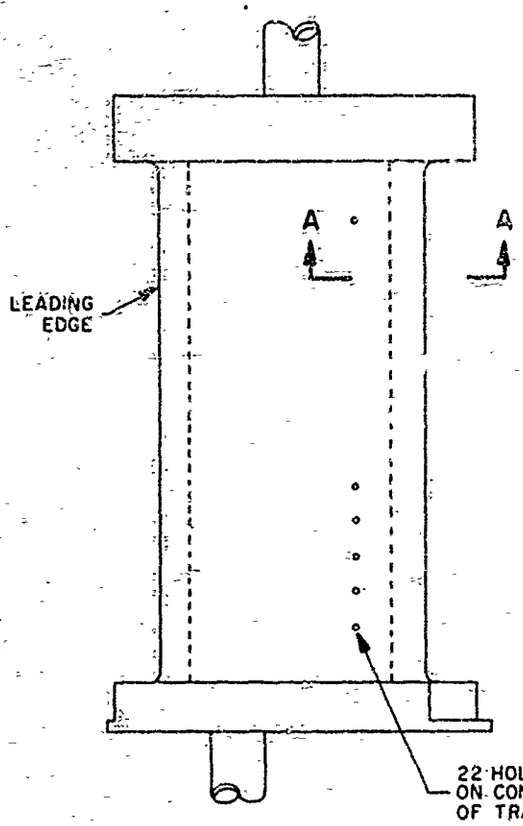
VIEW B-B

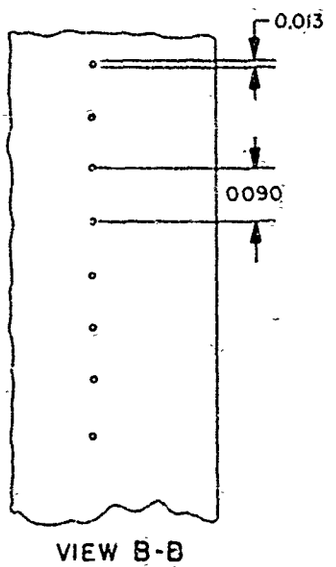
SCHEMATIC OF TURBINE VANE WITH FILM-COOLED TRAILING EDGE AS SHOWN ON FIGURE 6-33

Figure 6-54



SECTION A-A

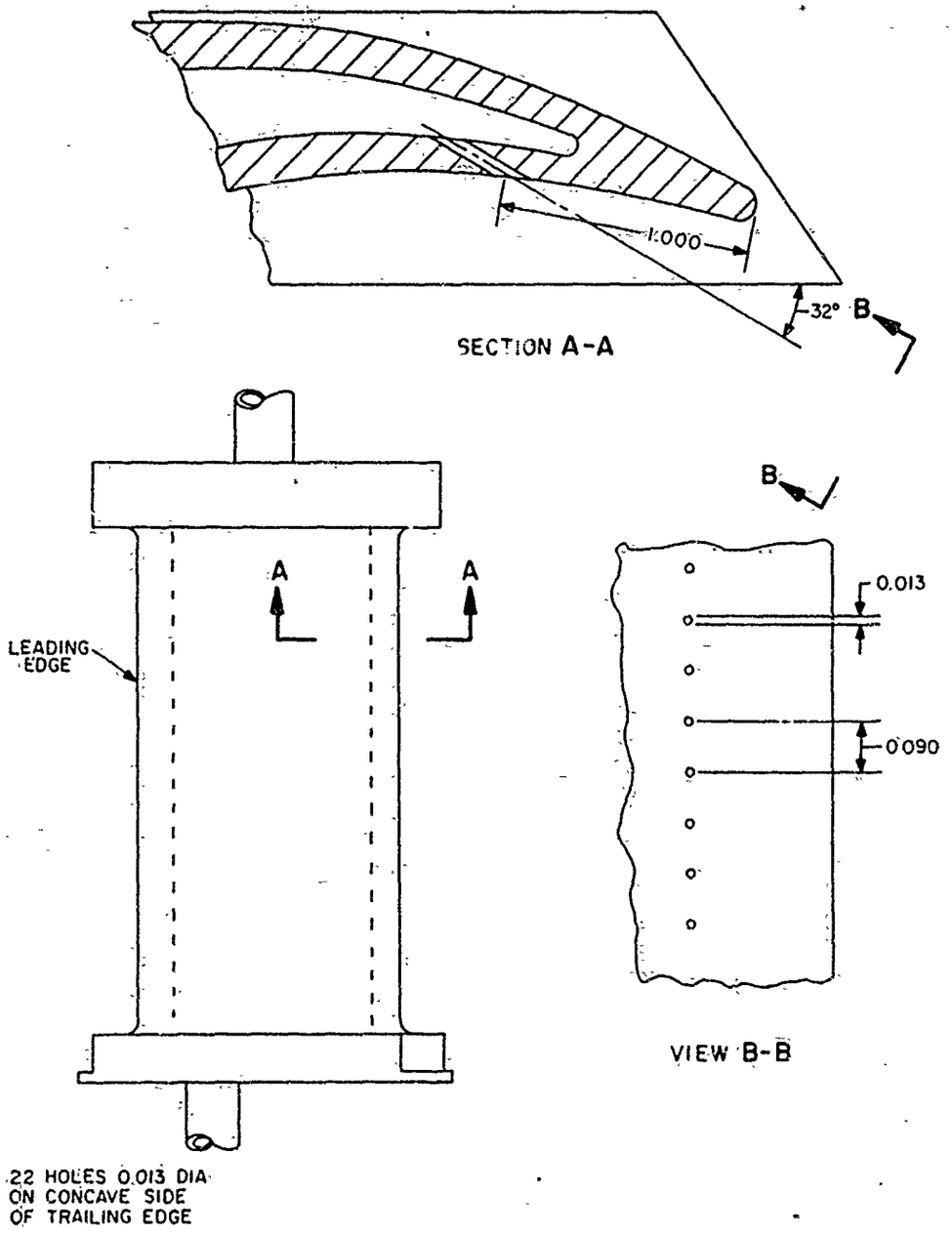




VIEW B-B

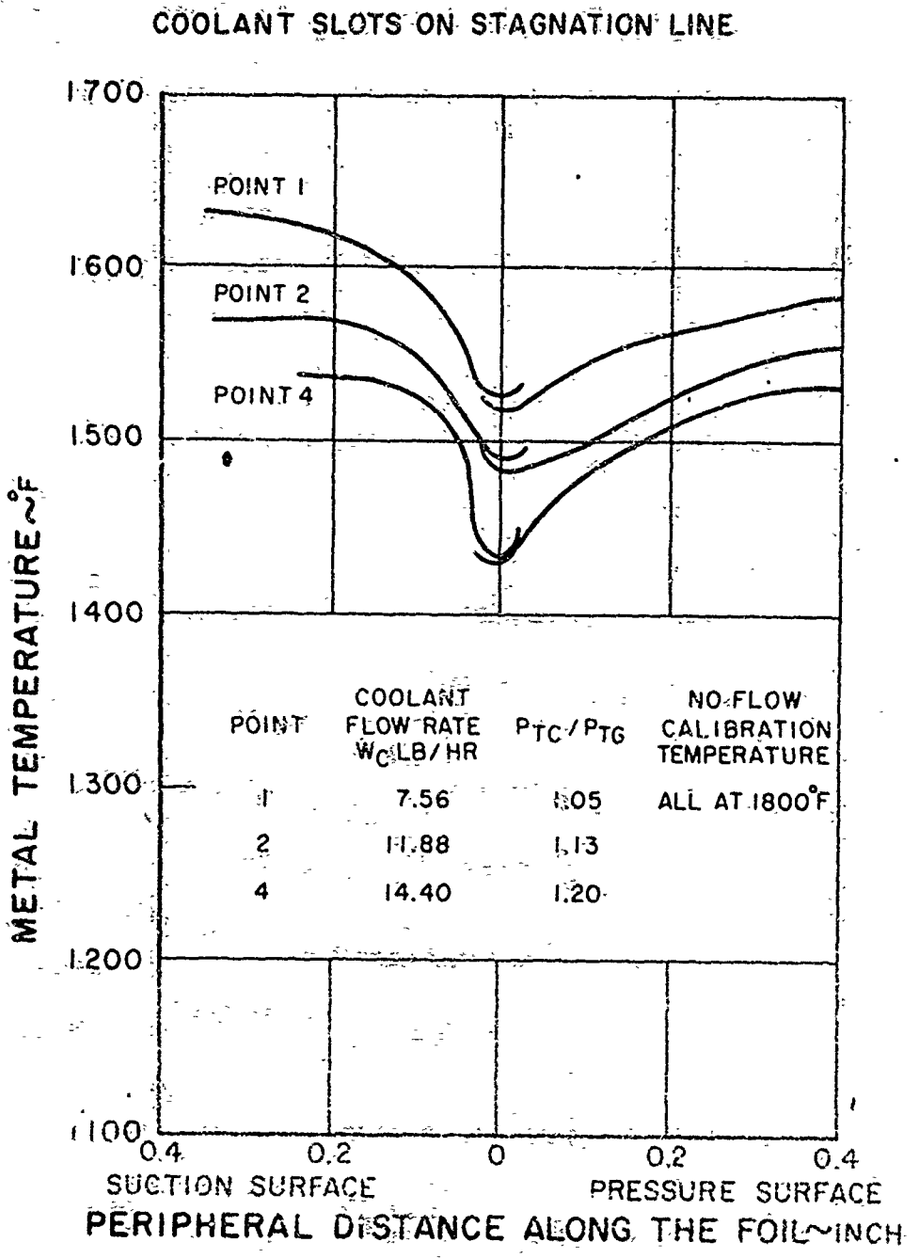
SCHEMATIC OF TURBINE VANE WITH FILM-COOLED TRAILING EDGE AS SHOWN ON FIGURE 6-31

Figure 6-55



SCHEMATIC OF TURBINE VANE WITH FILM-COOLING TRAILING EDGE AS SHOWN ON FIGURE 6-35

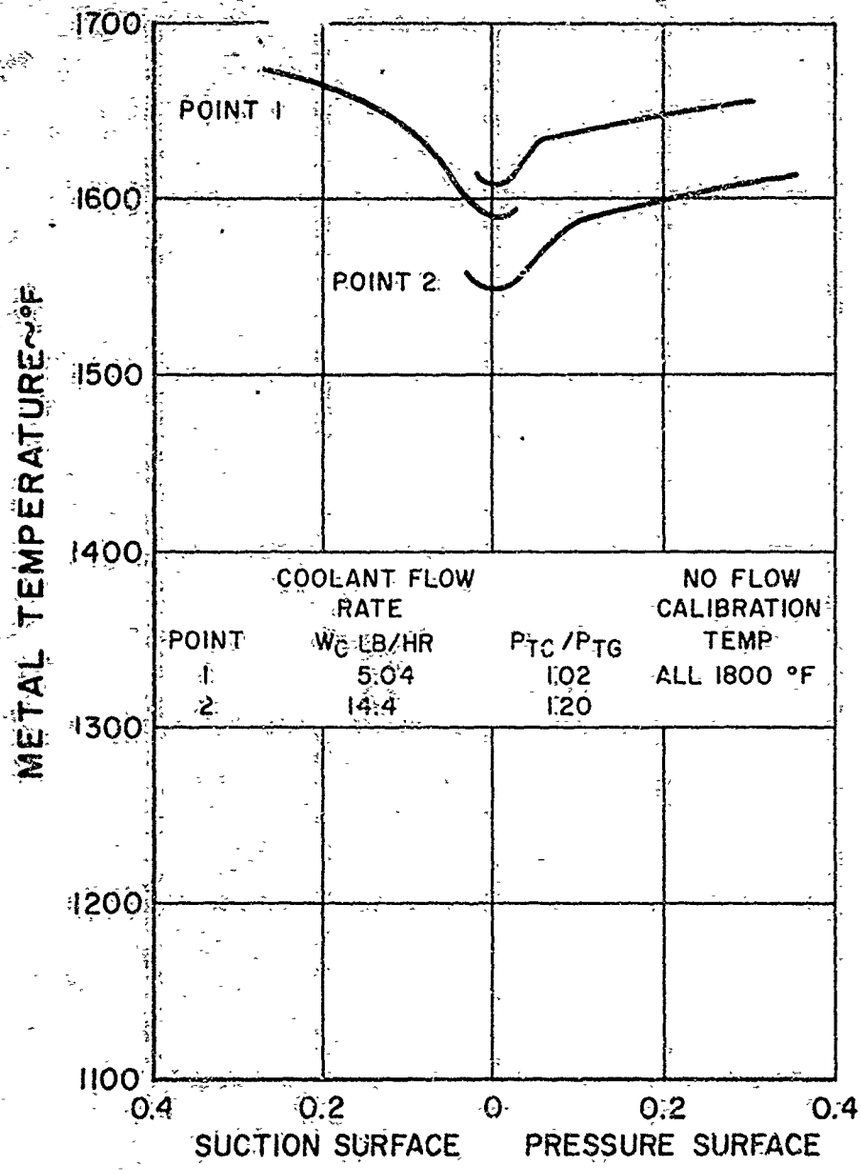
Figure 6-56



METAL TEMPERATURE VS. PERIPHERAL DISTANCE ALONG THE FOIL

Figure 6-57

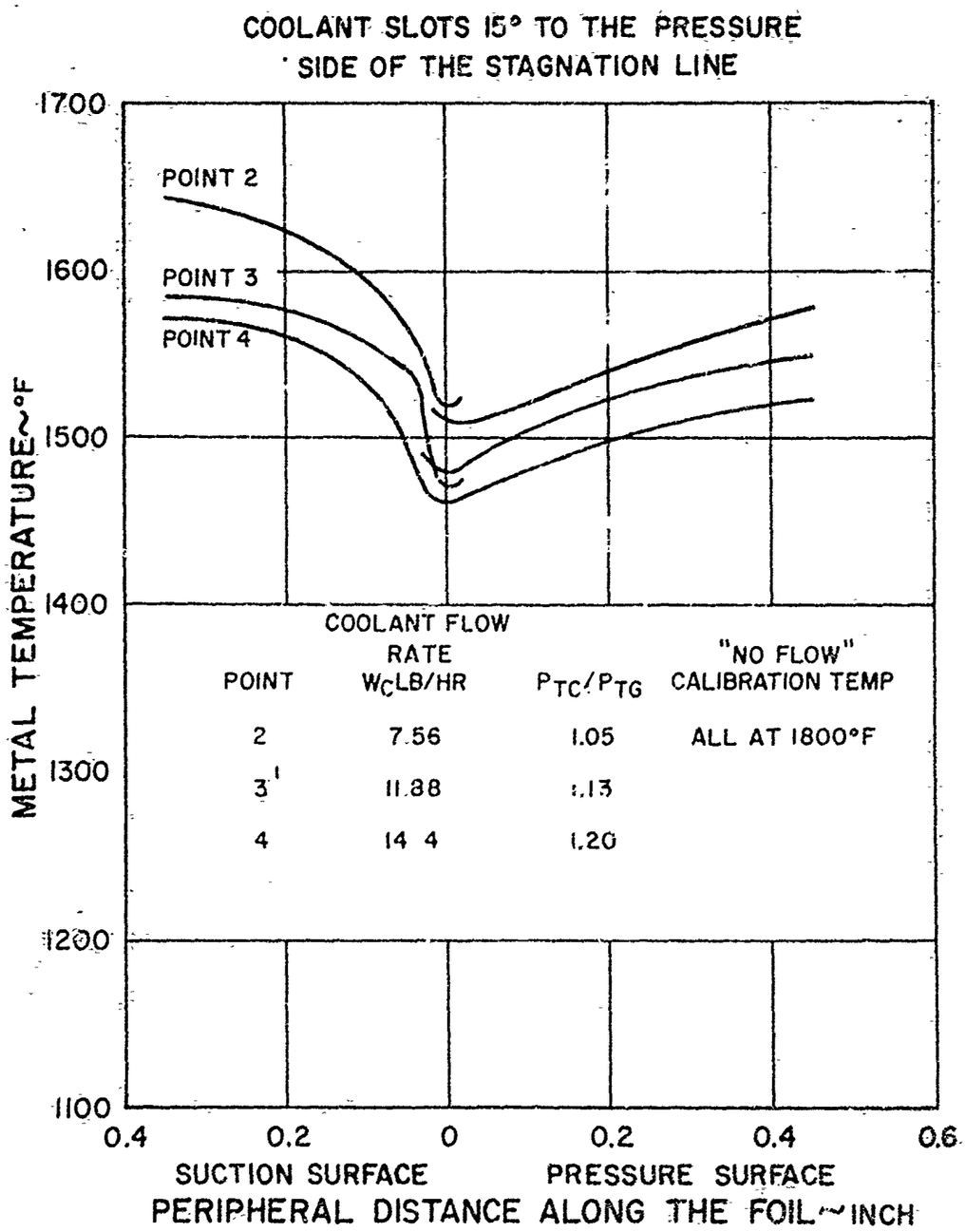
COOLANT SLOTS 15° TO THE SUCTION SIDE OF THE STAGNATION LINE



METAL TEMPERATURE VS. PERIPHERAL DISTANCE ALONG THE FOIL

Figure 6-58

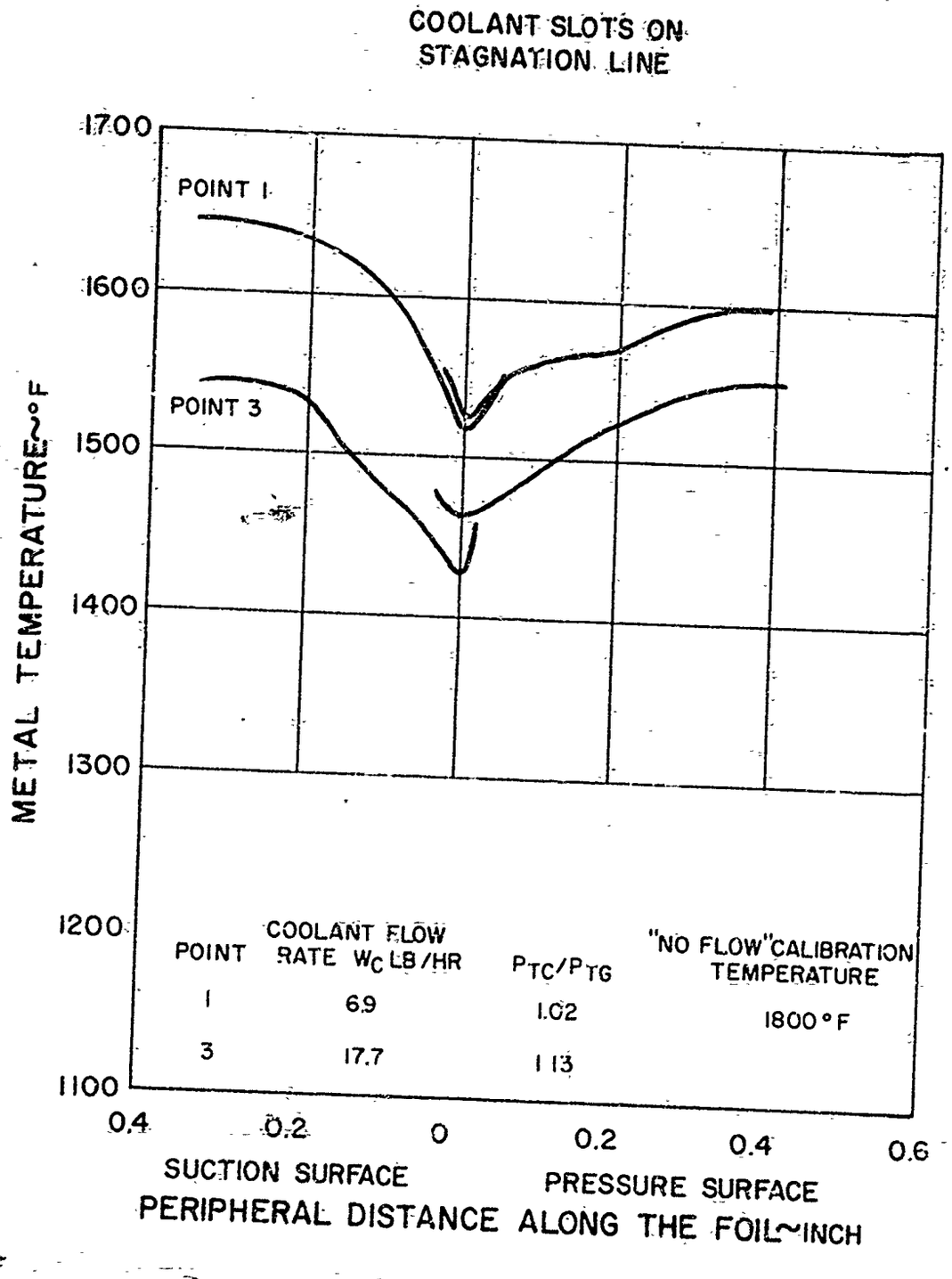
DOWNGRADED AT 3 YEAR INTERVALS
NOT AUTOMATICALLY DECLASSIFIED AFTER 12 YEARS
DOD DIR 5200.10



METAL TEMPERATURE VS. PERIPHERAL DISTANCE ALONG THE FOIL

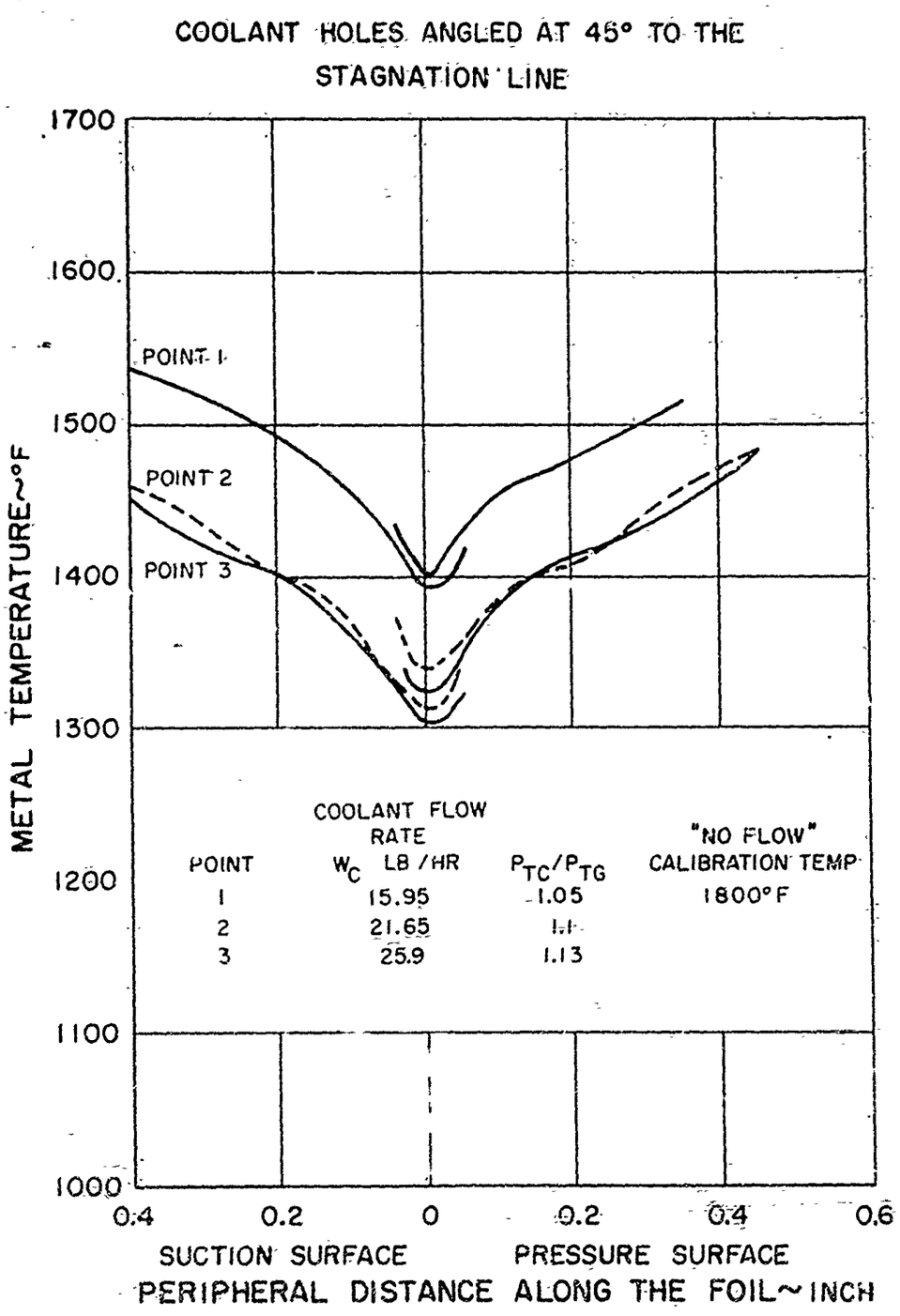
Figure 6-59

TECHNICAL DATA CONTAINED HEREIN
DECLASSIFIED AFTER 3 YEARS
DOD DIR 5200.1
THIS DOCUMENT CONTAINS INFORMATION AFFECTING THE NATIONAL DEFENSE OF THE UNITED STATES WITHIN THE MEANING OF THE ESPIONAGE LAWS, TITLE 18, U.S.C., SECTIONS 793 AND 794. THE TRANSMISSION OR THE REVELATION OF ITS CONTENTS IN ANY MANNER TO AN UNAUTHORIZED PERSON IS PROHIBITED BY LAW.



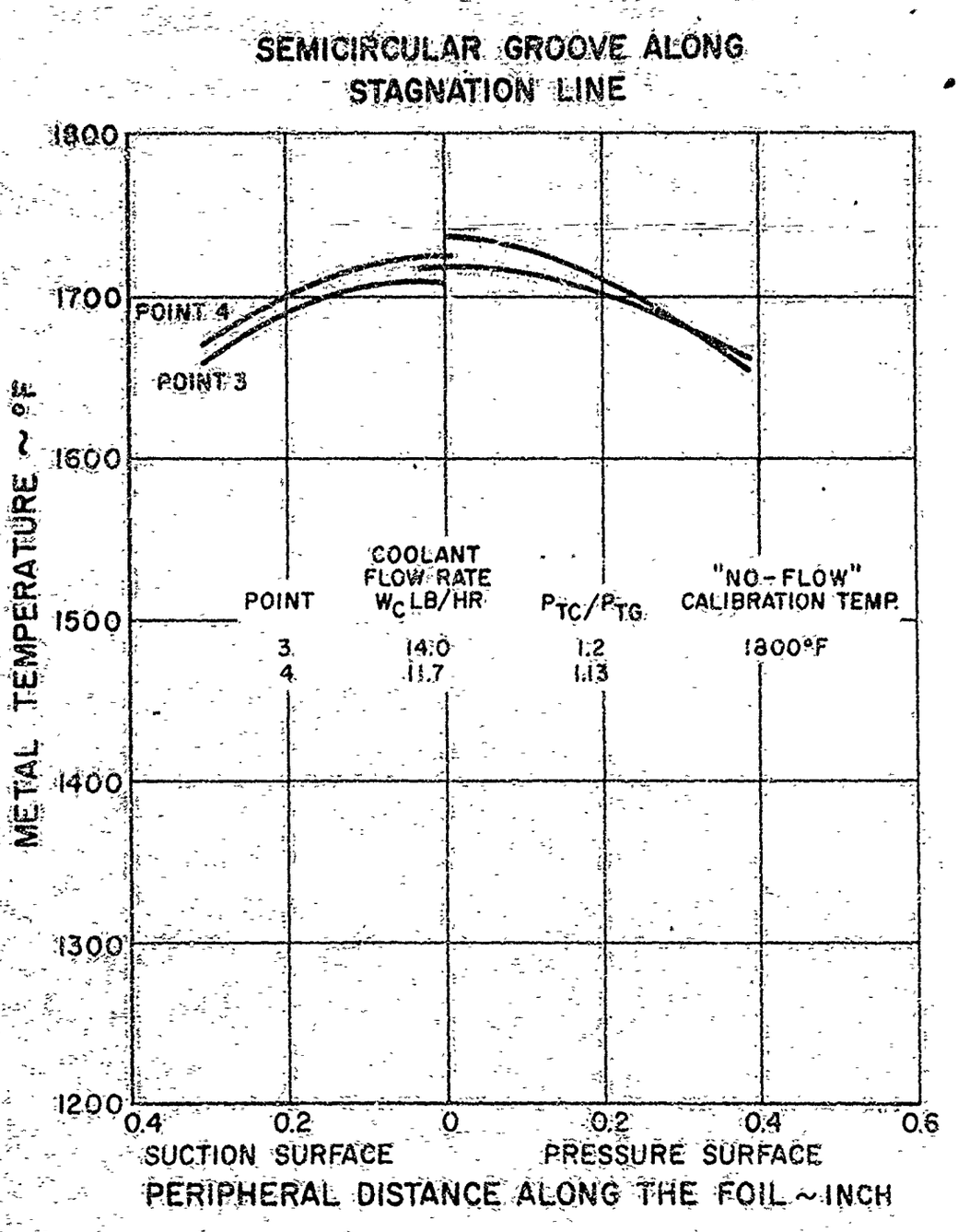
METAL TEMPERATURE VS. PERIPHERAL DISTANCE ALONG THE FOIL

Figure 6-60



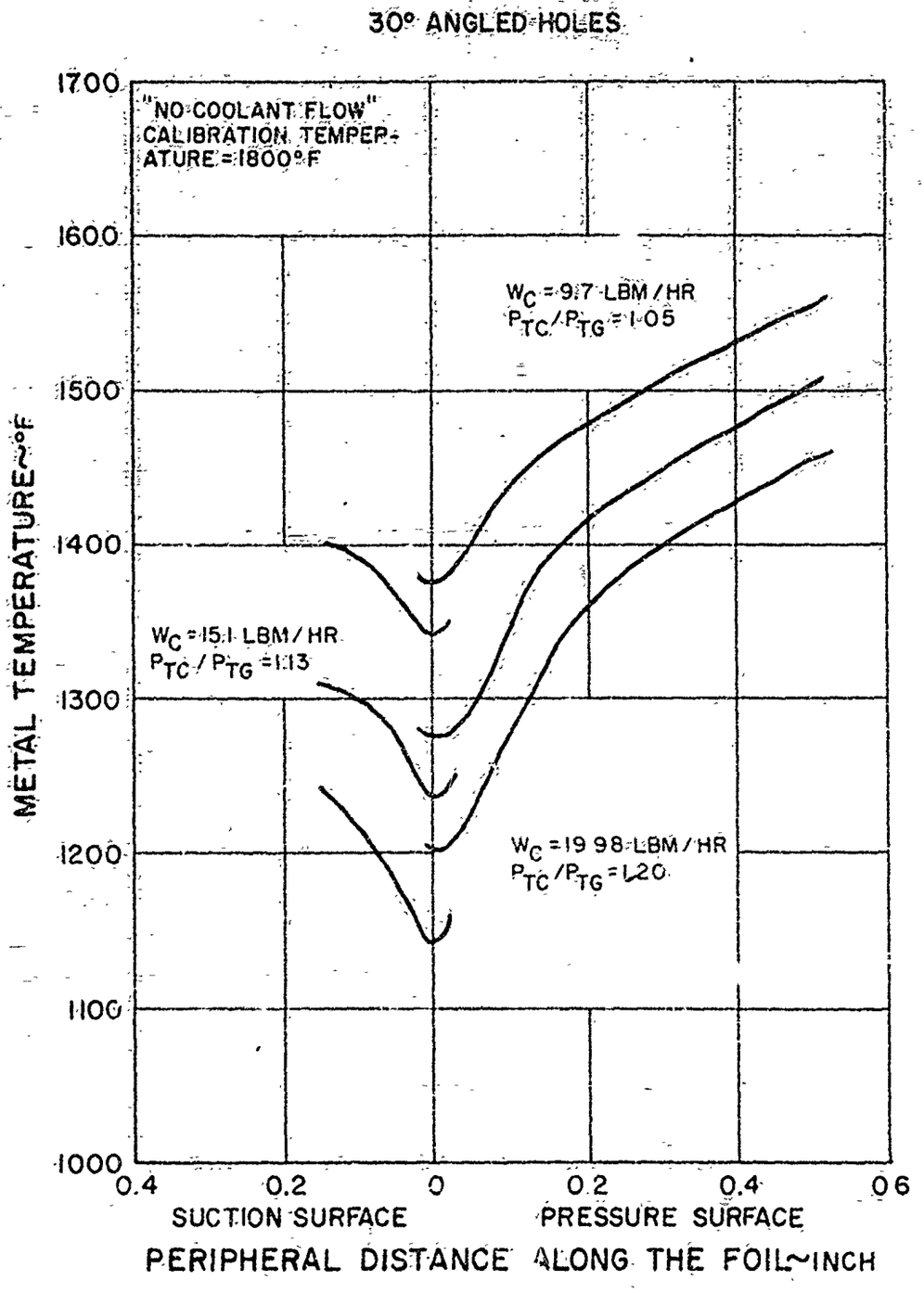
METAL TEMPERATURE VS. PERIPHERAL DISTANCE ALONG THE FOIL

Figure o-61



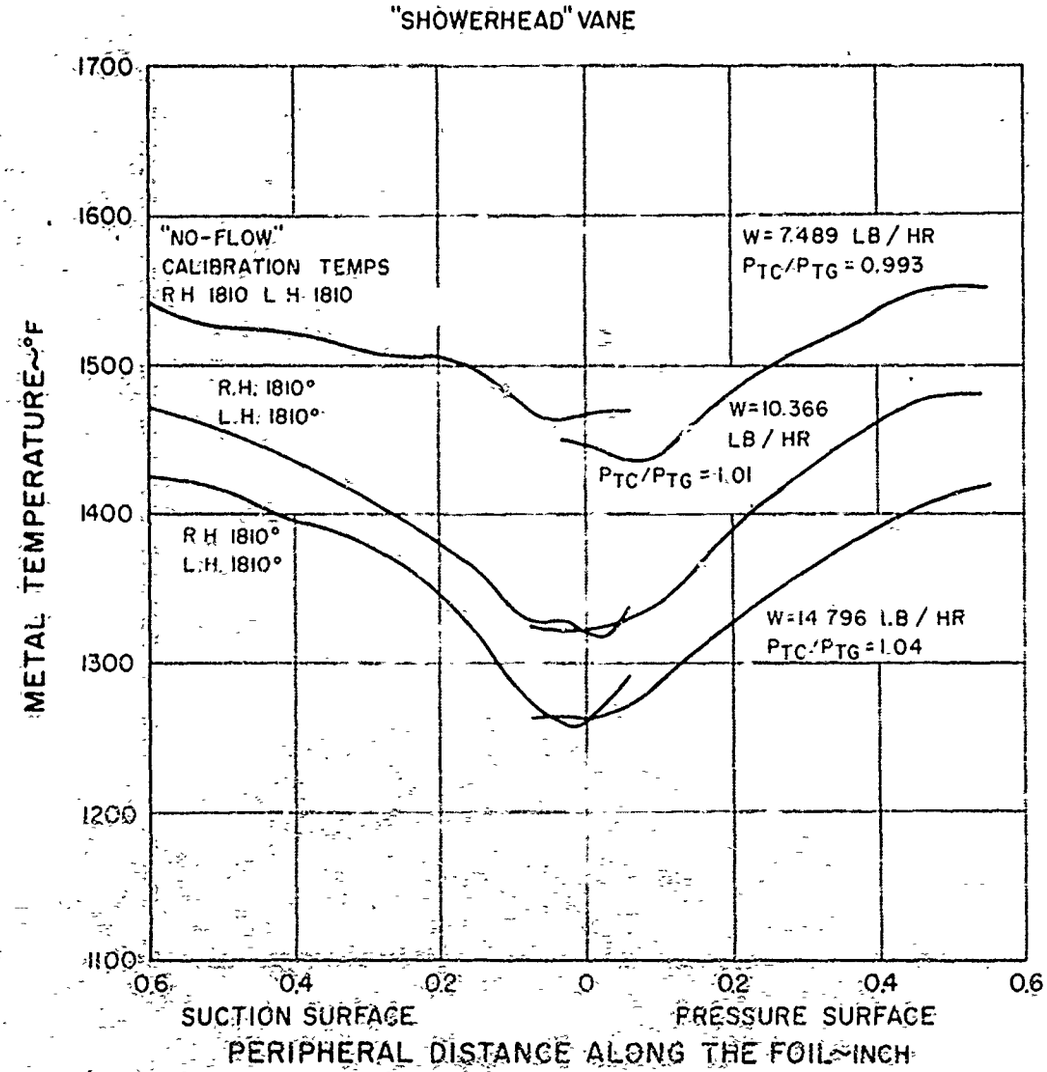
METAL TEMPERATURE VS. PERIPHERAL DISTANCE ALONG THE FOIL

Figure 6-62



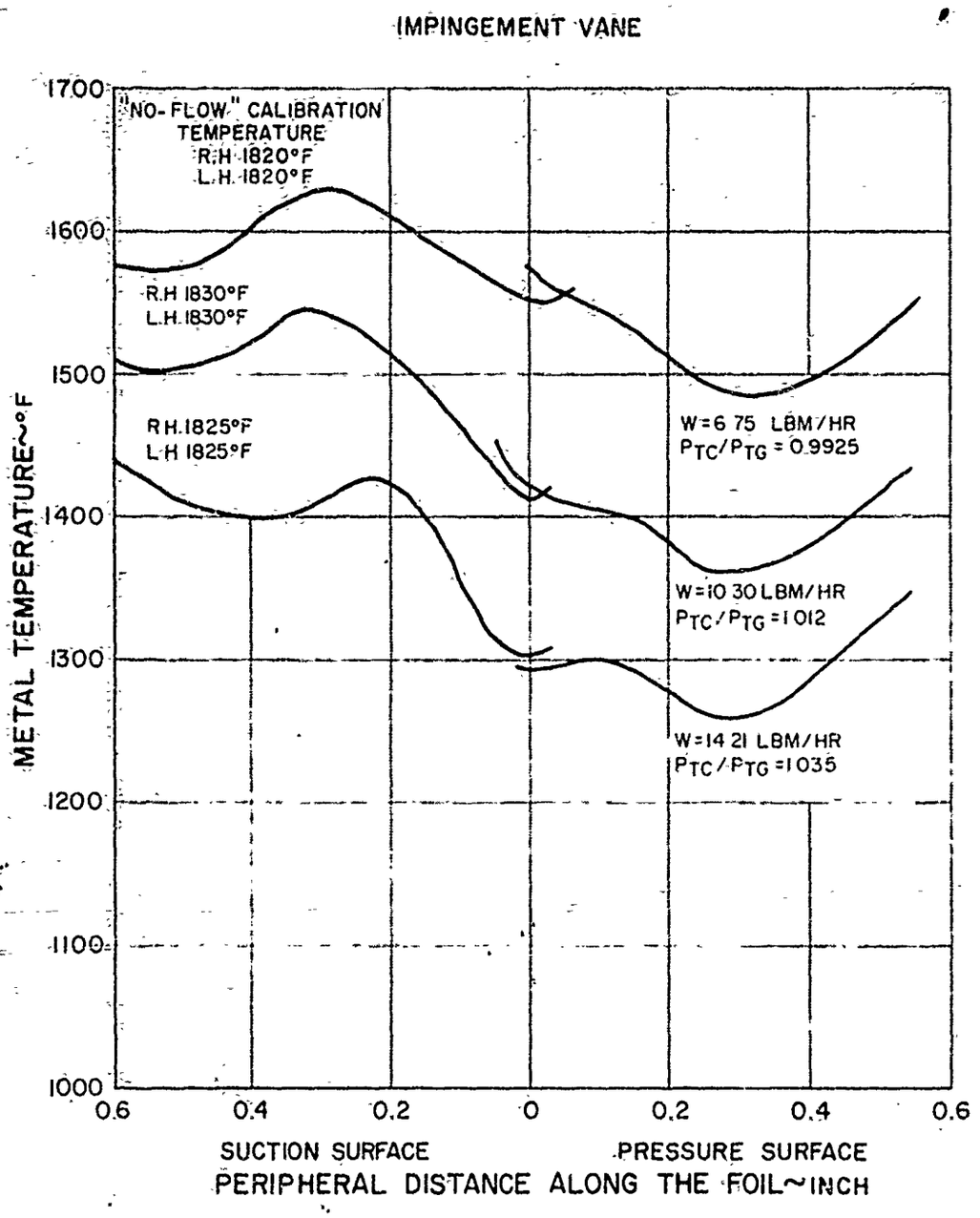
METAL TEMPERATURE VS. PERIPHERAL DISTANCE ALONG THE FOIL

Figure 6-63



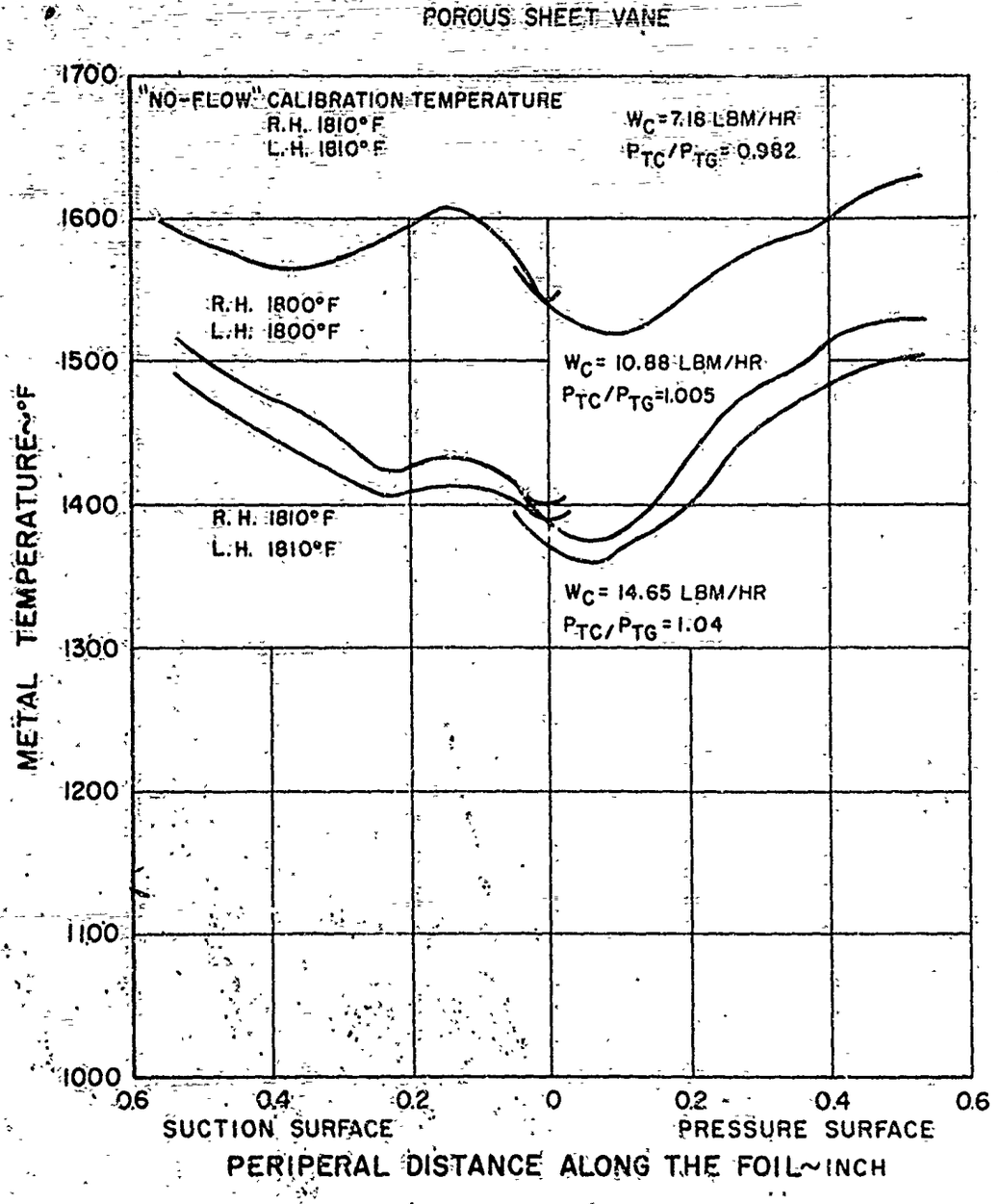
METAL TEMPERATURE VS. PERIPHERAL DISTANCE ALONG THE FOIL

Figure 6-61



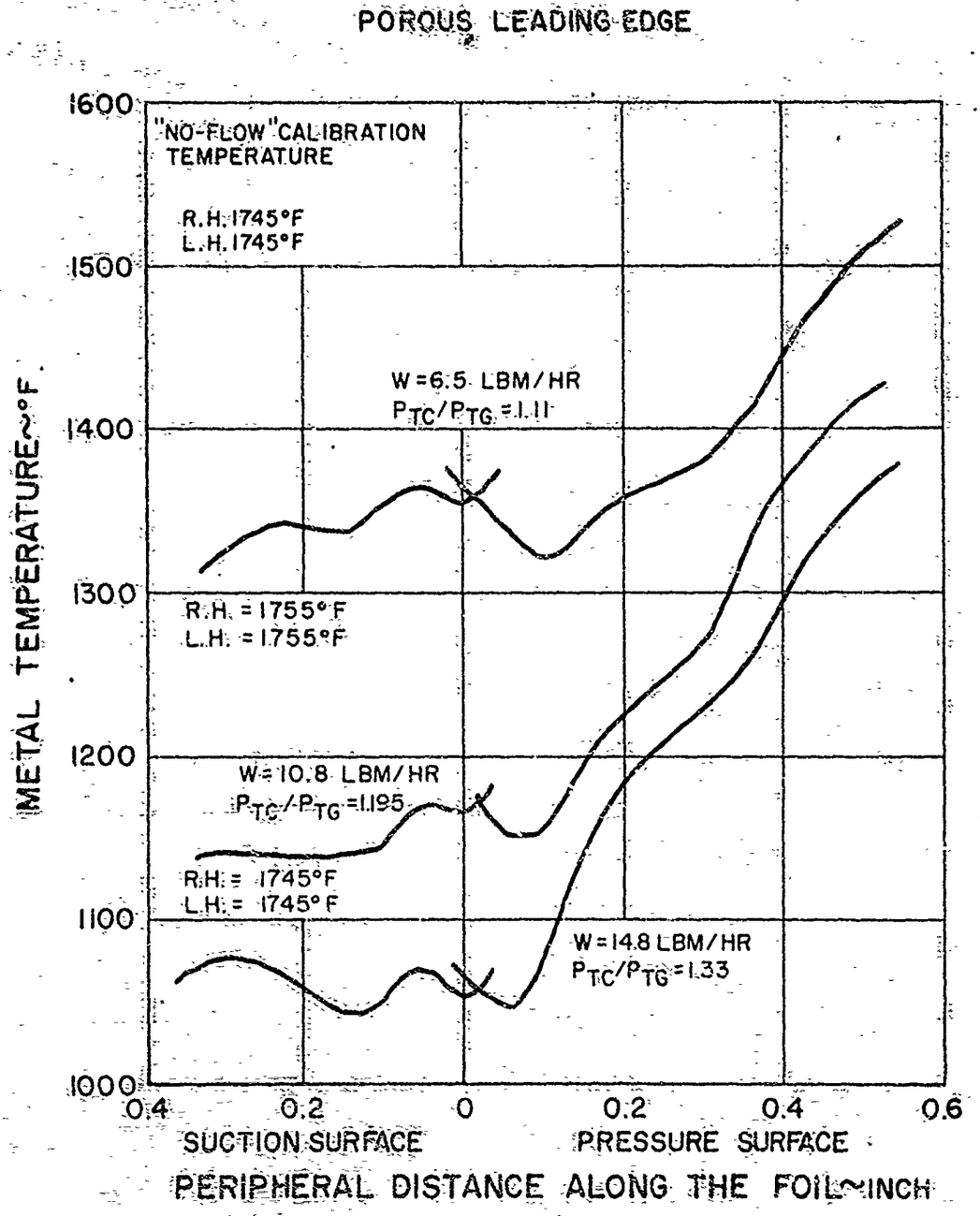
METAL TEMPERATURE VS. PERIPHERAL DISTANCE ALONG THE FOIL

Figure 6-65



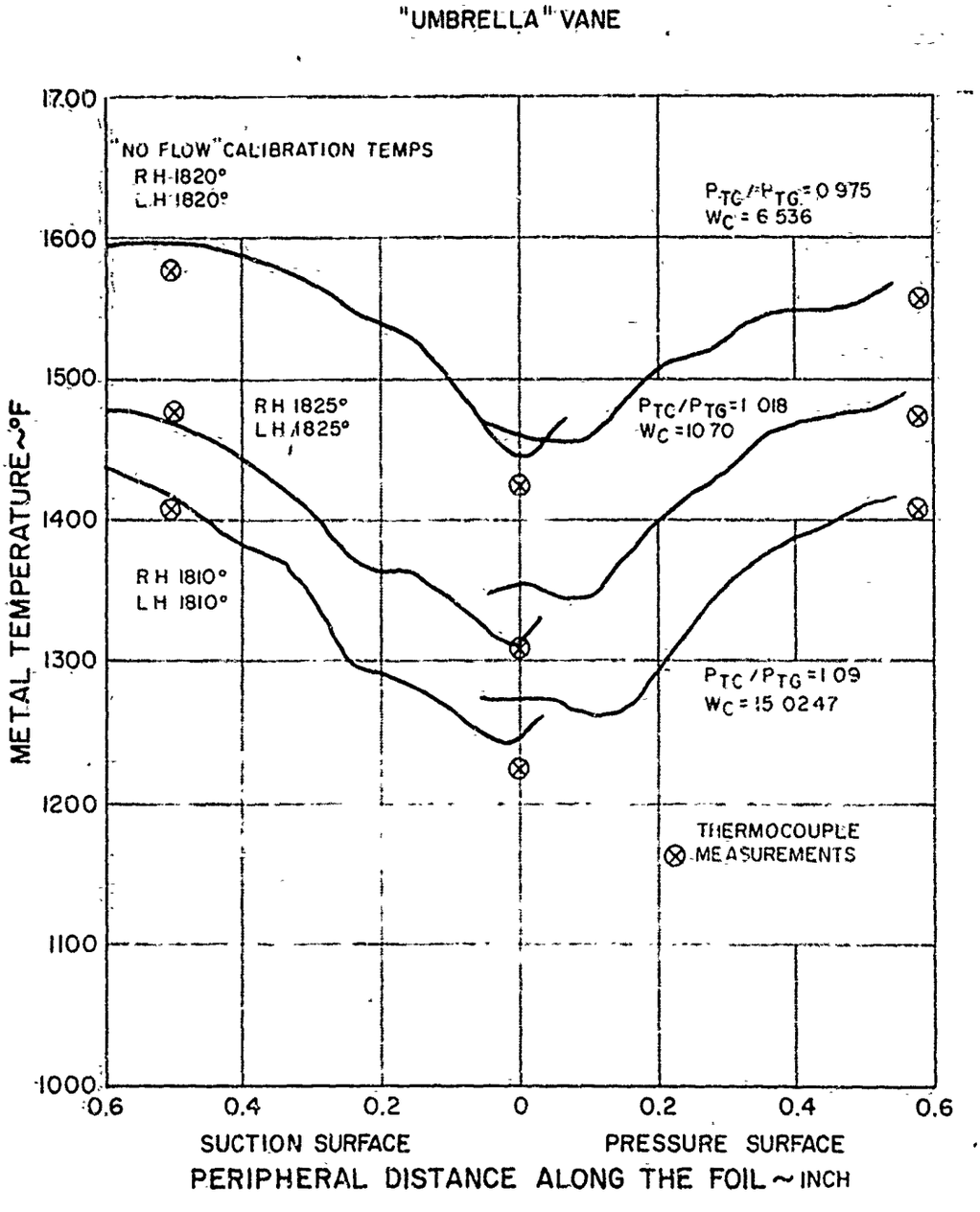
METAL TEMPERATURE VS. PERIPHERAL DISTANCE ALONG THE FOIL

Figure 6-66



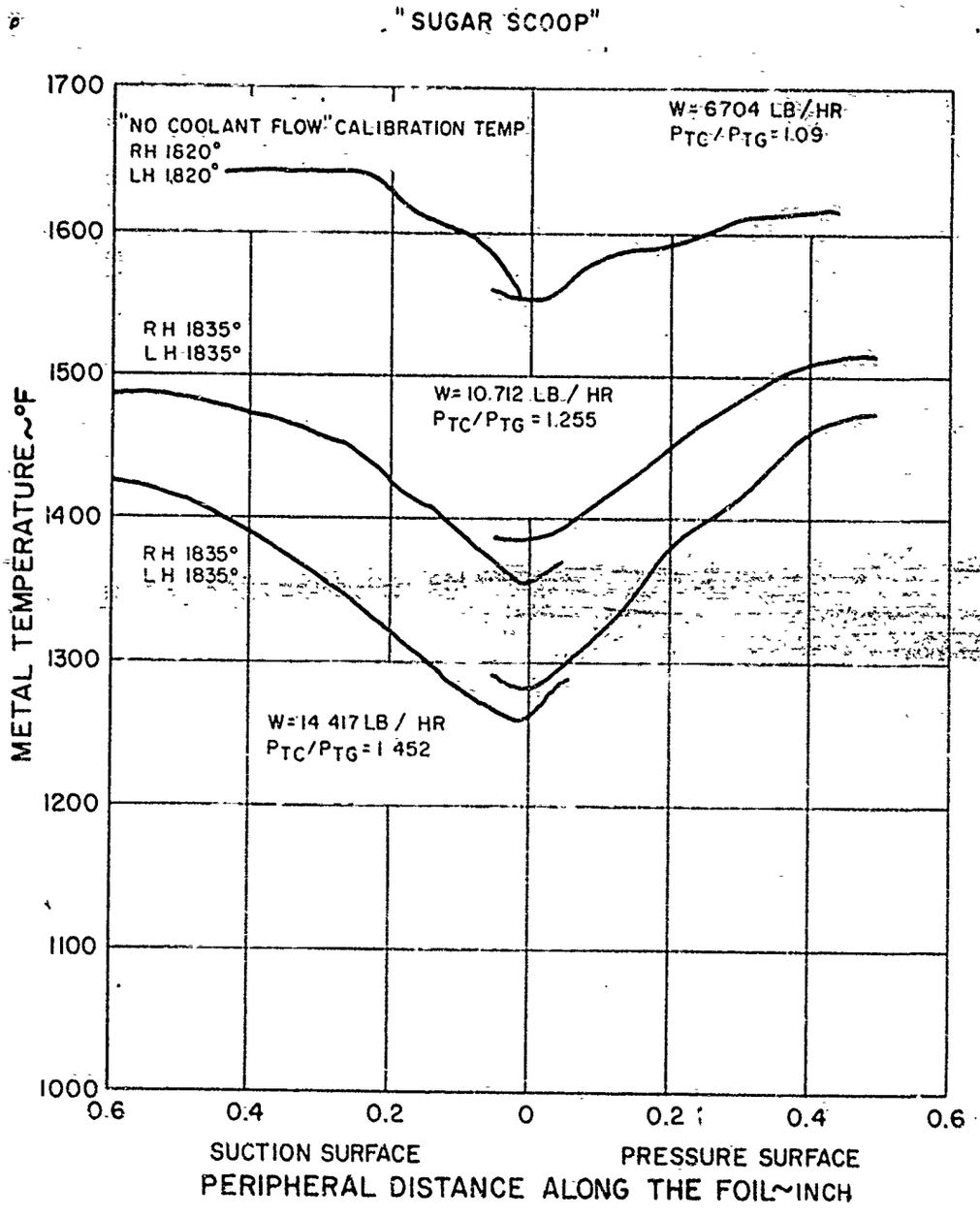
METAL TEMPERATURE VS. PERIPHERAL DISTANCE ALONG THE FOIL

Figure 6-67



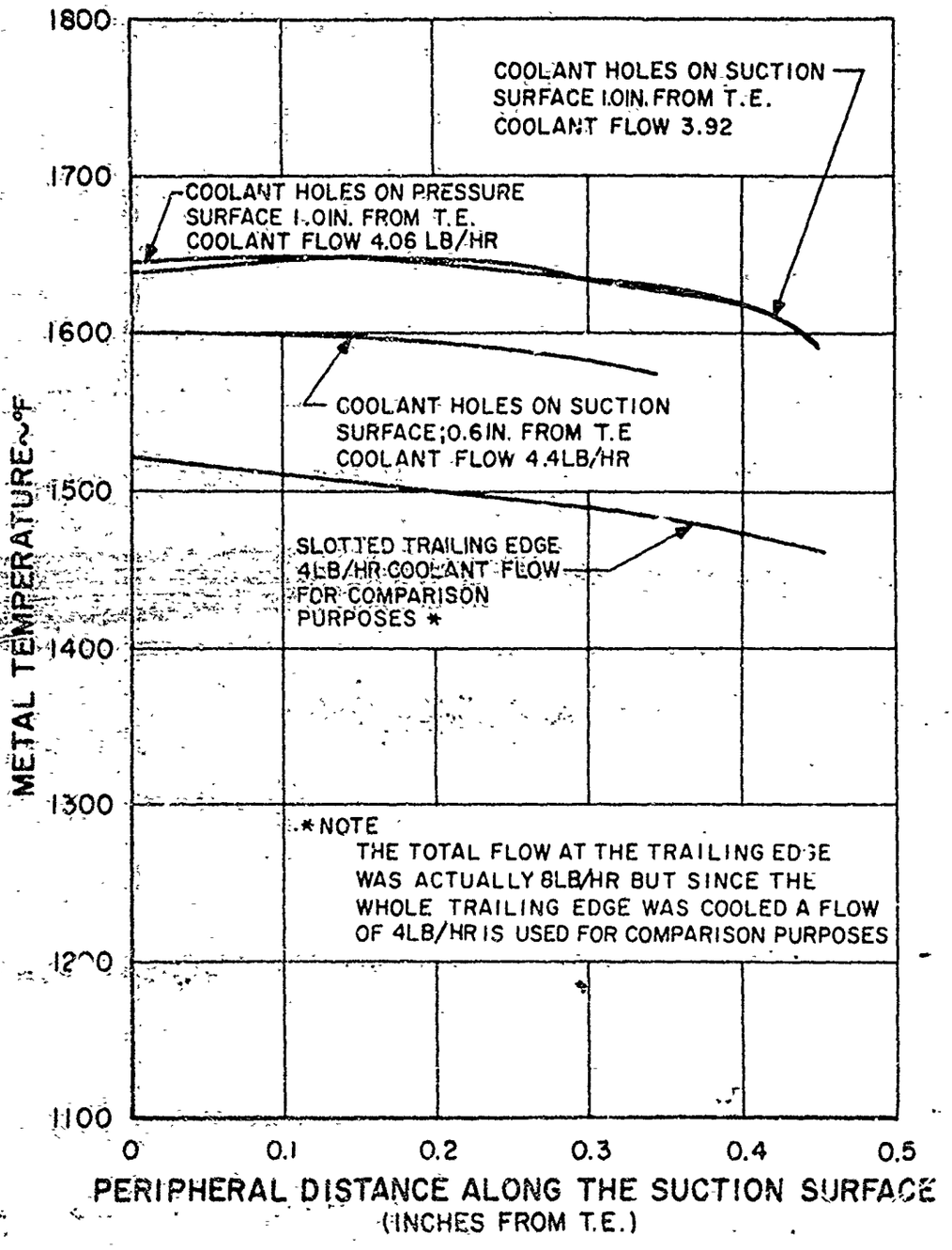
METAL TEMPERATURE VS. PERIPHERAL DISTANCE ALONG THE FOIL

Figure 6-68



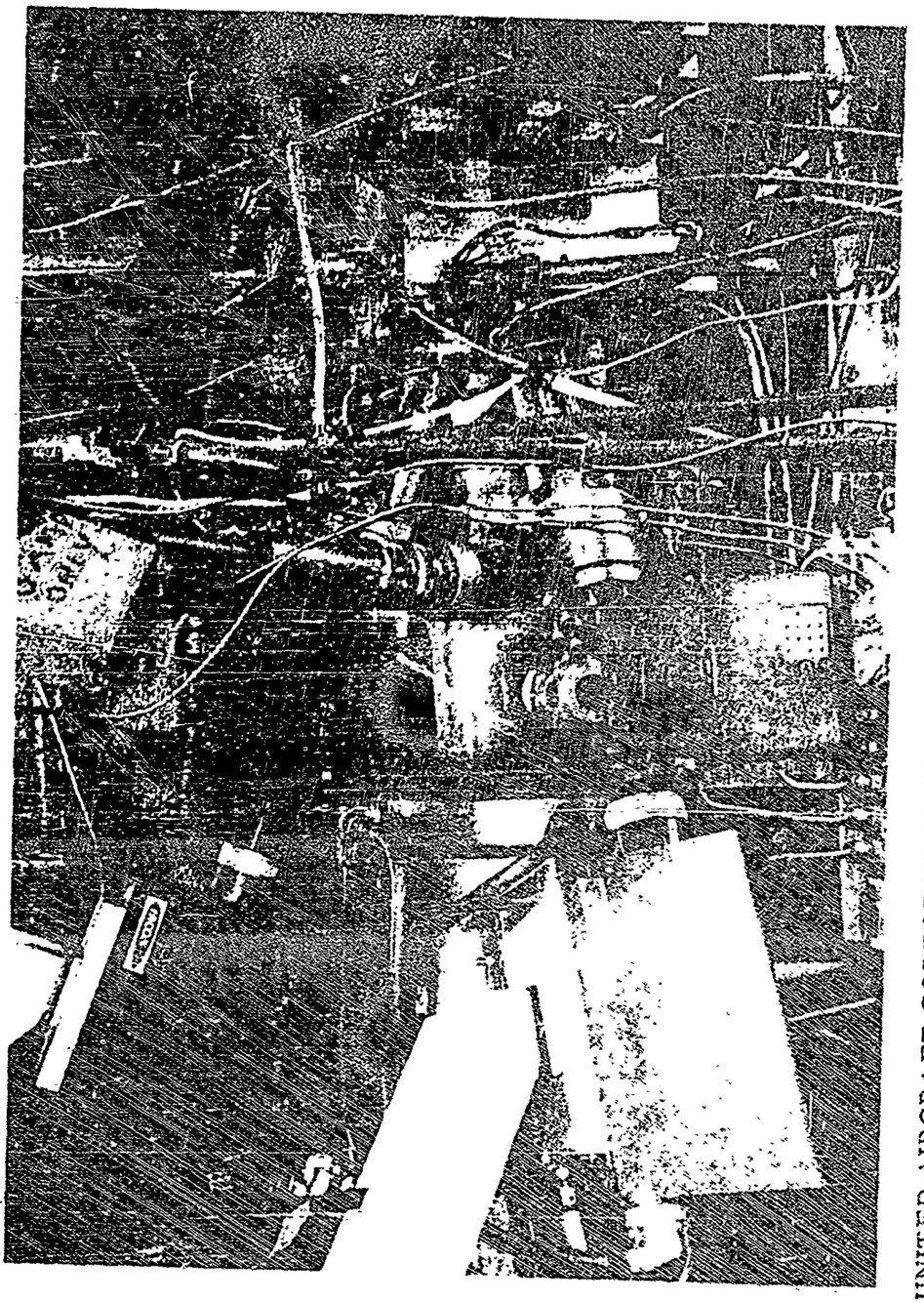
METAL TEMPERATURE VS. PERIPHERAL DISTANCE ALONG THE FOIL

Figure 6-69



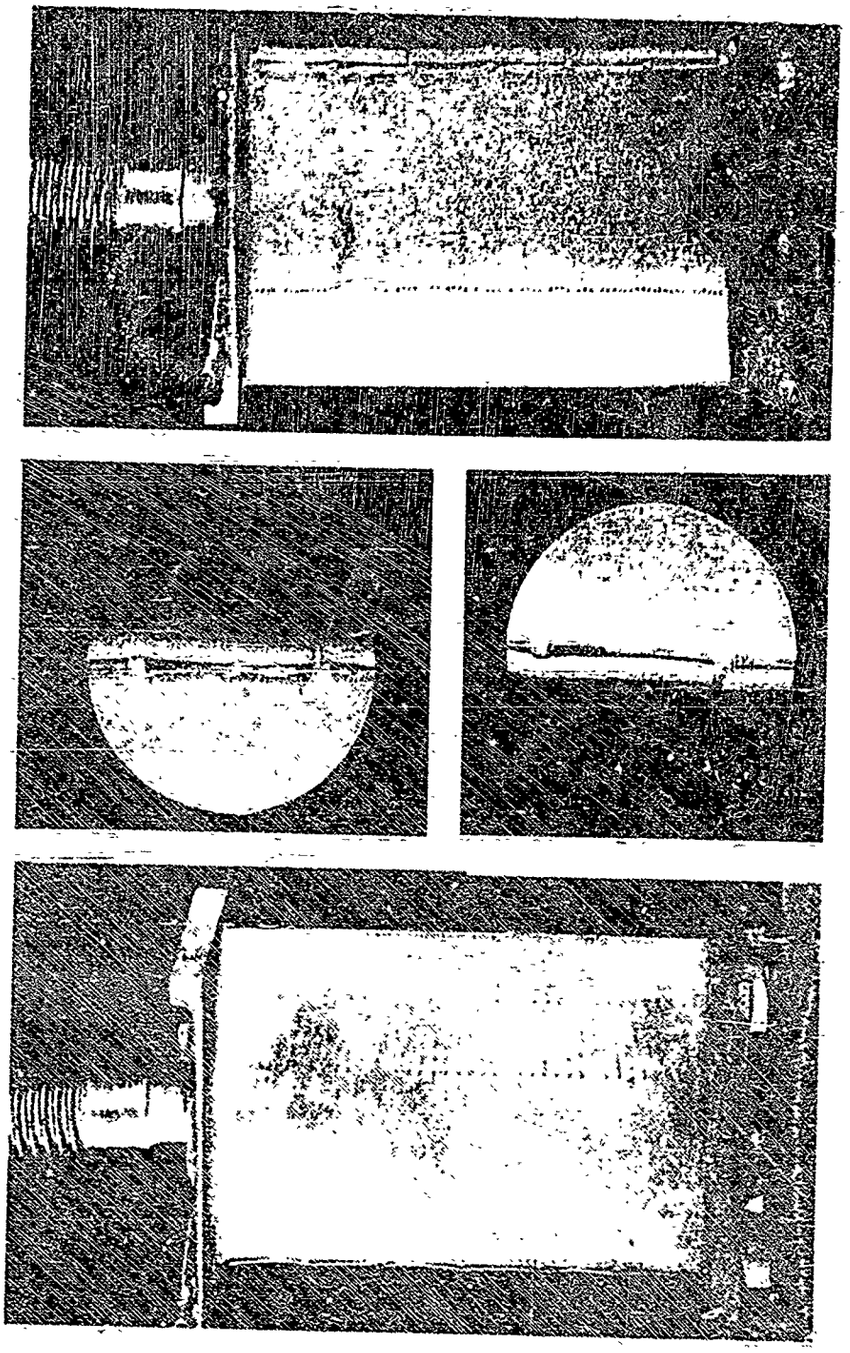
METAL TEMPERATURE VS. PERIPHERAL DISTANCE ALONG THE SUCTION SURFACE

Figure 6-70



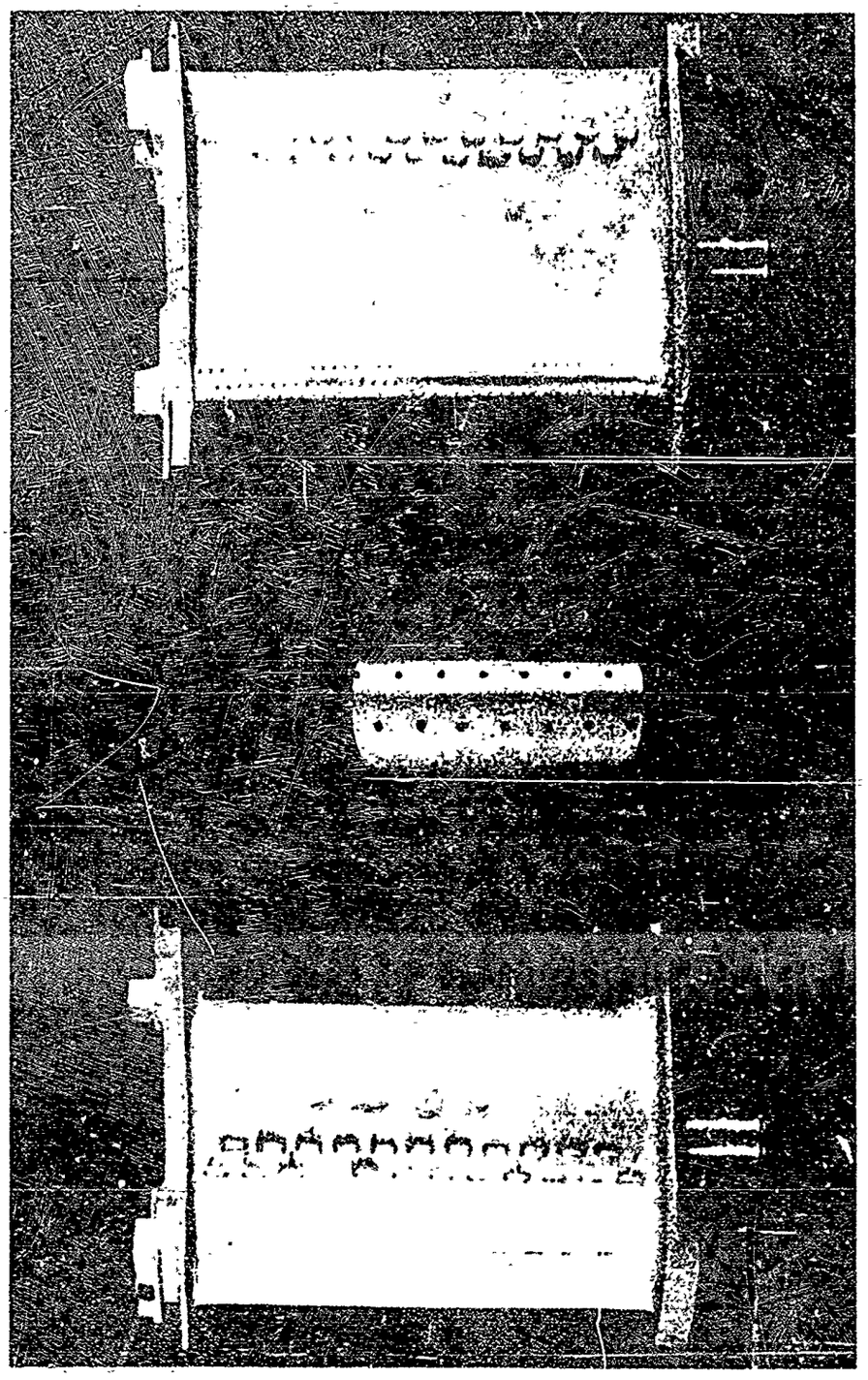
UNITED AIRCRAFT CORPORATION RESEARCH LABORATORY HIGH PRESSURE CASCADE SHOWING INFRA-RED SCANNING DEVICES

Figure 6-71



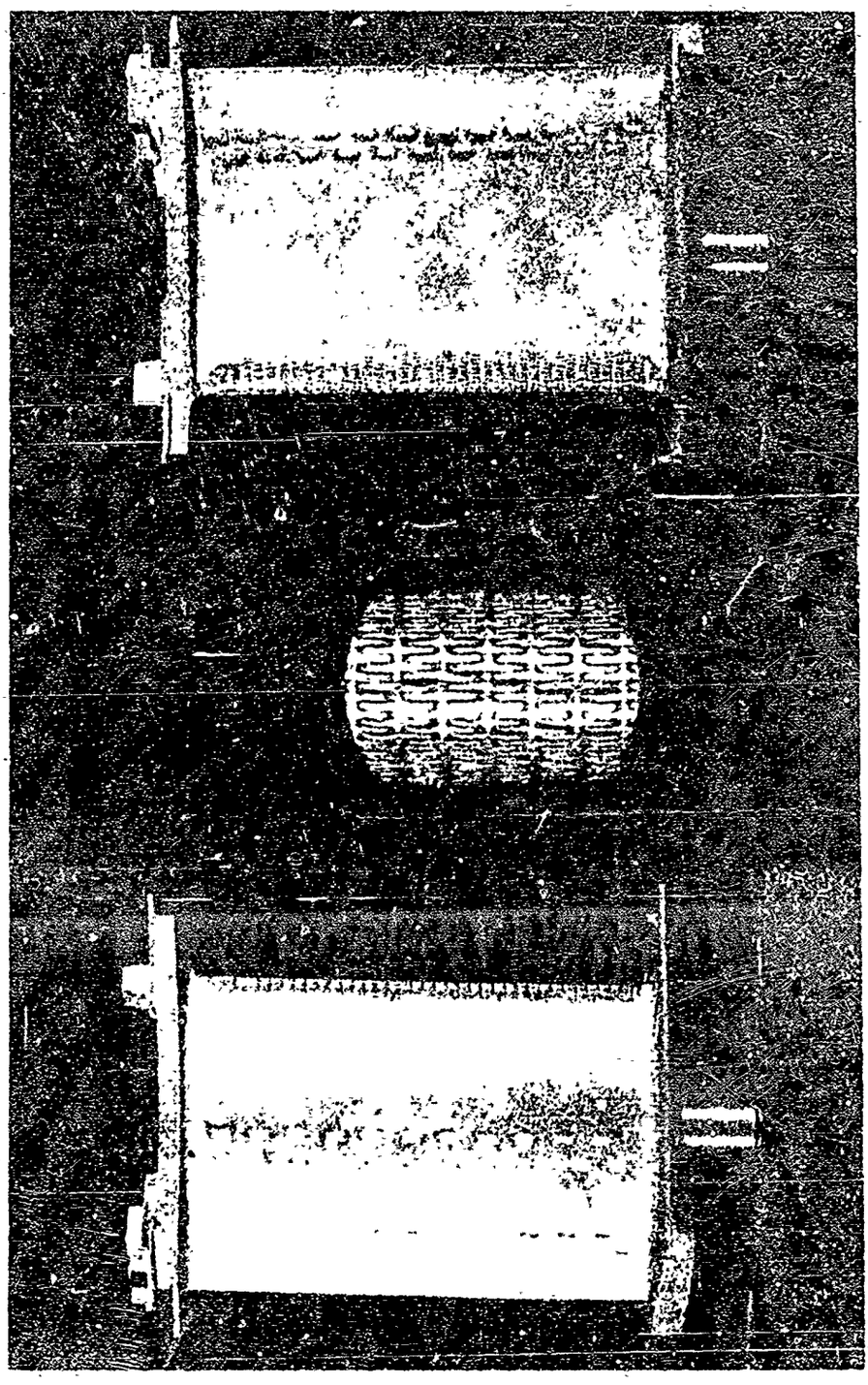
SHIELDED LEADING EDGE VANE TESTED IN
HIGH PRESSURE CASCADE RIG

Figure 6-72



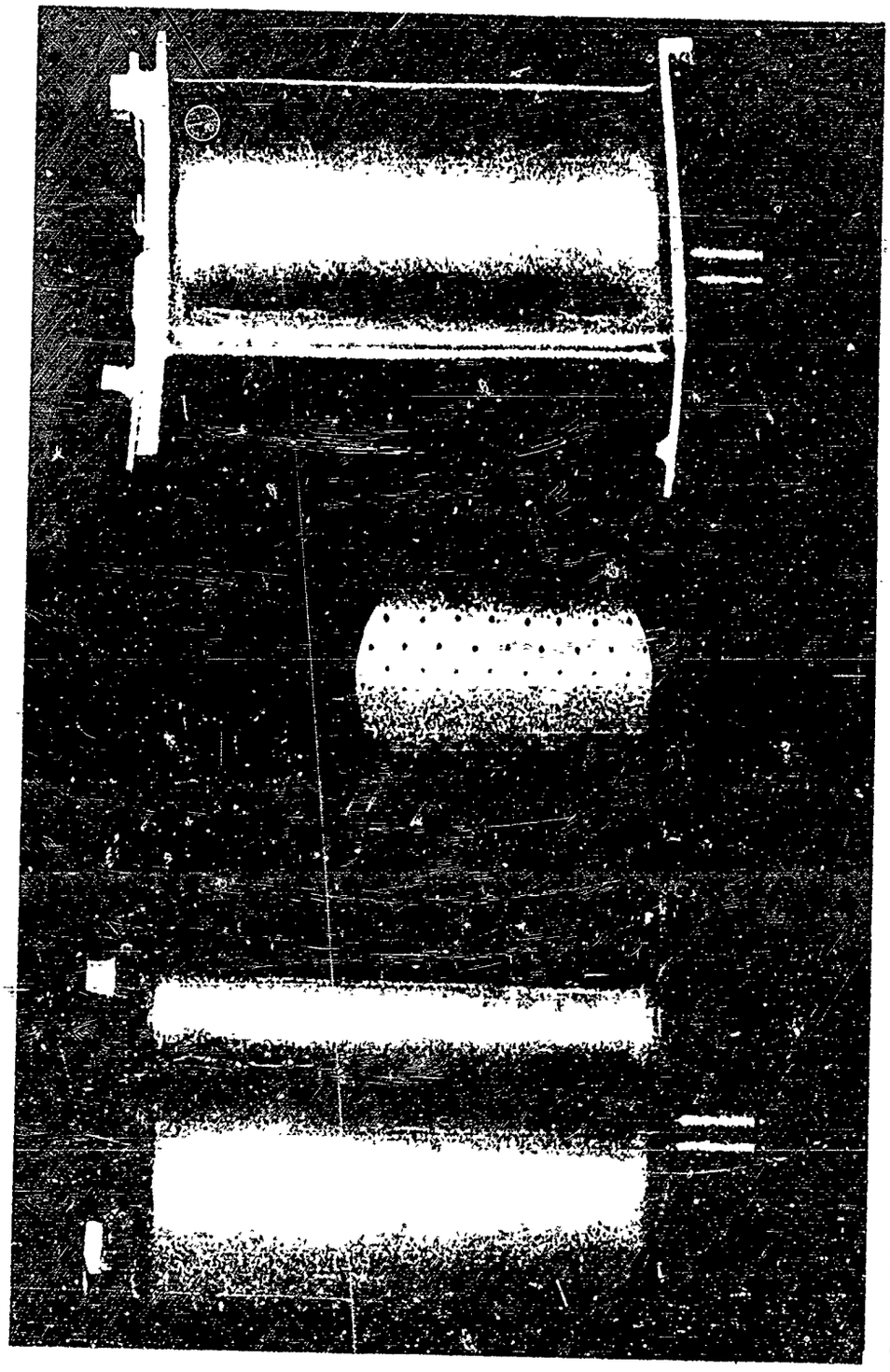
TURBINE VANE WITH LEADING EDGE (HOLES) AND TRAILING EDGE (SLOTS) COOLING SCHEMES

Figure 6-73



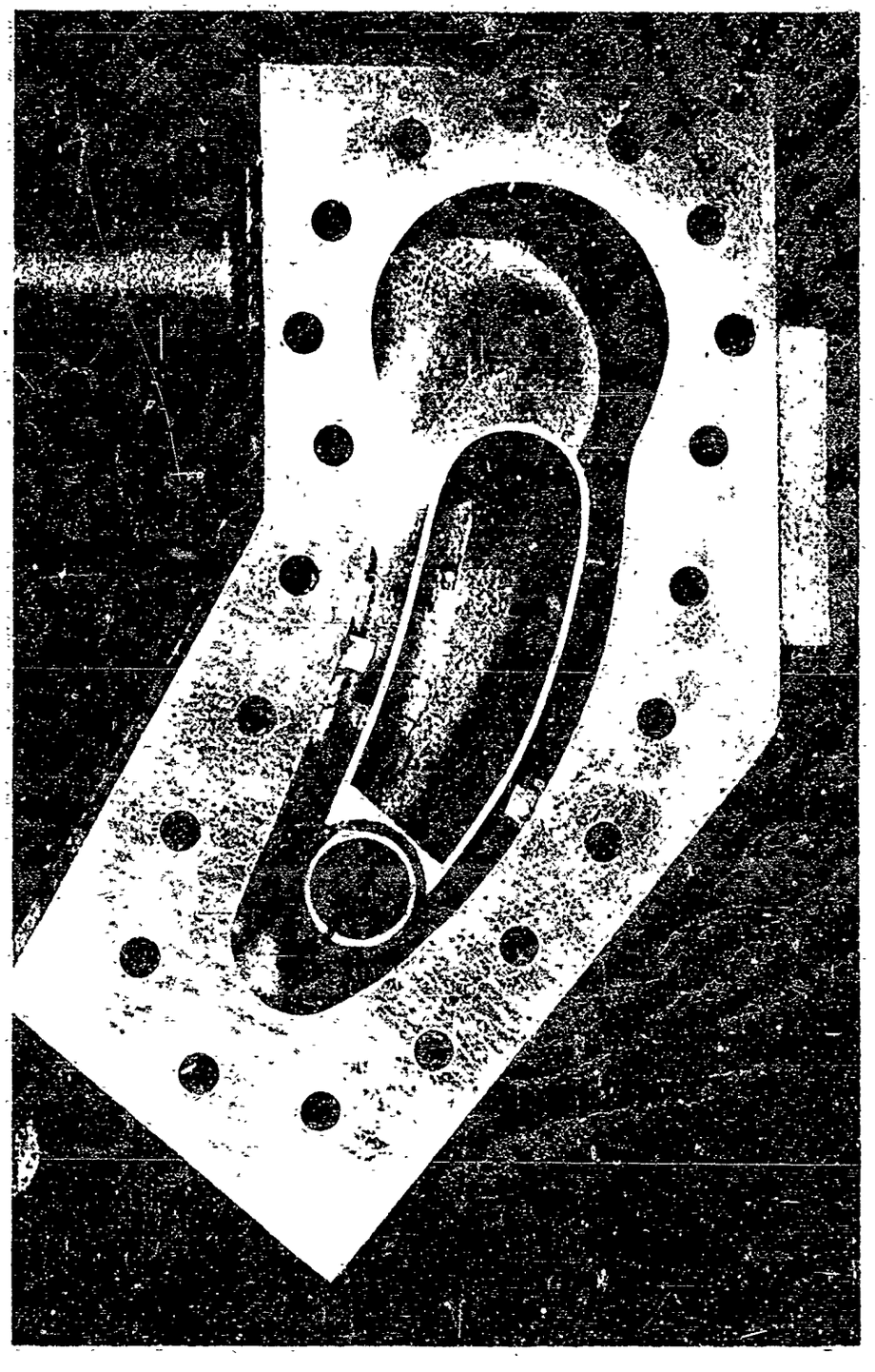
TURBINE VANE WITH FILM-COOLED POROUS LEADING EDGE AND SLOTTED TRAILING EDGE

Figure 6-74



FILM-COOLED TURBINE VANE WITH PIERCED-SHEET LEADING EDGE AND DRILLED-HOLE TRAILING EDGE

Figure 6-75



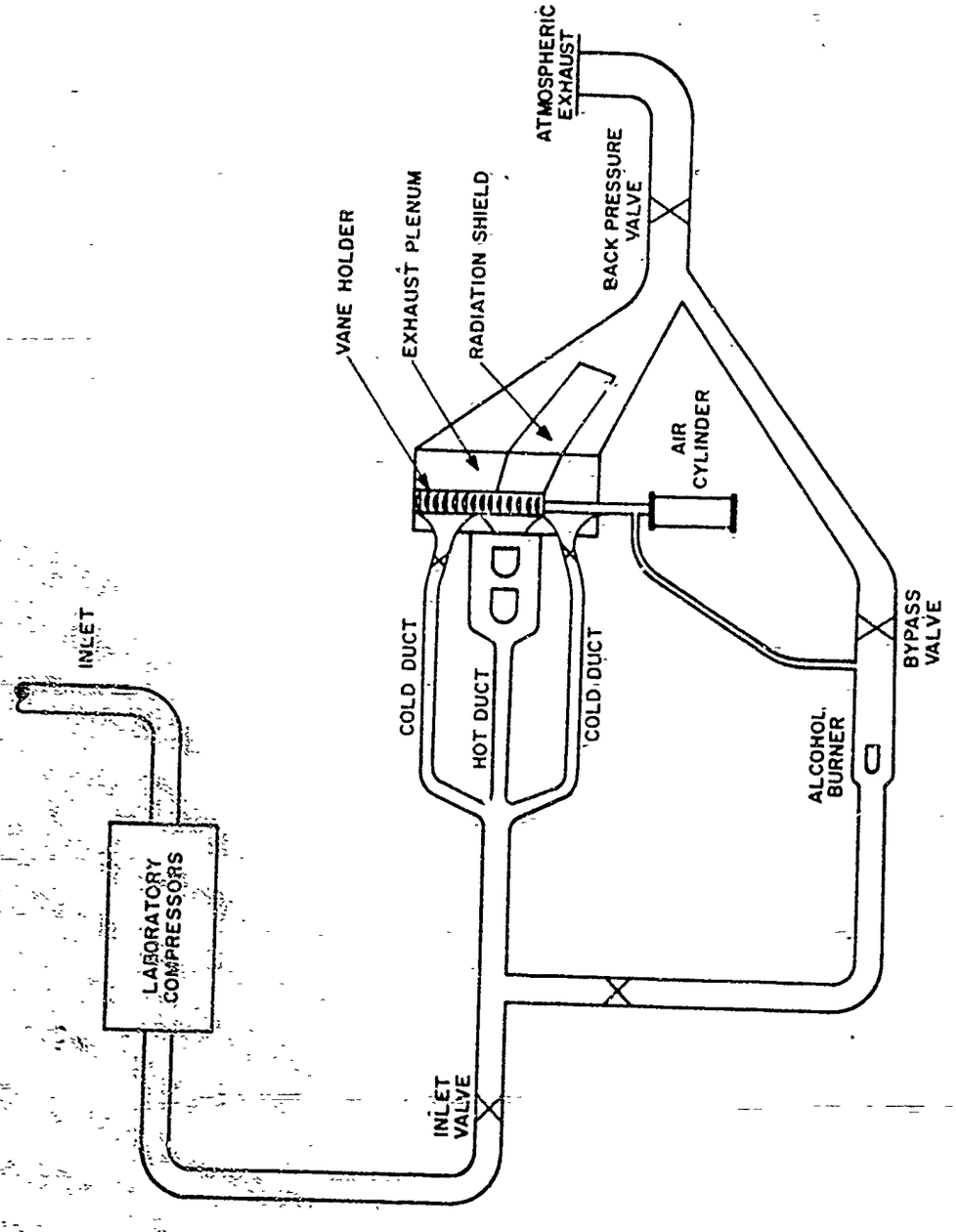
IMPINGEMENT RIG TEST SECTION

Figure 6-76



VIEW FROM REAR SHOWING VANE CASCADES IN CHOKED CASCADE THERMAL SHOCK RIG

Figure 6-77

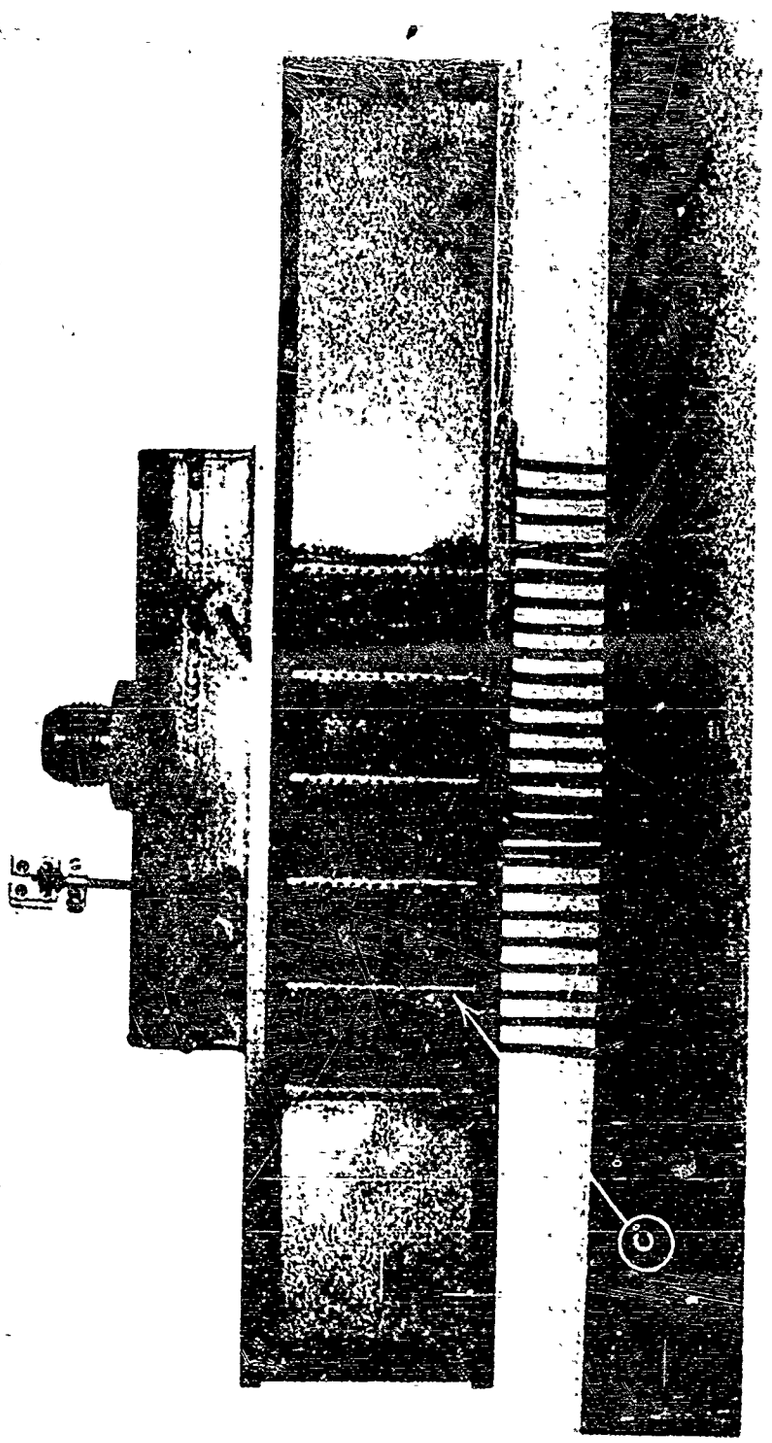


SCHEMATIC OF CHOKED CASCADE THERMAL SHOCK RIG

Figure 6-78

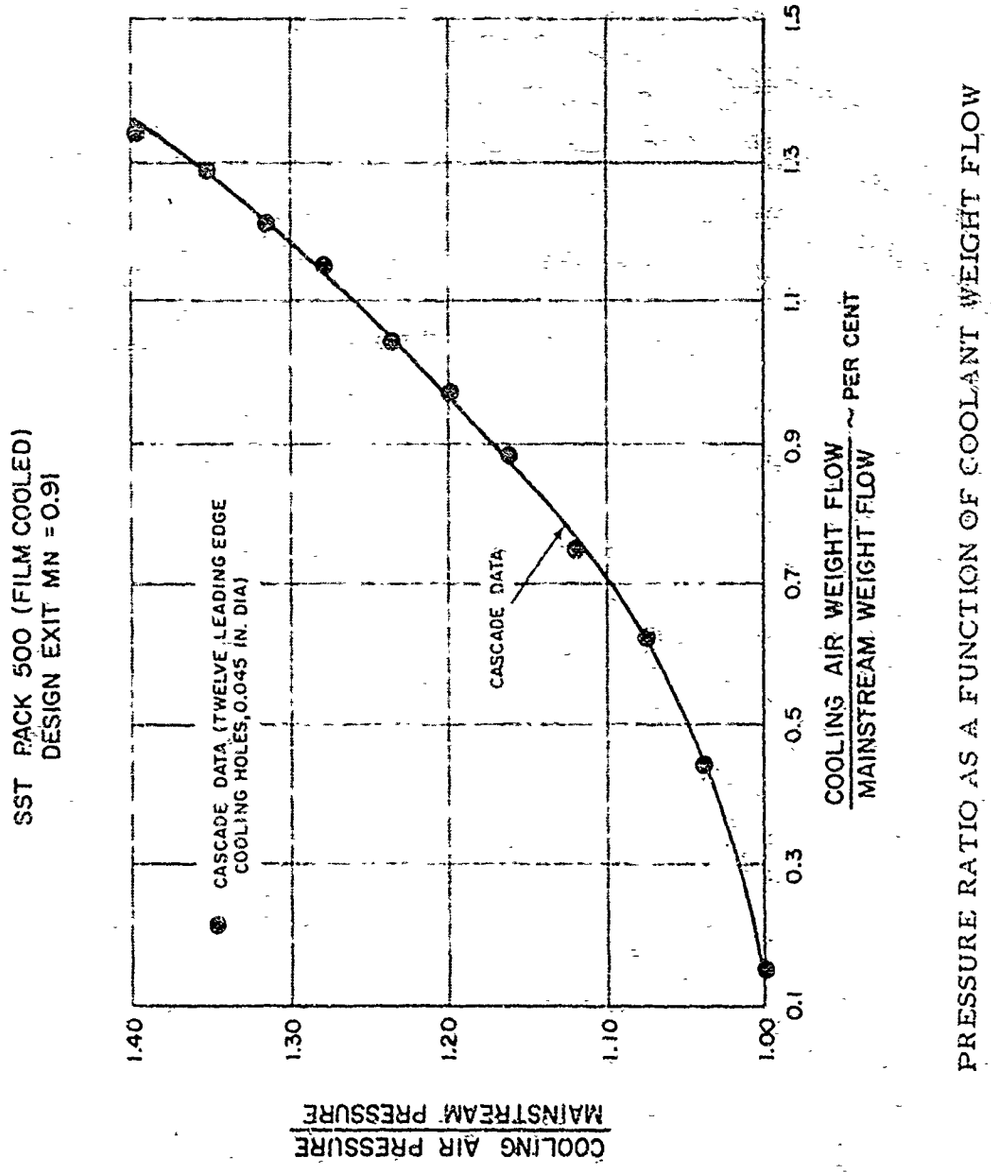
DOWNGRADED AT 3 YEAR INTERVALS
DECLASSIFIED AFTER 12 YEARS
DOD DIR 5200.10

THIS DOCUMENT CONTAINS INFORMATION AFFECTING THE NATIONAL DEFENSE OF THE UNITED STATES WITHIN THE MEANING OF THE ESPIONAGE LAWS, TITLE 18, U.S.C., SECTIONS 793 AND 794. THE TRANSMISSION OR THE REVELATION OF ITS CONTENTS IN ANY MANNER TO AN UNAUTHORIZED PERSON IS PROHIBITED BY LAW.



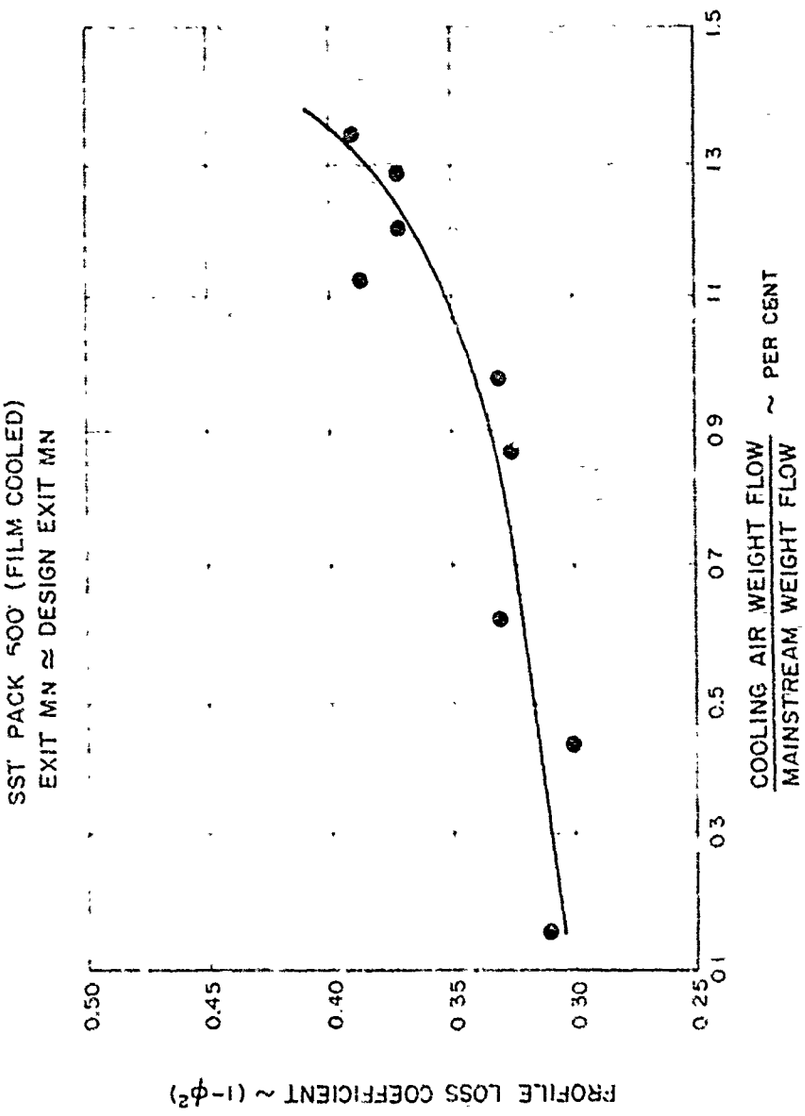
VANE PACK FOR FILM COOLED VANE TESTS A. PLENUM CHAMBER T/C. B. PLENUM CHAMBER
C. LEADING EDGE COOLING AIR HOLES

Figure 6-79



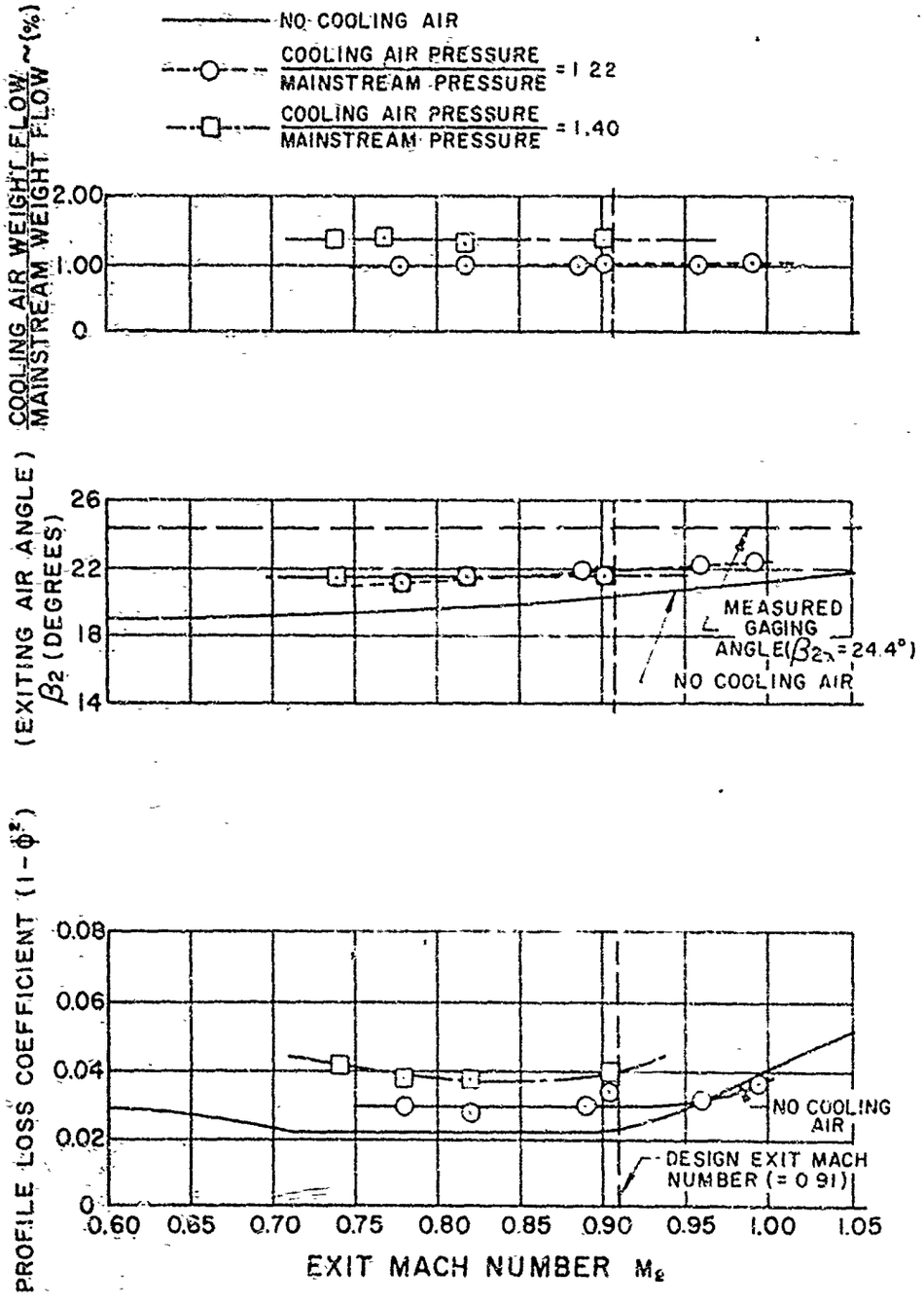
PRESSURE RATIO AS A FUNCTION OF COOLANT WEIGHT FLOW

Figure 6-80



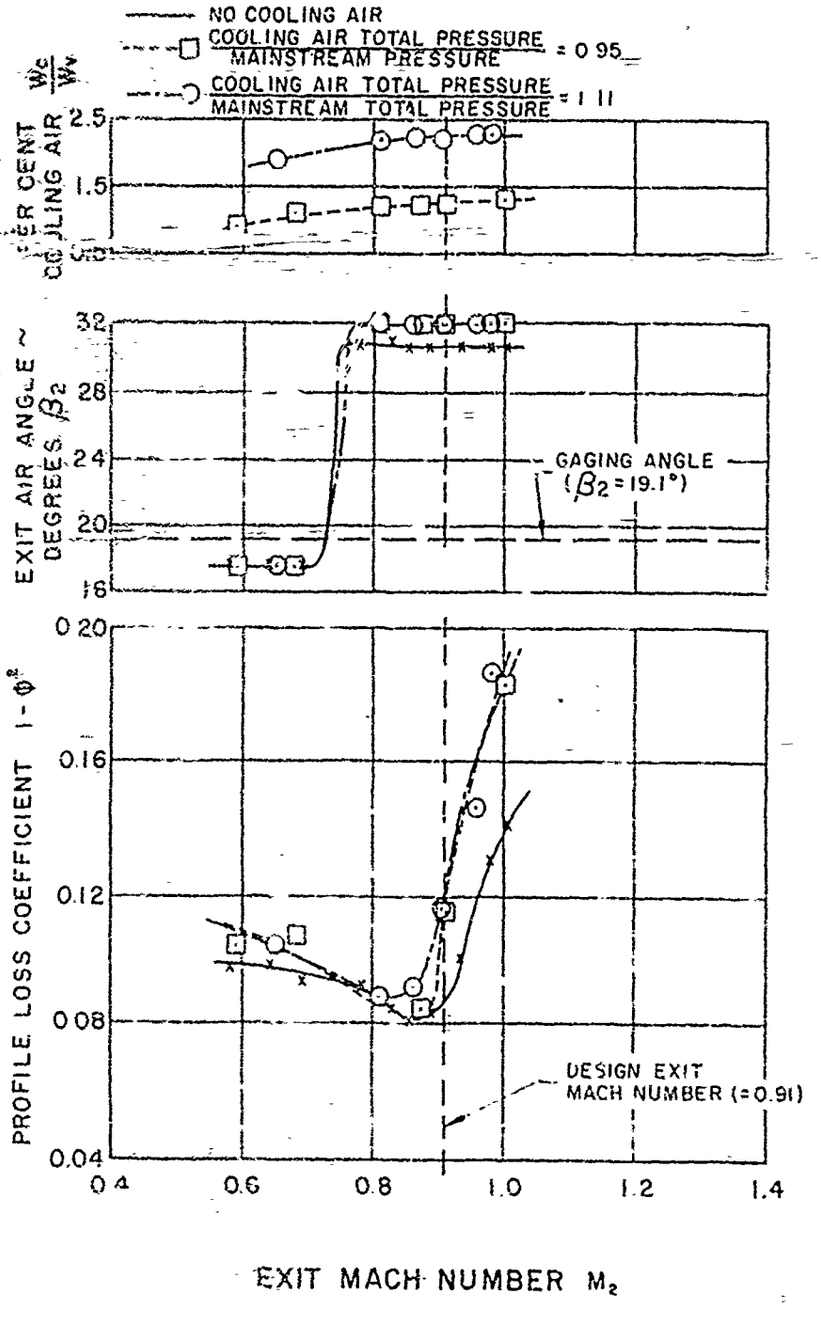
PRESSURE LOSS COEFFICIENT AS A FUNCTION OF COOLANT WEIGHT FLOW

Figure 6-81



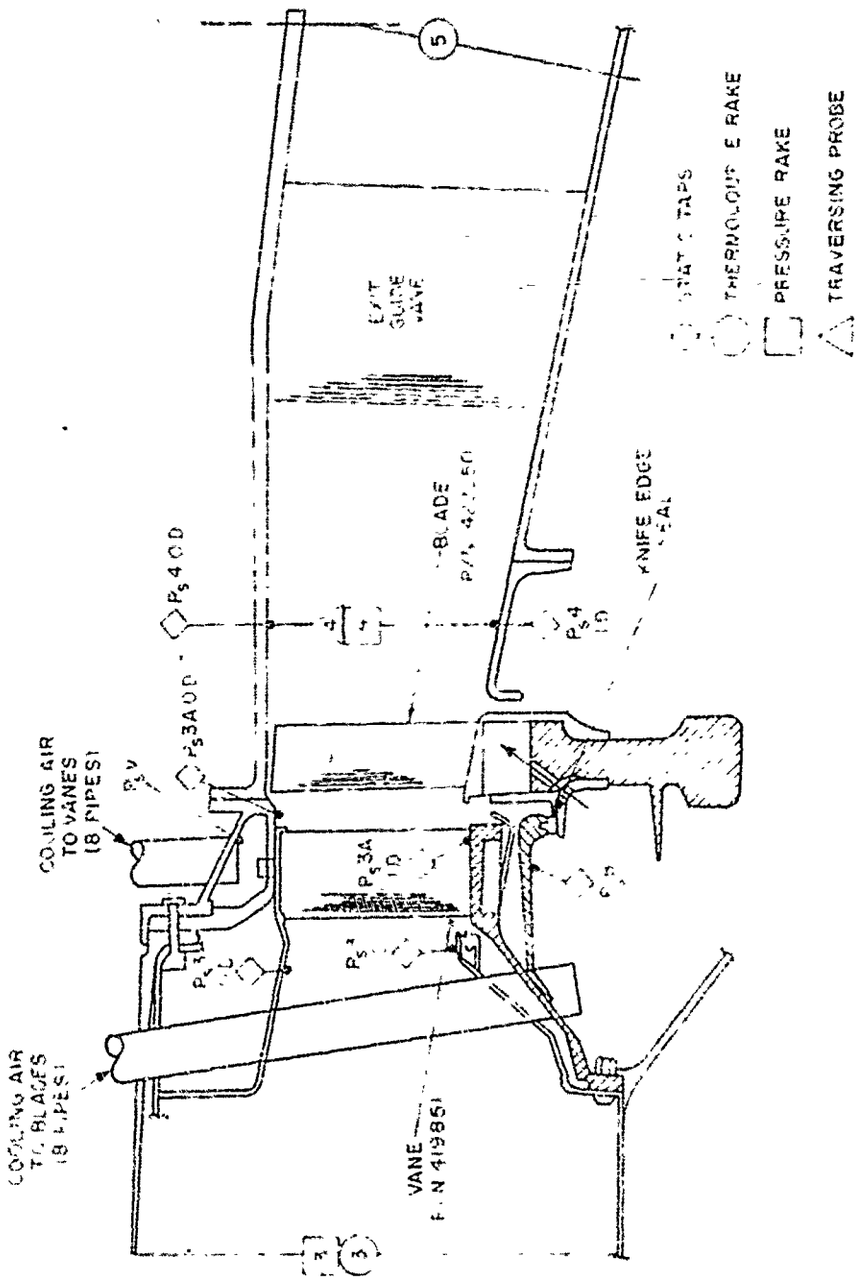
COOLANT PARAMETERS AS A FUNCTION OF EXIT MACH NUMBER

Figure 6-82



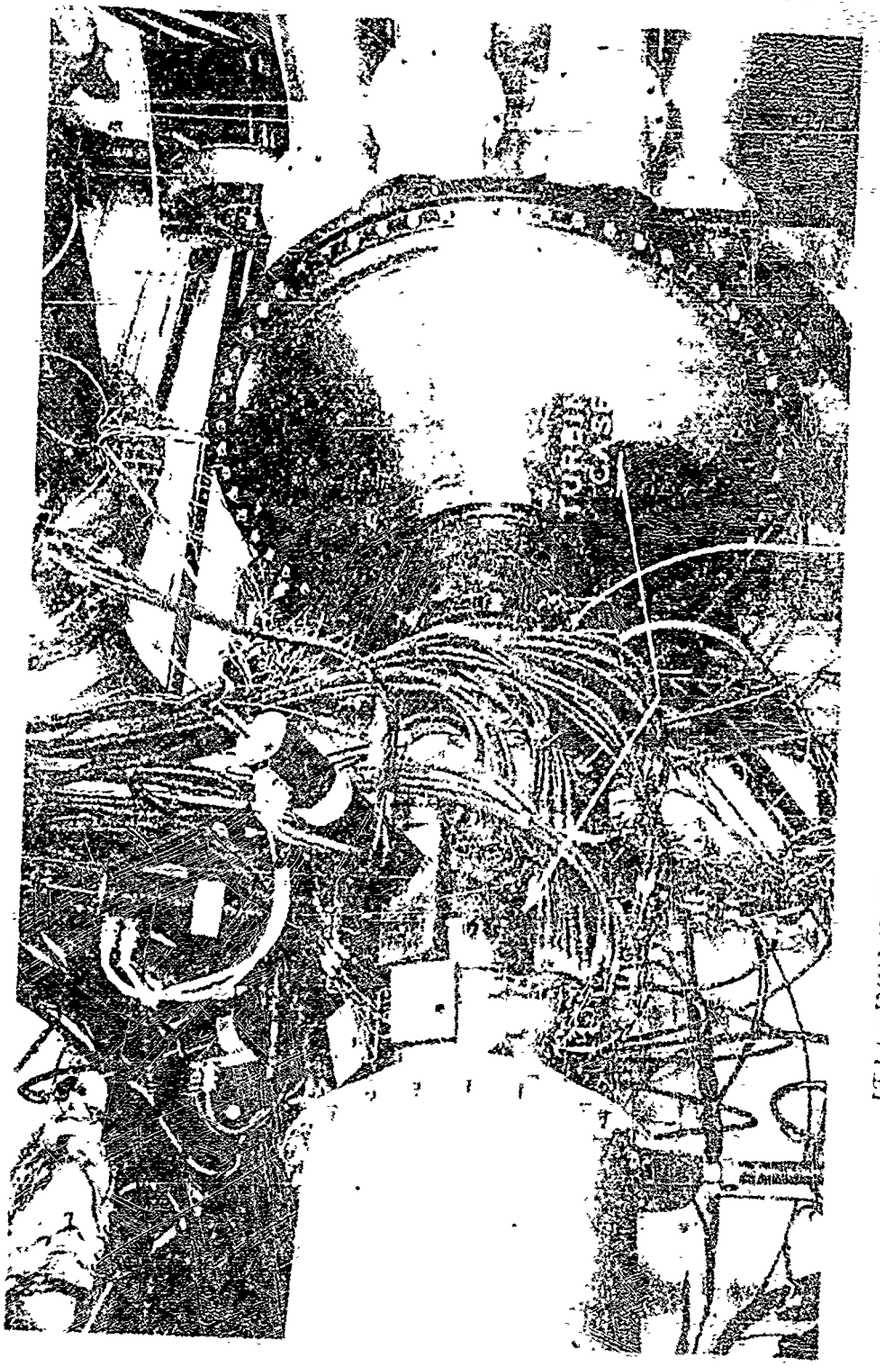
COOLANT PARAMETERS AS A FUNCTION OF EXIT MACH NUMBER

Figure 6-83



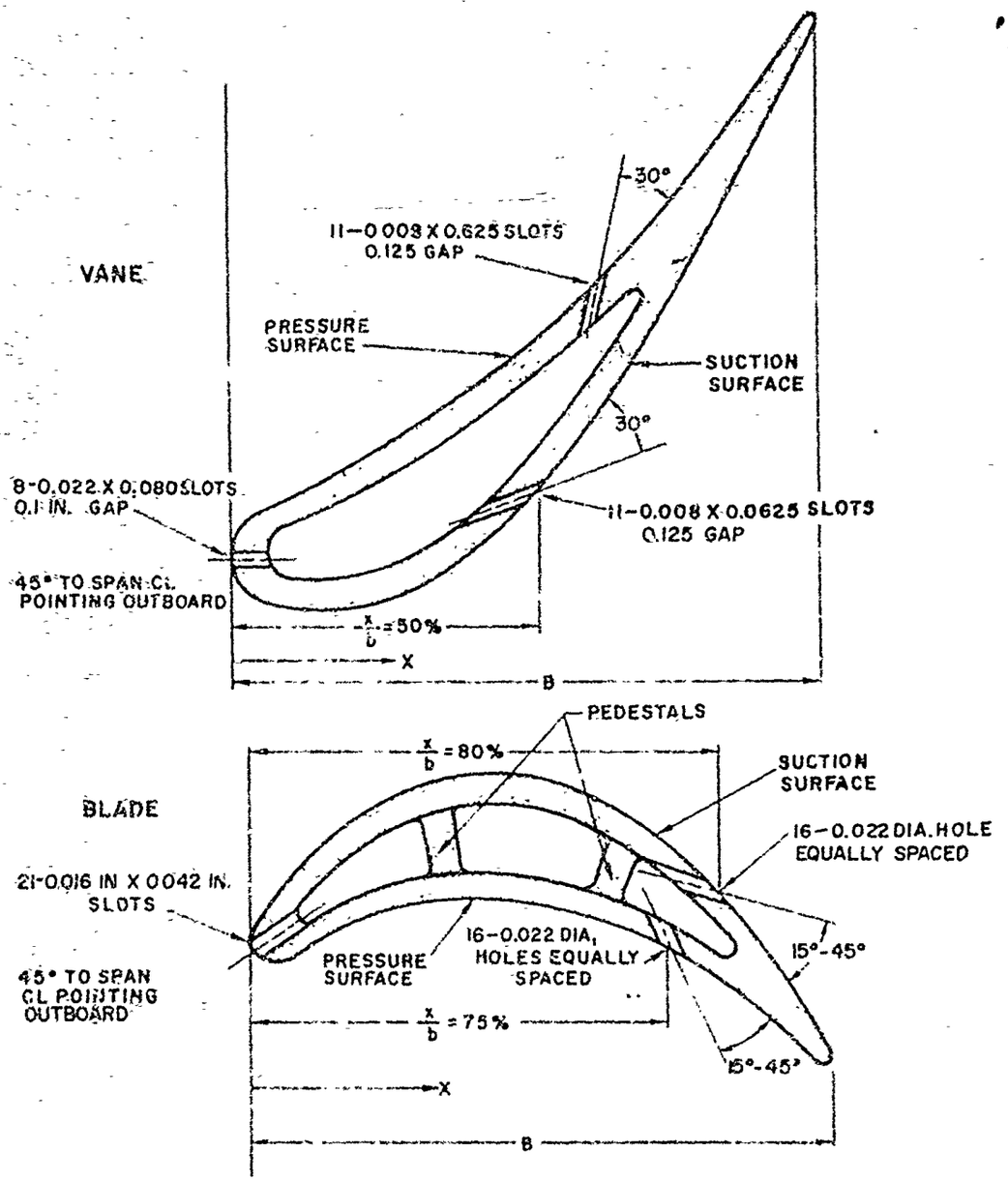
SCHEMATIC DIAGRAM OF J112 PERFORMANCE RIG SHOWING BLADE AND VANE COOLING AIR ARRANGEMENT AND INSTRUMENTATION SYSTEM

Figure 6-81



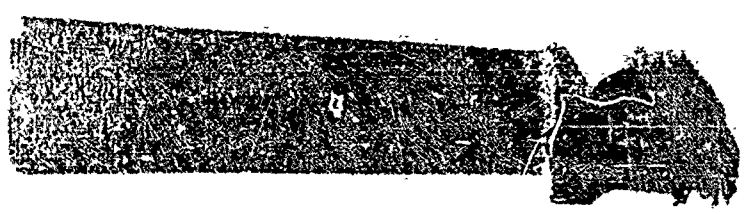
JT12 SINGLE-STAGE TURBINE PERFORMANCE RIG

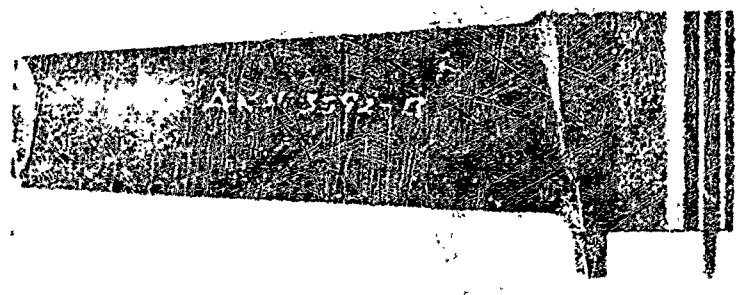
Figure [illegible]



BLADE AND VANE COOLING AIR PASSAGE CONFIGURATION
EVALUATED IN JT12 PERFORMANCE TESTS

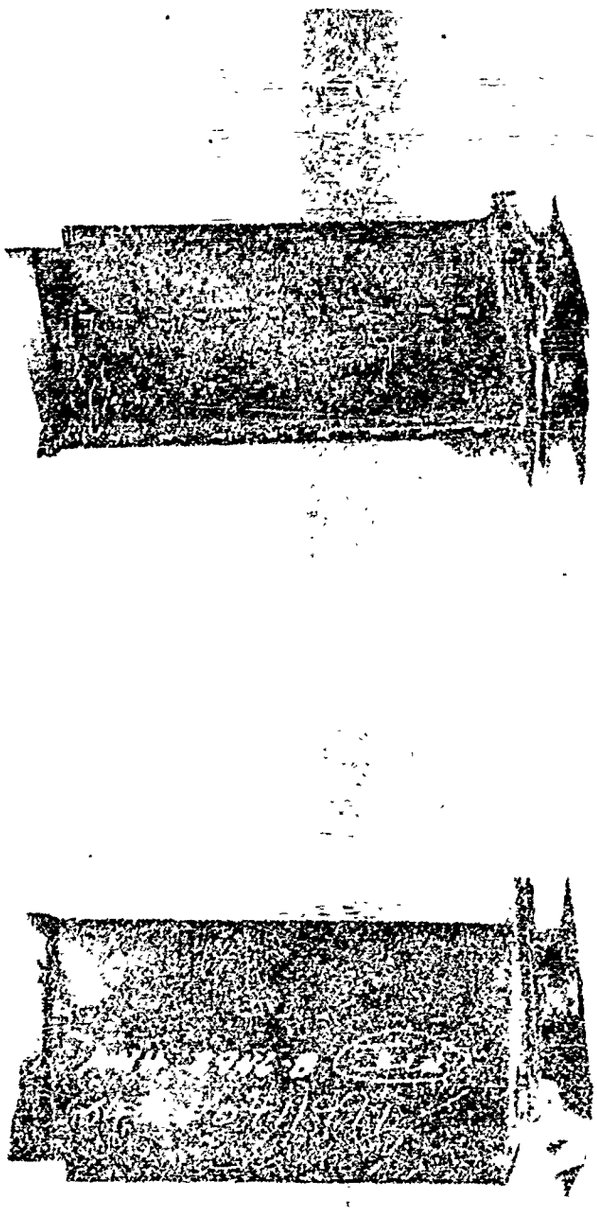
Figure 6-86





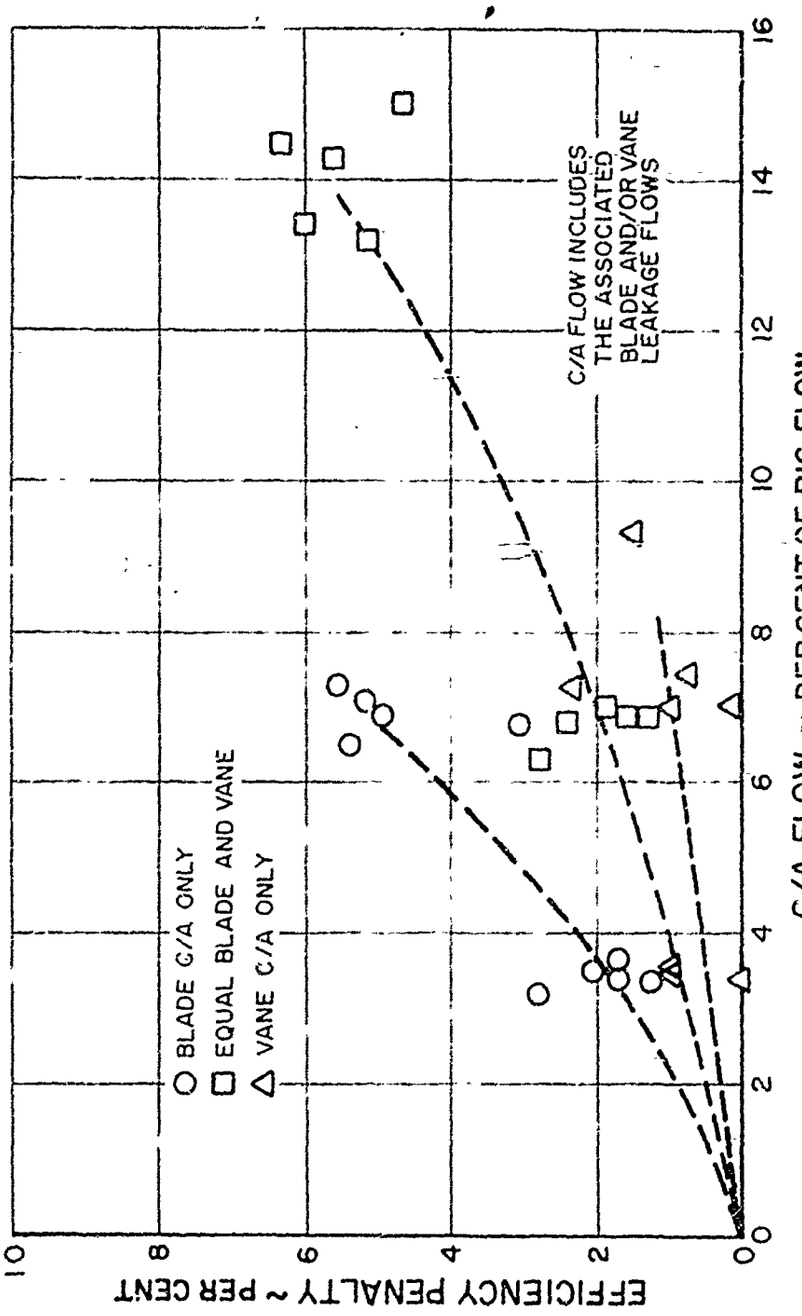
JT12-SIZED FILM COOLED FIRST-STAGE TURBINE BLADE FOR PERFORMANCE TEST

Figure 6-87



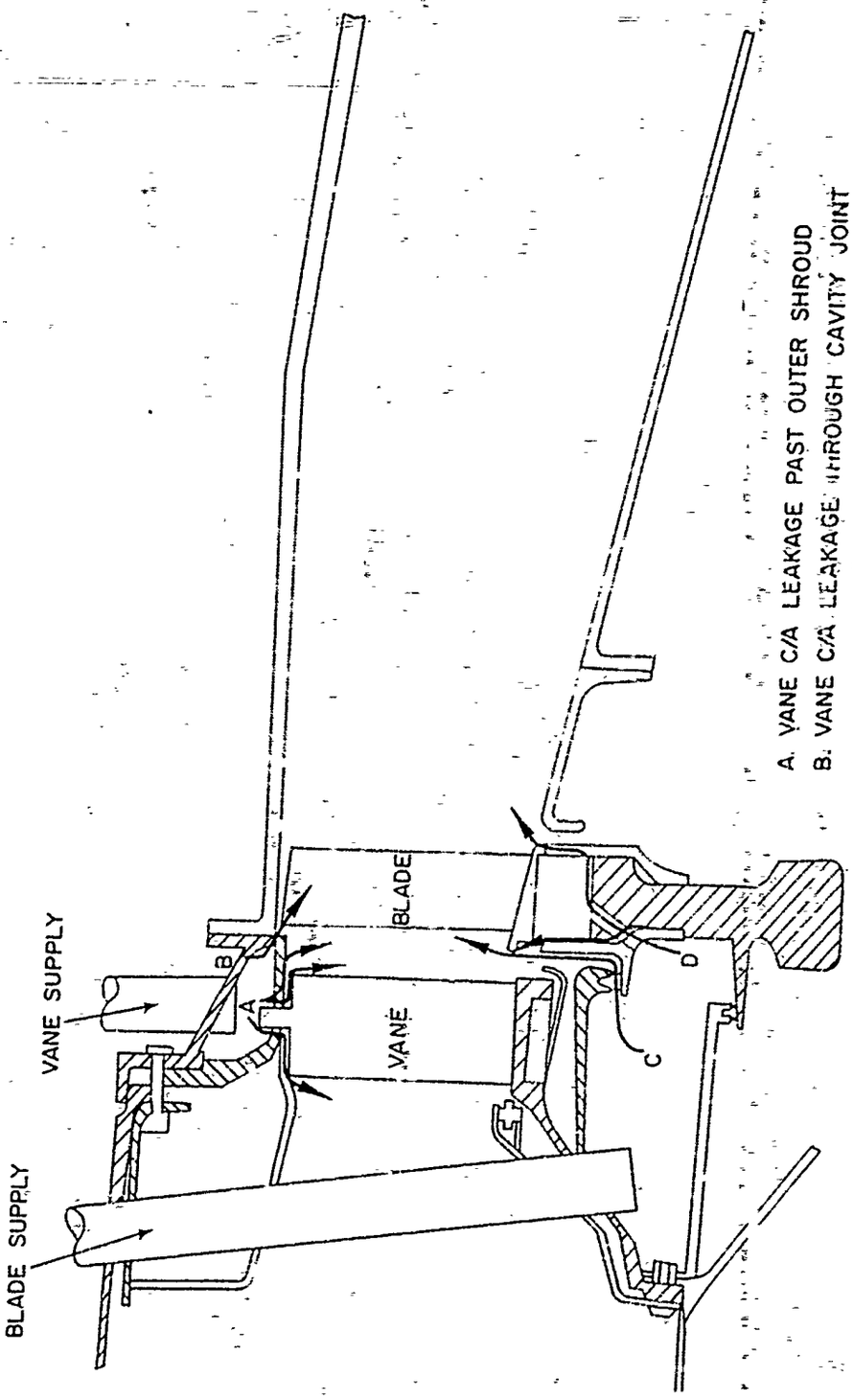
JT12-SIZED FILM COOLED FIRST-STAGE TURBINE VANE FOR PERFORMANCE TEST

Figure 6-88



EFFECT OF VANE AND BLADE COOLING AIR FLOW ON TURBINE PERFORMANCE

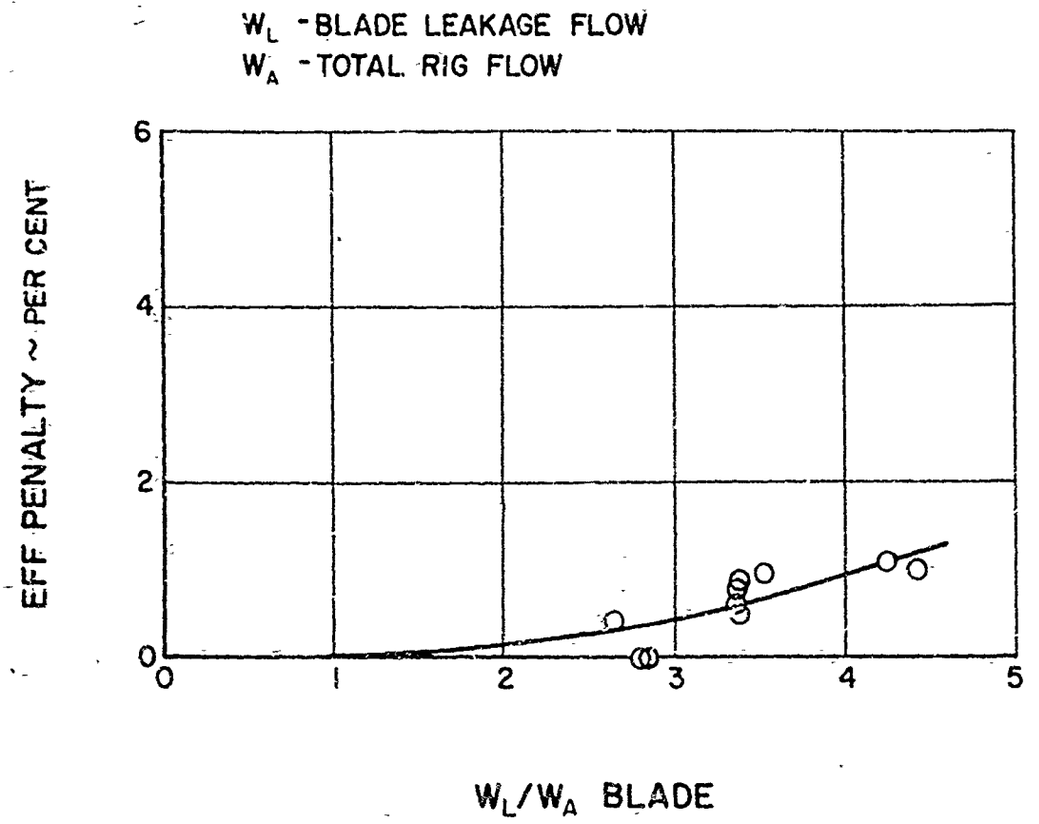
Figure 6-89



A. VANE C/A LEAKAGE PAST OUTER SHROUD
B. VANE C/A LEAKAGE THROUGH CAVITY JOINT
C. BLADE C/A LEAKAGE PAST LABYRINTH
D. BLADE C/A LEAKAGE BEHIND DISC PLATE

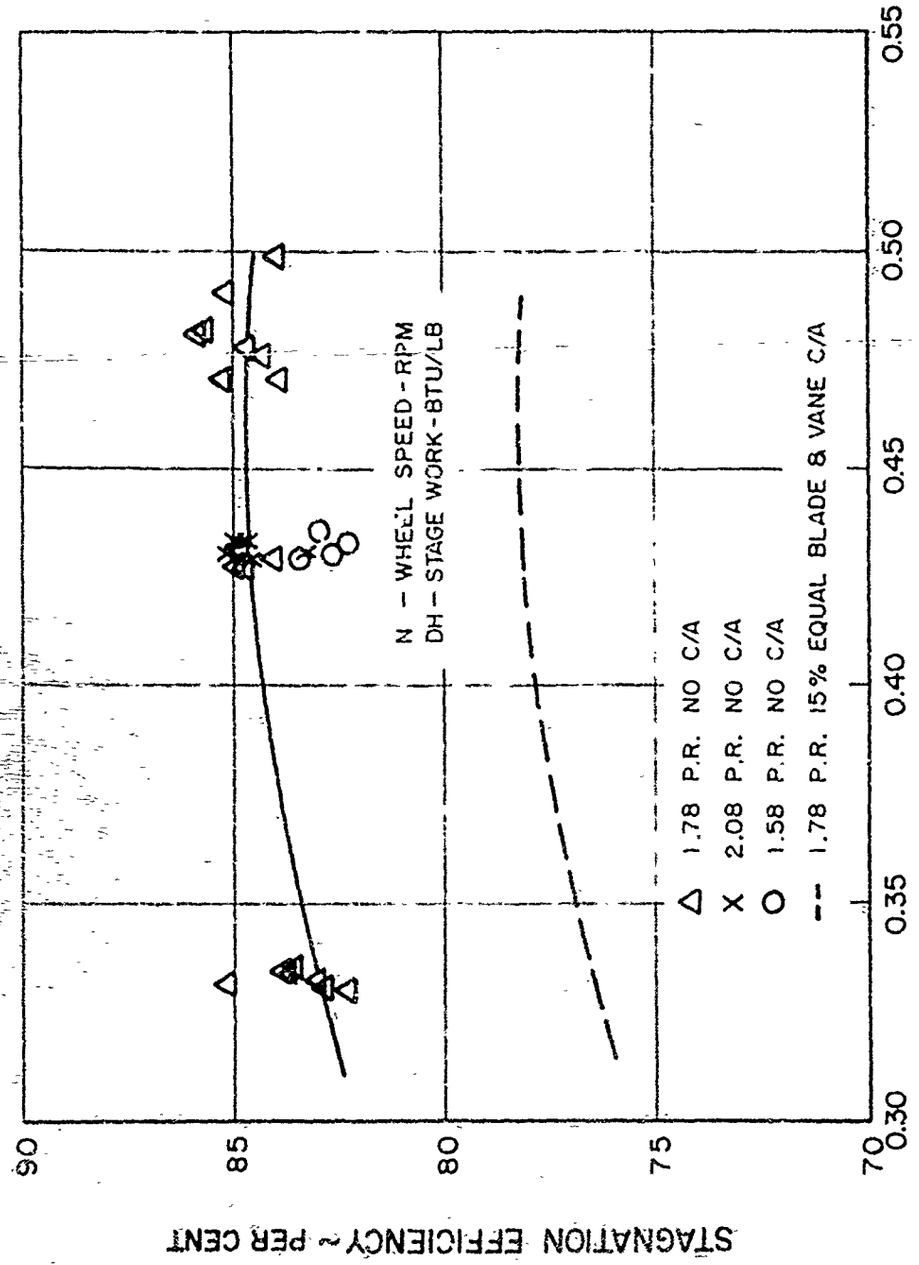
AIR LEAKAGE PATHS IN JT12 BURNER TURBINE RIG

Figure 6-90



EFFECT OF BLADE LEAKAGE ON TURBINE PERFORMANCE

Figure 6-91



COMPARISON OF THE EFFECT OF OFF-DESIGN OPERATION AND COOLING AIR BLEED ON TURBINE PERFORMANCE

Figure 6-92

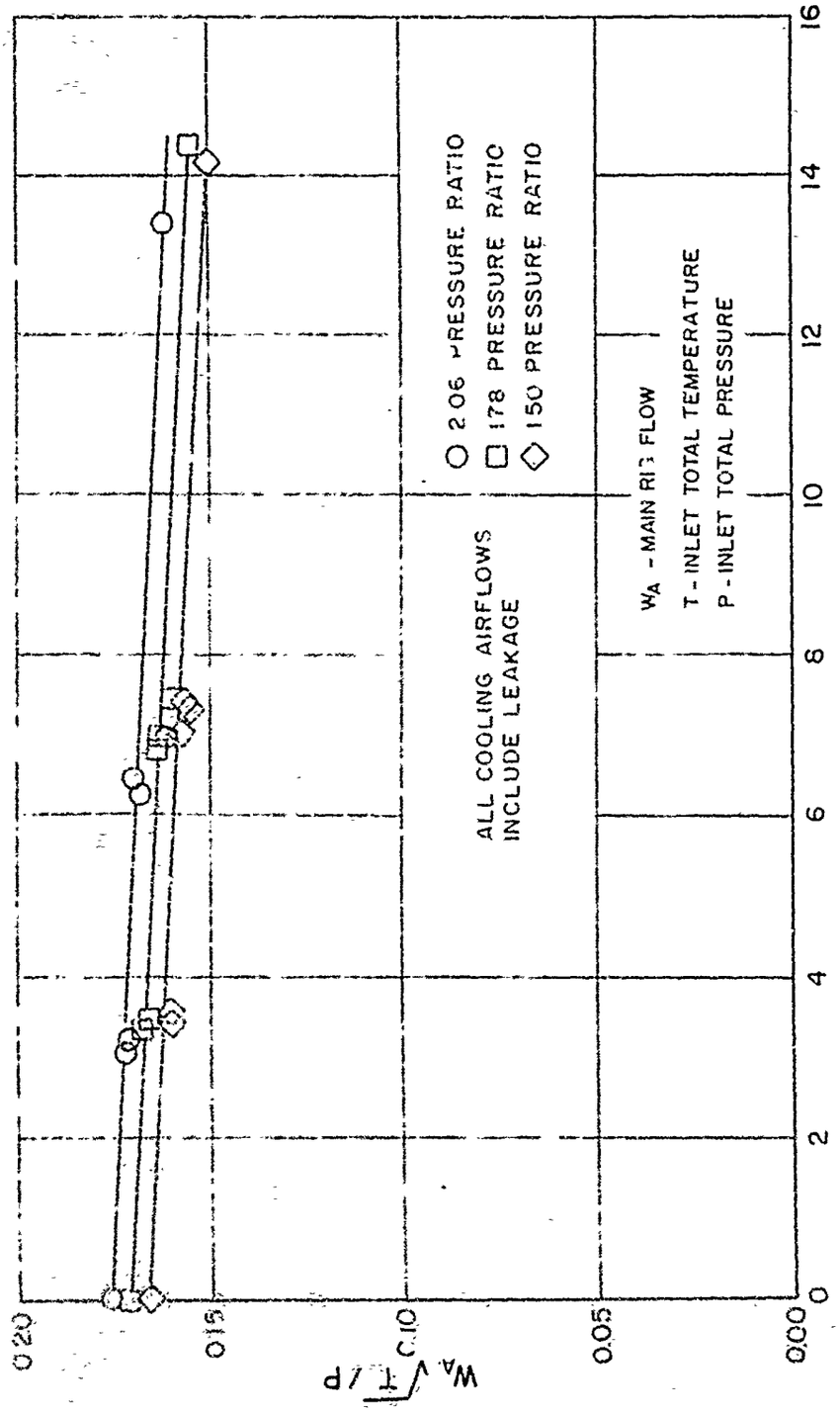
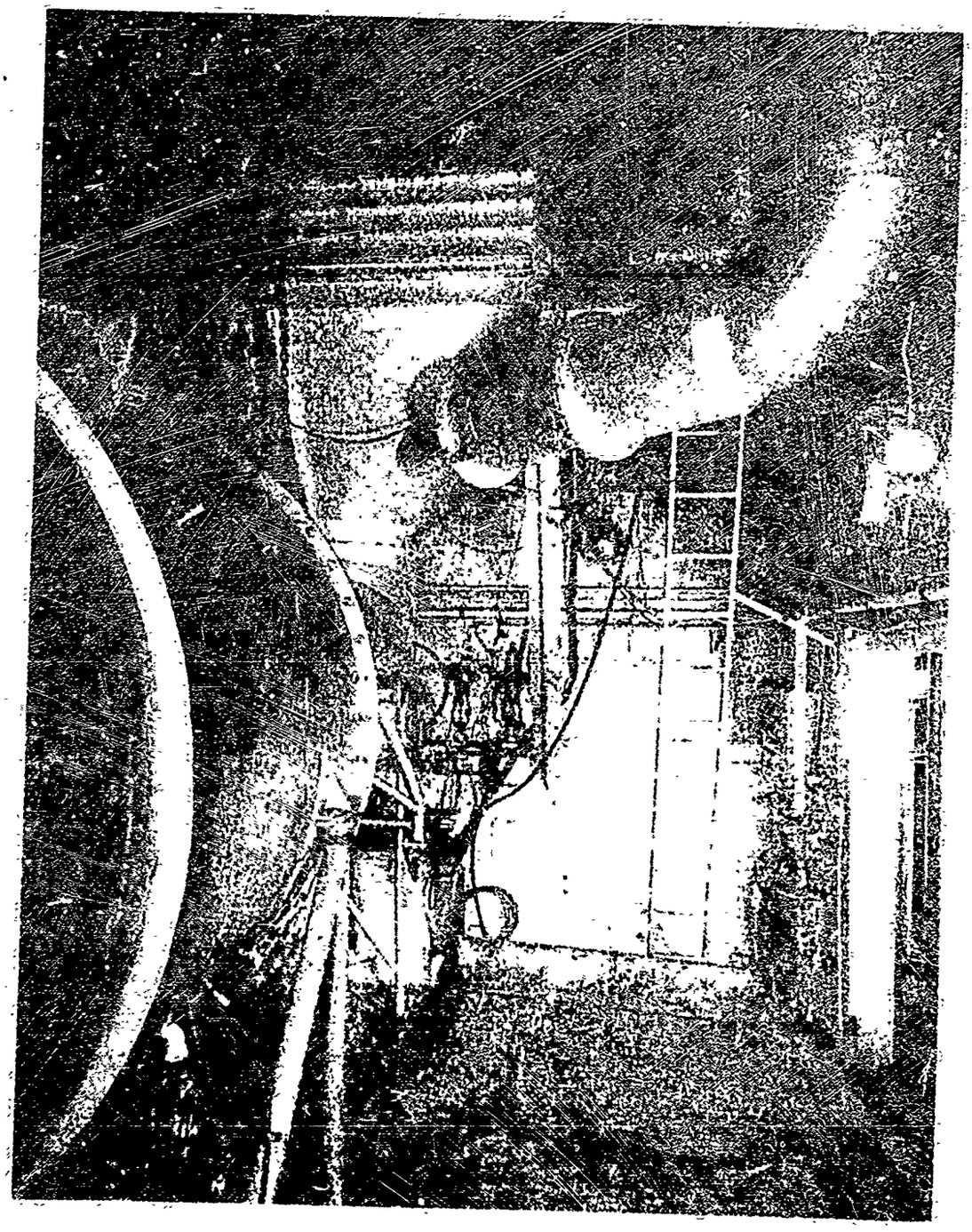

EFFECT OF BLADE AND VANE COOLING AIRFLOW ON RIG INLET FLOW PARAMETER
TOTAL PER CENT C/A FLOW
$W_A\sqrt{T}/P$
0.20
0.15
0.10
0.05
0.00
0
2
4
6
8
10
12
14
16
○ 2.06 PRESSURE RATIO
□ 1.78 PRESSURE RATIO
◇ 1.50 PRESSURE RATIO
ALL COOLING AIRFLOWS INCLUDE LEAKAGE
W_A - MAIN RIG FLOW
T - INLET TOTAL TEMPERATURE
P - INLET TOTAL PRESSURE

Figure 6-93

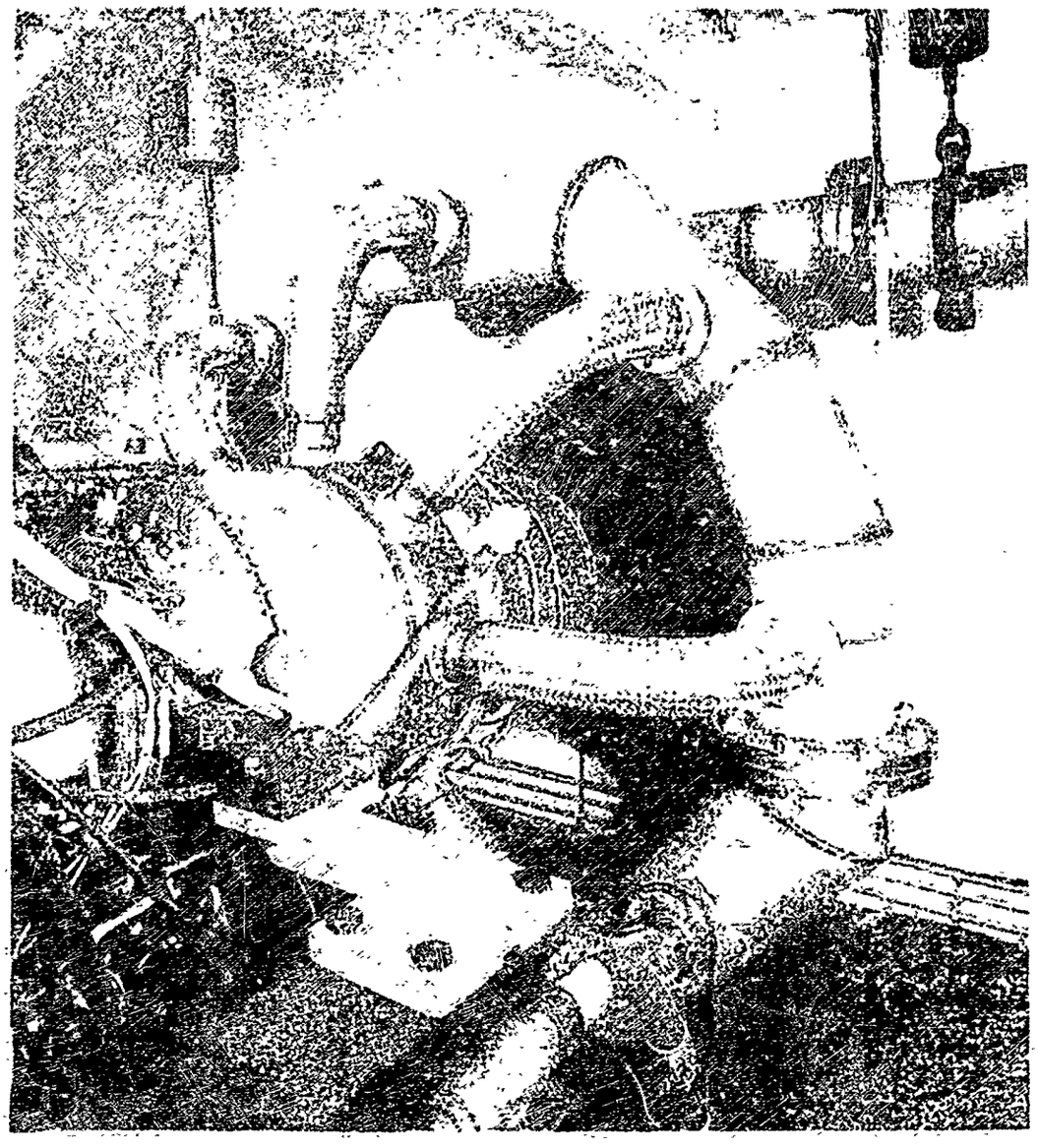


HEATED INLET HARDWARE ON TEST STAND FOR HIGH SPOOL ENGINE TEST

Figure 6-34

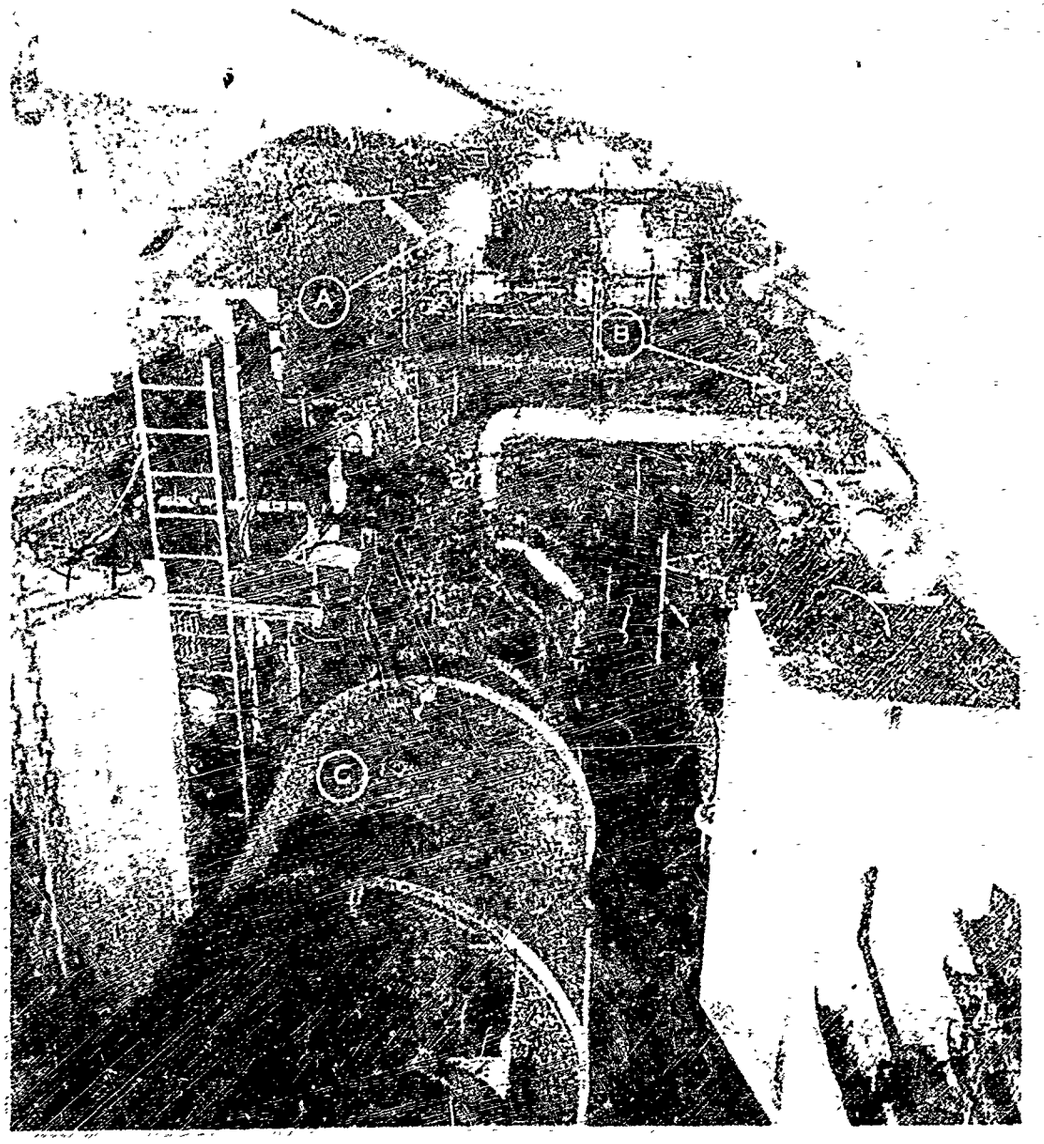
COOLED BLADE AND VANE TEST RIG SHOWING HEATED ENGINE-INLET AIR ARRANGEMENT AND COOLING AIR SUPPLY

Figure 6-43



JT12 COOLING AIR SUPPLY ENGINE SHOWING COOLING AIR BLEED DUCTING

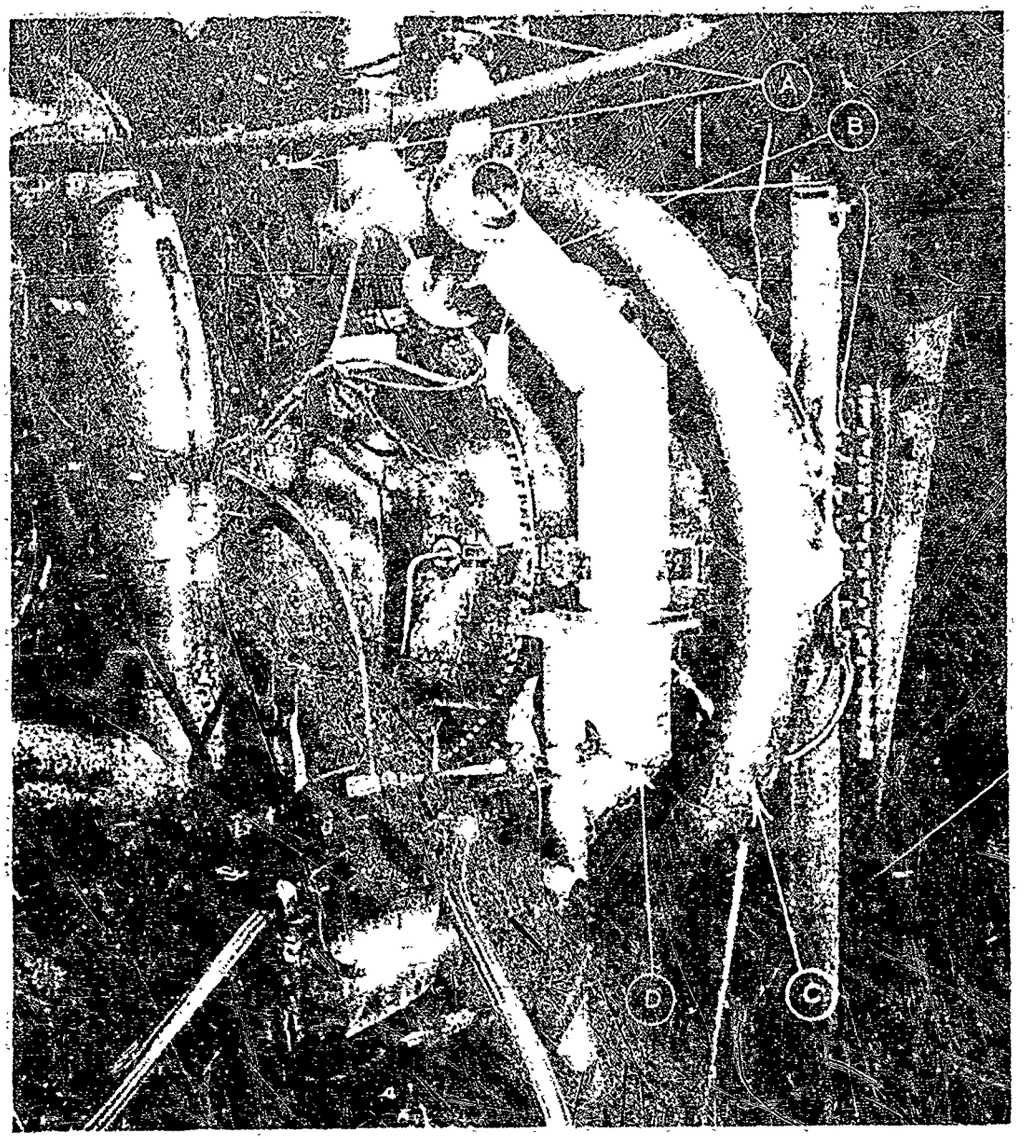
Figure 6-9o



JT4 HIGH SPOOL ENGINE SHOWING ENGINE AND VANE/BLADE COOLING AIR SUPPLY

A. JT12 COOLING AIR SUPPLY ENGINE
B. HEATER BURNER
C. PLENUM CHAMBER

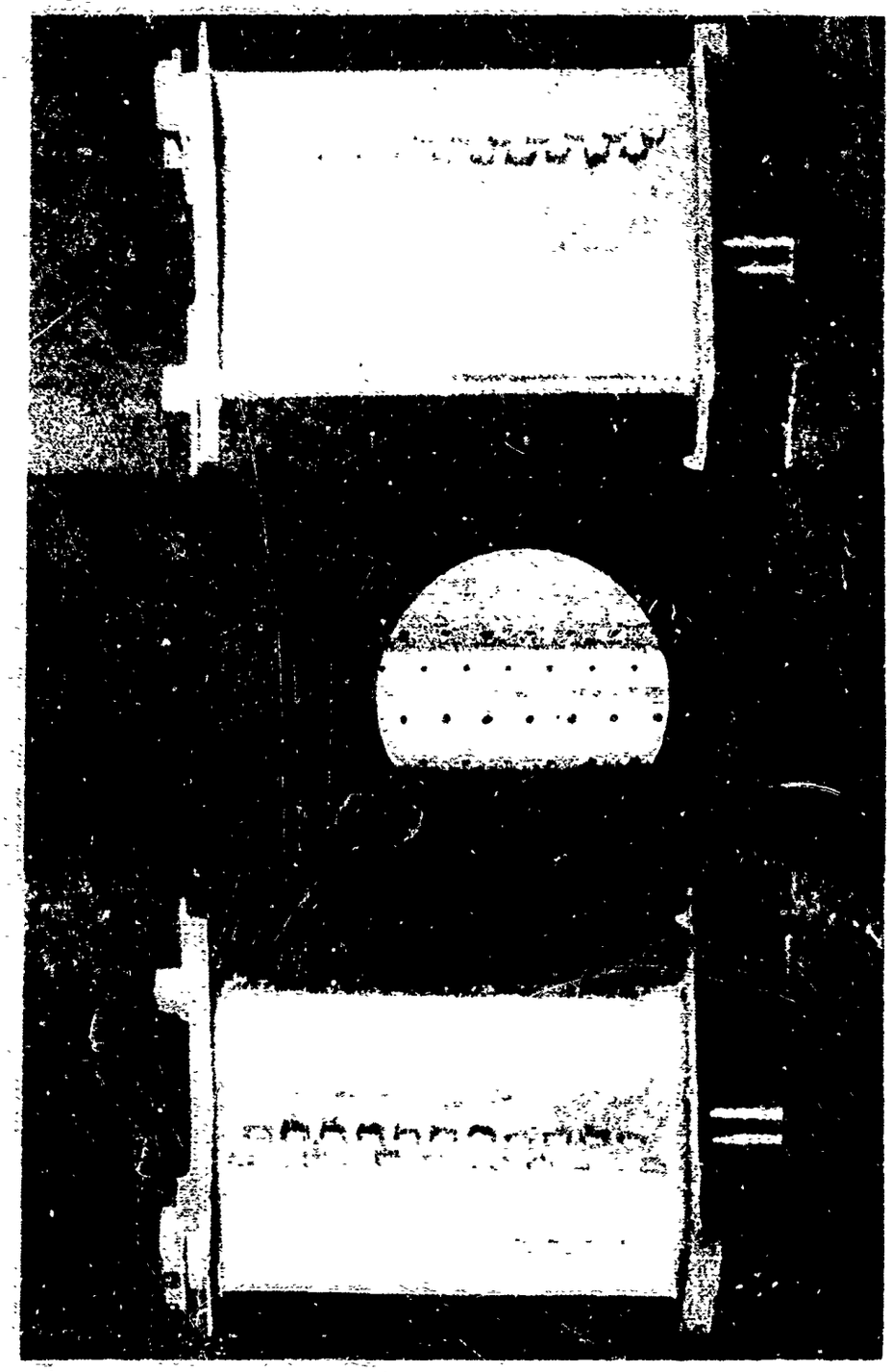
Figure 6-97



J14 HIGH SPOOL ENGINE SHOWING VANE AND BLADE COOLING AIR MANIFOLD

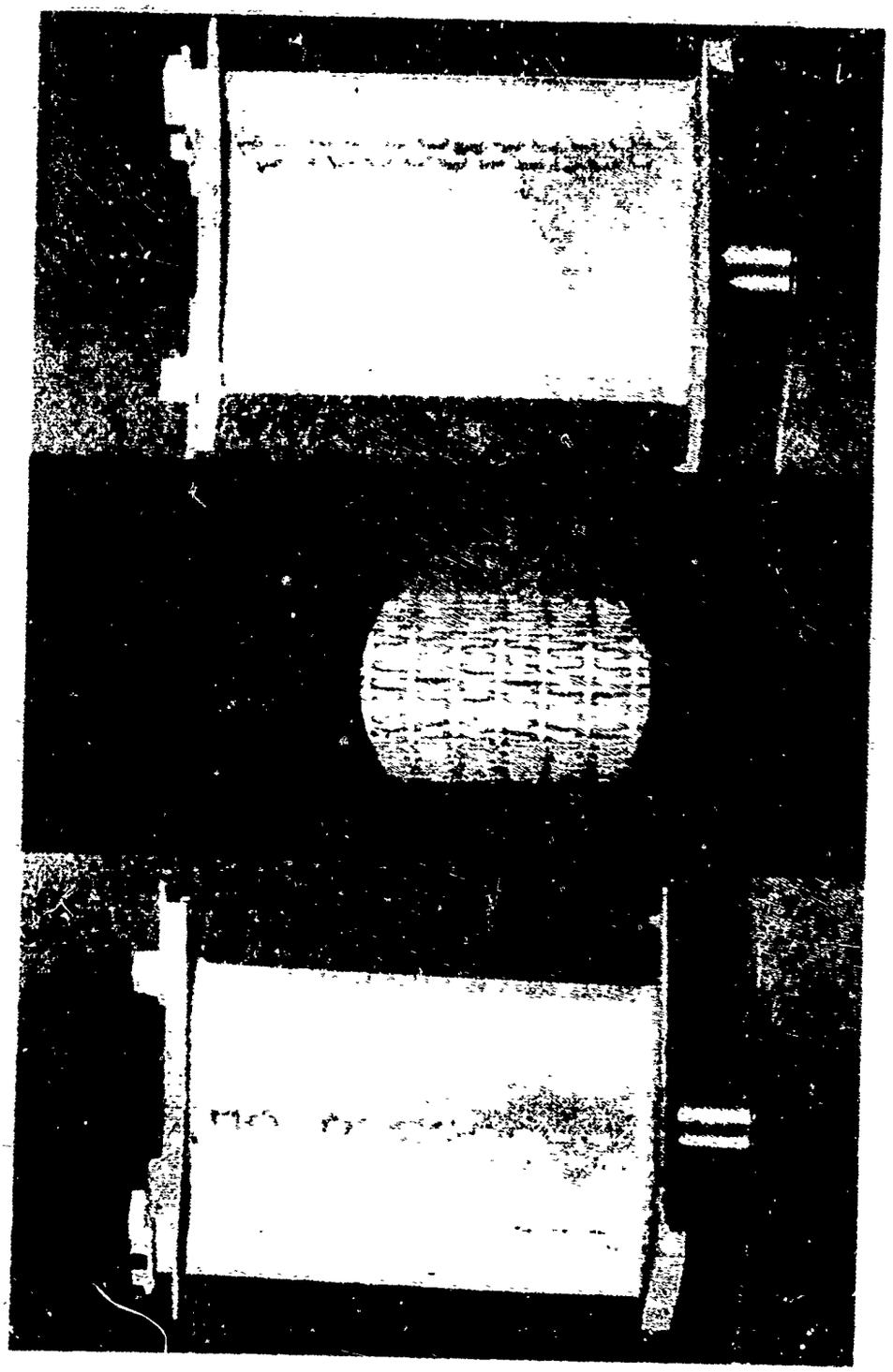
A. FLOW CONTROL
B. BLEED STACK
C. VANE COOLING AIR
D. BLADE COOLING AIR

Figure 6-98



JT4 FILM COOLED VANE FIVE-ROW SHOWER HEAD WITH 0.013-INCH HEADS

Figure 6-99



JT4 FILM COOLED VANE WITH BORON LEADING EDGE

Figure 6-100

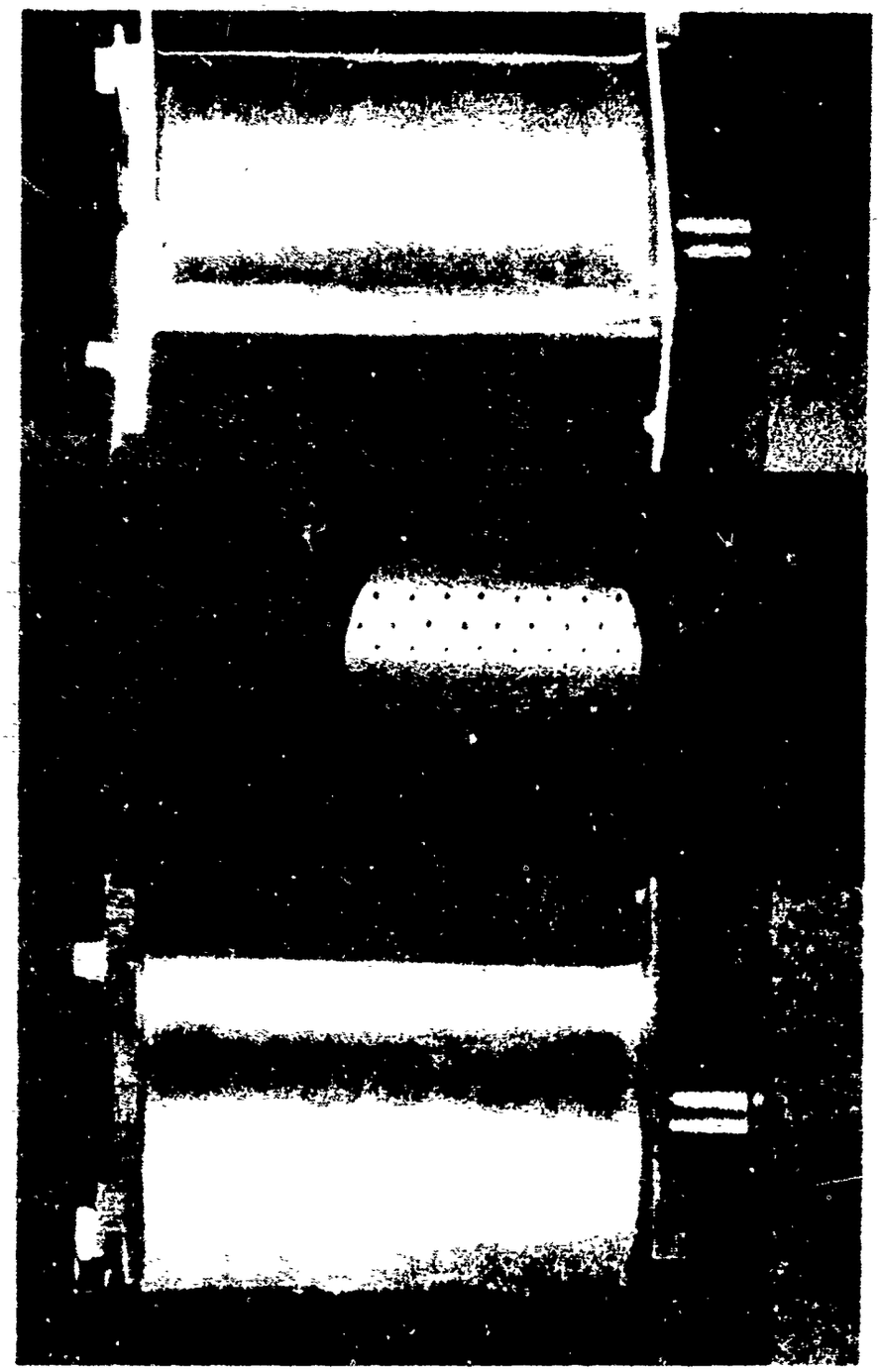
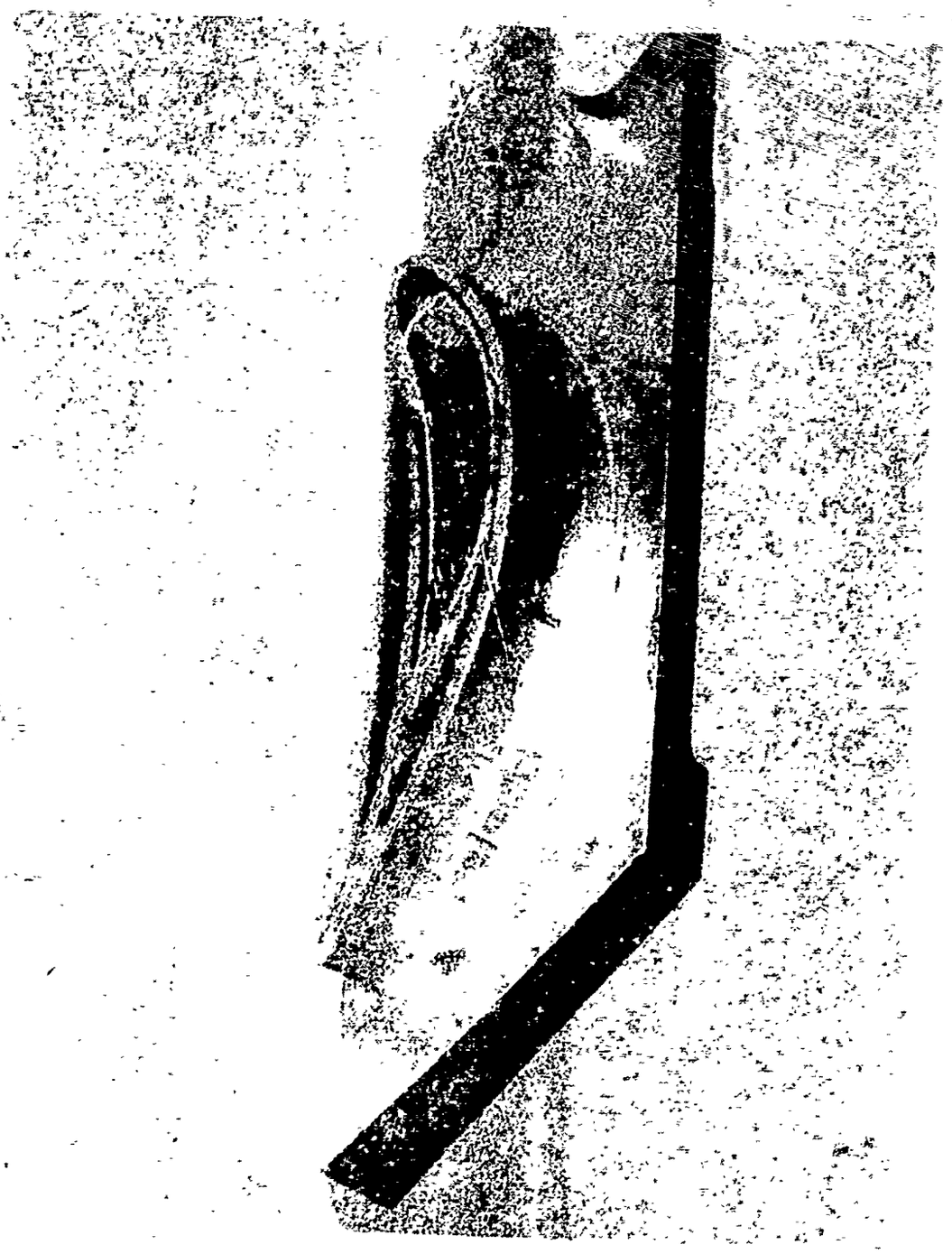
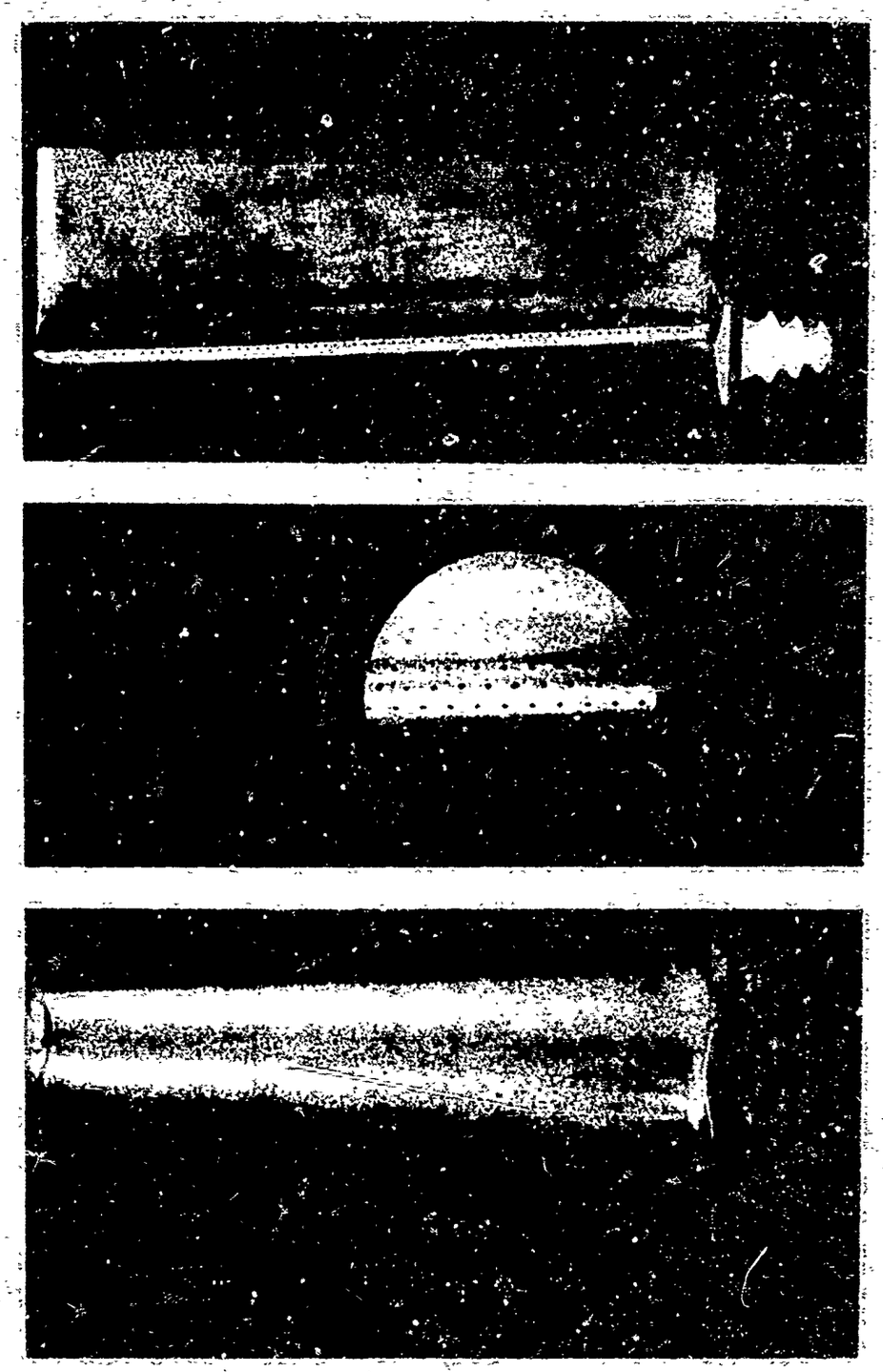


Figure 6-101



IMPINGEMENT VANE SECTIONED TO SHOW METHOD FOR COOLING LEADING EDGE

Figure 6-102

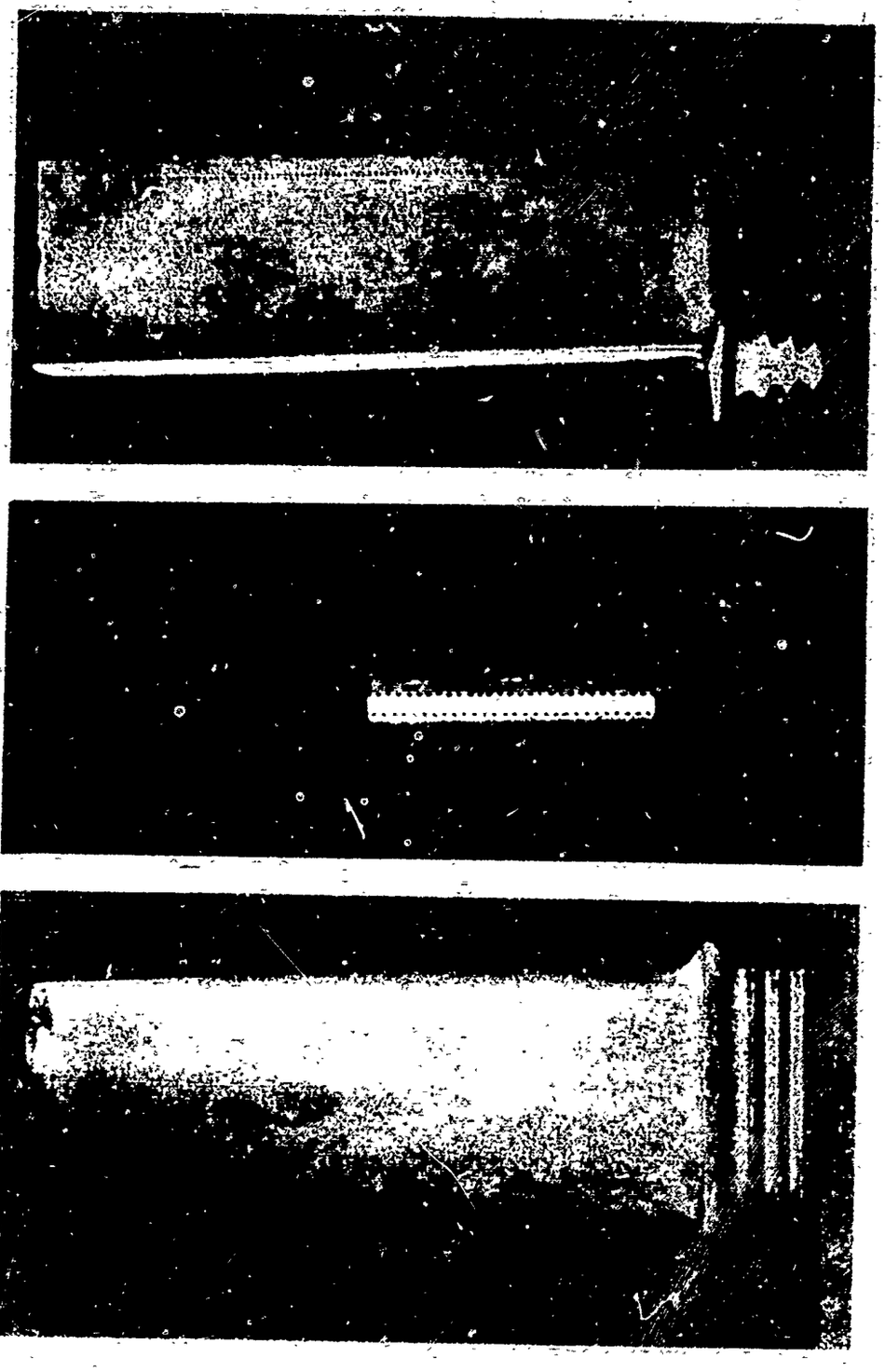


JT4 FILM COOLED BLADE - 3 ROW SHOWER HEAD (.013" DIA. HOLES AT 90° TO SURFACE AT LEADING EDGE) AND .010" DIA. HOLES AT TRAILING EDGE (PRESSURE AND SUCTION SIDES) AT 30° TO SURFACE

Figure 6-103

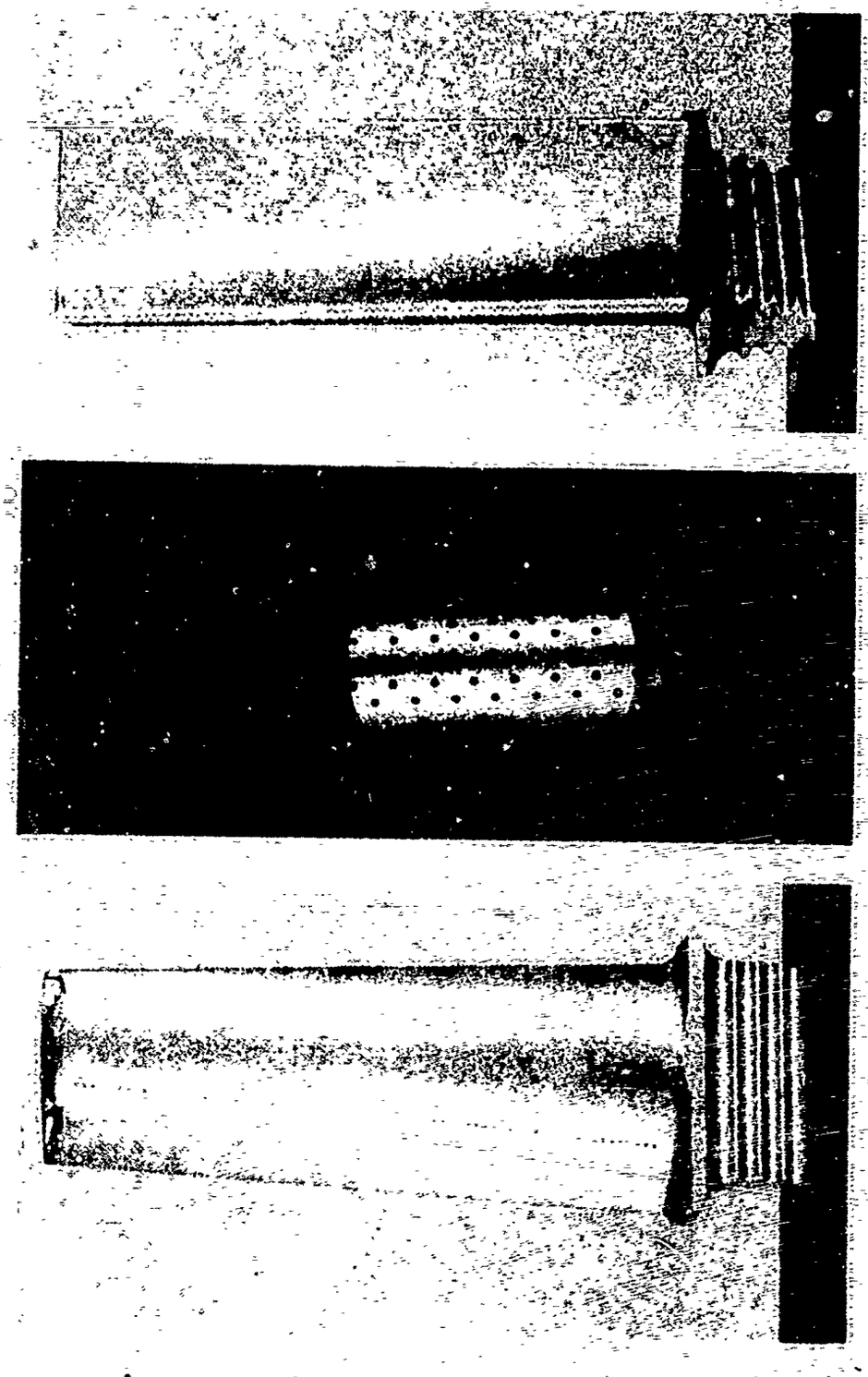
JT4 FILM COOLED BLADE - 3 ROW SHOWER HEAD (.013" DIA. HOLES AT 30° TO SURFACE AT LEADING EDGE) AND .010" DIA. HOLES AT TRAILING EDGE (PRESSURE AND SUCTION SIDE) AT 30° TO SURFACE

Figure 6-164



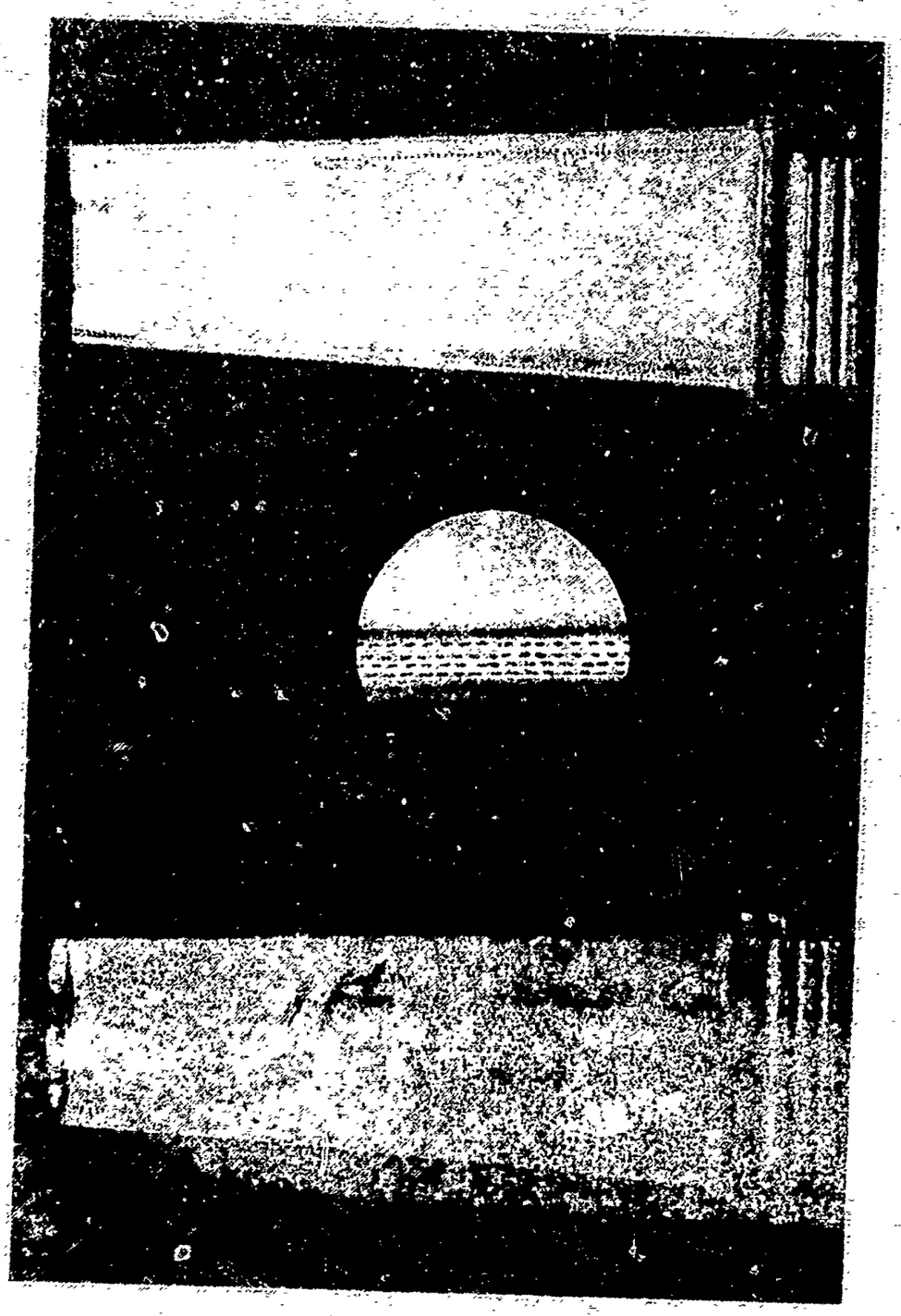
JT4 FILM COOLED BLADE - 3 ROW SHOWER HEAD (.008" DIA HOLES AT 90° TO SURFACE AT LEADING EDGE) AND .010" DIA. HOLES AT TRAILING EDGE (PRESSURE SIDE ONLY) AT 30° TO SURFACE

Figure 6-105



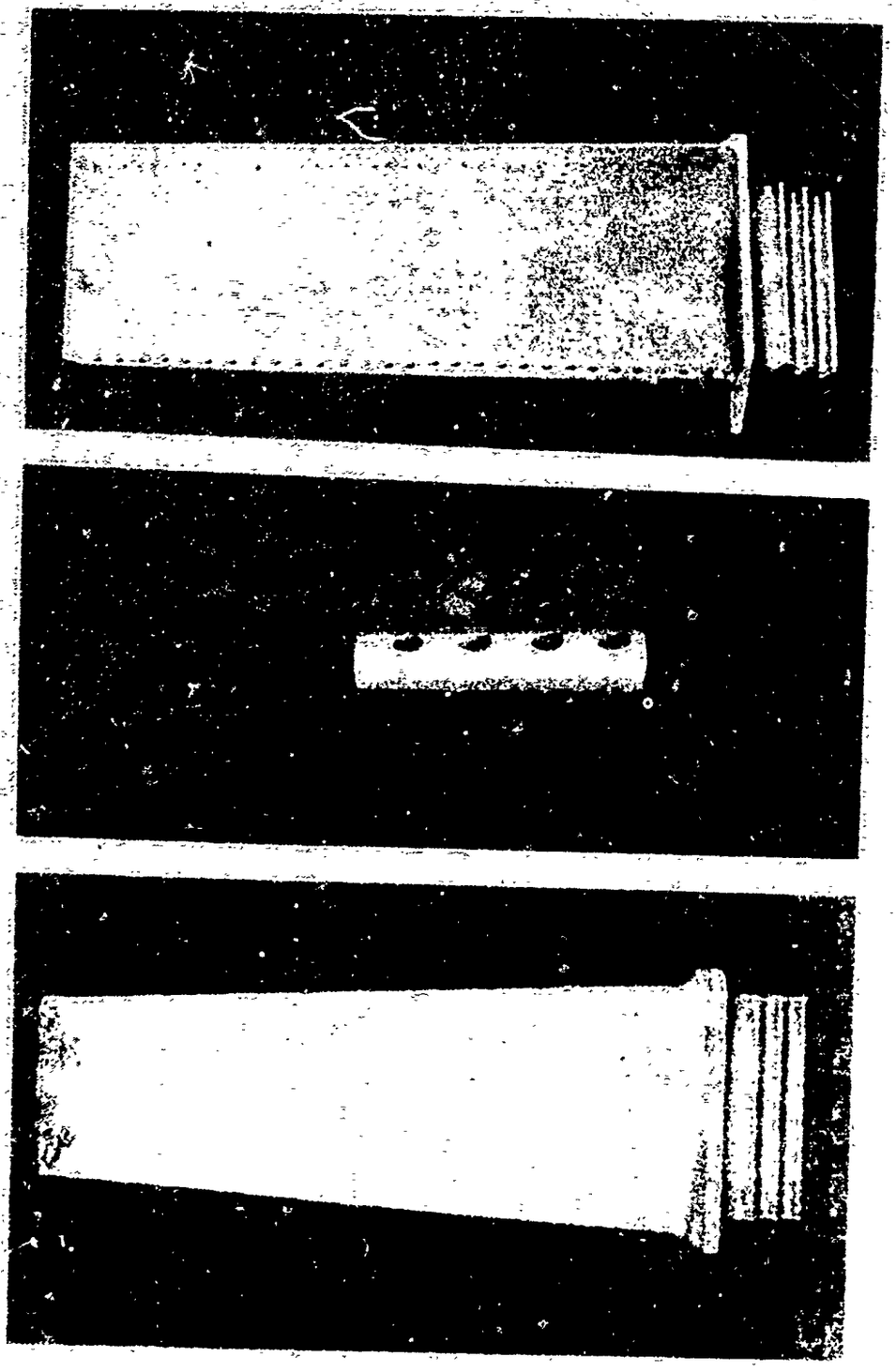
JT4 FILM COOLED BLADE - 5 ROW SHOWER HEAD (.008" DIA. HOLES AT 90° TO SURFACE AT LEADING EDGE) AND .013" DIA. HOLES AT TRAILING EDGE (PRESSURE AND SUCTION SIDES) AT 30° TO SURFACE

Figure 6-106



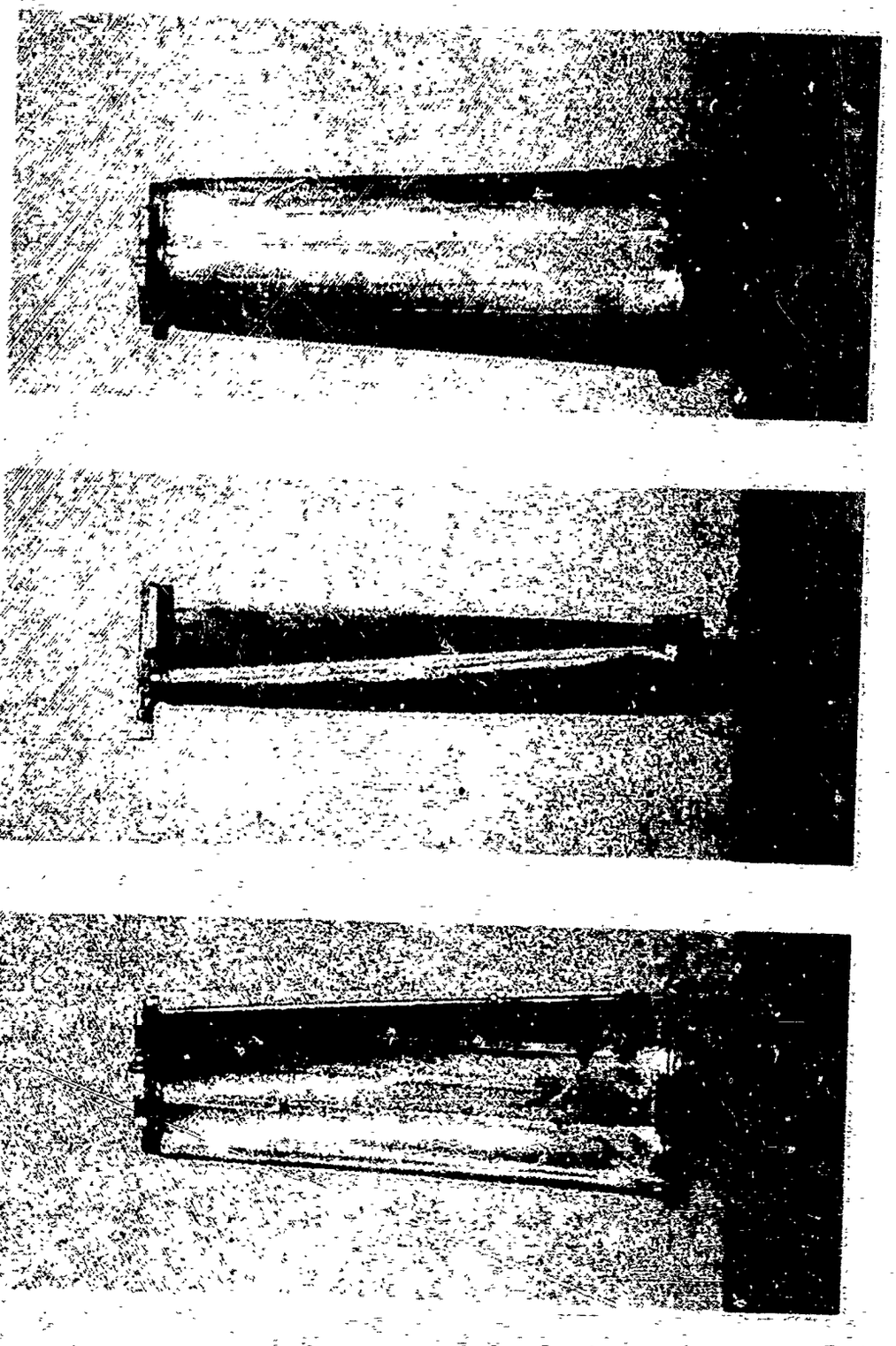
JT4 FIRST STAGE TURBINE BLADE - 5 ROW SHOWER HEAD (.008" DIA. HOLES AT 30° TO SURFACE AT LEADING EDGE) AND .010" DIA. HOLES AT TRAILING EDGE (PRESSURE AND SUCTION SIDES) AT 30° TO SURFACE

Figure 6-107



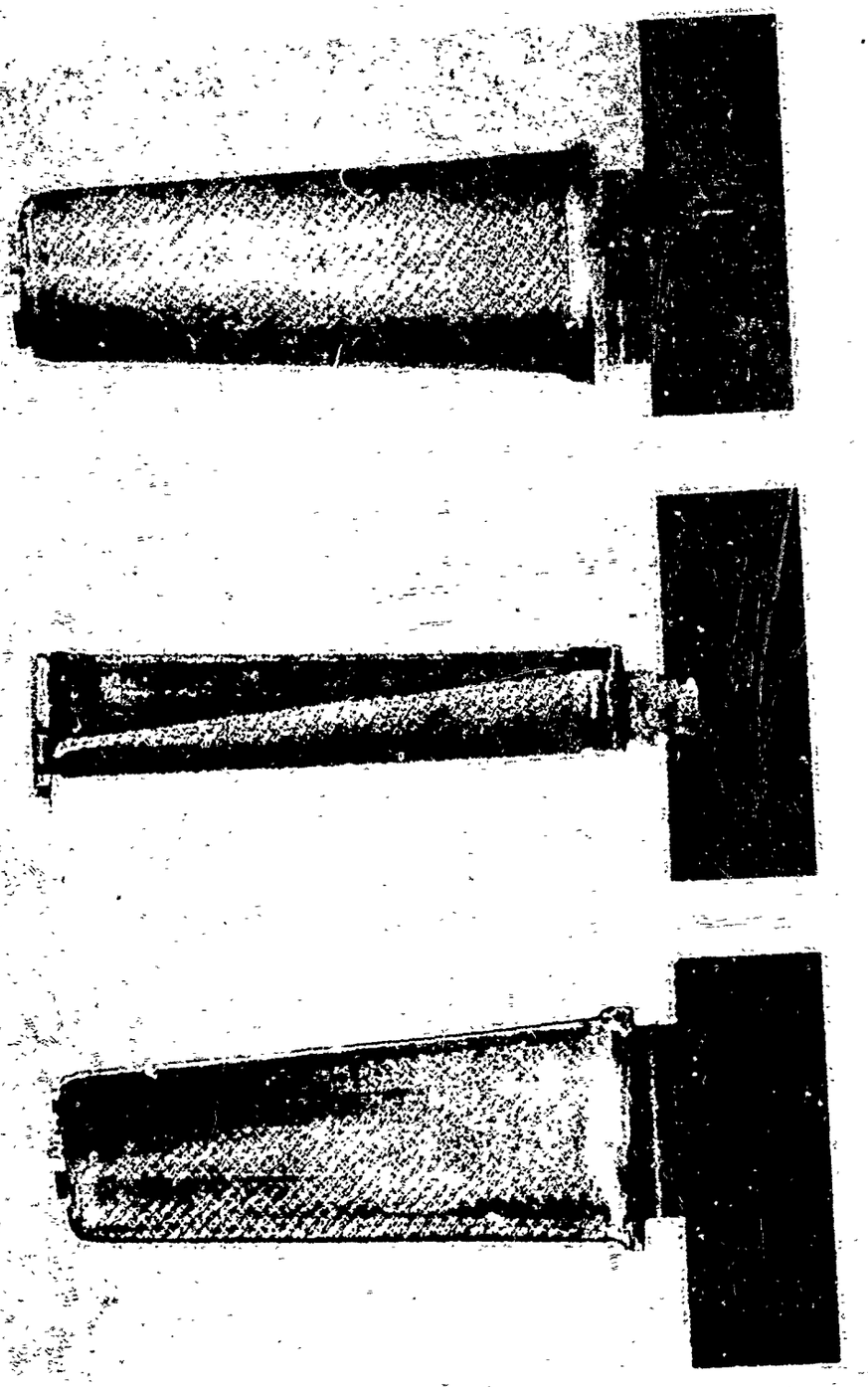
JT4 FILM COOLED BLADE, 0.04-INCH DIAMETER HOLES AT 30° TO LEADING EDGE

Figure 6-108



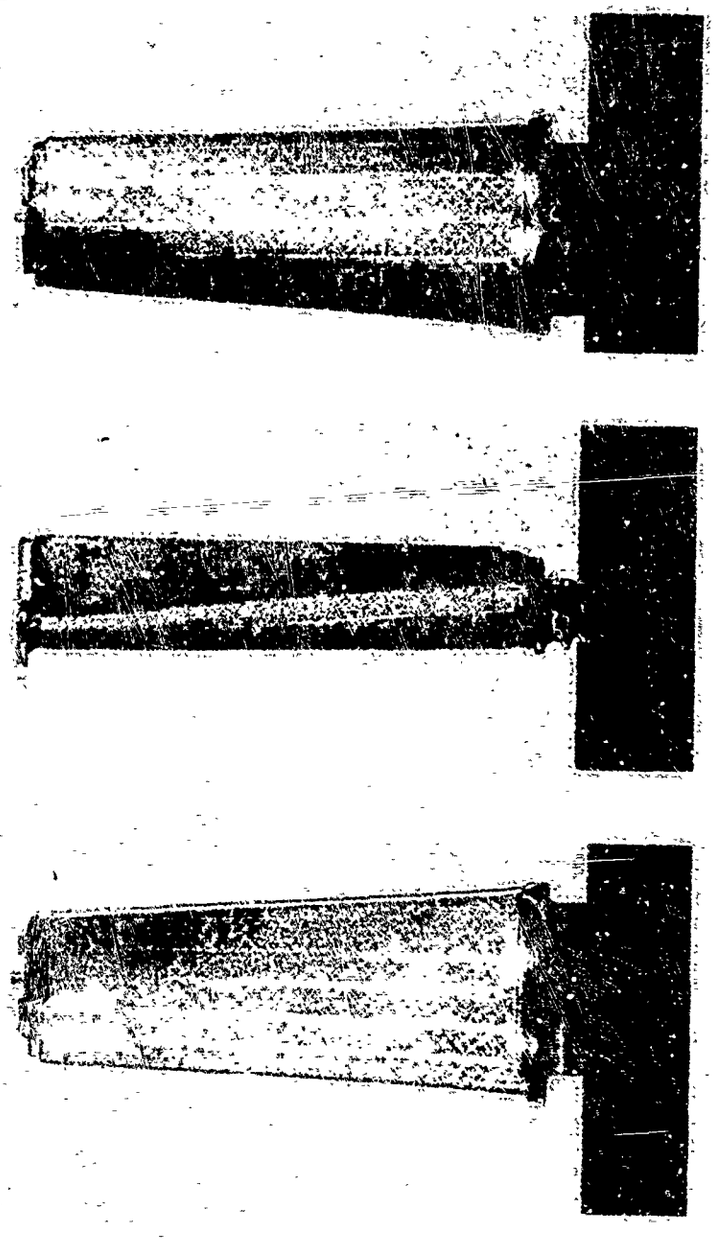
NARROW LAND BLADES - N155 POROLOY SKIN - EB WELD ATTACHMENT (.040" INTERFACE)
TRANSPIRATION COOLED

Figure 6-109



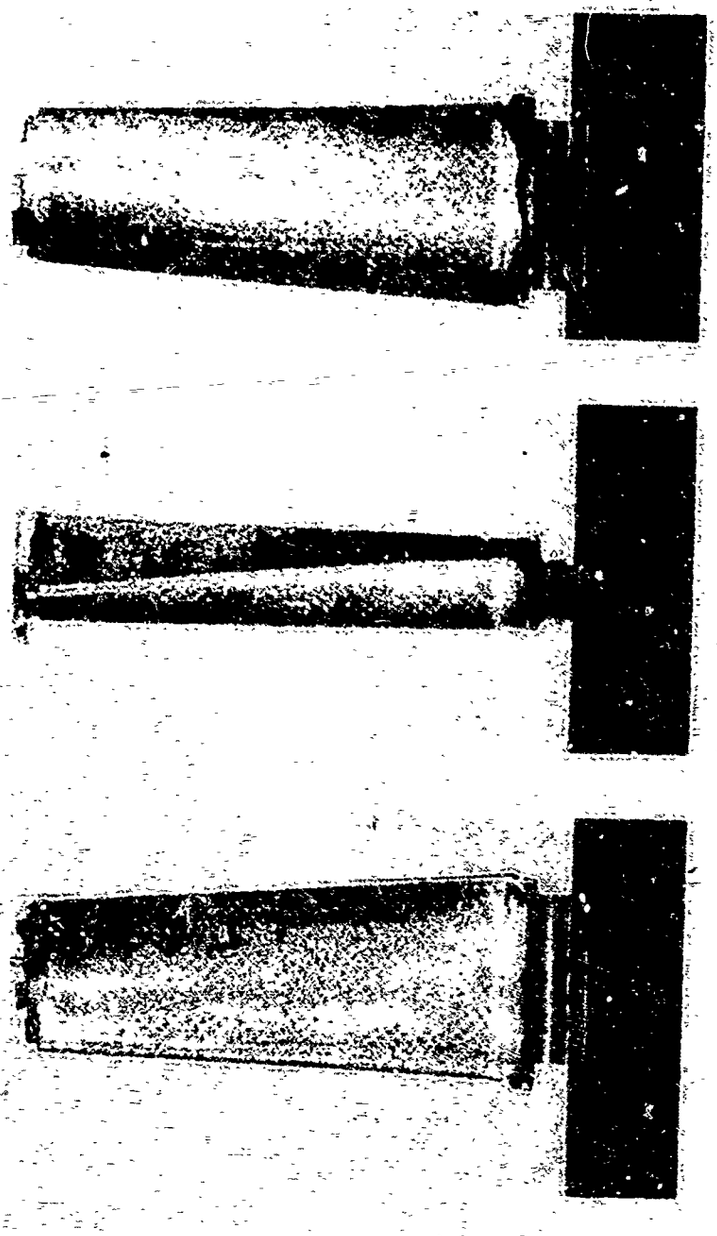
NARROW LAND BLADES - N155 REGIMESH SKIN - BRAZE 82-18 ATTACHMENT - TRANSPIRATION COOLED

Figure 6-110



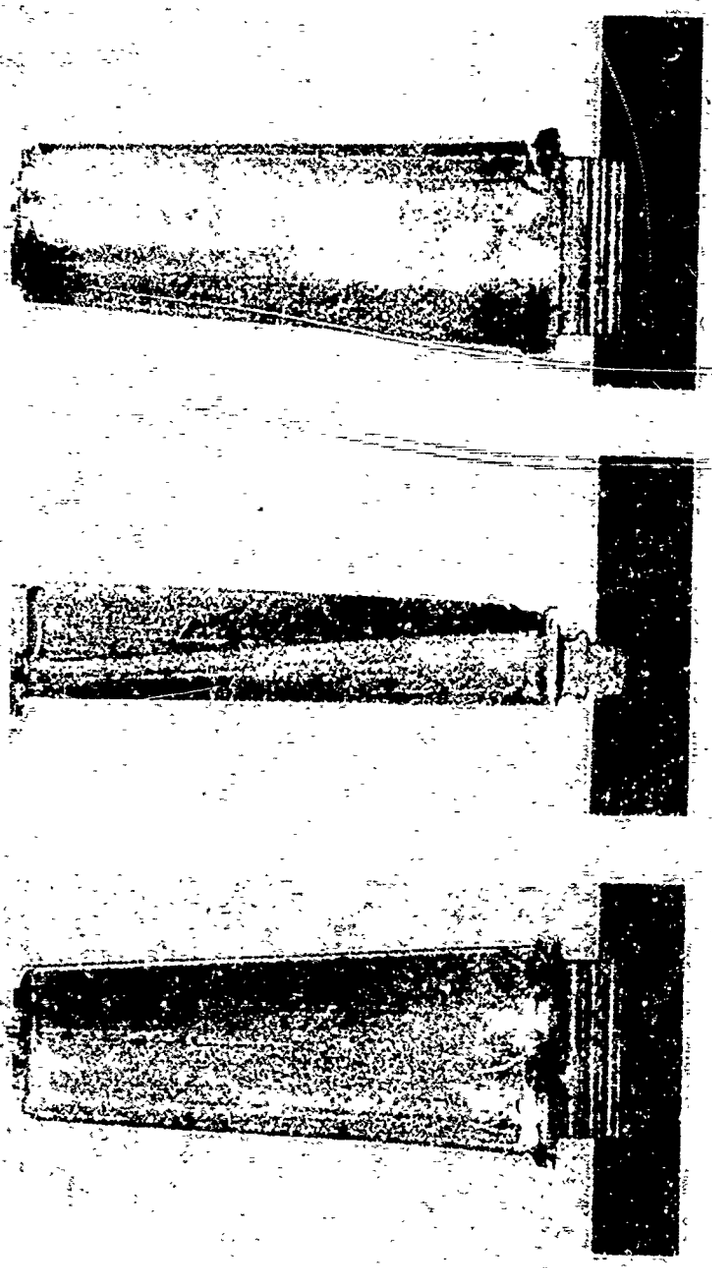
WIDE LAND BLADES - L605 REGIMESH SKIN - ER WELD ATTACHMENT (.040" INTERFACE) - TRANSPIRATION COOLED

Figure 6-111



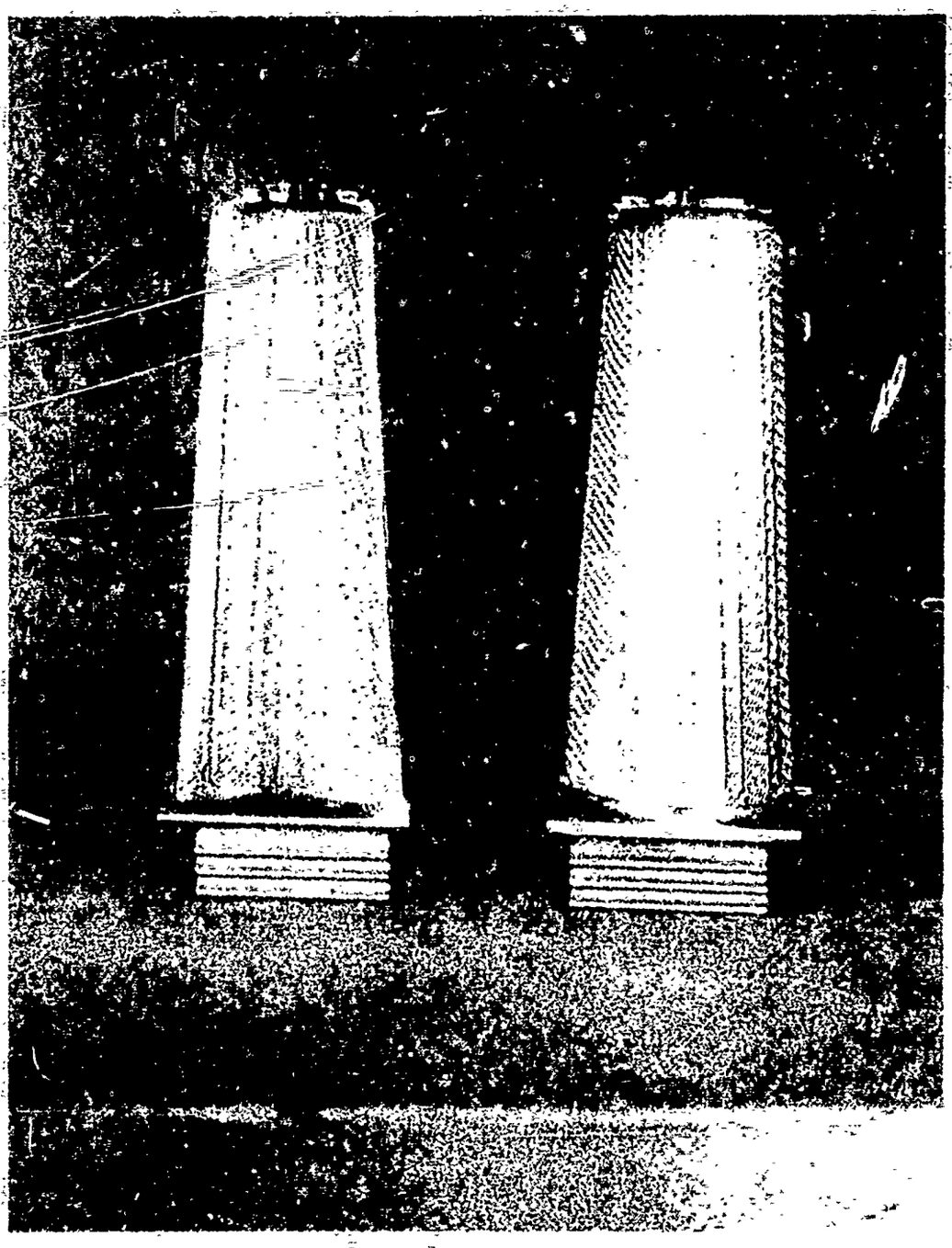
WIDE LAND BLADES - N155 REGIMESH SKIN - BRAZE 82-18 ATTACHMENT - TRANSPIRATION COOLED

Figure 6-112



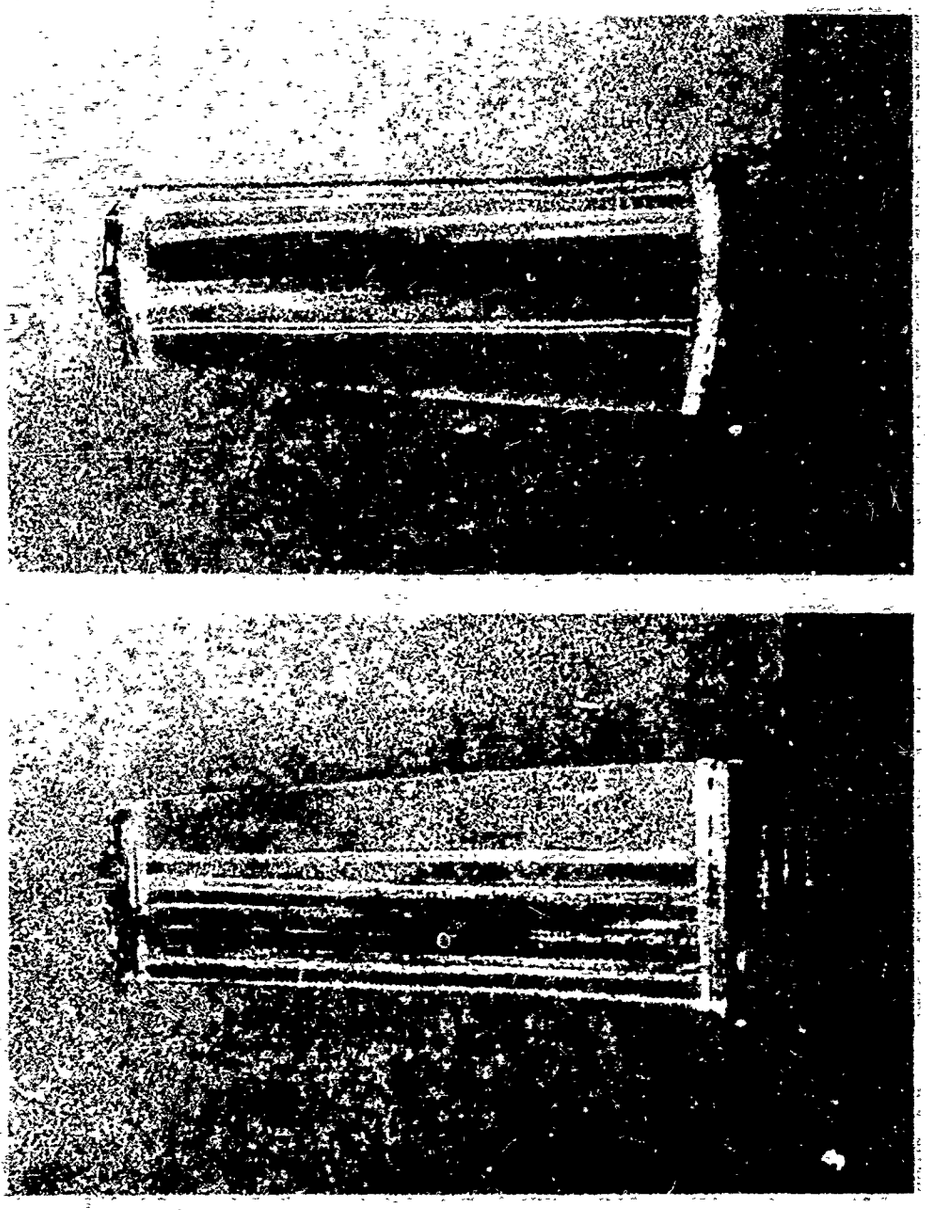
WIDE LAND BLADES - L605 REGIMESH SKIN - EB WELD ATTACHMENT (.072" INTERFACE) - TRANSPIRATION COOLED

Figure 6-113



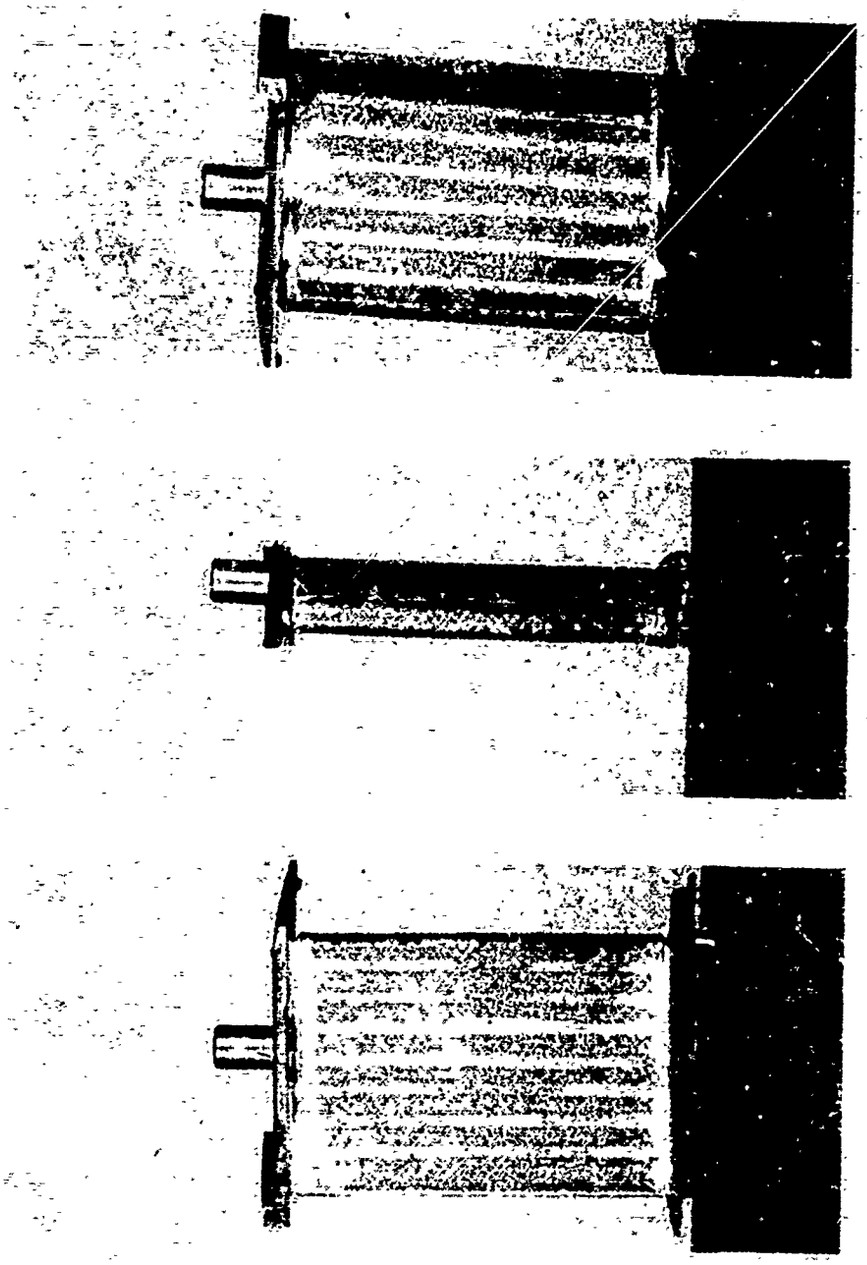
WIDE LAND BLADE - L605 REGIMESH SKIN - EB WELD
ATTACHMENT - H-47986 TRANSPIRATION COOLED

Figure 6-114



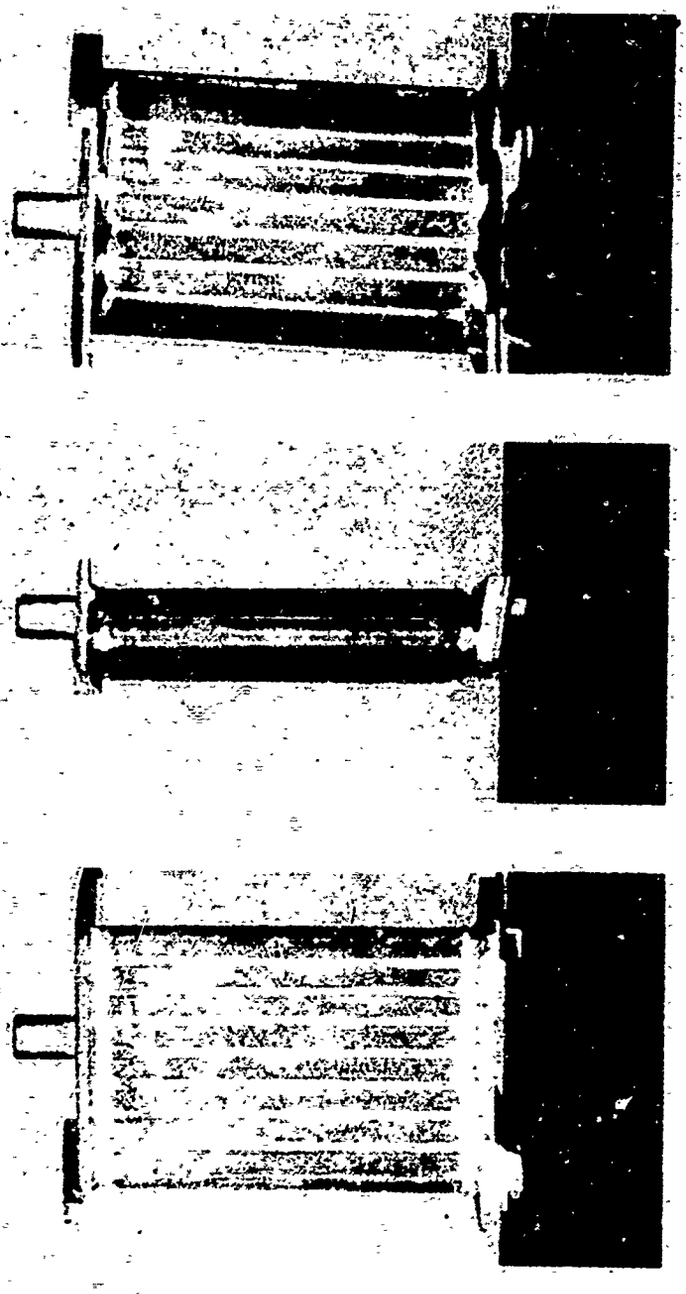
WIDE LAND BLADE - N155 POROLOY SKIN - EB WELD ATTACHMENT TRANSPIRATION COOLED

Figure 6-115



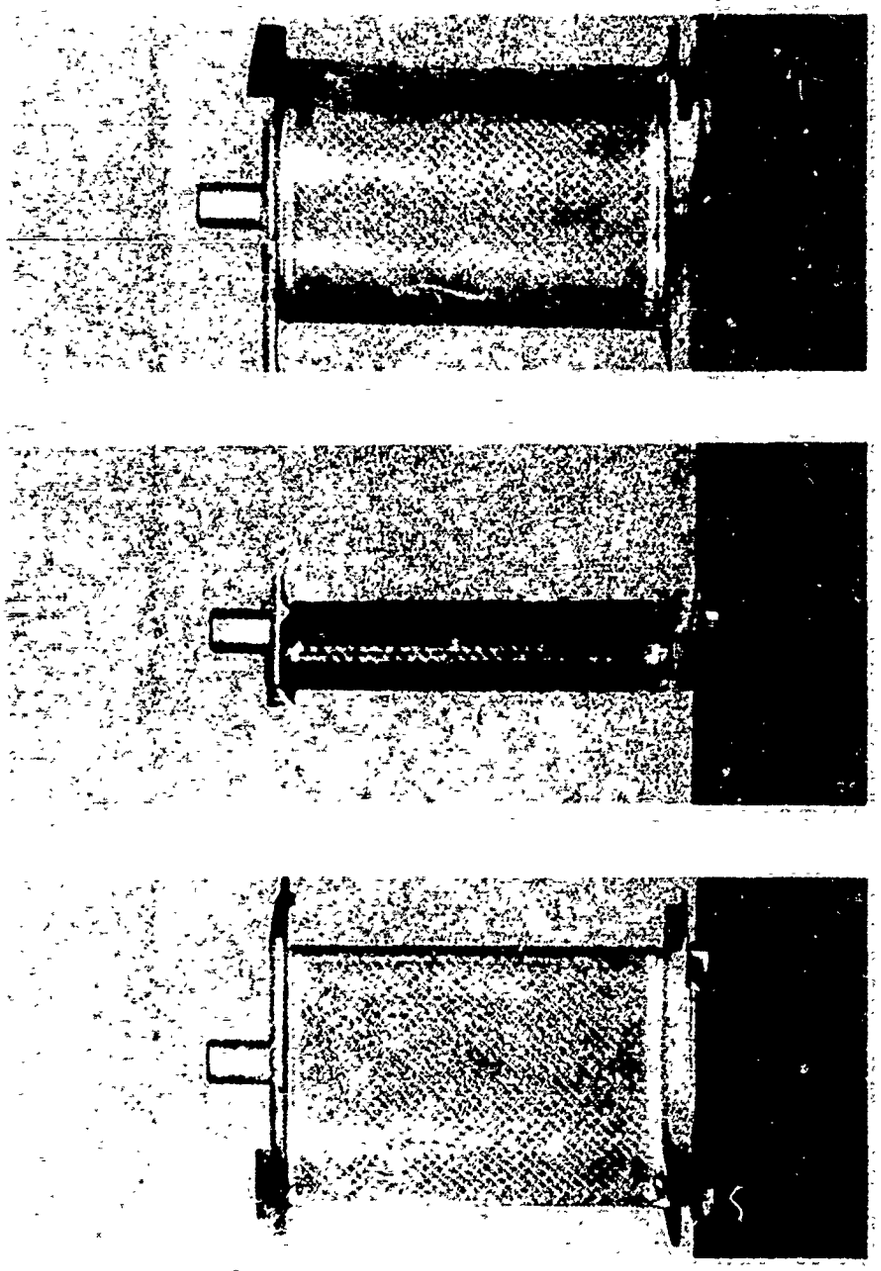
WIDE LAND VANES - L60[illegible] REGIMESH SKIN - EB[illegible]WELD ATTACHMENT - TRANSPIRATION COOLED

Figure 6-116



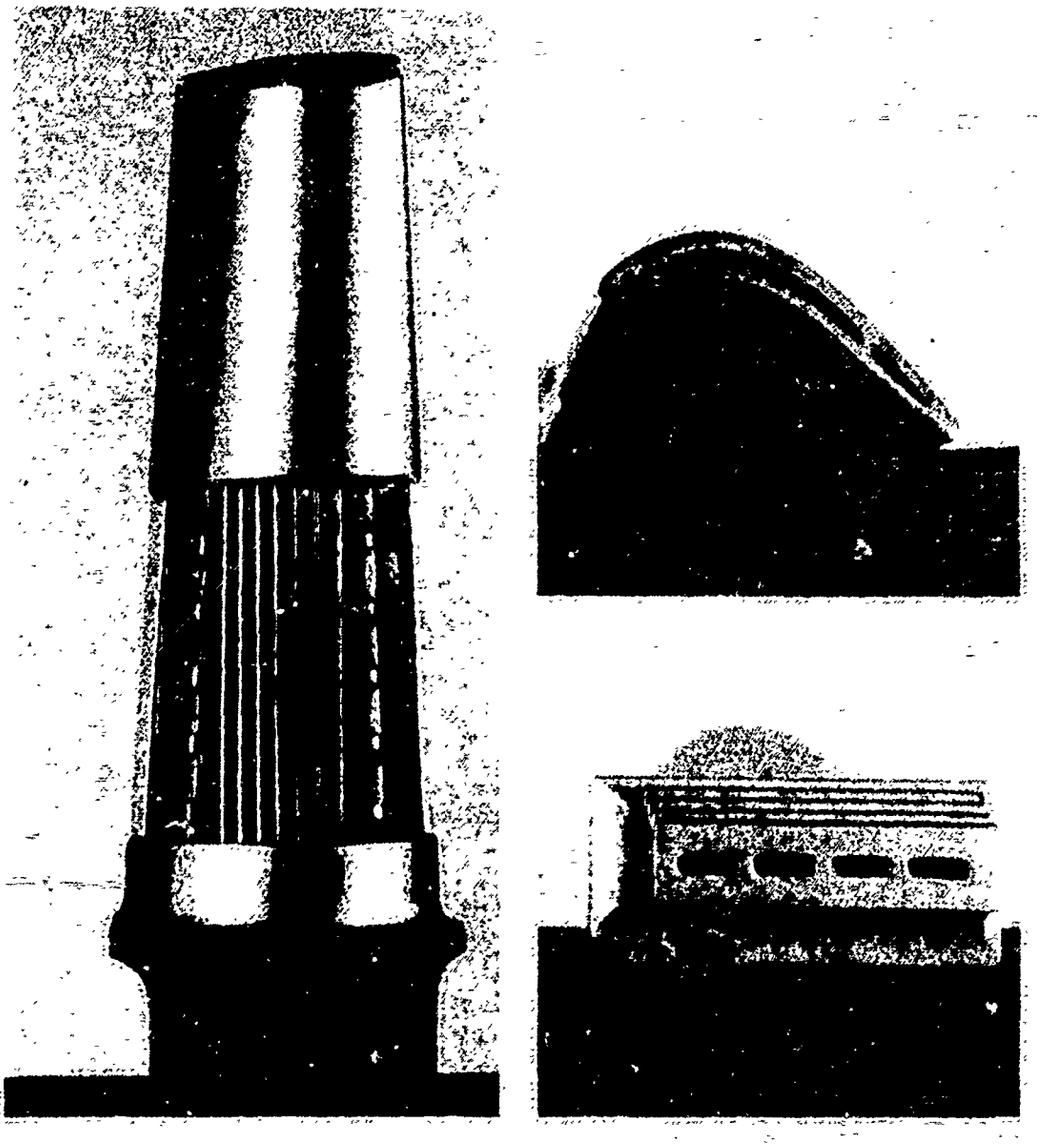
WIDE LAND VANE - N155 POROLOY SKIN - EB WELD ATTACHMENT - TRANSPIRATION COOLED

Figure 6-117



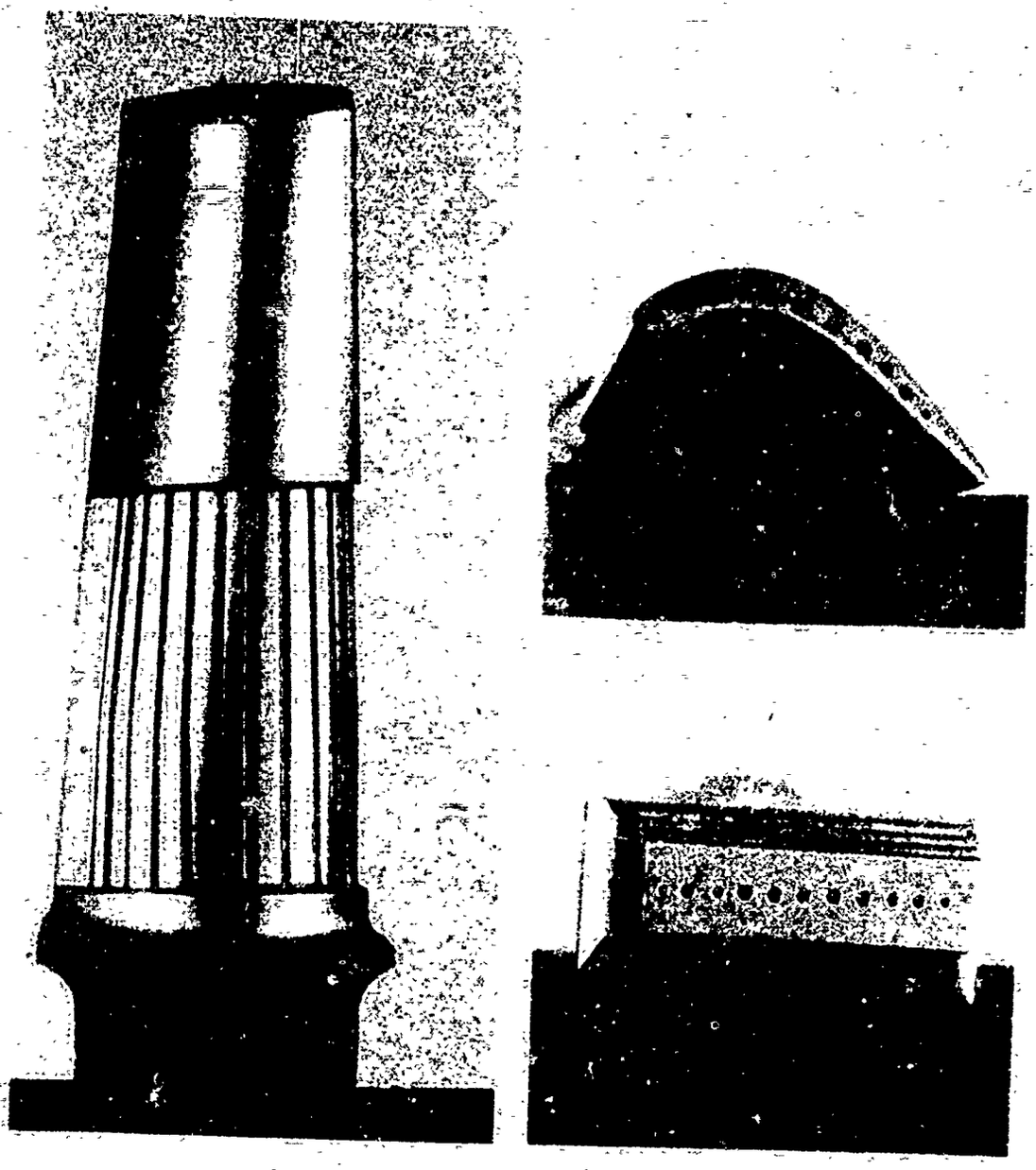
WIDE LAND VANE - N155 REGIMESH SKIN - BRAZE 82-18 ATTACHMENT - TRANSPIRATION COOLED

Figure 6-118



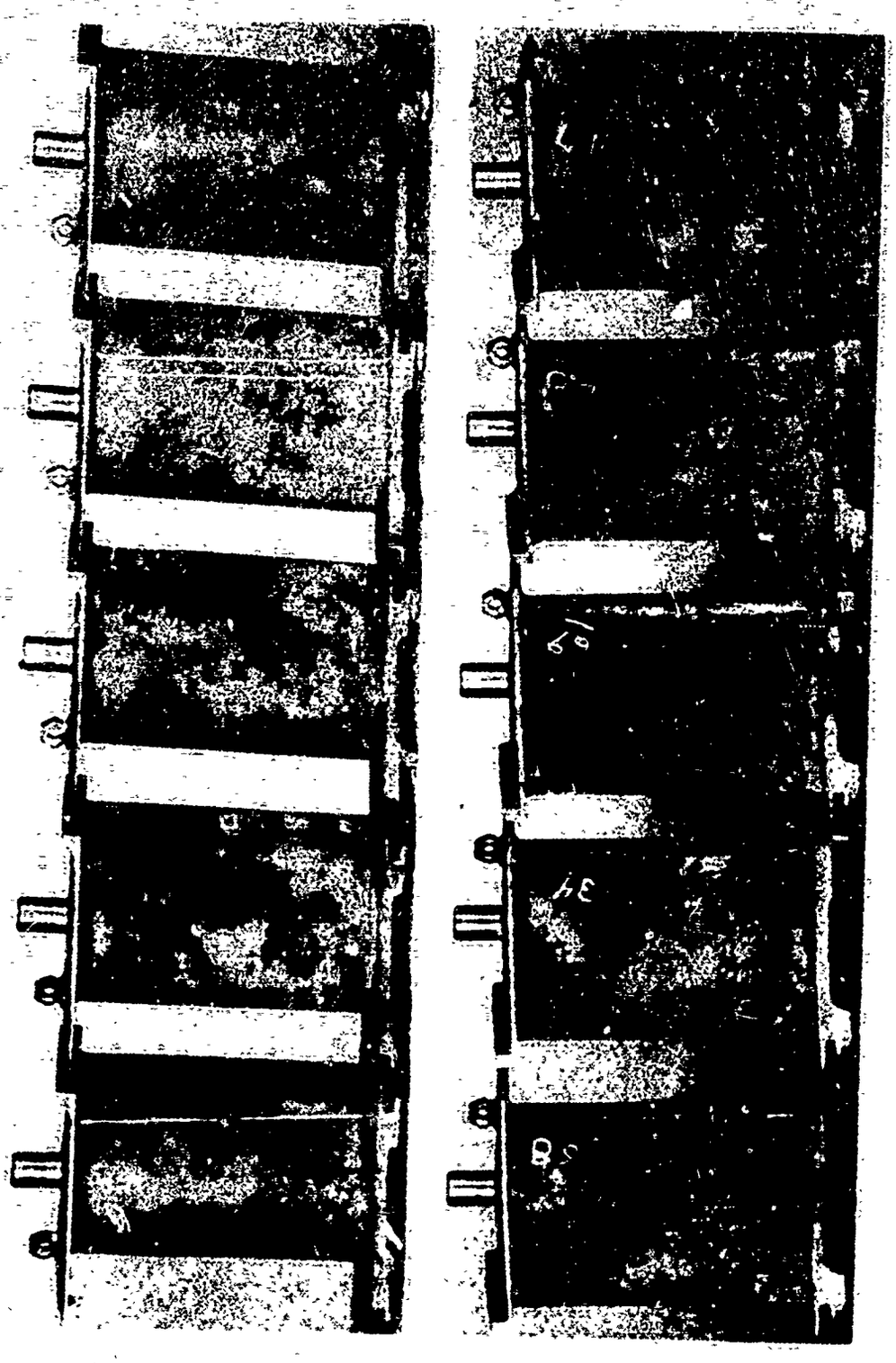
JT4 TURBINE BLADE, .030" SAWTOOTH COOLING PASSAGE DESIGN, MATERIAL PWA-655

Figure 6-119



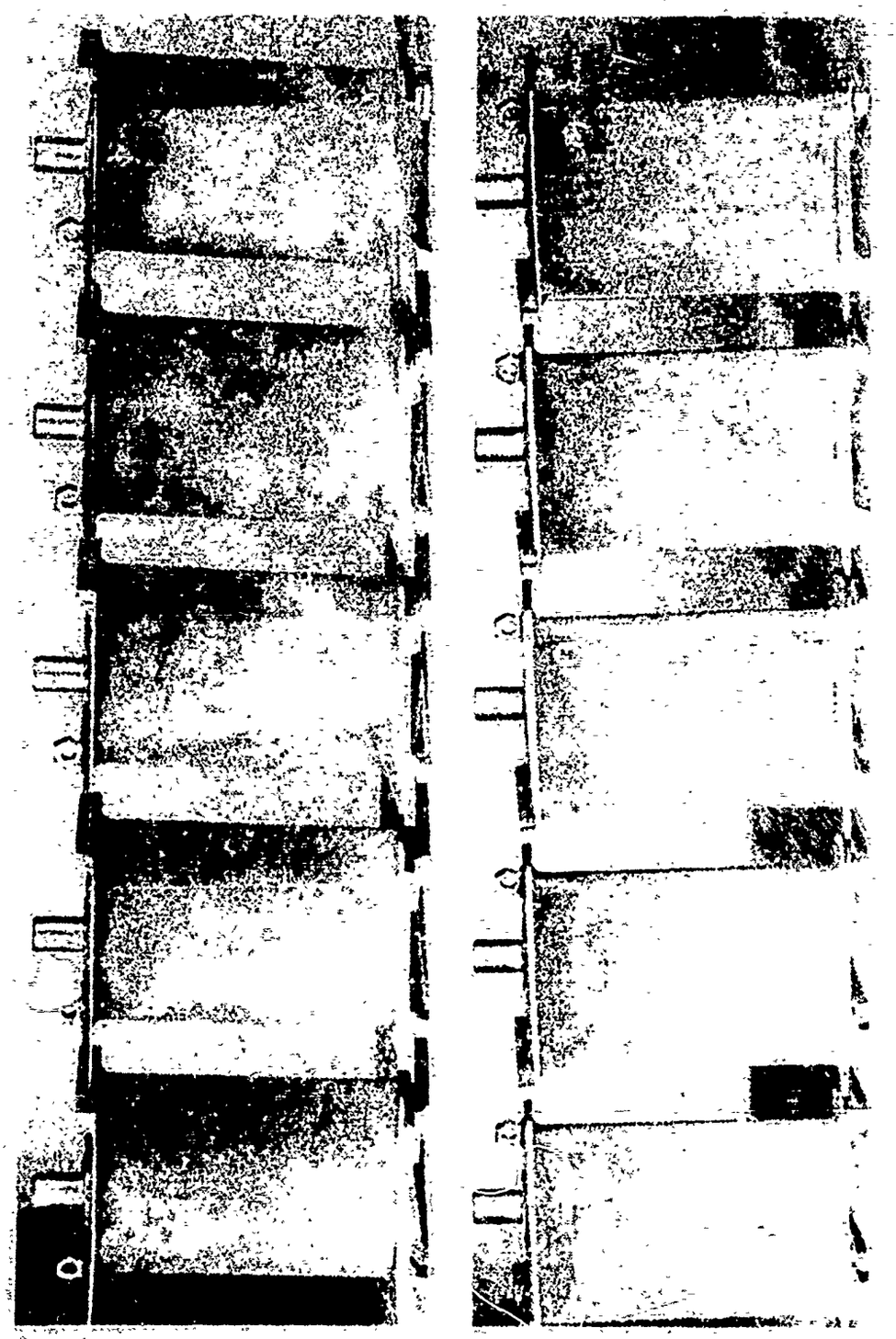
JT4 TURBINE BLADE, 11-HOLE COOLING PASSAGE DESIGN,
MATERIAL PWA-658 AND PWA-663

Figure 6-120



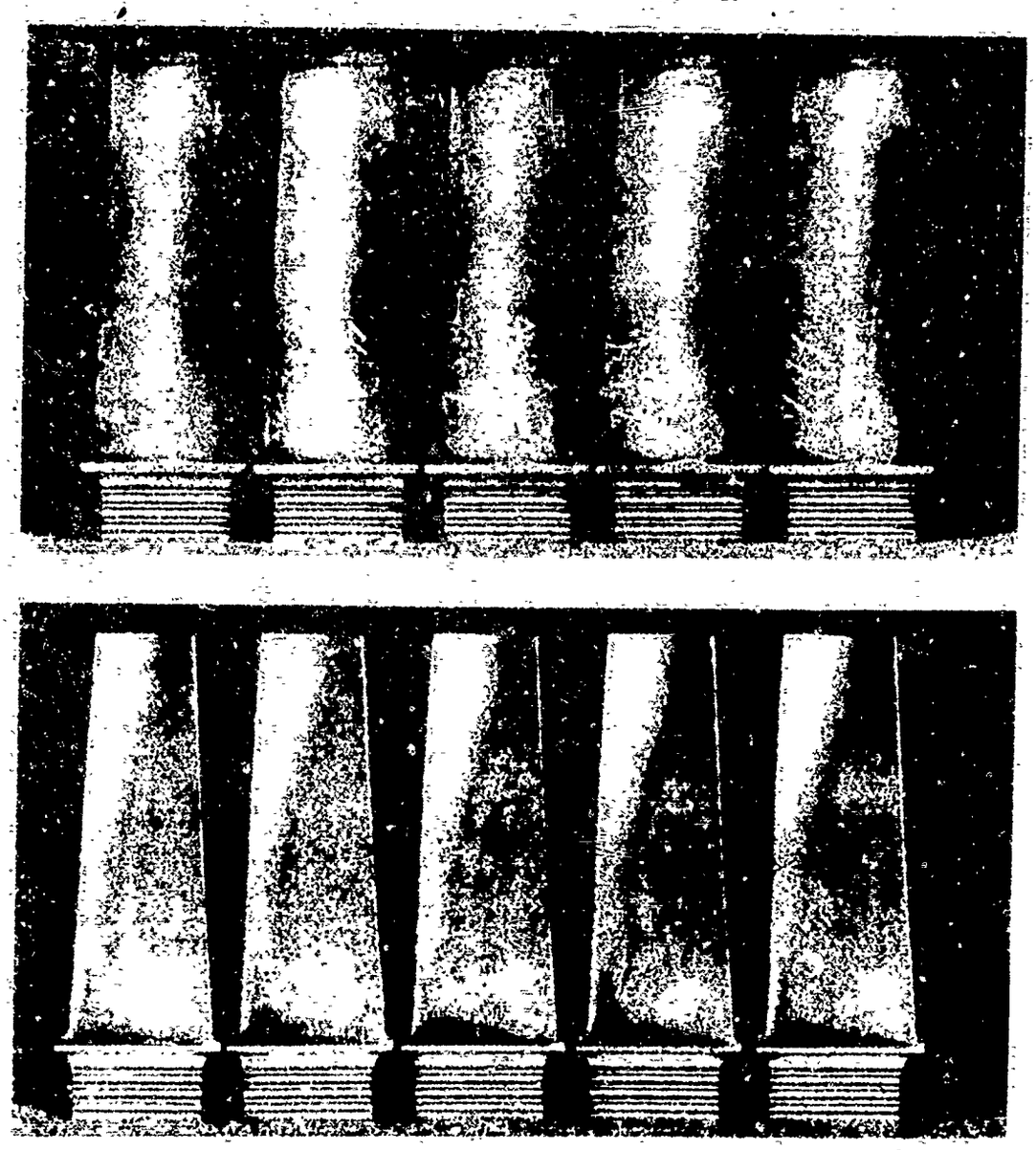
PWA 657 SLOTTED TRAILING EDGE VANES AFTER 155 CYCLES AT 2235°F

Figure 6-121



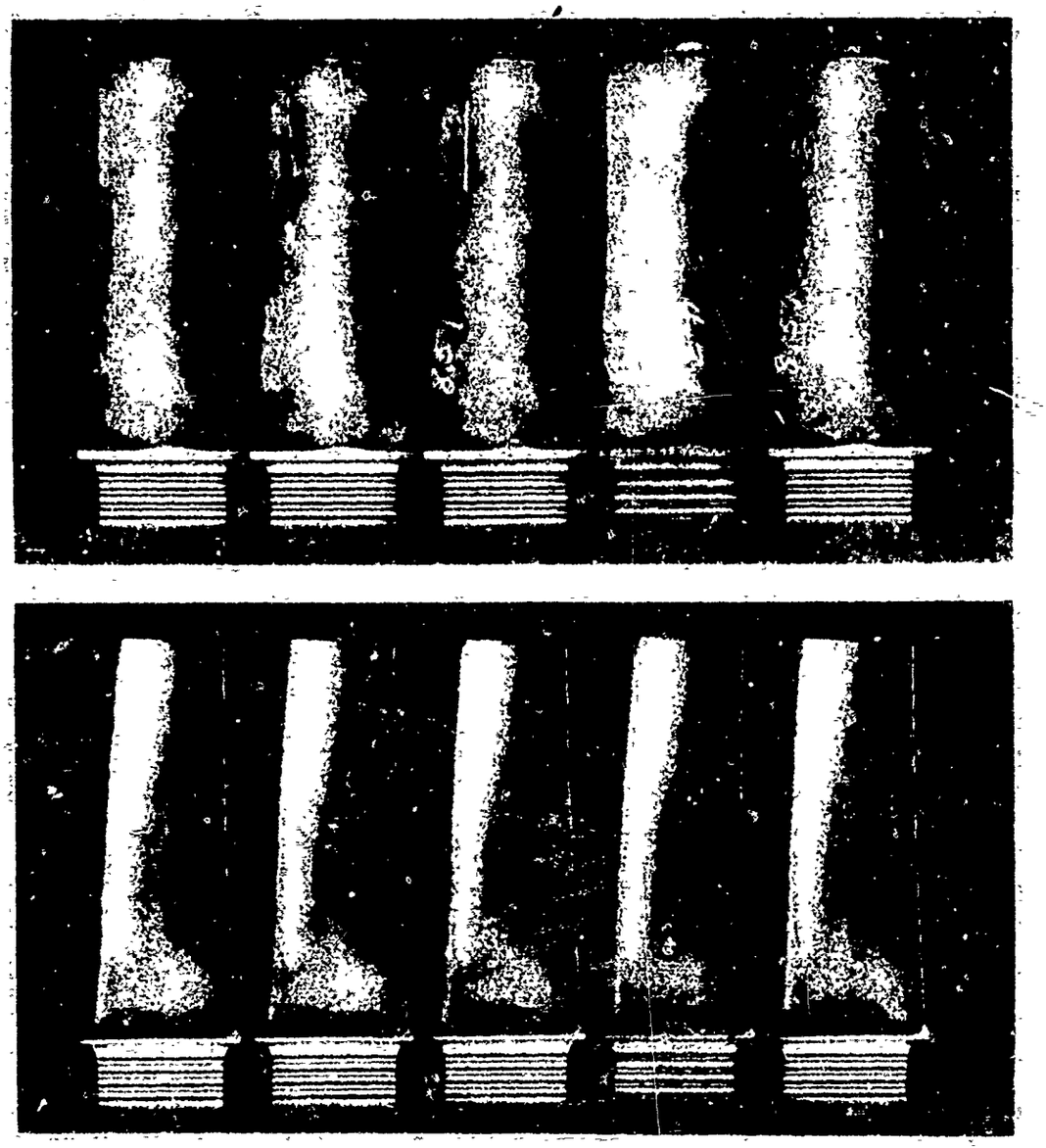
PWA 657 PEDESTAL TRAILING EDGE VANES AFTER 155 CYCLES AT 2235°F

Figure 6-122



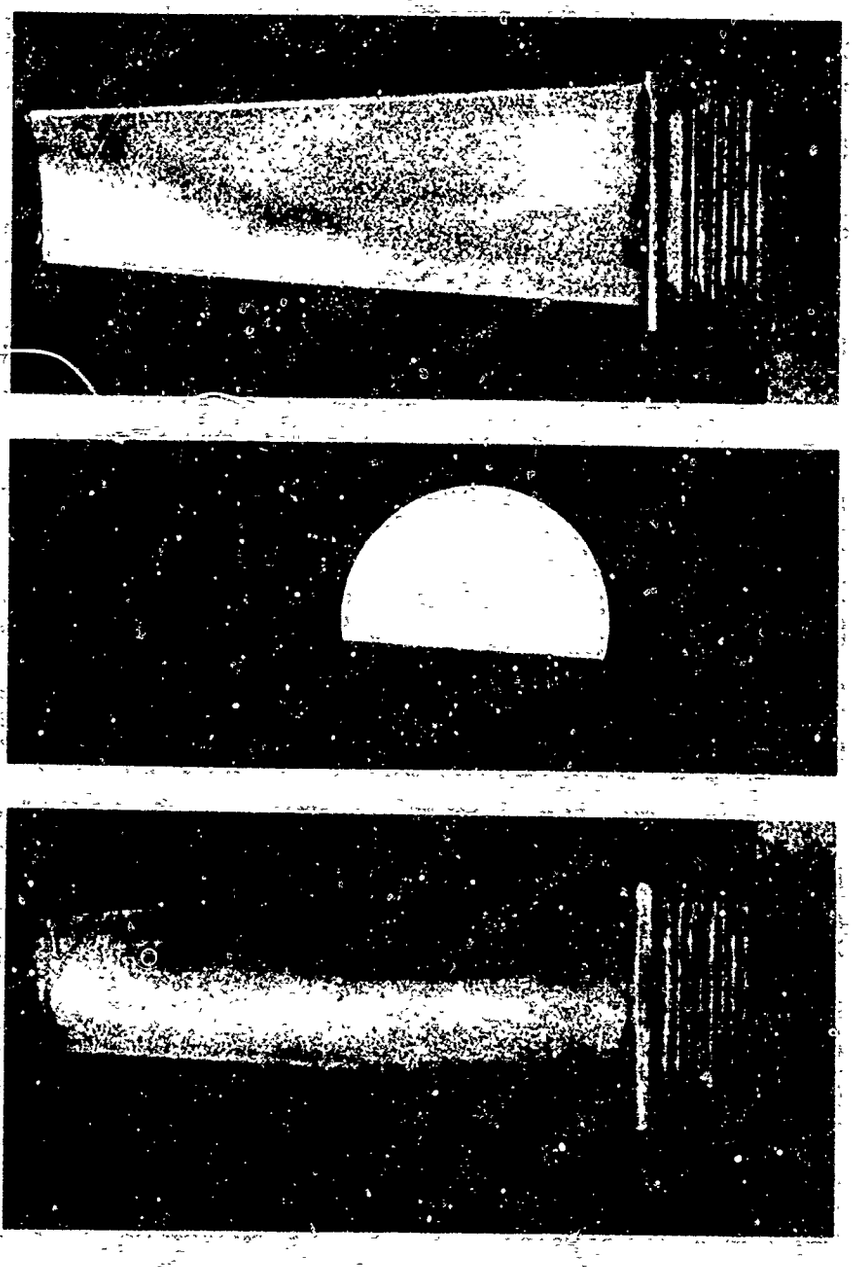
PWA 659 0.02-INCH SAWTOOTH BLADES AFTER 1030 CYCLES AT 2235°F

Figure 6-123



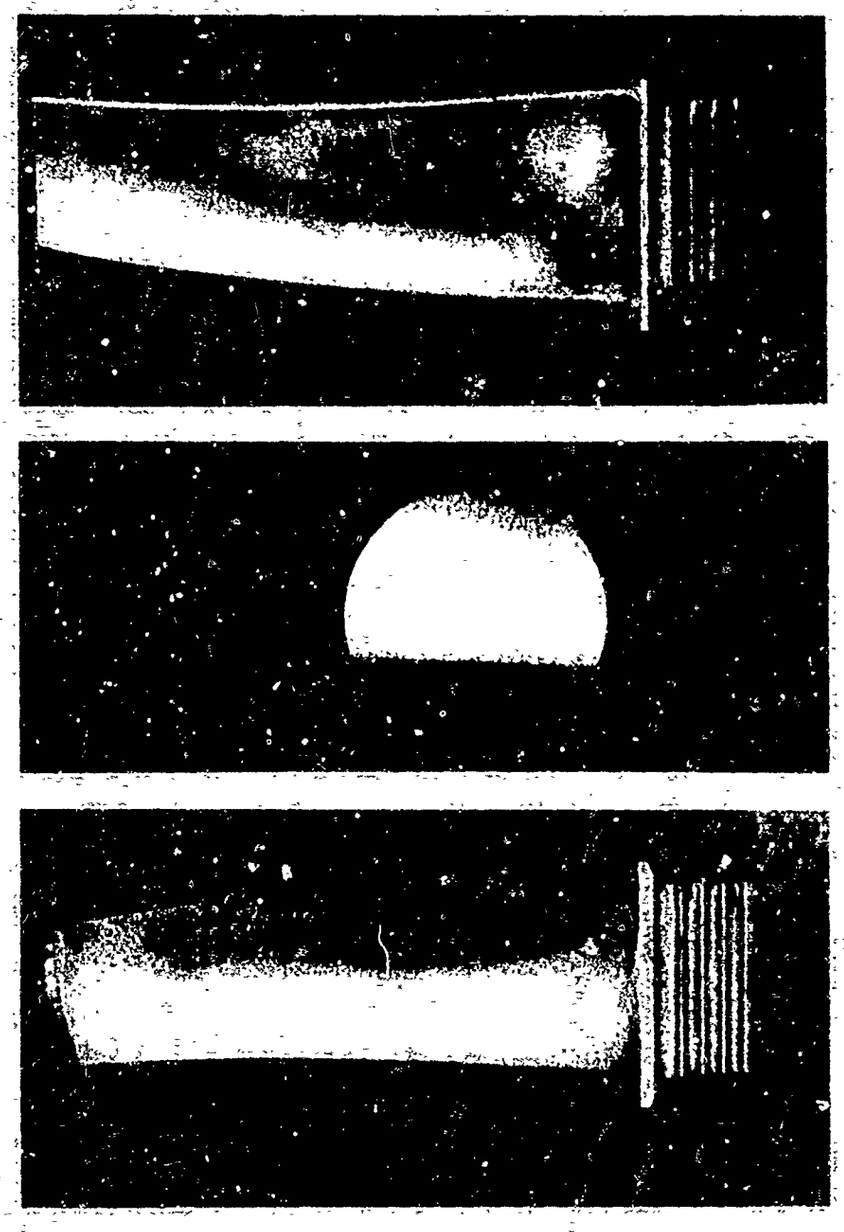
PWA 663 ELEVEN-HOLE BLADE AFTER 1030 CYCLES AT 2235°F

Figure 6-124



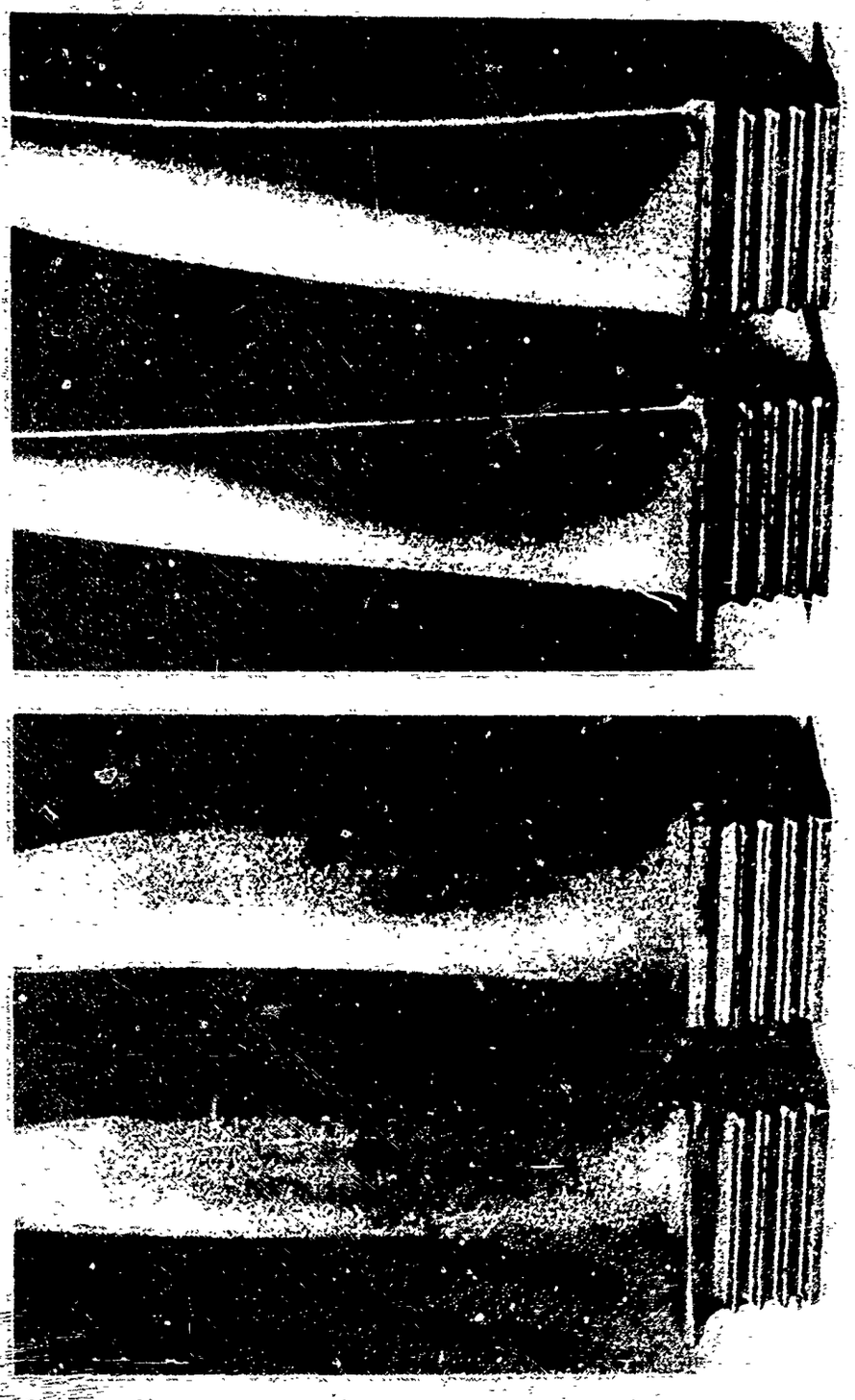
PWA 659 $TaAl_3$ COATED 0.02-INCH SAWTOOTH BLADE WITH LEADING EDGE CRACK

Figure 6-125



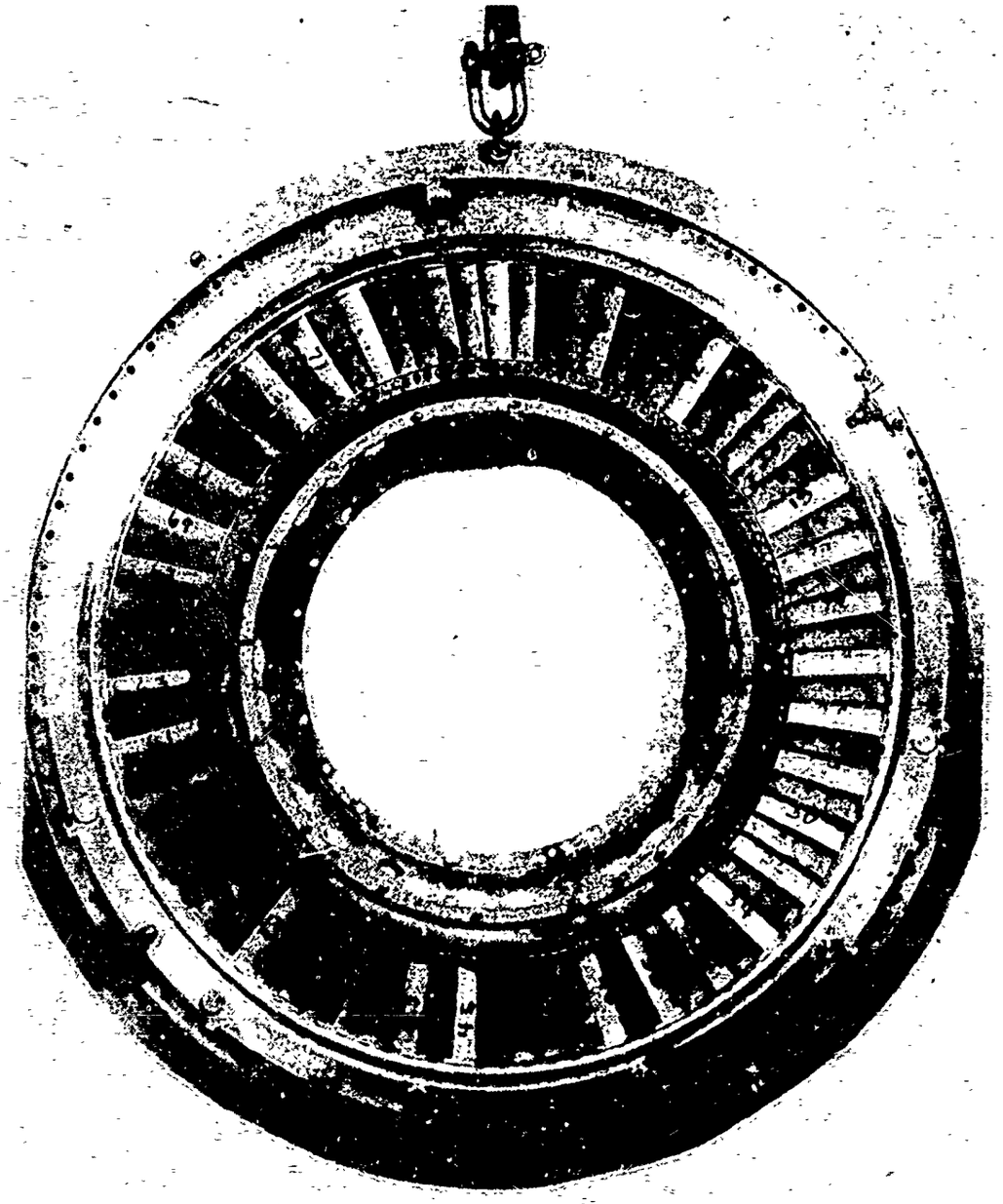
PWA 658 ELEVEN-HOLE BLADE SHOWING BOWING AND LEADING EDGE CRACK

Figure 6-126



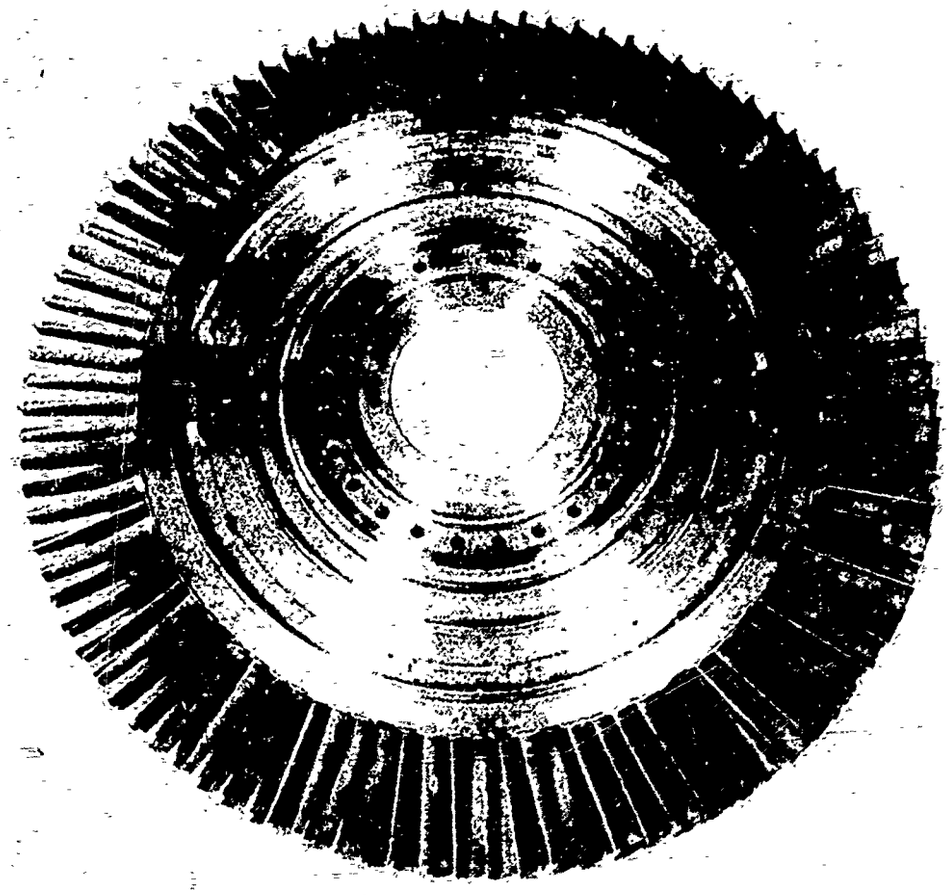
PWA 659 0.02-INCH SAWTOOTH BLADE (TOP) AND PWA 658 ELEVEN-HOLE BLADE (BOTTOM)
AFTER 1030 CYCLES AT 2235°F

Figure 6-127



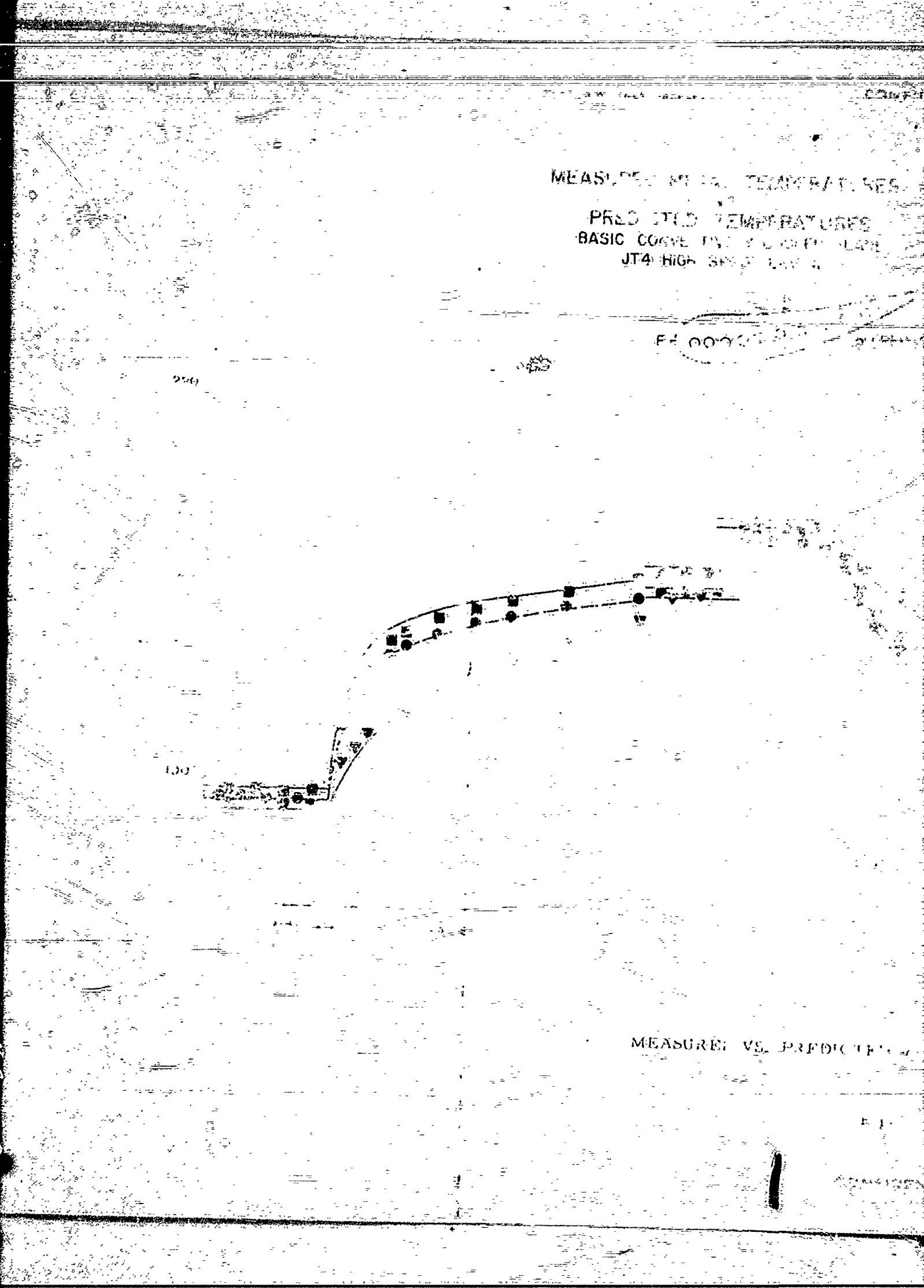
JT4 TURBINE VANE ASSEMBLY WITH FILM AND TRANSPIRATION COOLED VANES

Figure 6-128



JT4 TURBINE ROTOR ASSEMBLY WITH FILM AND TRANSPIRATION COOLED BLADES

Figure 6-129


MEASURED METAL TEMPERATURES
PREDICTED TEMPERATURES
BASIC COOLED
JT4 HIGH
250
150
MEASURED VS. PREDICTED

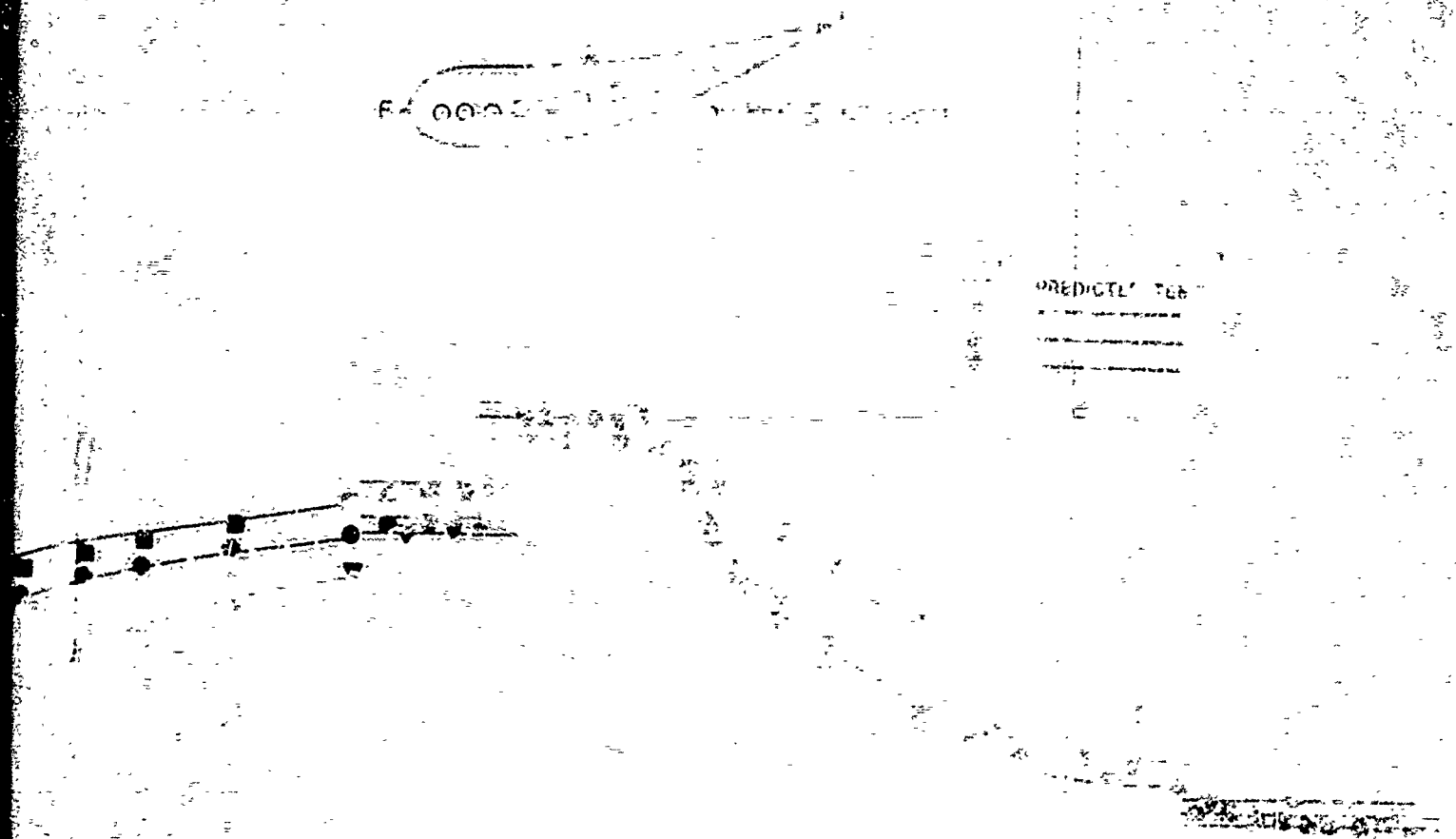
MEASURED VS. PREDICTED TEMPERATURES

VS.

PREDICTED TEMPERATURES

BASIC CONFIGURATION

JT4 HIGH SPEED



MEASURED VS. PREDICTED

AUGMENTOR



AUGMENTOR

ITEM 7 - AUGMENTORS

OBJECTIVE

The contractor has conducted experimental testing of the augmentor components which was directed toward verification of the augmentor performance.

The goal of this program was the development of an augmentation system having a 95% combustion efficiency at SST cruise conditions and a 93% efficiency during acceleration.

A. AERODYNAMIC FLAMEHOLDER TESTS IN SMALL-SCALE DUCT HEATER RIGS

1. INTRODUCTION

The augmentation system for the SST engine must be capable of achieving maximum combustion performance at cruise as well as at maximum augmentation flight conditions for economical aircraft operation. The low non-burning pressure losses of the aerodynamic or jet flameholder makes it especially suited to the SST mission for both the augmented and unaugmented conditions. The jet flameholder using small amounts of gas generator bleed flow has demonstrated stable combustion and attained the required combustion efficiencies at the most critical flight points and the most severe combustion conditions of the typical SST flight path.

Small scale tests with single, multiple and cross type aerodynamic flameholders and tests with various fuel injection techniques have revealed that several flameholder configurations are capable of high efficiencies and low pressure losses. The major effort, however, was concentrated on a spark ignited, cross type, externally fueled jet flameholder with an upstream secondary fuel system as shown by Figure 7-1.

In addition, information was obtained for application in the design and construction of the full scale duct heater rig and the designs of the SST duct burning engines.

A total of 580 test hours have been completed on the small scale duct heater rigs in Phase IIA.

DOWNGRADED AT 3 YEAR INTERVALS
DECLASSIFIED AFTER 12 YEARS
DOD DIR 5200.10

2. DESCRIPTION

a. Duct Heater

The most significant aspect of the duct heater is its flame stabilizer, the jet flameholder. The jet flameholder consists of an oval-shaped manifold through which approximately 3% bleed flow is injected normal to the duct flow. Compressor exit air has sufficient pressure and temperature to product stable operation with the jet flameholder. The air flow is controlled by means of a simple on-off valve located in the flameholder air line. Primary fuel is supplied through a sprayring located directly behind the flameholder. Flame is stabilized on the recirculation zone formed by air jets normal to the air stream. For high augmentation, a secondary fuel supply is injected into the combustion chamber upstream of the jet flameholder.

The combustion chamber is approximately 60 inches in length from the flameholder plane to the throat of the exit nozzle. The duct channel has been sized to provide a maximum cold Mach number of 0.175. Transpiration (porous metal) cooling liners are used to insure the optimum utilization of the cooling air in the full scale and engine application. The duct heater is ignited by either a simple spark plug or a torch ignitor at very lean fuel-air ratios. At these lean fuel-air ratios, the temperature rise and attendent pressure rise are very small.

b. Rig and Facility

The tests were performed in two small scale rigs. The small rig is a 6 1/2 x 8 inch rectangular cross section seal level research rig capable of flowing up to 50,000 lb/hr of air at 60"Hg pressure exhausting to the atmosphere. Inlet temperatures and jet flameholder flow conditions covering the SST range of interest can be simulated. The rig is water cooled, has interchangeable sections for altering chamber lengths and a set of fixed geometry exit nozzles for use in varying duct Mach numbers. The flameholder section has multiple bosses and viewing ports.

The majority of testing during Phase IIA was performed in the 12" x 16" two-dimensional altitude test rig. This rig closely simulates the SST duct heater channel and employs a vacuum system to operate between atmospheric pressure and 5"HgA. Interchangeability of rig sections, air or water cooling, and multi-boss flameholder sections with large viewing windows provide great flexibility of opera-

tion. An inlet air heat exchanger allows operation up to 600°F with unvitiated air. This rig is useful for simulating high altitude conditions and for obtaining minimum pressure blowout data. A variable area exit nozzle makes it possible to conduct tests at constant duct Mach numbers over a wide range of fuel-air ratios.

3. METHOD OF TEST

The combustion efficiency attained is computed from an aerodynamic measurement of the exhaust temperature. The rig is run choked at all times and using the choked flow parameter the exit temperature is accurately established by calculations. Combustion (thrust) efficiency is defined as the actual temperature rise divided by the ideal temperature rise.

The temperature is calculated from the following relationship:

$$T = \left(\frac{\overline{M} \quad P_T C_d A}{W_g} \right)^2$$

where:

$\overline{M}$ = Choking flow parameter
P_T = Total Pressure
C_d = Discharge Coefficient
A = Nozzle Area
W_g = Gas Stream Rate

This requires accurate measurement of gas flow, exit nozzle total pressure and exit nozzle effective area.

- The gas flow through the nozzle is the sum of the rig airflow, the rig fuel flow and the heater-burner fuel flow. Airflow in the rig is measured by a venturi; fuel flow measurements are made with standard fuel meters in each line.

- Exit nozzle total pressure is determined by averaging the total pressure readings taken with the exit pressure rake.

- Exit nozzle effective area is derived by calibrating the nozzle at cold flow conditions. By choking the nozzle and measuring flow, pressure and temperature, the nozzle effective area can be determined in a manner similar to the calculation of temperature.

Performance tests were made at constant inlet temperature, pressure and Mach number using the variable area exit nozzle. Minimum pressure data was obtained with pressure changing only. Hot and cold pressure loss data were obtained at various Mach numbers with various bleed flows.

4. TEST RESULTS

To demonstrate the ability of the duct heater combustion system to meet the performance requirements, a series of tests at the conditions to be found in the STF219 performance table were performed in the 12" x 16" two-dimensional altitude test rig. The results of these tests showed that the jet flameholder system has been sufficiently developed so that the required combustion (thrust) efficiency of 95% at cruise and 93% at acceleration is attainable.

The configuration utilized throughout this series of tests was a two zone system where the primary is a cross type aerodynamic jet flameholder, see Figure 7-1 and 7-2, with primary fuel sprayed upstream at the trailing edge of the jet flameholder and with the secondary fuel spraybar located approximately 2" upstrea of the leading edge of the jet flameholder. A schematic of the test setup is shown by Figure 7-3. The external primary fuel system was utili ed in this test series since it has been demonstrated to b superior by ior testing.

Since compressor bleed air is used to operate the jet fla r, a pressure loss from the large head available at the compres exit to the head desired at the jet flameholder is taken that ch es linearly with the head available. The jet flameholder pressure ratio then changes at various flight conditions directly with the compressor exit pressure. By using a 2.50 flameholder pressure ratio and a bleed flow of 4% of the duct flow at sea level take off, the bleed flow is 2.20% at a pressure ratio of 1.45 at the M = 3.0, 65,000 ft. cruise point. Throughout the t st series realistic conditions of combustion chamber Mach numbers, inlet temperatures, flameholder bleed flow, flameholder pressure ratios and combustion chamber length, have been maintained. The entire test series was performed at a pressure level of 25"HgA. The results presented in this report are conservative since only higher inlet Mach numbers were evaluated. At the low Mach numbers in the flight path, the measured efficiencies will be higher than those measured in this test series.

DOWNGRADED AT 3 YEAR INTERVALS
DECLASSIFIED AFTER 12 YEARS
DOD DIR 5200.10

a. Cruise Conditions

A test simulating the 3.0 flight Mach number at 65,000 feet, high airflow schedule, cruise point, was run. The results are shown by Figure 7-4, where combustion (thrust) efficiencies in excess of 95% for the range of $.002 \leq f/a \leq .022$ were measured using the primary fuel zone only. Stable burning was obtained for the range $.002 \leq f/a \leq .039$ and measured cold pressure loss was 1.9% with a flameholder bleed of 2.2%.

b. Sea Level Take-off Acceleration Conditions

Tests conducted at SLTO conditions produced results as shown by Figure 7-5. The system demonstrated combustion efficiencies in excess of 95% at the high augmentation conditions ($f/a \simeq .05$).

c. Transonic

The severest demand encountered by the duct heater system is the acceleration through transonic flight regime. The aircraft drag approaches the engine thrust capability at this point, hence the exit temperature must be maintained at the highest practical heat transfer limit. Further, the low inlet temperature makes flame stabilization more difficult. The results of a test performed at this condition are presented by Figure 7-6 along with a tabulation of the operating conditions. Combustion efficiencies in excess of 93% were demonstrated at maximum duct heater exit temperature.

d. Acceleration - Mach 2.0 at 55,000 Feet

To evaluate duct heater performance at the highest expected duct Mach number of 0.175, a test was performed at 2.0 flight Mach number, 55,000 feet. The results are presented in Figure 7-7 along with a tabulation of the test and STF 219 conditions. Since the desired efficiency is at richer conditions of $f/a \geq 0.050$ it was impossible to evaluate the system performance at these conditions. The richest point obtained was at $f/a = 0.045$ because of the limitation in the stand fuel supply system. Efficiencies between 90 and 95% were measured.

e. Duct Heater System Pressure Losses

Cold pressure losses of the configuration evaluated at the various SLF219 flight conditions were recorded and are presented by Figure 7-8. The results are higher than expected in full scale because of the high level of losses for the rig without flameholders. However, total losses are only 2% at maximum bleed flow and 0.15 Mach number, exclusive of diffuser losses.

f. Air Cooled Rig Test

A two dimensional rig was constructed to simulate the duct heater contours of the proposed SST engine and the air cooled liner. Tests were conducted to determine the following:

- Check wall cooling flow requirements.
- Compare flameholder performance without the usual water cooled rig walls.

The rig was sized to pass airflow comparable to the 12" x 16" rig and was installed in the same test facility. A convective-type liner was used with metering plates on the upstream end near the flameholder to control cooling flow rates. The cooling liner was instrumented at various axial locations downstream of the flameholder on the top and bottom. Cooling airflows were determined from calibrated static pressure drops across the liner inlet and cooling air temperatures were recorded. Tests were run at various inlet temperatures and flameholder pressure ratios with three exit nozzle sizes. Both the cross type flameholder and the conventional single element flameholder were tested.

A comparison of combustion efficiency for the water cooled and air cooled rig is shown on Figure 7-9. A significant improvement in efficiency was obtained with the air cooled walls. This was expected since the wall metal temperatures are unrealistically cold with water cooling.

g. Ignition Tests

Ignition tests of the cross jet flameholder with a 20 joule (28 volts, D.C. system) spark ignitor located near the trailing edge of the flameholder have been performed at various duct Mach numbers with the test rig discharge nozzle choked. The results are presented for constant flameholder airflows of 800 and 1600 lbs/hr on Figure 7-10. At these conditions successful lights were achieved at fuel-air

ratios less than 0.003. The cross jet flameholder utilized in the STF219 performance tests ignited smoothly at fuel-air ratios less than the maximum imposed by the fan surge margin.

A typical ignition transducer pressure trace for STF219 SLTO where ignition was achieved at a fuel-air ratio of 0.0030 is presented by Figure 7-11. This demonstrates a pressure pulse even less than that assumed in the Ignition-Control section of this report.

h. Stability of the Cross Jet Flameholder with External Primary Fuel

For the purpose of demonstrating the stability of a typical cross jet flameholder with external primary fuel, a minimum pressure blow-out loop has been obtained and the results presented on Figure 7-12. The results indicate stable operation to a total pressure of 9.4"HgA which is below the goal of 10.0"HgA and well below the pressure level at any normal STF219 operating condition.

5. DISCUSSION OF RESULTS

As a consequence of small scale duct heater tests, summarized by Table 7-1 the correlation between the small scale and the full scale rig, the following conclusions can be drawn:

- Combustion efficiencies in excess of the required value of 95% at cruise condition and 93% at acceleration have been demonstated.
- The aerodynamic jet flameholder is desirable for a duct burning turbofan because of its low pressure losses, simplicity of hardware, and low weight.
- Compressor exit air has sufficient temperature and pressure to operate the jet flameholder efficiently. Reasonable values of bleed flow are required.
- Tests with full scale hardware substantiated the efficiencies and pressure loss data obtained on the small scale research rigs.
- Sufficient heat transfer information indicates that structural integrity can be maintained with reasonable cooling flow rate.
- Ignition is accomplished easily even with a choked exit nozzle and design duct Mach numbers; soft lights have been demonstrated at all normal conditions.

TABLE 7-1

SUMMARY OF PERFORMANCE TESTS OF CROSS JET FLAMEHOLDER

WITH EXTERNAL FUEL AT CRITICAL STF219 OPERATING CONDITIONS

Flight Mach No.	0	0.9	2.0	3.0
Altitude (ft.)	0	36,000	55,000	65,000
Fuel-air ratio	0.045-0.055 (acceleration)	0.045-0.055 (acceleration)	0.045-0.055 (acceleration)	0.015-0.020 (cruise)
Pressure (psia)	12.3	12.3	12.3	12.3
Inlet temp. (F)	266	214	402	761
Combustion chamber Mach number	0.140	0.130	0.172	0.165
Bleed flow (%)	3.5	4.0	2.8	2.10
Combustion chamber length (in.)	62	62	62	62
Attained efficiency (%)	95.0-90.0	100.0-95.0	91.0	97.5-96
Pressure loss (%)	1.8	1.55	2.15	1.90

6. RECOMMENDATIONS

- Further small scale tests are desired to optimize the secondary fuel system.
- More experience is desired on full scale rig hardware over a range of flight conditions.

B. RAM INDUCTION BURNER TESTS IN SMALL-SCALE DUCT HEATER RIGS

1. INTRODUCTION

As an alternate to the jet flameholder system described above, tests were also conducted on low pressure loss can-type burners. The combustion system employs a piloting burner to achieve high cruise combustion efficiency while bypassing part of the air to reduce pressure loss. In addition, the "ram induction" air admission principle was employed to induct and mix air in the burner with a minimum pressure loss. The hot burner gases serve as a pilot zone to ignite additional fuel injected into the bypass air for maximum augmentation conditions.

2. DESCRIPTION

a. Duct Burner

Figure 7-13 is a photo of the initial duct burner design, model A. A photo of the latest duct burner, the model E, is shown in Figure 7-14. Air enters the burner through ram scoop openings. This feature not only reduces the pressure loss required to induce air into the burner, but permits the use of high inlet velocity air -- an essential requirement for a high Mach number fan duct burner. With high reference velocities, the inlet diffuser length and the duct cross section can be reduced for the same airflow.

The hot gases from the burner mix with the duct bypass air with the aid of vortex generators mounted in the bypass air passage at the rear of the burner. For maximum augmentation, additional fuel is injected into the bypass air by means of spray bars. The hot gases from the burner segment act as a pilot flame for burning this fuel. A total of 70 test hours on ram induction burners have been accumulated in Phase II-A.

b. Rig and Facility

The ram burner test rig is a 7" x 11" rectangular cross-section rig with water cooled duct sections. Rig airflow is metered through a choked venturi sized to produce a minimum duct Mach number of M = 0.12 at 500°F inlet temperature and 2 atmosphere inlet pressure. An inline heater burner is capable of heating inlet air temperature as

high as 1850°F. Overall combustor length is 66 inches to the throat of the variable area exhaust nozzle. Area variation in the exhaust nozzle will allow operation at duct Mach numbers between M = 0.12 and M = 0.20.

The rig is presently installed on a test stand, which uses a JT-4 turbojet engine as an air supply and an ejector. The engine is capable of supplying up to 20 lb/sec bleed air at a rig pressure of 100 psia. The air temperature is related to engine pressure ratio, but normally runs about 450°F for duct burner testing. The ejector is a two stage type capable of pulling down to 4 psia. When running on ejectors, the rig inlet pipe is normally removed and the rig draws in ambient air. Engine bleed air can be discharged to ambient in the vicinity of the open rig inlet, giving some control over rig inlet temperature. This arrangement allows testing with inlet temperatures from ambient to about 400°F. Higher inlet temperatures require the use of a direct fired heater burner installed ahead of the test section.

3. METHOD OF TEST

The combustion efficiency attained is computed from an aerodynamic measurement of the exhaust temperature. The rig is run choked at all times and using the choked flow parameter the exit temperature is accurately established by calculations. Combustion (thrust) efficiency is defined as the actual temperature rise divided by the ideal temperature rise.

The temperature is calculated from the following relationship:

$$T = \left(\frac{\bar{M} \; P_T C_d A}{W_g} \right)^2$$

where:

$\bar{M}$ = Choking flow parameter
P_T = Total Pressure
C_d = Discharge Coefficient
A = Nozzle Area
W_g = Gas-Stream Rate

This requires accurate measurement of gas flow, exit nozzle total pressure and exit nozzle effective area.

- The gas flow through the nozzle is the sum of the rig airflow, the rig fuel flow and the heater-burner fuel flow. Airflow in the rig is measured by a venturi; fuel flow measurements are made with standard fuel meters in each line.

- Exit nozzle total pressure is determined by averaging the total pressure readings taken with the exit pressure rake.

- Exit nozzle effective area is derived by calibrating the nozzle at cold flow conditions. By choking the nozzle and measuring flow, pressure and temperature, the nozzle effective area can be determined in a manner similar to the calculation of temperature.

The Mach number is set at the burner inlet and is held constant throughout the test. This is accomplished by adjusting the JT-4 engine speed and the area of rig exit nozzle. The nozzle area is adjusted at each fuel flow to give the same burner inlet pressure. Since air flow is held constant by running constant pressure at the venturi inlet, the burner Mach number is also constant.

4. TEST RESULTS

The test results of only the first and latest configurations will be discussed herein. These results are shown on Figures 7-15 and 7-16. Figure 7-15 shows the improvements made in combustion efficiency, and Figure 7-16 shows the improvements made in pressure loss. Another improvement is attributed to a successful reduction in the number of fuel injection zones from three to two.

The results show that the ram induction duct burner is capable of achieving outstanding combustion efficiency at both cruise and maximum augmentation fuel-air ratios. Modest pressure losses are encountered in the critical cruise region of operation. Pressure losses increase for maximum augmentation operation, apparently due to redistribution of the air flow splits in the burner system brought about by changing heat addition losses.

The latest and best performing burner, the model E, has undergone some very limited testing under the low temperature and pressure conditions encountered in transonic flight. Blow-out characteristics were found to be poor. However, the initial design, the model A was operated to pressures below 3 psia with 200°F inlet. It seems prob-

able that good performance and acceptable blowout limits can be combined in one configuration with further development effort.

A feature of the ram induction burner which is not apparent from the performance curves is that it is capable of very "soft" lights. The system has been lit with spark ignition at an overall fuel-air ratio of 0.0008. Such lean ignition capability eases the problem of coordinating the engine exhaust nozzle area with augmentation light off. Further, the almost flat combustion efficiency curve results in a near straight-line relationship between fuel-air ratio and augmentor temperature rise which simplifies exhaust nozzle control.

The configuration appears quite practical as an engine component because it is of reasonable length, uses a small amount of metal, requires only 2 stages of fuel ignition for an extremely wide operating range, and has exhibited good durability.

5. RECOMMENDATIONS

In view of the feasibility demonstrated by the ram induction duct burner, the program should be continued. Particular emphasis should be placed on the following areas:

- Improvement of Altitude Blowout Limits - This probably will require an increase in burner cross section or length and the revision in number, size and distribution of scoops. It may require a wider test burner segment to reduce rig wall quenching effects.

- I. D. and O. D. Wall Cooling Problems - The tests to date have been made with water cooled combustion chamber walls. By replacing these with walls cooled in the same manner as the engine, the existance of any hot streaks or other problems can be detected and action can be taken to relieve them.

- Ignition Limits Investigation - The ignition characteristics at normal cruise conditions have been determined, and are excellent. The low pressure, low temperature light off encountered in high altitude, low flight Mach number conditions should be investigated.

DOWNGRADED AT 3 YEAR INTERVALS
DECLASSIFIED AFTER 12 YEARS
DOD DIR 5200.10

C. HETEROGENEOUS BURNER TESTS IN SMALL-SCALE DUCT HEATER RIG

1. INTRODUCTION

As another alternate to the jet flameholder system previously described, tests were also conducted with low pressure-loss heterogeneous burners.

In heterogeneous burner designs, a hot zone that replenishes itself is maintained by using part of the air stream and part of the fuel. The rest of the fuel (the major part) is injected through the hot zone from nozzles or other devices in such a way that all fuel droplets are ignited as they cross the hot zone. Thus each droplet of fuel is ignited and burns separately.

The ignited droplets, by virtue of their ballistic trajectories and their entrainment in the gas flow pattern, enter the undisturbed air stream where they continue vaporizing and burning until complete combustion is achieved in the downstream section of the duct. For such a burner, only few boundaries are required for generation, maintenance and distribution of the hot zone, and only a small fraction of the air stream and fuel is utilized for this purpose. Because the bulk of the air stream remains undisturbed, the pressure loss is less than for conventional burners; also, because the fuel sprays are inflamed and mixed with the air stream early in the burner, the maximum volume (or length) required for complete vaporization and combustion is also less.

2. DESCRIPTION

a. Duct Burner

Figure 7-17 is a diagramatic illustration of the initial heterogeneous burner design for a round duct, Model A. Figure 7-18 is a photograph of the same burner. A photograph of Model B, the second heterogeneous burner built, is shown in Figure 7-19.

Part of the incoming air stream enters through a swirler and holes into the primary zone which is shielded by the centerbody. Part of the fuel is injected into the primary zone through the center nozzle. Upon ignition, the hot combustion product gases generated within the centerbody are distributed by the backplate behind the six hot zone anchoring devices.

DOWNGRADED AT 3 YEAR INTERVALS
DECLASSIFIED AFTER 12 YEARS
DOD DIR 5200.10

Secondary fuel is injected from the spraybars (or nozzles) and the resulting sprays cross the hot zones where all droplets are individually inflamed. Subsequently the inflamed droplets, by virtue of their ballistic trajectories and their entrainment in the gas flow pattern, enter the remainder of the air stream that had by-passed the centerbody between the hot zone anchoring devices. The droplets continue vaporizing and burning in the air stream until completely burned in the downstream duct section.

b. Rig and Facility

The tests were performed in a ten-inch diameter round-duct rig. Facilities supply an airflow of up to 100,000 pounds per hour at 150°F and 30 psia or up to 50,000 pounds per hour at 600°F and 30 psia; thus, inlet flow conditions simulating the SST range of interest can be simulated exactly in the rig. The rig is air cooled for the first four feet of length by use of a transpiration cooled liner, and is water cooled for the last foot of length. The length of the rig test section can be varied from three to six feet.

Viewing ports facilitate observation of the combustion processes along most of the length of the rig.

3. METHOD OF TEST

The Model A heterogeneous burner was tested at 18 psia and 500°F in a duct section that was five feet long. Inlet air was at 150°F and covered a velocity range that resulted in Mach numbers from 0.13 to 0.15.

Performance was measured by rake traverse with measurements of one pressure and one temperature per square inch of total duct exit cross-sectional area. All measurements were then averaged to obtain the mean exit temperature and pressure.

The Model B burner was tested using a duct section that was three feet long and a variable area converging-diverging nozzle. Choked conditions were maintained at the nozzle throat at all times that data were taken.

Reduction of data was accomplished by the techniques outlined in detail in the previous section.

4. TEST RESULTS

Heterogeneous burner test results, using unchoked data, are shown in Figure 7-20 and are briefly discussed below. The heterogeneous burner Model A demonstrated stable operation at both 500°F and 150°F inlet temperatures and, although unchoked, yielded good efficiencies as shown on Figure 7-20.

Model B burner tests were conducted with a choked exit nozzle. Test results are shown on Figure 7-21. The combustor operated over the fuel-air ratio range from 0.007 to 0.042 in a duct Mach number range of 0.12 to 0.2 at 500°F inlet air temperature. Combustion efficiencies are flat over a wide fuel-air ratio range.

DOWNGRADED AT 3 YEAR INTERVALS
DECLASSIFIED AFTER 12 YEARS
DOD DIR 5200.10

4. TEST RESULTS

Heterogeneous burner test results, using unchoked data, are shown in Figure 7-20 and are briefly discussed below. The heterogeneous burner Model A demonstrated stable operation at both 500°F and 150°F inlet temperatures and, although unchoked, yielded good efficiencies as shown on Figure 7-20.

Model B burner tests were conducted with a choked exit nozzle. Test results are shown on Figure 7-21. The combustor operated over the fuel-air ratio range from 0.007 to 0.042 in a duct Mach number range of 0.12 to 0.2 at 500°F inlet air temperature. Combustion efficiencies are flat over a wide fuel-air ratio range.

DOWNGRADED AT 3 YEAR INTERVALS
DECLASSIFIED AFTER 12 YEARS
DOD DIR 5200.10

D. FULL-SCALE DUCT HEATER TESTING

1. INTRODUCTION

The choice of a duct heater system utilizing the jet flameholding principle offers many advantages for the SST mission by providing the required augmentation for both acceleration and cruise without excessive weight or pressure loss penalties.

The initial development of the various elements of a duct heater has been conducted on small-scale, two dimensional test rigs. Such rigs offer the most efficient means of identifying the variables that affect duct heater combustion and of defining the parameters that describe its performance. However, at some point it is necessary to apply the design parameters derived from such rigs to a full-scale, three-dimensional system operating at realistic conditions. This may be done on an actual engine, but is more readily done on a full-scale, three-dimensional test rig. Test results from the rig using simulated engine hardware will provide accurate and authoritative performance verification of the proposed engine system. The total test time accumulated on the full-scale duct heater during the Phase II-A program was 56 hours.

2. DESCRIPTION

a. Test Rig

The full-scale duct heater test rig is designed to simulate an annular duct heater combustion system. It is typical of the turbofan supersonic transport power-plant in airflow capacity, size and geometry. The overall rig dimensions including inlet sections are roughly 18 feet in length and 6 feet in diameter. All ducting upstream of the exit nozzle is air cooled simulating actual powerplant conditions. The rig section downstream of the exit nozzle, is water cooled. See Figures 7-22 and 7-23. A fixed mount point is located at the upstream end of the diffuser with struts to support the inner body. Tubes, through which inner body instrumentation lines can be led, are also located in this region. Inlet temperature and pressure rakes, Figure 7-24, are located at the downstream end of the rig diffuser.

The initial testing has been performed with a long length of low angle diffuser. Provisions have been made for substituting the offset diffuser presently incorporated in the STF219 design. The offset diffuser design has been completed.

A short separate section downstream of the diffuser contains the secondary fuel system and the primary jet flameholder system. This section is designed to permit rapid changing of these components. The ignitor is also located in this section. These are shown by Figures 7-25, 7-26 and 7-27.

Combustion occurs in the annular combustion chamber which has a total length of 75 inches from the jet flameholder to the exit nozzle throat. Cooling liners shield both the inner and outer walls. Instrumentation to measure and record cooling air flow pressures, and structure temperature has been provided. Both inner and outer liners are made of porous material to provide transpiration cooling. See Figures 7-28, 7-29 and 7-30. The outer duct has been reinforced and the means of instrumenting the outer wall and liner, improved. Figure 7-31.

Alternate fixed area exit nozzles are used to vary test conditions. The converging section of the nozzle is 13.2 inches in length, and is split horizontally to facilitate nozzle replacement. Nozzles for performance testing are water cooled over this converging section. All nozzle convergence occurs on the outer duct wall as in the actual powerplant thus simulating the STF219 engine design. Alternate air-cooled nozzles are also available for use in optimizing the cooling air requirements for actual applications. A water-cooled diverging section extends downstream from the nozzle throat to the rear support section. Two different nozzle areas are available in both water-cooled and air-cooled versions to simulate typical acceleration and cruise conditions. Sixteen water-cooled exit total pressure rakes are installed at the exit nozzle throat.

Instrumentation provides information on combustor performance (exit temperature and efficiency), pressure loss, and cooling.

3. TEST FACILITY

The facility used in testing the full-scale duct heater rig is a stand in Pratt & Whitney Aircraft's Andrew Willgoos Laboratory. This stand has the capacity for high air flow at a range of pressure levels that simulate the bulk of the SST flight envelope. Air flow rates up to approximately 600 pounds per second and pressure levels up to 125" HgA are available in this facility.

Mainstream air flow is controlled by means of both inlet and exit valving in conjunction with regulating the speeds of the compressors and exhausters which supply the air flow. Air flow for this testing is measured by a standard orifice and/or calibrated venturi plate.

A separate high pressure air line provides secondary air flow to the jet flameholders at pressure ratios of 1.5 to 3.0 in quantities sufficient to simulate all bleed flow requirements. This air is heated by a small heater burner to the desired temperature level simulating either compressor bleed or turbine bleed.

Fuel systems supplying the duct heater primary, duct heater secondary and jet flameholder air line heater-burner are utilized during flow ranges of 2,000 to 67,000 PPH, 2,900 to 70,000 PPH and 0 to 800 PPH, respectively.

Water is used to cool duct work downstream of the exit nozzle and to cool the instrumentation.

4. METHOD OF TEST

The purpose of the test program is to obtain data on performance (efficiency and pressure loss), structural cooling and durability throughout the operating range encountered during SST operation.

The test procedure consists of setting the desired conditions, igniting the duct heater and setting desired jet flameholder air flow and fuel flow. Data are recorded after a sufficient time allowance to permit conditions to stabilize, additional points are obtained by varying the fuel flow (i.e., fuel/air ratio). A typical run consists of 6 to 8 performance points at varying fuel/air ratios.

The data taken at each point for the performance and cooling evaluation are as follows:

- Mainstream and jet flameholder air flow. (Calculated from measured pressure, pressure drop, and temperature across standard orifices).
- Fuel flows for heater burner, jet flameholder primary and secondary system. (Measured by turbine meters with electronic counters).

- Exit total pressures (44 measurements from four rakes recorded on standard manometers).

- Inlet total pressures (12 measurements located at the end of the diffuser upstream of the flameholder section). These measurements are used to calculate pressure loss. A number of pressure measurements in the combustion chamber, and in the cooling air passages, have been provided so that liner cooling air can be determined.

- Duct inlet temperatures (chromel-alumel thermocouples). Include the measurement of jet flameholder air, fuel, liner and wall temperatures.

6. TEST RESULTS

The test program that was conducted on the full-scale duct heater test rig during Phase II-A was devoted to low inlet temperature development of a typical duct heater. The configuration included a fiery cross jet flameholder configuration through which a premixed fuel-air mixture was injected into the main stream. Small-scale testing has indicated that the low inlet temperature conditions can impose a significant performance penalty reflected in decreased efficiency. All data obtained during this program were obtained at inlet temperatures ranging from 90 to 205°F.

The variables investigated included the effect of flameholder air temperature over a range from 200 to 1200°F, effect of pressure ratio across the jet flameholder over a range from 1.5 to 2.5, and the effect of lowering inlet pressure to 25" HgA from 40" HgA. Testing with secondary fuel flow in addition to the primary jet flameholder system was accomplished for the first time in the full scale configuration. Testing was conducted for a total of 56.33 hours of running time, including 16.28 hours of combustion time. The following significant conclusions resulted from this test program:

- Full-scale results agree quite closely with small-scale results. Figure 7-32 compares combustion efficiency levels of the full-scale and small-scale rigs for similar configurations operating at low inlet temperatures. Figure 7-33, based on Phase I test data, indicates similar small-scale to full-scale agreement for higher (540°F) inlet temperature. Measured pressure losses and the effect of changing such operating variables as flameholder air

temperature, rig inlet temperature, and rig inlet pressure also show agreement with small-scale rig data; these are more fully discussed in the following paragraphs. The effect of such agreement is to confirm that much of the development work pertaining directly to combustion variables can be accomplished on small-scale test rigs. The full-scale rig, then, offers the opportunity for demonstration and development of complete systems, and attention to other problems such as structural durability, and weight reduction.

- Combustion efficiencies in the range of 75 to 80 percent were recorded in full-scale testing as shown in Figure 7-34. Systems including separate injection of fuel and jet flameholder air were developed which have consistently exceeded 93 percent efficiency in small-scale testing. (See section on small-scale test results). Fabrication of a full-scale design based on this work was completed late in Phase II-A; this hardware is available for future full-scale programs.

- Pressure losses of three percent at a Mach number of 0.175 were measured for the nonburning system as shown in Figure 7-35. Measured pressure losses in the range of four to five percent for a Mach number range of 0.15 to 0.20 during combustion were also recorded. This represents close agreement with predicted pressure losses based on small-scale testing, and a more realistic measurement than that obtained in the previous program phase.

- There is apparently no effect of jet flameholder air temperature on performance. Figure 7-36 compares performance at 1200, 600 and 200°F flameholder air temperature, indicating no performance penalty whether compressor or turbine bleed airflow is used in the jet flameholder. Again, this fully confirms small-scale rig results.

- Results of testing at below-atmospheric pressure levels, at an inlet pressure of 25" HgA (which in combination with the low inlet temperatures represents the most severe inlet conditions to the combustor) were inconclusive. Efficiency levels 10 to 15 percent below comparable points at higher pressure (40" HgA) were recorded. However very high duct Mach numbers (ranging from 0.2 to 0.25) were incurred due to the use of the fixed area exit nozzle. Additional testing at a realistic Mach number is required to fully explore these inlet conditions.

- Jet flameholder pressure ratio apparently has little effect on jet flameholder performance, as indicated in Figure 7-37

- Testing with secondary fuel flow could not be conducted at high fuel-air ratios. Therefore, the data obtained are of little significance since the purpose of the secondary system is to achieve high fuel-air ratios. This inability to run at richer fuel-air ratios resulted from secondary fuel entering the outer liner cooling air annulus which resulted in over-temperaturing the outer liner at moderately high fuel-air ratios. This has tentatively been attributed either to recirculation of the secondary flow or to a leak at the spray ring feed-line. The testing that was conducted consisted of maintaining a constant duct fuel-air ratio contributed by the primary (jet flameholder) system, and adding secondary fuel in varying amounts. The results that were obtained indicated that the portion of duct fuel-air ratio contributed by the primary system should be maintained at or above minimum cruise fuel-air ratios of 0.015, and that no stability problems were encountered in adding secondary fuel-flow.

- No significant durability problems were encountered. In the previous test phase three problem areas were encountered, namely failure of the outer wall convective cooling liner, failure of the outer duct particularly around instrumentation bosses, and high vibration levels. During Phase II-A, a porous outer cooling liner was used which lasted throughout the test program without difficulty except for the conditions where secondary fuel was present in the cooling air annulus, which resulted in some liner distortion. The outer duct was replaced by a design in which duct thickness was increased, circumferential reinforcing bands were added, and instrumentation bosses were replaced by a number of small, tapped fittings. No difficulties with this duct, shown in Figure 7-38, were encountered. Investigation of vibration levels indicated a fairly high vibration level inherent in the rig whenever air was flowing, with no undue increase during combustion. No direct comparison can be made since vibration levels were not investigated during the previous phase.

- No additional liner cooling data were obtained. The porous inner liner was the same as previously used, and measured temperature distributions were similar to those reported previously. Many of the thermocouples on the outer porous liner did not last sufficiently long to provide adequate data for temperature evaluations. Pressure measurements taken in both inner and outer cooling air annuli provided checks of actual versus design cooling airflow.

7. RECOMMENDATIONS

This rig provides the essential step between small-scale testing and actual engine operation. After screening a large number of configurations in the small-scale two-dimensional rigs full-scale testing of only the most promising configurations is necessary. A concept where the jet flameholder air and fuel are not pre-mixed has been tested in small scale and appears to be attractive from the standpoint of simplification. It is recommended that this concept be evaluated in full scale. This will be done in conjunction with the offset diffuser utilized in the STF219 desi

E. SMALL-SCALE AFTERBURNER TESTING

1. INTRODUCTION

The possibility of using either a partially or fully augmented afterburning turbojet engine for the SST application was investigated. Due to cycle advantages and advances in cooling techniques the afterburner inlet temperature would go up to 1800°F. At these high temperatures it would not be necessary to stabilize flame in the afterburner using conventional vee-gutter systems. Flame can be stabilized with properly designed spraybars if the temperature is high enough. The purpose of this investigation was to determine the performance and stability characteristics of these low blockage augmentation systems. Part of the study consisted of reviewing past experience with high temperature afterburners and the remainder consisted of testing new configurations at various conditions.

Work was stopped after completion of 30 percent of the planned testing. This was done because the duct burning turbofan engine was determined to be the most promising cycle from the point of view of both Pratt & Whitney Aircraft and the major airframe manufacturers. A total of 25 hours of test time was accumulated on the small-scale afterburner.

2. DESCRIPTION

The afterburner is an augmentation device which takes advantage of the fact that only approximately 30 percent of the air passing through a turbojet engine is consumed by gas generator combustion. The remaining 70 percent is capable of supporting combustion if more fuel is added. An afterburner consists of fuel injection and flame stabilizing devices located at the exit of the basic turbojet and a lengthened tailpipe in which the additional combustion may take place. A photo of typical shielded spraybar used in the tests is shown in Figure 7-39.

The tests were performed in a 12" x 16" afterburner segment rig at the experimental test airport laboratory. The rig consisted of a series of removable and interchangeable water cooled sections which made it possible to perform tests at various combustion chamber lengths. It was necessary to water cool the entire rig due to the high temperatures involved.

Two pressure rakes were located in the rig. One was situated in front of the exit nozzle and the other was located immediately preceeding the flameholder section. There was also a thermocouple rake combined with the inlet pressure rake.

Exhausters located downstream of the rig provided the airflow making it necessary to perform all the tests at pressures less than one atmosphere. The airflow rates and pressure levels were regulated by the use of valves, one upstream and one downstream of the rig. A sketch of the rig is shown in Figure 7-40.

The inlet air was heated through the use of a heater-burner and a heat exchanger. Using this system temperatures from ambient up to 2000°F could be provided. Oxygen addition equipment was also used to restore the heated air to the proper oxygen concentration or to any desired amount of vitiation.

3. METHOD OF TEST

The combustion efficiency attained is computed from an aerodynamic measurement of the exhaust temperature. The rig is run choked at all times and using the choked flow parameter the exit temperature can be calculated. Combustion efficiency is then defined as the actual temperature rise divided by the ideal temperature rise.

The temperature is calculated from the following relationship:

$$T = \left(\frac{\overline{M} \quad P_t \, C_d \, A}{W_g} \right)^2$$

where $\overline{M}$ is the choking flow parameter.

P_t = Total Pressure
C_d = Coefficient of Discharge
W_g = Gas Flow Rate
A = Nozzle Area

This requires accurate measurement of gas flow, exit nozzle total pressure and exit nozzle effective area.

- The gas flow through the nozzle is the sum of the rig airflow, the rig fuel flow and the heater-burner fuel flow. Airflow in the rig was measured by a venturi. Fuel flow measurements were made with standard fuel meters in each line.

- Exit nozzle total pressure was determined by averaging the total pressure readings taken with the exit pressure rake.

- Exit nozzle effective area is derived by calibrating the nozzle at cold flow conditions. By choking the nozzle and measuring flow, pressure and temperature, the nozzle effective area can be determined in a manner similar to the calculation of temperature.

All performance tests were made at a rig inlet pressure of 20 in. Hg. and at inlet temperatures from 1400 to 1900°F. The degree of vitiation in the inlet air was varied from ramjet conditions to 15 percent of that found in a turbojet. Afterburner inlet mach numbers ranged from 0.2 to 0.35. All tests were performed using a fixed exit nozzle.

4. DISCUSSION OF RESULTS

The tests indicate that up to 1800°F it is necessary to utilize vee-gutters in order to stabilize flame. At or above this temperature the flame will hold on spraybars alone. It was determined however that at temperatures above approximately 1200°F it is necessary to use shielded spraybars as there is a tendency for the fuel to vapor lock. The exact point at which vapor lock will occur is not known as it is a function of the type of fuel being used, the fuel flow and the flight conditions.

At temperatures above 1700°F the rig lit very easily and smoothly without the use of a torch. There was no lean blowout at these conditions as even infinitesimal fuel flows lit and burned efficiently. All of the efficiency curves obtained had the same characteristic shape reaching very high efficiencies at very lean fuel-air ratios.

A curve showing the effect of the degree of inlet air vitiation is presented in Figure 7-41. Combustion efficiencies are plotted vs. afterburner fuel-air ratios for four different simulated engine fuel-air ratios. These different engine fuel-air ratios were obtained by varying the fuel flow to the rig heater burner. The inlet temperature was maintained at 1900°F by using a heat exchanger in conjunction with the heater burner. The curves indicate that there is a penalty of from 10 to 15 efficiency points in increasing the amount of vitiation from 0% to 50% of that found in the exhaust of a turbojet. At the points taken for rich fuel-air ratio each curve appears as a distinct line. However, at the lean points the scatter of the data seems to mask any distinct line.

A limited amount of testing was performed using different sized fuel sources. Figure 7-42 shows the results of testing two configurations which were identical in every respect except for the size of the fuel orifices. These curves indicate that much higher efficiencies are possible using the larger 0.030" diameter holes. More testing is necessary to determine what hole size and what number of holes is the optimum but there are definite indications that hole size has an important effect on the performance of a spray bar system.

A group of tests were performed using different numbers and sizes of conventional vee-gutters at 1700°F inlet. The results of these tests are shown in Figures 7-43 and 7-44. The two curves show the effect of changing the blockage in an afterburner system by two different means. The first curve shows that if the blockage in this particular system is halved by reducing the size of the flameholders by half the average decrease in efficiency is 15 percent. The second curve shows that if the blockage is halved by reducing the number of flameholders by half, the decrease in efficiency is 20 percent. One can conclude from these results that, from an efficiency point of view a large number of small flameholders is more desirable than a small number of large flameholders having an equal total blockage. This conclusion is in agreement with past experience with afterburning engines.

A limited amount of work was done on determining the effect of afterburner inlet air temperature on combustion efficiency. It was determined that raising the inlet temperature from 1800°F to 2200°F had a negligible effect on performance. Additional work will have to be done to determine the influence of temperature over a wider range. Figure 7-45 shows the results of this test.

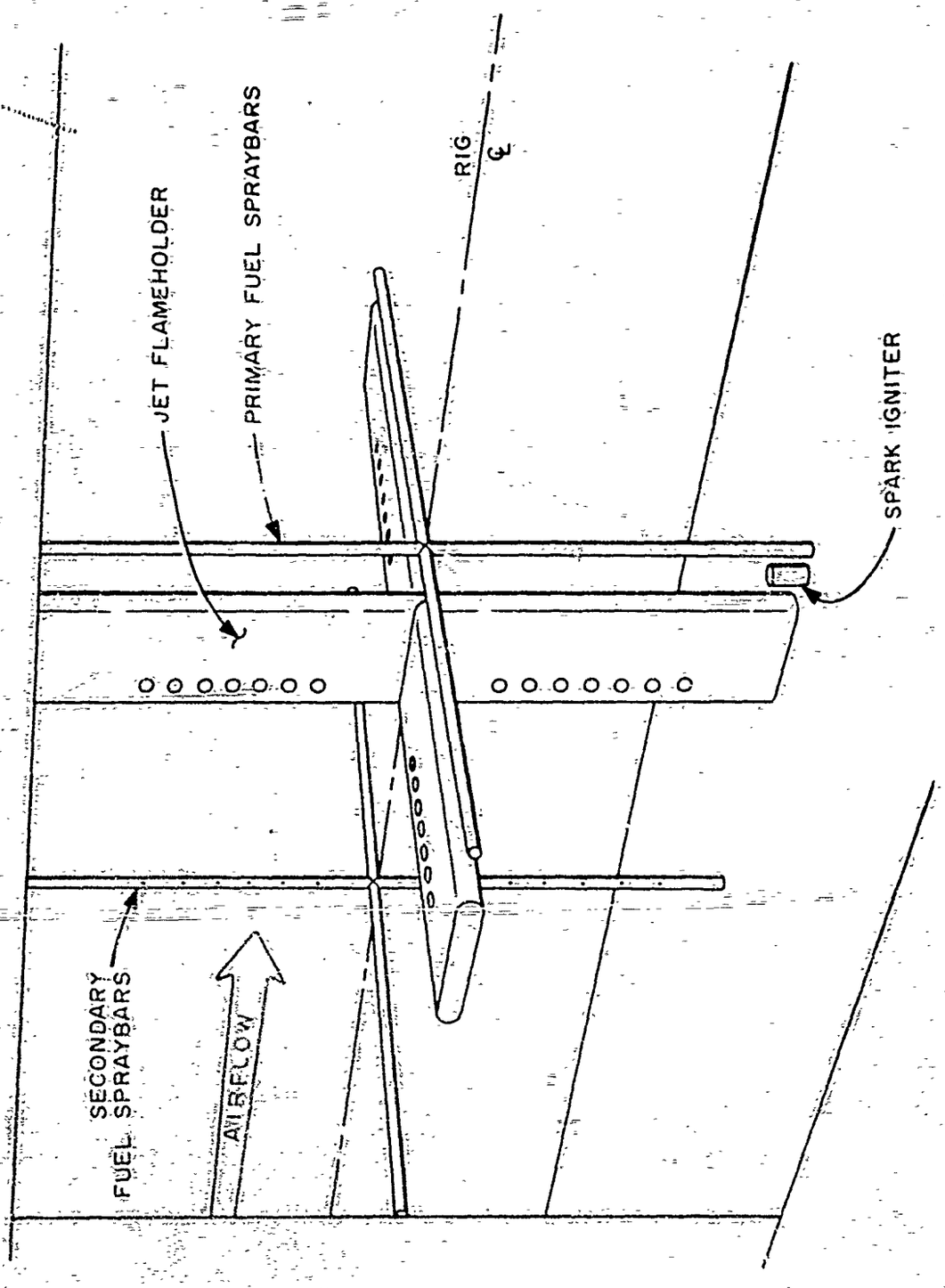
Minimum pressure blowout data was gathered for several of the configurations tested. In Figure 7-46 the blow out loop is shown for 2-5/8 inch spraybars at 1900°F. Under these conditions this system is very stable being capable of operation down to at least 6 in. Hg over a wide range of fuel-air ratios.

While the high efficiencies required have not been demonstrated over the entire fuel-air range there are indications that the goal of 95 percent efficiency at cruise and 93 percent efficiency during acceleration can be attained. The experience gained indicates that through a

more intensive testing program the high performance required can be had using extremely low pressure loss devices in short combustion chamber lengths at high mach numbers. Above auto-ignition temperature the major obstacle to high performance does not seem to be combustion but rather incomplete mixing. Also durability problems may be encountered as all parts of the system need to be cooled.

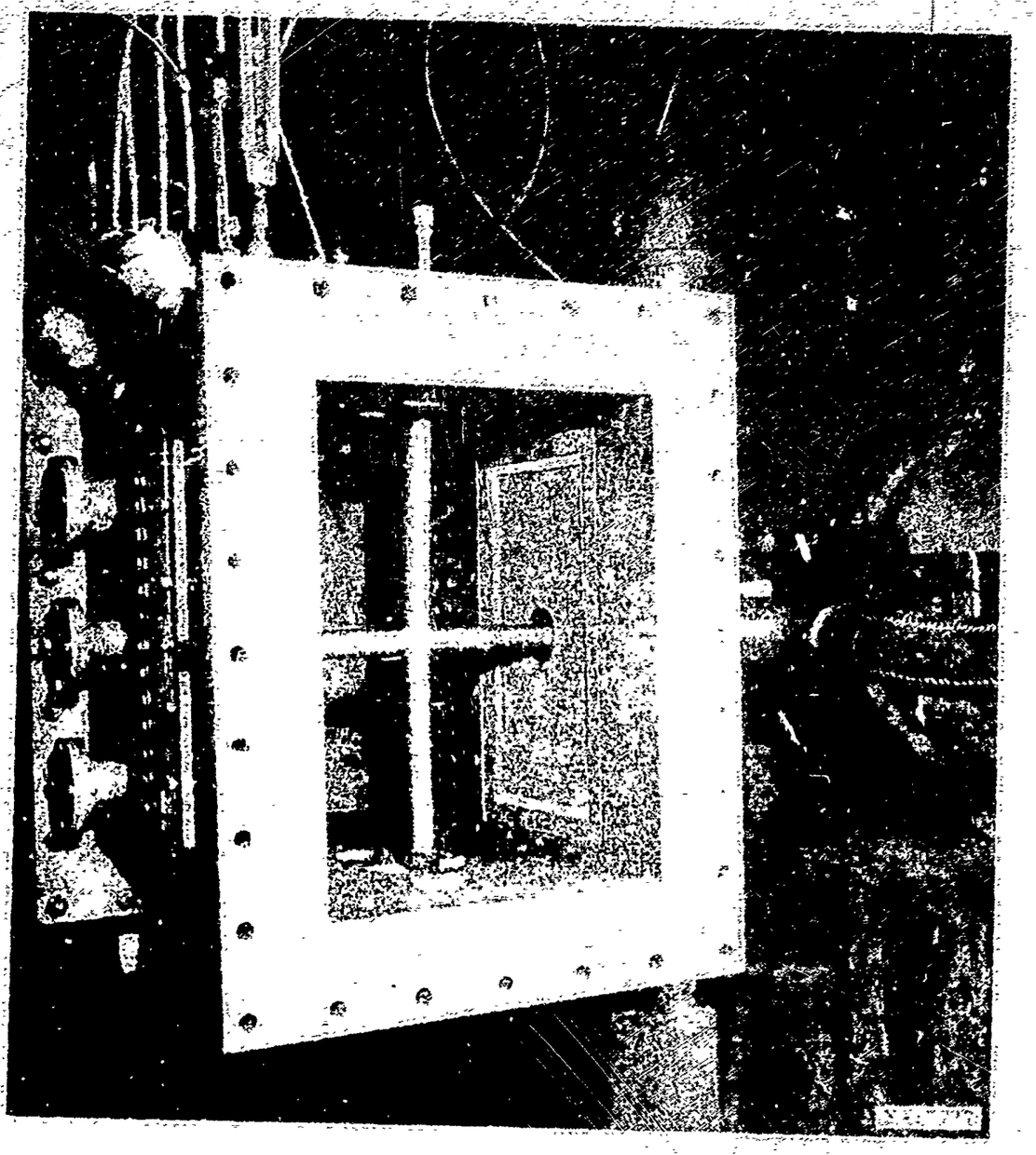
Since the spraybars perform very well at lean fuel-air ratios they are well suited for use in a partially augmented turbojet, that is, one in which relatively small amounts of fuel are injected directly into a slightly lengthened tailpipe of a turbojet.

It has been concluded from the testing done that spraybars alone are a very practical means of stabilizing flame in the afterburner of a SST turbojet. At the high temperatures involved there is no need for any conventional vee-gutter system as found in all afterburners being presently produced. A flameholding system consisting only of spraybars also offers the advantage of having a low cold pressure loss.



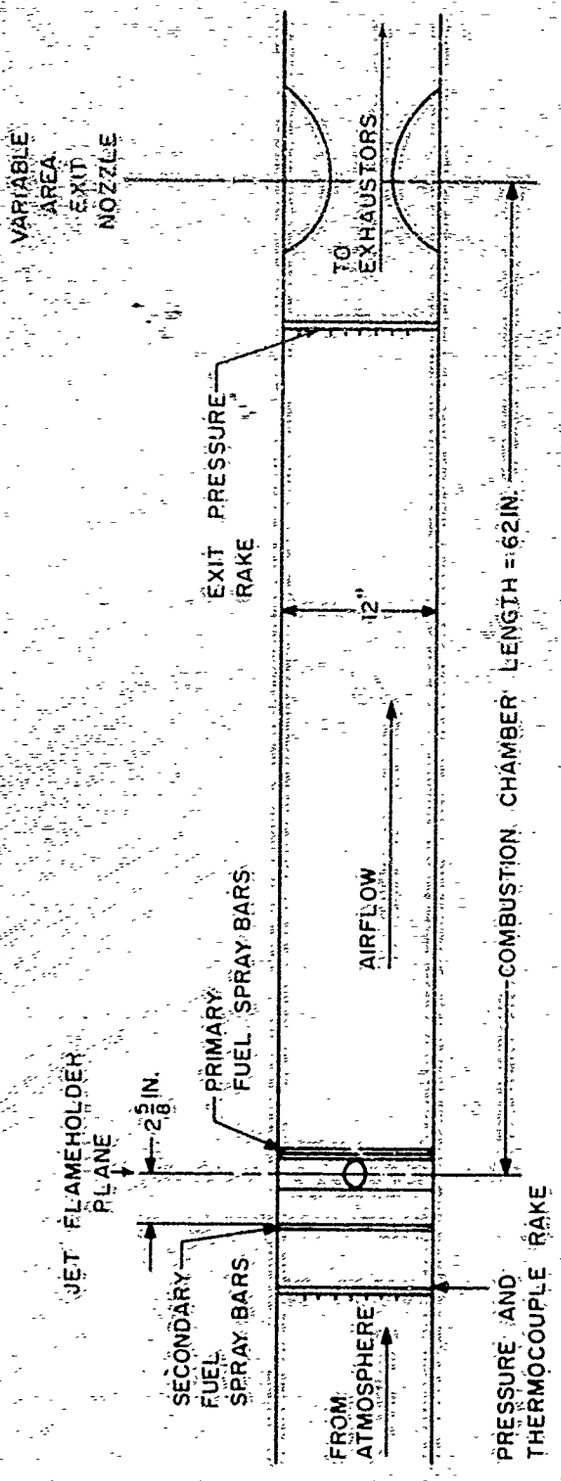
SCHEMATIC OF CROSS JET FLAMEHOLDER INSTALLED IN THE 12" X 16" RIG

Figure 7-1



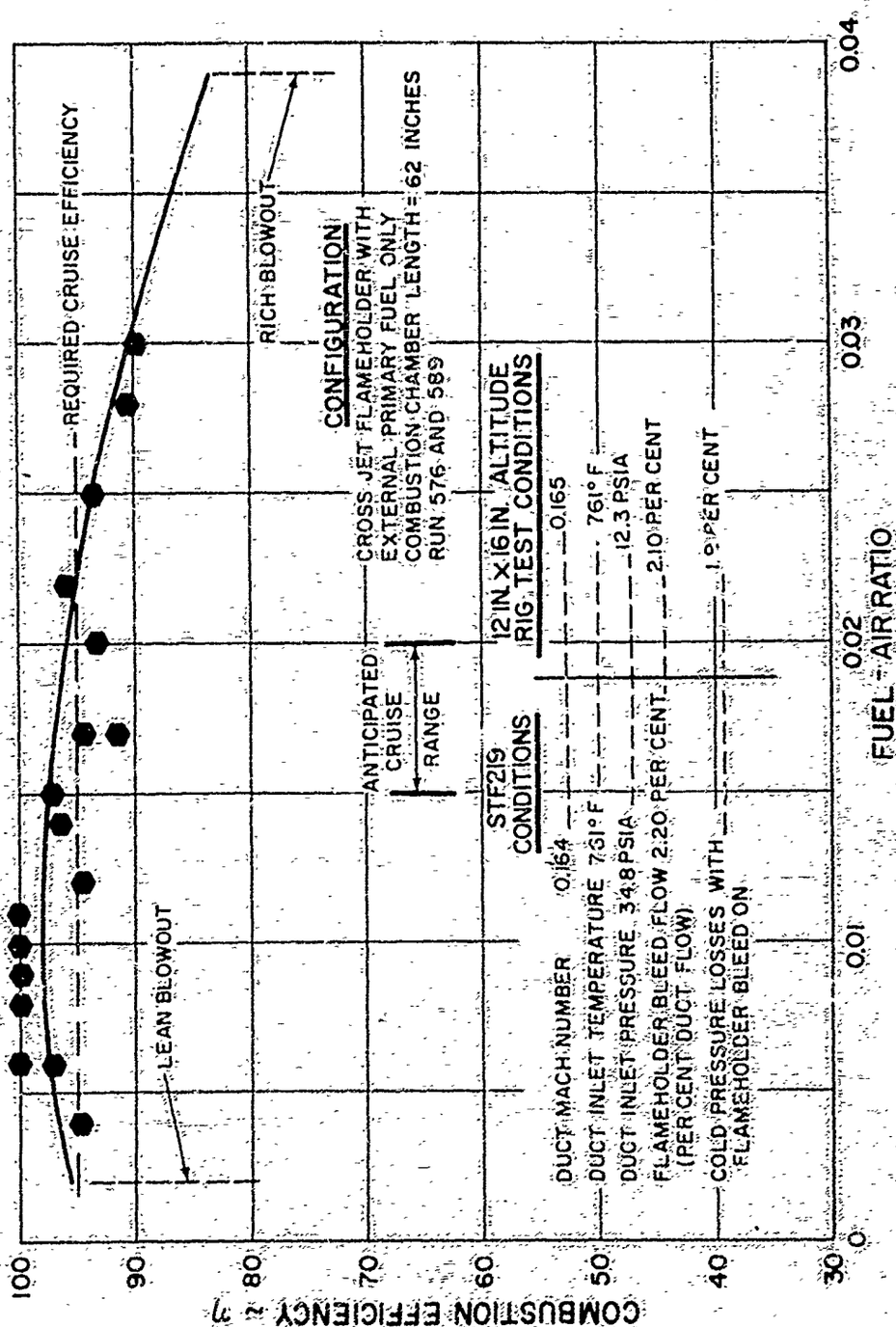
CROSS JET FLAMEHOLDER INSTALLED IN THE 12" X 14" RIG

Figure 7-2



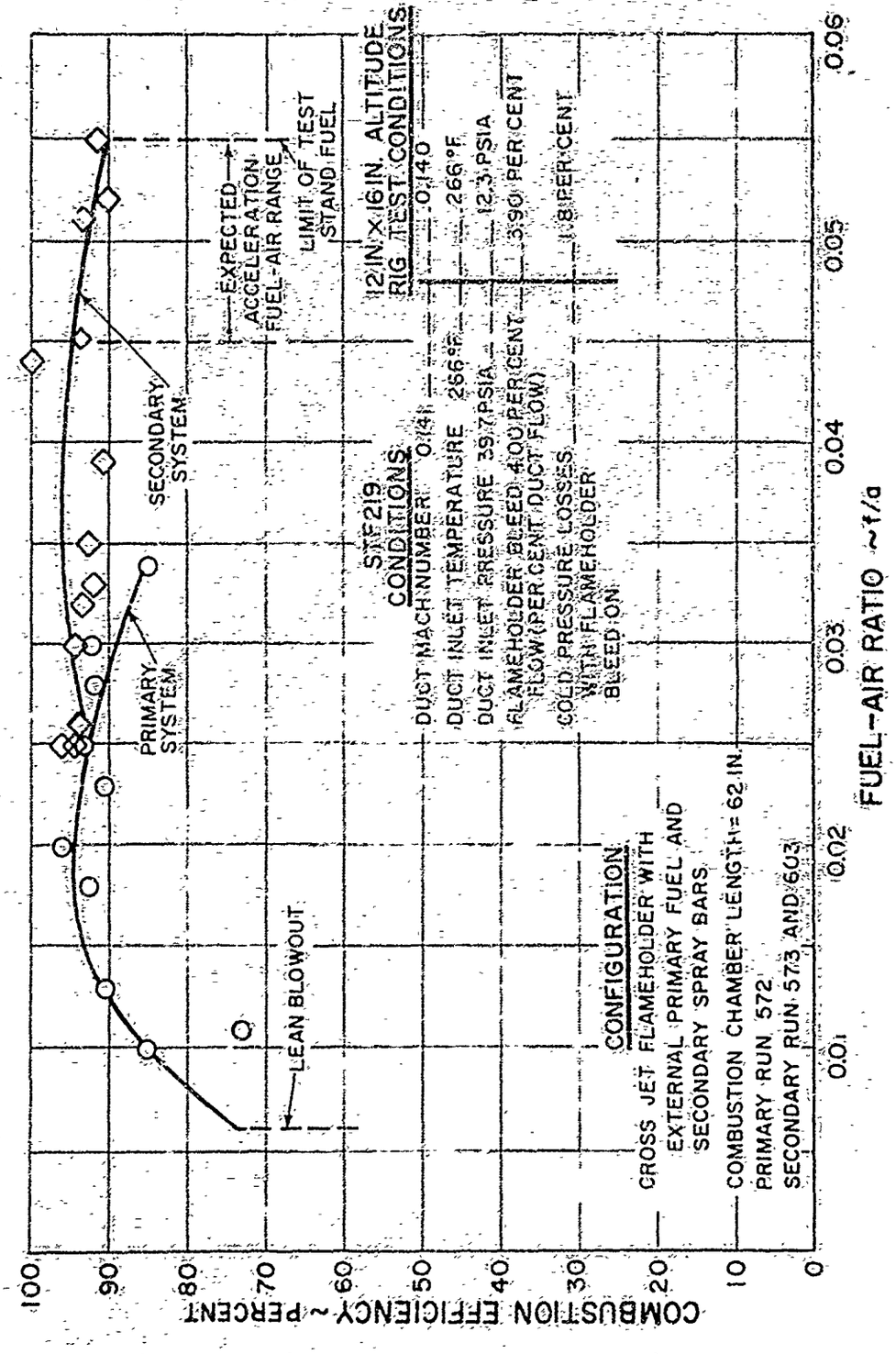
12" X 16" ALTITUDE RESEARCH RIG SIMULATING A 16" SEGMENT OF THE STF219 DUCT HEATER

Figure 7-3



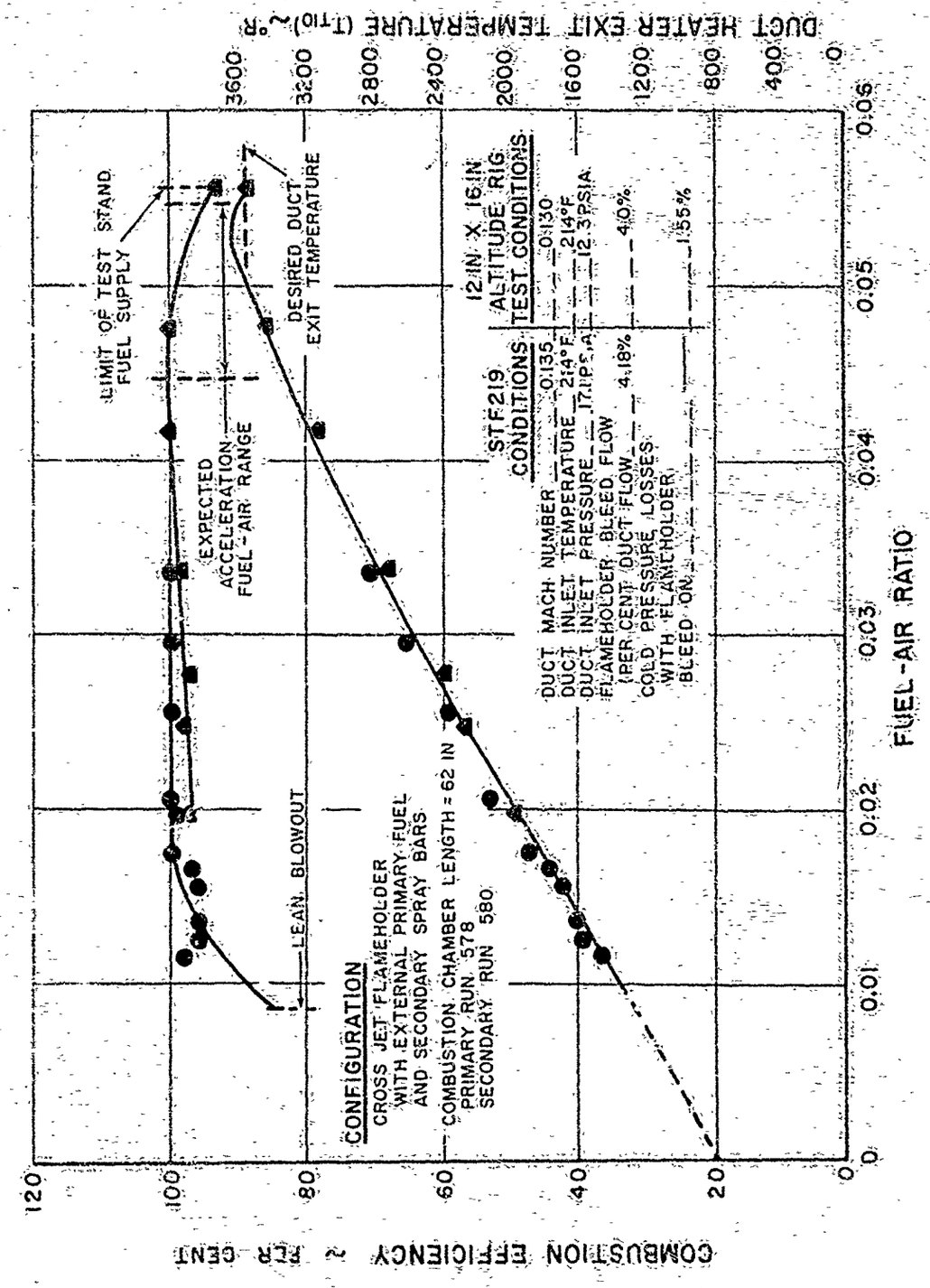
DUCT HEATER PERFORMANCE AT STF219 CRUISE CONDITIONS

Figure 7-4



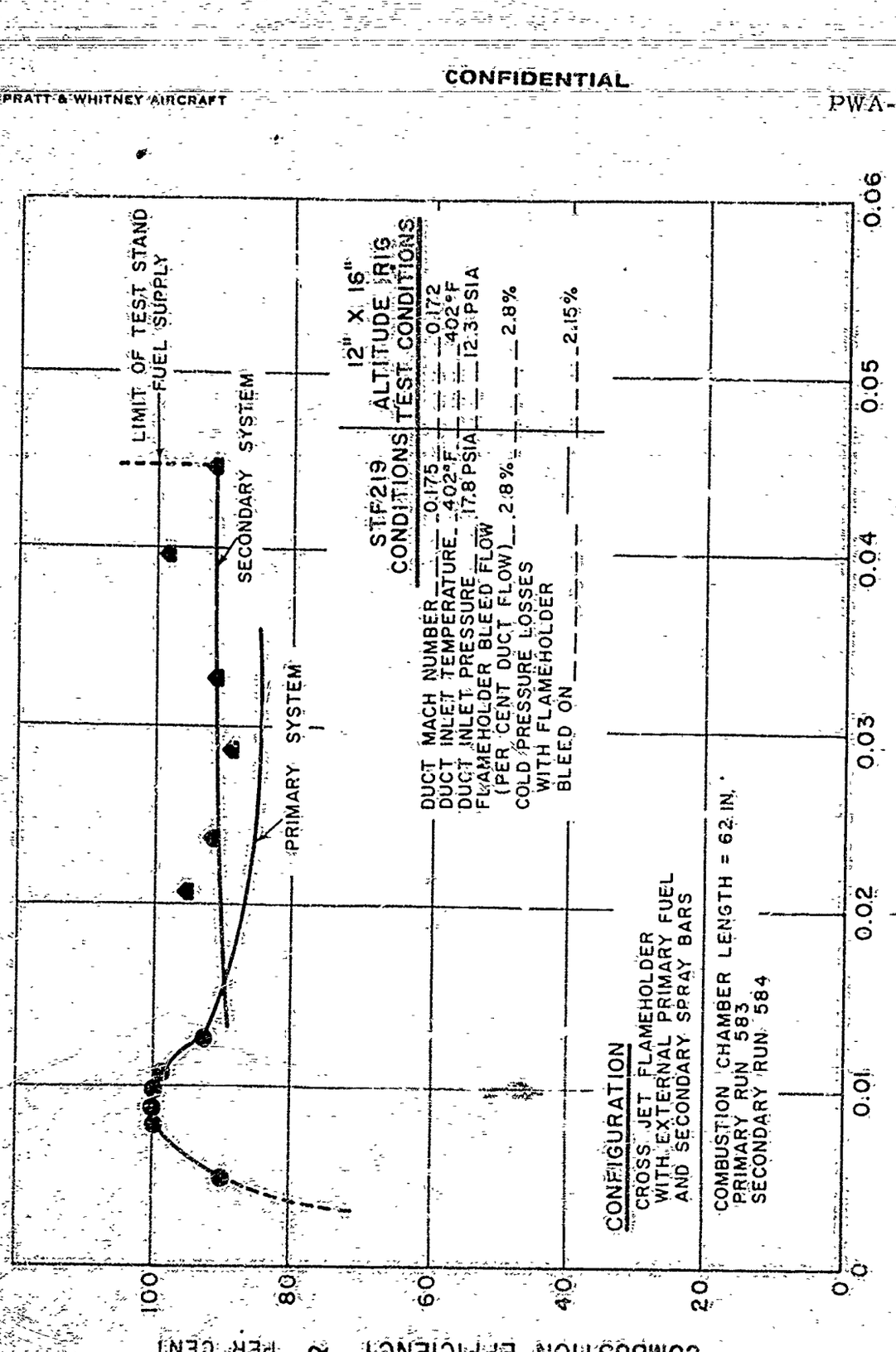
DUCT HEATER PERFORMANCE AT STF219 SEA LEVEL ACCELERATION CONDITIONS

Figure 7-6



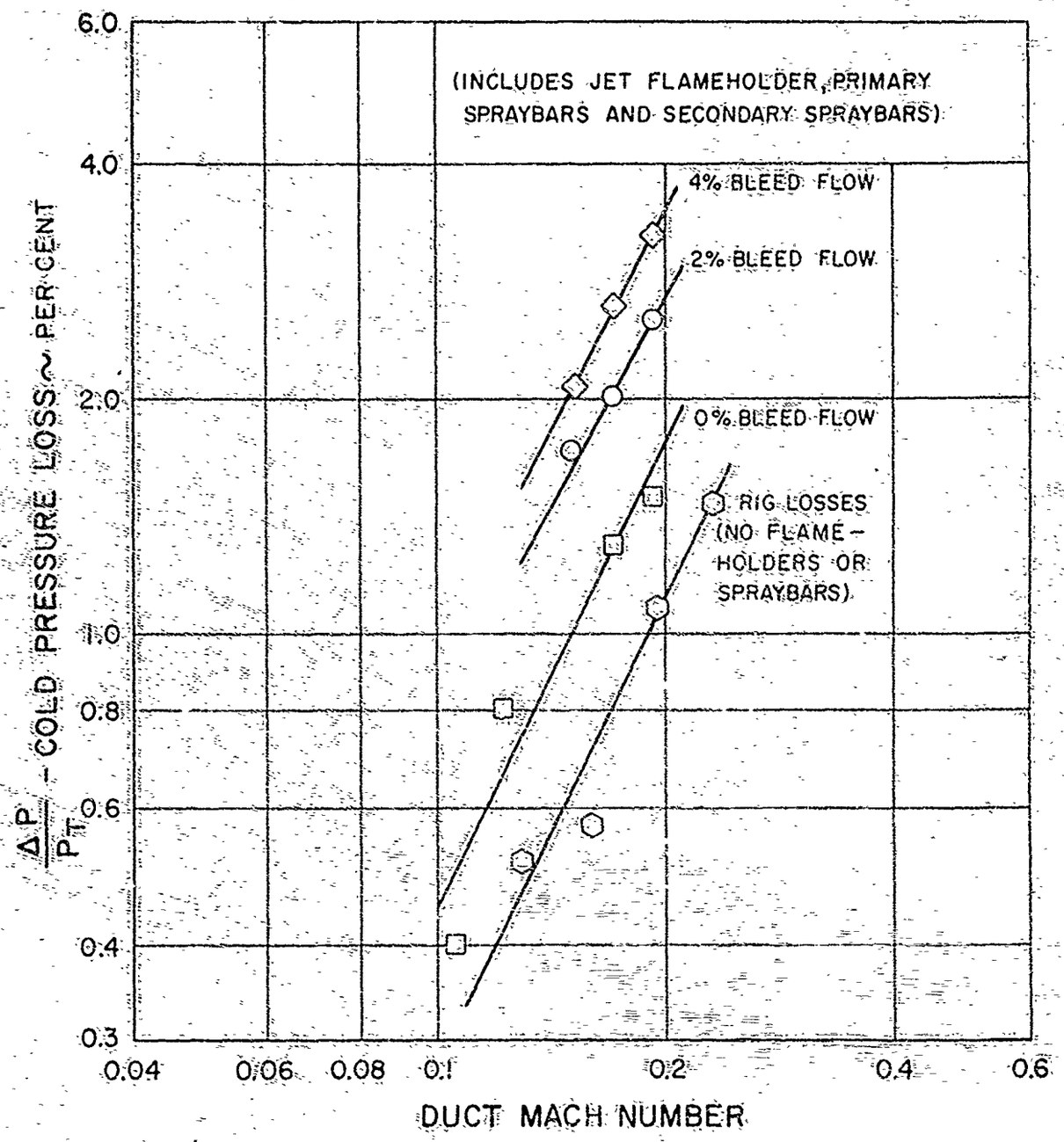
DUCT HEATER PERFORMANCE AT STF219 TRANSONIC CONDITIONS

Figure 7-6



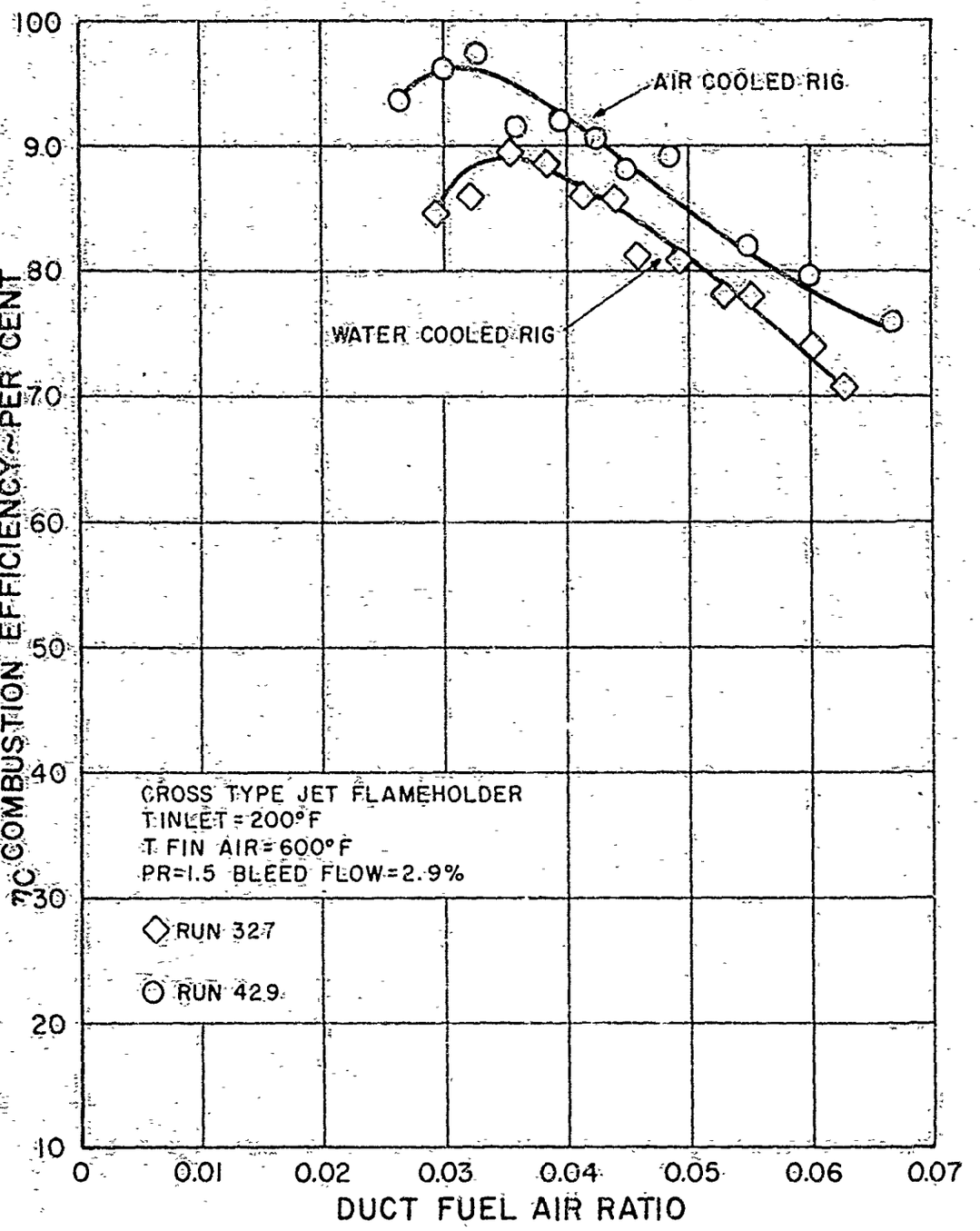
DUCT HEATER PERFORMANCE AT STF219 ACCELERATION CONDITIONS

Figure 7-7



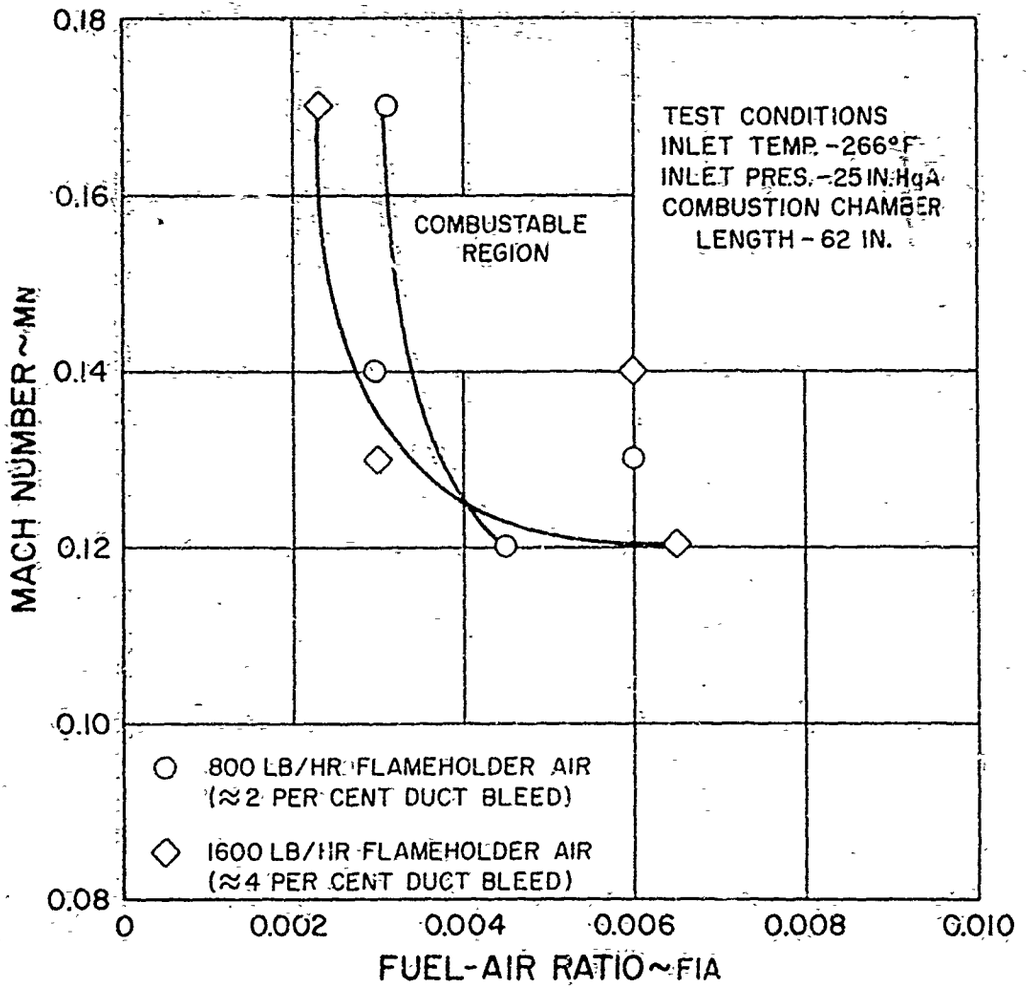
COLD FLOW LOSSES OF DUCT HEATER SYSTEM UTILIZED IN FLIGHT PERFORMANCE TESTS

Figure 7-8



COMPARISON OF JET FLAMEHOLDER PERFORMANCE IN AIR COOLED VS WATER COOLED RIGS

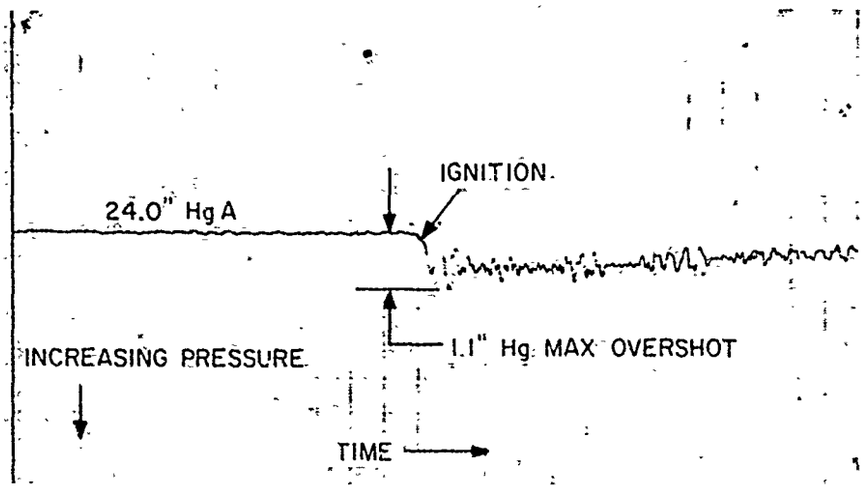
Figure 7-9



IGNITION CHARACTERISTICS OF THE CROSS JET FLAMEHOLDER WITH EXTERNAL PRIMARY FUEL

Figure 7-10

20 JOULE SPARK IGNITOR,
CHOKED EXIT NOZZLE SIMULATED
SEA LEVEL TAKEOFF CONDITIONS

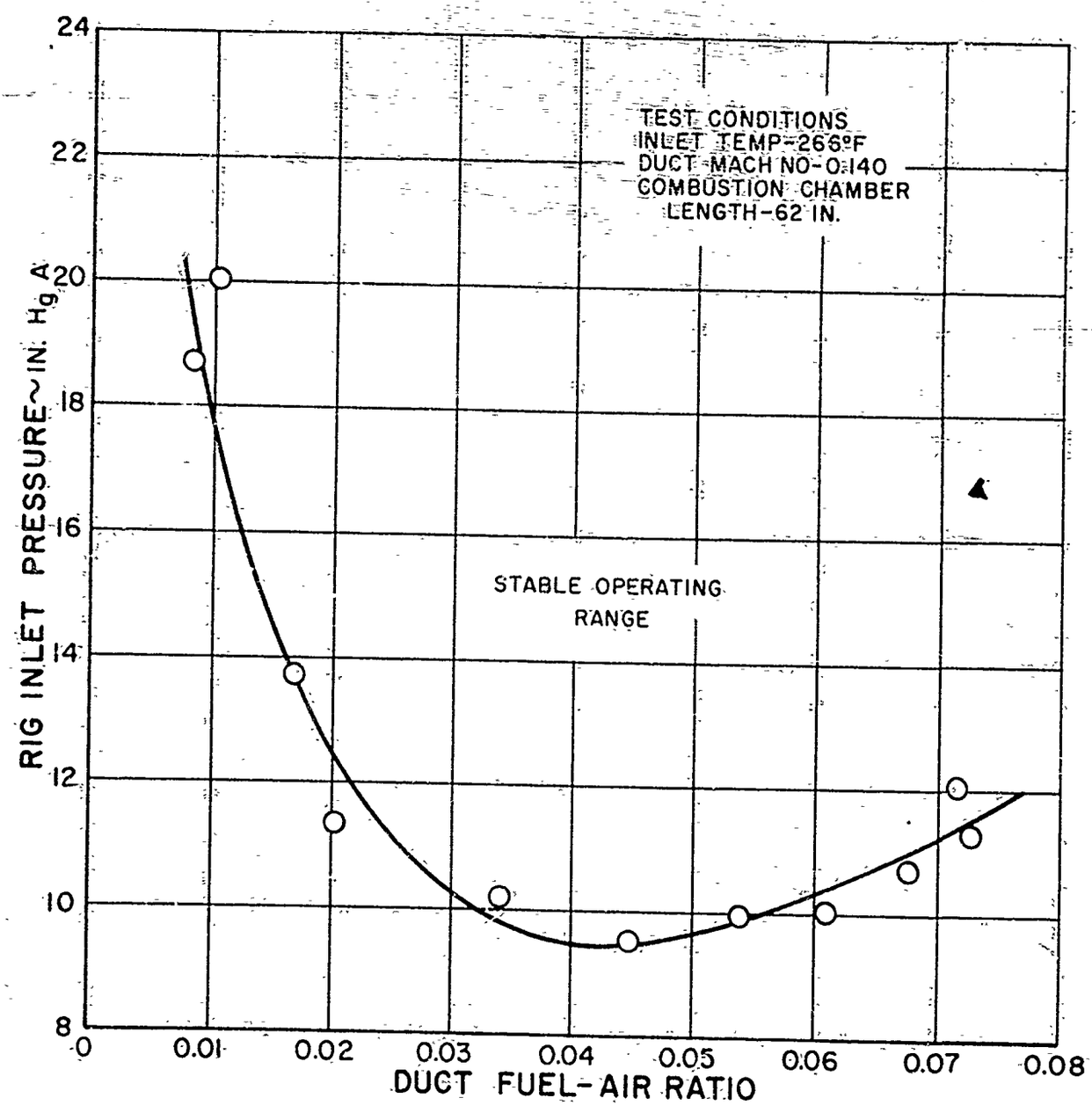


TEST CONDITIONS

STF219 ACCELERATION SIMULATION
DUCT MACH NO. = 0.148
DUCT INLET TEMPERATURE = 266°F
DUCT INLET PRESSURE = 24" Hg A
FLAMEHOLER AIR TEMPERATURE = 665°F
FLAMEHOLDER BLEED FLOW = 2.1%
IGNITION FUEL AIR RATIO = .0030
PRESSURE PULSE = 4.7%

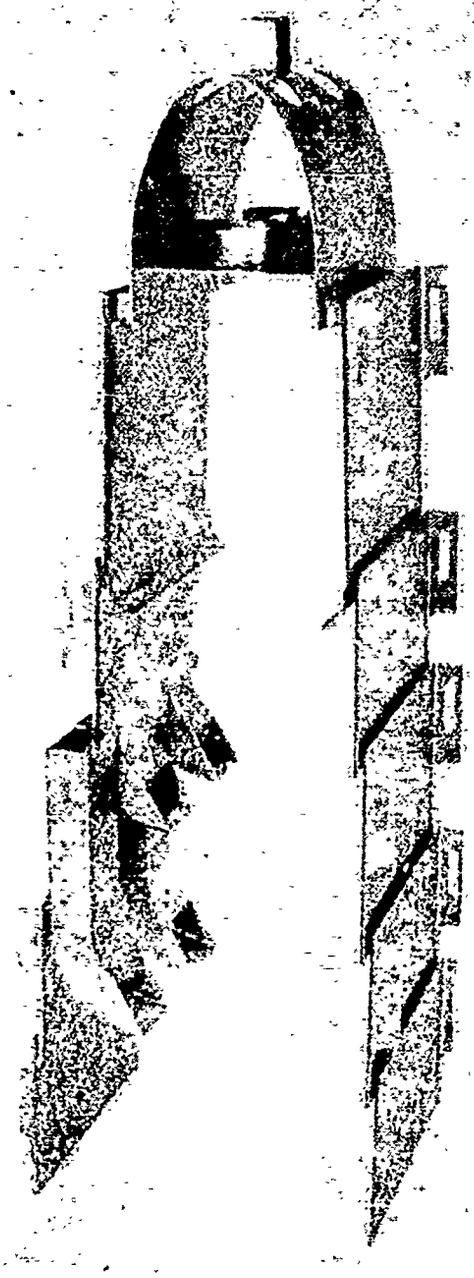
A TYPICAL HIGH SPEED TRANSDUCER TRACE OF THE IGNITION PRESSURE PULSE OF THE DUCT HEATER

Figure 7-11



MINIMUM PRESSURE BLOWOUT OF TYPICAL JET FLAMEHOLDER

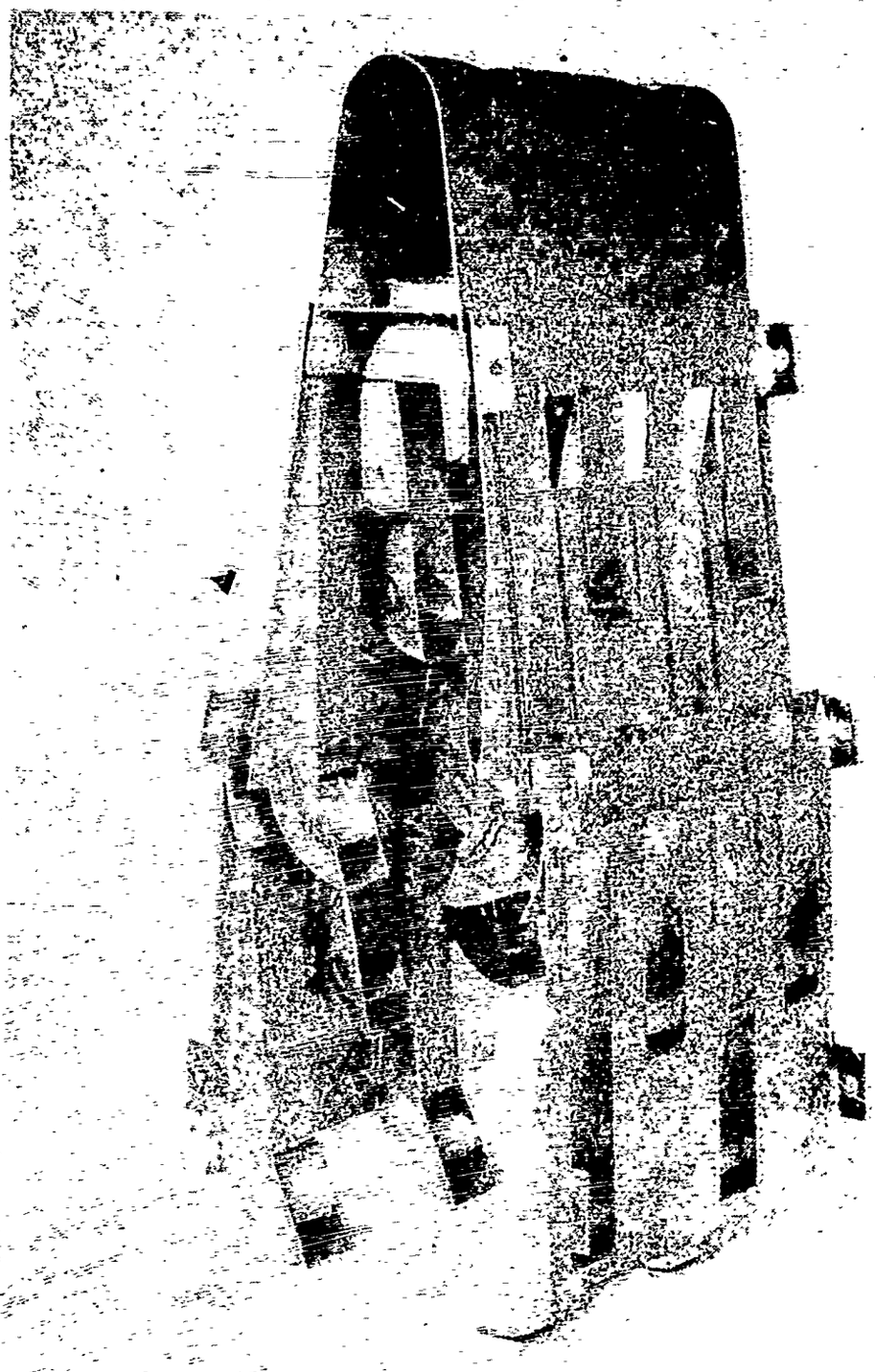
Figure 7-12



FE-7195

INITIAL DUCT BURNER DESIGN, MODEL A

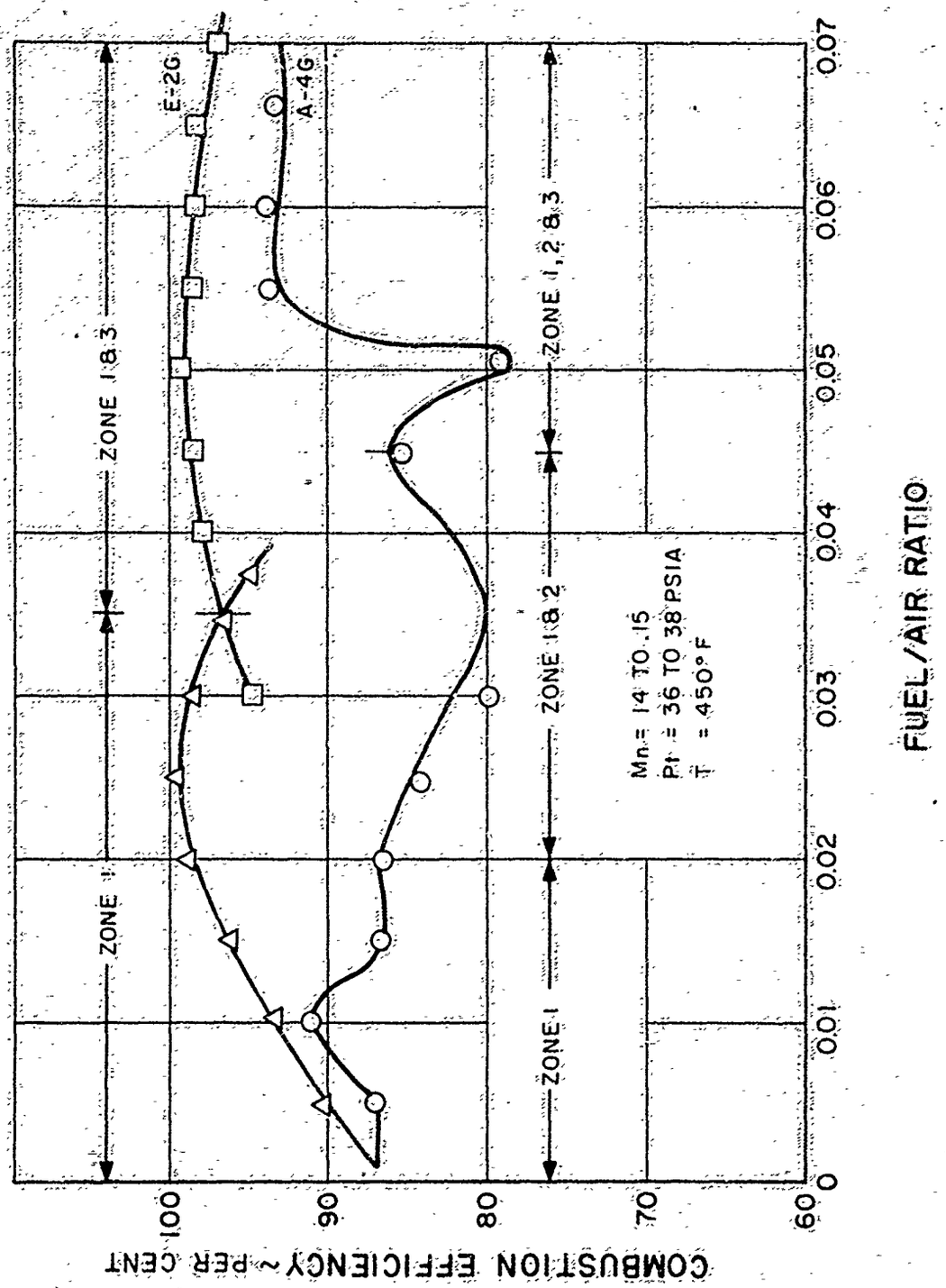
Figure 7-13



FE-44292

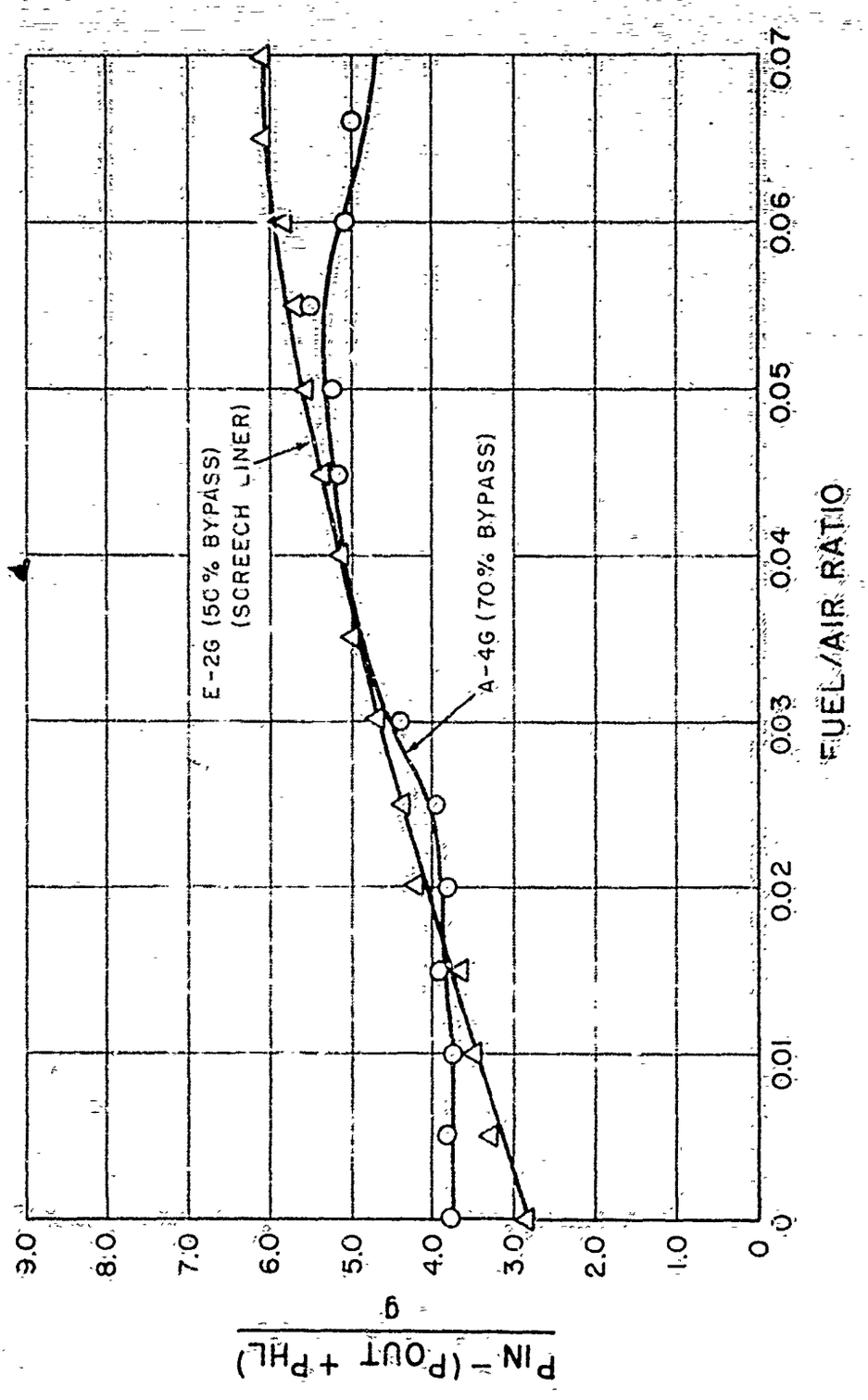
LATEST DUCT BURNER DESIGN, MODEL E

Figure 7-14



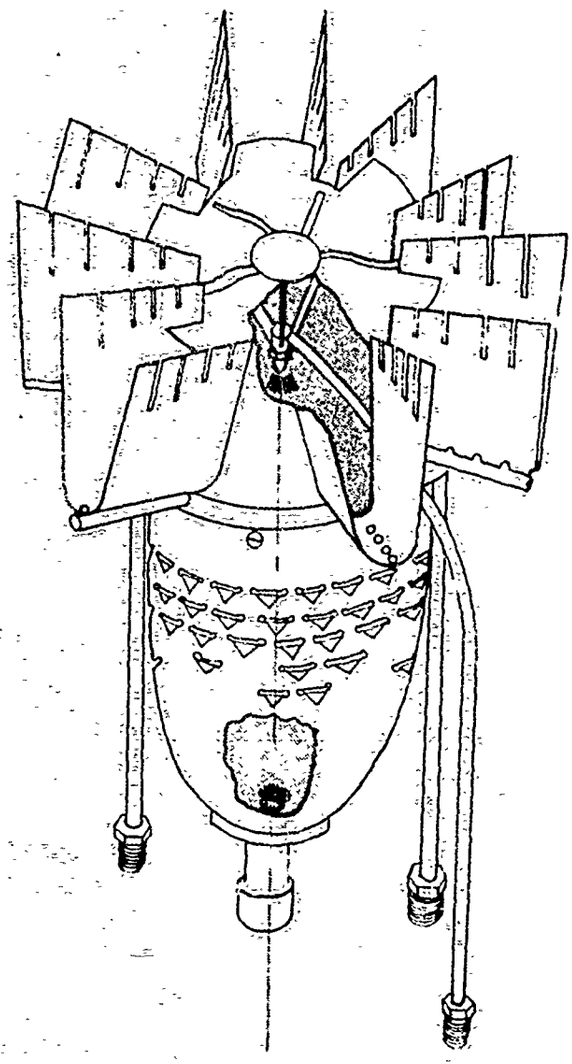
COMPARISON OF BURNER COMBUSTION EFFICIENCY

Figure 7-15



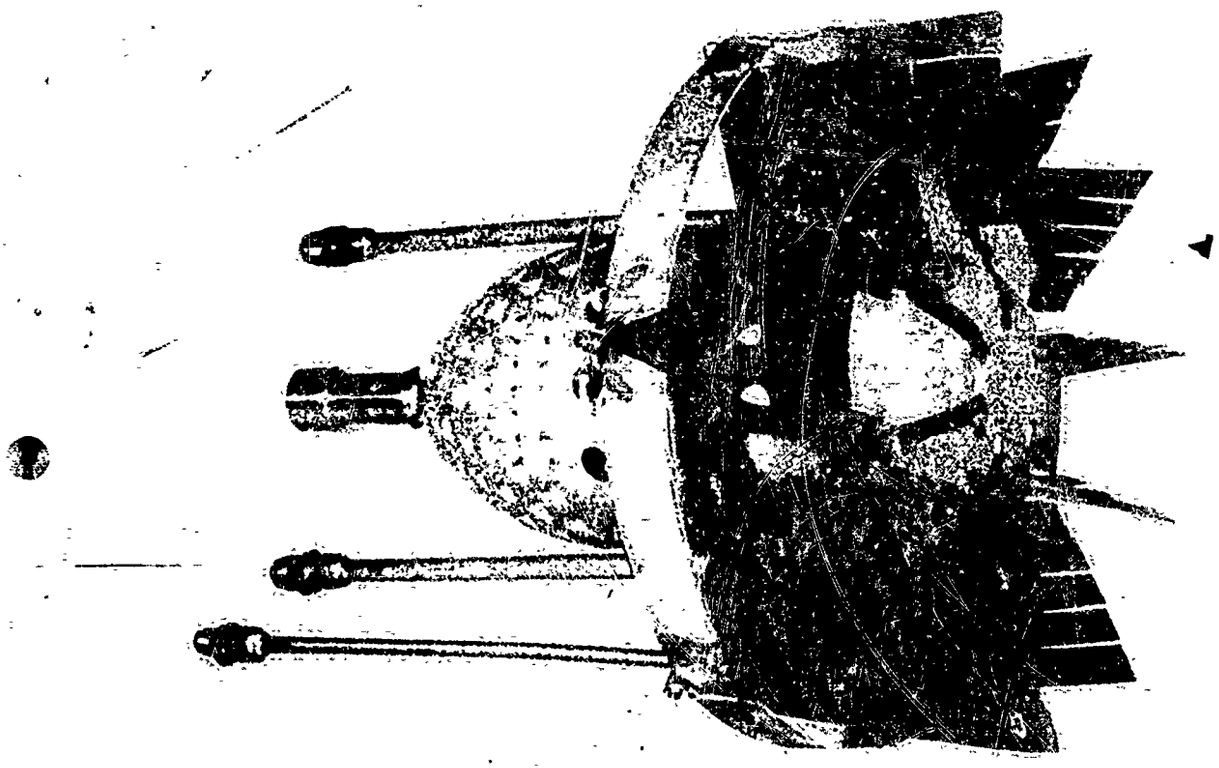
COMPARISON OF BURNER PRESSURE LOSS

Figure 7-16



DIAGRAMATIC ILLUSTRATION OF HETEROGENEOUS BURNER - MODEL A

Figure 7-17

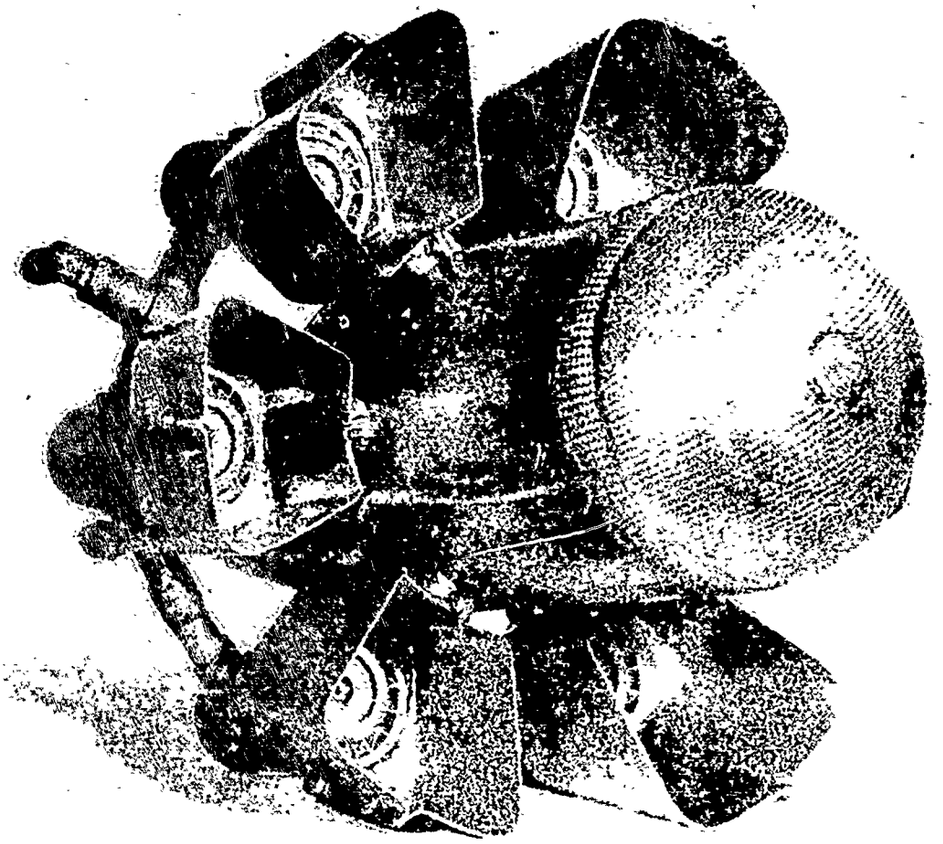


PHOTOGRAPH OF HETEROGENEOUS BURNER - MODEL A

Figure 7-18

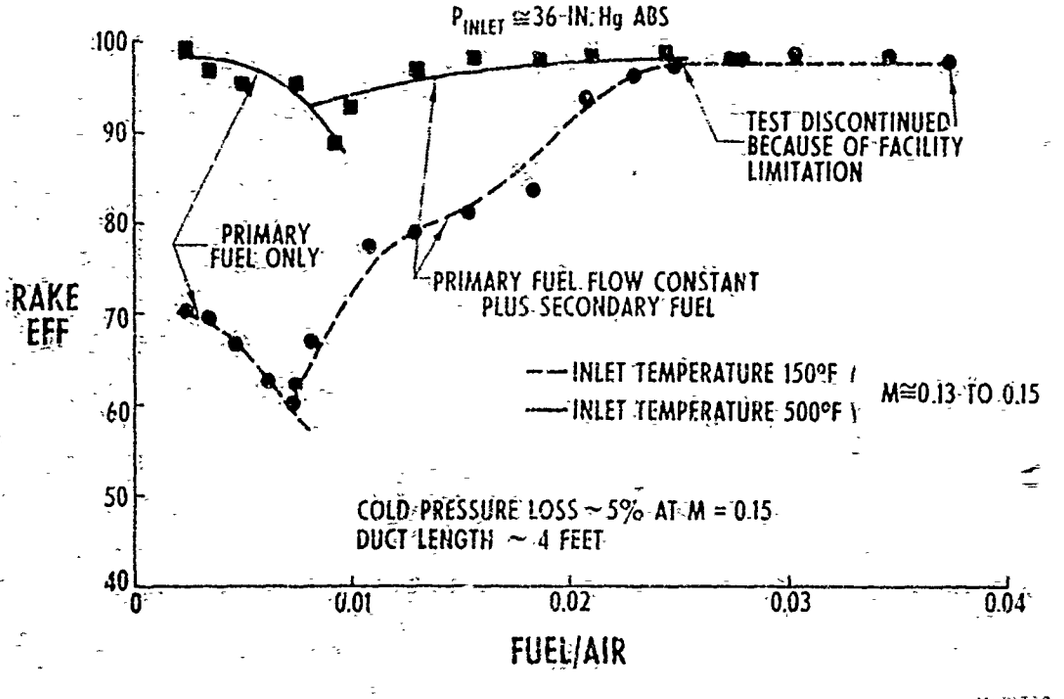
DOWNGRADED AT 3 YEAR INTERVALS
DECLASSIFIED AFTER 12 YEARS
DOD DIR 5200.10

THIS DOCUMENT CONTAINS INFORMATION AFFECTING THE NATIONAL DEFENSE OF THE UNITED STATES WITHIN THE MEANING OF THE ESPIONAGE LAWS, TITLE 18, U.S.C., SECTIONS 793 AND 794. THE TRANSMISSION OR REVELATION OF ITS CONTENTS IN ANY MANNER TO AN UNAUTHORIZED PERSON IS PROHIBITED BY LAW.



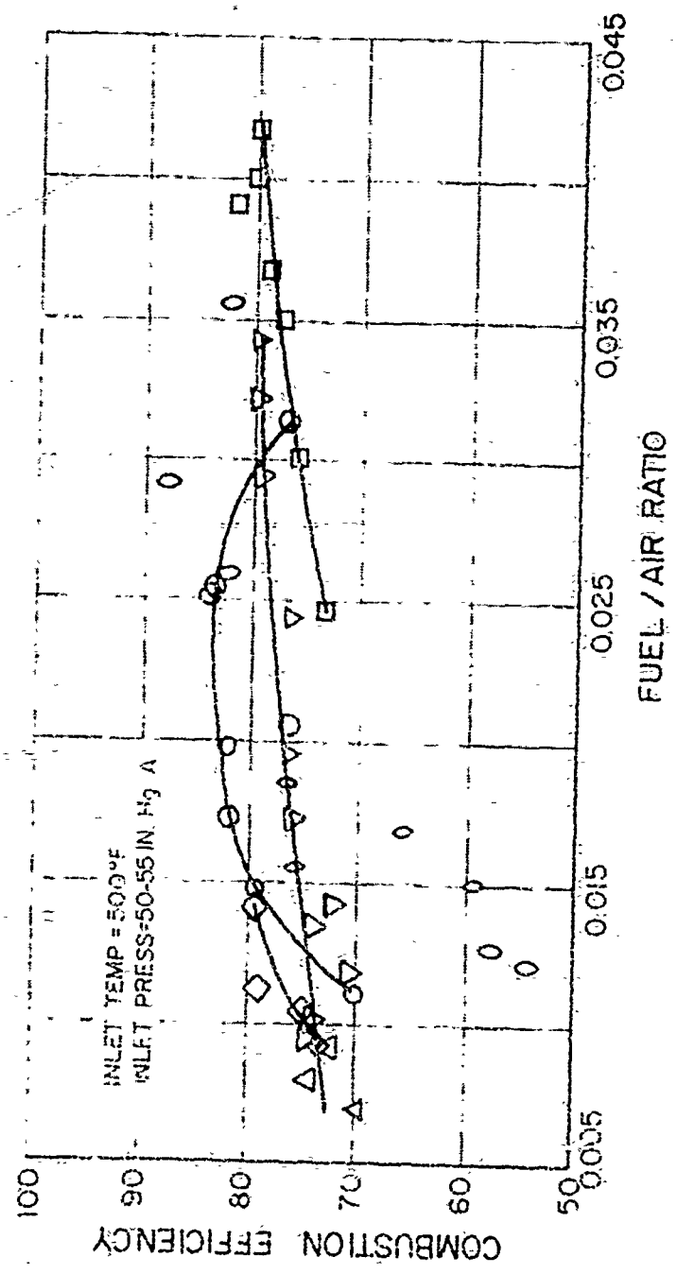
REAR VIEW OF HETEROGENEOUS BURNER - MODEL B

Figure 7-19



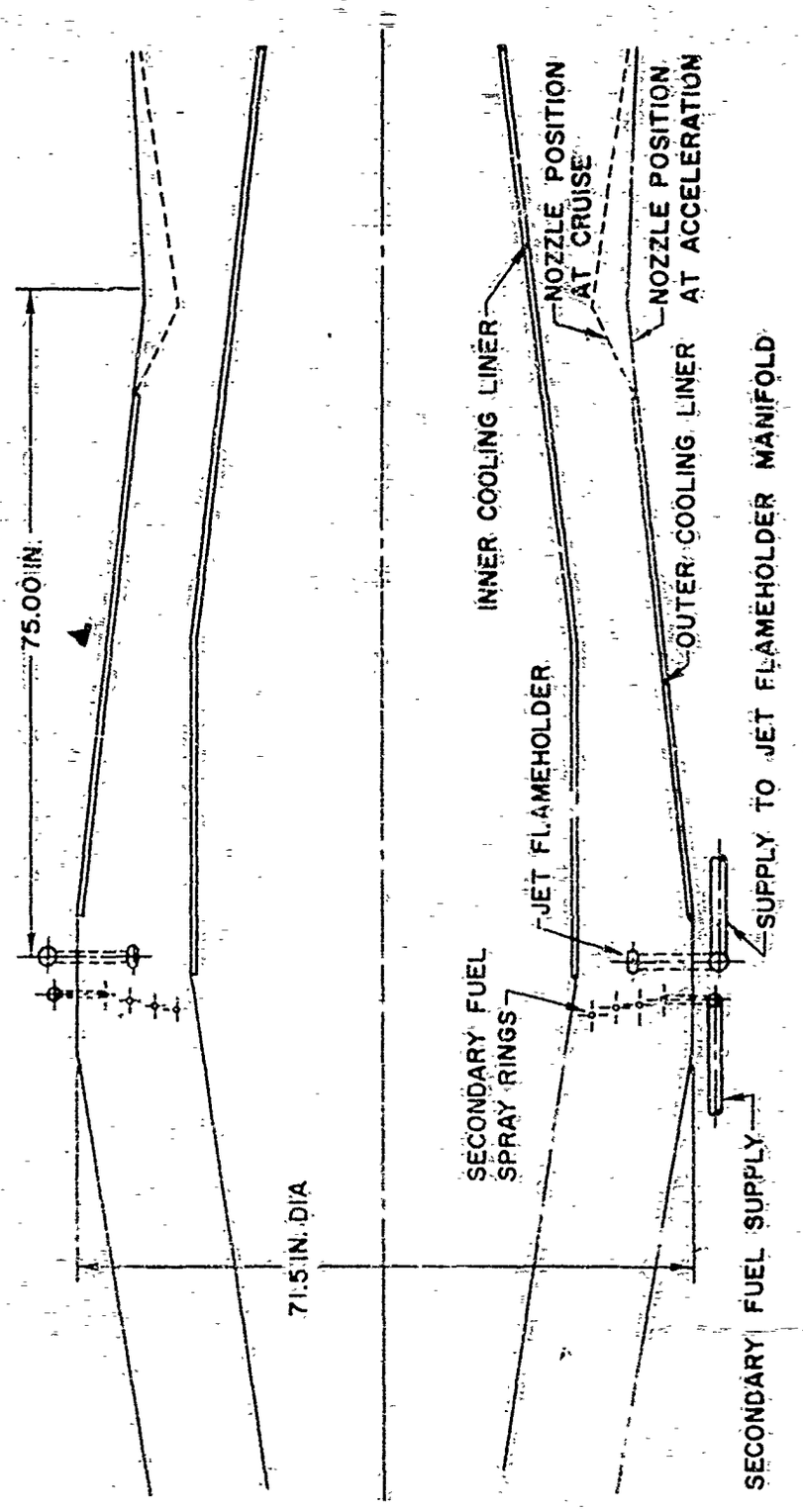
TEST RESULTS FROM MODEL A HETEROGENEOUS BURNER

Figure 7-20



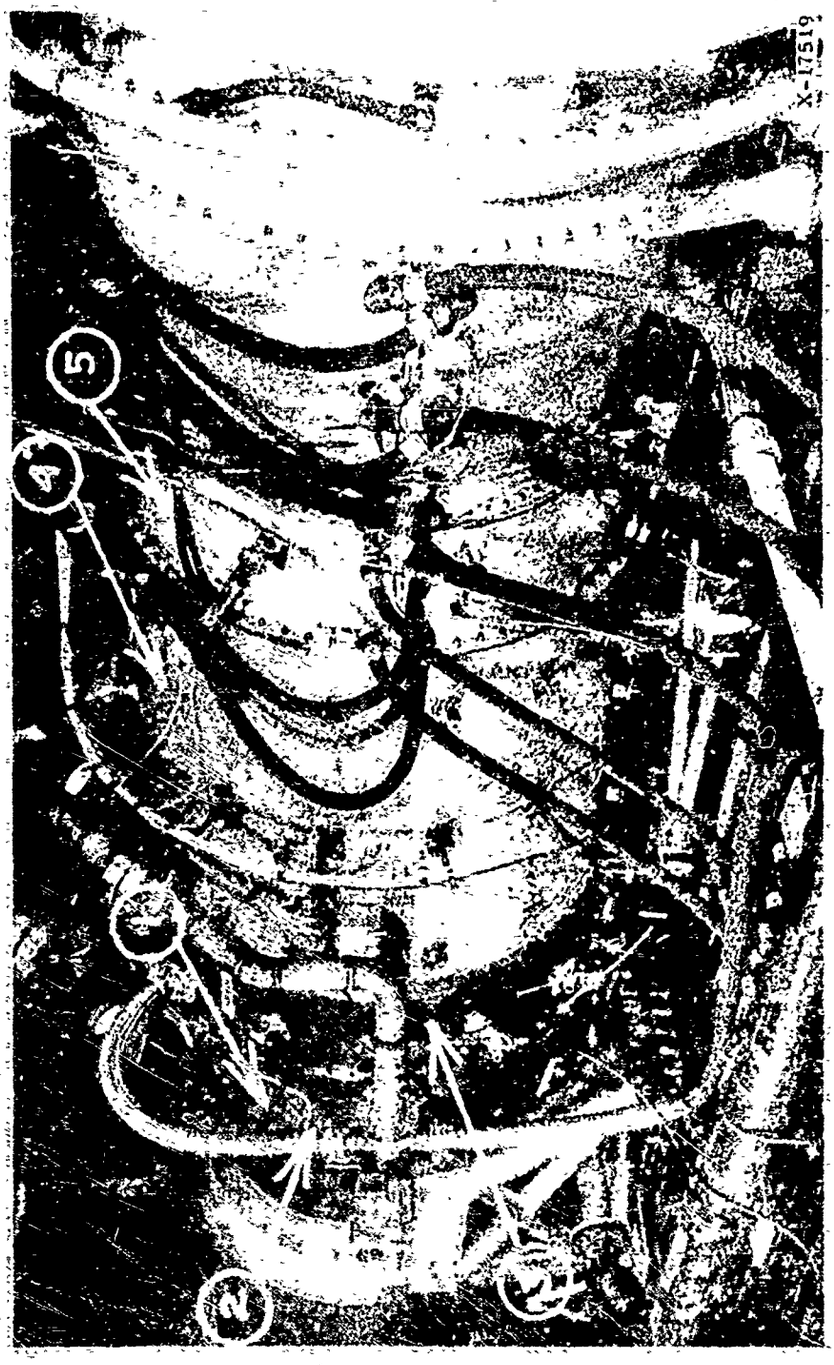
TEST RESULTS FROM MODEL B HETEROGENEOUS BURNER

Figure 7-21



SCHEMATIC OF FULL-SCALE DUCT HEATER TEST RIG

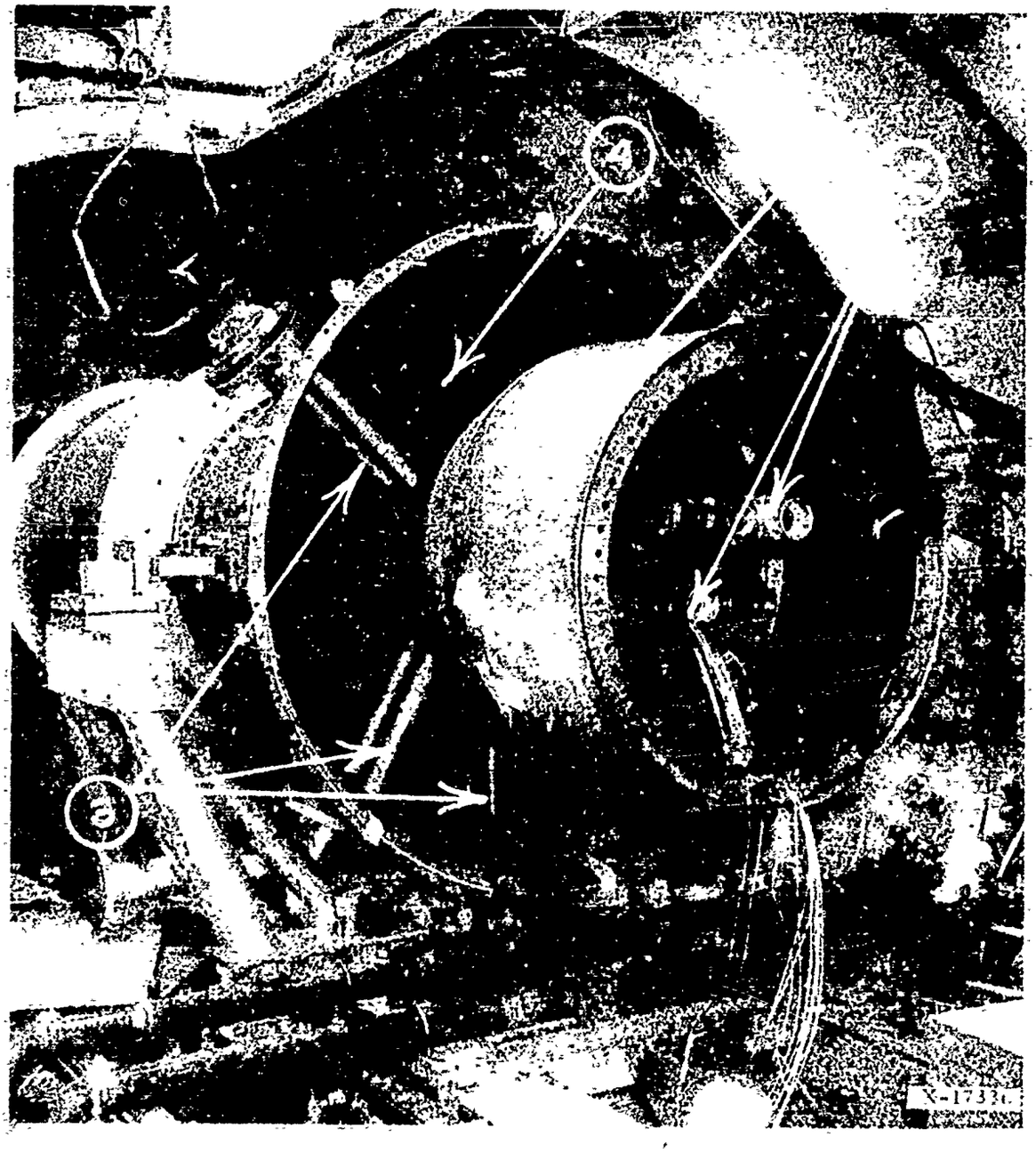
Figure 7-22



FULL SCALE DUCT HEATER TEST RIG

1. Inlet Diffuser
2. Jet Flameholder Manifold
3. Jet Flameholder Section
4. Combustion Chamber
5. Exit Nozzles

Figure 7-23



FULL SCALE DUCT HEATER RIG INLET DIFFUSER ASSEMBLY

1. Inner Body Fuel Baffle
2. Inner Body Cooling Water Pipes
3. Inner Body Instrumentation Tubes
4. Inner Body Support

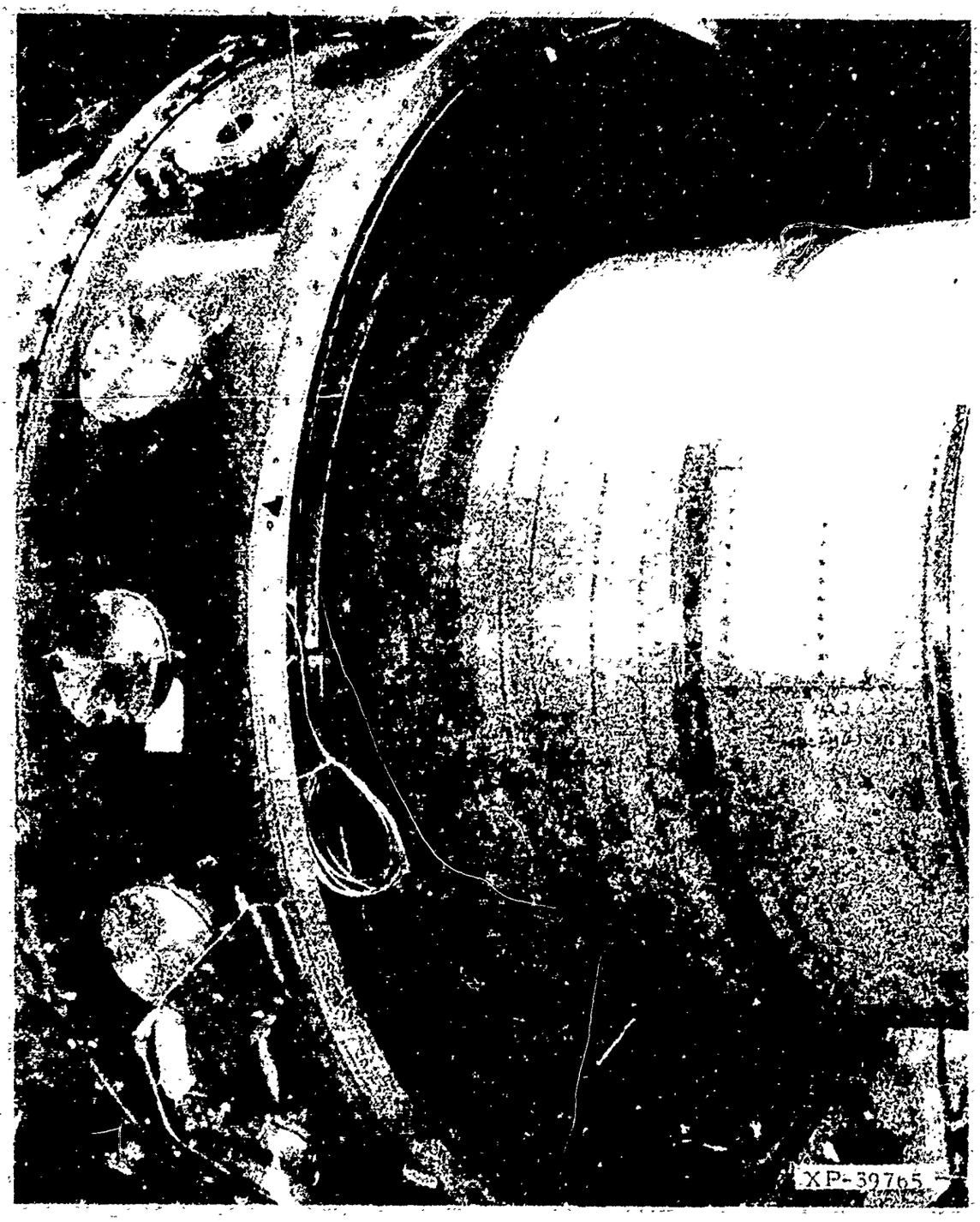
Figure 7-21



X-17285

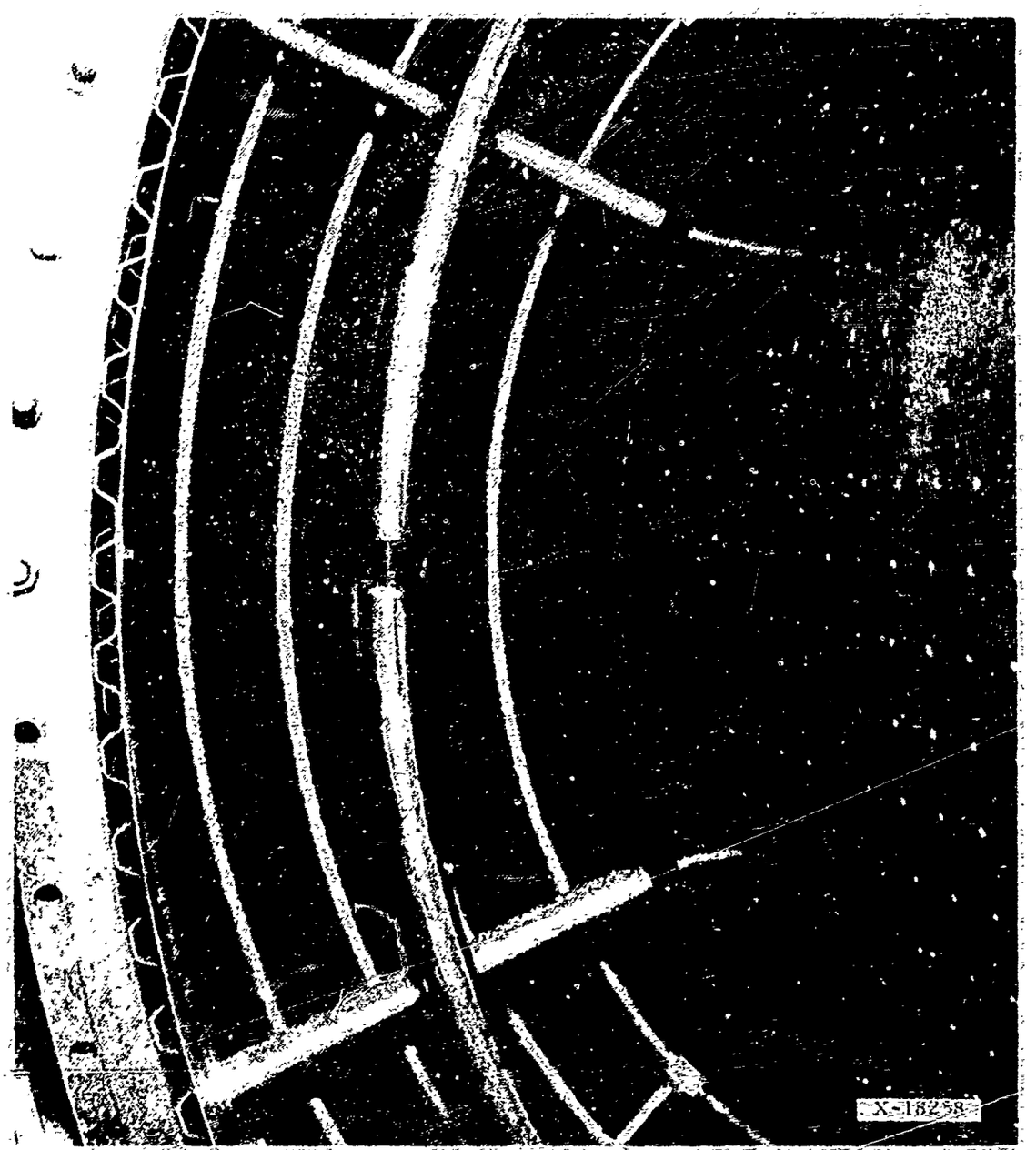
FULL SCALE DUCT HEATER RIG OUTER WALL FUEL BAFFLE

Figure 7-25



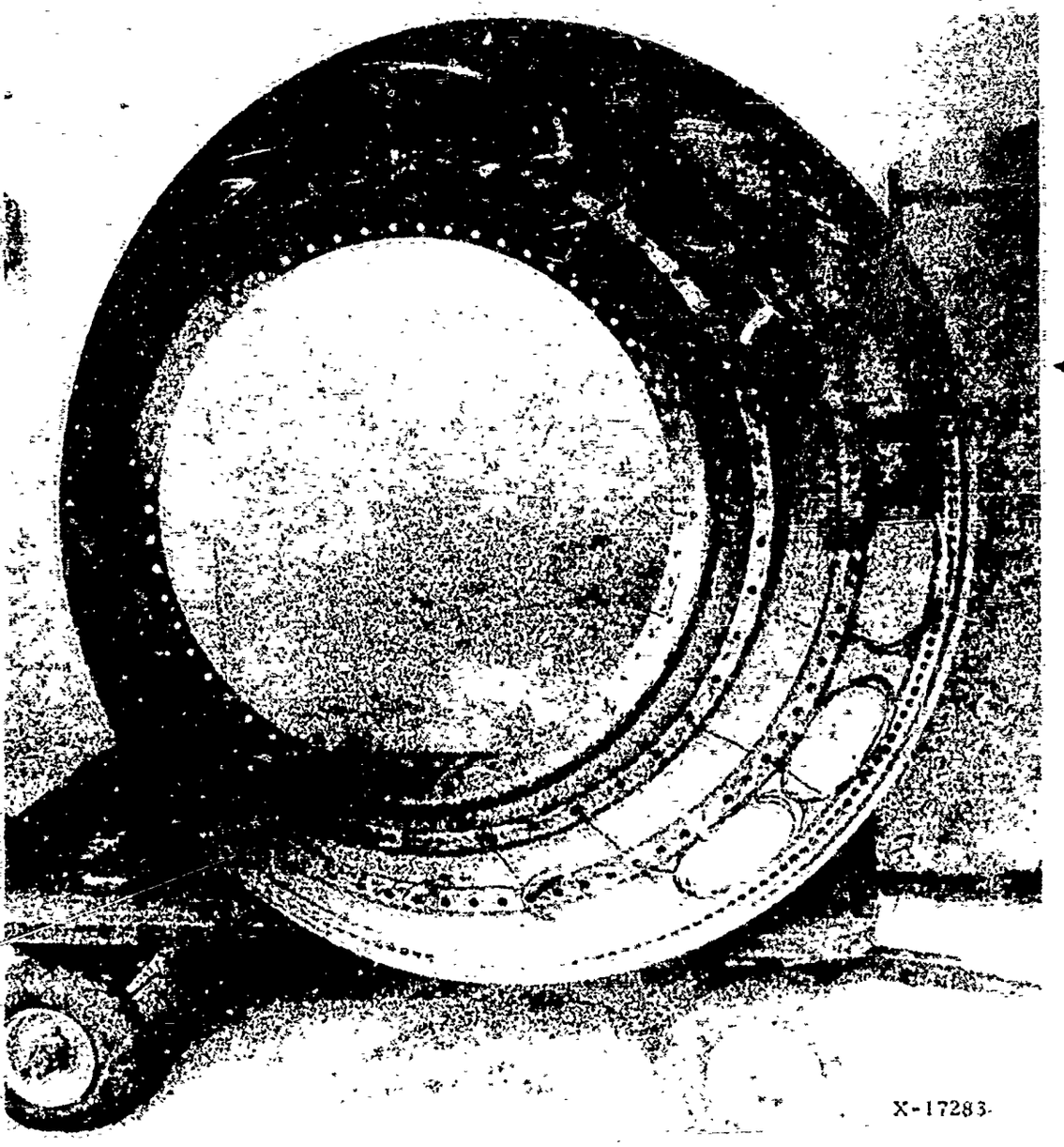
FULL SCALE DUCT HEATER RIG JET FLAMEHOLDER INSTALLED

Figure 7-26



SST FULL SCALE DUCT HEATER RIG JET FLAMEHOLDER AND SPRAY RINGS FIREY CROSS CONFIGURATION

Figure 7-27



X-17283

FULL SCALE DUCT HEATER RIG POROUS INNER COOLING LINER

Figure 7-28

DOWNGRADED AT 3 YEAR INTERVALS
DECLASSIFIED AFTER 12 YEARS
DOD DIR 5200.10



PARTIALLY ASSEMBLED FULL SCALE DUCT HEATER RIG SHOWING TRANSPIRATION COOLED INNER BODY

Figure 7-29



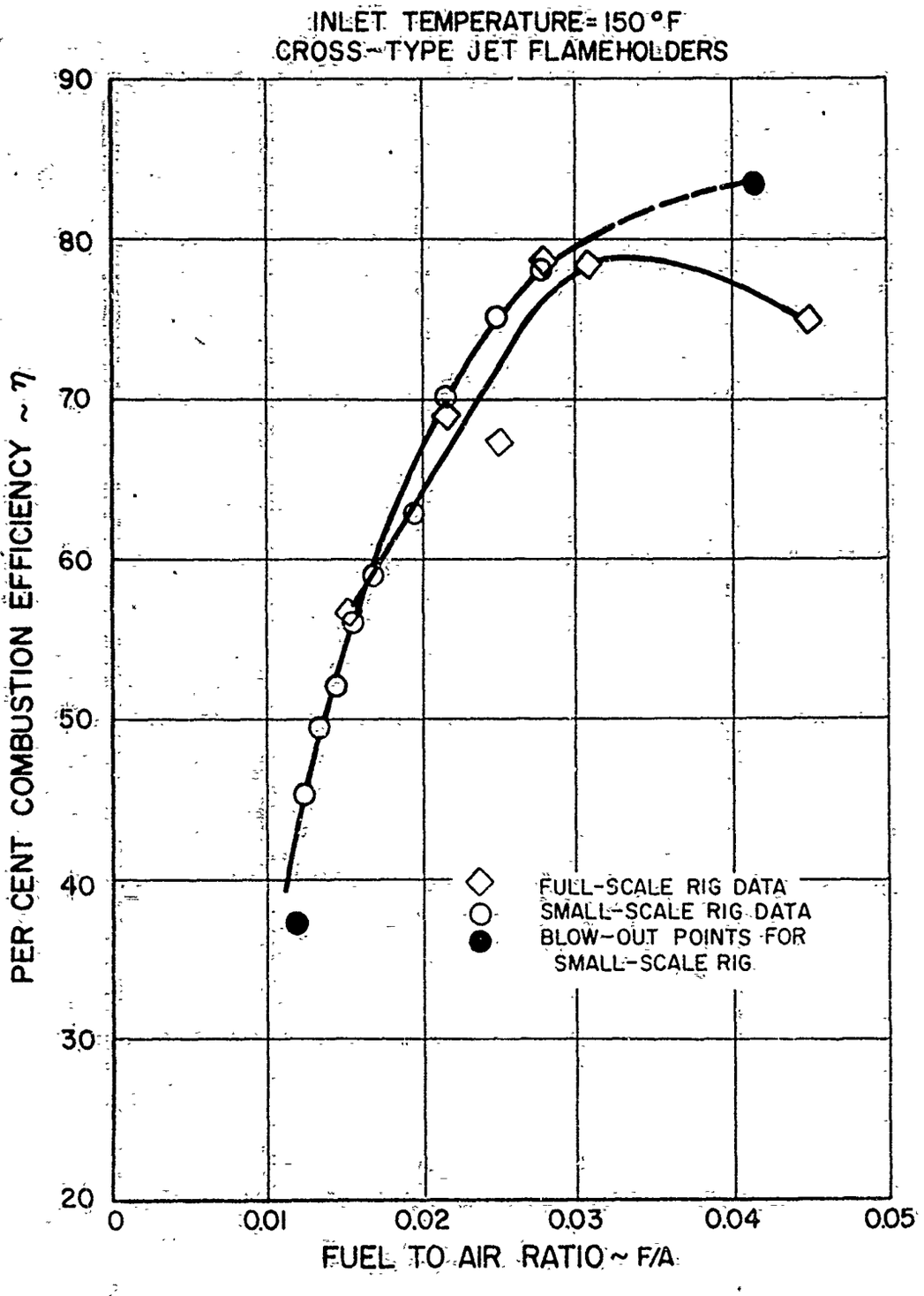
SST FULL SCALE DUCT HEATER RIG POROUS OUTER COOLING LINER

Figure 7-30



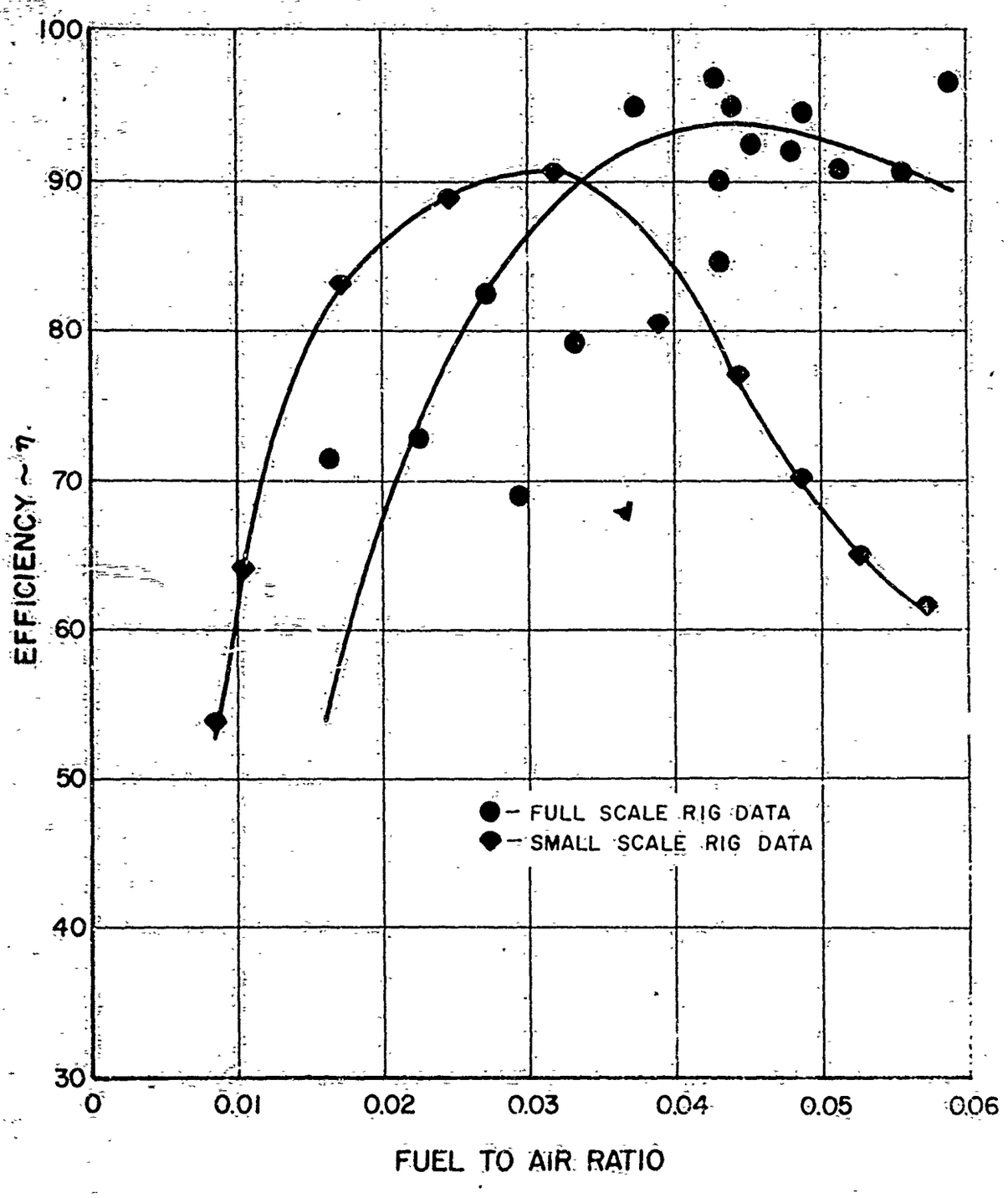
SST FULL SCALE DUCT HEATER RIG REINFORCED COMBUSTION CHAMBER OUTER DUCT

Figure 7-31



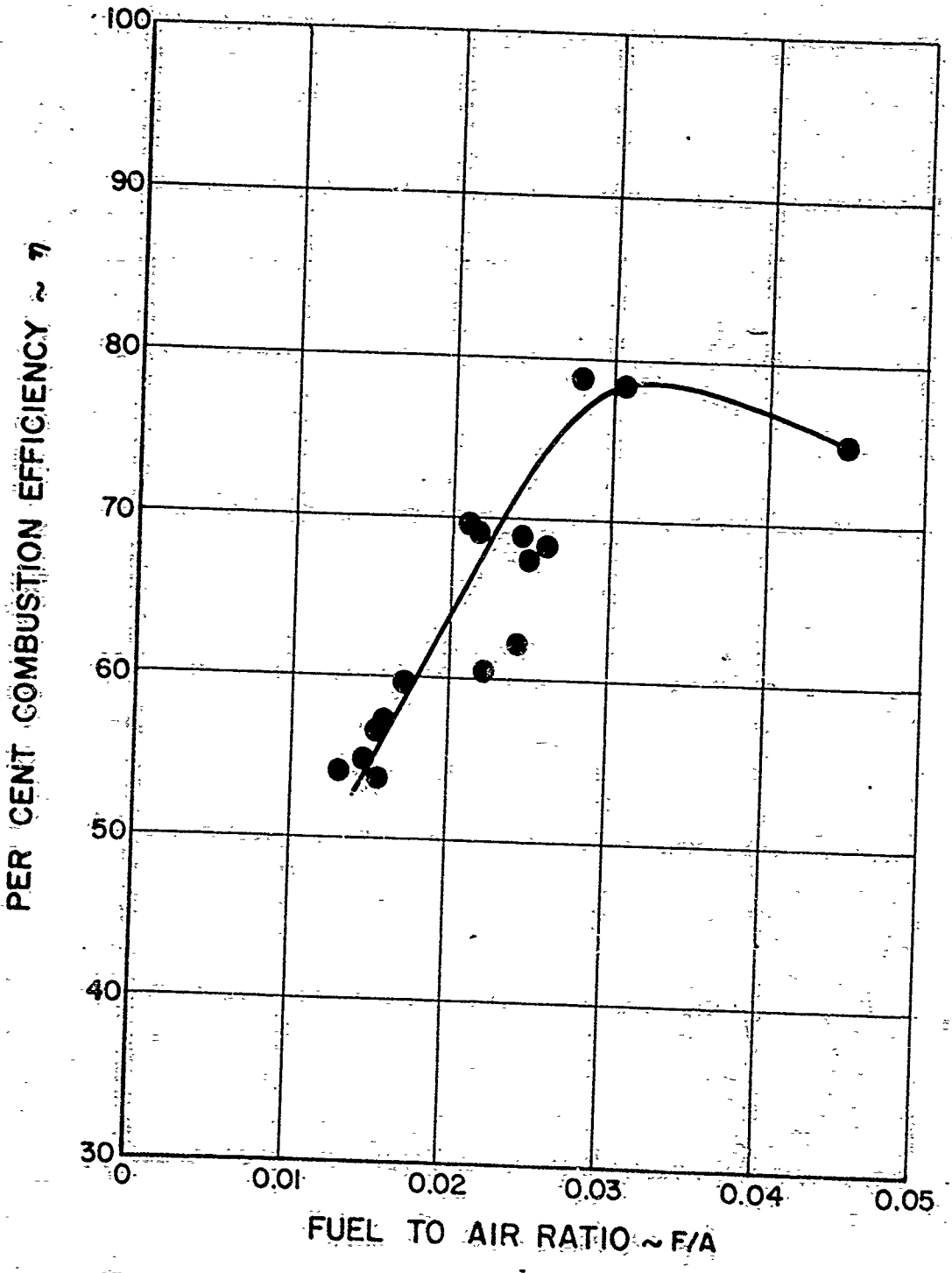
COMPARISON OF FULL-SCALE AND SMALL-SCALE DUCT HEATER TEST RESULTS AT LOW TEMPERATURE

Figure 7-32



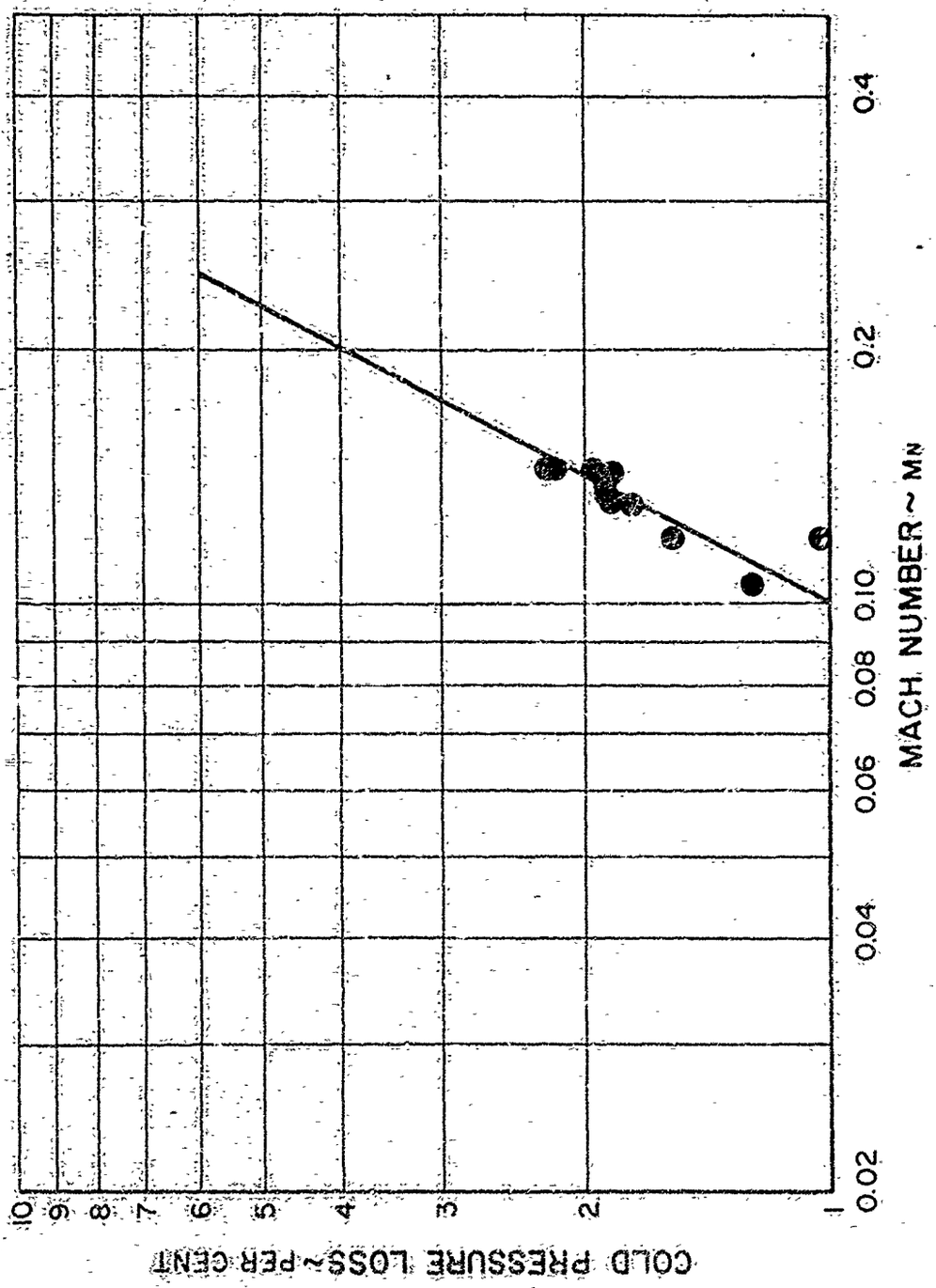
COMPARISON OF FULL-SCALE AND SMALL-SCALE DUCT HEATER TEST RESULTS AT HIGH TEMPERATURE

Figure 7-33



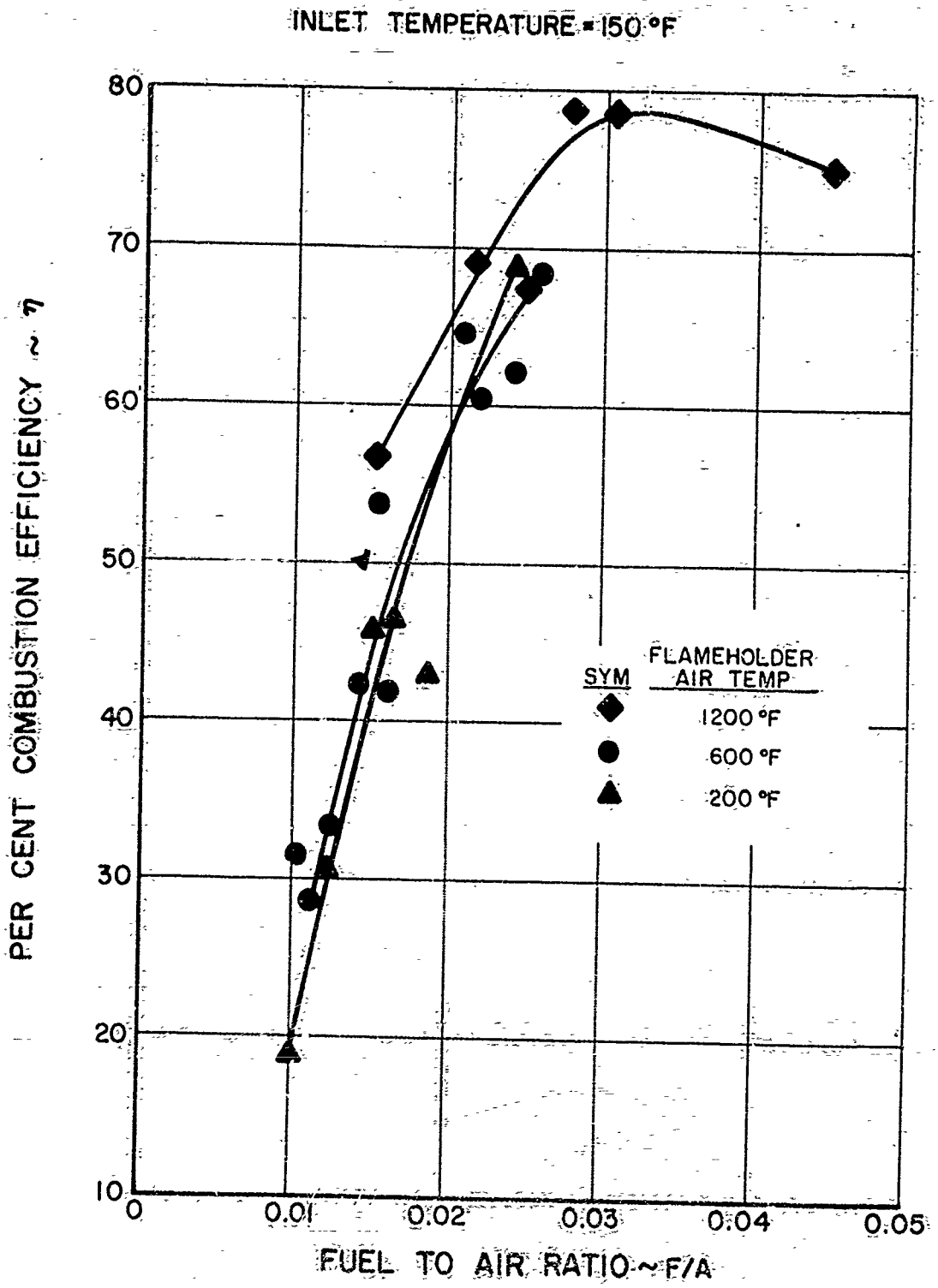
FULL-SCALE DUCT HEATER RIG PERFORMANCE

Figure 7-34



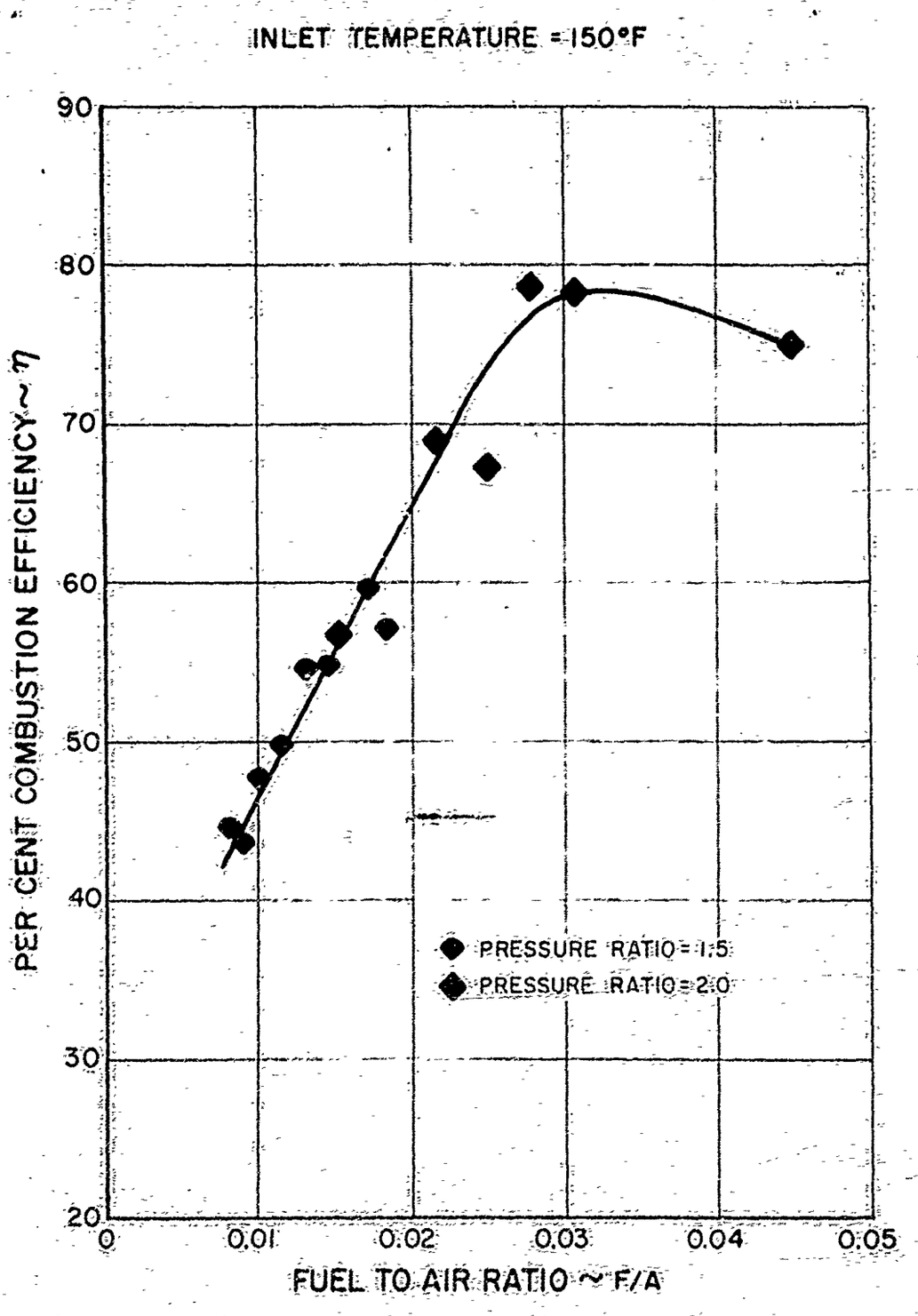
FULL-SCALE DUCT HEATER RIG COLD PRESSURE LOSS

Figure 7-35



EFFECT OF FLAMEHOLDER AIR TEMPERATURE ON FULL-SCALE DUCTHEATER TEST RESULTS

Figure 7-36



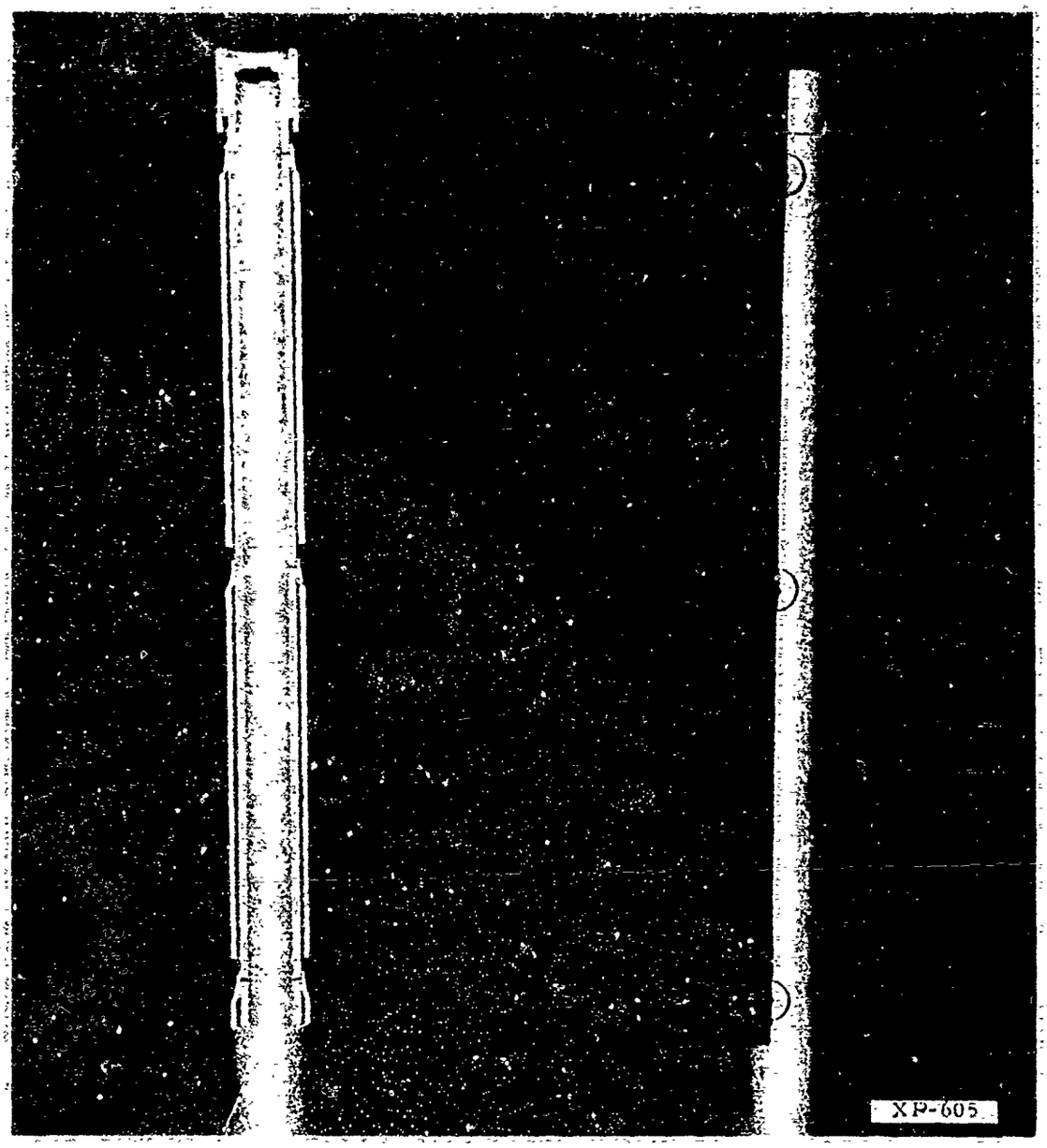
EFFECT OF FLAMEHOLDER PRESSURE RATIO ON FULL-SCALE DUCT HEATER TEST RESULTS

Figure 7-57



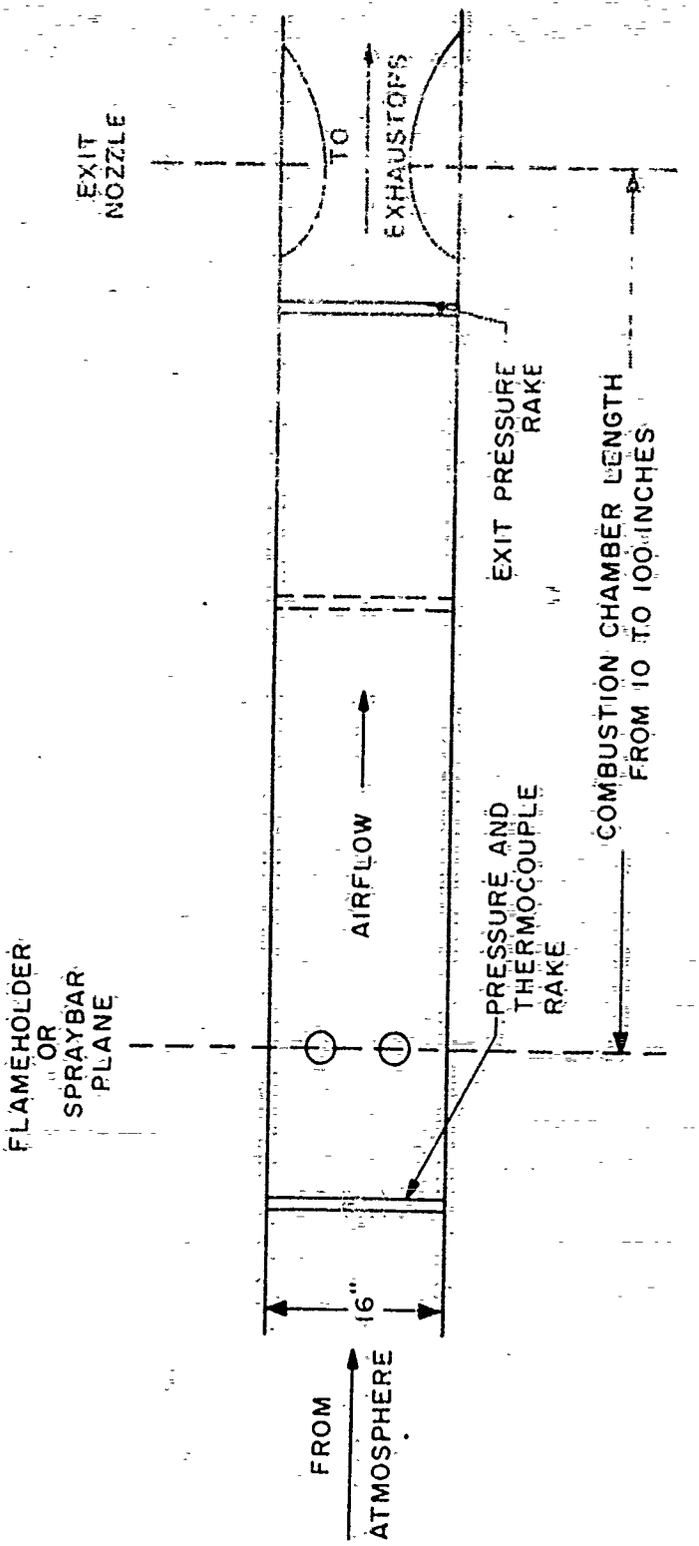
FULL-SCALE DUCT HEATER RIG

Figure 7-38



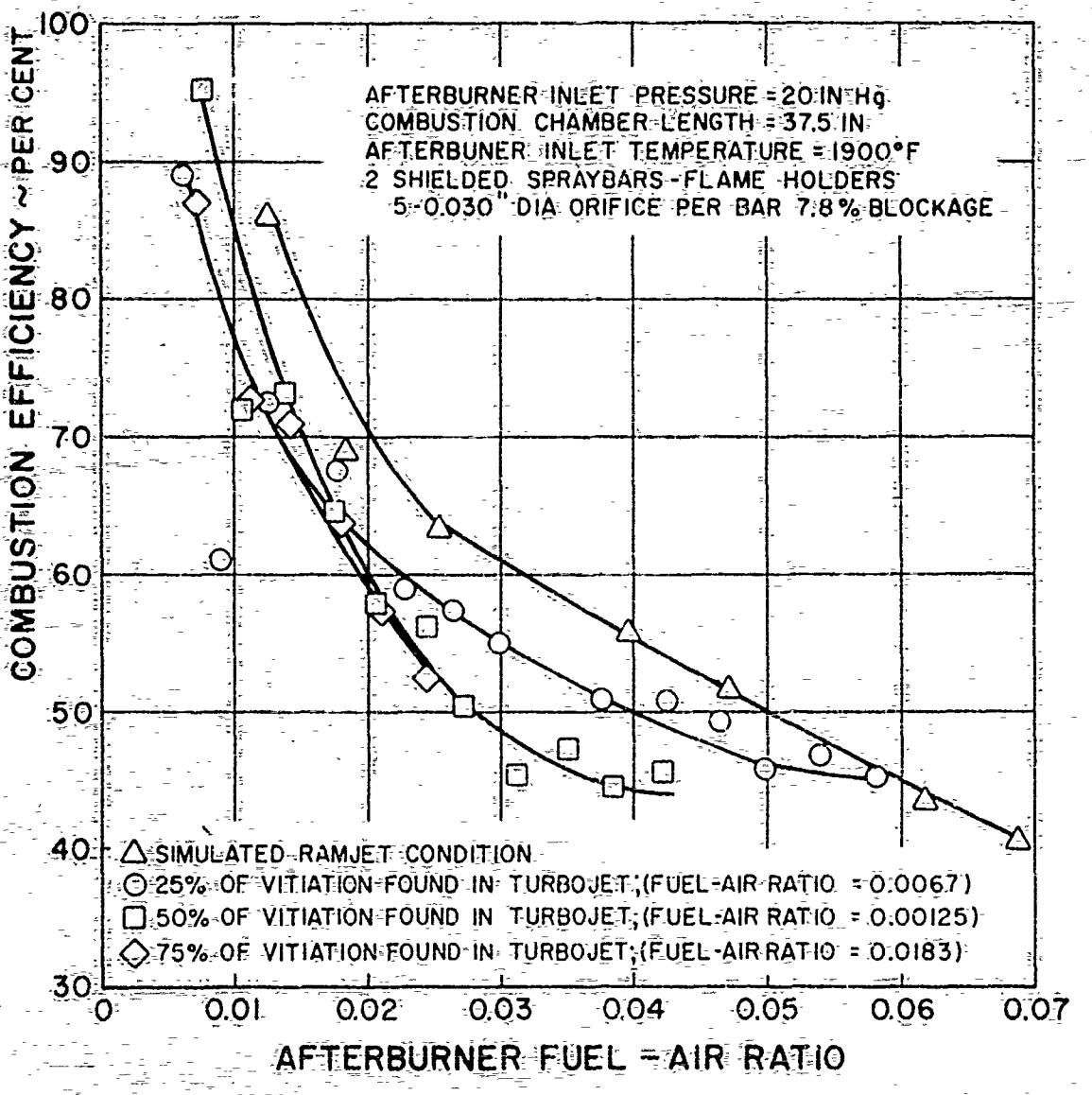
TYPICAL HEAT-SHIELDED ORIFICE-TYPE SPRAYBAR

Figure 7-39



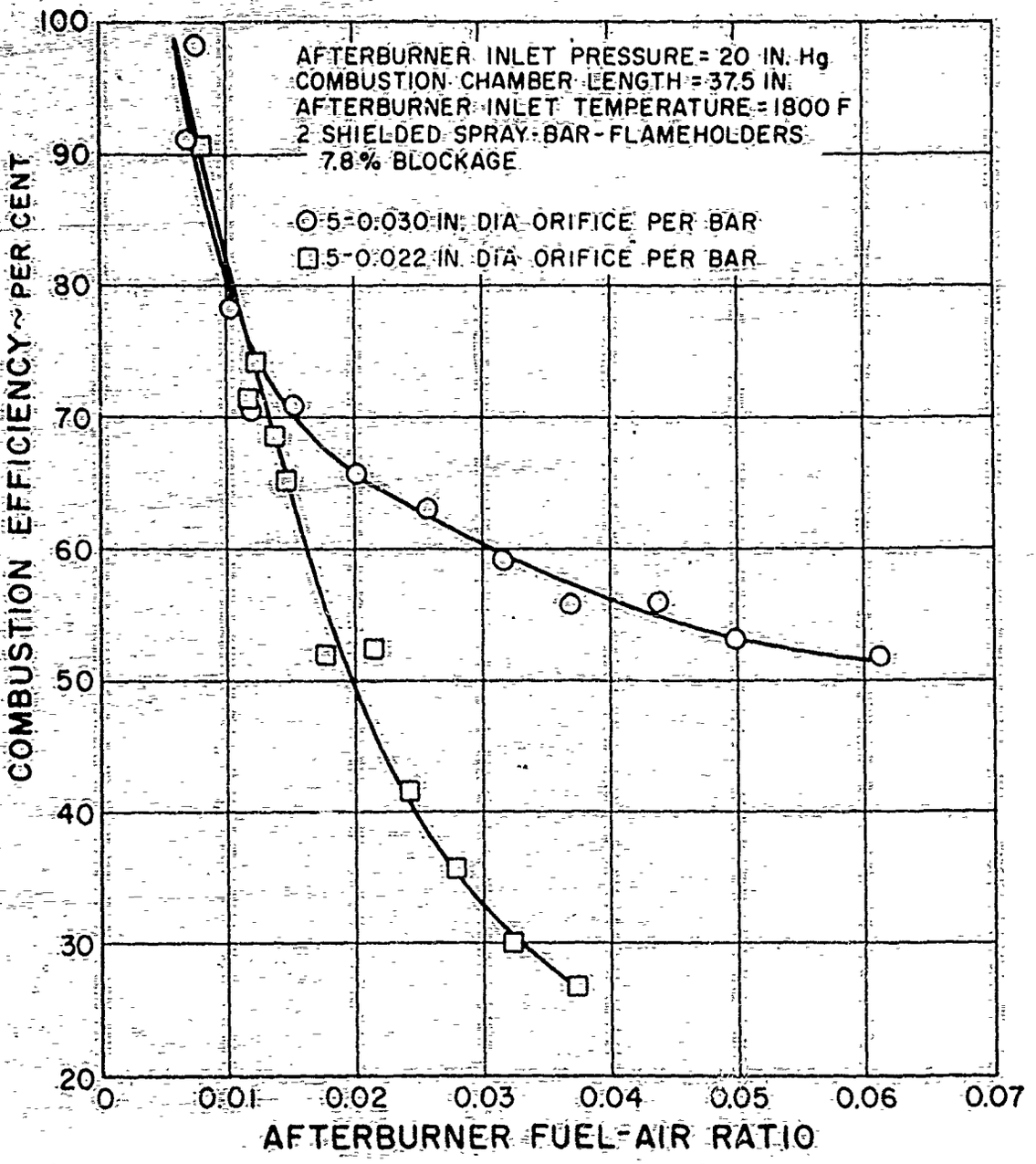
12" X 16" AFTERBURNER SEGMENT RIG

Figure 7-40



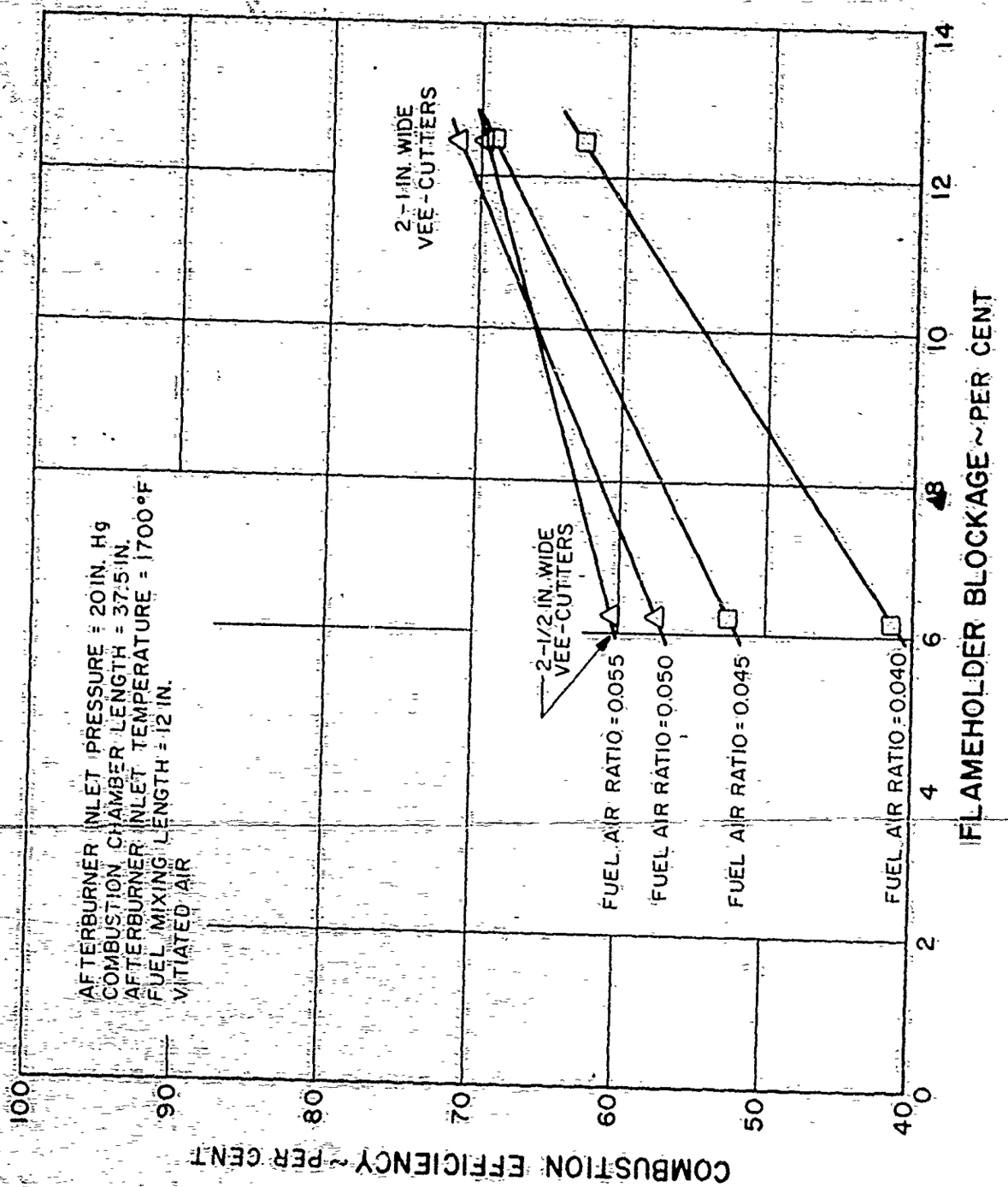
EFFECT OF VITIATION

Figure 7-41



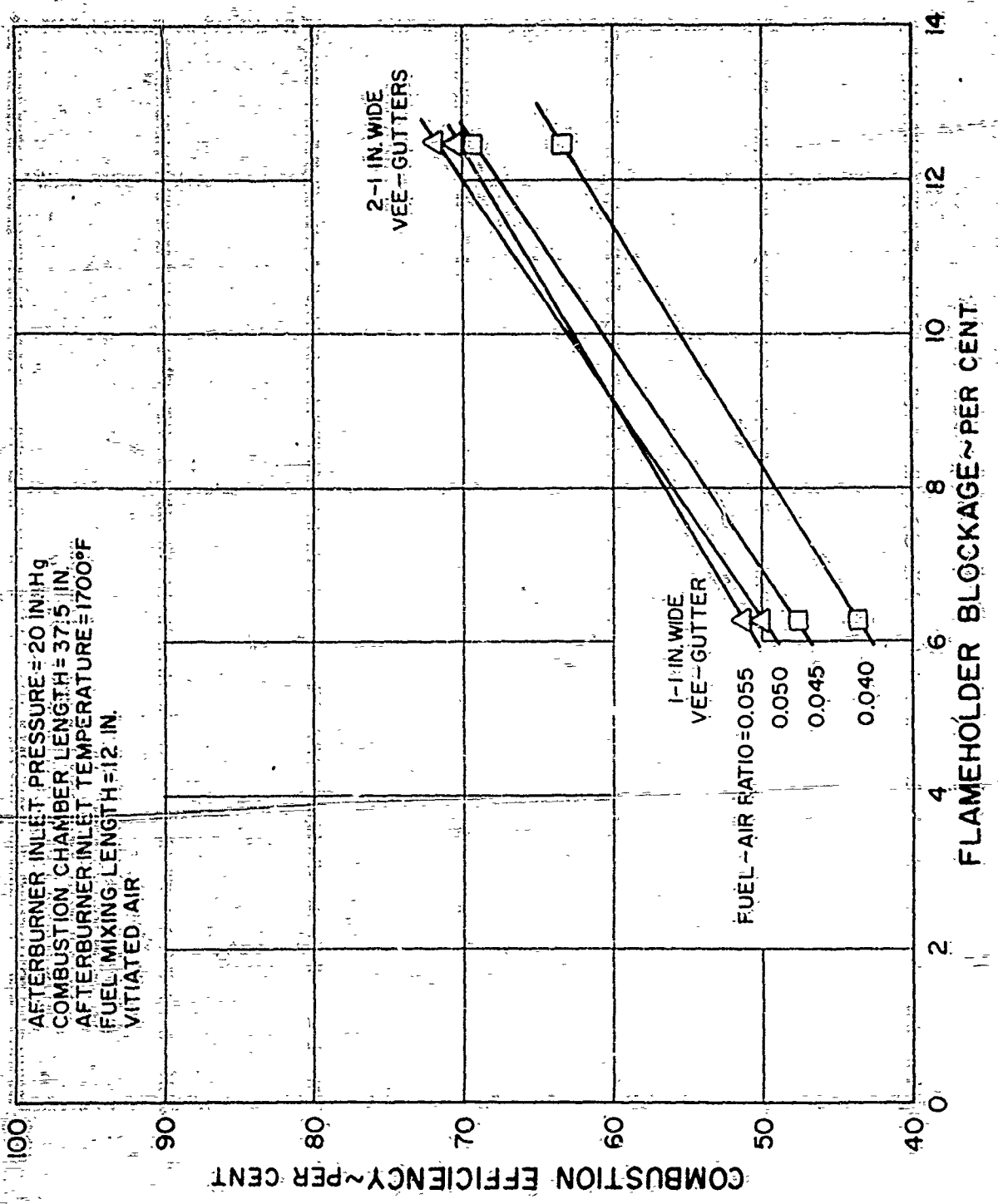
EFFECT OF ORIFICE SIZE

Figure 7-42



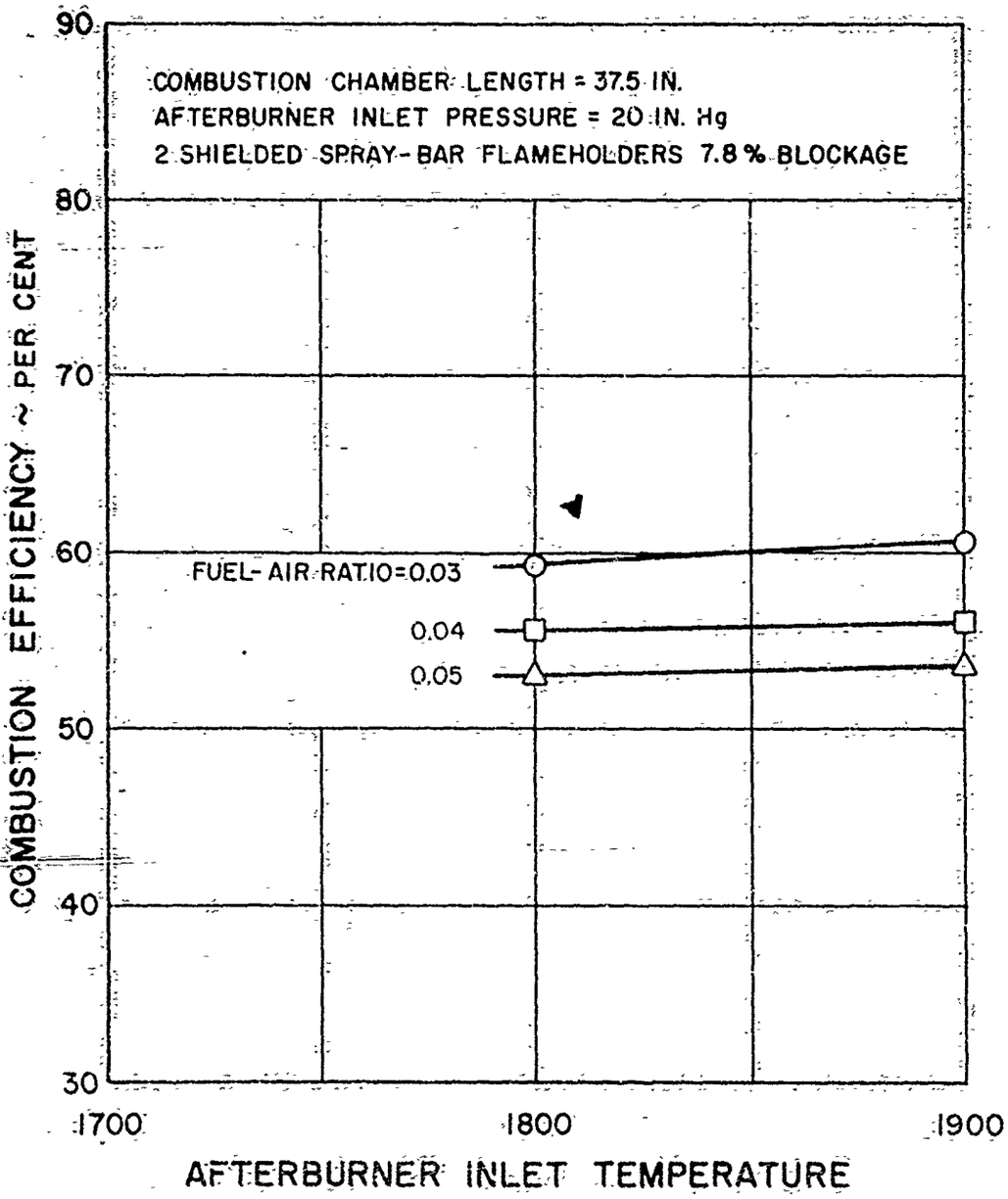
EFFECT OF INCREASING WIDTH OF F/H

Figure 7-43



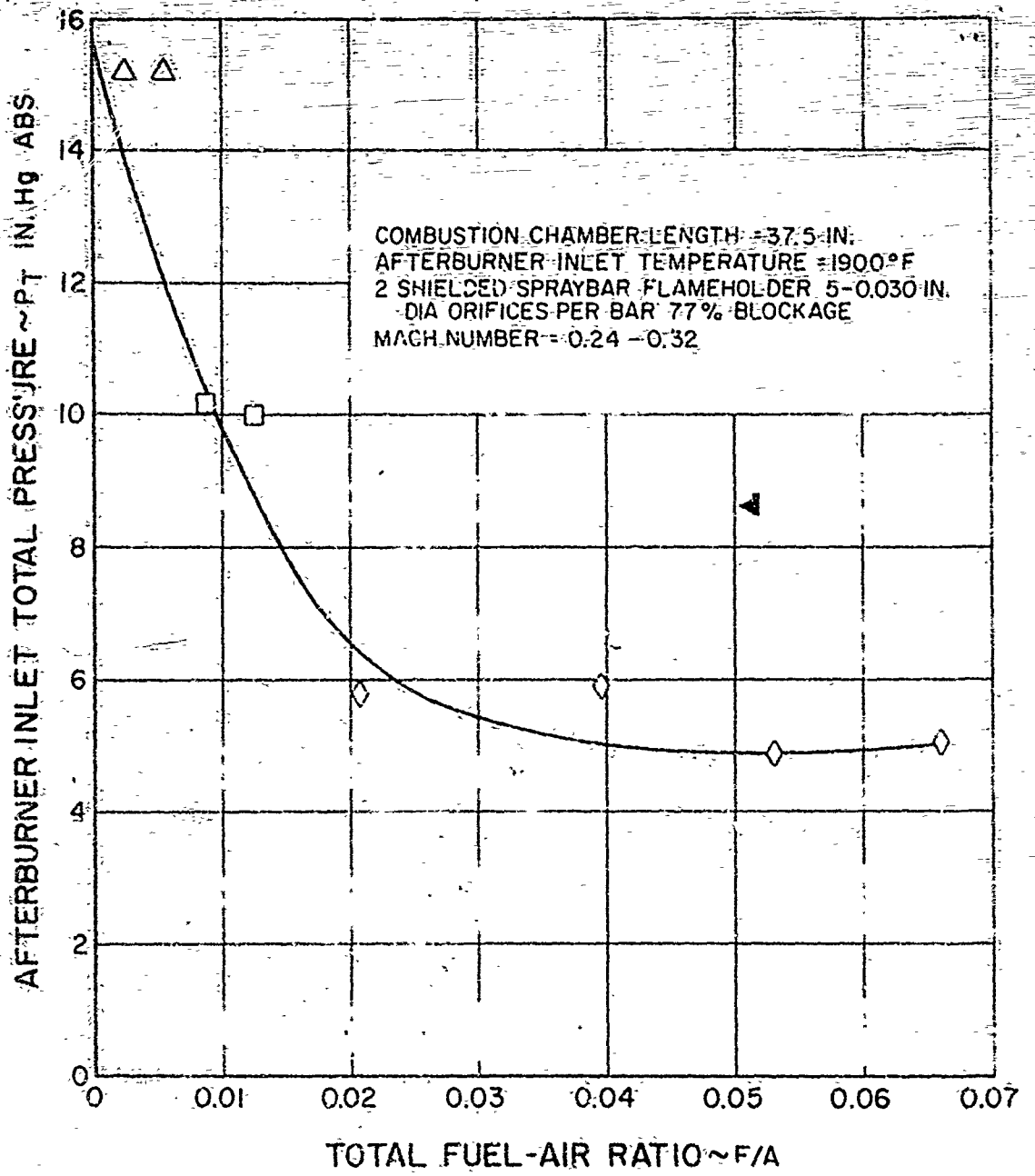
EFFECT OF INCREASING THE NUMBER OF FLAMEHOLDERS

Figure 7-41



EFFECT OF INLET TEMPERATURE ON COMBUSTION EFFICIENCY

Figure 7-45



STABILITY LIMITS

Figure 7-46